

BRITISH COLUMBIA

Geological Fieldwork 2005

A Summary of Field Activities and Current Research

Geoscience BC
Report 2006-1

Ministry of Energy, Mines and Petroleum Resources
Mining and Minerals Division
Paper 2006-1

BRITISH COLUMBIA

GEOLOGICAL FIELDWORK 2005

A Summary of Field Activities and Current Research

Geoscience BC

Report 2006-1

Ministry of Energy, Mines and Petroleum Resources
British Columbia Geological Survey

Paper 2006-1

Ministry of Energy, Mines and Petroleum Resources
Mining and Minerals Division
British Columbia Geological Survey

Parts of this publication may be quoted or reproduced if source and authorship is acknowledged. The following is the recommended format for referencing individual works contained in this publication:

Alldrick, D.J. (2006): Eskay Rift Project (NTS 103O, P, 104A, B, G, H) Northwestern British Columbia; *in* Geological Fieldwork 2005, *British Columbia Ministry of Energy, Mines and Petroleum Resources*, Paper 2006-1 and *Geoscience BC*, Report 2006-1, p 1-4.

This publication is also available, free of charge, as colour digital files in
Adobe Acrobat PDF format from the BC Ministry of Energy and Mines internet website at:

http://www.em.gov.bc.ca/Mining/Geolsurv/Publications/catalog/catfldwk.htm

COVER PHOTO: *Amy Boulton, a senior field assistant and currently attending the University of Manchester, United Kingdom, examines an outcrop south of Canam Lake, in central British Columbia, as part of an ongoing regional mapping program led by Paul Schiarizza.*

British Columbia Cataloguing in Publication Data

Main entry under title:

Geological Fieldwork: - 1974 -

Annual.

Issuing body varies

Vols. For 1978-1996 issued in series: Paper / British Columbia. Ministry of Energy, Mines and Petroleum Resources; vols for 1997- 1998, Paper / British Columbia. Ministry of Employment and Investment; vols for 1999- , Paper / British Columbia Ministry of Energy and Mines; vols for 2006- , Paper / British Columbia Ministry of Energy, Mines and Petroleum Resources.

Includes Bibliographical references.

ISSN 0381-243X=Geological Fieldwork

1. Geology - British Columbia - Periodicals. 2. Mines and mineral resources - British Columbia - Periodicals. 3. Geology - Fieldwork - Periodicals. 4. Geology, Economic - British Columbia - Periodicals. 5. British Columbia. Geological Survey Branch - Periodicals. I. British Columbia. Geological Division. II. British Columbia. Geological Survey Branch. III. British Columbia. Geological Survey Branch. IV. British Columbia. Dept. of Mines and Petroleum Resources. V. British Columbia. Ministry of Energy, Mines and Petroleum Resources. VI. British Columbia. Ministry of Employment and Investment. VII. British Columbia Ministry of Energy and Mines. VIII. Series: Paper (British Columbia. Ministry of Energy, Mines and Petroleum Resources). IX. Series: Paper (British Columbia. Ministry of Employment and Investment). X. Series: Paper (British Columbia Ministry of Energy and Mines). XI. Series: Paper (British Columbia Ministry of Energy, Mines and Petroleum Resources).

VICTORIA
BRITISH COLUMBIA
CANADA

JANUARY 2006

FOREWORD

The British Columbia Ministry of Energy, Mines and Petroleum Resources and Geoscience BC present the results of 2005 geoscience surveys and studies in this thirty-first edition of ***Geological Fieldwork: A Summary of Fieldwork and Current Research***. Many articles are contributions from staff of the BC Geological Survey. Geoscience field surveys and the provision of resulting geoscience data have led to claim staking and enhanced mineral exploration expenditures, which may ultimately lead to new mines and economic support for BC communities. As in previous years, the volume also publishes studies by university and industry authors.

This volume also includes 13 articles provided by Geoscience BC, a new, not-for-profit, nongovernment organization mandated to provide geoscience information to stimulate mineral, and oil and gas exploration in British Columbia. The province provided a grant of $25 million as start-up funding for the new organization.The articles span a wide spectrum from geochemical surveys and geological mapping to new tools for accessing provincial databases. For details of the Geoscience BC program, refer to the review, and the individual manuscripts, presented later in this volume.

This past year the BC Geological Survey regional field surveys and collaborative geoscience studies continued the tradition of partnerships with government, industry and universities. Articles in this volume include reports on continuing programs in the Iskut-Bowser Basin and Toodoggone areas, and new geoscience projects in the Canim Lake, coastal (industrial minerals), Greenwood, northeast (coal), northern Vancouver Island and Terrace areas. Industry partnerships provided operating funds and access to private-sector information, particularly for the porphyry copper-gold (Galore Creek and Mt Polley) and Toodoggone programs. This volume also reports on the results of a multiyear investigation into the province's diamond potential and highlights significant new information for the northeast corner of BC.

Over the past year, the BC Geological Survey published *Geological Fieldwork 2004*, *Exploration and Mining in British Columbia 2004*, 18 Open File maps and reports, 3 Geoscience Maps, 25 GeoFile maps, reports and data and 3 Information Circulars. One of the highlight products this year has been the new, 1:250 000-scale, digital geological map of the province — the first lithology-based map of the Province in over 25 years. All geoscience publications are now routinely posted to the Ministry of Energy, Mines and Petroleum Resources website. MapPlace, one of the world's premier Internet-based geoscience map systems, continues to improve with the addition of new tools and data layers; the site exceeded six million hits during the last year. MINFILE, the mineral deposits database system, has been reprogrammed and made more accessible with a new Internet interface. Clients can now access company mineral assessment reports from the ARIS database, on line for the years from 1947 to 1969, and from 1991 to the present.

This *Geological Fieldwork* volume reflects the hard work and expertise of numerous authors who have earned our thanks for their contributions. The articles have been improved by peer and supervisor review, and the quality services of RnD Technical are acknowledged for helping to put the volume together. The editor, Brian Grant, earns special commendation for being the key person in producing *Geological Fieldwork*, as he coordinates the organization and publication of the volume.

D.V. Lefebure
Chief Geologist
British Columbia Geological Survey

CONTENTS

Alldrick, D.J.: Eskay Rift Project (NTS 103O, P, 104A, B, G, H), Northwestern BC 1

Bath, A.B and Logan J.M.: Petrography and Geochemistry of the Late Triassic Bootjack Stock (NTS 093A/12), South-Central BC 5

Barresi, T. and Nelson, J.L.: Usk Map Area (NTS 103I/9), Near Terrace, BC: Cross-Sections and Volcanic Facies Interpretation. 21

Diakow, L.J. and Rhodes, R.: Geology Between the Toodoggone River and Chukachida Lake (Parts of NTS 094E/06, 07, 10 and 11), North-Central BC 29

Greene, A.R., Scoates, J.S., Nixon,G.T. and Weis, D.: Picritic Lavas and Basal Sills in the Karmutsen Flood Basalt Province, Wrangellia, Northern Vancouver Island, BC 39

Lett, R.E. and Friske, P.W.B.: Bowser Basin Geochemical Survey, North-Central BC: Anomaly Follow-up, 2005 . 53

Lett, R.E.: Geochemical Surveys in the Lillooet Area (NTS Areas 092J, 092I, 092O, 092P), Southwestern BC 63

Legun, A.S.: The Gates Formation in the Wolverine River Area, Northeastern BC 73

Logan, J.M. and Bath, A.B.: Geochemistry of Nicola Group Basalt from the Central Quesnel Trough at the Latitude of Mount Polley (NTS 093A/5, 6, 11, 12), Central BC . . . 83

Massey, N.W.D.: Boundary Project: Reassessment of Paleozoic Rock Units of the Greenwood Area (NTS 082E/02), Southern BC 99

Mihalynuk, M.G. and Friedman, R.M.: U-Pb Isotopic Ages of Intrusive Rocks Related to Mineralization North of Terrace, BC. 109

Nelson, J.L., Barresi, T., Knight, E. and Boudreau, N.: Geology and Mineral Potential of the Usk Map Area (NTS 103I/09), near Terrace, BC 117

Nixon, G.T., Kelman, M.C., Stevenson, D., Stokes, L.A. and Johnston, K.A.: Preliminary Geology of the Nimpkish Map Area (NTS 092L/07), Northern Vancouver Island, BC 135

Peterson, N.D., Russell, J.K. and Mahoney, J.B.: Mantle-Derived Peridotite Xenoliths from the Western Intermontane Belt, Whitesail Lake map area (NTS 093E), Western BC 153

Schiarizza, P. and Boulton, A.: Geology and Mineral Occurrences of the Quesnel Terrane, Canim Lake Area (NTS 092P/15), South-Central BC 163

Simandl, G.J., Robinson, N.D. and Paradis, S.: Iron (Magnetite) Ore Resources in Southwestern BC: Soft Niche or Steel-Hard Market? 185

Simandl, G.J., Robinson, N.D. and Paradis, S.: Dolomite in BC: Geology, Current Producers and Possible Development Opportunities along the West Coast . . . 197

Simandl, G.J., Ferbey, T., Levson, V.M., Robinson, N.D., Lane, R., Smith, R., Demchuk, T.E., Raudsepp, I.M. and Hickin, A.S.: Kimberlite and Diamond Indicator Minerals in Northeastern BC: A Reconnaissance Survey 209

GEOSCIENCE BC

Stevens, R.A.: Summary of Geoscience BC Program Activities 2005 231

Cook, S.J. and Dunn, C.E.: Preliminary Results of the Cordilleran Geochemistry Project: A Comparative Assessment of Soil Geochemical Methods for Detecting Buried Mineral Deposits, 3Ts Au-Ag Prospect (NTS 93F/3), Central BC 237

Dunn, C.E., Cook, S.J. and Hall, G.E.M.: Halogens in Surface Exploration Geochemistry: Evaluation and Development of Methods for Detecting Buried Mineral Deposits (NTS 93F/3), Central BC 259

Evenchick, C.A., O'Sullivan, P.B. and Waldron, J.W.F. : Targeted Energy-Resource Studies in the Bowser and Sustut Interior Basins of BC 281

Kilby, W.E. and Kilby, C.E.: ASTER Imagery for BC – An Online Exploration Resource. 287

Jackaman, W.: Drainage Sediment and Water Geochemical Surveys in the Anahim Lake and Nechako River Map Areas (NTS 93C and F), Central BC. 295

MacIntyre, D.: Geology and Mineral Deposits of the Skeena Arch, West-Central BC: A Geoscience BC Digital Data Compilation Project 303

Mahoney, J.B., Haggart, J.W., Hooper, R.L., Snyder, L.D. and Woodsworth, G.J.: Geological Setting and Mineralization Potential of the Southwestern Whitesail Lake Map Area (NTS 93E), Western BC: Preliminary Assessment 313

Marshall, D., Lesiczka, M., Xue, G. and Close, S.: Update on the Mineral Deposit Potential of the Nootka Sound Region (NTS 92E), West Coast of Vancouver Island, BC 323

Mortensen, J.K.: Stratigraphic and Paleotectonic Studies of the Middle Paleozoic Sicker Group and Contained VMS Occurrences, Vancouver Island, BC 331

Plouffe, A., Smith, I.R., McCurdy, M., Friske, P., Ferbey, T., Bednarski, J., Levson, V.M., Demchuk, T.E., Trommelen, M., Day, S. and Hickin, A.S.: Glacial and Stream Sediments Sampling in Support of Kimberlite Exploration in Northeastern BC 337

Nass, C.O.: 2005 Regional Geochemical Survey, NTS Areas 83C, 83D, 83E and 82N, Southeastern British Columbia. 343

Waldron, J.W.F., Gagnon, J.-F., Loogman, W. and Evenchick, C.A.: Initiation and Deformation of the Jurassic-Cretaceous Bowser Basin: Implications for Hydrocarbon Exploration in North-Central BC 349

Eskay Rift Project (NTS 103O, P, 104A, B, G, H), Northwestern British Columbia

By D.J. Alldrick

KEYWORDS: regional mapping, Eskay mine, Iskut, Eskay rift, lithogeochemistry, Hazelton Group, Bowser Basin, economic geology.

INTRODUCTION

Located in northwestern British Columbia, the Eskay Rift is the geological setting for the world's richest volcanogenic massive sulphide deposit: the Eskay Creek gold-silver mine (Fig. 1). The rift structure was first recognized by Geological Survey of Canada geologists (Anderson and Thorkelson, 1990), and they extended the structure southward in 1998 (Evenchick *et al.*, 1998; Evenchick and McNicoll, 2002).

The BC Geological Survey began detailed mapping of the northern half of the rift in 2003, combined with lithogeochemical studies at Dalhousie University. A series of reports (Alldrick *et al.*, 2005a, b; Barresi *et al.*, 2005; Barresi and Dostal, 2005; Alldrick *et al.*, 2004a, b) and coloured maps (Alldrick *et al.*, 2006a, b; Alldrick *et al.*, 2005a, b; Alldrick *et al.*, 2004a, b) present the field and laboratory work completed to date.

REGIONAL GEOLOGY

The Eskay Rift is a fault-bounded basin hosting thick accumulations of bimodal basalt and rhyolite flows, with intercalated sedimentary rocks. Rift strata record the final eruptive events of the Early to Middle Jurassic Hazelton Group, an island-arc complex that extends from the Yukon to Washington state. The rift hosts 60 VMS deposits and prospects, including two new VMS prospects discovered in outcrop in 2004.

2005 FIELD PROGRAM

This year's field program continued stratigraphic investigations within the rift (Mount Shirley, Sixpack Range, Todagin Plateau, Klastline Plateau, Mount Madge, Arctic Grid); reconnaissance investigation of Upper Hazelton strata beyond the Eskay Rift, where rift-indicator features had been noted (Treaty Glacier, Tim Williams Glacier, Oweegee Dome, Bait Range, Mount Dilworth); and examination of prospects and gossans (Table Mountain, Smitty, Knipple Glacier, Tim Williams Glacier, Bait North). Seven sites of economic interest deserve follow-up: a pyritic siltstone member within the Eskay-age basalt in the central Bait Range; the eastern stratigraphic extensions of the RAM prospect; the Timbit gossan east of Castle Rock; a recently exposed dacite cryptodome within pyritic Salmon River siltstone on Mount Dilworth; pyritic carbonate laminae with sandstone and siltstone members between basalt flows northeast of the toe of Tim Williams glacier; the Zinc Moss – Dome – Compass – Griz trend of prospects on Table Mountain; and pyritic rhyolite with minor intercalated basalt on northwestern Oweegee Dome.

Areas identified for investigations next season include the following:

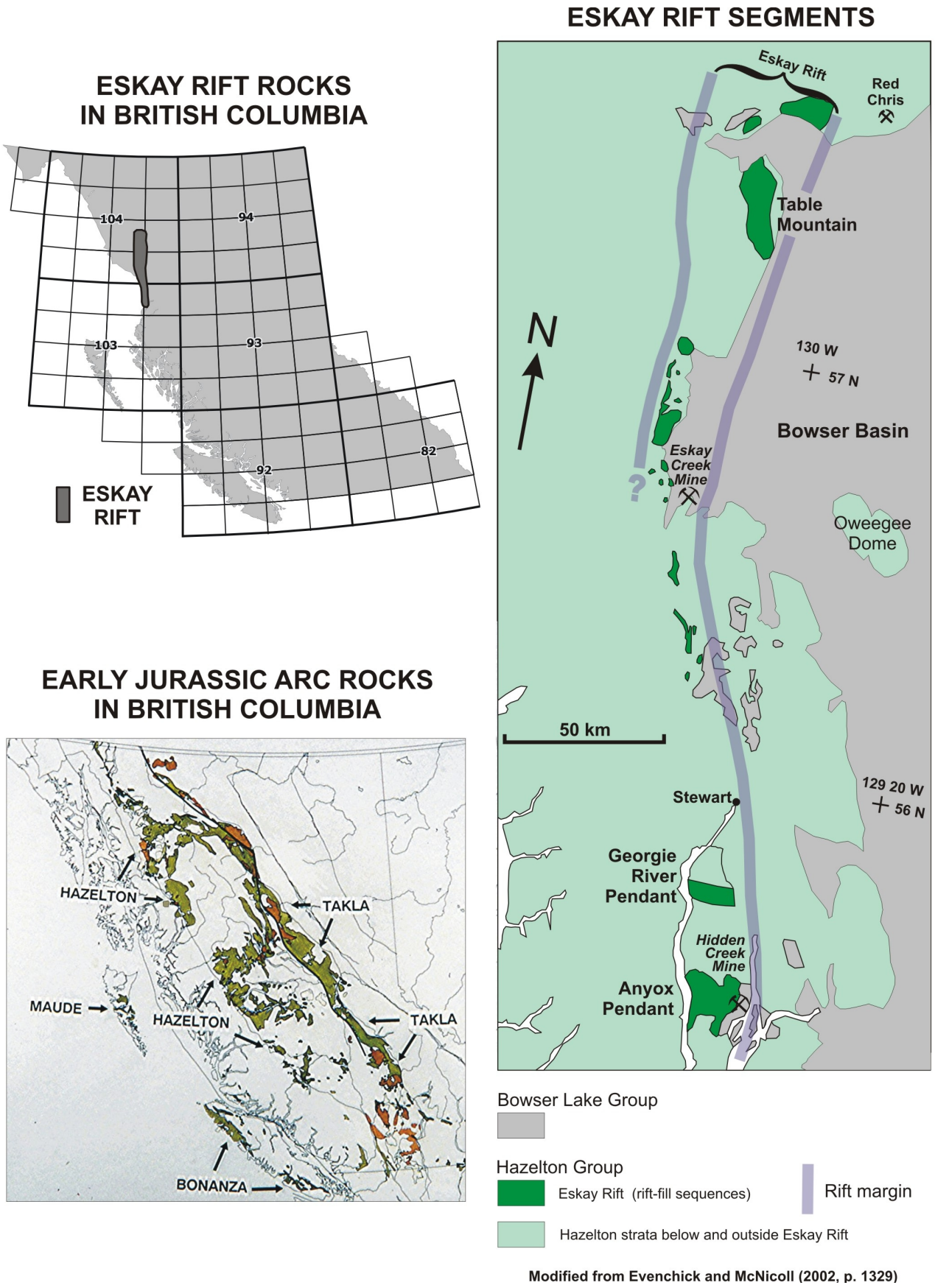
- Upper Hazelton stratigraphy north and east of Smithers
- An unmapped area with polymetallic prospects northeast of the Red Chris property and west of the Klappan River
- Rhyolite and pillow basalt within the Georgie River pendant
- Pyritic dacite in the upper Kitsault River valley
- The setting of the VMS prospects at Seneca, west of Harrison Lake
- Eskay-equivalent sedimentary strata outlined by Souther on the eastern flank of Mount Edziza
- The Eskay mine – Mount Madge corridor
- The area surrounding the Dome prospect on Table Mountain

SUMMARY

The Eskay Rift is preserved as a narrow, discontinuous, 250 km long belt extending from Klastline Plateau in the north to Anyox in the south (Fig. 1; Alldrick, 2000). There are 25 individual segments of these rift-fill-sequence rocks preserved. Detailed mapping along the northern half of the rift shows that most segments have generally similar lithological characteristics, but proportions of key rock types within and between rift segments vary widely. Some rift-fill sequences were clearly deposited in isolation from those of adjacent rift segments, suggesting that they occupied nearby but unconnected basins. Paleowater depth varied between these different rift segments, ranging from subaerial, to shallow to moderate water depth (0–500 m), to deep-water ocean floor settings (>1000 m). Associated VMS deposits reflect these varying water depths.

Exhalitive mineral deposits and prospects are known in three rift segments: Eskay Creek, Anyox and Table Mountain. The Eskay Creek and Anyox rift segments host producing and past-producing mines; the several exhalitive prospects in the Table Mountain rift segment were recently discovered, have limited outcrop exposure and have so far

This publication is also available, free of charge, as colour digital files in Adobe Acrobat PDF format from the BC Ministry of Energy, Mines and Petroleum Resources internet website at http://www.em.gov.bc.ca/Mining/Geolsurv/Publications/catalog/catfldwk.htm



Modified from Evenchick and McNicoll (2002, p. 1329)

Figure 1. Distribution of Eskay Rift strata in northwestern British Columbia.

yielded subeconomic assays. These exhalitive deposits and prospects developed at a range of water depths, accounting for pronounced differences in mineralogy and metal associations, and requiring different exploration strategies. The Georgie River and Downpour Creek rift segments have had limited exploration work to date and deserve further investigation due to their favourable lithological associations and prominent felsic volcanic centres. The five small, remote rift segments between Frank Mackie Icefield and the Granduc mine were last mapped and explored in the mid-1960s.

The Eskay Rift has been regarded as the final, brief (176–174 Ma) episode of Hazelton Arc history, but new mapping and dates from the Sixpack Range suggest that the onset of rifting may have started in early Hazelton time (191 Ma). In this particular rift segment, rift-fill strata rest directly on metamorphosed Paleozoic substrate.

The Eskay Rift records a major Early to Middle Jurassic crustal break that extended from a subaerial setting within island-arc rocks at its northern end to a near-continent, mid-ocean-ridge setting at its southern end. Analogous settings are preserved in Triassic arc rocks of the southeastern Alaska panhandle and along the east-trending arm of the Great African Rift.

REFERENCES

Alldrick, D.J. (2000): Geology of the Anyox Mining camp; BC Ministry of Energy, Mines and Petroleum Resources, Open File Map 2000-28, Scale 1:20 000.

Alldrick, D.J., Nelson, J.L., Barresi, T., Stewart, M.L. and Simpson, K.A. (2006a): Geology of upper Iskut River area, northwestern British Columbia; BC Ministry of Energy and Mines, Open File Map 2006-2, Scale 1:100 000.

Alldrick, D.J., Nelson, J.L. and Barresi, T. (2006b): Geology of the Volcano Creek – More Creek area, northwestern British Columbia; BC Ministry of Energy and Mines, Open File Map 2006-6, Scale 1:50 000.

Alldrick, D.J., Nelson, J.L. and Barresi, T. (2005a): Geology of the More Creek – Palmiere Creek area, northwestern British Columbia; *BC Ministry of Energy, Mines and Petroleum Resources*, Open File Map 2005-5, scale 1:50 000.

Alldrick, D.J., Nelson, J.L. and Barresi, T. (2005b): Tracking the Eskay Rift through northern British Columbia: geology and mineral occurrences of the upper Iskut River area; *in* Geological Fieldwork 2004, *BC Ministry of Energy, Mines and Petroleum Resources*, Paper 2005-1, pages 1–30.

Alldrick, D.J., Nelson, J.L., Barresi, T., Stewart, M.L. and Simpson, K.A. (2006b): Geology of upper Iskut River area, northwestern British Columbia; *BC Ministry of Energy, Mines and Petroleum Resources*, Open File Map 2006-2, scale 1:100 000.

Alldrick, D.J., Stewart, M.L., Nelson, J.L. and Simpson, K.A. (2004a): Geology and mineral occurrences of the upper Iskut River area: tracking the Eskay Rift through northern British Columbia; *in* Geological Fieldwork 2003, *BC Ministry of Energy, Mines and Petroleum Resources*, Paper 2004-1, pages 1–18.

Alldrick, D.J., Stewart, M.L., Nelson, J.L. and Simpson, K.A. (2004b): Geology of the More Creek – Kinaskan Lake area, northwestern British Columbia; *BC Ministry of Energy, Mines and Petroleum Resources*, Open File Map 2004-2, scale 1:50 000.

Anderson, R.G. and Thorkelson, D.J. (1990): Mesozoic stratigraphy and setting for some mineral deposits in Iskut River map area, northwestern British Columbia; *in* Current Research, Part E, Geological Survey of Canada, Paper 90-1E, pages 131–139.

Barresi, T. and Dostal, J. (2005): Geochemistry and petrography of Upper Hazelton Group volcanics: VHMS favourable stratigraphy in the Iskut River and Telegraph Creek map areas, northwestern British Columbia; *in* Geological Fieldwork 2004, *BC Ministry of Energy, Mines and Petroleum Resources*, Paper 2005-1, pages 39–48.

Barresi, T., Nelson, J.L., Alldrick, D.J. and Dostal, J. (2005): Pillow Basalt Ridge facies: detailed mapping of Eskay Creek equivalent stratigraphy in northwestern British Columbia; *in* Geological Fieldwork 2004, *BC Ministry of Energy, Mines and Petroleum Resources*, Paper 2005-1, pages 31–38.

Evenchick C.A. and McNicoll, V.J. (2002): Stratigraphy, structure and geochronology of the Anyox pendant, northwest British Columbia, and implications for mineral exploration; *Canadian Journal of Earth Sciences*, Volume 39, pages 1313–1332.

Evenchick C.A., McNicoll V.J., Holm K., Alldrick D.J. and Snyder L.D. (1998): Geology of the Observatory Inlet area; *Geological Survey of Canada*, Open File Map 3454, scale 1:50 000.

Souther, J.G. (1992): The Late Cenozoic Mount Edziza Volcanic Complex, British Columbia. *Geological Survey of Canada*, Memoir 420, 319 pages.

Petrography and Geochemistry of the Late Triassic Bootjack Stock (NTS 093A/12), South-Central British Columbia

Adam B. Bath[1, 2] and James M. Logan[1]

KEYWORDS: syenite, pseudoleucite, sulphide inclusions, Mount Polley, haüyne, bornite, chalcopyrite

INTRODUCTION

Establishing links between mineralization and causative intrusion(s) is an important and fundamental step to understanding mineralizing systems. In particular, the ability to distinguish petrological and geochemical characteristics of mineralized versus barren intrusive systems has important implications for the exploration geologist (*e.g.*, Frei, 1996).

This study investigated a Late Triassic alkalic intrusion, known as the Bootjack stock, from the south-central Canadian Cordillera. The Bootjack stock (BS) is part of the Quesnel arc complex (Fig. 1) that formed above an east-dipping subduction zone during the Late Triassic to Early Jurassic (Mortimer, 1987; Panteleyev *et al.*, 1996; Logan and Mihalynuk, 2005). Other K-rich or alkaline intrusions of similar age that occur along the Quesnel arc include the Copper Mountain intrusive rocks (Copper Mountain, Ingerbelle), White Mountain, Kruger syenite, Kamloops syenite and Iron Mask batholith (Afton, Ajax and Crescent in the south; and the Hogem batholith (Lorraine) in the north. In addition, the BS is age equivalent to syenite at Galore Creek, Copper Canyon, Zippa Mountain and Rugged Mountain, which are located within the Stikine arc terrane (Fig. 1). A number of the above intrusions are spatially and temporally coincident with Cu-Au mineralization. The BS, in particular, is spatially and temporally associated with the Cu-Au mineralizing event at Mount Polley; however, no direct links have been made between it and mineralization. The purpose of this study is to examine new major and trace element data from the BS, combined with petrographic descriptions, to determine if there are any features of the BS that could explain the alteration and mineralization events at Mount Polley. The study also compares the geochemistry of the BS with other intrusions of similar age at Mount Polley and in the Quesnel Lake area.

REGIONAL GEOLOGY

The Bootjack stock (BS) is located in the Quesnel Lake map area (NTS 093A/12) of south-central British Columbia and intrudes Triassic Nicola Group arc volcanic rocks and associated sedimentary rocks within the Quesnel Terrane (Fig. 1; Fraser, 1994; Panteleyev *et al.*, 1996; Logan and Mihalynuk, 2005). The intrusive body is closely associated, both spatially and temporally, with other alkalic intrusive phases at Mount Polley, which include diorite and plagioclase porphyry phases of the Mount Polley stock (Fraser, 1994). The BS outcrops further to the south (stratigraphically deeper) of the main mineralized centre and is separated from the Mount Polley stock and mineralization zones by a narrow belt (~2 km wide) of northwest-trending metavolcanic flows, breccia units, fine-grained bedded volcaniclastic units and a pyroxenite body, which was identified in drillcore and is located beneath Bootjack Lake (Hodgson *et al.*, 1976; Fraser, 1994). However, the northward extension of the BS is unknown, and the possibility that it intrudes rocks beneath Mount Polley cannot be ruled out.

GEOCHRONOLOGY

Intrusions

The relative timing of emplacement of the Bootjack and Mount Polley stocks is constrained by the presence of xenoliths. According to Fraser (1994), the BS and plagioclase porphyry include xenoliths of diorite and are therefore both younger. However, the age relationship between the BS and the plagioclase porphyry is unknown.

Estimated absolute ages suggest that the BS crystallized at 202.7 ±7.1 Ma (U-Pb date from pseudoleucite syenite; Mortensen *et al.*, 1995) or 200.8 ±2.8 Ma (U-Pb date from mafic pseudoleucite syenite; Mortensen *et al.*, 1995), and had cooled below 300°C by 203.1 ±2.0 Ma (Ar/Ar date from mafic pseudoleucite syenite; Bailey and Archibald, 1990), whereas the plagioclase porphyry crystallized at 204.7 ±3 Ma (U-Pb; Mortensen *et al.*, 1995). The diorite has been dated at 201.7 ±0.4 Ma (U-Pb; Mortensen *et al.*, 1995). These dates suggest that the crystallization ages of all these intrusive bodies are very similar. By combining the relative and absolute ages, it can be inferred that the BS crystallized between 202.0 and 198.0 Ma (using best U-Pb ages and errors).

Mineralization

Brecciation and mineralization are thought to be associated with the emplacement of the alkalic intrusive bodies (Fraser, 1994); however, a definitive link between the various intrusions and mineralization has not been established. The presence of diorite clasts within the breccia (dated at 201.6 ±0.5 Ma (U-Pb zircon; Fraser, 1994) and crosscutting lamprophyre dikes that have been dated regionally at approximately 130 Ma (Mortimer *et al.*, 1990) provide

[1] *British Columbia Ministry of Energy, Mines and Petroleum Resources, Victoria, BC*

[2] *University of Tasmania, Hobart, Tasmania, Australia.*

This publication is also available, free of charge, as colour digital files in Adobe Acrobat PDF format from the BC Ministry of Energy, Mines and Petroleum Resources internet website at http://www.em.gov.bc.ca/Mining/Geolsurv/Publications/catalog/catfldwk.htm

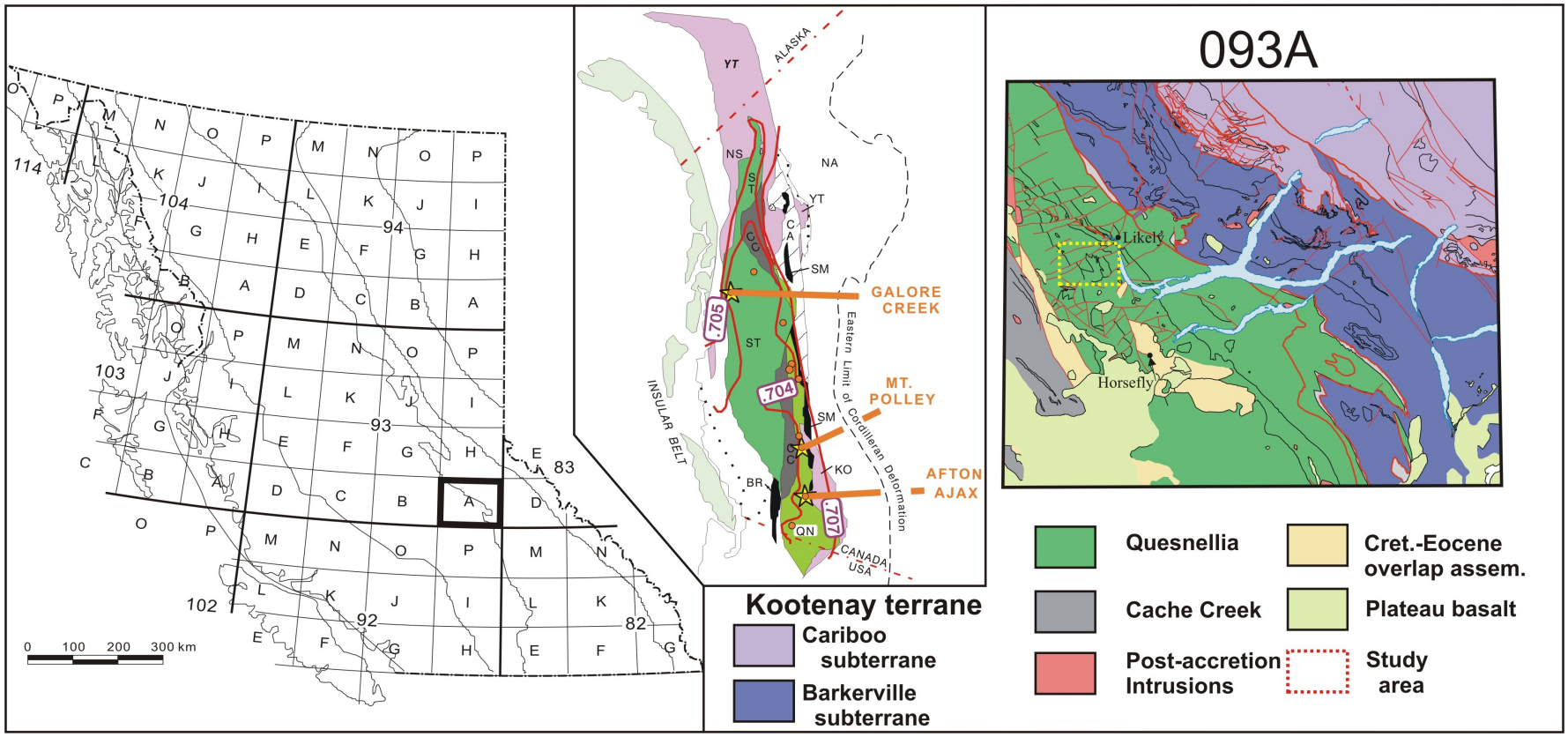


Figure 1. Location of the Mount Polley Cu-Au porphyry deposit in south-central British Columbia (NTS 092I). Insert is terrane map of the northern Cordillera (modified from Wheeler and McFeely, 1991), showing the tectonostratigraphic setting of the study area. Box on the right shows terrane relationships for NTS 093A and the project area (after Logan and Mihalynuk, 2005).

some relative age constraints. Absolute dates for mineralization have been estimated at 184 ±7 Ma for the Central zone (K-Ar biotite; Hodgson *et al.*, 1976), or more recently 205.2 ±1.2 Ma for the Northeast zone (Ar^{40}/Ar^{39} biotite; Logan and Ullrich, unpublished data, 2005) and 220.8 ±1.3 Ma for the Cariboo zone (Ar^{40}/Ar^{39} biotite; Logan and Ullrich, unpublished data, 2005).

GEOLOGY OF THE BOOTJACK STOCK

The Bootjack stock (BS) is an elliptical, northwest-trending body that covers an area of approximately 11 km² and consists of three main rock types: 1) medium-grained sparse pseudoleucite melasyenite (MS; =15% mafic minerals); 2) orbicular pseudoleucite syenite (OPS; <15% mafic minerals); and 3) equigranular coarse to medium-grained syenite (ES; <15% mafic minerals), which contains pegmatitic zones (Fig. 2).

Medium-grained melasyenite (MS; see Fig. 2), which makes up approximately 10% of the BS, forms a rim along the margin of the stock that is estimated to be 50–300 m wide. In gradational contact with the MS and making up approximately 85% of the central region of the stock is orbicular pseudoleucite syenite. The remaining 5% of the stock consists of equigranular syenite (ES), which crops out as a thin (150 mm) dike at station ABA05 32-259 or as wider (~50 m) late intrusive phases at station ABA05 33-267, where it shows pegmatitic textures. Pegmatitic texture within the ES was also identified at other locations (*e.g.*, ABA05 41-336; Fig. 2).

Hodgson *et al.* (1976) reported igneous foliation and phenocryst distribution that impart a gross layering to the intrusion. In addition, data collected during this study suggest that isolated cumulate layering is evident at numerous outcrops (*e.g.*, ABA05 32-260 and JLO05 30-232), and trends approximately east and dips steeply to moderately to the north.

PETROGRAPHY

Samples from the melasyenite, orbicular pseudoleucite syenite and equigranular syenite were collected, and standard thin sections, polished sections and epoxy mounts were made in order to determine mineral assemblages and identify texture, alteration assemblages and melt and fluid inclusions. Chemical tests were used to identify sodalite group minerals (sodalite, nosean and haüyne). The technique involved decomposition in nitric acid and evaporation. The precipitation of bladed colourless gypsum crystals confirmed the presence of haüyne in the samples (Deer *et al.*, 1992). To the best of the authors' knowledge, no other isotropic phase that is commonly found in nepheline syenite shows this behaviour.

Alteration is weak to moderate and assemblages are common throughout the Bootjack stock (one exception is JLO04 17-45, which is altered to sericite and cancrinite). Weakly altered samples show replacement of nepheline and haüyne with cancrinite, and of orthoclase with sericite. Mafic minerals (augite and hornblende) show reaction rims in which biotite and chlorite are common replacement phases. Some augite phases show amphibole replacement, which is evident from the relict euhedral augite crystal form with 60° and 120° cleavage angles. Minor calcite alteration, identified in two samples from the OPS, accounts for <2% of the rock.

Melasyenite

The melasyenite (MS) is light grey to dark green-grey, holocrystalline and contains crystals that are 0.5–3 mm in size. Pseudoleucite texture (pseudomorph after leucite, comprising a mixture of nepheline and orthoclase) is present in most samples, is 5–15 mm in size and light grey, and makes up 5–15% of the rock (Fig. 3C). The matrix is melanocratic, accounts for 85–95% of the rock and ranges from light grey to dark green-grey. At certain locations (*e.g.*, ABA05 34-274-4), the combined effect of a dominantly dark grey matrix and light grey orbicular pseudoleucite gives the MS a porphyritic texture. At other localities, the MS is finer grained and shows some cumulate layering (*e.g.*, JLO05 30-232).

In thin section, fresh samples consist of orthoclase (30–50%; Carlsbad twinning), nepheline (0–45%), haüyne (0–5%), biotite (0–5%) and augite (15–25%). Orthoclase, nepheline, haüyne and biotite are anhedral to subhedral and 0.5–3 mm in size, and have irregular to sharp grain boundaries, whereas augite is subhedral to euhedral and has sharp boundaries. Accessory phases include apatite, titanite and traces of fluorite; all ranging from <0.1 to 0.5 mm in size. Apatite commonly occurs as crystal inclusions within pyroxene. Opaque minerals include subhedral to anhedral magnetite, minor pyrite and tiny (<5 μm) bornite and chalcopyrite inclusions in haüyne. Haüyne occurs in the matrix as subhedral crystals in approximately 50% of the MS samples.

Orbicular Pseudoleucite Syenite

The orbicular pseudoleucite syenite (OPS) is a holocrystalline porphyritic rock consisting of pseudoleucite trapezohedrals that are 10–50 mm in diameter (Fig. 3A, B). The matrix constitutes 50–95% of the rock. It has a granitic texture and contains leucocratic phases, as well as subordinate mafic and opaque phases that are 0.5–3 mm in size. Four of the five samples are strongly dominated by pseudoleucite, which makes up 80–95% of the rock. One sample (ABA05 33-266) is more of a hybrid between OPS and ES, and contains only 50% pseudoleucite. Samples ABA05 33-266 and MMI04 18-1 differ from other samples in that their matrix includes a significant modal abundance of fresh interstitial haüyne (10–15%), which includes small (<5 μm) sulphide inclusions of bornite and chalcopyrite (Fig. 4A–D). Haüyne is present but less common in other samples. It occurs both in the matrix and as a constituent of the pseudoleucite region of the rock, but is mostly devoid of inclusions and is commonly weakly altered to cancrinite.

In thin section, fresh rocks include orthoclase (50–70%; Carlsbad twinning), nepheline (15–25%), biotite (0–1%), augite (4–8%), haüyne (2–15%), hornblende (trace–10%), plagioclase (0–1%), apatite (trace–1%), magnetite (2–3%) and pyrite (trace). All phases are anhedral to subhedral in crystal form and have irregular but sharp grain boundaries. An exception to this is apatite, which is euhedral to subhedral with sharp grain boundaries and commonly occurs as crystal inclusions within clinopyroxene.

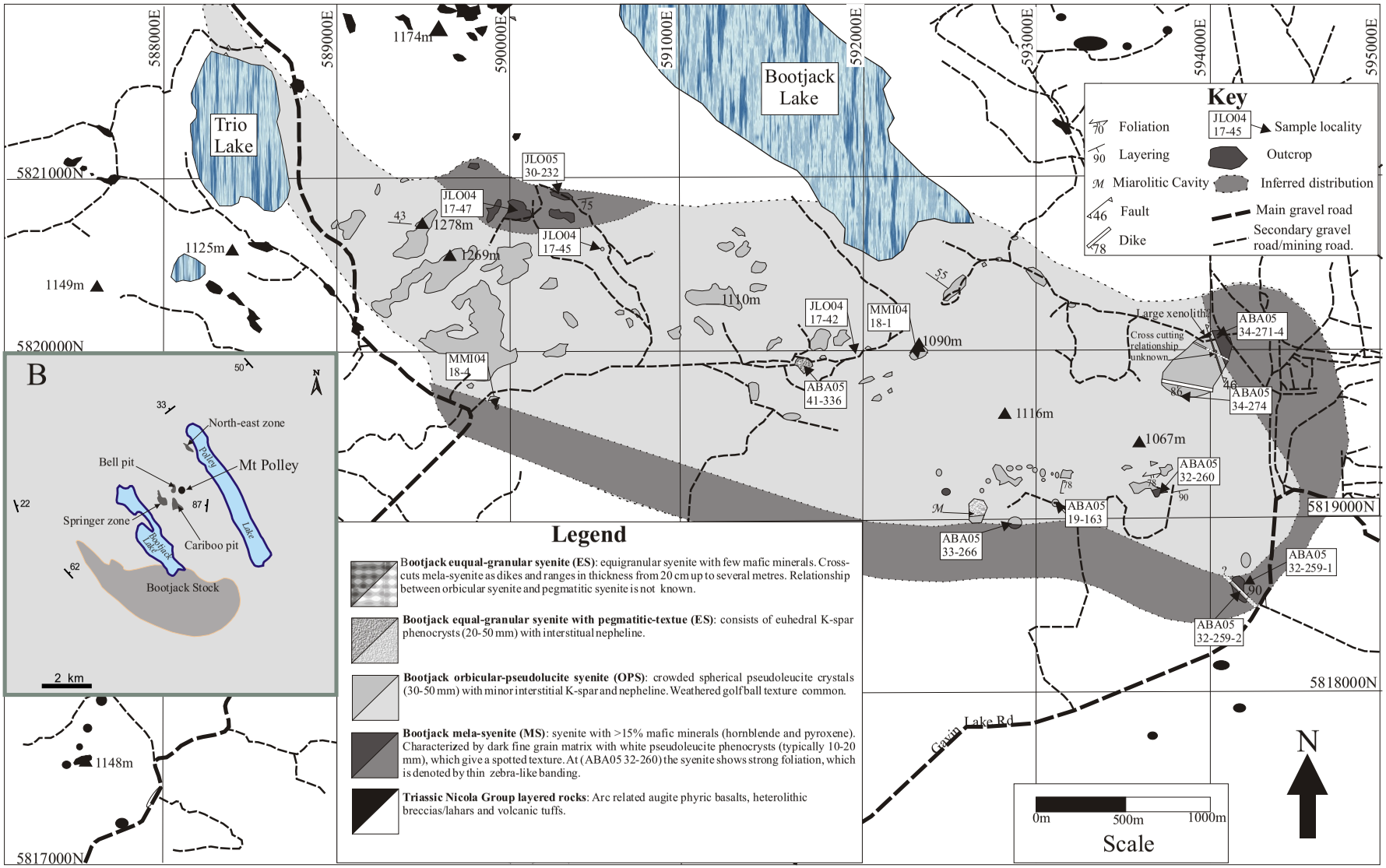


Figure 2. Geology of the Bootjack stock (NTS 093A/12), south-central British Columbia. Note that inset B shows the location of the Bootjack stock relative to Mount Polley.

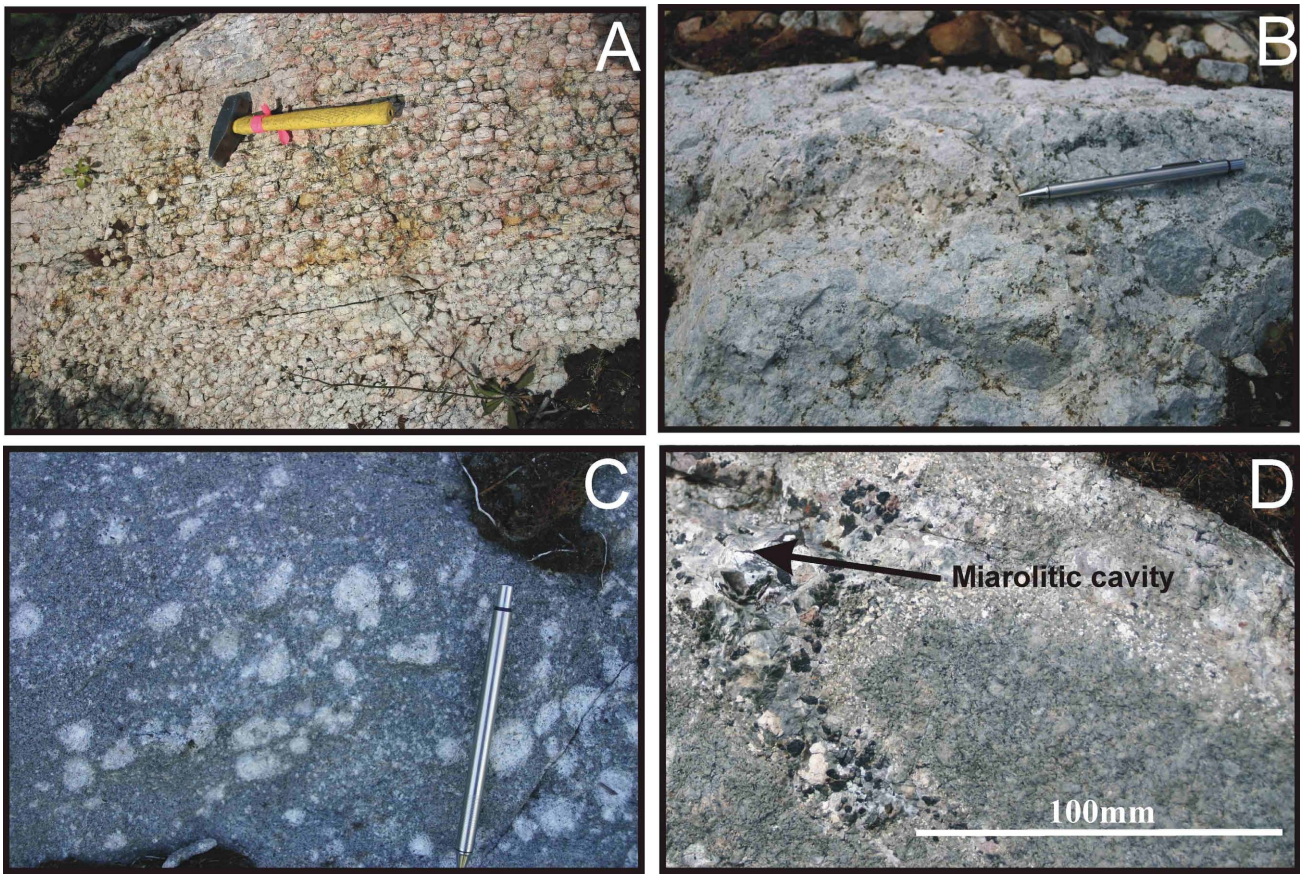


Figure 3. A) Outcrop of orbicular pseudoleucite syenite (OPS), which shows golf ball weathering. B) Fresh orbicular pseudoleucite syenite (OPS) from station ABA05 19-163. C) Melasyenite (MS) with pseudoleucite from station ABA05 32-259-1. D) Equigranular syenite (ES) with a miarolitic cavity from station ABA05 33-267. Miarolitic cavity consists of orthoclase, nepheline, magnetite, cancrinite, natrolite, sphene and fluorite.

Equigranular Syenite

The equigranular syenite (ES) is highly variable. It ranges from light to medium grey to pink, is holocrystalline and contains crystals that are 0.5–6 mm in size (Fig. 3D). Pegmatitic texture is common (*e.g.*, ABA05 41-336).

In thin section, fresh rocks contain orthoclase (40–60%; Carlsbad twinning), nepheline (25–35%), hornblende (1–3%), augite (1–4%), haüyne (2–7%), accessory apatite (trace) and magnetite (1%). Orthoclase, cancrinite and haüyne are anhedral to subhedral, whereas all other phases are subhedral to euhedral. In pegmatitic ES, haüyne is a common phases and includes sulphide inclusions of bornite and chalcopyrite.

MELT INCLUSIONS

Numerous types of melt and fluid inclusions were identified in apatite, sphene, pyroxene, hornblende and haüyne (usually less than 20 μm in size). Inclusions hosted in apatite, sphene, hornblende and pyroxene are dominated by silicate glass with small shrinkage bubble(s) and aqueous fluid inclusions, whereas inclusions in haüyne consist of sulphide minerals and unknown light green transparent material. This study will focus only on inclusions hosted in interstitial haüyne.

Three types of coexisting primary melt inclusions were identified in haüyne (types 1–3). Type 1 consists entirely of intergrown bornite and chalcopyrite (Fig. 4D). The bornite/chalcopyrite ratio is highly variable and, in many samples, inclusions exist entirely of bornite or chalcopyrite. Inclusions are mostly <5 μm in diameter and are irregular to globular.

Type 2 inclusions consist entirely of birefringent material (silicate, sulphate and carbonate?) and rarely contain a small shrinkage bubble (Fig. 4C). Type 2 inclusions range in shape from irregular to cubic to tabular and are mostly <5 μm in diameter.

Type 3 inclusions are composite inclusions comprising sulphide minerals (chalcopyrite and bornite), birefringent material (type 2 composition) and rarely a small shrinkage bubble (Fig. 4C). The ratio of sulphide minerals to birefringent material is highly variable. Type 3 inclusions are mostly <10 μm in diameter and range from irregular to globular in shape.

GEOCHEMISTRY

Analytical Methods

Fourteen samples from the Bootjack syenite were analyzed for major, minor and trace elements. Six samples

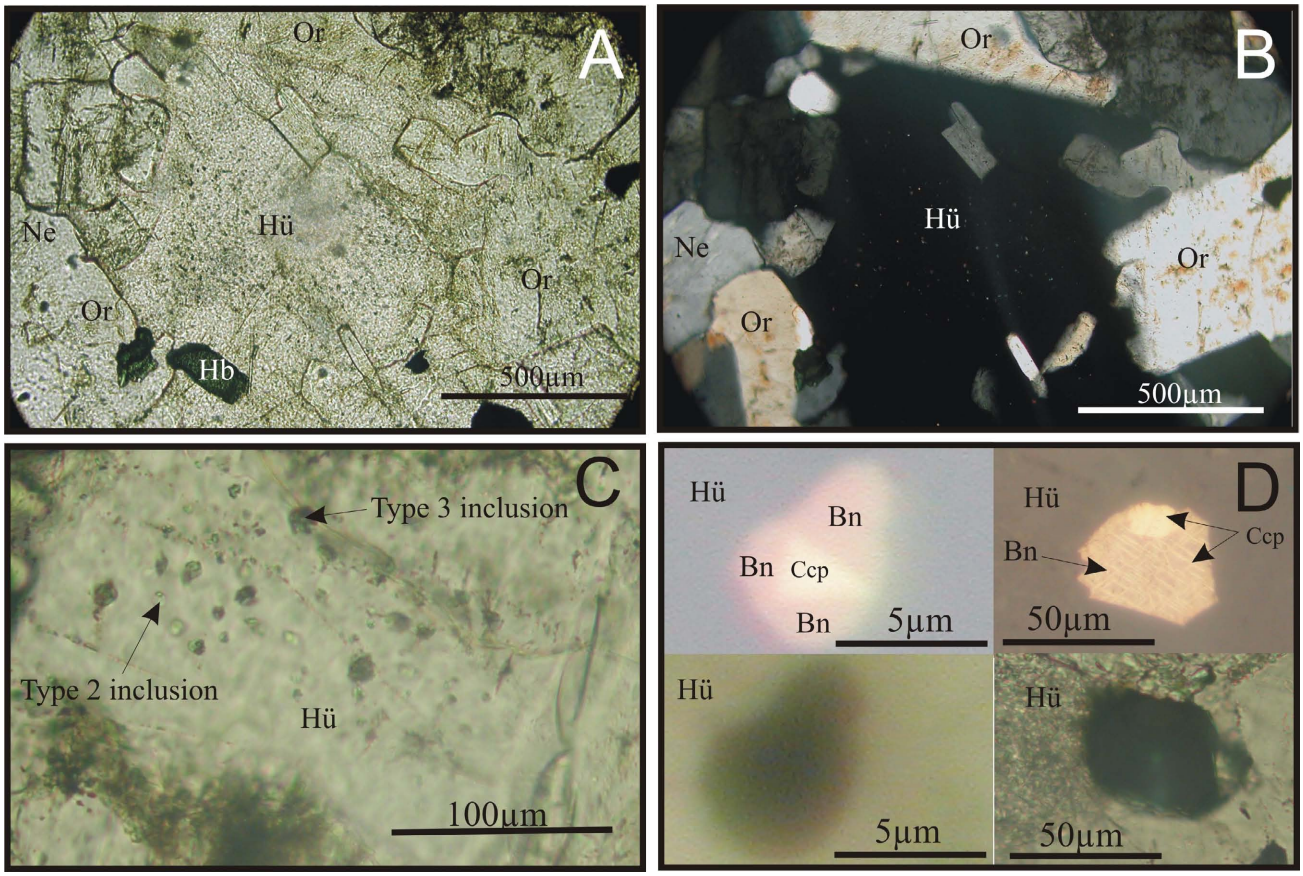


Figure 4. A) Photomicrograph of sample ABA05 33-266 (OPS) under plane-polarized light. Note the presence of orthoclase (Or), nepheline (Ne), haüyne (Hü) and hornblende (Hb). B) Photomicrograph of sample ABA05 33-266 (OPS) under cross-polarized light. Note the interstitial haüyne and the small birefringent inclusions (type 2 and 3) within haüyne (silicate, sulphate or carbonate material?). C) Type 2 and 3 inclusions in haüyne. D) Type 1 inclusions under plane-polarized light (bottom) and reflected light (top). The latter shows bornite (Bn) intergrown with chalcopyrite (Ccp), which is a common feature of type 1 inclusions.

were collected from the MS, six from the OPS and two from the ES. All samples were crushed and milled at the BC Geological Survey using a Cr-Fe plated jaw crusher, a tungsten carbide mill for major oxides (plus select trace elements) and a Cr-Fe mill for trace elements. In all cases, samples were free of xenoliths and weathered surfaces. For quality control, several hidden duplicates were included in the batch of samples to enable estimation of analytical precision, and several standard rock powders were included to allow estimation of analytical accuracy (Tables 1, 2).

Major oxides and Ba were determined by analyzing a fusion disc with a Siemens SRS-200 sequential X-ray fluorescence spectrometer (XRF) at Cominco Research Labs, Vancouver. Select trace elements (Rb, Sr, Y, Zr, Nb) were also analyzed by XRF using a pressed powdered pellet, and FeO was analyzed by titration at Cominco Research Labs. Analysis of rare earth elements (REE), Y, Th, Zr, Nb, Ba, Hf and Ta was carried out using the sodium peroxide sinter digestion technique and analyzed with a Hewitt Packard 4500plus ICP-MS at Memorial University, Newfoundland (MUN). The elements Mo, Cu, Pb, Zn, Ag, Ni, Co, As, U, Bi and W were all analyzed with a Perkin Elmer Elan 9000 ICP-MS at ACME Analytical Laboratories Ltd., Vancouver (four-acid [$HClO_4$, HNO_3, HCl and HF] digest ultra-trace method). Gold was determined by fire assay and ICP-ES (SpectroCirus Vision) at ACME.

It is important to note that trace elements Ba, Nb, Y and Zr were analyzed using both XRF and ICP-MS. However, according to P. King of MUN (pers. comm., 2005) the use of Ba, Nb, Ta, Hf and Zr data from the ICP-MS method should be treated only semiquantitatively (particularly Ba, Hf and Zr), as development work is still in progress to improve the reliability of these particular elements at MUN. Therefore, only XRF data for Zr and Nb will be used in this manuscript for interpretation purposes. Cominco Research Labs indicated that Ba values detected using XRF should also be treated with caution, so Ba has not been used in this manuscript for interpretation purposes. However, it is interesting to note that the comparison between the XRF and ICP-MS methods showed no correlation for Ba (*i.e.*, R^2 = <0.1), a very weak correlation for Nb (R^2 = 0.28, slope = 0.89), moderate correlation for Y (R^2 = 0.51, slope = 0.84) and a moderate to strong correlation for Zr (R^2 = 0.72, slope = 1.15). In the case of Zr, Nb and Y, some of the error can be attributed to the difference in detection limit between the two methods (see Tables 1, 2). This is particularly important for Y and Nb, where the measured values are not significantly greater than the detection limit for the XRF method (3 ppm).

TABLE 1. MAJOR OXIDE AND SELECT TRACE ELEMENT GEOCHEMISTRY FROM THE BOOTJACK STOCK AND OTHER INTRUSIONS FROM THE QUESNEL LAKE MAP AREA. ALL ELEMENTS WERE ANALYZED AT COMINCO RESEARCH LABS, VANCOUVER. ABBREVIATIONS FOR ANALYTICAL METHODS: XRF1, FUSED-DISC X-RAY FLUORESCENCE; TIT, HF DIGESTION – TITRATION; XRF2, PRESSED-PELLET X-RAY FLUORESCENCE. ROCK TYPE AND MINERAL ABBREVIATIONS: OPS, ORBICULAR PSEUDOLEUCITE SYENITE; MS, MELASYENITE; ES, EQUIGRANULAR SYENITE; MONZ, MONZONITE; SYN, SYENITE; DIO, DIORITE; HBL, HORNBLENDE; PX, PYROXENE; K-SPAR, K-FELDSPAR; MEG, MEGACRYSTIC. NOTE THAT SAMPLES ARE FROM UTM ZONE 10

			Element	SiO2	TiO2	Al2O3	Fe2O3	FeO	MnO	MgO	CaO	Na2O	K2O	P2O5	Ba*	LOI	Total	Nb	Rb	Sr	Y	Zr
			Units	%	%	%	%	%	%	%	%	%	%	%	%	%	%	ppm	ppm	ppm	ppm	ppm
			Method	XRF1	XRF1	XRF1	XRF1	TIT	XRF1	XRF1	XRF1	XRF1	XRF1	XRF1	XRF1	FUS	SUM	XRF2	XRF2	XRF2	XRF2	XRF2
Field Number			Detection Limit	0.01	0.01	0.01	0.01	0.01	0.01	0.01	0.01	0.01	0.01	0.01	0.01	0.01	0.01	3	3	3	3	3
Bootjack Stock	**LAT**	**LONG**	**Rock type**																			
JLO04-17-42	591968	5819970	OPS	53.72	0.14	22.94	0.91	0.61	0.05	0.43	1.4	5.26	11.8	0.07	0.18	2.11	99.69	bd	280	1487	bd	16
JLO04-17-45	590530	5820600	OPS	57.22	0.1	23.68	0.64	0.34	0.02	0.17	0.64	0.77	13.77	0.01	0.08	2.32	99.8	5	248	112	7	48
JLO04-17-47	590071	5820794	MS	50.24	0.43	20.73	3.86	1.85	0.2	2.22	4.05	2.75	7.38	0.23	0.41	3.96	98.52	3	119	7504	bd	113
JLO05 30-232	590281	5820887	MS	51.79	0.38	20.63	3.44	1.41	0.18	1.69	4.98	3.67	7.23	0.25	0.18	3.42	99.25	6	111	2592	10	21
MMI04-18-1	592290	5819991	OPS	54.08	0.12	22.31	1.1	0.45	0.07	0.23	0.89	6.65	10.39	0.01	0.04	2.81	99.21	10	315	626	7	48
MMI04-18-4	587880	5819740	MS	52.04	0.36	21.37	2.89	1.51	0.15	1.32	4.13	6.34	7.3	0.25	0.2	1.07	99.1	4	97	2474	12	53
ABA05 19-163	593070	5819099	OPS	53.2	0.18	22.61	1.55	0.73	0.05	0.69	2.04	4.55	12.39	0.14	0.16	1.45	99.74	4	283	1553	bd	9
ABA05 32-259-1	594205	5818538	MS	53.29	0.31	21.79	2.12	1.3	0.12	0.93	3.02	5.53	8.93	0.18	0.25	1.77	99.54	5	144	2621	3	bd
ABA05 32-259-2	594205	5818538	ES	52.52	0.3	21.62	2.45	1.23	0.15	1.07	3.09	5.15	8.36	0.18	0.18	3.16	99.46	4	82	2663	6	23
ABA05 32-260	593647	5819158	MS	52.06	0.41	21.21	3.29	2.02	0.18	1.64	5.44	6.9	5.01	0.31	0.23	1.05	99.75	3	57	3665	5	57
ABA05 33-266	592851	5818977	OPS	54.65	0.17	22.56	1.36	0.69	0.09	0.38	1.47	7.03	9.44	0.05	0.12	1.7	99.71	5	167	1582	bd	17
ABA05 34-271-4	593984	5820047	MS	50.95	0.33	21.73	2.76	1.34	0.14	1.32	3.9	5.01	8.78	0.28	0.26	2.62	99.42	bd	105	3733	bd	14
ABA05 34-274	593777	5819730	OPS	53.24	0.2	22.27	1.62	0.72	0.07	0.79	1.97	4.82	11.22	0.15	0.18	2.47	99.72	3	254	1651	bd	bd
ABA05 41-336	591661	5819901	ES	54.27	0.15	23.02	1.32	0.61	0.1	0.31	1.33	7.42	8.68	0.05	0.13	2.48	99.87	3	121	1408	44	39
Bullion pit																						
JLO04-11-4a	592526	5831352	monzosyn	60	0.41	18.37	2	0.96	0.01	0.72	2.48	6.03	6.07	0.07	0.17	2.18	99.58	7	72	246	25	130
JLO04-11-4b	592526	5831352	monzodior	46.65	1.2	16.54	6.36	4.94	0.17	5.07	10.46	3.01	2	0.36	0.1	2.24	99.65	3	31	602	23	43
ABA05 22-180	591987	5831743	monzosyenite	58.04	0.47	18.7	3.08	1.15	0.01	1.05	3.11	6.69	4.25	0.11	0.14	2.83	99.63	6	96	419	21	123
Mt Polley mine																						
JLO04-20-70b	590977	5825274	hbl monz	49.47	0.77	18.51	5.3	2.49	0.18	2.81	8.27	4.09	3.9	0.43	0.15	2.59	99.24	4	51	1277	24	64
JLO04-20-73	591572	5824216	diorite	50.25	0.81	17.34	5.58	3.5	0.18	3.64	8.42	3.51	3.57	0.38	0.24	1.73	99.54	bd	57	959	24	62
JLO04-23-100	592599	5823663	k-spr meg dike	56.2	0.43	18.93	3.7	1.17	0.23	1.41	4.36	4.03	6.63	0.18	0.15	1.6	99.16	6	124	1175	17	92
JLO04-24-111	589073	5824699	monz	53.66	0.68	18.04	3.17	3.41	0.18	2.88	5.46	4.86	3.44	0.27	0.19	2.69	99.31	bd	52	1049	24	85
MMI04-13-6	590925	5823526	diorite	48.33	0.75	18.3	6.14	3.25	0.2	4.01	10.19	3.17	2.5	0.34	0.18	1.76	99.49	bd	28	852	19	47
MMI04-23-5	592201	5826296	hbl monz	51.74	0.69	18.01	6.35	1.11	0.18	2.97	7.92	4.98	1.32	0.23	0.02	4.01	99.66	bd	17	302	25	58
ABA05 28-226	592752	5822168	Px Monz	54.93	0.5	18.4	3.39	1.55	0.15	1.42	6.21	5.13	4.75	0.23	0.13	2.56	99.35	4	94	1054	18	84
ABA05 28-227	592696	5822077	Monz	55	0.5	18.53	3.31	1.66	0.11	1.45	5.8	5.34	4.38	0.2	0.13	3.04	99.45	4	92	1178	21	85
ABA05 28-229	590942	5825302	Plg-Hb-K-spar	49.45	0.77	18.29	5.74	2.02	0.2	2.96	8.01	4.3	4	0.44	0.14	3.21	99.53	5	70	1159	23	56
ABA05 41-335	591011	5825166	Hb Monz	50.93	0.81	17.95	6.05	1.88	0.2	2.92	7.23	4.21	3.69	0.4	0.18	2.87	99.32	bd	63	1582	18	40
ABA05 16-130	598115	5820708	Syenite	51.72	0.69	17.63	5.03	2.53	0.18	3.09	7.69	4.19	3.3	0.37	0.09	2.83	99.34	4	59	893	23	63
JLO05 14-113	590883	5822789	Monzodiorite	52.7	0.62	18.55	5.12	2.45	0.18	2.85	6.51	3.7	4.55	0.31	0.19	1.93	99.66	bd	91	1234	21	62
Shiko Lake																						
JLO04-21-83a	603333	5813019	diorite	53.11	0.54	18.05	3.2	2.27	0.09	2.96	6.48	6.38	1.32	0.4	0.05	4.11	99.22	bd	16	1283	15	52
JLO04-21-83b	603333	5813019	syenmonz	59.04	0.36	17.95	2.67	1.2	0.05	1.3	3.48	4.94	6.34	0.18	0.16	1.41	99.22	6	70	665	21	85
JLO04-21-85a	603526	5813025	diorite	51.5	0.91	17.5	4.54	3.65	0.15	4.15	7.25	3.99	3.32	0.49	0.1	1.6	99.56	4	52	1000	18	46
JLO04-21-85b	603526	5813025	syenmonz	61.34	0.3	15.69	3.77	1.91	0.05	1.39	2.16	3.51	7.63	0.14	0.13	1.04	99.28	5	103	428	15	82
ABA05 12-95	603804	5813258	Diorite	49.58	0.82	16.75	6.43	3.18	0.14	4.84	8.27	3.48	3.23	0.52	0.12	2.1	99.46	3	65	940	12	20
ABA05 21-172	603087	5813197	Diorite	50.93	0.77	16.7	5.16	4.4	0.18	4.3	8.73	3.28	3.5	0.43	0.11	1.21	99.7	bd	64	932	16	44
ABA05 25-202	603999	5813318	Px Monz	51.43	0.64	16.46	4.04	2.89	0.14	3.89	8.47	3.73	3.39	0.37	0.16	3.42	99.03	3	51	756	18	46
Misc																						
JLO05 6-30	584642	5817415	Diorite	48.99	0.56	12.64	4.99	5.63	0.18	7.76	9.96	2.1	3.97	0.46	0.09	2.02	99.35	bd	103	951	9	26
JLO05 15-117	583081	5827617	Monz	51.65	0.64	18.3	6.06	1.15	0.18	2.48	6.73	5.71	2.65	0.38	0.12	3.43	99.48	bd	36	1719	20	54
JLO05 34-260	597806	5821024	Po Hrbl Monz	55.88	0.46	18.12	3.86	2.16	0.12	2.91	4.4	6.01	3.25	0.28	0.1	1.98	99.53	bd	52	827	19	48
ABA05 35-280	580735	5835899	Hb Diorite	49.38	0.85	17.2	2.16	7.07	0.15	4.42	8.35	2.86	3.61	0.37	0.14	3.29	99.85	bd	106	802	19	37
Q/C																						
CANMET SY4				49.69	0.28	20.59	3.11	2.69	0.10	0.51	7.98	7.03	1.60	0.11	0.03	5.41	99.10	10	54	1212	114	508
CANMET SY4	**Recommended**			49.9	0.287	20.69	3.35	2.86	0.108	0.54	8.05	7.1	1.66	0.131	0.034	4.56		13	55	1191	119	517
JLO 5-20				48.93	0.51	16.43	6.43	1.88	0.17	5.55	7.42	6.32	0.92	0.62	0.12	4.42	99.72	bd	17	1040	16	38
JLO 5-20rep				48.81	0.51	16.37	6.49	1.85	0.17	5.55	7.44	6.4	0.92	0.58	0.12	4.46	99.67	bd	11	1039	16	34
% Difference				0.25	0.00	0.37	0.93	1.61	0.00	0.00	0.27	1.26	0.00	6.67	0.00	0.90	0.05	0.00	42.86	0.10	0.00	11.11

Ba* = Fused disc analysis for XRF calibration. Values should be treated with CAUTION.

TABLE 2. TRACE ELEMENT DATA FOR THE BOOTJACK STOCK AND OTHER ALKALIC INTRUSIONS IN THE QUESNEL LAKE MAP AREA. NOTE THAT ELEMENTS AU TO W (LEFT SIDE OF TABLE) WERE ANALYZED AT ACME ANALYTICAL LABORATORIES LTD., VANCOUVER (ACME), WHEREAS ELEMENTS Y TO TH (RIGHT SIDE OF TABLE) WERE ANALYZED AT MEMORIAL UNIVERSITY, NEWFOUNDLAND (MUN). ABBREVIATIONS FOR ANALYTICAL METHODS: FAI, LEAD COLLECTION FIRE ASSAY – ICPES FINISH; TICP, FOUR-ACID DIGESTION – INDUCTIVELY COUPLED PLASMA – EMISSION/MASS SPECTROMETRY; PIMS, PEROXIDE FUSION – ICP-MS. ALSO NOTE THAT THE HIDDEN STANDARD FOR ACME WAS GSB TILL 99/GRX1, WHEREAS THE HIDDEN STANDARD FOR MUN WAS CANMET SY4 (GREY BACKGROUND). MMI04 21-1 WAS USED AS A HIDDEN REPEAT FOR ACME, WHEREAS SAMPLE ABA05 32-259-1 WAS USED FOR MUN (GREY BACKGROUND)

Element	Au	Mo	Cu	Pb	Zn	Ag	Ni	Co	As	U	Bi	W	Y	Zr	Nb	Ba	La	Ce	Pr	Nd	Sm	Eu	Gd	Tb	Dy	Ho	Er	Tm	Yb	Lu	Hf	Ta	Th
Units	ppb	ppm	ppm	ppm	ppm	ppb	ppm	ppm	ppm	ppm	ppm	ppm	ppm	ppm	ppm	ppm	ppm	ppm	ppm	ppm	ppm	ppm	ppm	ppm	ppm	ppm	ppm	ppm	ppm	ppm	ppm	ppm	ppm
Method	FAI	TICP	TICP	TICP	TICP	TICP	TICP	TICP	TICP	TICP	TICP	TICP	PIMS	PIMS	PIMS	PIMS	PIMS	PIMS	PIMS	PIMS	PIMS	PIMS	PIMS	PIMS	PIMS	PIMS	PIMS	PIMS	PIMS	PIMS	PIMS	PIMS	PIMS
Detection Limit	1	0.05	0.02	0.02	0.1	20	0.1	0.2	0.2	0.1	0.04	0.1	0.004	0.04	0.03	0.08	0.01	0.01	0.00	0.03	0.01	0.01	0.02	0.00	0.03	0.00	0.01	0.00	0.01	0.00	0.02	0.04	0.01
Bootjack Stock																																	
JLO04-17-42	4	0.22	54.36	6.04	29.6	32	0.9	3.7	28.0	0.4	bd	0.4	2.757	12.20	1.22	1939.29	3.90	6.29	0.76	2.98	0.57	0.22	0.55	0.08	0.50	0.10	0.30	0.04	0.32	0.05	0.28	0.05	0.51
JLO04-17-45	11	0.18	51.50	7.07	64.6	44	0.5	1.4	11.8	0.7	bd	0.7	4.940	38.14	3.82	843.72	6.03	9.17	1.04	3.66	0.66	0.20	0.66	0.11	0.70	0.17	0.58	0.10	0.70	0.10	0.67	0.20	2.88
JLO04-17-47	5	1.05	29.05	11.88	94.2	23	3.8	16.9	11.6	0.6	bd	1.5	9.943	34.81	2.82	8821.45	10.42	18.21	2.29	9.50	1.93	0.50	1.93	0.29	1.83	0.38	1.14	0.17	1.20	0.17	0.93	0.12	1.02
JLO05 30-232	5	0.88	14.39	11.88	88.1	bd	1.4	13.4	9.1	1.5	bd	0.6	11.673	60.62	5.00	2291.65	13.12	23.04	2.87	11.66	2.41	0.76	2.36	0.35	2.16	0.44	1.34	0.20	1.40	0.21	1.50	0.23	2.53
MMI04-18-1	6	0.87	43.54	13.62	53.3	47	0.7	2.3	9.9	1.4	bd	0.3	3.532	38.15	7.37	489.19	5.35	8.69	0.98	3.52	0.63	0.19	0.59	0.09	0.59	0.13	0.41	0.07	0.52	0.07	0.74	0.32	2.28
MMI04-18-4	3	2.12	87.81	12.97	90.9	61	0.8	12.6	5.4	1.8	bd	0.7	10.951	60.58	4.78	2363.35	12.97	22.36	2.70	11.01	2.06	0.68	2.02	0.31	1.97	0.41	1.26	0.19	1.31	0.19	1.27	0.21	2.46
ABA05 19-163	bd	0.26	78.60	6.97	38.3	57	1.5	6.7	48.2	0.4	bd	0.3	3.464	14.23	1.02	1902.49	4.82	8.09	0.98	3.98	0.78	0.32	0.73	0.10	0.61	0.13	0.38	0.06	0.34	0.06	0.31	0.04	0.44
ABA05 32-259-1	bd	1.79	50.78	9.23	68.9	bd	1.2	8.4	1.1	0.1	bd	0.7	7.815	23.86	1.31	3338.77	9.25	15.85	1.97	8.11	1.68	0.64	1.60	0.24	1.47	0.30	0.87	0.13	0.83	0.13	0.68	0.06	0.45
ABA05 32-259-2	3	0.69	28.47	14.08	85.6	22	0.8	9.4	4.4	1.5	bd	0.3	9.546	57.26	4.49	2998.02	11.12	18.88	2.27	8.96	1.80	0.65	1.73	0.27	1.72	0.36	1.10	0.17	1.19	0.18	1.33	0.20	1.64
ABA05 32-260	bd	1.97	108.67	13.93	104.7	70	1.4	16.0	2.8	0.6	bd	0.9	12.563	52.04	4.68	3054.12	15.86	27.38	3.35	13.73	2.70	0.93	2.60	0.38	2.36	0.48	1.40	0.21	1.40	0.21	1.34	0.19	1.24
ABA05 33-266	8	1.61	47.32	17.03	55.4	43	0.7	3.5	11.4	1.3	bd	0.5	6.702	69.01	3.86	1483.77	8.77	13.97	1.49	5.13	0.98	0.38	0.95	0.16	1.07	0.23	0.81	0.13	0.94	0.14	1.29	0.16	3.71
ABA05 34-271-4	2	2.15	185.71	12.22	81.1	265	1.4	11.1	1.9	0.7	bd	0.5	8.496	38.47	3.47	3495.31	13.09	21.82	2.55	10.18	1.93	0.69	1.84	0.25	1.56	0.32	0.94	0.14	0.97	0.14	0.89	0.16	2.18
ABA05 34-274	3	0.17	66.19	5.50	29.5	35	0.7	5.1	3.8	0.2	bd	0.1	4.116	13.28	0.83	2089.36	6.14	10.59	1.27	5.18	0.99	0.33	0.92	0.13	0.78	0.15	0.45	0.07	0.45	0.07	0.35	0.04	0.38
ABA05 41-336	5	0.90	49.85	18.52	61.2	42	0.3	3.0	8.7	2.4	bd	0.3	5.469	74.19	4.34	1532.70	8.64	12.78	1.36	4.72	0.86	0.33	0.78	0.13	0.85	0.19	0.66	0.11	0.85	0.13	1.45	0.13	4.05
Bullion pit																																	
JLO04-11-4a	17	0.59	806.22	1.96	9.5	361	3.2	5.1	10.0	1.4	bd	0.4	16.256	134.73	5.79	2025.56	13.85	27.17	3.36	13.31	2.57	0.77	2.70	0.44	2.85	0.59	1.82	0.29	2.06	0.31	2.98	0.33	4.54
JLO04-11-4b	5	0.69	68.87	1.58	60.1	33	10.2	36.6	9.5	0.7	bd	0.3	16.664	60.59	3.21	1209.73	9.11	19.67	2.76	12.80	3.06	1.03	3.54	0.55	3.41	0.67	1.90	0.27	1.79	0.26	1.66	0.14	1.27
Mt Polley mine																																	
JLO04-20-70b	3	1.22	145.30	8.82	108.9	99	1.9	22.2	6.8	1.2	0.04	0.5	19.708	70.78	3.23	1712.93	10.79	20.13	2.70	12.26	2.95	0.99	3.61	0.59	3.78	0.77	2.29	0.33	2.23	0.30	1.78	0.15	1.64
JLO04-20-73	8	0.78	185.44	4.82	89.0	48	2.9	28.4	9.1	0.6	bd	0.2	20.842	71.21	2.70	2761.67	8.97	18.54	2.63	12.28	3.07	1.00	3.85	0.63	4.06	0.82	2.37	0.34	2.28	0.32	1.96	0.12	1.20
JLO04-23-100	5	2.34	102.26	35.97	266.4	389	2.2	12.5	12.4	1.7	0.12	1.7	15.692	91.22	6.69	1876.47	15.30	27.29	3.51	14.55	2.99	0.89	3.10	0.49	3.05	0.61	1.84	0.28	1.91	0.26	2.24	0.23	3.85
JLO04-24-111	6	0.88	146.97	3.16	77.6	84	3.5	16.8	3.2	0.6	bd	0.4	21.852	98.37	5.57	2411.25	8.92	18.41	2.61	11.99	2.94	1.02	3.65	0.62	4.03	0.84	2.56	0.39	2.64	0.38	2.39	0.17	1.28
MMI04-13-6	6	0.75	203.10	5.16	92.3	82	4.6	30.4	2.9	0.7	bd	0.2	16.708	51.95	4.78	2190.61	7.57	15.33	2.18	10.30	2.56	0.91	3.13	0.51	3.28	0.66	1.92	0.28	1.82	0.26	1.41	0.13	0.96
MMI04-23-5	bd	1.28	11.01	6.20	115.0	51	0.4	15.9	5.4	0.8	bd	0.3	17.397	59.21	2.30	299.20	6.81	13.82	2.08	10.03	2.65	0.95	3.25	0.54	3.42	0.71	2.09	0.30	1.97	0.28	1.58	0.11	1.39
ABA05 28-226	5	8.31	38.28	12.86	125.8	134	0.8	6.5	9.8	1.3	bd	2.6	18.661	96.64	4.38	1672.12	11.88	21.75	2.78	12.05	2.81	0.92	3.02	0.51	3.39	0.70	2.19	0.33	2.21	0.35	2.46	0.18	2.12
ABA05 28-227	7	5.97	19.00	11.23	59.0	112	1.1	3.2	11.4	1.4	0.13	1.7	19.536	98.06	4.32	1779.47	13.18	24.36	3.15	13.37	3.13	1.00	3.46	0.54	3.65	0.76	2.31	0.35	2.36	0.36	2.52	0.21	2.00
ABA05 28-229	6	0.98	131.78	7.96	109.5	80	1.8	21.9	5.0	1.0	bd	0.4	21.134	75.77	3.63	1848.25	11.95	22.47	3.05	13.68	3.43	1.18	4.00	0.64	4.13	0.87	2.53	0.36	2.39	0.35	2.05	0.16	1.75
ABA05 41-335	bd	1.28	62.48	7.21	139.0	52	1.8	20.6	9.5	1.0	0.08	0.4	20.649	80.39	5.08	2330.76	13.05	24.56	3.30	14.61	3.56	1.15	4.02	0.63	3.97	0.83	2.39	0.35	2.30	0.35	2.20	0.17	1.84
ABA05 16-130	bd	0.44	63.82	8.97	95.3	71	7.1	21.8	4.1	1.2	0.05	0.2	19.715	84.02	3.78	1204.13	16.52	29.61	3.80	16.16	3.59	1.18	3.89	0.60	3.78	0.78	2.30	0.34	2.29	0.34	2.10	0.17	2.32
Shiko Lake																																	
JLO04-21-83a	27	0.37	256.50	4.65	36.3	96	4.1	13.7	7.0	0.9	bd	0.6	10.532	58.39	2.09	523.37	6.94	13.47	1.84	8.26	1.88	0.73	2.12	0.33	2.06	0.41	1.18	0.18	1.19	0.18	1.54	0.09	1.26
JLO04-21-83b	140	0.42	137.68	4.17	25.8	130	1.8	5.8	2.2	2.5	bd	0.2	11.933	103.51	6.67	1879.33	10.05	19.35	2.40	9.64	1.97	0.61	2.06	0.33	2.16	0.45	1.37	0.22	1.57	0.23	2.29	0.24	3.36
JLO04-21-85a	33	0.57	219.09	5.83	57.8	108	15.1	25.0	4.5	1.0	0.04	0.6	13.983	53.36	5.77	1254.46	10.93	20.71	2.71	11.94	2.62	0.82	2.93	0.45	2.81	0.55	1.59	0.24	1.55	0.22	1.47	0.18	2.24
JLO04-21-85b	214	0.50	1305.12	4.30	28.2	150	9.9	11.5	2.0	2.3	bd	0.2	7.974	83.32	5.16	1680.88	5.63	12.02	1.58	6.59	1.33	0.46	1.45	0.23	1.48	0.30	0.96	0.15	1.08	0.16	2.05	0.22	2.91
ABA05 12-95	2	0.49	103.76	3.24	62.4	72	20.2	30.8	3.5	0.5	bd	0.2	14.090	40.05	3.66	1709.92	10.71	21.18	2.83	12.55	2.81	0.90	3.01	0.44	2.84	0.56	1.62	0.22	1.48	0.22	1.13	0.15	1.55
ABA05 25-202	4	0.28	13.62	3.35	31.8	30	20.3	7.7	3.2	0.8	bd	0.3	15.717	67.18	3.00	2262.49	7.11	15.93	2.32	11.09	2.80	0.85	3.14	0.47	3.05	0.62	1.79	0.26	1.74	0.26	1.81	0.14	1.92
Misc																																	
JLO05 15-117	2	1.42	41.55	5.90	92.3	46	2.3	15.8	2.8	1.0	bd	0.5	21.606	103.85	4.09	1734.41	13.23	24.99	3.36	14.98	3.54	1.18	4.06	0.63	4.06	0.83	2.43	0.37	2.51	0.37	2.69	0.20	1.90
JLO05 34-260	7	0.23	58.06	4.40	65.6	23	13.1	14.7	2.7	0.4	bd	0.1	13.138	59.78	2.69	1268.30	7.74	14.76	1.93	8.55	1.98	0.69	2.22	0.36	2.40	0.51	1.54	0.23	1.60	0.24	1.56	0.13	0.97
ABA05 35-280	bd	1.62	163.46	4.15	67.5	241	16.0	37.5	2.3	1.3	bd	0.5	17.731	72.02	3.05	1922.88	10.10	20.95	2.94	13.51	3.20	0.99	3.56	0.56	3.48	0.72	2.02	0.29	1.97	0.28	1.99	0.16	2.35
Q/C																																	
Standard	35	19.04	1289.10	830.98	899.5	38425	38.9	8.7	473.3	36.2	1701	200	107.542	612.00	17.95	410.03	57.31	118.97	14.75	57.77	12.47	1.89	14.12	2.63	18.91	4.31	14.21	2.26	14.91	2.06	11.06	0.82	1.28
Recommended	36	18.00	1110.00	720.00	760.0	31000	41.0		401.0	33.0	1380	164	119.000	517.00	13.00	340.00	58.00	122.00	15.00	57.00	12.70	2.00	14.00	2.60	18.20	4.30	14.20	2.30	14.80	2.10	10.60	0.90	1.40
Sample	25	0.74	99.23	47.56	104.1	343	3.3	16.6	12.2	1.8	0.15	1.6	9.633	57.96	4.49	2990.90	11.23	19.02	2.28	9.07	1.80	0.65	1.75	0.27	1.74	0.36	1.10	0.18	1.22	0.18	1.36	0.20	1.61
Sample (rep)	24	0.84	99.56	47.37	110.5	363	3.3	16.7	12.1	2.0	0.14	1.6	9.458	56.56	4.49	3005.14	11.00	18.74	2.27	8.85	1.79	0.64	1.71	0.27	1.70	0.36	1.11	0.17	1.17	0.17	1.30	0.20	1.67
% Difference	4	12.66	0.33	0.40	6.0	6	0.0	0.6	0.8	10.5	6.90	0.0	1.833	2.45	0.03	0.48	2.07	1.46	0.44	2.53	0.32	0.70	2.36	1.83	2.00	1.46	0.69	3.89	4.85	5.80	4.11	0.31	3.91

Major Oxides and Normative Mineralogy

Major oxides data can be found in Table 1. These data are presented in order to 1) classify rocks from the BS using the IUGS system (Streckeisen, 1976); 2) determine if fractionation trends exist between the various rock types; and 3) compare the BS with other regional alkalic intrusions from the Quesnel Lake area (*i.e.*, Mount Polley stock, Bullion Pit, Gavin Lake, Shiko Lake, QR mine and Bootjack Lake pyroxenite), which are either assumed or known to be similar in age to the BS (Table 1; Fig. 5).

For classification purposes, CIPW normative calculations were used to plot each sample on a Streckeisen diagram (Fig. 6). Plots show that the BS is nepheline normative and ranges from Foid syenite to Foid monzonite. Exceptions to this are the finer grained MS and more altered OPS sample (JLO04 17-42) from the northeastern margin of the intrusion, which have normative compositions resembling Foid-bearing alkali-feldspar syenite to Foid-bearing syenite (Fig. 6; Streckeisen, 1976). Other discrimination plots used include the Ne-Q-Ka (nepheline-quartz-kalsilite) diagram (Fig. 7), which demonstrates that BS rocks plot in the leucite field (Rollinson, 1993), and the total alkali versus SiO_2 (TAS) plot, which demonstrates that the BS ranges from basic to intermediate (between 45 and 67 wt% SiO_2) and plots in the alkaline field (Wilson, 1989; Fig. 5J).

To test if fractionation trends exist between the various phases of the BS, MgO was selected as a common abscissa on a series of bivariant diagrams (Fig. 5A–I). The variation diagrams show that rocks of the BS are depleted in MgO (0.17–2.22 wt%) compared to other regional intrusions. The ES and the OPS have lower MgO values (0.17–1.07 wt% and 0.23–0.79 wt%, respectively) and the MS has higher MgO values (0.93–2.22 wt%), which directly reflects the mafic component of the rock (*i.e.*, rocks with greater than ~1 wt% MgO tend to have =15% mafic minerals). For plots of TiO_2, FeO_T, CaO and P_2O_5 versus MgO (Fig. 5), strong positive linear trends exist, which is consistent with the crystallization (subtraction) of pyroxene (Mg, Ca and Fe), Fe and Ti-oxides, amphibole (Ca), minor plagioclase (Ca) and apatite (Ca and P) during fractionation. In contrast, Al_2O_3, SiO_2 and total alkali show strong negative linear correlations with MgO (Fig. 5), whereas K_2O shows a weak negative correlation with SiO_2 and Na_2O shows no correlation. Overall, OPS rocks are the most fractionated and MS are the least fractionated.

Bivariant diagrams employing MgO are also used here to compare the BS with other alkalic intrusive phases from the Quesnel Lake area. The bivariant diagrams demonstrate that a single moderate to strong correlation exists for MgO versus TiO_2, FeO_T, CaO and P_2O_5 for all intrusive rocks, with the BS at the most evolved end of the spectrum and the pyroxenite at the least evolved end. In the case of Al_2O_3, SiO_2 and K_2O, there is a single trend for the regional intrusive rocks that differs from the BS. Alumina and K_2O are both significantly more enriched for the BS when compared to regional intrusions with equivalent MgO, whereas the BS is depleted in SiO_2 compared to regional intrusions with equivalent MgO. It is important to note that, although the regional intrusions are more enriched in SiO_2 compared with the BS, they are almost always silica undersaturated and tend to plot within the Foid-bearing syenite or monzonite field on the Streckeisen diagram (Fig. 6). One other significant difference between the BS and regional intrusions is that BS rocks plot in the leucite field on the Ne-Q-Ka diagram, whereas all regional intrusions plot in the feldspar field (Fig. 7).

Trace and Rare Earth Elements

Trace element data for the BS and regional intrusions can be found in Table 2. The data and various graphs are presented in order to 1) determine if fractionation trends exist for trace elements versus MgO; 2) compare primordial mantle – normalized data from the BS with other regional intrusions on a spider diagram; and 3) determine if any correlations exist between Cu, Au, Ag and other metals of commercial value.

Rocks from the BS show a positive correlation for MgO versus REE (R^2 = 0.53–0.75), Y (R^2 = 0.67), Ni (R^2 = 0.60), Zn (R^2 = 0.54), W (R^2 = 0.47) and Co (R^2 = 0.96). The positive correlation of REE and Y with Mg may be attributed to the fact that REE and Y tend to partition strongly into apatite, which commonly occurs as inclusions in clinopyroxene. This notion is supported by the relationship between REE-Y and P_2O_5, which show moderate (*e.g.*, Lu) to strong (*e.g.*, Eu) positive correlations (R^2 = 0.55–0.85). The positive correlation of Mg with Co and Ni is also consistent with fractionation.

Trace elements for OPS, MS, ES and regional intrusions were normalized to primordial mantle (PM; Sun and McDonough, 1989) and plotted on a spider diagram in order to compare trends between the various rock types (Fig. 8). Figure 8 demonstrates that the OPS, MS, ES and regional intrusions are all significantly enriched in large-ion lithophile elements (LILE; Rb, Ba, K and Sr), Pb and U compared to high field-strength elements (HFSE), which is a characteristic of arc rocks (*e.g.*, Kamenetsky *et al.*, 1997; Coulson *et al.*, 1999). It can also be concluded that all intrusions show a similar pattern across the diagram, although some intrusions are more depleted in certain elements compared to others. Of note are the heavy rare earth elements (HREE), medium rare earth elements (MREE) and Ti, which are significantly more depleted in the OPS compared with the MS and regional intrusions. The disparity can be attributed to the partitioning of these elements into the phases augite, apatite and hornblende, and the higher modal abundance of these phases in the MS relative to the OPS.

A variety of metal abundances from samples of the BS and regional intrusions (Table 2) were plotted on bivariant diagrams to evaluate their covariance (Fig. 9). Rocks from the BS show positive correlations for Ag versus Cu (R^2 = 0.86; Fig. 9A), Zn versus Pb (R^2 = 0.24), Ni versus Co (R^2 = 0.50) and Au versus As (R^2 = 0.69; Fig. 9B). No correlation exists for Au versus Ag or Cu. With the exception of Ni versus Co, there are no correlations between the BS and regional intrusions. In the case of Pb versus Zn, however, the regional intrusions show a steeper positive trend compared to the BS. Moreover, when Zn/Pb is plotted against MgO, there is a single positive linear trend for all intrusions, which suggests that Zn was depleted relative to Pb with fractionation.

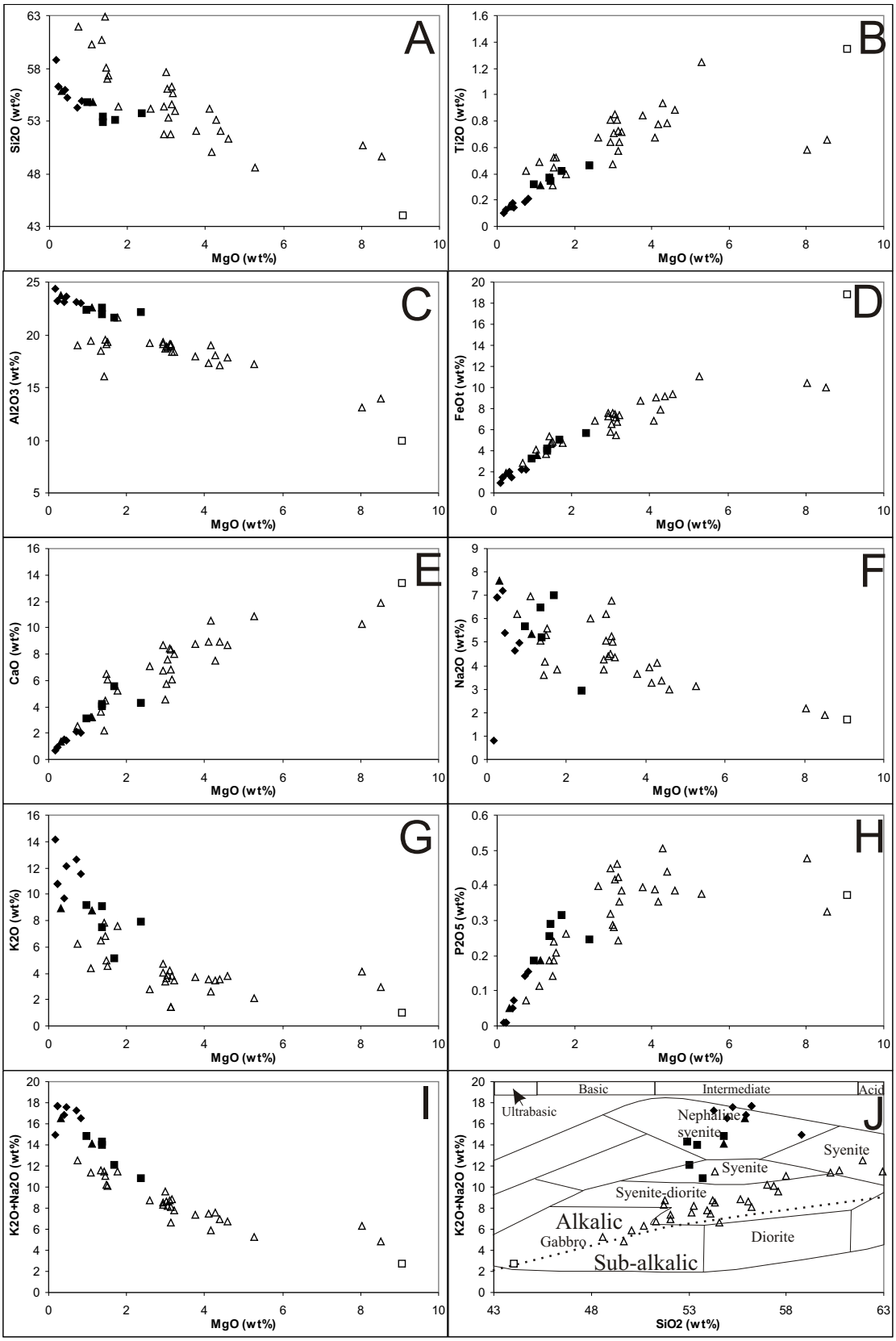


Figure 5. Major oxide bivariant diagrams for the Bootjack stock (MS, filled square; OPS, filled diamond; ES, filled triangle), regional intrusions (unfilled triangle) and a pyroxenite (sample MTP92-050 PX from Fraser, 1994). Part J is a total alkali versus silica (TAS) diagram. Note that the dotted line separates alkalic rocks from subalkalic rocks (after Wilson, 1989) and that all data are normalized to 100% anhydrous.

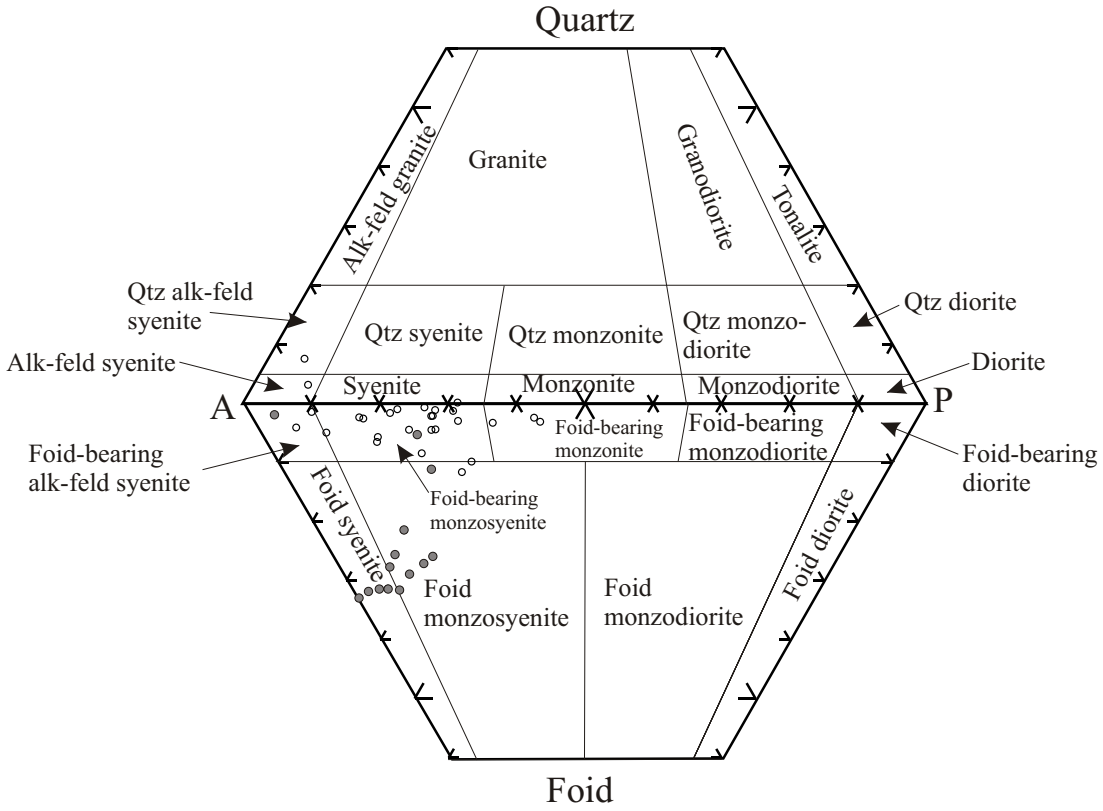


Figure 6. Rocks from the Bootjack stock (grey dots) and regional intrusions (colourless dots; see Table 1) plotted on an IUGS classification diagram using CIPW normative values. CIPW calculations were carried out using the same method as Le Maitre (1976). Note that BS rocks tend to plot in the Foid syenite to Foid monzosyenite field, compared with regional intrusions that plot mostly in the Foid-bearing monzosyenite field (after Streckeisen, 1976).

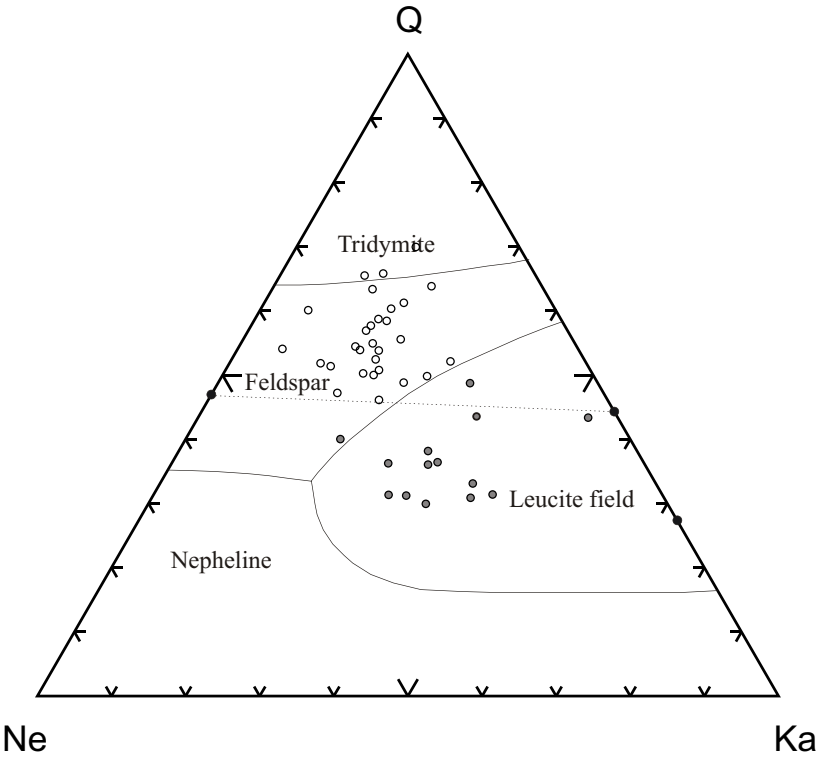


Figure 7. Rocks from the Bootjack stock and regional intrusions plotted on a nepheline-quartz-kalsilite (Ne-Q-Ka) diagram (assuming 1 Kb PH_2O) using CIPW normative values that were calculated using the same method as Le Maitre (1976). Note that BS rocks tend to plot in the leucite field, whereas regional intrusions tend to plot in the feldspar field (after Rollinson, 1993).

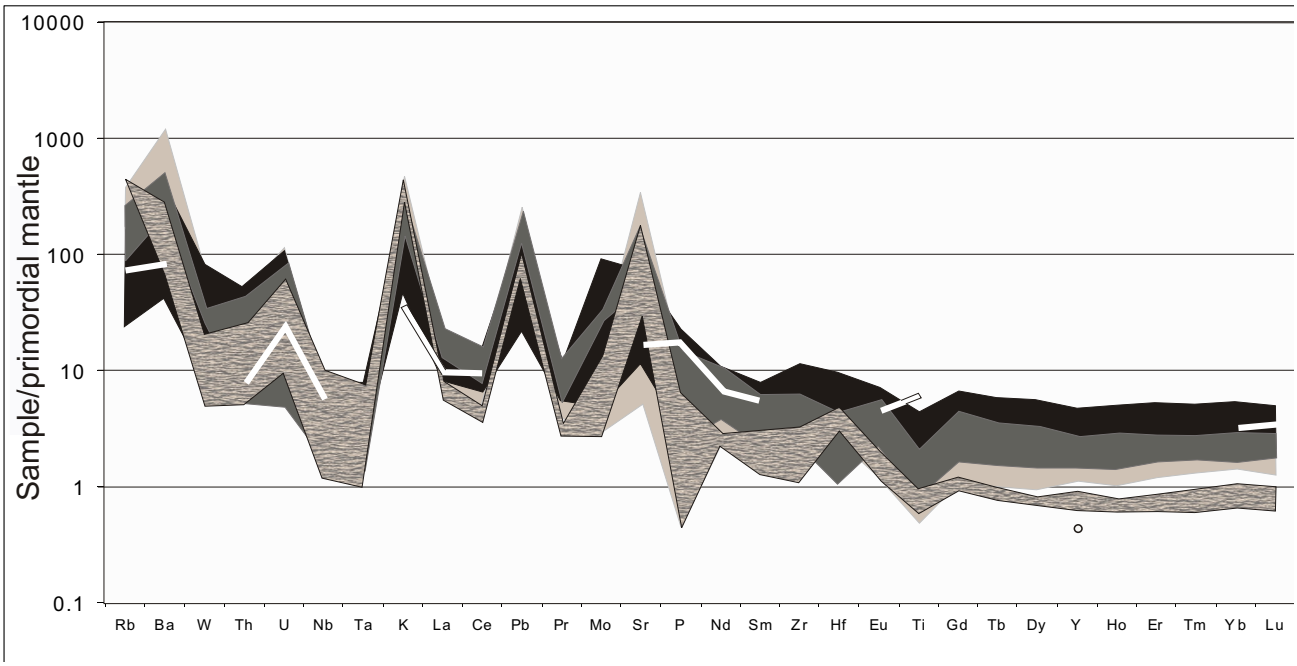


Figure 8. Spider diagram showing data from the Bootjack stock (MS, dark grey; ES, light grey; OPS, brick textured), regional intrusions (black) and Bootjack Lake pyroxenite (white line; sample MTP92-050PX from Fraser, 1994). All rocks are normalized to a primordial mantle (primordial mantle values from Sun and McDonough, 1989).

DISCUSSION

Petrological and Geochemical Features of the Bootjack Stock

Notably, one of the most significant aspects of the Bootjack stock (BS) is the existence of packed orbicular pseudoleucite syenite (OPS), which makes up an estimated 80% of the intrusion. Hence, an understanding of the genesis of pseudoleucite is particularly important with respect to understanding the BS. According to Deer *et al.* (1992), the genesis of pseudoleucite can be ascribed to two probable processes: 1) the breakdown of early-formed leucite with a Na-rich liquid; or 2) the breakdown of Na-rich leucite (or K-rich analcite) solid-solution series phase, which has been synthesized in experimental work. In natural systems, however, the composition of leucite does not depart significantly from the ideal formula ($KAlSi_2O_6$), and replacement of K by Na rarely exceeds 10% (Phillips and Griffen, 1981; Deer *et al.*, 1992); alternatively, though, analcite containing up to 20% of leucite component in basalt has been reported (Deer *et al.*, 1992).

The geochemistry of four fresh samples from the OPS, each containing approximately 80–95% pseudoleucite, was examined in order to estimate the composition of the pseudoleucite constituent of the rock. Optically, all four samples have a matrix mineral assemblage that closely resembles the pseudoleucite constituent of the rock, with the exception of subordinate aegirine-augite and magnetite. Hence, whole rock data are believed to closely represent pseudoleucite geochemistry, with the exception of minor Na and Fe enrichment. Geochemical data for four OPS samples show Si/Al molar ratios close to two (average = 2.02; standard deviation = 0.032), which is consistent with the chemical formula for leucite, but Al/K molar ratios average 1.82 (st. dev. = 0.12), which is significantly greater than the ideal leucite formula (1:1). Molar ratios for Al/(K+Na) are close to 1:1 (*i.e.*, avg. = 1.07; st. dev. = 0.04), suggesting that either the alkali substitution of Na for K was

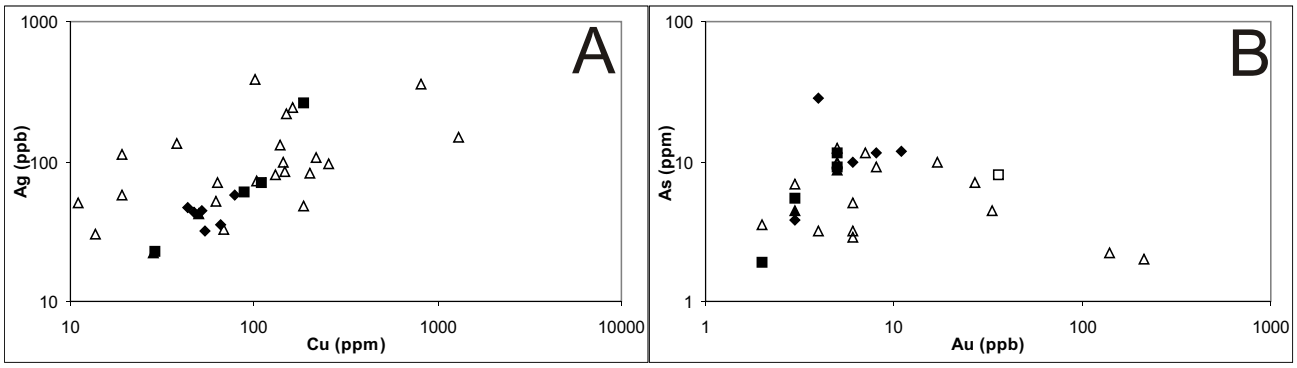
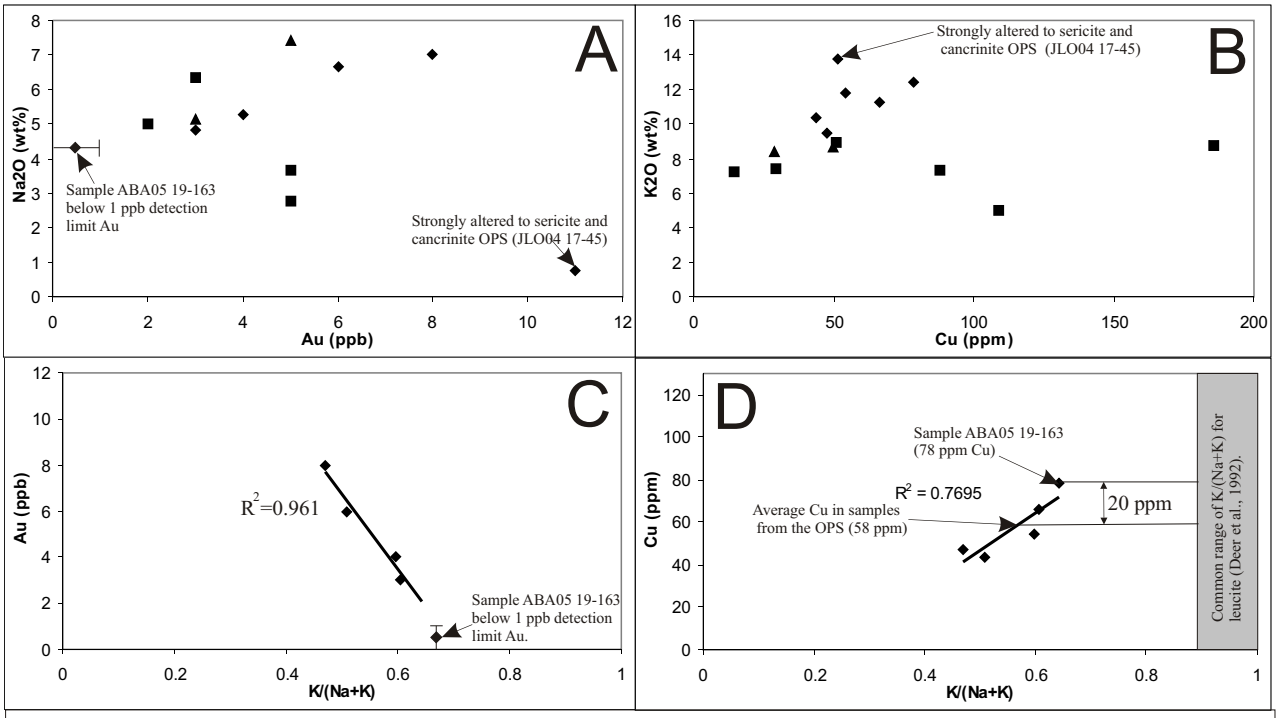


Figure 9. Bivariant diagrams for the Bootjack stock (MS, filled square; OPS, filled diamond; ES, filled triangle), regional intrusions (unfilled triangle) and Bootjack Lake pyroxenite (unfilled square; sample MTP92-050PX from Fraser, 1994).

efficient during the breakdown of leucite to form nepheline and orthoclase (see equation 1, after Deer *et al.*, 1992) or that the original leucite/analcite protolith composition ranged from 51–64% component leucite. Naturally occurring leucite or analcite are not known to exist with this range of composition, the inference being that pseudoleucite was formed as a result of leucite breakdown by Na-rich fluids, although the latter scenario cannot be entirely discounted. The presence of interstitial late-stage haüyne suggests that the final melt to crystallize was enriched in Na, Ca and S (both S^{2-} and S^{6+}), as well as minor Cl, and supports the notion of a Na-rich melt that could facilitate the breakdown of leucite to pseudoleucite.

$$2KAlSi_2O_6 + Na^+ \leftrightarrow NaAlSiO_4 + KAlSi_3O_8 + K^+ \quad (1)$$
(leucite) (nepheline + orthoclase)
(pseudoleucite)

One important characteristic of interstitial haüyne is that, in certain samples (*e.g.*, ABA05 33-266, MMI04 81-1



Calculation for the mass of Cu loss from the OPS during Na for K exchange reaction.

Assumptions: The loss of Cu was proportional to the loss of K during the alkali exchange reaction. That sample ABA05 19-163 represents the starting composition of Cu in the OPS prior to significant Cu loss during the alkali exchange reaction.

Average Cu in OPS = 58 ppm

Concentration of Cu in most K-rich sample (ABA05 19-163) = 78 ppm

Area of OPS = 10 km² (determined from map)

Thickness of OPS = 300 m (not well constrained but is known to be atleast 300 m thick based on topography relief)

E

Volume of OPS = 3 km³

Density (p) of OPS = 2.6 g/cm³ (approx density of nepheline and orthoclase)

Average loss of Cu from OPS = 20 ppm

Mass of Cu lost from OPS = vol x p x loss of Cu

Mass of Cu lost from OPS = 3 x 10 m³ x 2.6 tonnes/m³ x 20/1 000 000

Mass = 156 000 tonnes of Cu

Figure 10. Bivariant diagrams for alkalis, Cu and Au for rocks from the Bootjack stock (parts A–D; MS, filled square; OPS, filled diamond; ES, filled triangle) and calculations for Cu lost from BS (part E). Note that graphs A and B show Au versus Na and Cu versus K, respectively. In graph A, note the strong correlation between Au and Na for OPS samples (excluding sample JLO04 17-45, which is strongly altered). In graph B, note the moderate correlation between Cu and K for OPS samples. No correlation, however, exists for MS samples. Graphs C and D are alkali molar ratio versus Cu and Au. Note the linear decrease in Au with an increase in Na relative to K and the linear increase in Cu with increasing K relative to Na. Sample ABA05 19-63 is interpreted to be the sample least effected by the Na exchange for K reaction, which occurred during the breakdown of leucite to pseudoleucite (see text). Thus, the calculation in part E was carried out to determine on the average amount of Cu lost from the BS during the alkali exchange reaction.

and ABA05 41-336), haüyne displays type 1 inclusions, which represent trapped sulphide melt. Hence, there is strong evidence to suggest that the residual Na-rich melt, which facilitated the breakdown of leucite, also contained significant amounts of Cu.

Geochemical and Petrographic Links Between Haüyne, Cu and Au

The OPS samples containing the most interstitial haüyne tend to have the highest concentration of Au and Na and a positive linear trend for Au versus Na, suggesting an intimate link between Au and a residual Na- and S-rich melt (Fig. 10A, C). In contrast no correlation is evident between Cu and Na. Moreover, those samples containing the most interstitial haüyne tend to have lower concentrations of Cu and K (Fig. 10B, D). To explain this relationship, the authors suggest that haüyne crystallized from a S and Na-rich residual melt that actively scavenged Cu (with S) and replaced K (with Na) as it moved through the crystal mush. Thus, those parts of the magma chamber that were more affected by the interstitial late-stage melt tend to have less Cu and K. For OPS rocks, there is a moderate positive correlation for Cu versus K, which is interpreted to be related to the affect of the residual melt.

From the relationship between K and Cu, it is possible to approximate how much Cu may have been lost as a result of leucite breakdown and Na exchange. Based on the known extent of the OPS (~10 km^2) and assuming a thickness of 300 m, the loss of Cu from the OPS as a result of S scavenging is estimated to be approximately 156 000 t (see Fig. 10E). This calculation for Cu loss from the BS is not significantly different from estimated total Cu reserves and total Cu production at Mount Polley (Imperial Metals Corporation, 2004). However, the calculation is considered to be a minimum estimate, given that the absolute extent of the BS is poorly constrained and the likelihood that the overall loss of Cu (as well as Au and Ag) from the BS may have been significantly greater based on the high concentration of these metals in cogenetic, less evolved alkali basalt (see Logan and Bath, 2006), which likely resembles the composition of the parental melt for the BS.

Emplacement and Differentiation of the BS

The BS is a zoned intrusive body that is characterized by an OPS and ES core and an MS rim. The authors infer that the mafic-rich rim is a product of differentiation, where mafic phases accumulated along the walls of the intrusion. This idea is supported by the relative density of the mafic phases and the existence of cumulate layering at certain outcrops. Conversely, the OPS is interpreted to represent the accumulation of leucite crystals. Given the relatively low density of leucite (specific gravity = 2.47–2.50: Deer *et al.*, 1992), it is suggested that leucite, on crystallizing, floated to the top of the magma chamber and accumulated at the carapace of the intrusion (similar conclusion to Coulson *et al.* [1999] for Zippa Mountain). The ES is considered to be a late component of the system, as it is seen to crosscut the MS; however, it has not been observed to cut the OPS. The occurrence of pegmatitic texture within the ES, and also within local regions of the OPS, suggests that volatiles likely accumulated in the core of the magma chamber beneath the leucite layer and were then released as local pulses.

CONCLUSIONS

- Rocks from the Bootjack stock (BS) show geochemical fractionation trends, similar to those of coeval intrusions from the Mount Polley complex, Bullion pit, Shiko Lake and QR mine, that suggest a cogenetic relationship. However, the BS is more fractionated compared to other intrusions.
- Rocks from the orbicular pseudoleucite syenite (OPS) have Si/Al molar ratios that are close to 2, and Al/(Na+K) ratios of close to 1, which is consistent to that of leucite when Na for K substitution is taken into account. The transition from leucite to pseudoleucite occurred by the introduction of Na-rich melt, which is evident from the presence of interstitial haüyne.
- The presence of sulphide melt inclusions within interstitial haüyne from the BS is primary evidence of a Cu-rich sulphide melt, concentrated in a residual S and Na-rich melt, that could have migrated through the intrusive body and accumulated at the carapace of the intrusion along with magmatic volatiles and metals.
- The generation of excess K as a result of leucite breakdown to pseudoleucite may explain the pervasive early K alteration in the rocks at Mount Polley, whereas the late-stage S and Na- rich residual melt may represent the later Na alteration at Mount Polley.
- Further study on haüyne is required in order to accurately determine its crystal chemistry and the composition of type 2 inclusions (sulphate, silicate or carbonate?). These studies may help to establish whether an intimate link exists between the BS and mineralization at Mount Polley.
- As shown by Frei (1996), testing the ratio of oxidized and reduced sulphur in bulk rock as well as individual minerals (*e.g.*, apatite) can be an important indicator for distinguishing barren from mineralized intrusions. The authors wonder if unaltered haüyne from the BS could also be used as a tool for tracing the oxidation state of S, given the high concentration of S in its structure and its ability to readily host both S^{6+} and S^{2-}.

ACKNOWLEDGMENTS

First and foremost, we would like to thank the Mount Polley geology team of Pat McAndless, Chris Reese, Lee Ferreira, Leif Bjornson, Jacqueline Blackwell, Chris Taylor and Sheila Jonnes for bending over backwards for us this summer. Their efforts made this project much easier and we sincerely thank them. We would also like to genuinely thank Ray Lett for his help and advice with the geochemistry. Graham Nixon, George Simandl and Vadim Kamenetsky are all thanked for freely offering their time to discuss some of our queries.

REFERENCES

Bailey, D.G. and Archibald, D.A. (1990): Age of the Bootjack stock, Quesnel Terrane, south-central British Columbia (93A); *in* Geological Fieldwork 1989, *BC Ministry of Energy, Mines and Petroleum Resources*, Paper 1990-1, pages 79–82.

Coulson, I.M., Russell, J.K. and Dipple, G.M. (1999): Origins of the Zippa Mountain pluton: a late Triassic, arc-derived, ultrapotassic magma from the Canadian Cordillera; *Canadian Journal of Earth Sciences*, Volume 36, no 9, pages 1415–1434.

Deer, W.A., Howie, R.A. and Zussman, J. (1992): An Introduction to the Rock-Forming Minerals (2nd Edition); Longman.

Fraser, T.M. (1994): Geology, alteration and origin of hydrothermal breccias at the Mount Polley alkalic porphyry copper-gold deposit, south-central British Columbia; M.Sc. thesis, University of British Columbia, Vancouver, BC, 261 pages.

Frei, R. (1996): Sulfur in bulk rock and igneous apatite: tracing mineralized and barren trends in intrusions; *Schweizerische Mineralogische Und Petrographische Mitteilungen*, Volume 76, no 1, pages 57–73.

Hodgson, C.J., Bailes, R.J. and Versoza, R.S. (1976): Cariboo-Bell; *in* Porphyry Deposits of the Canadian Cordillera, Sunderland Brown, A., Editor, *Canadian Institute of Mining and Metallurgy*, Special Volume 15, pages 388–396.

Imperial Metals Corporation (2004): Mount Polley's Northeast zone expanded and mine restart economics robust; *Imperial Metals Corporation*, press release, August 3, 2004, URL < http://www.imperialmetals.com/s/News-2004.asp?ReportID=85638&_Type=News-Release-2004&_Title=Mount-Polleys-Northeast-Zone-Expanded-and-Mine-Restart-Economics-Robust> [09/12/2005].

Kamenetsky, V.S., Crawford, A.J., Eggins, S. and Muhe, R. (1997): Phenocryst and melt inclusion chemistry of near-axis seamounts, Valu Fa Ridge, Lau Basin: insight into mantle wedge melting and the addition of subduction components; *Earth and Planetary Science Letters*, Volume 151, no 3–4, pages 205–223.

Le Maitre, R.W. (1976): The chemical variability of some common igneous rocks; *Journal of Petrology*, Volume 17, pages 589–637.

Logan, J.M. and Bath, A.B. (2006): Geochemistry of the Nicola group basalts from Quesnel, at the latitude of Mount Polley; *in* Geological Fieldwork 2005, *BC Ministry of Energy, Mines and Petroleum Resources*, Paper 2006-1 and *Geoscience BC*, Report 2006-1.

Logan, J.M. and Mihalynuk, M.G. (2005): Regional geology and setting of the Cariboo, Bell, Springer and Northeast porphyry Cu-Au zones at Mount Polley, south-central British Columbia; *in* Geological Fieldwork 2004, *BC Ministry of Energy, Mines and Petroleum Resources*, Paper 2005-1, pages 249–270.

Mortensen, J.K., Ghosh, D.K. and Ferri, F. (1995): U-Pb geochronology of intrusive rock associated with copper-gold porphyry deposits in the Canadian Cordillera; *in* Porphyry Deposits of the Northwestern Cordillera of North America, Schroeter, T.G., Editor, *Canadian Institute of Mining and Metallurgy*, Special Volume 46, pages 142–158.

Mortimer, N. (1987): The Nicola Group: Late Triassic and Early Jurassic subduction-related volcanism in British Columbia; *Canadian Journal of Earth Sciences*, Volume 24, pages 2521–2536.

Mortimer, N., Van Der Heyden, P., Armstrong, R.L. and Harakal, J. (1990): U-Pb and K-Ar dates related to the timing of magmatism and deformation in the Cache Creek Terrane and Quesnellia, southern British Columbia; *Canadian Journal of Earth Sciences*, Volume 27, pages 117–123.

Panteleyev, A., Bailey, D.G., Bloodgood, M.A. and Hanckock, K.D. (1996): Geology and mineral deposits of the Quesnel River – Horsefly map area, central Quesnel Trough, British Columbia (NTS 93A/5, 6, 7, 11, 12, 13; 93B/9, 16; (93G/1; 93H/4); *BC Ministry of Energy, Mines and Petroleum Resources*, Bulletin 97, 156 pages.

Phillips, W.R. and Griffen, D.T. (1981): Optical Mineralogy: The Nonopaque Minerals; W.H. Freeman and Co., San Francisco, California, 677 pages.

Rollinson, H.R. (1993): Using Geochemical Data: Evaluation, Presentation, Interpretation; *Prentice Hall,* 352 pages.

Streckeisen, A. (1976): To each plutonic rock its proper name; *Earth Science Reviews*, Volume 12, pages 1–33.

Sun, S.S. and McDonough, W.F. (1989): Chemical and isotopic systematics of oceanic basalts: implications for mantle composition and processes; *in* Magmatism in Ocean Basins, Saunders, A.D. and Norry, M.J., Editors, *Geological Society of London*, Special Publication 42, pages 313–345.

Wheeler, J.O. and McFeely, P. (1991): Tectonic assemblage map of the Canadian Cordillera and adjacent parts of the United States of America; *Geological Survey of Canada*, Map 1712A, scale 1:2 000 000.

Wilson, M. (1989): Igneous Petrogenesis; Unwin Hyman, London, United Kingdom, 466 pages.

Usk Map Area (NTS 103I/09), Near Terrace, British Columbia: Cross-Sections and Volcanic Facies Interpretation

By T. Barresi[1] and J.L. Nelson

KEYWORDS: Terrace, Stikine Terrane, Usk, Telkwa Formation, Zymoetz group, volcanic facies, facies analysis, cross-section

INTRODUCTION

In the summer of 2005, one geologist and three geology students working for the British Columbia Geological Survey, along with three Kitselas First Nation resource technicians, surveyed the Usk map area, near Terrace, BC (Fig. 1). A major objective of the project was to identify subdivisions within the Telkwa Formation, a unit that had previously been undivided in the Terrace area. This article presents four cross-sections of the map area (Fig. 2); it is a companion article to Nelson *et al.* (2006), where a full examination of the physical features and exploration potential of the Usk map area is presented. This paper highlights the details of the newly distinguished units within the Telkwa, as well as their stratigraphic, (paleo)geographic and structural relationships to one another and to local intrusive and older Triassic and Paleozoic units. Special emphasis is placed on variations in volcanic facies that occur between and within the divisions of the Telkwa Formation. Twenty samples have been collected along these transects for whole-rock major, trace and isotope geochemical analyses. These will be incorporated into a Ph.D. thesis currently in progress by the senior author at Dalhousie University.

GEOLOGICAL SETTING

The Usk map area falls within the western portion of the Stikine Terrane, or Stikinia. Stikinia is the largest of the intermontane terranes and is composed of Paleozoic to Middle Jurassic, island-arc-related volcanic, plutonic and sedimentary rocks (Anderson, 1993). The map area also falls along the eastern boundary of the Coast Plutonic Complex, a linear belt of subduction-related plutonic rocks emplaced after the accretion of the intermontane terranes to the North American continent (van der Heyden, 1992).

The cross-sections in this paper depict three main stratigraphic units and two plutonic units. The oldest stratigraphic unit, the Zymoetz group, is correlative with Paleozoic rocks of the Stikine 'assemblage' in the Iskut-Stikine area (Nelson *et al.*, 2006; see also Logan *et al.*, 2000; Brown *et al.*, 1991). These units are overlain, in places, by thin, well-bedded sedimentary rocks, which are thought to be Triassic in age and are correlative with the Stuhini Group. The youngest, and by far the most voluminous, stratigraphic unit represented in these cross-sections is correlative with the Telkwa Formation, the oldest formation of the Hazelton Group (Richards and Tipper, 1976); it is composed mainly of intermediate coherent volcanic and volcaniclastic rocks. A large, multiphase, anastomosing pluton, informally named the Kleanza pluton (Gareau *et al.*, 1997a, b), is represented in these cross-sections. A second plutonic suite, belonging to the Eocene Coast Plutonic Complex, is only represented in cross-section D–D′–D″, as it outcrops mainly in the northwestern corner of the Usk map area (Carpenter Lake pluton, Fig. 2).

CROSS-SECTIONS

Detailed descriptions of the geological units that are shown in these cross-sections are presented in Nelson *et al.* (2006) and will not be repeated here; rather, this paper will focus on observations, made along the transects of the cross-sections, that may be important to the interpretation of the environment of emplacement/deposition.

Section A–A′

The A–A′ transect (Fig. 3), which crosses from Copper Mountain on the south side of the Zymoetz River to the O.K. Range on the north side of the river, highlights the features of the Paleozoic Zymoetz group, Triassic strata, and their internal structure and relationship to overlying and intrusive Jurassic units.

Apophyses of the Jurassic Kleanza pluton outcrop on Copper Mountain and in the O.K. Range. The margins of this intrusive body represent both original intrusive contacts and faulted contacts. The Kleanza pluton forms a laccolith in the northwestern and central parts of the Usk map area. The laccolith is present at a shallow depth, as depicted on the northeastern portion of this cross-section. Its geometry, in this portion of the map, is inferred from 1) its regional outcrop characteristics (for instance, plutonic rocks commonly outcrop in low lying drainages); and 2) high concentrations of dikes, up to 50% of all outcrop, with rock types similar to those of the pluton.

The Paleozoic Zymoetz group is composed of two units, a fossiliferous limestone and a volcanic unit that is composed of interbedded intermediate lapilli tuff and volcanic conglomerate and sandstone. These units are considered by Nelson *et al.* (2006) to be a subaqueous-arc edifice with limestone reefs and limy banks that were periodically inundated by volcaniclastic debris. Limestone of the Zymoetz group is coeval with the Permian Ambition For-

[1]*Department of Earth Sciences, Dalhousie University, Halifax, NS (john.barresi@dal.ca)*

This publication is also available, free of charge, as colour digital files in Adobe Acrobat PDF format from the BC Ministry of Energy, Mines and Petroleum Resources internet website at http://www.em.gov.bc.ca/Mining/Geolsurv/Publications/catalog/catfldwk.htm

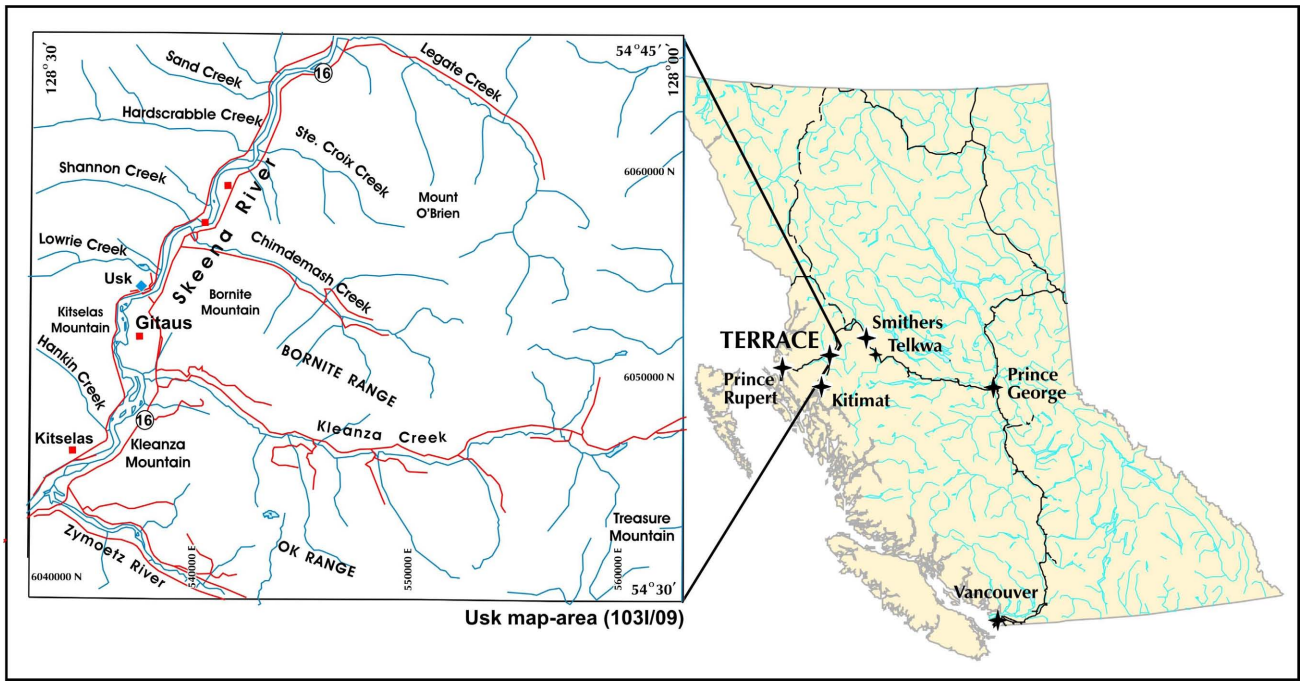


Figure 1. Location and geographic features of the Usk map area (NTS 103I/09), near Terrace, British Columbia.

mation in the Iskut-Stikine area (Gunning *et al.*, 1994); however, this limestone interfingers extensively with volcanic and volcanic-derived material, whereas the Ambition Formation postdates volcanic activity in the Iskut-Stikine area.

A thin band, less than 100 m thick, of well-bedded sedimentary rock overlies the Zymoetz group. These rocks bear a close likeness to other Triassic rocks in the Stikine Terrane. Radiolarians from this unit are currently being evaluated to confirm its age. These sedimentary rocks are composed of gray and black, pyritic radiolarian chert, in some areas interbedded with sooty black pyritic argillite. Beds are typically 5–15 cm thick and, in many outcrops, folded disharmoniously on a mesoscopic scale. These siliceous sediments represent an oxygen-starved marine depositional environment; they conspicuously lack any of the normally voluminous clinopyroxene porphyritic volcanic rocks that typify the Triassic elsewhere in the Stikine Terrane.

The Paleozoic and Triassic strata are characteristically thrust imbricated within the Usk map area. Repetitions of Paleozoic and Triassic rocks typically involve layer-parallel faults with up-to-the-south relative movement in the hangingwall. The thrust faults predate the deposition of the Jurassic Telkwa Formation and are overlain by basal conglomerate of the Telkwa Formation.

Paleozoic and Triassic strata are well exposed in the southwestern portion of the Usk map area, despite there being little evidence that this area is structurally lower than elsewhere in the map area, where they are not exposed. This leads to the interpretation that they formed a topographic high during the time of deposition of the Telkwa Formation. The presence of a proximal topographic high would explain the high-energy depositional environment of the Telkwa basal conglomerate, which is composed mainly of clasts derived from the Zymoetz group. The basal conglomerate has strong local variations in clast composition, which further supports the local presence of a Paleozoic and Triassic topographic high.

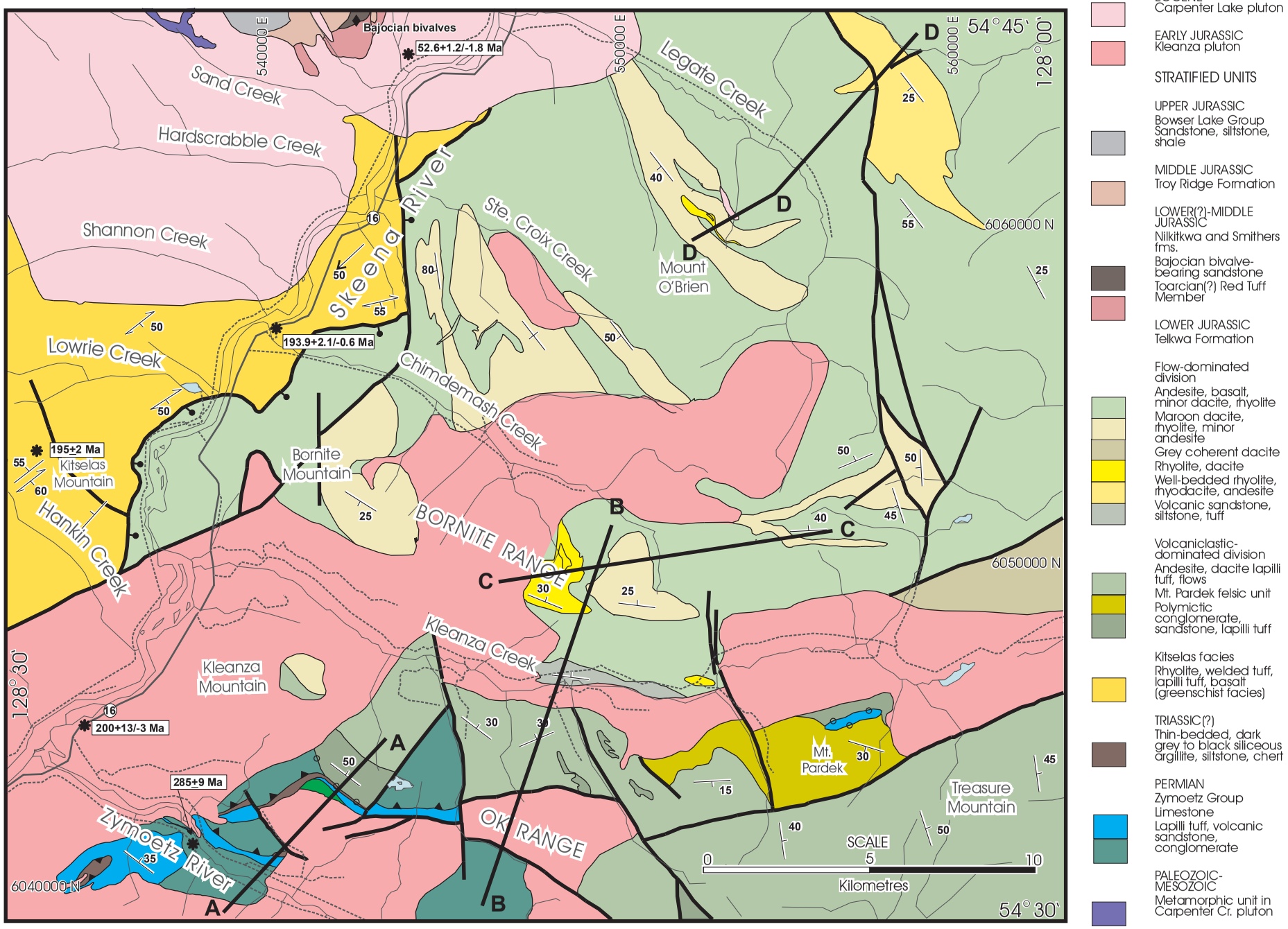
The Telkwa basal conglomerate and conglomerate of the Paleozoic volcanic unit are very similar and can easily be mistaken for one another, especially because they both contain the same types of clasts, and they may be structurally or stratigraphically in contact with one another. In general, conglomerate of the Zymoetz volcanic unit has a higher proportion of clinopyroxene porphyritic mafic rocks and quartz porphyritic dacite, and a lesser proportion of plagioclase porphyritic rocks; however, the Telkwa conglomerate can also contain these clasts where they are locally sourced from erosion of the Zymoetz group. Conglomerate of the Zymoetz volcanic unit is more commonly interbedded with volcanic sandstone with a limy matrix, and lapilli tuff. The basal Telkwa conglomerate can be uniquely identified where it contains clasts of the banded Triassic chert and sooty argillite (*e.g.*, along the northern end of this cross-section).

The basal Telkwa conglomerate is overlain by a thick unit of volcaniclastic rock composed mainly of andesitic lapilli tuff. This unit, and its relationship to the other coeval andesite unit in the map area, are described in the next cross-section.

Section B–B′

This transect (Fig. 3), which crosses from the O.K. Range on the north side of the Zymoetz River to the Bornite Range on the north side of Kleanza Creek, highlights the relationship between the two andesitic volcanic units within the Telkwa Formation, as well as other features of its internal stratigraphy.

The southwestern portion of this section shows the Zymoetz volcanic unit in faulted contact with a horst of the Kleanza pluton. Here, the pluton has been uplifted and offers a rare glimpse at its more homogeneous core, as op-



INTRUSIVE UNITS

EOCENE
Carpenter Lake pluton

EARLY JURASSIC
Kleanza pluton

STRATIFIED UNITS

UPPER JURASSIC
Bowser Lake Group
Sandstone, siltstone, shale

MIDDLE JURASSIC
Troy Ridge Formation

LOWER(?)-MIDDLE JURASSIC
Nilkitkwa and Smithers fms.
Bajocian bivalve-bearing sandstone
Toarcian(?) Red Tuff Member

LOWER JURASSIC
Telkwa Formation

Flow-dominated division
Andesite, basalt, minor dacite, rhyolite
Maroon dacite, rhyolite, minor andesite
Grey coherent dacite
Rhyolite, dacite
Well-bedded rhyolite, rhyodacite, andesite
Volcanic sandstone, siltstone, tuff

Volcaniclastic-dominated division
Andesite, dacite lapilli tuff, flows
Mt. Pardek felsic unit
Polymictic conglomerate, sandstone, lapilli tuff

Kitselas facies
Rhyolite, welded tuff, lapilli tuff, basalt (greenschist facies)

TRIASSIC(?)
Thin-bedded, dark grey to black siliceous argillite, siltstone, chert

PERMIAN
Zymoetz Group
Limestone
Lapilli tuff, volcanic sandstone, conglomerate

PALEOZOIC-MESOZOIC
Metamorphic unit in Carpenter Cr. pluton

Figure 2. Generalized geology of the Usk map area, showing the location of the cross-sections

posed to the heterogeneous border phases that are normally observed. The centre of the pluton is more evolved than the border phases: it is a relatively homogeneous, coarse grained, equigranular, biotite granite with up to 60% quartz. Border phases, such as those exposed in the Kleanza Creek valley, on this cross-section are typically more mafic and are composed of hornblende±biotite granodiorite and diorite, rare granite, green microdiorite and aplite. These border phases of the Kleanza suite show extreme local variability and mutual crosscutting relationships.

Juxtaposed across the Kleanza Creek valley are distinct units of the Telkwa Formation, which Nelson *et al.* (2006) refer to as the O.K. Range – Treasure Mountain facies and Kleanza Creek facies in the south, and the Mount O'Brien facies in the north. Both are composed mainly of andesitic volcanic rocks, but the O.K. Range and Kleanza Creek facies are mainly volcaniclastic rocks, whereas those to the north are mainly coherent volcanic flow units. The differences between these units are not the result of a stratigraphic relationship; rather, they represent a paleogeographic difference in volcanic environments and depositional settings. The northern Mt. O'Brien facies is proximal to eruptive fissures and centres, and is therefore composed mainly of coherent volcanic flows. In the southern Kleanza and O.K. Range facies, there is very little coherent volcanic material; instead, they are composed mainly of primary and resedimented volcaniclastic material, particularly andesitic lapilli tuff. These are more distal facies and represent a subsiding basin. The basin accommodated large amounts of volcanic debris that erupted directly into it or washed into it from the volcanic edifice.

There are no exposures of Triassic or Paleozoic rocks, or the basal Telkwa conglomerate, beneath the andesite of the Mt. O'Brien facies. On the northern slopes of Kleanza Creek, a sequence of finely bedded green and maroon volcanic sandstone grades transitionally upward into coherent flows.

Two locally occurring bodies of dacite and rhyolite are depicted on the northeastern portion of the cross-section. Both coherent and volcaniclastic facies of these felsic rocks form irregular and discontinuous bodies within the coherent Mt. O'Brien facies andesite unit. Felsic intervals are rare in the O.K. Range and Kleanza facies, due to the distance of these rocks from the local felsic eruptive centres located to the north in the Mt. O'Brien facies. The characteristics of the Mt. O'Brien facies felsic units and their relationships with the andesitic units are discussed in further detail in the following two sections.

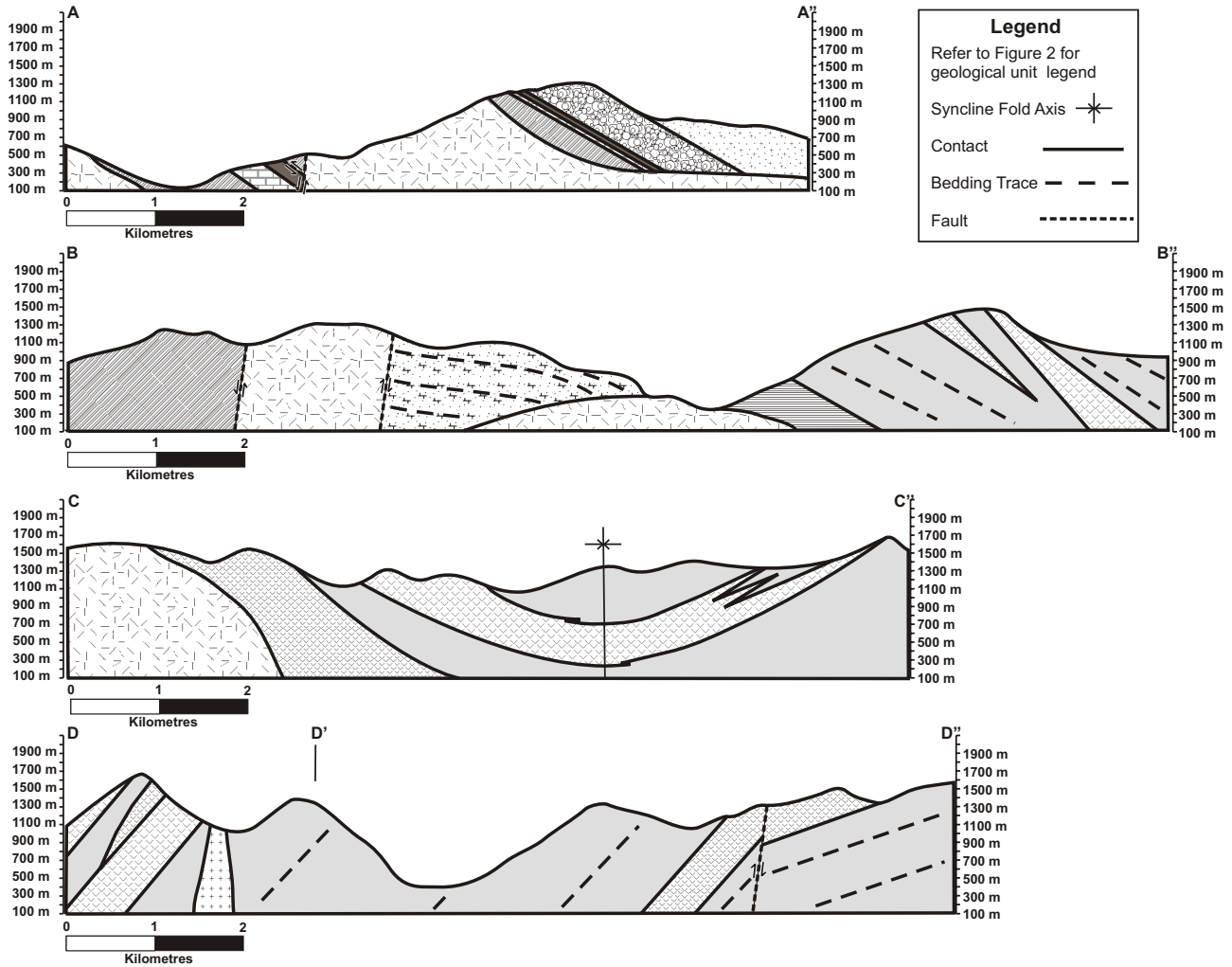


Figure 3. Cross-sections of the Usk map area. Rock unit patterns as on Figure 2.

Section C–C′

The C–C′ transect (Fig. 3), which spans a length of the Bornite Range between the headwaters of Chimdemash Creek to the north and Kleanza Creek to the south, depicts the physical distribution of dacitic and rhyolitic units within the Mt. O'Brien facies.

On the western portion of this cross-section, there is a contact between a body of the Kleanza pluton and a rhyolite volcanic unit. Closer to the centre of the intrusive body, the rock is relatively homogeneous, but, along its margin, it is composed almost entirely of dikes with variable composition, ranging from mafic to felsic. Of particular interest is the presence of highly epidotized, fine-grained, holocrystalline 'clasts'; these clasts are also found in abundance in certain tuff layers in the overlying rhyolitic units (Fig. 4). The close resemblance of many of the border phase felsic dikes to the rocks within the rhyolite unit, and the presence of holocrystalline epidotized clasts in both the pluton and the tuff layers, suggests that the contact between the pluton and the rhyolite may be transitional in the sense that the pluton was a feeder to the overlying eruptive volcanic unit.

The rhyolite unit is composed of laterally continuous layers of coherent, flow-banded white rhyolite, lapilli tuff and thin-bedded aphanitic siliceous sedimentary layers (Fig. 5). The fine-grained, well-bedded, siliceous sedimentary units may be intervals of felsic ash tuff or exhalitive chert. Lapilli tuff in this felsic unit is mono to polylithic, and some beds contain mafic as well as felsic lapilli. At least one 20 m thick bed is composed of resedimented lapilli tuff, which has scour-and-fill structures at its base and a coarsening-upward grading. Welding (*i.e.*, the flattening of pumice clasts due to compaction of hot volcanic material) is conspicuously absent in any of these beds. The continuity of beds in this unit, especially of the coherent rhyolite bodies, is unusual for these highly viscous volcanic rocks. It suggests that the section crosses very close to the volcanic centre but at a distance where beds can be deposited without being disrupted by further volcanic activity, probably on the moderately distal flanks of the eruptive edifice. The lateral continuity of beds, absence of welding, and presence of fine-grained, well-bedded sequences are all suggestive of a subaqueous depositional environment.

The dacitic unit in this cross-section is exposed on two limbs of what is interpreted to be a broad syncline. The syncline is inferred from the opposing dips of the rocks on each limb; however, within the dacitic unit, igneous layering orientations are highly variable. This can be explained by the viscous nature of the lava, the irregular topography of the underlying andesitic unit, and the general high-energy and chaotic nature of volcanic centres. The dacitic unit interfingers extensively with the surrounding andesite and typically fills paleotopographic depressions between large lobes of andesite that are typically hundreds of metres wide. In some places, thin veneers of fine-grained dacitic rock also cover paleotopographic highs. The dacitic unit is highly variable in its textures and individual facies are rarely laterally continuous. They are typically brick red or lavender in colour and variably feldspar phyric and vesicular. Coherent bodies are sometimes flow banded, spherulitic and rarely contain lithophysae (large vugs that form from the devitrification of volcanic glass). Volcaniclastic rocks include large breccia piles, lapilli tuff, and fine-bedded ash and crystal-ash tuffs. In at least two locations, lapilli tuff contains clasts of lapilli tuff (Fig. 6), an indication of multiple generations of explosive volcanism from the same centre. Other volcanic rocks are highly welded, with up to 1:10 aspect ratios on flattened pumice clasts. The overall geometry of deposition of the dacitic unit is consistent with subaerial pyroclastic flows (Wright *et al.*, 1980). The ubiquity of welded rocks in this unit also supports a subaerial depositional setting.

The andesite unit, which interfingers extensively with the dacitic unit, is composed mainly of green or maroon, vesicular, coherent flow units and minor amounts of lapilli tuff. The coherent units are fine grained to aphanitic and commonly have euhedral, lath-shaped plagioclase phenocrysts. The vesicles and amygdules, which range in size from 0.2 to 10 cm, occupy a large proportion of the coherent bodies, up to 60% by volume, and are filled with zeolite-facies metamorphic minerals, including chabazite, chlorite and natrolite (Fig. 7). These bodies form an irregular paleotopography composed of large flow units, as well as smaller flow lobes; no pillow forms were observed. The absence of pillow forms and the large vesicle size in these units is suggestive of a subaerial deposition. In addition, there is a virtual absence of interbedded sedimentary mate-



Figure 4. Holocrystalline epidotized clasts in the Kleanza pluton (left) and felsic lapilli tuff of the Telkwa Formation (right), Usk map area, near Terrace, BC.



Figure 5. Well-bedded rhyolitic ash and crystal ash tuff overlain by a 20 m thick bed of resedimented felsic lapilli tuff, Usk map area, near Terrace, BC.

rial, such as would be found in most proximal subaqueous depositional environments.

Section D–D′–D″

The D–D′–D″ transect (Fig. 3) crosses a cirque on the northern flank of Mt. O'Brien (D–D′) and then crosses Legate Creek, near its headwaters, to the northernmost mountain range in the Usk map area (D′–D″). This section crosses a small plug of probable Eocene age, and also two Telkwa rhyolitic units. It also crosses a major fault, which separates shallow-dipping strata in the north (Fig. 8) from more steeply dipping strata in the south. In addition, this section shows that regional trends in the orientation of beds are variable throughout the map area, as these beds dip to the southwest, whereas those in the other sections dip predominately to the northeast.

In the southwestern portion of this cross-section, a series of mainly coherent dacitic and rhyolitic units interfinger with andesite. These felsic units are similar to those described in cross-section C–C′. The andesite at this location also has similar characteristics to that on section C–C′; here, however, pipe vesicles may be present at the contacts between flows. Pipe vesicles commonly occur in subaerial environments where a flow passes over a moist surface, releasing vapours into the overlying lava (Wilmoth and Walker, 1993). The predominance of andesite shown in the lower slopes of the Legate Creek drainage is inferred, as this area is heavily forested and unexposed due to a thick Quaternary overburden.

The rhyolite unit in the northeastern portion of the cross-section is distinct from those elsewhere in the Usk map area. It is composed of a wide variety of coherent and volcaniclastic, 1–40 m thick beds of lapilli, ash and crystal-ash tuffs, and coherent rhyolite flows and domes that are transitional into flow breccias. This unit is also composed of approximately 30% dacite and 20% andesite beds. In one location, white flow-banded rhyolite was extruded through



Figure 6. Lapilli tuff with a 'clast' of a previously formed lapilli tuff, Usk map area, near Terrace, BC.



Figure 7. Amygdaloidal andesite, the vesicles partly filled with pink chabazite, Usk map area, near Terrace, BC.



Figure 8. Shallow-dipping, well-bedded layers in the northernmost rhyolitic unit (cross-section D'–D''), Usk map area, near Terrace, BC.

what was a nonlithified, red dacitic, crystal-ash tuff, creating an interval of peperitic white rhyolite in a red dacitic groundmass (Fig. 9). The andesite unit in this portion of the cross-section is composed of volcaniclastic and coherent flow rocks that are also bedded on a 1–40 m scale. Both the felsic and mafic rocks in this portion of the map area have been affected by high-angle, synvolcanic faults, which show between 1 and 10 m of vertical displacement. Rare welding of pumice clasts in rhyolitic beds suggests a subaerial depositional environment; however, limestone is found in the interstices of some andesite breccia, which suggests subaqueous deposition. In addition, rhythmic layering and normal grading of some tuff beds are also suggestive of subaqueous deposition by density currents. The volcanic rocks in this portion of the map area may have been deposited on a partly emergent, partly submerged volcanic edifice.

GEOLOGICAL HISTORY AND PALEOGEOGRAPHY OF THE STUDY AREA

The oldest rocks represented in the Usk map area belong to the Paleozoic Zymoetz group, which consists of limestone and volcanic rocks that were deposited on the limy shelf of an arc edifice. It was overlain by well-bedded Triassic chert and argillite in an oxygen-starved marine environment. These units were thrust imbricated prior to deposition of the Jurassic Telkwa Formation. During the Jurassic, they are interpreted to have formed an upstanding topographic high, which was present in the southwestern portion of the map area. These rocks were eroded and, along with a Telkwa volcanic influence, formed a basal Telkwa conglomerate, also exposed mainly in the southern portion of the map area. Overlying the basal conglomerate is a thick unit of mainly andesitic primary and resedimented lapilli tufts. These are interpreted to have been deposited in a mainly subaqueous, subsiding basin. Coeval, coherent volcanic rocks, which are voluminous to the north of Kleanza Creek, are the proximal and effusive equivalents of volcaniclastic rock deposited in the south. The northern section comprises andesite, dacite and rhyolite eruptive units, which interfinger extensively. Evidence of both subaerial and subaqueous deposition are present, often in close geographic or stratigraphic proximity to one another, suggesting that these rocks were deposited on a partly emergent arc edifice. Units of all ages have been intruded by the Jurassic Kleanza pluton and smaller bodies of Eocene age that relate to the eastern margin of the Coast Plutonic Complex. The relationship between the Kleanza pluton and the overlying Telkwa volcanic rocks is, in part, transitional, and similarities between the border phases of the pluton and Telkwa volcanic units suggest that these plutons were direct sources of volcanic magmas.

ACKNOWLEDGMENTS

We wish to thank Ellie Knight and Nicole Boudreau for their fine contributions to the Usk map; and Dan Parker, Richard Seymour and Chad Gerow of the Kitselas First Nations for their assistance in the field. The first author thanks Andrew McRae for his help in constructing the cross-sec-

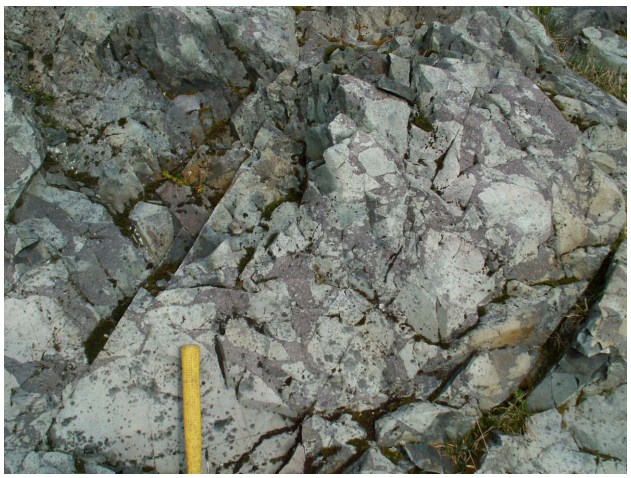


Figure 9. Peperitic, flow-banded white rhyolite in a red dacitic tuff groundmass, Usk map area, near Terrace, BC.

tions, and Jarda Dostal for his ever-present support and guidance.

REFERENCES

Anderson, R.G. (1993): A Mesozoic stratigraphic and plutonic framework for northwestern Stikinia, northwestern British Columbia, Canada; *in* Mesozoic Paleogeography of the Western United States – II; Dunne, G. and McDougall, K., Editors, Society of Economic Paleontologists and Mineralogists, Pacific Section, Volume 71, pages 477–494.

Brown, D.A., Logan, J.M., Gunning, M.H., Orchard, M.J. and Bamber, W.E. (1991): Stratigraphic evolution of the Paleozoic Stikine assemblage in the Stikine and Iskut rivers area, northwestern British Columbia; *Canadian Journal of Earth Sciences*, Volume 28, no 6, pages 958–972.

Gareau, S.A., Friedman, R.M., Woodsworth, G.J. and Childe, F. (1997a): U-Pb ages from the northeastern quadrant of Terrace map area, west-central British Columbia; *in* Current Research 1997-A/B, *Geological Survey of Canada*, pages 31–40.

Gareau, S.A., Woodsworth, G.J. and Rickli, M. (1997b): Regional geology of the northeastern quadrant of Terrace map area, west-central British Columbia; *in* Current Research 1997-A/B, *Geological Survey of Canada*, pages 47–55.

Gunning, M.H., Bamber, E.W., Brown, D.A., Rui, L., Mamet, B.L. and Orchard, M.J. (1994): The Permian Ambition Formation of northwestern Stikinia, British Columbia; *in* Pangea: Global Environments and Resources, Embry, A.F., Beauchamp, B. and Glass, D.J., Editors, *Canadian Society of Petroleum Geologists*, Memoir 17, pages 589–619.

Logan, J.M., Drobe, J.R. and McClelland, W.C. (2000): Geology of the Forrest Kerr – Mess Creek area, northwestern British Columbia; *BC Ministry of Energy, Mines and Petroleum Resources*, Bulletin 104, 164 pages.

Nelson, J.L., Barresi, T., Knight, E. and Boudreau, N. (2006): Geology and mineral potential of the Usk map area (NTS 103I/09), near Terrace, British Columbia; Geological Fieldwork 2005, *BC Ministry of Energy, Mines and Petroleum Resources*, Paper 2006-1 and *Geoscience BC*, Report 2006-1.

Richards, T.A. and Tipper, H.W. (1976): Jurassic stratigraphy and history of north-central British Columbia; *Geological Survey of Canada*, Bulletin 270, 73 pages.

van der Heyden, P. (1992): A Middle Jurassic to early Tertiary Andean-Sierran arc model for the Coast Belt of British Columbia; *Tectonics*, Volume 11, pages 82–97.

Wilmoth, RA and Walker, G.P.L. (1993): P-type and S-type pahoehoe: a study of vesicle distribution patterns in Hawaiian lava flows; *Journal of Volcanology and Geothermal Research*, Volume 55, pages 129–142.

Wright, J.V., Smith, A.L., and Self, S. (1980): A working terminology of pyroclastic deposits; *Journal of Volcanology and Geothermal Research*, Volume 8, pages 315–336.

Geology Between the Toodoggone River and Chukachida Lake (Parts of NTS 94E/6, 7, 10 and 11), North-Central British Columbia

By L.J. Diakow and R. Rhodes

KEYWORDS: Toodoggone Formation, Junkers member, Graves member, Pillar member, Belle member, Mount Gordonia, Toodoggone Peak, Chukachida Lake, epithermal veins, skarn

INTRODUCTION

Geological mapping at 1:20 000 scale, carried out from 2003 to 2005 as part of the Toodoggone Geoscience Partnership (Diakow and Shives, 2004), has expanded the distribution of the Early Jurassic Toodoggone Formation eastward, and subdivided volcanic and sedimentary rocks in a previously unknown upper part of the formation. This new mapping and complementary geochronology have significantly improved understanding of the internal stratigraphy and intrusive events, and the setting of new mineral occurrences in the central Toodoggone River area (NTS 094E). In 2005, detailed geological mapping was extended northward into a remote mountainous region of the Metsantan and Peak ranges, between the Toodoggone River in the south and Chukachida Lake in the north, an area originally mapped at regional scale by the Geological Survey of Canada (Gabrielse *et al.*, 1977). Except for a general absence of stratigraphic units representing the lower part of the Toodoggone Formation (*i.e.*, Duncan, Metsantan and overlying Saunders members), the stratigraphic framework in the current study region is similar to that established south of the Toodoggone River (Diakow *et al.*, 2005a). This report emphasizes the lateral lithostratigraphic changes in recently recognized rock units that make up the upper Toodoggone Formation north of the Toodoggone River. Figure 1 shows the local geology, and representative stratigraphic sections are portrayed in Figure 2.

EARLY PERMIAN AND LATE TRIASSIC BASEMENT ROCK UNITS

Limestone, siltstone and chert (unit PAl) of the Carboniferous to Early Permian Asitka Group are the oldest recognized strata. With the more extensive basaltic volcanic rocks of the overlying Late Triassic Takla Group, they constitute the basement succession for the Early Jurassic Toodoggone Formation.

Sedimentary rocks of the Asitka Group are localized in the footwall block of an east-trending fault, which in turn is truncated by regional northerly-trending faults traversing the valleys of Midas and Junkers creeks. Greyish white crystalline marble occupies the lower 175 m of a near-vertical fault scarp. The marble is overlain by a sequence of rusty weathered, black mudstone, siltstone and chert, which is between 25 and 75 m thick.

Rocks of the Takla Group are widespread north of the Toodoggone River, where they typically form craggy ridges and precipitous cliffs dominated by massive, chlorite and epidote-altered basaltic lavas, minor pyroclastic rocks and rare pods of limestone. With the exception of locally mappable intervolcanic sedimentary rocks, the Takla volcanic rocks are inherently difficult to subdivide.

The Takla Group depositionally overlies interlayered mudstone and chert exposed along a fault between Midas and Junkers creeks. Here the Takla Group consists of a sequence of basalt lavas distinguished by abundant plagioclase laths up to 3 cm long (unit uTTbb). This flow succession is at least 400 m thick, inclined gently toward the south. East of Contact Peak, the upper several hundred metres of basalt displays generally smaller plagioclase laths, which are between 2 and 5 mm long, and also contains up to 7% pyroxene. East of Mulvaney Creek, this bladed plagioclase-phyric basalt forms an entire mountain and directly underlies nearby rocks of the Jurassic Toodoggone Formation. Similar flows mapped about 60 km to the southeast near the Kemess North mineral deposit are interlayered with clinopyroxene-phyric lavas near the top of the Takla Group and overlain directly by basal conglomerate of the Toodoggone Formation. Bladed plagioclase porphyritic basalt in the study area differs in that it is generally coarser, more crystal rich (up to 60%) and appears to occupy a relatively low stratigraphic position within the Takla succession.

The most common rocks in the Takla are fine to medium-grained porphyritic to aphanitic basalt and subordinate andesite flows containing medium-grained plagioclase and clinopyroxene phenocrysts (unit uTTb). They occur both stratigraphically above and below the distinctive, coarsely bladed plagioclase porphyritic basalt.

Sedimentary rocks (unit uTTs), comprising siltstone and sandstone in shades of green or reddish brown, form well-layered, internally laminated intervals between the monotonous volcanic rocks. Intervolcanic sedimentary sections vary from several metres to more than 250 m in thickness. Angular crystal grains of plagioclase and pyroxene dominate the sedimentary rocks and suggest a local provenance from Takla volcanic rocks. Limestone lenses up to 1.2 m thick occur with fine clastic sedimentary rocks in several widely spaced localities south and east of Mount Gordonia. These thin carbonate units consist of fetid, black, impure limy bands alternating with resistant siliceous laminations.

This publication is also available, free of charge, as colour digital files in Adobe Acrobat PDF format from the BC Ministry of Energy, Mines and Petroleum Resources internet website at http://www.em.gov.bc.ca/Mining/Geolsurv/Publications/catalog/catfldwk.htm

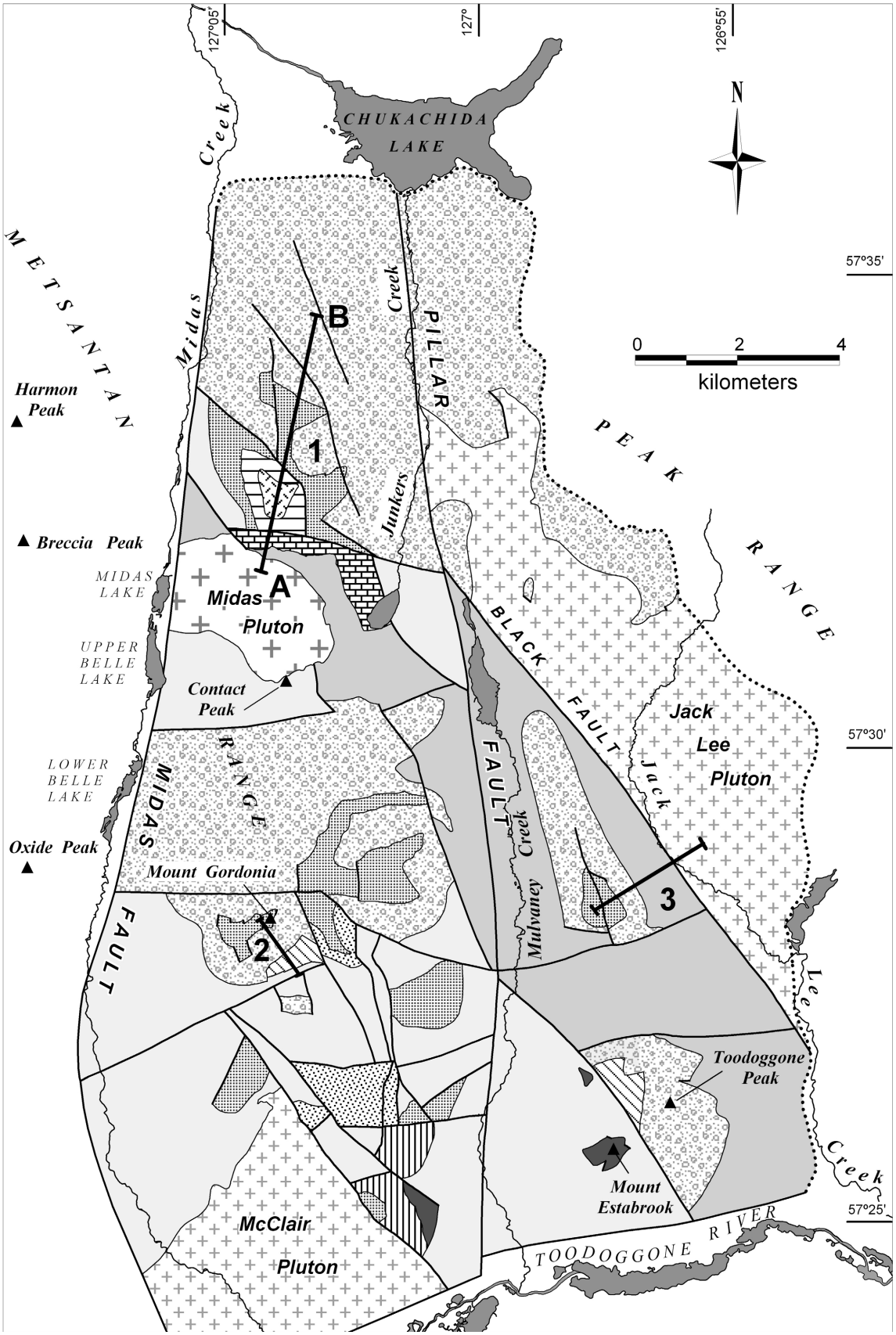
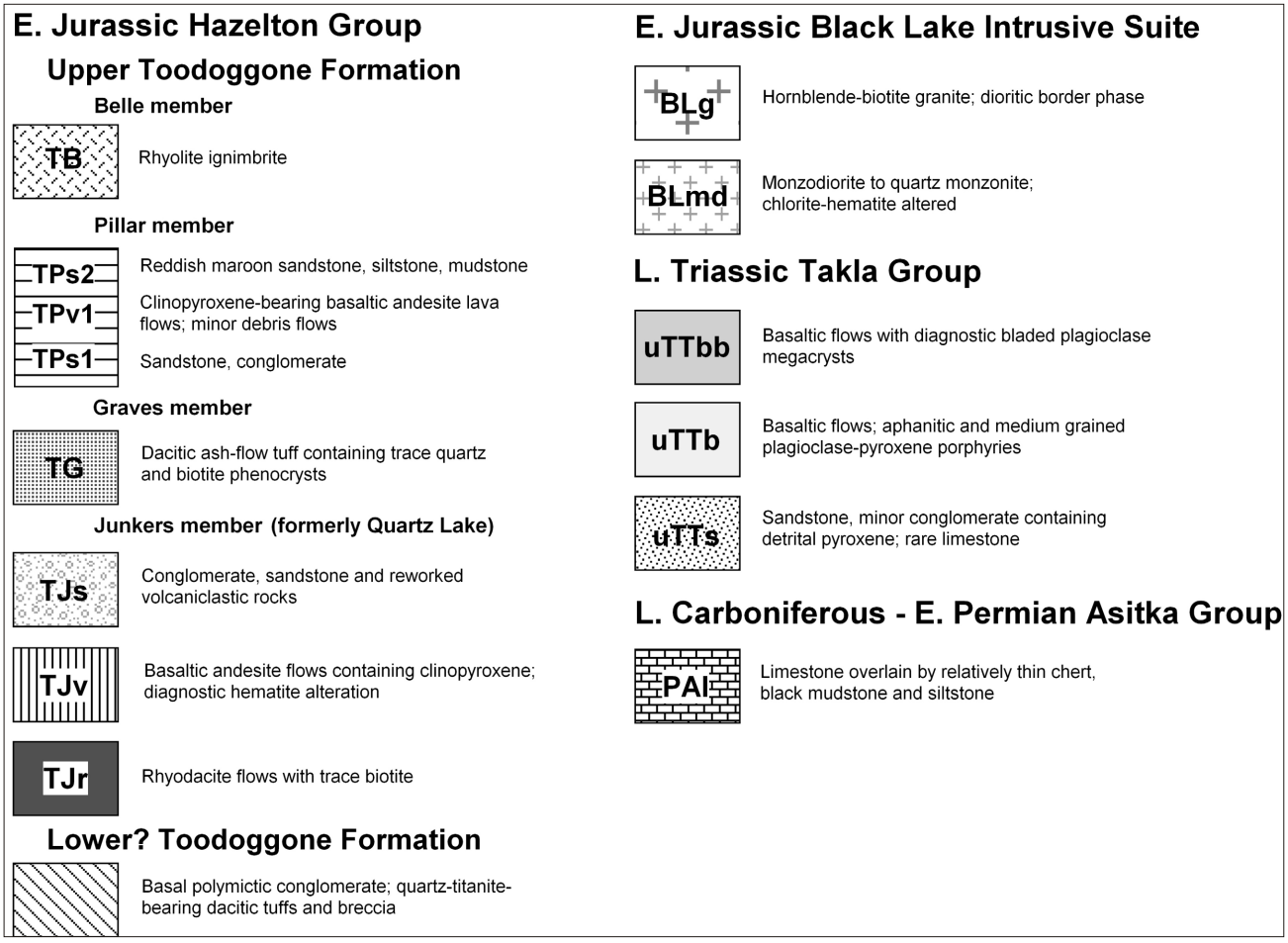


Figure 1. Simplified geology of the study region, located between the Toodoggone River in the south and Chukachida Lake in the north. Numbered transects correspond to representative stratigraphic sections shown in Figure 2 and schematic cross-section A–B, shown in Figure 3.



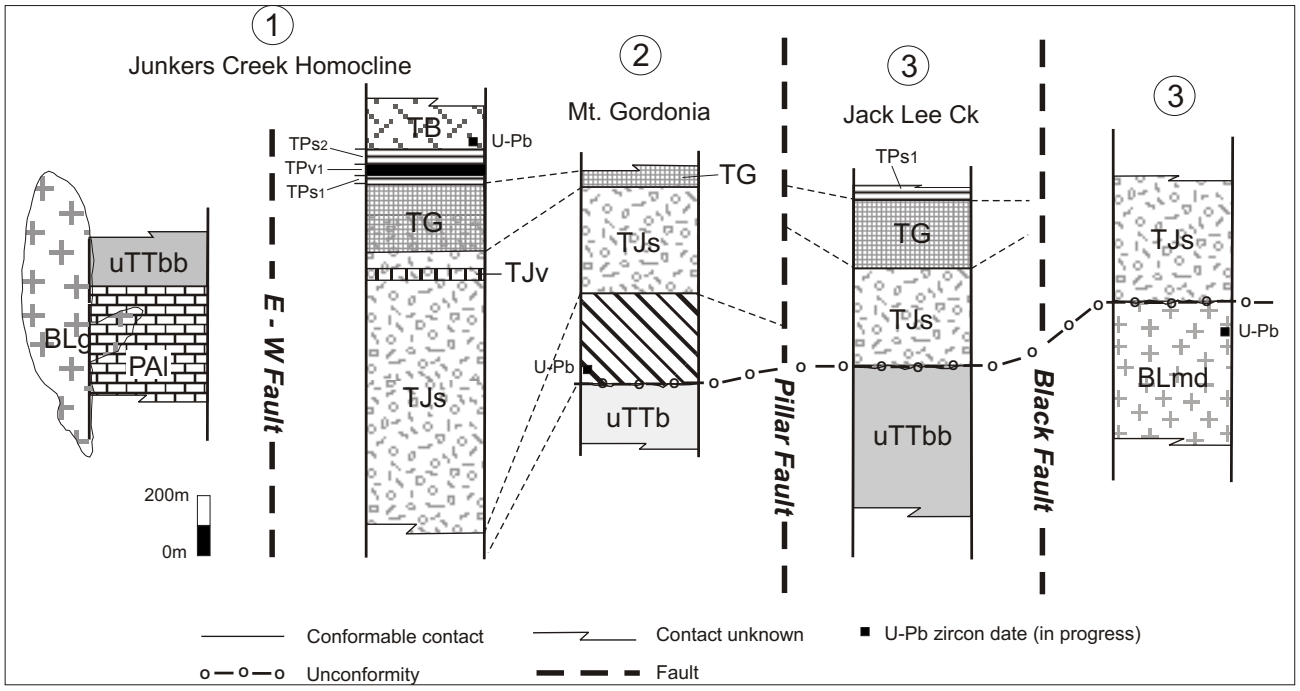


Figure 2. Generalized stratigraphic sections representative of the upper Toodoggone Formation. See Figure 1 for locations and legend.

EARLY JURASSIC TOODOGGONE FORMATION

The Pillar, Graves and Quartz Lake members, the latter renamed the Junkers member, represent much of the recently defined upper Toodoggone Formation (Diakow *et al.*, 2005a). The Belle member is a new unit proposed for an ignimbrite, which marks the highest volcanic member recognized in the Toodoggone Formation. The upper Toodoggone Formation dominates a region 40 km long, from southern localities near Jock Creek and east of the Pillar fault (Diakow *et al.*, 2005b) northwest into the current study area, east of the Midas fault and as far north as Chukachida Lake. These four members have stratigraphic continuity in a homocline immediately west of Junkers Creek and south of Chukachida Lake, shown in a north-south cross-section (Fig. 3). Several other localities containing exceptional sections of upper Toodoggone stratigraphy, which have not been significantly disrupted by faults, include the southeast slope of Mount Gordonia and the west slope of Toodoggone Peak. With the exception of the latter two sections, where upper Toodoggone stratigraphy apparently overlies strata presumed to be part of the lower Toodoggone Formation, the Junkers member rests unconformably on the Takla Group or Early Jurassic granitic rocks. This contrasts with the region south of the Toodoggone River, where Junkers (formerly Quartz Lake) strata overlie the Metsantan and Saunders members, subdivisions that form the upper two members of the lower Toodoggone Formation.

Lower (?) Toodoggone Formation

The base of the Jurassic section along part of the lower west slope of Toodoggone Peak is marked by a polymictic conglomerate up to 75 m thick, deposited upon mafic volcanic rocks assigned to the Takla Group. The conglomerate consists of rounded cobbles and boulders with mafic volcanic clasts derived from the Takla, scarce limestone pebbles from the Asitka and a variety of andesitic porphyries and red-brown volcanic rocks of uncertain provenance. Rare quartz grains in the red-maroon oxidized matrix suggest that it may have been derived, in part, from quartz-bearing volcanic rocks common in the lower Toodoggone Formation. Upsection from the conglomerate are various reddish lapilli tuffs and dacitic tuff-breccias that contain fine-grained porphyritic andesite and red-brown aphanitic volcanic fragments. Crystal fragments in these tuffs are plagioclase, rare quartz, minute yellow titanite and hornblende replaced by chlorite. The uppermost of these quartz-bearing beds is a dacitic lava-flow tuff, which was sampled to determine a U-Pb crystallization age (sample 05LDi 10.2). Based on the mineralogy of these rocks, they might be a remnant of the pre-193–194 Ma lower Toodoggone Formation. Similarly, at Mount Gordonia, dacitic tuff containing as much as 3% quartz and trace titanite phenocrysts, which occupies the lowest exposures below Junkers strata, resembles the lower Toodoggone Formation. This quartz-bearing tuff has also been sampled for a U-Pb age determination (sample 05LDi 30.1) that will establish a maximum depositional age for the overlying Junkers epiclastic-volcaniclastic succession.

Upper Toodoggone Formation

JUNKERS MEMBER (UNITS TJs, TJv, TJr; RENAMED AFTER QUARTZ LAKE MEMBER)

The Junkers member is proposed to replace the name 'Quartz Lake member'. This change reflects superior exposure of stratigraphy equivalent to the Quartz Lake member mapped north of the Toodoggone River, particularly on

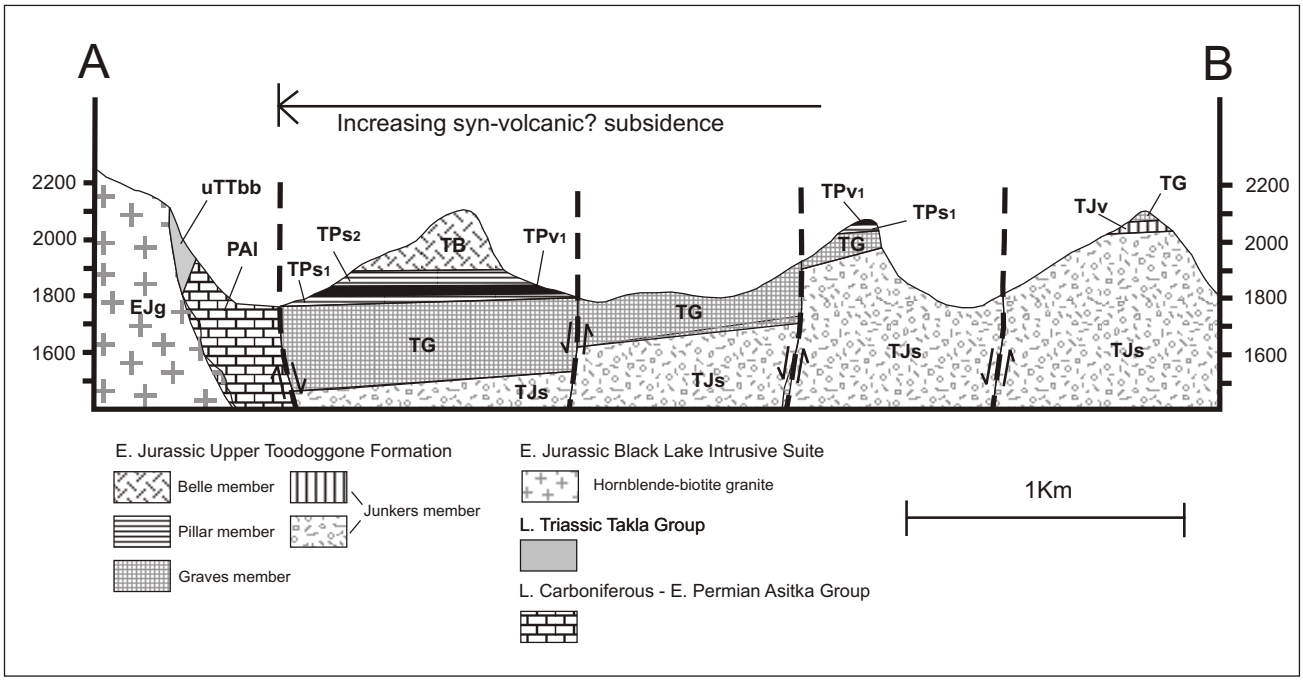


Figure 3. North to south cross-section of a homocline west of Junkers Creek that shows ash-flow tuff and epiclastic rocks increasing in thickness toward an east-trending fault that is interpreted to be synvolcanic with the Graves, Pillar and Belle members of the upper Toodoggone Formation.

ridges adjacent to Junkers Creek, which drains into the south side of Chukachida Lake. Strata of the Junkers member typically form thick, well-layered intervals that are locally more than 560 m thick at Toodoggone Peak and 370 m thick at Mount Gordonia. The unit thickens considerably farther north in the region of Junkers Creek, occupying the lower kilometre or more of a homocline. The lower contact of the Junkers unit is an unconformity, either above basaltic volcanic rocks of the Takla Group or an Early Jurassic (?) monzodiorite exposed east of Mulvaney and Junkers creeks. In sections at Mount Gordonia and Toodoggone Peak, the Junkers conformably overlies quartz-bearing dacitic tuff believed to be a vestige of the lower Toodoggone Formation.

Junkers strata are lithologically heterogeneous, composed of massively interbedded, reworked, polymict lapilli tuff, debris flows, volcanic conglomerate, sandstone-siltstone (95%; subunit TJs), pyroxene-bearing porphyritic basaltic andesite to andesite lava flows (5%; subunit TJv) and comparatively small-volume flows of rhyodacitic composition (subunit TJr). Unit TJs is dominated by conglomerate with interbedded sandstone and siltstone derived from basaltic lava flows and volcaniclastic rocks. Conglomeratic beds are typically poorly sorted and contain subrounded to subangular clasts that vary from cobble to boulder size. Except on weathered surfaces, the clasts are difficult to identify and blend into the dark green to maroon matrix. The clasts are wholly derived from a volcanic source, composed predominantly of fine-grained (0.5–2 mm) plagioclase-pyroxene-phyric basalt. Interbeds of maroon to reddish brown sandstone and siltstone are generally less than several metres thick. They display planar bedding, graded bedding and rare low-angle crosslaminations. Tube-shaped concretions have been found in some finer siltstone beds. Sandstone is typically rich in plagioclase with lesser amounts of pyroxene. However, locally common quartz, hornblende and titanite reflect different volcanic sources within the Toodoggone Formation. Clastic rocks containing mainly plagioclase and pyroxene grains with fine-grained basaltic lithic clasts may be derived locally from either basaltic flows that form part of the upper Toodoggone Formation or from the older Takla Group.

Rare accretionary lapilli tuff, found at the lowest exposure in the section south of Chukachida Lake, indicates the presence of ash fallout and suggests local deposition in a subaerial environment. Elsewhere, rocks suspected to have a pyroclastic origin include pyroclastic breccia and lapilli and finer, well-bedded ash-rich tuffs. Rounding of pyroclasts and mechanical sorting within these deposits, however, suggests varying degrees of syn to postdepositional reworking.

Pyroxene-bearing basaltic lavas (unit TJv) occur at the top of the Junkers unit in three localities and are sharply overlain by the Graves member. In the absence of intervening rocks of the Graves member, the Junkers basalt is indistinguishable in the field from a succession of similar flows stratigraphically higher within the Pillar member. At Mount Gordonia, these basaltic lavas are about 70 m thick and overlie a distinctive red epiclastic-volcaniclastic layered sequence about 100 m thick. In turn, they are sharply overlain by Graves ash-flow tuffs. The lavas are generally purplish grey-green, medium grained with plagioclase up to 4 mm (20–25%) and subvitreous pyroxene up to 3 mm (2%). Oxidation of the flows is apparent as reddish hematite staining that varies in intensity and manifests as Liesegang banding. Basaltic flows in the Gordonia section display a textural gradation not observed at any other locality. Near the bottom of this section, typical medium-grained porphyritic flows pass upsection into sparsely porphyritic to aphanitic lavas, then into a distinctive, coarse-bladed plagioclase-phyric variety at the top of the section. Slender plagioclase laths between 6 and 14 mm characterize these bladed flows. Although bladed plagioclase porphyry flows are locally voluminous in the Takla Group, those at Mount Gordonia are the only known occurrence in the Toodoggone Formation.

Lavas of dacitic to rhyodacitic composition (unit TJr) cap Mount Estabrook. Although unequivocal stratigraphic contacts have not been observed with nearby Junkers clastic rocks, these and other similar lavas west of Mulvaney Creek are believed to form lens-shaped deposits within the Junkers unit. Rhyodacite contains up to 20% plagioclase and several percent relict biotite and hornblende phenocrysts scattered in a dark reddish brown and greenish pink groundmass that commonly displays flow laminations.

Thick, lithologically varied and reworked volcaniclastic and epiclastic rocks characteristic of the Junkers member and resting on Takla and plutonic rocks likely coincided temporally with an interval of regional tectonic instability during which rocks of the lower Toodoggone succession were deeply eroded. The Junkers succession is interpreted as broad, low-angle alluvial fans built up along margins of uplifted fault blocks or, alternatively, represent the distal, largely clastic aprons of stratovolcano centres, prograding over older peneplaned rocks. Small-volume basaltic lava flows and their scattered distribution might suggest localization within irregular channels developed on coalescing fan surfaces. The Junkers member was deposited subaerially, with traction features in some sandstone beds suggestive of fluvial transport. The location of perceived central volcanoes, which fed the basaltic lavas and sourced the large volume of basaltic detritus occupying clastic deposits, likely lay east of present exposures of the Junkers member.

GRAVES MEMBER (UNIT TG)

The Graves member is named for lithic-rich ash-flow tuff deposits mapped within a series of half-graben fault blocks southeast of Mount Graves, south of the Toodoggone River (Diakow *et al.*, 2005a, b). The member consists primarily of a dacitic ash-flow tuff and locally prominent rhyolite lava flows or a rarely preserved, subaerial fallout, fine tuff facies. These rhyolitic flows and associated ash tuff deposits directly underlie a thick ash-flow sheet south of the Toodoggone River near the southern limit of the Graves member at Jock Creek. At a locality immediately north of Jock Creek, an ash-tuff bed about 1 m thick overlies thin intraformational conglomerate that was deposited at the top of pyroxene-phyric basalt of the Junkers member (Diakow *et al.*, 2005a). This ash layer yielded a U-Pb date of 192.0 +1/–2 Ma (sample 04LDi 22.9), corroborating the U-Pb date of 192.3 ±0.4 Ma on ash-flow tuff deposits (sample 03LDi 27.1) near Mount Graves.

North of the Toodoggone River, the Graves member is widespread, locally resting conformably on oxidized red-brown sections, up to 20 m thick, composed of bedded lapilli and fine tuffs. These rocks presumably are Plinian fallout deposits containing some synvolcanic reworking

that produced minor crystal-rich sandstone at the base of overlying massive ash-flow tuff. This distinctly bedded interval is evident immediately beneath ash-flow tuff at Mount Gordonia and along a low northwest-trending ridge several kilometres north of Toodoggone Peak. West of Junkers Creek, the pyroclastic flows overlie resistant, relatively thin lava flows (unit TJv) found locally near the top of a thick succession of maroon siltstone, sandstone and conglomerate typical of the Junkers member. The rhyolite-flow facies, mapped beneath the pyroclastic flows south of the Toodoggone River (Diakow *et al.*, 2005b), has not been observed at the bottom of the Graves member in the study area. However, isolated rhyolitic rocks, tentatively assigned to the Junkers member (unit TJr) and unconformable on the Takla Group on Mount Estabrook, might actually be part of the Graves member.

Ash-flow tuff deposits in the Graves member are typically unstratified and display variations in their pyroclast content, internal welding and thickness. South of the Toodoggone valley, the ash-flow tuff deposits are generally lithic rich and, except for isolated thin welded zones, typically occupy nonwelded sections between 100 and 150 m thick (Diakow *et al.*, 2005a). In contrast, pyroclastic flows north of the river commonly show a striking internal zonation in the degree of welding and thickness variability. Differential welding is exhibited best in pyroclastic flows east of Mulvaney Creek and west of Junkers Creek, where these deposits apparently thicken to more than 200 m. Pyroclastic flows at these localities consist of a lower, nonwelded zone abruptly superimposed by a significantly thicker welded zone.

The nonwelded zone weathers recessively and contains up to 10% lithic fragments 2–10 cm in diameter. The fragments consist primarily of dark green and brownish red aphanitic and porphyritic andesite. However, the most diagnostic fragments, found in the Graves member throughout the region, consist of relatively scarce, pink, fine-grained porphyritic dacite-rhyolite and hornblende monzonite to quartz monzonite. Crystal fragments consist mainly of plagioclase and minor angular and resorbed quartz. Rare titanite and sparse (1–2%) altered biotite and hornblende also occur in the ash flows.

The welded upper part of the ash-flow succession locally develops columnar-jointed cliffs with the upper surface of the columns weathering in places to spheroidal lobes a metre or more in diameter. Relatively scarce lithic fragments and the comparatively massive, resistant weathered appearance distinguish the welded zone. Chloritic fiamme and elongate cavities, the latter presumably derived from preferential weathering and removal of compressed pumiceous fragments, define dense welding. The welded zone is also distinguished by formerly glassy juvenile pumiceous pyroclasts and cuspate and plate shards devitrified to fibrous quartz and feldspar. In localities where the pyroclastic flows were presumably very thick, ghost outlines of vitroclastic components are obscured during granophyric crystallization by a mosaic of anhedral interlocking quartz and feldspar.

Lithic-rich ash-flow tuff deposits, resembling those in sections south of the Toodoggone River, occupy the top 75 m of Mount Gordonia, overlying a well-bedded fallout sequence that thins laterally from about 20 m to several metres. The fallout sequence sharply overlies red reworked tuff-breccia or volcanic conglomerate and locally stratigraphically higher, bladed-plagioclase andesite porphyry lava flows at the top of the Junkers unit. The base of the fallout sequence consists of whitish ash tuff, containing quartz and biotite grains. This is overlain by red lapilli-rich beds alternating with crystal-ash tuff. In thin section, a dark red ash-tuff bed that resembles mudstone is noted to consist of cuspate and plate shards, which suggests they originated from a vapour-rich silicic magma that produced juvenile pumiceous fragments. Except for a thin welded zone at the base of the ash-flow tuff section at Mount Gordonia, the bulk of the deposit is nonwelded and contains 40–60% subangular lapilli and a few blocks, as well as rare accidental fragments of the distinctive bladed plagioclase-phyric lavas from immediately beneath the Junkers member.

In general, the Graves member north of the Toodoggone River consists of pyroclastic flows varying in thickness and degree of welding between the scattered depositional sites. Columnar-jointed, densely welded ash-flow tuff deposits east of Mulvaney Creek, and exposures localized adjacent to an east-west fault west of Junkers Creek, represent several of the thickest accumulations, possibly ponded in depressions. It is uncertain whether these thick welded ash-flow tuff deposits represent infilled valleys of an irregular topography or ponded within depressions produced during syn-eruptive subsidence.

PILLAR MEMBER (UNITS TPv, TPs)

The Pillar member forms the top of the Toodoggone Formation south to the Toodoggone River, where it consists of two successive cycles of interstratified lava flows and epiclastic and volcaniclastic rocks (Diakow *et al.*, 2005a, b). The Pillar member north of the Toodoggone River is comparatively thinner with a more limited distribution. The best exposure of the unit is in the upper part of the homocline west of Junkers Creek, where it is approximately 130 m thick and forms a medial volcanic subdivision that separates similar stratified sedimentary sequences (Fig. 3). Thinner (<50 m thick) isolated exposures of the unit cap several ridges east of Mount Gordonia and one ridge northwest of Mount Estabrook. Everywhere, rocks of this unit conformably overlie the upper welded zone of pyroclastic flows that form the Graves member.

Two isolated sections of the lower sedimentary interval, approximately 25–40 m thick, depositionally overlie the Graves unit west of Junkers Creek. The lowest beds consist of maroon-coloured conglomerate up to 5 m thick, consisting mainly of cobble-size porphyritic andesite set in a matrix dominated by plagioclase. The matrix also contains sparse quartz and biotite grains, suggesting local erosion of the underlying Graves member. Red-maroon sandstone, siltstone and minor mudstone dominate the upper part of these sections. The finer clastic beds display internal, faint parallel laminations and textural grading. They have the appearance of minimally reworked airfall crystal-ash tuff deposits, but their primary pyroclastic origin has not been proven.

This lower sedimentary interval is sharply overlain by about 50 m of basaltic andesite lava flows, which pass upward locally into dacitic volcaniclastic rocks (unit TPv). These flows are light grey-green and characteristically oxidized, imparting a reddish maroon colour and hematitic Liesegang bands. Locally, the tops of individual flows are oxidized red and display vesicular texture and amygdules infilled with calcite. Phenocryst mineralogy consists of clinopyroxene (2%) and plagioclase up to 4 mm (25–30%). A monomict breccia that contains block-size fragments of

the underlying lavas encased in a muddy matrix is interpreted as a thin lahar locally overlying the lava flows. Because lava flows in the Pillar member closely resemble the appearance and mineralogy of those found locally near the top of the Junkers member (unit TJv), determining their respective stratigraphic positions is difficult without a reference relative to intervening pyroclastic flows of the Graves member. A 20 m thick dacitic pyroclastic flow, with a base of airfall crystal-ash tuff, locally overlies these lava flows. It contains small amounts of chlorite-altered biotite and quartz phenocrysts.

The volcanic interval passes upsection into an upper sedimentary sequence that, not unlike the lower one previously described, consists mainly of well-bedded brownish maroon sandstone and siltstone with minor interbeds of conglomerate. Siltstone in the section is friable, weathering recessively to angular fragments and displaying rounded, weathered forms. Sandstone commonly contains pyroxene grains and small lithic grains of basaltic lava, both possibly sourced from the underlying lava flows.

BELLE MEMBER (UNIT TB)

The highest subdivision presently recognized in the upper Toodoggone Formation is a rhyolitic ignimbrite occupying the top of the homoclinal succession located west of Junkers Creek and 3.5 km northeast of the more northerly of the Belle lakes (Fig. 1). The ignimbrite occupies a broad downwarp, defined by the shallow concave outline of underlying bedded epiclastic rocks that constitute the upper part of the Pillar member. The Belle ignimbrite covers an area of nearly a square kilometre, maintains a uniform thickness of approximately 125–150 m and dips gently southward. Extrapolating the ignimbrite sheet a short distance farther south, it is truncated by an east-west fault that juxtaposes the youngest strata of the Toodoggone Formation and oldest basement strata of the Asitka Group.

Ash and crystal-bearing tuff deposits containing juvenile bubble-wall shards occur in parallel-layered beds, locally 1 m thick at the base of the ash-flow tuff. These tuffs are interpreted as an airfall that preceded the overlying massive ash-flow tuff. The ash-flow contains mainly lapilli-size fragments and a few blocks, notably abundant aphanitic and laminated reddish and pink rhyolite. Also noted in thin section are juvenile devitrified glass fragments and shards scattered and deformed adjacent to broken crystal grains that include plagioclase, potassium feldspar and rare biotite.

A spectacular columnar-jointed cliff spanning the entire thickness of the ash-flow tuff is prominently displayed at the north-facing side of the deposit. Internally, the columns exhibit weak to moderate welded fabric. The glassy components at the base of the ash-flow tuff display granophyric crystallization, an interlocking mosaic of fine anhedral quartz and feldspar.

EARLY JURASSIC BLACK LAKE INTRUSIONS

Three stock-size intrusions mapped in the study area are assigned to the Black Lake intrusive suite. The McClair and Midas plutons exhibit sharp intrusive contacts with lava flows of the Takla Group. Unlike some mineralized plutons elsewhere in the Toodoggone region, which have attendant gossans in adjacent country rocks, the McClair and Midas plutons lack significant hydrothermal alteration on their margins. The Jack Lee is the largest of the plutons in the study area, covering roughly 30 km^2. In the west, it is extrapolated beneath the drift-covered valley of Jack Lee Creek, its contact coinciding with the trace of the Black fault. Several outliers of Junkers strata rest on the Jack Lee pluton, outboard of an extensively exposed nonconformable contact. Boulder-size clasts of monzodiorite, derived from the Jack Lee pluton, have been found at one locality in polymictic conglomerate deposited directly on the pluton.

The Jack Lee pluton consists mainly of medium-grained, inequigranular monzodiorite composed of plagioclase phenocrysts up to 4 mm set in a finer grained mosaic of anhedral potassium feldspar and quartz. Quartz constitutes up to 5% of plutonic specimens, and mafic minerals (hornblende, biotite and pyroxene, in decreasing relative abundance) make up 5–7%. Fresh exposures typically display a greenish coloration due to moderate to pervasive chlorite and epidote alteration of feldspars and mafic minerals, and coatings on joint and fracture surfaces. Locally intense oxidation of the pluton is imparted by hematite. Mineralogically this pluton resembles the Jock Creek pluton, a *ca.* 197 Ma monzonitic body mapped south of the Toodoggone River, where it is spatially and possibly genetically associated with important porphyry-style exploration targets at Sofia and Alexandra (Diakow *et al.*, 2005a). The Jack Lee pluton was sampled to determine a U-Pb crystallization age.

The McClair pluton, exposed in the southwest corner of the map area, intrudes mafic rocks of the Takla Group and, in the northeast, a steep fault places the intrusion against stratigraphy from the upper Toodoggone Formation. It is draped by a thin succession of pyroxene-phyric andesitic lava flows tentatively assigned to the Junkers member. Conglomeratic lenses that contain clasts derived from the underlying intrusion are found locally at the base of this flow unit, resting nonconformably on the McClair pluton. The McClair pluton is offset by the Toodoggone fault and, farther south, is bounded by the Pillar fault in the vicinity of the Pil North Au-Cu porphyry prospect. The intrusion contains xenoliths of fine-grained diorite, and aphanitic volcanic rocks presumably derived from the Takla Group.

The McClair pluton is composed of a pink hornblende-quartz monzonite with a medium to coarse-grained, equigranular texture. Subhedral and euhedral plagioclase phenocrysts up to 6 mm are variably replaced by sericite and calcite. Potassium feldspars occur both as phenocrysts and in an interlocking mosaic containing upwards of 15% quartz. Hornblende is the principal mafic mineral. Green unaltered prisms up to 8 mm may form 15% of the rock. Accessory titanite is visible in thin section.

Exposures of the Midas pluton cover 6 km^2, extending east from the valley bottom at Midas Lake into blocky-jointed, craggy ridges north of Contact Peak. The sharp intrusive contact dips steeply, with negligible contact metamorphism displayed in adjacent volcanic country rocks of the Takla Group. However, irregularly shaped exoskarns develop where the intrusion crosscuts nearby carbonate rocks of the Asitka Group.

The Midas pluton is mainly granite. A diorite phase is locally confined to the pluton margin and, nearby, also forms a plug-like apophysis that pierces the Asitka Group. The felsic main phase is light pink, medium grained, equigranular and composed roughly of subequal amounts

of plagioclase and potassium feldspar, and 15% quartz. Weakly chlorite-altered hornblende (5%) and subordinate biotite are ubiquitous. The mafic border phase consists of a fine-grained, biotite-bearing diorite that locally contains disseminated pyrite.

Plutons with a bulk composition of granite are unusual in the Black Lake suite, as most are in the compositional range of quartz monzonite and monzonite. The exception is the Fredrikson pluton, a large monzogranite stock with a minor quartz monzodiorite phase, located southeast of the Kemess minesite (Diakow and Rogers, 1998). This is one of the youngest isotopically dated plutons in the Toodoggone region, yielding a U-Pb zircon crystallization age of 191.0 ±0.4 Ma. The authors speculate that the Midas pluton, also sampled for U-Pb geochronology, might yield an equivalent age. Furthermore, it might be comagmatic with nearby rhyolite pyroclastic flows that form the Belle member and represent the youngest extrusive event in the Toodoggone Formation.

Dikes and a few sills occur throughout the map area, crosscutting larger plutons and all stratigraphic units. However, none has been observed in the youngest Belle member. Dike orientations generally correspond to the regional north-northwest structural fabric defined by major faults. They typically range from 0.5 to 2 m in width, although there are a number that are tens of metres wide. The dikes can be associated with chalcopyrite-pyrite-bearing quartz veins and brecciated veins along their margins.

A variety of dikes with differing compositions and textures has been recognized but not systematically classified or studied in detail. In general, the most common dikes consist of pink-orange, sparsely plagioclase porphyritic monzonite to porphyritic quartz monzonite. Most contain chlorite-altered biotite and hornblende, and negligible quartz phenocrysts. Other common varieties include aphanitic or fine-grained basaltic dikes, quartz-biotite-phyric rhyolite and flow-laminated rhyolite dikes. A dark grey-green dioritic variety, containing plagioclase and pyroxene, forms a major sill and dikes crosscutting the Pillar member northeast of Midas Lake. These may be feeders to basaltic flows within the unit.

STRUCTURE

Layered stratigraphy and major plutons throughout the map area are disrupted by a complex pattern of high-angle fault structures trending generally north-northwest and east-northeast. Major northerly-trending faults, including the Black, Pillar and Midas faults, have inferred traces through broad drift-filled valleys occupied by Jack Lee Creek, Mulvaney and Junkers creeks, and McClair and Midas creeks, respectively.

The presence of the Midas fault is speculative, based on a pronounced negative magnetic discontinuity corresponding to a prominent valley bordering the study area in the west (Shives *et al.*, 2004). The Black fault delineates the western margin of the Jack Lee pluton, placing it against monotonous mafic volcanic rocks of the Takla Group. The extension of this structure farther south between the Toodoggone and Finlay rivers displaces the Graves and overlying Pillar members.

The Pillar fault is a regional-scale feature extending south from Chukachida Lake for approximately 70 km to the southern limit of the Toodoggone volcanic belt, mapped near the Kemess mine. In the northern part of the study area, the fault follows Junkers Creek, separating gently northeast-inclined Junkers strata in the east from equivalent and younger overlying Toodoggone strata that form a south-inclined homocline in the west. Immediately south of the Toodoggone River, this fault defines a significant break separating generally west-inclined volcaniclastic and epiclastic strata of the upper Toodoggone succession in the east from older volcanic units that make up the lower Toodoggone Formation in the west. Several outliers of upper Toodoggone strata overlie lower Toodoggone strata west of the Pillar fault. It is believed that the Pillar fault was active throughout deposition of much of the upper Toodoggone Formation, confining the dominantly pyroclastic flow, volcaniclastic-epiclastic succession within a series of fault-controlled half grabens that incrementally step up east of the Pillar fault.

Generally easterly-trending faults in the study area form comparatively shorter segments truncated by the northerly-trending faults. Several significant east-west structures emphasize their underlying importance, influencing the distribution and local variation in thickness of ash-flow tuff deposits. For example, a segment of the Toodoggone fault mapped south and west of the study area is believed to define the northern structural margin of an asymmetric volcanic subsidence feature in which more than 250 m of moderately to densely welded ash-flow tuff deposits of the Saunders member ponded *ca.* 194 Ma. A similar scenario of synvolcanic faulting is envisaged farther north within the study area, in regions where thick sequences of columnar-jointed, welded ash-flow tuff deposits are localized adjacent to several well-defined east-trending faults. For example, an east-west fault near Junkers Creek places Permian sedimentary rocks of the Asitka Group against a stratified, south-inclined volcanosedimentary succession representing much of the upper Toodoggone Formation. This relationship suggests significant north-side-down displacement. Within the downdropped block, moving north away from this fault, the thickness of successive columnar-jointed, welded ash-flow tuff sequences of the Belle and Graves members and intervening Pillar lava flow–sedimentary sequence rapidly diminish, inferring half-graben or asymmetric subsidence (Fig. 3). Another parallel structure immediately north of Mount Gordonia apparently extends east to the Pillar fault, where a similarly oriented fault segment continues and is truncated farther east by the Black fault. The north side of these east-west structures is downdropped relative to uplifted Triassic basement strata widely exposed on the south side. Within the downdropped blocks, shallowly inclined strata of the Junkers member are overlain by pyroclastic flows of the Graves member. They form spectacular columnar-jointed cliffs representing the upper welded zone. The proximity of thick, welded pyroclastic flows adjacent to these east-west faults suggests ponding in fault-controlled depressions, as opposed to paleovalley depressions.

MINERAL PROSPECTS

The study area has 17 mineral occurrences described in MINFILE (2005) and a number of new mineral prospects. These prospects consist primarily of sulphide minerals in quartz veins and isolated skarns.

Quartz veins and vein breccia prospects are commonly localized along north and northwest-trending faults. These

faults also provide a locus for a variety of dikes, which share sharp contacts with adjacent quartz breccia and veins. Solitary veins typically vary from 10 to 50 cm in width. In broader fault zones, a series of narrow subparallel veins and veinlets occupy the zone. The veins generally consist of white, translucent crystalline quartz that sometimes displays diffuse banding and comb texture. Sulphide disseminations and less common massive crystalline concentrations include mainly pyrite, accompanied by generally small amounts of chalcopyrite, malachite, galena, sphalerite and pyrrhotite.

The tell-tale rusty gossanous surface expression prevalent adjacent to many porphyry occurrences south of the Toodoggone River is generally absent in the study area. This suggests the tract of mineralized monzonitic plutons might not extend beneath volcanic successions that underlie most of the study area. The Jack Lee and McClair plutons are biotite-hornblende-bearing intrusions more typical of large, sparsely mineralized plutons that constitute the Black Lake intrusive suite. These plutons generally contain only minor disseminated chalcopyrite and pyrite in quartz veinlets occupying fractures. The Midas pluton exhibits a sharp intrusive contact with either mafic flows of the Takla Group or limestone of the Asitka Group. This contact is weakly mineralized with malachite, which coats fractures in adjacent mafic country rocks. This feature is not necessarily unique to the contact zone of this intrusion, since malachite commonly coats fractures throughout the Takla volcanic succession.

Skarn mineralization occurs within limestone adjacent to a granite stock east of Midas Lake. Boulders, 40 cm in diameter and located in talus sourced from a rusty zone adjacent to a dioritic plug piercing limestone, consist of diopside-garnet-magnetite and rusty massive sulphide minerals. The sulphide boulders are composed of pyrrhotite, chalcopyrite, bornite and pyrite.

CONCLUSIONS

- The distribution of the Early Jurassic Toodoggone Formation extends into a previously little known region north of the Toodoggone River, where strata mainly representing the upper part of the formation unconformably overlie the Late Triassic Takla Group. Stratigraphy of the lower Toodoggone Formation is absent throughout most of the area. However, locally it consists of relatively thin volcaniclastic deposits that, in one locality, overlie a basal polymictic conglomerate containing clasts derived from older basement successions of the Takla and Asitka groups.
- The description of the upper Toodoggone Formation is revised from that in Diakow *et al.* (2005a) and is currently subdivided into four informal members. The lowest Junkers member replaces the earlier named Quartz Lake member. Conglomeratic and finer clastic beds containing fine porphyritic basalt clasts and pyroxene grains, and local volumetrically minor basalt and rhyodacite lava flows characterize crude, thick-bedded sections typical of the Junkers member. The overlying Graves member is composed of quartz-biotite-bearing dacitic ash-flow tuff deposits locally associated with rhyolitic flow and fallout facies. The Pillar member is a well-bedded, oxidized sequence dominated by clastic rocks that interfinger locally prominent basaltic flows and lesser dacitic volcaniclastic rocks. The newly recognized Belle member is composed of rhyolite ash-flow tuff that forms a columnar-jointed sheet in one locality at the top of Toodoggone stratigraphy.
- North-northwest-trending extensional faults extend from the south into the study area. These and smaller scale parallel features impart control regionally on intrusions and localize epithermal vein deposits in the Toodoggone Formation. East-west faults are thought to predate these northerly faults in the study area. These faults apparently demarcate the high wall of several half grabens in which ash-flow tuff deposits ponded and subsequently cooled, forming thick, welded, columnar-jointed exposures.
- The most common mineral prospects in the study area are pyrite-chalcopyrite±galena±pyrrhotite-bearing epithermal quartz veins and vein breccias. The veins are localized in northerly-trending faults and along dikes that crosscut strata of the upper Toodoggone Formation. Skarn is developed in Asitka limestone where it is intruded by an Early Jurassic granitoid.

ACKNOWLEDGMENTS

We thank Stealth Minerals Limited for their continued and significant financial and logistical support that enabled the mapping program to expand into more remote terrain of the Toodoggone region. We are grateful to the company for providing staff to assist in mapping, maintaining helicopter support and welcoming us in their base camp on the Finlay River. Stealth geologist April Barrios is gratefully acknowledged for her contributions and capable assistance during two weeks with the mapping team. Geological discussion with Dave Kuran, Paul Durring and Steve Rowins were always informative and appreciated. We also thank Northgate Minerals Corporation, particularly Carl Edmunds and Ron Konst at the Kemess mine, for geological discussions and their logistical support on our numerous trips to the minesite. Brian Grant is thanked for his editorial comments.

REFERENCES

Diakow, L.J., Nixon, G., Lane, B. and Rhodes, R. (2005a): Toodoggone Geoscience Partnership: preliminary bedrock mapping results from the Swannell Range: Finlay River – Toodoggone River area (NTS 94E/2 and 7), north-central British Columbia; *in* Geological Fieldwork 2004, *British Columbia Ministry of Energy, Mines and Petroleum Resources*, Paper 2005-1, pages 93–107.

Diakow, L.J., Nixon, G.T., Rhodes, R. and Lane, B. (2005b): Geology between the Finlay and Toodoggone rivers, Toodoggone River map area, north-central British Columbia (parts of NTS 94E/2,6 and 7); *British Columbia Ministry of Energy, Mines and Petroleum Resources*, Open File Map 2005-3.

Diakow, L.J and Rogers, C. (1998): Toodoggone-McConnell Project: geology of the McConnell Range — Serrated Peak to Jensen Creek, parts of NTS 94E/2 and 94D/15; *in* Geological Fieldwork 1997, *British Columbia Ministry of Energy, Mines and Petroleum Resources*, Paper 1998-1, p 8a-1–8a-13.

Diakow, L.J. and Shives, R.B.K. (2004): Geoscience partnerships in the Toodoggone River and McConnell Creek map areas, north-central British Columbia; *in* Geological Fieldwork 2003, *British Columbia Ministry of Energy, Mines and Petroleum Resources*, Paper 2004-1, p 27–32.

Gabrielse, H., Dodds, C.J., Mansy, J.L. and Eisbacher, G.H. (1977): Geology of Toodoggone River (94E) and Ware west-half (94F); *Geological Survey of Canada*, Open File 483.

MINFILE (2005): MINFILE BC mineral deposits database; *BC Ministry of Energy, Mines and Petroleum Resources*, URL <http://www.em.gov.bc.ca/Mining/Geolsurv/Minfile/> [Nov 18, 2005].

Shives, R.B.K., Carson, J.M., Dumont, R., Ford, K.L., Holman, P.B. and Diakow, L. (2004): Helicopter-borne gamma-ray spectrometric and magnetic total field geophysical survey (parts of NTS 94D/15, E/2,3,6,7,10,11); *Geological Survey of Canada*, Open File 4614.

Picritic Lavas and Basal Sills in the Karmutsen Flood Basalt Province, Wrangellia, Northern Vancouver Island, British Columbia

By Andrew R. Greene[1], James S. Scoates[1], Graham T. Nixon and Dominique Weis[1]

KEYWORDS: Wrangellia, Vancouver Island, large igneous province, oceanic plateau, flood basalt, picrite

INTRODUCTION

This paper presents the first evidence of high-MgO picritic lavas, herein named the Keogh Lake picrite, within the Triassic Karmutsen flood basalt province of Wrangellia on Vancouver Island. Previously published work has revealed MgO contents up to approximately 12 wt%, compared to the high-MgO contents (13–20 wt%) for mafic pillow basalt reported here. The recognition of picritic volcanism within the Middle Triassic Karmutsen Formation on northern Vancouver Island is strong evidence that the flood basalts originated from initiation of a mantle plume. The presence of the picrite also has important implications for mineral exploration, as there may well be a higher potential for magmatic Ni-Cu-platinum-group-element (PGE) mineralization in this part of Wrangellia. Accordingly, a preliminary examination was made of part of the sediment-sill complex at the base of the Karmutsen near Schoen Lake Provincial Park. The field studies conducted in these two separate areas increase understanding of the architecture and development of a large oceanic plateau. This contribution is a review of several significant geological features of an accreted oceanic plateau based on these new data.

WRANGELLIA: AN ACCRETED OCEANIC PLATEAU

The Triassic Karmutsen Formation on Vancouver Island is an extensive flood basalt province that is perhaps the thickest accreted section of an oceanic plateau worldwide. An ongoing study involves using this accreted oceanic plateau, which forms most of the Wrangellia Terrane, to address several major questions about the phenomena of oceanic plateaus and large igneous provinces (LIPs) in general. A great deal of research over the past several decades has focused on LIPs, which are defined as large-scale, transitory emplacements of predominantly mafic extrusive and intrusive rocks (Coffin and Eldholm, 1994). Most researchers believe that these vast volcanic fields originate by decompression melting in the head of a mantle plume (Condie, 2001). If mantle plumes rise beneath the continents, they form continental flood basalts, such as the Siberian Traps or Columbia River Basalts; if they rise beneath oceanic crust, they form oceanic plateaus, such as Kerguelen, Ontong Java and the Caribbean Plateau. These enormous magmatic events occur over geologically short time spans (several million years) and likely have catastrophic effects on the climate and biosphere (Wignall, 2001).

Continental flood basalts are more extensively studied than its oceanic counterpart because it is much more easily accessible. One of the major issues when studying oceanic plateaus in the ocean basins is the difficulty of sampling their interior, since only the uppermost flood basalts can be sampled by drilling. For example, although several small sections of the Ontong Java Plateau are exposed on land in the Solomon Islands, drilling of the oceanic plateau, which is estimated to be as much as 35 km thick, has only penetrated 338 m of the uppermost flows (Fitton *et al.*, 2004). In contrast, Wrangellia presents a thickness of more than 6 km of flood basalts on Vancouver Island and upwards of 4 km in large areas of Alaska (Wrangell Mountains and Alaska Range), allowing the opportunity to sample the complete succession of erupted flood basalts.

The Wrangellia oceanic plateau formed by vast outpourings of basaltic and Mg-rich picritic magmas (documented here) that appear to have been emplaced within several million years (*ca.* 230 Ma), and eventually became accreted to the western margin of North America (Richards *et al.*, 1991; Lassiter *et al.*, 1995). Currently, there is a lack of detailed information about the volcanic stratigraphy of oceanic plateaus. The Karmutsen offers an invaluable opportunity to explore the remnants of an oceanic plateau and thus gain an understanding of the internal volcanic stratigraphy. A better understanding of oceanic plateaus will provide insights into several important processes, including the generation of magmas in mantle plumes (White and McKenzie, 1995), the role of accretion of oceanic plateaus for the growth of continental crust (Albarède, 1998) and the climatic effects of such large-scale eruptions (Wignall, 2001).

This contribution is an initial step toward addressing three important aspects of flood basalt volcanism in oceanic settings: 1) the architecture of oceanic plateaus, 2) the source of basaltic magmas, and 3) the potential for magmatic Ni-Cu-PGE mineralization.

GEOLOGICAL HISTORY OF THE WRANGELLIA TERRANE

The Wrangellia Terrane consists of several distinct allochthonous blocks, extending from Vancouver Island to

[1]*Pacific Centre for Isotopic and Geochemical Research, Department of Earth and Ocean Sciences, University of British Columbia, Vancouver, BC*

This publication is also available, free of charge, as colour digital files in Adobe Acrobat PDF format from the BC Ministry of Energy, Mines and Petroleum Resources internet website at http://www.em.gov.bc.ca/Mining/Geolsurv/Publications/catalog/catfldwk.htm

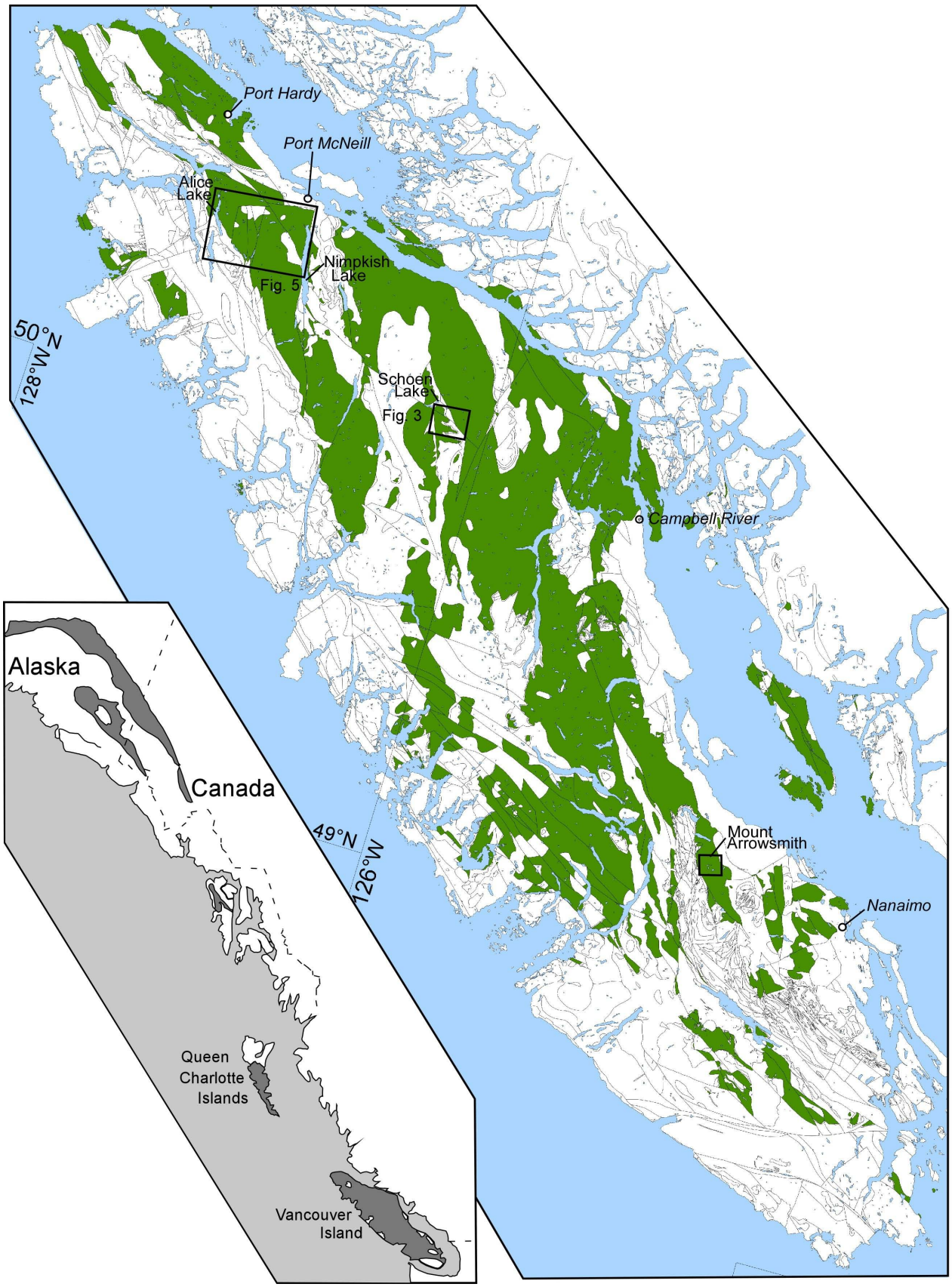


Figure 1. Simplified map of Vancouver Island showing exposures of flood basalts (green) of the Karmutsen Formation (after Massey *et al.*, 2003a, b). Areas of field study are outlined with solid boxes. Inset shows the extent of the Wrangellia Terrane (dark grey) in western Canada and Alaska (modified after Jones *et al.*, 1977).

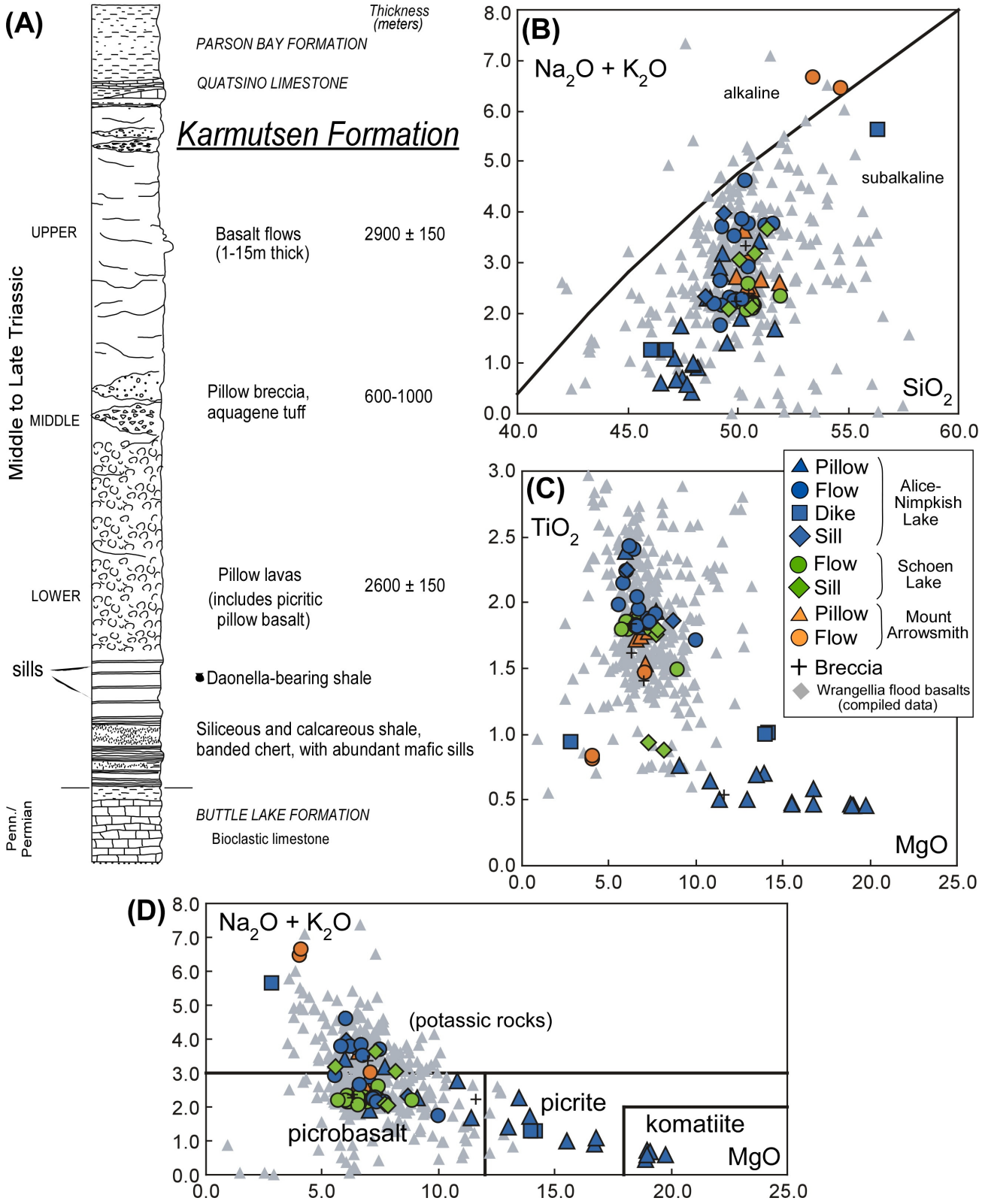
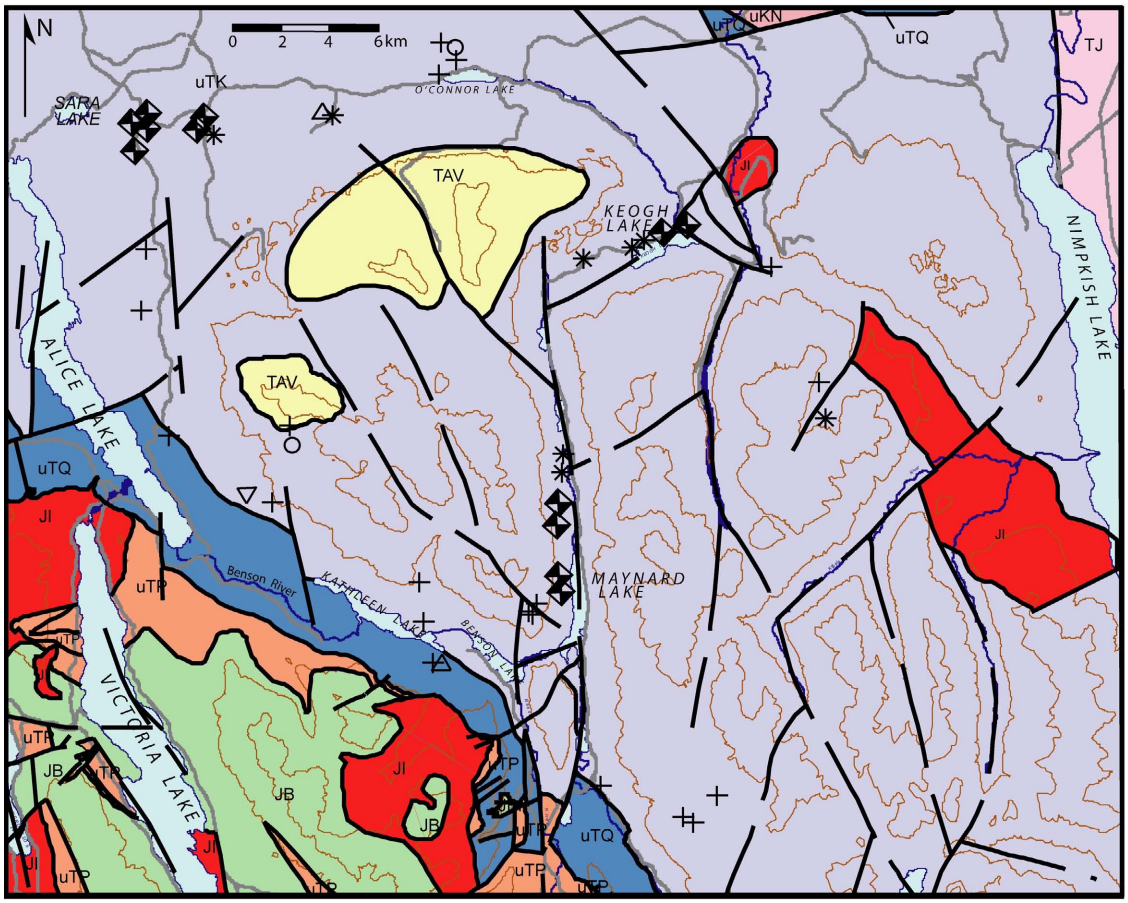


Figure 2. A) Composite stratigraphic column depicting flood basalt sequences of the Karmutsen Formation and major underlying and overlying sedimentary sequences on northern Vancouver Island (modified after Carlisle and Susuki, 1974). B) Total alkalis vs. silica diagram (wt%) for Keogh Lake picrite and other samples collected in 2004 and 2005, along with compiled data from published literature for the Karmutsen Formation and correlative Nikolai Formation. The vast majority of volcanic rocks is subalkaline basalt. Note that the Mount Arrowsmith flows are mildly alkalic. The boundary of the alkaline and subalkaline fields is that of Irvine and Baragar (1971). C) TiO_2 vs. MgO plot (wt%) for the samples shown in B. D) Plot of total alkalis vs. MgO (wt%), showing the IUGS classification fields (Le Bas, 2000). Note the Mg-rich nature of the Keogh Lake picrite. Oxides are plotted on an anhydrous, normalized basis in all diagrams.

central Alaska, that are related by widespread exposures of Triassic flood basalts and rarely their plutonic complements (Fig. 1; Jones *et al.*, 1977). Impressive successions of Middle Triassic flood basalts extend in a discontinuous belt from Vancouver Island and the Queen Charlotte Islands (Karmutsen Formation), through southeastern Alaska and the Kluane Ranges in southwest Yukon, and into the Wrangell Mountains and Alaska Range in eastern and central Alaska (Nikolai Formation). This belt of flood basalt sequences has distinct similarities and, as first suggested by Jones and et al. (1977), represents a once-contiguous terrane that probably formed within 15° of the paleoequator (Hillhouse, 1977).

Wrangellia developed as an extensive oceanic terrane with a geological history that extends from the middle Paleozoic through the Mesozoic (Richards *et al.*, 1991). The



Tertiary

TAV — Alert Bay Volcanics

Upper Cretaceous

uKN — Nanaimo Group Equivalents

Upper Triassic to Middle Jurassic

JB — Bonanza Group: Volcanics and Sediments

uTP — Parson Bay Formation

TJ — Undivided Parson Bay Formation and Bonanza Sediments

Upper Triassic

uTQ — Quatsino Formation

uTK — Karmutsen Formation

Early to Middle Jurassic

JI — Island Plutonic Suite

gabbro
massive lava
mafic dike
pillow lava
pillow lava - picrite
diabase

fault

road

Figure 3. Generalized geology of the region between Alice and Nimpkish Lakes, northern Vancouver Island (location shown in Fig. 1). Sample sites and rock types are denoted in the legend. Contour lines are at 500 m intervals.

flood basalts form the core of the terrane and is bounded above and below by marine sedimentary sequences. Continentally derived sedimentary rocks are almost entirely absent, with the exception of a kilometre-thick continental-margin sedimentary sequence at the base of flood basalts in the Talkeetna Mountains of Alaska (Schmidt *et al.*, 2003). The Wrangellia Terrane preserves two broad cycles of uplift and subsidence, beginning with a Paleozoic volcanic arc and succeeded by Middle Triassic volcanism (Ben-Avraham *et al.*, 1981). Triassic uplift and subsidence are recorded by chert, minor limestone and *Daonella*-bearing shale at the base of the flood basalts, and a limestone sequence above the flood basalts. These events are consistent with the rise and cessation of a mantle plume beneath the lithosphere (Richards *et al.*, 1991). Sedimentation and volcanism in the Wrangellia Terrane continued through the Early and Middle Jurassic with the resurgence of arc volcanism in the form of the Bonanza arc (Jeletzky, 1970; Northcote and Muller, 1972; DeBari *et al.*, 1999)

The Karmutsen Formation appears to represent a single flood basalt event (Richards *et al.*, 1989). A mantle plume initiation model has been proposed for the Wrangellia flood basalts based on 1) the nature of the underlying and overlying sedimentary rocks, 2) rapid uplift prior to volcanism, 3) the lack of evidence of rifting associated with volcanism (few dikes and abundant sills), 4) the short duration and high eruption rate of volcanism, and 5) relatively limited geochemical data (Richards *et al.*, 1991). The basalt flows are estimated to constitute a minimum volume of 1 x 10^6 km^3 (Panuska, 1990) and were originally interpreted to have erupted within 5 m.y. (Carlisle and Suzuki, 1974).

The timing and location of the accretion of Wrangellia to western North American and postaccretionary translation are highly debated (Trop *et al.*, 2002). Estimates of the timing of initial collision range from the Middle Jurassic to Late Cretaceous (*e.g.*, Tipper, 1984; Plafker *et al.*, 1989; Gehrels and Greig, 1991; McClelland *et al.*, 1992; van der Heyden, 1992; Monger *et al.*, 1982; Nokleberg *et al.*, 1994, 2000; Trop *et al.*, 2002). Paleomagnetic and faunal evidence indicate that the Wrangellia Terrane originated at low latitude, far to the south of its present position (Hillhouse,

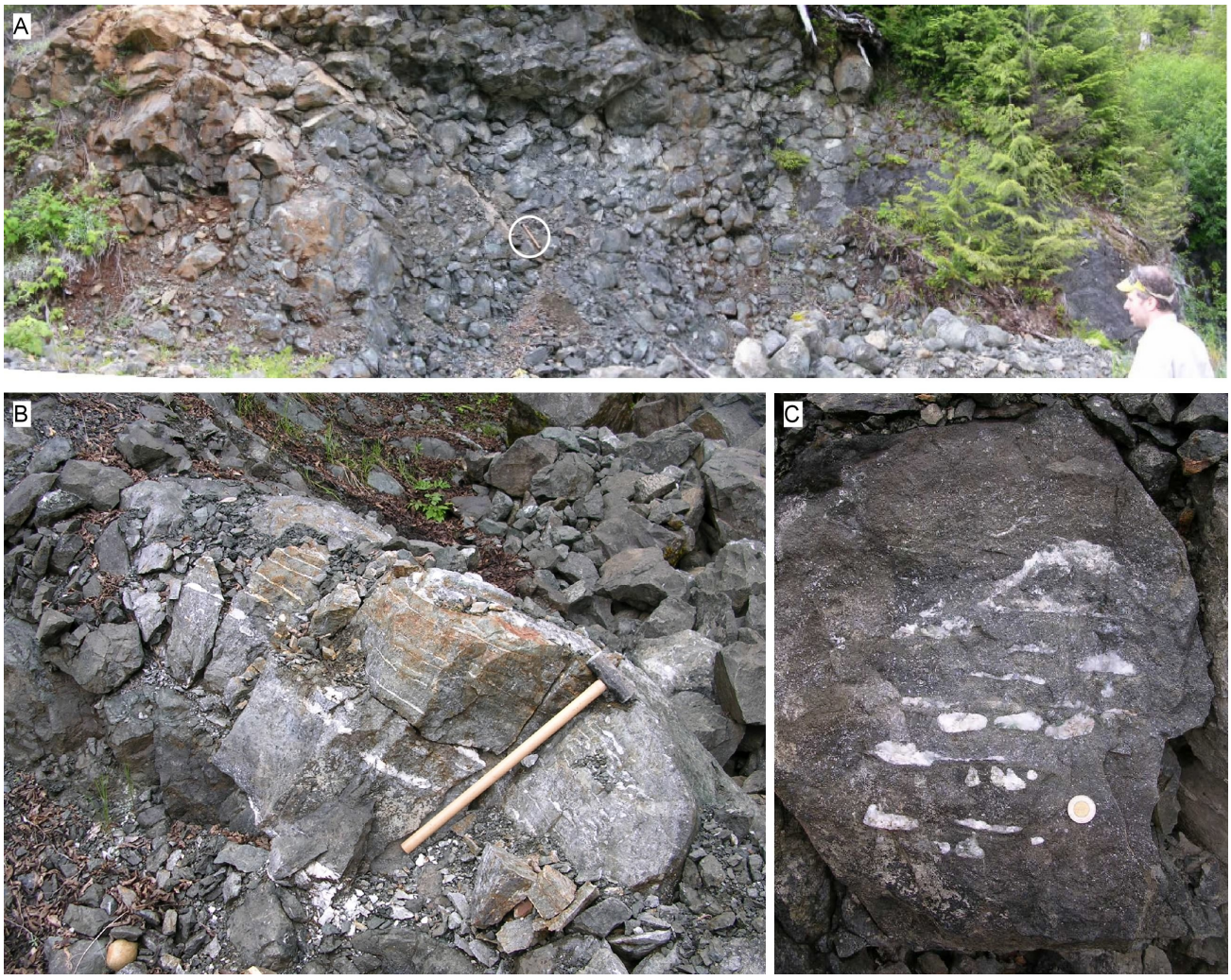


Figure 4. Photographs of picritic pillow basalt from the Alice-Nimpkish lakes area: A) stack of dense, closely packed, asymmetric picritic pillows with radial vesicle infillings (sledgehammer for scale [circled] ~80 cm long; UTM Zone 11, 626824E, 5586126N); B) cross-section of a large pillow lobe with infilling of quartz in tension cracks (sledgehammer for scale; UTM Zone 11, 616507E, 5598448N). C) drain-back ledges formed in a picritic pillow tube formed after lava drained from the pillow (shown by quartz infilling; coin for scale ~2.7 cm diameter; same location as B).

1977; Yole and Irving, 1980; Hillhouse *et al.*, 1982; Hillhouse and Gromme, 1984). Wrangellia may have joined or been in close proximity (stratigraphic continuity) with the Alexander Terrane by the Middle Pennsylvanian (Yorath *et al.*, 1985; Gardner *et al.*, 1988). As early as the Late Triassic, the oceanic Wrangellia Terrane amalgamated with the Taku Terrane of southeastern Alaska and the Peninsular Terrane of southern Alaska (Plafker *et al.*, 1989).

GEOLOGICAL SETTING OF THE KARMUTSEN VOLCANIC ROCKS

Approximately 35% of the area of northern and central Vancouver Island is directly underlain by the distinctive flood basalt sequences of the Karmutsen Formation (Fig. 1; Barker *et al.*, 1989). On Vancouver Island, the oldest rocks of Wrangellia are the Devonian arc sequences of the Sicker Group and Mississippian to Early Permian siliciclastic and carbonate rocks of the Buttle Lake Group (Muller, 1980; Brandon *et al.*, 1986; Sutherland Brown *et al.*, 1986). The Sicker and Buttle Lake groups and the Karmutsen Formation are intruded by gabbro and basaltic sills that are most likely related to Karmutsen flood basalts (Carlisle and Suzuki, 1974; Barker *et al.*, 1989). The uppermost part of the Karmutsen Formation is locally intercalated with small lenses of marine sedimentary rocks and overlain by the shallow-water Quatsino Limestone (Carlisle and Suzuki, 1974).

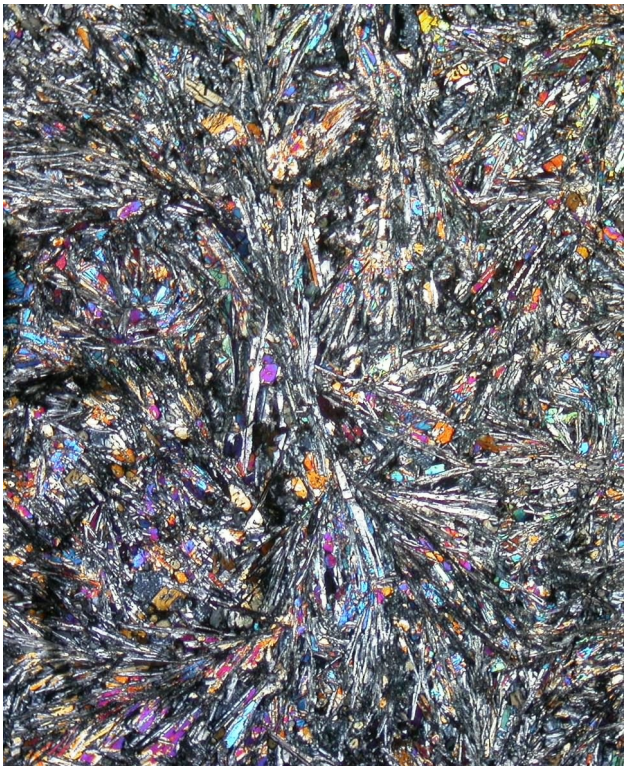


Figure 5. Photomicrograph under cross-polarized light (~10 mm high) of picrobasalt from just west of Maynard Lake (UTM Zone 11, 626698E, 5588266N). This sample shows the striking variolitic texture with wavy, branching sheaves of intergrown plagioclase and clinopyroxene that is typical of the picritic pillows (sample 4723A2; 10.8 wt% $MgO_{anhydrous}$).

The earliest in-depth studies of the Karmutsen Formation on Vancouver Island were made by H.C. Gunning (Gunning, 1930, 1932), J.A. Jeletzky (*e.g.*, Jeletzky, 1950, 1970), J.E. Muller and coworkers (Muller, 1967, 1977, 1981; Muller and Carson, 1969; Muller *et al.*, 1974, 1981) and D. Carlisle and students (Carlisle, 1963, 1972; Surdam, 1968; Kuniyoshi, 1972; Carlisle and Suzuki, 1974). This extensive work established the location, characteristics and depositional history of the Wrangellia Terrane on Vancouver Island. More recent descriptions of Karmutsen basalts were incorporated during regional mapping studies (1:50 000 scale) conducted by G.T. Nixon and coworkers (Nixon *et al.*, 1993, 1994a, b) on northern Vancouver Island and N.W.D. Massey and coworkers (Massey and Friday, 1988, 1989; Massey, 1995a, b, c) on central Vancouver Island.

The Karmutsen volcanic rocks represent perhaps the thickest accreted section of an oceanic plateau worldwide, along with the 3–4 km thick section of Ontong Java exposed in the Solomon Islands (Petterson *et al.*, 1997) and a 5 km thick section of the Caribbean Plateau on the island of Curacao, north of Venezuela (Klaver, 1987).

Within the densely forested regions of northern and central Vancouver Island, the volcanic stratigraphy of the Karmutsen Formation is estimated to exceed 6 km in thickness (Carlisle and Suzuki, 1974). Extensive faulting throughout this region makes reconstruction of the true stratigraphic thickness challenging. Nevertheless, the diagnostic units of the Karmutsen have been divided by Carlisle and Suzuki (1974) into 1) a lower member of exclusively pillow lava (2900 ±150 m), 2) a middle member of pillow breccia and aquagene tuff (600–1100 m), and 3) an upper member of massive basalt flows (2600 ±150 m; Fig. 2).

The Karmutsen volcanic rocks were emplaced in a predominantly submarine environment. Impressive successions of submarine pillow basalt at the base of the Karmutsen Formation overlie a thick sediment-sill unit comprising mafic sills intruding black shale of the Middle Triassic '*Daonella* beds'. Dense, picritic pillow lavas (described below) have been identified within the succession



Figure 6. Photomicrograph under cross-polarized light (~10 mm across) of a picrite pillow from the roadcut along the north side of Keogh Lake (UTM Zone 11, 629490E, 5595528N). This sample has abundant altered euhedral olivine phenocrysts up to several millimetres long (sample 4722A4; 19.0–19.8 wt% $MgO_{anhydrous}$, 4 analyses).

of pillow basalt. Massive amygdaloidal flows form most of the middle and upper crust of the Wrangellia plateau, interspersed with minor pillow-breccia units. Intravolcanic sedimentary rocks within the volcanic rocks of the uppermost Karmutsen are well-documented by Carlisle and Suzuki (1974).

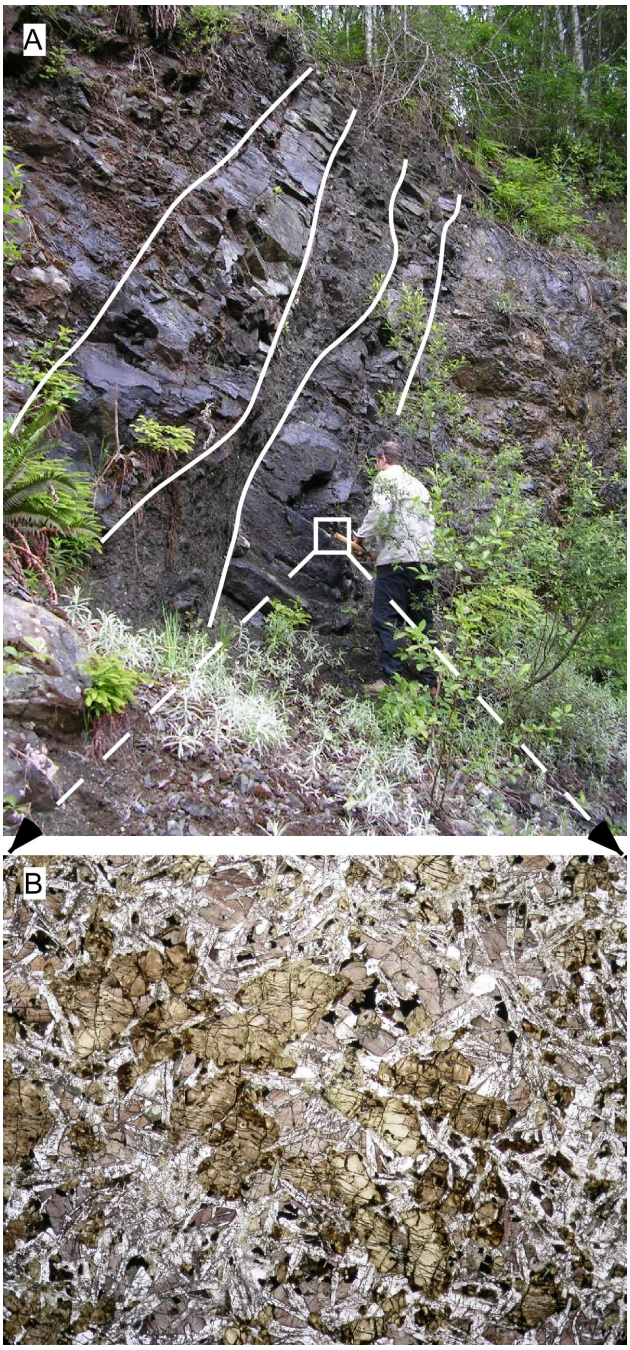


Figure 7. Olivine-rich dike cutting tholeiitic pillow basalt (UTM Zone 11, 620187E, 5599424N): A) photograph of subvertical mafic dikes approximately 1 m wide; B) photomicrograph under plane-polarized light (~10 mm across) of subophitic mafic dike from A with abundant, large, altered olivine crystals and altered plagioclase surrounded by clinopyroxene (sample 5615A2; 14.0–14.2 wt% $MgO_{anhydrous}$, 2 analyses).

AGE OF THE KARMUTSEN FORMATION AND CORRELATIVE FLOOD BASALTS

Despite its enormous size, there are relatively few precise geochronological constraints on the age and duration of Wrangellia flood basalt volcanism. Constraints on the age and duration of Karmutsen volcanism include fossils in the underlying and overlying sedimentary units and several isotopic age determinations. *Daonella*-bearing shale, 100–200 m below the base of the pillow basalt on Schoen Mountain, and *Halobia*-rich shale, interlayered with flows in the upper part of the Karmutsen, indicate that eruption of the flood basalts possibly occurred entirely within the early Upper Ladinian (Middle Triassic) to early Upper Carnian (Late Triassic; Carlisle and Suzuki, 1974). Uranium-lead zircon geochronology of several sills and dikes potentially related to the Karmutsen yields ages of 217–222 Ma (Isachsen *et al.*, 1985), 227 ±3 Ma (Parrish and McNicoll, 1992) and 228 ±2.5 Ma (Sluggett, 2003). Plutonic rocks related to the correlative Nikolai Formation in Yukon yielded K-Ar ages of 224 ±16 and 225 ±14 Ma (Campbell, 1981). A U-Pb zircon age from a gabbro sill considered to be con-

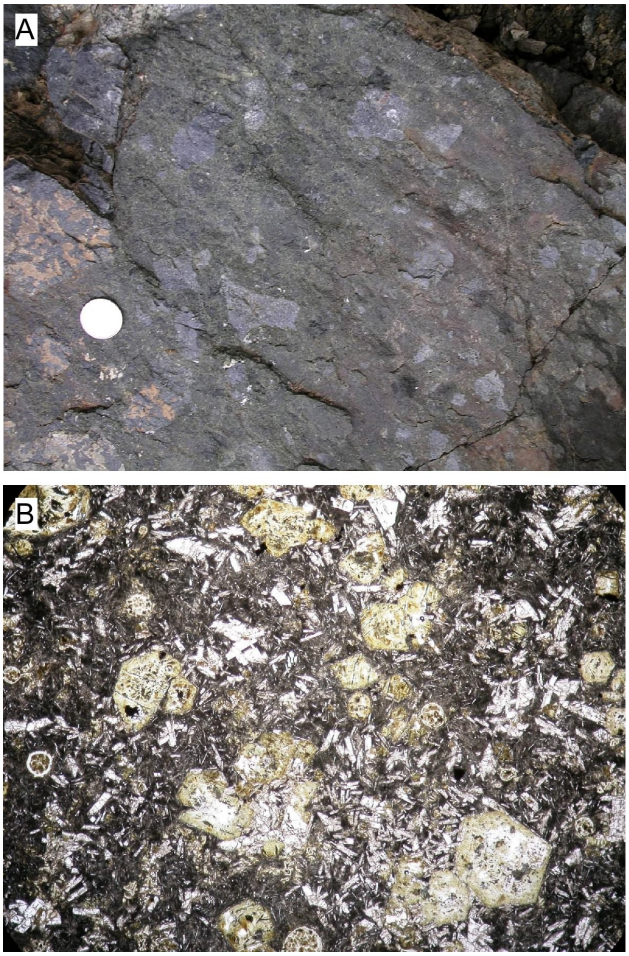


Figure 8. A) Photograph of pillow breccia with angular, blocky clasts in a fine-grained tuffaceous matrix east of Alice Lake (UTM Zone 11, 614756E, 5599192N; coin for scale ~2.7 cm in diameter). B) Photomicrograph under plane-polarized light (~10 mm across) showing altered euhedral olivine in seriate-textured basalt clasts within the pillow breccia from A (sample 5614A5; 11.6 wt% $MgO_{anhydrous}$).

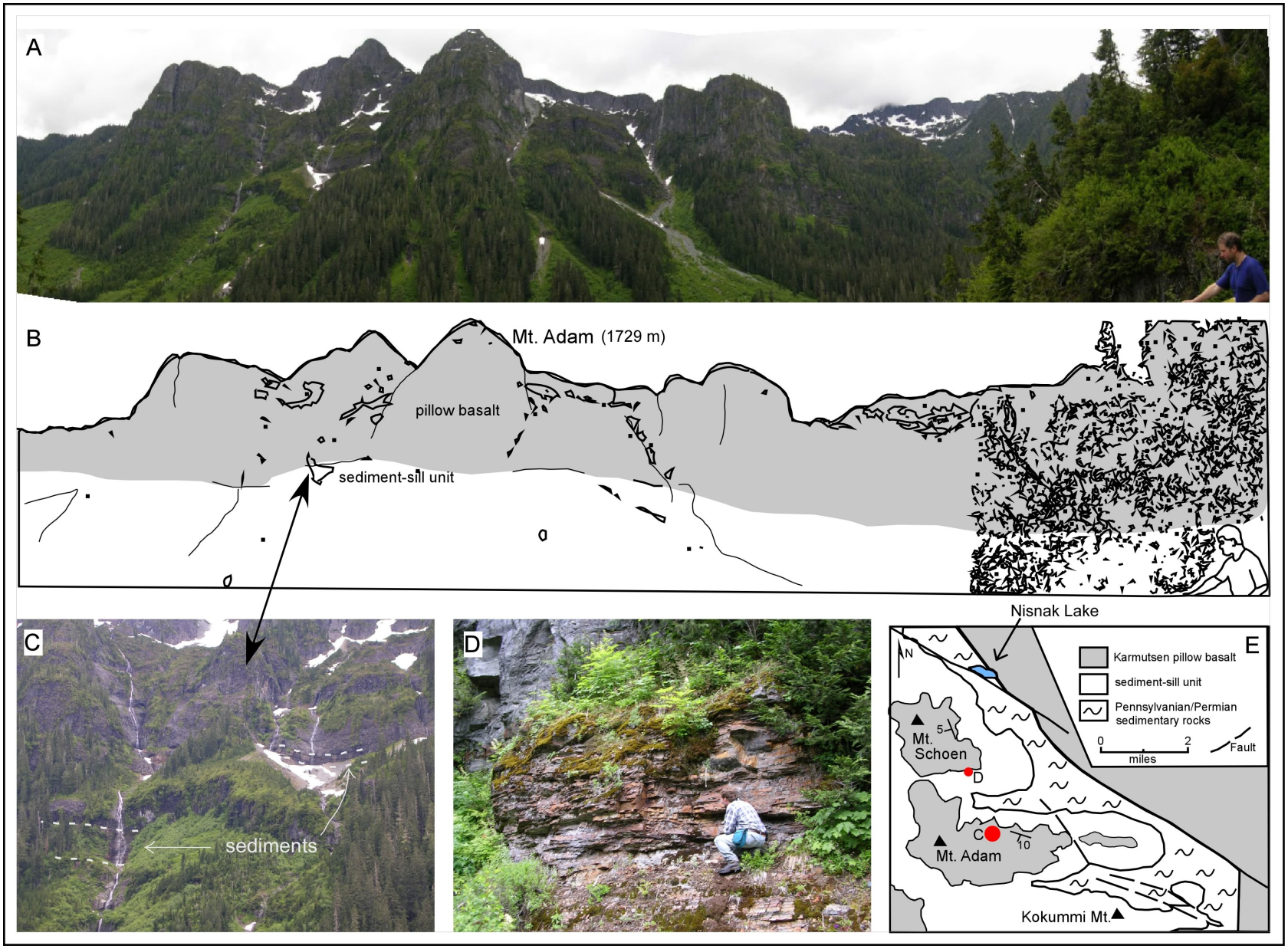


Figure 9. Sediment-sill unit around Schoen Lake Provincial Park (location shown on Fig. 1): A) Panorama of the north flank of Mount Adam. B) Interpretive sketch of A. C) Close-up view of sediment-sill unit. D) Laminated siliceous shale from sediment-sill unit on Mount Schoen. E) Simplified geological map of the area (modified from Carlisle, 1972, showing locations of photos in the figure.



Figure 10. Photograph of sediment-sill unit on Mount Schoen, location D on Figure 9D (UTM Zone 11, 700905E, 5557712N). Several mafic sills are interlayered with deformed, finely banded chert and shale.

temporaneous with eruption of the Nikolai volcanic rocks in the Yukon yielded an age of 232.2 ±1.0 Ma (Mortensen and Hulbert, 1991). Most recently, Bittenbender et al. (2002) published two Ar/Ar ages of 228.3 ±1.1 and 230.4 ±1.3 Ma from phlogopite in gabbro likely related to Wrangellia flood basalts in the Alaska Range. An additional Ar/Ar age from the Alaska Range of 231.1 Ma by J. Schmidt (pers. Comm., 2005) corroborates these ages. According to previously published geochronological results, the timing of emplacement of the plateau may have been between 233 and 217 Ma. This is based on very sparse data, however, and there are presently no ages for the entire succession of flood basalts from Vancouver Island to Alaska.

KEOGH LAKE PICRITE

During fieldwork in the summer of 2004, a succession of high-MgO picritic pillow lavas was discovered within the Karmutsen Formation on northern Vancouver Island. Fieldwork in 2005 was focused in the area where the picrite was found, west of the Karmutsen Range between Alice and Nimpkish Lakes (Fig. 3). The outcrops lie in a roughly triangular area (~28 km across) bounded by Keogh, Maynard and Sara lakes. An extensive network of logging roads provides good exposures in roadcuts and quarries adjacent to the roads. Excellent exposures of picritic pillow lavas occur in roadcuts along the north shore of Keogh Lake, the type locality. The picrite forms stacks of pillows (typically <1 m in diameter) close to tholeiitic pillows, massive flows, pillow breccia units and mafic dikes (Fig. 4).

The Keogh Lake picrite is geochemically distinguished from normal Karmutsen tholeiitic basalt pillows and flows by its elevated MgO contents (13–20 wt% MgO, on an anhydrous, normalized basis) and incompatible-element depletion (Fig. 2). In the IUGS classification scheme, the picrite has >12 wt% MgO, <3 wt% (K_2O+Na_2O), and <52 wt% SiO_2 (Le Bas, 2000). Picrite is a petrologically significant composition because it is the best candidate for least-modified partial melt of its mantle source region.

The picritic pillow basalt is distinguishable in the field by its density and nonmagnetic character. It appears to have a lower proportion of interpillow space than the more tholeiitic basalt pillows, perhaps resulting from the lower viscosity of the Mg-rich lava. The pillow lavas preserve numerous features from subaqueous eruption, such as spalled rims and drain-back ledges (Fig. 4). The picritic pillow lavas have striking features in thin section. The dense, closely packed pillows exhibit sheaf-like variolitic textures comprising numerous fans (or cone-shaped bundles) of diverging acicular plagioclase intergrown with clinopyroxene (Fig. 5). Many samples contain clusters of altered olivine (<2 mm in length) set in a matrix of curved and branching sheaves of plagioclase needles, commonly exhibiting swallow-tailed terminations. All the olivine has been replaced by serpentine (±talc), although plagioclase and clinopyroxene are mostly unaltered. Abundant pseudomorphs of euhedral olivine phenocrysts up to several millimetres long occupy 30–40 vol% of some picritic pillows (Fig. 6).

Mafic dikes in the Alice-Nimpkish lakes area may represent feeders to the Karmutsen flood basalts. Several of these dikes evidently fed the picritic lavas and comprise dense, fine-grained rocks containing up to 40 vol% coarse-grained olivine (Fig. 7). A volumetrically small proportion



Figure 11. Photograph of the base of the upper mafic sill in Figure 10. Note the presence of a prominent 25 cm thick sulphide-stained zone along the lower contact with the underlying shale.

of the rocks in this area is pillow breccia that incorporates broken pillow fragments containing abundant altered olivine phenocrysts (Fig. 8).

SIGNIFICANCE OF PICRITIC VOLCANISM IN THE WRANGELLIA OCEANIC PLATEAU

The Keogh Lake picrite of northern Vancouver Island may provide insight into the source of basaltic magmas and the potential for Ni-Cu-PGE mineralization in this part of Wrangellia. Picrite is usually linked to large igneous provinces (LIPs) and the initiation of mantle plumes, where mantle temperatures 200–300°C higher than ambient mantle result in higher degrees of partial melting (Herzberg and O'Hara, 1998). Picrite is much more common in Archean greenstone belts than in Phanerozoic LIPs because Archean mantle plumes were evidently hotter than Phanerozoic plumes (Nisbet *et al.*, 1993). Among Phanerozoic LIPs, picrite is commonly found in continental environments (*e.g.*, Deccan, Karoo, Paraná-Etendeka) and has only rarely been recognized in oceanic plateaus (*e.g.*, Caribbean plateau; Gibson, 2002).

Picrite is significant because it potentially originates near the axis of the plume where the temperature is highest (Campbell *et al.*, 1989) and, because it may result from high-temperature melting, it may preserve incompatible trace-element ratios of the mantle source (Campbell, 2002). The recognition of picritic volcanism within the Karmutsen Formation on northern Vancouver Island is strong evidence that the flood basalts originated from initiation of a mantle plume. The Keogh Lake picrite may represent the least differentiated rocks in Wrangellia.

BASAL SEDIMENT-SILL COMPLEX

During fieldwork in 2005, an exceptional sediment-sill complex was examined at the base of the Karmutsen Formation in the vicinity of Schoen Lake Provincial Park (Fig. 1, 9). Here, Middle Triassic marine sedimentary rocks overlie Pennsylvanian to Permian limestone and siliceous sedimentary rocks (Sicker Group), and both successions are intruded by thick mafic sills related to the overlying flood basalts (Carlisle, 1972). This sedimentary package represents the ocean floor at the initiation of Karmutsen volcanism and, indeed, presents a rare opportunity to examine the base of an oceanic flood basalt province.

Carlisle (1972) estimated the sediment-sill unit to be approximately 600–900 m thick, with a total thickness of roughly 150–200 m of pre-intrusive sedimentary rocks. The Triassic sedimentary rocks range from thinly bedded siliceous and calcareous shale to banded chert and finely laminated, *Daonella*-bearing shale (Fig. 9, 10; Carlisle, 1972). The younger, fissile Triassic units were more vulnerable to sill intrusion than the older, more massive underlying Paleozoic limestone (Carlisle, 1972). In some areas, the sills preserve evidence of intrusion into unlithified, wet sediments. The mafic sills (1–15 m thick) are fairly dense, coarse-grained intrusions, locally with columnar jointing. On Mount Schoen, a single sill is characterized by a prominent 25 cm thick sulphide-stained zone along the lower contact with the underlying shale (Fig. 11). A sample from this zone contains 1–2% blebby and interstitial sulphide composed of >95 vol% pyrrhotite with minor amounts of chalcopyrite. The restriction of pyrrhotite to the basal contact zone of the sill, combined with the petrographic observation that some of the sulphide blebs are cored by quartz within this 25 cm wide zone, suggests that local sulphide segregation occurred in the mafic magma in response to assimilation of the underlying shale during emplacement.

PICRITE AND Ni-Cu-PGE MINERALIZATION IN THE WRANGELLIA TERRANE OF BC?

This ongoing study will also provide insight into the potential for Ni-Cu-PGE mineralization for the portion of the Wrangellia Terrane on Vancouver Island. The continental equivalents of oceanic plateaus are the hosts of world-class ore deposits. The giant Ni-Cu-PGE deposits of the Noril'sk-Talnakh region in Siberia are located in picritic intrusions related to the Siberian continental flood basalt (CFB) province. In Wrangellia, some of the essential ingredients required to form a Noril'sk-type deposit — the emplacement of hot, picritic magmas into S-bearing sedimentary rocks — appear to be present. The S and Ba-rich Late Paleozoic and Middle Triassic sedimentary rocks underlying the Wrangellia flood basalts on Vancouver Island may have been assimilated by the picritic magmas and initiated sulphide liquid immiscibility. Future work will evaluate the PGE contents of the Wrangellia flood basalts from northern Vancouver Island and the extent and nature of any crustal contamination.

ACKNOWLEDGMENTS

We are grateful to Mikkel Schau for his insight and enthusiasm during fieldwork on northern Vancouver Island, and to Rob Mackie for his expertise in sulphide mineralogy. Funding for the fieldwork was generously provided by the BC Geological Survey in 2005, by the Rocks to Riches Program administered by the BC and Yukon Chamber of Mines in 2004, and by Natural Sciences and Engineering Research Council of Canada (NSERC) Discovery Grants to J. Scoates and D. Weis. We would also like to thank Nick Arndt and Nick Massey for inspiring this study.

REFERENCES

Albarède, F. (1998): The growth of continental crust; *Tectonophysics*, Volume 296, pages 1–14.

Barker, F., Brown, A.S., Budahn, J.R. and Plafker, G. (1989): Back-arc with frontal-arc component origin of Triassic Karmutsen basalt, British Columbia, Canada; *Chemical Geology*, Volume 75, pages 81–102.

Ben-Avraham, Z., Nur, A., Jones, D.L. and Cox, A. (1981): Continental accretion: from oceanic plateaus to allochthonous terranes; *Science*, Volume 213, pages 47–54.

Bittenbender, P.E., Bean, K.W. and Gensler, E.G. (2002): Mineral investigations in the Delta River mining district, east-central Alaska, 2001–2002; *Alaska Bureau of Land Management*, Open File Report 91, 88 pages.

Brandon, M.T., Orchard, M.J., Parrish, R.R., Brown, A.S. and Yorath, C.J. (1986): Fossil ages and isotopic dates from the Paleozoic Sicker Group and associated intrusive rocks, Vancouver Island, British Columbia; *in* Current Research, Part A, *Geological Survey of Canada*, Paper 86-1A, pages 683–696.

Campbell, I.H. (2002): Implications of Nb/U, Th/U and Sm/Nd in plume magmas for the relationship between continental and oceanic crust formation and the development of the depleted mantle; *Geochimica et Cosmochimica Acta*, Volume 66, pages 1651–1661.

Campbell, I.H., Griffiths, R.W. and Hill, R.I. (1989): Melting in an Archaean mantle plume: heads it's basalts, tails it's komatiites; *Nature*, Volume 339, pages 697–699.

Campbell, S.W. (1981): Geology and genesis of copper deposits and associated host rocks in and near the Quill Creek area, southwestern Yukon; Ph.D. thesis, University of British Columbia, 215 pages.

Carlisle, D. (1963): Pillow breccias and their aquagene tuffs, Quadra Island, British Columbia; *Journal of Geology*, Volume 71, pages 48–71.

Carlisle, D. (1972): Late Paleozoic to Mid-Triassic sedimentary-volcanic sequence on northeastern Vancouver Island; *in* Report of Activities, Part B, *Geological Society of Canada*, Paper 72-1B, pages 24–30.

Carlisle, D. and Suzuki, T. (1974): Emergent basalt and submergent carbonate-clastic sequences including the Upper Triassic Dilleri and Welleri zones on Vancouver Island; *Canadian Journal of Earth Sciences*, Volume 11, pages 254–279.

Coffin, M.F. and Eldholm, O. (1994): Large igneous provinces: crustal structure, dimensions, and external consequences; *Reviews of Geophysics*, Volume 32, pages 1–36.

Condie, K.C. (2001): Mantle Plumes and Their Record in Earth History; Cambridge University Press, Cambridge, United Kingdom, 306 pages.

DeBari, S.M., Anderson, R.G. and Mortensen, J.K. (1999): Correlation among lower to upper crustal components in an island arc: the Jurassic Bonanza arc, Vancouver Island, Canada; *Canadian Journal of Earth Sciences*, Volume 36, pages 1371–1413.

Fitton, J.G., Mahoney, J.J., Wallace, P.J. and Saunders, A.D. (2004): Origin and evolution of the Ontong Java Plateau: introduction; *in* Origin and Evolution of the Ontong Java Plateau, J.G. Fitton, J.J. Mahoney, P.J. Wallace and A.D. Saunders, Editors, *Geological Society of London*, Special Publication 229, pages 1–8.

Gardner, M.C., Bergman, S.C., Cushing, G.W., MacKevett, E.M. Jr., Plafker, G., Campbell, R.B., Dodds, C.J., McClelland, W.C. and Mueller, P.A. (1988): Pennsylvanian pluton stitching of Wrangellia and the Alexander terrane, Wrangell Mountains, Alaska; *Geology*, Volume 16, pages 967–971.

Gehrels, G.E. and Greig, C.J. (1991): Late Jurassic detrital zircon link between the Alexander-Wrangellia terrane and Stikine and Yukon-Tanana terranes; *Geological Society America*, Abstracts with Programs, Volume 23, page A434.

Gibson, S.A. (2002): Major element heterogeneity in Archean to Recent mantle plume starting-heads; *Earth and Planetary Science Letters*, Volume 195, pages 59–74.

Gunning, H.C. (1930): Geology and mineral deposits of Quatsino-Nimpkish area, Vancouver Island; *Geological Survey of Canada*, Summary Report 1929, Part A, pages 94–143.

Gunning, H.C. (1932): Preliminary report on the Nimpkish Lake Quadrangle, Vancouver Island, BC; *Geological Survey of Canada*, Summary Report 1931, Part A, pages 22–35.

Herzberg, C. and O'Hara, M.J. (1998): Phase equilibrium constraints on the origin of basalts, picrites, and komatiites; *Earth and Planetary Science Letters*, Volume 44, pages 39–79.

Hillhouse, J.W. (1977): Paleomagnetism of the Triassic Nikolai Greenstone, McCarthy Quadrangle, Alaska; *Canadian Journal of Earth Sciences*, Volume 14, pages 2578–3592.

Hillhouse, J.W. and Gromme, C.S. (1984): Northward displacement and accretion of Wrangellia: new paleomagnetic evidence from Alaska; *Journal of Geophysical Research*, Volume 89, pages 4461–4467.

Hillhouse, J.W., Gromme, C.S. and Vallier, T.L. (1982): Paleomagnetism and Mesozoic tectonics of the Seven Devils volcanic arc in northeastern Oregon; *Journal of Geophysical Research*, Volume B87, pages 3777–3794.

Irvine, T.N. and Baragar, W.R.A. (1971): A guide to the chemical classification of the common volcanic rocks; *Canadian Journal of Earth Sciences*, Volume 8, pages 523-548.

Isachsen, C., Armstrong, R.L. and Parrish, R.R. (1985): U-Pb, Rb-Sr and K-Ar geochronometry of Vancouver Island igneous rocks; *Geological Association of Canada – Victoria Section*, Symposium Abstracts, pages 21–22.

Jeletzky, J.A. (1950): Stratigraphy of the west coast of Vancouver Island between Kyuquot Sound and Esperanza Inlet, British Columbia; *Geological Survey of Canada*, Paper 50-57.

Jeletzky, J.A. (1970): Some salient features of Early Mesozoic history of Insular Tectonic Belt, western British Columbia*; Geological Survey of Canada*, Paper 69-14, 26 pages.

Jones, D.L., Silberling, N.J. and Hillhouse, J. (1977): Wrangellia: a displaced terrane in northwestern North America; *Canadian Journal of Earth Sciences*, Volume 14, pages 2565–2577.

Klaver, G.T. (1987): The Curacao lava formation: an ophiolitic analogue of the anomalous thick layer 2B of the mid-Cretaceous oceanic plateaus in the western Pacific and central Caribbean; Ph.D. thesis, University of Amsterdam, 168 pages.

Kuniyoshi, S. (1972): Petrology of the Karmutsen (Volcanic) Group, northeastern Vancouver Island, British Columbia; Ph.D. thesis, University of California, Los Angeles, 242 pages.

Lassiter, J.C., DePaolo, D.J. and Mahoney, J.J. (1995): Geochemistry of the Wrangellia flood basalt province: implications for the role of continental and oceanic lithosphere in flood basalt genesis; *Journal of Petrology*, Volume 36, pages 983–1009.

Le Bas, M.J. (2000): IUGS reclassification of the high-Mg and picritic volcanic rocks; *Journal of Petrology*, Volume 41, pages 1467–1470.

Massey, N.W.D., MacIntyre, D.G. and Desjardins, P.J. (2003a): Digital Map of British Columbia – Tile NM9 South-Coast BC; *BC Ministry of Energy, Mines and Petroleum Resources*, GeoFile 2003-4.

Massey, N.W.D., MacIntyre, D.G. and Desjardins, P.J. (2003a): Digital Map of British Columbia – Tile NM10 Southwest BC; *BC Ministry of Energy, Mines and Petroleum Resources*, GeoFile 2003-3.

Massey, N.W.D. (1995a): Geology and mineral resources of the Alberni-Nanaimo Lakes sheet, Vancouver Island (92F/1W, 92F/2E, and part of 92F/7E); *BC Ministry of Energy, Mines and Petroleum Resources*, Paper 1992-2, 132 pages.

Massey, N.W.D. (1995b): Geology and mineral resources of the Cowichan Lake sheet, Vancouver Island (92C/16); *BC Ministry of Energy, Mines and Petroleum Resources*, Paper 1992-3, 112 pages.

Massey, N.W.D. (1995c): Geology and mineral resources of the Duncan sheet, Vancouver Island (92B/13); *BC Ministry of Energy, Mines and Petroleum Resources*, Paper 1992-4, 112 pages.

Massey, N.W.D. and Friday, S.J. (1988): Geology of the Chemainus River – Duncan area, Vancouver Island (92C/16; 92B/13); *in* Geological Fieldwork 1987, *BC Ministry of Energy, Mines and Petroleum Resources*, Paper 1988-1, pages 81–91.

Massey, N.W.D. and Friday, S.J. (1989): Geology of the Alberni-Nanaimo Lakes area, Vancouver Island (91F/1W, 92F/2E and part of 92F/7); *in* Geological Fieldwork 1987, *BC Minis-*

try of Energy, Mines and Petroleum Resources, Paper 1989-1, pages 61–74.

McClelland, W.C., Gehrels, G.E. and Saleeby, J.B. (1992): Upper Jurassic – Lower Cretaceous basinal strata along the Cordilleran margin: implication for the accretionary history of the Alexander-Wrangellia-Peninsular terranes; *Tectonics*, Volume 11, pages 823–835.

Monger, J.W.H., Price, R.A. and Tempelman-Kluit, D.J. (1982): Tectonic accretion and the origin of the two major metamorphic and plutonic welts in the Canadian Cordillera; *Geology*, Volume 10, pages 70–75.

Mortensen, J.K. and Hulbert, L.J. (1991): A U-Pb zircon age for a Maple Creek gabbro sill, Tatamagouche Creek area, southwestern Yukon Territory; *in* Radiogenic Age and Isotopic Studies: Report 5, *Geological Survey of Canada*, Paper 91-2, pages 175–179.

Muller, J.E. (1967): Kluane Lake map area, Yukon Territory (115G, 115F/E 1/2); *Geological Survey of Canada*, Memoir 340, 137 pages.

Muller, J.E. (1977): Evolution of the Pacific Margin, Vancouver Island, and adjacent regions; *Canadian Journal of Earth Sciences*, Volume 14, pages 2062–2085.

Muller, J.E. (1980): The Paleozoic Sicker Group of Vancouver Island, British Columbia; *Geological Survey of Canada*, Paper 79-30, 22 pages.

Muller, J.E. (1981): Insular and Pacific Belts; *in* Cordilleran Cross-section — Calgary to Victoria, R.A. Price, J.W.H. Monger and J.E. Muller (eds.), *Geological Association of Canada – Mineralogical Association of Canada*, Joint Annual Meeting, Field Trip Guidebook, pages 261–334.

Muller, J.E., Cameron, B.E.B. and Northcote, K.E. (1981): Geology and mineral deposits of Nootka Sound map-area, Vancouver Island, British Columbia; *Geological Survey of Canada*, Paper 80-16.

Muller, J.E. and Carson, D.J.T. (1969): Geology and mineral deposits of the Alberni area, British Columbia; *Geological Survey of Canada*, Paper 68-50, 35 pages.

Muller, J.E., Northcote, K.E. and Carlisle, D. (1974): Geology and mineral deposits of Alert Bay – Cape Scott map area, Vancouver Island, British Columbia; *Geological Survey of Canada*, Paper 74-8, 77 pages.

Nisbet, E.G., Cheadle, M.J., Arndt, N.T. and Bickle, M.J. (1993): Constraining the potential temperature of the Archaean mantle: a review of the evidence from komatiites; *Lithos*, Volume 30, pages 291–307.

Nixon, G.T., Hammack, J.L., Hamilton, J.V. and Jennings, H. (1993): Preliminary geology of the Mahatta Creek area, northern Vancouver Island (92L/5); *in* Geological Fieldwork 1992, *BC Ministry of Energy, Mines and Petroleum Resources*, Paper 1993-1, pages 17–35.

Nixon, G.T., Hammack, J.L., Koyanagi, V.M., Payie, G.J., Panteleyev, A., Massey, N.W.D., Hamilton, J.V. and Haggart, J.W. (1994a): Preliminary geology of the Quatsino – Port McNeill map areas, northern Vancouver Island (92L/12, 11); *in* Geological Fieldwork 1993, *BC Ministry of Energy, Mines and Petroleum Resources*, Paper 1994-1, pages 63–85.

Nixon, G.T., Hammack, J.L., Payie, G.J., Snyder, L.D., Archibald, D.A. and Barron, D.J. (1994b): Quatsino – San Josef map area, northern Vancouver Island (92L/12W, 102I/8, 9); *in* Geological Fieldwork 1995, *British Columbia, Ministry of Energy, Mines and Petroleum Resources*, Paper 1995-1, pages 9–21.

Nokleberg, W.J., Parfenov, L.M., Monger, J.W.H., Norton, I.O., Khanchuk, A.I., Stone, D.B., Scholl, D.W. and Fujita, K. (2000): Phanerozoic tectonic evolution of the circum – North Pacific*; United States Geological Survey*, Professional Paper 1626, 122 pages.

Nokleberg, W.J., Plafker, G. and Wilson, F.H. (1994): Geology of south-central Alaska; *in* The Geology of North America, G. Plafker and H.C. Berg (eds.), *Geological Society of America*, volume G-1, pages 311–366.

Northcote, K.E. and Muller, J.E. (1972): Volcanism, plutonism, and mineralization, Vancouver Island; *Canadian Institute of Mining and Metallurgy Bulletin*, Volume 65, pages 49–57.

Panuska, B.C. (1990): An overlooked, world class Triassic flood basalt event; *Geological Society of America*, Abstracts with Programs, Volume 22, page A168.

Parrish, R.R. and McNicoll, V.J. (1992): U-Pb age determinations from the southern Vancouver Island area, British Columbia; *in* Radiogenic Age and Isotopic Studies: Report 5, *Geological Survey of Canada*, Paper 91-2, pages 79–86.

Petterson, M.G., Neal, C.R., Mahoney, J.J., Kroenke, L.W., Saunders, A.D., Babbs, T.L., Duncan, R.A., Tolia, D. and McGrail, B. (1997): Structure and deformation of north and central Malaita, Solomon Islands: tectonic implications for the Ontong Java Plateau – Solomon arc collision, and for the fate of oceanic plateaus; *Tectonophysics*, Volume 283, pages 1–33.

Plafker, G., Nokleberg, W.J. and Lull, J.S. (1989): Bedrock geology and tectonic evolution of the Wrangellia, Peninsular, and Chugach terranes along the Trans-Alaskan Crustal Transect in the northern Chugach Mountains and southern Copper River basin, Alaska; *Journal of Geophysical Research*, Volume 94, pages 4255–4295.

Richards, M.A., Duncan, R.A. and Courtillot, V. (1989): Flood basalts and hotspot tracks: plume heads and tails; *Science*, Volume 246, pages 103–107.

Richards, M.A., Jones, D.L., Duncan, R.A. and DePaolo, D.J. (1991): A mantle plume initiation model for the Wrangellia flood basalt and other oceanic plateaus; *Science*, Volume 254, pages 263–267.

Schmidt, J.M., O'Neill, J.M., Snee, L.W., Blodgett, R.B., Ridgeway, K.D., Wardlaw, B.R. and Blome, C.D. (2003): The northwestern edge of Wrangellia: stratigraphic and intrusive links between crustal blocks from the Peninsular Terrane to Broad Pass; *Geological Society of America*, Abstracts with Programs, Volume 35, No. 6, page 560.

Sluggett, C.L. (2003): Uranium-lead age and geochemical constraints on Paleozoic and Early Mesozoic magmatism in Wrangellia Terrane, Saltspring Island, British Columbia; B.Sc. thesis, *University of British Columbia*, Vancouver, BC, 84 pages.

Surdam, R.C. (1968): The stratigraphy and volcanic history of the Karmutsen Group, Vancouver Island, British Columbia; *University of Wyoming, Contributions to Geology*, Volume 7, pages 15–26.

Sutherland Brown, A., Yorath, C.J., Anderson, R.G. and Dom, K. (1986): Geological maps of southern Vancouver Island, LITHOPROBE I 92C/10, 11, 14, 16, 92F/1, 2, 7, 8*; Geological Survey of Canada*, Open File 1272.

Tipper, H.W. (1984): The allochthonous Jurassic – Lower Cretaceous terranes of the Canadian Cordillera and their relation to correlative strata of the North American craton; *Geological Association of Canada*, Special Paper 27, pages 113–120.

Trop, J.M., Ridgway, K.D., Manuszak, J.D. and Layer, P.W. (2002): Mesozoic sedimentary-basin development on the allochthonous Wrangellia composite terrane, Wrangell Mountains basin, Alaska: a long-term record of terrane migration and arc construction; *Geological Society of America Bulletin*, Volume 114, pages 693–717.

van der Heyden, P. (1992): A middle Jurassic to early Tertiary Andean-Sierran arc model for the coast belt of British Columbia; *Tectonics*, Volume 11, pages 82–97.

White, R.S. and McKenzie, D. (1995): Mantle plumes and flood basalts; *Journal of Geophysical Research*, Volume 100, pages 17543–17585.

Wignall, P.B. (2001): Large igneous provinces and mass extinctions; *Earth-Science Reviews*, Volume 53, pages 1–33.

Yole, R.W. and Irving, E. (1980): Displacement of Vancouver Island, paleomagnetic evidence from the Karmutsen Formation; *Canadian Journal of Earth Sciences*, Volume 17, pages 1210–1228.

Yorath, C.J., Clowes, R.M., Green, A.G., Sutherland Brown, A., Brandon, M.T., Massey, N.W.D., Spencer, C., Kanasewich, E.R. and Hyndman, R.D. (1985): LITHOPROBE – Phase 1, southern Vancouver Island: preliminary analyses of reflection seismic profiles and surface geological studies; *in* Current Research, Part A, *Geological Survey of Canada*, Paper 85-1A, pages 543–554.

Bowser Basin Geochemical Survey, North-Central British Columbia: Anomaly Follow-up, 2005

By R.E. Lett and P.W.B. Friske[1]

KEYWORDS: geochemistry, Bowser Basin, regional geochemical survey, gold anomaly, heavy minerals

INTRODUCTION

Reconnaissance-scale regional drainage surveys carried out as part of Canada's National Geochemical Reconnaissance (NGR) program routinely analyze the –80 mesh (<0.177 mm) fraction of sediment samples for trace elements. Standard sample preparation and analytical methods, maintained since the program was started in 1974, have minimized data levelling problems and have generated a large, uniform, high-quality stream and lake sediment geochemical database. Drainage sediment and water samples are collected at an average density of one sample per 13 km^2 in British Columbia as part of the NGR Program. This low-density sampling inevitably identifies areas of bedrock with higher geochemical values, indicating a greater mineral potential, but individual mineral occurrences may remain undetected. Sampling at a higher density or using a sediment heavy mineral concentrate (HMC) as a sample medium can increase the ability of low-density reconnaissance surveys to find individual mineral occurrences, but at a greater collection and analytical cost. Economical and practical methods that complement regional surveys to improve their success in discovering new mineral deposits in BC would clearly be attractive. The follow-up geochemical studies carried out jointly by the BC Geological Survey and the Geological Survey of Canada were therefore aimed at:

- characterizing the heavy mineral dispersal train related to polymetallic mineralization at the Eskay Creek Au mine and comparing it to the regional geochemical survey (RGS) silt response to establish if HMCs provide a spatially more extensive and/or stronger geochemical signature than the routinely collected silt;
- providing guidelines to the exploration community on the use of heavy minerals for drainage surveys;
- following up drainage sediment anomalies in the Bowser Lake area revealed by RGS results released in August 2005 (Friske *et al.*, 2005); and
- resampling historical RGS sites in northwestern BC to determine long-term geochemical variability and the source of unexplained sediment Hg and Ni anomalies.

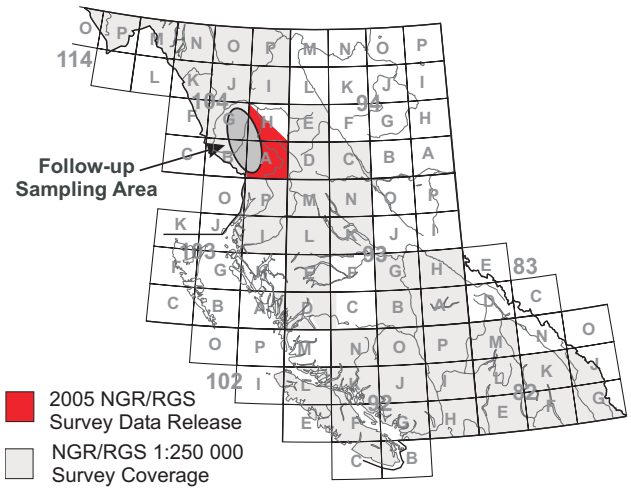


Figure 1. Location of the area covered by the 2005 regional geochemical survey (Friske *et al.*, 2005) and the follow-up sampling.

Preliminary results of these studies are described in this paper.

Follow-up geochemical sample sites are located in the Bowser Lake (NTS 104A), Iskut River (NTS 104B), and Telegraph Creek (NTS 104G) map sheets (Fig. 1). This is an area of high topographic relief flanked by the Skeena Mountains in the east and the Coast Range Mountains in the west. The Nass Basin, an irregularly shaped area of low relief drained by the Bell-Irving – Nass rivers system, separates these two ranges. The eastern part of the Iskut River and Telegraph Creek sheets is drained by the Unuk River and its tributaries (Holland, 1964). Regional geology comprises the Bowser Basin, a Middle Jurassic to Middle Cretaceous sedimentary basin filled by deltaic sedimentary rocks represented by the Bowser Lake, Skeena and Sustut Groups (Ferri *et al.*, 2004) and volcanic epiclastic and sedimentary rocks of the the Jurassic Hazelton Group. Along the western margin of the basin, the Early to Middle Jurassic Salmon River Formation forms a gradational contact with Bowser Lake sedimentary rocks (Alldrick *et al.*, 2004, 2005). Hazelton Group volcanic and sedimentary rocks also outcrop within the Bowser Basin in the Oweegee Dome inlier surrounding Delta Peak, located northeast of Bowser Lake. Geology of the Oweegee Dome comprises green volcanic conglomerate overlain by green volcanic flows, brown-black siltstone, mudstone, limestone, felsic to intermediate lapilli tuff, tuff-breccia and crystal lithic tuff (Alldrick *et al*,.2005). Typical of mineralization in these rocks is the Delta 2 showing (MINFILE 104A 166;

[1]*Geological Survey of Canada, Ottawa, ON.*

This publication is also available, free of charge, as colour digital files in Adobe Acrobat PDF format from the BC Ministry of Energy, Mines and Petroleum Resources internet website at http://www.em.gov.bc.ca/Mining/Geolsurv/Publications/catalog/catfldwk.htm

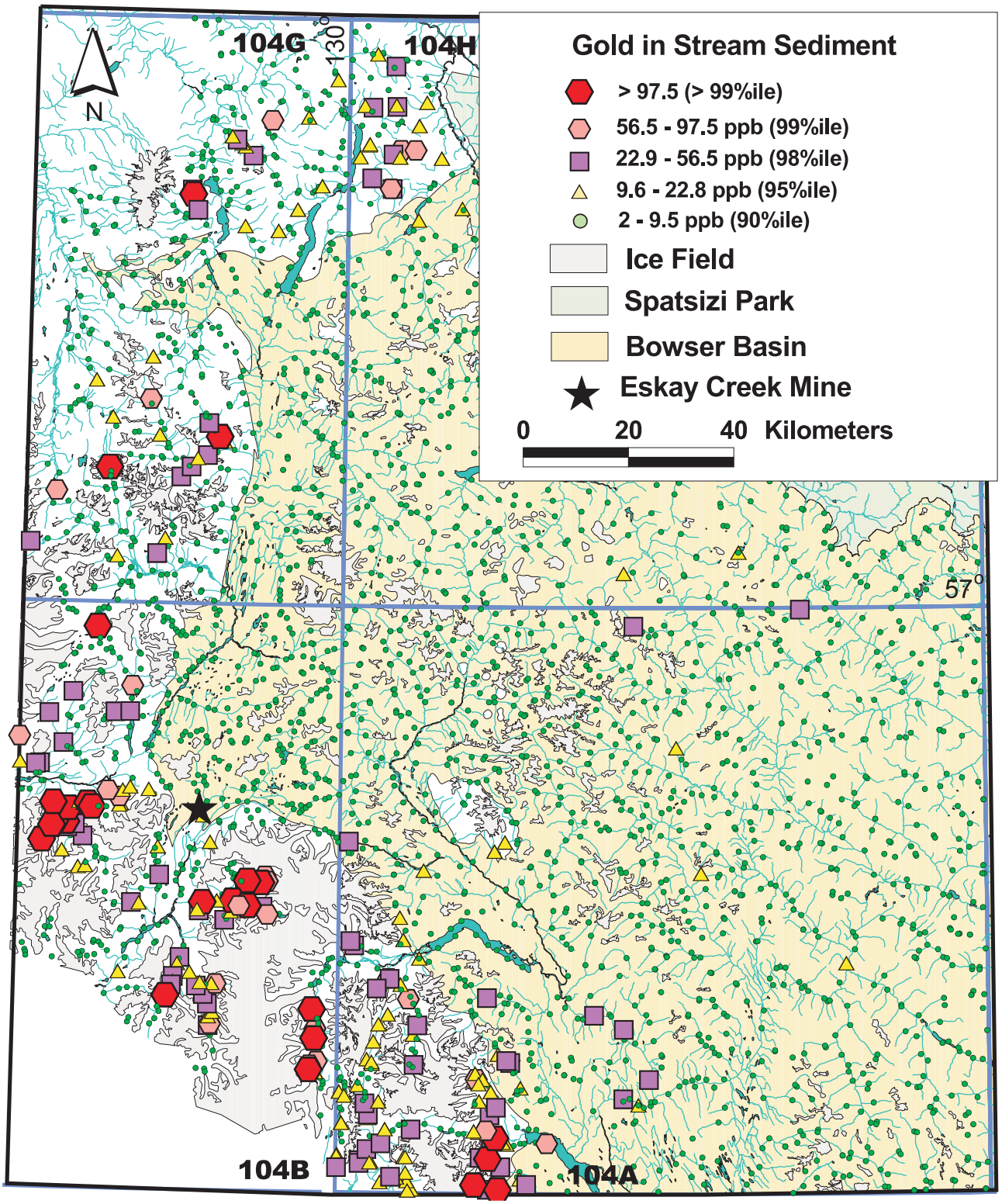


Figure 2. Gold in stream sediments from the Bowser Lake – Spatsizi River survey (Friske *et al.*, 2005; Jackaman, 2005) and regional geochemical surveys covering the adjacent NTS maps sheets 104B and G. Symbols show concentrations at the 90th, 95th, 98th and 99th percentile levels.

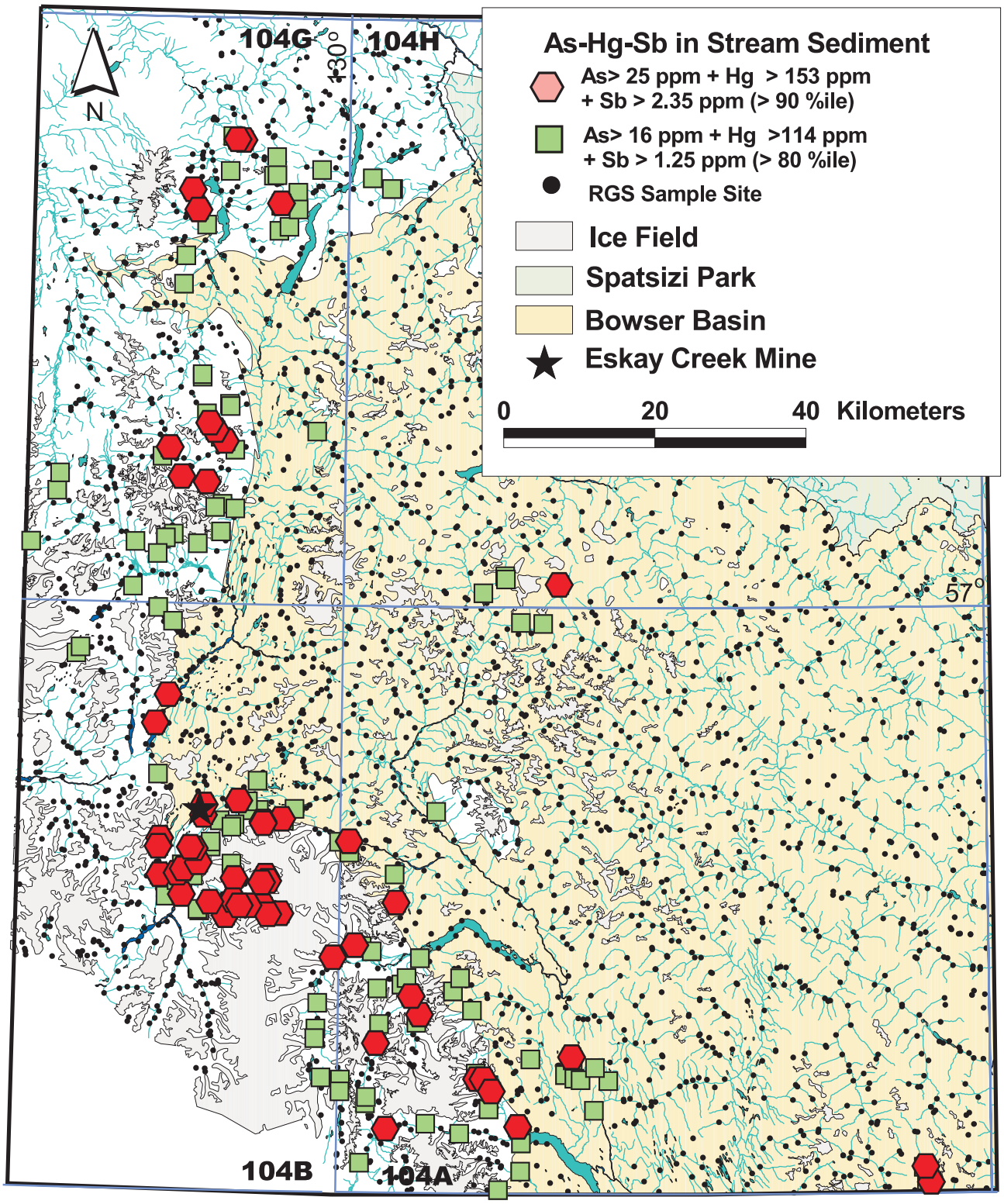


Figure 3. Multielement anomalies, Bowser Lake – Spatsizi River survey and regional geochemical surveys covering the adjacent NTS maps sheets 104B and G. Symbols show samples with As, Sb and Hg all above the 90th and 95th percentile levels.

MINFILE, 2005), where disseminated pyrite and localized chalcopyrite, malachite, azurite and sphalerite occur in northeast-trending faults and shears.

Hazelton Group rocks also host the world-class Eskay Creek Au mine and several past-producing Au-Cu mines, such as the Red Cliff, Goat and Roosevelt, located in the southwestern part of NTS 104A. The area also has potential for alkalic porphyry Cu-Mo-Au-Ag deposits similar to Red Chris (MINFILE 104H 022), epithermal volcanogenic massive sulphide deposits and, possibly, sedimentary-exhalitive Pb-Zn mineralization in Bowser Lake sedimentary rocks.

BOWSER LAKE – SPATSIZI RIVER REGIONAL SURVEY RESULTS

Results of a helicopter-supported stream sediment and water RGS completed in 2004 were released in August 2005 (Friske *et al.*, 2005). In total, 1463 stream sediment and 1458 water samples were collected from 1385 sites covering over 18 500 km^2 at a density of one sample per 13.5 km^2. Sediment samples were analyzed for Ag, Al, As, Au, Bi, Ba, Br, Ca, Cd, Ce, Co, Cr, Cu, Eu, Fe, Ga, Hf, Hg, K, La, Lu, Mg, Mn, Mo, Na, Ni, P, Pb, Rb, S, Sb, Sc, Se, Sm, Sr, Ta, Tb, Te, Th, Ti, Tl, U, V, W, Yb and Zn by a combination of instrumental neutron activation analysis (INAA) and aqua regia digestion – inductively coupled plasma mass spectrometry (ICP-MS) and for loss-on-ignition (LOI). Water samples were analyzed for pH, conductivity, Cl, F, NO_3, SO_4 and U. Filtered and acidified water samples from 320 of the sites were also analyzed for 52 major and trace elements (Friske *et al.*, 2005; Jackaman, 2005).

Figure 2 is a symbol plot of Au in the –80 mesh fraction of stream sediment samples from this RGS and from surveys covering the adjacent NTS 104B and G map sheets (Matysek *et al.*, 1988a, b). Stream sediment Au anomalies, where values exceed the 99th percentile (>97.5 ppb), cluster in the southwestern and western parts of the surveyed area, where the rocks are predominantly Hazelton Group. Many of the Au anomalies correspond to areas of known mineralization, such as those draining the Sulphurets camp. There are a smaller number of weaker (22.9–56.5 ppb Au) anomalies in Bowser Basin drainages, and the largest cluster is located in the southern part of the Bowser Lake map sheet. Sulphide mineralization typical of the Eskay Creek deposit is typically enriched in Hg, As and Sb, among other elements. Drainage sample sites where As, Sb and Hg values all exceed the 80th and 90th

TABLE 1. STATISTICS AND CONTRAST FOR AU, AG, AS AND HG IN –80 AND –230 MESH FRACTION OF STREAM SEDIMENT BASED ON GEOCHEMICAL DATA FOR 46 SAMPLES. CONTRAST = MAXIMUM/MEDIAN

Element	Mean	Median	Third Quartile	Maximum	95th Percentile	Contrast
Ag-80_MS	3752	264	686	>100000	2050	378
Ag-230_MS	4384	361	1098	>100000	3622	277
As-80_MS	46.2	17.0	40.8	623.5	161.6	37
As-230_MS	63.5	22.5	61.8	809.9	223.9	36
As-80_NA	10.8	13.5	30.8	91.6	67.7	7
As-230_NA	18.2	15.5	41.3	96.2	89.6	6
Au-80_MS	63.1	2.2	5.5	2138.5	45.8	972
Au-230_MS	140.8	1.8	6.9	4431.0	224.7	2461
Au-80_NA	178	6	14	5840	318	1062
Au-230_NA	236	8	25	6440	257	805
Hg-80_MS	2620	105	158	86756	2251	326
Hg-230_MS	3009	144	200	98406	2507	492

TABLE 2. STATISTICS CALCULATED FROM SELECTED ELEMENT DATA IN –80 MESH FRACTION OF 37 STREAM SEDIMENT SAMPLES. ABBREVIATIONS: ICP-MS, AQUA REGIA DIGESTION – INDUCTIVELY COUPLED PLASMA MASS SPECTROMETRY; INAA, INSTRUMENTAL NEUTRON ACTIVATION ANALYSIS; GRAV, LOSS-ON-IGNITION AT 550°C

Element	Units	Det. Limit	Method	Mean	Median	Third Quartile	Maximum
Ag	ppb	2	ICP-MS	4464	237	419	>100000
As	ppm	0.1	ICP-MS	28.1	15.5	36.7	167.5
As	ppm	0.5	INAA	15.7	19.0	42.0	91.6
Au	ppb	0.2	ICP-MS	76.9	2.2	4.8	2138.5
Au	ppb	2	INAA	223	7	21	5840
Ba	ppm	50	INAA	1392	1100	1500	3800
Bi	ppm	0.02	ICP-MS	0.19	0.11	0.16	1.72
Br	ppm	0.5	INAA	3.6	1.0	5.3	16.0
Cd	ppm	0.01	ICP-MS	1.95	0.57	0.86	18.14
Co	ppm	0.1	ICP-MS	18.2	17.4	21	25.8
Co	ppm	5	INAA	19	18	23	34
Cr	ppm	0.5	ICP-MS	41.9	30.9	54.8	103.4
Cr	ppm	2	INAA	149	120	210	630
Cu	ppm	0.01	ICP-MS	68.58	51.58	63.0	495.99
Fe	%	0.01	ICP-MS	4.37	4.18	4.82	7.46
Fe	%	0.02	INAA	5.30	4.90	5.90	9.20
Ga	ppm	0.2	ICP-MS	5.2	5.0	5.5	10.9
Hg	ppb	5	ICP-MS	3236	104	219	86756
LOI	%	0.1	Grav	5.45	4.30	6.80	14.50
Mn	ppm	1	ICP-MS	1036	942	1258	2057
Mo	ppm	0.01	ICP-MS	3.25	1.81	2.80	23.38
Ni	ppm	0.1	ICP-MS	60.9	57.3	94.9	147.3
Pb	ppm	0.01	ICP-MS	66.90	9.82	20.0	1453.11
S	%	0.02	ICP-MS	0.29	0.16	0.32	2.56
Sb	ppm	0.02	ICP-MS	29.18	1.34	3.59	762.60
Sb	ppm	0.1	INAA	40.5	2.3	6.8	1050.0
Se	ppm	0.1	ICP-MS	2.1	1.0	1.9	21.4
Te	ppm	0.02	ICP-MS	0.08	0.05	0.1	0.87
Th	ppm	0.1	ICP-MS	1.2	1.2	1.3	2.0
Th	ppm	0.2	INAA	4.1	3.9	4.9	8.0
Tl	ppm	0.02	ICP-MS	0.28	0.13	0.24	1.67
U	ppm	0.1	INAA	2.4	2.4	2.8	7.2
V	ppm	2	ICP-MS	65	54	70	191
Zn	ppm	0.1	ICP-MS	322.1	136.4	176.3	3763.2

TABLE 3. STATISTICS CALCULATED FROM SELECTED ELEMENT DATA FROM 35 HEAVY MINERAL CONCENTRATES ANALYZED BY AQUA REGIA DIGESTION ICP-MS AND 26 HEAVY MINERAL CONCENTRATES ANALYZED BY INAA. ABBREVIATIONS: ICP-MS, AQUA REGIA DIGESTION – INDUCTIVELY COUPLED PLASMA MASS SPECTROMETRY; INAA, INSTRUMENTAL NEUTRON ACTIVATION ANALYSIS

Element	Units	Method	Median	Third Quartile	Maximum
Ag	ppb	ICP-MS	4499	8145	>100000
As	ppm	ICP-MS	241.5	484.5	1737.8
As	ppm	INAA	279.5	523.0	1570
Au	ppb	ICP-MS	437.4	2301.9	>100000
Au	ppb	INAA	3095	8438	161000
Ba	ppm	ICP-MS	31.4	76.7	4289.9
Ba	ppm	INAA	18250	32625	92100
Bi	ppm	ICP-MS	0.54	1.85	10.94
Cd	ppm	ICP-MS	2.59	8.34	310
Co	ppm	ICP-MS	79.1	113.15	577.9
Co	ppm	INAA	81	143	615
Cr	ppm	ICP-MS	21.3	52.7	258.7
Cr	ppm	INAA	500	1225	46100
Cu	ppm	ICP-MS	337.05	765.47	>10000
Fe	%	ICP-MS	16.28	25.25	40
Fe	%	INAA	28.7	33.3	41.4
Hg	ppb	ICP-MS	1869	5257	>100000
Mn	ppm	ICP-MS	1096	2162	25909
Mo	ppm	ICP-MS	9.9	16.34	101.45
Mo	ppm	INAA	6	10	87
Ni	ppm	ICP-MS	94	239.2	793.2
Ni	ppm	INAA	71	95	730
S	%	ICP-MS	5.79	10	10
Sb	ppm	ICP-MS	12.41	24.79	2000
Sb	ppm	INAA	21.8	52.7	33000
Se	ppm	ICP-MS	10.8	17.65	100
Te	ppm	ICP-MS	0.18	0.7	4.17
Tl	ppm	ICP-MS	0.5	1.28	19.61
V	ppm	ICP-MS	80	160	361
W	ppm	ICP-MS	0.9	4.8	58.3
W	ppm	INAA	4	15.5	98
Zn	ppm	ICP-MS	374.3	1077.8	>10000
Zn	ppm	INAA	460	1100	116000

percentile levels are identified in Figure 3. Data used to create this map were combined from those reported in RGS 58 (Friske *et al.*, 2005) and results of the 104B and G sediment sample reanalysis previously reported by Lett and Jackaman (2003). Although most sites with this element signature are from streams draining the Hazelton Group, there are several anomalous drainages in the southeastern part of the Bowser Lake sheet (NTS 104A) underlain by sedimentary rocks.

FOLLOW-UP SAMPLING

Sample Collection

During the summers of 2004 and 2005, stream sediment, bulk sediment samples (for preparation of HMCs) and stream water samples were collected at 44 sites in NTS areas 104A, 104B and 104G. Information about the site, such as sediment texture, drainage size and water flow was recorded. Sediment typical of that collected during a reconnaissance-scale geochemical survey was taken from mid and lateral bars in active stream channels at locations selected to avoid high or low-energy extremes. Where abundant, living moss attached to boulders and logs from just above the stream high-water mark was also collected. Stream sediment and moss samples were stored in high-wet-strength Kraft paper sample bags for shipment to a commercial laboratory.

Ideally, sediment for preparation of a HMC fraction was taken at the upstream point of midchannel bars. At each site, a 5 gallon plastic pail was lined with a heavy-duty polyethylene plastic bag (18 x 24 inches, 4 mil) and sediment was wet sieved through a 12-mesh (1.68 mm) stainless steel sieve until a sample weight of 10–15 kg was obtained. The sample was weighed in the pail before the opening was taped shut with black plastic tape and placed in a second bag.

Water was also collected at each site in a rinsed Nalgene® bottle, and the pH and conductivity were measured within twenty-four hours. Later, a portion of the water sample was filtered through a 0.45 μm glass-fibre filter and the filtered water acidified to pH 2 with ISTAR® nitric acid.

Sample Preparation and Analysis

Fine-textured sediment and moss samples were air dried and the –18 mesh (<1 mm) fraction recovered by gently disaggregating the sediment or by pounding the moss before dry sieving through a 1 mm stainless-steel screen. Part of the –1 mm fraction was then screened to –80 mesh ASTM (<0.177 mm) and another portion screened to –230 mesh (<0.063 mm). A control reference material and analytical duplicate sample were inserted into each block of 20 samples before analysis. Any remaining –80 and –230 mesh material was archived for future analysis.

Bulk sediment samples were progressively reduced by different laboratory procedures to concentrate the heavy minerals. Initially, a 500 g character sample was taken and stored before a low-grade table concentrate was prepared from the remainder. Gold grains were observed at this stage and counted, measured and classified as to degree of wear (*i.e.*, distance of transport). The table reject was retabled to scavenge possible unrecovered massive sulphide indicator minerals. The concentrate from both tabling runs was separated in methylene iodide diluted with acetone to sp gr 3.20 to recover heavy minerals. Magnetite was removed after the heavy liquid separation and the remaining concentrate cleaned with oxalic acid to remove limonite stains. The dried concentrate was sieved into several size fractions, (<0.25 mm, 0.25 mm to <0.5 mm, 0.5 mm to <1.0 mm, =1.0 mm to 2.0 mm), with the <0.25 mm (60 mesh) fraction being used for chemical analysis.

The –80 and –230 mesh fractions of the stream sediment and moss samples and the <0.25 mm nonmagnetic fraction of the HMC were analyzed for trace and minor elements by aqua regia digestion – inductively coupled plasma mass spectrometry (aqua regia ICP-MS) at Acme Analytical Laboratories Ltd., Vancouver and by instrumental neutron activation analysis (INAA) at Becquerel Laboratories, Mississauga, Ontario. Analytical amounts of the HMCs ranged from 0.1 to 15 g. The filtered, acidified portion of each water sample was analyzed by inductively coupled

TABLE 4. ENHANCED (>3RD QUARTILE) CONCENTRATIONS OF ELEMENTS IN THE –80 MESH FRACTION OF STREAM SEDIMENT AND ELEMENTS ELEVATED IN STREAM WATER SAMPLES COLLECTED IN 2004. ABBREVIATION: REE, RARE EARTH ELEMENTS (*E.G.*, DY, ER, EU)

Year	Map Sheet	Site	Elements Enhanced (>3rd Quartile) in 80 Mesh Fraction of Sediment	Elements Elevated in Stream Water
2004	104A	7002	Mo	
2004	104A	7003		
2004	104A	7004		
2004	104A	7005	Pb, As, Bi	
2004	104A	7006	Cd, Pb	
2004	104A	7007		
2004	104A	7008		
2004	104A	7009		
2004	104A	7010		
2004	104A	7011	Mo	
2004	104B	7002	Au, Ag, Cd, Hg, Mo, Pb, Sb	Sb
2004	104B	7003	Cd, Pb	
2004	104B	7004	Bi	
2004	104B	7005	Au, As. Bi	
2004	104B	7006	Bi	
2004	104B	7007		
2004	104B	7008		
2004	104B	7009	Au, Ag, Bi, Cd, Cu, Hg, Mo, Pb, Sb, Zn	Sb
2004	104B	7010	Au, Ag, Bi, Cd, Cu, Hg, Mo, Pb, Sb, Se, Tl, Zn	Pb, Sb, Tl
2004	104B	7011	Au, Ag, Bi, Cd, Cu, Hg, Mo, Pb, Sb, Se, Tl, Zn	
2004	104B	7012	Au, Ag, Bi, Cd, Hg, Mo, Pb, Sb, Tl, Zn	Zn
2004	104B	7013	Ag, Bi, Cd, Hg, Mo, Pb, Sb, Zn	
2004	104B	7014	Cu, Hg, Pb	
2004	104B	7015	Au, Ag, Bi, Cd, Hg, Mo, Pb, Sb, Zn	Zn
2004	104B	7016		
2004	104B	7017	Au, Cu	
2004	104B	7018	As, Bi, Cu	
2004	104G	7002	Au, As. Cu, Hg, Sb	
2004	104G	7003		
2004	104G	7004		
2004	104G	7005	Au, Cd, Mo, Tl, Zn	
2004	104G	7006	Au. Cu, Mo	Al
2004	104G	7007	Au, Ag, Bi, Hg, Mo, Pb, Sb, Tl	Al, Cd, Cu, Zn, REE

plasma mass spectrometry at the Geological Survey of Canada, Ottawa.

DETAILED SAMPLING RESULTS

Size Fraction Chemistry

Element concentrations in the –230 mesh size fraction of sediment samples are typically higher than in the –80 mesh fraction. For some elements, such as V and Cr, the difference in median for the two size fraction populations is in the order of 10%. Other elements, such Au, Ag, As and Hg, have larger median differences (Table 1). Based on a population size of 46 samples, the Au median (INAA) for the –230 mesh fraction is 8 ppb, compared to 6 ppb for the –80 mesh fraction. Table 1 also compares anomaly contrast (maximum/median) for As, Ag, Au and Hg in the two size fractions. Arsenic contrast is almost identical for the two size fractions, whereas Au by aqua regia ICP-MS and Hg show a greater anomaly contrast for the –230 mesh fraction. Gold by INAA and Ag by aqua regia ICP-MS show larger contrast for the –80 mesh fraction. Depending on the analytical method, the –230 mesh fraction may have an advantage for improving anomaly contrast for Au and Hg, but not necessarily for other elements. Also, there are limitations to using the –230 mesh fraction, such as the need to collect a larger sample for screening enough material for analysis and the problem of levelling geochemical data produced from the –80 and –230 mesh fractions.

Multielement Associations in Sediment and Heavy Mineral Concentrates

The multielement signature of stream sediment and HMC anomalies can help characterize the source mineralization. Tables 2 and 3 list 3rd quartile values for selected elements calculated from the combined 2004 and 2005 –80 mesh sediment data and the 2004 HMC results. The 3rd quartile, rather than the more traditional 95th percentile, has been used as a threshold because it may be a more realistic value, given the small number of samples. Detection limit and mean, median and maximum concentrations are given in Table 2 for elements determined by aqua regia ICP-MS

TABLE 5. ENHANCED (>3RD QUARTILE) ELEMENTS IN THE <0.25 MM FRACTION OF HEAVY MINERAL CONCENTRATES AND GOLD GRAIN COUNTS FROM SEDIMENT SAMPLES COLLECTED IN 2004. SHAPE OF GOLD GRAINS REFLECTS RELATIVE DISTANCE FROM A SOURCE

Year	Map Sheet	Site	Elements Enhanced (>3rd Quartile) in Sediment Heavy Mineral Concentrates	Number of Visible Gold Grains			
				Total	Reshaped	Modified	Pristine
2004	104A	7002		0	0	0	0
2004	104A	7003		0	0	0	0
2004	104A	7004		0	0	0	0
2004	104A	7005	Au, Ag, As, Bi, Pb, Tl	9	6	2	1
2004	104A	7006	Bi, Pb	0	0	0	0
2004	104A	7007	Cd, Mo, Se	0	0	0	0
2004	104A	7008	Bi, Cu, Mo, Se	0	0	0	0
2004	104A	7009	Cd, Zn	0	0	0	0
2004	104A	7010	Mo	0	0	0	0
2004	104A	7011	Hg	0	0	0	0
2004	104B	7002	Ag, Sb	0	0	0	0
2004	104B	7003	Hg	0	0	0	0
2004	104B	7004	Cd, Cu, Se, Zn	0	0	0	0
2004	104B	7005	As, Sb, Pb	30	20	4	6
2004	104B	7006	Au, Bi	177	145	9	23
2004	104B	7007	Au, Se, Bi	7	5	1	1
2004	104B	7008	Au, Ag, Cu	2	2	0	0
2004	104B	7009	Au, Ag, Bi, Cd, Cu, Hg, Mo, Pb, Sb, Se, Tl, Zn	70	19	13	38
2004	104B	7010	Au, Ag, Bi, Cd, Cu, Hg, Mo, Pb, Sb, Se, Tl, Zn	413	204	0	209
2004	104B	7011	Cd, Cu, Hg, Mo, Pb, Sb, Se, Tl, Zn	36	4	0	32
2004	104B	7012	Au, Ag, Cd, Hg, Mo, Pb, Sb, Tl, Zn	0	0	0	0
2004	104B	7013	Ag, Cd, Cu, Hg, Mo, Pb, Sb, Tl, Zn	1	1	0	0
2004	104B	7014	Cd, Cu, Mo, Pb, Sb, Tl	0	0	0	0
2004	104B	7015	Ag, As, Cu, Cd, Mo, Se , Zn	0	0	0	0
2004	104B	7016		0	0	0	0
2004	104B	7017	Sb	0	0	0	0
2004	104B	7018	As, Bi, Se	2	2	0	0
2004	104G	7002	Au	1	1	0	0
2004	104G	7003		0	0	0	0
2004	104G	7004		0	0	0	0
2004	104G	7005	Mo	1	1	0	0
2004	104G	7006	As	2	1	0	1
2004	104G	7007	Ag, As, Bi, Hg, Sb, Se, Tl	2	2	0	0

and INAA techniques. In the case of Ag, the maximum value of >100 000 ppb reflects concentrations in excess of the ICP-MS upper limit.

Tables 4 and 5 list samples and corresponding elements that are above the 3rd quartile for the –80 mesh fraction (Table 4) and the <0.25 mm heavy mineral concentrate (Table 5). Also shown are elevated element levels in the filtered and acidified water samples (Table 4) and gold grain counts (Table 5). The number and morphology of gold grains in a sample are indicators of the proximity of the grain to the source. 'Pristine' grains are considered to be close to a source of Au mineralization, whereas 'reshaped' grains are considered to be more distant from a source.

Multielement associations are identified in Tables 4 and 5 for samples where concentrations exceed the 3rd quartile. Two samples, 104B7009 and 104B7010, with a large number of anomalous elements (*i.e.*, Au, Ag, Bi, Cd, Cu, Hg, Mo, Pb, Sb, Se, Tl, Zn) in both sediment and HMC are close the Eskay Creek mine. Their location and other sample sites described in this paper are shown in Figure 4. An abundance of pristine gold grains in these samples reflects a short transport distance from the source. Sample 104B7010 has elevated Pb, Sb and Tl in the stream water in addition to anomalous metals in sediment.

Anomalous samples with smaller multielement suites may also reflect mineralization in their drainages. Southwest of the Eskay Creek mine are several sites (104B7011, 7013, 7014, 7015) with HMC and sediment geochemical signatures that include Ag, Hg, Mo, Sb, Tl and Zn. The similarity of this signature to that in sediment and HMCs from

TABLE 6. ENHANCED (> 3RD QUARTILE) ELEMENTS IN THE MINUS 80 MESH FRACTION OF STREAM SEDIMENT SAMPLES COLLECTED IN 2005

Year	Map Sheet	Site	Elements enhanced (> 3rd Quartile) in the minus 80 mesh fraction of sediment
2005	104A	1002	
2005	104A	1003	Mo
2005	104A	1004	Ag, Cd, Se, Tl
2005	104A	1005	
2005	104A	1006	Ag, Bi. Cd, Cu, Pb, Sb, Zn
2005	104A	1007	Ag, Bi, Cu, Pb, Zn
2005	104A	1008	Au, Ag, As, Bi, Cd, Cu, Pb, Sb, Zn
2005	104A	1009	Au, Ag, As, Bi, Cd, Cu, Pb, Sb, Zn
2005	104A	1010	Au, Ag, As, Bi, Cd, Cu, Pb, Sb, Zn
2005	104A	1011	Ag, As, Cd, Pb
2005	104A	1012	Au, Ag, As, Bi, Cd, Cu, Pb, Sb, Zn
2005	104A	1013	
2005	104B	1002	Bi

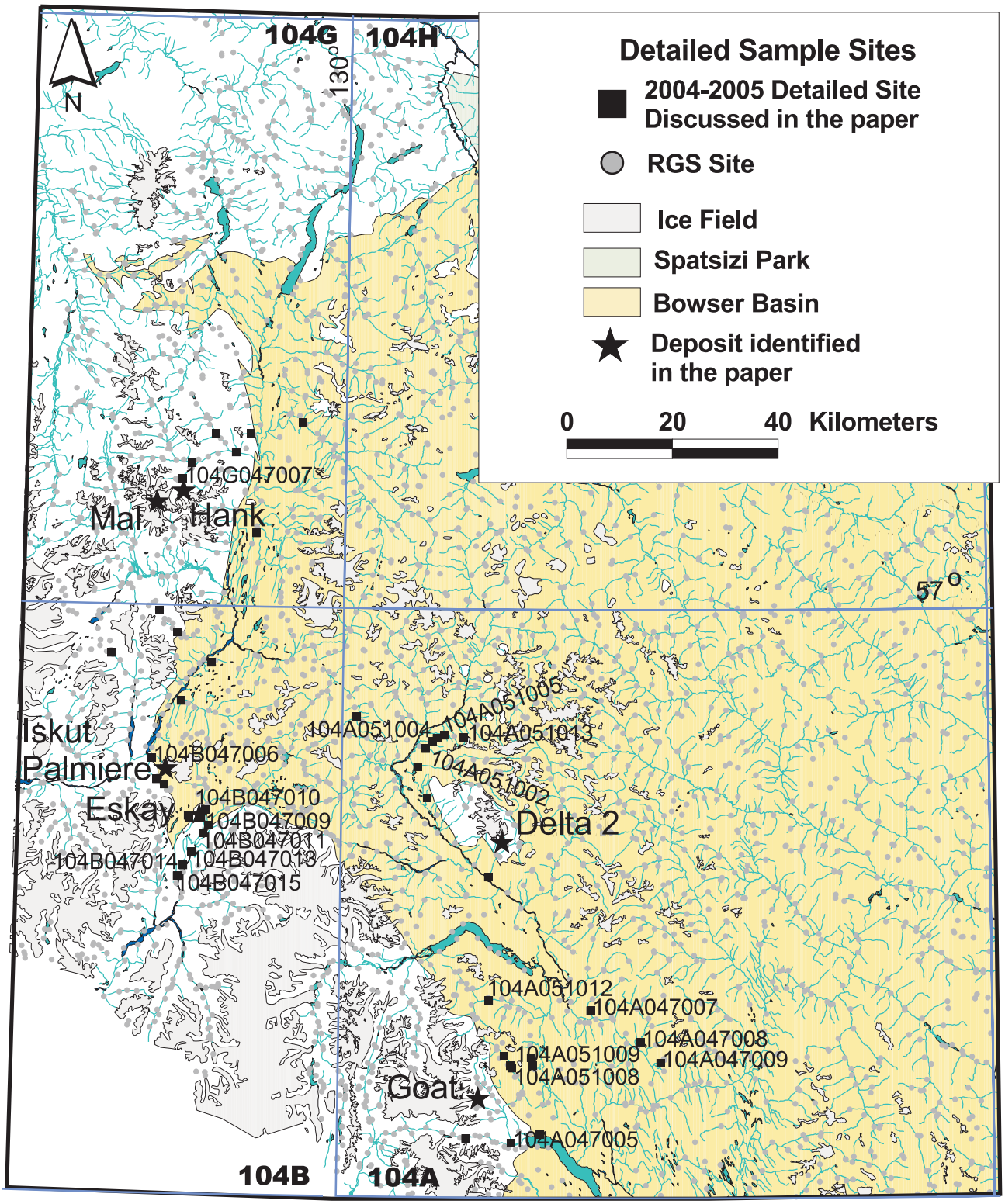


Figure 4. Mineral deposit and detailed sample locations discussed in the paper are identified on the map.

streams closer to the Eskay Creek mine suggests a similar epithermal mineral source for these anomalies. Northwest of the mine, sediment from a creek draining the area surrounding the Iskut Palmiere prospect contains 177 visible gold grains (Lett, at al., 2005). A more detailed examination of the chemistry and mineralogy of this sediment reveals a significant number of pristine gold grains in the HMC (*i.e.*, local source) and that Bi is the common anomalous element in both HMC and sediment. There are several single or multielement anomalies in the northwestern part of the follow-up survey area. Among them is sample 104G 7007, which has a distinct Au, Ag, As, Bi, Hg, Sb, Se and Tl association in sediment and HMC, and elevated Al, Cd, Cu, Zn and rare earth elements in the stream water. The source of this sediment-water geochemical anomaly may be Ag-Pb-Zn epithermal vein mineralization at prospects near the sample site, such as the Hank (MINFILE 104G07) and the MAL (MINFILE 104G147) prospects.

Sample 104A7005, located in the southwestern corner of the Bowser Lake map sheet (104A), has anomalous Au, Ag, As, Bi, Pb and Tl in the HMC and anomalous Pb, As and Bi in the sediment. This anomaly can be explained by geochemical dispersion from the past-producing Goat Ag-Pb-Zn-Au mine (MINFILE 104A02), located about 10 km upstream from the sample site. There are several sediment anomalies (*e.g.*. 104A 7007, 7008 and 7009) about 10 km northeast of the Goat deposit in an area underlain by Bowser Group sedimentary rocks. Among the elements characterizing these anomalies are Bi, Cd, Cu, Mo, Pb, Se and Zn. One possible source for these metals may be metal-rich shale.

Table 6 lists elements above the 3rd quartile for the –80 mesh fraction of sediment samples collected in 2005. Currently, no HMC or water geochemical data are available for the 2005 samples. However, water SO_4 was measured in the field using a Hach model SF-1 test kit. Several multielement anomalies defined by a 3rd quartile threshold are revealed in the –80 mesh fraction of the sediment. A number of these (*i.e.*, 2005104A 1008,1009,1012), located in the southwestern part of NTS 104A in an area underlain by Bowser Group sedimentary rocks, have a similar Au, Ag, As, Bi, Cd, Cu, Pb, Sb and Zn signature. There are currently no known sulphide mineral occurrences in the area. Among a cluster of anomalies in the northeastern part of the detailed survey area are one site (2005104A 1004) with a Ag, Cd, Se and Tl signature (Table 6), and three sites (2005104A 1002, 1005, 1013) with more than 50 ppm SO_4 in weakly alkaline water, but no corresponding elevated metal concentrations in the sediment. These samples are from streams draining the north side of the Oweegee Dome. The Delta 2 showing (MINFILE 104A166) is roughly 10 km to the south, but no mineralization has been found in the immediate area of the water anomalies.

CONCLUSIONS

Recently published regional stream sediment survey data for the Bowser Basin – Spatsizi River area reveals that most of the Au and pathfinder As-Sb-Hg element anomalies are in streams draining Hazelton Group rocks. However, there are also several weaker anomalies in drainages within the sedimentary Bowser Basin. Although many of the Hazelton anomalies can be traced to known base-precious metal mineralization, those in the Bowser Basin are still unexplained.

Detailed geochemical studies reveal a multielement Au, Ag, Bi, Cd, Cu, Hg, Mo, Pb, Sb, Se, Tl and Zn signature in the sediments and HMCs from streams draining the area around the Eskay Creek Au mine. The pristine shape of gold grains suggests a relatively local source for the grains. Stream waters typically have elevated Sb levels. A smaller Ag, As, Bi, Hg, Sb, Se, Tl ±Au element association characterizes sediment and HMC anomalies in streams draining other areas with known mineralization to the north of the Eskay Creek mine.

Heavy mineral geochemistry and the use of a smaller size fraction (–230 mesh) complements routine reconnaissance-scale regional geochemical surveys based on analysis of the –80 mesh fraction.

ACKNOWLEDGMENTS

Advice and assistance from Brian Grant during the fieldwork was very much appreciated. The authors would also like to thank Derek Weismiller of Lakelse Air for helicopter support, and the manager and staff of the Bell 2 Lodge for their hospitality. Acme Analytical Laboratories Ltd., Vancouver prepared the stream sediment samples and Overburden Drilling Management, Nepean, Ontario processed the heavy mineral concentrates.

REFERENCES

Alldrick, D., Jackaman, W. and Lett, R.E.W. (2004): Compilation and analysis of regional geochemical surveys around the Bowser Basin; *in* Geological Fieldwork 2003, *BC Ministry of Energy, Mines and Petroleum Resources*, Paper 2004-1, pages 163–166.

Alldrick, D., Nelson, J.L and Barresi, T. (2005): Geology and mineral occurrences of the upper Iskut River area — tracking the Eskay Rift through northern British Columbia; *in* Geological Fieldwork 2004, *BC Ministry of Energy, Mines and Petroleum Resources*, Paper 2005-1, pages 1–30.

Ferri. F, Osadetz. K and Evenchick, C. (2004): Petroleum source rock potential of Lower to Middle Jurassic clastic intermountain basins, British Columbia; *in* Summary of Activities 2004, *BC Ministry of Energy, Mines and Petroleum Resources*, pages 87–96.

Friske, P.W.B., Jackaman, W., Lett, R.E.W. and McCurdy, M.W. (2005): Regional stream sediment and water geochemical data, northwestern British Columbia, *Geological Survey of Canada*, Open File 5000, *BC Ministry of Energy, Mines and Petroleum Resources*, RGS Open File 58

Holland, S.S. (1964): Landforms of British Columbia; *BC Ministry of Energy, Mines and Petroleum Resources*, Bulletin 48, 138 pages.

Jackaman, W. (2005) Spatsizi River stream sediment and water survey; *in* Geological Fieldwork 2004, *BC Ministry of Energy, Mines and Petroleum Resources*, Paper 2005-1, pages 221–224.

Lett, R.E.W. and Jackaman, W. (2003): Re-analysis of regional stream sediment survey samples from the Iskut River area (NTS 104B and G); *BC Ministry of Energy, Mines and Petroleum Resources*, Geofile 2003-20, 14 pages.

Lett, R.E.W., Friske, P.W.B. and Jackaman, W. (2005): National Geochemical Reconnaissance Program in northwestern BC: Bowser Lake (NTS 104A) regional geochemical survey; *BC Ministry of Energy, Mines and Petroleum Resources*, Paper 2005-1, pages 61–66.

Matysek, P.F., Day, S.J., Gravel, J.L. and Jackaman, W. (1988a): 1987 regional geochemical survey: 104F (Sumdum) and

104G (Telegraph Creek): *BC Ministry of Energy, Mines and Petroleum Resources*, RGS 19, *Geological Survey of Canada*, Open File 1646.

Matysek, P.F., Day, S.J., Gravel, J.L. and Jackaman, W. (1988b): 1987 regional geochemical survey: 104B (Iskut River); *BC Ministry of Energy, Mines and Petroleum Resources*, RGS 18, *Geological Survey of Canada*, Open File 1645.

MINFILE (2005): MINFILE BC mineral deposits database; *BC Ministry of Energy, Mines and Petroleum Resources*, <http://www.em.gov.bc.ca/mining/Geolsurv/Minfile/> [Nov 2005].

Geochemical Surveys in the Lillooet Area (NTS Areas 092J, 092I, 092O, 092P), Southwestern British Columbia

By R.E. Lett

KEYWORDS: Lillooet, Spences Bridge Group, regional geochemical survey, geochemical samples

INTRODUCTION

Preliminary results of detailed drainage sediment, rock and soil sampling in a 500 km^2 area north of Lillooet, British Columbia (Fig. 1) are described in this paper. Volcanic and sedimentary rocks of the Spences Bridge Group underlie much of the area, and the group has been the recent focus of considerable exploration activity south of Lillooet. This activity started through the discovery of gold-mineralized quartz veins in 2002 by a company doing follow-up prospecting of government regional geochemical stream sediment survey data. The geochemical sampling described in this paper aimed to,

- find new mineral deposits,
- establish geochemical backgrounds for baseline determination,
- test other geochemical prospecting methods, and
- train First Nation and local community members in geochemical sampling methods.

SURVEY AREA

Physiography and Climate

Geochemical sampling focused on a 15 km wide corridor along the west side of the Fraser River between Lee and Ward Creeks (Fig. 2). Topography of the surveyed area is typical of the Camelsfoot Range that forms a transitional physiography between the Coast Mountains and the Fraser Plateau. The Camelsfoot Range is moderately rugged with steep and often precipitous slopes reflecting a change from elevations above 2000 m in the west to below 300 m along the Fraser River (Holland, 1964). There is a dissected plateau formed by Miocene volcanic rocks at about 1000 m elevation between McKay and Watson Bar creeks. Climate and vegetation are typical of transitional uplands between the Coast Mountains and the Fraser Plateau. Annual rainfall is less that 280 mm and temperatures range from –1°C in winter to above 40°C in summer. Vegetation along the Fraser River valley is typically steppe or bunchgrass prairie, with sagebrush or occasional ponderosa pine or Douglas-fir. Interior Douglas-fir, Montane Spruce and

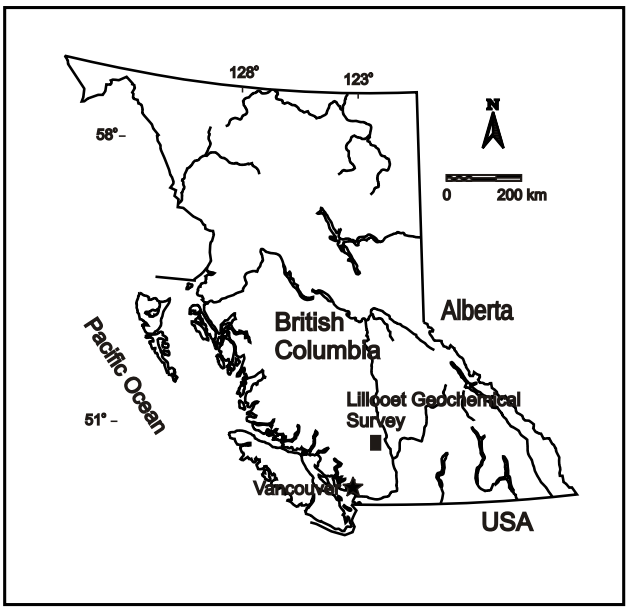


Figure 1. Location of the geochemical survey near Lillooet, British Columbia.

Engelmann Spruce are the dominant canopy species at higher elevations. Larger streams (*e.g.*, Slok Creek, McKay Creek and Leon Creek) flow east from the uplands through deeply incised, narrow valleys into the Fraser River. In late summer, the larger creeks have a diminished water flow and many of the second and first-order drainages are completely dry.

Surficial Deposits

Trettin (1961) suggested that more than 300 m of unconsolidated sediment, ranging from boulder gravel to mud, filled the Fraser River valley by the late Pleistocene. Deltaic crossbedded sediments, silt deposits and mudflows are evidence for braided streams, glacial lakes and alluvial fans formed from tributaries of the proto–Fraser River. Recent rejuvenation caused the river channel to erode through the Pliocene sediments to bedrock. At higher elevations above the Fraser River talus and colluvium mantle the steeper slopes. The absence of glacial ice-flow features and rare, localized till deposits in the surveyed area can be explained by minimal movement of the Pliocene ice sheet close to a major ice divide.

Geology

Rocks in the surveyed area comprise the Middle to Late Cretaceous (Albion) Spences Bridge Group, the Mid-

This publication is also available, free of charge, as colour digital files in Adobe Acrobat PDF format from the BC Ministry of Energy, Mines and Petroleum Resources internet website at http://www.em.gov.bc.ca/Mining/Geolsurv/Publications/catalog/catfldwk.htm

dle to Early Cretaceous Jackass Mountain Group, the Eocene Ward Creek assemblage and the Miocene to Pliocene Chilcotin Group. Spences Bridge and Jackass Mountain rocks are exposed as panels within the Fraser fault zone, a major northwest-trending dextral wrench fault system of Eocene age that comprises the Fraser fault, the Slok Creek fault, the Hungry Valley fault and the Watson Bar thrust (Trettin, 1961; Read, 1988). Offsets across the fault are most likely in the order of 130 km (Monger and Journeay, 1994). Cathro *et al.* (1998) described the Early Cretaceous Jackass Mountain Group as a southwest-dipping assemblage of volcaniclastic sedimentary rocks deposited as a submarine fan complex in a fore-arc environment represented by Tyaughton Basin. In the surveyed area, the Spences Bridge Group comprises an upper unit of grey to green dacite, andesite and minor basalt, and a lower unit of volcanic arenite, conglomerate, minor siltstone, phyllitic argillite and rare carbonaceous shale. Eocene rocks are volcanic pebble conglomerate, shale, rhyodacite flows and tuffaceous wacke. Pliocene to Miocene Chilcotin rocks are mainly vesicular and amygdaloidal basalt with minor conglomerate and sandstone (Read, 1988).

Mineral Deposits

A cluster of mineral occurrences in the northern part of the surveyed area forms part of the Watson Bar Au belt. Cathro *et al.* (1998) described five distinct styles of gold mineralization hosted by Jackass Mountain rocks:

- iron carbonate–silica alteration zones enriched in Au, As, Sb and Hg
- thrust-hosted quartz-sulphide mineralization

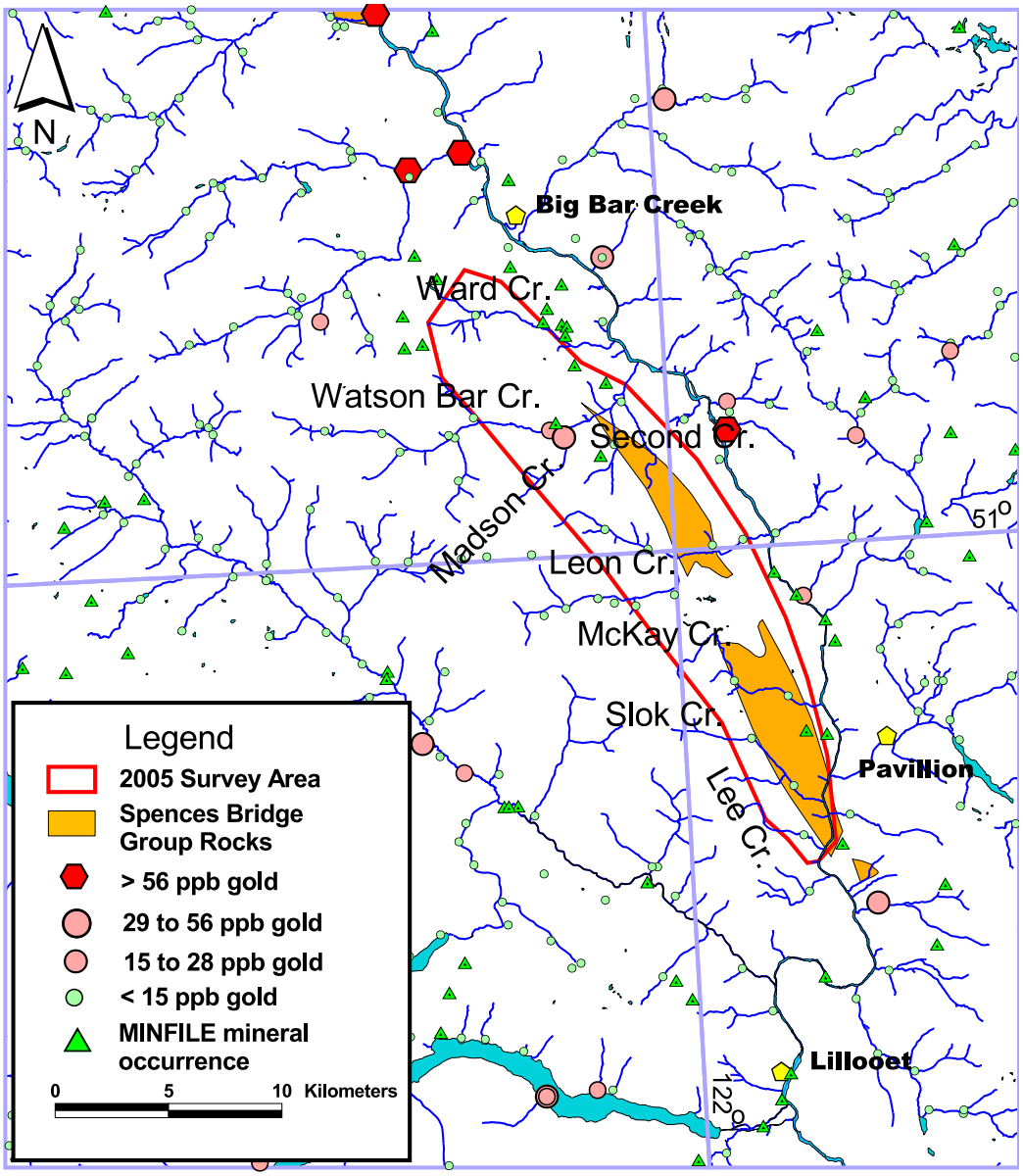


Figure 2. Gold by instrumental neutron activation analysis (INAA) in stream sediment samples taken during 1992 and 1994 regional geochemical surveys in the Lillooet area.

- quartz-sulphide veins related to quartz-feldspar porphyry sills intruding Jackass Mountain sedimentary rocks
- high-angle quartz-sulphide veins and stockworks
- Au-enriched horizons in the sedimentary rocks

The largest mineral occurrence in the surveyed area is the Watson Bar developed prospect (MINFILE 092O 051; MINFILE, 2005), where a shallow southwest-dipping thrust (zone V) contains an estimated 136 962 t grading 14.33 g/t Au (Cathro *et al.*, 1998). The Watson Bar prospect has been classified as an epithermal Au-Ag low-S deposit. Other smaller Au occurrences in the area are the MAD (MINFILE 092O 092), Buster (MINFILE 092O 055) and Astonisher (MINFILE 092O 054). Read (1988) documented a number of perlite, volcanic glass and bentonite industrial mineral occurrences in the surveyed area.

SURVEY METHODS

Sampling

In August 2005, 25 stream sediment, 25 stream water, 10 moss mat and 4 bulk sediment samples were collected from sites between Ward and Lee Creeks (NTS map sheets 092J, 092I, 092O and 092P). Sediment typical of that taken during reconnaissance-scale geochemical surveys was collected in high-wet-strength Kraft paper bags from mid and lateral bars in active stream channels at locations selected to avoid extremes of high or low energy. Water, taken from the active stream flow, was collected in a 12 mL Nalgene® bottle rinsed with stream water several times before collection. Living moss, where attached to boulders and logs, was collected in Kraft paper bags from just above the stream water surface. Field duplicate samples, generally 2–3 m apart, were collected from the same type of material and stream environment. Information about the sample, such as sediment texture, stream size and water flow, was recorded at each site.

Ideally, bulk sediment for preparation of a heavy mineral concentrate (HMC) fraction was taken at the upstream point of midchannel bars. At each HMC site a 5 gallon plastic pail was lined with a heavy-duty polyethylene plastic bag (18 x 24 inches, 4 mil) and sediment was wet-sieved through a 12-mesh (1.68 mm) stainless steel sieve until a sample weight of 10–15 kg was obtained. The sample was weighed in the pail before the opening was taped shut with black electrical tape and placed in a second bag. Bulk samples were shipped directly to the Geological Survey of Canada for preparation and analysis. Twenty-four rock samples were taken from outcrops in the surveyed area and five C-soil horizon samples were collected from pits dug close to roads.

Sample Preparation

Fine-textured sediment and moss mat sediment samples were prepared in the BC Geological Survey Laboratory in Victoria. The samples were air dried and the –18 mesh (<1 mm) fraction recovered by gently disaggregating the sediment or by pounding the moss mat before dry sieving through a 1 mm stainless steel screen. A split of the 1 mm fraction was then screened to –80 mesh ASTM (<0.177 mm) and a second split screened to –230 mesh (<0.063 mm). Control reference material and sieved analytical duplicate samples were inserted into each analytical block of 20 sediment samples. Any remaining –80 and –230 mesh sediment was archived for future analyses. Water samples were analyzed for pH and conductivity in the field using a calibrated Hanna model HI 98129 meter. A portion of the water sample was filtered though a 0.45 µm filter and acidified with Seastar Baseline 50% nitric acid.

TABLE 1. DETECTION LIMITS, PRECISION (% RSD) AND ACCURACY FOR ELEMENTS ANALYZED BY INSTRUMENTAL NEUTRON ACTIVATION (_INA) AND AQUA REGIA – INDUCTIVELY COUPLED PLASMA – MASS SPECTROMETRY (_ICP), LILLOOET AREA GEOCHEMICAL SURVEY. ABBREVIATIONS: DL, INSTRUMENTAL DETECTION LIMIT; GSBRM, ANALYSIS OF STSD 1 IDENTIFIED AS SAMPLE 92O20051008; STSD 1, RECOMMENDED ELEMENT VALUES BY LYNCH (1990) FOR CANMET REFERENCE MATERIAL; MEAN, MEAN OF TWO ANALYSES; % RSD, PERCENT RELATIVE STANDARD DEVIATION FOR TWO ANALYSES; % DIFF., PERCENT DIFFERENCE BETWEEN TWO ANALYSES; GRAV, LOSS-ON-IGNITION AT 550°C; ND, NOT DETERMINED BY CANMET

Element	Units	DL	Mean	% RSD	GSBRM	STSD 1	% Diff.
Ag_ICP	ppb	2	81	8	274	300	9.1
As_ICP	ppm	0.1	5.50	1.9	17.9	17	5.2
As_INA	ppm	0.5	4.8	23.6	23.8	23	3.4
Au_ICP	ppb	0.2	99.60	56.4	8.7	8	8.4
Au_INA	ppb	2	33	17.0	23	8	96.8
Ba_INA	ppm	50	410	6.9	780	630	21.3
Bi_ICP	ppm	0.02	0.51	1.4	0.44	N.D.	N.D.
Cd_ICP	ppm	0.01	0.23	6.2	0.9	0.8	11.8
Co_ICP	ppm	0.1	12.1	0.6	13.9	14	0.7
Co_INA	ppm	1	9.5	7.4	18	17	5.7
Cr_ICP	ppm	0.5	21.3	3.5	27.7	67	83.0
Cr_INA	ppm	5	37	0.0	58	67	14.4
Cu_ICP	ppm	0.01	178.50	0.6	34.22	36	5.1
Fe_INA	%	0.01	3.59	0.6	4.73	4.7	0.6
Hg_ICP	ppb	5	19	7	100	110	9.5
LOI_GRAV	%	0.01	4.15	2.6	29.5	31.6	6.9
Mn_ICP	ppm	1	459	0.1	3568	3740	4.7
Mo_ICP	ppm	0.01	14.25	2.9	1.06	2	61.4
Ni_ICP	ppm	0.1	13.35	0.8	19.5	18	8.0
Pb_ICP	ppm	0.01	6.90	0.46	33.11	34.00	2.70
Sb_ICP	ppm	0.02	0.19	9.6	2.3	2	14.0
Sb_INA	ppm	0.1	0.7	32.6	4.7	3.3	35.0
Se_ICP	ppm	0.1	3.50	1.0	1.9	N.D.	N.D.
V_ICP	ppm	2	101	0.4	46	47	2.2
Zn_ICP	ppm	0.1	54.40	1.2	154.2	165	6.8

Sample Analysis

Prepared stream sediment, moss sediment and rock samples, with quality-control replicate and standard reference materials, were analyzed at Acme Analytical Laboratories Ltd., Vancouver, BC for 37 trace and minor elements by a combination of inductively coupled plasma – mass spectrometry (ICP-MS) and inductively coupled plasma – emission spectrometry (ICP-ES) following aqua regia digestion. Selected –80 mesh fraction sediment samples were also analyzed for Au and 32 trace elements at Actlabs, Ancaster, Ontario by instrumental neutron activation analysis (INAA). Instrumental detection limits for selected elements are listed in Table 1. Filtered, acidified water samples, CANMET river water SLRS 3, unfiltered water

blanks and filtered blanks were analyzed for major and trace elements by ICP-MS at Acme Analytical Laboratories Ltd. Detection limits for trace elements in water range from 0.05 to 0.1 ppb. Preparation of a heavy mineral concentrate (HMC) from the bulk sediment samples and analysis of the HMC for Au and trace elements is still in progress.

Quality Control

Reliable data interpretation depends on discriminating between real geochemical trends and those variations introduced by sampling and analysis. Control reference standards and analytical duplicates are therefore routinely inserted into the batches of stream sediment, stream water and moss sediment samples submitted for commercial analysis to measure accuracy and precision. National Geochemical Reconnaissance (NGR) quality-control procedures used in this project are based on analysis of seventeen routine sediment or water samples, a field duplicate sample, an analytical duplicate sample or water blank, and A control reference sample in a block of 20 samples. Results from this project show that, for most elements, the combined analytical and sampling variation expressed as a percentage difference between duplicate sample values is less that 20%. Table 1 lists mean concentration and percent relative standard deviation (% RSD) for a duplicate pair of the BC Geological Survey sediment reference material for each element. Also shown in Table 1 is the percentage difference between analyses of stream sediment reference material STSD1 and the CANMET recommended value for this material (Lynch, 1990).

Precision (% RSD) for most elements other than Au, As (INAA) and Sb (INAA) is less than 10%. Lower preci-

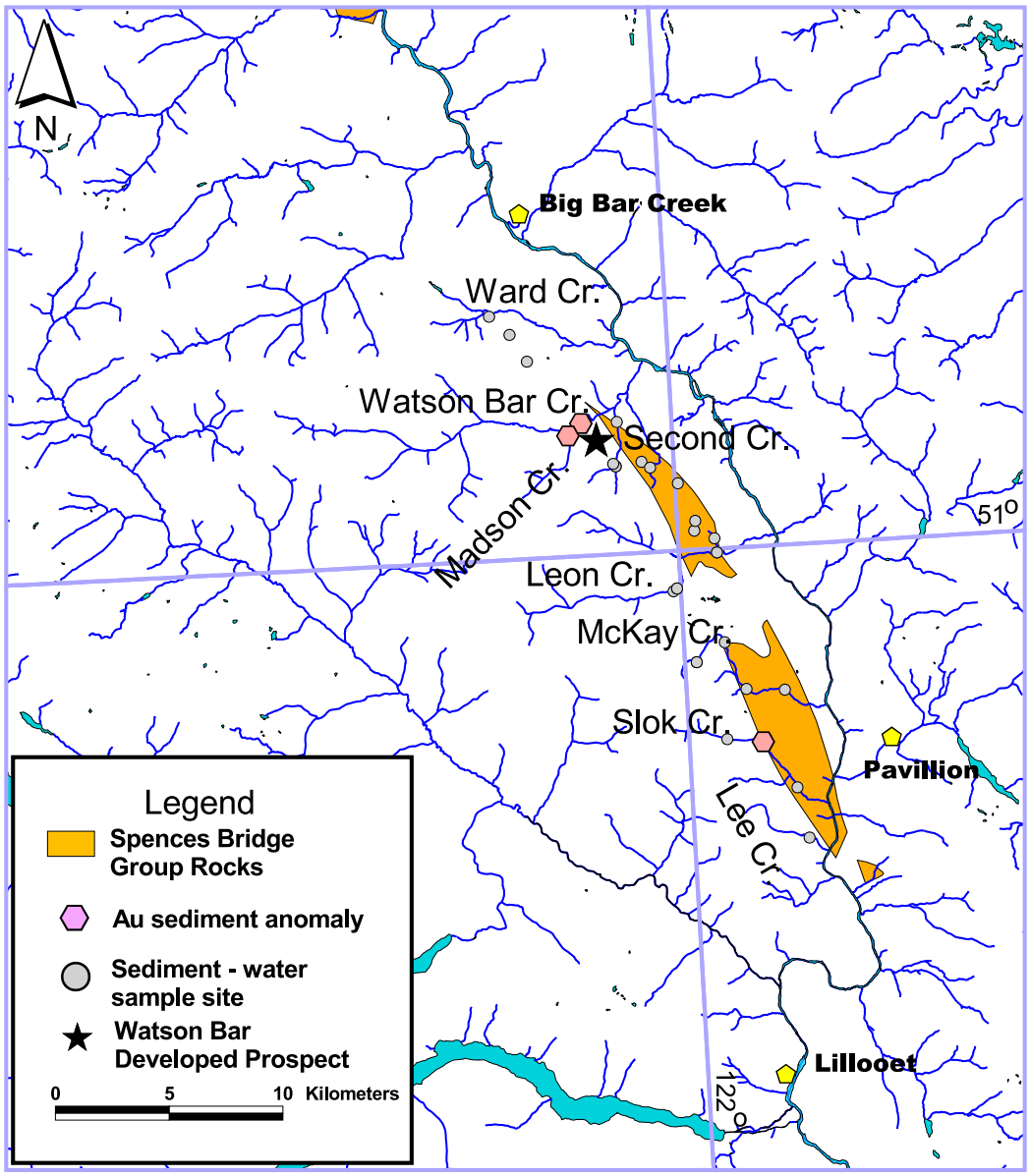


Figure 3. Stream sediment and water sample locations, 2005 detailed geochemical survey, Lillooet area. Symbols indicate sites with anomalous Au in stream sediment.

TABLE 2. MOSS SEDIMENT (MOSS) AND STREAM SEDIMENT (SED.) STATISTICS, LILLOOET AREA DETAILED GEOCHEMICAL SURVEY. MEAN, MEDIAN, 3RD QUARTILE, 95TH PERCENTILE, MAXIMUM AND MINIMUM VALUES HAVE BEEN CALCULATED FROM DATA FOR 25 SEDIMENT AND 10 MOSS MAT SAMPLES

Element	Units	Mean		Median		3rd Quartile		Maximum		95th Percentile	
		Sed.	Moss	Sed.	Moss	Sed.	Moss	Sed.	Moss	Sed.	Moss
Ag_ICP	ppb	53	71	46	76	73	82	110	103	88	94
As_ICP	ppm	31.4	69.3	4.5	5.8	17.8	66.3	289.2	353.9	184.1	290.4
As_INA	ppm	24.7	43.3	2.4	3.2	92.2	10.9	188.0	226.0	127.2	190.4
Au_ICP	ppb	2.6	6.7	0.7	0.7	1.5	7.9	29.6	28.8	9.6	27.0
Au_INA	ppb	17	92	2	5	3	6	331	494	23	426
Ba_INA	ppm	426	380	410	350	690	430	780	580	644	580
Bi_ICP	ppm	0.07	0.08	0.05	0.06	0.07	0.07	0.26	0.18	0.16	0.18
Cd_ICP	ppm	0.01	0.10	0.10	0.11	0.12	0.14	0.22	0.17	0.16	0.16
Co_ICP	ppm	13.7	14.6	13.7	12.1	15.4	14.8	29.5	24.7	21.5	24.1
Co_INA	ppm	11	10	11	8	19	13	22	17	19	17
Cr_ICP	ppm	40.2	45.1	41.6	46.8	46.9	51.6	54.2	54.1	52.7	54.0
Cr_INA	ppm	80	96	77	86	125	115	126	141	123	133
Cu_ICP	ppm	39.84	46.81	28.88	28.52	38.38	52.16	182.63	120.85	89.44	110.78
Fe_INA	%	2.76	2.66	2.60	2.43	4.74	3.27	5.46	3.50	4.38	3.49
Hg_ICP	ppb	204	214	32	59	60	242	3282	1035	461	739
LOI_GRAV	%	9.30	11.99	8.40	9.50	10.35	14.90	17.90	18.30	17.80	18.10
Mn_ICP	ppm	597	633	582	619	643	657	1080	821	897	796
Mo_ICP	ppm	0.64	0.73	0.40	0.54	0.48	1.01	2.58	1.41	2.04	1.37
Ni_ICP	ppm	32.4	34.6	33.1	34.4	36.7	38.0	43.4	41.0	41.7	40.4
Pb_ICP	ppm	4.70	5.55	4.58	4.81	5.12	5.38	8.49	12.61	7.72	9.43
Sb_ICP	ppm	0.8	1.6	0.2	0.4	0.4	2.2	7.8	6.9	3.4	5.5
Se_ICP	ppm	0.8	1.0	0.6	0.9	0.9	1.1	3.8	2.4	1.9	2.0
V_ICP	ppm	78	89	80	92	90	95	115	132	112	117
Zn_ICP	ppm	60.7	66.2	59.1	65.3	68.3	67.9	93.6	83.5	80.1	78.2

TABLE 3. STATISTICS FOR THE –80 AND –230 MESH FRACTIONS OF STREAM SEDIMENT, LILLOOET AREA DETAILED GEOCHECMICAL SURVEY. MEDIAN, 3RD QUARTILE AND MAXIMUM VALUES HAVE BEEN CALCULATED FROM DATA FOR TWENTY-FIVE –80 MESH AND THIRTEEN –230 MESH SEDIMENT SAMPLES. CONTRAST IS THE RATIO OF THE MAXIMUM VALUE TO THE 3RD QUARTILE

Element	Units	Mean		Median		3rd Quartile		Maximum		Contrast	
		-80	-230	-80	-230	-80	-230	-80	-230	-80	-230
Ag_ICP	ppb	54	124	46	68	73	80	110	826	1.5	10.3
As_ICP	ppm	31.3	46.2	4.5	20.9	17.8	48.0	289.2	260.1	16.2	5.4
Au_ICP	ppb	2.6	6.5	0.7	0.9	1.5	2.2	29.6	59.5	19.7	27.0
Bi_ICP	ppm	0.07	2.39	0.05	0.08	0.10	0.09	0.26	0.17	2.6	1.9
Cd_ICP	ppm	0.11	0.14	0.10	0.14	0.10	0.14	0.22	0.22	2.2	1.6
Co_ICP	ppm	13.7	14.2	13.7	13.2	15.4	16.5	29.5	25.9	1.9	1.6
Cr_ICP	ppm	40.2	40.8	41.6	40.5	46.9	41.9	54.2	52.8	1.2	1.3
Cu_ICP	ppm	39.8	46.6	28.9	41.3	38.4	63.1	182.6	106.3	4.8	1.7
Fe_ICP	%	3.05	3.07	2.98	3.13	3.40	3.38	5.61	4.66	1.7	1.4
Hg_ICP	ppb	204	371	32	262	60	588	3282	999	54.7	1.7
Mn_ICP	ppm	597	664	582	638	643	674	1080	1286	1.7	1.9
Mo_ICP	ppm	0.6	0.6	0.4	0.6	0.5	1.5	2.6	2.1	5.2	1.4
Ni_ICP	ppm	32.4	32.0	33.1	32.3	36.7	33.1	43.4	39.7	1.2	1.2
Pb_ICP	ppm	4.80	5.60	4.60	5.20	5.10	6.20	8.50	9.20	1.7	1.5
Sb_ICP	ppm	0.82	1.17	0.22	0.41	0.40	1.53	7.79	3.95	19.5	2.6
Se_ICP	ppm	0.8	1.1	0.6	0.6	0.9	1.6	3.8	4.4	4.2	2.8
V_ICP	ppm	78	74	80	71	90	91	115	109	1.3	1.2
Zn_ICP	ppm	60.7	65.7	59.1	64.3	68.3	76.3	93.6	82.7	1.4	1.1

sion for Au by ICP-MS (56%) reflects the small sample (1 g) used for the analysis. Accuracy (difference between reported and recommended) for Au, Ba, Cd, Cr, Mo and Sb is greater than 10%. Low accuracy (>10%) for some of the elements (*e.g.*, Cr) can be explained by a difference between the methods used to produce the reported and recommended value. The reason for a large difference (93%) between the reported and recommended Au value for STSD 1 is presently unknown. Percent relative standard deviation values for As, Ba, Cu, Ni, Pb and Zn calculated from duplicate analyses of the river water standard SLRS 3 are less than 10%. Mean values for these elements are less than 10% different than their CANMET recommended value in the water standard. Filtered water blanks analyzed with the stream water samples have less than 1.5 ppb Cu, less than 1.5 ppb Zn and detectable Pb and As.

RESULTS

Previous Regional Survey Results

Figure 2 shows the concentration of Au in stream sediment samples collected during previous regional geochemical surveys that covered the surveyed area (Jackaman *et al.*, 1992a, b; Jackaman and Matysek, 1994). The highest Au value (43 ppb) detected in the area covered by detailed sampling is in sediment from Madson Creek, a north-flowing tributary of Watson Bar Creek. This sediment also contains 343 ppm As and 14.2 ppm Sb in the sediment. The source of the Au and other anomalous metals in Madson creek is the Au mineralization at the Watson Bar developed prospect.

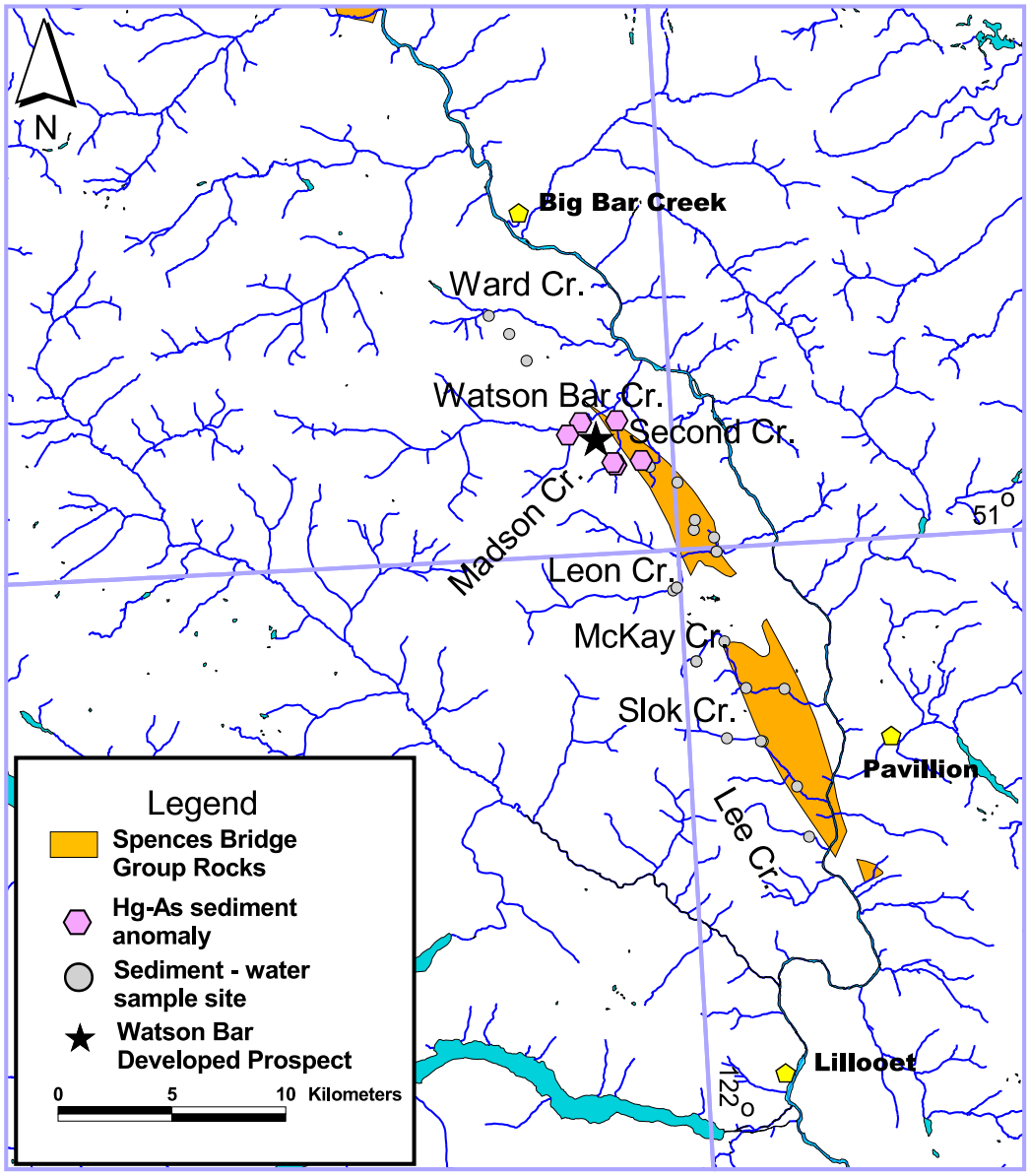


Figure 4. Stream sediment and water sample locations, 2005 detailed geochemical survey, Lillooet area. Symbols indicate sites with anomalous As-Hg in stream sediment.

Detailed Survey Results: Drainage Sample Type and Size Fraction Comparison

Figure 3 shows the location of the steam sediment and water samples collected during the detailed survey. Listed in Table 2 are selected element statistics for stream sediment and moss mat samples, including both 3rd quartile and 95th percentile values. The 3rd quartile can be a more realistic threshold for a small dataset than the more traditional 95th percentile. Both 3rd quartile and 95th percentile show that most elements (*e.g.*, Au, Ag, Cu, As, Hg, Mo, Pb) are higher in the moss sediment than in the stream sediment. Matysek and Day (1988) reported a similar pattern of element enhancement in the moss sediment from streams draining Cu and Au mineralization on Vancouver Island. Higher element values most likely reflect capture of metal-rich suspended sediment, including Au grains, by moss during periods of higher stream flow. Although moss sediment analysis can improve geochemical anomaly contrast (Matysek and Day, 1988), the moss is not present in every stream due to the relatively dry climate. It therefore has limited exploration application in the Lillooet area.

Table 3 compares the –80 mesh stream sediment geochemistry with that of the –230 mesh fraction. Third quartile values show that elements are higher in the –230 mesh fraction of the sediment, with the exception of Cr and Ni. Except for Ag and Au, however, the geochemical anomaly contrast (ratio of the maximum to 3rd quartile) is larger in the –80 mesh fraction. Although the ability of stream sediment geochemistry to detect Au mineralization is improved by using the –230 mesh fraction, there are limitations to using this fraction, such as 1) the need to collect a larger sample for preparation of enough material for analysis, 2) the problem of levelling data produced from the two

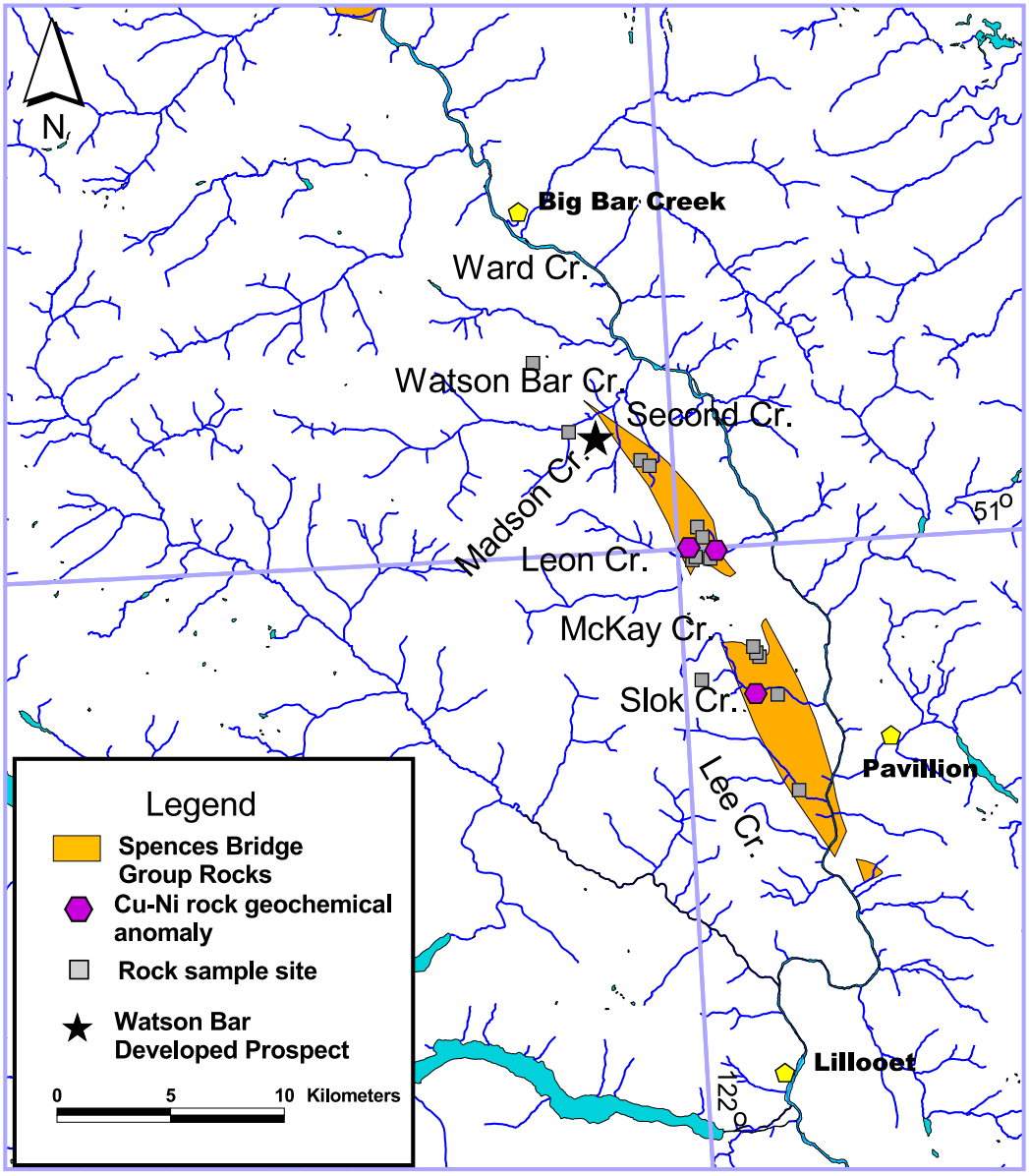


Figure 5. Location of rock samples collected during the 2005 detailed geochemical survey, Lillooet area. Symbols indicate sites with anomalous Cu-Ni in bedrock.

TABLE 4. STATISTICS CALCULATED FROM ANALYTICAL DATA FOR 21 SAMPLES OF VOLCANIC ROCK FROM THE SPENCES BRIDGE GROUP, LILLOOET AREA DETAILED GEOCHEMICAL SURVEY

Element	Mean	Median	3rd Quartile	Maximum	95th Percentile
Ag_ICP	47	35	46	259	72
As_ICP	4.8	4.9	7.0	12.2	10.7
Au_ICP	0.7	0.5	0.9	2.7	1.80
Bi_ICP	0.1	0.0	0.1	0.2	0.15
Cd_ICP	0.10	0.07	0.10	0.35	0.31
Co_ICP	18.4	17.9	20.9	39.9	33.3
Cr_ICP	49.4	37.0	67.0	128.5	115.7
Cu_ICP	52.0	46.1	65.9	129.61	88.78
Fe_ICP	3.5	3.6	4.4	6.27	5.05
Hg_ICP	10	7.0	14.0	45	35
Mn_ICP	665	664.0	820.0	1164	1064
Mo_ICP	0.38	0.35	0.49	0.59	0.58
Ni_ICP	41.2	28.0	48.2	180.7	125.8
Pb_ICP	3.53	3.24	3.39	12.63	5.42
Sb_ICP	0.15	0.14	0.18	0.43	0.36
V_ICP	121	110	163	252	228
Zn_ICP	59.7	54.6	71.6	125.3	77.20

TABLE 5. STATISTICS CALCULATED FROM ANALYTICAL DATA FOR FIVE C-HORIZON SOIL SAMPLES, LILLOOET AREA DETAILED GEOCHEMICAL SURVEY

Element	Mean	Median	3rd Quartile	Maximum	95th Percentile
Ag_ICP	76	60	101	135	128
As_ICP	6.7	6.1	8.3	9.4	9.2
Au_ICP	2.6	2.2	3.1	3.6	3.5
Bi_ICP	0.08	0.08	0.08	0.10	0.10
Cd_ICP	0.17	0.18	0.18	0.21	0.20
Co_ICP	18.00	19.20	19.40	22.40	21.80
Cr_ICP	64.7	64.8	67.4	73.0	71.9
Cu_ICP	49.76	48.70	55.34	56.72	56.44
Fe_ICP	4.24	4.19	4.20	4.70	4.60
Hg_ICP	46	39	55	93	85
Mn_ICP	576	611	619	806	769
Mo_ICP	0.63	0.60	0.61	0.82	0.78
Ni_ICP	65.60	62.80	67.00	78.70	76.40
Pb_ICP	4.85	4.47	4.97	6.40	6.11
Sb_ICP	0.36	0.35	0.37	0.51	0.48
Se_ICP	0.2	0.2	0.2	0.3	0.3
V_ICP	86	88	88	98	96
Zn_ICP	70.4	73.4	76.8	81.2	80.3

size fractions, and 3) the lower anomaly contrast for other elements.

Detailed Survey Results: Sediment and Water Geochemistry

Sediment samples (–80 mesh fraction) with more than 10 ppb aqua regia – ICP-MS Au or 23 ppb INAA Au are identified on Figure 3. The multielement signature of stream anomalies can help characterize the source mineralization. The highest Au value (311 ppb by INAA) is accompanied by 188 ppm As and 511 ppb Hg in sediment from Matson Creek, which flows from the Watson Bar epithermal Au-Ag deposit. Watson Bar creek sediment has only to 25 ppb Au but up to 210 ppm As in the sediment. This compares to sediment with 21 ppb Au, 38 ppm As and 230 ppb Hg taken from a similar site in the creek during the original regional survey. Samples of the –80 mesh sediment with more than 18 ppb As and 60 ppb Hg (3rd quartile) shown on Figure 4 cluster around the Watson Bar deposit. The sediment also has elevated As, Bi, Cu and Mo values, but only background Au levels. Anomalous As and Hg can be detected 2 km from the Au mineralization in Second Creek, a stream flowing north into Watson Bar Creek.

Although no other samples in the survey area have anomalous As and Hg, one sample from Slok Creek, close to the contact between the Spences Bridge and Jackass Mountain groups, has 29 ppb Au determined by aqua regia – ICP-MS but no detectable Au by INAA. This difference can be explained by the characteristic high variability or 'nugget effect' of Au in stream sediment. Stream waters are alkaline (median pH 8.3) and typically have a high (50–100 ppm) dissolved Ca-Mg concentration. Concentrations of most trace heavy metals (*e.g.*, Cr, Ag) are either below or just above instrument detection limit. Low concentrations of pathfinder metals (*e.g.*, As, Cd, Pb, Cu, Zn) are detectable in the stream water. For example, the highest amounts are 1.4 ppb Pb, 2.3 ppb Zn, 38 ppb Cu and 17.5 ppb As in water from the upper reach of a branch of Second Creek. Two kilometres downstream, the As level is 3.3 ppb and other metals are below detection limit.

Detailed Survey Results: Rock and Overburden Geochemistry

Table 4 lists statistics calculated from data for 21 samples of volcanic rock from the Spence's Bridge Group collected as part of the survey (Fig. 5). The maximum Au value detected in the sample suite is 2.7 ppb and there are no high concentrations of those pathfinder elements characteristically associated with Au mineralization in the area (*e.g.*, As, Hg). However, Table 4 reveals that the Spences Bridge Group has relatively high background levels for Cu, Ni and V. The actual background levels for these and other elements (*e.g.*, Cr and Ba) may be even higher because the aqua regia digestion will not dissolve all of the aluminosilicate and oxide minerals and therefore will not liberate all of the silicate-bound metal. Figure 5 shows the locations of samples with more than 65 ppm Cu and 48 ppm Ni. These samples also have elevated V and appear to cluster near the fault-bounded contact of the Spences Bridge Group. The anomalous Cu and Ni could be explained by fault-controlled serpentinization of mafic or ultramafic rocks in the volcanic stratigraphy. Further analysis of the rock samples by INAA is in progress. Table 5 lists statistics calculated from aqua regia – ICP-MS data for five C-horizon soil samples collected on plateau area underlain basalt. The C-horizon soil samples have a relatively uniform distribution of elements, and no anomalous Au values were detected.

CONCLUSIONS

Detailed stream geochemical studies in an area north of Lillooet reveal that,

- sediment and moss sediment in streams draining the Watson Bar Au-Ag deposit have anomalous As and Hg values, with varying amounts of Au. Arsenic and Hg are geochemical pathfinders for the epithermal Au-Ag min-

eralization. Dissolved metal in alkaline stream water flowing from the Au-mineralized area fall to levels approaching instrument detection limit within 2 km downstream.

- the –230 mesh fraction of stream sediment and –80 mesh fraction of moss sediment typically have higher metal contents than the –80 mesh fraction of stream sediment. However, except for Au and Ag, geochemical anomaly contrast for elements in the –80 mesh stream sediment is larger than the –230 mesh stream sediment fraction.
- Au and As levels in the sediment are similar to those found in a previous regional geochemical survey.
- one sediment sample from Slok Creek has detectable Au measured by aqua regia ICP-MS but no other anomalous metal. Rock and C-horizon soil samples have no anomalous Au, As or Hg, but elevated Cu and Ni values could reflect the presence of mafic rocks associated with faulting.

ACKNOWLEDGMENTS

The Ts'kw'aylaxw Band Council is acknowledged for supporting the survey carried out over their asserted traditional lands west of the Fraser River. Garrett Larochelle from the Ts'kw'aylaxw Band helped with much of the geochemical sampling, and his spontaneous enthusiasm in the field is very much appreciated. I learned much from Garrett about Ts'kw'aylaxw traditions and culture during the survey. I also appreciate the assistance from Colin Smith during the initial stages of the fieldwork and guidance from Mike Cathro on regional geology and survey logistics. Last, but not least, Rudi Durfeld is gratefully acknowledged for generously providing accommodation at his camp, for his hospitality and for his willingness to exchange information about the Watson Bar property. Nick Massey kindly edited a draft of the paper.

REFERENCES

Cathro, M.S., Durfeld, R.M. and Ray, G.E. (1998): Epithermal mineralization on the Watson Bar property (92/01E), Clinton Mining Division, southern BC; *in* Geological Fieldwork 1997, *BC Ministry of Energy, Mines and Petroleum Resources*, Paper 1998-1, pages 21-1–21-13.

Holland, S.S. (1964): Landforms of British Columbia; *BC Ministry of Energy, Mines and Petroleum Resources*, Bulletin 48, 138 pages.

Jackaman, W. and Matysek, P.F. (1994): British Columbia Regional Geochemical Survey, NTS 92I (Ashcroft); *BC Ministry of Energy, Mines and Petroleum Resources*, RGS 40 and *Geological Survey of Canada,* Open File 2666, URL <http://www.em.gov.bc.ca/Mining/Geolsurv/Geochinv/rgs/sheets/92i.htm> [Dec 2005].

Jackaman, W., Matysek, P.F. and Cook, S.J. (1992a): British Columbia Regional Geochemical Survey NTS 92P — Bonaparte Lake; *BC Ministry of Energy, Mines and Petroleum Resources*, RGS 36, URL <http://www.em.gov.bc.ca/Mining/Geolsurv/Geochinv/rgs/sheets/92p.htm> [Dec 2005].

Jackaman, W., Matysek, P.F. and Cook, S.J. (1992b): British Columbia Regional Geochemical Survey, NTS 92O (Taseko Lakes); *BC Ministry of Energy, Mines and Petroleum Resources*, RGS 35, URL <http://www.em.gov.bc.ca/Mining/Geolsurv/Geochinv/rgs/sheets/92o.htm> [Dec 2005].

Lynch, J. (1990): Provisional element values for eight new geochemical lake sediment and stream sediment reference materials: LKSD 1, LKSD 2, LKSD 3, LKSD 4, STSD 1, STSD 2, STSD 3, STSD 4; *Geostandards Newsletter*, Volume 14, no 1 pages 153–167.

Matysek, P.F. and Day, (1988): Geochemical orientation surveys: northern Vancouver Island, fieldwork and preliminary results; *in* Geological Fieldwork, 1987, *BC Ministry of Energy, Mines and Petroleum Resources*, Paper 1988-1, pages 493–502.

MINFILE (2005): MINFILE BC mineral deposits database; *BC Ministry of Energy, Mines and Petroleum Resources*, URL <http://www.em.gov.bc.ca/Mining/Geolsurv/Minfile/> [Nov 2005].

Monger, J.W.H and Journeay, J.M. (1994): Guide to the geology and tectonic evolution of the southern Coast Mountains; *Geological Survey of Canada*, Open File 2490, 77 pages.

Read, P.B. (1988): Tertiary stratigraphy and industrial minerals, Fraser River to Gang Ranch, southwestern British Columbia (92I/5, 92I12, 92I/13, 92J/16, 92O/1, 92O/8, 92 P/4); *BC Ministry of Energy, Mines and Petroleum Resources*, Open File 1988-29, map and notes.

Trettin, H.P. (1961): Geology of the Fraser River valley between Lillooet and Big Bar Creek; *BC Ministry of Energy, Mines and Petroleum Resources*, Bulletin 44, 109 pages.

The Gates Formation in the Wolverine River Area, Northeastern British Columbia

by A.S. Legun

KEYWORDS: coal, Gates Formation, Wolverine River, Fahler C, Fahler D, J seam, coal stratigraphy, depositional environment, Peace River coalfield

INTRODUCTION

The study area lies west of the town of Tumbler Ridge in the Peace River coalfield of northeastern BC (Fig. 1). It extends on either side of the Wolverine River, from Mt. Spieker in the northwest to Quintette Mountain in the southeast. The area encompasses new coal mine developments at Perry Creek (Western Canadian Coal Corp. [WCCC]) and Trend (Northern Energy & Mining Inc. [NEMI]) and significant exploration at Babcock (Quintette Coal Ltd.). The current development activity is near the existing transportation and power infrastructure, and load-out coal facilities of BC Rail at Tumbler Ridge. It is spurred by prices for metallurgical coal, which have doubled since early 2004 and at the time of writing are over $120/tonne freight on board (FOB). Old and potential coal pits, as well as those in development, in the Gates Formation in the study area are shown in Figure 1.

The two principal coal-bearing units in the area are the Gates and Gething formations of the Lower Cretaceous. The Gates Formation contains most of the economic coal resources at this latitude. Up to 18.5 m of coal may be found over 60 m of section in the Middle Member of the Gates Formation. The Gething Formation, characterized by more lenticular coals, gains economic prominence north of the Sukunka River.

Both formations represent material eroded from the Columbian Orogen in the west and deposited in the Rocky Mountains foreland basin during the Early Cretaceous. Deposits of the Gates Formation record shoreline migrations on a coastal plain that bordered the southern end of a boreal sea. In the Wolverine area, the sea shallowed at a transverse step in the basin, which marked an area of reduced subsidence to the south. Deltas, prograding from the south, were stalled at the margin by deeper waters and were affected by destructive wave, tidal and storm activity. As a result, nearshore stillstand and littoral drift deposits mark the limits of two marine tongues in the area. This report focuses on the relations of the marine tongues and nearshore deposits with coal measures to the south. Additional exploration data has become available since work done in the early 1980s.

This publication is also available, free of charge, as colour digital files in Adobe Acrobat PDF format from the BC Ministry of Energy, Mines and Petroleum Resources internet website at http://www.em.gov.bc.ca/Mining/Geolsurv/Publications/catalog/catfldwk.htm

Fieldwork also pursued other themes including 1) mapping in the Fortress Mt. area, 2) sampling the base of J seam to assess regional trends in Se, an element associated with coal interseam shales, and 3) sampling of conglomerates to assess carbonate content in relation to potential acid mine drainage (AMD) issues.

PREVIOUS WORK

Stott (1974) measured surface sections and noted that the basal sandstone of the Gates Formation varied in stratigraphic position. Stratigraphically lower sandstones underpinned the Gates Formation coal measures to the south. Duff and Gilchrist (1981) constructed regional lines of section using logs of petroleum wells, deep coal boreholes together with marine zones based on macrofossils and volcanic ash markers.

Smith *et al.* (1984), Cant (1984) and others noted upward coarsening cycles of regional extent in the subsurface of the plains. These 'Fahler' cycles were identified as deposits of marine incursion and retreat; a basal transgressive lag was followed by a thick regressive portion and capped by coals. Features further offshore were identified as barrier bar systems. Interpretations of cycles in eastern areas, for example the Elmworth area of Alberta, have become complex, with evidence of erosion and incision with sea level fall (Cant, 1995).

Leckie (1983, 1986) and Carmichael (1983, 1988) investigated the depositional environments of the coalfield. Leckie focussed on the northwest, placing coals in a "channel poor" strandplain environment, while Carmichael in the southeast saw evidence of deltaic distributary sedimentation, which influenced backswamps and floodbasins. Both authors identified the subsurface Fahler cycles in outcrop but did not quite meld their work north to south, particularly in relation to trends of Fahler C. Both investigated lithological components of the conglomerates, noting an erratic variation of carbonate content.

Kalkreuth and Leckie (1989) and Lamberson *et al.* (1991) investigated macerals of Gates Formation coals and interpreted types and conditions of the original peat swamps. Diessel *et al.* (2000) studied the wetting and drying cycles in Gates Formation coastal coals and their possible relationship to sea level changes.

On the industry side, personnel of Quintette Coal Ltd. made detailed seam correlations and collated summaries of total coal seam thicknesses, interseam thicknesses and coal quality data over the life of the pits at Shikano, Mesa, Wolverine and Transfer. Exploration drilling and related research on coalbed methane potential has provided additional data (Wyman, 1984; Lamberson and Bustin, 1993; Dawson and Kalkreuth, 1994; Ryan, 2000).

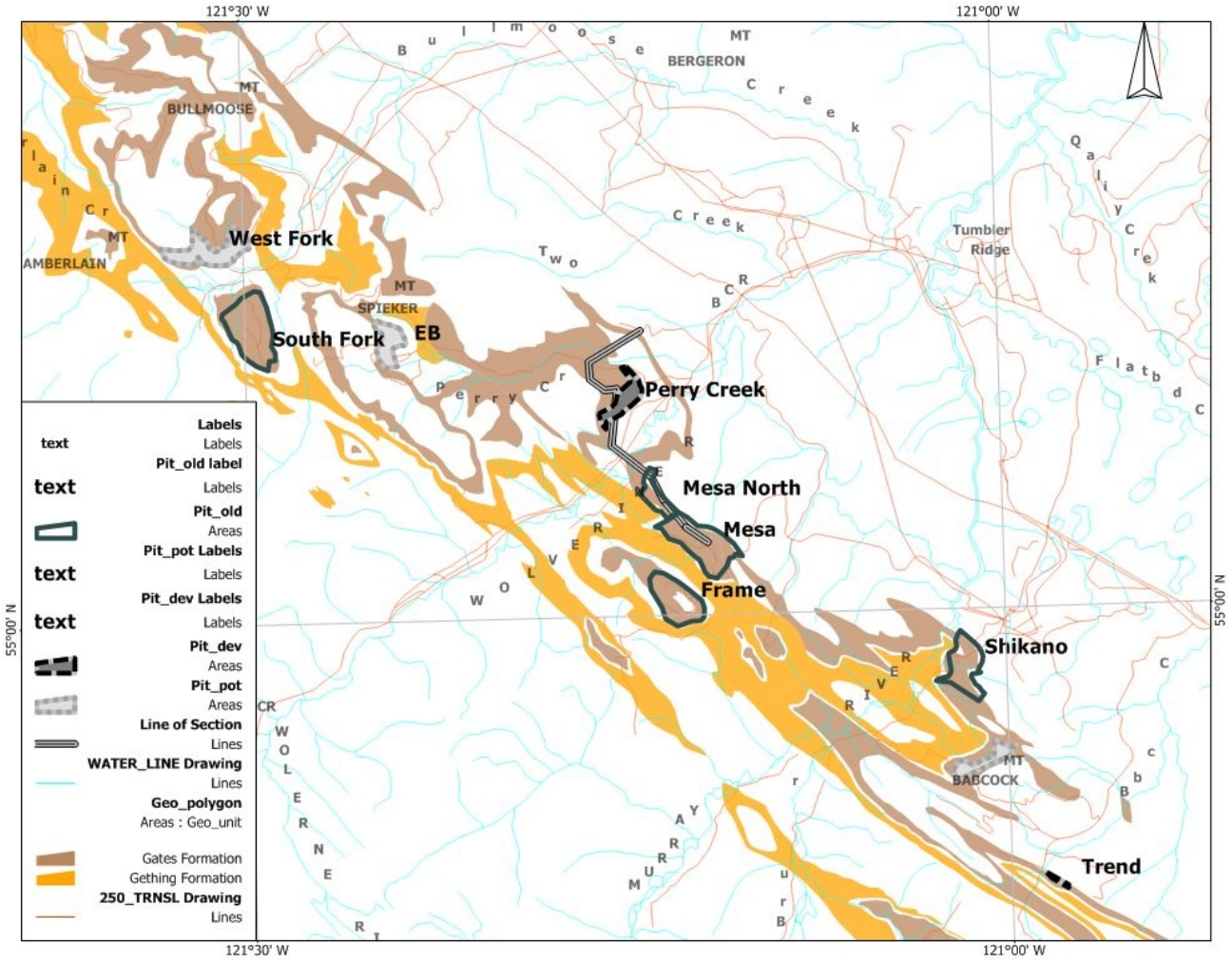


Figure 1. Study area with coal pit locations and the Gates and Gething formations.

REGIONAL STRATIGRAPHY

Table 1 shows the equivalence of various units between the coalfield, subsurface Fahler units, and local property terminology. The principal coal-bearing interval, between the base of J seam and the top of D seam, is described as the Middle Member of the Gates Formation. This Member ranges from 60 to 110 m in thickness and contains from 8 to 18.5 m of total mineable coal, as exposed in sections of various pits in the study area. The Middle Member corresponds to the interval between the top of the Quintette sandstone (Fahler F) and the base of the Notikewan conglomerate. The area south of Wolverine River (Quintette Mesa) lies landward of marine transgressions represented by Fahler D to A cycles.

J seam is the basal economic seam in the Wolverine area, resting on Fahler F marine cycle (Fig. 2, 3). It is often said to overly the 'Torrens'. However the Torrens corresponds to a sandstone 'leaf' below Fahler F. It is known as Fahler G in Alberta and a separate coal interval lies between it and Fahler F.

J seam is thick (often >5 m) and continuous. The seam can be traced from the Wolverine River for more than 70 km along the southeast margin of the coalfield (Carmichael, 1983). East of the coalfield, in subsurface, it comprises most of the interval known as the 4th coal. The 4th coal isopach appears to be based on Fahler D +100 m and thus may include additional coal strata (Wyman, 1984, Fig. 21). North of the Perry Creek area, J seam thins and splits under Fahler D with partings thickening. To the northwest, it divides into two significant plies known as seams A and B in the mined out South Fork deposit (Bullmoose mine).

In the Wolverine area, J seam often rests almost directly on sandstones of marine shoals (Fig. 4). These shoals may have comprised the wave-dominated delta-top environment in the area.

A total thickness of coal in each pit area was estimated from the sum of average thicknesses of each seam in the pit area (Table 2).

G seam is also a regionally persistent seam, often used as a datum in correlations through the coalfield. It lies above Fahler D.

E seam lies above Fahler C. It amalgamates with D seam in Quintette's Mesa area. It is thick and ashy, but

TABLE 1. STRATIGRAPHIC UNITS OF THE MIDDLE GATES FORMATION, WOLVERINE RIVER AREA.

Subsurface	Carmichael (1983)	Perry Creek Area	Quintette Mesa Area	Bullmoose Mine Area (adapted from Drozd [1985])
Notikewan	Babcock Member	Fortress Mt. unit?	Caprock conglomerate	
		D seam	D seam	E seam
Fahler A		Not present	not present	Not present
Fahler B		Not present	not present	Not present
		E,F seam	E seam interval	D seam
Fahler C		Wolverine unit	E congl	Not present
		G seam	G seam	C seam
Fahler D		J congl	not present	Unnamed congl in West Fork deposit
		J seam (J1,J2,J3 plies)	J seam	A,B seams
Fahler F	Sheriff Member	Quintette sandstone	Quintette sandstone	

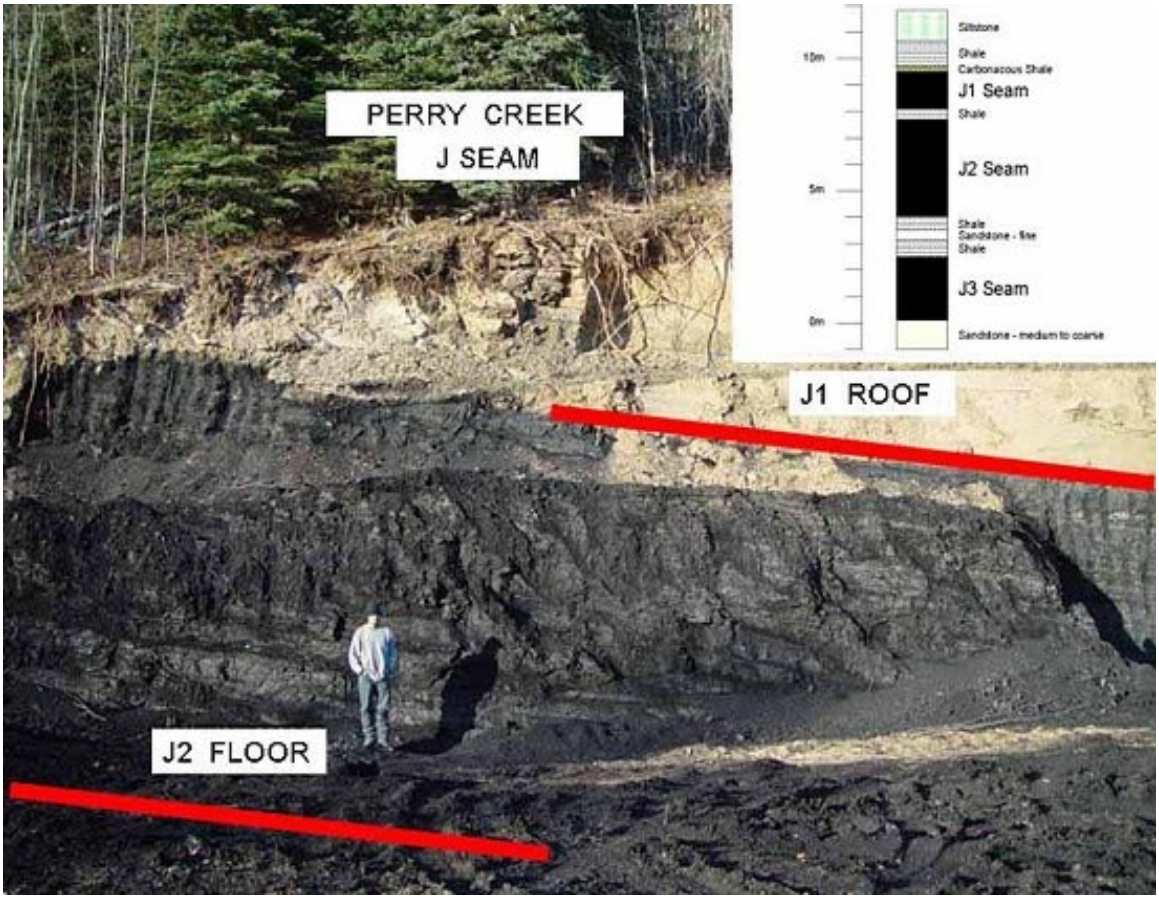


Figure 2. The J seam at Perry Creek thins, and partings thicken, below the Fahler D marine tongue to the north. Image from WCCC project description at http://www.westerncoal.com/properties.



Figure 3. Floor of J seam is exposed at Quintette's reclaimed Mesa pit.



Figure 4. Shoal megaripples are preserved at the top of Sheriff Member (Fahler F) and very close to base of J seam. These ripples are exposed in Quintette Coal Ltd.'s Wolverine pit wall. The view is looking up a steep (70°) face of the pit. Hammer is for scale.

locally eroded at the contact with the conglomerate of the Notikewan (Upper Gates Formation).

There is no formal seam correlation between the stratigraphy at South Fork (Bullmoose mine) and the various pits of the Quintette mine area south of the Wolverine River. However, J, G and E seams appear to persist. Their equivalents are shown in Table 1. J seam is equivalent to A and B seams at Bullmoose.

Depositional Setting

The Gates Formation is not a typical coal measure sequence because conglomerates, often associated with sandstones, occur in the coal measure sequence. The association of conglomerates, typical of deposits of higher gradients, and coals originating in peat deposits of shallow basins requires explanation, especially given the continuity of individual seams of the Gates Formation coal measures.

There is a change in the relation of conglomerate bodies to coals along the coalfield (Carmichael, 1988, Fig. 4). The trend described here is from the Alberta border northwest to the Wolverine River. Near the Alberta border (lat 54°15′), fluvial channels (of the upper delta plain) may incise coals. At about lat 54°45′ (Kinuseo Creek area), coals wrap up and below major distributary channel bodies. Carmichael (1983, Fig. 31, 32) documents the trends and overbank deposits of similar distributaries in the Babcock area (lat 54°55′). Channels with aprons of sediment on either side may have perched above the floodbasins. At Babcock, conglomerate channels also sit on sheet sands. This suggests basin fills by distributary lobes of sediment.

North of Babcock (lat 55°00′), channel bodies are infrequent in the Middle Gates Formation. The Wolverine-Babcock area shows a maximum development of coal over the stratigraphic interval, due to a lack of section-thickening channels. Somewhat enigmatically, the nearshore conglomerates of Fahler C and D lie adjacent to this area on the north. Leckie (1986) invokes a major channel at Mt. Spieker as a source for the nearshore conglomerate of Fahler D.

The continuity of the coals suggests floodbasins of considerable extent. J seam apparently formed under widespread limno-telmatic conditions (Diessel *et al.*, 2000). J seam can be traced southeast for over 70 km into facies of the upper delta plain, according to Carmichael (1983).

LOCAL STRATIGRAPHY

The local stratigraphic setting is illustrated in a north-south line of section extending from Quintette's Mesa pit area to the Perry Creek area (Fig. 5). A key coal borehole in the area is QWD 7115, within the area of the Perry Creek development. This borehole is utilized in lines of sections by Leckie (1983, 1986), Duff and Gilchrist (1981) and Quintette Coal Ltd. (1990). The section shows J seam overlain by Fahler D conglomerate. Fahler C is overlain by thick shaly coals of the D/E interval at Quintette. Fahler C can be traced as far south as the Mesa North pit in the Wolverine , while the southern limit

TABLE 2. SUMMARY OF COAL THICKNESS DATA, FROM OLD, DEVELOPING AND POTENTIAL PITS IN THE STUDY AREA

Area	J Seam Average (m)	Total Coal Average (m)
Shikano	5.26	18.43
Mesa North	5.73	18.48
Frame	3.46	16.66
Perry Creek	5.69	11.89
EB	5.6	11.6
South Fork	7.01	12.59
West Fork	5.2	<8
Trend (South)	4.68	17.53
Babcock	4.42	17.19

of Fahler D falls between drillholes QWD 7715 and 7719 in the Perry Creek area. New holes further constrain the trend of the southern bounds of Fahler C and D.

Fahler D and Fahler C

The coarse clastic units of Fahler D and Fahler C thicken rapidly northward, widen the stratigraphic separation between major coals, and reduce the mineable section. The cumulative effect is a fairly sharp northern boundary to economic coal resources in the Gates Formation.

The Fahler D and Fahler C marine tongues are exposed in cliff and ridge-forming sandstone and conglomerate units north of the Wolverine River. They are continuous bodies but not formally correlated across coal properties. Local terminology is used. Fahler C is the Wolverine sandstone at Perry Creek and E conglomerate in Quintette's Mesa North area. Fahler D is the J conglomerate at Perry Creek. No name is given to the equivalent conglomerate overlying B seam at West Fork.

Fahler C and D are massive conglomerates at their southern boundaries. The conglomerates extend seaward, fine seaward, and cap upward coarsening sequences. Further to the north (seaward), the upward coarsening interval includes shale at the base. Regional isopachs published by Leckie (1986) involve clean sand and conglomerate, and do not include shale of the marine interval.

The boundary of Fahler D is exposed on Mt. Spieker and this area of excellent exposures was chosen for reviewing the ground observations made by Leckie (1983). A number of closely spaced drillholes at the new Perry Creek development also illustrates Fahler D is at its limit here. The southern boundary of Fahler C is found in Mesa North pit of Quintette Coal Ltd. It is more accessible in cliff-wall exposures paralleling the Perry Creek road.

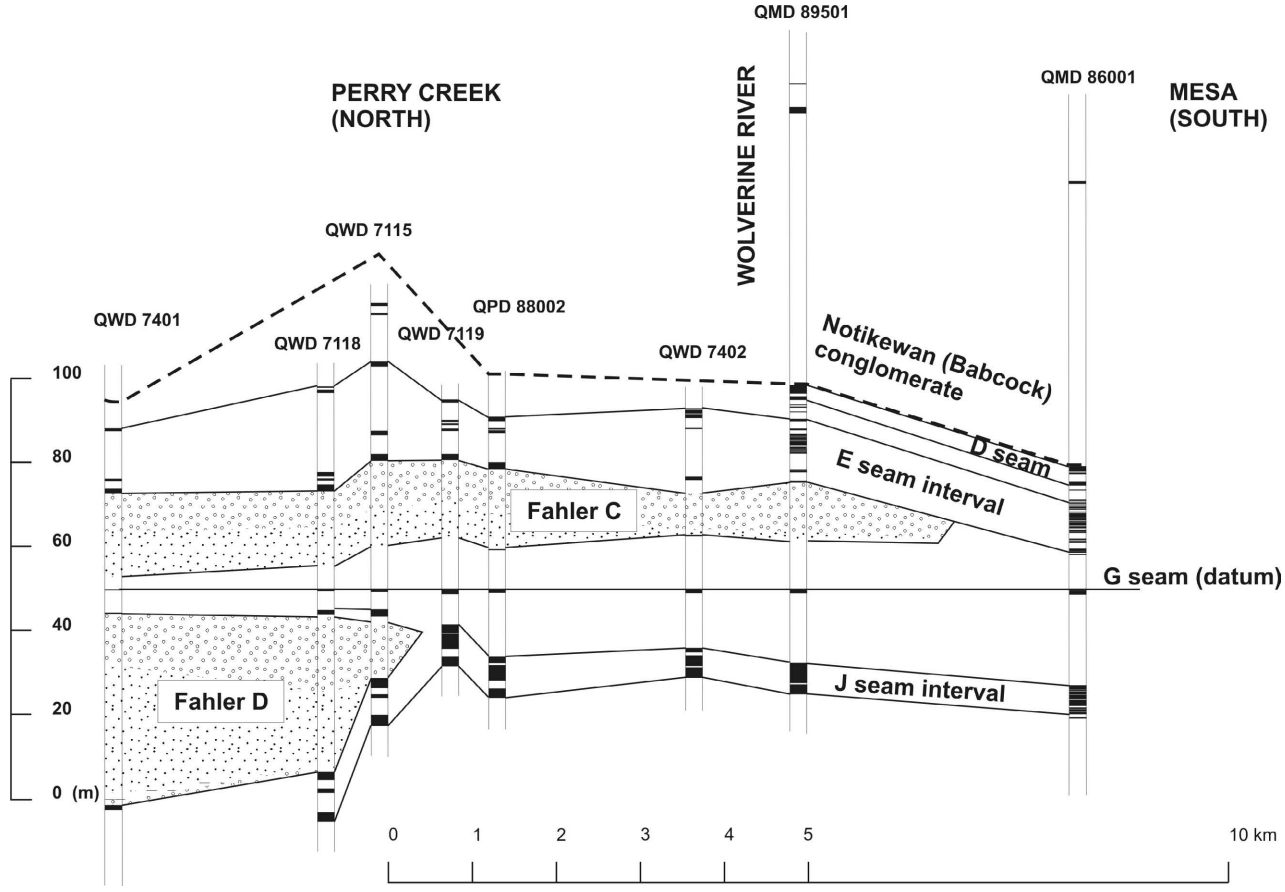


Figure 5. Line of section (Quintette Mesa pit to Perry Creek area). Location of line of section is shown in Figure 1.

Data Compilation and Contouring

Leckie's (1983) original data was reviewed and supplemented by data from Western Canadian Coal Corp., Quintette Coal Ltd. and the ministry's oil and gas database. Coal borehole data is being corrected for bedding angle so that a true thickness can be given (not all holes had been corrected at the time of writing so apparent thickness is included). Location data was checked and compiled in UTM NAD 83. Sixty-three records were available for Fahler D and thirty-seven for Fahler C. Thickness values ranged up to 43 m for Fahler D and 23 m for Fahler C. A bullseye thickness of 35 m for Fahler C, recorded by Leckie (1986) for well QUASAR MOBIL D- 057-D/093-P-02 (WA# 3194), appears to be a mistake.

Manifold software was utilized to manipulate database information, to create point data and to create a contoured surface. A triangulation algorithm was used for contouring. The base geology map was imported from AutoCad.

FAHLER D TRENDS

A contour plot (Fig. 6) emphasizes the rapid thinning to the south and the more gradual thinning to the north of the Fahler D unit, as well as the linear trend of the southern boundary.

The Fahler D boundary extends generally east-southeast across the coalfield. In the west, it lies within the area of the West Fork deposit (just north of the former Bullmoose mine). At Mt. Spieker, the trace cuts the saddle area just north of the EB pit area (see Mt. Spieker discussion). At Perry Creek, a straight east-trending segment is evident, constrained by numerous holes near QWD 7115 and 7119. This east-trending segment may continue to well # 15372 (SHELL B- 003-G/093-P-03), where the lithological log suggests a 10 m thickness of Fahler D. In the outer foothills, the boundary is constrained by well # 3319 (CNRL D- 080-A/093-P-03) and well # 3403 (KM ET AL B- 060-A/093-P-03) and then by the pair of well # 3814 (QUASAR MOBIL C- 076-D/093-P-02) and well # 3194 (QUASAR MOBIL D- 057-D/093-P-02 [0 m]).

FAHLER C TRENDS

Fahler C maintains a thickness of 15 to 20 m over a wide area (Fig. 7). The Fahler C boundary trends southeasterly, across the coalbelt. Its southern limit in the Wolverine area is marked by drillhole QMD 88003 in the Mesa North pit area. It is intersected just to the east in deep coal borehole Dupont Wolverine DDH-79-2. This suggests a more eastwardly trending segment. Its trace apparently continues southeast (outside the area of Fig. 7) and parallels the

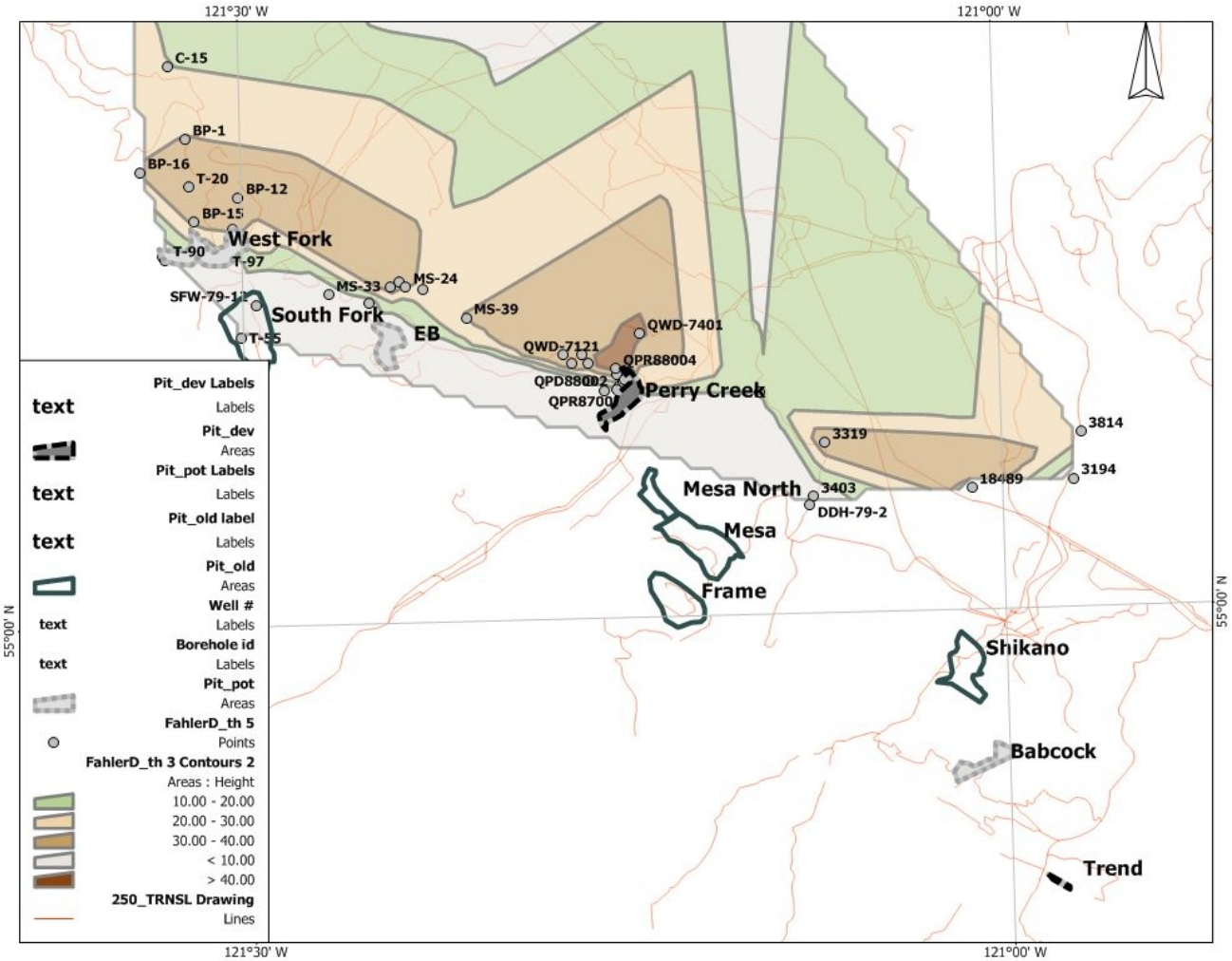


Figure 6. Contour plot of Fahler D using Manifold software triangulation algorithm.

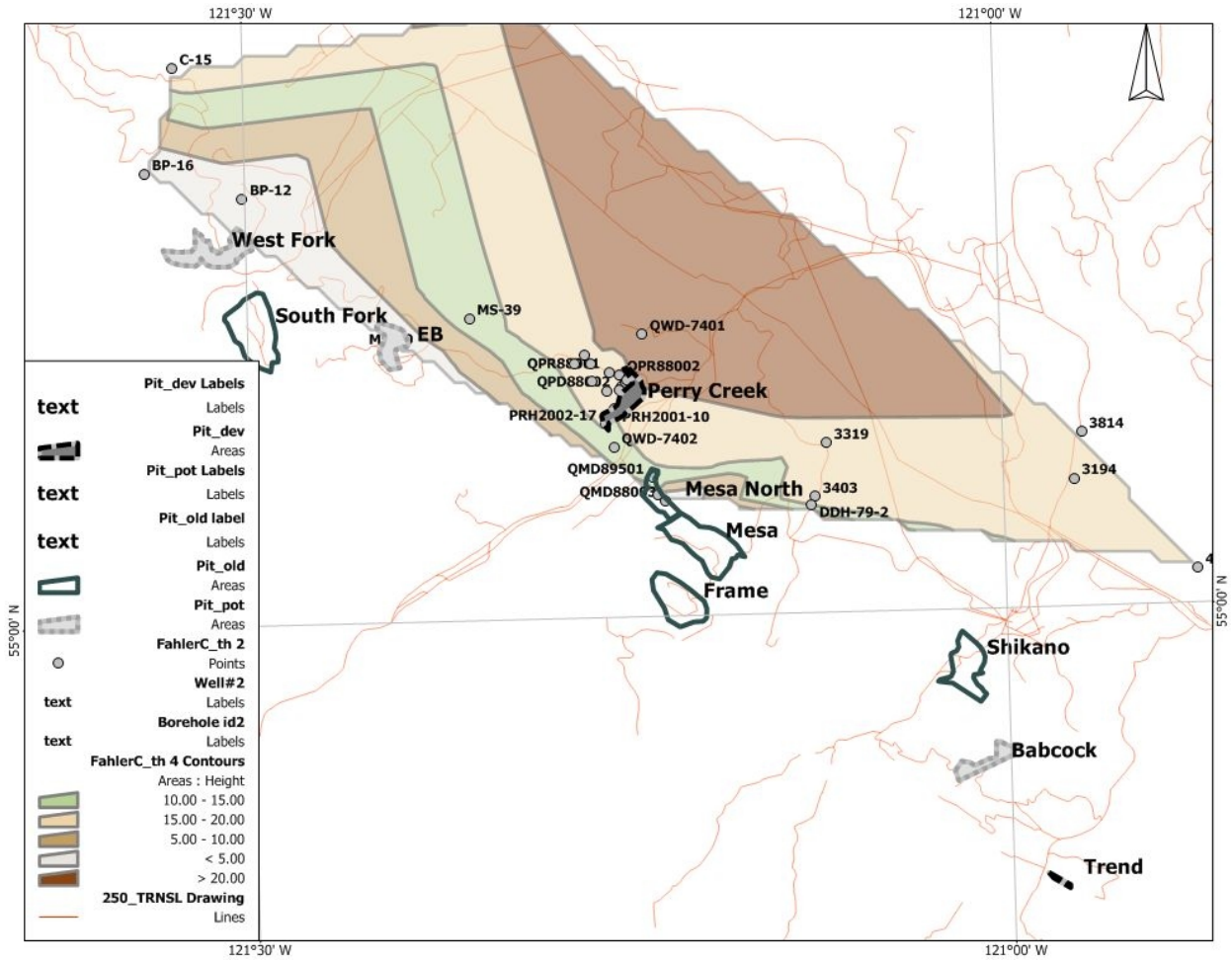


Figure 7. Contour plot of Fahler C using Manifold software triangulation algorithm.

coalfield in the subsurface. Carmichael (1983) shows it to be pinned by petroleum well KM ET AL B- 060-A/093-P-03l (WA #9439) in the Kinuseo Creek area.

Fahler D Exposures at Mt. Spieker

Fahler D at Mt Spieker is up to 38 m thick. The north to south facies changes of Fahler D are presented in a well known section diagram (Leckie and Walker, 1982, Fig. 3). In the north, in exposures along the west side and top of the mesa, shallow marine facies include subaqueous symmetrical and assymetrical gravel dunes, small-scale beach bars and ridges, herring bone (tidal) cross-stratification, pebble lag horizons, and finer beds containing the marine trace fossil *Rhizocorallium.*

At the south end, the most prominent features are long shallow dipping surfaces, which comprise over 15 to 18 m of section, dip to the south, and are exposed along a valley wall. They extend for several hundred metres to bluffs overlooking a topographic saddle (Fig. 8). Vertical tree casts are evident near the base of the bluff facing west (into the valley). Conglomerate, poorly to well sorted, is capped by well sorted (washed) sandstone and granule beds with current directions to the east. A few quartzitic clasts over 10 cm are randomly distributed. The writer found one sizable clast measuring 35 by 23 by 10 cm. This clast, which must weigh about 13 kg, is still cemented to granular matrix at one corner of the clast (Fig. 9).

Leckie and Walker (1982) noted small channel features trending 170° at the base of Fahler D.

The Fahler D conglomerate is missing on the south side of the saddle and apparently pinches out in the intervening few hundred metres where the section is not preserved. Coal seams provide stratigraphic control for the south side of the saddle (*e.g.*, drillhole MTSP MS 19, Robertson Research Limited [1978]). The shale above the Fahler D conglomerate has thickened and apparently takes up most of the interval, the conglomerate having thinned out.

INTERPRETATION

The low south-dipping surfaces are a major feature of Fahler D at its southern boundary. The boundary has a linear trend as shown in the contour plot (Fig. 6). Fahler D may represent a barrier bar and the dipping surfaces are the south-facing landward slope of the bar. As the dipping surfaces extend over 15 to 18 m of the stratigraphic section, a similar depth of water is implied. This would indicate a lagoon of some depth on the landward side.

The interpretation of these slopes as lateral accretion surfaces of a fluvial channel (Leckie 1983, 1986) implies



Figure 8. Low angle, south-dipping surfaces in Fahler D conglomerate, near southern limit of the conglomerate on Mt. Spieker.



Figure 9. A large, flat, ellipsoid clast sits in granule conglomerate of Fahler D at Mt. Spieker. The location of the clast is towards the base of the exposure shown in Figure 8.

an east-trending channel parallel to shore. However, the thickness of lateral accretion sets is greater than that described for most fluvial systems in the literature. It is possible that these sets might have been deposited in an estuarine channel.

Low-angle accretion bodies, of similar appearance, have been described by Carmichael (1988) as migrating shoals in estuaries normal to the shoreline. In this study area, accretion parallels the shoreline. The context suggests an alternative interpretation of a washover delta.

There are indications of marine influence south of the barrier bar. The barrier may have been broken by tidal channels, such as those suggested by small channel features oriented normal to the shoreline. Lagoonal sediments are preserved south of the barrier on Mt. Spieker. They include upward-coarsening shale, carbonaceous mudstones, some root zones but also forams and delicate echinoderms, which Leckie and Walker (1982, page 153) suggest have been washed in.

There are indications of a marine influence in other areas south of the Fahler D limit. Near Perry Creek, in the Perry Creek development, drilling by Quintette Coal Ltd. (Quintette Coal Ltd., 1989) showed sulphur to be elevated in J1 and J2 seam plies, when compared with values immediately south of the Wolverine River. The marine fossil *Psilomya peterpondi* (Duff and Gilchrist, 1981) overlies J seam in QWD 7402, located more than 2 km south of the boundary near the southern limit of the Perry Creek pit.

Further south, in the Mesa pit area, Carmichael (1983) notes lacustrine shales and freshwater fossils immediately above J seam, suggesting this area was outside the influence of coastal marine waters.

General Discussion of Fahler D and Fahler C

The overall trend of Fahler C is to the southeast while that of Fahler D is east-southeast. The coastal configuration had apparently changed by the time of the Fahler C transgression. However, both transgressions reached approximately the same position in the Mt. Spieker area.

The shoreline trends provide some explanation as to why an appreciable thickness of coal was mined in the South Fork deposit (Bullmoose mine), some 20 km northwest of the Quintette mine area at Wolverine River. The Bullmoose mine was landward of both Fahler C and D marine margins.

There are several indications of nearshore subsidence coinciding with stillstand deposits of Fahler D. The first is the burial of standing trees below 15 to 18 m of nearshore sediments. The second is the splits of J seam under the Fahler D edge. The third is the thickening of shale above the conglomerate, landward of a barrier bar. The presence of a bar, even submerged, would certainly have been able to compress peat deposits immediately below and to an uncertain lateral extent. Falini (1965) discusses the general as-

pects of the loading and compression of peats by sediments. At Mt. Spieker, the load on peat deposits at the barrier and landward of the bar might be appreciably different. The thickening of shale, landward of the conglomerate, suggests (subaqueous) relief that was eventually levelled with further sedimentation and prior to renewed peat formation. The concept of coastal loading is worth further investigation and modelling.

The presence of large quartzitic clasts in Fahler D raises questions as to the source of the sediment. It is difficult to envisage clasts approximately 35 cm long being carried through the channels of a low-gradient coastal plain. These channels did not incise the plain. The large clasts may have a common source, a point along the coast that was subjected to erosion, perhaps where the barrier bar approaches the western margin of the seaway. There is abundant evidence of storm activity and vigorous wave action in the seaway, in the form of swaley and hummocky cross-stratification (Leckie and Walker, 1982).

The source of Fahler D conglomerate is not clear. Channels are not evident in the EB pit area or in areas immediately south of the Perry Creek mine development. The area south of the Fahler D boundary has appreciable coal in a relatively thin and channel-free Middle Gates Formation. Further work needs to be done to answer the question – is the clast composition of Fahler D significantly different from other conglomerates?

FURTHER WORK

Mapping

There is scope for further mapping west of Fortress Mt. and the Bullmoose-Mesa thrust. This area (southern portion of Mt. Spieker syncline) has undergone minimal drilling. It is a prospective but underexplored area on the north side of the Wolverine River. It lies landward of Fahler D and C nearshore marine deposits. Mapping at a 1:20 000 scale has the potential to delineate additional resource areas that might be missed in 1:50 000-scale work.

Conglomerate Sampling

Gates Formation conglomerates are occasionally silicic and carbonate free. This effectively eliminates their neutralization potential and they have potential to generate acid mine drainage (AMD) depending on their pyrite content. Carbonate-free conglomerates have been noted at Babcock (Kim Bellfontaine, MEMPR Environmental Review Office, pers comm., 2005) and Perry Creek. For example, J2 conglomerate (Fahler D) at Perry Creek is recorded as containing 0.7% pyrite, 93.3% quartz and no carbonate (Lorax Environmental Services, 2004). Carbonate contents up to 11.4% are present in other sandstones and conglomerates, usually as dolomite. About 30 conglomerate samples, representative of marine, nonmarine and possibly estuarine depositional environments, were collected. Figure 10 illustrates estuarine conglomerate that buried the long-lived peat swamps of the D/E interval at Quintette. Sample processing at the time of writing is incomplete. The erratic distribution of carbonate lithic clasts in the Gates Formation, documented by both Leckie (1983) and Carmichael (1983), remains unexplained.

Sampling for Selenium

Selenium is a group 6a element that shares many similarities with sulphur. Coal mining releases the inorganic form of selenium. It is most likely to be present as selenate (SeO_4; +6 oxidation state) in oxygenated waste rock drainage waters. In low concentrations, selenium is required for good health. However, in high concentrations, in the organic form, it is a health hazard to wildlife and humans when absorbed. Generally speaking, fine-grained rocks, mudstones and shales, have higher selenium concentrations. At Wolverine, zinc and lead were found to have a strong positive correlation with selenium (EVS Consultants, 2004). Selenium is closely related to sulphur and sulphur-rich coals are often ascribed to marine influence. The thin shale overlying the marine Quintette sandstone and underlying J seam (base of coal measures) was chosen as a sampling horizon for Se. The sampling horizon is relatively easy to locate in the field as the Quintette sandstone (*i.e.*, top of Fahler F) forms a prominent ridge. The base of the coal measures is often recessive and covered but some carbonaceous shale is often preserved (or remains after mining) at the J seam's basal contact. Results of environmental sampling are not fully available at the time of writing and this will be the subject of a subsequent report.

ACKNOWLEDGMENTS

The writer thanks Al Kangas for providing access to the reclaimed pit areas of Quintette Coal Ltd. and the Babcock Mt. exploration site. Barry Ryan, Ray Lett, Brian Grant, Kim Bellfontaine are thanked for consultations regarding study themes.

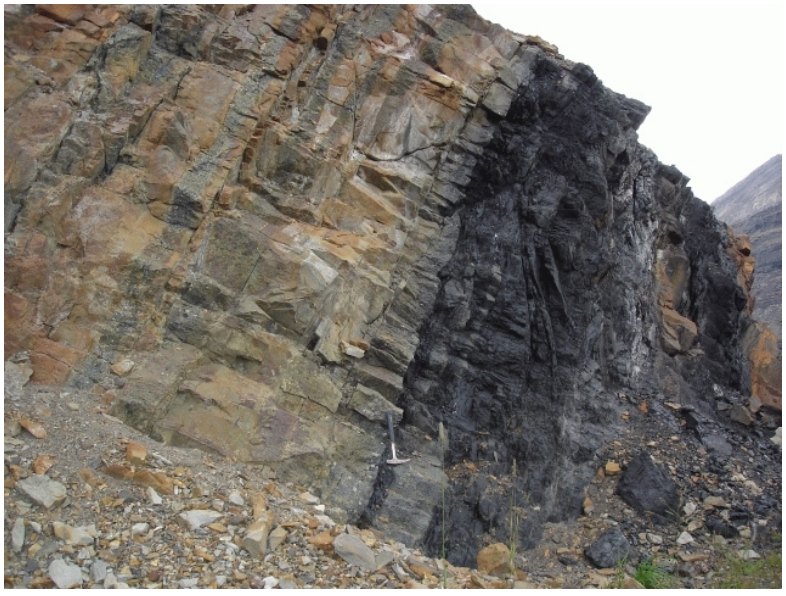


Figure 10. Silicic and pyritic conglomerate of Upper Gates Formation (Notikewan) overlying D/E seam in the Quintette Mesa pit.

REFERENCES

Cant, D.J. (1984): Development of shoreline-shelf sand bodies in a Cretaceous epeiric sea deposit; *Journal of Sedimentary Petrology*, Volume 54, pages 541–556.

Cant, D.J. (1995): Sequence stratigraphic analysis of individual depositional successions: effects of marine/nonmarine sediment partitioning and longitudinal sediment transport, Mannville Group, Alberta Foreland Basin, Canada; *American Association of Petroleum Geologists Bulletin*, Volume 79, no 5, pages 749–762.

Carmichael, S.M. (1983): Sedimentology of the Lower Cretaceous Gates and Moosebar formations, Northeast Coalfields, British Columbia; unpublished PhD thesis, *University of British Columbia*, 285 pages.

Carmichael, S.M. (1988): Linear estuarine conglomerate bodies formed during a mid-Albian marine transgression; "upper Gates" Formation, Rocky Mountain foothills of northeastern British Columbia; *in* Sequences, Stratigraphy, Sedimentology: Surface and Subsurface, James, D.P. and Leckie, D.A., Editors, *Canadian Society of Petroleum Geologists*, Memoir 15, pages 49–62.

Dawson, F.M. and Kalkreuth, W. (1994): Coal rank and coalbed methane potential of Cretaceous/Tertiary coals in the Canadian Rocky Mountain Foothills and adjacent Foreland: Hinton and Grande Cache areas, Alberta; *Bulletin of Canadian Petroleum Geology*, Volume 42, pages 544–561.

Diessel, C., Boyd, R., Wadsworth, J., Leckie, D. and Chalmers, G. (2000): On balanced and unbalanced accommodation/peat accumulation ratios in the Cretaceous coals from Gates Formation, western Canada, and their sequence-stratigraphic significance*; International Journal of Coal Geology*, Volume 43, pages 143–186.

Drozd, R. (1985): The Bullmoose mine project; *in* Coal in Canada, Patching, T.H., Editor, *Canadian Institute of Mining and Metallurgy*, Special Volume 31, pages 263-268.

Duff, P. McL. D. and Gilchrist, R.D. (1981): Correlation of Lower Cretaceous coal measures, Peace River Coalfield, British Columbia; *BC Ministry of Energy, Mines and Petroleum Resources*, Paper 1981-3.

EVS Consultants (2004): Selenium addendum report; *in* Addendum Report on the Application for the Wolverine Coal Project from Western Canadian Coal (prop) to Bob Hart (EAO) July 2004, *Western Canadian Coal Corp.*, URL <http://www.eao.gov.bc.ca/epic/output/html/deploy/epic_project_home_162.html>, Appendix 2, 23 pages, [Dec 2005].

Kalkreuth, W. and Leckie, D.A. (1989): Sedimentological and petrographical characteristics of Cretaceous strandplain coals: a model for coal accumulation from the North American western interior seaway; *in* Peat and Coal: Origin, Facies and Depositional Models, Lyons, P.C. and Alpern, B., Editors; *International Journal of Coal Geology*, Volume 12, pages 381–424.

Lamberson, M.N. and Bustin, R.M. (1993): Coalbed methane characteristics of Gates Formation coals, northeastern British Columbia: effect of maceral composition; *American Association of Petroleum Geologists Bulletin*, Volume 77, no 12, pages 2062–2076.

Lamberson, M.N., Bustin, R.M. and Kalkreuth, W. (1991): Lithotype (maceral) composition and variation as correlated with paleo-wetland environments, Gates Formation, northeastern British Columbia, Canada; *International Journal of Coal Geology*, Volume 18, pages 87–124.

Leckie, D.A. (1983): Sedimentology of the Moosebar and Gates formations (Lower Cretaceous); unpublished PhD thesis, *McMaster University*, 515 pages.

Leckie, D.A. (1986): Rates, controls, and sand-body geometries of transgressive-regressive cycles: Cretaceous Moosevale and Gates formations, British Columbia; *American Association of Petroleum Geologists Bulletin*, Volume 70, pages 516-535.

Leckie, D.A. and Walker, R.G. (1982): Storm and tide-dominated shorelines in Cretaceous Moosebar-Lower Gates interval-outcrop equivalents of deep basin gas trap in western Canada; *American Association of Petroleum Geologists Bulletin,* Volume 66, no 2, pages 138–157.

Lorax Environmental Services Ltd. (2004): ARD ML assessment, *in* Addendum report on the Application for the Wolverine Coal Project from Western Canadian Coal (prop) to Bob Hart (EAO) July 2004, *Western Canadian Coal Corp.*, URL <http://www.eao.gov.bc.ca/epic/output/html/deploy/epic_project_home_162.html>, Appendix 1, 23 pages, [Dec 2005].

Quintette Coal Ltd. (1989): 1988 Geological report of Transfer, Grizzly, Perry Creek, Marmot and Wolverine valley south areas; *BC Ministry of Energy, Mines and Petroleum Resources*, Coal Assessment Report 746.

Quintette Coal Ltd. (1990): 1989 Geological report of Transfer, Grizzly and Mesa North Extension areas; *BC Ministry of Energy, Mines and Petroleum Resources*, Coal Assessment Report 753.

Robertson Research Limited (1978): 1978 geological report for Ranger Oil Ltd., Mt. Spieker coal project; *BC Ministry of Energy, Mines and Petroleum Resources*, Coal Assessment Report 556.

Ryan, B.D. (2000): An introduction to coalbed methane potential in British Columbia; *in* Exploration and Mining in British Columbia 2000, *BC Ministry of Energy, Mines and Petroleum Resources*, pages 55–69.

Smith, D.G., Sneider, R.M. and Zorn, C.E. (1984): The paleogeography of the Lower Cretaceous of western Alberta and northeastern British Columbia adjacent to the deep basin of the Elmworth area; *American Association of Petroleum Geologists*, Memoir 38, pages 79–114.

Stott, D.F. (1974): Lower Cretaceous coal measures of the foothills of west-central Alberta and northeastern British Columbia; *Canadian Mining and Metallurgical Bulletin*, Volume 67, no 749, pages 87–101.

Wyman, R.E. (1984): Gas resources in Elmworth coal seams; *American Association of Petroleum Geologists*, Memoir 38, pages 173–187.

Geochemistry of Nicola Group Basalt from the Central Quesnel Trough at the Latitude of Mount Polley (NTS 093A/5, 6, 11, 12), Central British Columbia

By James M. Logan[1] and Adam B. Bath[1, 2]

KEYWORDS: Quesnel, Triassic, volcanic-arc basalt, geochemistry, alkaline, analcime-pyroxene basalt, porphyry copper-gold mineralization, Gibraltar, Copper Mountain, Mount Polley, hydrothermal breccia

INTRODUCTION

Alkaline magmas are important sources of Au and Cu (Muller and Groves, 1993) and are associated with a number of world-class porphyry (Dinkidi, Philippines; Skouries, Greece; Cadia, Australia) and epithermal-style deposits (Porgera and Landolam, Papua New Guinea; Emperor, Fiji; Cripple Creek, United States; see Jensen and Barton, 2000). British Columbia is well endowed with porphyry deposits that formed during two distinct periods in the development of the Cordillera: the first in the Late Triassic to Early Jurassic and the second in the Late Cretaceous to Eocene (McMillan *et al.*, 1995). Alkaline and cospatial calcalkaline Cu-Mo±Au porphyry deposits formed within island-arc settings, represented by the Quesnel and Stikine terranes, located on the fringes of ancestral North America, during Late Triassic to Early Jurassic time. These arcs may have extended for up to 3000 km prior to their collision with ancestral North America, between 185 and 173 Ma (Nixon *et al.*, 1993; Mihalynuk *et al.*, 2004), and they now account for more than half of the accreted crustal material within the BC Cordillera. Late Cretaceous to Eocene porphyry deposits formed in a continental-arc setting after amalgamation of the composite terranes to North America.

Elevated metal prices and recent exploration successes in BC have rekindled interest in Cu-Au porphyry deposits. Key exploration targets are the alkalic Cu-Au porphyry deposits similar to the Galore Creek, Mount Polley and Afton-Ajax deposits (Fig. 1).

Mineralized and unmineralized alkaline intrusions are common throughout the Intermontane Belt, in both Stikine and Quesnel terranes of the Canadian Cordillera (Barr *et al.*, 1976; Lueck and Russell, 1994). Alkaline intrusions associated with porphyry deposits include both silica-saturated and silica-undersaturated types (Lang *et al.*, 1995), but worldwide only the BC deposits are associated with small, complex, either nepheline or leucite normative, silica-undersaturated intrusions, and these contain almost no quartz. Late Triassic British Columbia deposits are unique end-members of a continuum of porphyry deposits associated with calcalkaline, high-K calcalkaline or alkaline systems. Understanding the conditions of alkaline porphyry formation and the distinction between barren and fertile alkaline intrusions is important for the evaluation of arc terranes and their economic potential in BC.

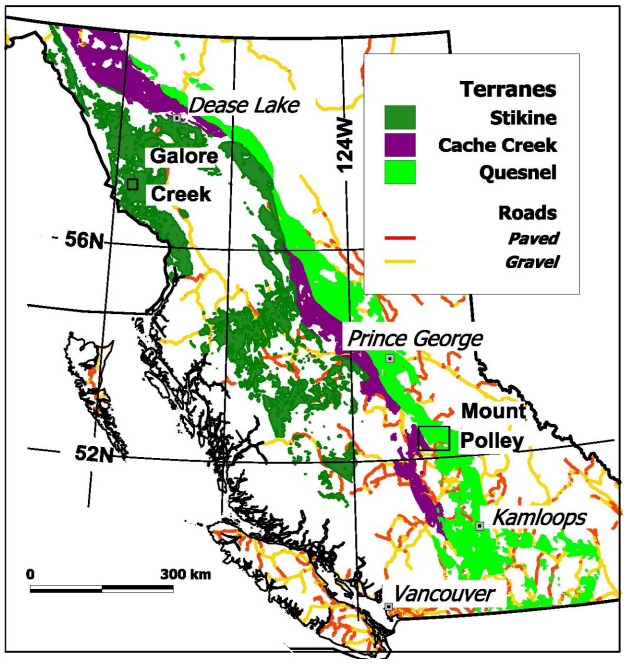


Figure 1. Location of study area, central Quesnel Trough, central British Columbia (modified from Wheeler and McFeely, 1991).

Regional geological mapping and sampling continued at Mount Polley as part of an ongoing study of alkaline Cu-Au porphyry deposits in BC. This report includes the results of mapping and rock geochemical data collected from the eastern side of Quesnel Terrane, in the vicinity of Mount Polley. Key objectives of the project are to complete a lithogeochemical transect across the central Quesnel Terrane at approximately 52.5°N, and to characterize Triassic to Jurassic evolution of the arc, similar to the study of the southern Quesnel by Mortimer (1987). It is also critical to establish the tectonic implications of overlapping calcalkaline and alkaline magmatism and related porphyry mineralization, and to refine the understanding of the petrological evolution of alkaline-arc magmatism that culminated in porphyry mineralization at the Triassic–Jurassic

[1]*British Columbia Ministry of Energy and Mines, Victoria, BC*

[2]*University of Tasmania, Hobart, Australia*

This publication is also available, free of charge, as colour digital files in Adobe Acrobat PDF format from the BC Ministry of Energy, Mines and Petroleum Resources internet website at http://www.em.gov.bc.ca/Mining/Geolsurv/Publications/catalog/catfldwk.htm

boundary. In addition, this study includes a melt – fluid inclusion study on volcanic and intrusive rocks associated with mineralized and barren alkalic centres in the Mount Polley area (Bath and Logan, 2006).

PREVIOUS WORK

The Geological Survey of Canada carried out regional geological studies in the Quesnel River area during the 1950s and 1960s (Tipper, 1959, 1978; Campbell, 1961, 1963, 1978; Campbell and Campbell, 1970), but it was not until the work by Fox (1975) that the alkaline composition of the volcanic rocks was recognized in the Quesnel area. Detailed mapping and mineral deposit studies in the Horsefly area by Morton (1976), and by Bailey (1978) in the area around Morehead Lake, provided the first stratigraphic descriptions of the rocks encompassing the Mount Polley deposit.

Bailey (1988a, b, 1990), Panteleyev (1987, 1988) and Panteleyev and Hancock (1989) carried out regional-scale geological mapping and mineral evaluation in the area located between Quesnel and the Horsefly River as part of the 1985–1990 Canada – British Columbia Mineral Development Agreement. The focus of their studies was to remap and reinterpret the central Quesnel volcanic belt and test the economic potential for Au and Cu deposits along its volcanic-intrusive axis (Panteleyev *et al.*, 1996). Deposit studies at Mount Polley by Hodgson *et al.* (1976), Fraser (1994, 1995) and Fraser *et al.* (1995) recognized three stages of breccia emplacement (pre, syn and postmineralization) and the distinctive alkaline porphyry alteration assemblages that separate the deposit into proximal and distal mineralized zones.

REGIONAL GEOLOGY

The study area lies along the eastern margin of the Intermontane Belt close to its tectonic boundary with the Omineca Belt, in south-central BC. At this latitude, the Intermontane Belt is underlain mainly by Late Paleozoic to Early Mesozoic arc volcanic, plutonic and sedimentary rocks of the Quesnel Terrane. Farther west are coeval rocks of the oceanic Cache Creek Terrane (Fig. 1). The Quesnel Terrane (Quesnellia) consists of a Late Triassic to Early Jurassic magmatic arc complex that formed above an east-dipping subduction zone (Mortimer, 1987). The Cache Creek Terrane, with its Late Triassic to Middle Jurassic (Patterson and Harakal, 1974; Ghent *et al.*, 1996) blueschist-facies rocks, represents the remnants of this subduction-accretionary complex (Travers, 1977; Mihalynuk *et al.*, 2004). Quesnellia is fault bounded, juxtaposed on the west with Paleozoic and Mesozoic rocks of the Cache Creek complex, and on the east by Mesozoic to Paleozoic and older metasedimentary, metavolcanic and metaplutonic rocks of the pericratonic Kootenay Terrane. The Barkerville and Cariboo subterranes of the Kootenay Terrane separated Quesnellia from North America until the Middle Jurassic, at which time they were imbricated and thrust eastward onto the North American craton (Nixon *et al.*, 1993). The tectonic boundary between the Kootenay and Quesnel terranes is intruded by the Jurassic–Cretaceous Raft batholith to the south. Tertiary volcanic rocks and feeder dikes of the Chilcotin Group are the youngest rocks in the region (Mathews, 1989).

Quesnel arc magmatism and associated porphyry mineralization migrated eastward with time, beginning in the west *ca.* 212 Ma with development of calcalkaline Cu-Mo±Au deposits at Highland Valley and Gibraltar. East of Gibraltar, submarine to subaerial Na and K-rich lava flows, cogenetic alkaline intrusions and 204 Ma, Cu-Au mineralization occupy the central axis of the arc. Mount Polley is hosted by a high-level, alkaline intrusive complex that is of latest Triassic age (202 Ma; Mortensen *et al.*, 1995). A chain of similar deposits extends the length of the Intermontane Belt (Barr *et al.*, 1976; Fig. 1). In the south, they are associated with the Iron Mask batholith (Afton, Ajax and Crescent) and Copper Mountain intrusions (Copper Mountain and Ingerbelle) and, to the north, with the Hogem batholith (Lorraine). Uplift and erosion of the forearc produced sub-Jurassic unconformities as magmatism shifted east and culminated with intrusion of 195 Ma calcalkaline plutons in the south (Takomkane, Thuya, Wild Horse and Pennask) and deposition of distal volcaniclastic and younger sedimentary rocks across the terrane.

NICOLA GROUP ROCKS

The central Quesnel belt consists of a twofold lithostratigraphic subdivision: a lower fine-grained sedimentary succession and an upper 'alkalic or shoshonitic' sequence of calcalkaline arc volcanic deposits that are gradational with and conformably overlie the sedimentary package. The volcanic succession occupies the central northwest-trending belt and is flanked on the east by 'black phyllite' and on the west by fine-grained volcanic sandstone, siltstone and conglomerate. The opposing regional dips of the Middle to Late Triassic sedimentary units beneath the younger, Upper Triassic volcanic succession provide the geometric definition for the Quesnel Trough (Roddick *et al.*, 1967; Campbell and Tipper, 1970; Panteleyev *et al.*, 1996). This twofold sedimentary-volcanic distinction of Quesnellia is recognized in the Mount Milligan and Manson Creek – Germansen Landing areas to the north (Ferri and Melville, 1994; Nelson and Bellefontaine, 1996) and as far south as Little Fort (Schiarizza and Israel, 2001).

Schiarizza *et al.* (2002) subdivided the Nicola Group rocks in the Clearwater – Little Fort area into five informal units: a central (lower) volcanic and (overlying) volcaniclastic package, an eastern sedimentary (Lemieux Creek) and two western sedimentary successions (Meridian and Wavey Lake). They recognized similar rock types and equivalent ages for the sedimentary rocks east and west of the volcanic axis and mapped them as facies-equivalent units. Relevant to the present study are the Anisian, Ladinian and Early Carnian conodont ages from limestone interbedded with grey phyllite, slate and slaty siltstone of their easternmost Lemieux Creek succession, which support correlation with the lithologically similar Middle to Late Triassic basal Nicola rocks of unit 1 (Panteleyev *et al.*, 1996) in the Quesnel Lake area.

The base of the Nicola, unit 1 (Fig. 2), forms a northwest-trending belt exposed east of Quesnel Lake. It has been estimated to constitute at least 2500 m (Rees, 1987), to locally 4000 m (Bloodgood, 1990), of fine-grained graphitic and quartzose sedimentary rocks that grade upward into (Carnian to Norian) basal units of the upper volcanic unit. Missing from the Lemieux Creek succession but well described by Bloodgood (1987), Rees (1987) and

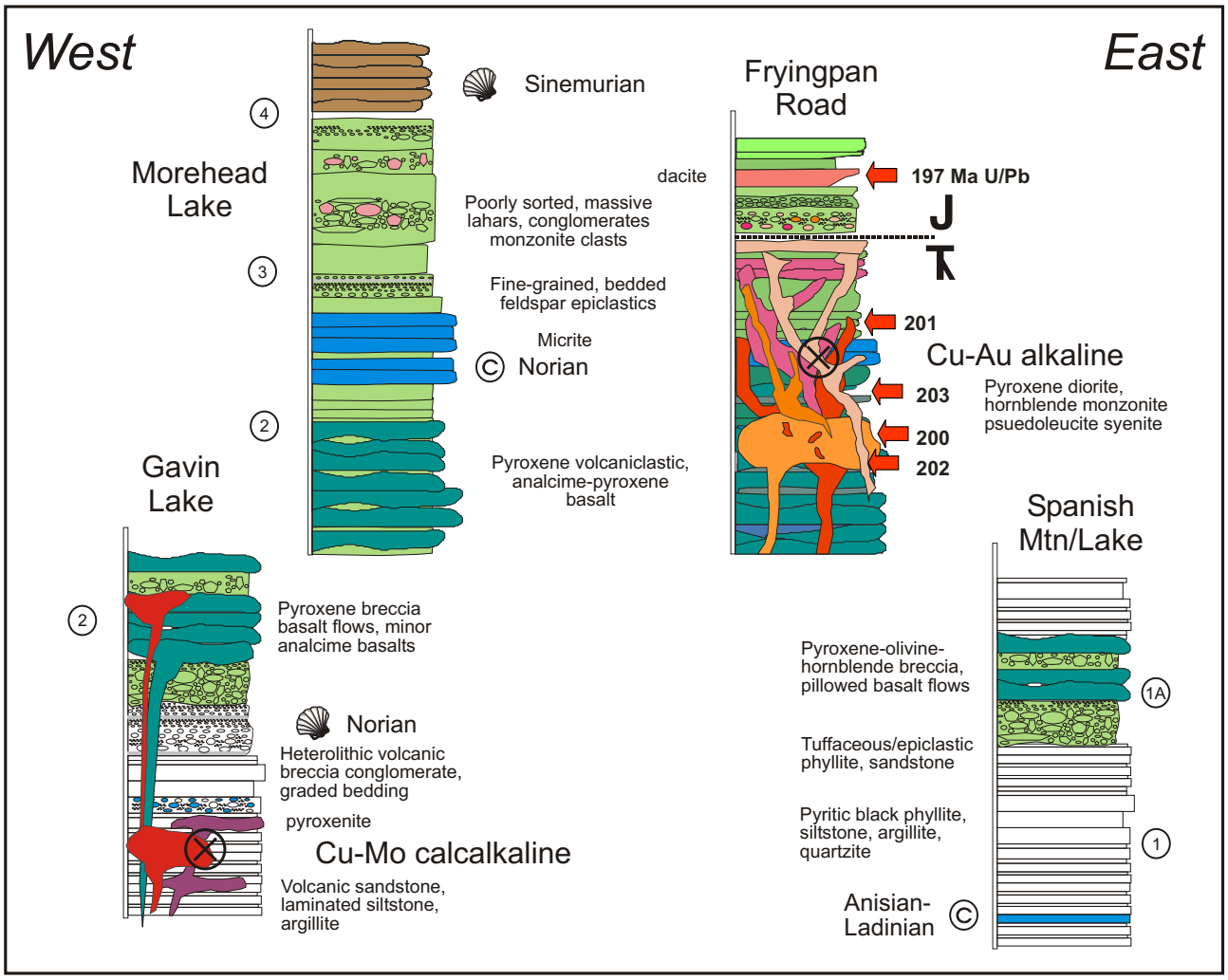


Figure 2. Stratigraphic sections for Nicola Group volcanic and sedimentary rocks in the Spanish Mountain, Fryingpan Road, Morehead Lake and Gavin Lake areas.

Panteleyev *et al.* (1996, unit 1A) in the Eureka Peak and Quesnel Lake areas are mafic hornblende, pyroxene volcanic breccia, conglomerate and tuffaceous argillite, which occur near the top of the sedimentary sequence (MLTNv).

Augite porphyritic flow, breccia and volcaniclastic units define a northwest-trending belt, up to 20 km wide, of subaqueous and subordinate subaerial volcanic rocks with an estimated thickness on the order of 5–6.5 km (Rees, 1987; Panteleyev *et al.*, 1996). Thickest accumulations of volcanic rocks and coeval subvolcanic intrusions define the magmatic axis of the Quesnel arc and show remarkable similarity in chemical affinity and geochronological correlations along the length of the arc, as well as with other Late Triassic arcs in the Cordillera (Mortimer, 1987; Mihalynuk et al., 1994, Nelson and Bellefontaine, 1996; Panteleyev *et al.*, 1996; this study). Green or maroon, clinopyroxene (augite)–phyric basalt to basaltic andesite (LTNpv) is the dominant and identifying rock type, but augite-olivine±plagioclase, augite-plagioclase-analcime (LTNav) and hornblende-plagioclase-augite (LTNhv) basalt compositions occur across the study area. Volumetrically, fine to medium-grained volcaniclastic deposits far exceed tuff and breccia units, and coherent lava and flow breccia units form the least abundant components of the arc within the study area.

West of the magmatic axis is a second package of fine-grained sedimentary and volcaniclastic rocks, the Gavin Lake succession, which underlies pyroxene volcanic breccia and flow rocks of the main volcanic facies (Fig. 2). It crops out north of Beaver Creek valley and extends about 20 km in a northwest-trending belt between Antoine and Gavin lakes. Panteleyev *et al.* (1996) mapped these as equivalent to their eastern sedimentary assemblage (unit 1). On its northern side, the contact between the Gavin Lake succession and overlying volcanic rocks trends northwest, orthogonal to the regional bedding in the lower sedimentary succession. At outcrop scale, however, the contact is gradational and conformable. The southern contact is poorly exposed and unconformably overlain and/or faulted against unnamed Jurassic sedimentary and Tertiary basalt units (units 6 and 11 of Panteleyev *et al.*, 1996).

The Gavin Lake succession is dominated by fine-grained, well-stratified, 25–30 mm thick beds of light and dark grey, wavy laminated siltstone, normal graded sandstone and cherty shale. Interbedded, massive or thick bedded pyroxene and plagioclase-rich crystal sandstone occurs locally or forms the matrix of thick-bedded debris flows.

The thin-bedded rocks are dark grey, black and rusty-weathering slate and dense cherty argillite that breaks with a conchoidal fracture. Interlayered with these are medium-bedded, pale and dark green, grey and brown cherty volcanic siltstone, brown medium-grained feldspathic sandstone with shale and siltstone rip-up clasts, and rare polylithic volcanic conglomerate. Also present, west of Antoine Lake, are coarse polymictic volcanic conglomerate, normal-graded beds of limestone, clast-dominated debris flows and finer grained laminar crossbedded sandstone-siltstone couplets. The conglomerate includes angular to subrounded pebbles of siltstone, green and maroon pyroxene-phyric basalt and pink hornblende–phyric subvolcanic monzonite supported by a silty or crystal-rich wacke matrix. Panteleyev *et al.* (1996) reported a Late Triassic (probably lower Norian) age for a suite of conodonts (GSC locality No. C-117644; Orchard, 1995). The colour alteration index (CAI) of 3.5 – 4.5 is slightly lower than the 5.0–5.5 CAI for Middle Triassic conodonts collected from the eastern sedimentary package of black phyllite.

North of Gavin Lake, the fine-grained sedimentary rocks are overlain conformably by bedded polymictic volcanic breccia and matrix-supported granule to pebble conglomerate, graded sandstone and cherty volcanic siltstone. Normal-graded beds and load structures indicate upright-facing, immature volcaniclastic units that contain pyroxene and plagioclase crystal-rich horizons and angular lithic fragments. Analcime and pyroxene flow breccias conformably cap the section (Fig. 2).

BASALT STRATIGRAPHY

The authors agree with the general stratigraphy of Bailey (1978) and Panteleyev *et al.* (1996), who recognized four main volcanic units in the study area (unit 1A and units 2, 3 and 4; see Fig. 2). Volcanic and epiclastic rocks of unit 1a were separated from the upper, dominantly volcanic sequence because they occur entirely within the Middle to Upper Triassic sedimentary unit 1, albeit near the top of the succession (Fig. 2), and on the basis of their petrochemical differences (Panteleyev *et al.*, 1996). They are interpreted to represent initiation of arc magmatism in a marginal-basin setting Bloodgood (1987). In the present study, these are referred to as Eastern arc basalt (MLTNv).

Units 2, 3 and 4 record the evolution of magmatism and the main construction period of the arc during the Late Triassic. These define the central axis of the arc and are referred to as Central arc basalt (LTNv). In general, the volcanic stratigraphy consists of a subaqueous pyroxene-phyric basalt unit, consisting mainly of flows and breccias; pyroclastic and lahar deposits of more evolved 'felsic' compositions; and an upper, subaerial, analcime-bearing olivine basalt unit (Logan and Mihalynuk, 2005). Ages of these three units were interpreted to span the Upper Triassic to Early Jurassic boundary. Subsequent U-Pb isotopic age dating of the various intrusive phases of the Polley and Bootjack stocks indicates that these intrusions are Late Triassic (Palfy *et al.*, 2000); therefore, they cannot intrude rocks younger than 200 Ma (Fig. 2).

Evidence for isolated Early Jurassic calcalkaline volcanism and plutonism is recognized in the area: for example, the 197 Ma (Logan *et al.*, in press) quartz-phyric dacite unit located immediately north of Mount Polley mine (Logan and Mihalynuk, 2005) and the 195 Ma quartz syenite dike at Shiko Lake. However, the majority of Early Jurassic strata within the study area are well-bedded sedimentary units that contain Early Sinemurian, Canadensis Zone fossils (GSC locality No. 93215b, 93960, 93961; Poulton and Tipper, 1991; Tipper, 1992) and mature, well-bedded, polylithic, monzonite-bearing conglomerate (Logan and Mihalynuk, 2005; Fig. 2). Provenance studies of Early Jurassic sedimentary sequences in the study area indicate immature arc-derived sandstone containing Late Triassic to Early Jurassic detrital zircons that suggest local sources dominated, or diluted and masked, any evolved North American continental sedimentary influence (Petersen *et al.,* 2004).

Middle to Late Triassic Metavolcanic Rocks (unit 1A)

Nine samples of metavolcanic rocks representing rocks from unit 1A (Panteleyev *et al.*, 1996) were collected from Spanish Mountain (n = 2), east of Spanish Lake (n = 3) and east of Horsefly in the vicinity of Viewland Mountain (n = 5). The rocks in the area of Spanish Mountain include plagioclase crystal tuffaceous siltstone, volcanic conglomerate and hornblende-plagioclase porphyritic breccia. Northeast of Spanish Lake, pale green foliated tuffaceous phyllite, massive greenstone and breccia dominate, with rare, thin pillowed flows of pyroxene porphyry basalt. Sections containing pyroxene basalt appear identical to the younger volcanic stratigraphy in the main Quesnel volcanic belt farther west. However, thin-section investigation reveals substantial recrystallization and low-grade metamorphism. Analcime basalt identified in the field is, in fact, metabasalt with secondary albite porphyroblasts filling vesicles. Panteleyev *et al*. (1996) showed a 1–2 km wide, northwest-trending belt of volcanic rocks extending between Horsefly and Quesnel lakes, centred on Viewland peak. Reconnaissance along the length of this belt collected representative samples of intermediate to mafic metavolcanic breccia and flow units. Deformation and lower greenschist metamorphism have also variably affected the massive breccia flow and tuffaceous units.

The volcanic rocks from the vicinity of Eureka peak (Bloodgood, 1987) comprise coarse porphyritic flows, breccia and fine-grained tuff. Phenocryst assemblages consist of pyroxene, hornblende and plagioclase. The volcanic rocks have been metamorphosed to lower greenschist facies. Metamorphic minerals include actinolite, albite, epidote, chlorite, quartz and calcite. Conodonts from limestone-bearing rocks southwest of Spanish Mountain have yielded Middle Triassic ages ranging from Anisian to Ladinian (Orchard, 1995), with conodont alteration indices (CAI) of 5.0–5.5. Bloodgood (1987) concluded that the chemistry suggested an island-arc origin with possible back-arc or marginal-basin affinities.

Late Triassic Augite-Phyric Volcanic Rocks

Maroon, green and grey pyroxene-phyric flow, breccia and pyroxene crystal–rich volcaniclastic units form the majority of the central volcanic belt. They are interfingered with augite-olivine, analcime and hornblende-bearing basalt units throughout the stratigraphic column (Panteleyev *et al.*, 1996; Logan and Mihalynuk, 2005) and near the top by limestone and felsic crystal tuffs (Fig. 2). Normal graded-bedding, crossbedding and load features are common in the sedimentary rocks; all indicate upright facing beds and a subaqueous environment of deposition.

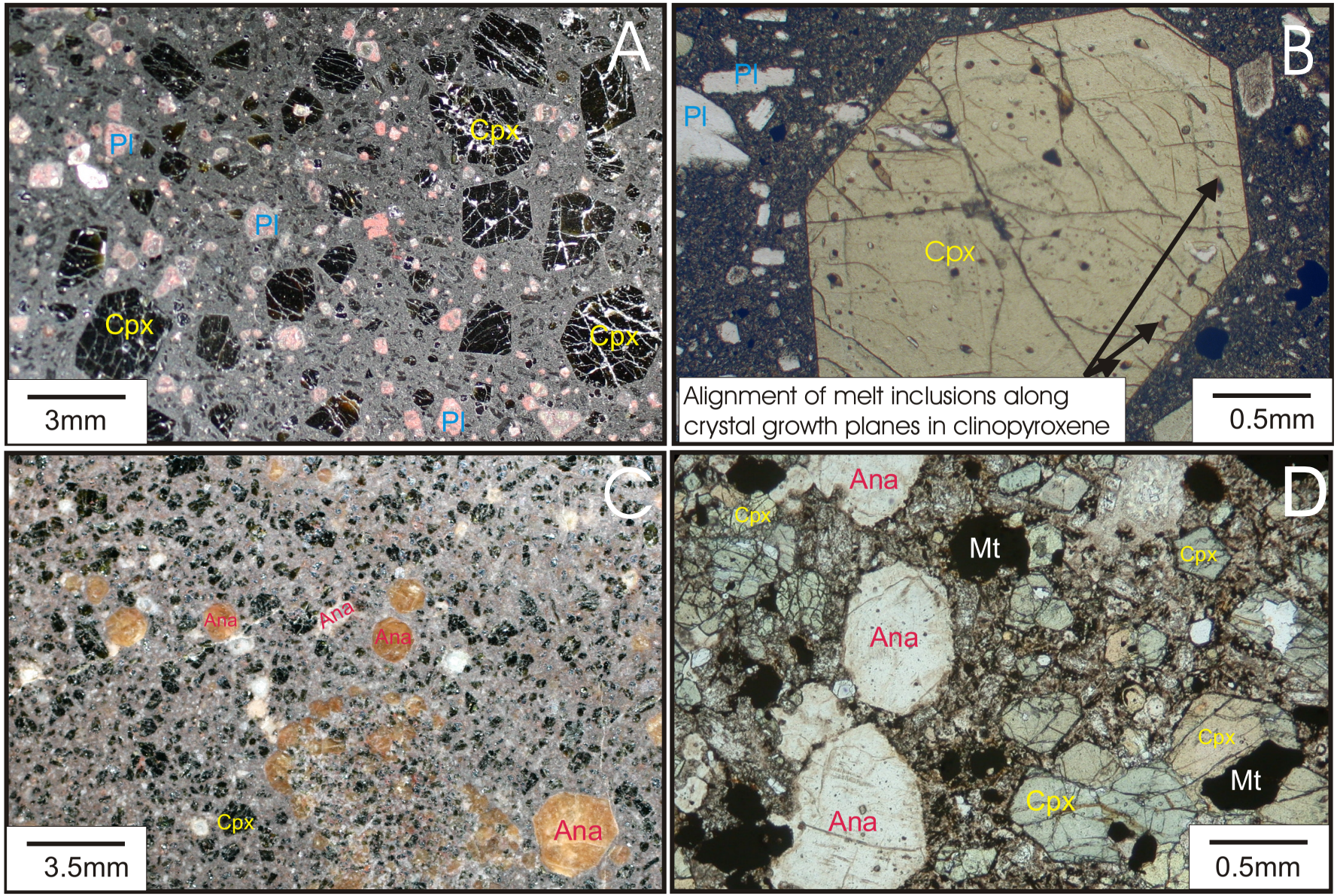


Figure 3. Hand samples (A and C) and thin sections (B and D) of typical alkaline basalt. Photomicrographs A and B are augite-plagioclase–phyric basalt; C and D are analcime-augite–phyric basalt with magnetite. Abbreviations: Ana, analcime; Cpx, augite; Mt, magnetite; Pl, plagioclase.

Coherent flows comprise 30% (to a maximum of 50%) medium to coarse-grained euhedral pyroxene (Fig. 3A, B), 20% subhedral plagioclase phenocrysts in a fine-grained felted seriate groundmass of plagioclase, pyroxene, ±olivine, magnetite and apatite. Euhedral coarse pyroxene crystals up to 5 mm in diameter are well zoned and often show alignment of melt inclusions along growth planes. Porphyritic augite flow breccia and flow tops are commonly amygdaloidal and exhibit trachytic alignment of plagioclase laths in a chloritic vitrophyric matrix.

Late Triassic Analcime-Phyric Volcanic Rocks

Analcime-bearing mafic flows crop out near Trio Lake, Mount Polley, west of Morehead Lake (Logan and Mihalynuk, 2005) and south of Antoine and Shiko lakes. South of Jacobie Lake, analcime-bearing basalt forms the basal flow unit that overlies the Gavin Lake succession. Excellent exposures are found along the highway north of Prior Lake within an ~260 m thick volcanic section dominated by dark grey-green to maroon, vesicular augite porphyry flows. Analcime content varies from one flow to the next, as do pyroxene and olivine contents.

Typical flows comprise 30% medium to coarse-grained euhedral pyroxene (up to 60%); 20–50% fine to coarse plagioclase, locally including coarse, trachytically aligned, bladed phenocrysts; 2–10% medium-grained olivine, commonly replaced by bright red iddingsite; up to 10% amygdules, mostly filled with calcite and chlorite; and 0–20% euhedral, salmon pink analcime up to 3 cm diameter (Fig. 3C, D).

Analcime occurs as euhedral phenocrysts, as irregular interstitial matrix material and as amygdule fillings in coherent basalt flows. In addition, it is present as euhedral grains in juvenile crystal lithic tuff and epiclastic units, which would support a primary origin for this phenocryst. The debate whether analcime is primary or secondary in similar Nicola lavas (Coates, 1960; Mortimer, 1987) or the younger Crowsnest Formation (Peterson and Currie, 1993) is inconclusive. Karlsson and Clayton (1991) presented strong isotopic and microprobe data to support low-temperature replacement of early leucite and a secondary origin for pristine analcime crystals.

Late Triassic to Early Jurassic (?) Hornblende-Phyric Volcanic Rocks

Hornblende-phyric basalt flows, dikes and breccia units form a subordinate but distinctive sequence exposed along the eastern side of the central volcanic belt at the QR deposit (Fox and Cameron, 1995) and north of Shiko Lake. Panteleyev *et al.* (1996) correlated these rocks (their unit 2d) with units 2a and 2b, which occupy a lower position in the Upper Triassic stratigraphy. Fossil or isotopic age constraints are lacking. From observations during the present study, similar hornblende-phyric flows and dikes are associated with sedimentary units high in the stratigraphy. These units are quartz poor and different from the Early Jurassic quartz-phyric hornblende dacite.

Hornblende-plagioclase porphyry dikes and diorite sills north of the Quesnel River at QR and Shiko Lake crosscut black and grey, thin laminated argillite and siltstone. The dikes are commonly rusty and contain 1–2% pyrite.

The rocks contain 3–5 mm euhedral grains of conspicuous hornblende, smaller euhedral pyroxene and plagioclase within a fine-grained seriate groundmass of the same minerals. Accessory minerals include magnetite, apatite, pyrite and the alteration minerals chlorite and carbonate. A white zeolite, possibly laumontite, occupies amygdules.

Intrusive Bodies

Dark green, 10–20 m wide pyroxenite bodies intrude fine-grained volcaniclastic rocks in two locales west of Gavin Lake. The pyroxenite occupies sill-like (conformable with bedding) bodies and dikes that crosscut bedding at high angles. The pyroxenite consists of coarse-grained, euhedral zoned pyroxene phenocrysts, altered subhedral olivine pseudomorphed by serpentine and talc, and plagioclase laths within a fine-grained, altered, opaque-rich (magnetite and pyrite) matrix of plagioclase, pyroxene and alteration minerals, including chlorite, talc and calcite. These intrusions are relatively rich in MgO (10.26 wt%; Table 1), represent a less fractionated magma, and contain similar major-element abundances as the pyroxenite at Mount Polley (*see* Bath and Logan, 2006; Fraser, 1994). They are likely feeder dikes to some of the early pyroxene-phyric basalt flows that stratigraphically overlie the western volcaniclastic sequence. Younger, texturally similar augite porphyry (AP) dikes that intrude the mine stratigraphy at Mont Polley have much lower MgO contents (5.26 wt% MgO; Fraser, 1994).

The western portion of the study area is intruded by metre to decimetre-wide quartz porphyritic monzonite dikes. The dikes consist of a fine-grained leucocratic matrix, variable amounts of finely disseminated pyrite and sparse to 10% euhedral quartz phenocrysts. Biotite (up to several percent) and rarely hornblende are present, but both are often completely replaced by sericite and carbonate. Weathering produces a distinctive limonitic-pinkish, fine-grained massive rock with conspicuous (2–8 mm) quartz phenocrysts. The largest concentration of these intrusive rocks occurs at Gavin Lake, where a coalescing swarm of east-trending dikes and small quartz monzonite porphyry plugs intrude an area approximately 0.5 km by 3 km immediately north of the lake. Chalcopyrite and molybdenite mineralization is associated with quartz and K-feldspar stockwork veining in the dikes. North-trending quartz veins, in places up to 5 m wide, cut the fine-grained volcaniclastic sequence. Mineralization includes chalcopyrite and galena with Au and Ag values reported (Hodgson, 1970). Bailey (1978) and Panteleyev *et al.* (1996) correlated these quartz-bearing calcalkaline intrusions with hornblende-biotite monzogranite of the Nyland Lake stock and included them in the Cretaceous Naver plutonic suite (Woodsworth *et al.,* 1991). A sample of quartz porphyritic monzogranite was collected for U-Pb geochronology; results are pending.

WHOLE-ROCK GEOCHEMISTRY

More than 100 representative samples were collected during the regional mapping of the Quesnel Lake area. These included samples of all major phases of the Mount Polley igneous complex, phases of equivalent (?) regional intrusive centres and a suite of the surrounding host lavas. Weathered surfaces or altered samples were screened by

TABLE 1. MAJOR-OXIDE AND SELECT TRACE-ELEMENT GEOCHEMISTRY FOR VOLCANIC AND INTRUSIVE ROCKS FROM THE QUESNEL LAKE AREA. ALL ANALYSES AT COMINCO LABS, VANCOUVER. ROCK AND MINERAL ABBREVIATIONS: pxnt, PYROXENITE; bslt, BASALT; brecc, BRECCIA; PX, PYROXENE; DORT, DIORITE; anal, ANALCIME; hnbl, HORNBLENDE; PO, PORPHYRY; epid, EPIDOTE; ALT, ALTERED; META, METAMORPHOSED; vlc, VOLCANIC. ANALYTICAL METHOD ABBREVIATIONS: XRF1, FUSED DISC – X-RAY FLUORESCENCE; TIT, HF DIGESTION – TITRATION; XRF2, PRESSED PELLET – XRF

			Element	SiO2	TiO2	Al2O3	Fe2O3	FeO	MnO	MgO	CaO	Na2O	K2O	P2O5	Ba*	LOI	Total	Nb	Rb	Sr	Y	Zr
			Units	%	%	%	%	%	%	%	%	%	%	%	%	%	%	ppm	ppm	ppm	ppm	ppm
			Method	XRF1	XRF1	XRF1	XRF1	TIT	XRF1	XRF1	XRF1	XRF1	XRF1	XRF1	XRF1	FUS	SUM	XRF2	XRF2	XRF2	XRF2	XRF2
Field Number			Detection limit	0.01	0.01	0.01	0.01	0.01	0.01	0.01	0.01	0.01	0.01	0.01	0.01	0.01	0.01	3	3	3	3	3
Western feeder dikes	Easting	Northing	Rock Type																			
L05-7-35	583391	5815847	pxnt	46.25	0.43	9.43	7.59	2.74	0.11	13.85	9.15	0.62	3.74	0.34	0.08	4.51	98.84	bd	108	420	7	26
L05-8-56	584508	5814773	pxnt	48.9	0.75	14.68	8.29	2.14	0.15	6.07	8.65	2.94	2.72	0.38	0.06	3.77	99.5	3	66	836	13	44
B05-38-309	581957	5816505	pxnt	46.74	0.5	11.6	3.75	6.5	0.14	10.86	8.53	1.11	4.26	0.37	0.08	4.62	99.06	bd	85	525	8	10
Eastern volcanics (MLTNv)																						
L05-31-242 B	617366	5815976	bslt	48.27	1.09	13.88	0.82	7.72	0.18	7.84	8.26	3.2	2.16	0.25	0.07	3.08	96.82	10	80	621	16	32
L05-31-244	624988	5812571	bslt-brecc	49.81	0.7	17.5	3.16	3.61	0.11	4.78	11.44	2.22	1.21	0.15	0.05	4.45	99.19	4	27	594	17	41
L05-31-245	627005	5809512	bslt	50.41	0.74	17.62	2.44	4.62	0.12	5.46	8	3.73	2.4	0.27	0.07	3.52	99.4	bd	38	964	22	44
L05-12-103	611942	5828360	bslt-brecc	48.91	0.75	14.01	1.77	5.99	0.11	11.27	7.69	2.1	2.04	0.23	0.11	4.42	99.4	7	96	197	19	127
L05-12-104	611789	5827866	bslt-brecc	55.5	0.73	14.23	0.99	4.19	0.09	5.71	6.78	5.09	2.09	0.57	0.12	3.35	99.44	10	56	352	32	127
L05-12-104-2	611789	5827866	bslt-brecc	51.22	1.01	16.79	1.36	5.85	0.1	6.92	4.59	3.95	3.27	0.43	0.17	3.94	99.6	14	143	273	30	180
L05-12-100	610588	5825008	plw-brecc	52.15	1.15	14.43	2.27	4.91	0.1	4.42	9.52	3.64	0.01	0.2	0.01	6.81	99.62	3	<3	243	32	84
Central volcanics (LTNv)																						
B05-13-105	586016	5819125	px bslt	47.43	0.63	13.35	6.31	3.97	0.17	8.14	11.32	1.82	2.78	0.31	0.06	2.73	99.02	bd	49	833	11	27
B05-17-137	598544	5831704	bslt brecc	48.56	0.69	13.85	0.07	9.4	0.18	8.4	10.69	2.31	1.54	0.23	0.05	3.6	99.57	4	42	578	17	35
L05-6-23	587770	5817263	bslt brecc	47.56	0.6	12.34	5.39	4.47	0.15	9.92	10.96	1.86	2.38	0.28	0.05	3.68	99.64	4	54	677	15	29
L05-9-69	592733	5831979	bslt brecc	47.97	0.63	13.01	3.94	4.62	0.15	8.42	13.06	1.96	1.6	0.2	0.07	3.95	99.58	4	50	495	16	43
L05-18-140	575825	5832707	bslt brecc	48.15	0.6	12.65	4.87	4.84	0.18	7.42	11.14	2.77	2.55	0.28	0.09	3.96	99.5	bd	51	614	12	31
L05-28-204	591320	5815000	px bslt	47.75	0.63	13.06	5.94	4.19	0.17	9.19	10.67	1.76	2.89	0.31	0.06	2.69	99.31	9	79	773	9	23
L05-29-210	592193	5808835	dort	48.18	0.66	14.97	5.82	3.97	0.18	7.23	8.97	2.11	3.46	0.33	0.08	3.2	99.16	7	84	1061	9	32
L04-14-24	594012	5820043	px dort	47	0.76	14.14	7.55	3.96	0.18	7.42	11.75	2.34	2.5	0.33	0.14	0.99	99.51	6	35	832	16	36
M04-19-6	594010	5820050	px dort	49	0.63	14.46	7.18	3.07	0.18	6.65	10.17	2.5	3.67	0.34	0.17	0.99	99.36	5	56	1263	17	40
L04-18-50	593810	5820137	px dort	48.7	0.76	18.01	5.58	4.32	0.17	4.51	9.89	3.06	2.65	0.28	0.13	1	99.55	-3	34	614	20	55
M04-21-1b	591861	5825326	bslt	49.13	0.62	16.37	5.09	3.61	0.15	5.17	7.13	2.57	5.15	0.44	0.2	3.23	99.27	6	88	1000	13	53
M04-22-4	605148	5812440	bslt brecc	49.79	0.67	14.71	4.63	4.13	0.15	7.75	9.55	2.24	2.48	0.41	0.15	2.54	99.66	3	34	773	17	71
M04-27-1	585709	5821580	bslt brecc	45.88	0.81	15.23	8.36	3.1	0.2	5.51	10.57	4.01	1.65	0.62	0.08	2.92	99.29	5	20	1207	19	57
L05-32-248	604402	5809833	px-po bslt	47.4	0.62	12.82	6.81	3.25	0.17	7.46	12.89	2.07	2.05	0.36	0.07	3.39	99.36	bd	50	1022	8	22
L04-12-10	582114	5826062	anal px bslt	45.75	0.81	12.13	7.83	4.48	0.2	7.71	12.85	3.44	0.93	0.64	0.06	2.48	99.81	7	8	912	14	53
L04-18-52	592046	5820432	anal px bslt	48.81	0.56	15.01	6.13	3.61	0.2	5.28	9.27	2.75	5	0.46	0.15	1.62	99.26	6	78	1764	9	41
L05-5-20	596421	5822497	anal px bslt	48.93	0.51	16.43	6.43	1.88	0.17	5.55	7.42	6.32	0.92	0.62	0.12	4.42	99.72	bd	17	1040	16	38
L05-13-109	603307	5811794	breccia	46.68	0.74	11.31	6.54	4.47	0.15	8.78	11.56	2.13	2.27	0.4	0.06	4.38	99.47	7	57	833	15	33
L05-29-216	602006	5804767	anal px bslt	47.72	0.66	14.52	7.5	2.38	0.15	6.03	9.25	4.34	1.66	0.34	0.15	4.64	99.34	bd	24	573	14	43
L05-32-246-2	600846	5804521	anal px bslt	46.47	1.04	13.81	9.62	2.45	0.28	5.53	10.63	3	2.74	0.75	0.11	3.27	99.7	bd	159	898	9	44
L05-17-133	602475	5815074	hnbl bslt	47.81	1.25	13.48	3.05	7.36	0.17	7.15	9.69	2.85	1.78	0.31	0.07	4.46	99.43	7	73	409	18	73
L05-26-194	589271	5815117	hnbl bslt	48.36	0.8	14.77	3.86	5.12	0.15	8.3	10.43	3.64	0.68	0.2	0.03	2.98	99.32	bd	17	862	18	55
L05-30-222	581841	5836202	hnbl bslt	51.27	0.91	17.12	3.65	3.75	0.1	3.44	8.06	2.81	4.94	0.4	0.2	2.71	99.36	4	105	530	19	83
B05-35-280	580735	5835899	hnbl dort	49.38	0.85	17.2	2.16	7.07	0.15	4.42	8.35	2.86	3.61	0.37	0.14	3.29	99.85	bd	106	802	19	37
L05-30-223	580758	5835905	hnbl dort	50.38	0.83	15.86	1.87	6.06	0.12	4.75	9.05	2.74	3.75	0.4	0.21	3.21	99.23	3	93	647	20	57
Early Jurassic Dacite																						
B05-28-230	591796	5826577	hnbl dacite	57.15	0.43	17.79	4.12	1.15	0.15	1.46	5	4.98	2.71	0.17	0.22	4.08	99.41	bd	50	514	15	66
M04-26-18	592800	5826580	dacite	57.91	0.43	17.81	4.06	1.13	0.14	1.48	4.59	4.82	2.76	0.18	0.22	3.95	99.61	7	27	487	17	67
Q/C																						
CANMET SY4				49.69	0.28	20.59	3.11	2.69	0.10	0.51	7.98	7.03	1.60	0.11	0.03	5.41	99.10	10	54	1212	114	508
CANMET SY4	**Recommended**			49.9	0.287	20.69	3.35	2.86	0.108	0.54	8.05	7.1	1.66	0.131	0.034	4.56		13	55	1191	119	517
L05 5-20				48.93	0.51	16.43	6.43	1.88	0.17	5.55	7.42	6.32	0.92	0.62	0.12	4.42	99.72	bd	17	1040	16	38
L05-20rep				48.81	0.51	16.37	6.49	1.85	0.17	5.55	7.44	6.4	0.92	0.58	0.12	4.46	99.67	bd	11	1039	16	34
% Difference				0.25	0.00	0.37	0.93	1.61	0.00	0.00	0.27	1.26	0.00	6.67	0.00	0.90	0.05	0.00	42.86	0.10	0.00	11.11

careful inspection of hand samples, and 75 were selected for analysis. Samples were milled in chrome steel (trace elements) and tungsten carbide (major oxides) at the BC Geological Survey laboratory in Victoria. Replicate samples and standards were included and the splits were shipped for analyses to Teck Cominco Laboratories, Vancouver for major-element and trace-element abundances (Ba, Rb, Sr, Nb, Zr and Y) by X-ray fluorescence (XRF); Acme Analytical Laboratories Ltd., Vancouver for trace-element analyses using inductively coupled plasma – emission spectrometry (ICP-ES); and Activation Laboratories Ltd., Ancaster, Ontario for trace-element analyses using instrumental neutron activation analysis (INAA). A subset of the samples was sent to Memorial University, Newfoundland (MUN) for trace-element analyses using inductively coupled plasma – mass spectrometry (ICP-MS). Detection limits, precision and accuracy are discussed in a companion paper (Bath and Logan, 2006).

This report focuses on the geochemical characterization of the Triassic basalt stratigraphy across the axis of the Quesnel arc at the latitude of Quesnel Lake, in the vicinity of the alkalic Cu-Au porphyry deposit at Mount Polley. Thirty-seven basalt samples are discussed in this report. Samples of the volcanic units have moderate to high loss-on-ignition values (0.99–4% LOI). This data set was complemented by whole-rock analyses from published sources (Bloodgood, 1987; Panteleyev *et al*., 1996; Fraser, 1995).

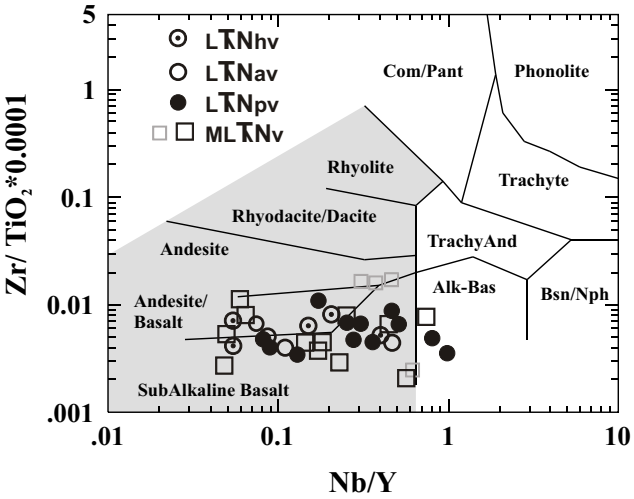


Figure 4. Zr/TiO2 *vs.* Nb/Y plot of Triassic Nicola Group volcanic rocks showing compositional range and classification for Mount Polley area (after Winchester and Floyd, 1977). Rock type codes: LTNhv, hornblende phyric basalt; LTNv, analcime-phyric basalt; LTNvpv, pyroxene-phyric basalt; MLTNv, hornblende-pyroxene metabasalt; small square, this study; large square, data from Bloodgood (1987).

RESULTS

Major Oxides

Major and trace-element compositions of representative volcanic rocks from the Nicola Group are provided in Table 1. Normative calculations, discriminant and bivariant plots use chemical data that are recalculated to 100% volatile free. Overall, the rock compositions are comparable to Nicola lavas from the southern (Mortimer, 1987), central (Barrie, 1993) and northern (Takla; Dostal *et al.*, 1999) Quesnel Terrane (Souther, 1977). The silica content varies between 45 and 52 wt%. The rocks have a moderately high content of alkalis (5–7 wt% Na_2O+K_2O) and plot as transitional to alkaline on the total alkali *versus* silica diagram (Irvine and Baragar, 1971) and as subalkaline basalt and andesitic basalt on the Zr/TiO_2 *versus* Nb/Y immobile element plot (Fig. 4) of Winchester and Floyd (1977), a result of the relatively depleted Nb and lower high field strength elements (HFSE; *e.g.*, <1.1 wt% TiO_2) that characterize volcanic arc rocks. Intraplate rifts and continental alkalic suites are enriched in Nb and TiO_2 relative to volcanic rocks formed at destructive plate boundaries, and plot to the right of the shaded area in the alkali basalt field.

An AFM plot (Fig. 5) shows a calcalkaline trend for the majority of the sample suite. Basalt from the Eureka peak area (Bloodgood, 1987) and stratigraphically equivalent lavas from the eastern side of the arc at Spanish Mountain (SM), east of Spanish Lake (SL) and in the Viewland Peak area (VP) straddle the tholeiitic-calcalkaline trend. These basalts are interlayered with Middle to Upper Triassic sedimentary rocks, and are older than the main arc and may therefore represent early volcanism and initiation of arc magmatism (Bloodgood, 1987; Panteleyev *et al.,* 1996). The typically high MgO contents (mean values of 7–10 wt%; Table 1) indicate that these volcanic rocks represent a primary magma that has not under gone substantial fractionation (see Fig. 6).

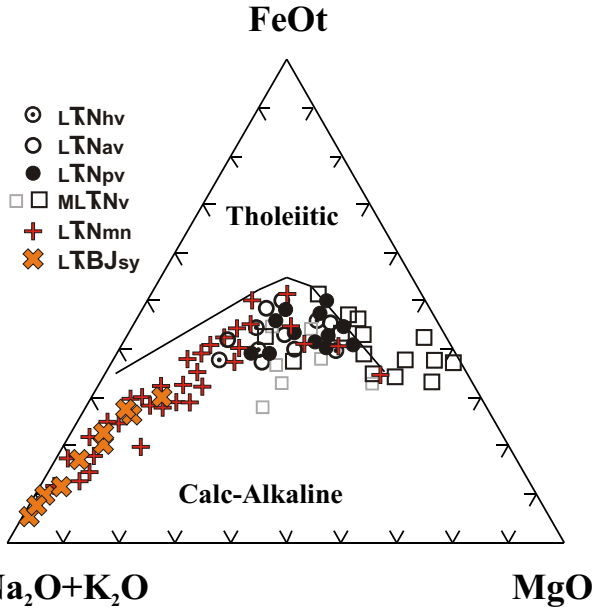


Figure 5. AFM ternary diagram showing calcalkaline nature of Mount Polley igneous rocks. Rock type codes as in Figure 4 plus LTNmn, Late Triassic regional intrusive rocks (diorite to monzonite) and LTBJsy, Bootjack stock syenite.

When plotted against an index of fractionation such as wt% MgO (Fig. 6), the major-element abundances can be used to determine the cogenetic relationships between different rock units. With the exception of a subset of the most primitive Eureka Peak basalt (Bloodgood, 1987; Panteleyev *et al.,* 1996, unit 1A), the smooth linear trends for the remaining samples suggest they can all be related by simple fractional crystallization. The FeO_T, TiO_2, P_2O_5,

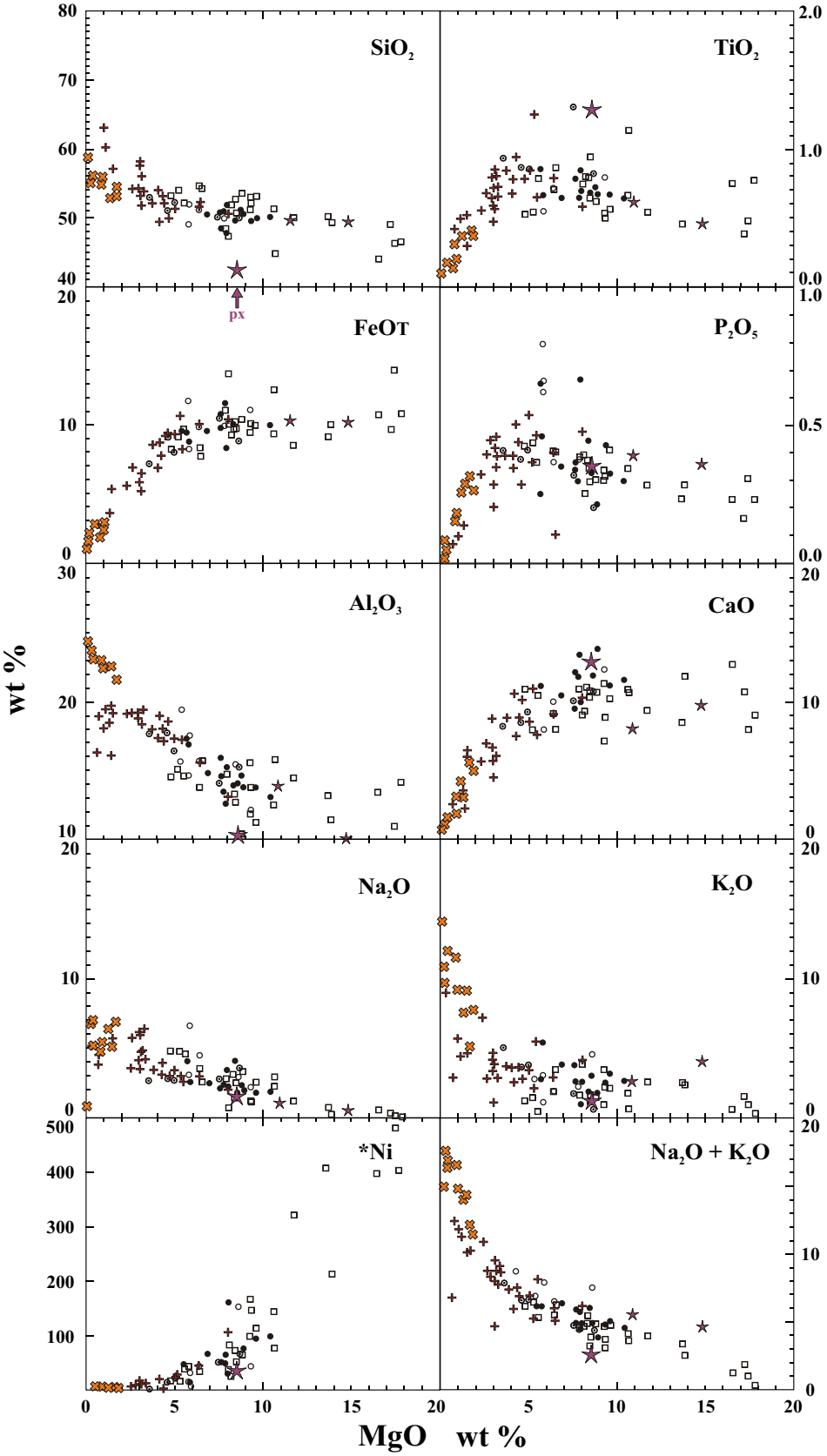


Figure 6. Major-element and trace-element bivariant diagrams for Nicola basalt, Eureka peak basalt (Bloodgood, 1987), pyroxenite (Fraser, 1994), regional intrusive units and Bootjack stock syenite. Symbols as in Figure 4 plus star, pyroxenite; large star, Fraser (1994). All analyses recalculated 100% volatile free. * Ni values in ppm.

TABLE 2. TRACE-ELEMENT DATA FOR VOLCANIC ROCKS FROM THE QUESNEL LAKE AREA. ELEMENTS ON LEFT SIDE OF TABLE (Au TO W) WERE ANALYZED AT ACME ANALYTICAL LABORATORIES, VANCOUVER; ELEMENTS ON RIGHT SIDE OF TABLE (Y TO Th) WERE ANALYZED AT MEMORIAL UNIVERSITY, NEWFOUNDLAND (MUN). ANALYTICAL METHOD ABBREVIATIONS: FAI, LEAD-COLLECTION FIRE ASSAY – ICP-ES FINISH; TICP, FOUR-ACID DIGESTION – INDUCTIVELY COUPLED PLASMA–EMISSION/MASS SPECTROMETRY ANALYSIS; PIMS, PEROXIDE FUSION – ICP-MS. HIDDEN STANDARDS (GSB TILL 99/GRX1 AND CANMET SY4) AND REPEAT ANALYSES (MMI04 21-1 AND ABA05 32-259-1) WERE USED TO EVALUATE ANALYTICAL ACCURACY FOR THE SUITE OF ELEMENTS ANALYZED AT ACME LABS AND AT MUN (GREY BACKGROUND)

Element	Au	Mo	Cu	Pb	Zn	Ag	Ni	Co	As	U	Bi	W	Y	Zr	Nb	Ba	La	Ce	Pr	Nd	Sm	Eu	Gd	Tb	Dy	Ho	Er	Tm	Yb	Lu	Hf	Ta	Th
Unit	ppb	ppm	ppm	ppm	ppm	ppb	ppm	ppm	ppm	ppm	ppm	ppm	ppm	ppm	ppm	ppm	ppm	ppm	ppm	ppm	ppm	ppm	ppm	ppm	ppm	ppm	ppm	ppm	ppm	ppm	ppm	ppm	ppm
Method	FAI	TICP	TICP	TICP	TICP	TICP	TICP	TICP	TICP	TICP	TICP	TICP	MUN	MUN	MUN	MUN	MUN	MUN	MUN	MUN	MUN	MUN	MUN	MUN	MUN	MUN	MUN	MUN	MUN	MUN	MUN	MUN	MUN
Detection Limit	1	0.05	0.02	0.02	0.02	20	0.1	0.2	0.2	0.1	0.04	0.1	0.004	0.042	0.028	0.077	0.006	0.008	0.003	0.030	0.014	0.006	0.017	0.004	0.026	0.002	0.010	0.003	0.012	0.003	0.021	0.042	0.008
Field Number																																	
Eastern volcanics (MLTNv)																																	
L05-31-244	10	0.43	67.55	3.43	78.6	54	27.6	23.3	0.6	0.4	bd	0.1																					
L05-31-245	2	0.35	125.54	3.5	76.4	70	33.8	24.5	1.1	0.5	bd	0.1	15.54	50.29	2.23	927.80	7.18	14.17	1.94	8.97	2.44	0.83	2.90	0.47	2.98	0.62	1.80	0.27	1.80	0.26	1.52	0.10	0.83
JLO 12-100	6	0.11	312.25	1.76	61.3	144	89.5	32.7	33.2	0.1	-0	0.5	28.28	88.90	2.14	37.96	3.42	8.74	1.82	9.86	3.26	1.31	4.68	0.78	5.14	1.09	3.17	0.46	3.00	0.42	2.30	#####	#####
L05-12-104	4	0.22	234.01	66.52	50.7	259	58.2	20.5	5	1.7	0.34	1.5	23.84	133.24	15.51	1688.75	47.21	76.74	9.51	36.03	5.88	1.31	4.96	0.67	4.01	0.83	2.44	0.36	2.41	0.38	3.24	0.67	14.31
Central volcanics (LTNv)																																	
L05-6-23	3	0.37	141.68	5.86	86.6	90	94.8	47.6	1.7	0.4	0.04	0.2	12.23	38.41	1.64	643.91	5.57	11.40	1.62	7.80	2.05	0.71	2.40	0.39	2.47	0.50	1.44	0.21	1.35	0.20	1.15	0.07	0.64
L05-9-69	6	0.53	101.23	3.8	67	74	73.6	37	1.3	0.5	bd	0.2	14.67	51.58	2.10	1040.24	5.51	12.37	1.78	8.68	2.45	0.79	2.93	0.47	2.97	0.59	1.74	0.25	1.58	0.23	1.48	0.11	0.97
L05-18-140	11	0.28	144	5.45	86.1	86	45.1	38.7	3	0.4	bd	0.1	12.29	41.25	1.55	1289.30	6.56	12.76	1.76	8.04	2.08	0.70	2.50	0.39	2.41	0.49	1.47	0.21	1.42	0.21	1.24	0.08	0.84
L05-28-204	5	0.48	150.12	5.09	89.8	83	92.8	44.8	1.4	0.4	bd	0.2	13.57	43.88	1.98	882.05	6.37	12.94	1.79	8.39	2.19	0.75	2.54	0.41	2.54	0.52	1.51	0.22	1.48	0.22	1.28	0.09	0.75
L05-29-210	7	0.49	158.7	6.37	91.1	95	57.1	38.8	2.1	0.6	bd	0.2	14.60	49.72	2.70	1164.59	7.51	14.97	2.05	9.40	2.43	0.82	2.73	0.44	2.78	0.58	1.68	0.24	1.64	0.25	1.23	0.12	1.04
L04-14-24	2	0.62	204.43	5.82	98.1	77	57.1	41.7	3.5	0.5	bd	0.2	13.63	34.05	1.59	1687.44	5.61	11.70	1.71	8.27	2.14	0.75	2.73	0.44	2.82	0.54	1.56	0.22	1.48	0.21	1.07	0.08	0.63
M04-19-6	5	1.63	42.69	5.21	82.8	37	62.8	35.4	2.2	0.7	bd	0.6	12.42	39.56	4.62	2092.92	6.26	12.54	1.75	8.16	1.99	0.68	2.42	0.38	2.43	0.50	1.44	0.21	1.39	0.20	1.12	0.12	0.92
L04-18-50	5	1.16	99.86	4.08	104.3	64	8.9	32.5	2.4	0.7	bd	0.4	16.65	56.91	2.48	1443.90	6.45	13.47	1.90	9.19	2.32	0.82	2.99	0.50	3.25	0.65	1.91	0.28	1.85	0.26	1.55	0.12	0.92
M04-21-1b	8	1.17	150.98	8.68	85.3	104	47.4	29.9	32.9	1	bd	0.7	12.40	52.10	4.77	2495.53	8.05	15.45	2.06	9.06	2.13	0.70	2.37	0.38	2.38	0.48	1.42	0.21	1.42	0.20	1.35	0.16	1.34
M04-22-4	5	0.66	135.96	7.57	74.6	83	158	36.7	3.4	1.2	bd	0.3	12.60	75.76	4.57	2068.57	10.78	21.41	2.84	12.22	2.66	0.81	2.73	0.42	2.46	0.49	1.43	0.21	1.40	0.20	1.87	0.16	2.11
M04-27-1	5	1.96	289.07	8.32	118.8	206	13.6	46.4	2.7	1.1	bd	0.5	16.22	68.62	3.75	1080.19	16.50	31.37	4.10	17.49	3.74	1.16	3.77	0.56	3.31	0.64	1.82	0.26	1.64	0.23	1.83	0.17	2.28
L05-32-248	bd	0.69	204.19	5.67	87.1	79	56.8	41.4	1.9	0.7	bd	0.2	12.98	40.66	1.70	897.37	8.42	16.75	2.29	10.38	2.41	0.80	2.70	0.41	2.58	0.52	1.51	0.21	1.39	0.20	1.21	0.07	0.94
L04-12-10	13	1.28	169.8	6.66	101.5	98	26.3	51.3	1.7	0.9	bd	0.3	13.84	55.28	3.24	764.32	13.54	26.84	3.56	15.69	3.40	1.04	3.57	0.52	3.02	0.55	1.49	0.21	1.34	0.19	1.55	0.14	1.72
L04-18-52	6	0.6	172.07	9	104.8	87	26.9	36.2	4.8	0.5	bd	0.5	11.47	44.97	2.73	1707.68	8.23	16.06	2.14	9.78	2.23	0.72	2.44	0.37	2.24	0.44	1.29	0.19	1.22	0.18	1.24	0.13	1.19
L05-5-20	8	0.35	232.27	9.83	93.1	111	24.6	28.7	1.6	1.8	0.07	0.2	11.40	54.54	3.83	1626.08	15.09	24.82	3.01	11.89	2.38	0.75	2.40	0.36	2.20	0.44	1.27	0.18	1.23	0.18	1.29	0.14	2.28
L05-13-109	4	0.77	132.41	4.44	92.1	38	45.9	50	7.1	0.8	bd	0.5	14.75	55.71	3.04	885.21	11.27	21.93	2.88	12.90	2.97	0.96	3.26	0.50	3.06	0.59	1.69	0.24	1.54	0.23	1.58	0.14	1.47
L05-29-216	9	0.74	54.28	5.8	121	40	38.1	37.1	2.9	0.7	bd	0.5	14.46	49.72	2.64	2172.05	7.47	14.81	2.04	9.43	2.39	0.78	2.65	0.43	2.75	0.56	1.63	0.24	1.56	0.23	1.35	0.12	1.12
L05-32-246-2	3	0.71	208.93	6.56	125.3	140	12.6	45.9	4.2	1.1	bd	0.2	15.46	55.10	3.63	1489.70	13.28	26.39	3.62	16.17	3.72	1.16	3.87	0.57	3.34	0.63	1.73	0.24	1.56	0.23	1.75	0.20	1.56
L05-17-133	bd	1.47	123.36	1.29	86.5	71	54.7	41	4.2	0.7	bd	0.2	22.10	80.70	4.21	1002.50	7.34	16.50	2.50	12.03	3.33	1.15	4.25	0.68	4.41	0.91	2.61	0.37	2.43	0.36	2.17	0.22	1.28
L05-26-194	5	0.73	102.72	5.34	86.1	55	66.3	39.3	2.2	0.6	bd	0.1	18.69	69.53	3.40	372.34	6.94	14.66	2.09	9.92	2.60	0.92	3.19	0.54	3.53	0.72	2.11	0.31	2.04	0.32	1.84	0.17	0.99
L05-30-222	11	2.41	13.92	3.62	43.8	45	4.3	11.4	6.8	1.2	0.04	3.3	21.57	98.48	4.31	2838.67	12.50	26.78	3.80	17.45	4.21	1.25	4.26	0.68	4.16	0.86	2.42	0.36	2.33	0.35	2.49	0.21	2.91
B05-35-280	bd	1.62	163.46	4.15	67.5	241	16	37.5	2.3	1.3	bd	0.5	17.73	72.02	3.05	1922.88	10.10	20.95	2.94	13.51	3.20	0.99	3.56	0.56	3.48	0.72	2.02	0.29	1.97	0.28	1.99	0.16	2.35
L05-30-223	3	2.27	48.24	5.03	53.8	101	22.1	21.9	1.2	1.9	bd	1.6	18.69	75.06	4.02	2966.24	13.82	27.91	3.83	17.22	3.99	1.33	3.92	0.59	3.62	0.75	2.12	0.31	1.99	0.30	1.96	0.17	3.66
Early Jurassic Dacite																																	
M04-26-18	2	1.16	57.71	5.79	77.9	113	1.6	10.5	2.6	0.8	bd	0.7	10.72	68.15	2.24	2727.23	6.83	13.81	1.91	8.54	1.97	0.68	2.05	0.33	2.00	0.41	1.24	0.19	1.31	0.19	1.63	0.13	1.38
Q/C																																	
Standard	35	19.04	1289.10	830.98	899.5	38425	38.9	8.7	473.3	36.2	1701	200	107.54	612.00	17.95	410.03	57.31	118.97	14.75	57.77	12.47	1.89	14.12	2.63	18.91	4.31	14.21	2.26	14.91	2.06	11.06	0.82	1.28
Recommended	36	18.00	1110.00	720.00	760.0	31000	41.0		401.0	33.0	1380	164	119.00	517.00	13.00	340.00	58.00	122.00	15.00	57.00	12.70	2.00	14.00	2.60	18.20	4.30	14.20	2.30	14.80	2.10	10.60	0.90	1.40
Sample	25	0.74	99.23	47.56	104.1	343	3.3	16.6	12.2	1.8	0.15	1.6	9.63	57.96	4.49	2990.90	11.23	19.02	2.28	9.07	1.80	0.65	1.75	0.27	1.74	0.36	1.10	0.18	1.22	0.18	1.36	0.20	1.61
Sample (rep)	24	0.84	99.56	47.37	110.5	363	3.3	16.7	12.1	2.0	0.14	1.6	9.46	56.56	4.49	3005.14	11.00	18.74	2.27	8.85	1.79	0.64	1.71	0.27	1.70	0.36	1.11	0.17	1.17	0.17	1.30	0.20	1.67
% Difference	4	12.66	0.33	0.40	6.0	6	0.0	0.6	0.8	10.5	6.90	0.0	1.83	2.45	0.03	0.48	2.07	1.46	0.44	2.53	0.32	0.70	2.36	1.83	2.00	1.46	0.69	3.89	4.85	5.80	4.11	0.31	3.91

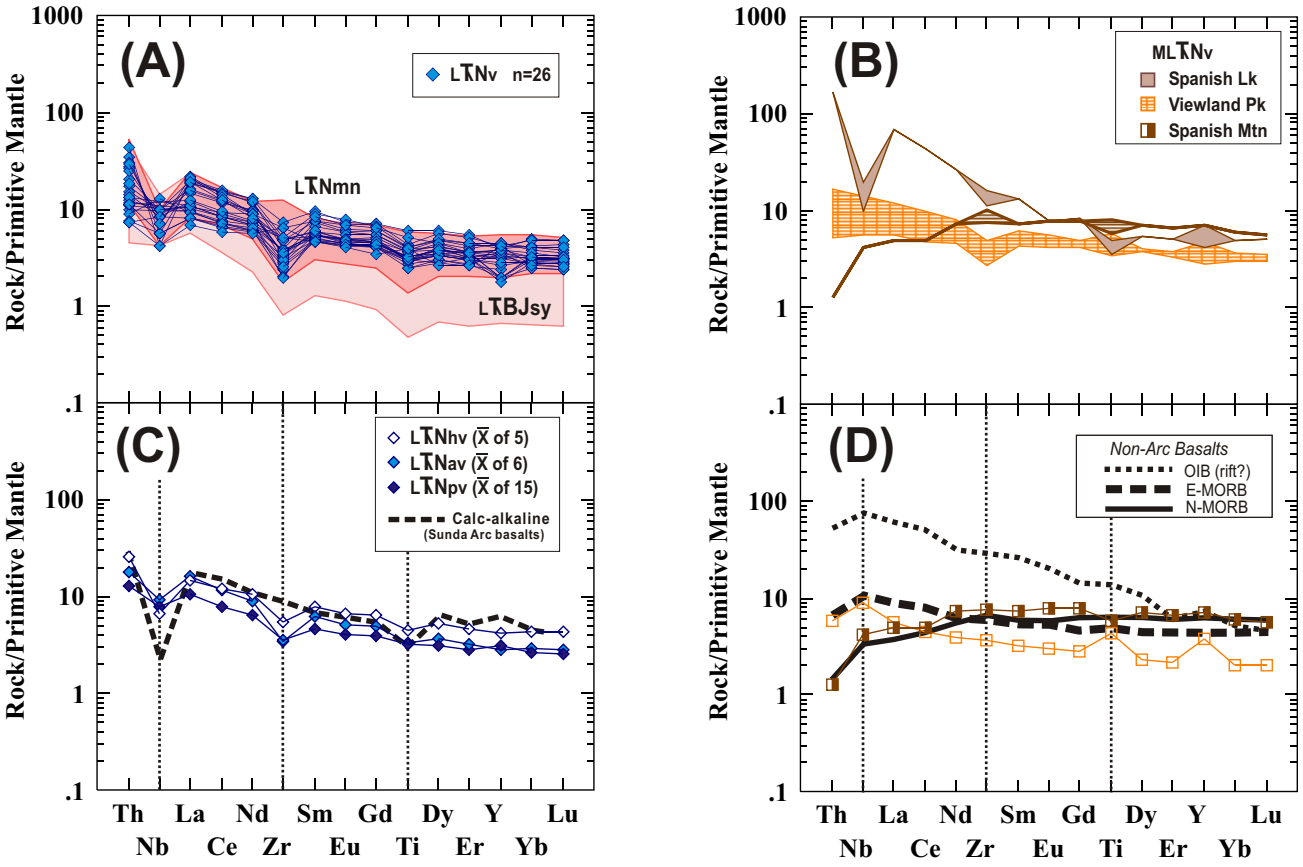


Figure 7. Primitive mantle–normalized (Sun and McDonough, 1989) multielement plots for Late Triassic Nicola Group basalt and basaltic andesite (LTNv) from the central part of the arc (A and C) and Middle to Late Triassic 'black phyllite'–hosted volcanic rocks (MLTNv) from the eastern side of the arc (B and D). Shaded areas in A correspond to the range of values for Late Triassic regional diorite to monzonite intrusive rocks (dark) and syenite of the Bootjack stock (light). Plot C compares average pattern of pyroxene, analcime and hornblende-phyric basalts with a typical calcalkaline island-arc basalt from the Sunda Arc (Jenner, 1996). Plot D compares average pattern of Viewland Peak metabasalt and pillowed basalt (L05-12-100) from Spanish Mountain with OIB, E-MORB and N-MORB from Sun and McDonough (1989).

CaO and Ni values display positive correlations, whereas Al_2O_3, Na_2O and SiO_2 and Na_2O+K_2O correlate negatively. The major-oxide trends show the least differentiated (*i.e.*, highest wt% MgO) to be the oldest basalt of unit 1A, and show progressive evolution and differentiation from pyroxene to analcime and finally hornblende-bearing basalt and the coeval/cogenetic intrusive suites of diorite-monzodiorite-syenite (Panteleyev *et al.*, 1996; this study). The pyroxenite that intrudes the Gavin Lake sedimentary succession is more primitive and shows better overall positive correlation with differentiation trends than the Mount Polley pyroxenite (Fraser, 1994). In fact, the Mount Polley pyroxenite sample has an intermediate MgO value relative to the most primitive basalt and the most fractionated syenite samples from the Bootjack stock (Bath and Logan, 2006). Overall, the differentiation trends are normal and consistent with fractional crystallization of olivine, clinopyroxene, Fe-Ti oxides, plagioclase and apatite. The increase in Al_2O_3 and SiO_2 and the sharp decrease in CaO and MgO beginning at approximately 9 wt% MgO probably reflect fractional crystallization (removal) of clinopyroxene. The sharp decline in Ni (and Cr) supports an early fractionation of olivine and clinopyroxene, and the general increase in P_2O_5 and TiO_2 contents with decreasing MgO reflects early suppression and subsequent crystal fractionation of apatite and sphene (Fig. 6).

The K_2O values show no correlation, whereas Na_2O shows a strong negative correlation, as does Na_2O+K_2O with the exception of the highly differentiated and potassic Bootjack stock syenite.

Trace Elements and Rare Earth Elements

Trace and rare earth element (REE) abundances of representative volcanic rocks from the Nicola Group are given in Table 2.

Mafic rocks from the central belt are basalt and basaltic andesite. They have TiO_2 contents of 0.7–0.85 wt% and low Nb contents ranging from <3 to 7 ppm (Table 1). The chondrite-normalized REE patterns for the basalt from the central belt are characterized by mean light rare earth element (LREE) enrichments (La/Yb_{CN} = 3.4, 3.9 and 5.6) and a downward sloping pattern toward the heavy rare earth elements (HREE). The HREE are essentially flat, (<10 times chondrite, not shown). Primitive mantle–normalized trace-element patterns of the Central arc basalt suite (LTNpv, LTNav and LTNhv) have broadly similar patterns (Fig. 7A, C). All are characterized by moderate negative Nb anomalies relative to Th and La, and all possess negative Ti anomalies and a generally downward sloping profile from LREE to HREE. The geochemical patterns for the basalt, and a

suite of Late Triassic diorite-monzonite-syenite intrusive rocks collected from the study area, are similar and suggest that they are cogenetic. Also shown is the trace-element pattern of the Late Triassic Bootjack syenite stock, with its higher concentrations of incompatible elements (left side of diagram) and lower concentrations of compatible elements (right side of diagram) compared to the regional diorite and basalt, which is consistent with fractionation from a dioritic parent magma (Bath and Logan, 2006). Primitive mantle–normalized mean trace-element values of the hornblende, analcime and pyroxene-phyric basalts (Fig. 7C) are variably depleted but closely parallel the pattern for calcalkaline-arc basalt from the Sunda arc (Jenner, 1996), which supports the field relationships (*i.e.*, interlayered breccia flows and coarse to fine tuff, polylithic breccia and epiclastic deposits).

The mafic volcanic rocks from the eastern volcanic belt (Spanish Lake, Spanish Mountain and Viewland Peak suites) are subalkaline basalt and andesite. They have similar TiO_2 contents of 0.7–1.0 wt% and low Nb contents of 3–14 ppm (Table 1), but show different trace-element abundances and multielement patterns when compared. Chondrite-normalized REE patterns for the basalt from the Viewland Peak suite are characterized by mean LREE enrichments (La/Yb_{CN} = 2.8) and a downward sloping pattern toward the HREE, but the basalt from Spanish Mountain is characterized by an upward sloping pattern toward the HREE. The HREE are essentially flat (~10 times chondrite for VP and 20 times chondrite for SM, not shown). The primitive mantle–normalized trace element patterns of the Viewland Peak and Spanish Mountain basalts (Fig. 7B, D) are characterized by depletions in the LREE (La, Ce) and most incompatible elements (Th, Nb), and therefore reflect typical depleted-mantle sources. Both have a positive Nb anomaly relative to Th and La, and positive Zr and Ti anomalies. They have flat or slightly negative slopes that closely overlap the global compilation patterns (Sun and McDonough, 1989) for enriched mid-ocean ridge basalt (E-MORB) and normal mid-ocean ridge basalt (N-MORB), respectively. The primitive mantle–normalized trace-element patterns for the Spanish Lake basalt are similar to patterns for subduction-generated arc basalt, but show elevated incompatible elements (Th, Nb) in comparison to central belt alkaline basalt.

On the Zr-Y-Ti tectonic discrimination diagram (after Pearce and Cann, 1973; Fig. 8), which is used to distinguish non-arc basalt (high Ti/Y ratios) from other magma types, all of the basalt from the central volcanic belt plots in arc-basalt fields, specifically fields A (tholeiitic volcanic-arc basalt, VAB) and B (MORB and calcalkaline VAB), with three metabasalt samples (MLTNv) from the eastern side of the arc (Viewland Peak area) plotting in field C (calcalkaline VAB). The distinction between fields A and B and field C can be modelled by upper crustal assimilation, which changes the composition from the average N-MORB mantle toward average upper crustal compositions (higher Zr values; Pearce, 1996). All of the basalt from the central volcanic belt has high-field-strength element (HFSE) abundances that are characteristic of VAB (high Th/Y ratios and Nb depletion) and plot in the calcalkaline (Hf/Th ratios <3) portion of the arc-basalt field on Figure 9 (after Wood, 1980). A single sample of pillowed basalt from Spanish Mountain falls into the MORB field (A).

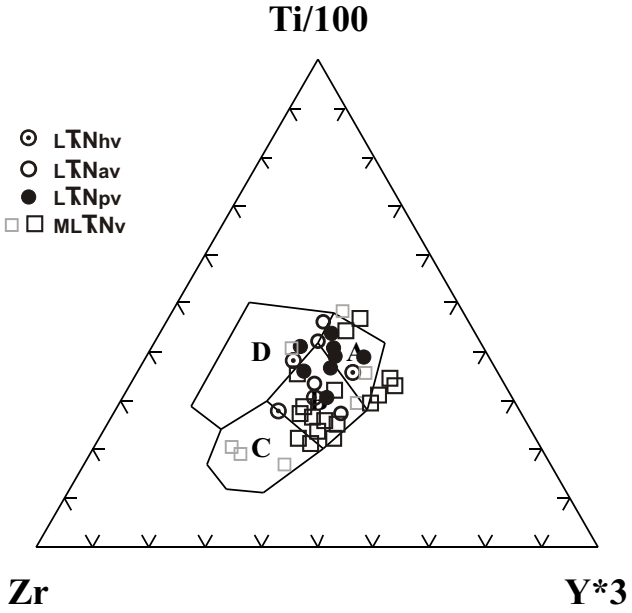


Figure 8. Tectonic discrimination diagram based on Zr, Ti, Y (after Pearce and Cann, 1973), used to distinguish non-arc basalt (high Ti/Y ratios) from other magma types and a partial separation of MORB and VAB. MORB plot in field B, calcalkaline VAB plot in fields B and C, tholeiitic VAB plot in field A and C, and non-arc within-plate basalt (WPB) plot in field D. Symbols as for Figure 3. All basalt and basaltic andesite from the central volcanic belt plot within fields A and B, with the exception of three basalt samples (MLTNv) from the eastern side of the arc (Viewland Peak area), which occupy field C.

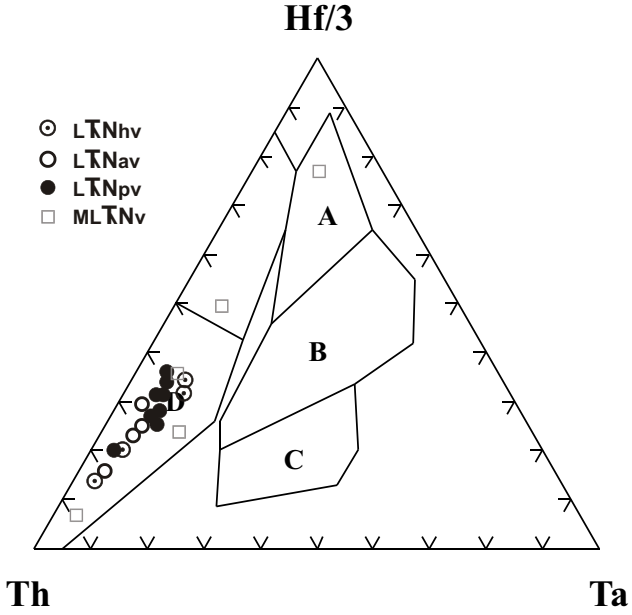


Figure 9. Tectonic discrimination diagram based on Th, Hf, Ta (after Wood, 1980), used to distinguish arc basalt (high Th/Ta) and theoretically between calcalkaline basalt, tholeiitic-arc basalt and non-arc basalt. Basalt and basaltic andesite from the central volcanic belt fall within the calcalkaline-arc basalt field (D). A single pillowed basalt sample from Spanish Mountain plots within the MORB field (A).

DISCUSSION

The Late Triassic Takla and Nicola rocks of Quesnellia have features of shoshonitic rocks derived from island arcs (de Rosen-Spence, 1985; Mortimer, 1987; Barrie, 1993; Pantelyev *et al.*, 1996; Nelson and Bellefontaine 1996), similar to the Late Triassic Stuhini rocks of Stikinia (Logan and Koyanagi, 1994; Logan, unpublished data, 2005). Low initial Sr ratios and εNd values (Preto *et al.,* 1979; Smith *et al.*, 1995; Lang *et al.*, 1995) indicate a primitive intraoceanic setting that was not underlain by continental (enriched-mantle) material.

Arc basalt is derived from essentially two sources; the subarc mantle wedge and an aqueous fluid and/or melt (adakitic lavas; Kay, 1981; Peacock *et al.,* 1994) derived from the subducted slab (Davies and Stevenson, 1992; Kerrich and Wyman, 1996). Dehydration of the slab at depths of approximately 100 km releases fluids that metasomatize the overlying subarc mantle wedge (MORB-like; Pearce and Peate, 1995), enriching it in the volatiles, S, SiO_2 and large-ion lithophile elements (LILE) such as Rb, K, Cs, Ba and Sr (Tatsumi *et al.*, 1986; de Hoog *et al.*, 2001). Certain high-field-strength elements (HFSE), such as Ti, Nb and Ta, are not mobilized (conservative elements; Pearce and Peate, 1995) but are retained in the downgoing slab. Melting of the subarc mantle wedge produces primary basaltic magmas that are distinguished from MORB by their higher H_2O and LILE and anomalously low Ti, Nb and Ta contents (Richards, 2003). These magmas rise to the base of the crust where they undergo a multistage process involving crustal **m**elting, **a**ssimilation, **s**torage and magma **h**omogenization ('MASH' model of Hildreth and Moorbath, 1988).

In southern BC, the Quesnel Terrane is an isotopic and geochemically primitive arc complex that formed above an east-dipping subduction zone (Cache Creek Terrane). Early Mesozoic magmatism responsible for construction of the arc is characterized by calcalkaline and alkaline stages of development. Arc magmatism migrated eastward with time, beginning in the west, *ca.* 212 Ma, with development of Cu-Mo±Au deposits at Highland Valley and Gibraltar that are related to calcalkaline intrusions of the Guichon plutonic suite (Woodsworth *et al.*, 1991). At the latitude of Mount Polley (east of Gibraltar), the majority of the arc consists of Na and K-rich, submarine to subaerial lava flows and cogenetic alkaline intrusions that represent ~20 m.y. (Norian stage) of alkaline magmatism. The chemical trends of the basaltic rocks change over time (up stratigraphy) from primitive eastern basalt (ML1Nv) and pyroxenite to more evolved/felsic central basalt (L1Nv). They overlap and parallel the chemical evolution of the Late Triassic intrusions and are likely cogenetic. Magmatism culminated between 204 and 200 Ma (Copper Mountain plutonic suite of Woodsworth *et al.*, 1991) with the intrusion of evolved monzonitic to syenitic bodies and Cu-Au porphyry mineralization. The causative magma in a mineralized porphyry system provides the heat, H_2O, S and metals to the system. These elements are exsolved from the magma and produce the brecciation, alteration and Cu mineralization. Bath and Logan (2006) present chemistry and petrography that favours the Late Triassic Bootjack stock (Bailey and Archibald, 1990) as a late fractionate/component of the causative magma responsible for mineralization at Mount Polley.

Uplift and erosion of the fore-arc produced sub-Jurassic unconformities as magmatism shifted east and culminated with intrusion of calcalkaline plutons at 195 Ma and deposition of distal volcaniclastic and younger sedimentary rocks across the terrane. In the study area, only small, high-level, quartz-bearing calcalkaline intrusions represent the voluminous Early Jurassic calcalkaline magmatism that is preserved in the southern and northern Quesnel Terrane. To the south, this magmatism is represented by an arc-parallel belt of 195 Ma calcalkaline batholiths (Takomkane, Thuya, Wild Horse, Pennask) in the eastern part of the Quesnel Terrane that represent the roots of this Early Jurassic magmatic arc.

CONCLUSIONS

The basalt and trachyte of the Nicola Group have well-developed high-field-strength element (Nb, Ta, Zr, Hf, Ti) depletions, and Th, U, and large-ion lithophile element (Rb, Ba, K, Sr) enrichment, which is typical of subduction-zone magmas in the central belt. They have REE concentrations similar to those of the Mount Polley igneous complex, consistent with a similar melt source and a cogenetic relationship through fractional crystallization.

The eastern volcanic belt contains metavolcanic units with geochemical characteristics of non-arc basalt that represent initiation of volcanism either in a back-arc basin or transitional volcanic arc-marginal basin setting. The latter model is supported by geochemistry and Nd isotope characteristics of Upper Triassic sedimentary rocks in the southern Quesnel Terrane (Unterschutz et al., 2002).

An interpretation that the rocks in the Quesnel Lake area may have been erupted within mature island-arc settings is consistent with the dominance of alkaline basaltic over intermediate andesitic compositions, the shoaling of the arc, and shallow-water deposition of limestone and reworked, locally derived volcaniclastic rocks.

The intrusive complex at Mount Polley represents one of a number of Cu-Au-mineralized magmatic centres that define the culmination of alkaline magmatism (Copper Mountain plutonic suite of Woodsworth *et al.*, 1991) in the Latest Triassic development of the Quesnel Terrane. An eastward shift of magmatism in the Early Jurassic and the return to mainly calcalkaline volcanism is marked by the appearance of a quartz-bearing dacite and Early Jurassic fossiliferous sedimentary rocks.

ACKNOWLEDGMENTS

Pat McAndless and the Mount Polley geology team of Chris Reese, Leif Bjornson, Jacquelline Blackwell, Lee Ferreira, Sheila Jonnes and Chris Taylor contributed to the success of this project through their ongoing efforts to educate us in the subtle relationships of alteration and mineralization at each of the Cariboo-Bell, Springer, NE and SE mineral zones. We thank them all, and Imperial Metals Corporation, for continuing to provide financial support for radiometric dating.

We thank Peter LeCouteur, consulting geologist, and Bob Lane, Regional Geologist with the BC Ministry of Energy, Mines and Petroleum Resources, for giving us a tour around the Woodjam (Megabucks showing) property. Brian Grant reviewed an earlier version of the manuscript and suggested improvements.

REFERENCES

Bailey, D.G. (1978): The geology of the Morehead Lake area; PhD thesis, *Queen's University*, Kingston, ON, 198 pages.

Bailey, D.G. (1988a): Geology of the Central Quesnel Belt, Hydraulic, south-central British Columbia (93A/12); *in* Geological Fieldwork 1987, *BC Ministry of Energy, Mines and Petroleum Resources*, Paper 1988-1, pages 147–153.

Bailey, D.G. (1988b): Geology of the Hydraulic map area, NTS 93A/12; *BC Ministry of Energy, Mines and Petroleum Resources,* Preliminary Map 67, scale 1:50 000.

Bailey, D.G. (1990): Geology of the Central Quesnel Belt, British Columbia; *BC Ministry of Energy, Mines and Petroleum Resources*, Open File 1990-31, 1:100 000-scale map with accompanying notes.

Bailey, D.G. and Archibald, D.A. (1990): Age of the Bootjack stock, Quesnel Terrane, south-central British Columbia (93A); *in* Geological Fieldwork 1989, *BC Ministry of Energy, Mines and Petroleum Resources*, Paper 1990-1, pages 79–82.

Barr, D.A., Fox, P.E., Northcote, K.E. and Preto, V.A. (1976): The alkaline suite porphyry deposits: A Summary; *in* Porphyry Deposits of the Canadian Cordillera, Sutherland Brown, A., Editor, *Canadian Institute of Mining and Metallurgy,* Special Volume 15, pages 359–367.

Barrie, C.T. (1993): Petrochemistry of shoshonitic rocks associated with porphyry copper-gold deposits of central Quesnellia, British Columbia, Canada; *Journal of Geochemical Exploration*, Volume 48, pages 225–258.

Bath A.B. and Logan, J.M. (2006): Petrography and geochemistry of the Late Triassic Bootjack stock (NTS 093A/12), south-central British Columbia; *in* Geological Fieldwork 2005, *BC Ministry of Energy, Mines and Petroleum Resources*, Paper 2006-1 and *Geoscience BC*, Report 2006-1.

Bloodgood, M.A. (1987): Deformational history, stratigraphic correlations and geochemistry of eastern Quesnel Terrane rocks in the Crooked Lake area, central British Columbia, Canada; MSc thesis, *University of British Columbia*, Vancouver, BC, 165 pages.

Bloodgood, M.A. (1990): Geology of the Eureka Peak and Spanish Lake map area, British Columbia; *BC Ministry of Energy, Mines and Petroleum Resources*, Paper 1990-3, 36 pages.

Campbell, K.V. and Campbell, R.B. (1970): Quesnel Lake map-area, British Columbia (93A); *in* Report of Activities, April to October 1969, *Geological Survey of Canada*, Paper 70-1, Part A, pages 32–35.

Campbell, R.B. (1961): Geology of Quesnel Lake, sheet 93A (west half), British Columbia; *Geological Survey of Canada*, Map 3-1961.

Campbell, R.B. (1963): Geology of Quesnel Lake, sheet 93A (east half), British Columbia; *Geological Survey of Canada*, Map 1-1963.

Campbell, R.B. (1978): Quesnel Lake (93A) map-area; *Geological Survey of Canada*, Open File Map 574.

Campbell, R.B. and Tipper, H.W. (1970): Geology and mineral potential of the Quesnel Trough, British Columbia; *Canadian Institute of Mining and Metallurgy Bulletin*, Volume 63, pages 785–790.

Coates J.A. (1960): Analcime-bearing volcanic rocks of the Quesnel River Group, Cariboo District, British Columbia; BSc thesis, *University of British Columbia*, Vancouver, BC, 56 pages.

Davies, J.H. and Stevenson, D. (1992): Physical model of source region of subduction zone volcanics; *Journal of Geophysical Research,* Volume 97, pages 2037–2070.

de Hoog, J.C.M., Mason, P.R.D. and van Bergen, M.J. (2001): Sulfur and chalcophile elements in subduction zones: constraints from a laser ablation ICP-MS study of melt inclusions from Galunggung Volcano, Indonesia; *Geochimica et Cosmochimica Acta*, Volume 65, pages 3147–3164.

de Rosen-Spence, A. (1985): Shoshonites and associated rocks of central British Columbia; *in* Geological Fieldwork 1984, *BC Ministry of Energy, Mines and Petroleum Resources*, Paper 1985-1, pages 426–437.

Dostal, J., Gale, V. and Church, B.N. (1999): Upper Triassic Takla Group volcanic rocks, Stikine Terrane, north-central British Columbia: geochemistry, petrogenesis, and tectonic implications; *Canadian Journal of Earth Sciences*, Volume 36, pages 1483–1494.

Ferri, F. and Melville, D. (1994): Geology of the Germansen Landing – Manson Creek area; *BC Ministry of Energy, Mines and Petroleum Resources*, Bulletin 91.

Fox, P.E. (1975): Alkaline rocks and related mineral deposits of the Quesnel Trough, British Columbia (abstract); *Geological Association of Canada, Cordilleran Section*, Symposium on Intrusive Rocks and Related Mineralization of the Canadian Cordillera, Program and Abstracts, page 12.

Fox, P.E. and Cameron, R.S. (1995): Geology of the QR gold deposit, Quesnel River area, British Columbia; *in* Porphyry Deposits of the Northwestern Cordillera of North America, Schroeter, T.G., Editor, *Canadian Institute of Mining, Metallurgy and Petroleum*, Special Volume 46, pages 142–158.

Fraser, T.M. (1994): Hydrothermal breccias and associated alteration of the Mount Polley copper-gold deposit; *in* Geological Fieldwork 1993, *BC Ministry of Energy, Mines and Petroleum Resources*, Paper 1994-1, pages 259–267.

Fraser, T.M. (1995): Geology, alteration and the origin of hydrothermal breccias at the Mount Polley alkalic porphyry copper-gold deposit, south-central British Columbia; MSc thesis, *University of British Columbia*, Vancouver, BC, 259 pages.

Fraser, T.M., Stanley, C.R., Nikic, Z.T., Pesalj, R. and Gorc, D. (1995): The Mount Polley copper-gold alkalic porphyry deposit, south-central British Columbia; *in* Porphyry Deposits of the Northern Cordillera, Schroeter, T.G., Editor, *Canadian Institute of Mining and Metallurgy*, Special Volume 46, pages 602–622.

Ghent, E.D., Erdmer, P., Archibald, D.A. and Stout, M.Z. (1996): Pressure-temperature and tectonic evolution of Triassic lawsonite-aragonite blueschists from Pinchi Lake, British Columbia; *Canadian Journal of Earth Sciences*, Volume 33, pages 800–810.

Hildreth, W. and Moorbath, S. (1988): Crustal contributions to arc magmatism in the Andes of central Chile, *Contributions to Mineralogy and Petrology*, Volume 98, pages 455–489.

Hodgson, C.J. (1970): Report on the Gavin Lake Cu-Mo property; *BC Ministry of Energy, Mines and Petroleum Resources*, Assessment Report 2733, 28 pages.

Hodgson, C.J., Bailes, R.J. and Versoza, R.S. (1976): Cariboo-Bell; *in* Porphyry Deposits of the Canadian Cordillera, Sutherland Brown, A., Editor, *Canadian Institute of Mining and Metallurgy*, Special Volume 15, pages 388–396.

Irvine, T.N. and Baragar, W.R. (1971): A guide to the chemical classification of the common volcanic rocks; *Canadian Journal of Earth Sciences,* Volume 8, pages 523–548.

Jensen, E.P. and Barton, M.D. (2000): Gold deposits related to alkaline magmatism; *Society of Economic Geology Reviews*, Volume 13, pages 279–314.

Jenner, G.A. (1996): Trace element geochemistry of igneous rocks: geochemical nomenclature and analytical geochemistry; *in* Trace Element Geochemistry of Volcanic Rocks: Applications for Massive Sulphide Exploration, Wyman, D.A., Editor, *Geological Association of Canada*, Short Course Notes, Volume 12, pages 51–77.

Karlsson, H.R. and Clayton, R.N. (1991): Analcime phenocrysts in igneous rocks: primary or secondary? *American Mineralogist*, Volume 76, pages 189–199.

Kay, R.W. (1981): Volcanic arc magmas: implications of a melting-mixing model for element recycling in the crust-upper mantle system; *Journal of Geology*, Volume 88, pages 497–522.

Kerrich, R. and Wyman, D.A. (1996):Trace element systematics: an overview; *in* Trace Element Geochemistry of Volcanic Rocks: Applications for Massive Sulphide Exploration, Wyman, D.A., Editor, *Geological Association of Canada*, Short Course Notes, Volume 12, pages 1–50.

Lang, J.R., Lueck, B., Mortensen, J.K., Russell, J.K., Stanley, C.R. and Thompson, J.F.H. (1995): Triassic–Jurassic silica-undersaturated and silica-saturated alkalic intrusions in the Cordillera of British Columbia: implications for arc magmatism; *Geology*, Volume 23, pages 451–454

Logan, J.M and Koyanagi, V.M. (1994): Geology and mineral deposits of the Galore Creek area (104G/3, 4); *BC Ministry of Energy, Mines and Petroleum Resources*, Bulletin 92, 96 pages.

Logan, J.M. and Mihalynuk, M.G. (2005): Regional geology and setting of the Cariboo, Bell, Springer and Northeast Porphyry Cu-Au Zones at Mount Polley, South-Central British Columbia; *in* Geological Fieldwork 2004, *BC Ministry of Energy, Mines and Petroleum Resources*, Paper 2005-1, pages 249–270.

Logan, J.M., Ullrich, T. and Friedman, R.M. (in press): U-Pb ages of intrusive rocks and $^{40}Ar/^{39}Ar$ plateau ages of copper-gold-silver mineralization associated with alkaline intrusive centres at Galore Creek and Mount Polley, northwest and central British Columbia; *BC Ministry of Energy, Mines and Petroleum Resources*, Geofile 2006-2.

Lueck, B.A. and Russell, J.K. (1994): Silica-undersaturated, zoned alkaline intrusions within the British Columbia Cordillera; *in* Geological Fieldwork 1993, *BC Ministry of Energy, Mines and Petroleum Resources*, Paper 1994-1, pages 311–315.

Mathews, W.H. (1989): Neogene Chilcotin basalts in south-central British Columbia: geology, ages, and geomorphic history; *Canadian Journal of Earth Sciences*, Volume 26, pages 969–982.

McMillan, W.J., Thompson, J.F.H., Hart, C.J.R. and Johnston, S.T. (1995): Regional geological and tectonic setting of porphyry deposits in British Columbia and Yukon Territory; *in* Porphyry Deposits of the Northwestern Cordillera of North America, Schroeter, T.G., Editor, *Canadian Institute of Mining, Metallurgy and Petroleum*, Special Volume 46, pages 40–57.

Mihalynuk, M.G., Erdmer, P., Ghent, E.D., Cordey, F., Archibald, D.A., Friedman, R.M. and Johannson, G.G. (2004): Coherent French Range blueschist: subduction to exhumation in <2.5 m.y.? *Geological Society of America Bulletin*, Volume 116, no 7/8, pages 910–922.

Mihalynuk, M.G., Nelson, J. and Diakow, L. (1994): Cache Creek Terrane entrapment: oroclinal paradox within the Canadian Cordillera; *Tectonics*, Volume 13, pages 575–595.

Mortensen, J.K., Ghosh, D.K. and Ferri, F. (1995): U-Pb geochronology of intrusive rocks associated with copper-gold porphyry deposits in the Canadian Cordillera; *in* Porphyry Deposits of the Northwestern Cordillera of North America, Schroeter, T.G., Editor, *Canadian Institute of Mining, Metallurgy and Petroleum*, Special Volume 46, pages 142–158.

Mortimer, N. (1987): The Nicola Group: Late Triassic and Early Jurassic subduction-related volcanism in British Columbia; *Canadian Journal of Earth Sciences*, Volume 24, pages 2521–2536.

Morton, R.L. (1976): Alkalic Volcanism and copper deposits of the Horsefly area, central British Columbia; PhD thesis, *Carleton University*, Ottawa, ON, 196 pages.

Muller, D. and Groves, D.I. (1993): Direct and indirect associations between potassic igneous rocks, shosohonite and gold-copper deposits; *Ore Geology Reviews*; Volume 8, pages 383–406.

Nelson, J.L. and Bellefontaine, K.A. (1996): The geology and mineral deposits of north-central Quesnellia; Tezzeron Lake to Discovery Creek, central British Columbia; Grant, B. and Newell, J.M., Editors, *BC Ministry of Energy, Mines and Petroleum Resources*, Bulletin 99, 112 pages.

Nixon, G.T., Archibald, D.A. and Heaman, L.M. (1993): ^{40}Ar-^{39}Ar and U-Pb geochronometry of the Polaris Alaskan-type complex, British Columbia: precise timing of Quesnellia–North America interaction; *Geological Association of Canada – Mineralogical Association of Canada*, Joint Annual Meeting, Edmonton 1993, Program and Abstracts, page A76.

Orchard, M.J. (1995): Report on conodonts and other microfossils from Quesnel Lake (93A, 93B and 93H); *Geological Survey of Canada*, Conodont Data File, Report MJO-1995-9.

Palfy, J., Smith, P.L. and Mortensen, J.K. (2000): A U-Pb ^{40}Ar-^{39}Ar time scale for the Jurassic; *Canadian Journal of Earth Sciences*, Volume 37, page 923–944.

Panteleyev, A. (1987): Quesnel gold belt — alkalic volcanic terrane between Horsefly and Quesnel lakes (93A/6); *in* Geological Fieldwork 1986, *BC Ministry of Energy, Mines and Petroleum Resources*, Paper 1987-1, pages 125–133.

Panteleyev, A. (1988): Quesnel Mineral Belt — the central volcanic axis between Horsefly and Quesnel lakes (93A/5E, 6W); *in* Geological Fieldwork 1987, *BC Ministry of Energy, Mines and Petroleum Resources*, Paper 1988-1, pages 131–137.

Panteleyev, A., Bailey, D.G., Bloodgood, M.A. and Hancock, K.D. (1996): Geology and mineral deposits of the Quesnel River – Horsefly map area, central Quesnel Trough, British Columbia (NTS 93A/5, 6, 7, 11, 12, 13; 93B/9, 16; 93G/1; 93H/4); *BC Ministry of Energy, Mines and Petroleum Resources*, Bulletin 97, 156 pages.

Panteleyev, A. and Hancock, K.D. (1989): Quesnel mineral belt: summary of the geology of the Beaver Creek – Horsefly River map area; *in* Geological Fieldwork 1988, *BC Ministry of Energy, Mines and Petroleum Resources*, Paper 1989-1, pages 159–166.

Patterson, I. and Harakal, J. (1974): Potassium-argon dating of blueschists from Pinchi Lake, central British Columbia; *Canadian Journal of Earth Sciences*, Volume 11, pages 1007–1011.

Peacock, S.M., Rushmer, T. and Thompson, A.B. (1994): Partial melting of subducting oceanic crust; *Earth and Planetary Science Letters*, Volume 121, pages 227–244.

Pearce, J.A. (1996): A user's guide to basalt discrimination diagrams, *in* Trace Element Geochemistry of Volcanic Rocks: Applications for Massive Sulfide Exploration, Wyman, D.A., Editor, *Geological Association of Canada*, Short Course Notes, Volume 12, pages 79–113.

Pearce, J.A. and Cann, J.R. (1973): Tectonic setting of basic volcanic rocks determined using trace element analyses; *Earth and Planetary Science Letters*, Volume 19, pages 290–300.

Pearce, J.A. and Peate, D.W. (1995): Tectonic implications of the composition of volcanic arc magmas; *Annual Reviews of Earth and Planetary Sciences*, Volume 23, pages 251–285.

Petersen, N.T., Smith, P.L., Mortensen, J.K., Creaser, R.A. and Tipper, H.W. (2004): Provenance of Jurassic sedimentary rocks of south-central Quesnellia, British Columbia: implications for paleogeography; *Canadian Journal of Earth Sciences*, Volume 41, pages 103–125.

Peterson, T.D. and Currie, K.L. (1993): Analcite-bearing igneous rocks from the Crowsnest Formation, southwestern Alberta; *in* Current Research, Part B, *Geological Survey of Canada*, Paper 93-1B, pages 51–56.

Poulton, T.P. and Tipper, H.W. (1991): Aalenian ammonites and strata of western Canada; *Geological Survey of Canada*, Bulletin 411, 71 pages.

Preto, V.A., Osatenko, M.J., McMillan, W.J. and Armstrong, R.L. (1979): Isotopic dates and strontium isotopic ratios for plutonic and volcanic rocks in the Quesnel Trough and Nicola Belt, south-central British Columbia; *Canadian Journal of Earth Sciences*, Volume 16, pages 1658–1672.

Rees, C.J. (1987): The Intermontane-Omineca belt boundary in the Quesnel Lake area, east-central British Columbia: tectonic implications based on geology, structure and paleomagnetism; PhD thesis, *Carleton University*, Ottawa, ON, 421 pages.

Richards, J.P. (2003): Tectono-magmatic precursors for porphyry Cu-(Mo-Au) deposit formation; *Economic Geology*, Volume 98, pages 1515–1533.

Roddick, J.A., Wheeler, J.O., Gabrielse, H. and Souther, J.G. (1967): Age and nature of the Canadian part of the Circum-Pacific Orogenic Belt; *Tectonophysics*, Volume 4, pages 319–337.

Schiarizza, P. and Israel, S. (2001):Geology and mineralization of the Nehalliston Plateau, south-central British Columbia (92P/7, 8, 9, 10); *in* Geological Fieldwork 2000, *BC Ministry of Energy, Mines and Petroleum Resources*, Paper 2001-1, pages 1–30.

Schiarizza, P., Heffernan, S. and Zuber, J. (2002): Geology of Quesnel and Slide Mountain terranes west of Clearwater, south-central British Columbia (92P/9, 10, 15, 16); *in* Geological Fieldwork 2001, *BC Ministry of Energy, Mines and Petroleum Resources*, Paper 2002-1, pages 83–108.

Smith, A.D., Brandon, A.D. and Lambert, R. St.J. (1995): Nd-Sr isotope systematics of Nicola Group volcanic rocks, Quesnel Terrane; *Canadian Journal of Earth Sciences*, Volume 32, pages 437–446.

Souther, J.G. (1977): Volcanism and tectonic environments in the Canadian Cordillera — a second look; *in* Volcanic Regimes in Canada, Baragar, W.R.A., Coleman L.C. and Hall, J.M., Editors, *Geological Association of Canada*, Special Paper 16, pages 3–24.

Sun, S.S., and McDonough, W.F. (1989): Chemical and isotopic systematics of oceanic basalts: implications for mantle composition and processes; *in* Magmatism in the Ocean Basins, Saunders, A.D. and Norry, M.J., Editors, *Geological Society of London*, Special Publication 42, pages 313–345.

Tatsumi, Y. Hamilton, D.L. and Nesbitt, R.W. (1986): Chemical characteristics of fluid phase released from a subducted lithosphere and the origin of arc magmas: evidence from high pressure experiments and natural rocks; *Journal of Volcanology and Geothermal Research*, Volume 29, pages 293–309.

Tipper, H.W. (1959): Quesnel, British Columbia; *Geological Survey of Canada*, Map 12-1959.

Tipper, H.W. (1978): Northeast part of Quesnel (93B) map-area, British Columbia; *in* Current Research, Part A, Geological Survey of Canada, Paper 78-1A, pages 67-68.

Tipper, H.W. (1992): Report on macrofossil collections from Quesnel Lake (93A, 93B and 93H); *Geological Survey of Canada*, Report No. J3-1992-HWT.

Travers, W.B. (1977): Overturned Nicola and Ashcroft strata and their relations to the Cache Creek Group, southwestern Intermontane Belt, British Columbia; *Canadian Journal of Earth Sciences*, Volume 15, pages 99–116.

Unterschutz, J.L.E., Creaser, R.A., Erdmer, P., Thompson, R.I. and Daughtry, K.L. (2002): North American margin origin of Quesnel Terrane strata in the southern Canadian Cordillera: inferences from geochemical and Nd isotopic characteristics of Triassic metasedimentary rocks; *Geological Society of America Bulletin*, Volume 114, no 4, pages 462–475.

Wheeler, J.O. and McFeely, P. (1991): Tectonic assemblage map of the Canadian Cordillera and adjacent parts of the United States of America; *Geological Survey of Canada*, Map 1712A, scale 1:2 000 000.

Winchester, J.A. and Floyd, P.A. (1977): Geochemical discrimination of different magma series and their differentiation products using immobile elements; *Chemical Geology*, Volume 20, pages 325–343.

Wood, D.A. (1980): The application of the Th-Hf-Ta diagram to problems of tectonomagmatic classification and to establishing the nature of crustal contamination of basaltic lavas of the British Tertiary volcanic province; *Earth and Planetary Science Letters*, 50, pages 11–30.

Woodsworth, G.J., Anderson, R.G. and Armstrong, R.L. (1991): Plutonic regimes; Chapter 15 *in* Geology of the Cordilleran Orogen in Canada, Gabrielse, H. and Yorath, C.J., Editors, *Geological Survey of Canada*, Geology of Canada, No 4, pages 491–531.

Boundary Project: Reassessment of Paleozoic Rock Units of the Greenwood Area (NTS 82E/02), Southern British Columbia

By N.W.D. Massey

KEYWORDS: Greenwood, Quesnellia, Knob Hill complex, Attwood Formation, Lexington porphyry

INTRODUCTION

The Boundary Project has been initiated with the purpose of better characterizing the lithological and geochemical variations within and between the various Paleozoic sequences in the southern Okanagan region along the United States border. These occur within the Quesnel Terrane, which is dominated by such Paleozoic mafic volcanic and pelitic rocks, unconformably overlain by Triassic and Jurassic volcanic and sedimentary rocks. In the Boundary District, such sequences include the Knob Hill Complex, Attwood Formation, Kobau Group and Anarchist Schist. These are exposed between down-faulted blocks of Tertiary volcanic and sedimentary cover preserved in structural keels between gneissic domes (Fig. 1). In 2005, fieldwork was concentrated in the Greenwood – Rock Creek area (NTS 082E/02). In future years, fieldwork will progress into the Osoyoos (NTS 082E/03) and Keremeos (NTS 082E/04) map sheets.

The Greenwood map sheet straddles Highway 3 between Osoyoos and Grand Forks. Five weeks of fieldwork in 2005 were restricted to areas immediately around and east of Greenwood, and to the area between Midway and Rock Creek (see Fig. 7 for locations). This includes most of the area mapped by Fyles (1989, 1990), upon which this study builds. Fieldwork was focused on,

- field checking previous mapping in order to produce a new compilation map for the Greenwood sheet (Massey, work in progress);
- collecting geochemical samples from volcanic rocks in the Knob Hill Complex and Attwood Formation;
- identifying and collecting suitable materials for paleontological or geochronological age determinations of the Paleozoic sequences; and
- investigating the reported occurrence of felsic volcanic rocks within the 'Lexington porphyry'.

PREVIOUS WORK

The Greenwood – Rock Creek area has a mining history dating from the first discoveries of placer gold in the 1860s and lode deposits in the 1880s. The first geological report was that of Bauerman (1885), prepared as part of the Boundary Commission Expedition of 1859–1861. Regional mapping has been undertaken by Brock (1902, 1903, 1905a, b), Daly (1912), Little (1957, 1983), Monger (1968), Church (1986), Templeman-Kluit (1989a, b) and Fyles (1990). Detailed mapping around individual mines and mining camps includes work by LeRoy (1912, 1913), McNaughton (1945), Seraphim (1956), Carswell (1957), Church (1970) and Nixon (2002).

PALEOZOIC STRATIGRAPHY OF THE GREENWOOD – ROCK CREEK AREA

Knob Hill Complex

The Knob Hill Complex dominates the Quesnellia Paleozoic rocks exposed in the Greenwood map sheet. Called the 'Knob Hill Group' by previous workers, the name is changed here to Knob Hill Complex, in line with modern accepted stratigraphic nomenclature, to reflect the inclusion of intrusive units with the layered rocks (Murphy and Salvador, 1999).

The complex is composed of chert, argillite, basalt, gabbro and serpentinite that together constitute a disrupted ophiolite (Little, 1983; Dostal *et al.*, 2001). It was included in the Okanagan subterrane of Quesnellia by Monger *et al.* (1991), along with other assemblages of oceanic affinity such as the Kobau and Old Tom – Shoemaker Groups. The stratigraphic thickness of the Knob Hill Complex is uncertain and difficult to estimate due to structural disruption. Little (1983) suggested "a minimum of a few thousands of metres", whereas Fyles (1990, 1995) estimated the complex to be more than 5 km thick.

The age of the Knob Hill Complex is still poorly determined. A Carboniferous to Permian age was assigned by Little based on a single macrofossil locality (Little, 1983, page 12, locality F7). However, this same limestone bed has yielded conodonts of Late Devonian (Frasnian) age (Orchard, 1993). Church (1986) reported a K-Ar whole rock age of 258 ±10 Ma (Permian) for uralitized gabbro from the Winnipeg mine. However, the reliability of such K-Ar whole rock ages is very suspect, and it is doubtful that this is recording a crystallization age. Refinement of the age of the complex awaits further paleontological and geochronological determinations.

Seven map units are recognized within the Knob Hill Complex in the Greenwood map sheet. Stratigraphic relationships between map units are not always clear. However, in the area north of Rock Creek, gabbro and serpentinite pass northward, and probably upward, into greenstone,

This publication is also available, free of charge, as colour digital files in Adobe Acrobat PDF format from the BC Ministry of Energy, Mines and Petroleum Resources internet website at http://www.em.gov.bc.ca/Mining/Geolsurv/Publications/catalog/catfldwk.htm

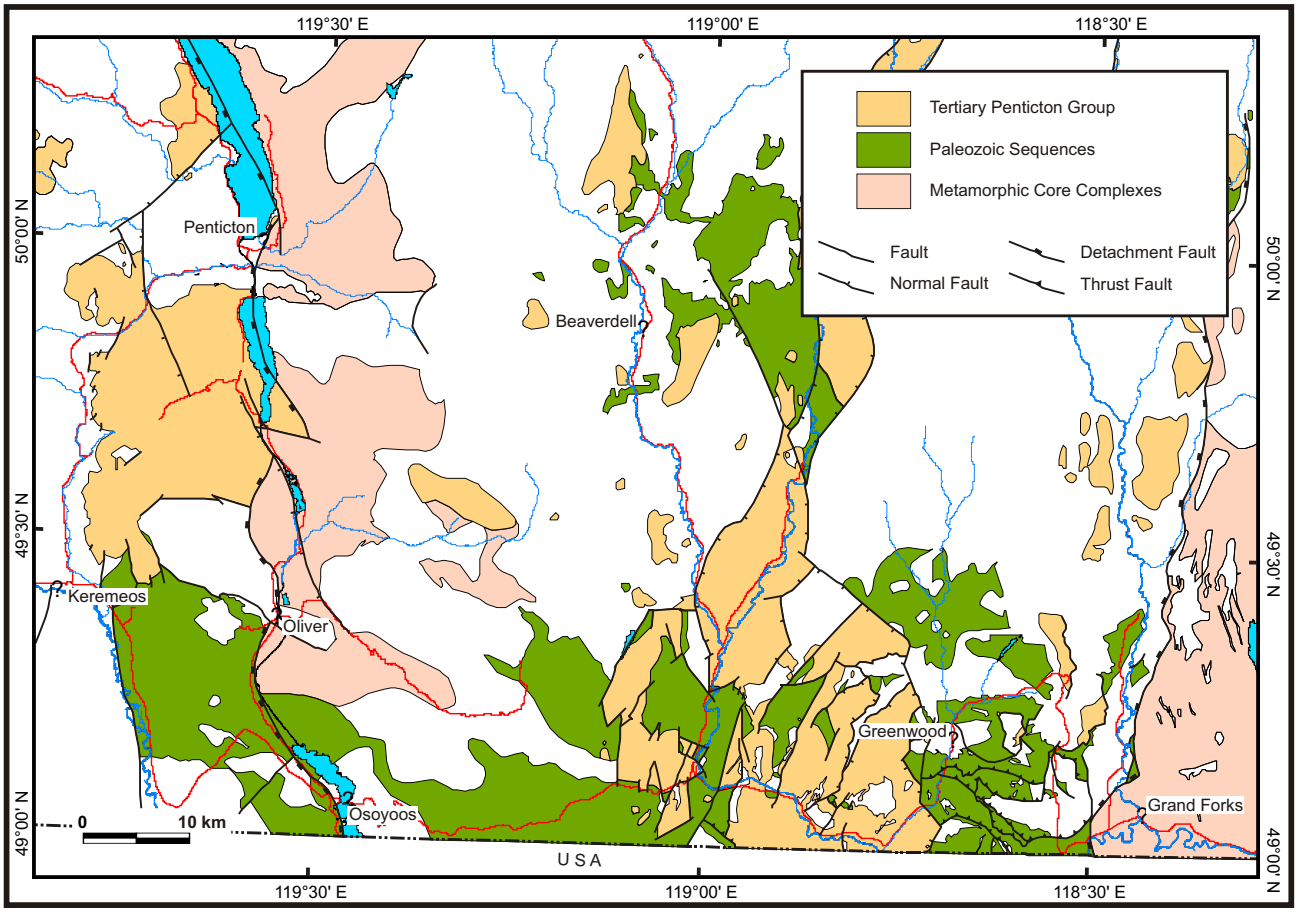


Figure 1. Distribution of Paleozoic Quesnellian rock suites in the Boundary District (south-central part of NTS 082E), amended from Massey *et al.* (2005).

mixed greenstone and chert, and finally chert and argillite. In the Greenwood area, Fyles (1990) suggested that the lower part of the Knob Hill Complex consisted of a highly variable mix of chert, argillite, conglomerate and breccia interfingering with greenstone flows. The upper part of the complex is mainly chert and greenstone. Due to the limited fieldwork undertaken in the area by the author, the following descriptions of the units draw heavily upon previous observations by Church (1986) and Fyles (1990).

GREENSTONE UNIT

The basaltic greenstone is mostly flows with minor breccia, agglomerate and tuffaceous sandstone. Chert, cherty argillite, jasper and rare limestone may occur between flows. Most flows are grey to green, massive and aphanitic. Chlorite, calcite and epidote are common alteration minerals in veins, fractures and within the rock. Pillow structures are rare, though they have been inferred by previous mappers (Fyles, 1990). Geochemically, the flows of the greenstone unit are oceanic basalt (Dostal *et al.*, 2001) and may have formed at a mid-ocean ridge or in a back-arc basin.

Medium-grained diabase to microgabbro bodies also occur within the greenstone unit. In general, these are featureless rock units in outcrop. However, outcrops along the power line adjacent to the Winnipeg mine show well-developed chilled margins, suggesting that they may be part of an unmapped sheeted dike complex (Fig. 2a). Dikes are also seen intruding the nearby gabbro (Fig. 2c).

CHERT-ARGILLITE UNIT

Sedimentary rocks in the Knob Hill Complex are typically fine grained, mainly grey to white chert interbedded with grey to black argillite and minor greenstone. The chert is highly fractured and jointed, tends to be massive to thickly bedded and only rarely shows ribbon structures. Radiolarians are reported in thin section (Church, 1986) but are rarely seen in hand specimen. Variable recrystallization of the chert produces a fine to medium-grained saccharoidal texture. Argillite is rarely bedded and may show gradational contacts with chert horizons. Thin white crystalline limestone forms occasional outcrops.

MIXED GREENSTONE AND CHERT UNIT

In the western part of the map sheet, between upper Nicholson Creek and Kettle River, a belt of mixed greenstone and chert in roughly equal proportions forms a transition between the greenstone unit to the south and the chert-argillite unit to the north (Fig. 3). Rock types are similar to those found in the other two units.

CHERT BRECCIA

Two areas of buff to cream and grey chert breccia and pebble conglomerate were outlined by Fyles (1990). They contain angular to subrounded chert clasts similar to the

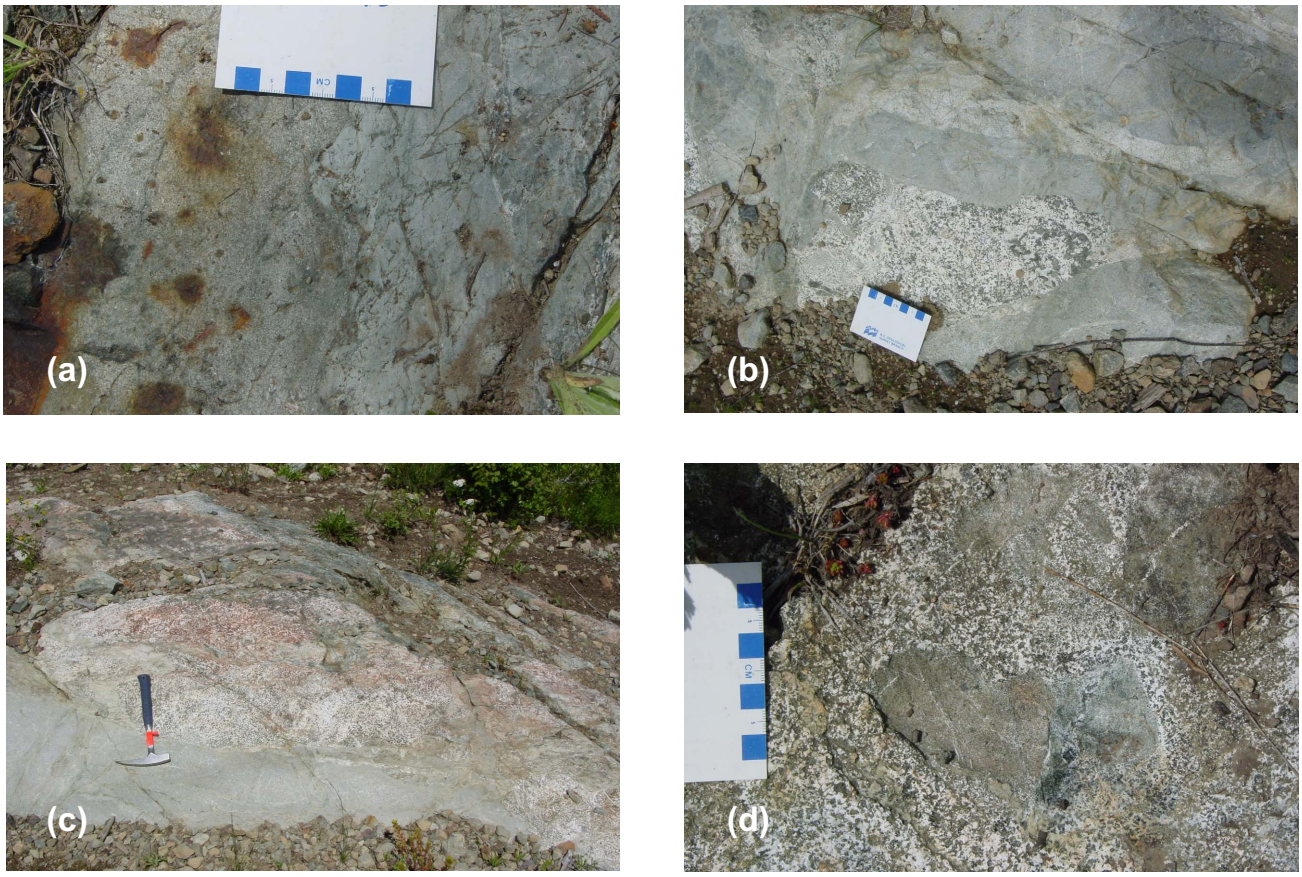


Figure 2: Diabase dikes in the Knob Hill Complex: a) chilled contact between diabase dikes (05NMA02-08; UTM Zone 11, 5436632N, 385389E, NAD83); b) gabbro screen between two diabase dikes (05NMA02-09; UTM Zone 11, 5436682N, 385375E, NAD83); c) diabase intruding gabbro body (05NMA02-09; UTM Zone 11, 5436682N, 385375E, NAD83); d) diabase inclusion within gabbro (05NMA02-10; UTM Zone 11, 5436766N, 385333E, NAD83).

chert of the chert-argillite unit. They lack the variety of other clast types, such as greenstone, serpentinite, jasper, and limestone, found in the Triassic Brooklyn Formation sharpstone conglomerate. Black siltstone and chert sandstone occur as interbedded lenses. Similar chert breccia also forms a prominent hill just south of Norwegian Creek, immediately west of the Sappho property, and is probably correlative.

GREENWOOD GABBRO

This unit was originally informally called the 'Old Diorite' by Church (1986) and renamed the 'Greenwood Gabbro' by Dostal *et al.* (2001). The latter term is preferred here as being in agreement with modern stratigraphic nomenclature.

The gabbro is composed of white plagioclase and green to black pyroxene that is extensively replaced by hornblende. Chlorite is common on fractures and in shears. The gabbro is generally massive and characteristically variable and patchy in texture, with coarse-grained gabbro phases grading into finer microgabbro or even coarser pegmatitic phases (Fig. 4). No chilled contacts are seen between phases. Light-coloured felsic veins (plagiogranite?) crisscross some outcrops. Occasional diabase xenoliths are included in the gabbro (Fig. 2d).

Greenwood Gabbro samples are geochemically comparable to oceanic plutonic rocks (Dostal *et al.*, 2001) and are probably comagmatic with the greenstone flows.

SERPENTINITE

Serpentinite occurs dominantly as fairly continuous sheets along faults, or as irregular lenticular bodies that are commonly spatially associated with gabbro bodies. The

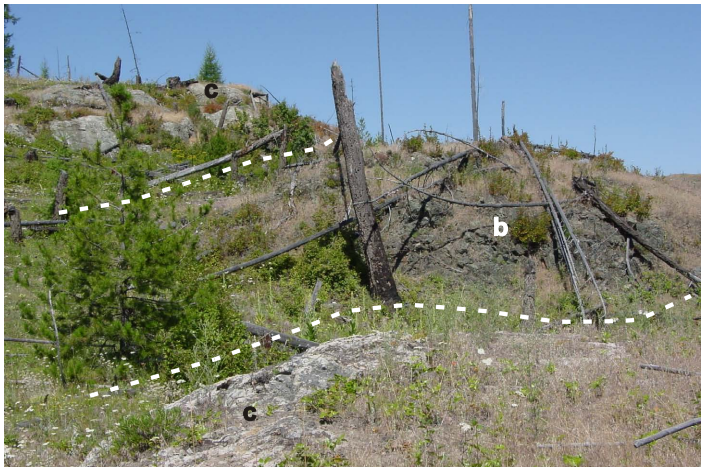


Figure 3. Interbedded chert (c) and greenstone flows (b) of the Knob Hill Complex, east side of the Kettle River valley (05NMA23-08; UTM Zone 11, 5443408N, 357292E, NAD83).

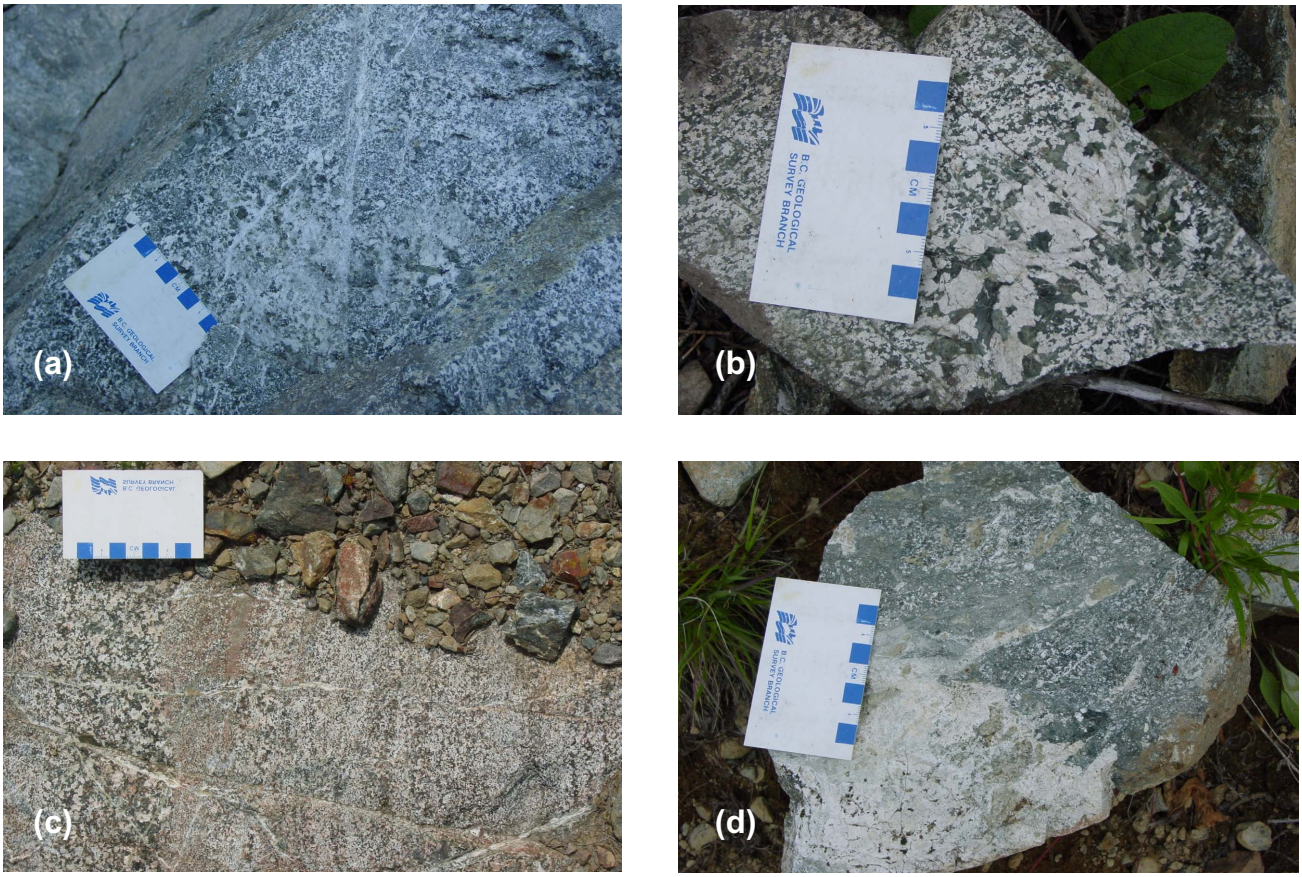


Figure 4. Greenwood Gabbro: a) typical variably textured gabbro, with white felsic vein network (05NMA21-02; UTM Zone 11, 5436561N, 353922E, NAD83); b) very coarse pegmatitic gabbro (05NMA02-03; UTM Zone 11, 5436880N, 385180E, NAD83); c) colour and grain-size layering in gabbro (05NMA02-11; UTM Zone 11, 5436808N, 385264E, NAD83); d) plagiogranite dike in variably textured gabbro (05NMA02-11; UTM Zone 11, 5436808N, 385264E, NAD83).

serpentinite is usually dark green to black and schistose to blocky, with greasy fracture coatings. Foliated serpentinite may contain boudins of blocky serpentinite. Original mineralogy is almost totally replaced by antigorite, though coarse relict pyroxene is seen in roadcuts along Highway 3 about 1.5 km south of the Phoenix Ski Hill turnoff. Talc and talc-carbonate are common in sheared margins of serpentinite bodies.

Listwanite is common in the western part of the map sheet along the Kettle River valley north of Rock Creek. This is a pale buff-white, crystalline, carbonate-rich rock that weathers to an orange-brown colour. There may be a soapy feel on some surfaces. Siliceous patches and veins weather positively and often show an apple green colour due to chlorite or mariposite(?). Late quartz veins contain minor sulphide minerals.

METAMORPHIC UNIT

Deformed and higher grade metamorphosed rocks ascribed to the Knob Hill Complex (Fig. 5) occur in three main belts. South of Rock Creek, the rocks comprise chert, quartzite, micaceous quartzite, greenstone, chlorite schist, limestone and dolomite. These are lithologically similar to chert-argillite and greenstone sequences found to the north of Rock Creek, although their structural relationship is uncertain due to lack of outcrop.

A second belt outcrops in the southeastern part of the map sheet, between Boundary Falls and Grand Forks, as a thrust slice between the Mount Wright and No 7 faults (see Fig. 7). This belt includes chlorite and chlorite-amphibole schists, quartz-biotite schist and phyllite, quartz-biotite gneiss, quartzite, chert, calcareous phyllite and crystalline limestone, minor greenstone and metagabbro.

The third belt of the metamorphic unit extends from Mount Roderick Dhu west to Windfall Creek. Metamorphic grade increases northwestward, from the greenstone and metachert found south of Jewel Lake into amphibolite, metagabbro, quartzite, micaceous quartzite, quartz-biotite schist, biotite-muscovite schist, quartz-biotite and quartz-feldspar-biotite gneiss.

Little (1983) referred to the latter two belts as a metamorphic assemblage of pre-Carboniferous (possible Proterozoic?) age. Church (1986), Fyles (1990) and this author include them in the Knob Hill Complex because of their lithological similarities to other mapped units in the Knob Hill. However, the contrast in structural styles to the undeformed lower grade Knob Hill rocks is still enigmatic and unexplained.

Attwood Formation

Rocks of the Attwood Formation are more restricted in the Greenwood area than the Knob Hill Complex, the main outcrop areas being around the northern slopes of Mount Attwood, the slopes of Rusty Mountain and Mount McLaren, and in the extreme southwestern corner of the map

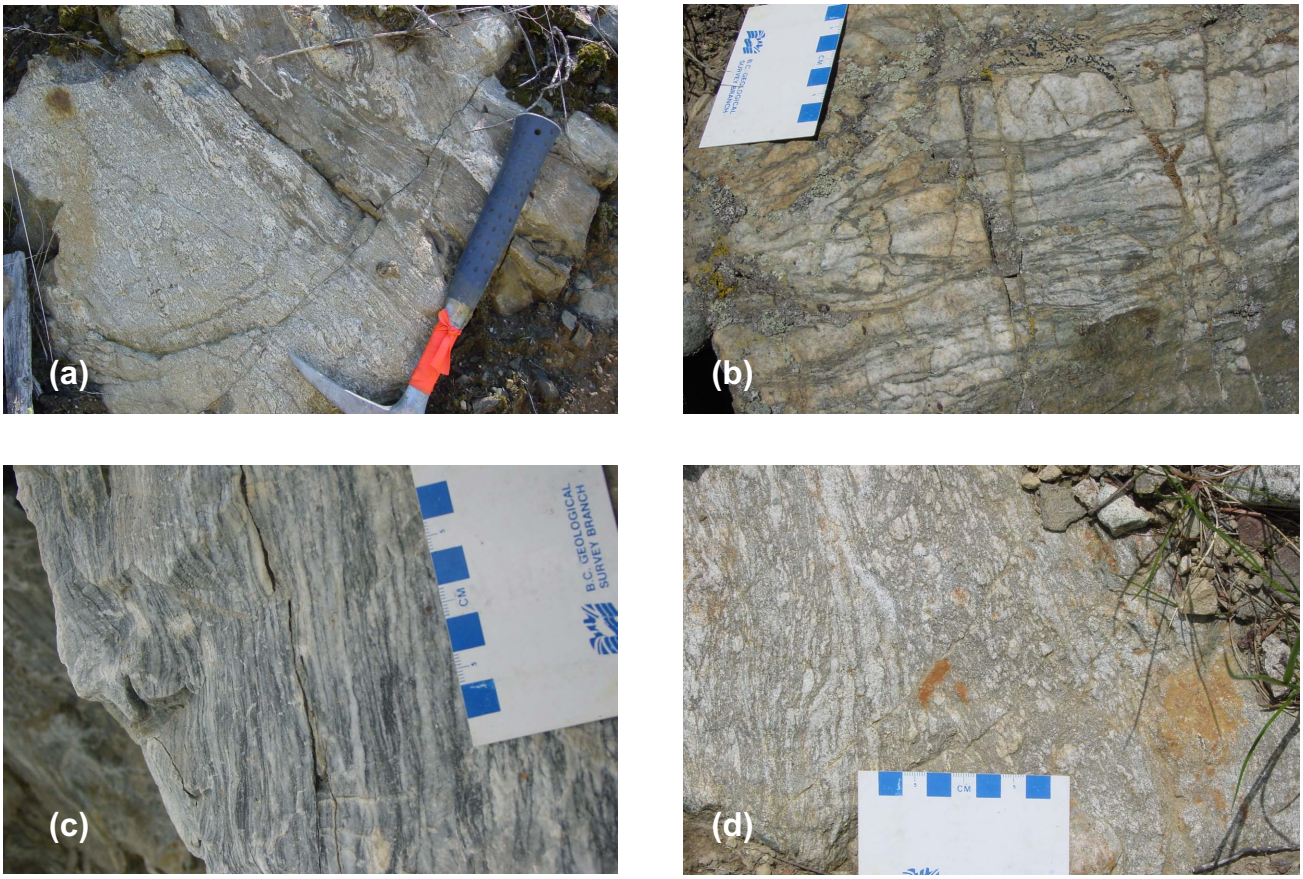


Figure 5. Rocks of the metamorphic unit of the Knob Hill Complex: a) biotite-quartz-feldspar gneiss, Windfall Creek (05NMA20-02; UTM Zone 11, 5430392N, 372191E, NAD83); b) metaquartzite (metachert?), Highway 3, Eholt Creek valley (05NMA26-12; UTM Zone 11, 5443713N, 383281E, NAD83); c) foliated marble, Highway 3, Boundary Falls (05NMA05-01; UTM Zone 11, 5435265N, 376209E, NAD83); d) quartz-biotite gneiss, Mount Roderick Dhu (05NMA09-22; UTM Zone 11, 5450126N, 382554E, NAD83).

sheet. The term Attwood 'Series' was introduced by Daly (1912) and refined by Little (1983) to Attwood Formation. Although the status of the Attwood was raised to the group level by Church (1986) and Fyles (1990), Little's definition is preferred here.

The Attwood Formation comprises an argillite-siltstone member, a limestone member and possible minor volcanic rocks. In all outcrop areas, the rocks are folded and the internal stratigraphy of the formation is unknown. Stratigraphic thickness is also unknown, though Little (1983) estimated it to be at least 400 m, with apparent thickness greater than 1200 m.

Fossil collections from the Attwood Formation limestone have yielded macrofossils and conodonts of Carboniferous to Permian age (Little, 1983; Church, 1986; Templeman-Kluit, 1989a). A Mississippian age is suggested for conodonts from a limestone along the Haulage Road (Orchard, 1997). No stratigraphic contact is found with the Knob Hill Complex and it is unclear what their original spatial or temporal relationships were. Monger *et al.* (1991) placed the Attwood, along with the Knob Hill, in the Okanagan subterrane of Quesnellia. However, Nelson *et al.* (1995) suggested that the clastic rocks of the Attwood show a greater affinity to the arc-derived clastic sedimentary rocks of the Harper Ranch subterrane.

ARGILLITE-SILTSTONE

The argillite-siltstone unit consists of fine-grained clastic sedimentary rocks, mostly black to grey argillite, lighter grey siltstone, dark grey to black chert and cherty argillite, and grey phyllite and slate. Laminations, thin bedding and graded beds are well developed in places, but may be obscured by slaty cleavage and fractures (Fig. 6). Minor sandstone, chert conglomerate and grey limestone also occur as interbeds.

Fine-grained dark grey siltstone or quartz wacke, with minor pebble conglomerate, crop out around Mount McLaren. This unit was assumed to be Jurassic by Little (1983), but included in the Attwood Formation by Church (1986) and Fyles (1990). Similar argillite, in a similar structural position in the footwall of the No 7 fault, is found around the Morning Star deposit in Washington, where they are correlated with the Lower Jurassic Archibald Formation of the Rossland Group (Caron, pers. comm., 2005).

LIMESTONE

Limestone is white to grey, fine to coarse-grained, variably recrystallized to saccharoidal marble. The limestone is generally massive, but may show faint streaking or laminations. Thin, pale green to white chert beds and black argillite occur as intercalations. Little (1983, page 8) also recorded the presence of chert granule limestone. Fossiliferous beds, occurring at various localities, have

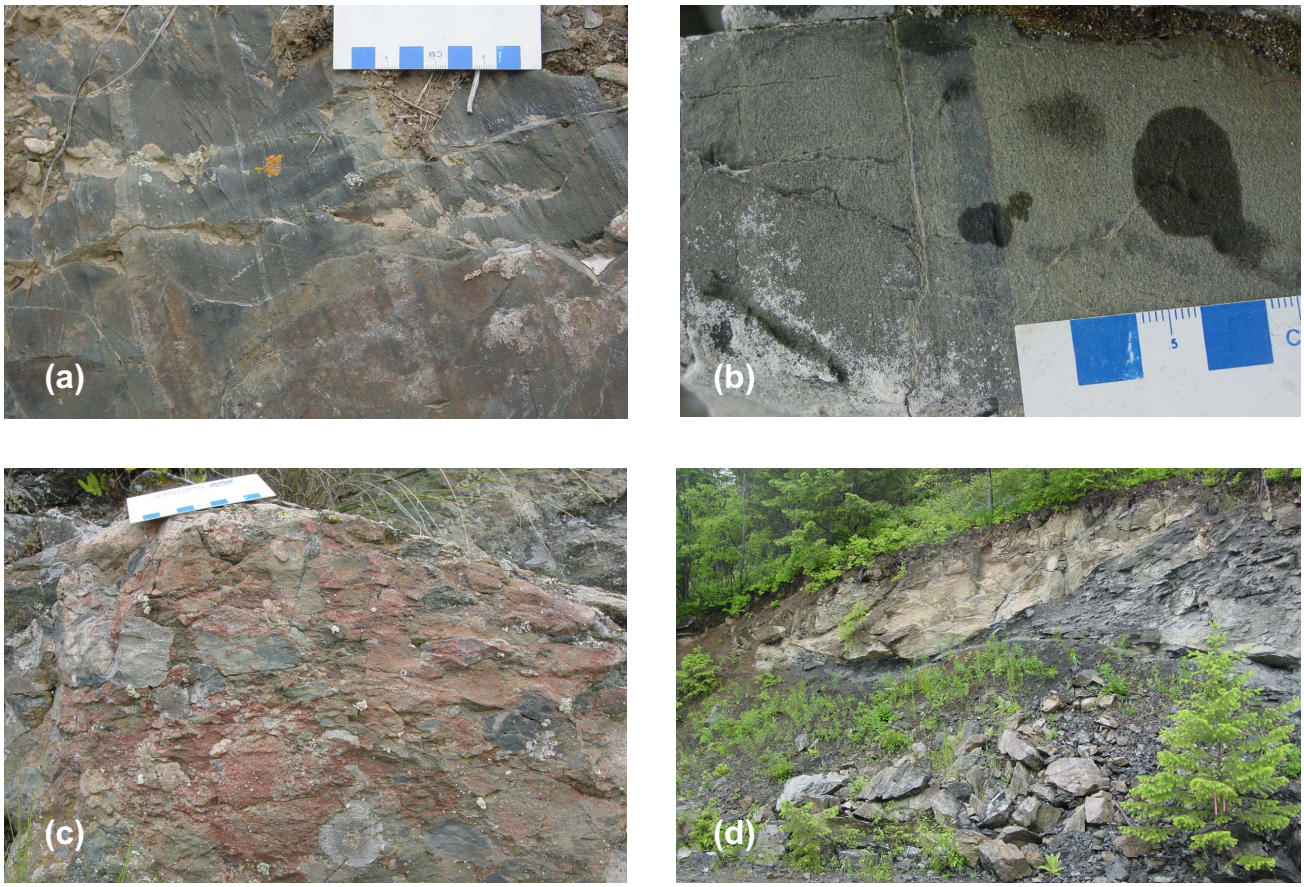


Figure 6. Attwood Formation rock types: a) slaty argillite-siltstone interbeds, Skomac mine (05NMA18-14; UTM Zone 11, 5435668N, 375126E, NAD83); b) graded sandstone-siltstone beds, Myers Creek area (05NMA 24-11; UTM Zone 11, 5430982N, 354727E, NAD83); c) limestone bed above argillite, Haulage Road (05NMA 03-10; UTM Zone 11, 5434200N, 384961E, NAD83); d) chert breccia, Skomac mine (05NMA 18-10; UTM Zone 11, 5435660N, 375038E, NAD83).

yielded corals, brachiopods, bryozoans and crinoids (Little, 1983).

VOLCANIC UNITS

A large proportion of the greenstone and metavolcanic rocks in the Greenwood area were assigned by Church (1986) to the Attwood Group [*sic*], though he later reassigned some to the Knob Hill (Dostal *et al.*, 2001). Fyles (1990), however, recognized some of the remaining 'Attwood' metavolcanic rocks as actually belonging to the Triassic Brooklyn Formation, and included the rest of the basalt in the Knob Hill, following the earlier suggestion of Little (1983).

However, a sliver of volcanic rocks, apparently in the immediate footwall of the Lind Creek fault (see Fig. 7 for location of faults), may be in the Attwood Formation (Fyles, 1990). Outcrops in this unit along the Haulage Road are fine-grained, massive aphanitic greenstone essentially indistinguishable from the Knob Hill greenstone. Contacts with limestone and argillite to the south were not found, and the status of this greenstone is presently unclear. Petrochemistry may help reveal whether or not it is akin to the Knob Hill greenstone.

Orange to buff-coloured muscovite schist and buff silty tuff are interbedded with grey argillite and cherty siltstone within the Attwood Formation in the Myers Creek area, in the southwest corner of the map sheet. These are believed to be felsic tuff horizons, although similar rocks are not seen elsewhere in the map area.

STRUCTURAL RELATIONSHIP OF PALEOZOIC UNITS

The Paleozoic rocks of the Greenwood area are preserved in a series of five northward-dipping thrust sheets (Fig. 7). Many of the bounding thrusts are marked by serpentinite layers or pods. Tertiary extensional faulting has disrupted and modified the thrust sheets and makes correlation uncertain between the western and eastern halves of the Greenwood map sheet. Detailed descriptions of the thrust sheets have been provided by Fyles (1990) and only a brief summary is given here. The sheets are informally numbered from south to north, structurally from bottom to top.

In the eastern part of the map area, sheet 1 straddles the Canada – United States border, being bounded to the north by the No 7 fault and to the south by the White Mountain fault (Stoffel *et al.*, 1991). It comprises probable Attwood Formation sedimentary rocks overlain by Triassic Brooklyn Formation volcanic rocks. In the west, a similar sheet of Attwood Formation rocks, bounded to the north by the Myers Creek fault, is here correlated with thrust sheet 1.

Sheet 2 is bounded by the No 7 fault as footwall and the North Mount Wright fault as hangingwall. Several other

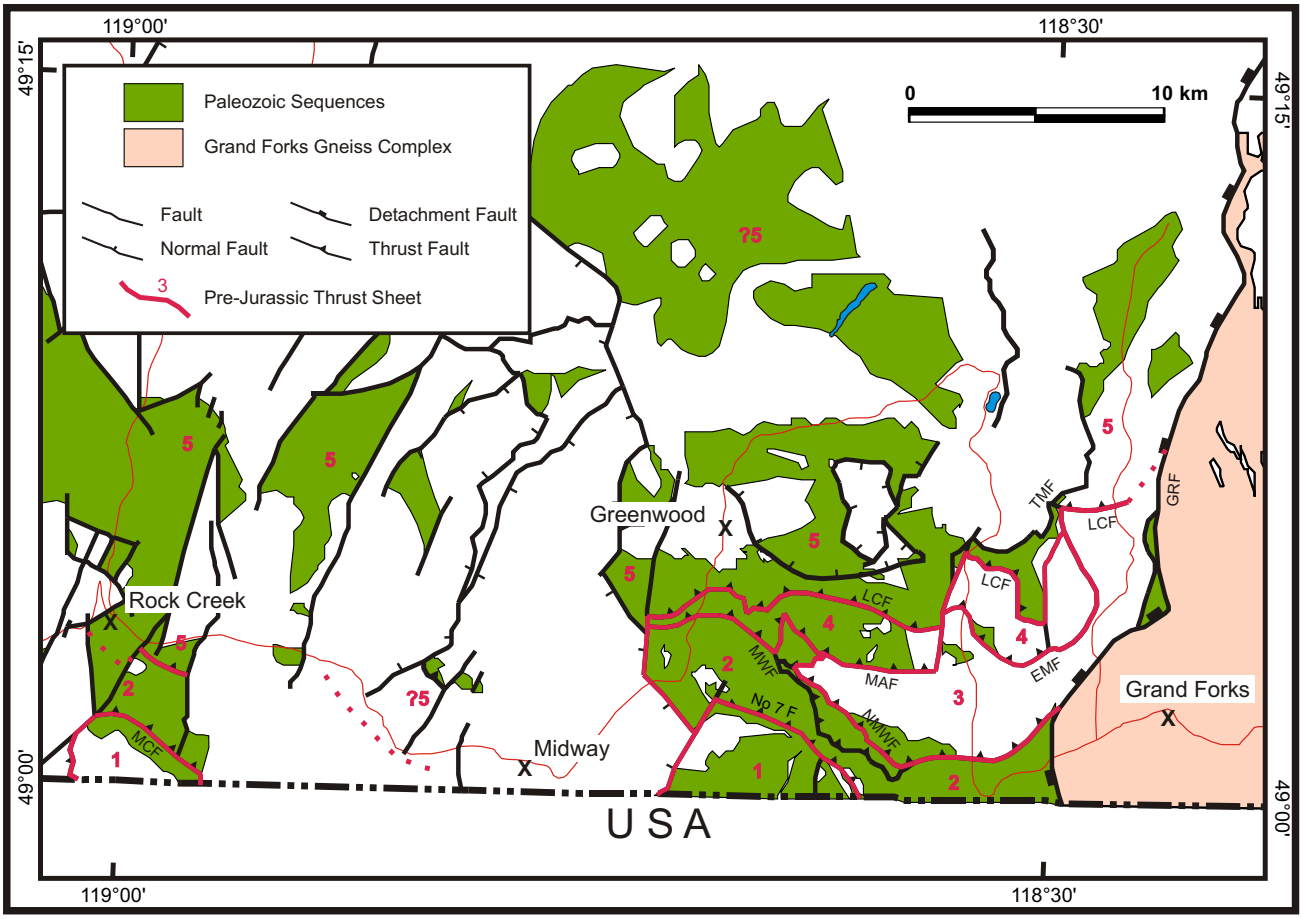


Figure 7. Main structural elements of the Greenwood area, outlining the five major thrust sheets (numbered 1–5) that contain the Paleozoic sequences (modified from Fyles, 1990). Abbreviations: GRF, Granby River fault; LCF, Lind Creek fault; MAF, Mount Attwood fault; MCF, Myers Creek fault; MWF, Mount Wright fault; NMWF, North Mount Wright fault; No 7 F, No 7 fault; TMF, Thimble Mountain fault.

mapped thrusts also occur internal to this sheet. The sheet comprises Knob Hill Complex metamorphic rocks with minor Brooklyn Formation. The Knob Hill Complex metamorphic rocks south of Rock Creek, and above the Myers Creek fault, are here correlated with sheet 2. The hangingwall thrust is not exposed but is postulated based on the contrast in metamorphism and deformation with the gabbro, greenstone and chert to the north of Rock Creek.

Sheets 3 and 4 only occur east of Greenwood. Sheet 3 comprises mostly Brooklyn Formation strata unconformable on Attwood Formation, bounded by the North Mount Wright and Mount Attwood faults. Sheet 4 similarly consists of Attwood and Brooklyn Formations, but is broken into several fragments by northerly trending Tertiary faults. The footwall thrust is the Mount Wright fault in the west and the Mount Attwood and Eagle Mountain faults to the east. The Lind Creek fault is the hangingwall thrust.

Sheet 5 contains the bulk of the Knob Hill Complex rocks in the map area, with unconformably overlying Brooklyn Formation. Knob Hill Complex outcrops north of the Kettle River in the western half of the map are part of this thrust sheet, although separated from the eastern area by Tertiary faults. The inlier of dominantly Brooklyn Formation rocks north of West Midway is also tentatively included in sheet 5, though it may belong to sheet 1.

Chert-argillite unit outcrops along the northern side of Highway 3 in the Eholt Creek valley are much higher in metamorphic grade and more deformed than Knob Hill units to the south on Montezuma Ridge, and are comparable to the rocks of the metamorphic unit. Such a sharp contrast of metamorphic grade may suggest a major structure along the Eholt Creek valley, perhaps another thrust. However, the Knob Hill units southeast of Jewel Lake are lower grade and appear to show a more gradual transition northward into the higher grade metamorphic rocks of Mount Roderick Dhu and Windfall Creek. Without more convincing evidence, all these units are considered to probably be part of thrust sheet 5.

The age of the thrust structures is still uncertain. Clasts of nearly all Paleozoic rock types, including serpentinite, are found in the Ladinian Brooklyn Formation conglomerate, indicating uplift and juxtaposition of the Paleozoic strata by the Middle Triassic. However, the involvement of Brooklyn Formation strata in the thrust sheets shows that the main thrusting event occurred, or continued, into post-Ladinian time. Diorite and granodiorite stocks of the Nelson suite intrude the thrust sheets, providing a minimum age for thrusting of 164–169 Ma (Lambert, 1989).

Church (1992) reported a discordant U-Pb zircon age of 199.4 ±1.4 Ma from the Lexington porphyry. This is possibly intrusive into the No 7 fault (see below), suggesting that thrusting took place prior to Jurassic time. The Chesaw fault in Washington is interpreted to be the continuation of the Myers Creek fault (Cheney *et al.*, 1994). It is apparently

cut by the Loomis pluton, which has yielded a discordant K-Ar hornblende age of 194 ±6 Ma (Rinehart and Fox, 1972; Stoffel, 1990). However, the Chesaw fault also cuts the Ellemehan Formation, which has been correlated with the Sinemurian to Pliensbachian Elise Formation of British Columbia (Read and Okulitch, 1977; Stoffel *et al.*, 1991), though lacking paleontological support.

LEXINGTON PORPHYRY REVISITED

The Lexington mining camp comprises up to eleven Cu-Au porphyry deposits in British Columbia and Washington, hosted by the Lexington porphyry within the No 7 fault zone. Mineralization stretches in a linear belt from the No 7 mine in the northwest to the Lone Star mine, in Washington, in the southeast. Exploration and development in this camp started in 1890 and continues to this day. Important reviews of mineralization and historical development were provided by Church (1970, 1986) and Seraphim *et al.* (1995).

The No 7 fault is marked by a thick serpentinite sheet along its length from McCarren Creek to the United States border. Along Goosmus Creek, the serpentinite is apparently split in two by the intrusion of a quartz porphyry body known as the Lexington porphyry (Church, 1992). The quartz-feldspar porphyry body in the footwall of the No 7 fault near the confluence of McCarren and Gidon creeks has been correlated with the Lexington quartz porphyry. The quartz-feldspar porphyry is, however, marked by large pink K-feldspar phenocrysts that are apparently absent from the type Lexington porphyry, which raises doubts about their correlation. Uranium-lead zircon geochronometry and petrochemistry are being conducted to help resolve this issue.

Several authors have mapped areas of andesitic to dacitic volcaniclastic rocks around some of the mines in the Lexington camp (*e.g.*, Church 1986, Fig. 9) and equivalents in Washington (*e.g.*, Morning Star deposit; Caron, pers. comm., 2005). Dacitic volcaniclastic rocks that host mineralization are also reported by company geologists in drillcore from the area (Butler, 1997; Cowley, 2004). Seraphim *et al.* (1995), however, asserted that these units at Lexington are not original volcanic rocks but the result of cataclasis of the porphyry within the fault zone, although they do allow for "the presence of xenoliths and screens of old volcanic rocks in the intrusion." Ongoing petrological and petrochemical studies are directed at this problem.

The recognition of these units as true volcanic rocks could have significant implications, not only for regional correlation and tectonic history but also for the possible potential for volcanogenic massive sulphide (VMS) deposits. Similar felsic volcaniclastic rocks are not found in the immediate map area and correlative equivalents are not easily recognized in the boundary region generally. Possible fine-grained buff tuff was found in the Attwood Formation in the Myers Creek area (see above), but no coarser lapilli tuff was found. If the volcaniclastic rocks are coeval with the 200 Ma Lexington porphyry, it may suggest that they are correlative with the Lower Jurassic Elise Formation of the Rossland Group. Church (1992) draws a comparison between the Lexington porphyry and felsic intrusions of similar age in the Nelson area (Dunne and Höy, 1992). Felsic volcanic rocks overlying the stratabound Lamefoot Cu-Au deposit have yielded an Ar/Ar plateau age of 195 Ma on sericite (Rasmussen, 2000) and have been correlated with the Elise Formation, as have felsic rocks at the Morning Star (Caron, pers. comm., 2005). However, in the Rossland area itself, the Elise Formation comprises mafic to andesitic volcanic rocks and lacks any significant felsic rocks (Höy and Andrew, 1989; Andrew *et al.*, 1990).

ACKNOWLEDGMENTS

The author is much indebted to Jim Fyles and Neil Church for all their invaluable help and advice during the planning stages of this project and since. The collaboration, support and ready welcome of the Boundary District exploration community were exceptional and, in particular, many thanks are extended to Bruce Laird of Merit Mining Corp. for his co-operation and enthusiastic assistance in sampling the Lexington rocks. The author also acknowledges the indispensable assistance of Ashley Dittmar during fieldwork and Sean Mullen in the office. Comments on an early version of this paper by JoAnne Nelson were much appreciated.

REFERENCES

Andrew, K.P.E., Höy, T and Drobe, J. (1990): Stratigraphy and tectonic setting of the Archibald and Elise formations, Rossland Group, Beaver Creek area, southeastern British Columbia (82F4E); *in* Geological Fieldwork 1989, *BC Ministry of Energy, Mines and Petroleum Resources*, Paper 1990-1, pages 19–27.

Bauerman, H. (1885): Geology of the country near the Forty-ninth Parallel of North Latitude, west of the Rocky Mountains; *Geological Survey of Canada*, Report of Progress, 1882–83–84, pages 5B–42B.

Brock, R.W. (1902): The Boundary Creek district, British Columbia; *Geological Survey of Canada*, Summary Report 1901, Volume XIV, pages 51A–69A.

Brock, R.W. (1903): Preliminary report on the Boundary Creek district, British Columbia; *Geological Survey of Canada*, Summary Report 1901, Volume XV, pages 92A–138A.

Brock, R.W. (1905a): Geological and topographical map of Boundary Creek Mining District, British Columbia; *Geological Survey of Canada*, Map 828, scale 1:63 360.

Brock, R.W. (1905b): Topographical map of Boundary Creek Mining District (economic minerals and glacial striae), British Columbia; *Geological Survey of Canada*, Map 834, scale 1:63 360.

Butler, S.P. (1997): Assessment report on the Lexington property, 1996, Greenwood Mining Division, British Columbia; *BC Ministry of Energy, Mines and Petroleum Resources*, Assessment Report 24901.

Carswell, H.T. (1957): Geology and ore deposits of Summit Camp, Boundary District, BC; M.Sc. thesis, *University of British Columbia*, 80 pages.

Cheney, E.S., Rasmussen, M.G. and Miller, M.G. (1994): Major faults, stratigraphy, and identity of Quesnellia in Washington and adjacent British Columbia; *Washington Division of Geology and Earth Sciences*, Bulletin 80, pages 49–71.

Church, B.N. (1970): Lexington; *in* Geology, Exploration, and Mining in British Columbia, *BC Ministry of Energy, Mines and Petroleum Resources*, pages 413–425.

Church, B.N. (1986): Geological setting and mineralization in the Mount Attwood – Phoenix area of the Greenwood mining camp; *BC Ministry of Energy, Mines and Petroleum Resources*, Paper 1986-2, 65 pages.

Church, B.N. (1992): The Lexington porphyry, Greenwood mining camp, southern British Columbia: geochronology

(82E/2E); *in* Geological Fieldwork 1991, *BC Ministry of Energy, Mines and Petroleum Resources*, Paper 1992-1, pages 295–297.

Cowley, P.S. (2004): Assessment report on the Lexington property diamond drilling, Greenwood Mining Division, British Columbia; *BC Ministry of Energy, Mines and Petroleum Resources*, Assessment Report 27393.

Daly, R.A. (1912): Geology of the North American Cordillera at the forty-ninth parallel; *Geological Survey of Canada*, Memoir 38.

Dostal, J., Church, B.N. and Hőy, T. (2001): Geological and geochemical evidence for variable magmatism and tectonics in the southern Canadian Cordillera: Paleozoic to Jurassic suites, Greenwood, southern British Columbia; *Canadian Journal of Earth Sciences*, Volume 38, pages 75–90.

Dunne, K.P.E. and Höy, T. (1992): Petrology of pre to syntectonic Early and Middle Jurassic intrusions in the Rossland Group, southeastern British Columbia (82F/SW); *in* Geological Fieldwork 1991, *BC Ministry of Energy, Mines and Petroleum Resources*, Paper 1992-1, pages 9–19.

Fyles, J.T. (1989): Geology of the pre-Tertiary rocks in the Rock Creek – Greenwood area, (82E/2); *in* Geological Fieldwork 1988, *BC Ministry of Energy, Mines and Petroleum Resources*, Paper 1989-1, pages 11–17.

Fyles, J.T. (1990): Geology of the Greenwood – Grand Forks area, British Columbia, NTS 82E/1, 2; *BC Ministry of Energy, Mines and Petroleum Resources*, Open File 1990-25, 19 pages.

Fyles, J.T. (1995): Day 3 (morning): Knob Hill Group, Attwood Group and Brooklyn Formation; *in* Victoria '95, Field Trip Guidebook B2, *Geological Association of Canada – Mineralogical Association of Canada*, Joint Annual Meeting, Victoria, BC, pages 40–49.

Höy, T and Andrew, K. (1989): The Rossland Group, Nelson map area, southeastern British Columbia (82F/6); *in* Geological Fieldwork 1988, *BC Ministry of Energy, Mines and Petroleum Resources*, Paper 1989-1, pages 33–43.

Lambert, R. St J. (1989): Tectonics and mineralization in southeastern British Columbia — tectonics of the Kootenay Arc; *in* Geological Guidebook for Washington and Adjacent Areas, Joseph, N.L. *et al.*, Editors, *Washington Division of Geology and Earth Resource Information*, Circular 86, pages 45–54.

LeRoy, O.E. (1912): The Geology and ore deposits of Phoenix, Boundary District, British Columbia; *Geological Survey of Canada*, Memoir 21, 110 pages.

LeRoy, O.E. (1913): Motherlode and Sunset mines, Boundary District, British Columbia; *Geological Survey of Canada*, Memoir 19, 56 pages.

Little, H.W. (1957): Kettle River (east half), British Columbia; *Geological Survey of Canada*, Map 6-1957, scale 1:253 440.

Little, H.W. (1983): Geology of the Greenwood Map-area, British Columbia; *Geological Survey of Canada*, Paper 79-29, 37 pages.

Massey, N.W.D., MacIntyre, D.G., Desjardins, P.J. and Cooney, R.T. (2005): Digital geology map of British Columbia, *BC Ministry of Energy, Mines and Petroleum Resources*, Open File 2005-2, DVD.

McNaughton, D.A. (1945): Greenwood-Phoenix area, British Columbia; *Geological Survey of Canada*, Paper 45-20, 23 pages.

Monger, J.W.H. (1968): Early Tertiary stratified rocks, Greenwood map-area (82E/2), British Columbia; *Geological Survey of Canada*, Paper 67-42, 39 pages.

Monger, J.H.W., Wheeler, J.O., Tipper, H.W., Gabrielse, H., Harms, T., Struik, L.C., Campbell, R.B., Dodds, C.J., Gehrels, G.E. and O'Brien, J. (1991): Part B. Cordilleran Terranes; *in* Chapter 8 (Upper Devonian to Lower Jurassic Assemblages) *of* Geology of the Cordilleran Orogen in Canada, Gabrielse, H. and Yorath, C.J., Editors, *Geological Survey of Canada*, Geology of Canada, no 4, pages 281–327.

Murphy, M.A. and Salvador, A. (1999): International stratigraphic guide – an abridged version; *Episodes*, Volume 22, pages 255–271.

Nelson, J., Ferri, F. and Roback, R. (1995) Introduction: raising the questions; *in* Late Paleozoic Arc and Oceanic Terranes and their External Relationships, Southern Quesnellia, Roback, R., Schiarizza, P., Nelson, J., Fyles, J., Ferri, F., Hoy, T., Ash, C. and Danner, W.R., Editors, *Geological Association of Canada – Mineralogical Association of Canada*, Joint Annual Meeting, Victoria, BC, Field Trip B2 Guidebook, pages 2–7.

Nixon, G.T. (2002): Alkaline hosted Cu-PGE mineralization: the Sappho Alkaline Plutonic Complex, south-central British Columbia; *BC Ministry of Energy, Mines and Petroleum Resources*, Open File 2002-7, 2 maps sheets at 1:5000 scale.

Orchard, M.J. (1993): Report on conodonts and other microfossils, Penticton (82E); *Geological Survey of Canada*, Report OF-1993-19.

Orchard, M.J. (1997): Report on conodonts and other microfossils, Penticton (82E); *Geological Survey of Canada*, Report OF-1997-9.

Rasmussen, M.G. (2000): The Lamefoot gold deposit, Ferry County, Washington (abstract); *in* Republic Symposium 2000, *Northwest Mining Association,* Dec 4–5, 2000.

Read, P.B. and Okulitch, A.V. (1977): The Triassic unconformity of south-central British Columbia; *Canadian Journal of Earth Sciences*, Volume 14, pages 606–638.

Rinehart, C.D. and Fox, K.F., Jr. (1972): Geology and mineral deposits of the Loomis Quadrangle, Okanagan County, Washington; *Washington Division of Mines and Geology*, Bulletin 64, 124 pages.

Seraphim, R.H. (1956): Geology and copper deposits of Boundary District, British Columbia; *Canadian Institute of Mining and Metallurgy Bulletin*, Volume 49, pages 684–694.

Seraphim, R.H., Church, B.N. and Shearer, J.T. (1995): The Lexington – Lone Star copper-gold porphyry: an Early Jurassic cratonic linear system, southern British Columbia; *in* Porphyry Deposits of the Northwestern Cordillera of North America, Schroeter, T.G., Editor, *Canadian Institute of Mining, Metallurgy and Petroleum*, Special Volume 46, pages 851–854.

Stoffel, K.L. (1990): Geologic map of the Republic 1:100 000 Quadrangle, Washington; *Washington Division of Geology and Earth Resources*, Open File Report 90-10, 62 pages, 1 map.

Stoffel, K.L., Joseph, N.L., Waggoner, S.Z., Gulick, C.W., Korosec, M.A. and Bunning, B.B. (1991): Geologic map of Washington — northeast quadrant; *Washington Division of Geology and Earth Resources*, Geologic Map GM-39, 36 pages and 3 maps at 1:250 000 scale.

Templeman-Kluit, D.J. (1989a): Geological map with mineral occurrences, fossil localities, radiometric ages and gravity field for Penticton map area (NTS 82E), southern British Columbia; *Geological Survey of Canada*, Open File 1969.

Templeman-Kluit, D.J. (1989b): Geology, Penticton, British Columbia; *Geological Survey of Canada*, Map 1736A, scale 1:250 000.

U-Pb Isotopic Ages of Intrusive Rocks Related to Mineralization North of Terrace, British Columbia

by Mitchell G. Mihalynuk and Richard M. Friedman

KEYWORDS: U-Pb zircon isotopic age, intrusive-related gold mineralization, Bowser Lake Group, molybdenum porphyry, copper porphyry

INTRODUCTION

In 2004, the BC Ministry of Energy, Mines and Petroleum Resources and Bootleg Exploration Inc. entered into a partnership agreement aimed at the evaluation of the regional potential for intrusive-related gold mineralization near Terrace, British Columbia. Bootleg Exploration Inc. is a wholly owned subsidiary of Eagle Plains Resources Ltd., and their area of interest is around Kitsum – Kalum Lake, centred approximately 35 km north of Terrace (Fig. 1). Preliminary results from that partnership were published in Mihalynuk and Friedman (2005). Geochronological data that have come available since then are reported here.

Six samples were collected for U-Pb geochronological work from widely separated localities (Fig. 2). Results from analyses of one sample were presented in Mihalynuk and Friedman (2005), four other samples are presented here, and one sample did not yield sufficient material to permit generation of an interpretable dataset. Readers interested in the geological setting of the intrusions and mineral deposits described herein are referred to Downie and Stephens (2003) or Mihalynuk and Friedman (2005).

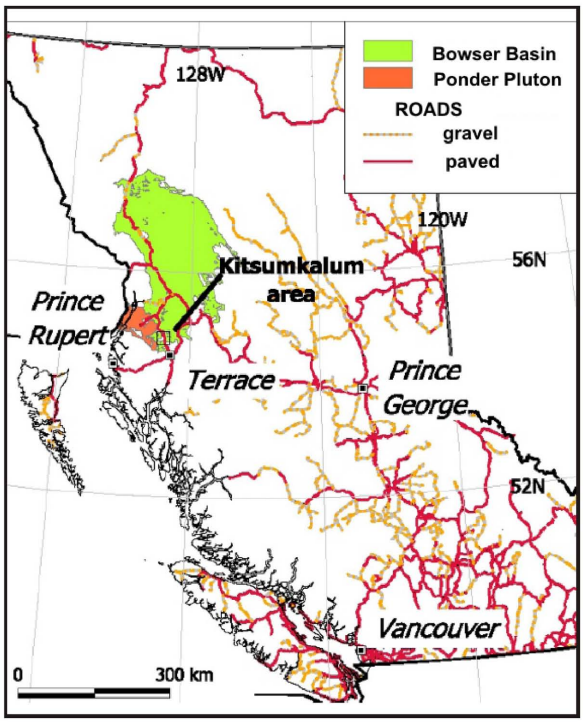


Figure 1. Location of the Kalum project area, approximately 35 km north of Terrace. Geology from Massey *et al.* (2003).

METHODS

Approximately 30 kg of unweathered intrusion was collected from each sample site to determine its crystallization age employing the isotope dilution – thermal ionization mass spectroscopy U-Pb method (ID-TIMS). All work was carried out at the Pacific Centre for Isotopic and Geochemical Research at the Department of Earth and Ocean Sciences, University of British Columbia.

Zircon was separated from rock samples using conventional crushing, grinding and Wilfley table techniques, followed by final concentration using heavy liquids and magnetic separations. Mineral fractions for analysis were selected based on grain morphology, quality, size and magnetic susceptibility. Except where noted, all zircon fractions were abraded prior to dissolution to minimize the effects of post-crystallization Pb-loss, using Krogh's (1982) technique. Samples were dissolved in concentrated hydrofluoric acid (HF) and nitric acid (HNO_3) in the presence of a mixed $^{233-235}U$-^{205}Pb tracer. Separation and purification of Pb and U employed ion exchange column techniques modified slightly from those described by Parrish *et al*. (1987). Pb and U were eluted separately and loaded together on a single Re filament using a phosphoric acid - silica gel emitter. Isotopic ratios were measured using a modified single collector VG-54R thermal ionization mass spectrometer equipped with a Daly photomultiplier. Measurements were done in peak-switching mode on the Daly detector. U and Pb total procedural blanks were in the range of 1 pg and 3 to 5 pg, respectively, during the course of this study. U fractionation was determined directly on individual runs using the $^{233-235}U$ tracer, and Pb isotopic ratios were corrected for a fractionation of 0.37%/amu for Faraday and Daly runs, respectively, based on replicate analyses of the NBS-981 Pb standard and the values recommended by Thirlwall *et al*. (2000). All analytical errors were numerically propagated through the entire age calculation using the technique of Roddick (1987). Concordia intercept ages and associated errors were calculated using a modified version of the York-II regression model (wherein the York-II errors are multiplied by the mean square of weighted deviates [MSWD]) and the algorithm of Ludwig (1980). All errors

This publication is also available, free of charge, as colour digital files in Adobe Acrobat PDF format from the BC Ministry of Energy, Mines and Petroleum Resources internet website at http://www.em.gov.bc.ca/Mining/Geolsurv/Publications/catalog/catfldwk.htm

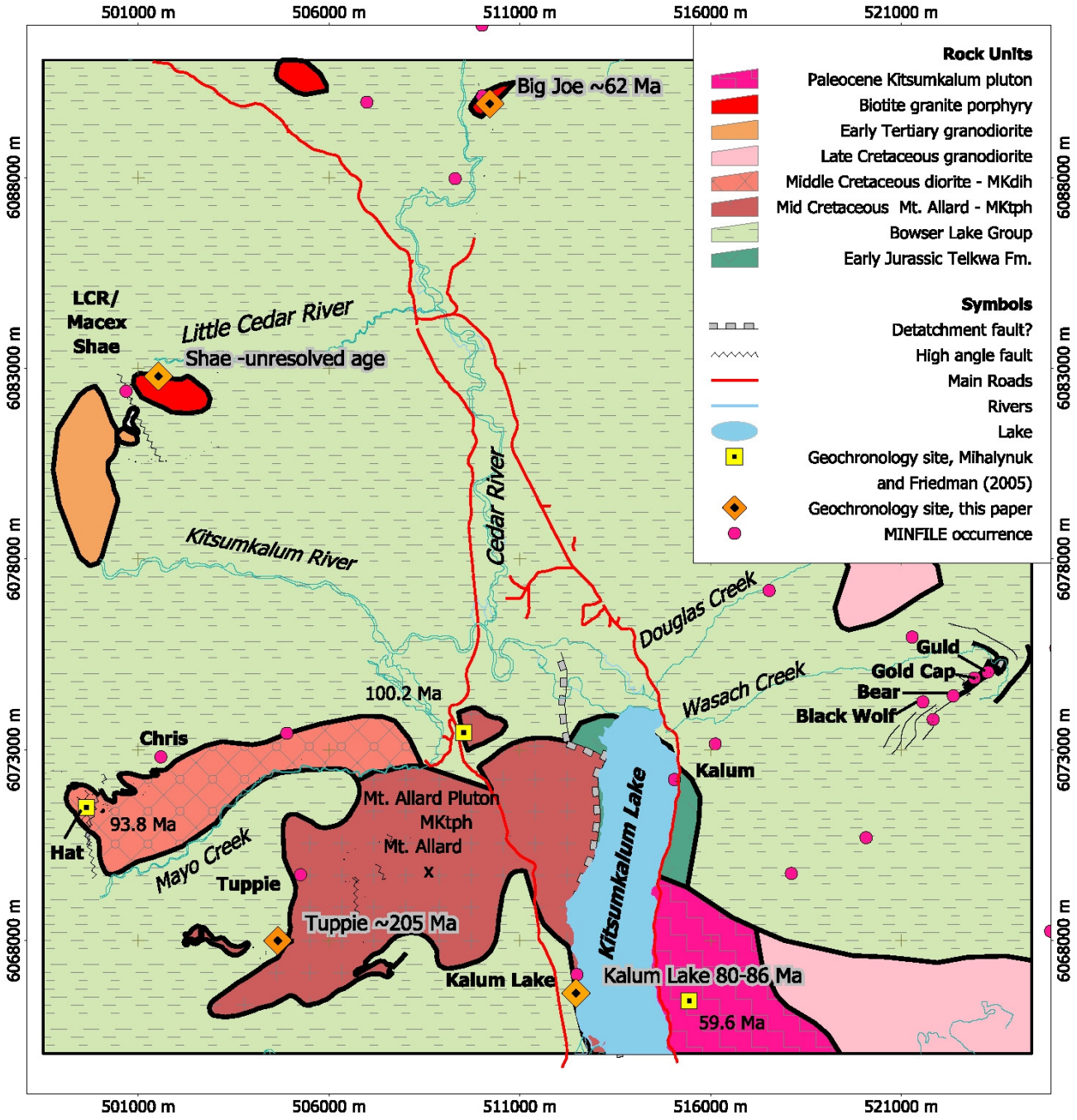


Figure 2. Generalized geology of the Kitsumkalum area. Sources of information: this project, Woodsworth *et al.* (1985), Downie and Stephens (2003) and Massey *et al.* (2003).

are quoted at the two sigma level. Results are plotted on a standard concordia diagram (Fig. 3) and listed in Table 1.

RESULTS OF GEOCHRONOLOGICAL ANALYSES

The locations of samples collected for geochronological study are shown in geological context on Figure 2. Analytical results are enumerated in Table 1, and concordia plots are shown on Figure 3.

Big Joe Biotite Granite

Molybdenite mineralization at the Big Joe occurrence is hosted by a biotite granite stock located within a kilometre of the east bank of the Cedar River, about 5 km upstream of its confluence with the Little Cedar River.

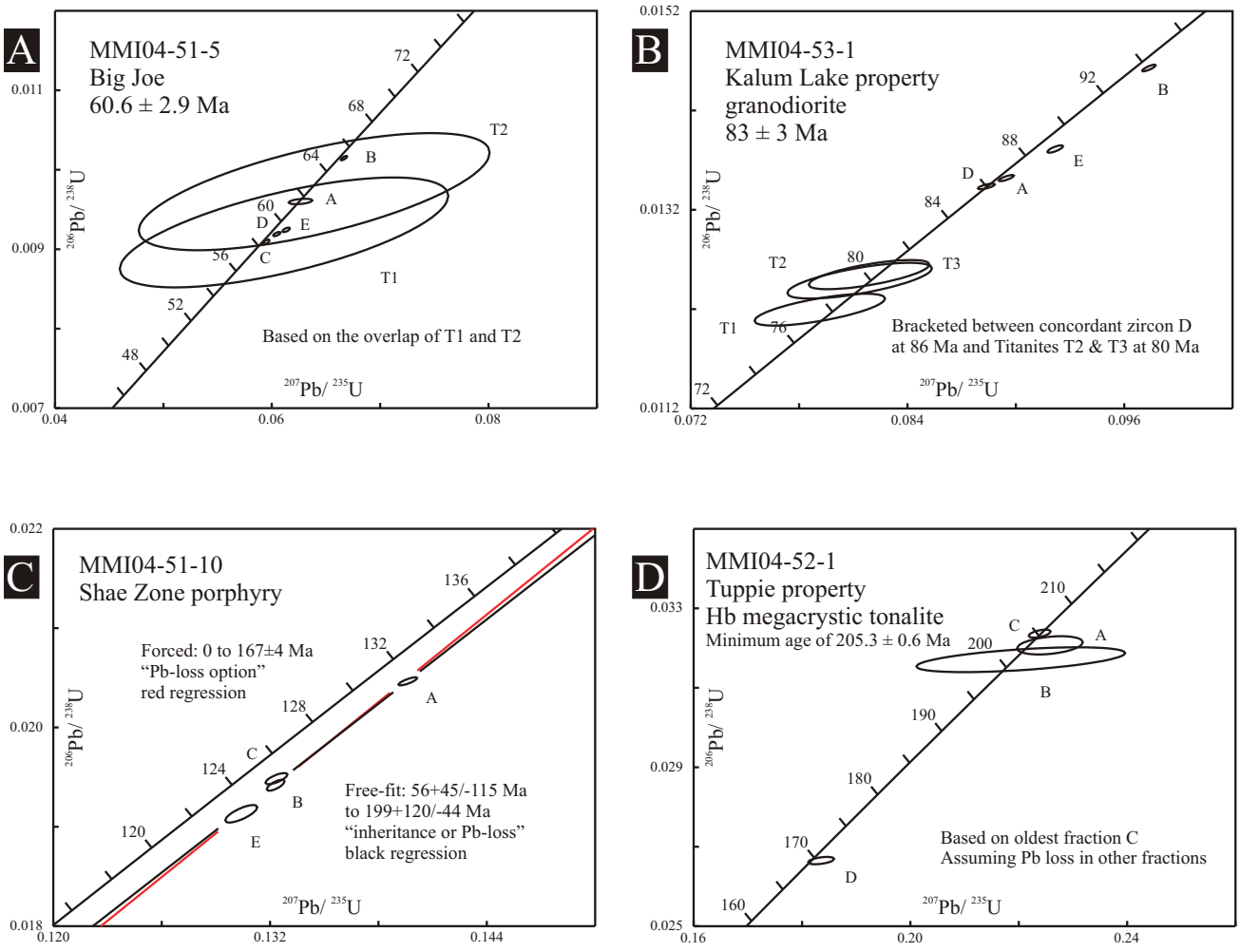


Figure 3. Concordia plots of isotopic data and interpreted ages. Data were obtained from analysis of samples from four intrusive bodies in the Kitsumkalum Lake area. See Figure 2 for locations and Table 1 for analytical data.

Medium-grained biotite granite comprises the poorly defined wedge-shaped intrusion, which has a long dimension of about 1 km. It is extensively affected by moderately intense phyllic alteration that has resulted in bleaching and yellow or rust weathering. Secondary white mica+/-pyrite is ubiquitous (Fig. 4). North-trending, centimetre-thick sheeted quartz veins are common. Some veins attain thicknesses of 35 cm. A west-trending subset of veins is locally well developed. Molybdenite occurs as fine rosettes and vein coatings, but it is not abundant in surface exposures. Fist-sized clots of molybdenite occur sporadically (Fig. 5).

A sample of the pluton was collected to date the molybdenite mineralization, assuming that the molybdenite is syngenetic. Both zircon and titanite were recovered and analyzed from this sample. Zircon results are scattered, reflecting the presence of minor inheritance and Pb loss, although fraction A is concordant at about 62 Ma (Fig. 3A). The overlap of two relatively imprecise titanite analyses at 60.6 ±2.9 Ma, which includes concordant zircon fraction A, provides the best estimate for the age of the rock.

Biotite Granodiorite at Kalum Lake Property

Medium-grained biotite granodiorite at the Kalum Lake property crops out near the east shore of southern Kalum Lake. Exposures show extensive carbonate alteration and weathered rock is orange in colour. The least altered parts of the exposures contain chloritized biotite and accessory magnetite, with average magnetic susceptibility values of 25 (versus 0.3 where altered). Mineralization displayed by excavated parts of the intrusion consists of quartz veins and tabular quartz stockworks, with a minimum 65 cm thickness, that carry pyrite, tetrahedrite and chalcopyrite as the principal sulphides. Mihalynuk and Friedman's (2005) analyses of these veins revealed approximately 1200 to 2300 ppb gold and 112 ppm silver; however,

TABLE 1. U-Pb ID-TIMS ANALYTICAL DATA FOR INTRUSIONS IN THE KITSUMKALUM LAKE AREA.

Fraction[1]	Wt	U[2]	Pb*[3]	$^{206}Pb/^{204}Pb$[4]	Pb[5]	^{208}Pb[6]	Isotopic ratios (1σ, %)[7]			Apparent ages (2σ, Ma)[7]		
	(mg)	(ppm)	(ppm)		(pg)		$^{206}Pb/^{238}U$	$^{207}Pb/^{235}U$	$^{207}Pb/^{206}Pb$	$^{206}Pb/^{238}U$	$^{207}Pb/^{235}U$	$^{207}Pb/^{206}Pb$
Big Joe granite MMI04-51-5: 60.6 +/-2.9 Ma												
A, 1	18	276	2.6	870	3	8.7	0.00960 (0.18)	0.0627 (0.87)	0.04733 (0.81)	61.6 (0.2)	61.7 (1.0)	65.8 (38/39)
B, 6	50	760	7.6	4772	5	8.0	0.01015 (0.13)	0.0667 (0.22)	0.04764 (0.15)	65.1 (0.2)	65.5 (0.3)	81.5 (7.1)
C, 5	37	958	8.4	3294	6	6.4	0.00909 (0.16)	0.0595 (0.24)	0.04746 (0.18)	58.4 (0.2)	58.7 (0.3)	72.3 (8.7)
D, 15	49	731	6.6	4739	4	7.7	0.00919 (0.14)	0.0605 (0.28)	0.04771 (0.21)	59.0 (0.2)	59.6 (0.3)	85 (10)
E, 20	37	540	4.8	2576	4	7.0	0.00924 (0.15)	0.0613 (0.28)	0.04812 (0.22)	59.3 (0.2)	60.4 (0.30	105 (10)
T1	343	155	1.5	33	2030	13.3	0.00921 (3.8)	0.0611 (12.4)	0.04813 (10.3)	59.1 (4.4)	60 (15)	106 (425/575)
T2	333	150	1.5	33	2030	14.6	0.00973 (3.8)	0.0639 (12.7)	0.04767 (10.5)	62.4 (4.7)	63 (15)	83 (436/595)
Kalum Lake prospect MMI04-53-1: 83 +/-3 Ma												
A 3	44	503	6.5	2548	7	5.4	0.01352 (0.11)	0.0895 (0.24)	0.04800 (0.16)	86.6 (0.2)	87.0 (0.4)	99.2 (7.6)
B, 7	64	636	8.9	5625	6	5.6	0.01463 (0.11)	0.0974 (0.19)	0.04828 (0.12)	93.6 (0.2)	94.3 (0.3)	112.8 (5.5)
D, 9	28	515	6.6	2616	5	6.0	0.01344 (0.10)	0.0884 (0.26)	0.04770 (0.20)	86.0 (0.2)	86.0 (0.4)	84.4 (9.7)
E, 4	24	815	10.9	4676	4	7.2	0.01381 (0.13)	0.0922 (0.23)	0.04840 (0.16)	88.4 (0.2)	89.5 (0.4)	118.9 (7.5)
T1	400	230	3.7	105	795	30.8	0.01220 (0.66)	0.0791 (2.3)	0.04707 (1.9)	78.1 (1.0)	77.3 (3.4)	52.7 (88/93)
T2	434	261	4.3	96	1110	31.4	0.01249 (0.72)	0.0813 (2.5)	0.04725 (2.0)	80.0 (1.2)	79.4 (3.8)	61.8 (94/100)
T3	396	252	4.3	115	793	33.6	0.01255 (0.59)	0.0819 (2.0)	0.04732 (1.7)	80.4 (0.9)	79.9 (3.1)	66 (79/83)
Shae Zone porphyry MMI04-51-10: minimum age of 167 +/–4 Ma												
A, 2	54	374	7.5	7696	3	7.8	0.02047 (0.10)	0.1396 (0.19)	0.04948 (0.12)	130.6 (0.3)	132.7 (0.5)	170.8 (5.6)
B, 3	69	475	8.9	7125	5	6.0	0.01942 (0.14)	0.1323 (0.19)	0.04942 (0.13)	124.0 (0.4)	126.2 (0.4)	167.6 (6.1)
C, 7	41	655	12.1	2552	13	4.7	0.01949 (0.14)	0.1324 (0.23)	0.04926 (0.16)	124.4 (0.4)	126.2 (0.6)	160.4 (7.5)
E, 7	31	510	9.2	2317	8	4.6	0.01913 (0.23)	0.1304 (0.34)	0.04801 (1.5)	122.2 (0.6)	124.5 (0.8)	169 (11)
Tuppie MMI04-52-1: minimum age of 205.3 +/-0.6 Ma												
A, 2	18	82	2.7	1321	2	12.7	0.03207 (0.36)	0.2257 (1.3)	0.05105 (1.3)	203.5 (1.4)	206.7 (5.0)	243 (58/60)
B, 9	14	35	1.1	120	9	12.4	0.03171 (0.49)	0.2204 (4.4)	0.05041 (4.1)	201.2 (2.00	202 (16)	214 (181/203)
C, 9	27	141	4.5	1242	6	8.2	0.03236 (0.15)	0.2239 (0.45)	0.05017 (0.39)	205.3 (0.6)	205.1 (1.7)	203 (18)
D, 12	16	140	3.8	962	4	11.8	0.02665 (0.6)	0.1835 (0.65)	0.04994 (0.60)	169.7 (0.6)	171.1 (2.1)	192 (27/28)

[1] Upper case letter is zircon fraction identifier, followed by the number of grains; titanite: T1, T2, etc. All zircon fractions were air abraded.

[2] U blank correction of 1 pg +/-20%; U fractionation corrections were measured for each run with a double ^{233}U-^{235}U spike (about 0.004/amu).

[3] Radiogenic Pb.

[4] Measured ratio corrected for spike and Pb fractionation of 0.0037/amu +/-20% (Daly collector), which was determined by repeated analysis of NBS Pb 981 standard throughout the course of this study.

[5] Total common Pb in analysis based on blank isotopic composition.

[6] Radiogenic Pb.

[7] Blank Pb was 3 to 5 pg throughout the course of this study; U <1 pg; common Pb composition for corrections based on Stacey and Kramers (1975) model Pb at the age of the rock or the $^{207}Pb/^{206}Pb$ age of the rock.

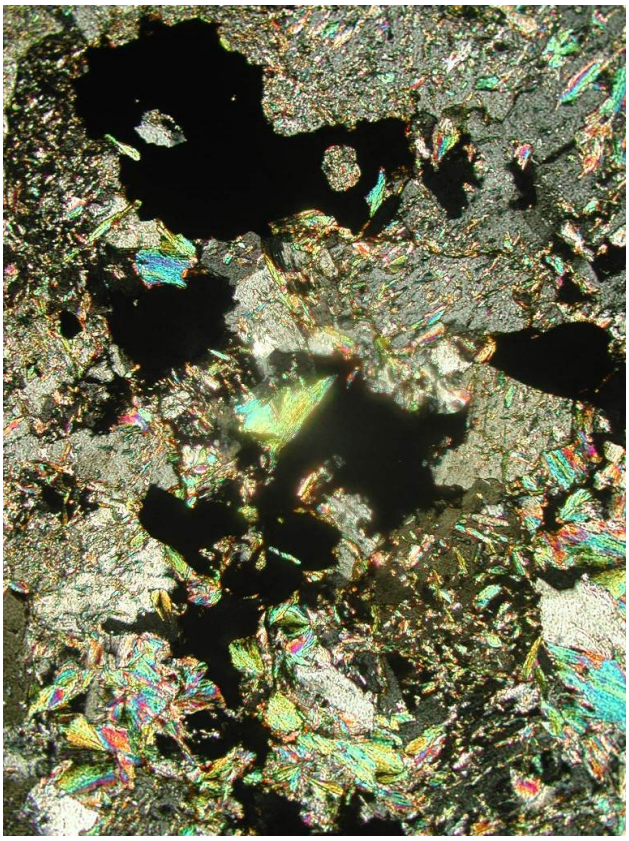


Figure 4. Photomicrograph of typical alteration assemblage in granite stock hosting molybdenite mineralization at the Big Joe. The long dimension of the photo represents approximately 4 mm and the photo was taken using cross-polarized light. Brightly coloured (high birefringence) mineral grains are white mica; opaques are mainly pyrite and minor molybdenite.



Figure 5. Blue-grey molybdenite occurs in irregular clots up to fist size at the Big Joe occurrence. Highly reflective mineral grains are pyrite and white mica.

spectacular assays were reported by Cavey and Howe (1984), 251 g/t gold and 226 g/t silver.

A sample of the least altered, intact intrusion was collected for determination of a magmatic crystallization that would provide a maximum age limit on the mineralization. This sample yielded abundant zircon and titanite. Of four analyzed multigrain zircon fractions, three are discordant due to the presence of minor inheritance (Fig. 3B; Table 1). The youngest fraction (D) is concordant and thus appears to be free of inheritance or may contain a trace of slightly older (Cretaceous) inheritance. Results for the three analyzed multigrain titanite fractions plot between 77 to 81 Ma. The two nearly identical older results (T2 and T3) represent the minimum age for the rock.

Shae Quartz-Biotite Porphyry

Quartz-biotite porphyry is exposed at low elevations in the Little Cedar River valley (Fig. 2). Porphyry-style copper-molybdenum mineralization is locally developed, and in several places the immediately adjacent country rocks are replaced by pyrrhotite, pyrite and chalcopyrite. Chilled phases are quartz-eye porphyry with quartz up to 8 mm in diameter, comprising up to 5% of the rock. Oxidation of finely disseminated pyrite produces rusty outcrops, which may be cut by sheeted or stockwork quartz veins (Fig. 6). Mihalynuk and Friedman (2005) interpreted this intrusion as coeval with pyritic quartz-biotite-feldspar porphyry dikes that intrude parallel to fold hinges in the Bowser Lake Group strata on the ridge to the south. If correct, the dikes post-date folding in the Bowser Lake Group strata.

Four multigrain zircon fractions were analyzed. All are discordant with early Cretaceous Pb-U dates; they define a quasi-linear array nearly parallel to this segment of the concordia curve. Both free-fit (black) and forced 0 Ma (red) regression lines are plotted on Figure 3C and the intercepts are listed in Table 1. The forced 0 Ma option implies Pb-loss, no inheritance and a Jurassic magmatic minimum age (167 ±4 Ma). The free-fit regression allows for either Pb-loss or inheritance interpretations. The former yields an Early Mesozoic to Late Palaeozoic age and the latter a Cenozoic to Cretaceous age with Jurassic to Palaeozoic inheritance. This sample requires more U-Pb work. Ar-Ar dating currently in progress may also provide verification of one of the interpretations.

Hornblende Megacrystic Tonalite

Dikes and sills of hornblende tonalite cut and thermally metamorphose siltstone and argillite at the Tuppie property (Downie and Stephens, 2003), about 7 km west of Kitsumkalum Lake (approximately 4 km southwest of Mount Allard). Contacts of these sills are commonly foliated, and some of the foliated zones are carbonate altered (Fig. 7), locally with quartz veining and base metal sulphide mineralization. One of the thickest sills, with a

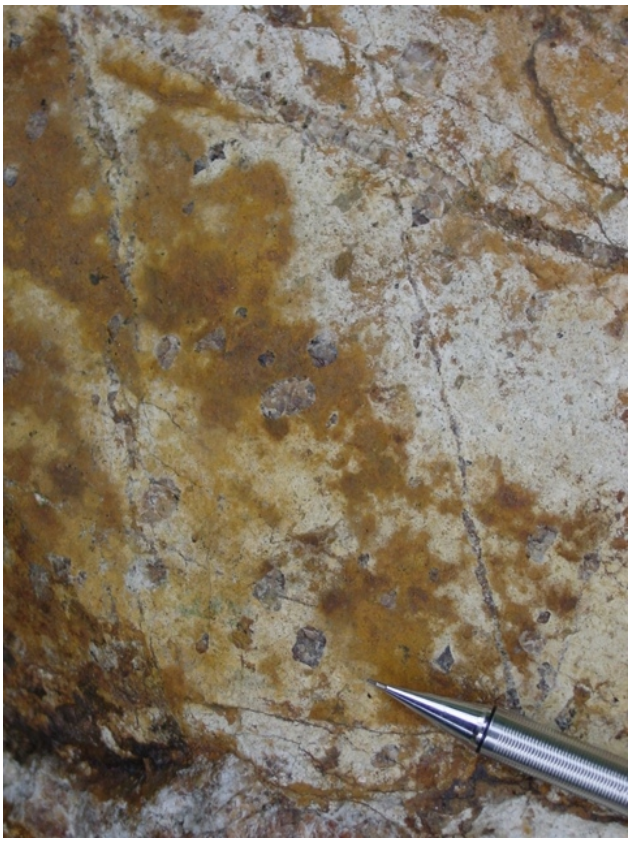


Figure 6. Quartz veining in altered biotite-quartz porphyry at the Shae occurrence. Coarse quartz eyes are well developed in chilled phases, as shown here.



Figure 7. Relatively fine-grained border of hornblende megacrystic tonalite at the Tuppie occurrence showing foliated and carbonate-altered equivalent.

foliated lower margin (270/22), was sampled for geochronological age determination. A date would place a maximum age constraint on this mineralization.

A conspicuous feature of these dikes and sills is a high proportion (~25%) of euhedral hornblende phenocrysts up to 5 cm long. Microscopic examination of these phenocrysts shows that they enclose biotite grains that may display a well-developed alignment (Fig. 8) and comprise up to a third of the phenocrysts. Whether or not this high biotite content is typical of the megacrystic tonalite is uncertain. If so, this helps to distinguish it from the tonalitic Mount Allard pluton, which also contains a high proportion of euhedral hornblende phenocrysts, but the Mount Allard phenocrysts contain abundant inclusions of quartz and feldspar as opposed to biotite.

Only a very small quantity of zircon could be extracted from the Tuppie sample, which was subdivided into four multigrain fractions on the basis of grain size. Fractions A and B consisted of euhedral prisms that were abraded prior to dissolution, while C and D were unabraded blocky anhedral to subhedral grains (Fig. 3D; Table 1). Results for the three coarser fractions overlap concordia between about 199 and 206 Ma. The finest unabraded grains comprise fraction D, which give significantly younger and discordant results suggesting strong Pb loss. If the dispersion of data can be attributed entirely to Pb loss, fraction C with Pb-U dates of about 205 Ma provides a minimum age for the rock.



Figure 8. Photomicrograph of an approximately 3.5 mm long hornblende phenocryst displaying a typical poikilitic enclosure of biotite.

If the Pb-loss interpretation is correct, the latest Triassic age determination leads to a geological impossibility. Regional mapping (Duffell and Souther, 1964; Woodsworth *et al*., 1985; Downie and Stephens, 2003) indicates that the sedimentary strata around the Tuppie are part of the Upper Jurassic Bowser Lake Group, the oldest parts of which are about 166 Ma (Evenchick and McNicoll, 2002). One possible explanation for this inconsistency is that the dated fractions are zircon xenocrysts. Until this problem can be resolved, the possibility of Late Triassic strata should be acknowledged because of the significant implications for mineral exploration. In particular, the limits of stratigraphy which bracket the age of the mineralized horizon at Eskay Creek, interpreted as a shallow submarine hydrothermal deposit (Alldrick, 1995), could be extended to the Kitsumkalum Lake area.

SUMMARY

Four new U-Pb age determinations are available for intrusive rocks in the Kitsumkalum area. Interpreted best ages for magmatic crystallization and constraint on the age of associated mineralization, from youngest to oldest, are

1) 60 ±2.9 Ma; Big Joe granite and ?syngenetic molybdenum mineralization;
2) 83 ±3 Ma; Kalum Lake granodiorite, which predates the mineralized quartz veins that cut it;
3) a tenuous and highly interpretive, low reliability minimum age of 167 ±4 Ma is suggested for the Shae biotite-quartz porphyry and disseminated plus replacement copper+/-molybdenum mineralization;
4) a provisional minimum age of 205.3 ±0.6 Ma is suggested for the hornblende megacrystic tonalite on the Tuppie property, which predates mineralized quartz veins that cut its foliated margin.

None of the samples analyzed yielded a straightforward geochronological dataset. All are subject to interpretation and more analytical work is needed to confirm the best ages suggested. Both of the older samples are particularly speculative. Nevertheless, the suggestion of Late Triassic to Middle Jurassic magmatic ages provided by these samples is important because it allows for the possibility of stratigraphy that is age equivalent to strata hosting the rich Eskay Creek deposit.

ACKNOWLEDGMENTS

This work was made possible through the financial contribution of a corporate partner, Eagle Plains Resources Ltd., and was conceived by its executive officers, Tim Termuende and Charles Downie. Geochronological sample collection was aided by David Lefebure. Geochronological analyses were conducted in partnership with the Pacific Centre for Isotopic and Geochemical Research at the Department of Earth and Ocean Sciences, University of British Columbia, which is funded in part by National Sciences and Engineering Research Council of Canada (NSERC) grants. Brian Grant helped to improve the manuscript.

REFERENCES

Alldrick, D.J. (1995): Subaqueous hot spring Au-Ag; *in* selected British Columbia Mineral Deposit Profiles, Volume 1 - Metallics and Coal, *BC Ministry of Energy, Employment and Investment*, Open File 1995-20, pages 55–58.

Cavey, G. and Howe, D. (1984): Report on the Kalum Lake claim group; submitted by Eagle Plains Resources Ltd., *BC Ministry of Energy, Mines and Petroleum Resources*, AR13,303.

Downie, C.C. and Stephens, J. (2003): Kalum gold-silver property; submitted by Eagle Plains Resources Ltd., *BC Ministry of Energy, Mines and Petroleum Resources*, AR27417, 54 pages (plus appendices).

Duffell, S. and Souther, J.G. (1964): Geology of Terrace map-area, British Columbia; *Geological Survey of Canada*, Memoir 329, 117 pages.

Evenchick, C.A. and McNicoll, V. (2002): Stratigraphy, structure, and geochronology of the Anyox Pendant, northwest British Columbia, and implications for mineral exploration; *Canadian Journal of Earth Sciences*, Volume 39, pages 1313–1332.

Krogh, T.E. (1982): Improved accuracy of U-Pb zircon ages by the creation of more concordant systems using an air abrasion technique; *Geochimica et Cosmochimica Acta*, Volume 46, pages 637–649.

Ludwig, K.R. (1980): Calculation of uncertainties of U-Pb isotopic data; *Earth and Planetary Science Letters*, Volume 46, pages 212–220.

Massey, N.W.D., MacIntyre, D.G. and Desjardins, P.J. (2003): Digital geology map of British Columbia: tile NM09 southcoast BC; *BC Ministry of Energy, Mines and Petroleum Resources*, Geofile 2003-4, scale 1:250 000.

Mihalynuk, M.G. and Friedman, R.M. (2005): Gold and base metal mineralization near Kitsumkalum Lake, north of Terrace, west-central British Columbia; *in* Geological Fieldwork 2004, *BC Ministry of Energy, Mines and Petroleum Resources*, Paper 2005-1, pages 67–82.

Parrish, R., Roddick, J.C., Loveridge, W.D. and Sullivan, R.W. (1987): Uranium-lead analytical techniques at the geochronology laboratory; *in* Radiogenic Age and Isotopic Studies, Report 1, *Geological Survey of Canada*, Paper 87-2, pages 3–7.

Roddick, J.C. (1987): Generalized numerical error analysis with application to geochronology and thermodynamics; *Geochimica et Cosmochimica Acta*, Volume 51, pages 2129–2135.

Stacey, J.S. and Kramer, J.D. (1975): Approximation of terrestrial lead isotope evolution by a two-stage model; *Earth and Planetary Science Letters*, Volume 26, pages 207–221.

Thirlwall, M.F. (2000): Inter-laboratory and other errors in Pb isotope analyses investigated using a ^{207}Pb–^{204}Pb double spike; *Chemical Geology*, Volume 163, pages 299–322.

Woodsworth, G.J., Hill, M.L. and van der Heyden, P. (1985): Preliminary geologic map of Terrace (NTS 103I, east half) map area, British Columbia; *Geological Survey of Canada*, Open File 1136, scale 1:125 000.

Geology and Mineral Potential of the Usk Map Area (NTS 103I/09), Terrace, British Columbia

JoAnne Nelson, Tony Barresi[1], Ellie Knight[2] and Nicole Boudreau[3]

KEYWORDS: Telkwa Formation, Terrace, Skeena River, Hazelton Group, Kitselas, Stikinia, vein deposits, copper deposits

INTRODUCTION

The Usk map area spans the valley of the Skeena River and its tributaries, over a 530 km^2 area north and east of the town of Terrace, British Columbia (Fig. 1, 2). It includes the lower parts of the Zymoetz (= Copper) River and Kleanza Creek, which flow southwest from their remote headwaters in the Howson Range between Terrace and Telkwa. Chimdemash, St. Croix and Legate creeks drain the Mount O'Brien massif east of the Skeena River. Tributaries west of the river are Carpenter, Sand, Hardscrabble, Shannon, and Lowrie creeks. The topographic names suggest episodes in a long history of settlement. Zymoetz is an ancient name describing the spread of translucent pale blue colour where its waters join the turbid, brown Skeena River. Hardscrabble refers to early placer mining work; Ste.-Croix and Legate were prospectors. Mount O'Brien was named for a young Terrace man killed in World War II.

Within the Usk map area, there are sites and communities that date from roughly 5000 BP to the present day (Berthiaume, 1999). The sites at Kitselas canyon range from ancient encampments to the prosperous village of Gitlaxdzawk, which dominated the Skeena's rocky western bank in historic times. Based on trade and taxation of river traffic, it flourished up to about 1860–1880, when disease and depopulation wiped the settlement out. In the late 1800s, steamboat traffic turned the Skeena River into a major corridor to the interior and a new town, also named Kitselas, was built south of the canyon. The construction of the railroad from 1910 to 1914 refocused communities: the new Kitselas was abandoned and small settlements grew up beside the railroad. Usk was one of these. It is now accessed by a reaction ferry from the highway that was built east of the river in the early 1940s. Terrace itself arose as the railroad and highway developed, and grew with the logging industry. Its northeastern suburb of Thornhill extends into the Usk map area (Fig. 2). A new community, Gitaus, sited on a gravel bench east of the Skeena, has been developed by the Kitselas First Nation over the last 15 years.

[1]*Department of Earth Science, Dalhousie University, Halifax, NS*

[2]*Department of Earth Science, Simon Fraser University, Vancouver, BC*

[3]*Department of Geology, St. Mary's University, Halifax, NS*

This publication is also available, free of charge, as colour digital files in Adobe Acrobat PDF format from the BC Ministry of Energy, Mines and Petroleum Resources internet website at http://www.em.gov.bc.ca/Mining/Geolsurv/Publications/catalog/catfldwk.htm

EXPLORATION HISTORY

The role of mineral exploration in the local economy has waxed and waned through time. The Tshimshian word Kleanza means 'gold', an indication of early placer activity. The opening of the Skeena as a major river route, and the construction of the railway, brought prospectors into the country. Discoveries followed. More than 10 prospects, mainly gold-quartz veins and copper-silver massive sulphide mineralization, eventually saw at least limited production between 1890 and 1942. On a voters list from Kitselas in 1909, 25% of the male population stated their profession as 'miner' (Bennett, 1997, p. 172). In the early 1900s, up to a hundred prospecting parties might be out in a given summer (W. McRae, pers. comm., 2005). Horse trails were built to access workings through tens of miles of arduous mountain valleys and over steep ridges. One such trail joined the headwaters of Chimdemash and Ste.-Croix creeks via 67 switchbacks.

The coming of the Depression and World War II put an end to most of the mining activity. Forest wealth fueled the next economic resurgence. Small mills had been built near the railroad beginning in 1910. During World War I, Sitka spruce from the Skeena River valley was in high demand for airplane construction. Mill development intensified with the opening of the highway during World War II. The Skeena Mill (originally Skeena Forest products) was built in 1960. Between 1950 and 1990, extensive networks of logging roads were constructed into all of the valleys in the area. They offer excellent access to remote locations; however, most of them are presently deactivated and becoming increasingly difficult as routes of travel.

Terrace has a small but active prospecting community. However, compared to well-known mining camps such as Smithers and the Iskut-Stikine region, the area has seen a modest level of modern mineral exploration. In the Usk area, for instance, there are 80 listed mineral occurrences (MINFILE, 2005), but only 25 assessment reports were filed during the period 1980–2004. Most of the work has been done on behalf of individuals and small companies.

In the last three years, there has been a minor resurgence in local mineral exploration. Between 2003 and 2005, Eagle Plains Resources Ltd. has been exploring the bulk tonnage Au and Cu-Mo potential of its large Kalum property north of Terrace (Mihalynuk and Friedman, 2005). The Dardanelle Au-quartz vein mine (MINFILE 103I107) and the Treasure Mountain Cu property (MINFILE 103I090), both of them located immediately south of the Usk map area, were explored and drilled in the summer of 2005. Exploration work continues on a system

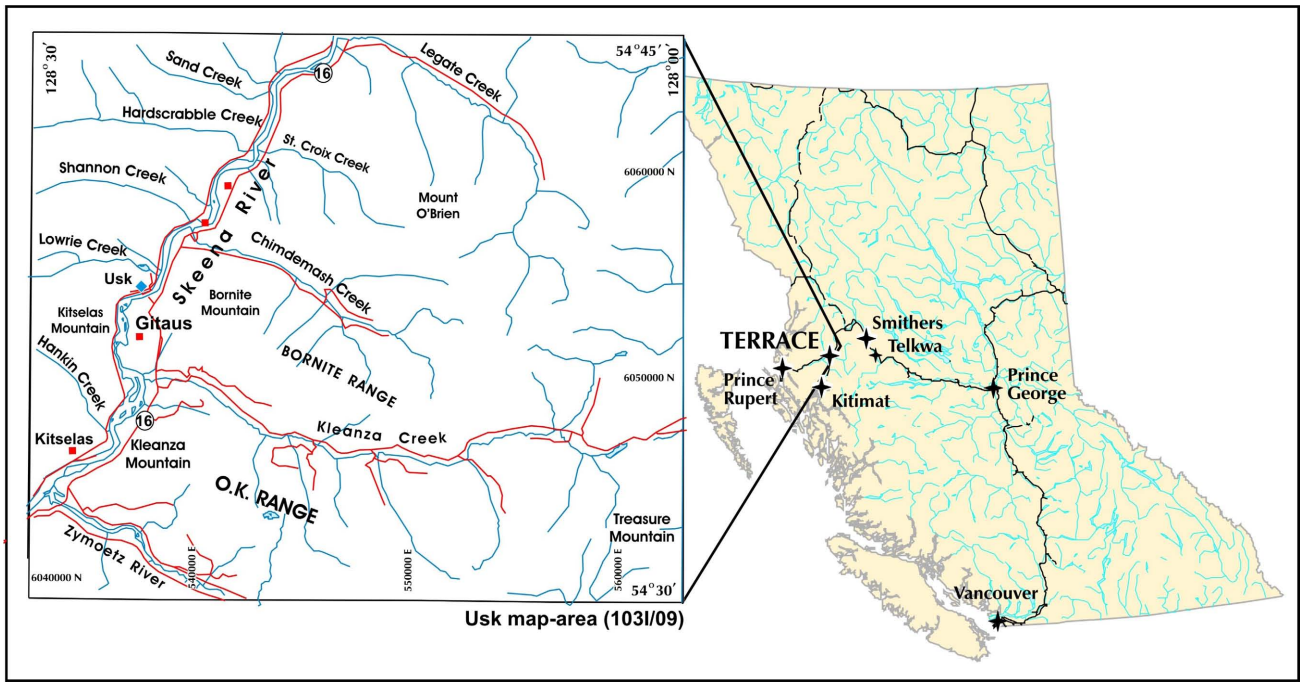


Figure 1. Location and physiography of Terrace, BC, and the Usk map area.

of veins and replacement-style occurrences, the Zona May (MINFILE 103I060) and M&K (MINFILE 103I065) in the upper Legate Creek drainage and Silver Basin in the upper Chimdemash drainage (MINFILE 103I065), by Argonaut Resources (Salat, 2005).

THIS PROJECT

Coastal and northwestern BC are relatively poorly covered by 1:50 000-scale regional geological mapping. At present, roughly 18% of the province has been mapped at 1:50 000 scale. Within NTS 103I, the large-scale sheet that includes Terrace, no 1:50 000-scale mapping is available, except for focused thesis work (Mihalynuk, 1987; Heah, 1991). The Terrace regional mapping project was initiated in 2005, in recognition of this knowledge gap and its potential effect on exploration interest in the area. Results for the Usk map area (NTS 103I/09) will be released as an open file map (Nelson *et al.*, 2006).

In connection with the present study, part of a Ph.D. thesis by Tony Barresi of Dalhousie University will address the volcanic stratigraphy and geochemistry of the Telkwa Formation (Barresi and Nelson, 2006), while an Honours B.Sc. thesis by Nicole Boudreau of St. Mary's University will examine the relationship between the Kitselas volcanic unit and the Hazelton Group.

This project was a cooperative effort between the BC Geological Survey Branch and the Resource Management Department of the Kitselas First Nation (KFN). In the summer of 2005, one BCGS geologist, three geology students and three KFN resource technicians surveyed the Usk map area, using trucks, bicycles and helicopter-supported fly camps. A total of 560 km^2 was mapped, including 160 linear kilometres of roads.

REGIONAL GEOLOGY

Terrace lies within the western extent of Stikinia, one of the intermontane terranes, a large crustal block dominated by the products of episodic Paleozoic through mid-



Figure 2. Looking north along the Skeena River from Thornhill, BC, with Kitselas Mountain on the western skyline and Bornite Mountain and Mount O'Brien on the east.

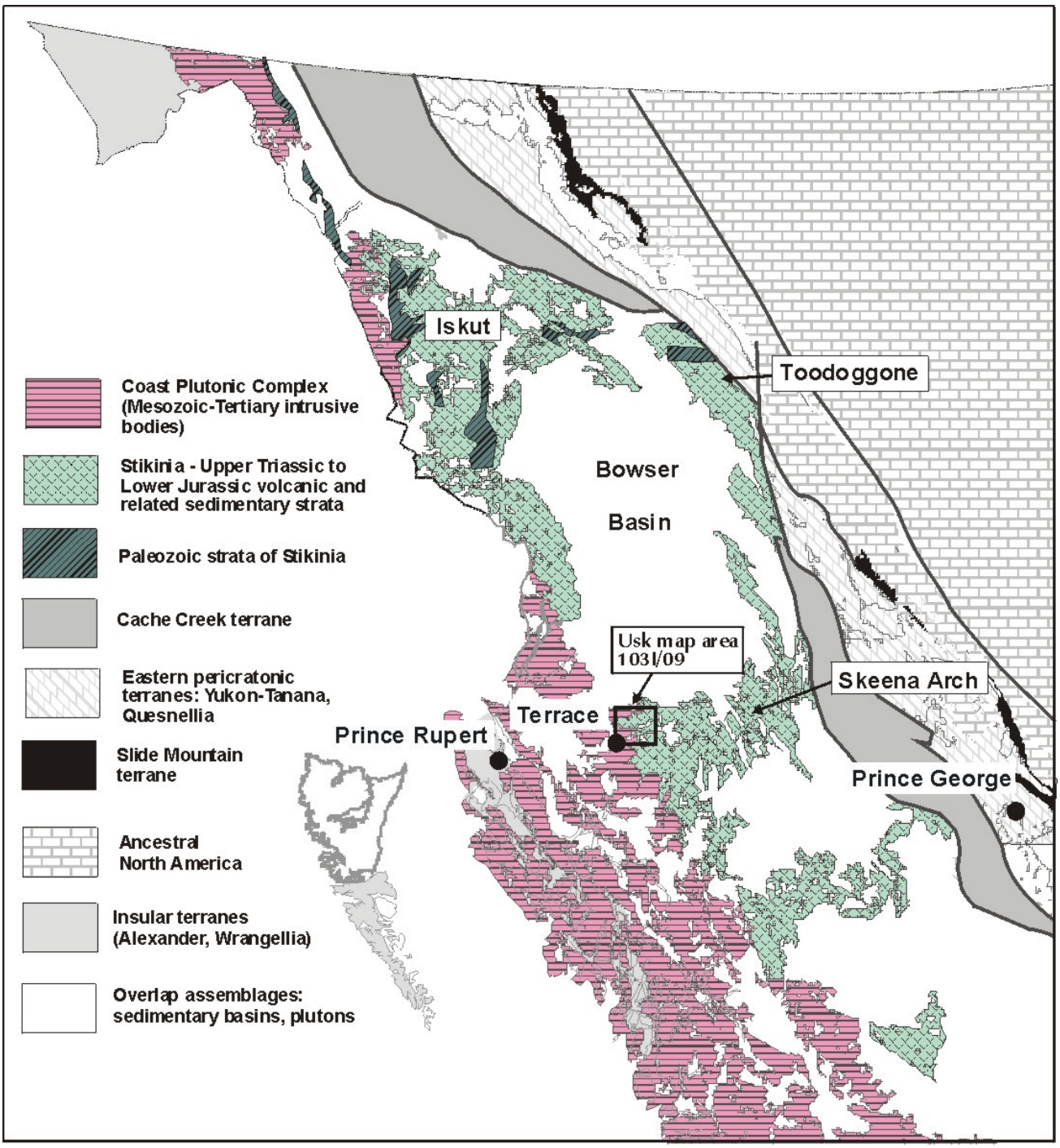


Figure 3. Tectonic setting of Terrace, BC in western Stikinia, on the eastern border of the Coast Plutonic Complex.

Jurassic island-arc magmatic activity (Fig. 3; Monger *et al.*, 1991).

Terrace also lies on the eastern fringe of the Coast Plutonic Complex, a linear belt dominated by granitoid and metamorphic rocks that occupies most of coastal BC. The Coast Plutonic Complex is the deeply eroded and tectonically denuded roots of the mid-Jurassic to Eocene successor arc, which developed along the new western margin of North America following accretion of the intermontane and insular terranes to the continent (van der Heyden, 1992).

Previous 1:250 000-scale mapping (Duffell and Souther, 1964; Woodsworth *et al.*, 1985) shows the general geological features of the Terrace area, which are refined by mapping of the present project (Fig. 4; see Nelson *et al.* [2006] for greater detail).

The oldest recognized stratigraphic unit is a section of upper Paleozoic volcanogenic rocks and limestone, corre-

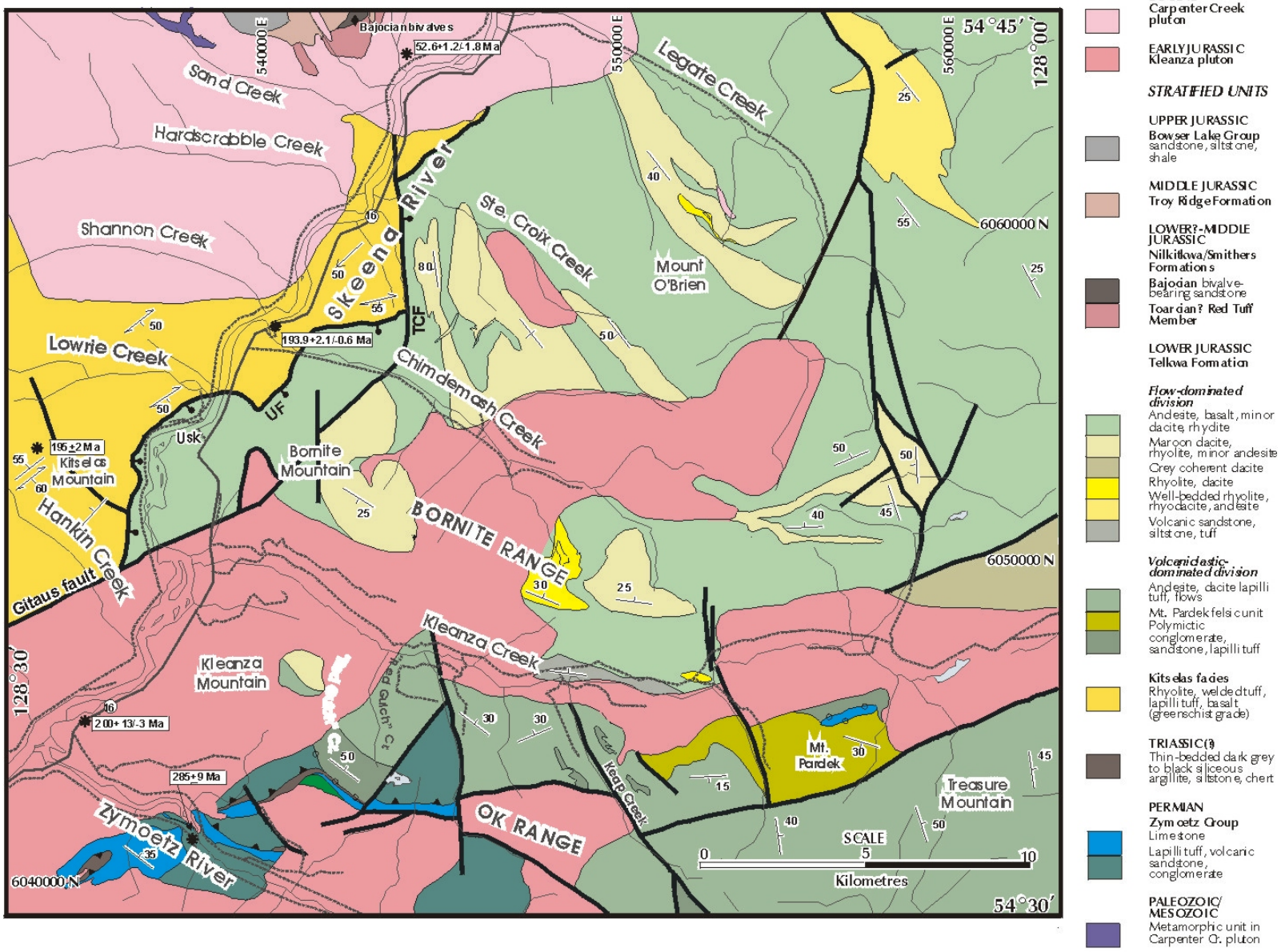


Figure 4. Geology of the Usk map area (NTS 103I/09), near Terrace, BC.

lative with younger strata in the Stikine 'assemblage' in the Iskut-Stikine area (Brown *et al.*, 1996; Logan *et al.*, 2000). It is overlain by Triassic sedimentary strata, which are in turn overlain by the primarily intermediate to felsic volcanogenic rocks that belong to a lower portion of the Hazelton Group, equivalent to the Telkwa Formation in the Smithers area (Tipper and Richards, 1976). North of the Usk map area, Telkwa strata are overlain by the Nilkitkwa, Smithers and Ashman formations and the Bowser Lake Group (Woodsworth *et al.*, 1985, and G. Woodsworth, unpublished mapping, 2006). Small exposures of these rocks occur within the Usk map area near Sand Creek.

Voluminous plutonic rocks occupy much of the drainages of the Zymoetz River and Kleanza Creek. Woodsworth *et al.* (1985) assigned them a Jurassic and/or Cretaceous age. Presently, published and unpublished zircon ages suggest that they are entirely Early Jurassic (*ca.* 200 Ma; Gareau *et al.*, 1997a; G. Woodsworth, pers. comm., 2005). The main body, termed the Kleanza pluton by Gareau *et al.* (1997b), is probably comagmatic with the Telkwa Formation. These rocks contrast with plutons in drainages to the west of the Skeena River, which are Eocene and belong to the Coast Plutonic Complex (Gareau *et al.*, 1997a, b).

A distinctive, mainly felsic volcanic unit underlies the Skeena valley between Gitaus and St. Croix Creek, and extends into the mountains west of the river. It has been named the Kitselas volcanic rocks, from a type locality on Kitselas Mountain (Gareau *et al.*, 1997b). Locally strong foliation and development of greenschist-facies mineral assemblages in this unit led to early interpretations of a Paleozoic age (Duffell and Souther, 1964). Gareau *et al.* (1997a) reported U-Pb zircon ages of *ca.* 194 and 195 Ma from this unit, coeval with the Telkwa Formation regionally (Marsden and Thorkelsen, 1992), and coeval with or slightly younger than the age of the Kleanza pluton locally. G. Woodsworth (unpublished data, 2006; pers. comm; see also Gareau *et al.*, 1997b) proposed that the comparatively high metamorphic grade and structural relationships of the Kitselas volcanic unit to the Telkwa Formation are suggestive of a detachment fault relationship. In this model, the Kitselas volcanic unit would lie in the footwall of an easterly-dipping detachment fault, with the zeolite-grade Telkwa Formation in its hangingwall.

A large, relatively undeformed bulbous pluton of Eocene age (53 Ma; Gareau *et al.*, 1997a) intrudes both the Kitselas volcanic unit and the Telkwa Formation in the northwestern part of the map sheet. Thus, motion on a fault between them must have ceased before this time. On the other hand, a 56 Ma pluton contains fabrics analogous to those in the Kitselas volcanic unit; Gareau *et al.* (1997a, b) considered it to be involved in the detachment-related deformation. Given these constraints, detachment faulting must have taken place in mid-Eocene time, coeval with other recognized crustal shear zones such as the Shames River shear zone west of Terrace (Heah, 1991).

LOCAL GEOLOGY

Detailed mapping of the Usk map area in 2005 (Fig. 4) focused on aspects of the regional geology that remain problematic, particularly those relating to mineral exploration models. The following questions formed the framework for investigation:

- What are the structural and stratigraphic relationships of the Triassic and Jurassic rocks to the underlying Paleozoic section? On one hand, the basal Telkwa Formation has been interpreted locally as Triassic to Jurassic in age (Gareau *et al.*, 1997b); regionally, on the other hand, it is restricted to the Early Jurassic (Tipper and Richards, 1976; Marsden and Thorkelsen, 1992).
- What was the nature and paleogeography of Telkwa volcanism? Prior to this study, the Telkwa Formation remained undivided in the Terrace area, except for one east-west transect south of the Usk map area (Mihalynuk, 1987).
- What are the nature and morphology of the Early Jurassic Kleanza pluton, and what is its relationship to the Telkwa Formation, which it intrudes?
- What are the volcanology and geochemistry the Kitselas volcanic unit, and what was its primary relationship to the Telkwa Formation?
- What is the nature of the structural boundary between the Kitselas volcanic unit and the Telkwa Formation?

Stratified Units

ZYMOETZ GROUP (NEW NAME)

A section of Permian volcanogenic and marine sedimentary strata, including thick limestone, outcrops within and south of the lower Zymoetz River valley (see Duffell and Souther, 1964; Woodsworth *et al.*, 1985). The authors propose that this isolated exposure, located 250 km south of the upper Paleozoic belt of northern Stikinia, be (informally) named the Zymoetz group.

Within the Usk map area, the Zymoetz group outcrops on Copper and Thornhill Mountains, and on the southern slopes of the OK Range (Fig. 4). It is divided into two units, limestone (uPls) and a mixed volcanogenic unit (Pvs) that includes pyroclastic and volcanic-derived sedimentary strata. The volcanogenic unit is highly variable; it includes coarse to fine lapilli and crystal-ash tuffs, well-bedded volcanic sandstone and polymictic volcanic conglomerate. Lapilli tuff ranges from mono to polymictic, and fragments range in size from dominantly sand to dominantly boulders. Clasts are mainly andesitic in composition, with subordinate quartz-phyric dacite and scattered limestone fragments. Plagioclase phenocrysts are ubiquitous; clinopyroxene is common in the andesite. Along the Zymoetz River, unstratified, dark green crystal-ash tuff predominates.

Conglomerate includes clasts derived from the lapilli tuff, as well as limestone and red to white, highly siliceous rocks that may be either rhyolite or chert, neither of which was observed *in situ*. They grade both into lapilli tuff and into volcanic sandstone. Green volcanic sandstone is well bedded and better sorted than the tuff. It interfingers with the limestone. Limy matrix is common, and aids in distinguishing it from Telkwa volcaniclastic units. Macrofossils occur on bedding planes in black shale, and isolated within volcanic sandstone beds.

Limestone in the Zymoetz group shows a strong variability in character. On top of Copper Mountain, outcrops are of pure, white to light grey crystalline marble with local

thin colour banding. This unit appears to be nonfossiliferous. On the northern slopes of Copper Mountain and along the road north of the Zymoetz River, thick-bedded grey limestone is interbedded with green volcanic sandstone that grades into crystal-lithic tuff. In both cases, the volcanogenic unit depositionally overlies the limestone. This limestone contains a wealth of macrofossils, including rugose corals, bryozoans and crinoids. Limestone in an isolated exposure southwest of Kleanza Lake is interbedded with laminated, siliceous green tuff and felsic conglomerate. Overall, the intimate relationships of limestone and volcanogenic strata are suggestive of a series of limy banks and small redeposited reefs that developed on an active arc edifice.

The Zymoetz group is dated both by macrofossils and by U-Pb zircon methods. Duffell and Souther (1964) reported extensive coral and brachiopod collections of Permian age, and Gareau *et al.* (1997a) obtained an Early Permian U-Pb age of *ca.* 285 Ma from lapilli tuff on the O.K. Range. These rocks correlate with Permian units in the Iskut-Stikine area (Brown *et al.*, 1996; Logan *et al.*, 2000). The limestone is age equivalent to the Ambition Formation of Gunning *et al.* (1994). One difference is that Zymoetz group limestone interfingers extensively with volcanic-derived clastic deposits, whereas the Ambition Formation contains almost no volcanic material and is interpreted to postdate arc volcanism.

TRIASSIC (?) SEDIMENTARY STRATA

Near the crest of the western O.K. Range, a distinctive unit intervenes between the highest exposure of Permian limestone and the Telkwa basal conglomerate. It consists of less than a hundred metres of thin-bedded, black and grey-laminated radiolarian chert. Bedding in it is roughly conformable with its external contacts, which are covered. This unit is considered to be of Triassic age (Duffell and Souther, 1964; G. Woodsworth, unpublished map, 2006). It resembles Middle Triassic chert in the Iskut-Stikine area (Logan *et al.*, 2000), as well as the Triassic Teh Formation on the BC-Yukon border (Roots *et al.*, in press). Radiolarians collected in this project will be evaluated paleontologically.

A band of thin-bedded black chert occurs in logging cut exposures farther downslope in the Zymoetz River valley, between two panels of Zymoetz group strata (Fig. 4). Bedding attitudes in it are highly variable and generally not parallel to its external contacts. The western contact is interpreted as a thrust fault that repeats Permian and Triassic strata. Similarly, coal black argillite and chert between Copper and Thornhill mountains, which lies structurally below white Permian marble, is interpreted as another Triassic unit in the footwall of a thrust fault.

TELKWA FORMATION (LOWER JURASSIC)

Overview

The Telkwa Formation of the Hazelton Group is the most widespread stratigraphic unit in the Usk map area (Fig. 4). It consists wholly of volcanic and volcanic-derived strata: mostly andesite and dacite but with some basalt and local rhyolitic centres. Stratigraphic relationships in it are complex, due to the irregularity of topography in volcanic environments, abrupt changes in volcanic facies, synvolcanic faulting and the localization of felsic accumulations.

At its base in the western O.K. Range, a polymictic conglomerate unconformably overlies thrust-imbricated Triassic and Paleozoic strata (Fig. 4). The conglomerate interfingers upward with a thick unit of andesitic and lesser dacitic volcaniclastic deposits and minor flows. This unit is divided into the informally named O.K. Range – Treasure Mountain and Kleanza Creek sections by an east-striking fault. The Kleanza Creek section underlies part of the southern slope of the Kleanza Creek valley, overlying (and interfingering with?) a local accumulation of felsic volcaniclastic rocks on Mount Pardek. Andesitic volcaniclastic and sedimentary strata north of Kleanza Creek are overlain by an extensive, flow-dominated unit, the Mount O'Brien section, which comprises andesite, dacite, rhyolite and basalt in decreasing order of abundance. Andesite constitutes about 70% of the unit, dacite 25% and rhyolite 5%. Three distinct rhyolitic centres have been identified in this section.

Conglomerate

Polymictic conglomerate is most abundant at the base of the Telkwa Formation, although lenses of it also occur



Figure 5. a) Polymictic conglomerate near the base of the Telkwa Formation in the western OK Range, containing pink and green siliceous volcanic rocks, chert, limestone, plagioclase and pyroxene-phyric andesite and dacite. b) Detail of pink, crinoidal limestone clast in conglomerate.

stratigraphically higher, interbedded with andesitic lapilli tuff and volcanic sedimentary intervals. It contains both intraformational (andesite, dacite and rhyolite) and extraformational (limestone, black chert, andesite, dacite and rhyolite) clasts (Fig. 5a).

Because both the Zymoetz group and Telkwa Formation are the remnants of mainly intermediate to felsic island arc edifices, distinction between clasts sourced from them must rely on subtle differences of composition and texture. For instance, clinopyroxene and quartz phenocrysts are much more abundant in the Permian volcaniclastic units, whereas well-formed, lath-shaped plagioclase predominates in the basal Telkwa.

Local clast composition of the conglomerate varies considerably. In some areas, limestone clasts are abundant; in others they constitute less than 1% of the population. Fossiliferous clasts contain corals, brachiopods and bryozoans, clearly reflecting their Permian source (Fig. 5b). Near the black Triassic chert band, the base of the conglomerate contains concentrations of black chert clasts.

The basal conglomerate is very coarse and thick bedded. Conglomerate higher in the section is finer grained, and interbedded with sandstone, siltstone and Telkwa lapilli tuff. Rare clasts of limestone in lapilli tuff on the west slope of Treasure Mountain, far upsection from the basal conglomerate, hint at continued (fault-related?) exposure of pre-Jurassic rocks during eruption and deposition of the Telkwa Formation.

O.K. Range – Treasure Mountain Section

From the middle of the O.K. Range east to Treasure Mountain and beyond, a section dominated by maroon and green andesitic volcaniclastic strata dips homoclinally to the east. In addition to andesite lapilli tuff, it comprises about 15% andesite flows, 5% thin intervals of fine-grained volcanic-derived sedimentary beds and 5% dacite lapilli and crystal-ash tuffs. Its basal contact with the conglomerate unit is an interpreted fault; however, rocks in this section are identical to those in the Kleanza Creek section, which demonstrably overlie and interfinger with the conglomerate. The two sections are separated by an east-striking, north-side-down normal fault (Fig. 4).

Andesitic lapilli tuff in the O.K. Range – Treasure Mountain section is thick bedded, ranging from coarse to fine clast dominated, and monomictic to polymictic. Overall, the clasts are mostly plagioclase phyric, with minor local hornblende and clinopyroxene (Fig. 6a).

Textural variations from unit to unit involve percentage and size of phenocrysts, which are typically lath shaped, euhedral and 2–5 mm long. Some tuff units contain crowded porphyritic and fine grained, holocrystalline clasts that tend to be strongly epidotized (Fig. 6b). The authors interpret these as hypabyssal clasts altered in place, prior to incorporation in an explosive eruptive unit. Similar alteration patches were observed in the Kleanza pluton in the Bornite Range.

Andesite flows are coherent, tabular to lensoid units 20–200 m thick, that in places grade through brecciated into lapilli tuff. Volcanic textures are identical to those in the tuff. These flows are only locally amygdaloidal, in contrast to flows in the Mount O'Brien section.

Thin units of bedded volcanic sandstone, siltstone and mudstone represent quiescent intervals. Subaqueous deposition is indicated by graded bedding and mudstone rip-up clasts.

Dacitic units are maroon, brick red, light grey, lavender and pink. They comprise lapilli and crystal-ash tuffs and minor coherent dacite. Clasts and coherent portions are very siliceous and aphanitic to glassy, and may contain sparse, very small (<1 mm) feldspar phenocrysts. West of Treasure Mountain, three thin dacitic units occur in association with thin-bedded volcanic sedimentary strata. One of them exhibits a polymictic base, involving andesite clasts from underlying units, and a monomictic top. Degree of welding increases upward within the unit.

Kleanza Creek Section and Mount Pardek

This section extends along the southern slopes of the Kleanza Creek valley, from Kleanza Mountain to Mount Pardek; its sedimentary upper part is exposed near the main logging road north of Kleanza Creek (Fig. 4). In the west, its base consists primarily of andesitic lapilli tuff that transitionally overlies and interfingers with polymictic conglomerate. To the east, the basal unit is the felsic tuff sequence exposed on Mount Pardek, which overlies Permian



Figure 6. a) Coarse-grained Telkwa Formation lapilli tuff from near Treasure Mountain, showing plagioclase-hornblende-phyric clasts with well-formed phenocrysts. b) Epidote-altered clasts in lapilli tuff.

limestone and conglomerate. This, in turn, is overlain by andesitic lapilli tuff and derived sedimentary layers. The authors interpret the Mount Pardek sequence as the products of a nearby felsic centre.

The Mount Pardek sequence consists of thin, quartz-feldspar-phyric flows, water-laid tuff units and resedimented volcaniclastic deposits (Fig. 7).

Although dominantly felsic, it also contains andesitic volcaniclastic layers. Felsic units are typically light pastel green. Unlike other felsic units in the Telkwa Formation, they contain up to 60% clear, euhedral quartz crystals. Evidence of subaqueous deposition includes grading and crude sorting in well-bedded units. They are probably of turbiditic origin. Overall, the sequence is up to 1200 m thick. The dominantly felsic unit grades upward into andesitic lapilli tuff, sandstone and siltstone that are identical to those of the O.K. Range – Treasure Mountain section.



Figure 7. Thick-bedded felsic lapilli tuff, Mount Pardek, looking north across Kleanza Creek to the main logging road.

West of Kipulta Creek, a lower felsic sequence consists of thin-bedded, colour-banded rhyolite tuff and waxy, translucent rhyolite. Lapilli tuff ranges from monomictic to polymictic, with green to pink rhyolite and also quartz-vein clasts. This sequence, like that on Mount Pardek, is overlain by volcaniclastic beds of intermediate composition, including lapilli tuff and maroon, well-bedded sandstone and siltstone.

Between Keap Creek and 'Red Gulch' Creek, andesite lapilli tuff with thin intervals of volcanic sandstone and siltstone overlies and interfingers with the basal Telkwa conglomerate. Polymictic conglomerate with limestone clasts occurs high in the section, particularly on the slopes west of Keap Creek. The conglomerate thickens southward, consistent with a topographic high south of the main Telkwa accumulation.

The northeast-facing sedimentary sequence north of Kleanza Creek is separated from the coarser lapilli tuff by an apophysis of the Kleanza pluton, although it is identical in lithology and bedding attitude to the volcanic-derived sedimentary intervals farther south. It is overlain by andesite flows and coarse lapilli tuff of the Mount O'Brien section along a transitional contact.

Mount O'Brien Section

This widespread unit extends from Kleanza Creek through the eastern and northern boundaries of the map area, including Bornite Mountain, Mount O'Brien and the ridges northeast of Legate Creek (Fig. 8a).

It is dominated by andesite and dacite flow/lapilli tuff eruptive units that alternate on scales of tens to hundreds of metres. The larger dacite bodies are shown on Figure 4. Rhyolite is also present in three separate centres, and aphyric basalt accompanies the andesite in places. In the western part of the section, beds are very thick and alternation between andesite/basalt, dacite and rhyolite occurs over hundreds of metres. East of Legate Creek and in the Treasure Creek area, the section is well bedded, individual flow units are thinner, and alternation between andesite and lesser dacite occurs at a scale too small to depict in regional mapping. These rocks are grouped with the andesite.

Andesite in this section is texturally (and compositionally?) different from that in the volcaniclastic-dominated sections to the south. Plagioclase is tabular rather than lath-shaped, and less euhedral. Synneusis (clumping of individual crystals due to weak attraction on flat faces) gives them a raggedly terminated appearance. Average plagioclase size varies from unit to unit, ranging from a few millimetres to, locally over a centimetre in length. Subsidiary clinopyroxene occurs in some of the flows. Mount O'Brien andesite flows tend to be amygdaloidal, from abundant tiny pinpricks to irregular, zeolite±quartz±epidote±chlorite±pumpellyite-filled cavities many centimetres across (Fig. 8b).

Dacite units are composite, consisting of coherent flows and flow breccias, lapilli tuff, welded to nonwelded tuff with lithic and pumice fragments, and less common crystal tuff (Fig. 8c). Texturally, they resemble the much less extensive dacite south of Kleanza Creek. Colours range from maroon to brick red to pastel shades of lavender, pink, cream and orange. All of these rocks are markedly more siliceous than the andesite. They are aphyric to finely porphyritic, with a small percentage of tiny, submillimetre plagioclase phenocrysts.

Three significant accumulations of rhyolitic volcanic rock occur within the Mount O'Brien section: they are located in the middle of the Bornite Range southwest of the headwaters of Chimdemash Creek, north of Mount O'Brien, on the northernmost ridge and cirques between St. Croix and Legate Creeks; and in the northeastern portion of the map area northwest of the headwaters of Legate Creek. These units are typically closely associated with minor amounts of dacite, basalt and andesite, but have been mapped at 1:50 000 scale wholly as rhyolite. Pyroclastic rocks within these units include nonwelded to strongly welded lapilli tuff with lithic and pumice fragments; coherent rhyolite (Fig. 8b,c) occurring as thin flows, minor domes and cryptodomes that commonly grade into flow breccia; beds of resedimented felsic debris ranging from conglomerate to sandstone; and local thin-bedded, aphani-

tic, highly siliceous units, which may represent felsic ash tuff or exhalitive chert.

Individual beds range in thickness from less than 1 m to more than 30 m and are normally laterally continuous with little change in volcanic or sedimentary facies. Coherent rhyolite and rhyolite fragments in volcaniclastic deposits are typically highly siliceous, flow banded, aphanitic, semitranslucent and white, pink, orange, lavender or brick red in colour. In these three locations, the high concentration of rhyolitic rocks, especially coherent rhyolite, leads to the interpretation that each location is proximal to a localized centre of felsic volcanism. These units lack the light green pastel colour, abundance of quartz phenocrysts and turbiditic sedimentary structures that characterize the Mount Pardek felsic unit located to the south.

Regional Variations in the Telkwa Formation

A dramatic regional change in the stratigraphy occurs between the O.K. Range – Treasure Mountain and Kleanza Creek sections located in the southern portion of the map area and the Mount O'Brien section in the north. The Mount O'Brien section is dominated by volcanic flows of intermediate composition, and local felsic accumulations that are proximal to eruptive centres; the O.K. Range – Treasure Mountain and Kleanza Creek sections are dominated by volcaniclastic deposits. It is clear that the southern sections represent a more distal volcanic facies than the coherent flows of the northern section (Barresi and Nelson, 2006). The authors propose that the southern sections are a thick accumulation of volcaniclastic material originating from volcanic centres in the Mount O'Brien section. This material was deposited in a subsiding basin south of Kleanza Creek. East-trending faults in the southern sections, particularly the fault separating the O.K. Range – Treasure Mountain section from the Kleanza Creek section, may be original basin-bounding faults. The differences in volcanic facies between the southern and northern sections are not due to a juxtaposition of different positions in a continuous stratigraphic sequence; rather, they represent a geographic change in facies (Barresi and Nelson, 2006).

Kitselas Facies (Lower Jurassic)

The Kitselas facies of the Telkwa Formation is well exposed in a homoclinal, northwest-facing sequence on Kitselas Mountain and the ridge between Shannon and Lowrie creeks. It also outcrops east of the Skeena River between Usk and the ridge north of St. Croix Creek. On Kitselas Mountain, cleavage development is spaced and original textures are very well preserved. The section is predominantly felsic, with >95% dacite or rhyolite along with a minor mafic component of basalt, andesite(?) and diabase. The base of the exposed section, which outcrops on the east side of the Skeena River and at the base of Kitselas Mountain, is primarily coherent rhyolite. The majority of the rocks higher in the section, which form Kitselas Mountain, are thick-bedded volcaniclastic units (Fig. 10a).



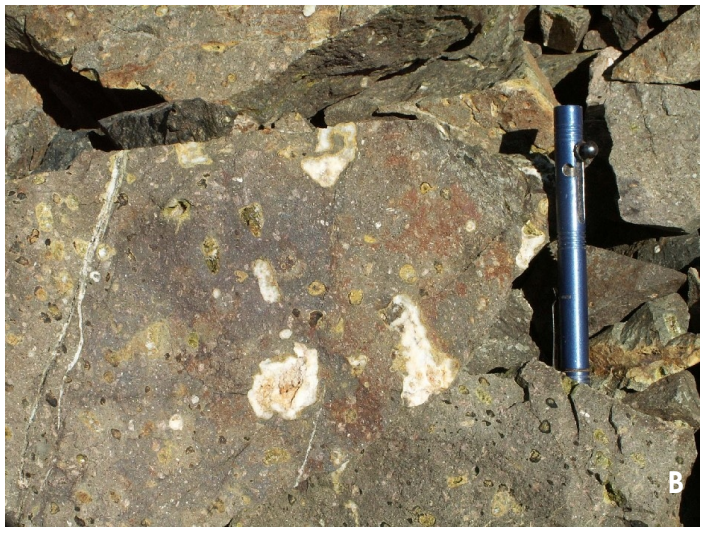




Figure 8. a) South face of Mount O'Brien, showing very thick, maroon andesite flows cut by a gently dipping diorite dike swarm related to the Kleanza pluton. b) Andesite with large, irregular amygdules from the Mount O'Brien section. c) Bright red dacite lapilli tuff with pale siliceous clasts.

The coherent rhyolite is typically medium grey to light purple and aphanitic with rare feldspar microphenocrysts. Flows, which are transitional into flow breccia, have similar characteristics to the larger coherent bodies but are colour and flow banded on a millimetre to centimetre scale. The volcaniclastic portion of the section includes rhyolitic to dacitic lapilli tuffs, welded tuff (Fig. 10b) and rare beds of crystal and/or ash tuffs and resedimented volcanic rocks. Lapilli and welded lapilli tuffs are monolithic, with dominantly sand to pebble-size lapilli. The dominant lapilli compositions are homogeneous aphanitic white, medium purple or grey rhyolite and pumice; minor plagioclase-phyric lapilli and scoriaceous bombs are locally present. Welded tuff exhibits both normal and normal-reverse grading, and the typical aspect ratio of pumice clasts is 1:5. One thin bed of resedimented volcanic rock grades upward from a laminated mudstone base to a conglomerate. Sedimentary structures within this section include flame structures, load casts and crossbeds, which together are suggestive of a subaqueous depositional environment.



Figure 9. Flow-banded rhyolite on the Bornite Range.

Basalt on Kitselas Mountain occurs as three continuous but thin (60–220 m) units. The thickest of these units caps the summit of Kitselas Mountain, and the other two outcrop on its western ridge. They are various shades of blue-grey and are defined by aphanitic, hackly and vesicular to scoriaceous textures. Several zones within the basalt on the Kitselas summit have been thoroughly epidotized, leaving them a brilliant pistachio green colour. These zones are texturally distinguishable from the unaltered basalt, as they have smaller and rarer amygdules and are holocrystalline as opposed to aphanitic. These zones are interpreted to represent proximity to eruptive fissures or centres where hydrothermal alteration would be concentrated. Other mafic rocks within the Kiteselas volcanic unit include minor diabase dikes on the southeast slope of Kitselas Mountain and thin concordant flows or sills exposed on the slopes east of the Skeena River.

Comparison of Kitselas Facies and Felsic Centres Elsewhere in the Telkwa Formation

The Kitselas facies is coeval with the Telkwa Formation (Gareau *et al.*, 1997a); however, its stratigraphic relationship to the Telkwa, locally or regionally, is uncertain. A brief comparison of the physical features of the Kitselas felsic rocks to felsic centres located within the Telkwa Formation in the Usk map sheet is presented here; a more detailed examination, including petrographic and geochemical comparisons is the subject of a B.Sc. thesis currently in progress by Nicole Boudreau.

The Kitselas volcanic rocks are dominantly rhyolitic in composition and consist of a thick section of coherent rhyolite at the base of the exposed section, overlain by an equally thick section of volcaniclastic rocks exposed on Kitselas Mountain. There is no analogue within the Usk map sheet for the thick coherent rhyolite body at the base of the section. However, the exposures of Telkwa felsic centres may be on the flanks of larger, unexposed rhyolite bodies, as is suggested by the thick accumulations of volcaniclastic material in these locations. The upper volcaniclastic section of the Kitselas volcanic rocks is very similar to Telkwa felsic rocks. Both are characterized by similar facies, textures and rock types, and are bedded on a similar scale. The most obvious differences between these rocks are that the Telkwa felsic rocks occur in a wide variety of colours and often have multiple rock types within individual tuff beds, whereas the Kitselas rocks are uniformly white to grey (or rarely purple) and are normally (apparently) monolithic.

Nevertheless, because the Kitselas rocks exhibit higher degrees of metamorphism and alteration, these features found in the Telkwa felsic rocks may simply be obscured in the Kitselas. Although there is no exact analogue for the Kitselas volcanic rocks within the Telkwa in the Usk map area, the physical features of the Kitselas volcanic rocks are consistent with those of the Telkwa.

NILKITKWA AND SMITHERS FORMATIONS

Along logging roads north of Sand Creek, inliers within the Carpenter Lake pluton consist of three units: bright maroon, thin-bedded felsic tuff and basalt; thin-bedded, siliceous and tuffaceous siltstone; and brown sandstone with large bivalve fossils. These units resemble, respectively, the 'Red Tuff' member of the Nilkitkwa Formation (Tipper and Richards, 1976); the so-called 'pyjama beds', correlative with the mid-Jurassic (Toarcian and Bajocian) Troy Ridge and Yuen formations (Tipper and Richards, 1976; Anderson, 1989); and the Smithers Formation (Tipper and Richards, 1976) and Toarcian to Bajocian sandstone intervals within the Eskay belt (Alldrick *et al.*, 2005).

The maroon felsic tuff-basalt unit is distinguished from Telkwa volcanic facies because of the uniformly thin-bedded, fine-grained character of the tuff, interbedded with thin, aphyric, amygdaloidal basalt flows. Accretionary lapilli were noted at one outcrop. The siliceous siltstone unit displays the dark and light colour banding typical of the 'pyjama beds', a lithotype also recognized within the Eskay belt (Alldrick *et al.*, 2005). The brown sandstone, with its lack of obvious chert detritus and abundance of large bivalves, more closely resembles mid-Jurassic clastic

units than it does the Bowser Lake Group. A collection of the bivalves was submitted to T. Poulton of the Geological Survey of Canada for identification. His report (Table 1) indicates a probable early Bajocian age, equivalent to the older part of the Smithers Formation.

In the area north of Sand Creek, G. Woodsworth *et al.* (unpublished mapping, 2006) showed Bowser Lake Group strata overlying the Nilkitkwa and Smithers units described above. These exposures were not visited in 2005.

METAMORPHIC UNIT IN SAND CREEK HEADWATERS

An enclave of metamorphic rocks lies within the Carpenter Lake pluton in the northeastern corner of the map area. They consist of brown, black and grey, variably pyritic hornfels with local limy pods. Microscopically, they contain grains of plagioclase, quartz and minor K-feldspar, along with metamorphic biotite, actinolite and diopside. Their protolith was probably thin-bedded tuffaceous wacke and dirty pelite. A strong, pre-contact metamorphic foliation is present. In character, the unit resembles impure clastic rocks of the Smithers Formation or Paleozoic volcaniclastic rocks of the Zymoetz group, but the exposure was too small to provide definitive information.

Intrusive Units

KLEANZA PLUTON (EARLY JURASSIC)

The Kleanza pluton is a large, sprawling, heterogeneous body with apophyses along the Zymoetz River, Kleanza Creek and southeast of Mount O'Brien (Fig. 4). It has been dated as Early Jurassic (*ca.* 200 Ma U-Pb date on zircon; Gareau *et al.*, 1997a). As is typical of intermontane plutons of this age (*cf.* Woodsworth *et al.*, 1991), it varies texturally from fine grained to porphyritic to coarse grained equigranular, and compositionally from gabbro to granite. Its marginal phases tend to be more mafic than those in its interior, and more variable. On Copper Mountain, for instance, microdiorite (a fine-grained, salt and pepper rock composed of 60% plagioclase and 40% pyroxene) alternates on a 10 m scale with porphyritic intrusive andesite, gabbro and very coarse grained hornblende pegmatite bodies. Microdiorite is common within the southwestern part of the pluton. Because of its fine-grained nature, it can be difficult to distinguish from similarly textured extrusive units. Key diagnostic features are the absence of phenocrysts, amygdules and fragmental textures.

South of Mount O'Brien, fine-grained border phases of the Kleanza pluton include pink plagioclase-phyric monzonite and green andesite that is texturally identical to nearby flows, except for its lack of amygdules and unstratified character. This part of the pluton is possibly a feeder to Telkwa extrusive units.

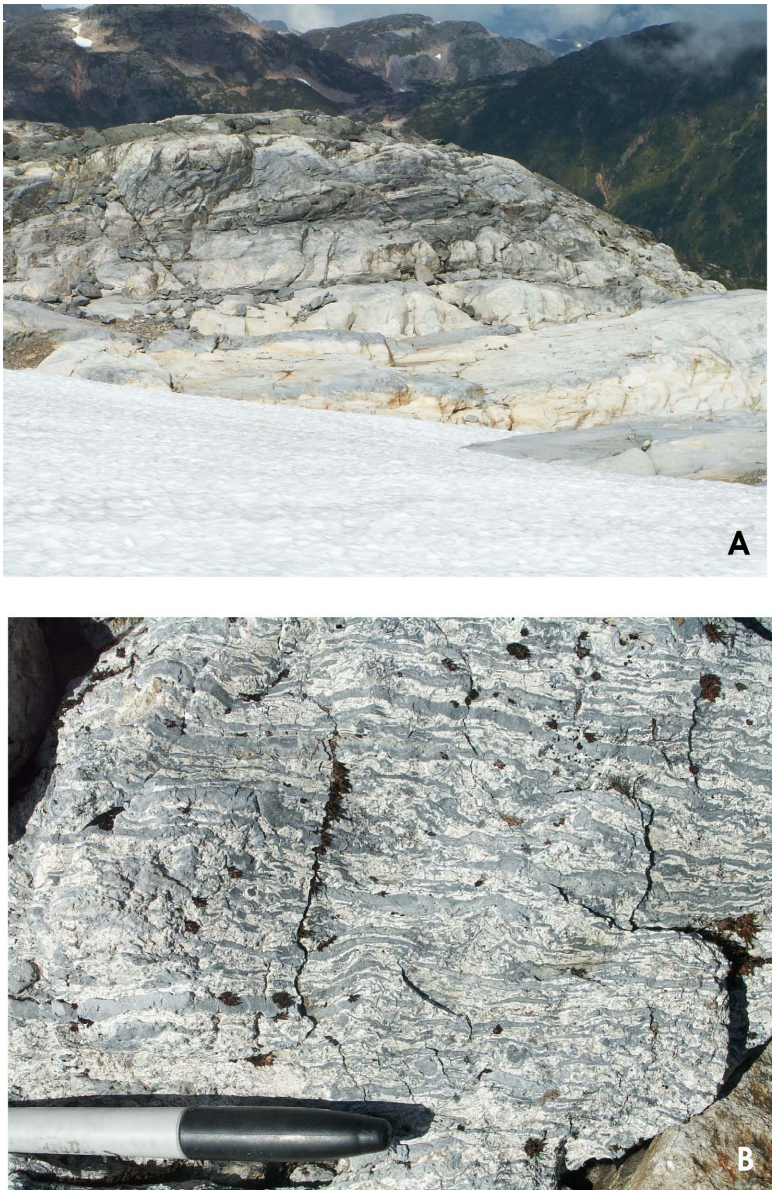


Figure 10. a) Part of the extensive, thick-bedded rhyolite to dacite volcaniclastic unit of the Kitselas member; looking west from near Kitselas Mountain. b) Welded tuff, Kitselas member.

Much of the interior of the Kleanza pluton consists of coarse-grained, equigranular hornblende-biotite granodiorite, with lesser diorite and granite.

The Kleanza pluton intrudes strata of the Zymoetz group, as well as the Telkwa Formation. Contacts both parallel and crosscut the stratigraphy. In the valley of Kleanza Creek, the pluton occurs at low elevations, flanked by Telkwa Formation on adjacent high ridges (Fig. 4; see also Barresi and Nelson, 2006). This configuration suggests a roof contact. Contacts in the Chimdemash Creek valley are steeper and more crosscutting. Overall, the pluton seems to have formed as a branching and possibly stacked set of laccolithic arms that delaminated and domed the stratigraphic section. It was probably emplaced at shallow depths. Contact metamorphism around its margins is only well developed in the Zymoetz group on Copper Mountain, where diopside-garnet assemblages occur in limestone. Farther

TABLE 1. REPORT ON MACROFOSSILS FROM SANDSTONE NEAR SAND CREEK.

Report No. J6-2005-TPP

Report on one collection of Jurassic bivalves collected by JoAnne Nelson, BC Geological Survey, in Terrace area, BC (NTS 103I/09), 2005

GSC Locality C-500768: Field no. 05NB5-6; UTM Zone 9V, 543161E, 6067163N

Identifications:

Plagiostoma sp. cf. *hazeltonense* McLearn
Ctenostreon(?) sp.
Lopha(?) sp.
other bivalves, indeterminate
belemnites, indeterminate
terebratulid brachiopod, indeterminate

Age: Early Bajocian probably

The fossils are very poorly preserved fragments and imprints. This fauna is represented best in British Columbia at Hudson Bay Mountain near Smithers and in central Whitesail Lake map area. It occurs in Early Bajocian beds of the Smithers Formation, together with the ammonite *Sonninia.* Other Middle Toarcian through Bathonian ages for these fossils are remotely possible, but very unlikely in the Terrace area.

T.P. Poulton
October 4, 2005

north, zeolite-facies assemblages persist to within metres of its margins.

CARPENTER LAKE PLUTON (EOCENE)

The Carpenter Lake pluton underlies a large area in the drainages of Carpenter, Sand and Hardscrabble creeks, as well as the lower reaches of Legate Creek. It has been dated as Eocene by a 53 Ma U-Pb date on zircon (Gareau *et al.*, 1997a), which is consistent with other plutons belonging to the Coast Plutonic Complex. It comprises large areas of homogeneous granodiorite, tonalite and granite, as well as areas of abundant dikes of variable compositions and textures. Among these, pink orthoclase-phyric granite, medium-grained granodiorite and diorite, and green andesite are most common. Pink pegmatite and aplite occur in parts of it, notably in the headwaters of Sand Creek.

STRUCTURE

The most important structure in the area is the Usk fault (UF), which abruptly separates footwall felsic rocks of the Kitselas volcanic unit from hangingwall Telkwa Formation andesite intruded by the Kleanza pluton (Fig. 4). It is an undulating surface that dips variably to the southeast, offset by the steep, east-side-down Gitaus and Tumbling Creek faults. The UF corresponds to an abrupt change in bedding attitudes. In its footwall, well-bedded Kitselas units strike uniformly southwest and dip and face northwest, away from the fault. In its hangingwall, Telkwa units strike southeast and dip moderately to steeply southwest, toward the fault. The UF is located within a metamorphic transition zone between greenschist and zeolite facies. Greenschist-facies assemblages are developed both within mafic rocks of the Kitselas volcanic unit and within the lower part of the Telkwa Formation, up to 300 m above the UF. Spaced, southeasterly-dipping zones of strong penetrative cleavage occur throughout the Kitselas volcanic unit. Strongly foliated zones are particularly well developed near its structural top (*e.g.*, in highway outcrops north of Chimdemash Creek). The broader shear zone persists hundreds of metres above the UF, expressed as strongly cleaved intervals and chloritic brittle shears within the Telkwa Formation and the Kleanza pluton.

Overall, the UF appears to be a discrete detachment fault corresponding to an abrupt lithological break, located within a broader zone of shearing and strong fabric development, the Usk shear zone. Attenuation occurred across the entire zone, with displacement focused on the UF. The original relationship of the Kitselas volcanic unit to the Paleozoic to Jurassic rocks in the hangingwall of the UF is still not known.

MINERALIZATION

The Usk map area contains about 80 documented mineral occurrences of several deposit types (Fig. 11; see also Kindle [1937a, b] for detailed descriptions of historic showings). Copper mineralization is common and widespread, and includes quartz vein, quartz-poor sulphide vein (bornite-chalcocite-epidote-specular hematite), shear-hosted, disseminated and replacement styles, in addition to the nearly ubiquitous malachite stains of uncertain origin. Silver is commonly associated with Cu minerals, particularly in veins and shears. Gold favours quartz veins, and occurs either with pyrite alone, as at Columario (MINFILE 103I077), or in polymetallic veins with chalcopyrite, bornite, sphalerite, galena, tetrahedrite and other sulphosalts. Molybdenite occurs within and near the Carpenter Lake pluton.

The origin and associations of the Cu and Au-bearing epigenetic mineralization are unclear, because the evidence is circumstantial. Four possibilities exist, listed in order of implied age of mineralization:

1) Copper-rich shear zone – hosted and replacement occurrences in the Telkwa Formation, notably on the north-south Treasure Mountain trend (Fig. 11) could be related to early fluid migration associated with Hazelton-age volcanic activity.
2) Hydrothermal systems associated with the Kleanza pluton could give rise to a broad spectrum of epigenetic occurrences, such as veins, shear-hosted, disseminated and replacement massive sulphide minerals.
3) The Early Tertiary Usk shear zone and Usk detachment fault could be implicated in the formation of local epigenetic mineralization.
4) Veins could relate to hydrothermal effects of the Eocene Carpenter Lake pluton.

The spatial distribution of Au and Cu-rich occurrences on Figure 11 points most strongly at the Kleanza pluton as a key factor in their formation. Most of the Au-rich veins concentrate in a band that corresponds to the northeast-trending northern lobe of the pluton, which extends from the mouth of the Zymoetz River to the headwaters of Legate Creek. This includes the cluster of veins on Kleanza Mountain, and the Silver Basin (MINFILE 103I067) to Zona May – Frisco area (MINFILE 103I063, 061).

The Kleanza pluton is a heterogeneous multiphase body. Outcrop patterns outline a curviplanar shallow top to both lobes. It was probably intruded as a sprawling, laccolith-shaped body to high crustal levels in zeolite-facies country rocks. The upper levels of the pluton and its volcanic cupola are extensively exposed in the area, constituting a highly favourable environment for mineralization. Major ankeritic alteration occurs in the Silver Basin area,

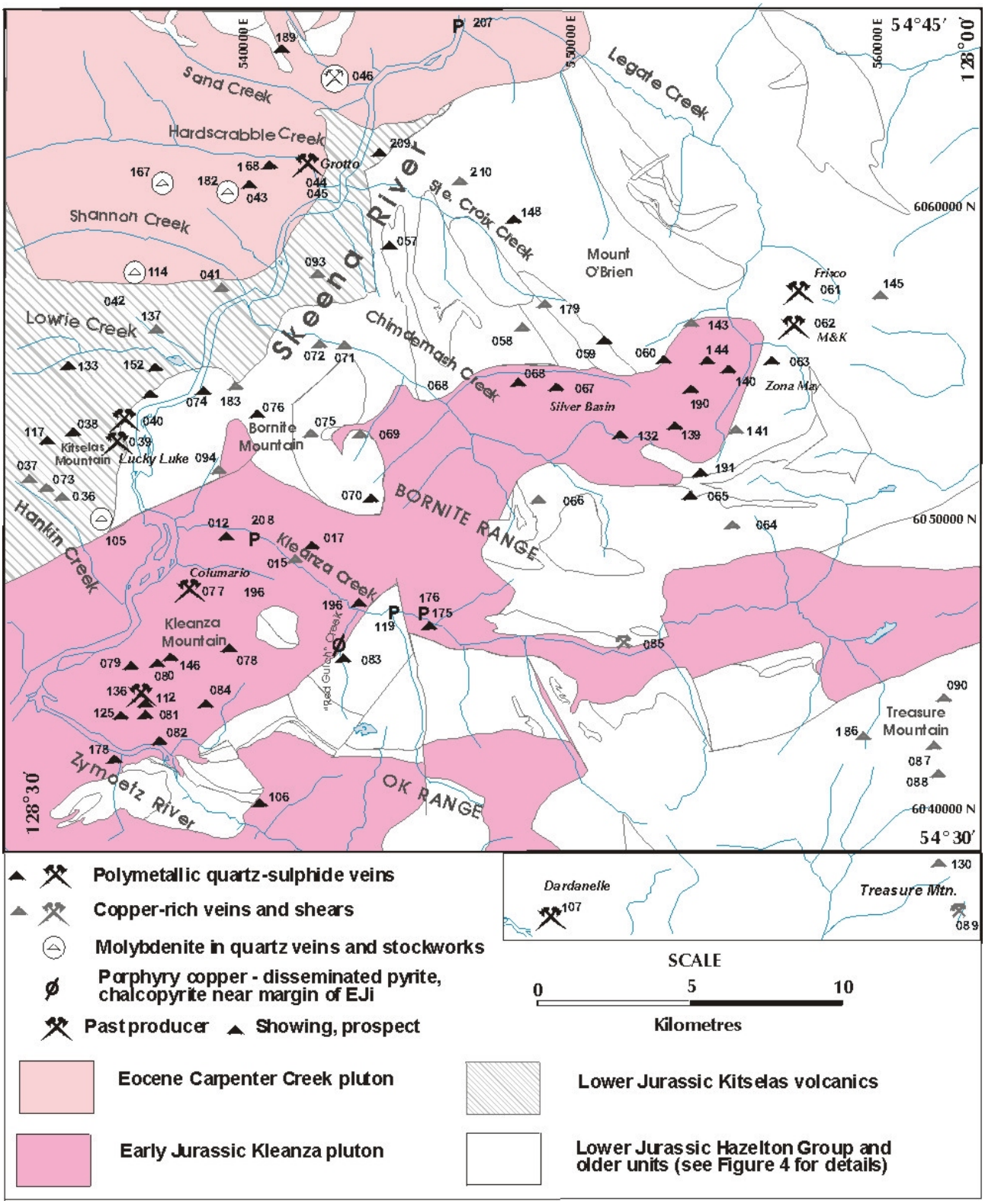


Figure 11. Mineral prospects in the Usk map area.

associated with an unusual porphyritic monzonite phase of the pluton. In 'Red Gulch' Creek and on the lower, western and southern slopes of Bornite Mountain, common occurrences of disseminated chalcopyrite and pyrite near the margins of the pluton may indicate a potential for porphyry-style mineralization.

The only cluster not clearly associated with the Kleanza pluton is that on Kitselas Mountain, including the Lucky Luke (MINFILE 103I039) and Gold Star veins (MINFILE 103I038; Carter, 1970). These crosscut S_1 fabrics in the Kitselas member, which are related to the Usk shear zone; therefore, they are probably of Eocene age and may relate to the detachment faulting event.

HIGHLIGHTS OF 2005 ROCK GEOCHEMICAL SAMPLING PROGRAM

As part of the regional mapping program, more than 70 samples were taken from mineralized zones and areas for geochemical and assay analysis (Table 2). Some correspond exactly or approximately to existing locations in the MINFILE database. Table 3 shows revised locations for selected mineral occurrences, based on the authors' work and that of Raymond Cook of Argonaut Resources.

Sampling carried out by the authors confirmed significant metal values from several known showings. Grab samples from the Columario (JN4-3; MINFILE 103I077) and Lucky Luke (JN2-5; MINFILE 103I039) returned 36.6 and 0.35 g/t Au, respectively. Many samples in the upper Chimdemash Creek area contain significant metal values, notably a vein float sample, TB-26-03, taken west of the Silver Basin (MINFILE 103I065) that contains 0.18 g/t Au. Showings on Treasure Mountain (EK 24 through 26 series; MINFILE 103I090, 086) returned high values of Cu and, in some cases, elevated Ag. The Alvija occurrence (MINFILE 103I089), located immediately north of the Kleanza Creek road, is a broad zone of fracturing and Cu mineralization. A representative sample contained 5.59% Cu and 99 g/t Ag. Quartz veins at the Shan occurrence (TB41-3, 4; MINFILE 103I167) contained up to 0.989% Mo.

Table 2 also shows many anomalies from samples not located near previously documented mineral occurrences. Although most are from thin veins and shear zones, some represent interesting new mineral potential for the area. They include the following:

- The highest Au value obtained from a new showing was 3670 ppb (3.6 g/t) from sample JN13-7, located on the ridge south of Mount O'Brien. It was obtained by digging through talus to a malachite-stained shear zone in rubble-crop. The width and length of this zone are unknown, because it is largely covered.
- Samples EK8-1 and 1a are from an outcrop on the north side of the Hardscabble Creek logging road, where several quartz veins with small, visible sulphide grains occur in a silicified zone associated with aplite dikes. The samples contain elevated values of W, Cu, Pb, Zn, Ag, Bi, Cd and Te (Table 2). The dike and vein system strike roughly east, subparallel to the road; they shortly disappear under cover in both directions. This locality is approximately 1 km west of the Grotto vein in the canyon of Hardscrabble Creek (MINFILE 103I044, 45).
- Samples from within and near the Silver Basin area tend to contain elevated base metal and silver values. These include JN7-3, JN8-2, TB26-3, TB26-6, TB26-13, TN27-5, TB27-8 and TB27-12. Combined with the widespread ankeritic alteration in the area, they indicate a significant metalliferous system.
- Samples of disseminated pyrite and chalcopyrite from near the borders of the Kleanza pluton include EK13-5, EK13-8, EK13-11, EK15-3, and TB4-2.They contain anomalous but sub-ore-grade Cu values, 419–3083 ppm, and negligible Au and Ag.
- Samples EK9-3 and 9-5, from the logging road south of Sand Creek, were of altered, quartz-veined granite of the Carpenter Lake pluton, with minor visible molybdenite. They returned anomalous Mo values of 38 and 164 ppm.

MINERAL POTENTIAL AND MODELS

Mineralization in the Usk area is controlled by the Early Jurassic Kleanza pluton, particularly its northern lobe; the Eocene Carpenter Lake pluton; possibly the Usk shear zone; and, in the case of the Cu(-Ag) occurrences on Treasure Mountain, fluid flow of unknown origin along a north-striking shear zone. The Kleanza system is generally expressed as polymetallic quartz veins and vein swarms with sporadic high values in Au and/or Ag. Replacement-style mineralization is reported in a tuff near its northeastern margin, at the Zona May occurrence (MINFILE 103I061; Salat, 2005; R. Cook, pers. comm., 2005). The widespread Silver Basin veins and alteration zones at the head of Chimdemash Creek provide a target of interest.

The Carpenter Lake pluton contains zones of molybdenite concentration, such as the Shan occurrence and the Sand Creek area.

Although, in general, the Treasure Mountain system is clearly shear related and shear controlled, there is an important zone south of the map area (MINFILE 103I090) from which stratabound zones have been reported (A. Burton, pers. comm., 2005). There, a 12.19 m surface chip sample assayed approximately 3.40% Cu and 18.6 g/t Ag (Sutherland Brown, 1965). Unclassified reserves are 28 120 tonnes grading 1.7% Cu (Sadlier-Brown, 1973). This zone offers the possibility of bulk-tonnage potential.

Exposures of Troy Ridge Formation equivalents in the northwestern corner of the map area hint at the potential for Eskay-equivalent stratigraphy along strike farther to the north.

SUMMARY AND CONCLUSIONS

Geological mapping by the BC Geological Survey in the area northeast of Terrace in 2005 has clarified stratigraphic, intrusive and structural relationships of upper Paleozoic, Triassic and Jurassic rock packages, including subdivision of the Jurassic Hazelton Group and Telkwa Formation.

It is suggested here that the Permian volcanogenic strata and limestone be informally named the Zymoetz group, as the nearest equivalent exposures (the Asitka Group and units in the Stikine 'assemblage') are 250 km distant.

The authors have recognized an unusual, volcanic-free Triassic section of black chert and basinal sedimentary strata. It, along with the underlying Permian rocks, was thrust imbricated prior to deposition of the basal conglomerate of the Lower Jurassic Telkwa Formation.

TABLE 2. GEOCHEMICAL AND ASSAY RESULTS FROM 2005 SAMPLING IN THE USK MAP AREA

						Element	Mo	W	Cu	Pb	Zn	Au	Ag	Bi	Cd	Te	As	Sb	Hg
						Units (note that assays in % and g/t are in bold)	ppm (%)	ppm	ppm (%)	ppm (%)	ppm (%)	ppb	ppb (g/tonne)	ppm	ppm	ppm	ppm (%)	ppm (%)	ppb %
						Method	ARMS	ARMS	ARMS	ARMS	ARMS	ARMS	ARMS	ARMS	ARMS	ARMS	ARMS	ARMS	ARMS
						Detection Limit	0.01	0.2	0.01	0.01	0.1	0.1	2	0.02	0.01	0.02	0.1	0.02	5
Station ID	**Easting**	**Northing**	**Sample Description**	**MINFILE name**	**MINFILE number**														
05EK03-2	536652	6041105	skarn? + chalcopyrite				0.36	-0.1	37.73	2	36.6	0.4	57	0.14	0.13	0.12	1.8	0.13	5
05EK04-1	549076	6046868	quartz vein + pyrite in microdiorite				0.96	2.3	18.92	2.18	28.4	2.2	149	1.06	0.11	0.37	0.7	0.12	5
05EK04-2	549227	6046833	quartz vein + pyrite in microdiorite				8.02	78.8	1518.63	2.5	31	17.8	1486	14.53	0.11	6.52	4.1	0.12	23
05EK08-01	540488	6062600	20 cm quartz vein in silicified aplite with pyrite, chalcopyrite, chalcocite, bornite, galena				4.17	>100	128.53	1042.78	370.5	17.4	30234	146.02	16.62	3.57	2	0.11	65
05-EK-08-01a	540488	6062600	20 cm quartz vein in silicified aplite with pyrite, chalcopyrite, chalcocite, bornite, galena				10.83	5.6	261.67	**0.41**	3137.3	41.3	**253**	646.65	159.04	19.87	2.6	21.93	204
05EK08-02	540593	6062598	quartz vein in silicified aplite with pyrite, chalcopyrite, chalcocite, bornite, galena				0.91	0.5	42.79	4.19	99	-0.2	75	0.71	0.67	0.04	1.1	0.21	13
05EK08-03	540646	6062609	quartz vein in silicified aplite with pyrite, chalcopyrite, chalcocite, bornite, galena				0.62	0.3	4.27	5.55	20.1	-0.2	69	0.39	0.06	-0.02	1.4	0.09	15
05EK08-10	543091	6062965	5 cm quartz vein with chalcopyrite wisps				61.78	0.1	2984.3	1.29	97.1	11.1	16081	1.83	1.81	0.39	-0.1	0.08	-5
05EK09-03	542074	6063990	quartz stockwork with molybdenite	Pitman	46		37.78	0.5	7.97	4.45	10.1	-0.2	227	4.39	0.06	0.33	0.6	0.12	-5
05EK09-05	541443	6064116	quartz stockwork with molybdenite	near Pitman	46		163.76	0.1	30.24	2.4	30.8	-0.2	83	1.56	-0.01	0.04	2.9	0.16	-5
05EK10-06	540517	6042837	pyritic zone at Kleanza pluton contact				1.12	-0.1	447.03	2.27	22.6	0.9	179	0.45	0.07	0.24	0.8	0.16	-5
05EK10-06rep	540517	6042837	pyritic zone at Kleanza pluton contact				0.97	-0.1	419.89	2.18	18.7	1.1	176	0.37	0.06	0.22	0.7	0.16	-5
05EK11-03	538339	6059735	altered Eocene granite with pyrite, azurite				1.92	-0.1	26.8	6.44	39.4	-0.2	264	0.76	0.06	0.13	0.5	0.06	-5
05EK13-05	543271	6046592	microdiorite with chalcopyrite, pyrite				43.58	0.3	481.64	4.21	44.6	5.9	336	0.12	-0.01	0.13	0.6	0.36	-5
05EK13-08	542834	6046628	microdiorite with chalcopyrite, pyrite				1.36	0.4	515.11	2.97	75.1	1.6	334	0.22	0.15	0.14	0.7	0.21	-5
05EK13-10	542936	6046450	microdiorite with chalcopyrite, pyrite				0.88	0.4	57.44	1.36	49.2	1	64	0.07	0.01	0.05	0.4	0.08	-5
05EK13-11	543211	6046552	andesite with chalcopyrite, pyrite				0.5	-0.1	699.52	631.29	55.9	17.4	2108	0.09	0.08	0.14	1.1	8.01	8
05EK15-03	540094	6053186	bornite with epidote alteration, quartz veining; in microdiorite				0.37	0.2	3038.05	3.32	90.2	55.2	3326	0.84	0.14	0.15	1.1	0.13	-5
05EK21-05	555527	6040284	thin quartz vein with malachite, azurite				1.45	0.2	**3.32**	7.25	38.7	6.6	**19**	0.03	2.82	0.02	1.2	0.04	74
05EK24-01	564027	6041719	Cu-stained shear zone	Treasure Mtn.	90		0.2	0.1	1409.7	10.68	130.5	0.8	1193	0.04	0.18	-0.02	2.2	0.27	6
05EK24-06	563187	6040694	Cu-stained shear zone - over 2 m wide	Treasure Mtn.	90		0.26	0.3	**5.091**	1.67	108.2	210.7	**34**	0.02	0.06	0.04	2.1	0.07	-5
05EK-24-06b	563187	6040694	second chip sample Cu-stained shear zone, 2 m	Treasure Mtn.			6.78	0.2	**1.853**	11.84	109.7	1092.2	**15**	1.36	0.39	0.06	1.6	0.85	7
05EK25-08	563061	6042263	malachite-stained andesite	Montana	88		1.17	-0.1	2597.7	40.73	79.7	13.3	1869	0.1	0.35	0.14	10.7	5.66	12
05EK26-01	563858	6042482	chalcocite+malachite in 30 cm+ shear	Treasure Mtn. - Wells showing	90		0.15	-0.1	**9.156**	3.95	101.2	339.7	**228**	0.12	0.21	0.1	0.9	0.1	65
05EK26-05	564139	6042351	bornite, chalcocite, chalcopyrite in shear	Treasure Mtn.	90		0.17	-0.1	**2.427**	1.31	76.8	136.2	**77**	0.09	0.67	0.03	1	0.13	28
05-EK-31-05	561796	6058684	1 m thick shear breccia with quartz veining				13.25	3.8	**3.2**	**0.44**	1640	364.3	10586	2.85	43.29	1.57	7.8	9.65	993
05-EK-31-05rep	561796	6058684	1 m thick shear breccia with quartz veining				13	2.9	**3.287**	**0.5**	1677.3	185.5	7714	2.78	46.16	1.4	6.9	2.93	1133
05EK35-12	561907	6062498	altered tuff with abundant malachite				0.32	-0.1	3750.53	31.78	140	13	25136	0.35	1.14	-0.02	78.7	116.86	162
05EK37-01	559887	6061626	rusty, malachite-azurite stained volcanic				0.35	-0.1	**1.341**	7.24	22.9	12.3	**270**	1.58	0.17	0.02	11.8	1.38	33
05EK41-02	562679	6043387	quartz stockwork with chalcopyrite, bornite, malachite, azurite				0.18	-0.1	2430.78	8.91	47.1	15.5	1270	0.07	0.14	-0.02	0.8	0.3	-5
05EK41-07	562848	6043929	minor chalcopyrite in shear	Copper King?	163		0.26	-0.1	118.3	0.7	14.9	6.6	447	0.02	0.06	-0.02	0.4	0.04	-5
05EK41-08	562893	6043778	20 cm shear with epidote, bornite, chalcocite, malachite, azurite	Copper King?	163		0.23	0.1	**6.116**	3.35	139	27.4	**88**	0.05	0.66	0.07	0.7	0.09	15
05JN02-5	536153	6052601	quartz vein with bornite, chalcocite, pyrite	Lucky Luke	39		17.52	1.4	**2.734**	3.68	34.2	3509.7	**70**	30.48	1.23	9	-0.1	0.09	8
05JN04-3	539757	6048084	quartz vein with coarse pyrite	Columario	77		1.23	0.1	**0.018**	7.09	28.1	38629.3	**137**	10.52	0.36	63.61	1.2	0.06	58
05JN05-3	560134	6043074	10 cm quartz vein with chalcocite, galena				0.47	-0.1	2094.4	2.23	22.7	34	1566	0.16	0.06	0.11	0.6	0.06	-5
05JN07-3	553460	6050340	20 cm quartz vein with epidote, hematite, chalcocite				0.25	<.1	**1.087**	**2.55**	**2**	113.5	**399**	0.1	778.5	0.7	**0.13**	**0.595**	**0.046**
05JN08-2	553704	6053780	quartz vein with pyrite, galena, trace chalcopyrite in altered monzonite porphyry				1.74	0.7	**0.06**	**0.53**	**1.41**	21.2	**10**	0.44	160.7	<.02	42.1	5.32	2965
05JN12-8	549820	6047287	40 cm rustry flat quartz vein				0.67	31.1	32.14	28.31	120.8	185.4	3646	23.23	0.61	11.15	8.8	0.07	18
05JN13-1	552164	6057440	frothy chalcedonic quartz vein 20 cm, irregular				0.88	0.5	41.62	5.81	113.5	1.4	475	0.95	1.78	0.05	0.8	0.09	39

TABLE 2 (CONTINUED)

						Element	Mo	W	Cu	Pb	Zn	Au	Ag	Bi	Cd	Te	As	Sb	Hg
						Units (note that assays in % and g/t are in bold)	ppm (%)	ppm	ppm (%)	ppm (%)	ppm (%)	ppb	ppb (g/tonne)	ppm	ppm	ppm	ppm (%)	ppm (%)	ppb %
						Method	ARMS	ARMS	ARMS	ARMS	ARMS	ARMS	ARMS	ARMS	ARMS	ARMS	ARMS	ARMS	ARMS
						Detection Limit	0.01	0.2	0.01	0.01	0.1	0.1	2	0.02	0.01	0.02	0.1	0.02	5
Station ID	**Easting**	**Northing**	**Sample Description**	**MINFILE name**	**MINFILE number**														
05JN13-7	551927	6056970	20 cm shear with chalcopyrite, pyrite	new showing		16.54	0.7	**5.314**	1413.18	929.7	3670	**17**	5	27.33	0.61	48.9	0.7	348
05NB04-3	536748	6044151	quartz vein with pyrite, molybdenite	New Harlequin	112	**0.214**	0.2	113	3.23	3.7	22.4	1118	0.75	0.55	0.45	0.1	0.03	30
05NB04-4	536890	6043614	coxcomb quartz vein with pyrite	Excelsior	181	9.14	3.4	733.1	9.2	81.8	959.7	13033	20.77	1.17	22.17	1	0.08	5
05NB06-4	546363	6063795	2 m fracture zone with chalcopyrite, malachite, chalcocite			0.66	0.4	2069.61	2.38	65.3	13.6	5110	2.59	0.91	0.27	0.2	0.07	-5
05-NB-07-06	545200	6062700	30 cm quartz vein with bornite			19.71	0.4	4165.32	1.88	27.5	246.9	11951	6.03	0.44	3.19	-0.1	0.28	-5
05NB10-6	540604	6045701	quartz vein in topographic linear, cryptocrystalline; stockwork			1.84	<.1	46.73	67.26	57.1	2.8	1314	0.04	1.37	0.02	3.7	8.77	1229
05NB10-8	540888	6045772	quartz stockwork			652.97	<.1	19.59	14.72	33.3	36.4	598	0.05	0.14	<.02	186	5.12	279
05NB24-3	534216	6065296	30 cm fine grained quartz vein + stockwork; in Eocene granite			0.78	-0.1	63.05	2.23	16	2.5	87	0.11	0.03	-0.02	0.2	0.03	-5
05TB03-7	552920	6046509	fractures with malachite, bornite: 20 m+wide zone	Alvija/ Lucky Jane?	85	3.23	0.1	**5.59**	36.42	184.6	14.7	**99**	0.23	1.68	0.57	1.4	0.2	660
05TB04-2	544488	6045917	disseminated pyrite in quartz veins; silicification	Kino	83	70.47	0.3	625.87	11.13	46.8	12.2	1276	0.17	0.4	0.12	1.6	1.27	7
05TB06-7	540244	6054066	flat quartz vein with pyrite, chalcopyrite, galena, sphalerite	Four Aces	76	0.3	-0.1	645.76	1433.4	6000.3	60.2	19066	9.29	195	7.79	0.1	0.04	11
05-TB-9-09	539333	6054456	quartz vein 2-3 m, with bornite, chalcocite	Emma	74	2.39	1.2	6271.25	3438.08	9155.5	43.6	61000	98.73	179.26	7.04	-0.1	1.36	16
05TB11-3	545285	6066873	1-2% visible pyrite in granodiorite			0.94	-0.1	928.45	8.92	108.8	1.2	11162	0.05	2.95	-0.02	23.4	117.19	210
05TB11-6	545706	6066895	thin quartz vein with pyrite, sphalerite, chalcopyrite			0.68	-0.1	890.26	10.14	120.5	0.7	10983	0.06	3.11	0.03	23	126.99	214
05TB13-3	541784	6050970	quartz vein with epidote alteration, chalcopyrite, bornite			1.19	0.1	9342.85	7.27	20	30.5	1754	0.21	1.84	0.74	0.6	0.56	-5
05TB13-5	541822	6050978	shear zone			0.36	-0.1	9309.3	1.61	40.9	11.3	3387	0.11	0.88	0.51	0.5	0.3	-5
05TB17-3	546337	6045678	5 m ankeritic shear zone with malachite, chalcocite			0.23	-0.1	1801.47	6.19	209.5	3.6	2820	0.07	0.07	0.02	0.8	0.78	-5
05TB22-6	557700	6044323	massive pyrite at dike margin			21.5	0.2	2222.15	8.05	21.8	9.4	840	4.22	0.03	5.22	59.8	2.15	66
05TB24-7	557660	6042014	40 cm zone of epidote veinlets with malachite, azurite, pyrite, chalcocite			0.44	0.1	**1.993**	1.7	42.5	2	8213	0.02	0.35	0.25	1.3	0.06	-5
05-TB-26-03	555087	6051416	polymetallic vein float, upper Chiimdemash Creek			4.69	17.6	**0.685**	4682.46	1326.6	1842.4	**1469**	0.5	149.35	0.02	125.3	**0.351**	2304
05TB26-6	555437	6051701	quartz veins with malachite, azurite, galena	Silver Basin	65	1.73	0.2	1362.83	8335.49	4974.6	102.4	96002	0.42	168.42	0.03	89.2	333.29	1213
05TB26-8	555673	6051584	chalcopyrite with epidote in amygdules	Silver Basin	65	0.3	<.1	66.15	12.91	196.6	1.6	603	0.03	3.9	0.02	1.4	0.73	26
05-TB-26-08	555673	6051584	barite-quartz vein 10 cm	Silver Basin	65	0.3	<.1	66.15	12.91	196.6	1.6	603	0.03	3.9	0.02	1.4	0.73	26
05-TB-26-13	555646	6051345	Main Trench vein 20 cm, with bornite, chalcopyrite, tetrahedrite	Silver Basin	65	9.04	0.5	**1.62**	79.43	1199.6	250.2	**1481**	0.28	279.63	0.03	180.7	9999	4472
05TB27-12	556713	6050629	rusty felsic dike			1.47	<.1	25.29	14.54	36.2	2.5	447	0.05	0.22	2.45	37.3	1.24	48
05TB27-5	554232	6051210	chalcocite, hematite and epidote in basalt			52.36	<.1	**1.412**	5	62.9	49	**55**	0.5	0.93	0.81	0.8	6.56	106
05TB27-8	553918	6050487	4 m patch of highly Cu-stained andesite			0.51	0.2	5418.61	12.73	65.8	0.8	4863	0.03	0.35	0.03	2.7	2.4	150
05TB39-10	559067	6065383	chalcopyrite-bornite in quartz vein breccia and epidote veins; sample is 2 - 1/2 m2 surfaces			0.7	-0.1	**4.28**	30.56	129.2	256.1	**161**	12.37	1.29	0.15	1.3	0.43	5
05TB39-10rep	559067	6065383	chalcopyrite-bornite in quartz vein breccia and epidote veins; sample is 2 - 1/2 m2 surfaces			8.27	-0.1	**4.507**	30.87	130.8	227.3	**166**	12.83	1.35	0.1	0.9	0.36	7
05TB41-3	536026	6058215	20 cm thick quartz vein with molybdenite in area of veining and disseminated pyrite-molybdenite			1328.84	0.2	115	1.24	2.9	-0.2	275	0.15	-0.01	0.04	0.1	0.04	-5
05TB41-4	536205	6058404	40 cm quartz vein with abundant pyrite, molybdenite	Shan	167	**0.989**	0.9	**0.035**	5.94	6.1	8	1380	4.88	0.26	0.53	0.4	0.11	6
05-TB-45-02	551591	6043380	one of several small sulfide (skarn?) zones in limestone olistolith within andesite tuff, each less than 30 cm wide			5.79	0.3	**1.123**	**1.28**	**10.94**	26.5	**2232**	0.43	1765.02	0.06	387.7	**0.686**	7393

TABLE 3. REVISIONS OF MINERAL DEPOSIT LOCATIONS FROM FIELD OBSERVATIONS, USK MAP AREA

MINFILE name	MINFILE number	Station	New easting	New northing	Description
Gold Star B zone	38	05JN11-2	534294	6053101	trench with quartz veins, chalcocite, bornite, chalcopyrite
Gold Star A zone	38	05JN11-3	534555	6052629	trench with quartz veins, chalcocite, bornite, chalcopyrite
Lucky Luke	39	05JN02-5	536153	6052601	quartz vein with bornite, chalcocite, pyrite
Pitman	46	05EK09-03	542074	6063990	quartz stockwork with molybdenite
Pitman	46	05EK09-05	541443	6064116	quartz stockwork with molybdenite
United St. Croix	59	05JN07-9	551722	6049346	complex quartz vein up to 1 m, with chalcopyrite, pyrite, chalcocite, malachite, azurite
Silver Basin main trench	65	05TB26-13	555646	6051345	quartz vein 20 cm with chalcocite, bornite; in WSW-striking shear zone
Emma	74	05TB09-9	539333	6054456	malachite-stained quartz veins in fault
Four Aces	76	05TB06-7	540244	6054066	flat quartz vein with pyrite, chalcopyrite, galena, sphalerite
Columario	77	05JN04-3	539757	6048084	quartz vein with coarse pyrite
Zymoetz	82	05NB04-5	536999	6043038	70 cm quartz vein with pyrite, galena, magnetite, sphalerite, chalcopyrite; in old adit
Kino	83	05TB04-2	544488	6045917	disseminated pyrite in quartz veins; silicification
Kino	83	05EK13-05	543271	6046592	microdiorite with chalcopyrite, pyrite
Kino	83	05EK13-08	542834	6046628	microdiorite with chalcopyrite, pyrite
Kino	83	05EK13-10	542936	6046450	microdiorite with chalcopyrite, pyrite
Kino	83	05EK13-11	543211	6046552	andesite with chalcopyrite, pyrite
Alvija	85	05TB03-7	552920	6046509	fractures with malachite, bornite; wide zone
Wells	87	05EK26-01	563858	6042482	chalcocite+malachite in 30 cm+ shear
Montana	88	05EK25-08	563061	6042263	malachite-stained andesite
Treasure Mtn. north	90	05EK24-06	563187	6040694	Cu-stained shear zone; over 2 m wide
New Harlequin	112	05NB04-3	536748	6044151	quartz vein with pyrite
Shan	167	05TB41-4	536205	6058404	40 cm quartz vein with abundant pyrite, molybdenite
Copper King	163	05EK41-08	562893	6043778	20 cm shear with epidote, bornite, chalcocite, malachite, azurite
Excelsior	181	05NB04-4	536890	6043614	coxcomb quartz vein with pyrite
Peerless	186	05JN06-3	560746	6044270	massive chalcocite vein in ankerite-altered andesite; 10 cm thick; flat dip
GPS locations of mineral occurrences established by Raymond Cook (pers. comm., 2005):					
Silver Basin headwall zone	65b		556552	6051171	disseminated tetrahedrite, bornite in amygdules
Pass	new		559633	6056738	gossan (breccia zone) 40 m wide, continuous 200 m in pass; assays pending
Frisco	61		558656	6058339	Cu, Ag in veins, stringers, disseminations in 12 m wide zone (MINFILE)
M&K main adit	62		558609	6057003	Quartz veins with Au, Ag values (0.38 g/t Au, 119 g/t Ag in grab sample; Salat, 2005) in sheared, brecciated zone
M&K (stratabound zone)	62b		558577	6056985	bedding-parallel mineralized zone, up to 1.2 m wide, in tuff; chalcopyrite, chalcocite, galena, bornite, minor tetrahedrite, pyrite, specularite
Zona May vein	60a		554523	6055208	0.2 3 m wide quartz vein over 700 (possibly 1800) m; strikes ESE; grab samples assayed 0.03 24 g/t Au, 0.3 3364 g/t Ag (Salat, 2005)
Zona May west wall breccia	60b		554296	6055299	see above
Zona May vein (glacier zone)	60c		554631	6055172	see above
Zona May east	60d		554674	6055172	see above
Dynasty	new		555343	6055033	extension of Zona May vein to east(?); east-striking quartz vein with Cu, Ag

The Telkwa Formation is regionally divisible into two distinct successions: a clastic-dominated section south of Kleanza Creek, and a flow-dominated succession north of Kleanza Creek. Although the flow-dominated section locally overlies the clastic section, the authors consider them to be volcanic facies variants as well: the flows were sourced locally within the map area and represent a major complex of andesite, dacite and rhyolite centres.

The Kitselas facies of the Telkwa Formation comprises mainly felsic volcaniclastic and coherent rocks, with minor basalt; it lies in the footwall of the Usk fault.

The top of the Hazelton Group comprises an equivalent of the 'Red Tuff' member of the Nilkitkwa Formation, sandstone fossil-dated as Bajocian, and banded siliceous strata equivalent to the Troy Ridge Formation. These are overlain by the Bowser Lake Group.

The 200 Ma Kleanza pluton is a sprawling laccolithic body with two major lobes. It is probably comagmatic with the Telkwa Formation, and may core the volcanic centre that generated flows in the Mount O'Brien section.

Mineralization in the area relates to the Kleanza pluton and the Eocene Carpenter Lake pluton, as well as possibly to the structures associated with the Usk shear zone and, in the case of Cu-Ag-rich shears and replacements, regional hydrothermal circulation in the Telkwa Formation.

ACKNOWLEDGMENTS

Glenn Woodsworth was generous with his knowledge of Terrace area geology, and it was our pleasure to confirm many of his observations and ideas in the field. Bill McRae, Jim Mulvey, George Chinn, Alex Burton and Ray Cook provided detailed information on mineral prospects in the area. We are deeply indebted to Bill and Helene McRae for every kind of help and support. This project was conducted in partnership with the Resource Management Department of the Kitselas First Nation. We thank Daniel Parker, Chad Gerow and Richard Seymour for able assistance in the field. Larry Diakow provided an insightful review of the text.

REFERENCES

Alldrick, D.J., Nelson, J.L. and Barresi, T. (2005): Geology and mineral occurrences of the upper Iskut River area: tracking the Eskay rift through northern British Columbia; *in* Geological Fieldwork 2004, *BC Ministry of Energy, Mines and Petroleum Resources*, Paper 2005-1, pages 1–30.

Anderson, R.G. (1989): A stratigraphic, plutonic and structural framework for the Iskut map area, northwestern British Columbia; *in* Current Research, Part E, *Geological Survey of Canada*, Paper 89-1E, pages 145–154.

Barresi, T. and Nelson, J.L. (2006): The Usk map area near Terrace, BC: Cross-sections and volcanic facies interpretation; *in* Geological Fieldwork 2005, *BC Ministry of Energy,*

Mines and Petroleum Resources, Paper 2006-1 and *Geoscience BC*, Report 2006-1.

Bennett, N., Compiler (1997): Pioneer Legacy: Chronicles of the Lower Skeena River; *R.E.M. Lee Hospital Foundation*, Terrace, BC, 240 pages.

Berthiaume, R. (1999): The Gitselasu: The People of Kitselas Canyon; *First Nations Education Centre*, Terrace, BC, 154 pages.

Brown, D.A., Gunning, M.H. and Greig, C.J. (1996): The Stikine Project: geology of western Telegraph Creek map area, northwestern British Columbia; *BC Ministry of Energy, Mines and Petroleum Resources*, Bulletin 95, 176 pages.

Carter, N.C. (1970): Gold Star; *in* Geology, Exploration and Mining in British Columbia 1970, *BC Ministry of Energy, Mines and Petroleum Resources*, pages 195–197.

Duffell, S. and Souther, J.G. (1964): Geology of Terrace map area, British Columbia; *Geological Survey of Canada*, Memoir 329, 117 pages.

Gareau, S.A., Friedman, R.M., Woodsworth, G.J. and Childe, F. (1997a): U-Pb ages from the northeastern quadrant of Terrace map area, west-central British Columbia; *Geological Survey of Canada*, Current Research 1997-A/B, pages 31–40.

Gareau, S.A., Woodsworth, G.J. and Rickli, M. (1997b): Regional geology of the northeastern quadrant of Terrace map area, west-central British Columbia; *Geological Survey of Canada*, Current Research 1997-A/B, pages 47–55.

Gunning, M.H., Bamber, E.W., Brown, D.A., Rui, L., Mamet, B.L. and Orchard, M.J. (1994): The Permian Ambition Formation of northwestern Stikinia, British Columbia; *in* Pangea: Global Environments and Resources, Embry, A.F., Beauchamp, B. and Glass, D.J., Editors, *Canadian Society of Petroleum Geologists*, Memoir 17, pages 589–619.

Heah, T.S.T. (1991): Mesozoic ductile shear and Paleogene extension along the eastern margin of the Central Gneiss Complex, Coast Belt, Shames River area, near Terrace, British Columbia; M.Sc. thesis, *University of British Columbia*, Vancouver, BC, 155 pages.

Kindle, E.D. (1937a): Mineral resources of Terrace area, Coast district, British Columbia; *Geological Survey of Canada*, Memoir 205.

Kindle, E.D. (1937a): Mineral resources, Usk to Cedarvale, Terrace area, Coast district, British Columbia; *Geological Survey of Canada*, Memoir 212.

Logan, J.M., Drobe, J.R. and McClelland, W.C. (2000): Geology of the Forrest Kerr – Mess Creek area, northwestern British Columbia; *BC Ministry of Energy, Mines and Petroleum Resources*, Bulletin 104, 164 pages.

Marsden, H. and Thorkelsen, D.J. (1992): Geology of the Hazelton volcanic belt in British Columbia: implications for the Early to Middle Jurassic evolution of Stikinia; Tectonics, Volume 11, pages 1266–1287.

Mihalynuk, M.G. (1987): Metamorphic, structural and stratigraphic evolution of the Telkwa Formation, Zymoetz River area (NTS 103I/08 and 93L/05), near Terrace, British Columbia; M.Sc. thesis, *University of Calgary*, Calgary, Alberta, 128 pages.

Mihalynuk, M.G. and Friedman, R.M. (2005): Gold and base metal mineralization near Kitsumkalum Lake, north of Terrace, west-central British Columbia; *in* Geological Fieldwork 2004, *BC Ministry of Energy, Mines and Petroleum Resources*, Paper 2005-1, pages 67–82.

MINFILE (2005): MINFILE BC mineral deposits database; *BC Ministry of Energy, Mines and Petroleum Resources*, URL <http://www.em.gov.bc.ca/mining/Geolsurv/Minfile/> [Nov 2005].

Monger, J.W.H., Wheeler, J.O., Tipper, H.W., Gabrielse, H., Harms, T., Struik, L.C., Campbell, R.B., Dodds, C.J., Gehrels, G.E. and O'Brien, J.A. (1991): Cordilleran terranes; Part B of Chapter 8 *in* Geology of the Cordilleran Orogen in Canada, Gabrielse, H. and Yorath, C.J., Editors, *Geological Survey of Canada*, Geology of Canada, No 4, p. 281–328 (also The Geology of North America, *Geological Society of America*, Boulder, Colorado, Volume G-2).

Nelson, J.L., Barresi, T., Knight, E. and Boudreau, N. (2006): Geology of the Usk map area, Terrace, British Columbia (103I/09); B.C. Ministry of Energy, Mines and Petroleum Resources, Open File 2006-3, 1:50,000 scale.

Roots, C.F., Nelson, J.L., Simard, R.-L., Mihalynuk, M., Harms, T.A., Friedman, R. and Heaman, L. (in press): Continental fragments, Paleozoic arcs and overlapping Triassic sediments in the pericratonic belt, northern British Columbia and southern Yukon; *in* Paleozoic Evolution and Metallogeny of Pericratonic Terranes at the Ancient Pacific Margin of North America, Canadian and Alaskan Cordillera, Colpron, M., Nelson J.L. and Thompson, R.I., Editors, *Geological Association of Canada*, Special Paper 45, in press.

Sadlier-Brown, T. (1973): Statement of material facts — Treasure Mountain; press release, prepared for *Spectroair Explorations Ltd*, June 16, 1973.

Salat, H.P. (2005): Report on the geological reconnaissance and evaluation of the Zona May – Silver Basin property, BC; submitted by Argonaut Resources Inc., *BC Ministry of Energy, Mines and Petroleum Resources*, AR 27786, 90 pages.

Sutherland Brown, A. (1965): Northwest Copper – Treasure Mountain; *BC Ministry of Energy, Mines and Petroleum Resources*, Minister of Mines Annual Report 1965, pages 71-72.

Tipper, H.W. and Richards, T.A. (1976): Jurassic stratigraphy and history of north-central British Columbia; *Geological Survey of Canada*, Bulletin 270, 73 pages.

van der Heyden, P. (1992): A Middle Jurassic to early Tertiary Andean-Sierran subduction model for the Coast Belt of BC; *Tectonics*, Volume 11, pages 82–97.

Woodsworth, G.J., Anderson, R.G. and Armstrong, R.L. (1991): Plutonic regimes; Chapter 15 *in* Geology of the Cordilleran Orogen in Canada, Gabrielse, H. and Yorath, C.J., Editors, *Geological Survey of Canada*, Geology of Canada, No 4, pages 491–531 (also *Geological Society of America*, The Geology of North America, Volume G-2).

Woodsworth, G.J., Hill, M.L. and van der Heyden, P. (1985): Preliminary geology map of Terrace (NTS 103I, east half) map area, BC; *Geological Survey of Canada*, Open File 1136, 1 map at 1:125 000 scale.

Preliminary Geology of the Nimpkish Map Area (NTS 092L/07), Northern Vancouver Island, British Columbia

By G.T. Nixon, M.C. Kelman, D. Stevenson[1], L.A. Stokes[2], and K.A. Johnston

KEYWORDS: Vancouver Group, Karmutsen Formation, Quatsino Formation, Parson Bay Formation, Bonanza Group, Bonanza volcanics, Island Plutonic Suite, Triassic, Jurassic, Vancouver Island, Nimpkish, Bonanza Lake, regional geology, stratigraphy, structure, skarn, mineral occurrences, mineral potential, mineralization

INTRODUCTION

Northern Vancouver Island is richly endowed in a variety of base and precious-metal deposits. For example, the Cu-Mo-Au porphyry deposit at the former Island Copper mine (1971–1994) produced approximately 345 million tonnes of ore with average head grades of 0.41 wt% Cu, 0.017% Mo, 0.19 g/t Au and 1.4 g/t Ag (Perello *et al.*, 1995). Other porphyry deposits are known to exist in the region (*e.g.*, Hushamu [MINFILE occurrence 92L 240] and Red Dog [92L 200]; MINFILE, 2005) and, thanks to a recent surge in metal prices, the potential for bringing these and future discoveries into production is currently high.

In order to improve understanding of the geological setting of mineral occurrences and the exploration potential of northern Vancouver Island, a regional mapping project (1:50 000 scale) was initiated this past summer in the Nimpkish map area (Fig. 1). The project encompasses the region between Nimpkish and Bonanza lakes, and extends northeast to Robson Bight and south to the Nimpkish River. The area is contiguous with regional mapping at the same scale completed more than a decade ago in the Quatsino Sound region (discussed below). This paper presents the preliminary results of the 2005 field season. Further details on the mapping and geological setting of the mineral occurrences are presented by Nixon *et al*. (in press).

The Nimpkish sheet covers an area of more than 1000 km^2 with moderate to rugged relief and heavy forest cover except for the higher ridges. Access is provided by an extensive system of active and decommissioned logging roads; however, road coverage is poor in the northeastern part of the project area. Outcrop is generally sparse. Thick deposits of glacial till and outwash typically occupy the main valley bottoms and form veneers on valley slopes. The best exposures are found in roadcuts, along ridge crests and forming bluffs on valley sides, and where streams have incised narrow canyons.

[1]*Department of Earth and Ocean Sciences, University of British Columbia, Vancouver BC*

[2] *Department of Earth Sciences, Memorial University of Newfoundland, St. John's, NL*

This publication is also available, free of charge, as colour digital files in Adobe Acrobat PDF format from the BC Ministry of Energy, Mines and Petroleum Resources internet website at http://www.em.gov.bc.ca/Mining/Geolsurv/Publications/catalog/catfldwk.htm

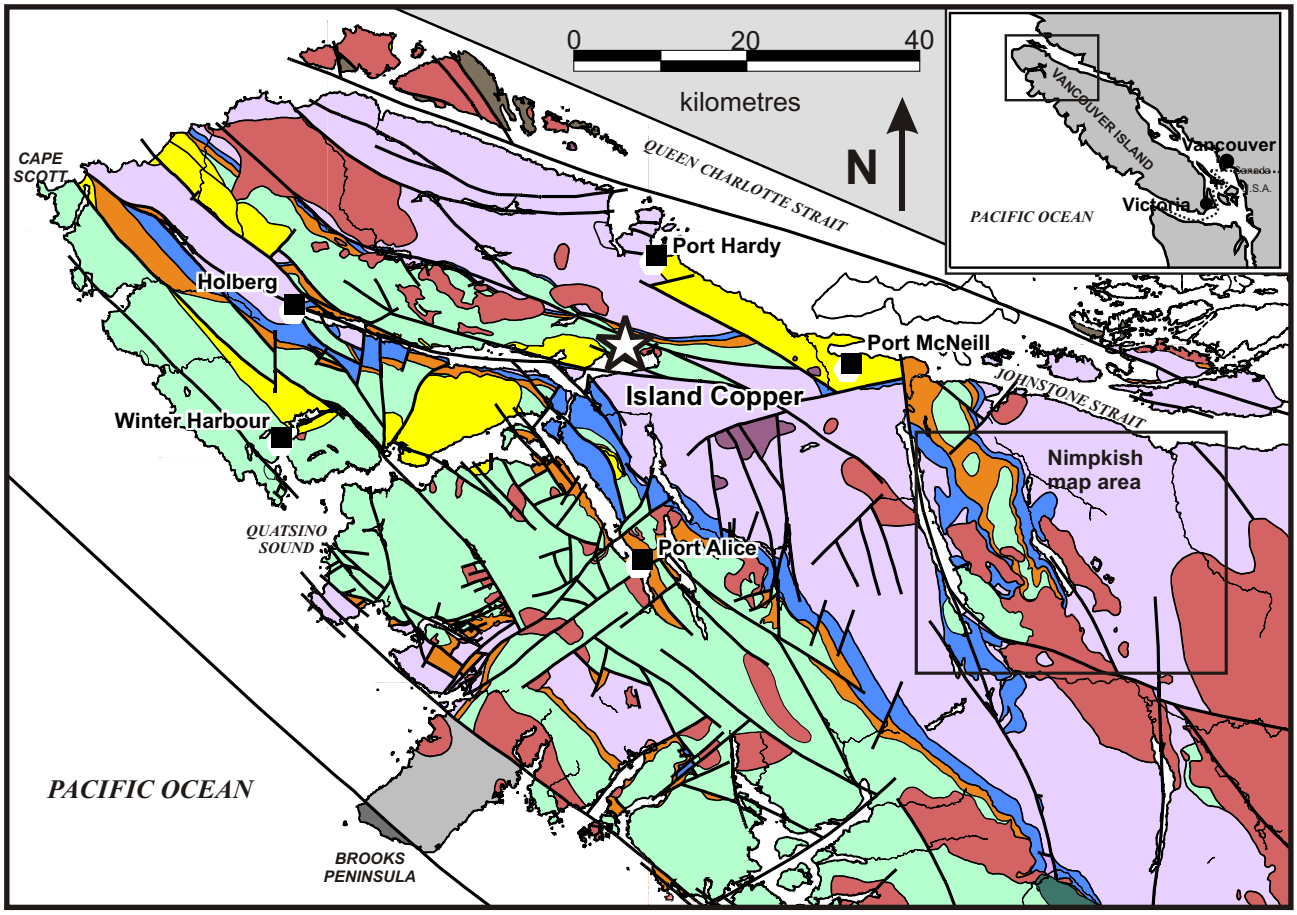
PREVIOUS WORK

The earliest recorded geological investigations of northern Vancouver Island were made by G.M. Dawson during his pioneering voyage (Dawson, 1887). Early mineral deposit studies were conducted by Dolmage (1919) and Gunning (1930), who carried out the first systematic mapping of the Nimpkish area (Gunning, 1930, 1932, 1938a, b). Hoadley (1953) incorporated much of Gunning's earlier work in his study of the geology and mineral deposits of the Zeballos-Nimpkish area. The most comprehensive reports dealing specifically with the geology and mineral deposits of northern Vancouver Island are those of Muller *et al*. (1974), Jeletsky (1976) and Muller and Roddick (1983). More recently, the results of 1:50 000-scale mapping combined with geochronological and biostratigraphic studies in the Quatsino Sound region have been published in a series of preliminary reports by Nixon and coworkers (Nixon *et al.*, 1993a, b, 1994a, b, 1995a, b; Friedman and Nixon, 1995; Archibald and Nixon, 1995). The lithostratigraphic nomenclature applied to the Nimpkish area (discussed below) draws upon this existing knowledge base.

TECTONIC SETTING AND REGIONAL GEOLOGY

The geology of Vancouver Island is characterized principally by Upper Paleozoic to Lower Mesozoic rocks of the Wrangell tectonostratigraphic terrane, which extends north through the Queen Charlotte Islands into southern Alaska (Fig. 1; Wheeler and McFeely, 1991). Wrangellia was amalgamated with the Alexander Terrane in the Alaska panhandle to form the Insular Superterrane as early as the Late Carboniferous time (Gardner *et al*., 1988), and was accreted to inboard terranes of the Coast and Intermontane belts as late as the mid-Cretaceous (Monger *et al*., 1982) or as early as the Middle Jurassic (van der Heyden, 1991).

At the latitude of the project area, Wrangellia is intruded to the east by granitoid rocks of the Coast Plutonic Complex and fault bounded to the west by the Westcoast Crystalline Complex, part of the basement to Wrangellia, and Pacific Rim Terrane (Wheeler and McFeely, 1991). The relatively low relief and high heat flow of northernmost Vancouver Island reflect tectonism associated with the development of the Queen Charlotte Basin, a Tertiary transtensional province related to oblique convergence of the Pacific and Juan de Fuca plates with the North American plate (Riddihough and Hyndman, 1991; Lewis *et al*.,



Neogene

Alert Bay volcanics

Eocene

Catface intrusions

Late Jurassic-Late Cretaceous

Nanaimo, Queen Charlotte and Kyuquot groups

Jurassic-Cretaceous

Pacific Rim complex

Early-Middle Jurassic

Island Plutonic Suite

West Coast Crystalline Complex

Late Triassic-Middle Jurassic

Bonanza Group

'Bonanza volcanics'

Harbledown Formation

Parson Bay Formation

Late Triassic

Vancouver Group

Quatsino Formation

Karmutsen Formation

Figure 1. Regional geology of northern Vancouver Island (after Massey *et al.*, 2005), showing the location of the Nimpkish map area.

1997). This geological history has resulted in the present crustal architecture: a dominant northwest-trending structural grain manifested by the distribution of major stratigraphic units, faults and granitoid batholiths (Fig. 1). Numerous fault-bounded blocks of homoclinal Early Mesozoic strata generally dip westward (Muller *et al.*, 1974). The northeasterly-trending Brooks Peninsula fault zone delineates the southern boundary of the Tertiary extensional regime in the Queen Charlotte Basin. This zone of tectonism also coincides with the southern limit of Tertiary (Neogene) dikes and remnants of effusive volcanism in the region (Armstrong *et al.*, 1985; Lewis *et al.*, 1997).

STRATIGRAPHIC NOMENCLATURE AND AGE RELATIONSHIPS

The stratigraphic nomenclature proposed for the Alert Bay – Cape Scott map sheet (NTS 092L) by Muller *et al*. (1974), as revised by Muller *et al.* (1981), is shown in Figure 2. Revisions to the Triassic–Jurassic lithostratigraphic nomenclature proposed in this study, shown in Figure 3, are based on previously published and unpublished geochronological and biostratigraphic data for the Quatsino Sound area (Nixon *et al.*, 1993a, b, 1994a, b, 1995a, b; Friedman and Nixon, 1995; Archibald and Nixon, 1995). The age ranges are based on recent improvements to the geological time scale (Palfy *et al*., 2000; Gradstein *et al*., 2004). The preliminary results of recent mapping in the Nimpkish area appear consistent with this new time-stratigraphic framework.

Devonian to Early Permian island-arc volcanic, volcaniclastic and sedimentary rocks that form the basement of Wrangellia (Sicker and Buttle Lake groups; Massey, 1995a, b, c) are not exposed on northernmost Vancouver Island. Lithostratigraphic units diagnostic of Wrangellian stratigraphy form the Triassic tripartite succession of the Karmutsen, Quatsino and Parson Bay formations (Jones *et al*., 1977), which Muller *et al*. (1974, 1981) placed in the Vancouver Group (Fig. 2). The Karmutsen tholeiitic flood basalts are currently interpreted to represent a thick (~6000 m) oceanic plateau formed by the activity of a mantle plume (Greene *et al.*, 2006). The overlying Quatsino limestone represents shallow-water carbonate deposition accompanying subsidence during the waning stages of Karmutsen volcanism (Carlisle and Suzuki, 1974; Muller *et al*., 1974). Sedimentation continued with the deposition of deeper water, impure limestone and siliciclastic rocks of the Parson Bay Formation. The volcanic, volcaniclastic and epiclastic strata of the Bonanza Group, and coeval intrusions of the Island Plutonic Suite, mark a renewed phase of island-arc magmatism and sedimentation (Carson, 1973; Muller *et al*., 1974; Woodsworth *et al*., 1991; Debari *et al*., 1999, 2000).

Lithostratigraphic evidence for including the Parson Bay Formation within the Bonanza Group is based on the occurrence of coarse volcaniclastic deposits, and rarely lavas, of basaltic to rhyolitic composition, intercalated with typical Parson Bay rocks. To the west, for example, in the adjoining Alice Lake map sheet (NTS 092L/06), basaltic lapilli tuff deposits, interpreted as the products of phreatomagmatic eruptions, are found close to the undisturbed contact with the Quatsino Formation and contain angular fragments of the limestone. In a measured section in the same area near Kathleen Lake, volcaniclastic debris flows and juvenile augite, hornblende and plagioclase-bearing crystal tuffs (partly reworked) are constrained by biostratigraphic evidence (conodont faunas and bivalves, including the Late Triassic fauna *Monotis subcircularis* Gabb; Nixon *et al*., 2000) to lie within the uppermost Middle to Upper Norian part of the Parson Bay section. Hornblende in these deposits has provided an Ar^{40}/Ar^{39} plateau age of 199.4 ±3.4 Ma (95% confidence limit; Nixon *et al*., 2000). According to recent time scales (Fig. 3), this date is essentially coincident with the Triassic–Jurassic boundary, and within error of the recommended age for the Norian–Rhaetian stage boundary (Gradstein *et al*., 2004). Some previous workers have also recognized that certain volcanic lithostratigraphic units of the Bonanza Group may be Upper Triassic (Rhaetian?) in age (*e.g*., Hecate Cove Formation; Jeletzky, 1976). Thus, recent biostratigraphic and geochronological evidence favours an Upper Triassic age for the initiation of volcanism in the Bonanza arc. As described below, volcanic breccias and lavas are also observed within typical Parson Bay rocks in the Nimpkish area. Accordingly, the authors have provisionally placed the entire Parson Bay Formation in the Bonanza Group (Fig. 3). Sedimentary strata of the Harbledown Formation, which are partly correlative with the Bonanza Group (Lower Jurassic; Carlisle, 1972; Muller *et al*., 1974), have not been recognized as a separate map unit within the Nimpkish area. Relationships between the Harbledown and Parson Bay formations in the Quatsino Sound area are currently under review.

The youngest isotopic ages for the Bonanza Group have been obtained on subaerial rhyolite lava and ash-flow tuff sequences exposed about 20 km west of the former Island Copper mine (described in Nixon *et al*., 1994a). These rocks have yielded U-Pb zircon dates of *ca*. 169 Ma or Middle Jurassic (mid-Bajocian; dates revised since originally reported by Friedman and Nixon, 1995). Currently, the oldest U-Pb zircon dates are 199–202 Ma (R.M. Friedman and G.T. Nixon, unpublished data, 1992-1996) from rhyolitic lavas on the west coast near Le Mare Lake (Nixon *et al*., 1993a) and south of Winter Harbour near Nose Peak (Nixon *et al*., 1995a). According to the time scale shown in Figure 3, these dates straddle the Triassic–Jurassic boundary. From previous work in the Quatsino Sound region, the authors consider it probable that the earliest juvenile volcanic components of the Bonanza arc may date back at least to the Early Norian, and that earlier (Carnian) fine-grained siliciclastic deposits in the Parson Bay Formation may have a distal arc-derived component.

Age relationships between the Bonanza Group and the Island Plutonic Suite were recently evaluated by Archibald and Nixon (1995) and DeBari *et al*. (1999, 2000), who concluded that the available geochronological and biostratigraphic data favour a comagmatic relationship. Previous dating studies of U-Pb zircon and Ar^{40}/Ar^{39} mineral separates (mainly hornblende and biotite) in granitoid rocks on northern Vancouver Island indicate crystallization ages of 197–167 Ma for the Island Plutonic Suite (Friedman and Nixon, 1995; Archibald and Nixon, 1995 and unpublished data 1992-1996). Thus, the oldest granitoid rocks are earliest Jurassic in age and lie within *ca.* 5 Ma of the oldest isotopic dates (latest Triassic) on volcanic rocks of the Bonanza Group.

STRATIFIED ROCKS

The main lithostratigraphic units in the Nimpkish map area belong to the Upper Triassic Karmutsen and Quatsino formations of the Vancouver Group and Parson Bay Formation of the Upper Triassic–Middle Jurassic Bonanza Group (Fig. 3 and 4). The youngest map units are volcanic and minor intercalated sedimentary rocks exposed in the core of a broad, northerly-trending syncline between Nimpkish and Bonanza lakes (Fig. 4). The latter rocks are tentatively assigned to the informally named, submarine to subaerial 'Bonanza volcanics' of the Bonanza Group (Muller *et al*., 1974, 1981). Younger, Upper Jurassic (?) to Cretaceous strata and Tertiary rocks of the Alert Bay volcanic belt that are exposed further north appear to be absent in the Nimpkish area.

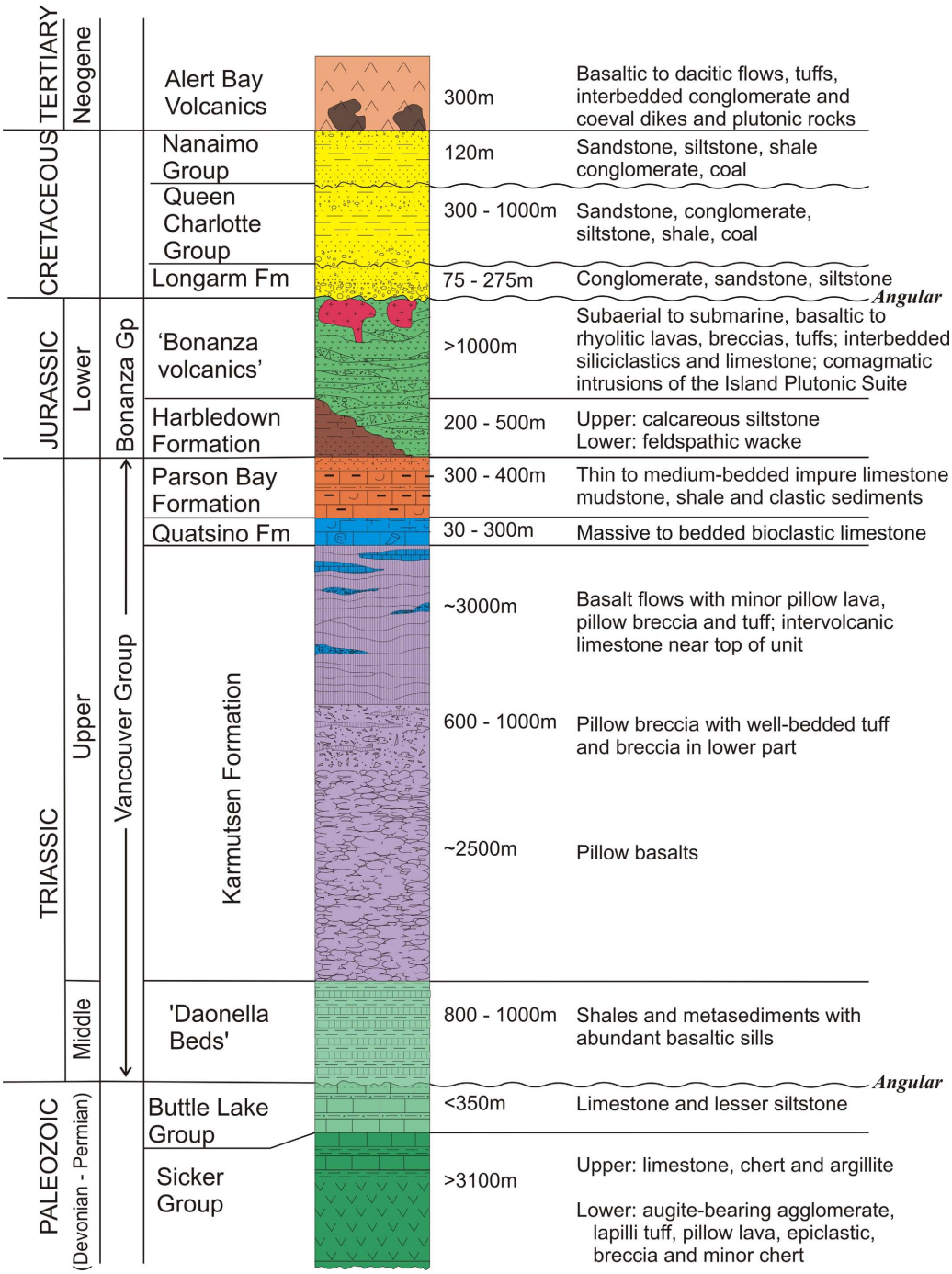


Figure 2. Stratigraphic nomenclature for northern Vancouver Island used by Muller *et al*. (1974, 1981).

Vancouver Group

Only the Upper Triassic Karmutsen and Quatsino formations of the Vancouver Group are exposed in the Nimpkish area.

KARMUTSEN FORMATION

The oldest rocks exposed in the area belong to the Karmutsen Formation, which underlies the northeastern half of the map sheet and the western shore of Nimpkish Lake. The Karmutsen basalts typically form terrain ranging from knobby hills to rugged mountains. The three major subdivisions described to the southeast in the Bute Inlet – Schoen Lake area comprise a lower pillow lava sequence overlain by pillow breccia and 'aquagene' tuff and breccia, in turn overlain by subaerial flows (Carlisle, 1972; Fig. 2). These subdivisions have not been delineated in the Nimpkish area due to limited access and disruption by faults. Layered flow sequences belonging to the youngest Karmutsen subdivision predominate, except in the extreme southwestern corner of the map area and possibly in the poorly accessible northeastern sector toward Robson Bight.

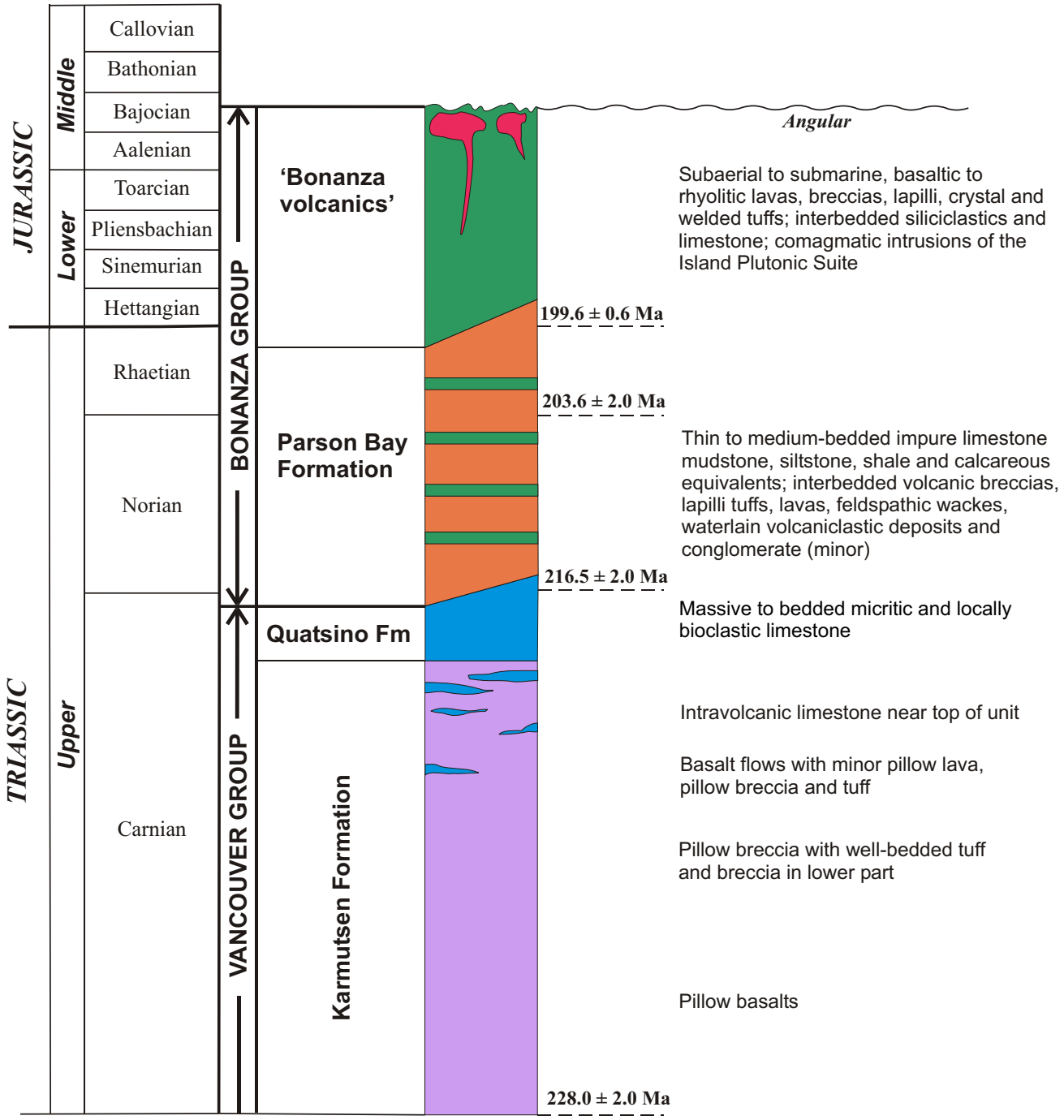


Figure 3. Revised stratigraphic nomenclature for Triassic–Jurassic lithostratigraphic units proposed in this study. The geological time scale is that of Gradstein *et al*. (2004).

Typical Karmutsen basalts are dark grey-green to almost black, aphanitic to plagioclase phyric and locally amygdaloidal. At least two varieties of plagioclase-phyric flows can be recognized: lavas that carry subequant to prismatic plagioclase phenocrysts that are generally 1–5 mm in length and 5–15% by volume; and megacrystic varieties containing blocky to lath-shaped plagioclase crystals 1–2 cm in length and up to 50% by volume (Fig. 5). The plagioclase-rich megacrystic flows generally weather medium to pale grey and locally exhibit strong trachytoid textures. They are confined to the uppermost part of the Karmutsen Formation and therefore serve as useful stratigraphic markers where intra-Karmutsen limestone or the Quatsino Formation is missing (Fig. 4).

The contacts between individual flows are typically sharp and unbrecciated, and there is no evidence for significant erosion or paleosol formation. Primary columnar jointing has not been observed. Certain lavas exhibit a pronounced flow foliation defined by a zone of stretched and flattened amygdules, or by centimetre-scale layering (1–

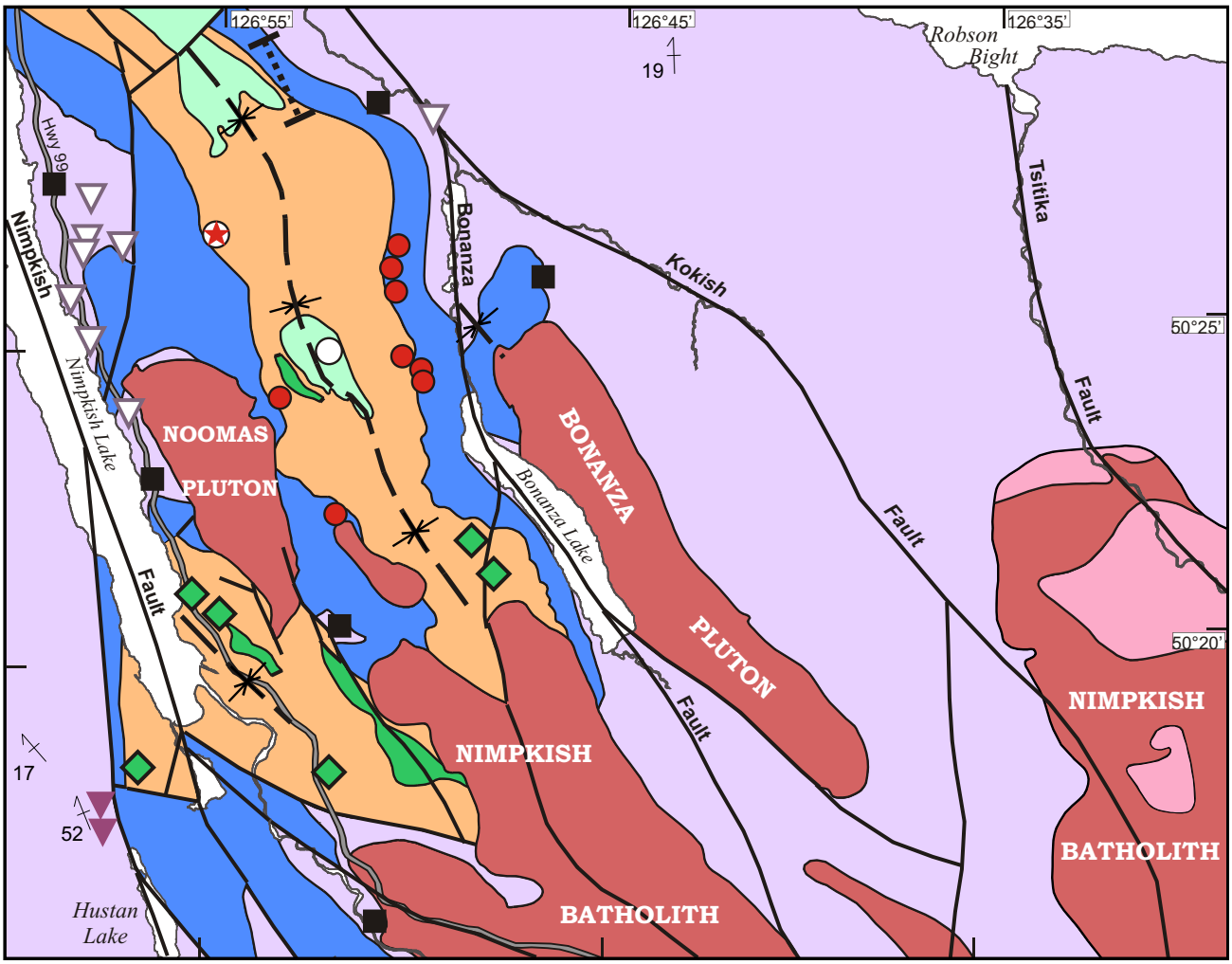


Figure 4. Generalized geology of the Nimpkish map area, northern Vancouver Island.

20 cm thick) of amygdule-rich and amygdule-free lava (Fig. 6).

Locally, significant volumes of volcanic breccia, possibly water-laid, contain matrix-supported clasts (1–10 cm across) of the adjacent lava in a very fine grained, grey-green, comminuted matrix. Where pillows occur, the interpillow material is dark grey to almost black, fine grained and commonly silicified, and coarse pillow fragments are very rare.

Relatively thick sequences of Karmutsen pillow basalt are exposed west of Hustan Lake and the southern tip of Nimpkish Lake in the southwestern corner of the map area. The pillows comprise slightly flattened ellipsoids averaging 0.5–1 m across (Fig. 7). Pillow-fragment breccia deposits occur locally but constitute only a small fraction of the total volume. The breccia comprises pillow fragments up to 0.4 m across in a finer grained hyaloclastite matrix. Rarely, these pillow lavas and breccia units enclose well-bedded, thin (3 m or less) sedimentary horizons consisting of black (fresh) to orange (weathered), thickly laminated to medium-bedded mudstone, shale and, rarely, fine sandstone, all of which can be calcareous and contain thin limestone interbeds. Similar sedimentary rocks were described by Carlisle and Suzuki (1974) intercalated within the upper part of the Karmutsen succession. However, the most common sedimentary units encountered near the top of the flow sequence are concentrated along the west shore of Nimpkish Lake. Here, small pods of pale to medium grey, massive to thinly bedded, micritic intra-Karmutsen limestone up to 4 m thick mark a transition to the overlying Quatsino Formation (Fig. 4).



Figure 5. Prismatic and subequant plagioclase megacrysts in a Karmutsen Formation flow, Kinman Creek (locality 05GNX-6-8-1); pencil magnet is 12 cm in length.

In thin section, phenocrysts of calcic plagioclase in Karmutsen basalt are partly replaced by sericite, epidote and clay minerals, and fine-grained chlorite – opaque mineral products generally replace former glass inclusions. Clinopyroxene forms either intergranular subhedral crystals or anhedral subophitic–ophitic grains, rarely up to 2 mm in length, enclosing plagioclase laths in the groundmass. Certain flows are distinctly enriched in clinopyroxene and, in some cases, basalt with coarsely ophitic textures may represent high-level sills. Euhedral to granular Fe-Ti oxides are a common primary accessory phase and account for the strongly magnetic character of many lavas. Amygdaloidal zones tend to be concentrated close to flow tops and near the chilled margins of pillows.

The effects of low-grade metamorphism, ranging from zeolite to prehnite-pumpellyite facies, are well documented in the Karmutsen Formation (*e.g.*, Surdam, 1973; Greenwood *et al.*, 1991). Numerous veins and amygdules are commonly filled with quartz, potassium feldspar, epidote, chlorite, carbonate, clay minerals and zeolites. Interpillow material may be almost totally replaced by one or more of these minerals, and pillow-fragment breccias locally contain replacement pods of coarse calcite crystals (up to 2 cm). Veins and diffuse zones of secondary silicate-carbonate may contain finely crystalline pyrite, which may form layers up to 1 mm thick within rare interbedded sedimentary rocks. Some joints and fractures are coated with acicular actinolite, which may reflect localized greenschist-facies conditions due to elevated temperatures of hydrothermal fluids influenced by granitoid emplacement. Strong alteration of Karmutsen basalt to epidote-amphibolite assemblages is usually found close to intrusive contacts with the Island Plutonic Suite, as documented elsewhere (Kuniyoshi and Liou, 1976).

QUATSINO FORMATION

The Quatsino Formation is well exposed east and south of Nimpkish Lake, where it is intruded by granitoid rocks of the Island Plutonic Suite, and in the higher ground border-



Figure 6. Amygdaloidal layering in Karmutsen Formation basalt flow just below the base of the Quatsino Formation limestone, northeastern shore of Nimpkish Lake (locality 05MEL-1-7-1).

ing Bonanza Lake, where it forms high cliffs. Around Bonanza Lake, Quatsino limestone reaches a thickness of about 350 m, comparable to that estimated by Muller and Rahmani (1970) in the Beaver Cove section (~320 m) near the northern edge of the map area (Fig. 4). This unit is much thicker to the west in the vicinity of Alice Lake (~750 m) but thins dramatically farther west on the coast around Klaskino Inlet (approx. 30–40 m; Muller *et al*., 1974; Nixon *et al*., 1993a).

The Karmutsen-Quatsino contact is exposed in roadcuts just north of Bonanza Lake near kilometre 18 on the main logging road. Here, massive grey limestone rests directly on dark grey-green, aphanitic to sparsely plagioclase-phyric, amygdaloidal basalt. The contact is sharp and appears conformable, but likely represents a nondepositional unconformity (paraconformity). A 1 m thick zone of epidote alteration is coincident with the contact. Local lenses and pods of intra-Karmutsen limestone, lithologically similar to the Quatsino, are found within flow sequences just below the basal contact and mark a transition to shallow-marine conditions.



Figure 7. Karmutsen Formation pillow lavas with interpillow quartz, west of Hustan Lake in the southwestern corner of the map area (locality 05GNX-20-3-1); hammer is 35 cm in length.

The lower part of the Quatsino Formation is typically a dark to medium grey, predominantly massive, fetid micritic limestone that weathers pale grey to white where recrystallized to marble. Stylolites are extremely common and, in many cases, are the only structure present. Ammonites have been collected at several localities but are too poorly preserved to be identified.

The uppermost part of the Quatsino Formation is generally composed of thinly laminated to medium or thickly bedded micrite to (rarely) calcarenite sequences that locally contain laminae enriched in bioclastic debris. Normally graded beds are observed locally and attest to deposition by the action of turbidity currents. Transported shell fragments, largely gastropods up to 1 cm across and thin-shelled pelecypods up to several centimetres across (predominantly *Halobia* sp.), occur in both the more massive and the well-bedded horizons but are more common near the top of the unit. Locally, dark grey to black chert concretions are present and some sequences exhibit pervasive silicification.

The Quatsino Formation in the Nimpkish area has undergone extensive reconstitution to a predominantly white and pale grey marble and, locally, dark grey and green varieties, due to the action of hydrothermal fluids apparently driven by heat from the granitoid bodies. In the vicinity of intrusive contacts, a dark grey and white layering, subparallel to bedding in some cases, is conspicuous in areas of skarn development (discussed below). Finely disseminated sulphide minerals and thin (<1 mm) stringers of pyrite are also found in these zones.

Bonanza Group

Lithostratigraphic units of the Bonanza Group in the Nimpkish area, as defined earlier in this report, include the Upper Triassic Parson Bay Formation and the informally named Upper Triassic to Middle Jurassic 'Bonanza volcanics'. As described below, volcanic rocks occur as both individual beds and mappable units within the mixed carbonate-siliciclastic Parson Bay sedimentary sequences. It is clear from the textures and mineralogy of the volcanic constituents that most, if not all, of these deposits represent the products of renewed volcanic activity and therefore record the encroachment and initial phases of Bonanza arc volcanism.

PARSON BAY FORMATION

The Parson Bay Formation is exposed in the core of a northerly-trending syncline in the high ground between Nimpkish and Bonanza lakes, and at the south end of Nimpkish Lake in a region of low to moderate relief. The thickness of this unit is difficult to estimate due to poor exposure combined with localized internal structural disruption and a plethora of hypabyssal dikes and sills that invade these rocks. In the Alice Lake area to the west, Muller *et al*. (1974) estimated a true stratigraphic thickness of about 600 m, whereas only the basal 50 m of Parson Bay strata are recorded in their Beaver Cove section (Fig. 4).

QUATSINO – PARSON BAY TRANSITION

The contact with the underlying Quatsino Formation limestone is conformable and sharply gradational to transitional over widths of 0.5–5 m. This thinly bedded interval is generally marked by intercalations of pale grey–weathering Quatsino limestone and dark grey, impure (siliceous to sandy) limestone, calcareous mudstone and siltstone, and minor, locally fossiliferous (*Halobia* sp.) black shale.

The age of the Parson Bay – Quatsino contact in the Nimpkish area has been established from collections of conodont fauna identified by M.J. Orchard, Geological Survey of Canada. Sample locations are plotted in Figure 4 where their age assignments are indicated. Most of the samples were collected in the northwestern part of the map area on both flanks of the major syncline. Micritic and impure limestone beds from the uppermost Quatsino and lowermost Parson Bay formations, including strata at several localities within 3–20 m of the contact, yield Late Carnian conodont faunas. A single site in the northeast, where Parson Bay rocks are tightly folded and faulted, has produced

an Early Norian fauna. Thus, the Quatsino – Parson Bay transition in the Nimpkish area may confidently be placed within the Late Carnian, possibly close to the Carnian–Norian boundary. This contact is regionally diachronous because, to the west in the Alice-Kathleen lakes area, it is straddled by late Early Norian conodont faunas (Nixon *et al*., 2000), and on the west coast is restricted once more to the Carnian, according to ammonite collections summarized by Muller *et al*. (1974).

SEDIMENTARY STRATA

Typical Parson Bay sedimentary rocks include grey to black, thinly laminated to thickly bedded, impure micritic limestone, mudstone, siltstone, shale, and grey-brown to pale buff, fine to coarse-grained feldspathic sandstone. Locally, thin (<5 cm), ochre to pale grey–weathering clay-rich beds may reflect layers rich in tuffaceous (vitric?) material. Clastic beds are commonly calcareous and shale beds may be distinctly carbonaceous; graphite commonly occurs where the latter rocks are cut by faults. Bedding is predominantly planar, and rare wavy laminations in limestone possibly represent the vestiges of algal mats. Certain beds are strongly silicified and pyritic, or impregnated by finely disseminated hematite, and finely disseminated diagenetic pyrite is widespread. Localized bleaching and recrystallization of impure limestone to marble occurs near intrusive contacts with the Island Plutonic Suite.

In the lower part of the Parson Bay Formation, thin-shelled pelecypods, tentatively identified as *Halobia* sp. (Carnian to Middle Norian), are commonly found in the fine-grained siliciclastic beds and are especially abundant in certain shaly horizons. Higher in the stratigraphy, bivalves, tentatively identified as *Monotis* sp. (Late Norian), are locally abundant in black fissile shale. Most of these strata probably represent a low-energy, shallow-marine environment, although mudstone at one locality exhibits desiccation cracks, which is indicative of intertidal conditions.

Volcanogenic rocks, including feldspathic wacke, breccia and rare conglomeratic beds, are a distinctive though subordinate component of the Parson Bay succession in the Nimpkish area (Fig. 4). These deposits are intercalated with typical, and locally fossiliferous, Parson Bay strata, and were obviously deposited in the same shallow-marine environment.

VOLCANIC ROCKS

A variety of bedded volcaniclastic deposits, including volcanic wacke and lithologically diverse breccia and minor lavas, is found at widely dispersed localities within the Parson Bay Formation. Some are mappable units of volcanic breccia, lava and interbedded sedimentary strata; others form more localized deposits at the scale of a bed, or thin sequence of beds, within the stratigraphic succession (Fig. 4).

Two northwesterly-trending volcanic sequences occur near the southern end of Nimpkish Lake and appear to sit conformably within the Parson Bay succession. The western sequence contains thickly bedded volcanic breccia, medium-bedded feldspathic wacke, laminated siltstone and massive lavas. The dark grey-green breccia contains poorly sorted, angular to subangular andesitic clasts (<1.5 cm) in a fine-grained plagioclase-bearing matrix. The clasts show similar textures: plagioclase microlites are set in a clay-sericite-altered and devitrified volcanic glass. Their matrix-supported character and preferred orientation suggests deposition by turbidites. The associated lavas are finely amygdaloidal, plagioclase-phyric andesite. Euhedral to subhedral plagioclase phenocrysts and glomerocrysts (<4 mm across and up to 15 vol%) are set in a devitrified and clay-sericite-altered glassy groundmass containing microlitic plagioclase. Irregular amygdules are lined with quartz and infilled with chlorite. Thin beds of water-laid volcanic breccia along strike to the northwest (Fig. 4) contain two basaltic clast types: angular to subangular lithic clasts with large (<5 mm) euhedral–subhedral plagioclase phenocrysts, and clasts enclosing euhedral clinopyroxene (<2 mm) that shows pronounced normal zoning. These deposits are also associated with feldspar-bearing and lithic-rich volcanic wacke.

The eastern volcanic sequence is partly fault bounded, and its exact stratigraphic position is uncertain. Although placed in the Parson Bay Formation, it may locally represent the base of the 'Bonanza volcanics'. The dominant rock types are variably reworked, dusky red to dark grey-green volcanic wacke and breccia. Two end-member types of monolithic breccia have been identified, both containing angular to subrounded volcanic clasts typically less than 1 cm across. Felsic volcanic breccia contains fragments with euhedral to subhedral phenocrysts (<3 mm) of plagioclase, minor euhedral mafic microphenocrysts (<0.5 mm) pseudomorphed by chlorite, and trace amounts of resorbed to subhedral quartz set in a devitrified glassy groundmass free of plagioclase microlites. Their mafic counterparts have clasts that are generally crowded with plagioclase microlites enclosed in a nearly opaque, oxide-charged groundmass. In one sample, these clasts contain subhedral phenocrysts of clinopyroxene with few feldspar microlites. The volcanic wacke is coarse to medium grained, thickly bedded to laminated, enriched in lithic fragments and plagioclase, and contains detritus of mixed parentage. Well-bedded sequences may be normally graded and locally contain worm burrows. Minor intercalated sedimentary strata include calcareous mudstone, siltstone and limestone.

Small outcrops of mafic volcanic breccia occur close to the contact with Quatsino limestone between Hustan and Nimpkish lakes (Fig. 4). Angular to subrounded, lapilli-size basaltic clasts are enclosed in a poorly sorted, massive deposit. The clasts are weakly amygdaloidal and sparsely feldspar porphyritic. Plagioclase microlites in the groundmass are set in an altered and recrystallized volcanic glass studded with granular secondary sphene. The fine-grained clastic matrix is cemented and partly replaced by carbonate, potassium feldspar, quartz, epidote, minor prehnite and opaque oxides. The clasts may represent formerly palagonitized hyaloclastite material redeposited in the shallow-marine environment.

West of Bonanza Lake, virtually monolithic volcanic breccia contains clasts of strongly amygdaloidal basalt with euhedral and sector-zoned clinopyroxene phenocrysts (<1 mm) and glomerocrysts (<2 mm) set in a devitrified glass rich in flow-aligned plagioclase microlites. The clastic matrix contains similar basaltic material, opaque oxides, trace subhedral hornblende and devitrified glass shards. Clinopyroxene phenocrysts are locally intergrown with a mafic mineral (olivine?) pseudomorphed by opaque oxide, carbonate, and cryptocrystalline serpentine-actinolite (?). These massive beds are overlain by thin to medium-bedded pyritic siltstone and lithic-crystal tuffaceous wacke.

Thin volcaniclastic sequences are interbedded with typical Parson Bay rocks on the western flank of the northerly-trending syncline east of Nimpkish Lake, and lie stratigraphically below the base of the central outlier of 'Bonanza volcanics' (Fig. 4). Dark grey-green, bedded volcanic breccia and buff-weathering feldspathic-lithic wacke are intercalated with dark grey calcareous mudstone and siltstone. Locally, dewatering structures are well developed in the sandstone and mudstone (Fig. 8). The volcanic breccia contains angular to subrounded basaltic clasts mineralogically and texturally similar to those observed in the overlying 'Bonanza volcanics' (described below). The transition from marine sedimentary strata to predominantly volcaniclastic deposits, which defines the base of the 'Bonanza volcanics' at this locality, appears conformable.



Figure 8. Well-developed load casts with ball and flame structures in calcareous mudstone – feldspathic lithic wacke sequence near top of Parson Bay Formation and just below the 'Bonanza volcanics' unit, central part of core of major syncline (locality 05MEL-22-21-1); hammer is 35 cm in length.

'BONANZA VOLCANICS'

In the Nimpkish area, the 'Bonanza volcanics' conformably overlie shallow-marine sedimentary strata of the Parson Bay Formation. The base of this map unit is taken as that point in the stratigraphic column at which volcanic rocks, either clastic or lavas, become dominant. Due to the rapidly changing nature of volcanic environments, particularly those straddling the land-water interface, lateral facies variations are expected to be diverse and abrupt. Thus, the base of this predominantly volcanic succession is anticipated to be diachronous and likely to be defined by different volcanic rocks in different areas. Furthermore, where sedimentary and volcanic rocks are interbedded and exposure is limited, as in the study area, this contact may be difficult to define precisely. This problem is further compounded by the superabundance of subvolcanic dikes and sills that intrude the Parson Bay succession.

The aerial extent of 'Bonanza volcanics' in the Nimpkish map sheet has been significantly reduced in comparison to earlier mapping (Muller *et al*., 1974; Muller and Roddick, 1983). This appears to be a direct consequence of adopting the above definition for the 'Bonanza volcanics', since Muller *et al*. (1974) placed the base of this unit where they encountered the first occurrence of volcanic breccia or lava in the stratigraphic succession. Since only the lowermost part of the 'Bonanza volcanics' appears to be preserved, their thickness in the Nimpkish area cannot be meaningfully estimated. However, based on a measured section near Cape Parkins at the entrance to Quatsino Sound, the average thickness of the volcanic succession is estimated to be 2600 m (Muller *et al*., 1974).

The 'Bonanza volcanics' in the study area are preserved in the northern and central sectors of the northerly-trending syncline between Nimpkish and Bonanza lakes (Fig. 4). Similar volcanic rocks exposed farther south in a structurally complex area near the western margin of the Nimpkish Batholith have tentatively been assigned to the Parson Bay Formation (discussed above). Lava flows predominate in the north and volcanic breccia units in the south; intercalated sedimentary strata are a minor component of both packages.

The northern outlier of 'Bonanza volcanics' is composed of pale grey to buff-weathering, massive, aphanitic to porphyritic basaltic lavas and minor fine-grained sedimentary rocks. The basalts are dark green-grey to reddish grey or maroon lavas that generally carry phenocrysts of pyroxene and rarely plagioclase, and commonly exhibit amygdaloidal textures. In thin section, subhedral phenocrysts (<1 mm) and monomineralic intergrowths (<4 mm) of clinopyroxene are set in a fine-grained groundmass of plagioclase, granular pyroxene and opaque oxides partially altered to clay and sericite. Some lavas contain mafic phenocrysts (olivine or orthopyroxene) completely pseudomorphed by microcrystalline oxides, chlorite and serpentine (?). Amygdules are commonly filled with chlorite, epidote, quartz, carbonate and zeolite.

The associated sedimentary rocks are dark grey to black fissile shale and thinly laminated to medium-bedded mudstone with poorly preserved bivalve fragments. Multiple thin basaltic dikes (<2 m in width) intrude the sedimentary strata but commonly cannot be seen to cut the overlying basalt. At one locality, the dense, bulbous base of the overlying lava clearly transects underlying shale without significant deformation. Rare internal flow structures have been observed, but no definitive flow contacts with surrounding sedimentary strata were found. The textures are clearly indicative of high-level emplacement, and these rocks may represent the roots of a small volcanic complex that preserves both intrusive and extrusive facies. The authors have therefore tentatively included this complex as a stratigraphic component of the 'Bonanza volcanics'.

The central outlier of 'Bonanza volcanics' is composed of basaltic volcanic breccia and interbedded marine sedimentary rocks. The breccia is yellowish to purplish brown or very pale grey weathering and dark grey-green on fresh surfaces. Angular to subrounded lapilli-size clasts in the massive to crudely bedded coarser breccia may reach 8 cm across; angular blocks up to 1 m in length are rarely observed. Maximum clast size in the finer grained deposits rarely exceeds ~1 cm and grades down into sub-millimetre-

size fragments. The breccia ranges from framework to matrix-supported types and is monolithic to weakly heterolithic with sparse, angular to subangular fragments of mudstone, wacke and limestone. The finely comminuted matrix is commonly cemented by carbonate and prehnite, and locally silicified. Most outcrops of coarse volcanic breccia show little sorting or bedding. However, thin intervals of finer grained, variably sorted volcanic breccia are generally well bedded, and locally exhibit trough-shaped bedding (Fig. 9). Intercalated with the volcanic breccia are pale grey to buff-weathering, dark grey to black, thinly laminated to medium-bedded mudstone, shale and limestone, and subordinate feldspar-lithic sandstone. Some clastic beds are calcareous or silicified, and locally yield poorly preserved fossils.

In thin section, basaltic clasts in the breccia commonly show amygdaloidal textures with carbonate and prehnite infillings, and contain abundant flow-aligned plagioclase microlites (<0.5 mm) and sparse clinopyroxene set in a groundmass of finely crystalline plagioclase, opaque oxides and grey-brown, clay-carbonate-altered devitrified glass. The interbedded sandstone is moderately to poorly sorted volcanic wacke rich in euhedral to anhedral and broken plagioclase and small (<2 mm) basaltic clasts mineralogically similar to their host volcanic breccia.

Although the carbonate and siliciclastic beds intercalated with the volcanic breccia are lithologically similar to the Parson Bay strata, these rocks have been provisionally placed within the 'Bonanza volcanics'. This assignment was influenced by the predominance of volcanic rocks and, though by no means definitive, the lack of conodont fauna in a single sample of interbedded limestone (Fig. 4).

The textural features of basaltic clasts in the breccia, specifically their amygdaloidal character, former glassy groundmass and hyalopilitic fabric displayed by plagioclase microlites, indicate that they formed by fragmentation of lavas flows and were deposited in a near-vent environment. Certain matrix-supported deposits were clearly emplaced by mass flowage. The clast-supported breccia is more difficult to interpret, but possible emplacement mechanisms include deposition by normal epiclastic processes and explosive hydromagmatic activity.

INTRUSIVE ROCKS

All the major intrusions in the Nimpkish area belong to the Island Plutonic Suite; the vast majority of the minor intrusive bodies in the Nimpkish area are apophyses of these granitoid rocks or high-level basaltic to rhyolitic dikes and sills related to Bonanza volcanism.

Island Plutonic Suite

Granitoid intrusions of the Island Plutonic Suite underlie significant tracts of terrain in the southern half of the map area and form the northern termination of the northwesterly-trending Nimpkish batholith and its satellite plutons (Carson, 1973; Muller *et al.*, 1974). Conventional K-Ar dates on hornblende and biotite from granitoid rocks in the Nimpkish map sheet have yielded isotopic ages of *ca.* 147–173 Ma (Wanless *et al.*, 1967, 1968, 1974; Breitsprecher and Mortensen, 2004). However, the reliability of these older K-Ar dates and their significance in terms of constraining the age of crystallization have been questioned (Archibald and Nixon, 1995; DeBari *et al.*, 1999, 2000). A more recent U-Pb zircon date of 168.6 ±5.6 Ma (95% confidence level) was reported by DeBari *et al.* (1999) for a sample of hornblende-biotite quartz diorite from the Nimpkish Batholith collected in a roadcut on Highway 19 approximately 5 km beyond the southeastern corner of the Nimpkish map sheet. This date is comparable to U-Pb and Ar^{40}/Ar^{39} dates on zircon and hornblende, respectively, which have been obtained for some of the youngest members of the Island Plutonic Suite on northern Vancouver Island (Friedman and Nixon, 1995; Archibald and Nixon, 1995).

In the Nimpkish area, intrusions of the Island Plutonic Suite are buff to pale grey or grey-green-weathering, medium to coarse-grained, heterogeneous granitoid bodies with equigranular to inequigranular or weakly porphyritic textures. According to the IUGS modal classification (LeMaitre, 1989), the principal rock types (estimated visually) are hornblende and biotite-bearing granodiorite and tonalite, with minor quartz diorite, diorite, granite and quartz-feldspar and potassium feldspar-megacrystic porphyry. Quartz forms anhedral, interstitial grains in the granitoid and rounded to subhedral phenocrysts in the porphyry. Euhedral megacrysts of subequant potassium feldspar (<2 cm) characterize a minor granite phase located near the southwestern margin of the eastern Nimpkish Batholith. Weakly chloritized mafic minerals, hornblende and biotite, generally occur in subequal proportions and constitute 5–15 vol% of the granodiorite-tonalite suite and up to 25 vol% of the dioritic rocks. Anhedral to euhedral bi-



Figure 9. Lenticular bedding in mafic, moderately sorted, water-laid volcanic breccia (cemented by calcite and zeolite) near the base of the 'Bonanza volcanics' unit in central part of core of major syncline (locality 05MEL-21-3-1); hammer is 35 cm in length.

otite crystals locally occur as well-developed books (<6 mm), and hornblende is generally prismatic and more abundant in the dioritic rocks. Locally, the Noomas pluton contains subhedral hornblende crystals up to 1 cm; and biotite is the dominant mafic constituent in the Bonanza pluton. A few samples of the latter intrusion exhibit poorly developed micrographic to granophyric textures. Colourless clinopyroxene crystals are rare and usually occur as resorbed relict grains within hornblende. Accessory minerals include Fe-Ti oxides, apatite and zircon. Alteration assemblages involve chlorite, epidote, sericite, carbonate, hematite, sphene and clay minerals, and minor disseminated pyrite.

Contacts with the country rock are generally sharp and steeply inclined to vertical. Locally, planar to irregular vein networks are well developed in hostrocks and some contacts are defined by faults. Dark grey-green, rounded to elongate dioritic xenoliths, typically less than 10 cm across and rarely reaching 1 m, are a common though generally sparse constituent of all plutons. Locally, xenolith-rich zones exhibit a pronounced magmatic flow foliation. In the eastern part of the Nimpkish batholith, extensive zones of agmatite are developed in Karmutsen wallrocks (Fig. 4). The agmatite involves subrounded to angular blocks (>1 m) of dark green-grey, aphanitic Karmutsen basalt set in a net-veined granitoid mesostasis. Although the xenoliths are amphibolitized and hornfelsed, original amygdaloidal textures are locally preserved. The occurrence of agmatite zones well within the batholith most likely indicates proximity to the roof.

Minor Intrusions

Dikes and sills (approx. 0.1–20 m in width) associated with the emplacement of volcanic sequences in the Bonanza Group cut older rocks of the Vancouver Group. They are typically fine grained and range in composition from basalt to rhyolite. The basaltic to andesitic intrusions are by far the most abundant. Some dikes branch repeatedly to form complex geometries without any deformation of adjacent bedding. Sill-like intrusive geometries are preferentially developed in the Parson Bay rather than the Quatsino and Karmutsen formations, presumably reflecting the well-bedded nature and lower lithostatic pressure of this part of the Bonanza Group at the time of intrusion.

The basaltic to andesitic intrusive rocks are dark grey-green to black, buff to pale green-grey-weathering rocks with aphanitic to porphyritic textures. These intrusions have well-developed chilled margins and commonly exhibit amygdaloidal interiors where amygdules are locally elongated to define a pronounced flow fabric parallel to their contacts. The porphyritic dikes generally carry euhedral to subhedral phenocrysts of plagioclase (<4 mm) that form up to 15 vol% of the rock. Subhedral clinopyroxene phenocrysts (up to 8 mm in size and 5 vol%) may coexist with feldspar, or represent the sole phenocryst phase, in which case glomeroporphyritic textures are common. The groundmass is typically very fine grained and usually carries devitrified and altered glass impregnated with opaque oxides.

The felsic intrusions are aphanitic to rarely feldspar phyric and may exhibit a marked flow lamination adjacent to their contacts. Dike interiors generally lack this fabric. Porphyritic intrusions contain sparse subequant plagioclase up to 3 mm in length and constituting up to 2 vol% of the rock. Many felsic dikes are intensely weathered and altered to assemblages of quartz, epidote, chlorite, carbonate, hematite, limonite and zeolite (?); pyrite may form up to 5 vol% of the rock.

Many of the dikes exploit fault zones where postemplacement motion has resulted in the growth of slickenfibres of secondary minerals, commonly epidote and quartz. These minerals, together with carbonate, zeolite, albite (?) and potassium feldspar (rare) are the most common vein minerals.

Minor apophyses of the Island Plutonic Suite are medium to coarse grained, equigranular to porphyritic, and dioritic to tonalitic. These dikes and sills range in thickness from less than 10 m to greater than 100 m. Most of the intrusions are hornblende diorite (locally clinopyroxene-bearing) or quartz diorite, leucocratic tonalite and quartz-plagioclase (±potassium feldspar) porphyries. Biotite and hornblende are the principal ferromagnesian minerals and typically constitute less than 5 vol% of the more leucocratic rock types and 15 vol% or more of the dioritic intrusions. Alteration minerals include chlorite, sericite, epidote, chlorite, sericite, actinolite and clay minerals. Silicification is locally pervasive and usually accompanied by minor disseminated pyrite.

The porphyritic rocks carry phenocrysts (<5 mm) of subequant plagioclase and resorbed quartz set in a microcrystalline quartzofeldspathic groundmass. Some display prominent macroscopic quartz-eye textures. A rare variety of granitic dike contains euhedral blocky megacrysts (1–2 cm in length) of potassium feldspar. Pale grey tonalite dikes at the southwestern margin of the Noomas pluton, just south of a large screen of Quatsino limestone, exhibit large (<10 cm in length) elongate gas cavities (miarolitic) infilled with coarsely crystalline dark green epidote, clearly indicative of high-level emplacement (Fig. 10).

STRUCTURE

The Nimpkish map area is underlain by a southwesterly to westerly-facing, moderately dipping, homoclinal succession cut by major high-angle faults trending northerly to northwesterly. This succession lies on the western flank of a major, northerly-trending anticlinal structure, the 'Victoria arch' (Muller *et al*., 1974), cored by Paleozoic basement rocks. This structure continues south as the Buttle Lake anticlinorium (Monger and Journeay, 1994).

The major faults are generally hidden by lakes and till-covered valleys but marked by strong lineaments. The Nimpkish-Hustan and Bonanza faults bound a downthrown block containing the youngest stratigraphic units ('Nimpkish block' of Muller *et al*., 1974). The amount of displacement by faulting is not well constrained. However, judging from the prevalence of shallowly dipping slickenfibres on fault planes throughout the area, the sense of motion was oblique slip.

The 'Nimpkish block' contains the axis of a major north-northwesterly-trending synform that preserves the Parson Bay Formation and the lowermost part of the 'Bonanza volcanics'. The strata on the flanks of this open fold dip moderately (20–30°) toward the core. Superimposed on this synclinal structure, and preferentially developed in the well-bedded sequences of the Parson Bay Formation, are tight, locally chevron-style folds, one to several metres in

amplitude with upright to recumbent or overturned attitudes. In outcrops with adequate exposure, these folds form discrete packages bounded by low-angle fault surfaces (with apparent thrust motion) oriented subparallel to the attitude of the bedding outside the zone of compressional deformation. Minor fold axes may be oriented at high angles to the trend of the major syncline. These structures appear to have a complex history and their origin is not well understood. They may have been formed during flexural-slip folding and compression in the cores of the larger structures, or generated by transpressional strike-slip faulting, or both.

The timing of regional, east to northeast-directed compressional deformation on northern Vancouver Island is constrained to be younger than Middle Jurassic (post-Bajocian, the age of the youngest volcanic rocks in the Bonanza Group; Friedman and Nixon, 1995) and older than the Early Cretaceous (Hauterivian–Valanginian) strata that rest with angular unconformity on the Bonanza Group (Nixon *et al*., 1993a, 1994a, 1995a). This episode of deformation may be further constrained to be late Middle to early Late Jurassic, since clastic strata ('White Point Beds') of Upper Jurassic age (late Oxfordian to Tithonian) underlie Lower Cretaceous sequences in the Queen Charlotte Islands (Gamba, 1993; Haggart and Carter, 1993). This contractional event was followed by uplift and erosion prior to deposition of Jurassic–Cretaceous sedimentary strata.

The history of faulting on northern Vancouver Island is complex and embodies Cretaceous transpression and Tertiary extension. Extensional faulting and diking evidently occurred early during Bonanza volcanism. Major northwesterly-trending faults displace (in a right-lateral sense), and locally fold, Early to early Late Cretaceous sedimentary sequences exposed in the Quatsino Sound area (Muller *et al*., 1974; Nixon *et al*., 1993a. 1994a, 1995a). In the Nimpkish area, the Kokish fault and northwesterly-trending structures that cut the Nimpkish batholith at the southern margin of the map area may well share a similar history. Northerly-trending structures, such as the Nimpkish-Hustan and Bonanza faults, may record Tertiary block-faulting near the southern margin of the Queen Charlotte Basin. Faulting appears to have continued through to the end of Neogene volcanism (Muller *et al*., 1974).

MINERAL OCCURRENCES

The Nimpkish area hosts a variety of base and precious-metal deposits, and is perceived as a region of future mineral potential (Massey, 1995d). The map area contains some 34 mineral occurrences (MINFILE, 2005), including skarn and manto deposits, Cu-Au-Mo porphyry, volcanic redbed Cu, and Au, magnetite and sulphide-bearing vein and stockwork systems (Fig. 11). The area also has a prior history of extraction of industrial minerals, notably limestone and marble.

The major metalliferous deposit types in the Nimpkish area are intrusion-related skarns and mantos clustered about the margins of the Island Plutonic Suite and hosted by Quatsino limestone and calcareous strata of the Parson Bay Formation. Mineralization is particularly extensive at the margins of the Noomas pluton and western part of the Nimpkish batholith. New skarns and a manto occurrence were also investigated during the 2005 field season



Figure 10. Flow-aligned miarolitic cavities filled with radiating epidote crystals in tonalitic dike at southwestern margin of Noomas pluton near Storey Creek (locality 05GNX-4-3-1); pencil magnet is 12 cm in length.

(Fig. 11). Lithogeochemical assays of selected known and new occurrences are given in Tables 1 and 2.

One of the largest Fe and Pb-Zn-Cu skarn systems is hosted by an enclave of Quatsino limestone at the southwestern margin of the Noomas Pluton (Fig. 11). The Smith Copper deposits (MINFILE 92L 037/208) have drill-indicated reserves of approximately 84 000 t grading 12.5 wt% Zn, 3.7% Pb, 1.69% Cu and 64.4 g/t Ag. The mineralization contains sphalerite, galena, pyrrhotite, chalcopyrite, pyrite and magnetite set in a gangue assemblage of pyroxene, garnet, epidote, chlorite, quartz and carbonate. Some of the thin (<2 m) calcsilicate skarns also contain subhedral to rounded crystals of chondrodite (?) up to 1 cm in size and coarsely prismatic diopside up to 3 cm. The main zone of mineralization trends ~340° and dips to the southwest, locally coincident with the attitude of the major lithostratigraphic units. Extensive calcsilicate skarn assemblages were also discovered at the northern margin of this pluton, although sulphide mineralization does not appear to be as common. A well-mineralized Fe-Zn skarn containing sphalerite, pyrite, malachite and magnetite from the eastern margin of this pluton, and close to the Wolf occurrence (MINFILE 92L 121), gave 2.3% Zn, 0.27% Cu, 7.5 g/t Ag and anomalous gold (50 ppb Au; Tables 1 and 2).

At the northwestern termination of the Nimpkish batholith, a Cu-Mo prospect (92L 207) and Fe-Cu-Au-Zn skarns (Nimpkish Copper; MINFILE 092L 036, plus 118–120) occur at the contact with Quatsino limestone (Fig. 11). Assays of drillcore reach 0.29% Cu and 85 g/t Au over

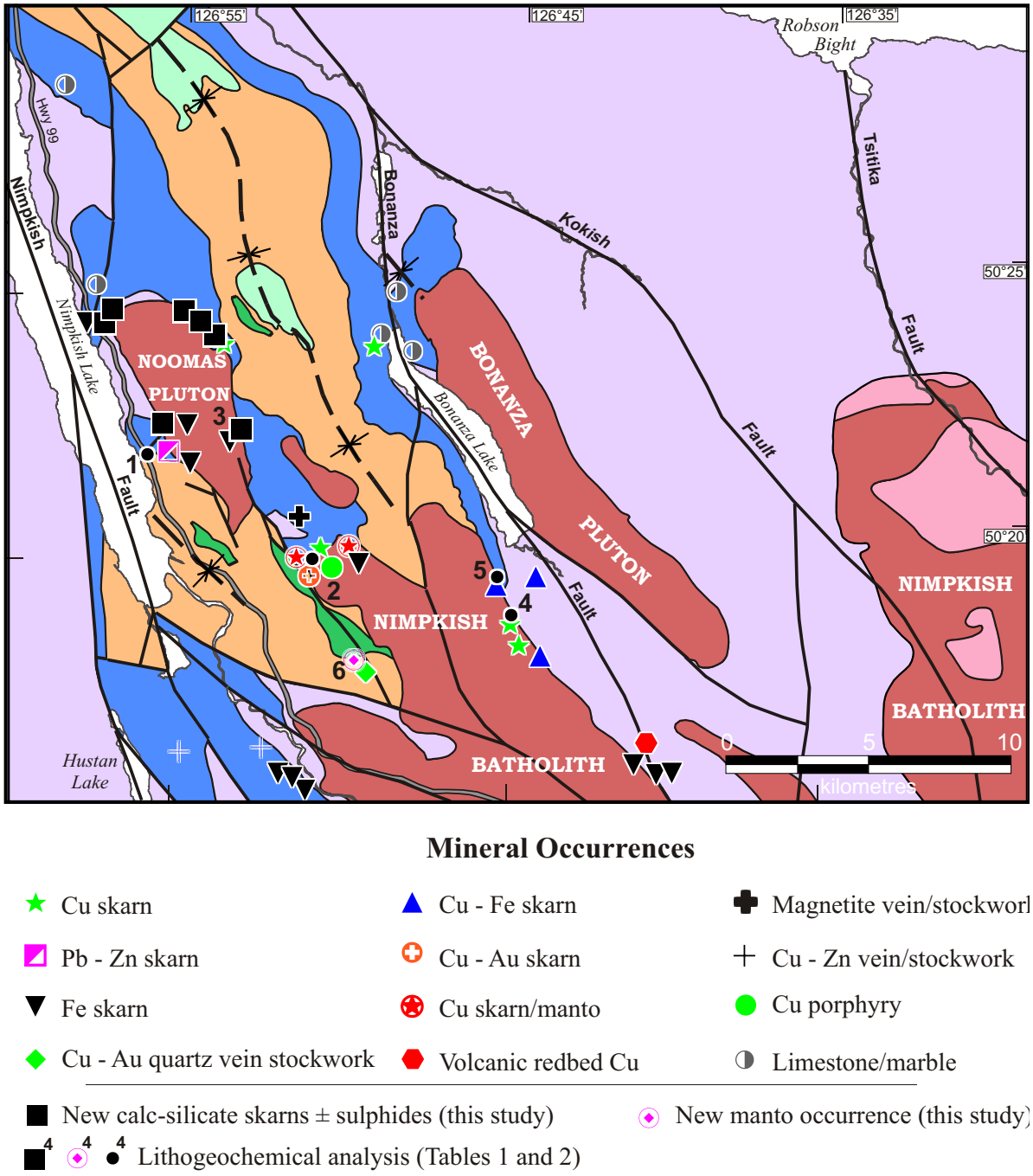


Figure 11. Geological setting of metallic and industrial mineral occurrences (MINFILE, 2005) and new showings (this study) in the Nimpkish area.

small widths (0.7 m), and a nearby trench has assayed 17.6% Zn and 0.73% Cu over 0.5 m. The mineralization occurs in small lensoid bodies (6 m long by 0.5 m thick) in Quatsino limestone that contain covellite, sphalerite, pyrrhotite, pyrite, malachite, molybdenite and bornite. A grab sample of massive pyrrhotite-pyrite ore in calcsilicate skarn collected during this study returned 0.18% Cu, 900 ppb Ag and 230 ppm Co (Table 1). The Cu-Mo porphyry-style mineralization is hosted by a shear zone where a quartz stockwork carries chalcopyrite and pyrite.

Copper-iron skarn deposits at the eastern margin of the Nimpkish batholith south of Bonanza Lake are hosted by Quatsino and intra-Karmutsen limestone (Fig. 11). The former Steele Creek open pit mine (MINFILE 92L 164) produced 4718 t of 2.48% Cu and 8.7 g/t Ag in 1968–1971. Drillcore samples taken in 1994 returned up to 0.38% Cu and 2.8 g/t Ag. The mineralization contains chalcopyrite, pyrite, malachite, and magnetite in a calcsilicate gangue. A high-grade grab sample collected during this study gave 23.3% Cu, 170 g/t Ag and 1330 ppm Co (Tables 1 and 2). Copper-iron skarn mineralization further north (MINFILE

TABLE 1. LITHOGEOCHEMISTRY OF MINERALIZED SAMPLES, NIMPKISH AREA

Map ID		1	2	3	4	5	6	6			
Sample		05GNX-2-8-1	05GNX-7-17-3	05DSV-4-1-1	05DSV-5-6-1	05DSV-6-2-1	05DSV-5-7-1	05DSV-5-7-1[1]	GSB Till 99	GSB Till 99	Difference (%)[2]
NAD83	Easting	646997	652808	650237	659796	654312	659273	659273	Internal	Mean of	
(Zone 9)	Northing	5581282	5577604	5582166	5575629	5574048	5577002	5577002	standard	10	
Ti	(wt%)	0.53	0.01	0.04	0.02	0.03	<0.001	0.001	0.54	1.13	71.1
Al	(wt%)	7.03	0.05	0.51	0.23	0.43	0.77	0.78	6.85	6.40	6.8
Fe	(wt%)	7.92	59.19	42.92	34.72	15.93	24.80	24.94	8.31	9.20	10.2
Mg	(wt%)	8.23	0.04	1.20	0.67	0.98	0.03	0.04	3.45	3.61	4.5
Ca	(wt%)	8.12	0.10	8.27	6.05	15.34	1.97	1.57	1.00	1.00	0.0
Na	(wt%)	0.97	0.01	0.05	0.01	0.03	0.01	0.01	1.90	1.85	2.6
K	(wt%)	0.04	<0.02	0.02	<0.02	<0.02	<0.02	<0.02	0.83	1.57	61.6
P	(wt%)	0.03	0.03	0.02	0.02	0.02	0.00	<0.001	0.12	0.12	0.9
S	(wt%)	0.11	>10	5.25	>10	3.46	>10	>10	0.01	0.01	0.0
Mo	(ppm)	0.3	2.1	1.3	0.7	0.4	19.6	18.9	0.9	0.8	11.8
Cu	(ppm)	63	1798	2733	>10000	208	>10000	>10000	190	186	2.2
Pb	(ppm)	0.8	3.7	4.3	174	4.7	574	656	236	241	2.1
Zn	(ppm)	63	34	>10000	768	>10000	>10000	>10000	438	388	12.2
Ag	(ppb)	50	919	7511	>200000	487	>200000	>200000	1366	1575	14.2
Au[3]	(ppb)	6	17	51	375	3	170	95	30	36	18.2
Li	(ppm)	2.7	0.2	0.8	0.1	1.2	0.4	0.4	35		
Cs	(ppm)	0.2	0.1	0.4	0.1	0.1	0.1	0.1	1.5	1.9	23.5
Ba	(ppm)	23	2	17	1	20	2	2	784	846	7.6
Rb	(ppm)	0.9	0.3	0.8	0.1	0.2	0.2	0.2	26	48	57.7
Sr	(ppm)	200	3	38	1	44	257	266	104		
Sc	(ppm)	38	0.1	1.7	0.6	1.1	<0.1	<0.1	28.2	13	73.8
V	(ppm)	261	<1	8	12	10	2	4	197	107	59.2
Cr	(ppm)	448	6	9	6	5	1	1	323	398	20.8
Ni	(ppm)	370	5	2	314	2	112	128	220	261	17.0
Co	(ppm)	67	234	37	1332	300	557	604	50	53	5.0
Mn	(ppm)	1520	117	17598	726	26017	671	600	1394	1516	8.4
Hf	(ppm)	0.83	0.02	0.33	0.15	0.10	0.02	<0.02	0.79	3.64	128.7
Zr	(ppm)	17	0.4	7	4	3	0.6	1	23	108	130.3
Nb	(ppm)	<1	<1	<1	<1	<1	<1	<1	9		
Y	(ppm)	18.2	0.2	2.9	1.1	2.8	1.2	1.5	16.7	27	47.1
U	(ppm)	0.1	10.8	1.8	1.3	0.9	0.2	0.3	0.9	1.4	43.5
Ce	(ppm)	4.46	0.35	2.67	2.13	1	0.48	0.58	37.74	52.73	33.1
Ga	(ppm)	13.98	1.11	3.8	4.49	1.63	2.74	2.69	17.69		
Cd	(ppm)	0.07	0.63	166	81.34	601	2164	2091	1.11	0.74	40.0
As	(ppm)	2.1	<0.2	11.8	77.4	22	5	5	64.3	70	8.5
Sb	(ppm)	0.08	0.08	3.21	0.2	1.5	0.52	0.53	13.66	15.28	11.2
Bi	(ppm)	<0.04	5.87	1.63	16.15	1.36	97.91	118.68	0.22	0.13	51.4
Sn	(ppm)	0.4	<0.1	0.6	13	0.1	0.5	0.6	1		
W	(ppm)	<0.1	0.6	58.5	4.8	0.4	8.4	4.3	0.5	0.1	133.3

Sample descriptions: 1, volcanic wacke with diseminations and veins of pyrite+chlorite; 2, massive pyrrhotite-pyrite ore in calcsilicate skarn; 3, pyrite-sphalerite-magnetite-malachite in calcsilicate skarn; 4, pyrite-chalcopyrite-malachite-magnetite in calcsilicate skarn; 5, massive stratiform sphalerite-greenockite-chalcopyrite-pyrrhotite manto; 6, chalcopyrite-pyrite-malachite-bornite-Native Cu in calcsilicate skarn

Samples jaw crushed at the BC Geological Survey (Victoria), then pulverized in a steel mill at Acme Analytical Laboratories Ltd. (Vancouver); glass wash between each sample; all analyses performed by four-acid digestion inductively coupled plasma emission/mass spectrometry

[1]hidden duplicate

[2]percent difference calculated as the difference between analyzed value of GSB Till 99 and the mean of ten previous analyses

[3]analysis by lead-collection fire-assay with ICP-ES finish

92L 134), near the Quatsino-Karmutsen contact, carries chalcopyrite, pyrite, bornite, sphalerite, malachite, native copper and magnetite. A high-grade grab sample gave 18.6% Cu, 17.5% Zn, 200 g/t Ag, 95–170 ppb Au, 600 ppm Co, 2100 ppm Cd and 100 ppm Bi (Tables 1 and 2).

A new mineral showing was discovered at the end of a short spur off a new logging road system near the western margin of the Nimpkish batholith. The mineralization is hosted by dark grey to black, medium to thinly bedded limestone, calcareous mudstone, siltstone and shale of the

TABLE 2. ASSAYS OF ORE-GRADE SAMPLES, NIMPKISH AREA

Map ID	3	4	5	6	6
Sample	05DSV-4-1-1	05DSV-5-6-1	05DSV-6-2-1	05DSV-5-7-1	05DSV-5-7-1[1]
Fe (wt%)	39.48	30.95	16.32	22.09	22.13
Mn (wt%)	1.72	0.07	2.60	0.06	0.06
Cu (wt%)	0.24	23.27	0.05	18.62	18.58
Pb (wt%)	<0.02	<0.02	<0.02	0.05	0.05
Zn (wt%)	2.27	0.06	8.06	17.52	17.11
Cd (wt%)	0.015	0.007	0.055	0.183	0.175
Ag (ppm)	9	170	<2	189	201

Sample locations and descriptions given in Table 1

Samples jaw crushed and pulverized in a steel mill at Acme Analytical Laboratories Ltd.; glass wash between each sample; all analyses (0.5 g sample) performed by four-acid digestion inductively coupled plasma emission spectrometry

[1]hidden duplicate

Parson Bay Formation near the contact with interbedded, mafic volcanic breccia (Fig. 11). The mineralization forms a thin (~0.5 m) stratiform horizon composed mainly of sphalerite with minor greenockite bloom and malachite staining. A grab sample assayed 8.1% Zn, 200 ppm Cu, 600 ppm Cd and 500 ppb Ag (Tables 1 and 2). The showing appears to represent a manto deposit associated with intrusion of the Nimpkish batholith. Interestingly, this occurrence lies about 600 m northwest of the Engl Cu-Ag showing (MINFILE 92L 296), where quartz-Ag veins are hosted by a 1 m wide fault zone. The latter mineralization also contains sphalerite and it is possible that the two systems are related.

ACKNOWLEDGMENTS

We wish to thank a number of people for geological discussions and assistance in the field and laboratory: Hiroyoshi Sano (Kyushu University) for sedimentological interpretations; Emily Hopkin for fossil identifications; Jim Laird for enthusiastically sharing his extensive knowledge of the terrain and mineral showings; Peter Krauss and Mike Orchard (Geological Survey of Canada) for conodont processing and identification, respectively; and Brian Grant, Jamie Pardy and Dave Lefebure for their field visits. Digital files for logging-road systems were kindly provided by Nina Baksh and Murray Ducheminski (International Forest Products); Patrick Bryant (Canadian Forest Products); Melody Wilson and Lisa Davidson (Cascadia Forest Products); and Dave Mogensen (Western Forest Products). We are especially grateful to Margaret Hanuse who provided incredible lodging in Port McNeill, and to Barbara Nixon and Lesley Stokes for providing an unforgettable Newfie dinner.

REFERENCES

Archibald, D.A. and Nixon, G.T. (1995): $^{40}Ar/^{39}Ar$ geochronometry of igneous rocks in the Quatsino – Port McNeill map area, northern Vancouver Island (92L/12, 11); *in* Geological Fieldwork 1994, *BC Ministry of Energy, Mines and Petroleum Resources*, Paper 1995-1, pages 49–59.

Armstrong, R.L., Muller, J.E., Harakal, J.E. and Muehlenbachs, K. (1985): The Neogene Alert Bay volcanic belt of northern Vancouver Island, Canada: descending-plate-edge volcanism in the arc-trench gap; *Journal of Volcanology and Geothermal Research*, Volume 26, pages 75–97.

Breitsprecher, K. and Mortensen, J.K. (2004): BCAge 2004A – a database of isotopic age determinations for rock units from British Columbia; *BC Ministry of Energy, Mines and Petroleum Resources*, Open File 2004-3.

Carlisle, D. (1972): Late Paleozoic to mid-Triassic sedimentary-volcanic sequence on northeastern Vancouver Island; *in* Report of Activities, November 1971 to March 1972, *Geological Survey of Canada*, Paper 72-1B, pages 24–30.

Carlisle, D. and Suzuki, T. (1974): Emergent basalt and submergent carbonate-clastic sequences including the Upper Triassic Dilleri and Welleri zones on Vancouver Island; *Canadian Journal of Earth Sciences*, Volume 11, pages 254–279.

Carson, D.J.T. (1973): The plutonic rocks of Vancouver Island, British Columbia: their petrography, chemistry, age and emplacement; *Geological Survey of Canada*, Paper 72-44, 70 pages.

Dawson, G.M. (1887): Report on a geological examination of the northern part of Vancouver Island and adjacent coasts; *Geological Survey of Canada*, Annual Report, 1886, Volume 2, Part B, pages 1–107.

DeBari, S.M., Anderson, R.G. and Mortensen, J.K. (1999) Correlation amongst lower to upper crustal components in an island arc: the Jurassic Bonanza arc, Vancouver Island, Canada; *Canadian Journal of Earth Sciences*, Volume 36, pages 1371–1413.

DeBari, S.M., Anderson, R.G. and Mortensen, J.K. (2000): Early to Middle Jurassic magmatism: new zircon U-Pb ages and comparative geochemistry from a crustal transect through the Bonanza arc on Vancouver Island, Canada; *Georesearch Forum*, Volume 6, pages 65–76.

Dolmage, V. (1919): Quatsino Sound and certain mineral deposits of the west coast of Vancouver Island, BC; *Geological Survey of Canada*, Summary Report, 1918, Part B, pages 30–38.

Friedman, R.M. and Nixon, G.T. (1995): U-Pb zircon dating of Jurassic porphyry Cu(-Au) and associated acid-sulphate systems, northern Vancouver Island, British Columbia; *Geological Association of Canada – Mineralogical Association of Canada*, Joint Annual Meeting, Victoria, BC, page A34.

Gamba, C.A. (1993): Stratigraphy and sedimentology of the Upper Jurassic to Lower Cretaceous Longarm Formation, Queen Charlotte Islands, British Columbia; *in* Current Research, Part A, *Geological Survey of Canada*, Paper 93-1A, pages 139–148.

Gardner, M.C., Bergman, S.C., Cushing, G.W., MacKevett, E.M. Jr., Plafker, G., Campbell, R.B., Dodds, C.J., McClelland, W.C. and Mueller, P.A. (1988): Pennsylvanian pluton stitching of Wrangellia and the Alexander Terrane, Wrangell Mountains, Alaska; *Geology*, Volume 16, pages 967–971.

Gradstein, F.M., Ogg, J.G. and Smith, A.G. (2004): A geologic time scale 2004; *Cambridge University Press*, Cambridge, United Kingdom, 610 pages.

Greene, A.R., Scoates, J.S., Nixon, G.T. and Weis, D. (2006): Picritic lavas and basal sills in the Karmutsen flood basalt province, northern Vancouver Island, British Columbia; *in* Geological Fieldwork 2005, *BC Ministry of Energy, Mines and Petroleum Resources*, Paper 2006-1 and *Geoscience BC*, Report 2006-1.

Greenwood H.J., Woodsworth, G.J., Read, P.B., Ghent, E.D. and Evenchick, C.A. (1991): Metamorphism; Chapter 16 *in* Geology of the Cordilleran Orogen in Canada, Gabrielse, H.

and Yorath, C.J., Editors, *Geological Survey of Canada*, Geology of Canada, No 4, pages 533–570.

Gunning, H.C. (1930): Geology and mineral deposits of Quatsino-Nimpkish area, Vancouver Island; *Geological Survey of Canada*, Summary Report, 1929, Part A, pages 94–107.

Gunning, H.C. (1932): Preliminary report on the Nimpkish Lake quadrangle, Vancouver Island, British Columbia; *Geological Survey of Canada*, Summary Report, 1931, Part A, pages 22–35.

Gunning, H.C. (1938a): Preliminary geological map, Nimpkish, east half; *Geological Survey of Canada*, Paper 38-2.

Gunning, H.C. (1938b): Preliminary geological map, Nimpkish, west half; *Geological Survey of Canada*, Paper 38-3.

Haggart, J.W. and Carter, E.S. (1993): Cretaceous (Barremian–Aptian) radiolaria from Queen Charlotte Islands, British Columbia: newly recognized faunas and stratigraphic implications; *in* Current Research, Part E, *Geological Survey of Canada*, Paper 93-1E, pages 55–65.

Hoadley, J.W. (1953): Geology and mineral deposits of Zeballos-Nimpkish area, Vancouver Island, British Columbia; *Geological Survey of Canada*, Memoir 272, 82 pages.

Jeletzky, J.A. (1976): Mesozoic and ?Tertiary rocks of Quatsino Sound, Vancouver Island, British Columbia; *Geological Survey of Canada*, Bulletin 242, 243 pages.

Jones, D.L., Silberling, N.J. and Hillhouse, J. (1977): Wrangellia – a displaced terrane in northwestern North America; *Canadian Journal of Earth Sciences*, Volume 14, pages 2565–2577.

Kuniyoshi, S. and Liou, J.G. (1976): Contact metamorphism of the Karmutsen volcanics, Vancouver Island, British Columbia; *Journal of Petrology*, Volume 17, pages 73–99.

LeMaitre, R.W., Editor (1989): A classification of igneous rocks and glossary of terms; *Blackwell Scientific Publications,* Oxford, United Kingdom, 193 pages.

Lewis, T.J., Lowe, C. and Hamilton, T.S. (1997): Continental signature of a ridge-trench-triple junction: northern Vancouver Island; *Journal of Geophysical Research*, Volume 102, pages 7767–7781.

Massey, N.W.D. (1995a): Geology and mineral resources of the Alberni-Nanaimo lakes sheet, Vancouver Island, 92F/1W, 92F/2E and part of 92F/7E; *BC Ministry of Energy, Mines and Petroleum Resources*, Paper 1992-2, 132 pages.

Massey, N.W.D. (1995b): Geology and mineral resources of the Cowichan Lake sheet, Vancouver Island, 92C/16; *BC Ministry of Energy, Mines and Petroleum Resources*, Paper 1992-3, 112 pages.

Massey, N.W.D. (1995c): Geology and mineral resources of the Duncan sheet, Vancouver Island, 92B/13; *BC Ministry of Energy, Mines and Petroleum Resources*, Paper 1992-4, 112 pages.

Massey, N.W.D. (1995d): The Vancouver Island Mineral Potential Project; *in* Geological Fieldwork 1994, *BC Ministry of Energy, Mines and Petroleum Resources*, Paper 1995-1, pages 435–447.

Massey, N.W.D., McIntyre, D.G., Desjardins, P.J. and Cooney, R.T. (2005): Digital geology map of British Columbia: whole province; *BC Ministry of Energy, Mines and Petroleum Resources*, Geofile 2005-1.

MINFILE (2005): MINFILE BC mineral deposits database; *BC Ministry of Energy, Mines and Petroleum Resources*, URL <http://www.em.gov.bc.ca/Mining/Geolsurv/Minfile/> [Nov 2005].

Monger, J.W.H. and Journeay, J.M. (1994): Basement geology and tectonic evolution of the Vancouver region; *in* Geology and Geological Hazards of the Vancouver Region, Southwestern British Columbia, Monger, J.W.H., Editor, *Geological Survey of Canada*, Bulletin 481, pages 3–25.

Monger, J.W.H., Price, R.A. and Tempelman-Kluit, D.J. (1982): Tectonic accretion and the origin of the two major metamorphic and plutonic welts in the Canadian Cordillera; *Geology*, Volume 10, pages 70–75.

Muller, J.E. and Rahmani, R.A. (1970): Upper Triassic sediments of northern Vancouver Island; *in* Report of Activities, Part B, *Geological Survey of Canada*, Paper 70-1B, pages 11–18.

Muller, J.E. and Roddick, J.A. (1983): Alert Bay – Cape Scott; *Geological Survey of Canada*, Map 1552A, scale 1:250 000.

Muller, J.E., Cameron, B.E.B. and Northcote, K.E. (1981): Geology and mineral deposits of Nootka Sound map-area, Vancouver Island, British Columbia; *Geological Survey of Canada*, Paper 80-16, 53 pages.

Muller, J.E., Northcote, K.E. and Carlisle, D. (1974): Geology and mineral deposits of Alert Bay – Cape Scott map-area, Vancouver Island, British Columbia; *Geological Survey of Canada*, Paper 74-8, 77 pages.

Nixon, G.T., Friedman, R.M., Archibald, D. A., Orchard, M.J. and Tozer, T. (2000): A contribution to the geologic time scale: the Triassic–Jurassic boundary, northern Vancouver Island, Canada; *Geological Society of America, Cordilleran Section*, Annual Meeting, Vancouver, BC, Abstract 80179.

Nixon, G.T., Hammack, J.V., Hamilton, J.V. and Jennings, H. (1993a): Preliminary geology of the Mahatta Creek area, northern Vancouver Island (92L/5); *in* Geological Fieldwork 1992, *BC Ministry of Energy, Mines and Petroleum Resources*, Paper 1993-1, pages 17–35.

Nixon, G.T., Hammack, J.V., Hamilton, J.V. and Jennings, H. (1993b): Preliminary geology of the Mahatta Creek area (92L/5); *BC Ministry of Energy, Mines and Petroleum Resources*, Open File 1993-10, scale 1:50 000.

Nixon, G.T., Hammack, J.L., Koyanagi, V.M., Payie, G.J., Panteleyev, A., Massey, N.W.D., Hamilton, J.V. and Haggart, J.W. (1994a): Preliminary geology of the Quatsino – Port McNeill map areas, northern Vancouver Island (92L/12, 11); *in* Geological Fieldwork 1993, *BC Ministry of Energy, Mines and Petroleum Resources*, Paper 1994-1, pages 63–85.

Nixon, G.T., Hammack, J.L., Koyanagi, V.M., Payie, G.J., Panteleyev, A., Massey, N.W.D., Hamilton, J.V. and Haggart, J.W. (1994b): Preliminary geology of the Quatsino – Port McNeill map areas (92L/5); *BC Ministry of Energy, Mines and Petroleum Resources*, Open File 1994-26, scale 1:50 000.

Nixon, G.T., Hammack, J.L., Payie, G.J. and Snyder L.D. (1995a): Quatsino – San Josef map area, northern Vancouver Island: geological overview (92L/12W, 102I/8, 9); *in* Geological Fieldwork 1994, *BC Ministry of Energy, Mines and Petroleum Resources*, Paper 1995-1, pages 9–21.

Nixon, G.T., Hammack, J.L., Payie, G.J. and Snyder L.D. (1995b): Quatsino – San Josef map area (92L/12W, 102I/8, 9); *BC Ministry of Energy, Mines and Petroleum Resources*, Open File 1995-9, scale 1:50 000.

Nixon, G.T., Kelman, M.C., Stevenson, D., Stokes, L.A. and Johnston, K.A. (in press): Geology of the Nimpkish map area, northern Vancouver Island (92L/07); *BC Ministry of Energy, Mines and Petroleum Resources*, Open File 2006-5, scale 1:50 000, in press.

Palfy, J., Smith, P.L. and Mortensen, J.K. (2000): A U-Pb and Ar^{40}/Ar^{39} time scale for the Jurassic; *Canadian Journal of Earth Sciences*, Volume 37, pages 923–924.

Perello, J.A., Fleming, J.A., O'Kane, K.P., Burt, P.D., Clarke, G.A., Himes, M.D. and Reeves, A.T. (1995): Porphyry copper-gold-molybdenum deposits in the Island Copper cluster, northern Vancouver Island, British Columbia; *in* Porphyry Deposits of the Northwestern Cordillera of North America, Schroeter, T.G., Editor, *Canadian Institute of Mining, Metallurgy and Petroleum*, Special Volume 46, pages 214–238.

Riddihough, R.P. and Hyndman, R.D. (1991): Modern plate tectonic regime of the continental margin of western Canada; *in* Geology of the Cordilleran Orogen in Canada, Gabrielse, H. and Yorath, C.J., Editors, *Geological Survey of Canada*, Geology of Canada, No 4, pages 435–455.

Surdam, R.C. (1973): Low-grade metamorphism of tuffaceous rocks in the Karmutsen Group, Vancouver Island, British Columbia; *Geological Society of America Bulletin* Volume 84, pages 1911–1922.

van der Heyden, P. (1991): A Middle Jurassic to Early Tertiary Andean-Sierran arc model for the Coast Belt of British Columbia; *Tectonics*, Volume 11, pages 82–97.

Wanless, R.K., Stevens, R.D., Lachance, G.R. and Delabio, R.N. (1974): Age determinations and geological studies: K-Ar isotopic ages, report 12; *Geological Survey of Canada*, Paper 74-2.

Wanless, R.K., Stevens, R.D., Lachance, G.R. and Edmonds, C.M. (1967): Age determinations and geological studies: K-Ar isotopic ages, report 7; *Geological Survey of Canada*, Paper 66-17.

Wanless, R.K., Stevens, R.D., Lachance, G.R. and Edmonds, C.M. (1968): Age determinations and geological studies: K-Ar isotopic ages, report 8; *Geological Survey of Canada*, Paper 67-2A.

Wheeler, J.O. and McFeely, P. (1991): Tectonic assemblage map of the Canadian Cordillera and adjacent parts of the United States of America; *Geological Survey of Canada*, Map 1712A.

Woodsworth, G.J., Anderson, R.G. and Armstrong, R.L. (1991): Plutonic regimes; *in* Geology of the Cordilleran Orogen in Canada, Gabrielse, H. and Yorath, C.J., Editors, *Geological Survey of Canada*, Geology of Canada, No 4, pages 491–531.

Mantle-Derived Peridotite Xenoliths from the Western Intermontane Belt, Whitesail Lake map area (NTS 093E), Western British Columbia

By N.D. Peterson[1], J.K. Russell[1] and J.B. Mahoney[2]

KEYWORDS: mantle petrology, volcanology, peridotite, dike, mantle xenoliths, Whitesail Lake, Hazelton Group

INTRODUCTION

Recently the Whitesail Lake map area (NTS 093E), immediately north and east of Bella Coola, BC has been the focus of regional mapping programs, including the current Geoscience BC funded mapping program of Mahoney *et al.* (2006) and the mapping conducted in 2004 under the Rocks to Riches program (Mahoney *et al.*, 2005). The regional mapping exercise discovered a new occurrence of mantle-derived peridotitic xenoliths in the BC Cordillera (Fig. 1). Specifically, they located a mafic dike near Mt. Preston that intrudes Hazelton Group rocks. The dike appears to post-date the regional metamorphism and deformation recorded by Hazelton rocks, and is therefore inferred to be Tertiary to Neogene in age. The dike contains abundant crustal and mantle-derived peridotite xenoliths, which are very fresh and unaltered in appearance.

The peridotite xenoliths are samples of lithospheric mantle, and they represent the only available means of directly studying the underpinnings of the crust. The Mount Preston dike has several attributes that make this particular suite of mantle xenoliths especially interesting. Firstly, the relatively young age of the dike suggests sampling of 'near-present-day' mantle lithosphere underlying this portion of British Columbia. The implication is that the petrological, structural and geochemical insights gathered from these xenoliths can be related directly to large-scale geophysical datasets (*e.g.*, seismic surveys). Secondly, the Mount Preston locality has a unique position geographically and geologically because it is on the western margin of the Intermontane Belt and within 40 km of Coast Belt rocks (Fig. 2). All other occurrences of mantle xenoliths from the northern Canadian Cordillera are situated well within the Intermontane Belt (*e.g.*, Edwards and Russell, 2000). Thus, this study of these mantle xenoliths will provide evidence for the thermal and structural state of the mantle lithosphere underlying the western margin of the Intermontane Belt. Furthermore, it should provide constraints on the nature of

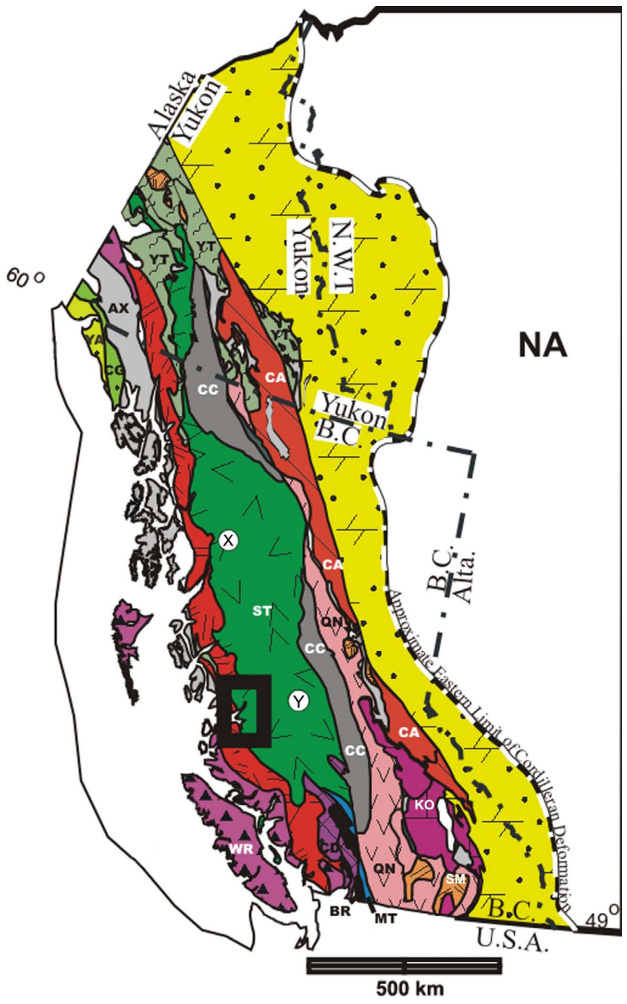


Figure 1. Location of area containing xenolith-bearing dike shown against the distribution of terranes that make up the Canadian Cordillera (modified from Wheeler and McFeely, 1991). Terranes are categorized as pericratonic (Kootenay [KO], Cassiar [CA] and Slide Mountain [SM]), Stikinia (Stikinia [ST], Quesnellia [QN], Cache Creek [CC] and Yukon-Tanana [YT]) and Insular (Alexander [AX], Wrangellia [WR], Chugach [CG] and Yukatat [YA]). Terranes that make up the southern Cordillera include the Cadwallader (CD), Bridge River (BR) and Methow (MT). Also shown are the approximate margin of ancestral North America and the eastern extent of Cordilleran deformation extending into western Canada. 'X' indicates the approximate location of Konigus Creek, the closest mantle xenolith – bearing edifice within the northern Cordilleran volcanic province (NCVP; Edwards and Russell, 2000; Evenchick and Thorkelson, 1993). 'Y' indicates the Itcha Mountains mantle xenolith locality of Nicholls *et al.* (1982). Outline indicates the area shown in Figure 2 (*i.e.*, NTS sheets 093D [Bella Coola] and 093E [Whitesail]).

[1]*Volcanology and Petrology Laboratory, Department of Earth and Ocean Sciences, University of British Columbia, Vancouver, BC (npeterson@eos.ubc.ca)*

[2]*Department of Geology, University of Wisconsin at Eau Claire, Eau Claire, WI*

This publication is also available, free of charge, as colour digital files in Adobe Acrobat PDF format from the BC Ministry of Energy, Mines and Petroleum Resources internet website at http://www.em.gov.bc.ca/Mining/Geolsurv/Publications/catalog/catfldwk.htm

the fundamental boundary between the Coast and Intermontane belts in this region. This will complement the new BATHOLITHS geophysical project, which is designed to explore the crustal structure of the Coast Belt but will also probe the underlying mantle lithosphere (Andronicos and Ducea, 2004). The BATHOLITHS operational area will encompass the Mt. Preston site (Fig. 2).

The purpose of this paper is to,

- report on the occurrence and properties of this young volcanic dike;
- describe the nature and distribution of mantle and crustal xenoliths within the dike; and
- explore some of the implications of these observations for the transport and emplacement of this mantle-derived magma.

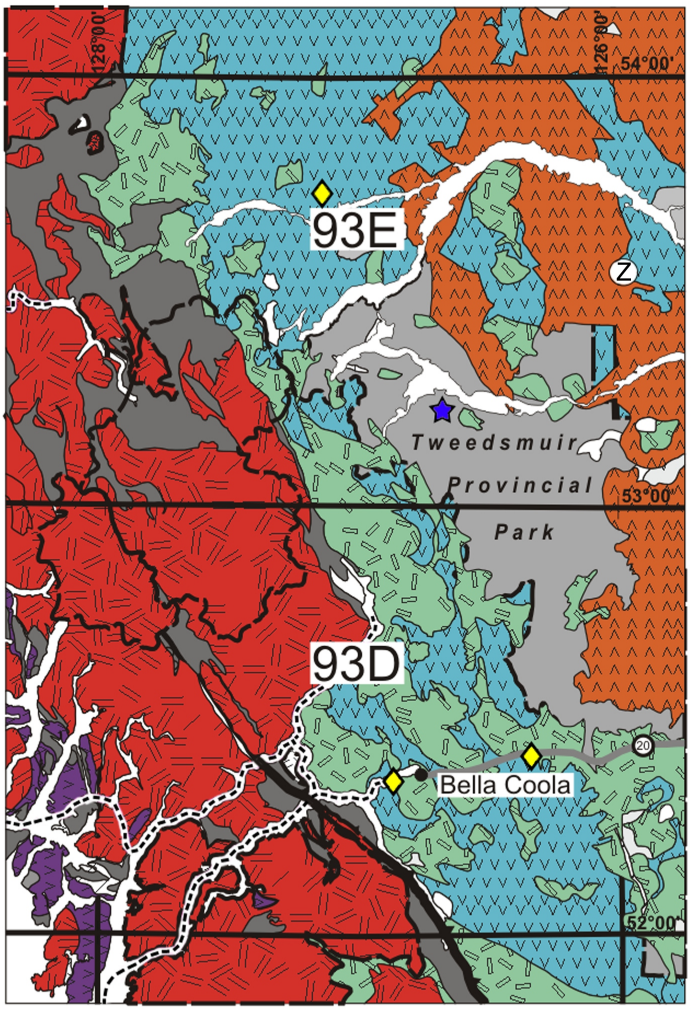


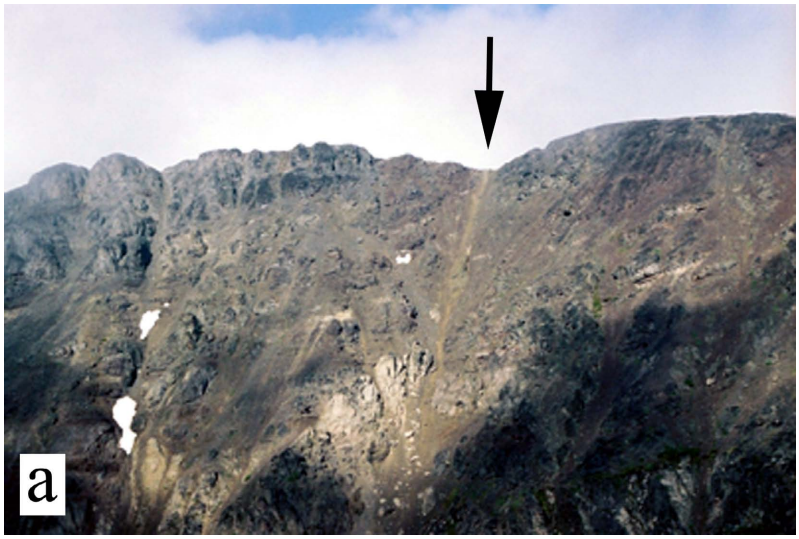
Figure 2. Schematic geology of the region surrounding Mt. Preston. The area is mainly underlain by Coast Belt plutonic rocks to the west and Jurassic (Hazelton) or Cretaceous (Monarch) volcanic and plutonic arc rocks to the north, immediate west and south. Cenozoic volcanic rocks of the Nechako Plateau outcrop in the extreme northeast. The study area (star) is situated immediately south of Eutsuk Lake, approximately 40 km east of the Coast Belt. Planned BATHOLITHS shot locations (diamonds) and marine geophysics survey tracks (dashed lines) are also shown. 'Z' indicates the nearest mantle xenolith occurrence to Mt. Preston, one of the Nechako River localities of Resnick *et al.* (1999).

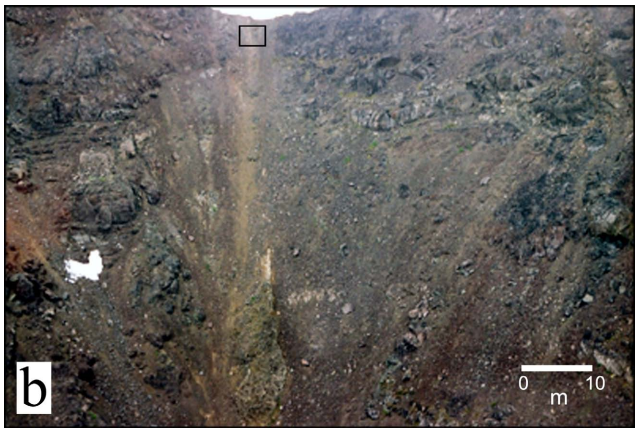
STRATIGRAPHIC RELATIONSHIPS

The focus of this work is a mafic dike that strikes 145° across a saddle on a ridge 3 km southeast of the peak of Mt. Preston (Fig. 3a). The dike is exposed on the ridge crest and in the south-facing cliff that forms the east-trending ridge. The ridge crest exposes the top of the dike and is situated 2063 m above mean sea level (amsl) at Zone 9, 653722E, 5898712N (NAD 27). Exposure begins at the top of the ridge, continuing intermittently down the southern face for about 110 m (60 m vertical; Fig. 3b, c). Much of the dike is covered by talus, but the contact between dike and country rock is locally well exposed. Where exposed, the contact dips steeply (between 50 and 64°). The dike is not exposed on the north side of the ridge.

The country rock to the dike comprises intermediate to felsic, subhorizontally bedded volcaniclastic rocks of the Early to Middle Jurassic Hazelton Group (Fig. 3b, c; Gordee *et al.*, 2005; Mahoney *et al.*, 2005). The Hazelton Group rocks are intruded by several sets of mafic dikes that, based on alteration and composition, appear to be Cretaceous or older. The mantle-xenolith – bearing dike crosscuts all other stratigraphic units and has a fresh, less altered appearance. A small normal fault, striking 102°, dipping 76°S and having an offset of ~1 m, crosscuts Hazelton stratigraphy in the nearby outcrop but does not crosscut the main dike.

Edwards and Russell (2000) have summarized xenolith localities in the northern Cordilleran volcanic province (NCVP). The nearest xenolith-bearing volcanic site in the NCVP is Konigus Creek (Fig. 1; Evenchick and Thorkelson, 1993). Several other papers (Littlejohn and Greenwood, 1974; Nicholls *et al.*, 1982; Ross, 1983; Mitchell, 1987) have summarized distributions in other parts of BC. The nearest occurrences of mantle peridotitic xenoliths to this new locale are the Nechako River centres (NTS 093F; Resnick *et al.*, 1999) and the Itcha Mountains complex (NTS 093C; Nicholls *et al.*, 1982; Fig. 1, 2).





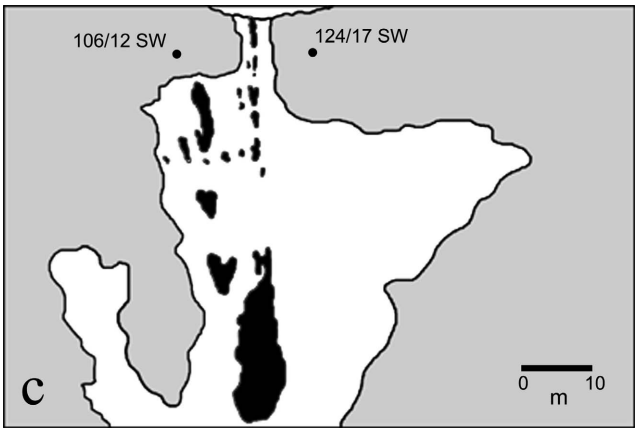


Figure 3. Field photographs showing the large-scale features of the mafic dike intruding older volcanic stratigraphic units: a) dike (arrow) exposed in a 300 m steep cliff face, its trace downslope highlighted by light green-grey talus; b) orientation of dike is approximately 145°/55°W and it intrudes Hazelton volcanic stratigraphic units that have bedding orientations of about 115°/15°S; dike is 1 m wide at the top of the cliff but widens downslope to 7 m; it appears to postdate regional metamorphism and deformation events that are recorded by the Hazelton Group rocks; solid box denotes portion of dike that is most enriched in mantle-derived xenoliths (see Fig. 6); c) geological sketch map of cliff face depicted in (b), showing distribution of dike and associated country rock outcrop (black) and layered Hazelton Group volcaniclastic rocks (grey); areas of talus are denoted by white; two approximate locations of bedding measurements on Hazelton rocks are shown.

GEOLOGY

Dike

The following observations are based on a five-day field mapping program designed to delineate the extent of the dike, its stratigraphic relationships and the physical nature of its contacts against country rocks, and to collect a comprehensive sample suite of the xenoliths of mantle lithosphere origin. The extent of the exposed dike was mapped to constrain the contacts and to understand the dike morphology (Fig. 4).

The mafic dike varies in thickness, from about 1 m where both contacts are visible to at least 7 m. At its widest point, only a single contact is exposed (Fig. 4). The outcrop is intermittent due to talus coverage, but visible outcrop extends 107 m downslope, or more than 60 vertical metres. At the lowest elevation of the exposure, the dike is defined by a large 7 m wide outcrop. At higher elevations, it bifurcates to form two lithologically identical, connected dikes separated by 2–3 m of talus. Specifically, the body splits at 2025 m elevation into a 1–4 m thick arm that strikes directly upslope (325°) to the ridge top and another wider, shorter arm that strikes 310° uphill but terminates at 2049 m absolute elevation (Fig. 3, 4).

The dike is aphanitic and grey to tan coloured on fresh surfaces. Weathered surfaces are light grey to dark brown, or sometimes oxidized to a reddish brown colour. The dike is vesicular in many places, locally up to 30% (Fig. 5a, b), with the vesicles varying from 0.5 to 10 mm in diameter. Flow banding on the scale of 5–10 cm is common, and is commonly accentuated by changes in vesicularity (Fig. 5c, d). The larger vesicles are sometimes stretched. Vesicles are frequently filled or coated; on the basis of powder x-ray diffraction, the minerals are vermiculite and calcite.

Locally, the dike has a fragmental character or appearance, with 'clasts' of melt visible within the dike. The clasts are commonly identified by changes in colour and vesicle characteristics (Fig. 5a, b). Clasts are only weakly vesicular but are surrounded by highly vesicular material. Clasts up to 10 cm in size were observed. The contact between clast and host magma is sharp and melting does not appear to have occurred. However, the clast boundaries are locally accentuated by oxidation rinds up to 1 cm in width. These melt clasts constitute <1% of the dike.

Contacts with country rock are abundant and sharply defined. The dike often displays one or more chilled margins (Fig. 5e, f). Physical properties such as xenolith content or vesicularity do not appear to change near the contact. Wherever contacts are visible, the country rock near the contact is partially melted. Melt is segregated into patches and lenses, which are sometimes vesicular. Commonly the lenses impart a foliation parallel to the contact. This contact zone varies in width from 10–30 cm.

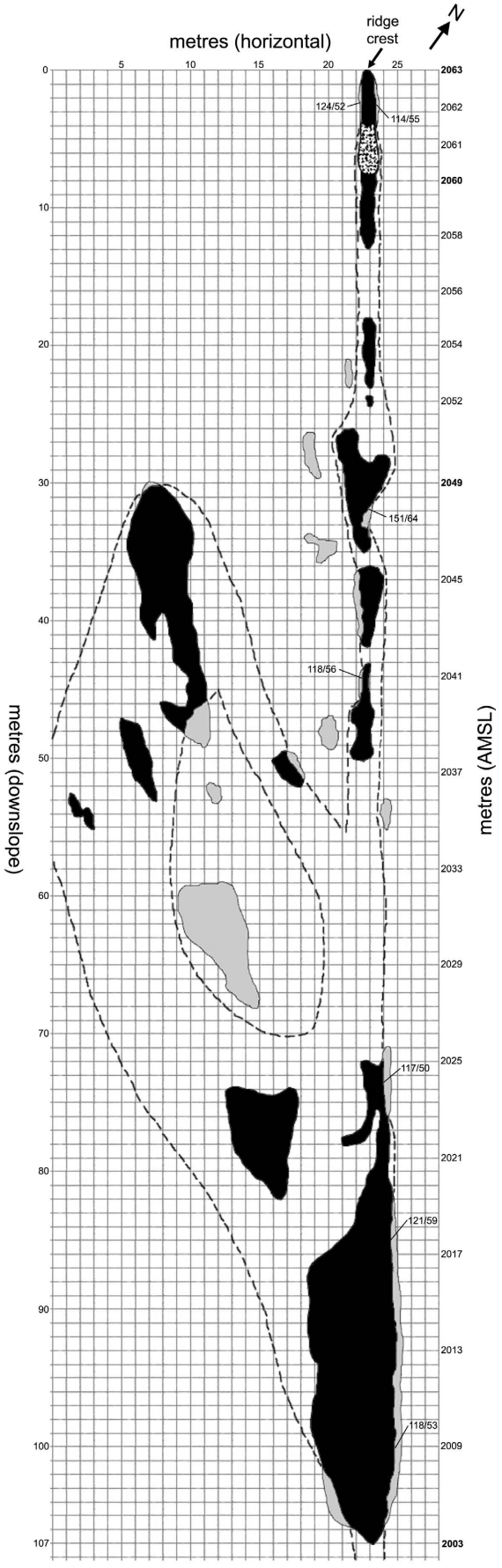


Figure 4. Geology of dike (black) and country rock (grey) outcrop, with xenolith-rich interval shown as textured. Dike exposures are limited by talus cover, but inferred contacts against Hazelton Group wallrocks are shown (dashed lines). The dike has an exposure length of 107 m and an apparent thickness ranging from 1 to >7 m. On the basis of the mapped exposure and the textural features of the dike, the body is interpreted to be a single dike below 2025 m and then to bifurcate into two main branches that terminate at 2049 m and 2063 m amsl. Absolute elevations listed in bold mark a change in slope (and thus scale of elevation markers).

Mantle Xenoliths

Peridotite xenoliths are especially abundant in the interval 4–8 m from the top of the outcrop, where the dike narrows to 1 m in width (Fig. 4, 6a, b). They constitute 50–80% of the dike over this interval and are present over the entire width of the dike (Fig. 6c, d). This concentration of xenoliths appears to often be clast supported within the dike rock. The mean diameter of xenoliths at this locality is ~15 cm; the largest peridotite was approximately 40 cm in diameter. There is no discernible sorting of the xenoliths down the dike or across it. In other areas of the dike, peridotite xenoliths constitute <1% and none are more than 5 cm in diameter. There is no gradient in xenolith concentration. The upper contact between xenolith-rich and xenolith-poor magma is horizontal, and the lower contact is unclear, though xenolith abundance drops suddenly (Fig. 6a, b). The peridotite xenoliths are very well preserved and show no signs of reacting with the host magma, although thin (1–5 mm) veins of melt are common within the peridotite blocks. Large xenoliths are rounded, but angularity increases with decreasing size. The xenoliths are dominantly lherzolite in composition, though some websterite and dunite were observed.

Individual xenoliths are equigranular, although there are substantial grain size variations (0.1–5 mm) between xenoliths. Larger grained xenoliths are more friable than fine grained ones. About a third of the xenoliths show planar fabrics at the hand-sample scale. These fabrics are most easily seen in the finer grained samples and are less apparent in coarser grained samples. Planar fabrics include mineralogical banding and mineral foliation. Banding is observed as 1–3 mm wide bands of spinel, repeating on a 1 cm scale, or 2–3 mm wide indistinct bands of clinopyroxene, repeating on an approximately 1–2 cm scale. Larger scale segregations or possibly bands of olivine and clinopyroxene (1 cm width or greater) also occur. Disaggregation of well-banded lherzolitic nodules may serve as an explanation for the small amounts of dunite and websterite that were found. Foliation tends to be strong in fine-grained samples, weakening with increasing grain size. Most commonly, the foliation is defined by flattened and elongated spinel grains, though clinopyroxene foliation was often noted in the same samples.

Xenocrysts and Crustal Xenoliths

Xenocrysts and crustal xenoliths also appear in the dike. Xenocrysts of olivine (1–2 mm), derived from the mechanical breakdown of peridotite, are ubiquitous, as are large (2–5 cm) xenocrysts of black augite (possibly from xenoliths), although both types make up <1% of the dike. Crustal xenoliths are more abundant and constitute more than 10% of the dike in some areas (Fig. 5g, h). Crustal xenoliths are generally <5 cm in diameter, although two were observed that were ~30 cm in diameter. Angularity seems inversely related to size, ranging from angular to rounded. Some crustal xenoliths resemble nearby country rock, and are not extensively altered. In contrast, others show textures indicating partial melting of the clasts and internal vesiculation, which cannot be correlated with observable wallrocks. One sample is of a 20 cm diameter granitoid xenolith; it is relatively fresh and does not resemble any observable country rock. At the upper contact of the short arm of the dike, the contact with country rock is well exposed; the country rock appears melted, and angular clasts of the same are entrained within the dike. Crustal xenoliths are more abundant in the lower, more massive parts of the dike; in the upper 25 m of outcrop, the dike is more vesicular to massive, with less crustal xenoliths. Where crustal xenoliths are most abundant, the dike surface often appears 'knobby' in texture.

DISCUSSION

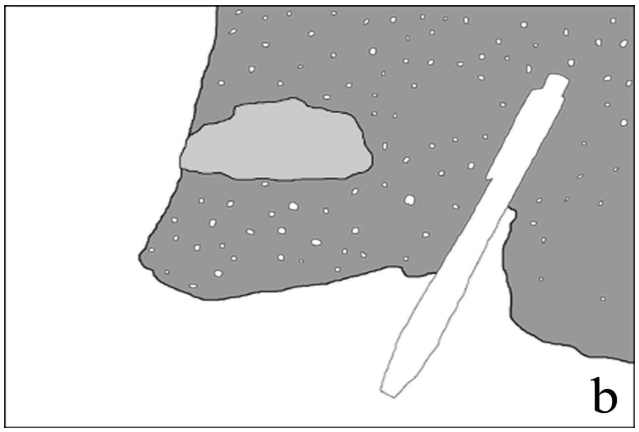
During magma transport, this dike was probably inflated to several times its current width. Melted wallrock implies sustained heat transfer from the dike, and thus sustained or possibly pulsed magma flow (Petcovic and Dufek, 2005). Discrete energetic pulses of magma within the dike may explain the abundance of crustal xenoliths and apparent autobrecciation: when flow waned and the dike relaxed, brittle failure of the wallrock margins and the chilled dike margin may have occurred. Another possibility is that there was sufficient vesiculation to promote fragmentation of the magma by primary vesiculation (Dingwell, 1996; Cashman *et al.*, 2000) or fragmentation of the wallrock and chilled margin (Tuffen *et al.*, 2003) by differential strain. The existence of flow banding indicates differential strain and possibly magma fragmentation followed by annealing. In any case, dike vesicularity indicates that the exposed portion of this dike was shallow (<1–2 km) during emplacement (Massol and Jaupart, 1999). Parrish (1983) calculated uplift in the area of approximately 1 km in the last 10 m.y., based on fission track data. The fact that the upper limit of mantle xenolith concentration is horizontal suggests that, if the high xenolith concentration was gravitationally controlled, no tectonic tilting has occurred since dike emplacement.

No young volcanic rocks have been reported in the immediate area (Mahoney *et al.*, 2005). There were also no young volcanic rocks noted in the talus on the top or north side of the ridge. As a high altitude area, this location would be subject to more intense erosion than surrounding lowlands. Any relatively fragile cinder cone would likely erode quickly, with any lava flows following. The vesicular nature of the dike, indicating shallow intrusion levels, and its significant size suggest that it would have produced surface volcanic rocks, though none are extant.

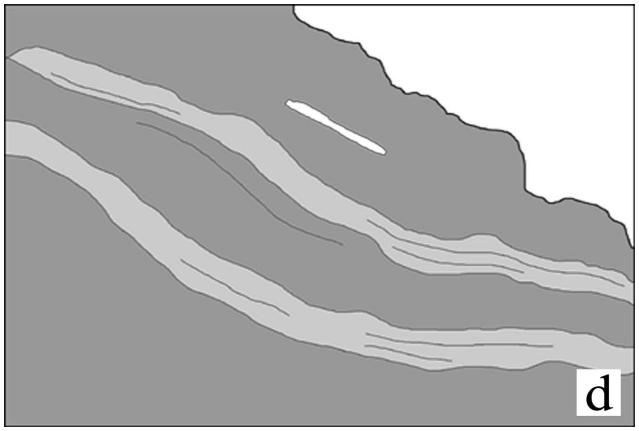
The only constraint on age of intrusion is that the dike crosscuts all Jurassic stratigraphy. However, the fresh appearance of the xenoliths and the absence of any crosscutting faults or other dikes suggest a young age, whereas the absence of a cinder cone or associated volcanic rocks, plus the large vertical exposure of the dike (indicating high erosion since intrusion) limits its youth. The tectonic regime of this part of BC has seen the production of many small volcanic centres in the last 15 m.y. (Edwards and Russell, 2000); a time of intrusion within the last 15 m.y. would be reasonable, allowing for subsequent erosion.

The concentration of peridotite xenoliths in a 4 m interval in the dike is very unusual and has not been reported previously in the Cordillera. Through this interval, the width of the dike is ~1 m. It is possible that this narrow passage resulted in a blockage of xenoliths, either as they were carried through this bottleneck or as they descended through the column of magma when flow became insufficient to buoy the rocks. Considering the grain-supported nature of the xenoliths in this interval, it may represent relaxation of the dike, trapping the xenoliths as the dike closed.

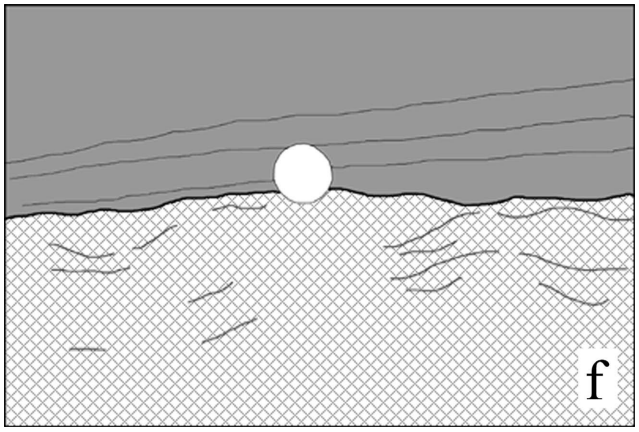

a


b

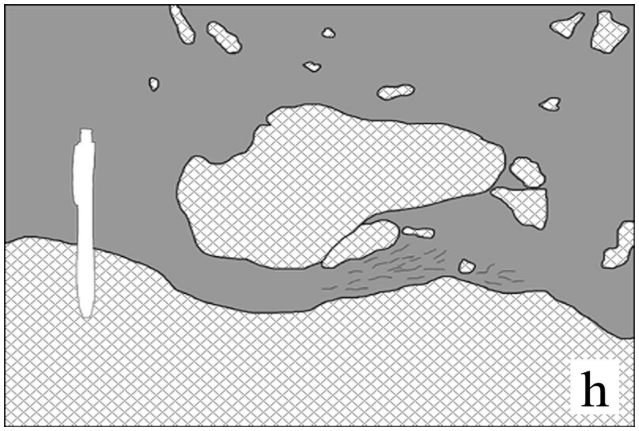

c


d


e


f


g


h

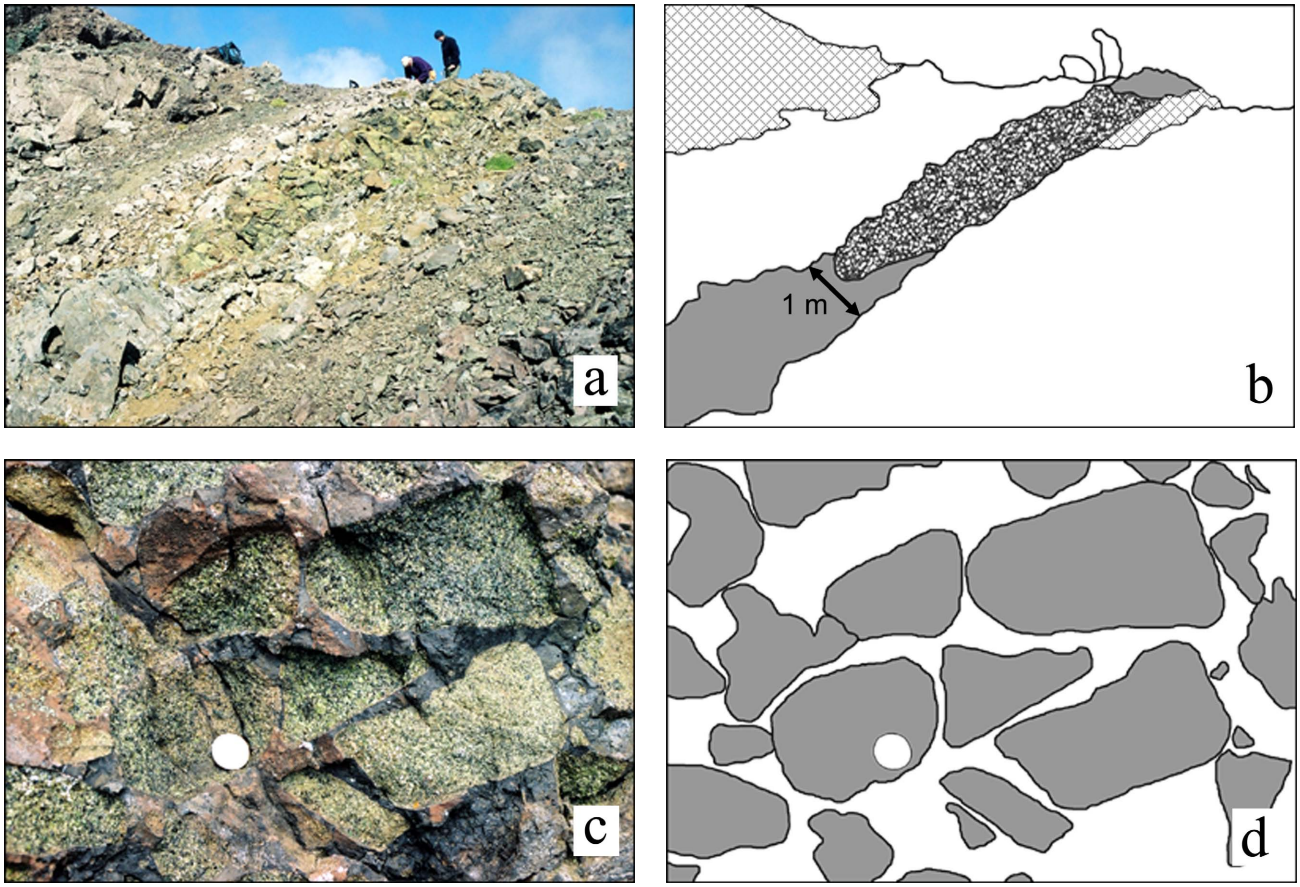


Figure 6. Field photographs and matching sketch maps showing the detailed aspects of the peridotite-bearing facies of the mafic dike: a) photo showing the width of the dike where it intersects the ridge top; the dike is very rich in xenoliths (green colour); b) sketch map of (a) showing the distributions of xenoliths (patterned) in the dike (dark grey) and in contact with Hazelton Group volcaniclastic rocks (patterned); much of the contact cannot be observed directly; locally, the exact contact relationships between the dike and country rocks can be observed (see Fig. 5e–h); c) photo showing the local relationships between the melt phase and the peridotitic mantle-derived xenoliths; xenoliths vary in diameter from 1 to 40 cm and appear to be clast supported; coin is 2.8 cm in diameter; d) sketch map of (c) showing the shapes and sizes of the xenoliths, the proportions of melt to xenolith, and the character of the peridotite clasts (see text); xenoliths make up ~60% of the view.

IMPLICATIONS

This site is well suited for mantle studies for several reasons. The largest xenolith transported to the surface is approximately 40 cm in diameter, indicating that all of the xenoliths were rapidly transported to the surface (Spera, 1984). The source for this magma is within or below the mantle lithosphere, thus providing an opportunity for this magma to sample the complete spectrum of rock types within the mantle lithosphere. North of this locale within the northern Cordilleran volcanic province (NCVP), geophysics and xenolith thermobarometry have constrained the crust-mantle boundary (CMB) to 30–40 km in depth (Welford *et al.*, 2001; Harder and Russell, 2005). Because the dike is aphyric and mafic in composition, it likely would have had a low yield strength (if any) and a high temperature during flow, and therefore low magma viscosity. This also implies rapid transport, if large, dense xenoliths are to be transported from the lithospheric mantle without settling out of suspension. Conventional ascent velocities for such magmas (Fujii and Scarfe, 1982; Spera, 1984) vary between 0.1 and 10 m/s, thus suggesting total transit times of between 1.4 hours and 5.8 days (assuming a source depth within the mantle lithosphere of 50 km). Given these estimated residence times, the xenoliths would have had limited time to react with the magma, ensuring preservation of pristine mantle mineral compositions (Edwards and Russell, 1998; Canil and Fedortchouk, 1999).

Figure 5. Field photographs and matching sketch maps showing specific volcanological aspects of the mafic dike: a), b) vesicular nature of the dike, with porosity estimated to be between 10 and 20%, rising up to 30% elsewhere in the dike; locally, the rock is amygdaloidal where vesicles are lined or infilled by vermiculite and calcite; photo also shows a subrounded clast of melt within the vesicular dike, the clast showing several amygdules and presumed to be accessory to juvenile in nature; pencil is 14 cm long; c), d) well-developed flow banding in the dike, defined by high (dark grey) versus low (light grey) vesicularity; e), f) nature of contact between the dike and the country rock, showing quenched margin(s) within dike and altered country rock; g), h) crustal xenolith derived from local country rock within the dike; contact between dike and wallrock is sharp.

The main goal of future research is to constrain mantle lithosphere properties. To that end, the 80 mantle xenoliths collected from Mt. Preston will be examined for composition, as well as equilibration T and P (using geothermobarometry). The fact that the mantle xenoliths on Mt. Preston are only weakly weathered indicates fairly recent exhumation and good potential for preservation of mantle mineral compositions. Consequently, the peridotitic samples will be ideal for geothermometric studies aimed at recovering mantle equilibration temperatures (Littlejohn and Greenwood, 1974). Although many mantle xenolith localities feature anomalously high concentrations of xenoliths, the host magmas, in all likelihood, sampled the lithospheric mantle randomly (Ross, 1983; Harder and Russell, 2005). Thus, geothermobarometry on a suite of nodules should provide a minimum temperature and pressure interval between the CMB and the asthenosphere (Ross, 1983), which constrains minimum lithospheric mantle thickness (Harder and Russell, 2005).

Variations in chemical composition (Littlejohn and Greenwood, 1974; Ross, 1983), texture and fabric (Ross, 1983) between xenolith localities (*e.g.* Edwards and Russell, 2000) allow regional mantle properties to be determined. The unique location of the Mt. Preston locality is fortuitous in this regard. A recently developed technique uses geothermobarometry along with geophysically derived heat-flow data to create an accurate geotherm and determine minimum lithospheric mantle thickness and depth (Russell and Kopylova, 1999; Russell *et al.*, 2001; Harder and Russell, 2005). When combined with heat-flow data from the BATHOLITHS seismic survey, the minimum depth and thickness of the mantle lithosphere will be obtained. Crustal xenoliths will also be examined for composition, in an attempt to correlate them with underlying stratigraphy and a possible source region for the dike magma. These results will be a powerful tool when combined with BATHOLITHS deep seismic data, which will image those interfaces.

ACKNOWLEDGMENTS

This research benefited from the capable assistance of Adam Kjos in the field. The project was funded by the Natural Sciences and Engineering Research Council (NSERC) through a Collaborative Research Opportunities (CRO) grant (BATHOLITHS: Generation and Evolution of Crust in Continental Magmatic Arcs) held by Ron Clowes and others. Geoscience BC funded J.B. Mahoney. N.D. Peterson was partially funded by the Egil H. Lorntzsen Scholarship.

REFERENCES

Andronicos, C.L. and Ducea, M. (2004): BATHOLITHS: An integrated geological, geochemical and geophysical study of the formation of continents; *in Geological Society of America*, Abstracts with Programs, volume 36, number 5, page 343.

Canil, D. and Fedortchouk, Y. (1999): Garnet dissolution and the emplacement of kimberlites; *Earth and Planetary Science Letters*, volume 167, pages 227–237.

Cashman, K.V., Sturtevant, B., Papale, P. and Navon, O. (2000): Magmatic fragmentation; *in* Encyclopedia of Volcanoes, Sigurdsson, H., Editor, *Academic Press*, San Diego, pages 421–430.

Dingwell, D.B. (1996): Volcanic dilemma: flow or blow? *Science*, volume 273, pages 1054–1055.

Edwards, B. and Russell, J.K. (1998): Time scales of magmatic processes: new insights from dynamic models for magmatic assimilation; *Geology*, volume 26, number 12, pages 1103–1106.

Edwards, B., and Russell, J.K. (2000): Distribution, nature, and origin of Neogene–Quaternary magmatism in the northern Cordilleran volcanic province, Canada; *Geological Society of America Bulletin*, volume 112, number 8, pages 1280–1295.

Evenchick, C.A. and Thorkelson, D.J. (1993): Geology, Spatsizi River, British Columbia (104H); *Geological Survey of Canada*, Open File 2719, scale 1:250 000.

Fujii, T. and Scarfe, C.M. (1982): Petrology of ultramafic nodules from West Kettle River, near Kelowna, British Columbia; *Contributions to Mineralogy and Petrology*, volume 80, pages 297–306.

Gordee, S.M., Mortensen, J.K., Mahoney, J.B. and Hooper, R.L. (2005): Volcanostratigraphy, lithogeochemistry and U-Pb geochronology of the upper Hazelton Group, west-central British Columbia: implications for Eskay Creek – type VMS mineralization in southwest Stikinia; *in* Geological Fieldwork, 2004, *BC Ministry of Energy, Mines and Petroleum Resources*, Paper 2005-1, pages 311–322.

Harder, M. and Russell, J.K. (in press): Thermal state of the mantle lithosphere beneath the Northern Cordilleran Volcanic Province, British Columbia; *Lithos*, in press, doi:10.1016/j.lithos.2005.05.002.

Littlejohn, A.L. and Greenwood, H.J. (1974): Lherzolite nodules in basalts from British Columbia, Canada; *Canadian Journal of Earth Sciences*, volume 11, pages 1288–1308.

Mahoney, J.B., Haggart, J.W., Hooper, R.L., Snyder, L.D. and Woodsworth, G.J. (2006): Geological setting and mineralization potential of the southwestern Whitesail Lake map area (NTS 93E), western British Columbia: preliminary assessment; *in* Geological Fieldwork, 2005, *BC Ministry of Energy, Mines and Petroleum Resources*, Paper 2006-1 and *Geoscience BC*, Report 2006-1.

Mahoney, J.B., Hooper, R.L., Gordee, S.M., Haggart, J.W. and Mortensen, J.K. (2005): Initial evaluation of bedrock geology and economic mineralization potential of southern Whitesail Lake map area (NTS 093E/02, 03), west-central British Columbia; *in* Geological Fieldwork, 2004, *BC Ministry of Energy, Mines and Petroleum Resources*, Paper 2005-1, pages 291–299.

Massol, H. and Jaupart, C. (1999): The generation of gas overpressure in volcanic eruptions; *Earth and Planetary Science Letters*, volume 166, pages 57–70.

Mitchell, R.H. (1987): Mantle-derived xenoliths in Canada; *in* Mantle Xenoliths, Nixon, P.H., Editor, *John Wiley and Sons*, New York, pages 33–40.

Nicholls, J., Stout, M.Z. and Fiesinger, D.W. (1982): Petrologic variations in Quaternary volcanic rocks, British Columbia, and the nature of the underlying upper mantle; *Contributions to Mineralogy and Petrology*, volume 79, pages 201–218.

Parrish, R.R. (1983): Cenozoic thermal evolution and tectonics of the Coast Mountains of British Columbia: 1. Fission track dating, apparent uplift rates, and patterns of uplift; *Tectonics*, volume 2, pages 601–631.

Petcovic, H.L. and Dufek, J.D. (in press): Modeling magma flow and cooling in dikes: implications for emplacement of Columbia River flood basalts; *Journal of Geophysical Research*, Volume 110, B10201, doi:10.1029/2004JB003432, 2005.

Resnick, J., Anderson, R.G., Russell, J.K., Edwards, B.R. and Grainger, N.C. (1999): Neogene basaltic flow rocks, xenoliths, and related diabase, northern Nechako River map area,

central British Columbia; *in* Current Research 1999-A, *Geological Survey of Canada*, pages 157–167.

Ross, J.V. (1983): The nature and rheology of the Cordilleran upper mantle of British Columbia: inferences from peridotite xenoliths; *Tectonophysics*, volume 100, pages 321–357.

Russell, J.K., Dipple, G.M. and Kopylova, M.G. (2001): Heat flow and heat production in mantle lithosphere from the Slave Craton; *Physics of Earth and Planetary Interiors*, volume 123, pages 27–44.

Russell, J.K. and Kopylova, M.K. (1999): A steady-state conductive geotherm for the north central Slave, Canada: inversion of petrological data from the Jericho kimberlite pipe; *Journal of Geophysical Research*, volume 104, pages 7089–7101.

Spera, F.J. (1984): Carbon dioxide in petrogenesis III: role of volatiles in the ascent of alkaline magma with special reference to xenolith-bearing mafic lavas; *Contributions to Mineralogy and Petrology*, volume 88, pages 217–232.

Tuffen, H., Dingwell, D.B. and Pinkerton, H. (2003): Repeated fracture and healing of silicic magma generate flow banding and earthquakes? *Geology*, Volume 31, pages 1089–1092.

Welford, J.K., Clowes, R.M., Ellis, R.M., Spence, G.D., Asudeh, I. and Hajnal, Z. (2001): Lithospheric structure across the craton-Cordilleran transition of northeastern British Columbia; *Canadian Journal of Earth Sciences*, volume 38, pages 1169–1189.

Wheeler, J.O. and McFeely, P. (1991): Tectonic assemblage map of the Canadian Cordillera and adjacent parts of the United States of America; *Geological Survey of Canada*, Map 1712A, scale 1:2 000 000.

Geology and Mineral Occurrences of the Quesnel Terrane, Canim Lake Area (NTS 092P/15), South-Central British Columbia

by P. Schiarizza and A. Boulton[1]

KEYWORDS: Quesnel Terrane, Nicola Group, Takomkane batholith, Iron Lake ultramafic-mafic complex, Raft batholith, copper, gold, molybdenum

INTRODUCTION

The Takomkane Project is a multiyear bedrock mapping program initiated by the BC Geological Survey in 2005. This program will concentrate on Mesozoic arc volcanic and plutonic rocks of the Quesnel Terrane in the vicinity of the Takomkane batholith, which straddles the Bonaparte Lake (92P) and Quesnel Lake (93A) map sheets (Fig. 1). Previous bedrock maps of the area are based on reconnaissance-scale mapping carried out by the Geological Survey of Canada in the 1960s. The purpose of the Takomkane Project is to provide more detailed maps and an improved geological framework for interpreting mineral occurrences and geochemical anomalies, and for predicting favourable settings for future discoveries.

This paper presents preliminary results from the first year of mapping for the Takomkane Project, which was carried out by the authors and two assistants from mid-June to the end of August, 2005. The area mapped covers about 1000 km^2 of generally subdued topography within the Fraser Plateau and adjacent Quesnel Highland of south-central British Columbia, including Canim Lake and the west end of Mahood Lake. Access to Canim Lake is by paved road that branches east from Highway 97 just north of 100 Mile House. Alternate access routes include the Camp 2 logging road, which originates at Clearwater on Highway 5, and the Drewry Lake road, which branches northward from Highway 24 near Sheridan Lake. Networks of secondary logging and Forest Service roads that branch from these main roads provide easy access to most parts of the map area.

The Canim Lake map area is contiguous with, and partially overlaps, an area that was mapped at 1:50 000 scale by the BC Geological Survey as part of the Bonaparte Project in 2000 and 2001 (Schiarizza and Israel, 2001; Schiarizza *et al*., 2002a, b, c). The Takomkane Project will build on the geological interpretations advanced during that work, and on the earlier 1:250 000 scale mapping by Campbell and Tipper (1971) in the Bonaparte Lake map area and the 1:125 000 scale map of Campbell (1978) for the Quesnel Lake map area. The history of geological work in the area also includes a study of Cenozoic volcanic rocks by Hickson and Souther (1984) and Hickson (1986), and numerous descriptions of individual mineral occurrences found in assessment reports on file at offices of the BC Ministry of Energy, Mines and Petroleum Resources in Victoria and Vancouver.

[1]*University of Manchester, Manchester, UK*

This publication is also available, free of charge, as colour digital files in Adobe Acrobat PDF format from the BC Ministry of Energy, Mines and Petroleum Resources internet website at http://www.em.gov.bc.ca/Mining/Geolsurv/Publications/catalog/catfldwk.htm

REGIONAL GEOLOGICAL SETTING

The Takomkane project area is within the Quesnel Terrane, which is characterized by a Late Triassic to Early Jurassic magmatic arc complex that formed along or near the western North American continental margin (Mortimer, 1987; Struik, 1988a, b; Unterschutz *et al*., 2002). To the east, the Quesnel Terrane is faulted against Proterozoic and Paleozoic siliciclastic, carbonate and volcanic rocks of the Kootenay Terrane, and locally an intervening assemblage of Middle to Late Paleozoic oceanic basalt and chert assigned to the Slide Mountain Terrane (Fig. 1). The Kootenay Terrane probably represents an outboard facies of the ancestral North American miogeocline (Schiarizza and Preto, 1987; Colpron and Price, 1995), whereas the Slide Mountain Terrane is interpreted as the imbricated remnants of a Late Paleozoic marginal basin (Schiarizza, 1989; Roback *et al*., 1994). Late Paleozoic through mid-Mesozoic oceanic rocks of the Cache Creek Terrane occur to the west of the Quesnel Terrane, and are interpreted as part of the accretion-subduction complex that was responsible for generating the Quesnel magmatic arc (Travers, 1978; Struik, 1988a). Younger rocks commonly found in the region include Cretaceous granitic stocks and batholiths, Eocene volcanic and sedimentary rocks, and flat-lying basalt of both Neogene and Quaternary age (Fig. 1).

In southern BC, the early Mesozoic arc of the Quesnel Terrane is represented mainly by Middle to Upper Triassic volcanic and sedimentary rocks of the Nicola Group, together with abundant Late Triassic to Early Jurassic calcalkaline to alkaline intrusions (Schau, 1970; Preto, 1977, 1979; Mortimer, 1987; Panteleyev *et al*., 1996; Schiarizza *et al*., 2002a). Much of the Nicola Group comprises volcanic rocks that belong to a high-potassium to shoshonitic rock series, although locally it also includes a western belt of mainly low-potassium calcalkaline volcanic rocks (Preto, 1977; Mortimer, 1987; Monger, 1989; Monger and McMillan, 1989). The younger stratigraphic component of the Quesnel Terrane includes locally exposed successions of Lower to Middle Jurassic sedimentary and less common volcanic rocks that overlie the Nicola Group unconformably (Travers, 1978; Monger and McMillan, 1989; Panteleyev *et al*., 1996; Schiarizza *et al.*, 2002a; Logan and Mihalynuk, 2005a). However, the easternmost part of the Quesnel Terrane in southern BC is, in part, represented by an assemblage of Lower Jurassic

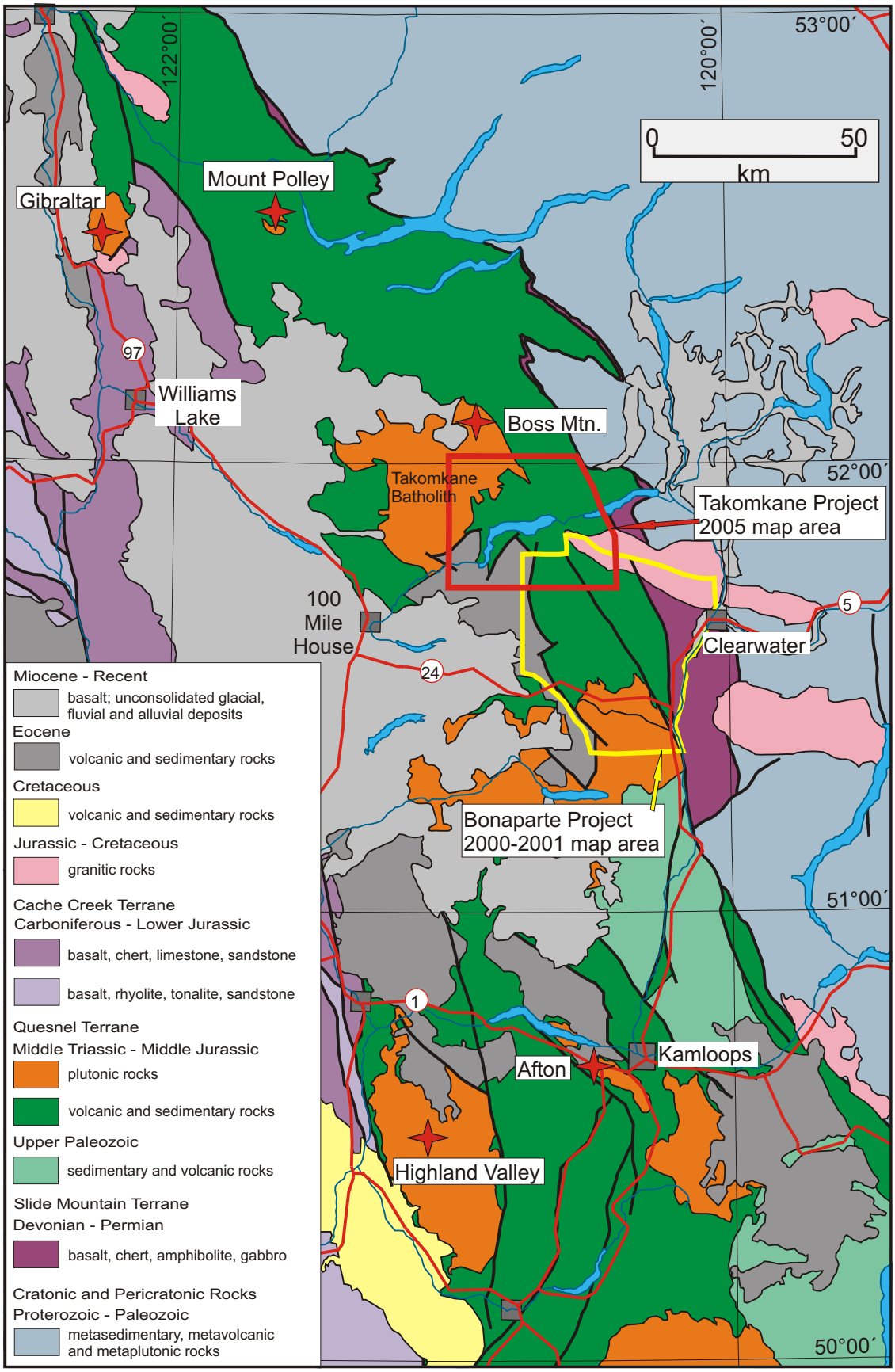


Figure 1. Regional geological setting of the Takomkane Project area, showing the area mapped in 2005, the area mapped in 2000 and 2001 during the Bonaparte Project, and the locations of selected major mineral deposits.

shoshonitic to calcalkaline arc volcanic rocks assigned to the Rossland Group (Höy and Dunne, 1997). These Lower Jurassic volcanic rocks occur well east of the axis of Triassic arc magmatism, but rest above Triassic sedimentary rocks that are correlated with an eastern sedimentary facies of the Nicola Group.

In southern BC, Mesozoic rocks included in the Quesnel Terrane rest stratigraphically above diverse assemblages of Paleozoic rocks, commonly across an angular unconformity (Read and Okulitch, 1977). These Paleozoic successions include arc-derived sedimentary and volcanic rocks of the Harper Ranch Group (Smith, 1979; Danner and Orchard, 2000), Attwood Group (Fyles, 1990; Dostal *et al*., 2001) and Mount Roberts Formation (Little, 1982; Roback and Walker, 1995); metamorphic rocks of the Spa Creek and Bob Creek assemblages (Erdmer *et al*., 2001, 2002); oceanic rocks included in the Slide Mountain Terrane (Campbell, 1971; Klepacki and Wheeler, 1985; Rees, 1987); and assemblages of oceanic rocks farther to the west that include the Knob Hill Group (Fyles, 1990; Dostal *et al*., 2001) and the Old Tom, Independence and Shoemaker formations (Bostock, 1941; Tempelman-Kluit, 1989). There is indirect evidence, mainly from provenance arguments, that some of these underlying Paleozoic successions formed above a basement with North American affinities (Roback and Walker, 1995; Ferri, 1997; Erdmer *et al.*, 2001, 2002). Tectonic models presented by Roback and Walker (1995) and Ferri (1997) suggest that Paleozoic arc rocks of the Quesnel Terrane formed on a fragment of continental crust that rifted away from ancestral North America during back-arc extension that produced the Slide Mountain marginal ocean basin. Subsequent collapse of the Slide Mountain basin in Permian–Triassic time may have brought this fragment back into proximity with the continental margin, and formed a complex, structurally imbricated basement on which the Triassic-Jurassic arc of the Quesnel Terrane formed (*e.*g., Schiarizza, 1989; Ferri, 1997; Dostal *et al*., 2001).

The structural geology of the Quesnel Terrane includes generally poorly understood faults that exerted controls on Late Triassic volcanic-sedimentary facies distributions and the localization of plutons and associated mineralization and alteration systems (Preto, 1977, 1979; Nelson and Bellefontaine, 1996; Logan and Mihalynuk, 2005b). In north-central BC, orogen-parallel sinistral strike-slip faults that may be broadly synchronous with arc magmatism (Schiarizza and Tan, 2005) occur outboard of east-directed thrust faults that formed during the latter stages of magmatism and juxtapose Quesnel Terrane above adjacent miogeoclinal rocks (Nixon *et al*., 1997). These structures may reflect transpressive deformation during construction of the Quesnel magmatic arc, perhaps reflecting oblique sinistral convergence between the arc system and the subducting oceanic tract to the west (Struik, 1993). In southern BC, late Early Jurassic east-directed thrust faults and associated folds are documented within the eastern part of Quesnel Terrane, and along the structural base of the terrane where it is juxtaposed above the Slide Mountain and Kootenay terranes (Struik, 1986, 1988b; Rees, 1987). Younger structures within the southern Quesnel Terrane include west to southwest-verging folds, in part of early Middle Jurassic age, that deform the east-directed thrust faults (Ross *et al*., 1985; Brown *et al*., 1986; Rees, 1987), and prominent systems of Eocene dextral strike-slip and extensional faults (Ewing, 1980; Panteleyev *et al*., 1996; Schiarizza *et al*., 2002a).

The Quesnel Terrane is an important metallogenic province, particularly for porphyry deposits containing Cu, Au and Mo. The world-class Highland Valley Cu-Mo porphyry deposits occur in calcalkaline plutonic rocks of the Late Triassic Guichon Creek Batholith (Casselman *et al*., 1995), which is hosted in the western calcalkaline belt of the Nicola Group (Fig. 1). The Gibraltar Cu-Mo mine, 240 km to the north-northwest, is associated with sodic calcalkaline plutonic rocks of about the same age but occurs in a structurally complex setting along the boundary between Cache Creek and Quesnel terranes (Bysouth *et al*., 1995; Ash and Reveros, 2001). Somewhat younger, latest Triassic alkaline plutons define a wide belt to the east of these calcalkaline deposits, and host important Cu-Au porphyry deposits, including the Afton mine and associated occurrences within the Iron Mask batholith near Kamloops, and the Mount Polley mine west of Quesnel Lake (Mortensen *et al*., 1995; Logan and Mihalynuk, 2005a, b). Cospatial with these latest Triassic alkaline plutons is a belt of large, Early Jurassic calcalkaline plutons that includes the Takomkane and Thuya batholiths in the Bonaparte Lake map sheet. Much younger calcalkaline plutons of mid-Cretaceous age crosscut terrane boundaries and host porphyry Mo deposits, including the past-producing Boss Mountain mine (Macdonald *et al*., 1995).

LITHOLOGICAL UNITS

The distribution of the main lithological units in the Canim Lake area is shown on Figure 2. Figure 3 combines the Canim Lake map area with the area mapped in 2000 and 2001, during the Bonaparte project, to summarize the authors' geological interpretation of the Quesnel belt between the Thuya and Takomkane batholiths. The Canim Lake area is underlain mainly by sedimentary and volcanic rocks assigned to the Middle to Upper Triassic Nicola Group. Lower Jurassic sedimentary rocks are restricted to a small area along the southern boundary of the map area. Intrusive rocks include Late Triassic to Early Jurassic suites that are part of the Quesnel magmatic arc, as well as younger granitic rocks of mainly Cretaceous age. Eocene volcanic and volcaniclastic rocks occupy a large area in the southwestern part of the map area, and outliers of Quaternary basalt, related to the Wells Gray – Clearwater volcanic rocks, occur in the eastern part of the area.

Nicola Group

The Nicola Group, named for exposures on the south side of Nicola Lake (Dawson, 1879), comprises a diverse assemblage of Middle and Upper Triassic volcanic, volcaniclastic and sedimentary rocks that crop out over a broad area in south-central BC. Campbell and Tipper (1971) assigned volcanic and associated sedimentary rocks of known or inferred Late Triassic age in the Bonaparte Lake map sheet to the group, including a belt of rocks on the northern margin of the Thuya batholith, and another, smaller belt, on the southeastern margin of the Takomkane batholith. However, they included most of the Mesozoic sedimentary and volcanic rocks between the Thuya and Takomkane batholiths in two Lower to Middle Jurassic map units, one of mainly sedimentary rocks (their unit 15) and the other dominated by volcanic rocks (unit 16). A fourth Mesozoic unit mapped by Campbell and Tipper in the northeastern Bonaparte Lake map sheet comprises Triassic sedimentary rocks that form a belt on the eastern mar-

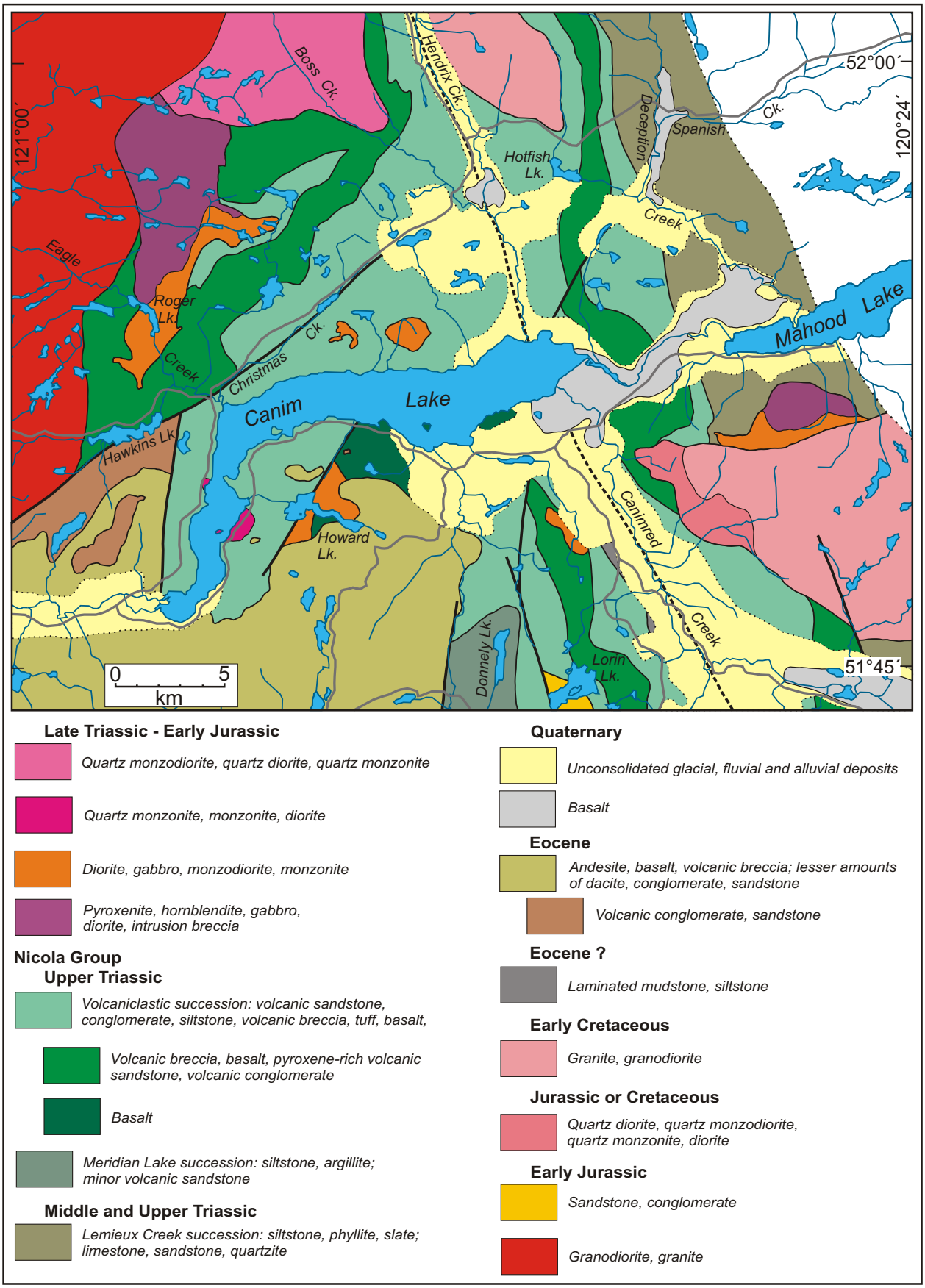


Figure 2. Generalized geology of the Canim Lake map area, based mainly on 2005 fieldwork.

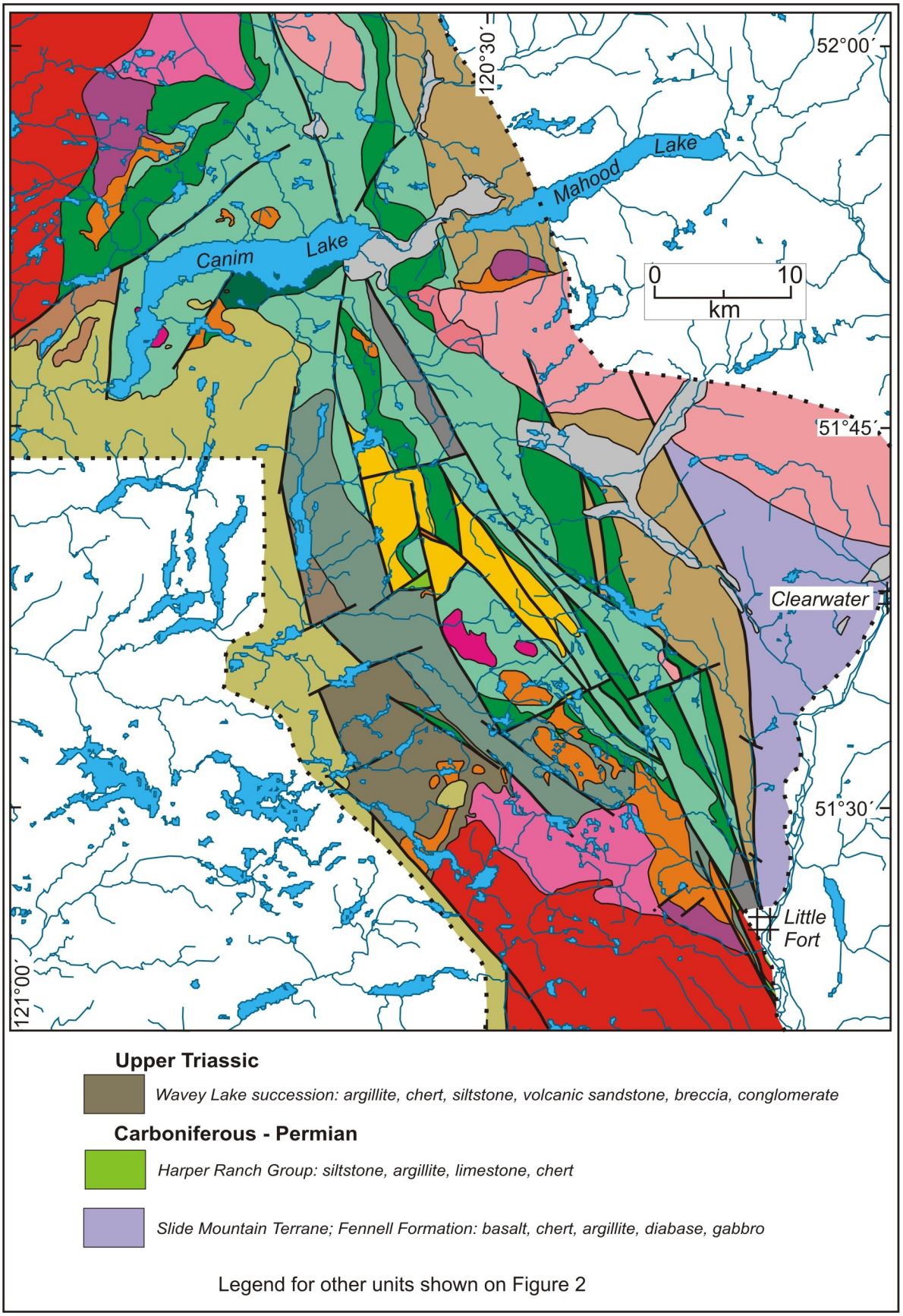


Figure 3. Generalized geology of the area between the Thuya and Takomkane batholiths, based on fieldwork conducted in 2000, 2001 and 2005.

gin of Quesnel Terrane (their unit 10). This unit was not included in the Nicola Group, in part because it was separated from Nicola exposures to the west by an extensive belt of rocks assigned to their Jurassic map units.

Schiarizza and Israel (2001) and Schiarizza *et al*. (2002a, b, c) reassigned most of Campbell and Tipper's (1971) Jurassic rocks in the Nehalliston Plateau – Bowers Lake area to the Triassic Nicola Group, based on lithological similarity to known Triassic rocks and a single new Late Triassic fossil age. They inferred that Jurassic sedimentary rocks were restricted to a narrow, northwest-trending belt centred on the fossiliferous localities at Windy Mountain (Fig. 3). Schiarizza *et al*. also included the eastern Triassic sedimentary belt (Campbell and Tipper's unit 10) in the Nicola Group, based partly on work to the north, where correlative rocks are interpreted as the stratigraphic base of the Nicola Group (Panteleyev *et al*., 1996), or an eastern sedimentary facies of the group (Struik, 1988b).

The subdivision of Mesozoic volcanic and sedimentary rocks in the Canim Lake map area follows, for the most part, the interpretation of Schiarizza *et al*. (2002a, b). Most rocks are assigned to the Middle to Upper Triassic Nicola Group, which includes two major subdivisions: the Lemieux Creek succession, comprising Middle and Upper Triassic sedimentary rocks in the eastern part of the group; and the volcaniclastic succession, a diverse assemblage of volcaniclastic and volcanic rocks that crop out over a broad area to the west. The Lemieux Creek succession is equivalent to unit 10 of Campbell and Tipper (1971). The volcaniclastic succession includes rocks assigned to the Nicola Group by Campbell and Tipper, but is dominated by rocks that they considered to be Jurassic (their units 15 and 16). The volcaniclastic succession includes two internal subunits, one dominated by coarse pyroxene porphyry breccia (breccia subunit) and one dominated by mafic volcanic flows (basalt subunit). Siltstone and argillite assigned to the Meridian Lake succession constitute an additional subdivision of the Nicola Group, restricted to a small area near the southern boundary of the Canim Lake map area. These rocks seem to underlie and interfinger with those of the volcaniclastic succession and may, in part, be correlative with the Lemieux Creek succession (Schiarizza *et al*., 2002a).

LEMIEUX CREEK SUCCESSION

The Lemieux Creek succession is dominated by dark grey slate, phyllite and siltstone that form the easternmost part of Quesnel Terrane in the Canim Lake map area. It forms a continuous, north-northwest-trending belt extending from the northern margin of the Raft batholith to the northern boundary of the map area. It also crops out on the southern margin of the batholith, and from there has been traced 34 km south to Little Fort, where it apparently pinches out between strands of the Rock Island Lake and Lemieux Creek fault systems (Fig. 3; Schiarizza and Israel, 2001). Rocks correlative with the Lemieux Creek succession extend far to the north of the Canim Lake map area, and include the informally named black phyllite unit of the Quesnel Lake area (unit 1 of Panteleyev *et al*., 1996), and the Slate Creek succession of the Takla Group in north-central BC (Ferri and Melville, 1994; Nelson and Bellefontaine, 1996).

The Lemieux Creek succession is well exposed in a canyon on lower Deception Creek and near the northern boundary of the map area along the east-flowing tributary to Deception Creek that contains the DL gold – quartz vein occurrence. It is also represented by abundant exposures of siltstone near the ridge top south of the west end of Mahood Lake. Elsewhere, it is represented by scattered small exposures, typically along logging roads, and by abundant fine rubble of black slate and phyllite, commonly accompanied by larger blocks of white vein quartz, which is a characteristic feature of the unit.

The Lemieux Creek succession in the Canim Lake map area consists mainly of dark grey to black slate and phyllite, commonly spotted with rusty porphyroblasts of siderite and/or pyrite, and locally containing small dark porphyroblasts of chlorite or chloritoid (Fig. 4). Veins and lenses of quartz or quartz-carbonate are a common feature. These range from a few millimetres to more than 1 m in thickness; most veins are subparallel to the slaty cleavage, but some crosscut cleavage at a high angle. Locally the slaty rocks include laminae and/or thin to medium interbeds of siltstone, slaty siltstone, slaty sandstone, calcareous sandstone and dark grey slaty to sandy limestone. Westernmost exposures of the succession adjacent to the Aqua Creek ultramafic-mafic complex, south of Mahood Lake, are dominated by dark to light grey, thin-bedded to laminated siltstone.

The Lemieux Creek succession is not dated within the Canim Lake map area, but limestone-bearing intervals to the north and south have yielded macrofossils and conodonts of Middle and Late Triassic age (Panteleyev *et al*., 1996; Schiarizza *et al*., 2002a). To the east, beyond the limits of the Canim Lake map area, the Lemieux Creek succession is in fault contact with Paleozoic rocks of the Slide Mountain and Kootenay terranes. To the west, the unit is in contact with the Nicola volcaniclastic succession, across what is interpreted as a west-facing stratigraphic contact.



Figure 4. Grey slate of the Lemieux Creek succession, west side of Deception Creek near northern boundary of the map area.

MERIDIAN LAKE SUCCESSION

Generally fine-grained sedimentary rocks of the Meridian Lake succession form a belt that extends from the northern margin of the Thuya batholith to the south-central part of the Canim Lake map area (Fig. 3). This succession consists mainly of thin-bedded siltstone and argillite, but also includes local beds of fine to coarse-grained volcanic sandstone and conglomerate. Intervals of dark grey limestone occur locally in more southerly exposures of the succession, and have yielded several conodont collections of Late Triassic (Carnian) age (Schiarizza *et al*., 2002a; conodonts identified M.J. Orchard, Geological Survey of Canada). External contacts are in large part faults, but the southern part of the succession is locally overlain to the east by volcanic rocks of the Nicola volcaniclastic succession, and stratigraphically underlain to the west by an assemblage of chert, volcanic sandstone and volcanic breccia assigned to the Wavey Lake succession (Schiarizza *et al*., 2002a).



Figure 5. Thin-bedded sandstone of the Nicola volcaniclastic succession, north of Canim Lake.

In the southern part of the Canim Lake map area, the Meridian Lake succession is represented by sparse exposures of siltstone, argillite and local fine to medium-grained sandstone in the vicinity of Donnely Lake. These fine-grained rocks pass into coarse volcanic sandstone and local breccia of the Nicola volcaniclastic succession to the north and east. The nature of these contacts is not well understood, although it appears that the Meridian Lake succession underlies and/or interfingers with the coarser volcaniclastic rocks.

VOLCANICLASTIC SUCCESSION

The volcaniclastic succession of the Nicola Group is the most widespread map unit in the Canim Lake map area. It forms a wide belt, locally more than 25 km across, bounded by the Lemieux Creek succession to the east and the Takomkane batholith and Eocene Skull Hill Formation to the west. It is the northward extension of rocks mapped mainly as the mixed volcanic-sedimentary unit (uTrNsv) of the Nicola Group by Schiarizza *et al*. (2002a–c). However, it also includes mappable units of volcanic breccia that Schiarizza *et al*. (2002a–c) mapped as two separate units underlying and overlying their mixed volcanic-sedimentary unit (their units uTrNv and lJb, respectively). These volcanic breccia units are here assigned to an internal subunit (breccia subunit) that probably occurs at several different stratigraphic levels within the volcaniclastic succession.

The volcaniclastic succession consists mainly of grey to green, fine to coarse-grained, commonly gritty, volcanogenic sandstone. Mineral grains of pyroxene, feldspar and locally hornblende, together with lithic fragments containing these same minerals, are the dominant constituents. In places, the sandstone forms well-defined thin to thick beds (Fig. 5), but it occurs elsewhere as massive units, up to several tens of metres thick, in which bedding is not apparent. The well-bedded intervals commonly include interbeds of green to grey siltstone or dark grey argillite, and locally display graded bedding, flame structures and rip-up clasts. Locally, siltstone and argillite, with little or no intercalated sandstone, dominate intervals up to several metres thick. Beds of calcareous sandstone to sandy limestone occur within some well-bedded intervals, particularly along the west shore of southern Canim Lake, and rare thin beds of green chert were noted within a section of thin-bedded sandstone and siltstone northwest of Howard Lake.

Coarse-grained intervals, including pebbly sandstone, pebble conglomerate and volcanic breccia, are common within the volcaniclastic succession, and include massive units many tens of metres thick, as well as medium to thick beds intercalated with volcanic sandstone. Conglomerate units contain angular to subrounded clasts of mainly pyroxene-feldspar-phyric mafic volcanic rocks, but also include clasts of siltstone, limestone and diorite. Volcanic breccia comprises angular to subangular fragments of pyroxene-feldspar porphyry within a matrix of mainly pyroxene and feldspar mineral grains. Pyroxene-feldspar porphyry also occurs as massive to rarely pillowed units, apparently derived from flows, sills and dikes, that are widespread but not abundant within the volcaniclastic succession.

The Nicola volcaniclastic succession is not dated within the Canim Lake map area, but similar rocks to the south have yielded Late Triassic macrofossils and conodonts (Campbell and Tipper, 1971; Schiarizza *et al*., 2002a, c). The contact between the volcaniclastic succession and the adjacent Lemieux Creek succession is not exposed, but is thought to be stratigraphic on the basis of concordant bedding orientations and some intercalation of characteristic rock types in adjacent outcrops of the respective units. West-facing stratigraphic tops indicators in easternmost exposures of the volcaniclastic succession indicate that it overlies the Lemieux Creek succession. A gradational stratigraphic contact has also been inferred by some workers to the north (Rees, 1987; Bloodgood, 1990; Panteleyev *et al*., 1996), although Struik (1988b) showed that the western volcanic belt is in part the same age as the eastern sedimentary belt, and suggested that they are separated by a regionally significant thrust fault.

Breccia Subunit

Breccia containing fragments of pyroxene-phyric basalt is fairly common throughout the Nicola volcaniclastic succession and, in three separate areas, forms thick accumulations of mappable thickness and strike-extent that are assigned to the breccia subunit (Fig. 2). These three breccia units occur in different fault panels, so their stratigraphic relationships to one another are unknown. However, the breccia unit in the eastern part of the area is near the base of the volcaniclastic succession, whereas the one west of Canimred Creek is apparently near the top. It is suspected, therefore, that they represent relatively proximal accumulations of coarse volcanic material at two or three spatially and stratigraphically distinct sites within the volcaniclastic succession.



Figure 6. Volcanic breccia containing pyroxene-phyric basalt fragments, breccia subunit, east of Hotfish Lake.

Volcanic breccia of the breccia subunit is medium to dark green or grey-green, and commonly forms relatively resistant, blocky, green-brown to rusty brown weathered exposures. Fragments are typically angular to subangular, and commonly range from a few centimetres to 10 cm in diameter (Fig. 6), although much larger fragments occur locally. In most exposures, the fragments are exclusively or dominantly pyroxene and pyroxene-feldspar-phyric basalt, but show considerable textural variation based on size, abundance and feldspar versus pyroxene proportions in the phenocryst population, as well as degree of vesiculation and presence or absence of amygdules. The matrix is dominated by pyroxene and feldspar grains, and the compositional similarity between clasts and matrix in many exposures obscures the fragmental texture. Locally, the clast population also includes hornblende (±feldspar±pyroxene) porphyry, diorite, aphyric basalt, pyroxenite, hornblendite, laminated siltstone and argillite. In some exposures east of the Boss Creek unit of the Takomkane batholith, the breccia fragments are mainly hornblendite, hornblende pyroxenite, gabbro and diorite, and the matrix is dominated by hornblende crystals. This breccia was derived from erosion of an ultramafic-mafic plutonic complex similar to the Iron Lake complex, which crops out just 8 km to the west.

The generally massive breccia of the breccia subunit locally includes intercalations of thin to thick-bedded pyroxene-rich sandstone and pebble to cobble conglomerate. The conglomerate resembles the breccia in composition, but contains a higher proportion of subrounded clasts and tends to be weakly stratified and/or include substantial interbeds of volcanic sandstone. Massive pyroxene-feldspar porphyry, probably derived from sills, dikes and flows, is fairly widespread in the breccia subunit, and pillowed basalt was noted locally within the northwestern and south-central belts (Fig. 7). Limestone occurs within the northwestern belt in a small area north of Hawkins Lake.

Basalt Subunit

A single mappable unit dominated by mafic flow rocks is assigned to the basalt subunit of the Nicola volcaniclastic succession. This unit is represented mainly by scattered small exposures of medium to dark green pyroxene-feldspar-phyric basalt that extend from Howard Lake north-northeastward to Canim Lake. These rocks are intruded by dioritic rocks of the Howard Lake stock, are overlain by Eocene volcanic rocks and are juxtaposed against sandstone typical of the volcaniclastic succession across the Howard Lake fault. The same belt of rocks may be represented by a few isolated exposures of silica-pyrite-altered basalt 5 km to the east, along and near the south shore of Canim Lake.



Figure 7. Pillowed basalt, breccia subunit, northeast of Hawkins Lake.

Lower Jurassic Sedimentary Rocks

A succession of Lower Jurassic sedimentary rocks is well exposed at Windy Mountain, 8 km south of the Canim Lake map area, where it includes a thick section of polymictic conglomerate, and overlying thin-bedded sandstone and siltstone that locally contain Early Jurassic ammonites (Campbell and Tipper, 1971; Schiarizza *et al*., 2002a, b). The most distinctive part of this succession is the conglomerate, which commonly includes clasts of granitic rock. Schiarizza *et al*. (2002a, b) mapped Lower Jurassic sedimentary rocks in several fault panels extending southeast and north-northwest from Windy Mountain, based on lithological correlation with the fossiliferous section (Fig. 3). They projected the westernmost panel of Jurassic rocks northward to within 6 km of Canim Lake, based on reconnaissance-scale mapping. More detailed work during the 2005 field season suggests that the rocks in the northern part of this belt are actually part of the Upper Triassic Nicola Group. The northernmost exposures that are confidently included in the Jurassic succession, based on the occurrence of granitoid-bearing conglomerate, are on the south side of Lorin Lake, near the southern boundary of the Canim Lake map area. These Lower Jurassic rocks are inferred to pinch out to the north, between the underlying Nicola Group to the east and a northerly-striking fault to the west (Fig. 2).

Intrusive Rocks

IRON LAKE ULTRAMAFIC-MAFIC COMPLEX

The Iron Lake complex comprises ultramafic and mafic plutonic rocks that crop out in the northwestern part of the Canim Lake map area. The complex is more than 13 km long and up to 6 km wide. It intrudes the Nicola volcaniclastic succession, mainly the breccia subunit, along its eastern, southern and southwestern margins, but is in contact with the Boss Creek and Schoolhouse Lake units of the Takomkane batholith to the north and northwest. The Iron Lake complex was not mapped by Campbell and Tipper (1971), who included part of it in the Takomkane batholith and part in the Nicola Group. The ultramafic rocks of the complex contain abundant magnetite, and correspond to a very strong positive anomaly on regional aeromagnetic maps.

At the scale of Figure 2, the Iron Lake complex is subdivided into an ultramafic unit and a mafic unit. The ultramafic unit consists mainly of dark green, medium to coarse-grained, commonly biotite or phlogopite-bearing clinopyroxenite and hornblende clinopyroxenite. Olivine clinopyroxenite and wehrlite, locally displaying cumulate textures, occur in the central part of the unit (Buskas, 1989; Morton, 2001). Dark grey to black, coarse-grained hornblendite is the predominant phase in some exposures of the ultramafic unit, and elsewhere occurs as centimetre-scale patches or dikes within pyroxenite. Plagioclase-bearing hornblendite and pyroxenite are also present, and locally grade into melanocratic gabbro. At one locality, near the northwest corner of the ultramafic unit, hornblende pyroxenite, hornblende-feldspar pyroxenite, gabbro and diorite occur as parallel sheets defined partly by modal layering and partly by dikes. Coarse-grained to pegmatitic, leucocratic hornblende-pyroxene gabbro is fairly common as irregular dikes and pods within the ultramafic rocks, and locally forms the matrix to intrusion breccia containing fragments of ultramafic rock and mafic gabbro (Fig. 8). Dikes of medium to fine-grained diorite and monzodiorite are also present but less common.

Mafic intrusive rocks predominate in a mappable unit that bounds the ultramafic unit to the south and southeast (Fig. 2). The mafic unit consists mainly of medium to coarse-grained hornblende-pyroxene gabbro to monzogabbro, and medium to fine-grained hornblende diorite and microdiorite. Dioritic rocks northeast of Roger Lake are commonly cut by a west-northwest-dipping foliation, and locally grade to amphibolite. Monzogabbro in the southern part of the unit locally includes centimetre-scale veins and patches of pegmatitic monzogabbro to monzonite, and locally displays vague concentric zones defined by modal variations in the feldspar versus mafic content. Dikes of hornblende-feldspar porphyry, monzonite and feldspar porphyry occur locally, and one exposure along the southwestern margin of the mafic unit comprises sheeted dikes of diabase, microgabbro and feldspar-hornblende clinopyroxenite.

The Iron Lake complex is not dated, but samples of diorite and hornblende gabbro collected during the 2005 field season have been submitted for U-Pb dating of zircons and Ar/Ar dating of hornblende, respectively.

AQUA CREEK ULTRAMAFIC-MAFIC COMPLEX

The Aqua Creek complex comprises ultramafic and mafic plutonic rocks that crop out on the north side of the Raft batholith, south of the western end of Mahood Lake. These rocks intrude the Lemieux Creek succession of the Nicola Group, and are themselves cut by the main monzogranite to granodiorite phase of the Raft batholith. The Aqua Creek complex was not mapped by Campbell



Figure 8. Intrusion breccia, Iron Lake ultramafic-mafic complex, east of Iron Lake.

and Tipper (1971), who included it in their unit 16, which consists of mafic volcanic and volcaniclastic rocks. They did note, however, that the rocks in this area contain a very high proportion of augite and resemble pyroxenite, and that they might be shallow intrusions. As with the Iron Lake complex, the ultramafic rocks of the Aqua Creek complex are rich in magnetite and generate a very strong positive anomaly on aeromagnetic maps.

The Aqua Creek complex is lithologically very similar to the Iron Lake complex, except that olivine-bearing rocks are not present. Ultramafic rocks dominate an apparently oval-shaped unit that forms the northeastern part of the complex; the northern limit of these rocks is not exposed, but is inferred from the regional aeromagnetic map. This ultramafic unit consists mainly of clinopyroxenite, hornblende clinopyroxenite, hornblendite, mafic gabbro and pegmatitic gabbro (Fig. 9). Most phases contain magnetite and either biotite or phlogopite as important accessory minerals. Mafic plutonic rocks, dominated by medium to coarse-grained hornblende-pyroxene gabbro and medium-grained hornblende diorite, form a mappable unit to the south and southwest of the ultramafic rocks. These rocks are locally converted to amphibolite along their contact with the Raft batholith. The northwestern boundary of the mafic unit is a complex zone of mafic plutonic rocks containing rafts of hornfelsed siltstone, passing northward into siltstone-dominated exposures containing dikes of gabbro and diorite.

Samples of pegmatitic gabbro and diorite from the Aqua Creek complex have been submitted for Ar/Ar dating of hornblende and U-Pb dating of zircons, respectively.

SMALL DIORITIC STOCKS

The Nicola volcaniclastic succession on the north side of Canim Lake is cut by an irregular stock and/or dike swarm of hornblende diorite south-southeast of Christmas Lake (Thompson, 1987), and by a roughly circular stock of similar composition 2 km to the east (Smith, 1976). To the south, at Howard Lake, poorly exposed diorite, monzonite, syenite and associated intrusion breccia form a mineralized intrusive body that cuts the basalt subunit of the Nicola Group. This intrusion is truncated by the Howard Lake fault to the west, and is partially overlapped by Eocene volcanic rocks to the south and southeast. Ten kilometres east of Howard Lake, a northwest-trending stock of hornblende-pyroxene gabbro cuts pyroxene porphyry breccia and conglomerate of the volcanic breccia subunit. All of these stocks, together with numerous smaller intrusive bodies of similar composition, are interpreted as part of the Quesnel magmatic arc and inferred to be Late Triassic and/or Early Jurassic in age.

TAKOMKANE BATHOLITH

The Takomkane batholith is a large, roughly equidimensional body of granitic rock that measures more than 40 km across (Fig. 1). The southeastern part of the batholith crops out within the Canim Lake map area, where it has been subdivided into two units. The most extensive unit consists of granodiorite to monzogranite assigned to the Schoolhouse Lake unit. A lithologically distinct suite dominated by quartz monzodiorite is well exposed on either side of Boss Creek, and is referred to as the Boss Creek unit. Crosscutting relationships were not observed, but the authors suspect that the Boss Creek unit is somewhat older. Both units cut the breccia subunit of the Nicola volcaniclastic succession, as well as the Iron Lake ultramafic-mafic complex. The Schoolhouse Lake unit is faulted against Eocene volcaniclastic rocks of the Skull Hill Formation west of Canim Lake.

The Schoolhouse Lake unit consists mainly of light grey to pinkish grey, coarse to medium-grained hornblende-biotite granodiorite, locally grading to monzogranite in the vicinity of Lang Lake, or to tonalite along the unit's eastern contact near Hawkins Lake. Textures vary from equigranular in granodiorite and tonalite, to K-feldspar porphyritic in monzogranite and some granodiorite. Mafic minerals typically form 10–20% of the rock, with hornblende commonly predominating over biotite. Weak, steeply dipping, margin-parallel foliations were locally observed in tonalite and granodiorite near the eastern contact of the batholith, but most rocks are isotropic. The Schoolhouse Lake unit is assigned an Early Jurassic age on the basis of a 193.5 ±0.6 Ma U-Pb zircon date reported by Whiteaker *et al*. (1998). The zircons were separated from a sample of granodiorite collected at Ruth Lake, just 2 km west of the Canim Lake map area. Similar granodiorite forms a major component of the Thuya batholith to the south, and has yielded an almost identical U-Pb zircon date of 192.7 ±0.9 Ma (Schiarizza *et al*., 2002a, c).

The Boss Creek unit comprises medium to coarse-grained, equigranular, biotite-hornblende quartz monzodiorite, locally grading to quartz diorite, granodiorite, tonalite or diorite. Mafic minerals commonly make up 15–25% of the rock, and biotite is generally more abundant than hornblende. Most rocks are isotropic, but weak south-southeast-dipping foliations were locally observed in the eastern part of the unit, and narrow north-northwest to north-northeast-striking mylonitic shear zones were observed in some exposures directly west of



Figure 9. Pegmatitic hornblende gabbro of the Aqua Creek ultramafic-mafic complex, south of Mahood Lake.

Boss Creek. The Boss Creek unit is undated, but a sample collected during the 2005 field season has been submitted for U-Pb dating of zircons. Similar rocks make up much of the northern part of the Thuya batholith, and have yielded a U-Pb zircon upper intercept date of 201.3 ±2.3 Ma, which is interpreted as a maximum crystallization age (R. Friedman, pers. comm., 2002).

SOUTH CANIM STOCK

The South Canim stock cuts volcanic sandstone and related rocks of the Nicola volcaniclastic succession along the southern part of Canim Lake. It consists mainly of light greenish grey to pinkish grey, medium to coarse-grained, hornblende-biotite monzonite, locally grading to quartz monzonite, monzodiorite and diorite. Textures are typically isotropic and equigranular, although K-feldspar crystals locally tend to be slightly larger than other mineral grains. The stock is best exposed as a series of bluffs on the east side of Canim Lake, but is also represented by exposures of monzonite to diorite on two islands in the eastern part of the lake. A single exposure along the Canim-Hendrix road, comprising a complex mixture of syenite to monzonite, diorite and microdiorite, with local hornblendite xenoliths and leucodiorite dikes, indicates that the northwestern tip of the stock extends to the west side of the lake.

The South Canim stock was mapped as Cretaceous by Campbell and Tipper (1971). However, its relatively alkalic composition suggests that it is more likely part of the Quesnel Terrane magmatic suite, and Late Triassic or Early Jurassic in age. A sample of quartz monzonite that was collected during the 2005 field season has been submitted for U-Pb dating of zircons.

RAFT BATHOLITH

The Raft batholith is an elongate granitic pluton that extends for about 70 km in a west-northwest direction, and cuts across the boundaries between the Kootenay, Slide Mountain and Quesnel terranes (Fig. 1). The Canim Lake map area includes the western end of the batholith, which crosscuts several mappable units of the Nicola Group and also truncates the Aqua Creek ultramafic-mafic complex. The batholith consists mainly of granite and granodiorite of mid-Cretaceous age, but a separate unit of mainly quartz monzodiorite makes up its western end.

Most of the Raft batholith within the Canim Lake map area consists of light grey, medium to coarse-grained biotite-hornblende granodiorite to monzogranite. Textures vary from equigranular to porphyritic, the latter characterized by pink orthoclase crystals up to 1.5 cm in size. Mafic minerals typically make up 10–20% of the rock, with biotite predominating over hornblende. At one locality near the northern margin of the batholith, however, modal layering on a scale of 10–30 cm is defined mainly by variations in the mafic mineral content, which ranges from 5–40%.

The lithologically distinct, western end of the Raft batholith consists mainly of medium to fine-grained, equigranular hornblende-biotite quartz monzodiorite, locally grading to quartz diorite, diorite or granodiorite. Crosscutting relationships between these rocks and the main granodiorite to monzogranite unit to the east were not observed. Both mappable units are cut by uncommon aplite dikes.

Previous mapping to the east-southeast indicates that biotite-hornblende granodiorite to monzogranite, as found in the Canim Lake map area, is the predominant rock type within the southern part of the Raft batholith as far east as the Clearwater River (Schiarizza *et al*., 2002a). A sample collected about 10 km east of the Canim Lake area in 2001 was submitted to Richard Friedman at the University of British Columbia for U-Pb dating of zircons, and yielded a concordia date of 105.5 ±0.5 Ma (Schiarizza *et al*., 2002b). This late Early Cretaceous date is interpreted as the crystallization age of the main part of the Raft batholith. However, Calderwood *et al*. (1990) obtained an upper intercept U-Pb zircon date of 168 +14/–12 Ma from a granodiorite sample collected from the west side of the Clearwater River, about 8 km north of Clearwater. They interpreted this Middle Jurassic date as a magmatic age, although the same sample yielded a biotite K-Ar date of 138 ±6 Ma and a Rb-Sr whole-rock mineral separates isochron date of 104.3 ±3.3 Ma (Jung, 1986).

The relationship between the granodiorite sample dated by Calderwood *et al*. (1990) and the granitic rocks here assigned a mid-Cretaceous age is not known. Although there is large analytical uncertainty in the Jurassic date, similar ages have been obtained from several Jurassic plutons associated with the arcuate belt of mid-Cretaceous granite that extends from the Raft batholith southeastward to the International Boundary (Logan, 2002). The closest such occurrence is about 50 km southeast of Clearwater, where quartz monzodiorite of the Honeymoon stock, on the southern margin of the mid-Cretaceous Baldy batholith, has yielded a Middle Jurassic U-Pb titanite date of 161 ±7.8 Ma (Logan, 2001). Therefore, it is possible that the predominantly mid-Cretaceous Raft batholith encompasses some older, Middle Jurassic phases. In light of this possible heterogeneity, a sample of quartz monzodiorite from the western unit of the Raft batholith was collected during the 2005 field season and submitted for U-Pb dating of zircons.

HENDRIX STOCK

A granitic pluton that intrudes the Nicola volcaniclastic succession at the north end of the map area, east of Hendrix Creek, is informally referred to as the Hendrix stock. The stock has an elliptical shape in plan view, with a northwest-trending major axis about 9 km long, although the northernmost portion lies beyond the limit of the present mapping. The western margin of the stock is obscured by Quaternary drift along Hendrix Creek; consequently, its relationship to the fault that is inferred to follow the creek is unknown.

The Hendrix stock consists mainly of light grey, medium to coarse-grained, equigranular biotite-hornblende monzogranite to granodiorite. Mafic minerals typically make up 10–20% of the rock, with biotite generally predominating over hornblende. Tonalite that was observed along the southern margin of the stock, however, has hornblende as the dominant mafic phase. The stock was assigned a Cretaceous age by Campbell and Tipper (1971). This interpretation is reasonable, as it is lithologically similar to Cretaceous rocks of the Raft batholith, but will be tested by U-Pb dating of zircons from a sample collected during the 2005 field season. The northern margin of the stock, which the authors anticipate mapping in 2006, is spatially associated with a zone of skarn-like mineral showings in the adjacent country rock (Dave Ridley, pers. comm., 2005).

Eocene (?) Sedimentary Rocks West of Canimred Creek

Thin-bedded sedimentary rocks, represented by sparse exposures west of Canimred Creek in the southeastern part of the map area, were first recognized by Schiarizza *et al*. (2002a), and tentatively correlated with an assemblage of Eocene lacustrine sedimentary rocks that crops out in the valley of the Horsefly River, about 60 km to the north-northwest (Wilson, 1977; unit 10 of Panteleyev *et al*., 1996). The rocks west of Canimred Creek comprise laminated to thin-bedded siltstone and mudstone, in pale shades of purple, grey and green. They dip eastward at moderate angles and are inferred to unconformably overlie Triassic volcaniclastic rocks of the Nicola Group, which crop out to the west. Relationships to the east are masked by a wide belt of unconsolidated Quaternary deposits, but it is suspected that the thin-bedded sedimentary rocks dip into, and are bounded by, a north-northwest-striking fault (Rock Island Lake fault) that follows the valley of Canimred Creek (Schiarizza *et al*., 2002a).

Eocene Volcanic and Volcaniclastic Rocks (Skull Hill Formation)

Campbell and Tipper (1971) assigned Eocene volcanic rocks in the Bonaparte Lake map sheet to the Skull Hill Formation of the Kamloops Group. The Skull Hill Formation is well represented in the southwestern part of the Canim Lake map area, where it forms a horseshoe-shaped belt, more than 20 km wide, that wraps around the south end of Canim Lake. These rocks form the north end of a continuous belt of Eocene exposures that extends 70 km south to Bonaparte Lake (Fig. 1). The Eocene rocks in the Canim Lake area typically flat lying and markedly less altered and deformed than the Mesozoic rocks. They rest unconformably above the Nicola Group and related intrusions, but are locally separated from the older rocks by north or north-northeast-striking faults. Two outliers of the Skull Hill Formation rest above the Nicola volcaniclastic succession on hilltops east of southern Canim Lake (Fig. 2).

The Skull Hill Formation in the Canim Lake map area consists mainly of grey to brown, red to brown-weathered, pyroxene-feldspar-phyric basalt or andesite, and related flow breccia. Hornblende-feldspar-phyric andesite occurs locally, and pink dacite containing angular fragments of sedimentary and volcanic rock was observed at one locality in the northeast corner of the main exposure belt. The mafic volcanic rocks are commonly vesicular, and vesicles are partially filled with chalcedony, calcite or zeolite minerals.

Sedimentary intervals, dominated by polymictic pebble to cobble conglomerate, occur as local interbeds within the volcanic rocks, and form two mappable subdivisions south of Hawkins Lake. The conglomerate typically consists of angular to subrounded clasts within a somewhat friable, yellow-brown sandy matrix. It is massive to weakly stratified, but locally displays well-defined medium to thick beds with interbeds of lithic wacke. Clast populations are dominated by basaltic to andesitic volcanic fragments derived from the Skull Hill Formation, but also include felsic volcanic rocks that are also suspected to be Eocene. Green chlorite-epidote-altered clasts of volcanic and volcaniclastic rock, probably derived from the Nicola Group, were observed in only one exposure, 1 km south of the east end of Hawkins Lake.

Quaternary Volcanic Rocks

Flat-lying basalt flows crop out in several valleys in the eastern part of the Canim Lake map area (Fig. 2). Campbell and Tipper (1971) assigned these rocks to the Miocene–Pliocene Chilcotin basalt, which covers much of the Interior Plateau to the west (Mathews, 1989). However, more detailed study by Hickson and Souther (1984) and Hickson (1986) indicated that they are outliers of the younger Clearwater – Wells Gray volcanic field, which is a prominent feature of Wells Gray Park to the east. The Clearwater – Wells Gray volcanic rocks are, like the Chilcotin basalt, mainly alkali olivine basalt, but are almost entirely Pleistocene and Holocene in age.

Actual exposures of Quaternary volcanic rocks are restricted to stream cuts along the Canim River and Hendrix and Deception creeks. Their distribution on Figure 2 is based on extrapolating these exposures to adjacent areas of flat, plateau-like topography, where the basalt is inferred to underlie a thin veneer of alluvium and/or glacial deposits; locally their extent can also be inferred from positive anomalies on regional aeromagnetic maps. The most extensive exposures are along the Canim River below the outlet of Canim Lake, including Canim and Mahood falls. These flows are inferred to extend eastward to Deception Creek, where small exposures occur on the west side of Deception Falls. An isolated outlier farther upstream, below the confluence of Spanish Creek, is represented by one small exposure in the creek bed, but its extent is shown by a well-defined aeromagnetic anomaly. This outlier may have once been continuous with the extensive flows exposed along Spanish Creek, 7 km to the east. Good exposures also occur along Hendrix Creek at and downstream from Hendrix Falls, where about 20 m of basalt represents an outlier of restricted aerial extent. Quaternary basalt inferred to underlie the southeast corner of the map area forms the west end of a broad volcanic plateau that extends westward from Mann Creek (Schiarizza *et al*., 2002a, b).

The Quaternary volcanic rocks exposed in the Canim Lake area consist mainly of dark grey vesicular basalt that commonly contains small olivine phenocrysts. The basalt occurs as multiple, thin, columnar-jointed subaerial flows, with an aggregate thickness of several tens of metres in the thickest sections exposed along the Canim River. The basal contact was observed at one locality, on the east side of Deception Falls, where the basalt is separated from the underlying Lemieux Creek succession by a thin veneer of unconsolidated till, confirming its Pleistocene or younger age.

STRUCTURE

Mesoscopic Structure

Mesoscopic structures observed in the Lemieux Creek succession include a well-developed slaty to phyllitic cleavage that is axial planar to folds of bedding, and a crenulation cleavage, with associated crenulation lineation and mesoscopic folds, that deforms the slaty cleavage. The crenulation cleavage strikes north-northwest to north, and dips steeply to the east or west. Associated folds and crenulations plunge at moderate angles to the north or northwest. Slaty cleavage and bedding are more variable in orientation, but commonly dip at moderate angles to the southwest or northeast. Folds associated with formation of the slaty cleavage were observed only rarely, northeast of

lower Deception Creek, where they plunge steeply to the south-southwest.

The polyphase mesoscopic structures within the Lemieux Creek succession are similar to structures documented within correlative rocks to the north (Bloodgood, 1990; Rees, 1987). This deformation is attributed to east-directed thrusting of the Quesnel and Slide Mountain terranes over the Kootenay terrane in late Early Jurassic time, and subsequent early Middle Jurassic folding of these thrust faults by west-verging folds (Ross *et al*., 1985; Brown *et al*., 1986).

Fabrics comparable to those of the Lemieux Creek succession are generally not apparent in the Nicola volcaniclastic succession, although slaty cleavage was observed within fine-grained intervals intercalated with coarse volcaniclastic rocks in a few areas just west of the contact between the two units. Elsewhere, outcrop-scale structures within the volcaniclastic succession consist mainly of brittle faults and fractures. Mesoscopic folds of bedding were noted only rarely, and penetrative foliations are, for the most part, restricted to local high-strain zones associated with faults and pluton margins. Foliated rocks are most common within the breccia subunit where it borders the Schoolhouse Lake unit of the Takomkane batholith, particularly in the north-tapering wedge between the batholith and the Iron Lake complex (Fig. 2).

Map-Scale Structure

The macroscopic structure of the Canim Lake map area is not well understood, in part due to poor exposure and in part because of the lack of reliable marker beds within either the Lemieux Creek succession or the Nicola volcaniclastic succession. Mapped structures consist of north-northwest to northeast-trending faults that cut the Nicola volcaniclastic succession. Eocene volcanic rocks of the Skull Hill Formation are cut by some of these faults but are generally flat lying and show little internal deformation. Eocene (?) sedimentary rocks west of Canimred Creek, however, dip at moderate angles to the east, presumably due to rotation along the adjacent Rock Island Lake fault. In contrast to the Eocene rocks, strata of the Nicola volcaniclastic succession show highly variable orientations, with common steep to overturned dips, indicating significant pre-Eocene deformation. It is suspected that much of this deformation was Early to Middle Jurassic and related to the regional events that generated the mesoscopic structural fabrics that are common in the Lemieux Creek succession.

Despite the lack of a detailed understanding, some general features of the structure of the Nicola rocks can be noted. East of the Rock Island Lake fault, the contact between the Lemieux Creek and volcaniclastic successions, together with a mappable breccia subunit within the volcaniclastic succession, strike northward, without major disruption, from the Raft batholith to the northern limit of the map area, suggesting that the Nicola rocks in the eastern part of the area form a coherent, west-facing panel. Bedding dips mainly at moderate to steep angles toward the west, but east-dipping overturned beds are common in the lower part of the volcaniclastic succession. In the southern part of the map area, the volcaniclastic succession east of the Rock Island Lake fault forms a predominantly west-facing and west-dipping panel that is overlain, to the west, by Early Jurassic rocks. East-facing beds were noted at one place in the northern part of this belt, however, suggesting that the internal structure may be complicated. Furthermore, the Nicola rocks are unconformably overlain by east-dipping Eocene (?) sedimentary rocks directly west of Canimred Creek, suggesting that this panel has undergone some rotation adjacent to the Rock Island Lake fault. The Nicola volcaniclastic succession south of the Hawkins Creek fault appears to form a northwest-facing homoclinal panel, with southeast-dipping overturned beds predominating in the section between Canim Lake and the Howard Lake fault. The panel of rocks north of the Hawkins Creek fault also faces to the northwest and, for the most part, dips at moderate angles in that direction. However, bedding swings to a north-striking, west-dipping orientation in the northern part of this domain, in the area between the Takomkane batholith and the Rock Island Lake fault.

ROCK ISLAND LAKE FAULT

The Rock Island Lake fault is the main component of a system of steep brittle faults that Schiarizza and Israel (2001) traced from Little Fort northwestward to Canimred Creek. These faults are best exposed near Little Fort, where they cut rocks as young as the Eocene Chu Chua Formation and display kinematic indicators suggesting mainly dextral strike-slip movement. It is suspected that the Rock Island Lake fault continues to the northern boundary of the Canim Lake map area along a system of topographic linears, locally coincident with truncations of aeromagnetic patterns, defined by the drift-covered valleys of Canimred Creek, lower Boss Creek and Hendrix Creek (Fig. 2, 3). The segment inferred along Canimred Creek may truncate the poorly exposed panel of east-dipping Eocene (?) siltstone and mudstone mapped west of the creek. The inferred trace in the northern part of the area separates a belt of northerly-striking stratigraphic units to the east from a belt with mainly northeast strikes to the west.

NORTHEAST-TRENDING FAULTS

The Hawkins Lake fault extends northeastward from the western boundary of the map area through a series of topographic lineaments that include Hawkins Lake, Christmas Creek and Christmas Lake. The southwestern segment of the fault separates the Takomkane batholith and adjacent Nicola rocks of the breccia subunit from Eocene conglomerate to the south. The northeastern segment is mainly within undivided rocks of the Nicola volcaniclastic succession, but is marked by an apparently broad area of poorly exposed quartz-pyrite and carbonate-altered rocks. An exposure of heavily fractured, faulted and chlorite-epidote-calcite-altered pillowed basalt on the north side of Canim-Hendrix road, east of Eagle Creek, is near the inferred trace of the fault. The most prominent faults cutting this exposure strike north-northeast to northeast, dip steeply and contain gently plunging calcite fibres with accretion steps indicating dextral strike-slip movement.

The north-northeast-striking Howard Lake fault extends through the west end of Howard Lake to Canim Lake. It separates volcanic sandstone of the Nicola volcaniclastic succession on its west side from the basalt subunit and Howard Lake stock to the east. The fault follows a prominent topographic lineament over much of its length north of Howard Lake. Rare isolated exposures observed near this trace are so highly fractured, calcite altered and weathered that their protolith could not be established with certainty. It is suspected, but not proven, that the fault is Eocene or

younger, because Eocene volcanic rocks are much more extensive on its east side and may be truncated by it south of Howard Lake. These relationships suggest that the fault has a component of east-side-down displacement.

A north-northeast-striking fault is inferred within the Nicola volcaniclastic succession north of the east end of Canim Lake, based on the apparent offset of the breccia subunit. The fault trace follows a prominent topographic depression, in part, and corresponds to an apparent dextral offset of the breccia subunit (Fig. 2).

NORTH-TRENDING FAULTS

A north-trending fault in the south-central part of the Canim Lake map area is part of a system of north to northwest-striking faults that define the eastern limit of Eocene volcanic rocks north of the Thuya batholith (Fig. 3). Displacement along this fault appears to die out northward within the current map area. However, 13 km to the west, a parallel fault is inferred to define the eastern limit of Eocene rocks on the west side of Canim Lake. Here, the contact between Eocene and Nicola rocks is fairly well defined but not exposed. Evidence for a fault is the apparent truncation of the contact between the conglomerate and volcanic units of the Eocene assemblage, and the abrupt development of a strong, steeply dipping, north-striking foliation in Nicola rocks near the Eocene contact. This north-striking fault is apparently truncated to the north by the northeast-trending Hawkins Lake fault.

MINERAL OCCURRENCES

The known mineral occurrences in the Canim Lake map area are shown on Figure 10. Many are Cu and/or Au showings, locally enriched in Pt-Pd, associated with ultramafic, dioritic and monzonitic plutonic rocks of the Quesnel Terrane. Others include vein and shear zone–hosted occurrences that are being explored for precious metals. Porphyry Mo occurrences are associated with mid-Cretaceous granitic rocks of the Raft batholith. The MINFILE (2005) number is included after the name of each occurrence for ease of reference.

Occurrences Associated with the Iron Lake Complex

IRON LAKE (092P 132)

The Iron Lake occurrence comprises Cu-Au-Pt-Pd-Co mineralization within ultramafic rocks of the Iron Lake complex. The area was staked as the Sheri claims by Pickands Mather and Company in 1972. Low-grade Cu mineralization was discovered during a 1972–1974 exploration program that included geological mapping, a soil geochemical survey, magnetometer and IP geophysical surveys, and 694 m of diamond drilling in eight holes. The Sheri claims were allowed to lapse, but the area was subsequently covered by the Ironhorse claims from 1983 to 1987, and the Horse and Canim claims from 1987 to 1992. Exploration work was carried out by a number of individuals and companies during this time period, and the focus shifted from Cu to precious metals when anomalous Au and Pt values were returned from multielement analyses of selected core samples from the 1974 Pickands Mather drill program. The Canim and Horse claims were allowed to lapse in the early 1990s, and the Iron Lake property was restaked by Eastfield Resources Limited in 2000. The property was subsequently optioned to Argent Resources Limited, who completed a helicopter-borne electromagnetic and magnetic survey in 2004, and a four-hole, 502.7 m diamond-drill program in the winter of 2005.

Visible low-grade Cu mineralization occurs sporadically within a west-northwest-trending belt 3 km long on the Iron Lake property, but is concentrated mainly in the eastern part of this belt, near Island Lake (Buskas, 1989). Mineralization includes pyrite and chalcopyrite as blebs and disseminations in clinopyroxenite, hornblendite and gabbro, and pyrite with traces of chalcopyrite in quartz-carbonate-altered shear zones. The quartz-carbonate-altered zones also contain Au, Pt, Pd and Co (Morton, 1984; Buskas, 1989). A different style of mineralization is represented by several large, angular pieces of mineralized rubble that were discovered southeast of Island Lake in 2000. The rubble consists of olivine pyroxenite containing disseminated bornite, chalcopyrite and magnetite. Analyzed samples of this material consistently graded about 0.60% Cu, 0.55 ppm Au, 0.20 ppm Pd and 0.10 ppm Pt (Morton, 2001).

Two of the four diamond-drill holes completed on the Iron Lake property by Argent Resources early in 2005 intersected massive sulphide mineralization (Eastfield Resources Limited, news release, March 15, 2005). In one hole, a section of hornblendite contained a 1.4 m intercept of mainly pyrrhotite with lesser chalcopyrite, and graded 0.66% Cu, 299 ppm Ni and 1349 ppm Co. In the other hole, a 17 m sulphide-rich intersection in peridotite contained 0.34% Cu and 359 ppm Ni, and included 1.4 m of massive sulphide that graded 0.95% Cu, 927 ppm Ni and 836 ppm Co. None of these sulphide intervals yielded significant platinum group element or Au values.

JULY (092P 112) AND BEER (092P 125)

The July and Beer occurrences comprise low-grade Cu mineralization within and adjacent to the Iron Lake ultramafic-mafic complex northeast of Roger Lake. The Beer showing is on ground that was covered by the Beer claims, which were staked in 1970 and explored by Aragon Resources Ltd. in 1971 and 1972 (Cukor, 1973). The July claims, which covered both the July and Beer showings, were staked and explored by Utah Mines Ltd. in 1972 (Gatchalian, 1972). Work performed by these two companies included geological mapping, soil geochemical surveys, magnetometer surveys, an IP survey and bulldozer trenching. Both claim groups were allowed to lapse in the early 1970s. The two occurrences were subsequently covered by the Straw claim group, which was staked in 1993 and explored with a small program that included prospecting and a soil geochemical survey (Ridley and Dunn, 1994a).

The July showings occur in an area that is underlain mainly by pyroxenite, hornblende pyroxenite and mafic gabbro, cut by numerous dikes of diorite, monzodiorite and monzonite. Local areas of intense diking grade into intrusion breccia, comprising fragments of ultramafic rock, mafic gabbro and diorite within a matrix of leucocratic monzodiorite to diorite. Chlorite-epidote alteration is ubiquitous, and calcite, magnetite and K-feldspar are also common in late-stage veinlets and alteration patches. Mineralization is widespread, but not common and of low grade. It comprises scattered grains and small blebs of chalcopyrite, bornite and malachite, commonly associated with magne-

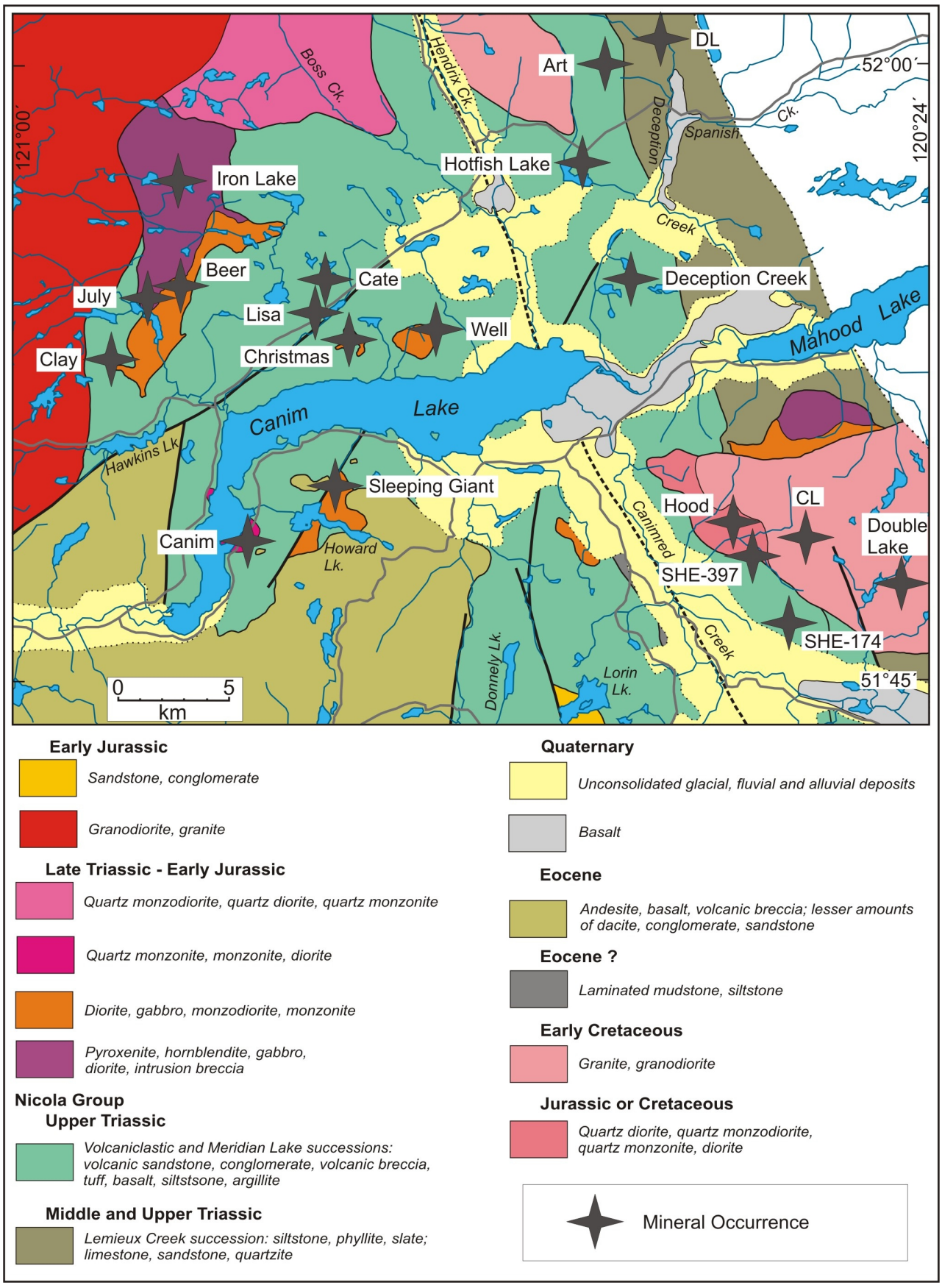


Figure 10. Mineral occurrences in the Canim Lake map area.

tite and/or disseminated pyrite (Gatchalian, 1972; this study). Host rocks are most commonly dioritic to monzonitic dikes or intrusion breccia matrix, but also include pyroxenite, gabbro and foliated volcanic breccia along the western contact of the intrusive complex.

The Beer showing comprises scattered occurrences of disseminated chalcopyrite and malachite that were identified on the Beer grid by Cukor (1973). The hostrocks were interpreted as mainly volcanic by Cukor (1973), but are herein interpreted as mainly variably altered medium to fine-grained diorite, monzodiorite and monzonite of the Iron Lake complex. However, some fine-grained, heavily chlorite-epidote-calcite-magnetite-altered rocks might be screens of volcanic country rock. The mineralization and alteration at the Beer showing is much the same as, and essentially a continuation of, the widespread but sparse and low-grade mineralization of the July showing.

CLAY (092P 155)

The Clay occurrence consists of Cu-Au mineralization within volcanic breccia of the Nicola volcaniclastic succession, adjacent to diorite and monzodiorite of the Iron Lake complex. The mineralization was discovered in 1978, and the property was explored by several different companies from then until 1994. Exploration work included geological mapping, soil geochemical surveys, magnetometer and IP surveys and trenching. It also included an 11 hole, 424 m diamond-drilling program carried out by Alcare Resources Inc. in 1982 (Werner, 1982) and a four hole, 397 m diamond-drilling program carried out by Noranda in 1985 (Baerg, 1985).

Mineralization at the Clay showing comprises disseminations, blebs and fracture coatings of bornite, malachite and, locally, chalcopyrite, commonly associated with pink calcite veins (Baerg, 1985). The hostrocks are chlorite-epidote-altered volcanic breccia, intercalated with a lens of skarny limestone and cut by diorite to monzonite dikes that are probably related to the adjacent Iron Lake complex. Mineralization is concentrated in a north-trending zone, 20–30 m wide, that has been traced discontinuously on surface and in drill holes for about 200 m (Baerg, 1985). The highest grades recorded in drillcore from the northern part of this zone came from a 61 cm intersection that yielded 2.17% Cu, 28 ppm Ag and 6.13 ppm Au (Werner, 1982). A 19.66 m intercept at the south end of the zone returned an average of 1190 ppm Cu, 1.92 ppm Ag and 233 ppb Au (Baerg, 1985).

Occurrences in the Christmas Lake Area

CHRISTMAS (092P 110) AND LISA

The Christmas occurrence, comprising gold mineralization within sulphide-rich hornfels adjacent to dioritic intrusions, is located about halfway between Christmas Lake and the north shore of Canim Lake. This area was covered by the RK claims and explored for porphyry Cu mineralization in the early 1970s. It was restaked as the Christmas claims by E&B Explorations Inc. in 1983, and from 1983 to 1987 explored with geological mapping, rock and soil geochemical surveys, and magnetometer, VLF-EM and IP geophysical surveys (Thompson, 1987). The property was optioned by Nustar Resources Inc. in 2002. Nustar explored the area of the main showing in 2002 and 2003 with trenching, rock sampling and 305 m of diamond drilling in two holes (McLeod, 2003). In 2004, they conducted soil geochemical and self-potential surveys over the Lisa showing, almost 2 km northwest of the main showing, where rubble of Au-arsenopyrite-mineralized quartz-ankerite vein material had been discovered in 1987 (Thompson, 1987; McLeod, 2004).

The area of the main Christmas showing is underlain by volcanic sandstone, siltstone, breccia and mafic flows of the Nicola volcaniclastic succession. These rocks are variably silicified and hornfelsed adjacent to a complex stock and/or dike swarm consisting mainly of hornblende diorite. The hornfelsed rocks commonly contain 1–2% disseminated pyrite. Gold mineralization is mainly associated with zones of higher sulphide content, which include pyrite, pyrrhotite and, locally, chalcopyrite and arsenopyrite. The highest assay value reported from the main zone is 5.910 ppm Au from a grab sample containing 30% pyrrhotite (Thompson, 1987).

The Lisa showing comprises rubble of arsenopyrite-mineralized quartz-ankerite vein material that was discovered during follow-up examination of a 4.027 ppm gold in soils anomaly. Two rock samples of the arsenopyrite-mineralized float returned assay values of 2.537 and 3.510 ppm Au, respectively (Thompson, 1987).

WELL (092P 144)

The Well occurrence is located on the north side of Canim Lake, 4.5 km west of Boss Creek. It consists of disseminated pyrite, with rare traces of chalcopyrite, within volcanic sandstone and breccia of the Nicola volcaniclastic succession, on the northeast margin of a diorite stock. It forms part of a prominent aeromagnetic high that was staked as the Well claim, and explored with geological mapping and a soil geochemical survey, by Du Pont of Canada Exploration Limited in 1975 (Smith, 1976). This exploration program failed to detect any significant mineralization and no subsequent work has been recorded in this area.

CATE (092P 182)

The Cate showing comprises a narrow, Au-bearing sulphide vein that is hosted in a shear zone exposed along a logging road about 1.5 km north of Christmas Lake. It is one of about a dozen vein and/or shear-related Cu±Au occurrences that have been identified on the Papoose claims, staked by Dave Ridley in 1993 and 1994. These claims cover an area that had previously been staked by Imperial Metals in 1983 (Senicar claims), and explored in 1984 through 1988 with geological mapping, soil and silt geochemical surveys, trenching and an IP survey.

The Papoose claims are underlain mainly by volcanic sandstone, breccia, siltstone and argillite assigned to the Nicola volcaniclastic succession, locally cut by dikes of diorite, gabbro and feldspar porphyry. Mineralization consists of local shear zones, quartz-carbonate veins and stockworks mineralized with variable amounts and combinations of pyrite, pyrrhotite, arsenopyrite and chalcopyrite (Ridley, and Dunn, 1993b; Ridley, 1995, 1997). These occurrences have been documented in a northwest-trending belt almost 1.5 km long. The Cate showing, discovered in 1993, comprises a steep, north-northeast-striking shear zone that includes a massive, 2 cm wide sulphide vein, consisting of pyrrhotite, arsenopyrite, pyrite and chalcopyrite. The shear zone separates diorite to the west from feldspar porphyry to the east, and is located at the southeast end of the belt of known mineralization. A 60 cm chip sample across the shear zone returned 1.32 ppm Au, 8985 ppm As

and 210 ppm Cu, whereas a grab sample of the massive sulphide vein contained 74.9 ppm Au, 20.6 ppm Ag, 1835 ppm Cu and greater than 1% As (Ridley and Dunn, 1993b). Ridley (1997) pointed out that mineralization at the Cate showing resembles, and is more or less along strike from, that at the Liza showing, 1.3 km to the south-southwest.

Occurrences in the Howard Lake Area

SLEEPING GIANT (092P 128)

The Sleeping Giant occurrence comprises disseminated and fracture-controlled Cu mineralization within the Howard Lake stock. The showings were covered by the RM claim group in 1972 and, over the next two years, explored with a program that included geological mapping; soil, silt and rock geochemical sampling; ground magnetometer and IP surveys; and bulldozer trenching (Fox, 1973). An 18 hole percussion-drill program, totalling 1222 m, was carried out in 1974, but the results were disappointing and the RM claims were allowed to lapse (Rebagliati, 1974). The area was covered by the Sleeping Giant claim group in 1989, and explored by rock and soil geochemical sampling in 1990 (Ridley, 1990). These claims were also allowed to lapse, but the showings were staked as the S.G. 1 claim in 1993, and a small area of previously untested ground was tested with 63 m of diamond drilling, which did not intersect any mineralization (Ridley and Dunn, 1994b).

The main Sleeping Giant showings are hosted in fractured dioritic intrusion breccia about 1 km north of Howard Lake. Mineralization occurs over an area 300–400 m in diameter, and consists of thin fracture fillings and disseminated grains of pyrite, chalcopyrite and local bornite (Fox, 1973; Ridley, 1990). The mineralization occurs in breccia fragments and matrix, and is accompanied by chlorite, epidote, K-feldspar and magnetite alteration. Pyrite and chalcopyrite also occur as disseminations and fracture fillings in syenitic rocks several hundred metres north of the breccia showings (Pat Lake showing; Ridley, 1990). Although the mineralization is quite widespread, geochemical analyses of percussion-drill cuttings from the main Sleeping Giant showings returned only low Cu values and no significant Au values (Rebagliati, 1974).

CANIM (092P 158)

The Canim showing consists of fracture-controlled Cu-Au-Ag mineralization within the South Canim stock. It was first described by Ridley (1986) following a prospecting survey of the Canim 1 mineral claim, although the south Canim stock is part of a broader area, stretching northeastward to Howard Lake, that underwent several phases of porphyry Cu exploration, beginning in the late 1960s.

Ridley (1986) described three separate mineralized zones within the South Canim stock. The main zone covers an area measuring about 120 m (north-south) by 50 m. Mineralization consists mainly of pyrite-chalcopyrite-magnetite-quartz within narrow (1–3 cm) fractures that dip at moderate angles to the northeast. Wallrocks are commonly altered to chlorite-epidote, and may be cut by sulphide-bearing veinlets oriented at high angles to the main mineralized fractures. A 1 m chip sample along one of the main mineralized fractures returned 19 556 ppm Cu and 16.6 ppm Ag (Ridley, 1986, sample 85-8). The highest precious metal values, 1420 ppb Au and 28.1 ppm Ag, came from a weathered fracture filling consisting of limonite with traces of pyrite, chalcopyrite and malachite (Ridley, 1986, sample 85-14). Stockwork-style veins mineralized with pyrite-chalcopyrite-magnetite-quartz were also located at the north showing, 200 m north of the main zone, and at the northernmost showing, 350 m north of the main zone (Ridley, 1986).

Occurrences in the Northwestern Part of the Map Area

DECEPTION CREEK (092P 130)

The Deception Creek occurrence comprises minor Cu and Zn mineralization within volcanic breccia, tuff, sandstone and argillite of the Nicola volcaniclastic succession near Christopher Lake, 3–4 km north-northeast of the east end of Canim Lake. The Chris claims were staked over the area by Pickands Mather and Company in the fall of 1972, and minor disseminated chalcopyrite was discovered during an exploration program in 1973, which included geological mapping and soil sampling (Pollmer and Dodd, 1973). More extensive exploration was carried out in the early to mid-1980s, after the area was restaked as the W claims by Archean Engineering Limited. This work included geological mapping; silt, soil and heavy mineral geochemical surveys; and VLF-EM surveys. It culminated in a four-hole diamond-drilling program in 1986, which tested two elongate VLF-EM conductors and coincident Zn soil anomalies for possible Cu-Zn massive sulphide mineralization. The holes encountered very minor mineralization, comprising pyrite, pyrrhotite and rare traces of chalcopyrite and sphalerite within quartz-calcite stringers. It was concluded that unmineralized graphitic argillite produced both the VLF-EM conductors and the Zn soil anomalies, and it was recommended that no further work be conducted on the property (Holmgren and Kowalchuk, 1986).

HOTFISH LAKE (092P 184)

The Hotfish Lake showing comprises mineralized quartz-carbonate veins located along and near the logging road northeast of Hotfish Lake. The veins were discovered during a 1994 exploration program on the Fish mineral claims that included line cutting; soil, silt and rock geochemical sampling; and a small amount of hand stripping (Wahl, 1994). There has been no subsequent work recorded on the claims.

The Hotfish Lake showing includes three separate quartz-carbonate veins, individually located in small isolated exposures that form a belt about 400 m long in a north-northwesterly direction (Wahl, 1994). The hostrocks observed during the present study are thin-bedded siltstone, calcareous siltstone and local volcanic sandstone of the Nicola volcaniclastic succession, although Wahl (1994) interpreted the vein hosts as mainly felsic volcanic rocks. The sedimentary rocks are complexly folded, mainly along westerly-plunging axes, and are faulted and fractured in multiple orientations. They are brecciated in fold hinges and along faults, and these breccias are typically altered to an assemblage that includes calcite, quartz, chlorite and pyrite. The three steeply dipping quartz-carbonate veins described by Wahl (1994) are 10 cm, 10–20 cm and 50–60 cm thick, respectively, and strike 170°, 235° and 198°. All are mineralized with pyrite and chalcopyrite, and one also contains sphalerite. An assay sample from the sphalerite-bearing vein, which is 10 cm wide, yielded 2175 ppm Cu,

1343 ppm Zn, 9.9 ppm Ag and 140 ppb Au (Wahl, 1994, sample SHF-3R).

ART (093A 200)

The Art showing is located near the northern boundary of the map area, about 1.5 km east of the Hendrix stock. The showing was discovered and staked by Dave Ridley in 1997, along the newly constructed Art Creek logging road. Subsequent work has included geological mapping, rock and soil geochemical surveys, a combined magnetometer and VLF-EM geophysical survey, and limited diamond drilling (Adamec, 1999; Ridley, 2001; Blann and Ridley, 2005).

Exposures in the general area of the Art showing are mainly volcanic breccia, with local pyroxene-phyric basalt, volcanic sandstone and siltstone, assigned to the breccia subunit of the Nicola volcaniclastic succession. The showing itself is within a light grey, tan-weathered, fine-grained felsite that forms a 30 m stretch of outcrop in the east bank of the Art Creek logging road. The felsite, together with diorite exposed 50 m to the south, appears to intrude the Nicola succession. The discovery showing, as presently exposed, comprises a 60 cm by 120 cm exposure in the ditch between the main felsite outcrop and the road. It consists of rusty, silicified, highly fractured felsite that contains clots, up to several centimetres across, of fine to coarsely crystalline pyrite-arsenopyrite. The predominant fracture orientation, parallel to the long axis of the showing outcrop, suggests that it is part of a north-northeast-striking fault zone within the felsite. A grab sample of mineralized material collected during the 2005 field season contained 50 ppb Au, 1914.6 ppm As and 7.02 ppm Sb; the moderate Au enrichment and high As values are consistent with values obtained from two separate 1 m chip samples reported by Adamec (1999). A shallow drillhole, collared on the road in 2001, was oriented to the south so did not crosscut the strongly mineralized zone, although the upper part of the hole cut moderately fractured felsite with calcite veinlets and local areas of disseminated sulphide minerals that include pyrite, arsenopyrite and traces of chalcopyrite. Samples from this interval returned an average of 167 ppb Au and 3500 ppm As over 12 m of core length (Ridley, 2001). Angular float of heavily pyrite-altered dioritic rock from near the diorite outcrop south of the felsite returned 1474 ppb Au (Blann and Ridley, 2005).

DL (093A 089)

The DL occurrence, in the northwest corner of the map area, comprises Au-bearing quartz veins hosted in phyllite of the Lemieux Creek succession. The showings are located about 400 m west of Deception Creek, along an east-flowing tributary stream. Gold mineralization from this general area is briefly mentioned in the BC Minister of Mines Annual Report for 1886 (Soues, 1887), and an old adit and trenches on the property may date from that time period (Ridley, 1992). These workings were staked as the REC claim in 1987, and evaluated with a limited program of mapping and rock sampling (Durfeld, 1988). The REC claim was allowed to lapse, and the showings were subsequently covered by the DL claim group, staked by their current owner, Dave Ridley, in 1991. Exploration since that time has included geological mapping, soil and rock geochemical sampling, magnetometer and VLF-EM geophysical surveys, and limited diamond drilling (Ridley and Dunn, 1993a; Christopher, 1999; Blann and Ridley, 2005).

The area of the DL showing is underlain by dark grey phyllite, commonly with small rusted porphyroblasts of Fe-carbonate. Cleavage is warped and variable in orientation, but it typically dips at moderate angles to the north or northeast. The phyllite is cut by tan-weathered feldspar±quartz porphyry dikes, and by lenses and veins of quartz which range from less than 1 cm to 2 m in width. Most dikes and veins are oriented approximately parallel to cleavage, but some narrow planar quartz veins are discordant. Many veins include knots of rusty carbonate, and some thicker veins contain fragments of wallrock. Most quartz veins do not contain sulphide minerals, but the Au-bearing veins in the area of the old workings locally contain pyrite, galena, tetrahedrite and chalcopyrite (Durfeld, 1988). Exploration to date has documented significant Au mineralization only in the immediate vicinity of these old workings, which include an adit oriented at about 015° in the north bank of the creek. There, the main mineralized zone is about 2 m wide and comprises several quartz veins, from 5 cm to 1 m thick, separated by thin lenses of phyllite (Ridley and Dunn, 1993a). A 1 m chip sample that included the main adit vein returned 42.9 ppm Au and 34.7 ppm Ag. (Ridley, 1992). A sample of pyrite-galena-mineralized vein material from an old trench about 20 m east of the adit yielded 1.22 ppm Au, 620 ppm Ag and 51 592 ppm Pb (Durfeld, 1988).

Occurrences Associated with the Raft Batholith

Mineral occurrences in the southeastern part of the Canim Lake map area are within and peripheral to the Raft batholith. These include porphyry Mo showings within the main monzogranite phase of the batholith. (CL and Double Lake occurrences), disseminated chalcopyrite ±molybdenite occurrences within the western quartz monzodiorite to diorite phase of the batholith (Hood and SHE-397 showings), and a base metal–bearing fault zone within the Nicola Group, near the south margin of the batholith (SHE-174 occurrence). All of these showings are described by Schiarizza *et al*. (2002a), so are not discussed here.

SUMMARY OF MAIN CONCLUSIONS

- The Canim Lake map area is underlain mainly by sedimentary and volcanic rocks of the Middle to Upper Triassic Nicola Group, together with Late Triassic to Early Jurassic ultramafic to granitic plutonic rocks. These rocks are all part of the Quesnel magmatic arc. Younger rocks in the map area include mid-Cretaceous granite and granodiorite of the Raft batholith and Hendrix stock, Eocene volcanic and sedimentary rocks, and Quaternary basalt.
- The Nicola Group in the Canim Lake map area includes two major subdivisions. The Lemieux Creek succession forms the eastern part of the belt and consists mainly of slate, phyllite and siltstone. It is assigned a Middle to Upper Triassic age based on correlation with rocks south of the Raft batholith. The volcaniclastic succession forms a wide outcrop belt to the west, and is inferred to stratigraphically overlie the Lemieux Creek succession. It consists of massive to well-bedded volcanic sandstone intercalated with pyroxene-rich volcanic breccia and mafic flows. It is not dated within the map area, but is as-

signed a Late Triassic age based on correlation with rocks to the south.

- Intrusive rocks assigned to the Quesnel magmatic arc include the Iron Lake and Aqua Creek ultramafic-mafic plutonic complexes, several small stocks of diorite to monzonite composition, and the Takomkane batholith, which is subdivided into a granodiorite phase (Schoolhouse Lake unit) and a quartz monzodiorite phase (Boss Creek unit). Only the Schoolhouse Lake unit of the Takomkane batholith is currently dated; it has yielded an Early Jurassic U-Pb zircon age of 193.5 ±0.6 Ma (Whiteaker *et al*., 1998). Dating of other plutonic units is in progress.
- Widespread, low-grade Cu mineralization, locally accompanied by Au, Pt and Pd, is found within and adjacent to the Iron Lake ultramafic-mafic complex. Disseminated and fracture-controlled Cu±Au mineralization also occurs within the Howard Lake and South Canim dioritic to monzonitic stocks. Other mineral occurrences in the Canim Lake map area include Au-bearing quartz±carbonate veins, mineralized shears, and porphyry Mo showings within mid-Cretaceous granite of the Raft batholith.

ACKNOWLEDGMENTS

We thank Fern Wager and Arthur Paul for their capable and enthusiastic assistance during fieldwork, and Mike and Jean Peake for their hospitality during our stay at Eagle Creek. We also thank Dave Ridley for showing us around many of the mineral showings in the area, and Brian Grant, Dave Ridley and Mike Cathro for geological discussions while in the field. Brian Grant reviewed an earlier version of the manuscript and suggested improvements.

REFERENCES

Adamec, J. (1999): Report on the Art property, Cariboo Mining Division, British Columbia; *BC Ministry of Energy, Mines and Petroleum Resources*, Assessment Report 25 800, 11 pages.

Ash, C.H. and Riveros, C.P. (2001): Geology of the Gibraltar copper-molybdenite deposit, east-central British Columbia (93B/9); *in* Geological Fieldwork 2000, *BC Ministry of Energy, Mines and Petroleum Resources*, Paper 2001-1, pages 119–133.

Baerg, R.J. (1985): Geological, geochemical and drilling report on the Hawkins Lake – Alcare Resources option, Clinton Mining Division; *BC Ministry of Energy, Mines and Petroleum Resources*, Assessment Report 13 751, 8 pages.

Blann, D.E. and Ridley, D. (2005): Geological report on the Art – DL mineral claims, Cariboo and Clinton Mining Division; *BC Ministry of Energy, Mines and Petroleum Resources*, Assessment Report 27 753, 14 pages.

Bloodgood, M.A. (1990): Geology of the Eureka Peak and Spanish Lake map areas, British Columbia; *BC Ministry of Energy, Mines and Petroleum Resources*, Paper 1990-3, 36 pages.

Bostock, H.S. (1941): Olalla area; *Geological Survey of Canada*, Map 628A.

Brown, R.L., Journeay, J.M., Lane, L.S., Murphy, D.C. and Rees, C.J. (1986): Obduction, backfolding and piggyback thrusting in the metamorphic hinterland of the southeastern Canadian Cordillera; *Journal of Structural Geology*, Volume 8, pages 255–268.

Buskas, A.J. (1989): Geochemical sampling, core logging and sampling, and geological mapping of the Canim 1-4 and Horse claims, Clinton Mining Division; *BC Ministry of Energy, Mines and Petroleum Resources*, Assessment Report 19 322, 21 pages.

Bysouth, G.D., Campbell, K.V., Barker, G.E. and Gagnier, G.K. (1995): Tonalite-trondhjemite fractionation of peraluminous magma and the formation of syntectonic porphyry copper mineralization, Gibraltar mine, central British Columbia; *in* Porphyry Deposits of the Northwestern Cordillera of North America, Schroeter, T.G., Editor, *Canadian Institute of Mining, Metallurgy and Petroleum*, Special Volume 46, pages 201–213.

Calderwood, A.R., van der Heyden, P. and Armstrong, R.L. (1990): Geochronometry of the Thuya, Takomkane, Raft and Baldy batholiths, south-central British Columbia; *Geological Association of Canada – Mineralogical Association of Canada*, Joint Annual Meeting, Vancouver, BC, Program with Abstracts, Volume 15, page A19.

Campbell, K.V. (1971): Metamorphic petrology and structural geology of the Crooked Lake area, Cariboo Mountains, British Columbia; Ph.D. thesis, *University of Washington*, 192 pages.

Campbell, R.B. (1978): Quesnel Lake, British Columbia; *Geological Survey of Canada*, Open File 574.

Campbell, R.B. and Tipper, H.W. (1971): Bonaparte Lake map area, British Columbia; *Geological Survey of Canada*, Memoir 363, 100 pages.

Casselman, M.J., McMillan, W.J. and Newman, K.M. (1995): Highland Valley porphyry copper deposits near Kamloops, British Columbia: a review and update with emphasis on the Valley deposit; *in* Porphyry Deposits of the Northwestern Cordillera of North America, Schroeter, T.G., Editor, *Canadian Institute of Mining, Metallurgy and Petroleum*, Special Volume 46, pages 161–191.

Christopher, P.A. (1999): Assessment report on the DL claims, Ledge property, Canim Lake area, Cariboo Mining Division, BC; *BC Ministry of Energy, Mines and Petroleum Resources*, Assessment Report 26 019, 13 pages.

Colpron, M. and Price, R.A. (1995): Tectonic significance of the Kootenay terrane, southeastern Canadian Cordillera: an alternative model; *Geology*, Volume 23, pages 25–28.

Cukor, V. (1973): Aragon Explorations Ltd. (N.P.L.) Canim Lake property, 92-P, Clinton Mining Division: Progress Report; *BC Ministry of Energy, Mines and Petroleum Resources*, Assessment Report 4265, 9 pages.

Danner, W.R. and Orchard, M.J. (2000): Paleontology of the Cache Creek and Quesnellia terranes, southwestern British Columbia; *in* Guidebook for Geological Field Trips in Southwestern British Columbia and Northern Washington, Woodsworth, G.J., Jackson, L.E. Jr., Nelson, J.L. and Ward, B.C., Editors, published by the *Cordilleran Section, Geological Association of Canada*, for the Geological Society of America, Cordilleran Section, 2000 Annual Meeting, Vancouver, BC, pages 117–173.

Dawson, G.M. (1879): Preliminary report on the physical and geological features of the southern portion of the interior of British Columbia; *in* Report of Progress, 1877–1878, Part B, *Geological Survey of Canada*, pages 1B–187B.

Dostal, J., Church, B.N. and Höy, T. (2001): Geological and geochemical evidence for variable magmatism and tectonics in the southern Canadian Cordillera: Paleozoic to Jurassic suites, Greenwood, southern British Columbia; *Canadian Journal of Earth Sciences*, Volume 38, pages 75–90.

Durfeld, R.M. (1988): Geochemical and geological report on the REC mineral claim, Cariboo Mining Division, British Co-

lumbia; *BC Ministry of Energy, Mines and Petroleum Resources*, Assessment Report 17 646, 4 pages.

Erdmer, P., Heaman, L., Creaser, R.A., Thompson, R.I. and Daughtry, K.L. (2001): Eocambrian granite clasts in southern British Columbia shed light on Cordilleran hinterland crust; *Canadian Journal of Earth Sciences*, Volume 38, pages 1007–1016.

Erdmer, P., Moore, J.M., Heaman, L., Thompson, R.I., Daughtry, K.L. and Creaser, R.A., (2002): Extending the ancient margin outboard in the Canadian Cordillera: record of Proterozoic crust and Paleocene regional metamorphism in the Nicola horst, southern British Columbia; *Canadian Journal of Earth Sciences*, Volume 39, pages 1605–1623.

Ewing, T.E. (1980): Paleogene tectonic evolution of the Pacific Northwest; *Journal of Geology*, Volume 88, pages 619–638.

Ferri, F. (1997): Nina Creek Group and Lay Range Assemblage, north-central British Columbia: remnants of late Paleozoic oceanic and arc terranes; *Canadian Journal of Earth Sciences*, Volume 34, pages 854–874.

Ferri, F. and Melville, D.M. (1994): Bedrock geology of the Germansen Landing – Manson Creek area, British Columbia (94N/9, 10, 15; 94C/2); *BC Ministry of Energy, Mines and Petroleum Resources*, Bulletin 91, 147 pages.

Fox, P.E. (1973): Geochemical and geophysical report on the RM claims, Clinton Mining Division; *BC Ministry of Energy, Mines and Petroleum Resources*, Assessment Report 4259, 14 pages.

Fyles, J.T. (1990): Geology of the Greenwood – Grand Forks area, British Columbia, NTS 82E/1, 2; *BC Ministry of Energy, Mines and Petroleum Resources*, Open File 1990-25.

Gatchalian, F.R. (1972): Geological, geochemical and geophysical report, July claims #1 to 32, Clinton Mining Division; *BC Ministry of Energy, Mines and Petroleum Resources*, Assessment Report 4496, 18 pages.

Hickson, C.J. (1986): Quaternary volcanism in the Wells Gray – Clearwater area, east-central British Columbia; Ph.D. thesis, *University of British Columbia*, Vancouver, BC, 357 pages.

Hickson, C.J. and Souther, J.G. (1984): Late Cenozoic volcanic rocks of the Clearwater – Wells Gray area, British Columbia; *Canadian Journal of Earth Sciences*, Volume 21, pages 267–277.

Holmgren, L.D. and Kowalchuk, J.M. (1986): Diamond drilling survey on the Deception Creek property, Clinton Mining Division, British Columbia; *BC Ministry of Energy, Mines and Petroleum Resources*, Assessment Report 15 142, 18 pages.

Höy, T. and Dunne, K.P.E. (1997): Early Jurassic Rossland Group, southern British Columbia: Part I — stratigraphy and tectonics; *BC Ministry of Energy, Mines and Petroleum Resources*, Bulletin 102, 123 pages.

Jung, A. (1986): Geochronometry and geochemistry of the Thuya, Takomkane, Raft and Baldy batholiths, west of the Shuswap metamorphic complex, south-central British Columbia; B.Sc. thesis, *University of British Columbia*, Vancouver, BC, 140 pages.

Klepacki, D.W. and Wheeler, J.O. (1985): Stratigraphic and structural relations of the Milford, Kaslo and Slocan groups, Goat Range, Lardeau and Nelson map areas, British Columbia; *in* Report of Activities, Part A, *Geological Survey of Canada*, Paper 85-1A, pages 277–286.

Little, H.W. (1982): Geology of the Rossland-Trail map area, British Columbia; *Geological Survey of Canada*, Paper 79-26, 38 pages.

Logan, J.M. (2001): Prospective areas for intrusion-related gold-quartz veins in southern British Columbia; *in* Geological Fieldwork 2000, *BC Ministry of Energy, Mines and Petroleum Resources*, Paper 2001-1, pages 231–252.

Logan, J.M. (2002): Intrusion-related mineral occurrences of the Cretaceous Bayonne magmatic belt, southeast British Columbia; *BC Ministry of Energy, Mines and Petroleum Resources*, Geoscience Map 2002-1.

Logan, J.M. and Mihalynuk, M.G. (2005a): Regional geology and setting of the Cariboo, Bell, Springer and Northeast Porphyry Cu-Au zones at Mount Polley, south-central British Columbia; *in* Geological Fieldwork 2004, *BC Ministry of Energy, Mines and Petroleum Resources*, Paper 2005-1, pages 249–270.

Logan, J.M. and Mihalynuk, M.G. (2005b): Porphyry Cu-Au deposits of the Iron Mask batholith, southeastern British Columbia; *in* Geological Fieldwork 2004, *BC Ministry of Energy, Mines and Petroleum Resources*, Paper 2005-1, pages 271–290.

Macdonald, A.J., Spooner, E.T.C. and Lee, G. (1995): The Boss Mountain molybdenum deposit, central British Columbia; *in* Porphyry Deposits of the Northwestern Cordillera of North America, Schroeter, T.G., Editor, *Canadian Institute of Mining, Metallurgy and Petroleum*, Special Volume 46, pages 691–696.

Mathews, W.H. (1989): Neogene Chilcotin basalts in south-central British Columbia: geology, ages, and geomorphic history; *Canadian Journal of Earth Sciences*, Volume 26, pages 969–982.

McLeod, J.W. (2003): Report on the Christmas Lake project, Canim Lake area, Clinton Mining Division, British Columbia; *BC Ministry of Energy, Mines and Petroleum Resources*, Assessment Report 27 272, 12 pages.

McLeod, J.W. (2004): Report on the Christmas Lake project, Canim Lake area, Clinton Mining Division, British Columbia; *BC Ministry of Energy, Mines and Petroleum Resources*, Assessment Report 27 544, 12 pages.

MINFILE (2005): MINFILE BC mineral deposits database; *BC Ministry of Energy, Mines and Petroleum Resources*, URL <http://www.em.gov.bc.ca/Mining/Geolsurv/Minfile/> [Nov 2005].

Monger, J.W.H. (1989): Geology, Hope, British Columbia (92H); *Geological Survey of Canada*, Map 41-1989, sheet 1, 1:250 000 scale.

Monger, J.W.H. and McMillan, W.J. (1989): Geology, Ashcroft, British Columbia (92I); *Geological Survey of Canada*, Map 42-1989, sheet 1, 1:250 000 scale.

Mortensen, J.K., Ghosh, D.K. and Ferri, F. (1995): U-Pb geochronology of intrusive rocks associated with copper-gold porphyry deposits in the Canadian Cordillera; *in* Porphyry Deposits of the Northwestern Cordillera of North America, Schroeter, T.G., Editor, *Canadian Institute of Mining, Metallurgy and Petroleum*, Special Volume 46, pages 142–158.

Mortimer, N. (1987): The Nicola Group: Late Triassic and Early Jurassic subduction-related volcanism in British Columbia; *Canadian Journal of Earth Sciences*, Volume 24, pages 2521–2536.

Morton, J.W. (1984): Geophysical report, Ironhorse 1-2, 92P/15W; *BC Ministry of Energy, Mines and Petroleum Resources*, Assessment Report 11 088, 9 pages.

Morton, J.W. (2001): Report on the Iron Lake property, Clinton Mining Division, BC; *BC Ministry of Energy, Mines and Petroleum Resources*, Assessment Report 26 534, 15 pages.

Nelson, J.L. and Bellefontaine, K.A. (1996): The geology and mineral deposits of north-central Quesnellia; Tezzeron Lake to Discovery Creek, central British Columbia; *BC Ministry of Energy, Mines and Petroleum Resources*, Bulletin 99, 112 pages.

Nixon, G.T., Hammack, J.L., Ash, C.H., Cabri, L.J., Case, G., Connelly, J.N., Heaman, L.M., Laflamme, J.H.G., Nuttall, C, Paterson, W.P.E. and Wong, R.H. (1997): Geology and platinum-group-element mineralization of Alaskan-type ultramafic-mafic complexes in British Columbia; *BC Minis-*

try of Energy, Mines and Petroleum Resources, Bulletin 93, 141 pages.

Panteleyev, A., Bailey, D.G., Bloodgood, M.A. and Hancock, K.D. (1996): Geology and mineral deposits of the Quesnel River – Horsefly map area, central Quesnel Trough, British Columbia; *BC Ministry of Energy, Mines and Petroleum Resources*, Bulletin 97, 155 pages.

Pollmer, A. and Dodd, G. (1973): Exploration report on the Chris claims, Clinton Mining Division; *BC Ministry of Energy, Mines and Petroleum Resources*, Assessment Report 4733, 10 pages.

Preto, V.A. (1977); The Nicola Group: Mesozoic volcanism related to rifting in southern British Columbia; *in* Volcanic Regimes in Canada, Baragar, W.R.A., Coleman, L.C. and Hall, J.M., Editors, *Geological Association of Canada*, Special Paper 16, pages 39–57.

Preto, V.A. (1979): Geology of the Nicola Group between Merritt and Princeton; *BC Ministry of Energy, Mines and Petroleum Resources*, Bulletin 69, 90 pages.

Read, P.B. and Okulitch, A.V. (1977): The Triassic unconformity of south-central British Columbia; *Canadian Journal of Earth Sciences*, Volume 14, pages 606–638.

Rebagliati, C.M. (1974): Report on the Canim Lake copper prospect; *BC Ministry of Energy, Mines and Petroleum Resources*, Property File, 11 pages.

Rees, C.J. (1987): The Intermontane-Omineca belt boundary in the Quesnel Lake area, east-central British Columbia: tectonic implications based on geology, structure and paleomagnetism; Ph.D. thesis, *Carleton University*, 421 pages.

Ridley, D.W. (1986): Prospecting report on the Canim #1 (four units) mineral claim near Canim Lake, Clinton Mining Division; *BC Ministry of Energy, Mines and Petroleum Resources*, Assessment Report 14 924, 11 pages.

Ridley, D.W. (1990): Soil geochemistry, geology and prospecting of the Sleeping Giant group (89 metric units), Canim Lake area, Clinton Mining Division; *BC Ministry of Energy, Mines and Petroleum Resources*, Assessment Report 20 452, 25 pages.

Ridley, D.W. (1992): Prospecting report on the Deception Ledge property, DL 1-8 two post mineral claims, Cariboo Mining Division; *BC Ministry of Energy, Mines and Petroleum Resources*, Assessment Report 22 460, 14 pages.

Ridley, D.W. (1995): Prospecting report on the Papoose 2 mineral claims, Clinton Mining Division; *BC Ministry of Energy, Mines and Petroleum Resources*, Assessment Report 23 925, 8 pages.

Ridley, D.W. (1997): Geological and geochemical report on the Papoose 1 and 2 mineral claims, Clinton Mining Division; *BC Ministry of Energy, Mines and Petroleum Resources*, Assessment Report 24 952, 11 pages.

Ridley, D.W. (2001): Diamond drilling report on the Art 1-4 mineral claims, Art Creek area, Cariboo-Clinton Mining Divisions; *BC Ministry of Energy, Mines and Petroleum Resources*, Assessment Report 26 821, 7 pages.

Ridley, D. and Dunn, D. (1993a): Geological and geochemical report on the Deception Ledge property (DL 1-8 mineral claims), Cariboo Mining Division; *BC Ministry of Energy, Mines and Petroleum Resources*, Assessment Report 23 201, 12 pages.

Ridley, D. and Dunn, D. (1993b): Prospecting report on the Papoose property (Papoose 1 mineral claim), Clinton Mining Division; *BC Ministry of Energy, Mines and Petroleum Resources*, Assessment Report 23 269, 14 pages.

Ridley, D. and Dunn, D. (1994a): Prospecting and geochemical report on the Straw group (Straw 1-20 two-post mineral claims), Clinton Mining Division; *BC Ministry of Energy, Mines and Petroleum Resources*, Assessment Report 23 279, 15 pages.

Ridley, D. and Dunn, D. (1994b): Drilling report on the Sleeping Giant property (S.G. 1 mineral claim), Clinton Mining Division; *BC Ministry of Energy, Mines and Petroleum Resources*, Assessment Report 23 280, 10 pages.

Roback, R.C., Sevigny, J.H. and Walker, N.W. (1994): Tectonic setting of the Slide Mountain terrane, southern British Columbia; *Tectonics*, Volume 13, pages 1242–1258.

Roback, R.C. and Walker, N.W. (1995): Provenance, detrital zircon U-Pb geochronometry, and tectonic significance of Permian to Lower Triassic sandstone in southeastern Quesnellia, British Columbia and Washington; *Geological Society of America Bulletin*, Volume 107, pages 665–675.

Ross, J.V., Fillipone, J., Montgomery, J.R., Elsby, D.C. and Bloodgood, M. (1985): Geometry of a convergent zone, central British Columbia, Canada; *Tectonophysics*, Volume 119, page 285–297.

Schau, M.P. (1970): Stratigraphy and structure of the type area of the Upper Triassic Nicola Group in south-central British Columbia; *in* Structure of the Southern Canadian Cordillera, Wheeler, J.O., Editor, *Geological Association of Canada*, Special Paper 6, pages 123–135.

Schiarizza, P. (1989): Structural and stratigraphic relationships between the Fennell Formation and Eagle Bay Assemblage, western Omineca Belt, south-central British Columbia: implications for Paleozoic tectonics along the paleocontinental margin of western North America; M.Sc. thesis, *University of Calgary*, Calgary, Alberta, 343 pages.

Schiarizza, P., Heffernan, S. and Zuber, J. (2002a): Geology of Quesnel and Slide Mountain terranes west of Clearwater, south-central British Columbia (92P/9, 10, 15, 16); *in* Geological Fieldwork 2001, *BC Ministry of Energy, Mines and Petroleum Resources*, Paper 2002-1, pages 83–108.

Schiarizza, P., Heffernan, S., Israel, S. and Zuber J. (2002b): Geology of the Clearwater–Bowers Lake area, British Columbia (NTS 92P/9, 10, 15, 16); *BC Ministry of Energy, Mines and Petroleum Resources*, Open File 2002-15, 1:50 000 scale.

Schiarizza, P., Israel, S., Heffernan, S. and Zuber, J. (2002c): Geology of the Nehalliston Plateau (92P/7, 8, 9, 10); *BC Ministry of Energy, Mines and Petroleum Resources*, Open File 2002-4, 1:50 000 scale.

Schiarizza, P. and Israel, S. (2001): Geology and mineral occurrences of the Nehalliston Plateau, south-central British Columbia (92P/7, 8, 9, 10); *in* Geological Fieldwork 2000, *BC Ministry of Energy, Mines and Petroleum Resources*, Paper 2001-1, pages 1–30.

Schiarizza, P. and Preto, V.A. (1987): Geology of the Adams Plateau–Clearwater–Vavenby area; *BC Ministry of Energy, Mines and Petroleum Resources*, Paper 1987-2, 88 pages.

Schiarizza, P. and Tan, S.H. (2005): Geology and mineral occurrences of the Quesnel Terrane between the Mesilinka River and Wrede Creek (NTS 94D/8, 9), north-central British Columbia; *in* Geological Fieldwork 2004, *BC Ministry of Energy, Mines and Petroleum Resources*, Paper 2005-1, pages 109–130

Smith, F.M. (1976): Geological and geochemical report on the Well claim, Clinton Mining Division, BC; *BC Ministry of Energy, Mines and Petroleum Resources*, Assessment Report 5807, 5 pages.

Smith, R.B. (1979): Geology of the Harper Ranch Group (Carboniferous–Permian) and Nicola Group (Upper Triassic) northeast of Kamloops, British Columbia; M.Sc. thesis, *University of British Columbia*, Vancouver, BC, 211 pages.

Soues, F. (1887): Lillooet; *in* Annual Report for 1886, *BC Ministry of Energy, Mines and Petroleum Resources*, pages 206–209.

Struik, L.C. (1986): Imbricated terranes of the Cariboo gold belt with correlations and implications for tectonics in southeast-

ern British Columbia; *Canadian Journal of Earth Sciences*, Volume 23, pages 1047–1061.

Struik, L.C. (1988a): Crustal evolution of the eastern Canadian Cordillera; *Tectonics*, Volume 7, pages 727–747.

Struik, L.C. (1988b): Regional imbrication within Quesnel Terrane, central British Columbia, as suggested by conodont ages; *Canadian Journal of Earth Sciences*, Volume 25, pages 1608–1617.

Struik, L.C. (1993): Intersecting intracontinental Tertiary transform fault systems in the North American Cordillera; *Canadian Journal of Earth Sciences*, Volume 30, pages 1262–1274.

Tempelman-Kluit, D.J. (1989): Geological map with mineral occurrences, fossil localities, radiometric ages and gravity field for Penticton map area (NTS 82E), southern British Columbia; *Geological Survey of Canada*, Open File 1969.

Thompson, D.A. (1987): Geological, geophysical and geochemical report on the Christmas 1-8 mineral claims, Canim Lake area, British Columbia, Clinton Mining Division; *BC Ministry of Energy, Mines and Petroleum Resources*, Assessment Report 16 170, 9 pages.

Travers, W.B. (1978): Overturned Nicola and Ashcroft strata and their relations to the Cache Creek Group, southwestern Intermontane Belt, British Columbia; *Canadian Journal of Earth Sciences*, Volume 15, pages 99–116.

Unterschutz, J.L.E., Creaser, R.A., Erdmer, P., Thompson, R.I. and Daughtry, K.L. (2002): North American margin origin of Quesnel terrane strata in the southern Canadian Cordillera: inferences from geochemical and Nd isotopic characteristics of Triassic metasedimentary rocks; *Geological Society of America Bulletin*, Volume 114, pages 462–475.

Wahl, H. (1994): Report on initial geological work on the Fish group of claims, Clinton Mining Division; *BC Ministry of Energy, Mines and Petroleum Resources*, Assessment Report 23 869, 11 pages.

Werner, L.J. (1982): Diamond drilling report on the Clay property, Hawkins Lake, Clinton Mining Division; *BC Ministry of Energy, Mines and Petroleum Resources*, Assessment Report 11 055, 11 pages.

Whiteaker, R.J., Mortensen, J.K. and Friedman, R.M. (1998): U-Pb geochronology, Pb isotopic signatures and geochemistry of an Early Jurassic alkalic porphyry system near Lac La Hache, BC; *in* Geological Fieldwork 1997, *BC Ministry of Energy, Mines and Petroleum Resources*, Paper 1998-1, pages 33-1–33-13.

Wilson, M.V.H. (1977): Paleoecology of Eocene lacustrine varves at Horsefly, British Columbia; *Canadian Journal of Earth Sciences*, Volume 14, pages 953–962.

Iron (Magnetite) Ore Resources in Southwestern British Columbia: Soft Niche or Steel-Hard Market?

George J. Simandl, Nicole D. Robinson and Suzanne Paradis[1]

KEYWORDS: industrial minerals, magnetite, iron ore, skarn, niche markets, exploration and development potential, production

EXECUTIVE SUMMARY

There are two types of market for iron ore: an international market, where large quantities of ore are used for iron and steel making, and niche markets, where small quantities of ore are custom processed to optimize the properties of the concentrate for a specific industrial mineral application.

The main market for iron ore is iron and steel making. The iron ore industry is truly international because of the availability of large high-grade mines and large ocean-going ore-carrying vessels.

Niche markets represent less than 5% of the total production, but the oxides sold within these markets command higher prices than the international market will tolerate.

Coal beneficiation, coloured pigments, radiation shielding, sand blasting, heavy aggregate, and ballast for pipelines and offshore oil and gas platforms are examples of existing and future potential niche markets for British Columbia magnetite.

The producers supplying iron oxides to niche markets who are able to provide custom processing, and the associated technical services, to meet clients' needs have a competitive edge over suppliers of exclusively raw material.

Before the development of large, high-grade iron deposits in Australia and Brazil, small to mid-size iron skarn deposits were mined successfully along the coast of BC. Several of these past producers closed down during periods of low iron prices. Because of this, magnetite-rich rock, or magnetite in form of tailings, may be available for future recovery. The re-examination of selected past producers, existing prospects, and magnetite-bearing tailings may represent an acceptable risk and low capital requirement if future production is aimed at niche markets.

In the long term, offshore placer deposits also represent a potential source of magnetite. If such deposits could be economically exploited under the current strict environmental regulations, placer magnetite could be potentially recovered as a co-product from the extraction of titanium oxide, garnet, zircon, silica sand and, possibly, gold or platinum.

British Columbia skarns are high-grade deposits able to supply magnetite for niche markets. Worldwide, banded iron formations and their enriched equivalents are, and will remain, the main source of iron ore for steel making, but small iron ore shipments could be extracted from BC's skarn deposits as well.

WORLD IRON ORE RESOURCES AND PRODUCTION LEVELS

World iron ore resources are estimated at over 800 billion tonnes, containing more than 230 billion tonnes of iron (Jorgenson, 2005a). Estimates for the United States alone are 110 billion tonnes of iron ore representing 27 billion tonnes of iron. Most of the known US reserves are low-grade taconite ores that require upgrading and agglomeration (Jorgenson, 2005a). Fifty countries produce iron ore, but 96% of the global total is produced by only 15 of those countries. In 2004, Brazil (220 million tonnes), China (280 million tonnes), Australia (220 million tonnes), India (110 million tonnes), Russia (95 million tonnes), Ukraine (66 million tonnes), United States (54 million tonnes), South Africa (40 million tonnes) and Canada (31 million tonnes) were among the largest iron-ore-producing nations. Seaborne iron ore trade for 2004 is estimated at 593 million tonnes, equivalent to approximately US$25 billion per year (Minesite, 2005).

Magnetite and Hematite Production in British Columbia

British Columbia's iron ore production in 2004 was approximately 87 000 t and, in the first six months of 2005, an estimated 51 000 t (Jorgenson, 2005b). Most, if not all, came from tailings of the Craigmont mine. A large proportion of the material produced by the mine is sold for coal washing. Plans to produce sandblasting media (+70 mesh) were put on hold. Craigmont Mines is also considering the production of specular hematite for surface coatings (Craigmont Mines, 2005).

During the summer of 2005, approximately 4500 t of magnetite in two sizes, ¾" × ¾" and <¼", were barged to an industrial user from Kelsey Bay, North Vancouver Island. The shipment originated from one of the magnetite zones that are located close to the Iron Mike deposit, described by BC Minister of Mines (1961, 1965) and Shearer (2002, 2004). It is currently referred to as Iron Ross. The shipment is likely the bulk sample collected in 2002 and described by Shearer (2002).

[1]*Geological Survey of Canada, Mineral Resources Division, Pacific Geoscience Centre, Sidney, BC.*

This publication is also available, free of charge, as colour digital files in Adobe Acrobat PDF format from the BC Ministry of Energy, Mines and Petroleum Resources internet website at http://www.em.gov.bc.ca/Mining/Geolsurv/Publications/catalog/catfldwk.htm

Magnetite began to be recovered as part of routine limestone aggregate processing by Texada Quarrying Ltd. at their Gillies Bay operation on Texada Island. The magnetic material is currently stockpiled for potential use as heavy aggregate but, with additional processing, may also be suitable for a number of other known uses. According to the company, as the quarrying progresses toward the limestone-granodiorite contact, magnetite pockets will be encountered and magnetite will be recovered. The current stockpile is estimated at 3000 t of magnetite-rich rock.

Iron and Steel-Making Market

Most of the world's iron ore production (probably over 95%) is used in iron and steel making. Major iron ore importers are China, Japan and the Republic of South Korea. These three countries account for more than 60% of the world's iron imports (Ericsson, 2004). In 2003, China's imports reached 148.1 million tonnes, relative to Japan's 132.1 million tonnes, and China became the largest iron ore importer in the world. In recent years, an unprecedented increase in iron ore demand from China resulted in corresponding increases in iron ore prices. The price increase of 18.6% for Carajas fines, FOB Europe to US$0.379 per dry metric tonne unit (dmtu) from 2003 to 2004 (Ericsson, 2004), and a more recent 71.5% increase in the price of Mt. Newman high-grade fines to US$0.6172 per dmtu (Anonymous, 2005a; CNN, 2005), are excellent examples of recent market tendencies. Such price increases are attracting the interest of the mining industry. Consequently, BHP Billiton has raised its output from 82 million tonnes in 2003 to 110 million tonnes in 2004 (Xinhua News Agency, 2005), and projects that are expected to come 'on stream' by 2009 represent more than 450 million tonnes of new capacity (Erickson, 2004). A good example of this is a recently announced development of Hope Downs iron ore deposits in Australia by Pilbara Iron, a subsidiary of the Rio Tinto Group. Hopes Downs 1 alone has reserves of 470 million tonnes grading more than 62% iron (Louthean, 2005). Another example is the Cape Lambert magnetite project, also in Australia (Anonymous, 2005b). To what extent this additional capacity will be justified depends largely on the future rate of increase in Chinese iron requirements. Many analysts believe that growth in demand will remain positive but at much lower rates than have been witnessed during recent years.

As far as steel production in BC goes, there are simply not enough known iron ore resources. Integrated mills are typically designed to produce more than 2 million tonnes of steel products per year, which requires about 4 million tonnes of iron ore in 60% Fe range. This figure is not in line with the currently known conventional iron resources in BC. Mini-mills have smaller capacity, typically on the order of 200 000–400 000 t of steel per year; however, in most cases, their primary feed is scrap steel.

IRON ORE FOR NICHE MARKETS

The use of iron ores in industrial applications (non-iron or steel) represents a small but significant proportion of the total market. These markets are particularly important for small exploration/development companies. In addition to the chemical specifications that are so important in iron making, the industrial mineral use of iron ores is also strongly constrained by physical properties of the final concentrate. The main iron-ore-forming minerals are oxides: hematite (Fe_2O_3) magnetite ($Fe^{2+}Fe_2^{3+}O_4$), goethite ($Fe^{3+}O(OH)$) and limonite (hydrous iron oxides). The use of iron carbonate minerals, including siderite ($Fe^{2+}CO_3$), has been nearly discontinued for iron and steel making, but they are still mined for their industrial mineral applications.

Hematite, or 'red iron ore', varies in colour from shiny black to red; the lamellar variety is highly sought after for its use in surface coatings. Magnetite ore is black and its freshly broken surfaces have a metallic lustre. Magnetite is characterized and easily identified by its magnetic properties. Goethite is highly variable in habit and form. It has a brown streak and is easily recognized when it has a botryoidal texture. Limonite varies in colour from brown or black to yellow. Siderite ranges in colour from grey to yellow, beige or shades of reddish brown, but is most commonly brown. The density of these minerals varies from more than 5 g/cm^3 for magnetite and hematite to as low as 3.3 g/cm^3 for some varieties of goethite. Magnetite is the hardest, while siderite is the softest. Because most of the iron ore deposits along the coast of BC are iron skarns containing mainly magnetite or magnetite placer deposits, this paper will focus largely on magnetite.

Industrial mineral applications of magnetite include coal-washing, production of heavy aggregates, sand-blasting media, ballast in marine structures, counterweights, roofing granules, drilling-fluid media, black pigment, radiation shielding, heat exchangers, water purification and as a source of iron in cement. Selected industrial mineral uses of iron oxides that represent promising niche markets, with emphasis on magnetite, are described below.

Magnetite Use in Coal Beneficiation

Coal beneficiation is a procedure that extracts impurities from raw coal. It improves burning efficiency and reduces unwanted air emissions, homogenizes shipments and reduces transportation costs. Lumps of crushed coal from 1 to 2 cm in size are commonly treated by dense-medium separation. The high-density medium is commonly a suspension of finely ground magnetite or ferrosilicon. Because coal is lighter, it floats and is separated off, while heavier rocks and other impurities sink and are removed as waste. Any magnetite mixed with the coal is separated using water sprays and is then recovered, using magnetic drums, and recycled. Specifications for magnetite concentrate used in the coal industry varies from one coal producer to the next, but data presented below can be considered representative (Kilborn Engineering (BC) Ltd., 1986). No more than 5 wt% of the particles should exceed 45 μm (325 mesh) and no more than 30 wt% should be finer than 10 μm. Density of the magnetite concentrate is expected to be in the range 4.9–5.2 g/cm^3. More than 95 wt% of the particles in the concentrate should be magnetic, and the moisture of the concentrate should be less than 10 wt%. Most of magnetite products currently in use in coal beneficiation exceed 95 wt% of Fe_3O_4.

The 2004 magnetite production in BC totalled 87 000 t and, for the first 6 months of 2005, production reached 51 000 t (Jorgenson, 2005b).

A substantial portion of this material was sold for coal beneficiation. In 1986, magnetite requirements in the combined Alberta and BC coal industries were estimated at 70 000–75 000 t (Kilborn Engineering (BC) Ltd., 1986), and demand is projected to reach 100 000 t by 1990.

An independent approach to constrain the current magnetite requirements for coal washing is by looking at BC's coal production, which was estimated at 27.1 million tonnes in 2004 (Schroeter *et al.*, 2005) and is projected to be 27.5 million tonnes for 2005 (Barry Ryan, pers. comm., 2005).

As a first approximation, magnetite losses from the circuit reported in other jurisdictions vary from 1 to 3.5 kilograms per tonne of coal washed, depending on the engineering design, maintenance level of the plant and quality of the coal. These figures, in combination with a partial user survey in BC, suggest that, if no ferrosilicon was used as the heavy medium, then actual magnetite losses in coal-cleaning circuits of BC's coal producers for 2005 would be between 28 000 and 84 000 t. The most likely range is 50 000–60 000 t of magnetite per year. The coal production of Alberta is traditionally slightly higher than that of BC. For both provinces combined, the magnetite market for coal washing is in the 56 000–168 000 tonne range, with the most likely consumption between 100 000 and 120 000 t per year. This estimate is in agreement with the estimate of 100 000 t of magnetite per year made by Kilborn Engineering (BC) Ltd. for 1990. However, it is necessary to take into consideration the ongoing research into recovery of heavy minerals from Alberta's tar sand operations. Magnetite market conditions for coal washing would change abruptly if one of the by-products from the tar sands was a coal-washing-grade magnetite.

Coloured Pigments

The demand for coloured pigments is closely linked to the economic cycles of the industrialized nations. Iron oxides are an important segment of the overall pigment market. These oxides are found in their natural state and, after fine grinding, they are suitable for use as pigments (Anonymous, 2005c). They are used in a variety of industrial applications; however, building products (masonry cement, ready mix, mortar and roofing granules) and surface coatings account for more than 90% of this market by volume. In most applications, natural iron oxides now compete with their synthetic counterparts that offer a more consistent product in terms of particle shape, particle size and distribution, as well as chemical composition, including lower heavy metal content. Representative chemical analyses are provided in Podolsky and Keller (1994).

Iron oxides are typically nonreactive. Oil absorption, surface area, particle size, shape of the particles, optical properties and magnetic properties are important parameters if the concentrate is intended for the pigment market (Podolsky and Keller, 1994). Magnetite is typically used as black pigment. Goethite and limonite (ochre) are traditional yellow pigments and hematite, calcined siderite and calcined pyrite are used as red pigments.

In 2000, the total iron oxide consumption for pigment applications was estimated at 1.5 million tonnes (O'Driscoll, 2004). Although there is no consensus regarding the size of the natural iron oxide pigment market, the United States Geological Survey's estimate for 2002 was 500 000 t.

The main advantage of natural iron oxide pigments over their synthetic equivalents is lower price. The prices for technical-grade natural iron oxide vary from Euro(€)190 to 310 per tonne (ex-works). These prices increased by 15–20% between 2002 and 2004 (O'Driscoll, 2004). Cement-grade natural iron oxide ranges in price from €30 to 40 per tonne (bulk, FOB). Specular hematite (sought after because of its platy nature) was selling in the range €600–800 per tonne (FOB; O'Driscoll, 2004). In North America, prices are expected to have similar ranges for comparable products.

Radiation Shielding

The negative effects of X-rays on humans were recognized in 1895, a few months after Roentgen's discovery, and substantial progress has been achieved in radiation shielding since that time (Shultis and Faw, 2005). The use of magnetite, ilmenite, limonite, goethite, iron ore pellets, barite, steel and iron shot as heavy aggregates in radiation-shielding concrete is relatively common (Cement Association of Canada, 2005a, b). The use of such materials in the construction of nuclear power plants is well documented. Recently, however, the innovative use of heavy aggregates started to expand into construction of facilities such as cancer-care buildings and research laboratories (Finkelstein and Gray, 1995). The radiation-shielding efficiency of construction materials is approximately proportional to their density. Heavy concrete (commonly incorporating magnetite aggregate), with a density of approximately 3.69 g/cm^3, is used in radiation barriers where space is critical. Common concrete has a density around 2.35 g/cm^3. In most situations, magnetite aggregate has a cost advantage over other heavy mineral aggregates (Kase, 2003).

Ballast in Construction of Offshore Oil and Gas Installations

Magnetite is one of the materials that competes with olivine in the ballast market, particularly where the development of offshore oil and gas resources is involved. The best example of the use of magnetite as ballast in Canada relates to the construction of the Hibernia platform. A Newfoundland company called Lodestone Limited obtained a contract to supply 300 000 t of magnetite ballast from the Bishop deposits in western Newfoundland (Boyd, 1997). A total of 411 000 t of magnetite was shipped from St. George's Bay to the Hibernia platform, located off the Grand Banks approximately 300 km southeast of St. John's. The ore was unloaded as slurry consisting of 8% magnetite and 92% water.

Heavy ballast concrete coatings for pipelines represent another important but relatively new market. For example, approximately 620 000 t of magnetite from the famous Kiruna iron mine in Sweden is required for coating the 650 km Nyhamna-Sleipner stretch of Langeled, the pipeline serving the Ormen Lange gas development in the Norwegian and North seas (Lindwall, 2004).

Depending on the type of technology used, if oil and gas drilling starts in BC's offshore, even relatively small magnetite deposits along the coast may become viable sources of magnetite.

Sand Blasting

Before the health and safety regulations regarding 'free silica' were implemented, silica sand had a near monopoly as a sand-blasting medium. Today, besides silica sand, there is a variety of sand-blasting materials in use, including garnet, olivine, slag, staurolite, magnetite and he-

matite. Both magnetite and hematite are now produced and marketed in Canada for these applications.

GEOLOGY OF IRON ORE DEPOSITS

Banded iron formations (BIFs) provide the bulk of the iron ore currently mined worldwide. They include the Superior and Algoma types (Gross, 1993, 1996), their hypogene or supergene-enriched portions (Morey, 1999; Taylor *et al.*, 2001, 2002) and their metamorphosed equivalents, such as those currently mined in the Wabush area of Quebec and Labrador. Algoma-type deposits are generally smaller than those of Superior type, yet they are commonly 30–100 m thick and extend for several kilometres along strike and average 25% Fe (Gross, 1996). Economic portions of primary (not enriched) BIF consist typically of silica-rich iron ore and are commonly referred to as taconites. Taconites are harder, have lower iron content and require more costly processing than their enriched counterparts. Nevertheless, these primary ores can be upgraded to produce concentrates containing about 65% iron. Taconites are mined mainly in the United States and China but are found throughout the world, including Canada. They currently account for most of the world's known undeveloped iron resources. The iron-oxide facies of BIF is a preferred iron source, since it typically has a lower content of sulphur and other deleterious elements than skarn deposits.

Some geographic areas are known to contain magmatic (Jiang *et al.*, 2004) and/or hydrothermal iron deposits. Iron-oxide breccias (Lefebure, 1995), including the famous Kiruna (Sweden) and Olympic Dam deposits (Australia), and iron-rich skarns (Ray, 1995), represented by BC's Tasu mine on Moresby Island (the last major magnetite producer in BC), Iron Mike and Brynnor (Kennedy Lake), are good examples. At least the last two deposits may still contain economically recoverable iron resources for industrial mineral applications. Skarns were historically important sources of iron ore but, from a worldwide perspective, their importance is continuously declining.

In addition, several other types of iron oxide deposits that supply hematite, goethite, limonite, umber and specular hematite for pigment applications are described by Harben and Kuzvart (1996). In today's global market, these deposits have limited potential as sources of ore for iron and steel making, but they still supply material for a variety of industrial applications. Placer deposits, as summarized by Levson (1995), represent a potential source of magnetite derived as a by-product of gold, platinum, garnet, zircon or ilmenite mining.

Iron Ore Deposits along the Southwestern Coast of British Columbia

Most of the iron deposits located along the coast of BC are iron-rich skarns (Fe skarns), characterized by the presence of magnetite and hematite as ore minerals and by chalcosilicates as gangue or characteristic rock-forming minerals within the host rock. The most common chalcosilicate gangue minerals are diopside, hedenbergite, garnet, wollastonite, the tremolite-actinolite series of amphiboles, serpentine group minerals, epidote group minerals, scapolite, idocrase, chlorite and, less commonly, prehnite. Calcite, dolomite, quartz and sulphide minerals, including pyrite, chalcopyrite and bornite, are also common accessory minerals. Brucite is present in some of the magnesian (dolomitic) skarns. Magnetite itself is typically distributed within the skarn zone in a manner that is difficult to predict. It may form lenses, pods, veins and stringers (Fig. 1) of massive ore (Fig. 2, 3), or it may be disseminated through carbonates. Figure 4 shows the main excavation at Iron Mike, from which pockets of massive iron ore were mined.

Globally, Fe-skarn deposits range from 3 to more than 250 million tonnes and grade between 40 and 50% iron (Ray, 1995). In BC, Fe-skarn deposits average approximately 4 million tonnes, with the largest deposits being in the 20 million tonne range (Ray, 1995). Table 1 shows the production levels of Fe-skarn mines operating in BC in the early 1960s and provides information on the average iron content and major element composition of ore concentrates that were produced. It also provides information on the size ranges of particles that made up the concentrate. The concentrate from the Empire development was very coarse (<15 cm); the concentrate from Nimpkish Iron Mines Ltd. consisted of particles finer than 0.6 cm; and the concentrate from Texada Mines Ltd. was the finest of the three, with particles finer than 1.91 mm.

Common impurities include SiO_2, CaO, MgO and Al_2O_3. Impurities such as P_2O_3, TiO_2, S, As, Cr, Ni and Cu were highly undesirable in the early 1960s (Gross, 1965), and the same restriction applies today.

There is no good reason to dismiss the possibility that larger Fe-skarn deposits will be discovered along BC's coast in the future, since a large number of known magnetite deposits were discovered during gold and copper exploration. Some of these skarns were mined in part for their copper and gold content. Under current market conditions, these small Fe skarns have a limited iron ore potential, ex-

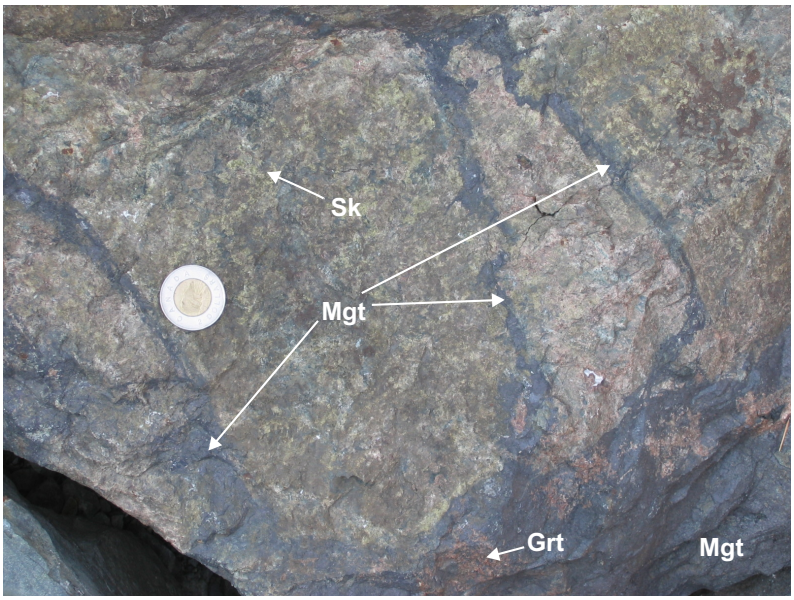


Figure 1. Magnetite stringers cutting clinopyroxene and epidote-rich skarn hostrock, Iron Mike deposit; two-dollar coin for scale. Abbreviations: Mgt, magnetite; Grt, garnet; Sk, skarn.

cept where they are located close to the market or tidewater. Several of these deposits may have industrial mineral potential if they can satisfy specific niche market requirements.

Although the BIFs are the main source of iron ore worldwide, the largest known deposit of this type in BC, Falcon, contains an inferred resource of less than 5.3 million tonnes grading 37.8% Fe (Gross, 1996). These reserve estimates are, however, not compliant with National Instrument 43-101.

In the long term, magnetite could be also derived as a by-product of heavy mineral sand deposits. Such deposits were described by Barrie *et al.* (1988) and Barrie (1991, 1994). Barrie *et al.* (1988) summarized the situation as follows: "Bottom sediments of the northern BC continental shelf contain, on average, 10% of heavy minerals by weight within the dominant sand fraction. Anomalous concentrations occur within selected sand samples from Queen Charlotte Sound (>25%) and Hecate Strait (>18%). The heavy mineral suite here is dominated by amphibole and the titanium minerals ilmenite, sphene and titaniferous magnetite."

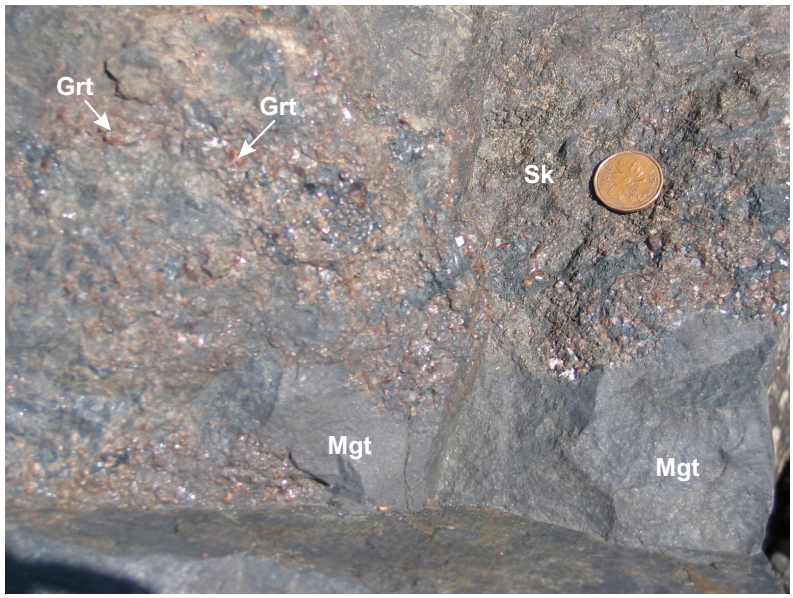


Figure 2. Massive magnetite ore, split along a vein composed mainly of garnet, clinopyroxene, carbonate and epidote, Iron Mike deposit; penny for scale.. Abbreviations: Mgt, magnetite; Grt, garnet; Sk, garnet-clinopyroxene-carbonate skarn.

Current knowledge of these deposits is extremely limited and it remains to be seen if they could be developed in a manner consistent with the strict environmental regulations that apply to any development of BC's offshore resources. In these deposits, magnetite would likely be a co-product of titanium oxide, garnet, gold or platinum, zircon, silica sand and possibly other industrial minerals or gemstones.

The potential of beach sand deposits, mainly around Queen Charlotte Islands, is described by Mandy (1934), Robertson (1956), Russel (1956), Holland and Nasmith (1958), Nickel (1956) and Thompson and Howard (1957). None of these reports is particularly optimistic, but some of these placers are known to contain gold, ilmenite-hematite, magnetite, garnet, staurolite and zircon.

Location and Description of Iron Occurrences in Southwestern British Columbia

According to MINFILE (2005), there are 296 occurrences in BC with magnetite listed as one of the commodities. A compilation by Hancock (1988) covered 90 of these occurrences. Although this compilation is not up to date, it is worthwhile examining, because it contains maps and sketches that are not readily available from MINFILE.

Figure 5 shows iron deposits located along the coast in southwestern BC. From the 157 magnetite occurrences covered by this figure and listed in MINFILE, 129 are of the skarn variety. From the 129 skarn occurrences, 37 are classified as Fe skarns, although they may also contain reported gold and base metal values. The remainder of skarns are identified either as Cu, Pb-Zn or Mo skarns, or simply as skarn. Lady A (A, C and D zones) and Mesabi are tentatively classified as Algoma-type iron formations, although their resources are very limited if compared to tonnages of typical Algoma-type iron deposits.

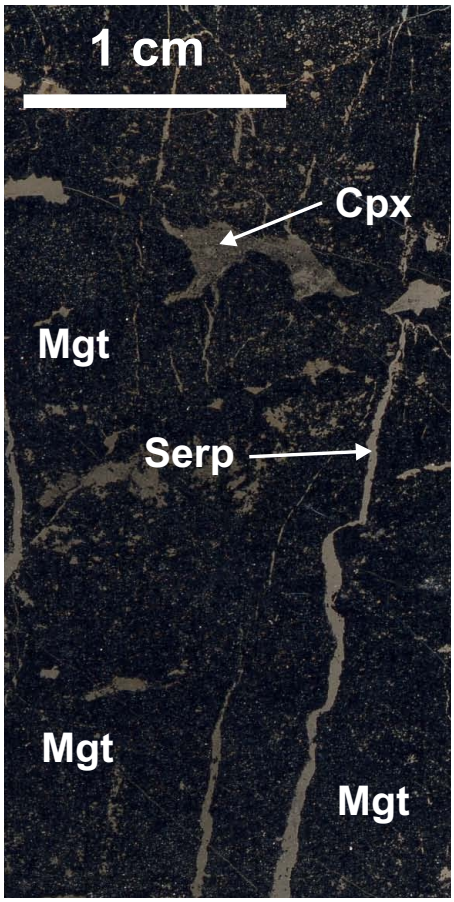


Figure 3. Cut and polished section of massive magnetite ore, Kennedy Lake mine. Gangue minerals are light coloured; the main gangue mineral is clinopyroxene altering to serpentine, with subordinate carbonate. Veinlets consist mainly of serpentine and carbonate, but they also contain amphibole and vestiges of clinopyroxene. Abbreviations: Cpx, clinopyroxene; Mt, magnetite (black); Serp, serpentine.

The skarn zones are typically located near the contact of carbonate and/or volcanic rocks with intrusive bodies. Two of the best known examples are Kennedy Lake, which was documented by Shang and Menzies (1961), and the Iron Mike group of deposits (BC Ministry Mines and Petroleum Resources, 1961, 1965; Hancock, 1988; Shearer, 2004). Both of these deposits are past producers and have some resources left in the ground.

Selected examples of magnetite deposits are listed in Table 2. The MINFILE database indicates that some of the past producers have magnetite resources left in the ground, some of the deposits have partially documented resources, and others are simply occurrences located in favourable geological settings. Follow-up prospecting, modern geophysical surveys or drilling may be justified in a number of these cases.



Figure 4. Main excavation at Iron Mike group of deposits. Massive magnetite ore is still visible in the walls of the excavation. Geologist for scale. Abbreviation: Mgt, magnetite.

As with all regional reconnaissance commodity assessments, the uneven quality of available data, the need to produce a compact shortlist, and a large degree of subjectivity involved in the compilation may have resulted in undue omissions from the Table 2. There are also some inconsistencies between inventory reports, MINFILE descriptions and, in some cases, between different sources of primary information. These inconsistencies are most apparent when resource figures are compared. The uncertainty is highest in cases where several deposits are located adjacent to one another and have changed names many times. There is a possibility that resource estimates were assigned to the wrong deposit, especially in the cases of deposits with very long exploration histories. Most of the resource figures that are part of this compilation are not compliant with National Instrument 43-101. This table should not be used to select exploration targets without considering all the information and references provided in MINFILE, Ray and Webster (1997) and Hancock (1988), and from ground verification.

In a number of occurrences listed in the Table 2, the main exploration driver may be the presence of copper, gold or molybdenum rather than the magnetite content. Magnetite may still be an important by-product.

CONCLUSION

Most of the iron occurrences and deposits in the study area are skarns. Virtually all of these skarns contain some

TABLE 1. CHARACTERISTICS OF CONCENTRATES PRODUCED FROM SKARN DEPOSITS IN BRITISH COLUMBIA AND SHIPMENT LEVELS FROM 1960 TO 1962 (GROSS, 1965)

Company and Property Location	Ore Mineral / Grade	Year	Concentrate Shipped				
			Shipment ($x10^3$ tonnes)	Average Analyses (%)			
				Fe	SiO_2	P	Mn
Kennedy Lake, Vancouver Island	Magnetite / >50% Fe	1960	-	-	-	-	-
		1961	-	-	-	-	-
		1962	417	61.4	5.0	0.05	-
Empire Development Company, Ltd., Benson R., 40 km southwest of Port McNeill, Vancouver Island	Magnetite / 48.4% Fe	1960	421	58	6.38	0.025	-
		1961	269	57.84	6.81	0.039	-
		1962	22	56.49	4.27	0.025	-
Jedway Iron Ore Ltd., Moresby Island, Queen Charlotte Islands	Magnetite / 51 52% Fe	1960	-	-	-	-	-
		1961	-	-	-	-	-
		1962	49	58.97	0.57	0.02	0.17
Nimpkish Iron Mines Ltd.	Magnetite / 41.6% Fe	1960	257	59.3	5.22	0.013	0.016
		1961	384	59.1	5.1	0.014	-
		1962	329	58.6	5.4	0.013	0.15
Texada Mines Ltd., Texada Island	Magnetite / 41.20% Fe	1960	381	61.39	3.93	0.014	0.13
		1961	449	61.42	3.93	0.11	0.13
		1962	547	61.81	3.92	0.011	0.13
Zeballos Iron Mines Limited, Vancouver Island	Magnetite / 48% Fe	1960	-	-	-	-	-
		1961	-	-	-	-	-
		1962	230	62.6	5.45	0.01	-

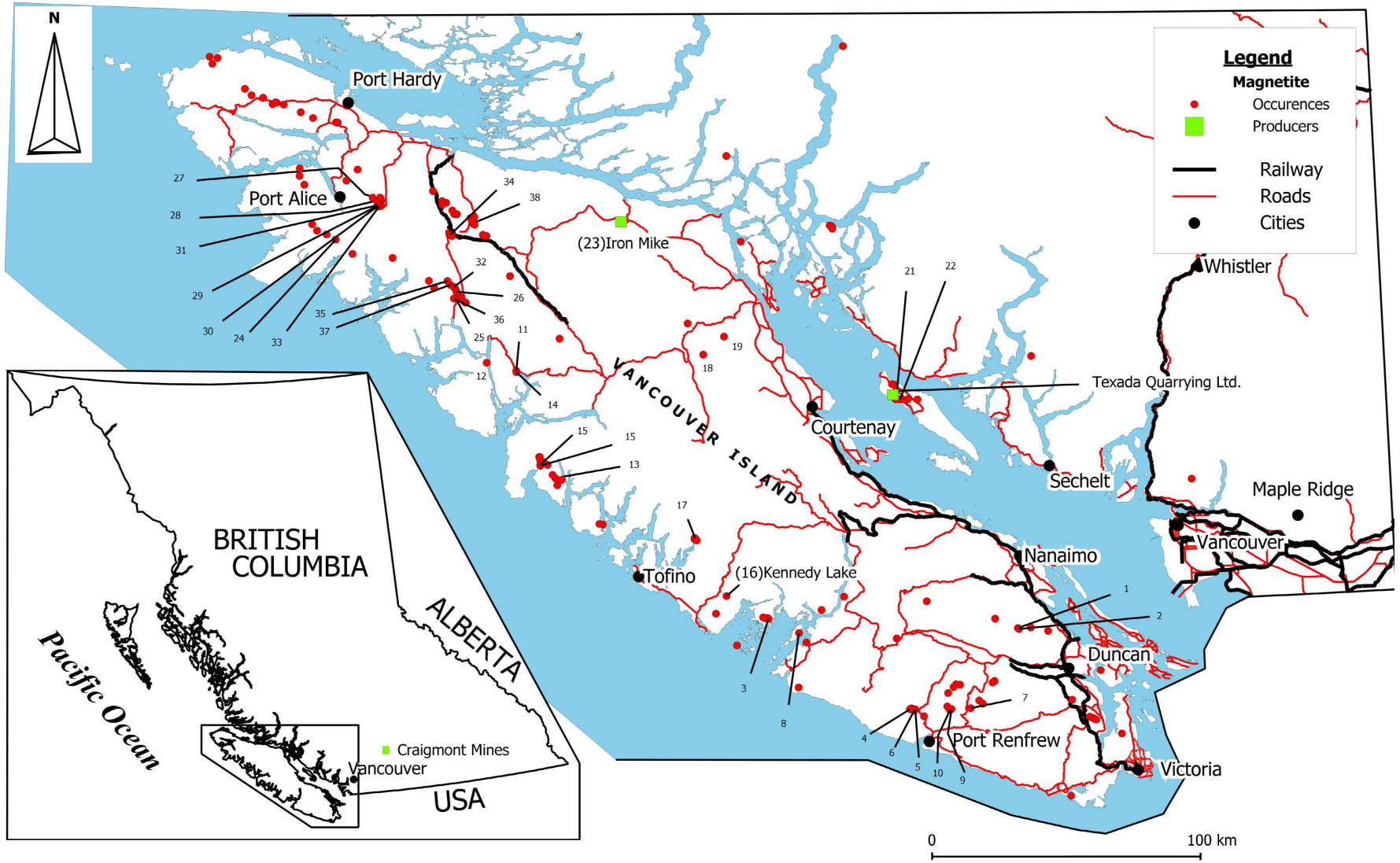


Figure 5. Location of selected magnetite producers, deposits and occurrences in southwestern British Columbia. The deposits that are identified by numbers are listed and characterized in Table 2.

TABLE 2. PARTIAL LIST OF MAGNETITE DEPOSITS IN THE COASTAL AREA OF SOUTHWESTERN BRITISH COLUMBIA. RESOURCE ESTIMATES ARE COMPILED FROM OLD REPORTS OF UNEQUAL QUALITY, LARGELY NOT COMPLIANT WITH NATIONAL INSTRUMENT 43-101. MINFILE NUMBERS ARE PROVIDED IN THE SECOND COLUMN OF THE TABLE FOR SO THAT INTERESTED PARTIES CAN CONSULT MINFILE (2005). LOCATION NUMBERS FOR THE DEPOSITS CORRESPOND TO THOSE ON FIGURE 5

Location Number	MINFILE Number	Name	Deposit Code[1]	Status[2]	Resources[3]	Grade	Selected Sample	Mineralization[4]	Reference
1	092B 029	Lady A (A Zone)	G01	DP	estimated: 366 000 t	25% Fe	-	Mgt	BC Minister of Mines (1956a)
2	092B 033	Lady A (C Zone)	G01	DP	estimated: 2 150 000 t	18% Fe	-	Mgt	Buckham (1953)
3	092C 002	Crown Prince	K03	DP	inferred: 67 500 t possible: 180 000 t	50% Fe	-	Mgt	BC Minister of Mines (1916a)
4	092C 022	Bugaboo	K03	DP	possible and probable: 4 400 000 t	55.67% Fe, 3.61% S (Daniel) 54.31% Fe, 2.21% S (Conqueror)	-	Mgt	Menzie and Nichols (1960); Gilmour and McKinley (2003)
5	092C 025	Sirdar	K03	DP	proven: 9000 t probable: 8900 t possible: 69 000 t	-	56.57% Fe, 8.52% insolubles, 2.75% S, 0.121% P (ore)	Mgt	Young and Uglow (1926); Gilmour and McKinley (2003)
6	092C 027	Baden Powell	K03	DP	proven: 33 800 t probable: 56 000 t	-	59.34% Fe, 5.93% insolubles, 2.57% S, 0.012% P, 1.14% MnO (high grade)	Mgt	Gilmour and McKinley (2003)
7	092C 031	Tally	K	SH	-	-	<1.5% Cu, <0.5% Co, <17.14 g/t Ag (grab) <3.5% Cu (from the pit)	Mgt, Cu, Co, Ag	092C 031 Property File Mineral Deposit Inventory Card
8	092C 033	Mountain	K03	DP	-	-	50.4% Fe (representative)	Mg	BC Minister of Mines (1902)
9	092C 090	Reko 3	K	PR	zone 8 estimated: 33 000 t	-	-	Cu, Mgt	Eastwood (1975); Gilmour and McKinley (2003); Roscoe (1973)
10	092C 110	Reko 38	K	PR	zone 5 estimate: 35 000 t, zone 4 & 6 also substantial	-	-	Mgt, Cu	Eastwood (1975), Roscoe (1973); Gilmour and McKinley (2003)
11	092E 001	Glengarry	K03	PP	possibly 270 300 t remaining	42.7% Fe	-	Mgt, Cu	BC Minister of Mines (1956b); MINFILE Production Report, 092E 001
12	092E 010	Geo	K01, K03	PR	-	-	13.71 g/t Ag, 6.17 g/t Au, 5.2% Cu (680 t bulk sample), minor mgt	Au, Ag, Cu, Mgt, Gms, Pb, Zn, Mo	BC Minister of Mines and Petroleum Resources (1962a); Coombes (1992)
13	092E 011	Indian Chief	K01, K03	PP	possible and potential: 1 900 000 tonnes	23.2 g/t Ag, 0.31 g/t Au, 1.5% Cu, mgt may be in tailings (mgt. grade unavailable)	-	Cu, Ag, Au, Mgt	Agnew (1962)
14	092E 015	Rob Roy	K03	PR	probable reserves: 45 359 t	56.8% Fe	-	Mgt	BC Minister of Mines (1916b)
15	092E 016, 031	Brown Jug, Thelma	K03	DP	potential: 500 000 t 1.5 million t	40% Fe 30% Fe	-	Mgt, Au, Ag, Zn, Cu, Pb	Agnew (1962); Chaplin (1962)
16	092F 001	Brynnor (Kennedy Lake)	K03	PP	some remaining	56% Fe	-	Mgt, Agg	Hancock (1988)
17	092F 015	Hetty Green	K01, K07	PP	-	0.5110% Mo	0.5110% Mo (chip - 20 m)	Cu, Mgt, Mo, W, Ag, Au	Ostler (1979); BC Minister of Mines and Petroleum Resources (1963); Hancock (1988)
18	092F 075	Iron Hill (Argonaut)	K03	PP	possibly some remaining resources	60% Fe	-	Grt, Mgt	Hancock (1988)
19	092F 076	Iron River	K03, K01	DP	east: indicated: 1 450 000 t west: indicated: 3 175 000 t varies widely depending on source of information	1.4 1.7 g/t Au, 2.4 3.4 g/t Ag	Cu concentrate Cu concentrate	Mgt, Cu, Ag, Au	Durek and Nordin (1972); McCullough (1974); http://www.info-mine.com/mining/

TABLE 2 (CONTNUED)

Location Number	MINFILE Number	Name	Deposit Code[1]	Status[2]	Resources[3]	Grade	Selected Sample	Mineralization[4]	Reference
20	092F 130	Iron Mountain	K03	DP	possible resource: 250 000 t, reserves: 18 000 t	50% Fe	-	Mgt	BC Minister of Mines (1916c)
21	092F 258	Yellow Kid-Texada Mines	K03, K01	PP	possibly a small resource left underground	-	-	Cu, Ag, Au, Mgt, Zn	BC Minister of Mines (1952)
22	092F 259	Lake-Texada Mines	K03, K01	PP	possibly a small resource left underground	-	-	Ag, Au, Cu, Mgt, Zn, Co	British Columbia Minister of Mines (1952)
23	092K 043	Iron Mike	K03	PP	possible resource: 786 530 t	43.5% Fe	-	Mgt, Cu	H.L. Hill and Associates (1965); MINFILE Production Report, 092K 043
24	092L 003	Little Lake	K03	DP	inferred: 2 846 000 t	0.0270% Cu, 47.82% Fe, 1.113% S	-	Mgt, Cu	Deleen and Durek (1974)
25	092L 028	Ford	K03	PP	-	-	-	Mgt	MINFILE Production Report, 092L 028; Hancock (1988)
26	092L 031	Churchill Magnetite	K03	DP	726 000 t	35 40% Fe	-	Mgt	Saukko (1967)
27	092L 035	Old Sport	K01	PP	some mgt in tailings	-	4.41 g/t Ag, 1.45 g/t Au, 8.65% Cu, 38.6 g/t Ag, 0.03% Co (grab)	Mgt, Cu, Ag, Au, Co	Hancock (1988); BC Minister of Mines and Petroleum Resources (1960)
28	092L 040	Shamrock	K03	DP	resource: 180 000 t	26.0% Fe	-	Mgt	Lamb (1961)
29	092L 044	Merry Widow 5	K03, I05	PP	-	17% Cu, 2.9% Zn, 0.2% As, 0.16% Co, 200 g/t Ag, 32 g/t Au	17% Cu, 2.9% Zn, 0.2% As, 0.16% Co, 200 g/t Ag, 32 g/t Au (sulphide-rich)	Mgt, Cu, Au, Zn, Co, As, Ag	Ettlinger and Ray (1989)
30	092L 045	Kingfisher	K03	PP	-	-	-	Mgt	Hancock (1988)
31	092L 046	Raven	K03	PP	-	-	-	Mgt, Cu, Au, Ag, Zn	Ettlinger and Ray (1989)
32	092L 068	Artlish	K03	DP	inferred: 635 000 t	0.08% Cu, 44.1% Fe, 3.16% S	-	Mgt, Cu	Saukko (1965)
33	092L 091	Benson Lake	K01	PP	possibly 272 154 t	1.0 g/t Au, 1.6% Cu, 30.0% Fe	-	Cu, Mgt, Au, Ag	Carter (1991)
34	092L 123	Klaanch	K	SH	-	-	-	Mgt, Cu, Zn	Tipper (1959); Hoadley (1953)
35	092L 127	Hiller 4-5	K03	DP	3 357 000 t	35.9% Fe, 0.66% S, <0.02% Cu	-	Mgt	Saukko (1967)
36	092L 128	Ridge	K03	DP	45 359 t	-	68.84% Fe	Mgt	BC Minister of Mines and Petroleum Resources (1962b); Stevenson, 1950
37	092L 301	Hiller 8-12	K03	DP	180 000 t	30% Fe	-	Mgt	McDougall (1965)
38	092L 337	Bob 17	K01, K03	PR	inferred: 12 608 t	3.0% Cu, 30% Mgt	-	Cu, Mgt, Au, Ag	McDougall (1961)

[1] Deposit code key:
K - skarn (unclassified)
K01 - copper skarn
K03 - iron skarn
G01 - algoma-type iron formation

[2] Status key:
SH = showing
PR = prospect
DP = developed prospect
PP = past producer

[3] Resource estimates are from a variety of technical reports, most of them not compliant with National Instrument 43-101.

[4] Mineralization key:
As = Arsenic
Co = Cobalt
Cu = Copper
Grt = Garnet
Gms = Gemstones
Au = Gold
Fe = Iron
Pb = Lead
Mgt = Magnetite
Mo = Molybdenite
Ag = Silver
W = Tungsten
Zn = Zinc

magnetite, but a large number were discovered during the exploration for copper and gold. Some of the past-producing iron mines in southwestern BC still contain magnetite-rich rocks in the ground and others contain magnetite in tailings. Such resources are expected to have limited tonnage, but they require minimal capital investment and offer relatively low risk as short term sources of magnetite, especially if the contract to deliver the magnetite can be obtained prior to mining. The most recent example of such activity is the extraction of a bulk sample from the Iron Ross deposit, which is covered in this document as one of Iron Mike group of deposits. In a number of cases, the remaining reserves may be too deep or so small that they could be entirely extracted under the bulk-sampling permit.

Although the prices of iron ore increased drastically over the last two years, banded iron-formation-type deposits and their enriched equivalents will remain the main worldwide source of iron ore for steel making. Small shipments from BC skarn deposits could be sold as a direct shipping ore, but will more likely be used as a concentrate for industrial mineral niche markets.

As exploration in BC is on the rise, exploration for base and precious-metal-bearing skarn deposits along the coast may result in the discovery of new magnetite deposits.

The lack of detailed information regarding BC's offshore placer resources makes it impossible to predict if magnetite could be recovered from them as a by-product. If the offshore oil and gas developments go ahead, magnetite-bearing skarns located near the coast may become suppliers of heavy mineral aggregate.

With the expansion of coal production in British Columbia and worldwide, there may be potential for a new magnetite producer along the northwestern coast, who could take advantage of the Prince Rupert terminal and railway to supply magnetite to the future coal mines of northern BC and Alberta.

ACKNOWLEDGMENTS

The manuscript benefited from a critical review by Brian Grant of the BC Ministry of Energy, Mines and Petroleum Resources. George Walton from Camosun College, Victoria and Laura Simandl from St. Margaret School, Victoria, provided outstanding field assistance. Without them this paper would not have been possible.

REFERENCES

Agnew, H. (1962): A report on the mineral occurrences in the Hesquiat Lake – Stewardson Inlet areas, Alberni Mining Division; *BC Ministry of Energy, Mines and Petroleum Resource*s, Assessment Report 462, 22 pages.

Anonymous (2005a), BHP Billiton settles iron ore prices; 13 April 2005, URL <http://www.bhpbilliton.com/bb/investorsAndMedia/newsReleaseDetail.jsp?id=News/2005/NR_BHPBilliton130405.html&title=BHP+Billiton+Settles+Iron+Ore+Prices> [Dec 2005].

Anonymous (2005b): Fox buys Cape Lambert magnetite project; *Mining Journal*, April 29, 2005, page 8.

Anonymous (2005c): Riverside Ochre at 100; *Industrial Minerals*, no 453, page 73.

Barrie, J.V. (1991): Contemporary and relict titaniferous sand facies on the western Canadian continental shelf; Continental Shelf Research, Volume 11, pages 67–80.

Barrie, J.V. (1994): Western Canadian marine placer potential; *Canadian Institute of Mining, Metallurgy and Petroleum Bulletin*, Volume 87, pages 27–30.

Barrie, J.V., Emory-Moore, M., Luternauer, J.L. and Bornhold, B.D. (1988): Origin of heavy mineral deposits, northern BC continental shelf; *Marine Geology*, Volume 84, pages 43–51.

BC Minister of Mines (1902): Copper Island group; *BC Ministry of Energy, Mines and Petroleum Resource*s, Annual Report, 1902, pages 218–219.

BC Minister of Mines (1916a): Crown Prince; *BC Ministry of Energy, Mines and Petroleum Resource*s, Annual Report, 1916, pages 291–292.

BC Minister of Mines (1916b): Fido; *BC Ministry of Energy, Mines and Petroleum Resource*s, Annual Report, 1916, page 294.

BC Minister of Mines (1916c): Henderson Lake Deposits; *BC Ministry of Energy, Mines and Petroleum Resource*s, Annual Report, 1916, page 286.

BC Minister of Mines (1952): Prescott, Paxton, Lake (Texada Mines Limited); *BC Ministry of Energy, Mines and Petroleum Resource*s, Annual Report, 1952, page 218–221.

BC Minister of Mines (1956a): Lady A; *BC Ministry of Energy, Mines and Petroleum Resource*s Annual Report, 1956, page 135.

BC Minister of Mines (1956b): Glengarry; *BC Ministry of Energy, Mines and Petroleum Resource*s, Annual Report, 1956, pages 131-133.

BC Minister of Mines and Petroleum Resources (1960): Old Sport; *BC Ministry of Energy, Mines and Petroleum Resource*s, Annual Report, 1960, page 98.

BC Minister of Mines and Petroleum Resources (1961): Iron Mike; *BC Ministry of Energy, Mines and Petroleum Resources*, Annual Report, 1961, page 91-92.

BC Minister of Mines and Petroleum Resources (1962a): Star of the West (Belle Tahsis Mines Ltd.); *BC Ministry of Energy, Mines and Petroleum Resource*s, Annual Report, 1962, page 104.

BC Minister of Mines and Petroleum Resources (1962b): F.L., Ridge, Cordova (Zeballos Iron Mines Limited); *BC Ministry of Energy, Mines and Petroleum Resource*s, Annual Report, 1962, pages 100–103.

BC Minister of Mines and Petroleum Resources (1963): Sun West Minerals Limited; *BC Ministry of Energy, Mines and Petroleum Resource*s, Annual Report, 1963, pages 115–116.

BC Minister of Mines and Petroleum Resources (1965): Iron Mike (Orecan Mines Ltd.); *BC Ministry of Energy, Mines and Petroleum Resource*s, Annual Report, 1965, pages 225–227.

Boyd, B. (1997): Iron ore; *in* Canadian Minerals Yearbook, 1996, Minerals and Metals Sector, *Natural Resources Canada*, pages 32.1–32.5.

Cement Association of Canada (2005a): Physical properties of high-density aggregates and concrete; *Cement Association of Canada*, EB101-7, Table 18-3, URL <http://www.cement.ca/cement.nsf/37693a7697922813852567b6006c2e36/56b4f0a3941f5e9d85256be2004dffb7?OpenDocument> [Dec 2005].

Cement Association of Canada (2005b): Radiation-shielding; *Cement Association of Canada*, URL <http://www.cement.ca/cement.nsf/searchFinal/1DB9D0B7AD895E6885256BF4004B999F?OpenDocument> [Dec 2005].

Chaplin, R. (1962): A report on the preliminary geological and magnetometer surveys in the Hesquiat Lake area, Alberni

Mining Division; *BC Ministry of Energy, Mines and Petroleum Resources,* Assessment Report 464, 16 pages.

CNN (2005): Global iron ore price set to soar; Cable News Network, online article, February 23, 2005, URL <http://edition.cnn.com/2005/BUSINESS/02/22/nippon.steel/> [Dec 2005].

Coombes, S. (1992): Geological, geochemical and geophysical report on the Extra 1-4 claims; *BC Ministry of Energy, Mines and Petroleum Resources,* Assessment Report 22130, 118 pages.

Craigmont Mines (2005): Products supplied by Craigmont Mines; URL <http://www.craigmontmines.com/prods.html> [Dec 2005].

Dasler, P.G. (1986): Assessment report of drilling on the Iron River property, Searchlight Resources Inc.; *BC Ministry of Energy, Mines and Petroleum Resource*s, Assessment Report 15877, 48 pages.

Deleen, J.L. and Durek, J. (1974): Geological and geophysical report on the Power River property, Port Alice area; *BC Ministry of Energy, Mines and Petroleum Resources,* Assessment Report 5375, 49 pages.

Durek, J.J. and Nordin, E. (1974): Iron River Project geological report; *Kaiser Exploration and Mining Co.*, confidential report.

Eastwood, G.E.P. (1975): Reko; *in* Geology, Exploration and Mining in British Columbia 1974, *BC Ministry of Energy, Mines and Petroleum Resources*, pages 166–167.

Ericsson, M. (2004): Iron ore; *in* Mining Annual Review 2004, Ellis, R., Editor, *Mining Communications Ltd.*, London, pages Iron Ore 1–8.

Ettlinger, A.D. and Ray, G.E. (1989): Precious metal enriched skarns in British Columbia: an overview of geological study; *BC Ministry of Energy, Mines and Petroleum Resources,* Paper 1989-3, 128 pages.

Finkelstein, K.D. and Gray, S.W. (1995): CHESS upgrade 1995: improved radiation shielding; *in* SRI '95 APS X-ray Centennial Symposium (Seventh Users Meeting for the Advanced Photon Source); *United States Department of Energy*, abstract D44.

Gilmour, W.R. and McKinley, S.D. (2003): Geological, geochemical and geophysical assessment report on the Pearson property; *BC Ministry of Energy, Mines and Petroleum Resources*, Assessment Report 27246, 136 pages.

Gross, G.A. (1965): Geology of iron deposits in Canada, Volume 1 — general geology and evaluation of iron deposits; *Geological Survey of Canada*, Economic Geology Report 22, 181 pages.

Gross, G.A. (1993): Industrial and genetic models for iron ore in iron-formations; *in* Mineral Deposit Modeling, Kirkham, R.V., Sinclair, W.D., Thorpe, R.I., and Duke J.M., Editors., *Geological Association of Canada*, Special Paper 40, pages 151–170.

Gross, G.A. (1996): Algoma-type iron formation; *in* Selected British Columbia Mineral Deposit Profiles, Volume 2 — Metallic Deposits, Lefebure, D.V. and Höy, T., Editors, *BC Ministry of Energy, Mines and Petroleum Resources*, Open File 1996-13, pages 25–28.

Hancock, K. (1988): Magnetite occurrences in British Columbia; *BC Ministry of Energy, Mines and Petroleum Resources*, Open File 1988-28, 153 pages.

Harben, P.W. and Kuzvart, M. (1996): Global Geology — Industrial Minerals; *Industrial Minerals Information Ltd.*, London, United Kingdom, 462 pages.

Hill, H.L and Associates (1965): Reports and maps, May 15, 1965; *BC Ministry of Energy, Mines and Petroleum Resources* Property File 092K 043.

Hoadley, J.W. (1953): Geology and mineral deposits of the Zeballos-Nimpkish area, Vancouver Island, British Columbia; *Geological Survey of Canada*, Memoir 272, 82 pages.

Holland, S.S and Nasmith, H.W. (1958): Investigation of beach sands; *BC Ministry of Energy, Mines and Petroleum Resources*, 6 pages.

Jiang, N., Chu, X., Mizuta, T., Ishiyama, D. and Mi, J. (2004): A magnetite-apatite deposit in the Fanshan alkaline ultramafic complex, northern China; *Economic Geology*, Volume 99, pages 397–408.

Jorgenson, J.D. (2005a): Iron ore; *United States Geological Survey*, Mineral Commodity Summaries (January 2005), pages 84–85.

Jorgenson, J.D. (2005b): Iron ore in July 2005; *United States Geological Survey*, Mineral Industry Surveys, October 2005, 7 pages.

Kase, K.R., Nelson, W.R., Fasso, A., Liu, J.C., Mao, X., Jenkins, T.M. and Kleck, J.H. (2003): Measurements of accelerator-produced leakage neutron and photon transmission through concrete; *Health Physics*, Volume 84, no 2, pages 180–187.

Kilborn Engineering (B.C.) Ltd. (1986): Characteristics of Canadian magnetite resources for optimum utilization in coal heavy media process — report on survey of magnetite medium usage in heavy media coal cleaning; submitted to *CANMET*, contract serial number OSQ85-00189.

Lamb, J. (1961): Report in 092L 044 Merry Widow; *BC Ministry of Energy, Mines and Petroleum Resources* Property File, page 9.

Lefebure, D.V. (1995): Iron oxide breccias and veins P-Cu-Au-Ag-U; *in* Selected British Columbia Mineral Deposit Profiles, Volume 1 — Metallics and Coal, Lefebure, D.V. and Ray, G.E., Editors, *BC Ministry of Energy, Mines and Petroleum Resources*, Open File 1995-20, pages 33–36.

Levson, V.M. (1995): Marine placers; *in* Selected British Columbia Mineral Deposit Profiles, Volume 1 — Metallics and Coal, Lefebure, D.V. and Ray, G.E., Editors, *BC Ministry of Energy, Mines and Petroleum Resources*, Open File 1995-20, pages 29–31.

Lindwall, E. (2004): High density concrete to coat world's longest subsea pipeline; *Offshore*, URL <http://www.gasnet.com.br/artigos/artigos_view2.asp?cod=375> [Dec 2005].

Louthean, R. (2005): Expansion boom for Pilbara Iron; *Mining Magazine*, Volume 193, no 2, pages 19–21.

Mandy, J.T. (1934): Gold-bearing black-sand deposits of Graham Island, Queen Charlotte Islands; *Canadian Institute of Mining and Metallurgy* and *Society of Nova Scotia* – Transactions, volume 37, 1934, pages 563-72.

McCullough, P.T. (1974): Review of Iron River, Vancouver Island; *Texada Mines Ltd.*, confidential report.

McDougall, J.J. (1961): Report on Bonanza Lake Copper, Falconbridge Ltd; *BC Ministry of Energy, Mines and Petroleum Resources* Property File 092L 164, page 2.

Minesite (2005): Canaccord's iron ore conference provides timely excuse for some Australians to visit London; *Minesite*, URL <http://www.minesite.com/storyFull5.php?storySeq=288> [Dec 2005].

MINFILE (2005): MINFILE BC mineral deposits database; *BC Ministry of Energy, Mines and Petroleum Resources*, URL <http://www.em.gov.bc.ca/Mining/Geolsurv/Minfile/> [Nov 2005].

Morey, G.B. (1999): High-grade iron ore deposits of the Mesabi Range, Minnesota — product of a continental-scale Proterozoic ground-water flow system; *Economic Geology*, Volume 94, pages 133–142.

Nickel, E.H. (1956): Queen Charlotte Island sands; *BC Ministry of Energy, Mines and Petroleum Resources*, Property File 103J 035, 40 pages.

O'Driscoll, M. (2004): Iron's true colours; *Industrial Minerals*, no 444, pages 34–41.

Ostler, J. (1979): Diamond drilling report of the Tofino Pawnee claims, Tofino Inlet; *BC Ministry of Energy, Mines and Petroleum Resources,* Assessment Report 8138, 23 pages.

Podolsky, G. and Keller, D.P. (1994): Pigments, iron oxide; *in* Industrial Minerals and Rocks (6th edition), Carr, D.D., Editor, *Society for Mining, Metallurgy, and Exploration Inc.*, Littleton, Colorado, pages 765–781.

Ray, G.E. (1995): Fe skarns; *in* Selected British Columbia Mineral Deposit Profiles, Volume 1 — Metallics and Coal, Lefebure, D.V. and Ray, G.E., Editors, *BC Ministry of Energy, Mines and Petroleum Resources*, Open File 1995-20, pages 63–65.

Ray, G.E. and Webster, I.C.L. (1997): Skarns in British Columbia; *BC Ministry of Energy, Mines and Petroleum Resources*, Bulletin 101, 260 pages.

Robertson, J.M. (1956): Report on Queen Charlotte Islands black sands, Skeena Mining Division; *BC Ministry of Energy, Mines and Petroleum Resources*, Property File 103G, J and K, 6 pages.

Roscoe, R.L. (1973): Diamond drilling report on the Reko 38, Granite Creek, Port Renfrew area; *BC Ministry of Energy, Mines and Petroleum Resources*, Assessment Report 5029, 32 pages.

Russel, F.T. (1956): Report on Queen Charlotte Islands black sands, Skeena Mining Division; *BC Ministry of Energy, Mines and Petroleum Resources*, Property File 103G, J and K, 2 pages.

Saukko, R.N. (1965): Hiller-Churchill properties, Zeballos area, Vancouver Island; *BC Ministry of Energy, Mines and Petroleum Resources*, Property File 092L 127.

Saukko, R.N. (1967): Hiller-Churchill properties, Zeballos area, Vancouver Island; *BC Ministry of Energy, Mines and Petroleum Resources*, Property File 092L 127.

Schroeter, T., Cathro, M., Grieve, D., Lane, R., Pardy, J., Ryan, B., Simandl, G. and Wodjak, P. (2005): BC Mining and Mineral Exploration Overview 2004; *BC Ministry of Energy, Mines and Petroleum Resources*, Information Circular 2005-1, 16 pages.

Shang, C.C. and Menzies, M.M. (1961): A study of the Kennedy Lake iron mine; *BC Ministry of Energy, Mines and Petroleum Resources*, Property File 092F 001, 13 pages.

Shearer, T.J. (2002): Geological and trenching report on the Iron Ross project; *BC Ministry of Energy and Mines*, Assessment Report 26874, 39 pages.

Shearer, T.J (2004): Geological, drilling and magnetometer assessment report on the Iron Ross project; *BC Ministry of Energy, Mines and Petroleum Resources*, Assessment Report 27438, 39 pages.

Shultis, J.K. and Faw, R.E. (2005): Radiation shielding technology; *Health Physics*, Volume 88, no 4, pages 297–322.

Stevenson, J.S. (1950): Geology and mineral deposits of the Zeballos mining camp, British Columbia; *BC Ministry of Energy, Mines and Petroleum Resources,* Bulletin 27, page 128.

Taylor, D., Dalstra, H.J. and Harding, A.E. (2002): Genesis of high-grade hematite orebodies of the Hamersley Province, Western Australia — a reply; *Economic Geology*, Volume 97, pages 179–181

Taylor, D., Dalstra, H.J., Harding, A.E., Broadbent, G.C. and Barley, M.E. (2001): Genesis of high-grade hematite orebodies of the Hamersley Province, Western Australia; *Economic Geology*, Volume 96, pages 837–873.

Thompson, R.M and Howard, H.M. (1957): Testing of Queen Charlotte sands; *Western Canada Steel Ltd*., 40 pages.

Tipper, H.W. (1959): Revision of the Hazelton and Takla groups of central British Columbia; *Geological Survey of Canada*, Bulletin 47.

Xinhua News Agency (2005): Oversupply to drive down iron ore prices: experts; *Xinhua News Agency*, April 15, 2005, URL <http://www.china.org.cn/english/BAT/125884.htm> [Dec 2005].

Dolomite in British Columbia: Geology, Current Producers and Possible Development Opportunities along the West Coast

George, J. Simandl, Nicole D. Robinson and Suzanne Paradis[1]

KEYWORDS: dolomite, dolostone, markets, exploration potential, deposit descriptions, prospects, mines, current suppliers

INTRODUCTION

Dolomite crystals most commonly form rhombohedrons when filling open spaces. They are translucent to transparent, have a pearly lustre and are commonly white, but can be pink, colourless, yellow, grey or brown. Dolomite is characterized by perfect cleavage, and has a white streak, an approximate density of 2.86 g/cm^3 and hardness in the range 3.5 to 4 on the Mohs scale. It does not effervesce when in contact with cold, diluted hydrochloric acid unless it is powdered. Dolomite's theoretical chemical formula is $CaMg(CO_3)_2$, which is equivalent to 54.35% $CaCO_3$ and 45.65% $MgCO_3$. This may also be expressed as 30.4% CaO, 21.7% MgO and 47.9% CO_2.

Specifications of the materials currently marketed as dolomite vary substantially from one producer to the next. This is partly due to the product not being a mineral, but rather crushed dolostone or dolomitic marble with small concentrations of calcite or magnesite, accessory silicates, oxides, barite, and sulphides as impurities. Some of the chemical variation may be due to the incorporation of impurities such as iron or manganese into the dolomite crystal structure. Dolomite is a well-known industrial mineral used for its physical and chemical properties, and is also one of the ore minerals used for production of magnesium metal. Some of the material marketed as dolomite may have been formed by extreme substitution of magnesium into the calcite structure. A high magnesium calcite may contain up to 18 mol% $MgCO_3$ incorporated into the calcite structure by substitution for calcium, depending largely on temperature and the Mg/Ca ratio of ambient water (Stanley *et al.*, 2002). High magnesium calcite is not stable during late diagenesis and metamorphism, and it dissociates into an assemblage of calcite and dolomite.

USES OF DOLOMITE

Dolomite is one of the major ores of magnesium metal (Coope, 2004). It competes with magnesite, brines, carnallite, brucite and a number of other magnesium-rich minerals. British Columbia has large magnesite resources that are concentrated in the southeastern portion of the province (Simandl and Hancock, 1996; Simandl, 2004).

Dolomite is also calcined to produce dead-burned dolomite, dolomite refractory bricks, refractory gunning and ramming mixes, and mortars, as well as flux in steel making (Moore, 2002). Large tonnages of dolomite are sold for soil conditioning, as a compost additive and plant nutrient, as animal feed additive (with some restrictions), and for fluegas desulphurization. Dolomite is also used as filler in a variety of plastics, paints, coatings and sealants. Other applications include mine-dust suppression, roofing granules, insecticide/fungicide and fertilizer carrier. In the chemical industry and fibreglass and glass manufacturing, dolomite is used as a source of CaO and MgO (Moore, 2002; Crossley, 2003). The use of dolomite in environmental rehabilitation, in its natural or calcined form as 'dolime', is also steadily growing. Dolomite rocks that do not meet industry specifications for the above uses are commonly sold as aggregate for concrete, terrazzo chips or other landscaping applications.

SPECIFICATIONS OF DOLOMITE PRODUCTS ON THE MARKET

Knowledge of products that are currently available on the market is essential in the evaluation of new deposits. Although the CaO and MgO content of dolomite are reported for all applications, there is no published information, in a number of cases, on other major oxides or trace elements. Detailed information is provided to potential buyers upon request. Particle-size distribution, oil absorption, surface area, bulk density (loose and tapped), pH, neutralizing value relative to $CaCO_3$, base metal and free moisture content, and dry brightness are reported for most of the products intended for the filler market.

Table 1 contains information on pulverized natural dolomite products (*i.e.*, products 1 and 3–10). The products that have the widest range of applications tend to approach the stoichiometric composition of dolomite. Product 9 differs from other materials in its high SiO_2 content and above-average Al_2O_3 content. This product is an exceptional functional filler derived from pulverizing rock that consists dominantly of dolomite, with subordinate talc, tremolite, pale mica and antigorite (Goldberg and Wehrung, 1981). In this particular case, the minor constituents, especially talc and tremolite, enhance the properties of dolomite in a number of filler and ceramic applications. Product 2 is a dolomite derivative (dead-burned dolomite). It is characterized by higher overall CaO and MgO content than the other products, which is achieved by a reduction in the CO_2 content during the calcining process. Rock used in the production of dead-burned dolomite is expected to contain more

[1]*Mineral Resources Division, Geological Survey of Canada, Sidney, BC*

This publication is also available, free of charge, as colour digital files in Adobe Acrobat PDF format from the BC Ministry of Energy, Mines and Petroleum Resources internet website at http://www.em.gov.bc.ca/Mining/Geolsurv/Publications/catalog/catfldwk.htm

TABLE 1. REPRESENTATIVE EXAMPLES OF CHEMICAL COMPOSITIONS OF DOLOMITE AND RELATED VALUE-ADDED PRODUCTS CURRENTLY AVAILABLE ON THE MARKET.

Oxide	Sample									
	1	2	3	4	5	6	7	8	9	10
CaO	30.8	57.2	30.1	>30.0	31.2^	30.8*	30.6*	34.45	25.48	30.9
MgO	21.5	40.1	21.5	>20.0	20.8	20.5	19.8	18.04	19.95	19.3
Al_2O_3	0.02	0.5	0.1	<1.0	0.05	-	-	0.31	0.41	0.26
Fe_2O_3	0.008	0.9	0.2	-	0.14	0.6	-	0.2	0.33	0.13
SiO_2	0.02	1.3	4.7	<1.5	0.7	-	-	0.07	22.95	5.9
TiO_2	0.01	-	-	-	-	-	-	0.01	-	0.02
K_2O	0.01	-	-	-	-	-	-	0.01	-	0.1
Na_2O	0.02	-	-	-	-	-	-	0.01	-	0.02
P_2O_5	0.01	-	-	-	-	-	-	0.01	-	-
LOI	47.7	-	42.8	-	46.9	44	-	46.6	30.3	41

- = not reported * = recalculated from $CaCO_3$ = recalculated from $MgCO_3$ ^ = typical analysis

Sample notes:

1 - Dolomitwerk Jettenberg: natural crushed rock; >99.1% dolomite, 0.8% calcite; used for glass, ceramics and other uses
2 - Jebcoram TL - Usha Martin procurement requirements for refractory monolithic materials; granular calcined magnesia product coated with nontoxic resin binder
3 - Colca processed - micronized, raw dolomite, brightness > 95
4 - The Ocean Command International Trading Co. Ltd: dead-burned dolomite in -120, -100, -200, and -325 mesh
5 - Reade Advanced Materials: 100 Dolowhite
6 - Imasco Minerals Inc: dry-ground dolomite produced in 100, 140, 200, 325, and 400 mesh sizes; used in joint fillers, putties, and caulking, building products and stucco, paints, rubber and adhesives, as well as in glass making; dry brightness (ASTM C110-92) for filler materials varies from 92.5 to 93; cattle feed supplement also available in 100, 250 and 325 mesh
7 - Imasco Minerals Inc: soil conditioners
8 - Ashgrove Cement Company: material currently used in agricultural, environmental and construction applications
9 - Dynatec Canada Talc DOLFIL 50-90, used mainly as functional filler and in ceramics
10 - Mighty White Dolomite - sample quarried in 1987 (Fishl, 1992)

than 18% MgO by volume; the CaO/MgO ratio should be less than 1.6; and the SiO_2 content should be less than 1.5%, preferably less than 1%.

Products 6, 7, 8 and 10 are from BC. Product 10 is considered representative of the Mighty White Dolomite operation, which is located near Rock Creek in southern BC (Fig. 1). It is a white, high purity dolomite. Product 8 is mined by the Ashgrove Cement Company on Texada Island. It has lower MgO content than most of the products listed in Table 1, but also an extremely low silica content. The mine is favourably located, permitting low-cost transportation by barging along the west coast of North America. Products 6 and 7 are products from Imasco Minerals, Inc. Product 6 represents a wide range of products varying mainly in particle size and distribution. Soil conditioners (product 7) do not require such tight specifications as products used as mineral fillers or in other industrial applications.

This brief survey of the literature suggests that there is little or no processing of dolomite besides selective mining, crushing, screening, ± hand-picking, milling and blending, as the chemical specifications of products marketed by a given company vary mainly in particle size and particle distribution. The chemical composition of materials from a given deposit varies only slightly from one product to the next or remains the same. In general, the producers try to provide products to supply to a wide range of consumers.

Large unfractured dolomite blocks can be used as dimension stones; smaller blocks are typically sold as riprap and armour stone; and dolomite that is in the 1–20 cm size range is used as aggregate for concrete. Material in the 4–30 mm range is used commonly as roofing granules, stucco, terrazzo chips, etc. In functional filler applications, dolomite competes with limestone, which is better known and more widely used. Filler-grade dolomite products typically sell in the 1 μm to 0.4 mm particle range. Fine-grained material is used mainly in paint, plastics and rubber, while coarser material is used for roofing carpet backing and joint cements. Glass producers commonly use the material in the 20–200 mesh rage. Where there is no market for fines, the dust is commonly pelletized and marketed for horticultural applications. For a global overview, the reader is referred to Carr *et al.* (1994) and Harben and Kuzvart (1996).

GEOLOGY OF DOLOMITE

Worldwide, most dolomite products currently on the market are derived from sedimentary, hydrothermally formed or metamorphic rocks, as described below. In some countries, dolomite is derived from carbonatite, where it is either recovered as a byproduct or mined because there are no conventional local dolomite resources. In BC, most of the carbonatite bodies are located in the same geographic areas as abundant sedimentary dolomite deposits, so this paper will not consider carbonatite but rather concentrate on traditional sedimentary and hydrothermal dolomite sources. The classification of carbonate rocks is described in many textbooks (Folk, 1959, 1962; Dunham, 1962;

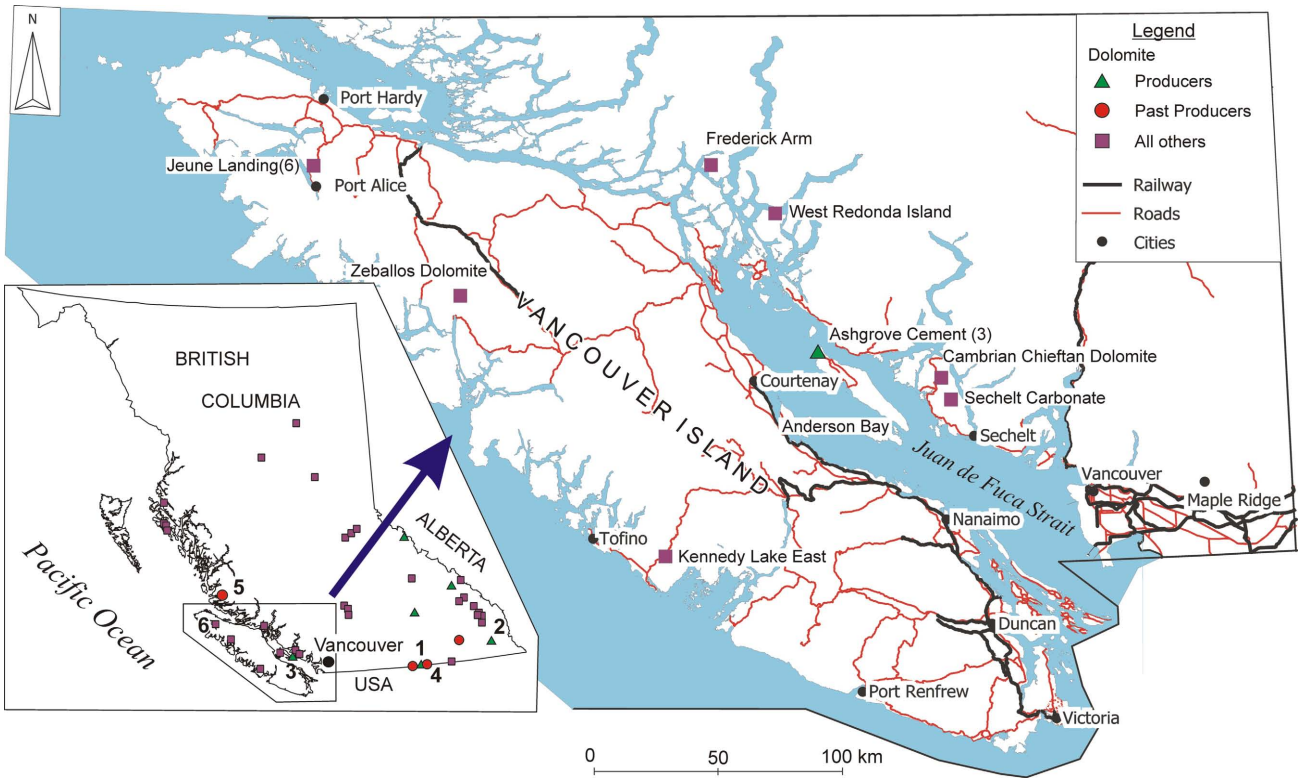


Figure 1. Geographic distribution of dolomite resources in British Columbia. Current dolomite producers: 1, Mighty White Dolomite operation at Rock Creek; 2, Imasco Minerals Ltd. (Crawford Bay); 3, Ashgrove Cement. Other deposits mentioned in the text: 4, Grand Forks Dolomite; 5, Smith Inlet; 6, approximate location of Jeune Landing Dolomite occurrence.

Strohmenger and Wirsing, 1991). This classification is, however, not practical when dealing with finely ground materials, or with recrystallized dolomites where textures are completely destroyed.

Dolostone

Dolostone (also called dolomite) is a sedimentary rock, consisting mainly of the mineral dolomite, which has a chemical composition approaching the theoretical composition of dolomite. Dolomite rocks are commonly divided into penecontemporaneous and replacive dolomites. The penecontemporaneous and replacive dolomite bodies are fine grained and form beds, often interbedded with limestone or dolomitic limestone. Penecontemporaneous dolomite, also called syndepositional dolomite, is relatively rare. Its deposits are restricted in size, and correspond to evaporitic lagoonal or lacustrine settings. The beds and lenses are usually a few centimetres to 20 m in thickness, although they may be substantially thicker and dolomitization within individual bodies in commonly incomplete.

Replacive dolomite forms during burial and is volumetrically the most important. It forms beds or lenses that are commonly more than 100 m thick. This type of deposit offers the best exploration potential for the large-volume, mainstream dolomite markets. The most accepted models for replacive dolomitization are reflux and thermal convection in open half-cell, also referred to as the Kohout convection model (Machel, 2004).

Depending on the level of exposure, availability of regional geological maps and textural information, a definitive distinction between replacive and penecontemporaneous dolomites may not be possible based on rapid field evaluation.

Hydrothermal Dolomite

Hydrothermal dolomite bodies can be formed in most postdepositional and postlithification settings. They are commonly superimposed over earlier replacive dolomite. Hydrothermal dolomite can form sizable bodies. In most cases, the contacts between hydrothermal dolomite and the surrounding rock are at least partially discordant to local stratigraphy, the dolomite zones are highly irregular, and their shape is difficult to predict unless there is a dominant structural control. Individual crystals within bodies of hydrothermal dolomite are typically coarse grained and, in some geological settings, saddle-shaped hydrothermal dolomite is used as an indirect indicator of Mississippi Valley – type Pb-Zn deposits, although, in many districts, it can be found tens or hundreds of kilometres from the nearest Pb-Zn deposit (Leach and Sangster, 1993; Davies, 1996).

Dolomitic Marble

When dolostone is affected by regional or contact metamorphism, it recrystallizes and forms dolomitic marble. The chemical composition of the dolomitic marble does not change significantly from that of its protolith during regional metamorphism; however, the marble formed in the contact metamorphic aureole of an igneous intrusion

may have substantially different chemistry than its protolith. This is largely due to the fact that contact metamorphism is most marked in a near-surface environment where the system is open (*i.e.,* fluids and elements may enter or leave the system). Both regional and contact metamorphisms result in major changes in mineralogy, texture and physical properties of the rock. If silica (chert or quartz) or clay impurities are present in the dolomitic protolith, the resulting dolomitic marble, depending on metamorphic conditions, may contain forsterite, diopside, hedenbergite, amphibole of tremolite-actinolite series, garnet or brucite. In most cases, the recrystallization is also accompanied by 'bleaching': a change in colour from grey or beige to white.

DOLOMITE IN BRITISH COLUMBIA

There are 39 known dolomite occurrences (Fig. 1) currently listed in MINFILE (2005). These occurrences are described either as showings, prospects, developed prospects, past producers or producers (*i.e.,* currently operating mines). The distribution of the main carbonate zones in BC was compiled by Fishl (1992, map 1). This map suggests that the best geological potential for dolomite is in the northeastern part of BC. Large quantities of dolomite are also known to occur in the southeastern portion of the province and in the Rocky Mountains between Golden and Canal Flats, where a substantial proportion of the Jubilee, Beaverfoot, Cathedral and Eldon formations is uniformly dolomitized over thicknesses of tens to hundreds of metres. As with most industrial minerals, proximity to the market is essential and the presence of other minerals competing for the same market should be taken into consideration. The southeastern part of the province also holds large sedimentary-hosted magnesite resources and the only magnesite producer in Canada, Mount Brussilof, which is owned by Baymag Inc.

For these reasons, the paper will briefly describe current dolomite producers and then highlight known occurrences along the west coast. In most cases, the descriptions of individual properties are largely based on MINFILE (2005), so the MINFILE numbers are provided in the text. Southwestern BC has a lower geological potential for dolomite than the southeastern part of the province, but its market potential is far better than that of the rest of the province due to its favourable geographic location relative to dolomite users and competitive transportation costs, facilitated by barging.

To put southwestern BC into perspective, it contains, according to MINFILE, two dolomite showings, one prospect, one developed prospect and one past producer. There is also Ash Grove Cement Company, which produces a material with approximately 18% MgO that approaches dolomite in composition and can compete with it in a number of applications. This deposit will be described in the next section.

Dolomite occurrences located in southwestern BC are shown on Figure 1. There is no formal market study, and precise statistics for dolomite are not available because dolomite production is commonly reported together with that of limestone; therefore, any reported dolomite production data are likely underevaluated. Nevertheless, according to United States Geological Survey (USGS) mineral commodity surveys for 2002, Washington State and California produced 537 000 and 316 000 tonnes of crushed dolomite, at average prices of US$4.72 and 7.79 per tonne, respectively. Dolomite production statistics for Oregon were withheld and it is possible that there was no dolomite recently produced in that state. It is not clear what proportion of crushed dolomite went directly to the construction industry versus being milled and otherwise upgraded. Furthermore, the authors' interactions with the American manufacturing industry indicate that the Seattle area of Washington State will need more than 40 000 tonnes of additional high-purity dolomite in the glass and fibreglass industries over the next two years.

Current Producers and Advanced Projects

There are currently only three active operations in BC that produce dolomitic material (Fig. 1). Mighty White Dolomite Ltd., near Rock Creek, and Imasco Minerals Ltd., at its Crawford Bay underground operation on Kootenay Lake, produce high-quality dolomite. Ashgrove Cement Company's operation on Texada Island is renowned as a limestone producer, and the same property also produces material with a high MgO content that can best be described as limy dolomite. Such material has lower MgO content than typical dolomite and, depending on the application, this may be to its advantage, as long as the product is consistent. For example, in flat glass industry, the ideal ratio of CaO/MgO is 3:2 (Moore, 2002). This ratio is commonly achieved by mixing limestone and dolomite; therefore, the Ashgrove Cement deposit should not be disqualified from many potential uses based strictly on higher than normal CaO content.

Pan Pacific Aggregates Ltd. proposes to construct and operate a quarry on the Sechelt Peninsula, approximately 15 km northwest of Sechelt (Fig. 1). Dolomite is one of the many rock types reported from this property, which is described in more detail in the occurrences section under 'Sechelt Carbonate' (MINFILE 092GNW031). Based on currently available data, it is difficult to predict if the dolomite produced from this property could be used for applications other than soil conditioner or aggregate. The project proposal includes processing plant, conveyor system and loading facility.

Albrit Minerals and Materials Corp. owns a quarry (MINFILE 082ESE036) located 250 m north of Highway 3, just east of Morrissey Creek and approximately 4 km due east of Grand Forks, which in the past supplied dolomite for rock wool. It is referred to in this publication as Grand Forks Dolomite.

A newly discovered dolomite deposit near Port Alice, referred to as 'Jeune Landing Dolomite' (Village of Port Alice, 2005), is also discussed in this section.

MIGHTY WHITE DOLOMITE LTD.

Mighty White Dolomite Ltd. operates a dolomite quarry near Rock Creek (MINFILE 082ESE200). The deposit consists of a dolomite lens in altered metasedimentary and volcanic rocks of the Carboniferous or Permian Knob Hill Group that outcrops over a 100 m by 100 m area along the top of a knoll, 4.5 km south-southeast of the community of Rock Creek (Fig. 1). The lens is largely embedded in hornblende gneiss (amphibolite). An irregular band of talc-chlorite schist lies along the hangingwall contact. Bedding strikes 157–180° and dips 40–80°E. A schistosity strikes 150° and dips 30–50°W (Fishl, 1992).

The lens contains massive, white, fine to very fine grained dolomite. Scattered grains, patches and veinlets of quartz and a trace of talc were reported in Fishl (1992). During a property visit, however, yellowish serpentine appeared to be the main impurity (<0.5%). Two samples of crushed dolomite taken from a stockpile averaged 30.73% CaO, 18.16% MgO, 6.55% insoluble material, 0.32% R_2O_3, 0.135% Fe_2O_3, 0.01% MnO, 0.0025% P_2O_5, 0.015% SO_3 and 44.04% loss-on-ignition (McCammon, 1972).

A chemical analysis of a sample of dolomite quarried in 1987 is listed in Table 1 (product 10). In 1972, the deposit was estimated to contain 15.4 million tonnes of proven (measured geological) reserves and 9.0 million tonnes of probable (indicated) reserves (Anonymous, 1972; Melville *et al.*, 1992). These reserve estimates are not compliant with National Instrument 43-101, and they were reduced by active mining.



Figure 2. Mighty White Dolomite Ltd. processing plant, Rock Creek, southern British Columbia.

Mighty White Dolomite Ltd. currently produces crushed dolomite for agricultural, landscaping and decorative uses, and for a variety of other markets (Boulton *et al.*, 2001) at its plant, which is located near Rock Creek (Fig. 2).

IMASCO MINERALS LTD.

The Crawford Creek Dolomite (MINFILE 082FNE113) underground mine (Fig. 1, 3) is located in the Kootenay Lake area, 600 m south of Crawford Creek, and is operated by Imasco Minerals Ltd. The orebody is hosted by a band of limestone and dolomite of the Lower Cambrian Badshot Formation, which extends north-northeast from the head of Crawford Bay for at least 12 km. The bed outcrops along the east flank of the Preacher Creek antiform: a tight, overturned, eastward-closing fold cored by overlying gneiss, schist and amphibolite of the Lower Cambrian and younger Lardeau Group. Underlying quartzite and schist of the Hadrynian – Lower Cambrian Hamill Group outcrops along the flanks of the fold.

The deposit consists of white medium-grained dolomite containing scattered crystals of metamorphic minerals, especially tremolite. The dolomite develops a brown staining on weathered surfaces. Numerous randomly oriented fractures occur with spacings of 10–15 cm. A sample of chips collected from the quarry contained 30.26% CaO, 20.17% MgO, 2.14% insoluble materials, 0.77% R_2O_3, 0.92% Fe_2O_3, 0.021% MnO, 0.012% P_2O_5, 0.01% S and 46.37% LOI (BC Ministry of Mines and Petroleum Resources, 1965). The chemical analyses of two of the products (6 and 7) are shown in Table 1.

Imasco initially quarried dolomite on the south side of Crawford Creek, 600 m north of the current mine site, during 1962 and 1963. Quarrying began at the current site in 1964, and underground mining began in 1969. Between 1962 and 1988, 734 500 tonnes of dolomite were mined. The dolomite is trucked to the company's plant in Sirdar, where it is crushed and screened for a variety of products: agricultural soil conditioner, a component in stucco and roofing materials, and white ornamental aggregate rock.

ASHGROVE CEMENT

Ashgrove Cement Company has opened a new quarry on Texada Island. This quarry, named Pit #7 (Fig. 4), is located adjacent to the main pit, commonly referred to as Pit #6. The deposit is only partially delimited. The drilling



Figure 3. Crawford Creek Dolomite mine, operated by Imasco Minerals Ltd.

done in 2003 suggested that rocks with the highest MgO content are probably located outside the current limit of the Pit #7. Further drilling is planned in early 2006 to define this new area. The rock is pale grey or white on fresh surfaces and pale buff on a weathered surfaces. A representative sample taken from this pit by the senior author assayed 16.93% MgO, 35.63% CaO, 1.7% SiO_2, 0.44% Al_2O_3, 0.7% Fe_2O_3, 0.03% Na_2O, 0.07% K_2O, 0.02% TiO_2, 0.03% P_2O_5, 0.04% MnO, 0.001% Cr_2O_3, 5 ppm Ni, 1 ppm Sc and 44.4% LOI. Based on this chemical analysis, the rock can best be described as calcitic dolomite. Pyrite, present in trace amounts, appears to be the main source of Fe_2O_3. The company uses this product to satisfy its in-house needs and is marketing this stone on the open market for a variety of applications. Most recent data point to higher MgO content and lower Fe_2O_3 content than previously reported. An analysis of a composite sample, consisting of 50 subsamples taken with an auto sampler on a 12 500 tonne barge load, assayed 18.04% MgO, 34.45% CaO, 0.07% SiO_2, 0.01% TiO_2, 0.31% Al_2O_3, 0.20% Fe_2O_3, 0.01% MnO, 0.01% Na_2O, 0.01% K_2O, 0.01% P_2O_5, 0.01% Ba and 46.59% LOI. According to the company, this sample also contained a dirty surface muck-pile, which may have contaminated the load. The material satisfies or exceeds requirements for a number of agricultural and environmental applications.



Figure 4. Quarry (Pit #7) on Texada Island, operated by the Ashgrove Cement Company.

GRAND FORKS DOLOMITE

Albrit Minerals and Materials Corp. owns a quarry (MINFILE 082ESE036) located 250 m north of Highway 3, just east of Morrissey Creek and approximately 4 km due east of Grand Forks, which in the past supplied dolomite for rock wool. A 30–60 m thick bed of biotite schist (mica gneiss) containing several 10–30 m thick lenses of dolomite extends eastward from Morrissey Creek along the base of a bluff for at least 488 m. The bed lies within high-grade metamorphic rocks of the Proterozoic and possibly Paleozoic Grand Forks gneiss. The bedding in a quarry just east of Morrissey Creek strikes 110° and dips 75°S. Across the creek to the west, a 30 m thick band of dolomitic limestone and overlying biotite-hornblende migmatite strike north and dip 30°W (Fishl, 1992).

The deposit comprises medium to coarse-grained (2–6 mm), brownish weathering white dolomite that contains scattered streaks and spots of light green to yellowish green serpentine, flakes of yellow to light brown phlogopite and vein-like bodies of feldspar. Other minor constituents include calcite, forsterite, diopside, spinel, anthophyllite, tremolite, biotite and apatite. A sample of randomly collected chips from the quarry east of Morrissey Creek contained 30.86% CaO, 20.69% MgO, 1.19% insoluble material, 0.98% R_2O_3, 0.49% Fe_2O_3, 0.039% MnO, 0.03% P_2O_5, 0.004% S and 46.20% LOI (McCammon, 1971). Dolomite reserves are estimated at 1 million tonnes (Gunter, 1984). These reserve estimates, however, are not compliant with National Instrument 43-101.

The dolomitic limestone west of Morrissey Creek is medium grained and white in colour. Chert beds are prominent within this unit. The limestone contains minor diopside, mica and serpentine. Dolomite and limestone were initially quarried here for building stone and lime as early as 1916. Ramshead Quarries Ltd. quarried the dolomite for building stone from 1968 to 1971. V.T.S. Quarry Ltd. performed some minor exploration work for agricultural lime in 1984. More recently, in the 1990s, the material was extracted by Roxul West International's predecessor for use in the Grand Forks insulation plant. The last assessment report from this property was produced by Caron (1998).

JEUNE LANDING DOLOMITE

A 30 m thick dolomite bed was reported near the village of Port Alice, in the same geological setting as the well-known limestone deposit called Jeune Landing (MINFILE 092L 151). No other geological data were available at the time of writing.

The project has the support of the Village of Port Alice Council. During its regular meeting of September 14, 2005, the council approved a motion to support Sechelt Industrial Minerals Corporation in establishing a dolomite quarry near Jeune Landing and request that the permit be expedited (Village of Port Alice, 2005).

Dolostone Occurrences on Vancouver Island and the Sunshine Coast

At first glance, dolomite resources along the west coast may appear to be limited. This is largely due to a regional geological setting that is not as favourable for dolomite exploration as that of eastern BC. An overwhelming focus on high-calcium carbonate during past exploration may also be a factor. For example, Mathews and McCammon (1957) highlighted at least two zones on Texada Island that they labelled as "chiefly magnesian limestone". Interestingly, their definition of 'magnesian limestone' included carbonate with MgO content of 4.79–19.15%. They also defined 'dolomitic limestone' as carbonate with MgO content in the range 19.15–21.86%. These definitions are not in line with modern terminology or even with the terminology of their

era, because 21.86% MgO corresponds to the stoichiometric composition of pure dolomite. It is therefore possible that a number of zones, other than those on Texada Island, with high exploration potential for dolomite may have been overlooked.

ANDERSON BAY (MINFILE 092F 088)

The Anderson Bay occurrence consists largely of a limestone-marble deposit. It is located just west of Anderson Bay on the southeast coast of Texada Island (Fig. 1). Marble was produced from several quarries until 1917.

A 37–60 m thick limestone bed of the Mississippian–Permian Buttle Lake Group extends northward for 1.7 km and is unconformably overlain by amygdaloidal basaltic flows of the Upper Triassic Karmutsen Formation (Vancouver Group), and underlain by mafic volcanic breccia, grey argillite and aphanitic volcanic rocks of the Paleozoic Sicker Group. Bedding strikes north to northwest and dips 30–60°W. The limestone bed pinches out to the south and is truncated to the north by a fault extending northwest from Anderson Bay (Fishl, 1992).

The deposit consists of coarse to fine-grained, white to reddish brown crinoidal limestone. The lower 12–15 m consists of white to pink crinoidal limestone that grades upward into 9–15 m of banded, pink to red crinoidal limestone containing some jasper. This is overlain by red and green tuffaceous limestone (Fishl, 1992).

Magnesian and high-calcium beds are found in the upper portion of the deposit. Lenticular masses of fine-grained pink dolomite veined with white calcite occur near the north end of the deposit. A sample from one of these lenses assayed 33.02% CaO, 16.20% MgO, 4.94% SiO_2, 0.85% Al_2O_3 and 1.56% Fe_2O_3 (Goudge, 1944). Four chip samples taken in succession across a total stratigraphic thickness of 53 m averaged 48.4% CaO, 2.8% MgO, 2.9% insoluble material, 1.7% R_2O_3, 0.92% Fe_2O_3, 0.065% MnO, 0.13% P_2O_5, 0.004% S and 42.95% LOI (Mathews and McCammon, 1957).

Two small quarries were opened in the early 1900s in this area. Nootka Quarries operated one quarry, 380 m northwest of the head of Anderson Bay. Continental Marble operated a second quarry about 540 m to the south. Until 1916, 96.7 tonnes (1265 cu. ft.) of marble were produced from this quarry for ornamental stone (Goudge, 1944).

SECHELT CARBONATE (MINFILE 092GNW031)

Dolomite and limestone are reported over a distance of 3 km in a northwest-trending pendant of metavolcanic and metasedimentary rocks of the Upper Triassic Karmutsen Formation (Roddick *et al.*, 1979) just northwest of Carlson Lake, 13 km east of Pender Harbour on the Sechelt Peninsula (Fig. 1). This pendant lies in diorite and quartz diorite of the Jurassic–Tertiary Coast Plutonic Complex. The beds within the pendant strike north and dip moderately to steeply east. The beds comprise mostly carbonate outcropping over widths in excess of 150 m with several amphibolite, skarn-altered metavolcanic rocks. They are cut by north-trending, steeply dipping andesitic to basaltic dikes.

The carbonate consists of fine to coarse-grained, white to medium grey, banded limestone and fine to medium-grained, massive to mottled dolomite. Minor to trace amounts of quartz, muscovite, serpentinite, diopside, olivine, talc, graphite and pyrite are present in the limestone. The dolomite contains minor chlorite and quartz, and is commonly cut by veins of dolomite and calcite. Ten composite samples collected from various limestone outcrops averaged 55.3% CaO, 0.5% MgO, 0.7% SiO_2, 0.2% R_2O_3 and 43.3% LOI (Wright Engineering Ltd., 1983; Candol Development Ltd., 1984). Assays of dolomite samples ranged from 16.8 to 20.0% MgO (Ditson, 1987).

Candol Development Ltd. carried out an extensive program of mapping, sampling and diamond drilling (1423 m) between 1983 and 1987. Drilling indicated a 30–80 m wide zone of dolomite at least 500 m long that is bounded to the west by limestone and to the east by an andesitic dike. The deposit is estimated to contain geological reserves of 3.5 million tonnes of dolomite averaging 19.2% MgO over an average width of 55 m, a strike length of 500 m and down to 50 m in depth (Ditson, 1988; Melville *et al*., 1992). These reserve estimates, however, predate National Instrument 43-101.

Additional investigations are described by Murphy (2003). Chemical analyses done independently by Ashgrove Cement Company confirmed the presence of dolomite but did not provide information about SiO_2, Al_2O_3, Fe_2O_3 or other potential impurities in the dolomite. The project is currently under environmental assessment and more information can be found at http://www.eao.gov.bc.ca/epic/output/html/deploy/epic_project_home_271.html. Results of the drilling in 2005 are not yet available.

CAMBRIAN CHIEFTAN DOLOMITE (MINFILE 092GNW054)

This occurrence is located 8.3 km northeast of the community of Garden Bay, near the old Cambrian Chieftan Mine (MINFILE 092GNW011) on the Sechelt Peninsula.

A dolomite lens lies in a northwest-trending roof pendant of volcanic and sedimentary rocks of the Upper Triassic Vancouver Group (probably Karmutsen and/or Quatsino formations) within diorite and quartz diorite of the Jurassic–Tertiary Coast Plutonic Complex. The sedimentary rocks strike due north and dip vertically to steeply east. They are cut by a few vertically dipping andesitic and dioritic porphyritic dikes that commonly strike 140°.

The dolomite lens is at least 311 m long and up to 37 m wide on the surface, averaging 30 m in exposed thickness. The lens is composed of white to grey, mottled crystalline dolomite containing epidote and calcite veinlets and sparse pyrite grains. Nine 4.5 kg samples randomly collected over the dolomite lens assayed 18.8–21.1% MgO, with an average MgO content of 19.8% (Bacon, 1957). Assays of six of these samples are found in Table 2 (Bacon, 1957), and show consistent CaO, MgO and SiO_2 contents.

TABLE 2. ANALYSES OF DOLOMITIC ROCKS FROM THE CAMBRIAN CHIEFTAN DEPOSIT (BACON, 1957

	Sample					
	1	2	3	4	5	6
CaO	32.3	31.5	33.1	31.7	30.6	30.9
MgO	19.3	20	18.8	20.1	21.1	20.7
SiO_2	3.3	5.1	3.4	3.4	2.1	2.9
R_2O_3	0.5	0.9	0.6	0.6	0.4	0.8
Fe_2O_3	0.6	0.6	0.4	0.4	0.4	0.5
H_2O at 105 C	0.1	0.1	0.1	0.1	0.2	0.1
Loss-on-ignition	44	41.9	43.5	43.6	45.1	44.2
Totals	**100.1**	**100.1**	**99.9**	**99.9**	**99.9**	**100.1**

A mass of thinly bedded, white to grey crystalline limestone outcrops just west of the dolomite lens. The north end hosts magnetite-chalcopyrite skarn zones that were sporadically mined as part of the Cambrian Chieftan deposit.

FREDERICK ARM (MINFILE 092K 136)

A 300 m wide band of limestone and dolomite enclosed in granitic rocks of the Jurassic–Tertiary Coastal Plutonic Complex extends northwestward from the west shore of Frederick Arm up the side of Treble Mountain (Fig. 1) for at least 800 m. The carbonate rocks strike 125° and dip vertically. The band is cut by fine-grained diabase dikes.

The carbonate is composed of bluish grey fine-grained limestone containing a few beds of white to yellowish white dolomite. In places, dolomite and pyrite grains are disseminated in the limestone. A chip sample across a 30 m section of limestone contained 48.52% CaO, 2.77% MgO, 5.92% SiO_2, 1.16% Al_2O_3, 0.50% Fe_2O_3 and 0.46% S (Goudge, 1944). A chip sample across a 3.7 m thick dolomitic bed on the west side of the carbonate deposit contained 32.78% CaO, 17.94% MgO, 2.60% SiO_2, 0.55% Al_2O_3, 0.46% Fe_2O_3 and 0.38% S (Goudge, 1944).

SMITH INLET (MINFILE 092M 008; 2005)

A band of limestone, hosted in granitic rocks of the Jurassic–Tertiary Coast Plutonic Complex, outcrops on both sides of Smith Inlet in the vicinity of Nalos Landing (Fig. 1). The limestone strikes 110° and dips nearly vertically to the northeast.

On the north side of the inlet, the limestone band is 700 m wide, continues inland for 800 m and is intruded by mafic dikes (Fishl, 1992). Medium to coarse-grained carbonate rocks consist of high-calcium limestone interbedded with dolomite that contains traces of disseminated pyrite (Fishl, 1992). Dolomite forms irregular masses, up to 7.6 m in diameter, within the limestone, which becomes more siliceous and dolomitic along the edges of the deposit (Fishl, 1992).

A sample taken across a 15 m width in the centre of the deposit on the north shore of the inlet contained 53.39% CaO, 1.14% MgO, 1.08% SiO_2, 0.02% Al_2O_3, 0.08% Fe_2O_3 and no S (Goudge, 1944). A sample of white dolomitic rock contained 32.48% CaO, 19.61% MgO, 0.058% SiO_2, 0.19% Al_2O_3, 0.09% Fe_2O_3 and no S (Goudge, 1944).

In 1929, two quarries were opened along the north shore of Smith Inlet by Coast Calcite Co. Ltd. Operations were suspended a short time afterward and no production figures are available.

ZEBALLOS DOLOMITE (MINFILE 092L 214) AND NOMASH RIVER

Limestone and dolomite are reported in the 900 crosscut of the Central Zeballos mine (MINFILE 092L 212), located 7 km northeast of the community of Zeballos and 110 km due west of the town of Campbell River (Fig. 1). The deposit lies within a discontinuous belt of limestone of the Upper Triassic Quatsino Formation that extends for 120 km from Quatsino Sound in a southeasterly direction to Tlupana Inlet. The belt is locally intruded along its southwestern flank by quartz diorite and granodiorite of the Jurassic Island Intrusions to the northeast. Underlying basaltic flows of the Upper Triassic Karmutsen Formation (Vancouver Group) outcrop to the northeast. The limestone strikes northwest and dips moderately southwest. The 900 crosscut is situated near the west end of a mass of medium to coarse-grained recrystallized limestone that extends westward from the Nomash River for 2000 m along the northern margin of a stock of granodiorite. The crosscut exposes grey calcium limestone intermingled with white dolomite and magnesian limestone. Most of the white carbonate is confined to a zone between 46 and 122 m from the portal. Laboratory studies indicate that the white carbonate comprises mostly dolomite with interstitial calcite (Stevenson, 1950). The dolomite and magnesian limestone occur as white streaks commonly ranging from a few centimetres to 10 m in thickness, the thickest being 21 m. These lenses may be the result of hydrothermal dolomitization. Stevenson (1950) reported that a white crystalline dolomitic limestone in the crosscut assayed 32.70% CaO, 19.6% MgO, 0.05 R_2O_3 and 1.1% insoluble material. Samples taken along a section of white carbonate between 57.9 and 85.3 m from the portal averaged 36.2% CaO, 17.0% MgO, 0.93% insoluble material and 0.28% R_2O_3 (Stevenson, 1950). Samples from a section of grey limestone between 182.9 and 201.2 m from the portal averaged 47.3% CaO, 7.26% MgO, 1.8% insoluble material and 0.25% R_2O_3 (Stevenson, 1950). Various grab samples were collected by Impact Resources Inc., the analyses of which are found in Table 3 (Econotech Services Ltd., 1981, 1982; Kent, 1989).

Dolomite reserves were estimated at several million tonnes (Econotech Services Ltd., 1981, 1982; Kent, 1989), but are not compliant with National Instrument 43-101.

Zones of garnet-diopside skarn, sometimes containing magnetite and sulphide minerals, are frequently formed along the intrusive contacts. The deposit was sampled in 1981 and diamond drilled in 1982 by Impact Resources, Inc.

When the property was visited in 2005, the adit was open and appeared to be in good condition (Fig. 5). The road that leads to the adit is overgrown but well preserved.

Stevenson (1950) also indicated that cream-coloured carbonate in a bed of the Nomash River, approximately 1.3 km upstream from the north fork of the Zeballos River, contains 35.00% CaO, 17.1% MgO, 0.76% R_2O_3 and 0.94 % insoluble material.

Two carbonate samples collected in 2005 from the mountain face, within 10 m of the portal, contain 0.75 and

TABLE 3. ANALYSES AND RESULTS OF BRIGHTNESS TESTS ON CARBONATE ROCKS COLLECTED BY IMPACT RESOURCES INC. FROM THE ZEBALLOS DOLOMITE (ECONOTECH SERVICES LTD., 1981, 1982)

	Sample			
	A	B	C	D
$CaCO_3$	87.9	61.95	61.2	93
$MgCO_3$	9.5	37.35	38.5	1.76
SiO_2	-	-	-	0.5
Insoluble material	2.6	0.78	-	-
H_2O	-	-	0.13	-
Brightness:				
Blue light	90.4	90.8	84.6	-
Green light	91.25	92.1	-	-
Unspecified	-	-	-	89.6

0.72% SiO_2, 0.03 and 0.08 Al_2O_3, 0.20 and 0.13% Fe_2O_3, 1.05 and 1.38% MgO, 1.05 and 1.38% MgO, 55.44 and 54.67% CaO, 0.02 and 0.02% Na_2O, 0.04 and 0.04% K_2O, 0.01 and 0.01% TiO_2, 0.02 and 0.08% P_2O_5, 0.001 and 0.001% Cr_2O_3, and 42.4 and 42.8% LOI, indicating that they are limestone in composition.

Other Dolomite Occurrences Along the Coast

A number of dolomite occurrences were also described along the north coast of BC. All other factors being equal, however, these deposits become less economically viable with increasing distance from the market. The descriptions provided below indicate that at least some of these occurrences are worth following up. Refer to Roddick (1970a, b) for local and regional geology.

CLAXTON (MINFILE 103J 033)

The area is underlain by Permian–Triassic feldspathic schist with a northerly trend and 80°W dip. A large dolomitic deposit is reported to occur 300 m from the water at Claxton, 24.0 km south of Prince Rupert. A sample contained 41.9% $MgCO_3$ (Fishl, 1992).

BANKS ISLAND (L.797, MINFILE 103H 062)

A 180 m wide band of white coarse-grained limestone and dolomite outcrops on Lot 797 on the east coast of Banks Island, 2.5 km south of Gale Point. The bed is contained in a roof pendant of gneissic diorite and migmatite within granodiorite of the Coast Plutonic Complex. The deposit strikes 125° and dips steeply to the northeast. Numerous inclusions of country rock are present along the northeastern edge of the band. Sinuous quartzite fragments are sometimes found floating in the limestone. The dolomite commonly contains veins of white quartz (Goudge, 1944).

BANKS ISLAND (L.2224, MINFILE 103H 039)

A 180 m thick, bed of limestone that strikes 130–140° and dips steeply outcrops on Lot 2224 on the north coast of Banks Island, 12 km northwest of Keecha Point. The limestone lies within quartz diorite of the Coast Plutonic Complex. It contains interbeds of schist that become numerous toward the edges of the deposit. The bed consists of erratically intermingled, white high-calcium limestone and dolomite. The dolomite occurs as thin beds to large lenses that become more frequent near the margins of the bed. A chip sample taken across 30 m of high-calcium limestone contained 54.56% CaO, 0.72% MgO, 0.24% SiO_2, 0.18% Al_2O_3, 0.07% Fe_2O_3 and no S, while a sample across a 9 m thick dolomite lens contained 31.84% CaO, 20.77% MgO, 0.24% SiO_2, 0.08% Al_2O_3, 0.23% Fe_2O_3 and trace S (Goudge, 1944).

LIMESTONE BAY (MINFILE 103H 038)

A 240–300 m wide band of limestone outcrops on Despair Point on the northeast coast of Banks Island and continues in a southeasterly direction for 1.2 km. The band is in contact with gneissic diorite and migmatite to the northwest and quartz diorite to the west. The limestone strikes 100° and dips vertically. It is occasionally split into two bands by quartzite mineralized with pyrrhotite and banded silicified schist.



Figure 5. Adit at Zeballos Dolomite was open during the visit in 2005.

The deposit comprises mostly white coarse-grained limestone and minor grey medium-grained limestone with irregular interbeds and masses of dolomite. A 15.2 m chip sample taken across light grey limestone on the northeast side of the deposit contained 52.80% CaO, 0.85% MgO, 1.66% SiO_2, 0.53% Al_2O_3, 0.20% Fe_2O_3 and 0.03% S, while a sample taken across a 4.6 m thick bed of coarse-grained white dolomite near the southwest edge of the deposit contained 31.72% CaO, 20.62% MgO, 0.78% SiO_2, 0.15% Al_2O_3, 0.08% Fe_2O_3 and no S (Goudge, 1944).

EXPLORATION GUIDELINES

In general, exploration programs for industrial minerals that have relatively low unit value ($/tonne) are not justified, unless they are backed by conceptual and market studies. In certain circumstances, large established companies incorporate extra properties into their portfolios for strategic reasons. Such properties are important in strategic planning and typically offer material of exceptional grade and are located near low-cost transportation corridors. The motivation to hold such properties is to ensure the long-term supplies of raw materials for established or captive markets, or to tie up the deposit to limit potential competition. Long-term holding of such undeveloped resources is, however, not an option for junior companies or individual prospectors, who cannot afford to cover the cost of maintaining the property in good standing for several decades.

Knowledge of the specifications of dolomite currently on the market is necessary for the design of new exploration programs. Material from the new deposits should match or exceed current consumer specifications. In most applications, dolomite is considered a low-cost material; therefore, deposits that do not require processing other than crushing and milling are preferred. Mineralogy and physical proper-

ties of the final product are extremely important, especially where dolomite is expected to be used as a filler or extender.

The proximity of the deposit to the market is essential, unless it is adjacent to low-cost transportation corridors, such as the one provided by barging along the west coast of British Columbia.

The distinction between sedimentary-diagenetic and hydrothermal origins of dolomite formation provides important clues to the geological potential of any given area on the conceptual or grassroots exploration level, when looking for world-class dolomite deposits. In the areas where dolomitization appears erratic or limited to a specific, narrow stratigraphic horizon and where detailed geological maps are not available, the best starting points for exploration are the investigation of known dolomite occurrences, followed by tracing or projecting dolomitic rocks along stratigraphic or structural controls into geographic areas with the best possible existing infrastructure.

The acid test, in conjunction with the use of non-toxic heavy liquid or staining, provides fast reconnaissance-level information in exploration for magnesite (Simandl *et al.*, 1993). It can also be applied to other carbonate minerals, such as dolomite. Shortwave infrared spectroscopy was successfully used to distinguish dolomite from magnesite-rich rocks (Thompson and Simandl, 2004), and the same method may reflect variations in magnesium content within the calcite-dolomite range of carbonate rocks. Beyond the reconnaissance stage, there is still no substitute for chemical analyses, especially if material is required for its magnesia content rather than its physical properties.

If the carbonate rock was metamorphosed, the presence of diagnostic metamorphic minerals, such as forsterite, tremolite, diopside and talc, can indicate the presence of a magnesium component in marble, but the concentration of these minerals is not directly proportional to magnesium content because it also depends on other parameters.

Methods used in advanced stages of exploration must match the needs dictated by field conditions and other factors. They are best handled by a specialist and are outside the scope of this paper.

CONCLUSION

The best geological potential for dolomite appears to be in southeastern British Columbia, where thick uniform beds of dolomitic rocks are common. Since dolomite competes with magnesite in a number of markets, it is important to recognize that southeastern BC is also known for important magnesite resources, including the world-class Mount Brussilof magnesite mine, the only magnesite producer in Canada.

There are only three active operations in BC producing dolomitic rock. Coastal areas of southern BC have moderate geological potential to host a world-class, high-grade dolomite deposit, but their potential to host mid-sized dolomite deposits that can sustain a production level in the 50 000 to 100 000 tonnes of dolomite per year is excellent. There is no formal market study regarding dolomite in BC, but the development of deposits located along the coast is economically favourable because of low-cost transportation to potential markets in the Pacific Northwest of the United States. Recent requests from potential American dolomite consumers suggest that the market in Washington State alone is large enough to accommodate a new mid-size BC-based coastal dolomite producer. New glass and fibreglass plants are expected to begin production in the Seattle area within a year.

One of the known dolomite occurrences in southwestern BC (such as those listed in this paper) or another favourably located dolomite occurrence may become a new dolomite supplier on west coast of BC. Texada Island is well known for its high-calcium limestone resources; however, its potential in terms of 'dolomite-type' resources is probably underestimated.

If no new potential producer is identified in southwestern BC, areas further north along the coast (*e.g.*, Banks Island) should be further explored for dolomite. Unfortunately, transportation costs from northwestern BC to the west coast of United States will be higher than from the southwestern part of the province, resulting in a higher delivered price, and consequently lower number of potential industrial users in the US Pacific Northwest.

ACKNOWLEDGMENTS

George Walton from Camosun College, Victoria and Laura Simandl of St. Margaret's School, Victoria provided field assistance.

REFERENCES

Anonymous (1972): New Dolomite White Mining Ltd.; *Financial Post Survey of Mines 1972*, page214.

Bacon, W.R. (1957): Geology of Lower Jervis Inlet, British Columbia; *BC Ministry of Energy, Mines and Petroleum Resources,* Bulletin 39, 45 pages.

Boulton A.S., Simandl G.J., Hamilton, W.N. and Dixon Edwards, W.A. (2001): Cordilleran transect: Calgary, Alberta to Victoria, British Columbia; *BC Ministry of Energy, Mines and Petroleum Resources*, 37th Forum on the Geology of Industrial Minerals, Field Trip #5 Guidebook, 26 pages.

British Columbia Ministry of Mines and Petroleum Resources (1965): Annual Report 1964; *BC Ministry of Energy, Mines and Petroleum Resources*, page 184.

Candol Development Ltd. (1984): Prospectus; *BC Ministry of Energy, Mines and Petroleum Resources*, Property File 092GNW031.

Caron, L. (1998): Grand Forks dolomite and silica quarries: updated mine plan, geology and reserve estimate; *BC Ministry of Energy, Mines and Petroleum Resources*, Assessment Report 25684, 29 pages.

Carr, D.D. Rooney, L.F. and Freas, C. (1994): Limestone and dolomite; D.D. Carr, Chief Editor, Industrial Minerals and Rocks, 6th Edition; Society for Mining, Metallurgy, and Petroleum Exploration, Inc., pages 605-630.

Crossley, P. (2003): Opportunities in energetic growth markets propel the glass fibre industry onwards, as minerals suppliers face up to changing batch formulations; *Industrial Minerals*, No 425, pages 34–41.

Coope, B. (2004): Magnesium metal — sources, processes and markets; *in* Proceedings of 37th Annual Forum on Industrial Minerals, With Emphasis on Western North America; G.J. Simandl, W.J. McMillan and N.D. Robinson, Editors, *BC Ministry of Energy, Mines and Petroleum Resources*, Paper 2004-2, pages 51–56.

Davies, G.R. (1996): Hydrothermal dolomite (HTD) reservoir facies, global perspectives on tectonic-structural and temporal linkage between MVT and SEDEX Pb-Zn ore bodies, and subsurface HTD reservoir facies; short course notes pre-

pared by Graham Davies Geological Consultants, *Canadian Society of Petroleum Geologists*, 167 pages.

Ditson, C. (1987): Geological, geochemical and drilling report on the Plain property; *BC Ministry of Energy, Mines and Petroleum Resources*, Assessment Report 15593, 27 pages.

Dunham, R.J. (1962): Classification of carbonate rocks according to depositional texture; *in* Classification of Carbonate Rocks, Hamm, W.E, Editor, *American Association of Petroleum Geologists*, Memoir 1, pages 108–121.

Econotech Services Ltd. (1981): Sample evaluation results, April 28, 1981; *BC Ministry of Energy, Mines and Petroleum Resources*, Property File 092L 214.

Econotech Services Ltd. (1982): Letter to R.F. Kent, June 22, 1982; *BC Ministry of Energy, Mines and Petroleum Resources*, Property File 092L 214.

Fishl, P.S. (1992): Limestone and dolomite resources of British Columbia; *BC Ministry of Energy, Mines and Petroleum Resources*, Open File 1992-18, 150 pages.

Folk, R.L. (1959): Practical petrographic classification of limestones; *Bulletin of the American Association Petroleum Geologists*, Volume 43, pages 1–38.

Folk, R. L. (1962): Spectral subdivisions of limestone types; *in* Classification of Carbonate Rocks, Hamm, W.E, Editor, *American Association of Petroleum Geologists*, Memoir 1, pages 62–85.

Goldberg, R.J. and Wehrung, J.M. (1981): Analysis of two talc samples by SEM, EDXA; consultant report to W.R. Barnes Company Ltd., Waterdown, Ontario, 18 pages.

Goudge, M.F. (1944): Limestones of Canada: their occurrence and characteristics, Part V, Western Canada; *Canada Department of Mines and Resources, Mines and Geology Branch*, Report 811, 233 pages.

Gunter, R. (1984): Beaver, Beaver 3; *BC Ministry of Energy, Mines and Petroleum Resources*, Assessment Report 13176, 13 pages.

Harben, P.W. and Kuzvart, M. (1996): Industrial Minerals — A Global Geology; *Industrial Minerals Information Ltd.*, 462 pages.

Kent, R.F. (1989): Letter to Peter Fischl with assays by Calcium Carbonate Company, December 17, 1989; *BC Ministry of Energy, Mines and Petroleum Resources*, Property File 092L 214.

McCammon, J.W. (1971): Ramshead quarries; *in* Geology, Exploration and Mining in BC 1970, *BC Ministry of Energy, Mines and Petroleum Resources*, pages 491–492.

Leach, D.L, and Sangster, D.F. (1993): Mississippi Valley – type lead-zinc deposits; *in* Mineral Deposit Modelling, Kirkham, R.V., Sinclair, W.D., Thorpe, R.I. and Duke, J.M., Editors, *Geological Association of Canada*, Special Paper 40, pages 289–314.

Machel H.G. (2004): Concepts and models of dolomitization: a critical paper; *in* The Geometry and Petrogenesis of Dolomite Hydrocarbon Reservoirs, Braithwaite, C.J.R., Rizzi, G. and Darke, G., Editors, *Geological Society*, London, Special Publication 235, pages 7–63.

Mathews, W.H. and McCammon, J.W. (1957): Calcareous deposits of southwestern British Columbia; *BC Ministry of Energy, Mines and Petroleum Resources*, Bulletin 40, 155 pages.

McCammon, J.W. (1972): Dolo; *in* Geology, Exploration and Mining in BC 1971, *BC Ministry of Energy, Mines and Petroleum Resources*, page 456.

Melville, D.M., Faulkner, E.L, Meyers, R.E., Wilton, H.P. and Malott, M-L. (1992): 1991 producers and potential producers, mineral and coal; *BC Ministry of Energy, Mines and Petroleum Resources*, Open File 1992-1, scale 1:2 500 000.

MINFILE (2005): MINFILE BC mineral deposits database; *BC Ministry of Energy, Mines and Petroleum Resources*, <http://www.em.gov.bc.ca/mining/Geolsurv/ Minfile/> [Nov 2005]

Moore, P. (2002): Dolomite value reflected in glass; *Industrial Minerals,* no 422, pages 22–32.

Murphy, K.G. (2003): Report on the limestone and dolomite potential of the central Sechelt Peninsula; *BC Ministry of Energy, Mines and Petroleum Resources*, Assessment Report 27095, 23 pages.

Roddick, J.A. (1970a): Douglas Channel – Hecate Strait map-area, British Columbia; *Geological Survey of Canada*, Paper 70-41, 56 pages.

Roddick, J.A. (1970b): Douglas Channel – Hecate Strait map-area, British Columbia; *Geological Survey of Canada*, Map 23-1970, scale 1:250 000.

Roddick, J.A., Woodsworth, G.J. and Hutchinson, W.W. (1979): Geology of Vancouver west half and mainland part of Alberni, British Columbia; *Geological Survey of Canada*, Open File 611, scale 1: 125 000.

Simandl, G.J. (2004): Magnesite and related opportunities in British Columbia, Canada; *in* Proceedings of 37th Annual Forum on Industrial Minerals, With Emphasis on Western North America, Simandl, G.J., McMillan, W.J., and Robinson, N.D., Editors, *BC Ministry of Energy, Mines and Petroleum Resources*, Paper 2004-2, pages 57–60.

Simandl, G.J. and Hancock K.D. (1996): Magnesite in British Columbia, Canada: a neglected resource; *Mineral Industry International*, No 1030, pages 33–44.

Simandl, G.J., Hancock, K.D., Paradis, S. and Simandl, J. (1993): Field identification of magnesite-bearing rocks using sodium polytungstate; *CIM Bulletin*, no 966, pages 68–72.

Stanley, S.M., Ries, J.B. and Hardie, L.A. (2002): Low-magnesium calcite produced by coralline algae in seawater of Late Cretaceous composition; *Proceedings of the National Academy of Sciences of the United States of America*, Volume 99, pages 15323–16326.

Stevenson, J.S. (1950): Geology and mineral deposits of the Zeballos mining camp, British Columbia; *BC Ministry of Energy, Mines and Petroleum Resources*, Bulletin 27, 145 pages.

Strohmenger, C. and Wirsing, G. (1991): A proposed extension of Folk's (1959, 1962) textural classification of carbonate rocks; Carbonate and Evaporites, Volume 6, pages 23–28.

Thompson, A. and Simandl, G.J. (2004): Short-wave infrared spectroscopy (SWIR) in magnesite exploration; *in* Proceedings of 37th Annual Forum on Industrial Minerals, With Emphasis on Western North America, Simandl, G.J., McMillan W.J. and Robinson, N.D., Editors, *BC Ministry of Energy, Mines and Petroleum Resources*, Paper 2004-2, pages 77–80.

Village of Port Alice (2005): Sechelt Industrial – Dolomite Quarry 318/05; *in* Village of Port Alice, minutes of the Regular Council Meeting; September 14, 2005, 6 pages <http://www.portalice.ca/pdf/050914%20-Reg.pdf> [Dec 2005].

Wright Engineering Ltd. (1983): Candol Development Ltd. — Sechelt mineral claims primary report; *BC Ministry of Energy, Mines and Petroleum Resources*, Property File 092GNW 031, 8 pages.

Kimberlite and Diamond Indicator Minerals in Northeastern British Columbia: A Reconnaissance Survey

by G.J. Simandl, T. Ferbey, V.M. Levson, N.D. Robinson, R. Lane, R. Smith[1], T.E. Demchuk, I.M. Raudsepp[2] and A.S. Hickin

KEYWORDS: diamond, kimberlite, lamproite, indicator minerals, exploration potential, G10, G11, G12, garnet, Cr-spinel, Cr-diopside, ilmenite, olivine

EXECUTIVE SUMMARY

Northeastern British Columbia is underlain by Precambrian basement that belongs to the North American craton (Fig. 1). It has diamond exploration potential, particularly if the modified 'diamondiferous mantle root model' is considered (Simandl, 2004). This heavy mineral reconnaissance project expands on an earlier study, which was restricted to kimberlite indicator minerals (KIMs) present in Late Pleistocene glaciofluvial sands and gravels sampled in the Fort Nelson region (Levson *et al.*, 2004; Simandl *et al.*, 2005). A variety of media were sampled and tested during this study, including bedrock and regolith of partially consolidated conglomerates of the Dunvegan Formation, active river or stream sediments, and glaciofluvial or glaciolacustrine deposits. Of the 58 samples processed, 38 contain KIMs, such as purple pyrope garnet, Cr-diopside, olivine, ilmenite or spinel. In contrast with the earlier study, no eclogitic garnets were recovered. At least a portion of the KIMs recovered from these samples may be derived from local igneous sources or from secondary or tertiary sources that originated by weathering, transportation and natural preconcentration of protolith-derived constituents. The fact that the Dunvegan Formation contains Cr-spinel, but no other indicator minerals, is noteworthy. The chemical composition of some of these spinels is suggestive of a lamproite/kimberlite provenance.

Concentrations of KIMs located east of the maximum extent of the Laurentide glaciation, as delineated by Mathews (1980; Fig. 2), may have been locally derived and reworked or brought into the region from the Northwest Territories and Alberta by Late Pleistocene glacial and/or glaciofluvial systems. Samples from the Etsho Plateau area yield a wide spectrum and relatively high concentration of potential kimberlite indicator minerals. Follow-up sampling in this area is warranted.

[1]*Geological Survey of Canada, Calgary, AB*

[2]*Department of Earth and Ocean Sciences, University of British Columbia, Vancouver, BC*

This publication is also available, free of charge, as colour digital files in Adobe Acrobat PDF format from the BC Ministry of Energy, Mines and Petroleum Resources internet website at http://www.em.gov.bc.ca/Mining/Geolsurv/Publications/catalog/catfldwk.htm

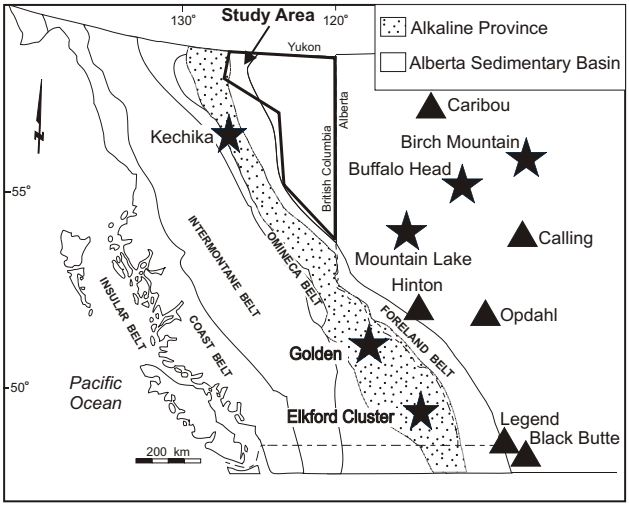


Figure 1. Location of the study area; corresponds approximately to BC's portion of the Western Canada Basin. Known primary (star) and secondary (triangle) diamond occurrences in BC and Alberta are also shown. The Crossing Creek diatreme, within the Elkford Cluster, is the only confirmed kimberlite in BC (*modified from* Simandl, 2004).

Samples NEBC-1, 7, 23, 43 and 44 are noteworthy because of their high concentrations of Cr-spinels (chromites). Some of these spinels have the same chemical characteristics as chromites that plot within the diamond inclusion field. Samples NEBC-1 and 7 are active river sediments, and upstream prospecting is justified.

An intriguing, but problematic, aspect of this study is the recovery of a diamond during the processing of sample NEBC-11, which did not contain any indicator minerals. This stone is a clear diamond nearly 0.8 mm in size (Fig. 3). Because of its size and colourless nature, the diamond may have been lodged within the screen during the processing for an unspecified number of samples without being detected by the laboratory personnel. If the diamond did not belong to sample NEBC-11, as suggested by a lack of associated KIMs, it may have come from any of the samples that were processed prior to it, or from samples belonging to the previous client. Ten BC Geological Survey samples, numbered NEBC-1 to 10, were processed before sample NEBC-11. Several of these samples did contain KIMs.

BACKGROUND

Northeastern BC is an underexplored portion of the North American continent with respect to diamonds, other

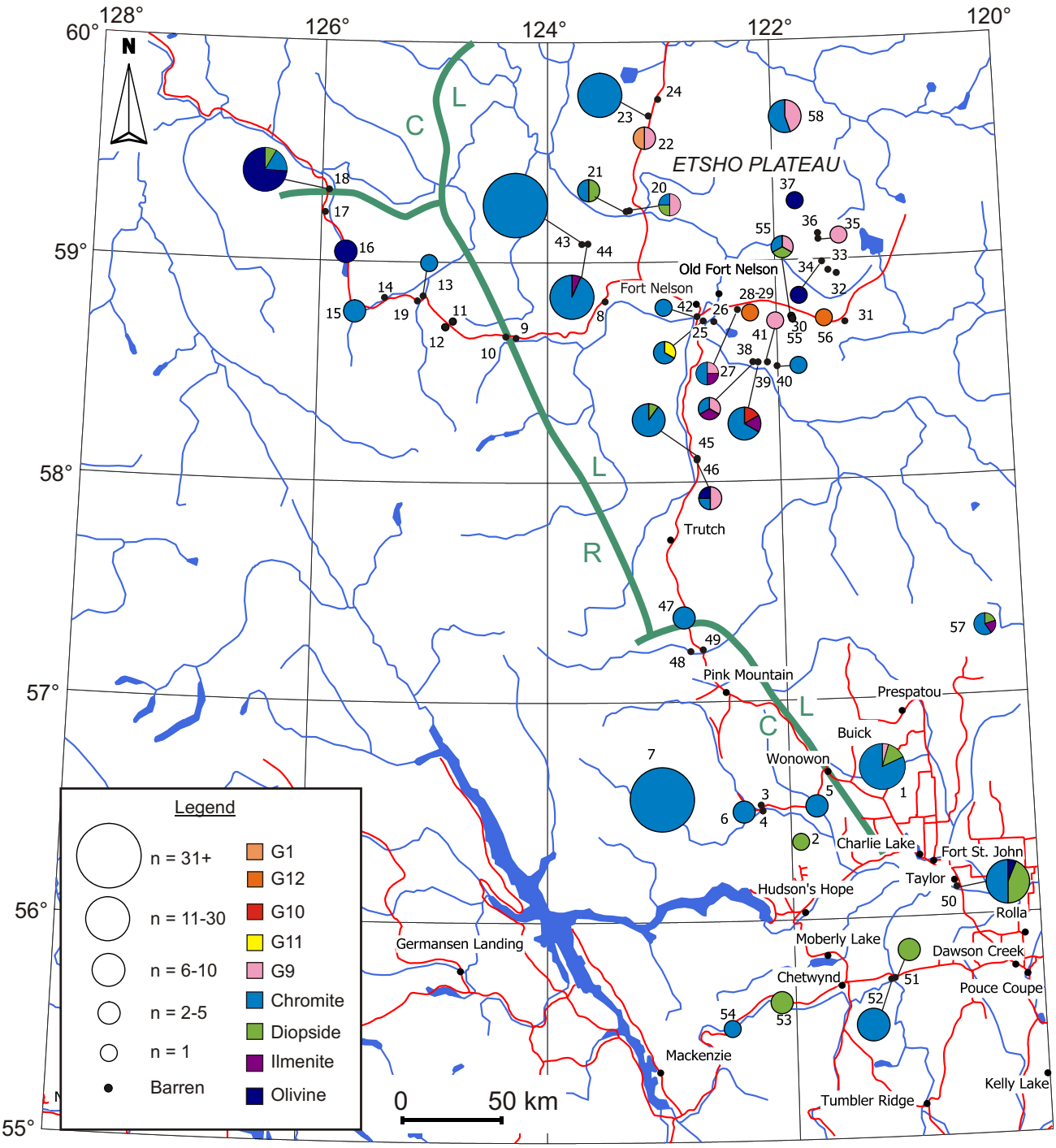


Figure 2. Location of glaciofluvial, stream sediment and bedrock samples. The circle diameter is proportional to the number of indicator mineral grains. Colours correspond to specific kimberlite indicator minerals (KIMs). The green line separates the glacial systems: L - Laurentide glacial system; C - Cordilleran glacial system; R - Rocky Mountain glacial system.

gemstones and non-energy minerals. It is characterized by low relief and has a rapidly developing infrastructure, which supports the oil and gas industry. High-quality diamonds are presently mined within the Slave Craton of the Northwest Territories (Carlson *et al.*, 1999; Lockhart *et al.*, 2004), approximately 600 km northeast of Fort Nelson. Diamond deposits have also been discovered in the Buffalo Head Terrane in neighbouring Alberta (Eccles *et al.*, 2004; Hood and McCandless, 2004), approximately 400 km southeast of the Fort Nelson area. Several alluvial diamond occurrences have also been reported in the Northwest Territories and in Alberta (Simandl, 2004). There are reports of diamond occurrences within the BC Alkaline Province (Northcote, 1983a, b; Anonymous, 1994; McCallum, 1994; Pell, 1994; Allan, 1999, 2002; Roberts, 2002). Recent dating (Simandl and Davis, 2005) indicates that Precambrian crystalline basement similar in age to the Buffalo Head Terrane extends farther west than previously ex-

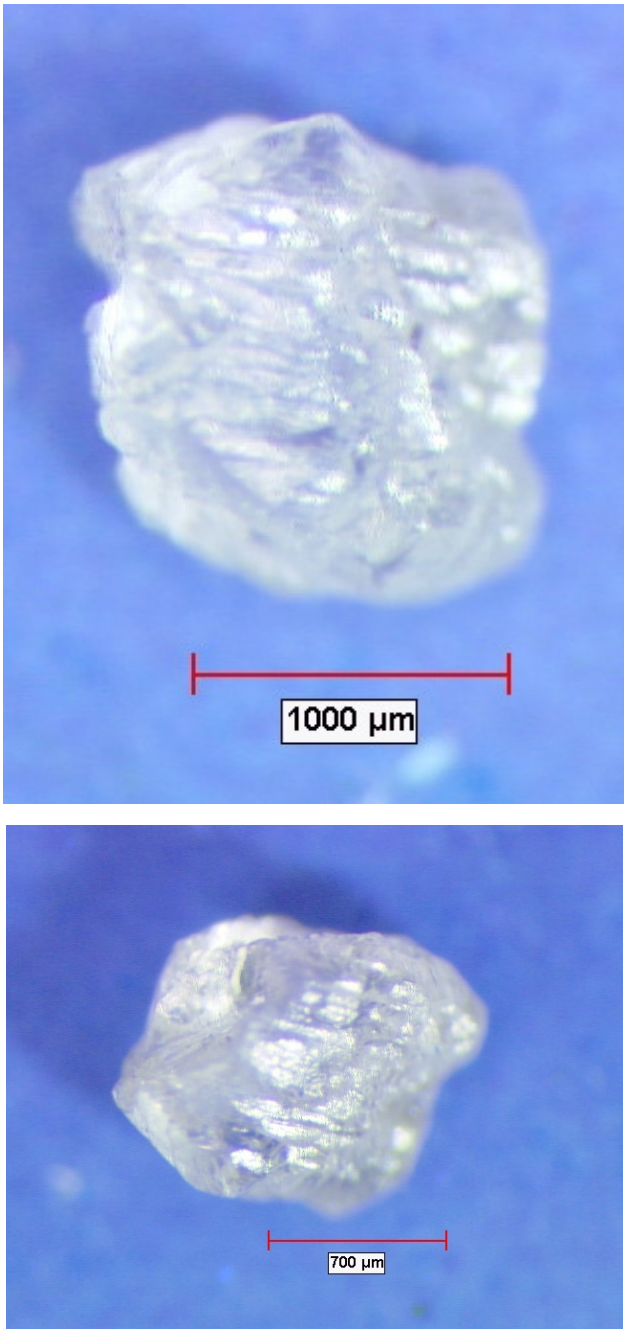


Figure 3: Colourless diamond identified in the heavy mineral concentrate of sample NEBC-11. There is a distinct possibility that this diamond was derived from samples processed prior to sample NEBC-11 or may have come from samples belonging to a previous client (contamination). See sections "Diamond and Fluorite" and "Discussion and Recommendations" for possible implications of this find on diamond exploration in northeastern BC.

pected, supporting the hypothesis that northeastern BC may have been underlain by a thick cold lithosphere prior to rifting of the Rodinia Supercontinent. The diamondiferous root, as described by Haggerty (1986) and Mitchell (1991), may have been destroyed after the diamonds were brought to the surface by kimberlites, lamproites or other diamond elevators (Simandl, 2004). The results of this heavy mineral reconnaissance/orientation survey, when considered in conjunction with the findings of a previous KIM study (Simandl *et al.*, 2005), provide support for the use of the diamondiferous mantle root exploration model in northeastern BC.

BEDROCK GEOLOGY, POTENTIAL DIAMOND ELEVATORS AND THEIR AGE

Northeastern BC is underlain by a Precambrian basement that belongs to the North American craton (Hoffman, 1988, 1989, 1991; Ross *et al.*, 1991, 1995; Villeneuve *et al.*, 1993; Simandl and Davis, 2005). Traditionally, northeastern BC was regarded as being 'too close to the edge' of the continent to apply the diamondiferous mantle root concept; however, recent dating indicates that Precambrian crystalline basement of similar age as the Buffalo Head Terrane extends farther west than was previously thought (Simandl and Davis, 2005).

The Precambrian basement in northeastern BC is overlain by a thick sedimentary sequence. Outcropping in the study area are major stratigraphic elements of this sedimentary package: the Toad and Grayling formations (Triassic, 208–245 Ma) the Wapiti Formation (Upper Cretaceous, 65–97 Ma), the Fort St. John Group or Smokey Group (Cretaceous, 65–145.6 Ma), the Dunvegan Formation (Upper Cretaceous, 65–97 Ma), the Sikanni Formation of the Fort St. John Group (Cretaceous, 65–145.6 Ma) and Kotaneelee Formation (Upper Cretaceous, 65–97 Ma), in a compilation by Massey *et al.* (2005). The Fort Nelson area is underlain predominantly by marine shales of the Shaftsbury Formation, part of the Lower Cretaceous Fort St. John Group. These shales are interpreted to have been deposited in a prodelta or shelf environment during a transgression of an embayment in the Cretaceous (Thompson, 1977).

Directly overlying the Fort St. John Group and forming the resistive cap of the Etsho Plateau are sandstones of the Dunvegan Formation of the Upper Cretaceous Smokey Group. These sandstones are part of an assemblage of clastic rocks that range texturally from clay-rich shales and mudstones to boulder conglomerates. The contact between the Dunvegan and Shaftsbury formations is gradational and consists of sandy siltstones and fine-grained sandstones interbedded with silty shales (Thompson, 1977; Stott, 1982). The stratigraphy and sedimentology of the Dunvegan Formation have been discussed in detail by Plint *et al.* (2001), Plint (2002) and Plint and Wadsworth (2003).

There are no known kimberlite or lamproite occurrences in the study area. The closest examples of extensive alkaline volcanic activity are in the Lac de Gras area (Northwest Territories), the Buffalo Head Hills area (Alberta) and BC's Alkaline Province. Most kimberlite pipes in the Northwest Territories were emplaced between 45 and 75 Ma (Lockhart *et al.*, 2004). In northern Alberta, the radiometric ages of kimberlite emplacement range from 70.3 ±1.6 to 88 ±5 Ma (Eccles *et al.,* 2004). The known radiometric ages of lamprophyres, lamproites and kimberlites within BC's Alkaline Province vary from 391 ±12 Ma for the HP pipe to 240 to 250 Ma for the Cross kimberlite (Smith *et al.*,1988; Pell, 1994) and are older than sedimentary rocks that outcrop in northeastern BC. It is possible that pipes of similar ages to those of the Lac de Gras and Buffalo Head Hills areas cut sedimentary units of comparable or older ages in northeastern BC. It is also possible that the

pyroclastic material ejected from craters or eroded from the pipes was incorporated into the sedimentary sequence.

This is the first report substantiating that indicator minerals may occur in the sedimentary rocks of northeastern BC. The presence of indicator minerals within the outcropping sedimentary sequence may complicate the interpretation of KIM anomalies in surficial materials; however, if confirmed, this report will provide invaluable information for the exploration of possible secondary (placer) diamond targets.

SURFICIAL GEOLOGY

Quaternary History

A recent account of the glacial history of the North American continent is provided by Dyke (2004). For detailed information regarding the Quaternary geology of portions of northeastern BC and the surrounding areas, the reader is referred to Smith *et al.* (1988), Bednarski (1999, 2000, 2001), Levson *et al.* (2004) and Plouffe *et al.* (2004). The text that follows is a simplified glacial history of northeastern BC, with emphasis on aspects directly related to diamond exploration using glacial or glaciofluvial deposits.

According to Mathews (1980), three glacial systems (*i.e.*, the Laurentide, Rocky Mountain and Cordilleran) coexisted in northeastern BC during the last glaciation. During the Late Pleistocene, the Laurentide ice sheet advanced westward up the regional slope into northeastern BC. Its western boundary with the Rocky Mountain and Cordilleran glacial systems is approximated on Figure 2. Most, if not all, of the region was covered by ice during the last glacial maximum. The configuration of late glacial ice fronts and lobes is indicated by cross-cutting relationships observed in large-scale landforms (*e.g.*, flutes, crag and tails, recessional moraines, etc.). Although the Laurentide ice sheet generally moved into the region from the east and northeast, its advance was not uniform. Differing orientations of these landforms suggest that multiple ice-flow events occurred in the region during the Late Wisconsinan and that ice lobes were active during the later stages of glaciation. During the eastward retreat of the Laurentide ice sheet, numerous meltwater channels, flowing towards the west, incised the landscape. Glacial lakes commonly developed along the ice margin, as drainage down the regional slope to the east was blocked by ice (Mathews, 1980).

Based on clast lithologies, glacial deposits within the study area can be divided into three groups. The first group of deposits were those affected by the Laurentide system during the last glacial advance, east of Mathews' line (Fig. 2). These deposits contain a variety of rock types and are characterized by the presence of pink granitic and gneissic clasts that originated within the Canadian Shield. Deposits affected by the Cordilleran system, west of Mathews' line, are characterized by grey granite fragments, quartzite/sandstone pebbles and boulders, and schist and slate clasts. The deposits that were affected by the Rocky Mountain system are characterized by fragments and pebbles of locally derived sedimentary rocks including chert, quartzite, limestone, dolomite, shale and minor diabase. These areas are devoid of pebbles of either Cordilleran or shield-derived plutonic rocks (Mathews, 1980).

SAMPLE LOCATION AND COLLECTION

The 58 samples analyzed for this study were collected across northeastern BC, from as far as 200 km west of Muncho Lake Park to 350 km south of Dawson Creek (Fig. 2). These samples were collected during the 2004 field season and included material from modern stream and river deposits, and glaciofluvial sand and gravel deposits.

The spatial distribution of the glaciofluvial samples was affected by the scarcity of glaciofluvial material in the region and accessibility constraints. This material was collected from vertical exposures in gravel pits, trenches and roadcuts. Samples of modern stream or river sediments were, in most cases, collected upstream from bridges or where river valleys were easily accessed from nearby roads. Sample weights typically ranged from 15 to 30 kg, but some samples were over 40 kg. The samples were sieved in the field to exclude clasts greater than 4 mm. Sample depths were typically 20 to 50 cm below surface and samples were collected from undisturbed material.

Samples from modern river and stream sediments were collected from fluvial systems that drain significant basins. These systems may have incorporated indicator minerals from primary diamond deposits, till, glaciofluvial and glaciolacustrine deposits, or sedimentary bedrock. In samples where KIMs are present, it is expected that river and stream sediment samples will have higher counts of KIMs relative to till samples, as flowing water will tend to naturally preconcentrate heavy minerals. Modern stream or river sediments are particularly useful sample media for assessing the potential of inaccessible areas within well-defined topography and catchment areas.

Information on the samples collected for this study is summarized in Table 1. Clast lithologies are provided for samples that contained pebble and cobble-sized clasts only. This information is important to establish the provenance of the sediments that host the KIMs. The clasts were invariably well-rounded, with the exception of clasts of shales or locally derived sediments. Samples that did not contain any clasts are described as sand-sized or clay-rich material. The table also lists the type and frequency of grains that were confirmed to be potential KIMs, based on their chemical composition.

Samples NEBC-23 and 43 must be considered separately. The former was sampled from a regolith derived from a conglomerate facies of the Dunvegan Formation, whereas the latter was sampled from lithified Dunvegan Formation conglomerate.

Figure 4 summarizes the sample processing procedure. A 500 g sample split was taken from the original sample and archived prior to processing by SGS Lakefield Research Limited's laboratory. Each sample was then wet-screened at 20 and 60 mesh. The +20 mesh material and approximately 500 g of the -60 mesh material were dried and stored. The -20+60 mesh fraction was further concentrated using the Wilfley table and the tail fractions were dried and stored. The concentrates were subjected to heavy liquid separation (methylene iodide at 3.1 g/cm^3) followed by dry screening (35 mesh) and magnetic separation by hand-magnet and Frantz electromagnetic separator.

Using a binocular microscope, the mineral concentrates were picked for diamond indicator mineral species. All picked indicator minerals were put into standard 1-inch polished grain mounts and returned to the BC Ministry of

TABLE 1. SAMPLE DESCRIPTION, LOCATION AND KIMBERLITE INDICATOR MINERAL (KIM) SUMMARY. KEY: DIOP=DIOPSIDE, ILM=ILMENITE, CHR=CHROMITE, OL=OLIVINE, GN=GNEISS, GR=GRANITE, SH=SHALE, LS=LIMESTONE, SS=SANDSTONE, CL=CLAY, CONGL=CONGLOMERATE, UMF=ULTRAMAFIC, CB=CRYSTALLINE BASEMENT, SED=SEDIMENTARY, QTZ=QUARTZITE, CH=CHERT, SI=SILTSTONE, IS=IRONSTONE, MAF=MAFIC, (P)=PINK, (G)=GREY, >=GREATER THAN, >=MUCH GREATER THAN, COMMAS INDICATE SIMILAR ABUNDANCES.

					KIMs									
Sample Number	UTM - Northing	UTM - Easting	Composition of Clasts	Sample Type	G10	G9	G11	G1	G12	Cr Diop	Ilm	Chr	Ol	Total
NEBC-01	6282870	608712	ss/si > gr (p), gn (p), ls, is	River		1				3		18		22
NEBC-02	6264810	575052	ss > sh > gr > gr gn > umf > ch > maf	River						1				1
NEBC-03	6262791	546990	sand-sized material	River										0
NEBC-04	6262536	547022	ss > ls > sh > is	River										0
NEBC-05	6265576	573653	ss >> ls, sh > is > gr	Stream								4		4
NEBC-06	6297889	522801	mainly sed	Stream								2		2
NEBC-07	6304336	520920	ss >> sh, ls > ch, congl	River								71		71
NEBC-08	6520367	471424	ss, si > gr > sh > ch, gn	Pit										0
NEBC-09	6502598	426083	ss >> ls > congl	River										0
NEBC-10	6503318	420959	ss >> ls > sh, ch	Pit										0
NEBC-11	6508859	390131	ls > ss > ch > sh	Pit										0
NEBC-12	6501947	400528	ls > ss > ch	Pit										0
NEBC-13	6524807	379408	ls, ss, sh > qtz > ch > maf	Pit								1		1
NEBC-14	6524322	359904	ls >> sh, ch, ss > congl, qtz	Flood Plain										0
NEBC-15	6518192	344777	ls >> maf, ss, sh, (g)	Pit								2		2
NEBC-16	6548532	340361	ls >> ss, qtz, ch	Pit									5	5
NEBC-17	6568296	330650	cl (clay-rich)	River										0
NEBC-18	6579659	332851	ls >> ss, si, sh > gr	River						2		4	17	23
NEBC-19	6522313	376458	ls > qtz > sh, gn > ch > maf	Flood Plain (River)										0
NEBC-20	6566238	484386	gn >> maf > qtz, sh	Pit		2				1		1		4
NEBC-21	6565844	482724	gr gn >> qtz, ss > is	Pit						1		1		2
NEBC-22	6603120	492464	qtz, ss, gn	Pit		1		1						2
NEBC-23	6614075	494595	congl, ls, ss, sh >> qtz > gn	pit, Dunvegan Fm, regolith								25		25
NEBC-24	6622371	499465	ss, sh > gr gn > qtz	Pit										0
NEBC-25	6510030	520870	gn (p) > qtz > gr > ch	Pit			1					2		3
NEBC-26	6509616	526229	gr gn >> qtz > sh	Stream										0
NEBC-27	6515567	538244	gn > qtz > sh, ss	Roadcut		1					1	2		4
NEBC-28	6514501	544774	ss, cb (p)	Pit					1					1
NEBC-29	6514501	544774	ss, cb (p)	Pit										0
NEBC-30	6512127	565471	gn (p), qtz > maf, umf	Pit										0
NEBC-31	6509051	592514	cb (p)	Trench										0
NEBC-32	6533569	588526	gr gn >> qtz	Pit										0
NEBC-33	6535231	584300	cl (clay-rich)	Surface										0
NEBC-34	6539551	581206	cb (p) > sh	Pit									1	1
NEBC-35	6551005	579502	sand-sized material	Stream		1								1
NEBC-36	6553888	578755	cb (p)	Stream										0
NEBC-37	6570249	567872	cb (p)	Small Pit									1	1
NEBC-38	6489088	545698	gr (p) > qtz > maf	Pit		1					1	1		3
NEBC-39	6488921	548332	cb (p)	Esker	1						1	4		6
NEBC-40	6486881	557911	sand-sized material	Pit								1		1
NEBC-41	6488850	553059	cb (p)	Pit		1								1
NEBC-42	6512245	517785	cb (p)	Pit								1		1
NEBC-43	6549892	460825	ch, congl, ss > qtz	pit, Dunvegan Fm, hard rock								37		37
NEBC-44	6549887	461981	congl, sh > 70% >> cb (p)	Stream							2	25		27
NEBC-45	6440574	516839	gn (p) > gn (g) > ss > maf, sh > is, congl	Stream						1		9		10
NEBC-46	6439810	516735	cb (p) > ss	Pit		2						1	1	4
NEBC-47	6360037	509264	ss, ls > sh > gr gn >> maf	River								3		3
NEBC-48	6342957	512200	ls+sh > 97%	Pit										0
NEBC-49	6343737	518469	ss >> is	River										0
NEBC-50	6222613	645018	ss > sh > qtz > is > gr gn (p)	Stream						7		8	1	16
NEBC-51	6176752	613163	qtz/ss >> 70% > congl, is > gr	Pit						2				2
NEBC-52	6176129	611299	ss, sh > is > maf >> gr (p)	River								8		8
NEBC-53	6165753	556133	ss > sh > ls, congl >> is	River						2				2
NEBC-54	6152653	530479	qtz > ls >> sh, is, maf	Stream								1		1
NEBC-55	6510906	565930	gr (p), qtz	Pit		1				1	1			3
NEBC-56	6539487	581232	gr (p), qtz	Pit					1					1
NEBC-57	6354768	661877	gr (p), qtz	Pit						1	1	3		5
NEBC-58	6612910	564017	gr (p), qtz	Pit		4						5		9
Total Indicators					1	15	1	1	2	22	7	240	26	315

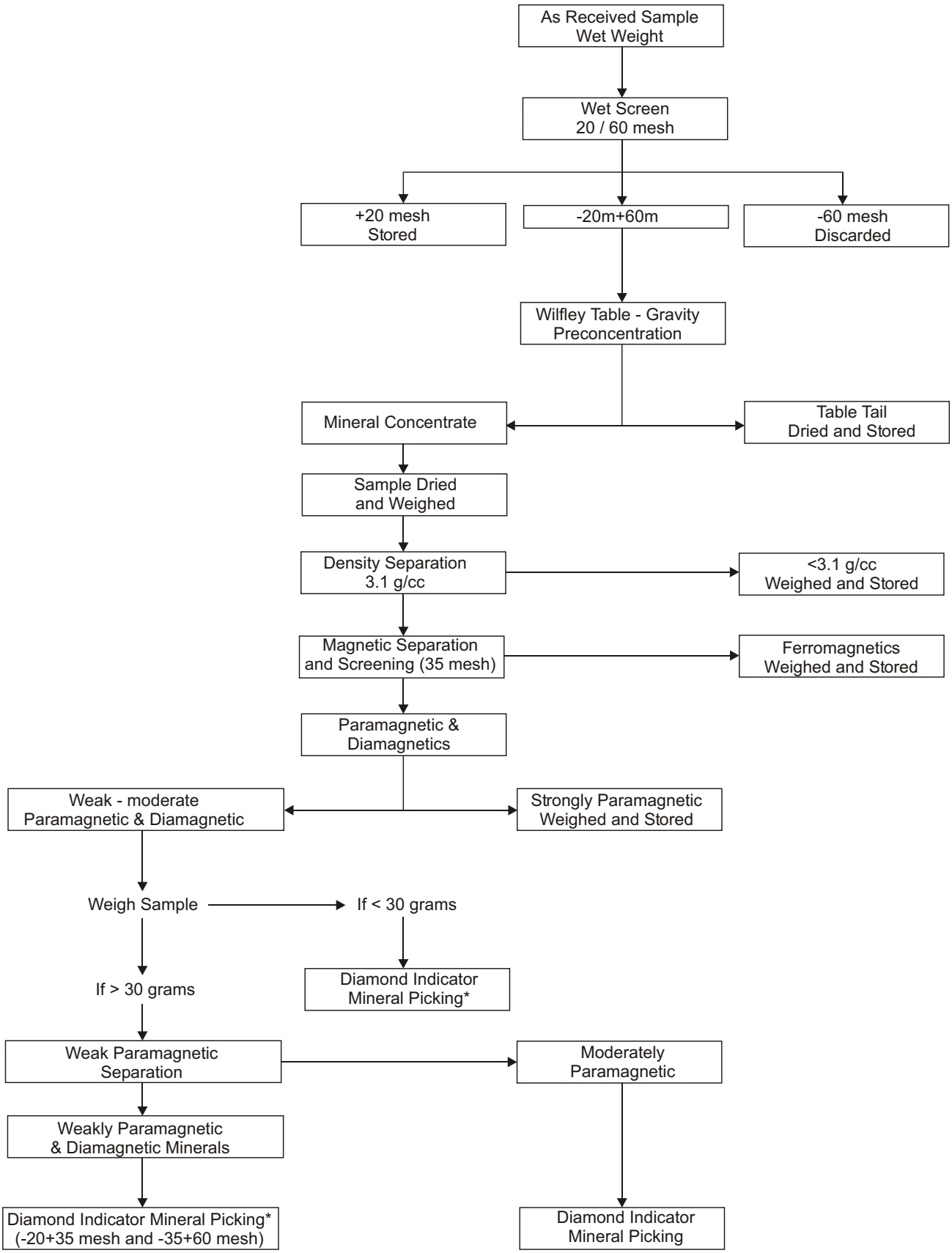


Figure 4. Diamond indicator mineral extraction flow sheet. * indicates primary diamond indicator mineral fraction. Source: SGS Lakefield Research Limited.

Energy, Mines and Petroleum Resources. Microprobe analyses were then conducted on these mounts by M. Raudsepp at the University of British Columbia to determine the major element composition of the visually picked mineral grains. Chemical composition of mineral grains is required to determine if a mineral is a diamond or kimberlite indicator.

In total, 381 mineral grains were subjected to microprobe analyses. Of these, 315 grains were identified as potential KIMs. The locations of sample sites and number of KIM grains at each site are provided in Figure 2 and Table 1.

INTERPRETATION OF MICROPROBE ANALYSES

Interpretation of the data from northeastern BC is more complex than from areas such as Lac de Gras (NWT) or Buffalo Head Hills because sediments in northeastern BC contain clinopyroxenes, olivines and chromites with chemical compositions that may not be unique to kimberlites or lamproites. For example Cr-spinel can be also derived from Alaskan intrusions, ophiolites, boninites, xenoliths within alkali basalts, or from other lithologies typical of BC's Alkaline Province. Of the 58 samples collected for this study, 38 contain potential KIMs. Of these, 28 contain more than one indicator mineral variety and often more than one grain of each. The following section presents microprobe data on visually picked minerals and includes a discussion of the KIMs identified in this study.

Garnet

Mantle-derived garnet is considered to be the most important kimberlite and diamond indicator mineral. The two most recent studies on garnet classification and interpretation are those of Schulze (2003) and Grütter *et al.* (2004). Methods presented in these studies are very effective in distinguishing pyrope, eclogitic and crustal garnets. The key elements used to identify and interpret mantle-derived garnets, and to estimate the diamond potential of an area or individual pipe, are Cr, Ca, Mg, Fe, Ti and Na.

In this paper, different garnet species are classified in accordance with the method described by Grütter *et al*. (2004). This scheme divides garnets into 12 categories (G1 to G12). Of these, harzburgitic (G10), lherzolitic (G9), pyroxenitic, websteritic and eclogitic garnets (G4, G5 and G3) are commonly associated with diamonds. Wehrlitic garnets are referred to as G12, low-chromium megacrysts as G1, and titanium-rich peridotitic varieties as G11. The garnets that do not fit any of the 12 categories, including crustal garnets, are referred to as G0. The scheme is in part empirical; it was tested on a large dataset and is robust.

The results of the microprobe analyses of the hand-picked garnets, using the classification method outlined by Grütter *et al.* (2004), are provided in Table 2. The locations of garnet-bearing samples identified in this study are presented in Figure 2. Of the 21 garnets visually picked and analyzed, at least 20 can be considered as KIMs. There is one G10 garnet (sample NEBC-39). Fifteen of the mantle-derived garnets are lherzolitic (G9), two are wehrlitic (G12), one is a G11 and one is a G1 garnet (Fig. 5). Eclogitic (G3) garnets were previously reported from this area by Simandl *et al.* (2005); however, no eclogitic garnets were picked in this study. Follow-up picking is required to confirm the lack of eclogitic garnets. Kelyphitic rims were not observed on any of the visually picked garnets, and some garnets did have an orange-peel texture, suggesting that they were subject to some degree of transport, or at least local reworking, after being liberated from their host rock.

Clinopyroxene

Chrome-bearing, green to bright green clinopyroxenes are typically easy to visually identify in heavy mineral concentrates and can be associated with diamonds. For these reasons, clinopyroxenes are considered effective KIMs. Unfortunately, clinopyroxenes with similar characteristics to those present in kimberlitic rocks are also found in a variety of ultramafic rocks, such as ophiolitic-layered intrusions, Alaskan-type intrusions and basalt-hosted xenoliths. Consequently, microprobe analyses are required to differentiate kimberlite-related clinopyroxene grains from those associated with other lithologies, and clinopyroxene is therefore considered a less significant KIM than garnet or ilmenite. The chemical compositions of the 24 clinopyroxene grains that were visually picked from concentrates are provided in Table 3.

All of the clinopyroxenes, except one (a clinoenstatite), plot within the kimberlite indicator field on the Quirt (2004) Wo-En-Fs diagram. The Mg numbers [100*Mg^{2+}/(Mg^{2+}+Fe^{2+})] of these clinopyroxenes vary from 85.42 to 93.33 with an average higher than 90 (Table 3). Cr-diopside grains with an Mg number greater than 88 are likely to be from mantle peridotite, particularly if they have elevated Cr_2O_3 levels (> 0.5 wt %), as do most of the grains analyzed.

The Cr_2O_3-Al_2O_3 discrimination plot of Ramsey and Tompkins (1994) and the Cr_2O_3-CaO plot of Fipke *et al.* (1989) were used to further refine this interpretation. Globally, most clinopyroxenes found as solid inclusions or intergrowths in and/or with diamond, plot in the on-craton garnet-peridotite field seen in Figure 6, but clinopyroxenes plotting in the off-craton garnet peridotite and spinel peridotite field are also recovered from kimberlite concentrates. On the Cr_2O_3-CaO plot (Fig. 7), with the exception of three grains, all the clinopyroxenes visually picked from heavy mineral concentrates plot within the field representative of diopsides found as inclusions in diamonds. If the Cr-Al-Na ternary diagram of Morris *et al.* (2002) is consid-

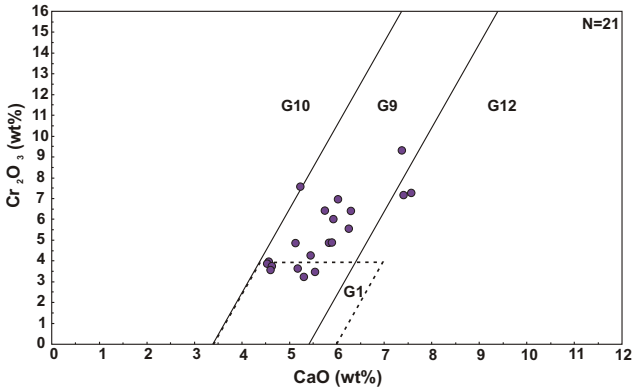


Figure 5. Garnet Cr_2O_3-CaO discrimination plot. One grain plots in the G10 field, and 15 plot within the G9 field. Fields from Gurney and Moore (1994) and Grütter et al. (2004).

TABLE 2. CHEMICAL COMPOSITION OF GARNETS; FOR SAMPLE LOCATIONS SEE TABLE 1 AND FIGURE 2.

Sample ID	UTM Northing	UTM Easting	Na_2O	MgO	Al_2O_3	SiO_2	CaO	TiO_2	Cr_2O_3	MnO	FeO	Total	Garnet Type
NEBC-1	6282870	608712	0.01	19.10	19.59	41.10	6.29	0.02	6.41	0.44	7.58	100.55	G9
NEBC-20	6566238	484386	0.02	19.50	20.49	41.05	5.87	0.00	4.89	0.43	8.29	100.55	G9
NEBC-20	6566238	484386	0.02	20.01	20.83	41.10	5.45	0.05	4.26	0.41	8.51	100.65	G9
NEBC-22	6603120	492464	0.07	20.83	19.38	41.73	5.16	1.00	3.64	0.29	8.04	100.14	G1
NEBC-22	6603120	492464	0.04	19.70	20.65	41.36	5.13	0.11	4.85	0.38	8.66	100.90	G9
NEBC-25	6510030	520870	0.05	20.45	18.23	41.63	5.74	0.63	6.44	0.23	7.03	100.43	G11
NEBC-27	6515567	538244	0.02	19.62	19.81	41.09	6.26	0.05	5.56	0.35	8.00	100.74	G9
NEBC-28	6514501	544774	0.00	18.38	18.32	40.57	7.40	0.00	7.18	0.41	8.27	100.53	G12
NEBC-35	6551005	579502	0.04	20.32	20.72	41.62	5.86	0.01	4.88	0.38	7.09	100.89	G9
NEBC-38	6489088	545698	0.03	20.23	21.42	41.19	5.55	0.01	3.47	0.41	8.07	100.39	G9
NEBC-39	6488921	548332	0.05	20.10	18.42	40.74	5.24	0.30	7.57	0.39	7.58	100.39	G10
NEBC-41	6488850	553059	0.03	19.87	18.77	41.10	6.01	0.09	6.96	0.35	8.37	101.55	G9
NEBC-46	6439810	516735	0.02	19.50	19.05	41.38	5.92	0.16	6.01	0.32	7.79	100.14	G9
NEBC-46	6439810	516735	0.01	19.85	21.82	40.87	5.30	0.03	3.25	0.33	8.03	99.50	G9
NEBC-55	6510906	565930	0.02	17.74	16.62	40.04	7.36	0.06	9.32	0.42	7.47	99.06	G9
NEBC-56	6539487	581232	0.01	16.94	18.62	40.94	7.57	0.01	7.28	0.57	8.50	100.44	G12
NEBC-58	6612910	564017	0.06	20.74	20.98	41.53	4.56	0.28	3.96	0.29	7.84	100.24	G9
NEBC-58	6612910	564017	0.06	20.66	21.15	41.64	4.60	0.29	3.58	0.39	7.93	100.30	G9
NEBC-58	6612910	564017	0.05	20.85	21.10	41.29	4.54	0.26	3.85	0.30	7.58	99.82	G9
NEBC-58	6612910	564017	0.06	20.78	21.01	42.15	4.62	0.31	3.77	0.36	7.54	100.60	G9

TABLE 3. COMPOSITION AND MG# OF CLINOPYROXENES (CR-DIOPSIDES); FOR SAMPLE LOCATIONS SEE TABLE 1 AND FIGURE 2.

Sample ID	UTM Northing	UTM Easting	Na_2O	MgO	Al_2O_3	SiO_2	K_2O	CaO	TiO_2	Cr_2O_3	MnO	FeO	Total	Mg #
NEBC-1	6282870	608712	1.21	15.80	6.17	51.31	0.00	20.91	0.30	0.83	0.03	2.79	99.36	0.909978
NEBC-1	6282870	608712	1.85	15.16	7.29	51.70	0.01	19.74	0.43	0.71	0.06	3.01	99.96	0.89966
NEBC-1	6282870	608712	1.41	15.68	6.17	51.34	0.00	20.74	0.26	1.05	0.07	2.74	99.45	0.910806
NEBC-2	6264810	575052	0.16	17.83	1.16	53.32	0.02	23.22	0.10	0.92	0.14	2.90	99.76	0.916483
NEBC-18	6579659	332851	1.44	15.78	6.45	51.27	0.00	19.57	0.42	1.10	0.10	2.71	98.85	0.912209
NEBC-18	6579659	332851	0.16	18.04	0.84	53.55	0.00	22.89	0.13	0.45	0.07	2.89	99.01	0.917638
NEBC-20	6566238	484386	0.70	16.79	1.11	53.13	0.00	22.13	0.03	0.74	0.20	3.55	98.38	0.893889
NEBC-21	6565844	482724	0.70	16.31	1.54	53.56	0.00	22.50	0.06	0.51	0.08	3.91	99.18	0.881399
NEBC-45	6440574	516839	0.45	15.94	2.80	51.96	0.00	22.37	0.16	0.77	0.13	4.85	99.43	0.854281
NEBC-45	6440574	516839	1.44	16.08	6.63	51.17	0.00	19.50	0.38	1.04	0.13	3.19	99.57	0.899722
NEBC-50	6222613	645018	0.16	17.74	1.48	53.24	0.00	23.19	0.12	0.65	0.09	3.03	99.70	0.912654
NEBC-50	6222613	645018	1.64	15.65	6.71	50.99	0.00	19.53	0.46	0.64	0.09	3.10	98.81	0.900126
NEBC-50	6222613	645018	0.47	17.31	3.43	52.52	0.01	21.98	0.01	1.11	0.02	2.21	99.06	0.93332
NEBC-50	6222613	645018	1.50	15.11	7.00	50.95	0.00	20.42	0.35	1.00	0.10	2.61	99.04	0.911777
NEBC-50	6222613	645018	1.24	15.82	5.79	51.91	0.00	21.37	0.36	0.96	0.09	2.79	100.33	0.910081
NEBC-50	6222613	645018	1.18	16.91	4.91	52.43	0.01	20.25	0.13	1.36	0.05	2.74	99.97	0.916749
NEBC-50	6222613	645018	1.55	15.55	6.20	51.41	0.00	20.65	0.30	1.07	0.12	2.48	99.32	0.917881
NEBC-51	6176752	613163	1.47	16.30	7.13	50.98	0.01	18.68	0.37	0.84	0.05	3.36	99.18	0.896459
NEBC-51	6176752	613163	1.38	15.85	5.89	51.72	0.01	20.81	0.26	1.22	0.09	2.56	99.80	0.91698
NEBC-52	6176129	611299	0.11	33.40	4.80	54.15	0.01	0.64	0.09	0.31	0.14	6.50	100.15	0.901617
NEBC-53	6165753	556133	1.29	15.87	6.79	50.79	0.00	19.54	0.42	0.77	0.13	3.19	98.79	0.898615
NEBC-53	6165753	556133	1.65	15.17	6.98	51.02	0.00	19.87	0.62	0.94	0.09	2.73	99.08	0.908319
NEBC-56	6539487	581232	0.31	17.36	2.03	51.55	0.00	21.81	0.30	0.85	0.14	4.47	98.82	0.873772
NEBC-57	6354768	661877	0.69	16.87	1.90	53.36	0.00	22.63	0.15	0.92	0.07	3.10	99.70	0.906524

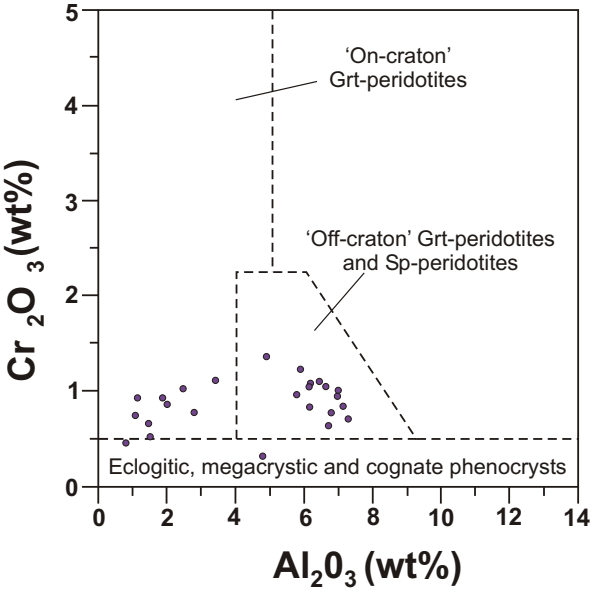


Figure 6. Clinopyroxene Cr_2O_3-Al_2O_3 discrimination plot (*after* Ramsey and Tompkins, 1994). Eight of the grains from this study plot within the on-craton field, further refining interpretations based on the Mg number. Fourteen grains plot within the spinel peridotite and off–craton garnet peridotite fields. Two grains have Cr_2O_3 content below 0.5 wt% and plot within the field of 'eclogitic, megacrystic and cognate phenocrysts.'

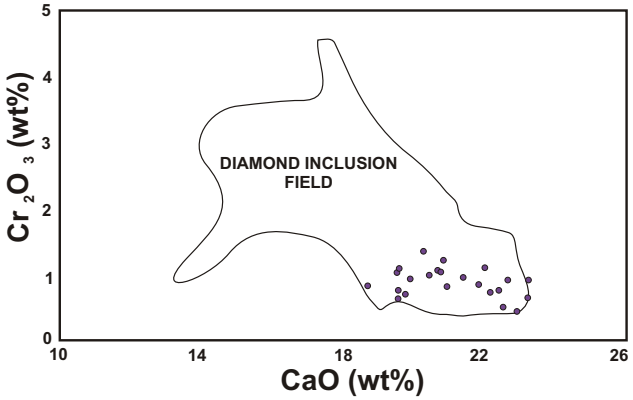


Figure 7. Clinopyroxene Cr_2O_3-CaO plot. The outlined field represents the composition of clinopyroxenes found as inclusions in diamonds (Fipke *et al.*, 1989).

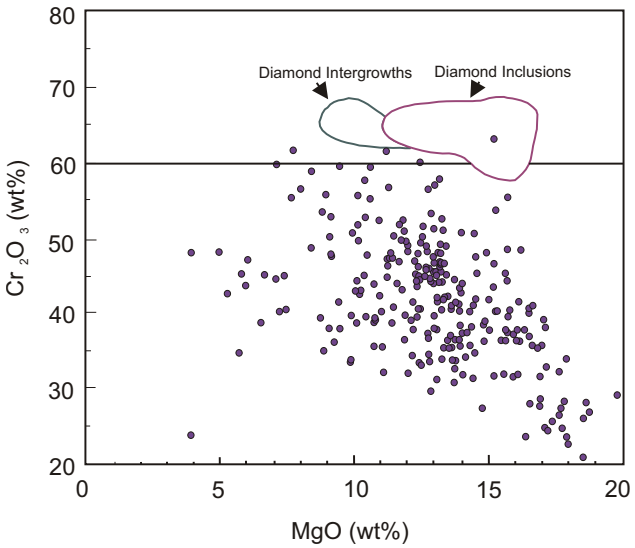


Figure 8. Cr-spinels, Cr_2O_3-MgO diagram. Most of the grains appear to follow the peridotite trend and five of these grains have Cr_2O_3 content of 60 wt% or more. Compositions of spinels found as intergrowths with or inclusions in diamonds from Fipke *et al.* (1989).

ered, only one of the clinopyroxenes plot within the Cr-diopside field for kimberlite xenoliths and xenocrysts; however, when this discrimination plot is applied to parts of the world other than Ontario, it achieves only limited success (Quirt, 2004, Fig. 10B). If the Na-Ca-Cr-Fe diagram of Thorleifson *et al.* (1994) and Quirt (2004) is considered, depending on the plot, about half of the diopsides from northeastern BC would be peridotitic. Normally, Cr-diopsides do not carry as much weight as garnets during the interpretation of heavy mineral data; however, if clinopyroxene of appropriate chemical composition occurs in the same sample with other indicators such as pyrope or ilmenite (or at least in the same geographic area as G9 or G10), it is appropriate to consider it as a full-fledged KIM. A detailed investigation that leads to the Cr-diopside interpretation is underway and it will be published as a separate document. For the purpose of this study, all the clinopyroxenes listed in Table 3 are considered KIMs.

Spinel

As with Cr-diopside, the distinction of kimberlite-related spinels from spinels derived from other sources is not straightforward. Spinels are found in a variety of settings, including layered intrusions, Alaskan-type intrusions, ophiolites, xenoliths within alkali basalts, and boninites. Of the 275 Cr-spinels (chromite) grains picked, 240 grains can be considered as potential KIMs based on their chemical composition. These chromite grains consist mainly of Al_2O_3 (4.70–36.26%), Cr_2O_3 (29.15–62.91%), FeO (13.22–44.45%) and MgO (3.91–19.77%). Smaller constituents are TiO_2 (<4.89%), MnO (<1.74%), NiO (<0.47%) and SiO_2 (<0.30%). The chemical analyses of potential KIM chromite grains can be found in Table 4.

The majority of these grains appear to follow the peridotite trend (Fig. 8). Five of the grains have high chrome content (>60% Cr_2O_3) and an appropriate MgO content to fit the compositional fields of chromite inclusions in diamonds. On the TiO_2 versus 100[Cr/(Cr+Al)] diagram (Fig. 9), the majority of the chromites plot within the garnet peridotite field and at least 16 grains have compositions compatible with chromites found as inclusions in diamonds. To further improve the discrimination between kimberlite-related spinels and spinels from a variety of other sources, additional criteria were selected based on the database of spinels published by Barnes and Roeder (2001, 2004) and other factors, such as the grain-size of spinels from a variety of non-kimberlite/lamproite environments (Grütter and Apter, 1998; McCandless and Dummett, 2003). Details of this enhanced interpretation method will be published as a separate paper, but the results are already incorporated into the current interpretation (Fig. 2). Samples NEBC-1, 7, 23, 43 and 44 contain 18, 71, 25, 37 and 25 chromites, respectively. Sample NEBC-1 also contains Cr-diopside and a G9 garnet, and sample NEBC-44 contains ilmenite that has an appropriate chemical composition to be

TABLE 4. CHEMICAL COMPOSITION OF Cr-SPINELS (CHROMITES); FOR SAMPLE LOCATIONS SEE TABLE 1 AND FIGURE 2 .

Sample ID	UTM Northing	UTM Easting	MgO	Al_2O_3	SiO_2	CaO	TiO_2	V_2O_3	Cr_2O_3	MnO	FeO	NiO	Nb_2O_5	Ta_2O_5	Total
NEBC-1	6282870	608712	12.48	30.72	0.06	0.00	0.56	0.12	33.15	0.09	21.70	0.10	0.05	0.00	99.03
NEBC-1	6282870	608712	9.10	19.06	0.10	0.00	0.25	0.08	47.76	0.00	20.72	0.11	0.00	0.00	97.18
NEBC-1	6282870	608712	14.29	30.05	0.03	0.01	0.12	0.15	35.70	0.03	18.59	0.20	0.02	0.00	99.18
NEBC-1	6282870	608712	19.77	29.97	0.10	0.00	0.27	0.11	29.15	0.15	19.21	0.25	0.00	0.00	98.97
NEBC-1	6282870	608712	12.34	13.07	0.17	0.01	2.65	0.00	46.01	0.03	24.68	0.16	0.00	0.00	99.13
NEBC-1	6282870	608712	7.11	8.24	0.06	0.00	0.04	0.30	59.60	0.16	22.93	0.00	0.00	0.00	98.44
NEBC-1	6282870	608712	8.80	10.11	0.07	0.01	0.10	0.15	53.27	0.04	25.93	0.10	0.00	0.00	98.57
NEBC-1	6282870	608712	9.87	19.45	0.09	0.00	1.02	0.27	39.62	0.19	27.81	0.23	0.04	0.00	98.58
NEBC-1	6282870	608712	9.43	9.35	0.07	0.02	0.04	0.19	59.32	0.01	20.48	0.03	0.05	0.00	98.98
NEBC-1	6282870	608712	15.54	35.36	0.09	0.02	0.16	0.19	31.93	0.04	16.51	0.21	0.03	0.00	100.08
NEBC-1	6282870	608712	5.26	19.11	0.04	0.00	0.32	0.14	42.54	0.04	30.83	0.10	0.08	0.00	98.46
NEBC-1	6282870	608712	11.67	15.16	0.06	0.02	0.07	0.20	51.67	0.00	20.44	0.15	0.00	0.00	99.45
NEBC-1	6282870	608712	3.91	16.75	0.09	0.00	0.09	0.24	47.91	0.00	29.73	0.02	0.00	0.00	98.73
NEBC-1	6282870	608712	15.76	25.98	0.11	0.01	0.60	0.17	40.30	0.00	16.28	0.24	0.03	0.00	99.47
NEBC-1	6282870	608712	10.72	24.24	0.04	0.01	0.70	0.16	35.58	0.09	27.11	0.23	0.00	0.00	98.88
NEBC-1	6282870	608712	12.91	24.67	0.06	0.01	0.13	0.17	43.84	0.00	18.04	0.04	0.09	0.00	99.96
NEBC-1	6282870	608712	10.06	20.08	0.05	0.00	1.22	0.21	38.64	0.00	28.11	0.20	0.00	0.00	98.57
NEBC-1	6282870	608712	13.93	23.93	0.03	0.00	0.04	0.22	43.43	0.03	17.58	0.16	0.00	0.00	99.35
NEBC-5	6265576	573653	13.86	24.51	0.21	0.00	0.75	0.08	41.12	0.11	19.37	0.22	0.06	0.00	100.30
NEBC-5	6265576	573653	13.03	26.59	0.05	0.00	0.31	0.20	37.81	0.04	21.04	0.09	0.00	0.00	99.17
NEBC-5	6265576	573653	13.23	30.65	0.05	0.03	0.65	0.15	33.91	0.11	21.27	0.19	0.00	0.00	100.23
NEBC-5	6265576	573653	13.72	30.39	0.03	0.00	0.29	0.10	32.70	0.07	21.83	0.13	0.07	0.00	99.32
NEBC-6	6297889	522801	13.40	9.88	0.15	0.00	2.67	0.00	48.74	0.00	23.68	0.11	0.02	0.00	98.65
NEBC-6	6297889	522801	13.19	9.68	0.10	0.03	3.29	0.00	47.83	0.03	25.30	0.26	0.00	0.00	99.72
NEBC-7	6304336	520920	16.06	34.79	0.11	0.00	0.43	0.07	31.77	0.05	16.15	0.32	0.08	0.00	99.84
NEBC-7	6304336	520920	7.65	5.67	0.11	0.00	2.75	0.00	55.18	0.00	25.57	0.19	0.00	0.00	97.11
NEBC-7	6304336	520920	15.70	26.96	0.14	0.00	0.59	0.06	39.44	0.00	16.29	0.30	0.03	0.00	99.51
NEBC-7	6304336	520920	12.10	15.29	0.11	0.00	3.67	0.00	39.02	0.05	28.29	0.17	0.02	0.00	98.72
NEBC-7	6304336	520920	16.30	27.74	0.19	0.00	0.78	0.07	37.75	0.00	16.48	0.20	0.00	0.00	99.53
NEBC-7	6304336	520920	12.41	13.45	0.13	0.00	2.84	0.00	44.46	0.00	25.00	0.15	0.00	0.00	98.44
NEBC-7	6304336	520920	15.14	23.33	0.10	0.00	0.07	0.17	43.35	0.00	17.38	0.17	0.06	0.00	99.79
NEBC-7	6304336	520920	17.01	29.47	0.09	0.02	0.19	0.12	39.10	0.04	13.22	0.24	0.05	0.00	99.55
NEBC-7	6304336	520920	12.61	13.85	0.16	0.01	2.61	0.00	44.89	0.06	24.62	0.17	0.00	0.00	98.98
NEBC-7	6304336	520920	7.98	14.56	0.13	0.00	0.25	0.11	56.38	0.03	19.86	0.11	0.00	0.00	99.40
NEBC-7	6304336	520920	12.31	13.08	0.15	0.00	3.04	0.00	43.57	0.00	25.99	0.11	0.04	0.00	98.29
NEBC-7	6304336	520920	11.26	6.06	0.11	0.00	1.98	0.00	56.47	0.00	20.57	0.15	0.00	0.00	96.59
NEBC-7	6304336	520920	12.94	14.17	0.14	0.02	2.58	0.00	45.33	0.00	23.41	0.18	0.00	0.00	98.77
NEBC-7	6304336	520920	11.38	12.58	0.13	0.02	3.22	0.00	38.65	0.17	32.40	0.20	0.02	0.00	98.76
NEBC-7	6304336	520920	12.62	13.29	0.16	0.01	2.57	0.00	45.62	0.05	24.43	0.17	0.00	0.00	98.92
NEBC-7	6304336	520920	12.62	12.39	0.11	0.00	2.90	0.00	45.78	0.03	24.90	0.15	0.00	0.00	98.88
NEBC-7	6304336	520920	16.94	30.17	0.18	0.00	0.75	0.10	35.72	0.00	16.34	0.26	0.00	0.00	100.45
NEBC-7	6304336	520920	17.13	32.37	0.21	0.01	0.62	0.11	32.80	0.00	15.70	0.19	0.00	0.00	99.13
NEBC-7	6304336	520920	11.87	13.90	0.11	0.00	4.04	0.00	39.68	0.12	29.29	0.16	0.07	0.00	99.24
NEBC-7	6304336	520920	10.73	7.49	0.11	0.02	3.40	0.00	43.80	0.10	32.26	0.12	0.00	0.00	98.03
NEBC-7	6304336	520920	10.03	8.88	0.06	0.00	3.87	0.00	42.90	0.21	32.15	0.08	0.00	0.00	98.18
NEBC-7	6304336	520920	12.41	13.24	0.13	0.00	2.66	0.00	44.85	0.03	25.00	0.15	0.03	0.00	98.50
NEBC-7	6304336	520920	16.17	19.81	0.19	0.00	0.71	0.05	48.24	0.00	13.70	0.15	0.00	0.00	99.03
NEBC-7	6304336	520920	13.19	14.36	0.14	0.02	2.44	0.00	45.30	0.14	22.97	0.16	0.01	0.00	98.72
NEBC-7	6304336	520920	13.28	8.22	0.16	0.00	2.90	0.00	50.91	0.02	23.28	0.23	0.01	0.00	99.01
NEBC-7	6304336	520920	13.10	14.97	0.08	0.00	2.83	0.00	43.95	0.05	23.85	0.19	0.06	0.00	99.08
NEBC-7	6304336	520920	12.80	7.84	0.10	0.00	3.58	0.00	44.33	0.09	29.62	0.10	0.00	0.00	98.45
NEBC-7	6304336	520920	15.92	27.67	0.18	0.00	0.87	0.11	37.22	0.00	16.80	0.25	0.04	0.00	99.06
NEBC-7	6304336	520920	17.08	28.27	0.16	0.01	0.71	0.12	38.04	0.00	14.99	0.20	0.03	0.00	99.61
NEBC-7	6304336	520920	12.71	12.17	0.08	0.00	2.33	0.00	48.08	0.01	22.95	0.18	0.11	0.00	98.62
NEBC-7	6304336	520920	13.15	14.07	0.17	0.00	2.44	0.00	46.25	0.00	22.58	0.13	0.00	0.00	98.80
NEBC-7	6304336	520920	13.06	13.99	0.15	0.00	2.60	0.00	45.38	0.00	23.81	0.17	0.02	0.00	99.18
NEBC-7	6304336	520920	12.52	8.26	0.12	0.00	2.70	0.00	51.32	0.06	23.36	0.30	0.00	0.00	98.64
NEBC-7	6304336	520920	16.45	25.58	0.21	0.00	1.00	0.03	40.52	0.00	15.36	0.34	0.01	0.00	99.51
NEBC-7	6304336	520920	9.23	8.51	0.11	0.00	4.57	0.00	36.27	0.29	38.83	0.13	0.06	0.00	98.01
NEBC-7	6304336	520920	13.29	8.10	0.12	0.02	3.92	0.00	41.79	0.05	30.94	0.22	0.00	0.00	98.46

TABLE 4 (CONTINUED)

Sample ID	UTM Northing	UTM Easting	MgO	Al_2O_3	SiO_2	CaO	TiO_2	V_2O_3	Cr_2O_3	MnO	FeO	NiO	Nb_2O_5	Ta_2O_5	Total
NEBC-7	6304336	520920	12.32	13.65	0.17	0.01	2.78	0.00	44.14	0.11	24.94	0.19	0.01	0.00	98.30
NEBC-7	6304336	520920	12.30	13.17	0.15	0.02	2.67	0.00	45.04	0.00	24.98	0.16	0.00	0.00	98.49
NEBC-7	6304336	520920	15.60	22.83	0.07	0.00	0.08	0.14	45.29	0.00	15.42	0.11	0.00	0.00	99.56
NEBC-7	6304336	520920	16.61	30.55	0.14	0.00	0.76	0.08	35.79	0.00	15.14	0.24	0.00	0.00	99.30
NEBC-7	6304336	520920	14.97	24.89	0.09	0.00	0.63	0.13	41.68	0.00	17.09	0.12	0.00	0.00	99.60
NEBC-7	6304336	520920	13.03	14.34	0.16	0.00	2.39	0.00	45.03	0.02	22.98	0.15	0.04	0.00	98.14
NEBC-7	6304336	520920	11.21	7.36	0.09	0.00	4.89	0.00	46.17	0.00	28.85	0.25	0.00	0.00	98.83
NEBC-7	6304336	520920	13.24	14.21	0.16	0.01	2.32	0.00	46.43	0.00	22.92	0.17	0.00	0.00	99.48
NEBC-7	6304336	520920	12.16	12.98	0.13	0.02	3.81	0.00	41.46	0.02	28.41	0.23	0.00	0.00	99.22
NEBC-7	6304336	520920	12.36	15.15	0.12	0.00	3.26	0.00	40.50	0.14	27.27	0.20	0.08	0.00	99.08
NEBC-7	6304336	520920	13.15	14.06	0.17	0.01	2.41	0.00	46.46	0.00	22.75	0.16	0.00	0.00	99.17
NEBC-7	6304336	520920	16.04	28.35	0.09	0.01	0.47	0.08	37.65	0.05	15.87	0.20	0.00	0.00	98.80
NEBC-7	6304336	520920	13.18	14.23	0.15	0.01	2.38	0.00	45.37	0.00	22.89	0.21	0.00	0.00	98.41
NEBC-7	6304336	520920	13.70	16.34	0.12	0.00	1.43	0.01	44.38	0.04	22.63	0.18	0.00	0.00	98.84
NEBC-7	6304336	520920	10.11	15.12	0.18	0.00	0.21	0.10	51.55	0.09	21.79	0.13	0.00	0.00	99.30
NEBC-7	6304336	520920	14.84	23.36	0.20	0.02	1.40	0.03	38.89	0.08	19.60	0.25	0.00	0.00	98.66
NEBC-7	6304336	520920	13.15	7.35	0.12	0.01	2.98	0.00	49.03	0.02	25.93	0.27	0.00	0.00	98.85
NEBC-7	6304336	520920	13.08	11.67	0.13	0.01	1.59	0.00	48.00	0.05	24.01	0.24	0.00	0.00	98.78
NEBC-7	6304336	520920	14.44	16.44	0.08	0.04	1.15	0.04	50.49	0.00	15.92	0.09	0.00	0.00	98.70
NEBC-7	6304336	520920	16.48	28.88	0.23	0.01	0.51	0.07	36.89	0.00	15.39	0.14	0.00	0.00	98.61
NEBC-7	6304336	520920	12.72	5.86	0.15	0.01	2.21	0.00	56.31	0.00	21.55	0.09	0.00	0.00	98.90
NEBC-7	6304336	520920	11.19	9.60	0.07	0.01	3.04	0.00	44.71	0.00	29.62	0.19	0.00	0.00	98.43
NEBC-7	6304336	520920	14.89	17.82	0.09	0.01	1.96	0.00	47.89	0.02	16.68	0.16	0.00	0.00	99.50
NEBC-7	6304336	520920	11.32	7.77	0.11	0.00	3.28	0.00	47.29	0.05	28.13	0.09	0.00	0.00	98.04
NEBC-7	6304336	520920	12.59	14.65	0.19	0.01	2.28	0.00	44.83	0.06	23.63	0.16	0.00	0.00	98.40
NEBC-7	6304336	520920	10.44	8.11	0.09	0.00	3.51	0.00	47.63	0.03	28.55	0.08	0.00	0.00	98.42
NEBC-7	6304336	520920	12.66	11.26	0.13	0.00	2.32	0.00	48.79	0.04	23.58	0.17	0.02	0.00	98.98
NEBC-7	6304336	520920	12.51	8.98	0.13	0.01	2.50	0.00	50.10	0.00	23.61	0.13	0.00	0.00	97.97
NEBC-7	6304336	520920	15.21	25.62	0.22	0.00	0.35	0.16	40.08	0.07	17.07	0.20	0.02	0.00	99.00
NEBC-7	6304336	520920	16.48	28.98	0.11	0.01	0.15	0.12	39.95	0.02	13.77	0.19	0.00	0.00	99.76
NEBC-7	6304336	520920	12.91	9.45	0.12	0.00	1.76	0.00	51.04	0.00	23.02	0.12	0.00	0.00	98.43
NEBC-7	6304336	520920	12.85	7.76	0.14	0.03	2.36	0.00	53.08	0.00	22.91	0.17	0.02	0.00	99.33
NEBC-7	6304336	520920	12.78	13.93	0.13	0.00	2.68	0.00	44.57	0.00	23.77	0.20	0.00	0.00	98.05
NEBC-7	6304336	520920	12.72	12.88	0.14	0.00	2.87	0.00	45.79	0.00	24.95	0.20	0.00	0.00	99.56
NEBC-7 float	6304336	520920	12.46	10.16	0.10	0.00	2.36	0.00	49.32	0.01	23.27	0.09	0.03	0.00	97.80
NEBC-13	6524807	379408	15.65	27.54	0.15	0.02	0.67	0.10	37.43	0.00	17.79	0.25	0.09	0.00	99.67
NEBC-15	6518192	344777	11.64	7.57	0.15	0.07	4.00	0.00	46.76	0.00	27.86	0.13	0.00	0.00	98.19
NEBC-15	6518192	344777	13.91	25.04	0.08	0.00	1.36	0.02	35.57	0.07	22.86	0.21	0.02	0.00	99.13
NEBC-18	6579659	332851	10.91	15.00	0.07	0.01	0.28	0.18	52.17	0.08	20.81	0.03	0.00	0.00	99.55
NEBC-18	6579659	332851	14.00	29.87	0.03	0.00	0.06	0.16	37.35	0.00	18.35	0.07	0.04	0.00	99.92
NEBC-18	6579659	332851	10.35	9.49	0.07	0.00	0.24	0.08	57.45	0.13	21.69	0.06	0.06	0.00	99.64
NEBC-18	6579659	332851	16.62	27.49	0.09	0.00	0.15	0.13	40.89	0.00	14.68	0.26	0.02	0.00	100.32
NEBC-20	6566238	484386	15.24	14.64	0.13	0.00	0.32	0.11	53.56	0.00	15.32	0.32	0.00	0.00	99.64
NEBC-21	6565844	482724	7.07	15.35	0.08	0.00	0.43	0.10	44.46	0.16	30.68	0.05	0.00	0.00	98.39
NEBC-23	6614075	494595	8.86	23.07	0.08	0.01	0.38	0.14	35.00	0.05	31.20	0.28	0.05	0.00	99.12
NEBC-23	6614075	494595	5.70	10.36	0.07	0.00	1.60	0.12	34.73	0.11	44.45	0.13	0.00	0.00	97.27
NEBC-23	6614075	494595	12.30	24.53	0.04	0.00	0.36	0.14	39.47	0.08	22.06	0.15	0.03	0.00	99.17
NEBC-23	6614075	494595	15.19	34.28	0.04	0.00	0.24	0.18	31.71	0.04	17.38	0.12	0.00	0.00	99.19
NEBC-23	6614075	494595	11.98	20.85	0.07	0.00	0.03	0.28	48.09	0.00	18.57	0.03	0.00	0.00	99.90
NEBC-23	6614075	494595	15.88	36.26	0.03	0.03	0.07	0.15	31.54	0.06	15.32	0.21	0.00	0.00	99.56
NEBC-23	6614075	494595	10.14	17.73	0.08	0.02	0.27	0.09	49.54	0.10	21.64	0.09	0.06	0.00	99.75
NEBC-23	6614075	494595	10.19	21.62	0.08	0.03	0.07	0.24	42.51	0.16	23.93	0.15	0.06	0.00	99.03
NEBC-23	6614075	494595	9.91	15.39	0.09	0.00	0.14	0.17	50.51	0.03	22.48	0.10	0.04	0.00	98.86
NEBC-23	6614075	494595	8.73	24.29	0.14	0.00	0.55	0.04	39.31	0.19	26.05	0.11	0.00	0.00	99.40
NEBC-23	6614075	494595	12.93	18.98	0.09	0.00	0.05	0.28	47.42	0.00	19.04	0.16	0.00	0.00	98.94
NEBC-23	6614075	494595	11.87	19.09	0.08	0.00	0.08	0.20	49.38	0.00	19.13	0.09	0.07	0.00	99.98
NEBC-23	6614075	494595	13.30	28.45	0.06	0.00	0.31	0.18	35.42	0.08	20.69	0.10	0.02	0.00	98.61
NEBC-23	6614075	494595	13.24	13.51	0.15	0.02	0.22	0.23	52.38	0.00	18.92	0.12	0.03	0.00	98.80
NEBC-23	6614075	494595	13.91	26.46	0.06	0.00	0.39	0.11	38.33	0.10	19.97	0.27	0.02	0.00	99.62
NEBC-23	6614075	494595	12.78	28.47	0.08	0.01	0.47	0.14	33.61	0.12	23.09	0.21	0.00	0.00	98.98

TABLE 4 (CONTINUED)

Sample ID	UTM Northing	UTM Easting	MgO	Al_2O_3	SiO_2	CaO	TiO_2	V_2O_3	Cr_2O_3	MnO	FeO	NiO	Nb_2O_5	Ta_2O_5	Total
NEBC-23	6614075	494595	10.76	21.98	0.04	0.02	1.01	0.21	39.29	0.18	25.93	0.22	0.00	0.00	99.65
NEBC-23	6614075	494595	14.48	30.03	0.06	0.00	0.46	0.16	34.77	0.08	19.62	0.18	0.00	0.00	99.85
NEBC-23	6614075	494595	15.61	26.89	0.09	0.00	0.79	0.10	37.66	0.02	17.83	0.20	0.00	0.00	99.20
NEBC-23	6614075	494595	13.96	24.38	0.09	0.00	0.25	0.21	42.68	0.01	17.85	0.14	0.02	0.00	99.60
NEBC-23	6614075	494595	15.17	20.23	0.10	0.00	0.18	0.11	46.43	0.03	16.95	0.20	0.00	0.00	99.40
NEBC-23	6614075	494595	7.72	5.62	0.11	0.00	0.13	0.14	61.40	0.20	23.51	0.04	0.01	0.00	98.88
NEBC-23	6614075	494595	13.88	23.90	0.05	0.00	0.03	0.25	43.24	0.04	18.42	0.20	0.00	0.00	100.01
NEBC-23	6614075	494595	13.33	14.87	0.11	0.00	1.42	0.00	46.57	0.00	22.08	0.19	0.00	0.00	98.57
NEBC-23	6614075	494595	12.82	34.61	0.04	0.00	0.10	0.15	29.66	0.10	21.65	0.08	0.01	0.00	99.24
NEBC-25	6510030	520870	5.94	14.31	0.03	0.00	0.09	0.09	43.53	0.17	35.02	0.13	0.00	0.00	99.31
NEBC-25	6510030	520870	10.12	8.13	0.07	0.02	0.61	0.17	55.48	0.01	23.23	0.04	0.00	0.00	97.88
NEBC-27	6515567	538244	11.32	10.35	0.09	0.00	2.29	0.00	47.82	0.07	27.23	0.21	0.05	0.00	99.43
NEBC-27	6515567	538244	16.11	31.88	0.08	0.03	0.06	0.10	36.27	0.00	16.10	0.32	0.00	0.00	100.95
NEBC-38	6489088	545698	9.82	26.04	0.01	0.00	0.24	0.18	33.48	0.16	29.45	0.18	0.04	0.00	99.62
NEBC-39	6488921	548332	6.52	23.31	0.10	0.00	0.82	0.05	38.63	0.16	29.55	0.10	0.00	0.00	99.25
NEBC-39	6488921	548332	9.44	9.68	0.12	0.00	4.12	0.00	37.89	0.23	36.32	0.04	0.00	0.00	97.83
NEBC-39	6488921	548332	11.07	30.71	0.07	0.00	0.11	0.11	32.16	0.12	25.08	0.17	0.00	0.00	99.60
NEBC-39	6488921	548332	6.02	11.52	0.06	0.00	0.18	0.13	46.99	0.13	32.82	0.08	0.00	0.00	97.93
NEBC-40	6486881	557911	11.95	14.60	0.08	0.00	0.38	0.11	48.91	0.04	22.01	0.10	0.05	0.00	98.24
NEBC-42	6512245	517785	7.19	15.17	0.07	0.00	0.45	0.08	40.21	0.23	34.98	0.17	0.02	0.00	98.58
NEBC-43	6549892	460825	13.73	31.05	0.06	0.00	0.26	0.18	33.72	0.10	20.72	0.16	0.02	0.00	99.98
NEBC-43	6549892	460825	13.25	16.77	0.11	0.01	1.48	0.02	44.14	0.00	23.41	0.20	0.00	0.00	99.37
NEBC-43	6549892	460825	14.40	33.32	0.04	0.00	0.08	0.22	31.32	0.06	20.58	0.17	0.04	0.00	100.24
NEBC-43	6549892	460825	12.34	21.18	0.07	0.01	0.42	0.09	47.79	0.00	18.15	0.02	0.00	0.00	100.08
NEBC-43	6549892	460825	17.60	34.79	0.15	0.00	0.45	0.11	32.21	0.00	14.63	0.13	0.00	0.00	100.08
NEBC-43	6549892	460825	15.00	28.82	0.10	0.01	0.03	0.17	37.68	0.03	17.59	0.22	0.00	0.00	99.65
NEBC-43	6549892	460825	13.61	30.49	0.05	0.01	0.67	0.20	33.76	0.07	21.37	0.14	0.03	0.00	100.40
NEBC-43	6549892	460825	12.71	27.47	0.10	0.00	0.23	0.12	37.23	0.07	22.18	0.19	0.00	0.00	100.30
NEBC-43	6549892	460825	13.72	29.13	0.07	0.00	0.32	0.18	36.49	0.04	20.02	0.06	0.03	0.00	100.06
NEBC-43	6549892	460825	15.66	12.20	0.15	0.02	0.61	0.04	55.15	0.00	15.55	0.26	0.08	0.00	99.71
NEBC-43	6549892	460825	15.15	5.14	0.17	0.00	0.19	0.00	62.91	0.00	15.05	0.25	0.01	0.00	98.86
NEBC-43	6549892	460825	13.75	23.13	0.05	0.00	0.62	0.19	41.44	0.00	20.43	0.15	0.01	0.00	99.76
NEBC-43	6549892	460825	13.41	16.86	0.10	0.00	1.78	0.03	45.02	0.07	23.08	0.21	0.00	0.00	100.57
NEBC-43	6549892	460825	10.09	13.72	0.12	0.03	1.72	0.00	44.25	0.09	28.71	0.12	0.12	0.00	98.97
NEBC-43	6549892	460825	10.25	18.20	0.08	0.00	1.18	0.02	42.92	0.09	26.68	0.07	0.00	0.00	99.49
NEBC-43	6549892	460825	9.40	16.99	0.12	0.00	1.61	0.05	41.43	0.02	30.21	0.21	0.00	0.00	100.04
NEBC-43	6549892	460825	12.16	25.35	0.03	0.00	0.10	0.14	37.75	0.07	23.37	0.14	0.05	0.00	99.18
NEBC-43	6549892	460825	12.74	29.54	0.06	0.03	0.04	0.25	36.69	0.07	19.70	0.10	0.00	0.00	99.21
NEBC-43	6549892	460825	10.99	23.46	0.07	0.01	0.13	0.18	40.22	0.13	24.50	0.13	0.01	0.00	99.83
NEBC-43	6549892	460825	12.24	12.86	0.14	0.01	2.21	0.00	46.85	0.00	24.83	0.22	0.01	0.00	99.36
NEBC-43	6549892	460825	15.61	30.27	0.09	0.01	0.19	0.16	36.32	0.07	16.13	0.27	0.00	0.00	99.12
NEBC-43	6549892	460825	13.44	28.49	0.06	0.00	0.27	0.19	36.36	0.07	21.12	0.18	0.03	0.00	100.21
NEBC-43	6549892	460825	7.45	16.44	0.07	0.00	1.59	0.01	40.46	0.13	32.79	0.12	0.00	0.00	99.07
NEBC-43	6549892	460825	13.57	27.14	0.08	0.00	0.11	0.19	40.56	0.04	18.75	0.17	0.05	0.00	100.66
NEBC-43	6549892	460825	12.92	22.50	0.05	0.01	0.14	0.10	46.61	0.03	17.95	0.12	0.00	0.00	100.42
NEBC-43	6549892	460825	13.49	31.93	0.04	0.00	0.01	0.15	35.33	0.00	18.57	0.09	0.03	0.00	99.63
NEBC-43	6549892	460825	13.68	33.26	0.05	0.00	0.24	0.15	30.84	0.00	20.78	0.17	0.03	0.00	99.22
NEBC-43	6549892	460825	14.12	30.68	0.08	0.00	0.34	0.16	34.23	0.09	20.49	0.13	0.03	0.00	100.36
NEBC-43	6549892	460825	9.13	14.26	0.08	0.02	0.43	0.14	47.50	0.08	27.20	0.09	0.00	0.00	98.93
NEBC-43	6549892	460825	10.39	14.36	0.30	0.00	0.02	0.21	52.59	0.10	21.81	0.07	0.09	0.00	99.94
NEBC-43	6549892	460825	14.26	28.30	0.15	0.00	0.10	0.17	40.21	0.06	16.26	0.09	0.02	0.00	99.62
NEBC-43	6549892	460825	13.55	27.96	0.03	0.01	0.08	0.19	37.02	0.10	21.41	0.14	0.00	0.00	100.50
NEBC-43	6549892	460825	13.05	24.51	0.04	0.00	0.04	0.21	42.04	0.03	19.52	0.10	0.00	0.00	99.55
NEBC-43	6549892	460825	15.67	16.11	0.12	0.00	1.35	0.00	48.29	0.00	17.33	0.33	0.08	0.00	99.27
NEBC-43	6549892	460825	11.78	13.23	0.13	0.03	0.22	0.08	52.25	0.06	22.16	0.21	0.02	0.00	100.16
NEBC-43	6549892	460825	11.16	5.98	0.11	0.02	0.20	0.01	61.26	0.11	19.96	0.10	0.10	0.00	99.02
NEBC-43	6549892	460825	13.45	25.24	0.08	0.02	0.04	0.22	42.15	0.00	19.08	0.23	0.00	0.00	100.50
NEBC-44	6549887	461981	10.79	26.39	0.07	0.01	0.34	0.15	39.02	0.06	22.33	0.07	0.00	0.00	99.24
NEBC-44	6549887	461981	12.42	16.79	0.13	0.01	2.03	0.00	40.52	0.09	26.23	0.19	0.03	0.00	98.43
NEBC-44	6549887	461981	12.96	11.66	0.09	0.00	0.23	0.04	56.90	0.00	16.87	0.09	0.00	0.00	98.83

TABLE 4 (CONTINUED)

Sample ID	UTM Northing	UTM Easting	MgO	Al_2O_3	SiO_2	CaO	TiO_2	V_2O_3	Cr_2O_3	MnO	FeO	NiO	Nb_2O_5	Ta_2O_5	Total
NEBC-44	6549887	461981	11.03	25.59	0.07	0.00	0.32	0.15	35.51	0.05	26.09	0.19	0.00	0.00	98.99
NEBC-44	6549887	461981	12.41	10.27	0.07	0.00	0.27	0.03	59.80	0.00	16.76	0.11	0.00	0.00	99.72
NEBC-44	6549887	461981	14.19	29.75	0.07	0.00	0.34	0.13	37.45	0.01	17.36	0.13	0.10	0.00	99.52
NEBC-44	6549887	461981	10.70	27.66	0.14	0.00	0.07	0.20	38.72	0.50	21.51	0.08	0.07	0.00	99.64
NEBC-44	6549887	461981	15.25	28.68	0.05	0.01	0.05	0.22	40.15	0.00	15.39	0.16	0.04	0.00	100.01
NEBC-44	6549887	461981	9.87	28.02	0.03	0.00	0.43	0.20	33.78	0.13	26.52	0.20	0.02	0.00	99.19
NEBC-44	6549887	461981	10.58	10.04	0.07	0.00	0.19	0.05	59.24	0.00	19.14	0.02	0.00	0.00	99.32
NEBC-44	6549887	461981	9.05	18.28	0.05	0.00	1.94	0.05	37.96	0.10	31.60	0.19	0.00	0.00	99.21
NEBC-44	6549887	461981	4.95	8.21	0.06	0.00	0.24	0.12	47.99	0.22	36.59	0.04	0.00	0.00	98.42
NEBC-44	6549887	461981	9.04	14.60	0.05	0.00	0.23	0.08	50.01	0.75	23.70	0.05	0.00	0.00	98.51
NEBC-44	6549887	461981	14.79	30.22	0.04	0.00	0.09	0.20	38.46	0.04	15.58	0.11	0.00	0.00	99.51
NEBC-44	6549887	461981	11.77	16.37	0.13	0.01	1.67	0.02	43.09	0.00	25.74	0.19	0.00	0.00	99.00
NEBC-44	6549887	461981	8.37	4.70	0.11	0.02	1.63	0.00	48.51	0.15	34.13	0.29	0.00	0.00	97.91
NEBC-44	6549887	461981	11.83	27.40	0.07	0.01	0.34	0.22	36.43	0.30	22.57	0.12	0.03	0.00	99.33
NEBC-44	6549887	461981	16.00	30.06	0.09	0.02	0.23	0.08	36.41	0.00	15.48	0.17	0.05	0.00	98.57
NEBC-44	6549887	461981	15.67	23.12	0.16	0.01	0.28	0.09	44.26	0.00	15.27	0.29	0.04	0.00	99.19
NEBC-44	6549887	461981	14.34	30.33	0.09	0.00	0.00	0.16	38.18	0.01	16.54	0.11	0.03	0.00	99.81
NEBC-44	6549887	461981	13.12	9.02	0.13	0.00	0.32	0.04	57.62	0.00	19.14	0.19	0.00	0.00	99.59
NEBC-44	6549887	461981	13.98	17.34	0.13	0.00	1.59	0.00	43.87	0.00	21.69	0.28	0.04	0.00	98.91
NEBC-44	6549887	461981	13.15	12.82	0.12	0.00	0.53	0.06	46.63	0.09	25.19	0.12	0.00	0.00	98.70
NEBC-44	6549887	461981	14.52	24.10	0.10	0.00	0.43	0.17	41.94	0.00	17.79	0.16	0.00	0.00	99.20
NEBC-44	6549887	461981	11.71	18.24	0.05	0.01	0.06	0.24	49.57	0.04	20.98	0.08	0.00	0.00	100.97
NEBC-45	6440574	516839	16.81	32.17	0.12	0.00	0.05	0.18	35.20	0.00	14.98	0.27	0.00	0.00	99.78
NEBC-45	6440574	516839	15.44	29.91	0.11	0.01	0.61	0.19	36.31	0.02	17.15	0.20	0.00	0.00	99.95
NEBC-45	6440574	516839	12.39	29.42	0.07	0.00	0.25	0.22	33.46	0.06	22.84	0.18	0.00	0.00	98.88
NEBC-45	6440574	516839	12.13	27.69	0.03	0.01	0.16	0.18	34.33	0.10	24.88	0.13	0.00	0.00	99.64
NEBC-45	6440574	516839	14.50	16.39	0.14	0.00	1.34	0.00	47.33	0.00	19.21	0.17	0.00	0.00	99.08
NEBC-45	6440574	516839	12.95	28.00	0.06	0.01	0.01	0.19	37.90	0.07	20.67	0.16	0.00	0.00	100.02
NEBC-45	6440574	516839	14.82	32.88	0.04	0.03	0.01	0.21	36.26	0.01	15.77	0.19	0.00	0.00	100.20
NEBC-45	6440574	516839	13.90	27.78	0.05	0.00	0.08	0.16	40.25	0.00	18.08	0.08	0.00	0.00	100.38
NEBC-45	6440574	516839	13.33	27.09	0.08	0.00	0.00	0.26	41.94	0.05	17.31	0.12	0.06	0.00	100.23
NEBC-46	6439810	516735	13.05	33.85	0.02	0.03	0.18	0.25	31.22	0.09	20.48	0.15	0.07	0.00	99.40
NEBC-47	6360037	509264	17.87	33.35	0.18	0.00	0.09	0.13	33.96	0.07	13.23	0.23	0.00	0.00	99.10
NEBC-47	6360037	509264	11.58	16.85	0.10	0.00	1.26	0.00	43.86	0.05	25.25	0.12	0.00	0.00	99.06
NEBC-47	6360037	509264	12.74	28.42	0.08	0.00	0.35	0.17	34.53	0.08	22.06	0.12	0.00	0.00	98.55
NEBC-50	6222613	645018	13.98	19.51	0.13	0.02	0.00	0.14	50.52	0.00	15.26	0.07	0.00	0.00	99.63
NEBC-50	6222613	645018	10.58	6.81	0.12	0.02	0.33	0.06	55.04	0.12	25.13	0.14	0.10	0.00	98.44
NEBC-50	6222613	645018	9.12	8.52	0.06	0.00	0.25	0.00	52.63	0.12	26.50	0.05	0.00	0.00	97.24
NEBC-50	6222613	645018	11.44	20.42	0.06	0.00	1.26	0.24	40.77	0.08	23.75	0.21	0.00	0.00	98.23
NEBC-50	6222613	645018	8.93	11.73	0.08	0.00	0.04	0.21	55.50	0.03	22.52	0.05	0.00	0.00	99.09
NEBC-50	6222613	645018	10.41	9.66	0.12	0.00	0.84	0.11	39.47	0.04	36.83	0.11	0.00	0.00	97.58
NEBC-50	6222613	645018	10.93	24.43	0.07	0.00	0.03	0.21	42.20	0.05	21.05	0.06	0.00	0.00	99.02
NEBC-50	6222613	645018	11.81	8.10	0.10	0.00	0.28	0.00	50.75	0.12	27.17	0.18	0.00	0.00	98.49
NEBC-52	6176129	611299	8.40	7.47	0.12	0.00	0.06	0.23	58.66	0.05	23.42	0.13	0.05	0.00	98.58
NEBC-52	6176129	611299	11.40	20.28	0.08	0.01	0.03	0.21	47.25	0.02	20.64	0.05	0.07	0.00	100.04
NEBC-52	6176129	611299	14.54	18.37	0.13	0.02	0.83	0.10	45.25	0.01	19.88	0.18	0.00	0.00	99.30
NEBC-52	6176129	611299	11.44	16.53	0.09	0.01	0.16	0.16	50.09	0.02	20.95	0.03	0.00	0.00	99.48
NEBC-52	6176129	611299	13.58	26.74	0.06	0.00	0.11	0.19	40.90	0.05	18.51	0.10	0.00	0.00	100.23
NEBC-52	6176129	611299	12.95	18.62	0.12	0.00	1.65	0.02	39.56	0.00	26.03	0.14	0.00	0.00	99.09
NEBC-52	6176129	611299	7.37	13.23	0.08	0.02	0.31	0.26	44.89	0.20	31.74	0.13	0.05	0.00	98.29
NEBC-52	6176129	611299	10.36	21.98	0.08	0.00	0.04	0.19	44.91	0.05	22.04	0.03	0.00	0.00	99.67
NEBC-54	6152653	530479	11.20	14.64	0.08	0.00	0.58	0.09	47.08	0.00	25.65	0.06	0.04	0.00	99.43
NEBC-57	6354768	661877	16.88	32.72	0.13	0.03	0.53	0.08	31.56	0.07	17.14	0.29	0.00	0.00	99.43
NEBC-57	6354768	661877	13.22	26.29	0.09	0.01	0.23	0.29	40.37	0.04	18.68	0.22	0.00	0.00	99.43
NEBC-57	6354768	661877	16.08	26.44	0.15	0.01	0.39	0.15	41.45	0.05	16.23	0.19	0.03	0.00	101.18
NEBC-58	6612910	564017	13.89	29.38	0.07	0.02	0.20	0.18	36.46	0.15	19.78	0.14	0.04	0.00	100.30
NEBC-58	6612910	564017	5.80	11.10	0.07	0.01	0.34	0.12	45.14	0.23	35.90	0.13	0.00	0.00	98.84
NEBC-58	6612910	564017	6.64	15.57	0.07	0.01	0.36	0.13	45.04	0.17	30.52	0.17	0.00	0.00	98.67
NEBC-58	6612910	564017	13.09	24.42	0.14	0.01	0.59	0.13	41.49	0.08	19.08	0.17	0.00	0.00	99.20
NEBC-58	6612910	564017	14.40	20.02	0.16	0.00	1.60	0.05	40.96	0.02	22.17	0.18	0.00	0.00	99.57

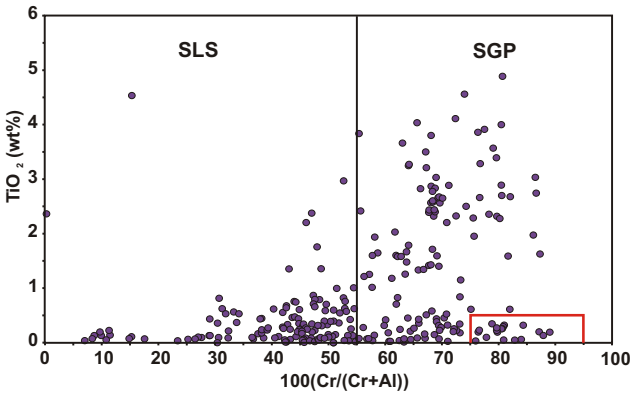


Figure 9. Cr-spinel TiO_2-100[Cr/(Cr+Al)] diagram. The majority of the chromites plot within the garnet peridotite field. At least 16 grains have compositions compatible with chromites found as inclusions in diamonds, indicated by the rectangle. SLS – spinels from spinel peridotites, SGP – spinels from garnet peridotites; fields from Ramsey and Tompkins (1994).

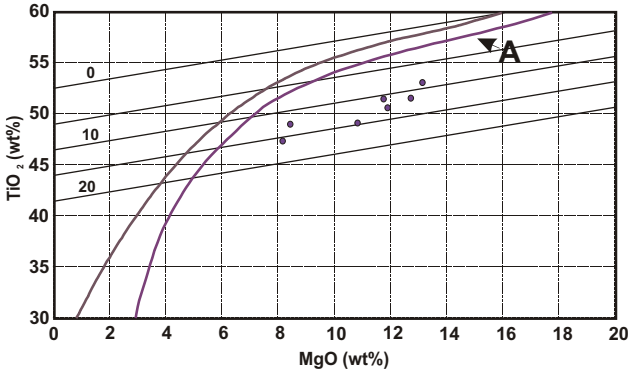


Figure 10. Ilmenite TiO_2-MgO discrimination plot (*after* Wyatt *et al.*, 2004). Seven grains plot within the kimberlite field, which is located to the right of the curve marked 'A'.

interpreted as kimberlite related. A substantial portion of spinels from these samples have the characteristics of lamproite-derived spinel; however, it is possible that some of the spinel from NEBC-7 originated from lamprophyre dikes or diatremes related to the Aley carbonatite complex (also referred to as the Ospika pipe), which is located less than 100 km from the sample site. At this stage, microprobe analyses of spinels from this complex have not been undertaken.

Ilmenite

Ilmenite is one of the most widely used KIMs. It is a common member of the megacryst suite, and the major compounds TiO_2, MgO, CrO_2, MnO_2 and Fe_2O_3 are used to distinguish kimberlitic ilmenites from those that are non-kimberlitic (Wyatt *et al.*, 2004). Seven grains of ilmenite were picked and analyzed (Table 5). Based on the TiO_2-MgO plot (Fig. 10), all the analyzed ilmenite indicator grains plot within the kimberlite field (*i.e.,* to the right of the curve marked 'A').

As shown in Figure 11, the Cr_2O_3-MgO plot also suggests that the same seven grains identified in Figure 10 are associated with kimberlite. The fields of typical North American, South African (on- and off-craton) and Australian kimberlitic ilmenites are provided in Figure 11 for reference, and are based on data from Wyatt *et al.* (2004). Six of these ilmenites come from samples collected in the Etsho Plateau region east of Fort Nelson and one originates from a sample collected approximately 110 km north of Fort St. John near the BC-Alberta border (Fig. 2).

Olivine

Olivine is considered a useful KIM in cold climates. Olivine is the most common rock-forming mineral in kimberlites; however, it is also present in a variety of other ultramafic rocks, basalts and mantle xenoliths in BC (Voormeij and Simandl, 2004a, b). Due to its occurrence in diverse rock types, olivine is less diagnostic and it does not provide as much information regarding the diamond potential of northeastern BC as do garnets, ilmenites, spinels or Cr-diopsides. Nevertheless, in association with other indicator minerals, olivine may play an important role in the evaluation of indicator mineral anomalies. Olivine from kimberlites and peridotites is MgO-rich (close to the forsterite end-member of the olivine solid solution series) and is colourless to pale yellow or pale green. Its chemistry is characterized by Mg numbers [$100*Mg^{+2}/(Mg^{+2}+Fe^{+2})$] between 84 and 95 and notable traces of NiO. Most of the olivines from the study area fall within that range (Table 6; Fig. 12). Olivines that are found as inclusions in diamonds

TABLE 5. CHEMICAL COMPOSITION OF ILMENITES; FOR SAMPLE LOCATIONS SEE TABLE 1 AND FIGURE 2.

Sample ID	UTM Northing	UTM Easting	MgO	Al_2O_3	SiO_2	CaO	TiO_2	V_2O_3	Cr_2O_3	MnO	FeO	NiO	Nb_2O_5	Ta_2O_5	Total
NEBC-27	6515567	538244	8.16	0.10	0.00	0.02	47.39	0.00	1.68	0.26	41.06	0.06	0.16	0.00	98.89
NEBC-38	6489088	545698	11.87	0.55	0.05	0.03	50.60	0.00	1.81	0.26	33.07	0.11	0.22	0.02	98.59
NEBC-39	6488921	548332	12.70	0.58	0.05	0.01	51.54	0.00	0.95	0.19	32.01	0.07	0.15	0.00	98.25
NEBC-44	6549887	461981	8.42	0.16	0.04	0.00	48.97	0.00	0.97	0.27	40.09	0.10	0.31	0.01	99.35
NEBC-44	6549887	461981	13.11	0.37	0.05	0.04	53.05	0.00	1.07	0.24	30.73	0.12	0.16	0.03	98.97
NEBC-55	6510906	565930	10.82	0.48	0.00	0.05	49.09	0.00	0.10	0.28	36.87	0.03	0.15	0.02	97.89
NEBC-57	6354768	661877	11.75	0.61	0.06	0.01	51.48	0.00	0.42	0.26	33.93	0.00	0.13	0.00	98.64

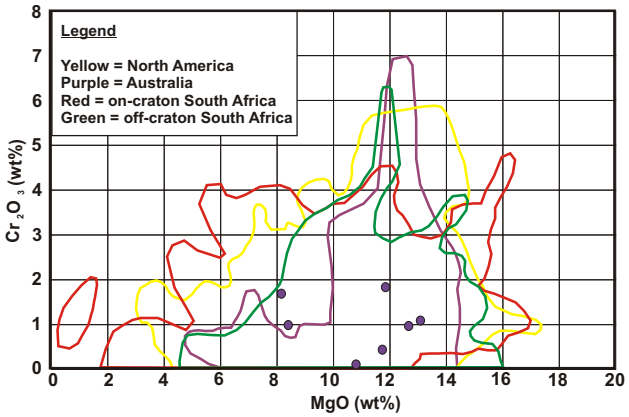


Figure 11. Ilmenite Cr_2O_3-MgO discrimination plot (*after* Haggerty, 1991). Simplified fields representing North American, Australian and South African (on- and off-craton) kimberlitic ilmenites derived from plots by Wyatt *et al*. (2004). All seven ilmenite grains from northeastern BC plot within the fields representing South African and North American kimberlitic ilmenites. Five of the seven grains also fall within the field of Australian kimberlitic ilmenites.

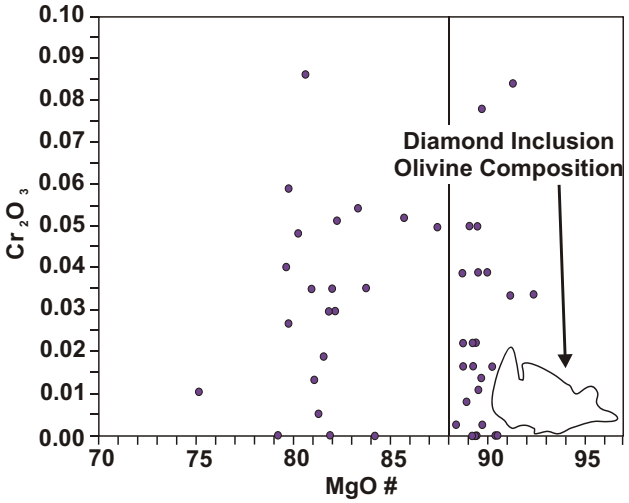


Figure 12. Olivine Cr_2O_3-Mg# discrimination plot. Olivines with an Mg# >88 are commonly, but not uniquely, associated with kimberlites. Twenty-six grains from this study have an Mg# >88. The outline of olivine compositions found as solid inclusions in diamonds is from Fipke *et al.* (1995). None of the grains recovered during this study fit that profile.

commonly plot in an irregularly shaped field on Fipke *et. al.*'s (1995) Cr_2O_3-Mg# discrimination plot (Fig. 12).

The Mg-rich variety of olivine, identified in samples from northeastern BC, is commonly pale yellow-green in colour, equidimensional, subrounded to rounded, and has a fresh appearance. Microprobe data on 47 olivine grains recovered from collected samples are presented in Table 6 and plotted on the Cr_2O_3-Fo diagram (Fig. 12). None of the olivine grains collected during this study fall within the compositional field of olivines found as inclusions in diamonds.

The concentrations of olivine in samples NEBC-16 and 18 suggest that these olivines may be derived from known ultramafic rocks west of the study area, rocks that are part of the Cache Creek and Slide Mountain terranes, or from alkaline pipes or dikes in the Kechika River area. This interpretation is consistent with Mathew's (1980) inference of the glacial history of the area and thus expected sediment transportation patterns.

DIAMOND AND FLUORITE

One of the most intriguing aspects of this study is a recovery of a clear diamond that cannot be attributed to a specific sample. It was recovered from the -1.18+0.85 mm fraction of heavy mineral concentrate derived from sample NEBC-11. The stone is a transparent diamond (Fig. 3) with crystal faces measuring 1.05×1.03×0.73 mm and weighing 1.34 mg (0.0067 carat). Apparently, because of its size and colourless nature, this diamond may have been sitting on the screen (or lodged within the screen) for an unspecified length of time without being detected and before making its way through the screen. If this explanation is correct, the diamond may have come from any of the ten samples numbered from NEBC-1 to 10, which were processed before sample NEBC-11 entered the system. This diamond may have also come from samples belonging to a previous client (contamination). Therefore, the sample from which this diamond was recovered cannot be established.

Besides the above described diamond, the heavy mineral fraction of sample NEBC-11 also contained abundant fluorite. Fluorite (CaF_2) is a relatively soft (4 on Moh's hardness scale), brittle mineral with well-developed cleavage. Fluorite is commonly found as an ore or gangue mineral in Mississippi Valley-type Pb-Zn deposits (Leach and Sangster, 1993), vein-type fluorite, fluorite-barite veins (Hora, 1996a, b) and carbonatite deposits (Birkett and Simandl, 1999). It is relatively common in samples from northeastern BC, and it is particularly abundant in concentrates from samples NEBC-11 and 12, where it is the most abundant nonmagnetic heavy mineral. The fluorite is most likely derived from local sources, such as the known fluorite occurrences of Mile 397, Stone, Rep 6, Ctv T-7 and Hope H-3 (Fig. 13).

There is no established association between diamonds and fluorite in classical kimberlite or lamproite-hosted diamond deposits; however, both of these minerals have a similar density (3.52 and 3.13 g/cm^3, respectively) and are nonmagnetic. The lack of obvious genetic association between diamond and fluorite in primary diamond deposits is probably the main reason why the SGS Lakefield Research laboratory interpreted this diamond as probable contamination. The diamond does not show visible signs that are characteristic of alluvial diamonds, such as scuffing and scratching concentrated at the edges of the crystals, percussion marks and green or brown spots, which are related to radiation damage. The lack of these signs prevent speculation whether this diamond was derived directly from a primary diamond deposit (with little glacial or glaciofluvial or fluvial transport) or if it was transported for long distances from its primary source.

DISCUSSION AND RECOMMENDATIONS

The geology of the Precambrian basement in northeastern BC is poorly understood, but there are indications that it could be more favourable for diamond exploration than previously reported (Simandl, 2004; Simandl and Davis, 2005). Therefore, the results of this study are important, particularly if the modified diamondiferous mantle

TABLE 6. CHEMICAL COMPOSITION AND MG# OF OLIVINES; FOR SAMPLE LOCATIONS SEE TABLE 1 AND FIGURE 2.

Sample ID	UTM Northing	UTM Easting	Na_2O	MgO	Al_2O_3	SiO_2	K_2O	CaO	TiO_2	Cr_2O_3	MnO	FeO	Total	Mg #
NEBC-16	6548532	340361	0.02	49.91	0.00	40.08	0.01	0.06	0.02	0.00	0.14	10.19	100.44	0.897276791
NEBC-16	6548532	340361	0.02	41.66	0.03	38.44	0.00	0.28	0.01	0.00	0.19	19.48	100.11	0.792166542
NEBC-16	6548532	340361	0.03	50.06	0.03	40.05	0.00	0.05	0.02	0.00	0.12	9.44	99.79	0.904375441
NEBC-16	6548532	340361	0.00	50.00	0.00	40.72	0.00	0.05	0.00	0.02	0.14	9.66	100.59	0.902232176
NEBC-16	6548532	340361	0.01	50.56	0.16	40.52	0.00	0.13	0.00	0.08	0.09	8.60	100.16	0.912901199
NEBC-16	6548532	340361	0.00	48.76	0.02	39.92	0.01	0.11	0.00	0.00	0.14	11.42	100.39	0.883907029
NEBC-17	6568296	330650	0.03	39.01	0.04	37.16	0.00	0.24	0.03	0.01	0.22	23.02	99.76	0.751307804
NEBC-18	6579659	332851	0.00	49.16	0.04	40.27	0.02	0.07	0.01	0.01	0.15	10.90	100.62	0.889381538
NEBC-18	6579659	332851	0.02	48.79	0.04	39.74	0.01	0.11	0.02	0.04	0.10	11.07	99.95	0.887062621
NEBC-18	6579659	332851	0.00	49.71	0.01	40.53	0.00	0.04	0.03	0.04	0.13	10.37	100.86	0.895221689
NEBC-18	6579659	332851	0.00	48.84	0.03	40.02	0.00	0.06	0.00	0.02	0.18	11.04	100.20	0.887437969
NEBC-18	6579659	332851	0.00	48.98	0.03	40.15	0.00	0.05	0.00	0.00	0.18	10.50	99.88	0.892654771
NEBC-18	6579659	332851	0.00	44.09	0.02	38.25	0.01	0.22	0.04	0.03	0.19	17.05	99.89	0.821757035
NEBC-18	6579659	332851	0.03	43.75	0.04	38.96	0.00	0.24	0.00	0.00	0.17	17.21	100.40	0.819268606
NEBC-18	6579659	332851	0.01	49.19	0.02	39.89	0.00	0.07	0.01	0.00	0.16	10.50	99.85	0.893045135
NEBC-18	6579659	332851	0.02	49.11	0.04	40.21	0.00	0.07	0.00	0.02	0.11	10.54	100.12	0.892556252
NEBC-18	6579659	332851	0.01	49.09	0.01	39.82	0.00	0.06	0.02	0.00	0.21	10.55	99.78	0.892381564
NEBC-18	6579659	332851	0.01	43.59	0.05	38.51	0.02	0.21	0.02	0.01	0.19	18.13	100.76	0.810864545
NEBC-18	6579659	332851	0.00	48.90	0.05	39.72	0.01	0.11	0.01	0.05	0.18	10.69	99.71	0.890753872
NEBC-18	6579659	332851	0.04	49.03	0.05	40.23	0.01	0.09	0.03	0.00	0.19	10.33	99.99	0.894318803
NEBC-18	6579659	332851	0.02	42.46	0.04	38.19	0.00	0.21	0.00	0.05	0.24	18.59	99.80	0.802767803
NEBC-18	6579659	332851	0.05	43.16	0.03	38.80	0.01	0.24	0.02	0.04	0.27	18.08	100.70	0.809688989
NEBC-18	6579659	332851	0.01	45.25	0.06	38.96	0.00	0.22	0.00	0.04	0.21	15.63	100.37	0.837703925
NEBC-18	6579659	332851	0.02	43.51	0.04	38.91	0.01	0.20	0.02	0.02	0.20	17.51	100.43	0.815819074
NEBC-18	6579659	332851	0.03	41.85	0.05	38.24	0.00	0.22	0.05	0.06	0.27	18.94	99.72	0.79751405
NEBC-18	6579659	332851	0.02	46.55	0.04	39.47	0.00	0.09	0.01	0.05	0.21	13.86	100.30	0.856846945
NEBC-18	6579659	332851	0.02	45.39	0.03	38.78	0.00	0.08	0.02	0.00	0.17	15.18	99.66	0.8420612
NEBC-18	6579659	332851	0.03	49.35	0.06	40.58	0.00	0.09	0.03	0.02	0.14	10.60	100.90	0.892413402
NEBC-18	6579659	332851	0.01	43.65	0.05	38.79	0.00	0.24	0.01	0.03	0.18	17.26	100.21	0.818503832
NEBC-18	6579659	332851	0.00	45.09	0.03	39.13	0.02	0.22	0.02	0.05	0.21	16.06	100.83	0.833500275
NEBC-18	6579659	332851	0.02	49.48	0.03	40.00	0.02	0.08	0.00	0.08	0.12	10.12	99.94	0.897045379
NEBC-18	6579659	332851	0.01	49.73	0.03	40.28	0.00	0.11	0.00	0.05	0.13	10.44	100.78	0.894647235
NEBC-18	6579659	332851	0.00	43.65	0.04	38.59	0.00	0.21	0.00	0.01	0.25	17.89	100.63	0.81304251
NEBC-18	6579659	332851	0.00	43.70	0.05	38.79	0.00	0.24	0.00	0.04	0.20	17.10	100.11	0.819991566
NEBC-18	6579659	332851	0.01	42.87	0.07	38.11	0.00	0.26	0.05	0.09	0.22	18.31	99.99	0.806682982
NEBC-18	6579659	332851	0.00	47.65	0.05	39.73	0.01	0.07	0.04	0.05	0.13	12.23	99.96	0.874143503
NEBC-18	6579659	332851	0.00	49.38	0.02	40.00	0.00	0.07	0.00	0.02	0.15	10.44	100.09	0.893974877
NEBC-18	6579659	332851	0.00	42.61	0.08	38.64	0.00	0.24	0.00	0.03	0.19	19.26	101.06	0.797693604
NEBC-18	6579659	332851	0.00	50.25	0.02	40.55	0.01	0.05	0.00	0.00	0.14	9.41	100.42	0.904945707
NEBC-18	6579659	332851	0.00	49.28	0.02	40.28	0.01	0.08	0.04	0.01	0.15	10.28	100.13	0.895254953
NEBC-18	6579659	332851	0.02	49.09	0.02	39.94	0.01	0.08	0.00	0.02	0.15	11.10	100.43	0.887455775
NEBC-34	6539551	581206	0.02	49.82	0.04	40.58	0.02	0.06	0.01	0.04	0.21	9.88	100.68	0.899918975
NEBC-37	6570249	567872	0.02	51.57	0.00	41.06	0.00	0.04	0.00	0.03	0.13	7.61	100.46	0.923568485
NEBC-46	6439810	516735	0.01	50.61	0.00	40.63	0.00	0.00	0.00	0.03	0.08	8.76	100.14	0.911496993
NEBC-50	6222613	645018	0.00	49.18	0.02	39.99	0.00	0.06	0.01	0.01	0.15	10.12	99.54	0.896521253
NEBC-50	6222613	645018	0.00	44.25	0.04	38.82	0.00	0.22	0.00	0.05	0.25	17.01	100.64	0.822622844
NEBC-52	6176129	611299	0.01	42.31	0.02	38.37	0.01	0.21	0.02	0.04	0.23	19.24	100.47	0.796719761

root exploration model is applied to northeastern BC (Simandl, 2004).

There are several areas with anomalous counts of kimberlite indicator minerals (Fig. 2). As indicated in the text, these minerals may not have the same source, a concept supported by the glacial history of the area. Samples collected from areas close to the Etsho Plateau are of particular interest because they contain a variety of indicator minerals, including pyrope garnets, Cr-spinel, olivine, ilmenite and Cr-diopside.

Sample NEBC-50, from south of Taylor (Fig. 2), contains 16 indicator grains consisting of Cr-spinel, Cr-diopside and olivine. Sample NEBC-7, from about 100 km northwest of Hudson Hope, is unique because it contains 71 Cr-spinel grains. A direct correlation between the number of indicator mineral grains and proximity to their source is unlikely, as different sampling media were used. As expected, some of the highest indicator mineral counts come from active river sediments, where natural concentration was anticipated.

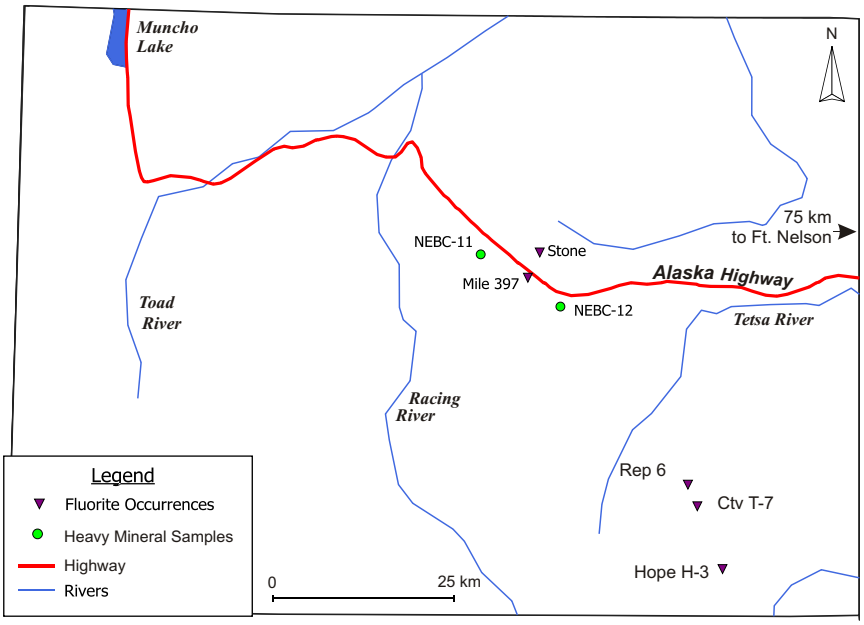


Figure 13. Detailed map showing the location of samples NEBC-11 and 12, which contain the highest concentrations of fluorite grains. Sample NEBC-11 was originally reported to contain a diamond. The known fluorite occurrences are shown as triangles. Their descriptions are available through the BC Ministry of Energy, Mines and Petroleum Resources website at http://www.em.gov.bc.ca/mining/geolsurv/minfile/search/.

In the following discussion, the distribution of anomalous glaciofluvial samples in relation to the maximum extent of the Laurentide, Cordilleran and Rocky Mountain glacial systems, which is approximated by Mathews' line on Figure 2 (Mathews, 1980), is considered.

The first important observation is that all the samples that contain pyrope garnets are located east of Mathews' line, mostly between Fort Nelson and the Etsho Plateau. The samples from this region are characterized by a variety of indicator minerals. They contain G9, G10, G12 and G1 garnets, ilmenite, Cr-spinel and Cr-diopside, as well as G3 garnets recovered during the previous field season (Levson *et al.*, 2004; Simandl *et al.*, 2005). Possible sources for these garnets are known diatremes located northeast of the study area within the Slave Craton, known diatremes of the Buffalo Head Terrane, or undiscovered pipes cutting the Mesozoic to Paleozoic sedimentary rocks in the Etsho Plateau region. Some of these grains may have been previously reworked and incorporated into the sedimentary sequence itself. There is a rapid decline in KIM concentrations in stream sediments with increasing distance from pipes in the Buffalo Head Hills area (Friske *et al.*, 2003). This suggests that these kimberlites are unlikely sources for high concentrations of indicator minerals reported in this study and in Simandl *et al.* (2005). Currently, there are no high concentrations of KIMs reported along the BC-Northwest Territories border. This makes the local origin of the garnets a viable hypothesis. The northern portion of BC's Alkaline Province is not known to contain primary lithologies such as those described by Canil *et al.* (2005); therefore it is an unlikely source of these garnets.

If the samples west of Mathews' line with the highest KIM contents are examined, Cr-spinel and olivine with some Cr-diopside are the potential indicator minerals. The source of these minerals is more difficult to interpret than pyrope garnets or ilmenites because the distinction between Cr-spinels associated with kimberlites and lamproites from those associated with other ultramafic rocks, such as layered intrusions, ophiolites, Alaskan complexes, boninites and minerals from xenoliths in basalt, is a complex procedure. Ultramafic rocks are common in the Cache Creek and the Slide Mountain terranes (Voormeij and Simandl, 2004a, b), but these terranes occur well to the west of the study area.

The details of the interpretation will be the subject of a related paper; however, results of the discrimination procedure are incorporated into Figure 2. The results of this study indicate that a number of Cr-diopsides and Cr-spinels may be related to alkaline intrusions located within the northern portion of the Alkaline Province, as described in Pell (1994) and Simandl (2004).

Based on a combination of discrimination methods (Simandl and Robinson, work in progress), it is possible that some of the Cr-spinels from samples NEBC-1, 7, 23, 44, 50, 52 and 58 are lamproite-related. A more detailed study of chromite morphology, as described by Lee *et al.* (2004), and some trace element analyses are required to corroborate this.

Samples from the Fort St. John area are characterized by dominant Cr-spinels and Cr-diopside kimberlite indicators. Sample NEBC-1, from northeast of Fort St. John, is an exception. It contains 22 indicator grains consisting of Cr-spinel, Cr-diopside and one G9 garnet. Sample NEBC-23 is regolith and sample NEBC-43 is bedrock, both corresponding to the Dunvegan conglomerate and containing numerous Cr-spinel grains. This finding is extremely significant because it demonstrates that at least some of the Cr-spinels were incorporated into the Upper Cretaceous Dunvegan Formation before being incorporated into surficial deposits. If these Cr-spinel grains are indeed related to kimberlites or lamproites, then the age of primary alkaline

rocks from which they were derived is upper Cretaceous or older. Under those circumstances, detailed studies of the Dunvegan Formation may reveal potential heavy mineral traps favourable for formation of paleoplacer diamond deposits. Deep incisions into the Dunvegan Formation, described by Plint and Wadsworth (2003), may represent invaluable information that can help to zero in exploration on potential diamond paleoplacer targets.

The following is a series of other important points and recommendations:

- The Etsho Plateau region contains several samples that warrant further investigation. This region is particularly interesting because of the wide range of KIMs retrieved. Before designing a follow-up exploration program, samples from Simandl *et al.* (2005) should be incorporated into the database generated by this study. There are also high concentrations of non-garnet indicators in the southern part of the study area worth following up.
- Because of the uncertainty regarding the provenance of the diamond recovered, it is recommended that sites NEBC-1 to 11 be resampled and the new samples analyzed. The diamond recovered from sample NEBC-11 may have originated at any of these sites. The samples from these sites that contain high concentrations of potential KIMs are particularly worthy of follow-up. However, the possibility remains that the diamond was derived from one of the samples submitted by the previous client.
- Further studies should pay close attention to the indicator mineral content of sedimentary bedrock. Such information is invaluable in establishing the provenance of Cr-spinel and potentially other indicators in surficial materials commonly sampled by exploration companies and to assigning an age to the potential primary sources of diamonds (including possibly yet undiscovered kimberlite or lamproite pipes). It is therefore recommended to sample material from the strategically located, large-diameter boreholes that are drilled for oil and gas in the Fort Nelson and Fort St. John areas and study recovered heavy minerals.
- Heavy mineral samples should also be examined for the presence of fluorite, barite, sulphides (base metals), gold and platinum. Mississippi Valley-type (MVT) deposits and sedimentary exhalative (SEDEX) type mineralization have been reported in a number of boreholes drilled in this area for oil and gas and a number of known fluorite and barite deposits were reported in this area.
- Many samples are worthy of follow-up. Of particular interest are the samples in the Fort Nelson area that contain several indicator minerals (pyrope garnets, including G10, ± Cr-spinels, ± Cr-diopside ± olivine ± ilmenite). Samples NEBC-38 and 39 are good examples in spite of their low total indicator grain content. The final interpretation of kimberlite potential should also incorporate the data of Simandl *et al*. (2005).
- A number of samples, such as NEBC-1 and 7, contain high concentrations of Cr-spinel. Preliminary interpretation indicates that these Cr-spinels may be lamproite-derived, but this interpretation should be tested using international databases. When a potential source is identified, the composition of Cr-spinels from this source should be compared with that of spinels from anomalous samples. For example, it would be worth comparing the compositions of spinels from the Ospika pipe with those of spinels recovered from sample NEBC-7.
- Available geophysical data obtained during oil and gas exploration, particularly in the Etsho Plateau region, should be re-examined to locate anomalies that may correspond to diatremes and/or dikes.
- There is a major gap in sample coverage in the central portion of the study area, on both sides of the Mathews' line, and in the Trutch and Pink Mountain areas. At least 15 helicopter-supported samples would be required to complete reconnaissance-scale coverage in this region, east of the Mathews' line. There may not be a need for helicopter support west of this line. Samples from this area may contain indicator minerals as well.
- If the Dunvegan Formation is confirmed to contain indicator minerals, as indicated by samples NEBC-23 and 43, then paleogeomorphology could be used to focus exploration on paleoplacer deposits.

SUMMARY

Kimberlite indicator minerals, including peridotitic garnets, ilmenite, Cr-diopside, spinel (chromite) and olivine, were recovered from the -0.5+0.25 mm size fraction of heavy mineral concentrates from northeastern BC. The same indicator minerals, plus corundum and eclogitic garnets, were previously recovered from the Fort Nelson area (Simandl *et al.*, 2005). The concentrates in this study were produced from glaciofluvial sand and gravel and stream sediments. Thirty-eight of the fifty-eight samples collected in this study contain potential KIMs, some with more than one mineral type. Most of the indicator grains appear fresh and subrounded or subangular, but several have sharp edges. Garnets do not appear to have kelyphitic rims, but a few may have an orange-peel texture, suggesting that they were subject to some degree of transportation or at least local reworking.

Indicator minerals present in some samples proximal to, or on, the Etsho Plateau, occur in small-scale, low-energy glaciofluvial systems, and may have a local source perhaps somewhere on the plateau itself, as described by Simandl *et al.* (2005). A number of these samples have several types of kimberlite and diamond indicators. Other samples, particularly those occurring in large-scale, high-energy glaciofluvial systems, may not contain locally derived KIMs. Ongoing studies east of the BC-Alberta border by the Alberta Geological Survey and the Geological Survey of Canada will aid in determining if an eastern provenance for the KIMs in the Etsho Plateau area is a viable hypothesis. The Northwest Territories are another potential source of these indicator minerals. It remains to be established to what degree the till and regional stream sediment

sampling will constrain these reconnaissance-scale anomalies.

For anomalies located west of Mathews' line, the indicator minerals could be locally derived or derived from diatremes located within the Alkaline Province, as reviewed by Simandl (2004). If there are no anomalies upstream or within tributaries of the rivers that were sampled, then the indicator minerals are most likely local. More work is required to determine the source of these anomalies and to confirm if these Cr-spinels are lamproite/kimberlite derived.

The Dunvegan Formation in the Fort Nelson area contains Cr-spinels (*e.g.*, samples NEBC-23 and 43). Systematic sampling and analyses of cuttings from oil and gas wells for heavy minerals is recommended to gain better background information about potential sources of these KIMs.

If the glaciofluvial and fluvial sampling in the neighbouring regions of Alberta and the Northwest Territories do not reveal high concentrations of indicator minerals, then the significance of the indicator anomalies presented on Figure 2 will be further enhanced, pointing to a local provenance.

CONCLUSION

The results of this reconnaissance kimberlite/diamond indicator mineral study, in combination with the tectonic setting of northeastern BC and most recent basement age dates, suggests that northeastern BC has potential to contain kimberlite/lamproite-hosted diamonds.

The presence of potential indicator minerals (Cr-spinels) within the Dunvegan Formation supports the hypothesis that paleoplacer diamond deposits may be present. However, this also opens the possibility that some of the KIMs in glaciofluvial or fluvial sediments may have been derived from sedimentary bedrock, rather than directly from kimberlite or lamproite pipes. Cr-spinel is particularly resistant to weathering and to transport-induced abrasion; it is a mineral that is relatively prone to recycling. Most pyrope garnets (mainly G9 and one G10), encountered in this study, come from glaciofluvial samples that are located in the Etsho Plateau region. These pyropes are associated with a variety of other KIMs, including Cr-diopside, suggesting a more proximal source. As expected, active river sediments have a high, largely Cr-spinel indicator mineral content.

The diamond reported from sample NEBC-11 may have been derived from any of the samples in the NEBC-1 to 11 series. Another possibility is that it came from samples submitted by a previous client (*i.e.*, contamination). Follow-up geological, geochemical and geophysical studies related to KIMs and diamond targets are justified in northeastern BC.

ACKNOWLEDGMENTS

The document benefited from the constructive comments of Suzanne Paradis of the Geological Survey of Canada at the Pacific Geoscience Centre, Sidney, BC, and Brian Grant of the BC Ministry of Energy, Mines and Petroleum Resources, Victoria, BC. Enriching discussions with Herman Grütter, Mineral Services Canada and John Gurney from Mineral Services Laboratories, South Africa, are gratefully acknowledged. Jan Bednarski, Geological Survey of Canada, Sidney, BC, is thanked for his insights into the Quaternary history of the region. Laura Simandl from St. Margaret's School, Victoria, BC, is thanked for photographic documentation of the fieldwork and meticulous sampling.

This study was possible due to financial support from the Rock to Riches program of the BC and Yukon Chamber of Mines and support from the BC Geological Survey and Resource Development and Geoscience Branch of the BC Ministry of Energy, Mines and Petroleum Resources.

REFERENCES

Allan, R.J. (1999): Micro-diamond results from Ice Claim project, BC; *Skeena Resources Limited*, news release, August 20, 1999.

Allan, R.J. (2002): Diamond exploration corporate up-date; *Skeena Resources Limited*, news release, March 22, 2002.

Anonymous (1994): BC diamonds discovered; *in* George Cross News Letter, *Consolidated Ramrod Gold Corporation,* No. 225.

Barnes, S.J. and Roeder, P.L. (2001): The range of spinel compositions in terrestrial mafic and ultramafic rocks; *Journal of Petrology*, Volume 42, pages 2279–2302.

Barnes, S.J. and Roeder, P.L. (2004): Barnes and Roeder global spinel database; *Commonwealth Scientific and Industrial Research Organization (CSIRO),* URL <http://www.em.csiro.au/terrain_studies/aboutus/people/stephen_barnes/BR_spinel_database_dec04.zip> [Jul 2005].

Bednarski, J. (1999): Preliminary report on mapping surficial geology of Trutch (94G), northeastern British Columbia; *Geological Survey of Canada*, Current Research 1999A, pages 35–43.

Bednarski, J.M. (2000): Surficial geology Trutch, British Columbia; *Geological Survey of Canada*, Open File 3885, scale 1:250 000.

Bednarski, J.M. (2001): Drift composition and surficial geology of the Trutch map area (94G) northeastern British Columbia; *Geological Survey of Canada*, Open File D3815, CD-ROM.

Birkett, T.C. and Simandl, G.J. (1999): Carbonatite-associated deposits: magmatic, replacement and residual; *in* Selected British Columbia Mineral Deposit Profiles, Volume 3, Industrial Minerals, Simandl, G.J., Hora, Z.D. and Lefebure, D.V., Editors, *BC Ministry of Energy, Mines and Petroleum Resources*, Open File 1999-10, pages 73–76.

Canil, D., Mihalynuk, M.G. and Charnell, C. (2005): Heavy mineral sampling and provenance studies for potentially diamond-bearing source rocks in the Jurassic Laberge Group, Atlin-Nakina area, northwestern British Columbia (104N); *in* Geological Fieldwork 2004, *BC Ministry of Energy, Mines and Petroleum Resources*, pages 83–92.

Carlson, S.M., Hillier, W.D., Hood, C.T., Pryde, R.P. and Skelton, D.N. (1999): The Buffalo Hills kimberlites: a newly-discovered diamondiferous kimberlite province in north-central Alberta, Canada; *in* Proceedings of the VIIth International Kimberlite Conference, Gurney, J.J., Gurney J.L., Pascoe, M.D. and Richardson, S.H., Editors, Volume 1, pages 109–116.

Dyke, A. (2004): An outline of North American deglaciation with emphasis on central and northern Canada; *in* Quaternary Glaciations-Extent and Chronology, Part II, Ehlers, J. and Gibbard, P.L., Editors, Developments in Quaternary Science, *Elsevier*, Volume 2b, pages 373–424.

Eccles, D.R., Heaman, L.M., Luth, R.W. and Creaser, R.A. (2004): Petrogenesis of the Late Cretaceous northern Alberta kimberlite province; *Lithos*, Volume 76, pages 435–459.

Fipke, C.E., Gurney, J.J., Moore, R.O. and Nassichuk, W.W. (1989): The development of advanced technology to distinguish between diamondiferous and barren diatremes; *Geological Survey of Canada*, Open File 2124, 1175 pages.

Fipke, C.E., Gurney, J.J. and Moore, R.O. (1995): Diamond exploration techniques emphasising indicator mineral geochemistry and Canadian examples; *Geological Survey of Canada*, Bulletin 423, 86 pages.

Friske, P.W.B., Prior, G.J., McNeil, R.J., McCurdy, M.W. and Day, S.J.A. (2003): Relative proportion of kimberlite indicator minerals in stream sediment bulk samples (parts of NTS 84B, 84C, 84F, 84G); *Alberta Geological Survey*, Special Report 66 / *Geological Survey of Canada*, Open File 1790.

Grütter, H.S. and Apter, D.B. (1998): Kimberlite and lamproite-borne chromite phenocrysts with "diamond-inclusion"-type chemistries; Extended Abstract, 7th International Kimberlite Conference, South Africa, pages 280–288.

Grütter, H.S., Gurney, J.J., Menzies, A.H. and Winter, F. (2004): An updated classification scheme for mantle-derived garnet, for use by diamond explorers; *Lithos*, Volume 77, pages 841–857.

Gurney, J.J and Moore, R.O. (1994): Geochemical correlation between kimberlitic indicator minerals and diamonds as applied to exploration; *in* Proceedings of the 5th International Kimberlite Conference, Araxa, Brazil, *Companhia de Pesquisa de Recursos Minerais - CPRM*, Volume 1, page 125.

Haggerty, S.E. (1986): Diamond genesis in a multiply constrained model; *Nature*, Volume 320, pages 34–38.

Haggerty, S.E. (1991): Oxide mineralogy of the upper mantle. Oxide Minerals; *in* Short Course Notes, 3, *Mineralogical Society of America*, pages Hg 101–Hg 300.

Hoffman, P.F. (1988): United plates of America: the birth of a craton; *Annual Reviews in Earth and Planetary Sciences*, Volume 16, pages 543–603.

Hoffman, P.F. (1989): Speculations on Laurentia's first gigayear (2.0-1.0 Ga); *Geology*, Volume 17, pages 135–138.

Hoffman, P.F. (1991): Did the breakout of Laurentia turn Gondwanaland inside-out?; *Science*, Volume 252, pages 1409–1412.

Hood, C.T.S. and McCandless, T.E. (2004): Systematic variations in xenocryst mineral composition at the province scale, Buffalo Hills kimberlites, Alberta, Canada; *Lithos*, Volume 77, pages 733–747.

Hora, Z.D. (1996a): Vein barite; *in* Selected British Columbia Mineral Deposit Profiles, Volume 2 - Metallic Deposits, Lefebure, D.V. and Hõy, T., Editors, *BC Ministry of Employment and Investment*, Open File 1996-13, pages 81–84.

Hora, Z.D. (1996b): Vein fluorite-barite; *in* Selected British Columbia Mineral Deposit Profiles, Volume 2 - Metallic Deposits, Lefebure, D.V. and Hõy, T., Editors, *BC Ministry of Employment and Investment*, Open File 1996-13, pages 85–88.

Leach, D.L. and Sangster, D.F. (1993): Mississippi Valley-type lead-zinc deposits; *in* Mineral Deposit Modeling, Kirkham, R.V., Sinclair, W.D., Thorpe, R.I. and Duke, J.M., Editors, *Geological Association of Canada,* Special Paper 40, pages 289–314.

Lee, D.C., Maddren, J. and Griffin, B.J. (2004): The importance of chromite morphology in diamond exploration; Long Abstract, 8th International Kimberlite Conference, Victoria, Canada, 5 pages.

Levson, V.M., Ferbey, T., Kerr, B., Johnsen, T., Bednarski, J., Smith, I.R., Blackwell, J. and Jonnes, S. (2004): Quaternary geology and aggregate mapping in northeast British Columbia: applications for oil and gas exploration and development; *in* Summary of Activities 2004, *BC Ministry of Energy, Mines and Petroleum Resources*, pages 29–40.

Lockhart, G., Grütter, H. and Carlson, J. (2004): Temporal, geomagnetic and related attributes of kimberlite magmatism at Ekati, Northwest Territories, Canada; *Lithos*, Volume 77, pages 665–682.

McCallum, M.E. (1994): Lamproitic (?) diatremes in the Golden area of the Rocky Mountain Fold and Thrust Belt, British Columbia, Canada; *in* Kimberlites, Related Rocks and Mantle Xenoliths, Proceedings of the 5th International Kimberlite Conference, Araxa, Brazil, *Companhia de Pesquisa de Recursos Minerais - CPRM*, 1, pages 195–209

Massey, N.W.D, MacIntyre, D.G., Desjardins, P.J. and Cooney, T. (2005): Digital geology map of British Columbia; DVD documentation utilities; *BC Ministry of Energy, Mines and Petroleum Resources,* Open File 2005-2.

Mathews, W.H. (1980): Retreat of the last ice sheets in northeastern British Columbia and adjacent Alberta; *Geological Survey of Canada*, Bulletin 331, 22 pages.

McCandless, T.E and Dummett, H.T. (2003): Some aspects of chromian spinel (chromite) chemistry in relation to diamond exploration; Special Session 13: Canadian diamond deposits: History and techniques of their discovery – A Tribute to Hugo Dummett (abstract), *Geological Association of Canada-Mineralogical Association of Canada*, Vancouver.

Mitchell, R.H. (1991): Kimberlites and lamproites: primary sources of diamonds; *Geoscience Canada*, Volume 18, pages 1–16.

Morris, T.F., Sage, R.P., Ayer, J.A. and Crabtree, D.C. (2002): A study in clinopyroxene composition: implications for kimberlite exploration; *Geochemistry: Exploration, Environment, Analysis*, Volume 2, pages 321–331.

Northcote, K.E. (1983a): Report on Mark property, Pangman Peek (82N/15W); submitted by Dia Met Minerals Ltd., *BC Ministry of Energy, Mines and Petroleum Resources,* Assessment Report 13596.

Northcote, K.E. (1983b): Report on Jack Claims Lens Mountain (82N/14E); submitted by Dia Met Minerals Ltd., *BC Ministry of Energy, Mines and Petroleum Resources,* Assessment Report 13597.

Pell, J. (1994): Carbonatites, nepheline syenites, kimberlites and related rocks in British Columbia; *BC Ministry of Energy, Mines and Petroleum Resources*, Bulletin 88, 136 pages.

Plint, A.G., McCarthy, P.J. and Faccini, U.F. (2001): Nonmarine sequence stratigraphy; updip expression of sequence boundaries and systems tracts in a high-resolution framework, Cenomanian Dunvegan Formation, Alberta foreland basin, Canada; *American Association of Petroleum Geologists,* Bulletin, Volume 85, pages 1967–2001.

Plint, A.G. (2002): Paleovalley systems in the Upper Cretaceous Dunvegan Formation, Alberta and British Columbia; *Bulletin of Canadian Petroleum Geology*, Volume 50, pages 277–296.

Plint, A.G. and Wadsworth, J.A. (2003): Sedimentology and palaeogeomorphology of four large valley systems incising delta plains, Western Canada foreland basin; implications for Mid-Cretaceous sea-level changes; *Sedimentology*, Volume 50, pages 1147–1186.

Plouffe, A., Smith, I.R., Paulen, R.C., Fenton, M.M. and Pawlowicz, J.G. (2004): Surficial geology, Bassett Lake, Alberta (NTS 84L/SE); *Geological Survey of Canada*, Open File 4637, scale 1:100 000.

Quirt, D.H. (2004): Cr-diopside (clinopyroxene) as a kimberlite indicator mineral for diamond exploration in glaciated terrains; *in* Summary of Investigations 2004, Volume 2, *Saskatchewan Geological Survey, Saskatchewan Industry Resources,* Miscellaneous Report 2004-4.2, CD-ROM, Paper A-10, 14 pages.

Ramsey, R.R. and Tompkins, L.A. (1994): The geology, heavy mineral concentrate mineralogy, and diamond prospectivity of Boa Esperanca and Cana Verde pipes, Corrego D'anta, Minas Gerais, Brazil; *in* Kimberlites, Related Rocks and Mantle Xenoliths, Proceedings of the 5th International Kimberlite Conference, *Companhia de Pesquisa de Recursos Minerais - CPRM*, Volume 2, pages 329–345.

Roberts, W.J. (2002): Diamond discovery at Xeno; *Pacific Ridge Exploration Limited,* news release, March 13, 2002.

Ross, G.M., Parish, R.R., Villeneuve, M.E. and Bowring, S.A. (1991): Geophysics and geochronology of the crystalline basement of the Alberta Basin, western Canada; *Canadian Journal of Earth Sciences*, Volume 28, pages 512–522.

Ross, G.M., Milkerreit, B., Eaton, D., White, D., Kanasewich, E.R. and Buryanyk, M.J.A. (1995): Paleoproterozoic collisional orogen beneath Western Canada Sedimentary Basin imaged by LITHOPROBE crustal seismic reflection data; *Geology*, Volume 23, pages 195–199.

Schulze, D.J. (2003): A classification scheme for mantle-derived garnets in kimberlite: a tool for investigating the mantle and exploring for diamonds; *Lithos*, Volume 71, pages 195–213.

Simandl, G.J. (2004): Concepts for diamond exploration in "on/off craton" areas - British Columbia, Canada; *Lithos*, Volume 77, pages 749–764.

Simandl, G.J. and Davis, W. (2005): Cratonic basement in northeastern British Columbia, new age dates and their significance for diamond exploration; *in* Geological Fieldwork 2004, *BC Ministry of Energy, Mines and Petroleum Resources*, pages 337–346.

Simandl, G.J., Ferbey, T., Levson, V.M., Demchuk, T.E., Smith, I.R. and Kjarsgaard, I. (2005): Kimberlite indicator minerals in the Fort Nelson area, northeastern British Columbia; *in* Geological Fieldwork 2004, *BC Ministry of Energy, Mines and Petroleum Resources*, pages 325–336.

Smith, C.B., Colgan, E.A., Hawthorne, J.B. and Hutchinson G. (1988): Emplacement age of the Cross kimberlite, southeastern British Columbia, by Rb-Sr phlogopite method; *Canadian Journal of Earth Sciences*, Volume 25, pages 790–792.

Stott, D.F. (1982): Lower Cretaceous Fort St John Group and Upper Cretaceous Dunvegan Formation of the foothills and plains of Alberta, British Columbia, District of MacKenzie and Yukon Territory; *Geological Survey of Canada*, Bulletin 328, 124 pages.

Thompson, R.I. (1977): Geology of Beatton River, Fontas River and Petitot River map-areas, northeastern British Columbia; *Geological Survey of Canada*, Paper 75-11, 8 pages.

Thorleifson, L.H., Garrett, R.G. and Matile, G.L.D. (1994): Prairie kimberlite study - indicator mineral geochemistry; *Geological Survey of Canada*, Open File 2875, 1 diskette.

Villeneuve, M.E., Ross, G.M., Thérialt, R.J., Miles, W., Parrish, R.R. and Broome, J. (1993): Tectonic subdivision and U-Pb geochronology of the crystalline basement of the Alberta basin, western Canada; *Geological Survey of Canada*, Bulletin 447, 93 pages.

Voormeij, D.A. and Simandl, G.J. (2004a): A map of ultramafic rocks in British Columbia: applications in CO_2 sequestration and mineral exploration; *BC Ministry of Energy, Mines and Petroleum Resources*, Geofile 2004-1.

Voormeij, D.A. and Simandl, G.J. (2004b): Ultramafic rocks in British Columbia: delineating targets for mineral sequestration of CO_2; *in* Summary of Activities, *BC Ministry of Energy, Mines and Petroleum Resources*, pages 157–167.

Wyatt, B.A., Baumgartner, M., Ancar, E. and Grütter, H. (2004): Compositional classification of "kimberlitic" and "non-kimberlitic" ilmenite; *Lithos*, Volume 77, pages 819–840.

Summary of Geoscience BC Program Activities 2005[1]

by Robert A. Stevens[2]

KEYWORDS: geochemistry, archived data, ASTER, Bowser Basin, Skeena arch, Whitesail Lake, Anahim Lake, Nechako River, Nootka Sound, Lillooet, Sicker Group, kimberlite, halogens

INTRODUCTION

Geoscience BC is an innovative and applied geoscience centre formed in 2005 and dedicated to the collection, interpretation and marketing of geoscience expertise, information and products in support of resource exploration in British Columbia. The mandate is to attract investment in the mineral and oil and gas industries in BC through applied geoscience work. In support of this mandate, Geoscience BC is pleased to present its first set of technical progress reports for projects funded during the spring and summer of 2005. These projects build on previous geoscience work completed and supported by the BC Geological Survey and the Resource Development and Geosciences Branch of the BC Ministry of Energy, Mines and Petroleum Resources, by the Geological Survey of Canada and by universities and industry.

The Geoscience BC projects (Fig. 1) include

- regional geochemical survey programs (the BC portions of six 1:250 000-scale NTS sheets were completed);
- geochemical studies to develop methods for detecting blind deposits in central BC;
- northeastern BC kimberlite indicator mineral study;
- mapping and mineral potential projects on Vancouver Island and in central BC;
- hydrocarbon potential study of the Bowser Basin;
- Advanced Spaceborne Thermal Emission and Reflection Radiometer (ASTER) imagery project;
- community geoscience needs for the Lillooet – Lytton area; and
- Placer Dome archived data capture project in central BC.

The Geoscience BC programs presented in this volume are one and two-year projects. Final data releases will be as early as January 2006 for the ASTER project by Kilby and Kilby (2006) and April 2006 for the RGS programs by Jackaman (2006) and Naas (2006). Other projects will produce final results from the fall of 2006 through to the spring of 2007. All data will be released through the publication systems of the BC Geological Survey and will be made available for viewing on their MapPlace website (www.MapPlace.ca) and on Geoscience BC's website (www.geosciencebc.com).

GEOCHEMISTRY PROJECTS

Regional geochemical survey (RGS) programs have a history of success in BC, and targets produced by these surveys are well known to generate grass-roots exploration that leads to new mineral deposit discoveries. During the 2005 field season, Geoscience BC completed RGS programs over two 1:250 000-scale NTS map sheets in central BC (NTS 093C, F; Jackaman, 2006) and over the BC parts of four 1:250 000-scale, NTS map sheets in the southeastern part of the province (NTS 083C, D, E and 082N; Naas, 2006). The RGS program in central BC covers a large portion of the Nechako Plateau, and these two sheets are the last remaining NTS sheets in the interior of BC to receive RGS coverage. The Nechako Plateau is a relatively flat interior region with poor drainage and an abundance of lakes; as a result, most of the samples collected in this area are lake sediments. In total, 1885 lake sediment and water samples and 102 stream sediment and water samples were collected at 1957 sites (Fig. 2). This program was the largest lake sediment sampling program ever completed in BC. The NTS map sheets completed in southeastern BC are the first of what is expected to be a series of programs to complete RGS coverage in the eastern part of the province. In total, 1409 sites were sampled for stream sediment and water. The RGS results from both survey areas are expected to be released in April 2006.

A significant part of the central interior of BC is covered by unconsolidated Quaternary cover and Tertiary volcanic rocks that hinder exploration for mineral deposits in the underlying, potentially productive bedrock. Even though the central interior of BC contains prospective geology, a map of known mineral occurrences (MINFILE, 2005) shows a dearth of occurrences in this drift-covered area. To address these challenges to mineral exploration, two Geoscience BC projects were undertaken during 2005 (Cook and Dunn, 2006; Dunn *et al.,* 2006) to develop geochemical methods for detecting blind deposits. The project by Cook and Dunn (2006) was designed to determine and recommend the most effective geochemical methods of exploration for buried mineral targets in drift-covered terrain in central BC by evaluating the most suitable soil horizons for field sampling, and evaluating and comparing commercially available analytical methods. In 2005, 7 samples were collected at each of 36 sample sites along profiles across epithermal veins on a Au-Ag epithermal prospect

[1] *Geoscience BC contribution GBC001*

[2] *Geoscience BC, 410 - 890 West Pender Street, Vancouver, BC V6C 1J9 (rstevens@geosciencebc.com)*

This publication is also available, free of charge, as colour digital files in Adobe Acrobat PDF format from the BC Ministry of Energy, Mines and Petroleum Resources internet website at http://www.em.gov.bc.ca/Mining/Geolsurv/Publications/catalog/catfldwk.htm

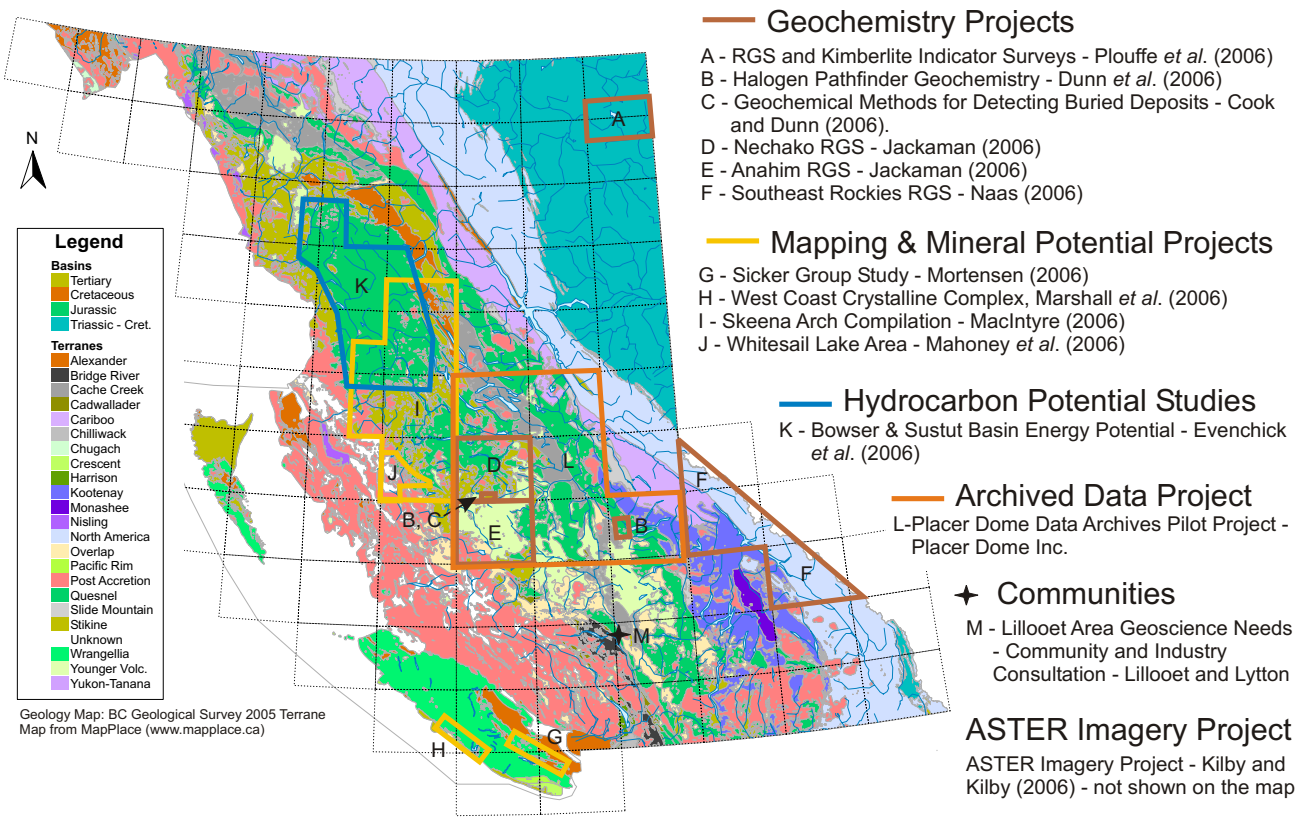


Figure 1. Location of Geoscience BC projects initiated in 2005.

(3Ts prospect). The samples will be analyzed using 6 different analytical methods, including selective extraction methods. The project, outlined in Dunn *et al.* (2006), will evaluate the use of halogens in both soils and vegetation as a means of detecting buried deposits. The use of halogens in geochemical exploration has received little attention in Canada; however, the results of studies recently translated from Russian suggest they may be effective for detecting buried deposits (Trofimov and Rychkov, 2004). As a first step in evaluating the use of halogens, Dunn *et al.* (2006) will determine the response of halogens in soils and vegetation to known mineralization and compare these responses to multielement inductively coupled plasma – mass spectrometry (ICP-MS) data on the same samples. In 2005, over 450 vegetation samples and almost 200 soil samples were collected from three properties, the 3Ts, QR and Mt. Polley deposits, in central BC.

The announcement of kimberlite indicator minerals (KIMs) from glaciofluvial samples in northeastern BC (Simandl, 2005a, b) has highlighted the possibility of diamond occurrences in this part of the province. To evaluate this potential, the project by Plouffe *et al.* (2006) involves the collection of glacial sediment, as well as stream sediment, water and heavy mineral concentrate samples, that will be used to better understand the potential sources of KIMs in this region. The samples will also be used to investigate the potential for gold, base metal and other economic commodities. In addition, this project will help evaluate aggregate resources in this region, resources that are critical to the development of infrastructure for oil and gas exploration in northeastern BC. In 2005, 123 glacial sediment samples, comprising 25



Figure 2: Regional lake sediment and water sampling in the Nechako Plateau using a float-equipped helicopter. Photo courtesy of W. Jackaman.



Figure 3: Glacial sediment sampling in support of kimberlite exploration in northeastern BC. Photo courtesy of I.R. Smith.



Figure 4: Chatsquot layered mafic intrusion on the southern flank of Chatsquot Mountain in the Whitesail Lake map area. Photo courtesy of Robert L. Hooper.

glaciofluvial samples and 98 till samples, were collected (Fig. 3). Analytical results are pending.

MAPPING AND MINERAL POTENTIAL PROJECTS

Detailed geological mapping has long been recognized as an important geoscience tool to improve exploration activity and success in a given region. To this end, Geoscience BC has supported three mapping projects in key geological areas, in order to improve the understanding of basic geology and mineral potential in these regions. The project reported by Mortensen (2006) will evaluate the Sicker Group on Vancouver Island, which is known to host volcanogenic massive sulphide (VMS) occurrences and deposits, such as the Myra Falls deposit. Despite the potential of the Sicker Group, exploration activity within it has been at a low level for the past decade. In addition to low commodity markets, this is likely due to a poor overall understanding of the geology and a lack of identification of the key stratigraphic level(s) that may host mineralization. The project by Mortensen (2006) will address these challenges through detailed geological mapping, lithogeochemistry, stratigraphic correlation, Pb-isotope geochemistry and geochronology. During the 2005 field season, 42 samples were collected for major, trace and rare earth elements, and 15 samples for U-Pb dating.

Also on Vancouver Island, Marshall *et al.* (2006) outlined a study to evaluate the geology and mineralization in the Nootka Sound area. Recent work by Marshall *et al.* (2005) suggests that a number of the rock units in the area correlate with volcanic assemblages and intrusive rocks that are known to host mineralization outside the area (*e.g.,* Zeballos or Myra Falls deposits). The primary goals of this study are to better understand the mineral potential of the area through improved geological mapping, lithogeochemistry, and metallogenic and mineral deposit studies. A number of potential exploration targets were identified during mapping in 2005.

The third mapping and mineral potential project is outlined by Mahoney *et al.* (2006). This project involves detailed geological mapping and mineral deposit studies of Mesozoic volcanic rocks of the western Stikinia Terrane and Mesozoic plutonic rocks along the eastern edge of the Coast Plutonic Complex in the Whitesail Lake map area (NTS 093E). This area has high mineral potential: stream sediment geochemistry and MINFILE (2005) data and detailed geological mapping to the north and south indicate potential for volcanogenic massive sulphide, Cu±Mo±Au porphyry and Ni-Cu-Cr-platinum group element mineralization (Mahoney *et al.,* 2006). Work during 2005 focused on bedrock mapping and preliminary evaluation of min-

eral potential in the southwestern corner of the Whitesail Lake map area (Fig. 4).

In addition to the mapping projects outlined above, MacIntyre (2006) discusses a project to produce a digital data compilation of the geology and mineral deposits of the Skeena arch in west-central BC. The Skeena arch is a belt of uplifted Jurassic and older rocks in central BC exposing a long-lived magmatic arc that has produced a diverse range of mineral deposits in a wide variety of geological settings. This area represents some of the most richly endowed terrain in BC and has been the site of extensive mineral exploration. This project will compile all geoscience data relevant to mineral exploration into a comprehensive GIS database that will include definition of exploration targets based on the positive correlation of indicators such as geochemical and geophysical anomalies and stratigraphic setting. A set of updated and standardized 1:100 000-scale maps will be generated for the Skeena arch, and all products will be provided on CD and available on the MapPlace website.

HYDROCARBON POTENTIAL STUDY

The interior sedimentary basins of BC, such as the Nechako, Bowser and Sustut basins, have generally been underexplored for hydrocarbon resources, largely due to the reconnaissance nature of geoscience data that evaluates this potential. Geoscience BC will address this need for more geoscience data to evaluate the hydrocarbon potential of the interior sedimentary basins over the coming few years. In 2005, one multicomponent project was initiated to address the hydrocarbon potential in the Bowser Basin (Evenchick *et al.,* 2006; Waldron *et al.,* 2006). One component of this project involves fission-track thermochronolgy studies in the southern part of the basin (Evenchick *et al.,* 2006). These studies are important to establish the timing of hydrocarbon maturation relative to the development of structures in the basin. In the 2005 field season, 29 samples were collected for fission track studies. The second component of the project includes an integration and publication of all field data from geoscience and hydrocarbon potential studies undertaken in the Bowser and Sustut basins over the past several years by the Geological Survey of Canada and the BC Ministry of Energy, Mines and Petroleum Resources (Evenchick *et al.,* 2006).

The third component of the project, outlined in Waldron *et al.* (2006), involves a detailed study of the early geological history and structural development of the Bowser Basin. This study will focus on better understanding the stratigraphic succession at the base of the Bowser Basin, which is thought to contain the best potential source rocks for hydrocarbon deposits. In addition, it will examine the structural development and character of the Cretaceous–Tertiary Skeena fold belt, which will assist in identifying potential hydrocarbon traps. In particular, the study will examine the development of structural domes and the relationship between folds and faults in the Bowser Basin.

ASTER IMAGERY PROJECT

The Advanced Spaceborne Thermal Emission and Reflection Radiometer (ASTER) imagery project by Kilby and Kilby (2006) will make available 100 new ASTER images of BC for analysis and download through the Image Analysis Toolbox (IAT) on the BC Geological Survey's MapPlace website. The ASTER instrument captures readings from the surface of the Earth in a range of wavelengths within the electromagnetic spectrum. The information captured in these images can be processed to produce a number of different products that are useful for the exploration industry. This project will provide the raw ASTER imagery for download, as well as a number of derived products, including a rock-mask filter, alteration images, a digital elevation model, 3-D images and digital stereo pairs. In addition, several of the products from this project can be incorporated into Google Earth for an enhanced level of data viewing.

OTHER PROJECTS (COMMUNITIES AND ARCHIVED DATA)

In addition to the projects summarized above, for which papers are presented in this volume, Geoscience BC initiated two other innovative projects in 2005. One of these projects was co-sponsorship of a community geoscience forum in Lillooet in October 2005. This project stemmed from a proposal submitted to Geoscience BC from the communities of Lillooet and Lytton. The forum brought together community leaders, industry, local prospectors, government and local First Nations to examine the geoscience needs of the Lillooet – Lytton area. The aim was to develop an updated list of key geoscience projects in the area that would help to increase exploration within the region and thus diversify and strengthen the local economy. A total of 25 projects was identified and prioritized during the meeting (see www.geosciencebc.com for the list of projects). The list of projects will assist the communities, industry, consultants, government and others with formulating project proposals, which may be submitted to Geoscience BC in response to future requests for proposals.

Geoscience BC has also initiated an archived data capture pilot project in partnership with Placer Dome Inc. The scope of this project is to publicly release Placer Dome's geoscience data from undeveloped properties within an area of central BC that incorporates seven 1:250 000-scale NTS map sheets. The data will be scanned, converted into a modern GIS database and made publicly available through MapPlace. Geoscience BC hopes to use this pilot project to establish the most effective means of capturing, organizing and disseminating large quantities of diverse geoscience data. Once an optimum process is established, the intention is to expand the pilot project to include Placer Dome's archived data in the rest of BC and to encourage other companies to move their archived data into the public domain.

SUMMARY

Geoscience BC is pleased to present the technical progress reports found in this volume. These reports highlight the high-quality projects that are underway in partnership with industry, universities and government. The results of these projects will enhance the geoscience database for the province of BC and encourage new and more exploration for minerals and oil and gas.

ACKNOWLEDGMENTS

Geoscience BC would like to thank the authors of the Geoscience BC reports for the excellent progress on their

respective projects and for the timely reporting of preliminary results, and the members of the Technical Advisory Committee for their help with review and evaluation of project proposals. Geoscience BC would also like to thank the BC Geological Survey, in particular Brian Grant, for help and support in preparing the Geoscience BC publications and for publishing these papers in this volume.

REFERENCES

Cook, S.J. and Dunn, C.E. (2006): Preliminary results of the Cordilleran geochemistry project: a comparative assessment of soil geochemical methods for detecting buried mineral deposits, 3Ts Au-Ag prospect (NTS 093F/3), central British Columbia; *in* Geological Fieldwork 2005, *BC Ministry of Energy, Mines and Petroleum Resources*, Paper 2006-1 and *Geoscience BC*, Report 2006-1.

Dunn, C.E., Cook, S.J. and Hall, G.E.M. (2006): Halogens in surface exploration geochemistry: evaluation and development of methods for detecting buried mineral deposits (NTS 093F/3), central British Columbia; *in* Geological Fieldwork 2005, *BC Ministry of Energy, Mines and Petroleum Resources*, Paper 2006-1 and *Geoscience BC*, Report 2006-1.

Evenchick, C.A., O'Sullivan, P.B. and Waldron, J.W.F. (2006): Targeted energy-resource studies in the Bowser and Sustut interior basins of British Columbia; *in* Geological Fieldwork 2005, *BC Ministry of Energy, Mines and Petroleum Resources*, Paper 2006-1 and *Geoscience BC*, Report 2006-1.

Jackaman, W. (2006): Drainage sediment and water geochemical surveys in the Anahim Lake and Nechako River map areas (NTS 093C and F), central British Columbia; *in* Geological Fieldwork 2005, *BC Ministry of Energy, Mines and Petroleum Resources*, Paper 2006-1 and *Geoscience BC*, Report 2006-1.

Kilby, W.E. and Kilby, C.E. (2006): ASTER imagery for British Columbia – an online exploration resource; *in* Geological Fieldwork 2005, *BC Ministry of Energy, Mines and Petroleum Resources*, Paper 2006-1 and *Geoscience BC*, Report 2006-1.

MacIntyre, D. (2006): Geology and mineral deposits of the Skeena arch, west-central British Columbia: a Geoscience BC digital data compilation project; *in* Geological Fieldwork 2005, *BC Ministry of Energy, Mines and Petroleum Resources*, Paper 2006-1 and *Geoscience BC*, Report 2006-1.

Mahoney, J.B., Haggart, J.W., Hooper, R.L., Snyder, L.D. and Woodsworth, G.J. (2006): Geological setting and mineralization potential of the southwestern Whitesail Lake map area (NTS 093E), western British Columbia: preliminary assessment; *in* Geological Fieldwork 2005, *BC Ministry of Energy, Mines and Petroleum Resources*, Paper 2006-1 and *Geoscience BC*, Report 2006-1.

Marshall, D., Podstawskyj, N. and Aichmeier, A. (2005): Gold mineralization and geology in the Zeballos area, Nootka Sound, British Columbia; *in* Geological Fieldwork 2004, *BC Ministry of Energy, Mines and Petroleum Resources*, Paper 2005-1, pages 301–310.

Marshall, D., Lesiczka, M., Xue, G. and Close, S. (2006): Update on the mineral deposit potential of the Nootka Sound region (NTS 092E), west coast of Vancouver Island, British Columbia; *in* Geological Fieldwork 2005, *BC Ministry of Energy, Mines and Petroleum Resources*, Paper 2006-1 and *Geoscience BC*, Report 2006-1.

MINFILE (2005): MINFILE BC mineral deposits database; *BC Ministry of Energy, Mines and Petroleum Resources*,URL <http://www.em.gov.bc.ca/Mining/Geolsurv/Minfile/> [Nov 2005].

Mortensen, J.K. (2006): Stratigraphic and paleotectonic studies of the Middle Paleozoic Sicker Group and contained VMS occurrences, Vancouver Island, British Columbia; *in* Geological Fieldwork 2005, *BC Ministry of Energy, Mines and Petroleum Resources*, Paper 2006-1 and *Geoscience BC*, Report 2006-1.

Naas, C.O. (2006): 2005 Regional geochemical survey, southeastern British Columbia (NTS 083C, D, E and 082N); *in* Geological Fieldwork 2005, *BC Ministry of Energy, Mines and Petroleum Resources*, Paper 2006-1 and *Geoscience BC*, Report 2006-1.

Plouffe, A., Smith, I.R., McCurdy, M., Friske, P., Ferbey, T., Bednarski, J., Levson, V.M., Demchuk, T.E., Trommelen, M., Day, S. and Hickin, A.S. (2006): Glacial and stream sediments sampling in support of kimberlite exploration in northeastern British Columbia; *in* Geological Fieldwork 2005, *BC Ministry of Energy, Mines and Petroleum Resources*, Paper 2006-1 and *Geoscience BC*, Report 2006-1.

Simandl, G.J., Ferbey, T., Levson, V.M., Demchuk, T.E., Hewett, T., Smith, I.R. and Kjarsgaard, I. (2005a): Heavy mineral survey and its significance for diamond exploration, Fort Nelson area, British Columbia, Canada; *BC Ministry of Energy, Mines and Petroleum Resources*, Geofile 2005-13, 1 map sheet.

Simandl, G.J., Ferbey, T., Levson, V.M., Demchuk, T.E., Mallory, S., Smith, I.R. and Kjarsgaard, I. (2005b): Kimberlite indicator minerals in the Fort Nelson area, northeastern British Columbia; *in* Geological Fieldwork 2004, *BC Ministry of Energy, Mines and Petroleum Resources*, pages 325–343.

Trofimov, N.N. and Rychkov, A.I. (2004): Iodine and bromine: geochemical indicators of deep ore deposits; *Colorado Mountain Publishing House*, Denver, CO, 205 pages.

Waldron, J.W.F., Gagnon, J.-F., Loogman, W. and Evenchick, C.A. (2006): Initiation and deformation of the Jurassic–Cretaceous Bowser Basin: implications for hydrocarbon exploration; *in* Geological Fieldwork 2005, *BC Ministry of Energy, Mines and Petroleum Resources*, Paper 2006-1 and *Geoscience BC*, Report 2006-1.

Preliminary Results of the Cordilleran Geochemistry Project: A Comparative Assessment of Soil Geochemical Methods for Detecting Buried Mineral Deposits, 3Ts Au-Ag Prospect (NTS 093F/03), Central British Columbia[1]

By Stephen J. Cook[2] and Colin E. Dunn[3]

KEYWORDS: exploration, geochemistry, till, soil, humus, overburden, geochemical survey, geochemical anomaly, Au-Ag epithermal mineralization

INTRODUCTION

Effective mineral exploration in the Nechako Plateau and adjoining regions of central British Columbia has for many years been hindered by thick forest cover, an extensive blanket of till and other glacial deposits and, locally, widespread Tertiary basalt cover. Where undertaken, regional till and lake sediment geochemical surveys have been effective as reconnaissance exploration techniques. However, few publicly available studies have been conducted here into the use of surficial geochemistry to aid in prioritizing regional geochemical anomalies, or in carrying out the most effective geochemical surveys at a property scale in areas of exotic cover. In this respect, BC has lagged far behind other provincial and international jurisdictions in undertaking applied geochemical exploration research.

In response to a call from Geoscience BC for geoscience projects to promote resource investment in BC, this project investigates the geochemical response, in soil and Quaternary materials, of a Au-Ag epithermal prospect (3Ts prospect) in central BC (Fig. 1). This region is highly prospective for the discovery of epithermal Au deposits, among other mineral deposit types, and the low-sulphidization 3Ts prospect is one of the more significant examples of this type in the region. The objective of the project is to determine and recommend the most effective field and laboratory geochemical methods for property-scale evaluation of buried mineral targets in drift-covered terrain, by 1) evaluating the most suitable soil media and horizons for field sampling, and 2) evaluating and comparing commercially available analytical methods.

The study comprises an integrated field and laboratory investigation of comparative soil horizons, analytical digestions and selective extraction methods on soil from transects across two of the 3Ts mineralized vein systems, the Tommy vein and the Ted vein. Geochemical analyses

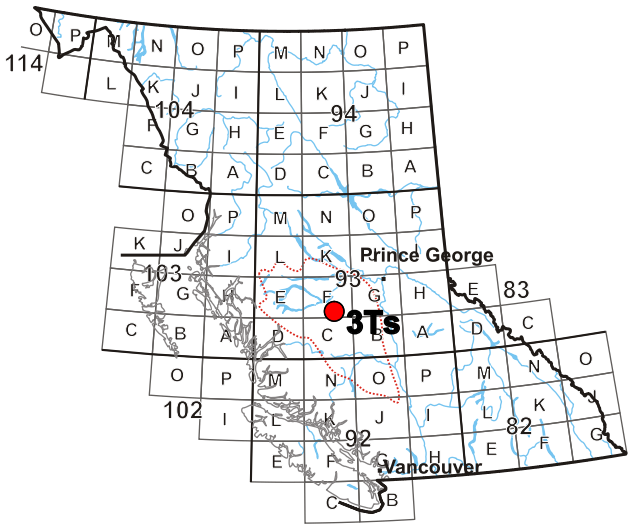


Figure 1. Location of the 3Ts epithermal Au-Ag prospect and the Cordilleran Geochemistry Project study site in the southern Nechako Plateau area of central BC.

were conducted on samples from a range of soil horizons spanning the 3Ts prospect using several commercially available partial and selective extraction methods, including

- aqua regia digestion – inductively coupled plasma–mass spectrometry (ICP-MS),
- Na-Pyrophosphate Leach[SM],
- Enzyme Leach (EL)[SM],
- Mobile Metal Ion (MMI)[SM],
- Soil Gas Hydrocarbons (SGH)[SM], and
- Soil Desorption Pyrolysis (SDP)[SM].

This progress report will outline the full field and analytical methodology scope of the project, but preliminary results reported here will focus solely on comparative aqua regia digestion – ICP-MS Au and Ag results for LFH horizon humus, B horizon soil and underlying C horizon till.

This project is envisioned as a smaller, more restricted, Cordilleran analogue of the successful central Canadian CAMIRO 'Deep Penetrating Geochemistry' project and its successors. These and similar projects, spearheaded by the Geological Survey of Canada and the Ontario Geological Survey, have provided a wealth of objective data and valuable interpretive results for effective geochemical exploration beneath exotic overburden (*e.g.*, Cameron *et al.*, 2004; Bajc, 1998). No similar, publicly available, comparative

[1] *Geoscience BC contribution GBC002*

[2] *Cook Geochemical Consulting, Victoria, BC*

[3] *Consulting Geochemist, Sidney, BC*

This publication is also available, free of charge, as colour digital files in Adobe Acrobat PDF format from the BC Ministry of Energy, Mines and Petroleum Resources internet website at http://www.em.gov.bc.ca/Mining/Geolsurv/Publications/catalog/catfldwk.htm

geochemical methodology studies have been conducted in the western Cordillera, and it is this vacuum that the project attempts to fill. As well, this project complements the parallel Geoscience BC research project 'Halogens in surface exploration geochemistry: method development' (Dunn *et al.*, 2006); The 3Ts prospect is one of three mineral deposits of varying types selected for this study of halogen geochemical responses in B horizon soil and vegetation.

Project deliverables are to include practical recommendations on the most appropriate field sampling, preparation and analytical techniques for epithermal Au deposit exploration in this environment. Where and what to sample? Which analytical methods reflect the presence of buried mineralization, and which do not? Which of the methods provide the greatest and optimal geochemical contrast for property-scale exploration? Answering these questions will assist mineral exploration companies in conducting the most effective geochemical exploration programs for blind targets, thereby increasing the likelihood of discovery.



Figure 2. South-facing view toward 3Ts Au-Ag project area, showing the Little Adrian Lake drainage and the effects of mountain pine beetle damage on lodgepole pine trees, June 2005.



Figure 3. Typical lodgepole pine and white spruce forest, showing ubiquitous thick cover of surface moss at 3Ts property, eastern portion of Ted vein geochemical orientation line (site 570) near Adrian Lake, July 2005.

LOCATION, ACCESS AND PHYSIOGRAPHY

The 3Ts Au-Ag prospect is located in the Fawnie Creek map area (NTS 093F/03), about 125 km south of Vanderhoof, in the southern Nechako Plateau region of the Interior Plateau of central BC. The property is reached by following the Kenny Dam Road and then the Kluskus Forestry Road south from Vanderhoof for about 161 km, and then by the Green 9000 Road to the old Tsacha exploration road to the former Teck Corporation campsite. As truck access to the property via the Green 9000 Road is prevented by the recent removal of a bridge, current access is by all-terrain vehicle from the Teck campsite along old exploration roads (Fig. 2). Poor access brought about by removal of the bridge caused a significant increase in the time and expense needed to complete the project.

The prospect is located in the Tommy Lakes region of the Naglico Hills, an area of rolling hills, small lakes and ponds, and minor wetland areas (elevation 1065–1250 m). It is just north of the Blackwater River, which separates the Nechako Plateau to the north from the Fraser Plateau to the south. Quartz veining and associated alteration systems are relatively resistant to weathering and locally form small but prominent ridges between Tommy Lake to the north and Adrian Lake to the east. Lodgepole pine (*Pinus contorta*) and white spruce (*Picea glauca*) are the most common trees on the property (Fig. 3). They were the object, in part, of the parallel halogen geochemistry study by Dunn *et al.* (2006). Aspen (*Populus tremuloides*) is also locally present. The dominant lodgepole pine here has, as elsewhere in central BC, been affected by the recent mountain pine beetle infestation.

BEDROCK GEOLOGY AND MINERAL DEPOSITS

Exploration History

The original Tommy vein discovery of what is now the 3Ts project area was staked in early 1994 by Teck Corpora-

tion as the Tsacha property (MINFILE 093F 055; MINFILE, 2005), following the release of BC Geological Survey surface rock geochemical data (up to 3.7 g/t gold and 41.8 g/t silver) by Diakow *et al.* (1994). A bedrock mapping party had discovered an auriferous quartz vein system outcropping on hummocky moss-covered rock knobs in the Tommy Lakes area, and released the gold results at the Cordilleran Roundup conference in Vancouver in January 1994. Other properties staked included the Taken property (MINFILE 093F 068). Release of regional lake sediment geochemical data (Fig. 4) for the southern Nechako area during the summer of 1994 (Cook and Jackaman, 1994) helped bring about additional staking in the area. Initial surface sampling across the Tommy vein by Teck returned assays of up to 61.9 g/t gold and 292.5 g/t silver (Pautler, 1995). Exploration of the Tsacha (Teck) and Taken (Phelps Dodge) properties during the period 1994–1999 expanded the known mineralized vein system to include several additional veins, including the Ted vein. During this period, 81 holes totalling more than 16 000 m were drilled on the Tsacha property, primarily on the Tommy vein. The inferred resource on the Tsacha property is 470 700 t grading 7.4 g/t Au and 65.2 g/t Ag, based on a 4 g/t Au cutoff grade (Wallis and Fier, 2002).

After a period of inactivity, Southern Rio Resources Ltd. staked the adjacent Tam property in 2001, optioned the Tsacha and Taken properties in 2002 from Teck Cominco and Phelps Dodge, respectively, and consolidated the claim groups (~34 km^2) as the 3Ts project. Recent work by Southern Rio has included the continued drilling of the Tommy and Larry veins, and the discovery of several areas of mineralized boulders.

Regional and Property Bedrock Geology

Regional geology of the southern Nechako Plateau was first mapped by Tipper (1963) and more recently by Diakow *et al.* (1994, 1995) and Diakow and Levson (1997). This part of the Stikine Terrane is dominated by volcanic and sedimentary units of the Lower to Middle Jurassic Hazelton Group. These are intruded by the Late Jurassic Capoose batholith to the north, and locally overlain by Eocene volcanic units of the Ootsa Lake Group. Miocene-Pliocene Chilcotin Group basalt flows are present in low-lying areas to the south, obscuring the presence of older, more prospective rock units.

Property-scale mapping was carried out by Pautler *et al.* (1999). Hazelton Group rocks hosting epithermal quartz

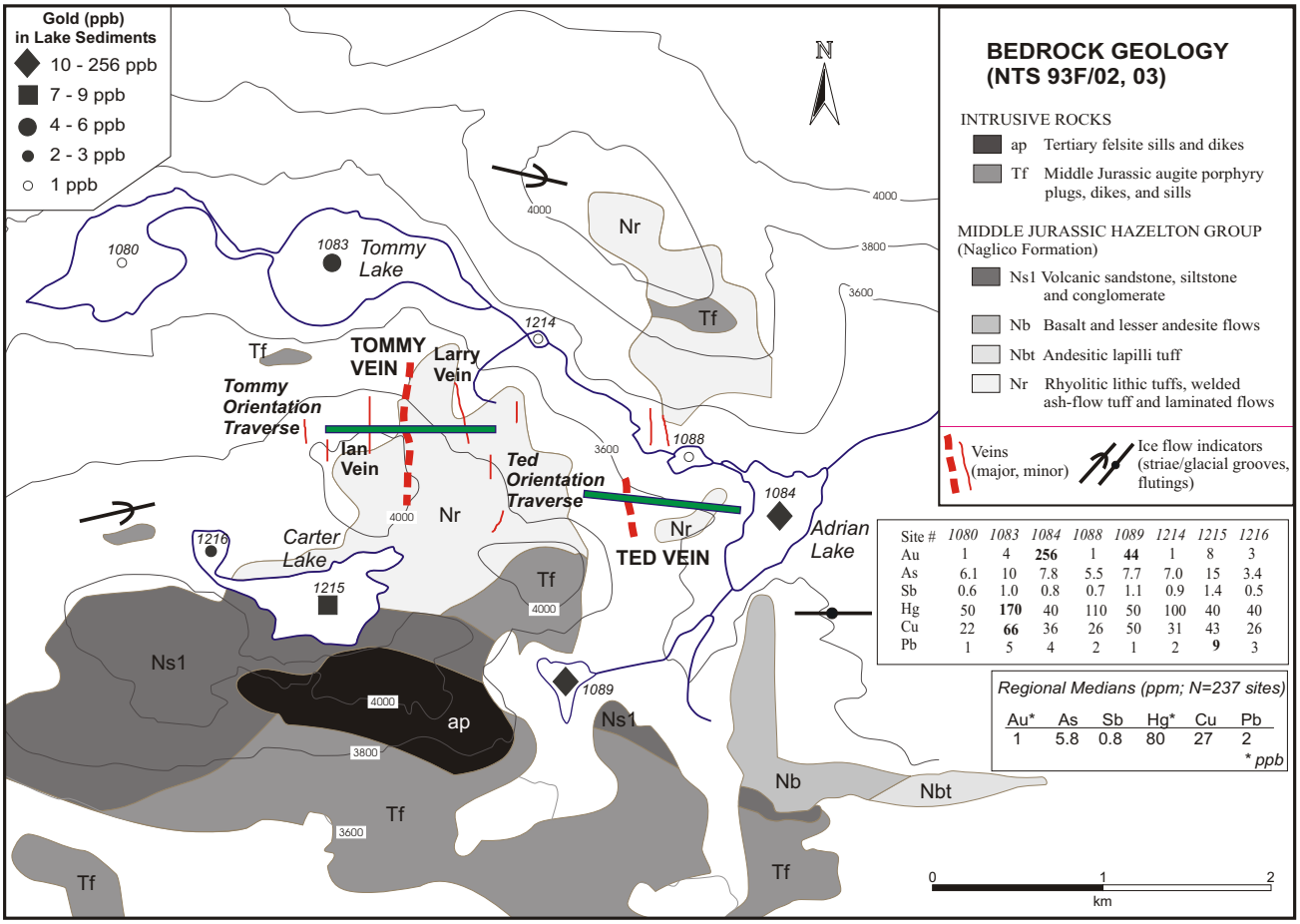


Figure 4. Bedrock geology of the 3Ts epithermal Au-Ag project area, southern Nechako Plateau (NTS 093F/02, 03), showing locations of mineralized veins and 2005 soil orientation traverses over the Tommy and Ted veins; regional geology after Diakow *et al.* (1994, 1995); regional lake sediment geochemical data showing elevated Au concentrations (regional median: 1 ppb) around 3Ts vein system from Cook and Jackaman (1994); glacial striae and flutings from Levson and Giles (1994) and Giles and Levson (1995). Refer to Rhys (2003) for all names of minor veins. Diagram modified from Cook and McConnell (2001).

vein mineralization in the area of the Tsacha and Tam properties are characterized by rhyolite ash-flow tuff and lapilli tuff of the Entiako Formation. Of these, the dominant host unit is a maroon quartz-phyric lapilli tuff approximately 400 m thick. Late Cretaceous felsite sills and a Middle Jurassic augite porphyry plug are exposed to the south of the 3Ts vein system. Lane and Schroeter (1997) reported a preliminary U-Pb zircon date of 73.8 ±2.9 Ma for the biotite-phyric felsite sill that intrudes the Tommy vein. Cretaceous fine-grained diorite sills and dikes are exposed to the north of the vein system near the south side of Tommy Lake. One of these, a shallowly dipping sill that is likely analogous to felsite mapped to the south, is approximately 100–150 m thick and cuts the Tommy and Ted veins at depth. Smaller dikes and sills <5 m in thickness are also commonly observed in drillcore (Rhys, 2003).

Epithermal Au-Ag Mineralization

The 3Ts Au-Ag prospect is a low-sulphidization epithermal Au-Ag prospect that comprises the former Tsacha (MINFILE 093F 055; MINFILE, 2005) and Tam/Taken (MINFILE 093F 068) showings. Epithermal precious metal deposits in central BC have been classified as being hosted by either 1) rocks of Eocene or younger age, primarily felsic volcanic rocks of the Ootsa Lake Group, such as the Wolf (MINFILE 093F 045) or Clisbako (MINFILE 093C 016) prospects, or 2) older Lower to Middle Jurassic Hazelton volcanic rocks (Lane and Schroeter, 1997). The 3Ts vein mineralization here is Late Jurassic in age and belongs to the latter, less well-known group of older epithermal Au deposits. Argon-argon dating of potassium feldspar from the altered margin of the Tommy vein at the University of British Columbia returned a Late Jurassic age of 144.7 ±1.0 Ma (Bottomer, 2003a), similar to that of the Capoose intrusive event.

The Tommy and Ted veins are the best explored of at least nine parallel veins and stockworks that make up the 3Ts quartz vein system (Fig. 4). These, which also include the Larry, Johnny, Ian, Bobby, Barney, Goofy and Alf veins (Tsacha property) and the Mint vein (Tam property), occur over an area of approximately 2 km^2 within the host felsic tuff of the Entiako Formation. In general, subvertically dipping mineralized quartz-calcite-potassium-feldspar veins on the property strike north-northwesterly and exhibit typical epithermal textures, including vein breccia fragments, crustiform banding and comb crystal structures consistent with a shallow depth of formation (Pawliuk, 2005). They are associated with potassium-feldspar(?)-quartz-sericite-pyrite alteration haloes of variable thickness. Gold in quartz vein mineralization has also been intersected below the crosscutting microdiorite sill at both the Tommy and Ted veins, and each remains open at depth beneath this. The Tommy vein is considered to represent a higher level in the hydrothermal system than the Ted vein, based on differences in Ag:Au ratio, base metal content and the extent of wallrock alteration (Bottomer, 2003b). The following descriptions are taken from several sources, including Lane and Schroeter (1997), Southern Rio reports (*e.g.*, Pawliuk, 2005) and the structural study of Rhys (2003).

TOMMY VEIN

The Tommy vein, the largest on the property, is located on the Tsacha claim (MINFILE 093F 055) and is a north-northwesterly-striking, subvertical, quartz-adularia-calcite-potassium-feldspar vein. It is up to 8 m wide (average width 4 m) and has a known strike length of about 640–700 m (Fig. 4). The vein remains open along strike. It exhibits typical epithermal textures, such as breccia features, local crustiform banding, comb crystal structures and drusy cavities, and is cut by a diorite sill at an average depth of about 120 m. The Tommy vein has also been traced below the sill, and an 11.3 m drill intersection at 280 m vertical depth returned 8.83 g/t Au and 62.6 g/t Ag.

The vein shows some local relief (Fig. 5). It consists of massive, clear to milky white crystalline quartz and subordinate calcite with locally developed colloform bands of pale grey chalcedony, adularia and rare amethyst (Lane and Schroeter, 1997), as well as potassium feldspar (Rhys, 2003). Precious metal mineralization occurs as fine-grained disseminations in colloform banding and bladed veins. Massive vein mineralization is typically flanked by quartz stringer, stockwork or breccia zones. It is of the low-sulphidization type and contains less than 1% metallic minerals, including chalcopyrite, pyrite, stephanite, argentite, galena, native gold (±electrum), specularite and magnetite. Hematite and malachite are minor constituents. The Ag:Au ratio in the vein varies form <1 to 50, with a mean of about 10.

Wallrock hydrothermal alteration associated with the Tommy vein is patchy, and clay and sericite alteration are only sporadically and distally developed. Lane and Schroeter (1997) reported narrow and locally intense zones of silicification to be associated with broad zones of weak, red-coloured clay alteration associated with hematite. However, Rhys (2003) stated that both the Tommy and adjacent Larry vein are enveloped by broad zones of pale grey



Figure 5. View of Tommy vein, showing the sampling of LFH horizon humus (site 591), July 2005.

to pink potassium feldspar-quartz-sericite-pyrite alteration extending, in some cases for up to tens of metres into the felsic volcanic host. Alteration was stated to be widest in the central and southern parts of the Tommy and Larry vein system, and weaker in the north. In addition to these, a large (approx. 1000 m by 300–500 m) potassium-feldspar(?)-quartz-sericite-pyrite alteration zone has been mapped within the host rhyolite tuff to the west of the Tommy vein (Rhys, 2003).

The Larry vein, about 200 m east of the Tommy vein, was traversed by the same Tommy geochemical orientation line during this study, as was the Ian vein system to the west. The Larry vein has been traced 590 m along strike and 100–200 m downdip, and is open in all directions. No resource estimate has been completed. Rhys (2003) noted that Larry stockwork more closely resembled a sheeted vein system than a true stockwork.



Figure 6. Sampling site just downslope of the Ted vein (site 559), July 2005.

TED VEIN

The Ted vein is located on the Tam 2 claim (MINFILE 093F 068) about 1 km east-southeast of the Tommy vein. It is a similarly north-northwesterly-striking (150–170°), subvertical, quartz-calcite-sulphide vein with epithermal textures. The vein has been traced along strike for at least 300 m and over an average width of 10 m, and is the widest of the 3Ts veins. It is open along strike both north and south, and to depth. The original Ted vein showing consists of a 50 m wide zone of small outcrops and subcrop (Fig. 6) of altered rhyolite and quartz stockworks, one vein of which reached 15 m in width. Surface rock samples from this showing were reported to contain 1.5 g/t Au, 82 g/t Ag, 0.1% Zn and 0.3% Pb (Schimann, 1994). The Ted vein is of the intermediate-sulphidization type and may represent a lower level within the hydrothermal system than the Tommy vein on the basis of several factors. These include a higher Ag:Au ratio, higher Mn and base metal contents, greater gangue carbonate component and more extensive wallrock alteration (Bottomer, 2003b, pers. comm., 2005).

Initial drilling of the Ted vein by Phelps Dodge in 1996 returned a 6.46 m true width intersection of 8.88 g/t Au and 393.6 g/t Ag (Fox, 1996). The upper contact of the 70 m thick intrusive sill cutting the Ted vein is at 120–140 m depth, and an above-sill initial inferred resource of 273 800 t grading 2.0 g/t Au and 133 g/t Ag has been prepared (Wallis and Fier, 2004). More recent drilling (hole TT-04-37) has encountered Au mineralization beneath the sill, at a depth of 388.3–399.3 m, intersecting 11 m (estimated true width 6.5 m) of quartz-carbonate vein returning 3.74 g/t Au and 59.3 g/t Ag (Pawliuk, 2005).

The following description of the Ted vein is paraphrased from Pawliuk (2005) and Rhys (2003). Quartz-calcite veining varies widely in colour from pale grey to creamy white, is finely banded, and exhibits textural evidence for at least three episodes of veining and brecciation. Vein material typically contains 10–40% variably silicified fragments of rhyolite porphyry wallrock and about 5–10% variably coloured calcite, which occurs as late-stage infilling of brecciated zones and open cavities. Open cavities are reported to form up to 2% of the rock volume. The Ted vein contains approximately 0.5% finely disseminated sulphide minerals, primarily pyrite but also including variable amounts of chalcopyrite, sphalerite, galena, Ag-sulphides, tellurides and sulphosalts. Chalcopyrite and sphalerite occur as irregular wispy masses and 2–5 mm blebs, respectively, and both are rimmed by later sulphosalt (?). Early quartz vein fragments within the Ted vein breccia commonly have greater sulphide and sulphosalt (?) mineral contents than do later generations of quartz-calcite infilling. Disseminated red hematite is also locally present within the vein.

Much higher sulphide concentrations are also locally present. Pawliuk (2005) reported a 0.45 m drill intersection of deep hole TT-04-37 containing 30% galena and 10% disseminated sulphosalt (?); another galena-bearing vein intersected in the same hole returned 171 g/t Ag and 2.27% Pb over a narrow 0.43 m wide intersection.

Hydrothermal alteration of the host rhyolite tuff at the Ted vein is similar to that at the Tommy. Pervasive silicification, and potassium-feldspar-quartz±pyrite alteration, grades outward from the vein to pale bleached alteration (Rhys, 2003).

SURFICIAL GEOLOGY AND SOILS

Regional Surficial Geology and Quaternary History

Surficial geology of the Fawnie Creek and adjacent Tsacha Lake map areas (NTS 093F/02, 03) was mapped by Levson and Giles (1994) and Giles and Levson (1995), respectively. The sediments comprise mainly basal till with subordinate colluvial and glaciofluvial deposits. The entire region was ice covered during the Late Wisconsinan glacial maximum, and ice-flow studies indicate that the dominant glacial direction was to the east-northeast (Giles and Levson, 1994a). Mapped surficial cover at the 3Ts area is mainly thin till veneer (<1 m thick) and thin colluvial veneer (<1 m thick) over discontinuous bedrock. Till veneer

predominates in the area around the Tommy vein, whereas colluvium and adjacent areas of till blanket were mapped nearer Adrian Lake in the area of the Ted vein (Levson and Giles, 1994). A drift-prospecting potential map of the Fawnie Creek map area (Giles and Levson, 1994b) highlighted the 3Ts area, among others, as having a high to very high potential for the use of near-surface geochemical methods in tracing surficial sediment back to its bedrock source. Localized areas of exotic glaciofluvial sand and gravel are restricted to small stream valleys between the lakes. Small Holocene organic wetland deposits occur in a few areas of lower relief. No systematic property-scale Quaternary mapping or section interpretation was attempted as part of this study, but profiling of sample pits here generally confirms, at a property scale, the regional mapping results of Levson and Giles (1994).

Till and Soil Development

TILL AND OTHER PARENT MATERIALS

Till is present at most soil profile sites along the Tommy transect, other than over the relatively weathering-resistant Tommy vein. It occurs as both basal and colluviated tills. Basal till (Fig. 7) is typically grey, overconsolidated, locally sandy and is most common on the western part of the transect. In contrast, colluviated till is more widespread on the steeper slope to the east of the Tommy vein. The distribution of parent materials is more complex on the Ted transect line. Most profiles of glacial deposits examined on the Ted transect consist of basal till, but glaciofluvial outwash sand (Fig. 8) was encountered in three pits along the line. These samples were included with till samples for aqua regia digestion and ICP-MS analysis. Several of the Ted basal till horizons are classed as IIC horizons due to the widespread occurrence of coarse, angular, near-surface colluvium deposits over pre-existing till. No samples of C horizon till or other parent material were obtained from four thin rubbly soil sites on the Tommy transect, mostly near the Tommy vein, and from one site on the Ted transect.

SOIL DEVELOPMENT

Two main near-surface soil horizons are found above the widespread basal or colluviated tills at all sample sites: 1) an organic-rich LFH horizon humus layer, and 2) a thin B horizon mineral soil of variable genetic origin. All such soils were classified in accordance with the Canadian System of Soil Classification (Agriculture Canada, 1987).

Samples of LFH horizon humus comprise a mixture of partially decomposed twigs, needles, cones, moss and other fine-grained organic debris above the underlying mineral soil. They are thin, typically in the range of 2–4 cm, and do not exceed 5 cm at any site. The LFH horizon lies beneath a widespread cover of surface moss, which was not sampled here, and is marginally thicker at sites on the more subdued topography of the Ted transect than on the steeper Tommy transect.

The B horizon mineral soils on the 3Ts property are predominantly brunisols (Fig. 9, 10). They take the form of thin, brown to red-brown, near-surface Bm horizons, typically 10–20 cm in thickness. No podzolic Bf horizons were observed at any site, although there is some evidence for local development of eluviated Aej horizons in rare outwash sand and gravel.

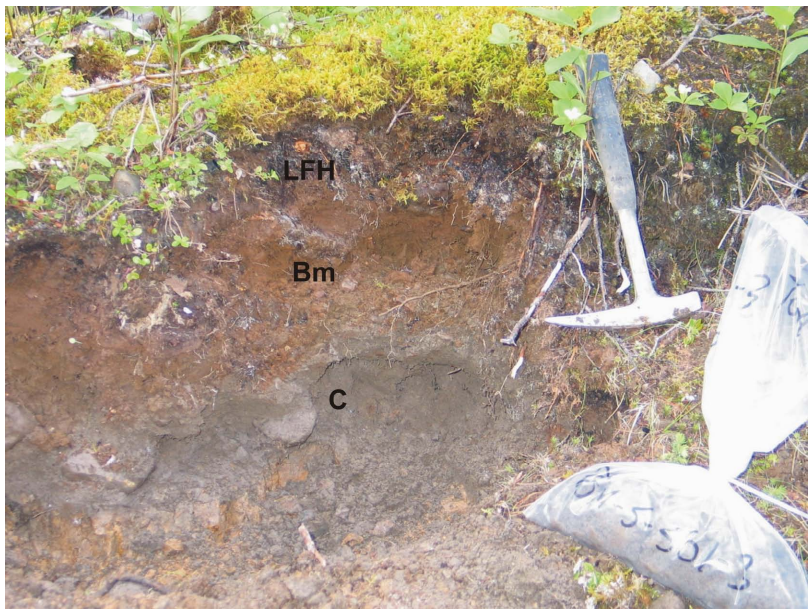


Figure 7. Typical basal till (site 501) from background area at western end of the Tommy orientation line, showing typical brunisolic Bm soil horizon and LFH horizon humus development.



Figure 8. Glaciofluvial outwash sand and Bm soil development (site 576) at western end of the Ted orientation line.

Most Bm horizon soils profiled on the Tommy orientation transect are within relatively simple till or colluviated till parent materials. Four of the soils are, however, developed in angular rubble±colluvium in rocky areas where no till is present; three of these are immediately around the Tommy vein exposure. Soil development is much more complex on the Ted traverse line, where brunisolic B horizons are developed within till, rubble and colluvium (Fig. 11), colluvium (?) and localized glaciofluvial outwash sand parent materials. Furthermore, composite soil profiles are present at several sites where Bm horizons are preferentially developed in coarse, gravelly, near-surface colluvium deposits above IIC horizon till (Fig. 12). The colluvium is from an upslope source, in this case to the south, whereas the underlying till has originated from an up-ice source to the west. Several such sites are present along the eastern part of the Ted transect line near Adrian Lake, all of which have since been stabilized by forest growth.

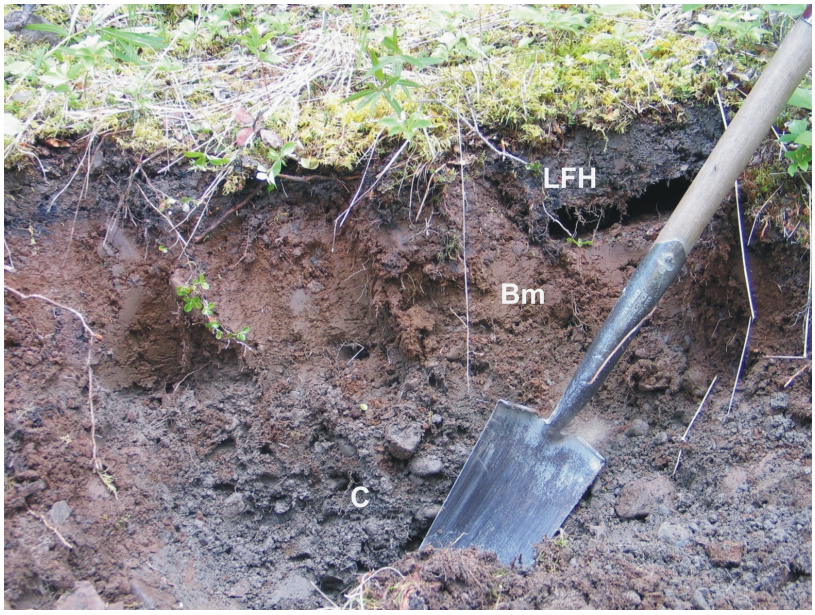


Figure 9. Typical soil profile in the 3Ts area, showing surface humus (LFH horizon) above brunisolic Bm horizon and underlying C horizon till (site 505), western portion of the Tommy orientation line.

Previous Geochemical Surveys and Studies

The southern Nechako River area, including the Fawnie Creek (NTS 093F/03) map area, was the object of a series of reconnaissance geochemical programs carried out by the BC Geological Survey during the period 1992–1995. These projects, carried out with bedrock mapping programs under the banner of the Interior Plateau Project, included regional lake sediment geochemical surveys (Cook and Jackaman, 1994), lake water geochemical surveys (Cook *et al.,* 1999), Quaternary mapping and till geochemical surveys (Levson *et al.*, 1994; Cook *et al.,* 1995) and till orientation studies (Levson, 2001). Distribution of lake sediment Au results in the Tommy Lakes area clearly outlines the location of the original Tommy vein (Fig. 2). The single lake sediment sample collected from Adrian Lake returned the highest total (INAA) Au value (256 ppb) in that geochemical survey (regional median 1 ppb Au). In all, four small lakes containing moderately elevated to highly elevated gold concentrations in the range 4–256 ppb were found to encircle the small hills hosting the original Tommy Au vein discovery at what is now the 3Ts project. In addition to the high Au concentration, which was confirmed by subsequent INAA reanalysis of the sample, this Adrian Lake sediment was also characterized by very low or background-level abundances of other elements, including As (7.8 ppm), Cu (36 ppm) and Pb (4 ppm). Regional till geochemical data of Levson *et al.* (1994) also show the down-ice dispersal of Au in till from the deposit. Of several till samples collected by the BC Geological Survey in 1993 northeast of the Tommy vein, two returned elevated Au values of 23 ppb.

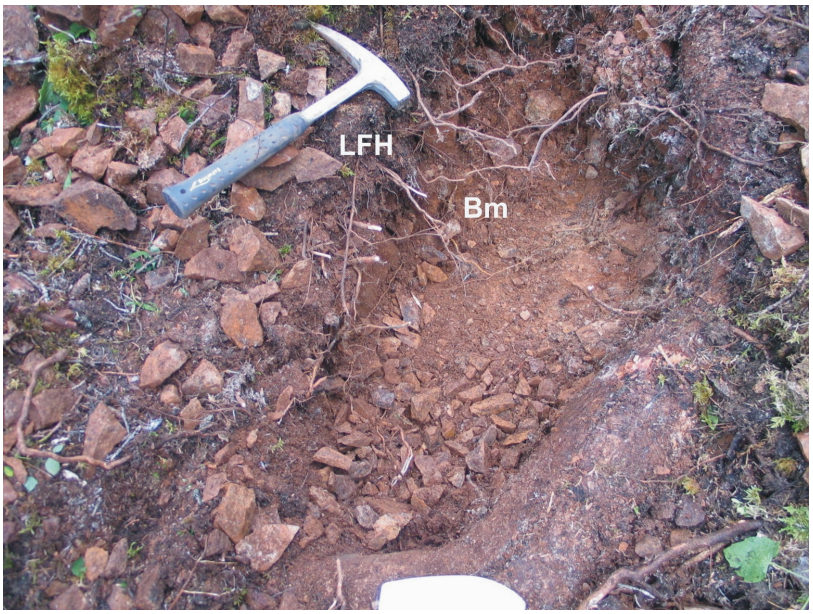


Figure 10. Thin Bm soil horizon developed in rubble and colluvium directly atop bedrock at the Tommy vein (site 591); no till present at this site.

Little in the way of soil geochemical surveys appears to have been conducted near the Tommy vein. However, at least three near-surface B horizon soil geochemical surveys of the adjacent Tam and Taken properties were carried out during 1994–1998 by Fox Geological (Fox, 1994, 1995, 1996, 1999) on behalf of Phelps Dodge and others. They include two overlapping soil grids and subsequent infill work (N = 832 samples). Line orientations of the two grids (east-west and 060°, respectively) are roughly transverse to the strike of the vein systems. However, they are also roughly

parallel to the dominant east or northeast-trending ice-flow direction on the property, suggesting the possibility that any Au or Ag geochemical signatures of soil potentially derived from any Au-bearing till dispersal plumes may have been missed in the gaps between the 200 m or 100 m gridline spacings. Nevertheless the soil sampling appears to have been carried out consistently from year to year, and it successfully delineated the areas of the Ted and Mint vein systems.

FIELD AND LABORATORY METHODS

Quality Control – Quality Assurance Procedures

A variety of standard QA-QC procedures was used in both the field and the laboratory to ensure a uniformly high quality of data. A 20-sample block method of sampling was used, in which field duplicates and standards were collected and inserted at regular intervals. Field duplicates (n = 5 pairs) were collected at a rate of 1 every 10 samples, and appropriate CANMET and other control standards inserted at a rate of at least 1 in every 20 samples. For those selective extraction methods for which standards are either unavailable or poorly constrained, such as Mobile Metal Ion (MMI) or Enzyme Leach procedures, multiple insertions of a B horizon bulk sample, prepared as a control, were included as blind drift monitors in batches to monitor analytical precision. This bulk sample was obtained from a soil profile near the Tommy vein. In addition to these proactive QA-QC initiatives, some of the laboratories also reported the results of their internal QA-QC procedures, such as those for internal standards and analytical replicates.

Field Sampling Procedures

Fieldwork at the 3Ts property was conducted during late June to early July 2005. A series of soil profiles (N = 36 sites) were conducted on two approximately 750 m long east-west lines transecting each of the Tommy and Ted veins (Fig. 2). The Tommy transect comprises 20 sites; the Ted transect comprises an additional 16 sites. Sample sites (Fig. 13) are spaced at roughly 50 m intervals, although tighter 25 m site spacings were used nearer the vein systems, and distal sites are locally telescoped to 75–100 m spacings. One of the sites directly over the Tommy vein is offset to the south relative to the sampling line. The eastern end of the Tommy soil transect is at a small wetland area, but the vegetation transect of the halogen geochemistry study continues for another 1.5 km to the east (Dunn *et al.,* 2006).

Three types of organic and mineral samples, exclusive of vegetation (Dunn *et al.,* 2006), were collected at each profile site:

- LFH horizon humus
- B horizon soil
- C horizon till

The two sampling transects were purposely chosen to cross the veins at rather arbitrary points, so as not to bias fieldwork toward those parts of the veins known to be most prospective. All-terrain vehicle road access was utilized



Figure 11. Brunisolic Bm horizon soil developed in loose rubble and colluvium atop weathering bedrock at site 570, near the eastern end of the Ted orientation line; no till present at this site.

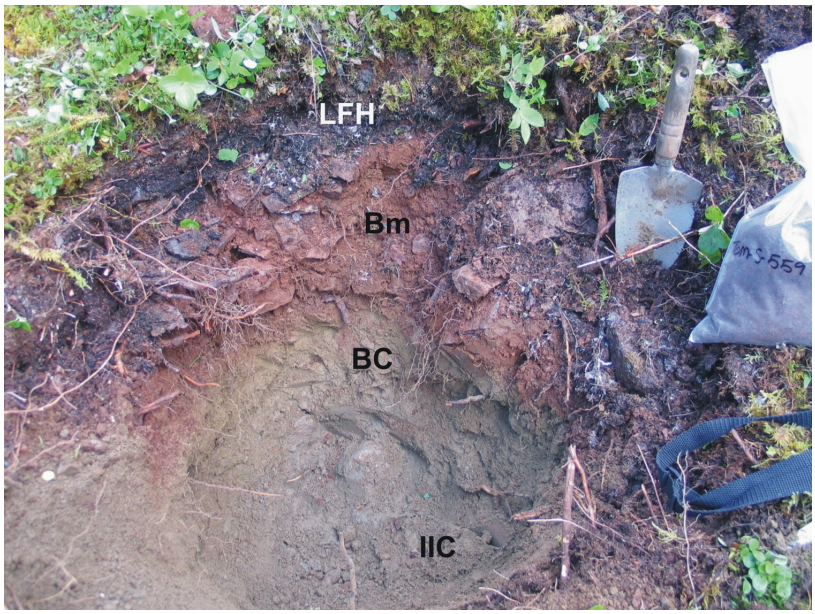


Figure 12. Composite soil profile, showing preferential development of brunisolic Bm horizon within stabilized near-surface angular colluvium atop IIC horizon till; site (559) located immediately down-ice and downslope from Ted vein exposure.

where possible, but was not a major factor in siting of the transects. In all, 7 separate samples were collected at each site for the range of intended analytical procedures; a total of 14 such samples were collected at each field duplicate site.

A single LFH horizon humus sample was collected at each site, using Hubco® breathable bags to prevent rotting of the sample before reaching the lab. Humus samples comprise a mixture of partially decomposed twigs, needles, cones, moss and other fine-grained organic debris above the underlying mineral soil. Surface forest mosses over humus were stripped off prior to humus collection, and were not sampled as part of this study. Humus samples were collected first at each site so as to prevent any inadvertent contamination of this thin horizon (typically <5 cm thick) from the underlying mineral soil. Each site was closely inspected prior to sampling to ensure that it was pristine and there had been no prior surface disturbance. In the case of roadcut sample sites, the LFH sample was taken farther back from the bank to eliminate any possibility of inadvertently collecting material contaminated by soil during earlier road-building operations.

A total of 5 samples of B horizon or adjacent near-surface soil were collected at each site. One B horizon sample was collected for each of aqua regia digestion, Enzyme Leach (EL), Soil Gas Hydrocarbons (SGH), and Soil Desorption Pyrolysis (SDP). In addition, a fifth sample was collected at constant depth of 10–25 cm at each site for Mobile Metal Ion (MMI) analysis. In practice, this constant depth typically, although not always, corresponded to a mixed sample of the Bm horizon with the underlying transitional BC horizon. All soil samples obtained for proprietary selective extractions were sampled and preserved in accordance with the appropriate laboratory protocols. For example, all samples for MMI, SGH and SDP analysis were collected using Zipoc® bags; these were then placed within a protective outer poly bag which was secured with a zap strap. Samples collected for aqua regia digestion were also used for other determinations including LOI, pH and, where applicable, Au fire assay. Note that these B horizon samples are also, in part, the subject of the parallel halogen geochemistry study of Dunn *et al.* (2006). All soils were classified in accordance with the Canadian System of Soil Classification (Agriculture Canada, 1987).



Figure 13. Typical till pit (site 525) in basal till at the eastern end of the Tommy orientation line; note absence of outcrop and the extensive forest moss cover.

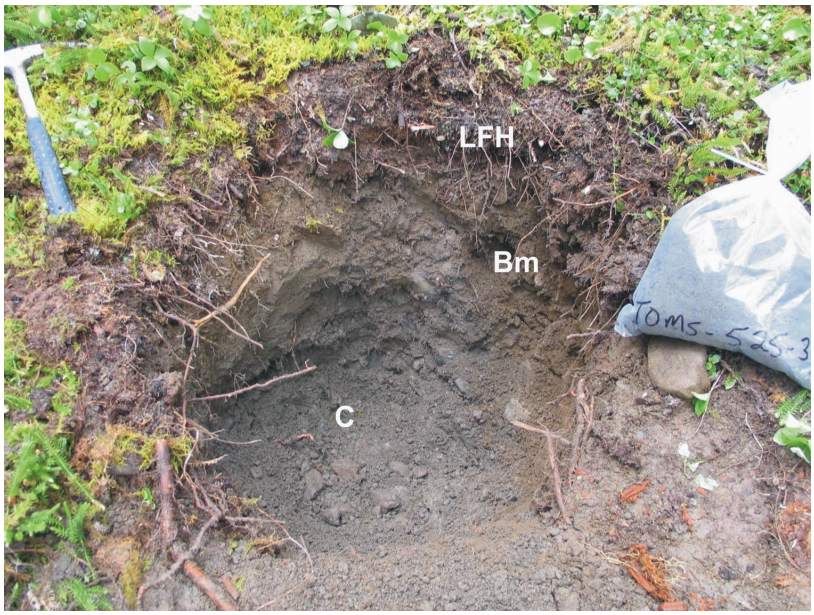


Figure 14. Till profile from same site as previous photo on Tommy orientation line, showing LFH humus and brunisolic Bm soil horizons above grey basal till; sample bag at right is C horizon till sample TOM-S-525-3.

A single C horizon till sample (mean weight 4.85 kg) was collected from shallow oxidized till material at most sites (Fig. 14). Till samples were typically obtained from a depth of approximately 45–60 cm on the Tommy transect, and from about 40–60 cm on the Ted transect. No till samples were obtained from four rubbly near-bedrock sites on the Tommy transect, mostly near the Tommy vein, and from one site on the Ted transect. In addition, a few of the C horizon samples on the Tommy line are of glaciofluvial origin. All samples were collected in large poly bags and secured with a zap strap. All samples were shipped to their respective laboratories in hard plastic cases to prevent any possible damage to the samples.

Field duplicate samples (n = 5 pairs) of all media were typically collected from pits dug a few metres apart at relevant sites. Overstorey vegetation samples were also collected at each site as part of the parallel halogen geochemistry study (Dunn *et al.*, 2006). These biogeochemical samples consisted of lodgepole pine (*Pinus contorta*) outer bark and white spruce (*Picea glauca*) foliage.

Sample Preparation and Analytical Procedures

Samples from each horizon were analyzed for a range of commercially available partial digestions and proprietary selective extractions (Table 1). Aqua regia digestion – ICP-MS multielement analyses and both pH and LOI determinations were common to all three types of soil media, but the majority of the selective extractions were conducted solely on the near-surface B horizon mineral soil samples that have traditionally been used for property-scale geochemical exploration in BC. These included Enzyme Leach (EL), Mobile Metal Ion (MMI), Soil Gas Hydrocarbons (SGH) and Soil Desorption Pyrolysis (SDP), as well as total Au determination by Pb-collection fire assay – ICP-MS. Samples of the LFH horizon humus were also analyzed by Na-pyrophosphate leach and conductivity in addition to aqua regia – ICP-MS. All C horizon samples were analyzed by aqua regia digestion – ICP-MS and for total Au by Pb-collection fire assay – ICP-MS only.

Aqua regia geochemical work on humus, soil and till, as well as Au fire assay, pH, LOI and other determinations, were conducted at Acme Analytical Labs, Vancouver. Specialized proprietary selective extractions were carried out at ALS Chemex, Perth, Australia (MMI); Activation Laboratories, Ancaster, Ontario (EL and SGH); and SDP Pty., Brisbane, Australia (SDP).

SAMPLE PREPARATION

Sample preparation procedures for all humus, soil and till samples prepared and analyzed for trace elements by aqua regia digestion – ICP-MS at Acme Analytical Labs are outlined here. Preparation procedures for those LFH and B horizon soils submitted for proprietary selective extractions (Na-pyrophosphate, EL, MMI, SGH and SDP) are described in the appropriate sections that follow. Note that all sample preparation activities were carried out at the relevant laboratories; no prior preparation work was conducted in the Tatelkuz Lake field camp on any samples.

TABLE 1. SUMMARY OF DIGESTION AND OTHER METHODS USED FOR ANALYSIS OF ORGANIC AND MINERAL SOIL HORIZONS: FIRE ASSAY FUSION, AQUA REGIA, NA-PYROPHOSPHATE, ENZYME LEACH (EL), MOBILE METAL ION (MMI-M), SOIL GAS HYDROCARBON (SGH) AND SOIL DESORPTION PYROLYSIS (SDP)

	LFH Horizon Humus	B Horizon Soil	C Horizon Till
Au by fire assay		X	X
Aqua regia ICP-MS	X	X [1]	X
Na-pyrophosphate	X		
Enzyme Leach		X	
Mobile Metal Ion Multi-element (MMI-M)[SM]		X [2]	
Soil Gas Hydrocarbons (SGH)[SM]		X	
Soil Desorption Pyrolysis (SDP)[SM]		X	
pH	X	X	X
Conductivity	X		
Loss-on-ignition	X	X	X

[1] with halogen geochemistry project of Dunn et al. (2006)

[2] sampled at constant depth, typically from Bm/BC horizons

Note that aqua regia ICP-MS determinations were conducted on both 80 mesh and 230 mesh fractions of B horizon soils.

All LFH horizon humus samples were first allowed to air dry in the field prior to shipping, and were then dried in the laboratory at low heat (40°C), disaggregated within their original bags by pounding with a mallet, and screened to <250 µm (–60 mesh ASTM) using stainless steel sieves.

All B horizon soil samples were dried at low heat (40°C) and sieved in their entirety to <180 µm (–80 mesh ASTM) using stainless steel sieves, with 30 g splits being taken for each of group 1F aqua regia – ICP-MS analysis and group 3B-MS Pb-collection Au fire assay. The widely used –80 mesh soil fraction was used here to facilitate comparisons with most exploration industry soil datasets.

The C horizon till samples were dried at low heat (40°C) and then sieved in their entirety to <63 µm (–230 mesh ASTM) using stainless steel sieves in accordance with standard till preparation procedures of the Geological Survey of Canada and the BC Geological Survey. Splits of 30 g were taken for each of group 1F aqua regia – ICP-MS analysis and group 3B-MS Pb-collection Au fire assay.

AQUA REGIA (AR) DIGESTION

Aqua regia digestions with ICP-MS finish (Acme group 1F) were conducted on all prepared 3Ts humus (LFH horizon), mineral soil (B horizon) and till (C horizon) samples at Acme Analytical Labs, Vancouver. In each case, 30 g analytical subsamples were digested with 180 ml 2-2-2 HCl-HNO_3-H_2O at 95°C for 1 hour, diluted to 600 ml and then analyzed for a 53-element suite by both ICP-MS and ICP-ES on Perkin-Elmer Elan 6000 and SpectroCirus instrumental units, respectively. This relatively weak aqua regia digestion is a partial digestion, providing a partial recovery of numerous silicate-bound and refractory elements such as Ni, Ba and Cr. It is typically near-complete, however, for sulphide-associated elements such as Cu, Zn, Pb, Ag and Co.

Analytical subsamples of 30 g were used in each case here in an attempt to increase sample representativeness and minimize Au particle sparcity effect, but aqua regia – digestible Au as reported here may or may not be complete, depending on the nature of the silicate host. At the time of writing, total Au determinations by Pb-collection fire assay were underway on all mineral soil and till samples to verify earlier results.

Subsequent to this, 20 g of prepared B horizon soil pulp was supplied in most cases to the halogen geochemistry study (Dunn *et al.*, 2006), a further 15–30 g removed for Au fire assay purposes and the remaining <180 µm (–80 mesh ASTM) fraction then further sieved to <63 µm (–230 mesh ASTM) for further group 1F aqua regia – ICP-MS trace element determination of the finer soil fraction. This work was in progress at time of writing.

MOBILE METAL ION (MMI)

The Mobile Metal Ion (MMI) method is a proprietary commercial selective extraction method of Wamtech Pty. Ltd., Australia; analyses are conducted under license at a number of laboratories around the world. There is a paucity of published case studies on the use of MMI geochemistry in the search for epithermal Au deposits in the Cordillera and, in fact, there are only a few such studies of any sort in northern glaciated terrain (*e.g.*, Fedikow, 2005; Bajc, 1998). The MMI-M partial extraction suite was conducted on near-surface soil samples by ALS Chemex at their facility in Perth, Western Australia. The MMI-M method (ALS

Chemex code ME-MS17) is one of several MMI analytical suites that use proprietary leach reagents stated to be suitable for the extraction of target elements, in this case a multielement suite. Analytical finish is by ICP-MS. Results are to be reported by Cook and Dunn (work in progress).

ENZYME LEACH (EL)

The Enzyme Leach (EL) method is a proprietary commercial selective extraction method of Activation Laboratories Ltd., Ancaster, Ontario. Enzyme Leach has attracted much attention from the mineral exploration industry but, as with MMI, most published case studies are confined to nonglaciated areas. Enhanced Enzyme Leach analyses (Actlabs code 7EnhEL) of all B horizon soil samples were conducted by Activation Laboratories using an ICP-MS finish. The method, although proprietary, is considered to be selective for those metals associated with the amorphous manganese oxide phase that coats mineral particles in the near-surface environment. A 1 g sample of <250 μm (–60 mesh) soil material is leached in a glucose oxidaze solution containing a proprietary enzyme, which reacts with and dissolves any amorphous manganese oxide present. Any metals are reported to be complexed with gluconic acid, and the solutions are analyzed using a Perkin-Elmer Elan 6000 or 6100 ICP-MS unit. Results will be reported at a later date by Cook and Dunn (work in progress).

SOIL GAS HYDROCARBONS (SGH)

The Soil Gas Hydrocarbons (SGH) method is a proprietary commercial analytical method of Activation Laboratories Ltd., Ancaster, Ontario. Sample preparation and analysis for SGH was conducted on all B horizon soil samples by Activation Laboratories. Samples were air dried at no more than 40°C, sieved to <250 μm (–60 mesh) and a 0.5 g sample extracted and analyzed by gas chromatography – mass spectrometry. The method, although proprietary, targets a range of 162 organic compounds that are thought to be adsorbed onto clay minerals and amorphous iron and manganese oxides present in the soil. Hydrocarbons in the C5–C17 range are measured, as these are stated to be more robust from a field sampling perspective, and less affected by decaying biogenic material than hydrocarbons in the C1–C4 range. The SGH method has been the subject of a recent CAMIRO research study (Sutherland and Hoffman, 2003), but, to the knowledge of the authors, no published case studies on the use of the SGH method are known from the western Cordillera. Results for 3Ts are to be reported by Cook and Dunn (work in progress).

SOIL DESORPTION PYROLYSIS (SDP)

Soil Desorption Pyrolysis (SDP) is a proprietary commercial analytical method of SDP Pty. Ltd., Brisbane, Australia. The B horizon soil samples were shipped to Australia by air to minimize elapsed time between collection and analysis, and preparation and SDP analysis of the samples was conducted at that facility. The SDP method is stated to measure trace amounts of volatile compounds, such as light hydrocarbons and other gases, which are adsorbed onto clay-size soil particles. Samples are dried at 40°C, the 0.2–2 μm clay-size particle fraction separated using a centrifuge, and total adsorbed gases determined by pyrolysis at 450°C. Study of the SDP response here is timely, as most SDP orientation studies have been confined, with a few exceptions, to deposits in arid desert environments of Australia, Chile and Nevada. Results from the 3Ts prospect will be reported by Cook and Dunn (work in progress).

SODIUM PYROPHOSPHATE LEACH

Sodium pyrophosphate leaches (Acme group 1SLO) were conducted on all LFH horizon humus samples at Acme Analytical Labs, Vancouver. This is a nonproprietary selective extraction method for organic-rich samples that is widely available at commercial laboratories. The procedure used here involves the leaching of a 1 g prepared humus sample with 10 ml 0.1M Na-pyrophosphate ($Na_3P_2O_7$), bottle rolling for two hours and ICP-MS determination of a 58-element analytical suite using a Perkin-Elmer Elan 6000 unit. The leach is selective for elements adsorbed by organic matter (humic and fulvic compounds) and was carried out on organic-rich humus samples only. Results will be reported at a later date by Cook and Dunn (work in progress).

FIRE ASSAY FOR TOTAL AU DETERMINATION

Lead-collection Au fire assays (Acme group 3B-MS) were conducted at Acme Analytical Labs, Vancouver on all 3Ts mineral soil and till samples to 1) verify the presence of elevated Au concentrations in soil; and 2) ascertain, by total decomposition of the samples, what differences, if any, might exist between the partial (aqua regia digestion) and total Au determinations. Fire assays of 30 g subsamples of <180 μm (–80 mesh ASTM) B horizon prepared soil and <63 μm (–230 mesh ASTM) prepared till, with ICP-MS finish, were in progress at time of writing.

OTHER DETERMINATIONS

In addition to the above partial and selective extractions, other determinations, including pH and loss-on-ignition (LOI), were carried out on all organic and mineral soils at Acme Analytical Labs. Conductivity was also determined on only the humus samples.

Soil pH was determined in the lab on a 5 g sample slurry in 10 ml of distilled-deionized water. Field pH was not determined. Loss-on-ignition, an approximate measure of organic matter content, was determined at 500°C. Conductivity of humus samples was measured by conductivity electrode.

PRELIMINARY RESULTS AND DISCUSSION

Quality Control – Quality Assurance Results

For the purposes of this preliminary report, quality control – quality assurance results presented here are limited to an assessment of analytical accuracy and precision for selected elements determined by aqua regia digestion – ICP-MS. Analytical accuracy is monitored by the insertion of control standards of known composition and evaluation of the results. Replicate analyses of these standards also provide an estimation of analytical precision at various concentration levels. Certified CANMET till and lake sediment standards were used, as were a variety of internal till and organic soil standards from both BC Geological Survey and exploration industry sources.

Analytical accuracy for selected elements is well within acceptable limits for most elements of economic interest. For example, multiple insertions (n = 3) of CANMET till standard TILL-3 in the B horizon soil suite returned mean ±1σ results of 1410 ±54 ppb Ag, relative to the recommended value of 1.4 ±0.2 ppm (1400 ±200 ppb) Ag reported by Lynch (1996). At the lower end of the Ag concentration range, multiple insertions of CANMET till standard TILL-1 in each of the B horizon soil (n = 4) and till (n = 3) suites returned mean ±1σ results of 206 ±8 ppb and 210 ±12 ppb Ag, respectively, relative to a recommended value of <0.2 ppm (<200 ppb) Ag. Three insertions of each of TILL-1 and TILL-4 in the till suite returned Cu results of 48.6 ± 1.3 ppm and 224.5 ± 9.5 ppm relative to recommended values of 49 ±2 ppm and 254 ±15 ppm Cu, respectively. Accuracy of humus analyses are similarly within acceptable limits. For example, three insertions of the organic-rich CANMET standard LKSD-4 in the LFH horizon suite returned mean ±1σ results of 209 ±7 ppm Zn, 34.6 ±1.3 ppm Cu and 238 ±4 ppb Ag relative to recommended values of 195 ±16 ppm Zn, 31 ±2 ppm Cu and 0.2 ±0.1 ppm (200 ± 100 ppb) Ag, respectively (Lynch, 1999).

Examination of precision results shows that analytical precision, as determined by replicate analyses of standards, is generally better than 10% for most trace elements of economic interest, such as Ag, Zn, Pb and Cu. For example, replicate analyses of five sets of CANMET and other standards in the till and mineral soil suites by aqua regia digestion – ICP-MS returned precision results in the range 5.3–11.1% for Ag, 3.1–10.0% for Zn and 3.9–9.8% for Pb. Replicate blind analyses (n = 5) of the B horizon field standard returned very similar precision results of 8.3% for Ag, 5.2% for Zn and 5.1% for Pb. Precision results for these same three elements in the LFH horizon humus suite, as determined by three analyses of LKSD-4, are 3.0% for Ag, 7.1% for Zn and 2.4% for Pb.

Summary Statistics and Overview of Results

Summary statistics for selected elements determined by aqua regia digestion – ICP-MS for each of LFH horizon humus, B horizon soil and C horizon till and other parent materials are shown for the combined orientation lines (Table 2) and for both the Tommy (Table 3) and Ted (Table 4) transects. Discussion here of the results for the geochemical orientation lines will be confined to comparative aqua regia digestion data, particularly Au and Ag, for each of the three soil horizons sampled. Remaining selective extraction and other geochemical results will be reviewed in the final project report (Cook and Dunn, work in progress).

Elevated Au concentrations in mineral soil and humus are present in all Tommy transect horizon suites, and in most Ted transect horizon suites. In most cases, the highest Au concentrations are on the Tommy transect. Here, up to 41 ppb Au is present in LFH horizon humus (median 1 ppb), up to 223 ppb Au in B horizon soil (median 5.3 ppb) and up to 41 ppb Au in C horizon till and other parent materials (median 3.2 ppb). Somewhat lower but nevertheless elevated Au concentrations are also present in Ted transect sample media. These include up to 24 ppb and 85 ppb Au in B horizon soil (median 1.8 ppb) and C horizon till (median 3.1 ppb), respectively. In the case of till, samples from both transects returned similar background median results (3.2 ppb and 3.1 ppb), but the highest concentrations are on the Ted transect. Only LFH humus horizons on the Ted transect failed to yield any elevated Au concentrations (maximum 2.5 ppb).

Box plots showing Au and Ag (ppb) distribution in each of humus, B horizon soil and C horizon till parent materials for the combined Tommy and Ted orientation transects (Fig. 15) indicate that elevated Au concentrations (>50 ppb) are restricted to B and C horizon mineral soil, although one humus sample (41 ppb Au) from directly over the Tommy vein does approach this level. Conversely, all but one of those samples containing >2000 ppb (2 ppm) Ag are organic-rich humus from the LFH horizon; mineral soil had substantially lower background Ag concentrations.

Downprofile Geochemical Variations with Soil Horizon

Some general downprofile geochemical relations are apparent in the summary of statistical results for the combined lines. A few elements (*e.g.*, Mo) have near-constant median concentrations (range of medians 0.82–1.00 ppm) with depth, regardless of soil horizon, but absolute concentrations of most elements increase with increasing depth in 3Ts soil. Median concentration of many elements, including those related to epithermal mineralization (*e.g.*, Au and As), in mineral soil are several times those in organic-rich humus, but there is little difference in median results from one mineral horizon to another. In the case of Au (Fig. 15), for instance, median concentrations in B horizon soil (3.7 ppb) and C horizon till (3.2 ppb) do not differ appreciably from one another, but are 8–9 times that of the overlying humus (0.4 ppb Au). Other elements, including Cu, Ce, Y and Zr, show a more gradual increase in median concentration with increasing depth in the soil profile.

Median concentrations of several elements, notably Ag, Cd, Hg and S, are much higher in surface humus relative to underlying mineral soil. For example, median, or background-level, Ag concentrations are 4 times greater in humus (582 ppb) than in the C horizon (145 ppb), as shown in Figure 15. Similarly, the median concentration of Hg in humus (214 ppb) is more than 10 times that present in B horizon mineral soil (19 ppb) and more than 23 times that of the C horizon (9 ppb). Median loss-on-ignition (LOI) results are similarly much greater in organic-rich humus (90.8%) relative to the underlying B horizon soil (11 times) and C horizon parent material (21 times).

Geochemical Contrast Over Gold Mineralization

Elevated Ag (Fig. 16, 17) and Au (Fig. 18, 19) geochemical responses in all orientation soil media reflect, to varying degrees, the presence of epithermal Au mineralization associated with quartz veins on both the Tommy and Ted properties. In general, Ag tends to form more coherent multisite anomalies, whereas Au, perhaps as a consequence of the particle sparcity effect, more commonly occurs as single-site anomalous values.

The absolute concentrations of elements in soil horizons may be the product of a host of factors, such as bulk composition, lithological origin, surficial cover, topography, weathering and biogeochemical cycling. It is not the absolute magnitude of Au, Ag or other elements in a soil horizon that determines its effectiveness for geochemical exploration, but rather the extent of geochemical contrast

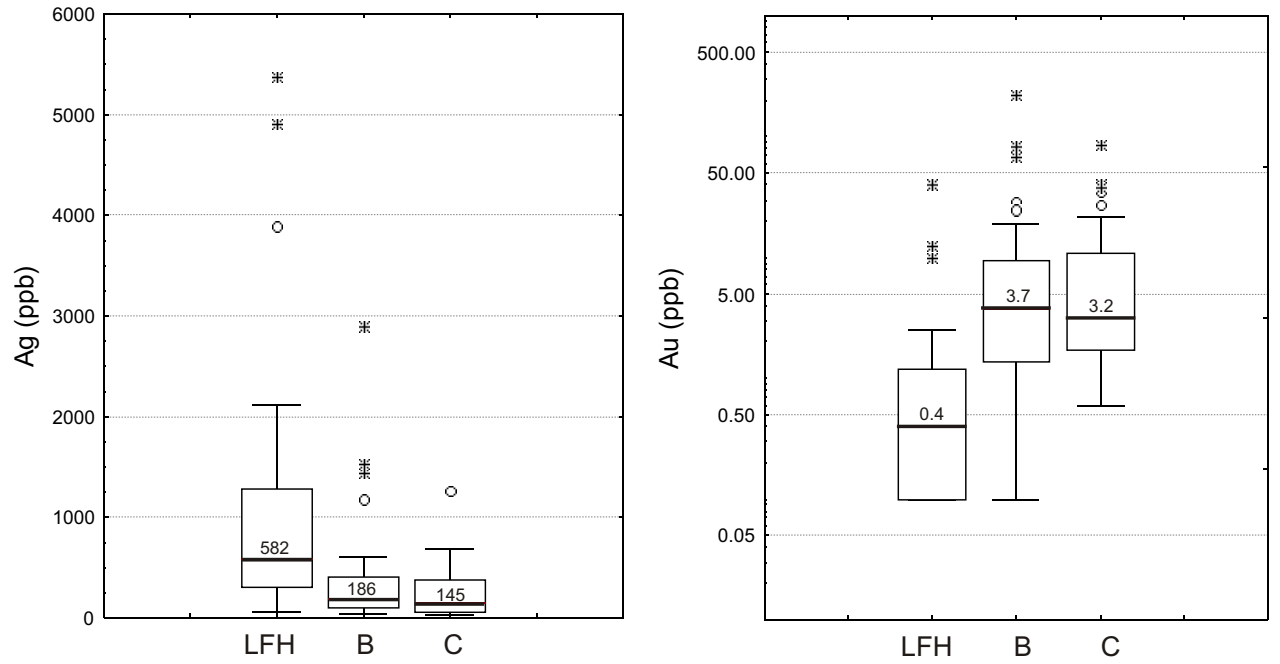


Figure 15. Box plots showing distribution of Ag (left) and Au (right; log scale) in each of humus (n = 36), B horizon soil (n = 36) and C horizon till parent materials (n = 31) for the two combined Tommy and Ted vein orientation transects, 3Ts project. Median Ag and Au concentrations are shown for each. Fifty percent of the data for each lies within the box; the median is denoted by the horizontal line.

between results from mineralized and unmineralized areas. Contrast is measured here with response ratios, which are shown in transect plots for all Ag and Au in humus, B horizon and C soil results at each vein (Fig. 16–19). Response ratios level all sets of results to a common baseline for comparison. They are calculated, for each element, by calculating the ratio for each site concentration to the median value for that orientation line. For example, a response ratio of 1 indicates a sample concentration at the median, or 50th percentile, of the dataset; a response ratio of 4 indicates a concentration of 4 times the median, regardless of the absolute magnitude.

TOMMY VEIN RESULTS

Soil geochemical results at the Tommy vein show highly elevated Ag concentrations in humus of up to 5380 ppb (site 591), which are more than 11 times that of background humus Ag concentrations (median 475 ppb) along the Tommy orientation line. Perhaps even more significantly, elevated levels of Ag in humus in excess of 2000 ppb persist in humus samples down ice and downslope along the line for a further 75–80 m to the east. This pattern mimics a similar, although slightly lower in magnitude and less coherent, Ag distribution in B horizon soil; soil Ag concentrations here of up to 2899 ppb (site 591) have response ratios of 8–16 times background (median 182 ppb) and occur directly over and adjacent to the Tommy vein at two sites. Highly elevated soil Ag concentrations do not persist as far to the east downslope and down ice as they do in humus, but nevertheless provide greater geochemical contrast, as shown by the response ratios (Fig. 16).

Elevated Au values of up to 223 ppb are present in B horizon soil (median 5.3 ppb) at two sites directly above and adjacent to the Tommy vein, and up to 41 ppb in LFH horizon humus (median 1 ppb). Despite the differences in magnitude between Au results in the two sample media, response ratios indicate that geochemical contrast levels of the two are almost identical. Response ratios for soil at two sites are in the range 13–43 times, whereas those for humus at an overlapping set of sites are in the range 10–41 times. Consideration of all adjacent sites with response ratios >5, however, shows that B horizon soil offers a slightly more coherent geochemical response to Tommy vein mineralization than does humus.

There is no direct Ag or Au response in till at the Tommy vein, as no till is developed directly over the outcropping and moss-covered vein along the sampling line (Fig. 5, 10). However, elevated Ag concentrations up to 571 ppb, up to 8 times background levels (median 72 ppb), are present at two down-ice sites to the east. Similarly elevated Au concentrations up to 41 ppb at two sites here would seem to indicate a local down-ice dispersal of mineralized till material from the Tommy vein of approximately 100 m, although the spotty occurrence of till in this area makes it difficult to quantify more precisely.

In addition there is a local Au response in till (39 ppb; site 521) at the Larry vein to the east. Silver concentrations in till here are a modest 363–392 ppb, but these nevertheless correspond to elevated response ratios of approximately 5 times background at three sites over about 60 m at and adjacent to the Larry vein. Corresponding Au response ratios in till are 3–12 times background here. Interestingly, neither humus nor B horizon soil at the Larry vein showed any elevated Ag or Au concentrations.

Conversely, elevated Ag and Au in both humus and B horizon soil do define a single-site anomalous zone (site 518) between the Tommy and Larry veins. Highly elevated Ag concentrations up to 3888 ppb in humus and 1182 ppb in B horizon soil, for example, are reported from predominantly rubble and colluvium; no till was encountered at the

TABLE 2. SUMMARY STATISTICS FOR SELECTED ELEMENTS BY AQUA REGIA DIGESTION – ICP-MS FOR COMPARATIVE SOIL HORIZONS, COMBINED ORIENTATION LINES, ALL DATA

LFH Horizon Humus	Au ppb	Mo ppm	Cu ppm	Pb ppm	Zn ppm	Ag ppb	Co ppm	Mn ppm	Fe ppm	As ppm	U ppm	Cd ppm	Sb ppm	La ppm	Al ppm	S %	Hg ppb	Cs ppm	Nb ppm	Y ppm	Ce ppm	LOI %	pH
Median	**0.4**	**0.89**	**5.54**	**4.2**	**57.5**	**582**	**0.8**	**885.5**	**0.19**	**0.3**	**0.1**	**0.79**	**0.08**	**0.9**	**0.11**	**0.10**	**214**	**0.42**	**0.28**	**0.45**	**1.4**	**90.8**	**4.6**
Mean	2.28	1.97	5.83	4.49	66.86	1119.47	1.02	1144.47	0.23	0.45	0.25	0.93	0.09	1.98	0.12	0.11	218.31	0.57	0.34	2.68	2.03	89.12	4.82
1s	7.09	6.34	2.51	1.39	35.17	1276.32	0.70	864.28	0.17	0.46	0.60	0.80	0.07	6.21	0.09	0.02	50.35	0.42	0.27	12.14	3.35	6.50	0.56
CV (%)	*311.2*	*321.4*	*43.0*	*30.9*	*52.6*	*114.0*	*68.8*	*75.5*	*74.7*	*101.8*	*236.5*	*85.2*	*77.2*	*314.5*	*70.4*	*19.1*	*23.1*	*74.6*	*78.6*	*453.7*	*165.0*	*7.3*	*11.7*
Minimum	0.1	0.18	3.01	2.57	18.8	54	0.2	235	0.04	0.1	0.1	0.2	0.03	0.5	0.03	0.07	145	0.15	0.07	0.13	0.4	70.4	4
Maximum	40.8	38.9	16.42	8.25	189.3	5380	3.1	3742	0.65	2.5	3	3.66	0.45	38.1	0.46	0.14	344	1.68	1.16	73.28	20.9	96.4	6
N=sites	36	36	36	36	36	36	36	36	36	36	36	36	36	36	36	36	36	36	36	36	36	36	36

B Horizon Soil	Au ppb	Mo ppm	Cu ppm	Pb ppm	Zn ppm	Ag ppb	Co ppm	Mn ppm	Fe ppm	As ppm	U ppm	Cd ppm	Sb ppm	La ppm	Al ppm	S %	Hg ppb	Cs ppm	Nb ppm	Y ppm	Ce ppm	LOI %	pH
Median	**3.7**	**1.00**	**8.68**	**12.3**	**103.0**	**185.5**	**9.8**	**558.5**	**3.24**	**6.1**	**0.3**	**0.36**	**0.26**	**8.55**	**1.53**	**0.01**	**19**	**2.12**	**2.99**	**4.37**	**15.55**	**8.3**	**5.2**
Mean	15.62	1.31	10.30	21.62	136.58	384.94	9.35	745.69	3.34	10.98	0.48	0.65	0.37	9.53	1.43	0.02	22.22	3.39	2.90	5.78	18.19	8.93	5.18
1s	39.70	1.36	5.74	23.36	145.18	563.14	1.97	596.73	0.99	13.92	0.75	0.85	0.29	4.69	0.43	0.02	11.67	2.72	0.88	6.92	7.17	2.96	0.57
CV (%)	*254.2*	*103.7*	*55.7*	*108.0*	*106.3*	*146.3*	*21.1*	*80.0*	*29.6*	*126.8*	*154.9*	*129.6*	*80.0*	*49.2*	*30.0*	*103.6*	*52.5*	*80.2*	*30.5*	*119.8*	*39.4*	*33.2*	*11.1*
Minimum	0.1	0.68	5.38	7.45	37.4	38	4.8	229	2.09	2.6	0.2	0.14	0.14	4	0.49	0.01	6	0.91	0.37	1.03	7.5	5.3	3.8
Maximum	223.1	8.89	33.58	112.5	891.1	2899	14.7	2668	8.27	78	4.5	4.26	1.56	30.4	2.22	0.09	62	10.99	5.5	43.6	43.7	20	6.5
N=sites	36	36	36	36	36	36	36	36	36	36	36	36	36	36	36	36	36	36	36	36	36	36	36

C Horizon Till	Au ppb	Mo ppm	Cu ppm	Pb ppm	Zn ppm	Ag ppb	Co ppm	Mn ppm	Fe ppm	As ppm	U ppm	Cd ppm	Sb ppm	La ppm	Al ppm	S %	Hg ppb	Cs ppm	Nb ppm	Y ppm	Ce ppm	LOI %	pH
Median	**3.2**	**0.82**	**13.10**	**11.0**	**61.9**	**145**	**9.5**	**368**	**3.14**	**6.4**	**0.4**	**0.11**	**0.28**	**12.4**	**1.45**	**0.01**	**9**	**1.27**	**1.16**	**8.13**	**29.9**	**4.3**	**6.2**
Mean	11.15	0.84	13.09	21.18	66.08	250.19	9.20	362.42	3.12	8.97	0.48	0.13	0.36	12.42	1.41	0.02	11.19	2.80	1.41	8.49	29.99	4.75	6.11
1s	18.00	0.21	2.39	43.30	15.17	272.05	1.29	70.31	0.27	8.38	0.29	0.07	0.27	2.58	0.38	0.03	7.39	2.59	0.74	2.44	6.16	1.56	0.38
CV (%)	*161.5*	*24.5*	*18.3*	*204.5*	*23.0*	*108.7*	*14.0*	*19.4*	*8.6*	*93.4*	*59.4*	*57.9*	*77.2*	*20.7*	*26.9*	*191.5*	*66.0*	*92.7*	*52.1*	*28.8*	*20.5*	*32.8*	*6.3*
Minimum	0.6	0.58	8.32	6.45	41.8	30	6.9	150	2.46	4.7	0.3	0.06	0.2	8.3	0.53	0.01	5	0.61	0.52	4.75	18.4	2.8	5.1
Maximum	84.9	1.67	19.1	250.2	124.5	1271	12.3	549	3.56	52.2	1.7	0.46	1.6	18.8	2.1	0.2	36	9.12	3.34	17.2	45.2	9.2	6.8
N=sites	31	31	31	31	31	31	31	31	31	31	31	31	31	31	31	31	31	31	31	31	31	31	31

TABLE 3. SUMMARY STATISTICS FOR SELECTED ELEMENTS BY AQUA REGIA DIGESTION – ICP-MS FOR COMPARATIVE SOIL HORIZONS, TOMMY ORIENTATION LINE

LFH Horizon Humus	Au ppb	Mo ppm	Cu ppm	Pb ppm	Zn ppm	Ag ppb	Co ppm	Mn ppm	Fe ppm	As ppm	U ppm	Cd ppm	Sb ppm	La ppm	Al ppm	S %	Hg ppb	Cs ppm	Nb ppm	Y ppm	Ce ppm	LOI %	pH
Median	**1.0**	**1.04**	**5.94**	**4.2**	**59.6**	**474.5**	**0.9**	**885.5**	**0.21**	**0.4**	**0.1**	**0.92**	**0.07**	**0.85**	**0.10**	**0.10**	**188.5**	**0.58**	**0.33**	**0.45**	**1.45**	**90.7**	**5.0**
Mean	3.89	1.08	6.04	4.59	74.54	1087.15	1.09	1195.10	0.22	0.41	0.12	1.20	0.07	0.91	0.11	0.11	200.10	0.66	0.37	0.50	1.54	89.84	5.00
1s	9.28	0.37	1.67	1.58	39.44	1362.36	0.65	864.84	0.15	0.32	0.07	0.94	0.02	0.39	0.06	0.02	43.53	0.45	0.26	0.25	0.86	4.72	0.57
CV (%)	*238.9*	*34.4*	*27.6*	*34.5*	*52.9*	*125.3*	*59.8*	*72.4*	*65.2*	*77.1*	*58.3*	*78.4*	*33.2*	*43.4*	*53.8*	*18.5*	*21.8*	*69.3*	*70.7*	*49.7*	*55.9*	*5.3*	*11.3*
Minimum	0.1	0.53	3.82	2.57	29.6	54	0.4	241	0.04	0.1	0.1	0.39	0.03	0.5	0.03	0.08	145	0.15	0.09	0.18	0.5	78.2	4.2
Maximum	40.8	1.89	10.81	8.25	189.3	5380	2.5	3132	0.6	1.5	0.4	3.66	0.13	1.8	0.23	0.14	301	1.68	0.89	1.16	3.3	95.4	6
N=sites	20	20	20	20	20	20	20	20	20	20	20	20	20	20	20	20	20	20	20	20	20	20	20

B Horizon Soil	Au ppb	Mo ppm	Cu ppm	Pb ppm	Zn ppm	Ag ppb	Co ppm	Mn ppm	Fe ppm	As ppm	U ppm	Cd ppm	Sb ppm	La ppm	Al ppm	S %	Hg ppb	Cs ppm	Nb ppm	Y ppm	Ce ppm	LOI %	pH
Median	**5.3**	**0.94**	**8.84**	**11.5**	**113.0**	**182**	**10.1**	**593.5**	**3.27**	**6.0**	**0.3**	**0.39**	**0.21**	**9.3**	**1.60**	**0.01**	**20**	**1.90**	**3.26**	**5.46**	**19.9**	**8.8**	**5.4**
Mean	24.34	1.47	10.50	18.25	132.61	460.00	9.91	791.65	3.59	12.61	0.38	0.69	0.32	9.76	1.63	0.01	24.50	3.66	3.19	5.58	19.82	9.67	5.34
1s	51.79	1.80	6.07	18.22	57.04	685.15	0.98	564.70	1.17	17.88	0.26	0.70	0.33	3.55	0.26	0.00	13.08	3.21	0.42	2.47	7.14	3.49	0.47
CV (%)	*212.8*	*122.3*	*57.8*	*99.8*	*43.0*	*148.9*	*9.9*	*71.3*	*32.6*	*141.8*	*69.2*	*101.6*	*103.0*	*36.4*	*16.2*	*0.0*	*53.4*	*87.8*	*13.2*	*44.2*	*36.0*	*36.1*	*8.7*
Minimum	0.6	0.68	5.38	7.45	77.2	70	7.8	262	2.85	2.7	0.2	0.17	0.14	6.2	1.03	0.01	9	0.91	2.21	3.03	11.7	6.4	4.7
Maximum	223.1	8.89	33.58	82.72	321.3	2899	11.5	2455	8.27	78	1.3	3.2	1.56	22.4	2.22	0.01	62	10.99	3.94	14.97	43.7	20	6.5
N=sites	20	20	20	20	20	20	20	20	20	20	20	20	20	20	20	20	20	20	20	20	20	20	20

C Horizon Till	Au ppb	Mo ppm	Cu ppm	Pb ppm	Zn ppm	Ag ppb	Co ppm	Mn ppm	Fe ppm	As ppm	U ppm	Cd ppm	Sb ppm	La ppm	Al ppm	S %	Hg ppb	Cs ppm	Nb ppm	Y ppm	Ce ppm	LOI %	pH
Median	**3.2**	**0.83**	**13.51**	**10.7**	**64.4**	**72**	**9.5**	**383.5**	**3.23**	**6.4**	**0.4**	**0.12**	**0.26**	**13**	**1.51**	**0.01**	**7.5**	**1.30**	**1.03**	**8.71**	**33.15**	**4.2**	**6.2**
Mean	9.20	0.81	13.64	10.90	69.68	181.13	9.47	394.19	3.25	7.48	0.40	0.14	0.28	13.33	1.53	0.01	9.38	2.39	1.29	8.86	33.40	4.69	6.08
1s	12.80	0.07	1.77	3.42	16.22	175.82	1.06	51.22	0.19	2.46	0.05	0.09	0.07	2.39	0.25	0.00	4.16	2.04	0.78	1.52	5.16	1.46	0.29
(CV%)	*139.1*	*8.7*	*13.0*	*31.4*	*23.3*	*97.1*	*11.1*	*13.0*	*6.0*	*32.9*	*12.9*	*68.3*	*26.1*	*18.0*	*16.3*	*0.0*	*44.4*	*85.4*	*60.6*	*17.1*	*15.4*	*31.0*	*4.8*
Minimum	0.8	0.69	10.75	6.78	57.1	30	8.1	334	2.98	4.7	0.3	0.06	0.2	9.5	1.17	0.01	5	0.61	0.56	6.25	23.1	3.1	5.5
Maximum	40.6	0.92	16.3	19.2	124.5	571	11.6	549	3.56	13.3	0.5	0.46	0.47	18.8	2.1	0.01	16	7.48	3.34	11.85	45.2	8.3	6.7
N=sites	16	16	16	16	16	16	16	16	16	16	16	16	16	16	16	16	16	16	16	16	16	16	16

TABLE 4. SUMMARY STATISTICS FOR SELECTED ELEMENTS BY AQUA REGIA DIGESTION – ICP-MS FOR COMPARATIVE SOIL HORIZONS, TED ORIENTATION LINE

LFH Horizon Humus	Au ppb	Mo ppm	Cu ppm	Pb ppm	Zn ppm	Ag ppb	Co ppm	Mn ppm	Fe ppm	As ppm	U ppm	Cd ppm	Sb ppm	La ppm	Al ppm	S %	Hg ppb	Cs ppm	Nb ppm	Y ppm	Ce ppm	LOI %	pH
Median	**0.1**	**0.75**	**4.55**	**4.1**	**48.9**	**620.5**	**0.7**	**849.5**	**0.17**	**0.3**	**0.1**	**0.48**	**0.09**	**0.9**	**0.11**	**0.10**	**233**	**0.39**	**0.24**	**0.43**	**1.40**	**91.5**	**4.5**
Mean	0.27	3.09	5.57	4.36	57.26	1159.88	0.93	1081.19	0.23	0.51	0.43	0.60	0.11	3.31	0.14	0.10	241.06	0.46	0.31	5.40	2.65	88.21	4.60
1s	0.60	9.56	3.32	1.14	27.19	1202.87	0.77	887.61	0.20	0.60	0.88	0.38	0.10	9.29	0.11	0.02	50.21	0.37	0.29	18.16	4.95	8.29	0.49
CV (%)	*223.1*	*309.5*	*59.7*	*26.0*	*47.5*	*103.7*	*82.8*	*82.1*	*86.7*	*119.1*	*206.6*	*62.8*	*84.1*	*280.6*	*82.3*	*20.5*	*20.8*	*79.9*	*91.8*	*336.6*	*186.9*	*9.4*	*10.7*
Minimum	0.1	0.18	3.01	2.6	18.8	234	0.2	235	0.04	0.1	0.1	0.2	0.05	0.5	0.04	0.07	149	0.2	0.07	0.13	0.4	70.4	4
Maximum	2.5	38.9	16.42	6.35	117.2	4907	3.1	3742	0.65	2.5	3	1.37	0.45	38.1	0.46	0.14	344	1.67	1.16	73.28	20.9	96.4	5.5
N=sites	16	16	16	16	16	16	16	16	16	16	16	16	16	16	16	16	16	16	16	16	16	16	16

B Horizon Soil	Au ppb	Mo ppm	Cu ppm	Pb ppm	Zn ppm	Ag ppb	Co ppm	Mn ppm	Fe ppm	As ppm	U ppm	Cd ppm	Sb ppm	La ppm	Al ppm	S %	Hg ppb	Cs ppm	Nb ppm	Y ppm	Ce ppm	LOI %	pH
Median	**1.8**	**1.05**	**8.41**	**14.3**	**79.75**	**185.5**	**9.1**	**463**	**2.98**	**6.6**	**0.3**	**0.29**	**0.36**	**7.55**	**1.17**	**0.01**	**19**	**2.20**	**2.66**	**3.40**	**13.80**	**7.5**	**5.0**
Mean	4.72	1.10	10.05	25.84	141.53	291.13	8.64	688.25	3.03	8.93	0.61	0.61	0.43	9.25	1.17	0.02	19.38	3.05	2.53	6.04	16.16	8.01	4.98
1s	7.20	0.34	5.49	28.61	212.16	358.41	2.62	648.56	0.61	6.26	1.09	1.02	0.24	5.93	0.46	0.02	9.24	1.98	1.16	10.20	6.89	1.85	0.64
CV (%)	*152.5*	*30.6*	*54.6*	*110.7*	*149.9*	*123.1*	*30.4*	*94.2*	*20.0*	*70.0*	*178.0*	*168.3*	*56.5*	*64.1*	*39.6*	*100.7*	*47.7*	*64.9*	*45.7*	*169.0*	*42.7*	*23.1*	*13.0*
Minimum	0.1	0.68	6.61	7.47	37.4	38	4.8	229	2.09	2.6	0.2	0.14	0.19	4	0.49	0.01	6	0.96	0.37	1.03	7.5	5.3	3.8
Maximum	24.4	1.99	29.45	112.52	891.1	1523	14.7	2668	4.05	27	4.5	4.26	0.94	30.4	2.09	0.09	40	8.03	5.5	43.6	37.2	11.5	6.3
N=sites	16	16	16	16	16	16	16	16	16	16	16	16	16	16	16	16	16	16	16	16	16	16	16

C Horizon Till	Au ppb	Mo ppm	Cu ppm	Pb ppm	Zn ppm	Ag ppb	Co ppm	Mn ppm	Fe ppm	As ppm	U ppm	Cd ppm	Sb ppm	La ppm	Al ppm	S %	Hg ppb	Cs ppm	Nb ppm	Y ppm	Ce ppm	LOI %	pH
Median	**3.1**	**0.78**	**12.14**	**16.5**	**58.5**	**156**	**9.0**	**329**	**3.00**	**6.8**	**0.4**	**0.11**	**0.31**	**11**	**1.21**	**0.01**	**10**	**1.25**	**1.43**	**7.32**	**28.5**	**4.5**	**6.2**
Mean	13.23	0.88	12.50	32.14	62.25	323.87	8.91	328.53	2.98	10.55	0.57	0.12	0.44	11.45	1.29	0.03	13.13	3.23	1.54	8.09	26.35	4.80	6.14
1s	22.59	0.29	2.86	61.28	13.45	337.94	1.48	73.47	0.27	11.78	0.40	0.05	0.38	2.47	0.46	0.05	9.52	3.09	0.69	3.16	5.03	1.71	0.47
CV (%)	*170.8*	*33.0*	*22.9*	*190.7*	*21.6*	*104.3*	*16.6*	*22.4*	*9.1*	*111.6*	*69.3*	*39.4*	*85.9*	*21.6*	*35.8*	*184.1*	*72.5*	*95.6*	*44.5*	*39.1*	*19.1*	*35.5*	*7.7*
Minimum	0.6	0.58	8.32	6.45	41.8	55	6.9	150	2.46	5.2	0.3	0.06	0.23	8.3	0.53	0.01	5	0.78	0.52	4.75	18.4	2.8	5.1
Maximum	84.9	1.67	19.1	250.2	92.6	1271	12.3	476	3.38	52.2	1.7	0.22	1.6	17.6	2.02	0.2	36	9.12	2.7	17.2	34.9	9.2	6.8
N=sites	15	15	15	15	15	15	15	15	15	15	15	15	15	15	15	15	15	15	15	15	15	15	15

site. It is not presently known whether these precious metal concentrations reflect the location of a previously unknown zone or are simply the product of downslope colluviation of mineralized material from the Tommy vein.

TED VEIN RESULTS

Gold and silver in humus, B horizon soil and till all reflect the presence of precious metals mineralization at the Ted vein to varying degrees, although the magnitudes of the

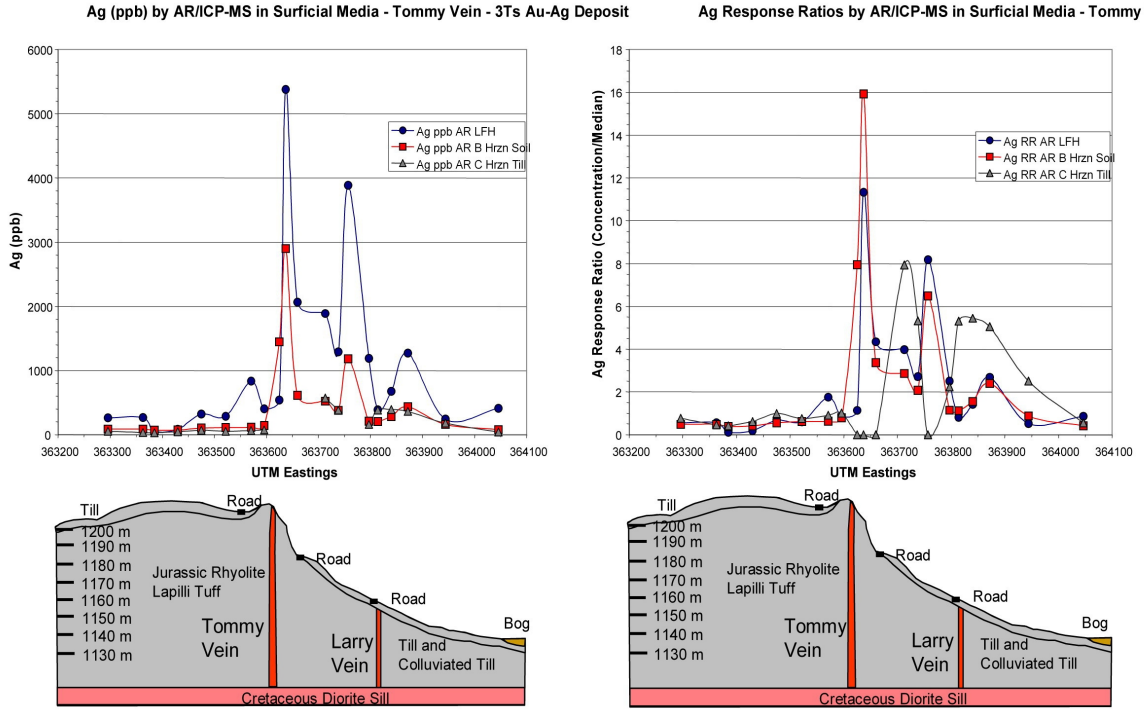


Figure 16. Distribution of Ag concentrations (left) and calculated response ratios (right) in humus, B horizon soil and C horizon till and other parent materials along the east-west Tommy vein orientation transect.

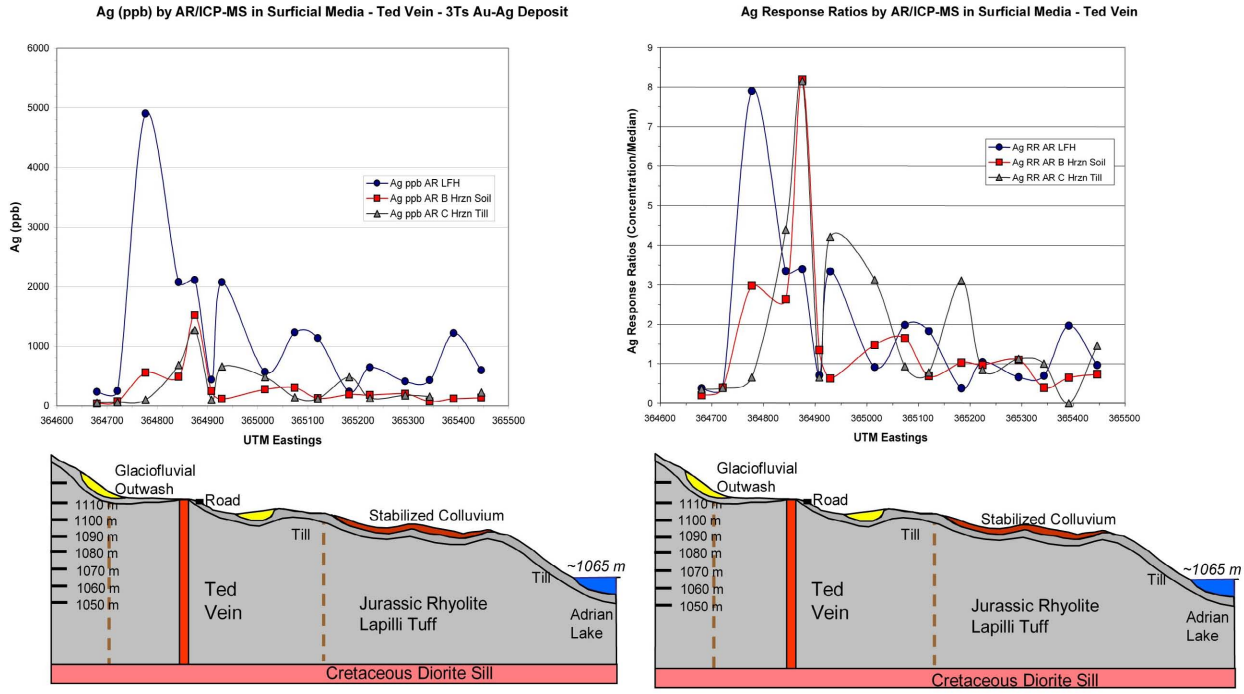


Figure 17. Distribution of Ag concentrations (left) and calculated response ratios (right) in humus, B horizon soil and C horizon till and other parent materials along the approximately east-west Ted vein orientation transect.

geochemical responses for these elements are slightly less than those reported for the Tommy vein. Conversely, soil at Ted vein contains higher concentrations of certain base metals such as Zn (maximum 891 ppm) and Pb (maximum 113 ppm) than does soil at the Tommy vein. These results are consistent with the reported higher sulphide mineral content of the Ted relative to the Tommy vein, where disseminated sulphide minerals are not always observed to be present (Rhys, 2003). Such aqua regia base metal relations are not the subject of this preliminary report, which centres on precious metals geochemistry results, but they will be addressed in the final project report (Cook and Dunn, work in progress).

The Ted vein is bracketed by two orientation sites (sites 558 and 559), with the highest precious metals con-

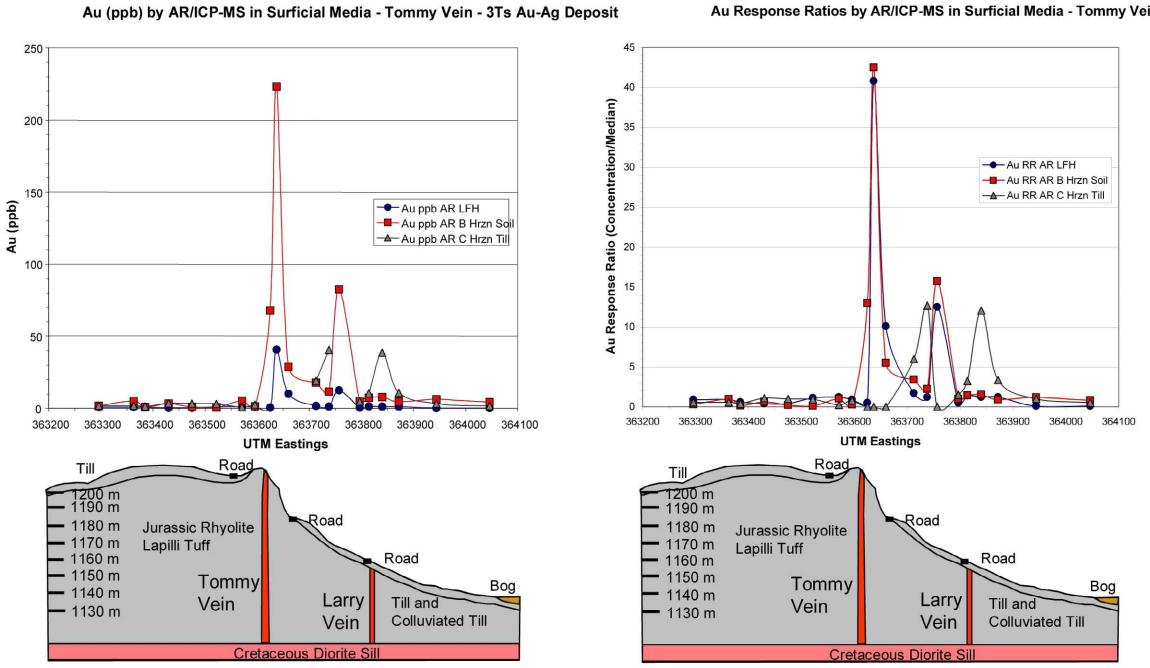


Figure 18. Distribution of Au concentrations (left) and calculated response ratios (right) in humus, B horizon soil and C horizon till and other parent materials along the east-west Tommy vein orientation transect.

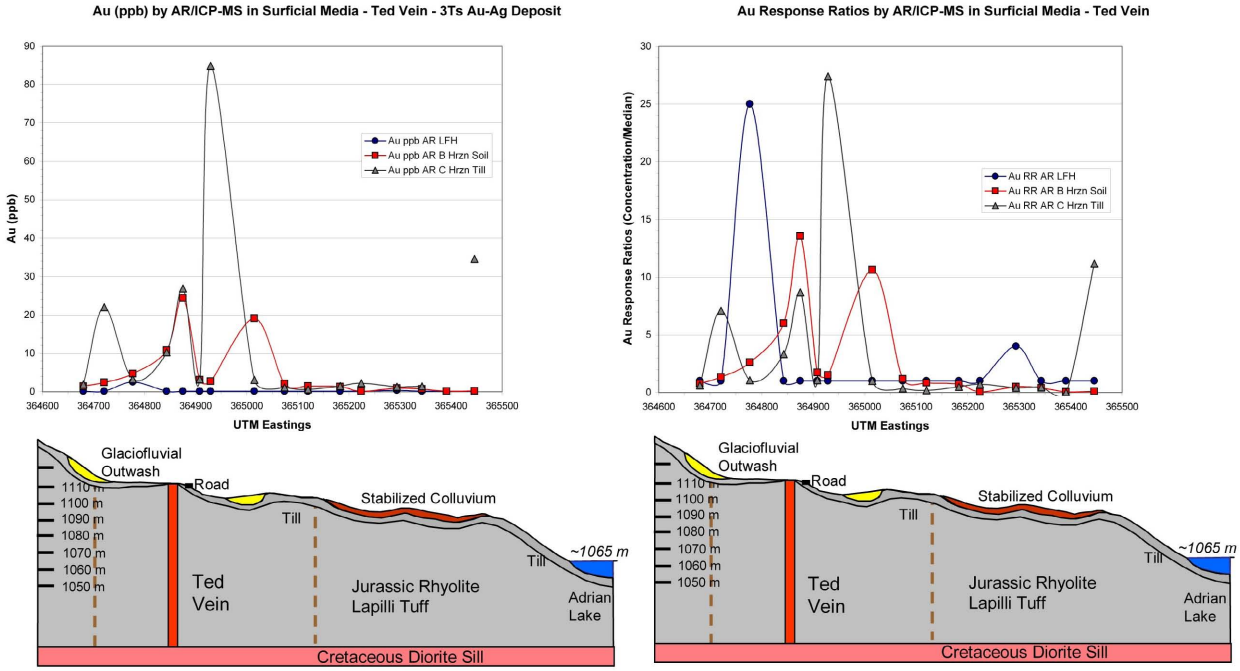


Figure 19. Distribution of Au concentrations (left) and calculated response ratios (right) in humus, B horizon soil and C horizon till and other parent materials along the approximately east-west Ted vein orientation transect.

centrations generally reported at the easternmost of the two (site 559; Fig. 6, 12), immediately downslope and down ice. Elevated Au concentrations are present in a B horizon soil (24.4 ppb; site 559) at the Ted vein and at two sites in C horizon till (26.9–84.9 ppb), both above and down ice of the vein. These correspond, at site 559 closest to the vein, to highly elevated response ratios of 9 and 14 times background in soil and till, respectively. In the case of Ag, elevated values are present in all three media, particularly at the easternmost site 559. Silver concentrations of 1523 ppb in B horizon soil (median 186 ppb) and 1271 ppb in till (median 156 ppb) both represent response ratios of about 8 times those of background values. Silver concentrations in LFH horizon humus at both of the Ted vein sites are also very high, in the order of 2000 ppb, but yield response ratios of only about 3 times due to the relatively high Ag background concentrations in humus on the Ted orientation line (median 621 ppb) relative both to the underlying mineral soil and to humus on the Tommy. Interestingly, there are no coincident elevated Au concentrations in LFH horizon humus at the Ted vein, although Au concentrations up to 41 ppb were reported from similar humus above the Tommy vein (Fig. 5).

Elevated Au and Ag concentrations in both B horizon soil and till at site 559 on the Ted orientation line are of very similar magnitude (*e.g.*, 24–27 ppb Au), even though the soil in this composite profile is developed in a stabilized colluvial sediment (Fig. 12) rather than the underlying IIC horizon till. This is likely, in this particular case, due to the site being both downslope of (to the northeast) and down ice of (to the east) the same Ted vein. Elsewhere, the lower background Au concentrations of B horizon soil on the Ted line (median 1.8 ppb) relative to those on the Tommy line (median: 5.3 ppb) may be, at least in part, due to the widespread presence, overlying the till, of now-stabilized surface colluvium from a southerly, apparently unmineralized source area. Similar relations were reported by Cook and Fletcher (1994) for varying Pt contents of ultramafic colluvium overlying till in the Tulameen area of southern BC.

Perhaps the most intriguing aspect of precious metals distribution on the Ted orientation line is the very high Ag content (4907 ppb) of humus at one site (574), located west of the Ted vein. This highly elevated Ag concentration is the highest on Ted line and corresponds to a response ratio of almost 8 times the median concentration in humus (621 ppb). This LFH horizon is developed on a till-based soil profile in relatively flat terrain. The Au concentration, although only 2.5 ppb, is nevertheless the highest of any of the sixteen humus samples on the Ted line (median: 0.1 ppb) and it yields a response ratio of 25 times background. The underlying B horizon soil contains only background Au levels but does yield an elevated Ag content of 554 ppb, the second highest on the line after the Ted vein itself, with a response ratio of almost 3 times background (median 186 ppb). The proximity to adjacent humus sites on the Ted line with high Ag suggests two possible explanations. It may reflect the presence of a parallel or peripheral mineralized zone. Alternatively, given the similar site elevation to the adjacent Ted vein, it may instead simply reflect local hydromorphic scavenging of metals derived from weathering of Ted vein mineralization.

In addition to the above, locally elevated single-site Au concentrations of unknown origin occur in till on the Ted line, both near its western end (22 ppb) and at its eastern end (34.6 ppb). Neither B horizon soil nor humus are similarly enriched in Au at these sites.

PRELIMINARY CONCLUSIONS

Preliminary results from a geochemical orientation study carried out at the 3Ts epithermal Au-Ag prospect in central BC show that Au and Ag determined by aqua regia digestion – ICP-MS in humus, B horizon soil and C horizon till all reflect, to varying degrees, the presence of Au in epithermal quartz vein mineralization at both the Tommy and Ted veins. In addition to this, Au and Ag in till alone reflect the presence of the Larry vein, which is transected by the Tommy orientation line.

Results suggest that, for property-scale geochemical exploration, B horizon mineral soil and LFH horizon organic-rich humus offer similar levels of geochemical contrast for aqua regia – digestible Au and Ag, with the B horizon soil offering slightly superior contrast overall. Brunisolic Bm horizon soil is commonly developed around the 3Ts property, primarily in the basal and colluviated tills that are the dominant glacial parent material in the area. However, they are also found to be developed in rubbly near-bedrock colluvium, stabilized colluvium and glaciofluvial sediments, underlining the importance of the proper identification of Quaternary deposits in interpreting source directions of any anomalous geochemical patterns.

Geochemical results vary slightly from vein to vein with variations in primary mineralogy, topography and surficial cover. In general aqua regia – digestible Au and Ag results at the Tommy vein show slightly greater geochemical contrast, as measured by response ratios, than do those at Ted vein. At the Tommy vein, Au response ratios for B horizon soil and humus over the vein are almost identical. Elevated Ag results in humus provide a larger geochemical footprint, but elevated Ag in B horizon soil offers slightly better anomaly contrast over the mineralization. Rubbly B horizon soil and LFH humus are developed directly over subcopping and outcropping quartz vein mineralization here, and likely incorporate a significant component of near-residual mineralized fragments. There is no direct till response, as neither basal nor colluviated till is preserved directly over the vein. However, elevated Au and Ag values in till immediately to the east are tentatively interpreted to represent, at least in part, glacially transported material that was locally derived from the Tommy vein.

Surficial cover is more complex on the Ted orientation line. Localized glaciofluvial outwash sediments and more widespread stabilized near-surface colluvium are present in addition to basal and colluviated tills. As with the Tommy vein results, B horizon mineral soil here provides the best overall anomaly contrast for property-scale geochemical exploration. Gold and silver in humus, B horizon soil and till all reflect the presence of precious metals mineralization at the Ted vein to varying degrees, although the magnitudes of the geochemical responses are slightly less than those reported for Tommy vein. In addition, highly elevated Au and Ag concentrations are present in both B horizon soil and C horizon till, both above and down ice of the vein. Elevated Ag is similarly present in LFH horizon humus here, although Au itself is absent. Readers are referred to the companion paper of Dunn *et al.* (2006) for additional information on corresponding lodgepole pine and white spruce biogeochemical results at 3Ts.

Although the results of this study demonstrate that the locations of both the Tommy and Ted veins may be successfully delineated using mineral soil and organic-rich humus, they do not necessarily indicate that similar, but blind, deposits may be detected at greater depths. The felsic tuff that hosts epithermal Au-Ag mineralization at 3Ts is only poorly exposed at surface beneath the widespread till veneer, stabilized colluvium and abundant forest moss cover that hinder effective prospecting here. However, the positive aqua regia – digestible geochemical results here are strongly influenced by the near-surface outcropping and subcropping of subvertical, highly resistant quartz veins beneath a thin near-residual soil. Continuation of further field studies in areas where the Tommy and Ted veins are known to exist at greater depth may, however, help provide some of these answers.

A final report to Geoscience BC, incorporating comparative results of all analytical methods employed in this study (Cook and Dunn, work in progress), will be submitted by March 31, 2006. The final report will ascertain which of the partial and selective extraction methods described here delineate the presence of mineralization and provide the greatest levels of geochemical contrast over each of the Tommy and Ted veins at the 3Ts prospect. Specific field sampling and analytical recommendations will be provided for conducting the most effective property-scale geochemical surveys for similar epithermal Au deposits in the BC interior plateau.

ACKNOWLEDGMENTS

Funding for the project was provided by Geoscience BC. The authors thank Karen Hulme of the University of Adelaide, Australia for her able assistance during the field program. Lindsay Bottomer and Dan Meldrum of Southern Rio Resources Ltd., Vancouver, are thanked for their support of and assistance with the project. Kerry Kennedy also assisted during fieldwork, and crew accommodation was provided by Tatelkuz Lake Ranch. John Barr of Anglo American Exploration (Canada) Ltd., Vancouver, and Ray Lett of the BC Geological Survey, Victoria, provided some of the control standards used in this project. Lindsay Bottomer, Ray Lett and Rob Stevens reviewed and commented on earlier versions of the manuscript.

REFERENCES

Agriculture Canada (1987): The Canadian system of soil classification (second edition); *Agriculture Canada*, Expert Committee on Soil Survey, Publication 1646, 164 pages.

Bajc, A.F. (1998): A comparative analysis of Enzyme Leach and Mobile Metal Ion selective extractions: case studies from glaciated terrain, northern Ontario; *Journal of Geochemical Exploration*, volume 61, pages 113–148.

Bottomer, L. (2003a): Epithermal gold-silver mineralization in the Nechako plateau, central British Columbia; North West Mining Association, Annual Meeting, Program with Abstracts, December 2003.

Bottomer, L. (2003b): The 3Ts epithermal gold-silver project, Nechako region, central BC; Cordilleran Round-Up 2003, Program with Abstracts, January 2003.

Cameron, E.M., Hamilton, S.M., Leybourne, M.I., Hall, G.E.M. and McClenaghan, M.B. (2004): Finding deeply buried deposits using geochemistry; *Geochemistry: Exploration, Environment, Analysis*, volume 4, pages 7–32.

Cook, S.J. and Fletcher, W.K. (1994): Platinum distribution in soil profiles of the Tulameen ultramafic complex, southern British Columbia, Canada; *Journal of Geochemical Exploration*, volume 51, pages 161–191.

Cook, S.J. and Jackaman, W. (1994): Regional lake sediment and water geochemistry of part of the Nechako River map area (93F/2, 3; parts of 93F/6, 11, 12, 13, 14); *BC Ministry of Energy, Mines and Petroleum Resources*, Open File 1994-19, 31 pages.

Cook, S.J. and McConnell, J. (2001): Lake sediment geochemical methods in the Canadian shield, cordillera and appalachia; *in* Drift Exploration in Glaciated Terrain; McClenaghan, M.B., Bobrowsky, P.T., Hall, G.E.M. and Cook, S.J., Editors, *The Geological Society of London*, Special Publication 185, pages 125–149.

Cook, S.J., Jackaman, W., Lett, R.E.W., McCurdy, M.W. and Day, S.J. (1999): Regional lake water geochemistry of parts of the Nechako plateau, central British Columbia (93F/2, 3; 93K/9, 10, 15, 16; 93L/9, 16; 93M/1, 2, 7, 8); *BC Ministry of Energy, Mines and Petroleum Resources*, Open File 1999-5.

Cook, S.J., Levson, V.M., Giles, T.R. and Jackaman, W. (1995): A comparison of regional lake sediment and till geochemistry surveys: a case study from the Fawnie Creek area, central British Columbia; *Exploration and Mining Geology,* volume 4, no 2, pages 93–110.

Diakow, L.J. and Levson, V.M. (1997): Bedrock and surficial geology of the southern Nechako plateau, central British Columbia (NTS 93F/2, 3, 6, 7); *BC Ministry of Energy, Mines and Petroleum Resources,* Geoscience Map 1997-2.

Diakow, L.J., Webster, I.C.L., Levson, V.M. and Giles, T.R. (1994): Bedrock and surficial geology of the Fawnie Creek map area (NTS 93F/3); *BC Ministry of Energy, Mines and Petroleum Resources*, Open File 1994-2.

Diakow, L.J., Webster, I.C.L., Whittles, J.A., Richards, T.A., Levson, V.M. and Giles, T.R. (1995): Bedrock and surficial geology of the Tsacha Lake map area (NTS 93F/2); *BC Ministry of Energy, Mines and Petroleum Resources*, Open File 1995-16.

Dunn, C.E., Cook, S.J. and Hall, G.E.M. (2006): Halogens in surface exploration geochemistry: evaluation and development of methods for detecting buried mineral deposits (NTS 093F/03), central British Columbia; *in* Geological Fieldwork 2005, *BC Ministry of Energy, Mines and Petroleum Resources*, Paper 2006-1 and *Geoscience BC*, Report 2006-1.

Fedikow, M.A.F. (2005): Discriminating barren and productive geophysical targets using partial digestion soil geochemistry: discovery of the Hunt gold zone, Manitoba, Canada; *Association of Applied Geochemists*, 22nd International Geochemical Exploration Symposium, Program and Abstracts, page 51.

Fox, P.E. (1994): Geochemical report on the Taken claim, Omineca Mining Division; *BC Ministry of Energy, Mines and Petroleum Resources*, Assessment Report 23758, 29 pages.

Fox, P.E. (1995): Geological report on the Taken 1 claim, Omineca Mining Division; *BC Ministry of Energy, Mines and Petroleum Resources*, Assessment Report 24203, 21 pages.

Fox, P.E. (1996): Diamond drilling, geological and soil geochemical report on the Tam property, Omineca Mining Division; *BC Ministry of Energy, Mines and Petroleum Resources*, Assessment Report 24710, 92 pages.

Fox, P.E. (1999): Geological, geochemical and geophysical report on the Taken property, Omineca Mining Division; *BC Ministry of Energy, Mines and Petroleum Resources*, Assessment Report 25810, 33 pages.

Giles, T.R. and Levson, V.M. (1994a): Surficial geology and drift exploration studies in the Fawnie Creek area (93F/03); *in*

Geological Fieldwork 1993, *BC Ministry of Energy, Mines and Petroleum Resources*, Paper 1994-1, pages 27–37.

Giles, T.R. and Levson, T.M. (1994b): Drift prospecting potential of the Fawnie Creek area (93F/03); *BC Ministry of Energy, Mines and Petroleum Resources*, Open File 1994-10.

Giles, T.R. and Levson, T.M. (1995): Surficial geology and Quaternary stratigraphy of the Tsacha Lake area (93F/02); *BC Ministry of Energy, Mines and Petroleum Resources*, Open File 1995-10.

Lane, R.A. and Schroeter, T.G. (1997): A review of metallic mineralization in the Interior Plateau, central British Columbia (parts of NTS 93C, B and F); *in* Interior Plateau Geoscience Project: Summary of geological, geophysical and geochemical studies, Diakow, L.J., Newell, J.M. and Metcalfe, P., Editors, *BC Ministry of Energy, Mines and Petroleum Resources*, Paper 1996-2.

Levson, V.M. (2001): Regional till geochemical surveys in the Canadian Cordillera: sample media, methods and anomaly evaluation; *in* Drift Exploration in Glaciated Terrain, McClenaghan, M.B., Bobrowsky, P.T., Hall, G.E.M. and Cook, S.J., Editors, *Geological Society of London*, Special Publication 185, pages 45–68.

Levson, V.M. and Giles, T.R. (1994): Surficial geology and Quaternary stratigraphy of the Fawnie Creek area (93F/03); *BC Ministry of Energy, Mines and Petroleum Resources*, Open File 1994-9.

Levson, V.M., Giles, T.R., Cook, S.J. and Jackaman, W. (1994): Till geochemistry of the Fawnie Creek map area (93F/03); *BC Ministry of Energy, Mines and Petroleum Resources*, Open File 1994-18.

Lynch, J. (1996): Provisional elemental values for four new geochemical soil and till reference materials TILL-1, TILL-2, TILL-3 and TILL-4; *Geostandards Newsletter*, Volume 20, no 2, pages 277–287.

Lynch, J. (1999): Additional provisional elemental values for LKSD-1, LKSD-2, LKSD-3, LKSD-4, STSD-1, STSD-2. STSD-3, STSD-4; *Geostandards Newsletter*, Volume 23, no 2, pages 251–260.

MINFILE (2005): MINFILE BC mineral deposits database; *BC Ministry of Energy, Mines and Petroleum Resources*, URL <http://www.em.gov.bc.ca/Mining/Geolsurv/Minfile/> [Nov 2005].

Pautler, J.M. (1995): 1995 Spotlight Session on Interior Plateau of British Columbia; *Cordilleran Roundup*, Abstracts, page 42.

Pautler, J.M., Smith, S.W. and Lane, R.A. (1999): Exploration and geology of the Tsacha epithermal gold deposit; *in* Exploration and Mining in British Columbia 1998, *BC Ministry of Energy, Mines and Petroleum Resources*, pages B1–B10.

Pawliuk, D.J. (2005); Summary report on the Ted vein diamond drilling program — November 2004, Tam property, 3Ts Project, Omineca Mining Division; report prepared for Southern Rio Resources, April 2005, filed on SEDAR July 8 2005, 28 pages.

Rhys, D. (2003): Tsacha and Tam properties — structural study; internal consulting report prepared by Panterra Geoservices Inc. for Southern Rio Resources, July 10, 2003, 18 pages.

Schimann, K. (1994): Geological and geochemical report on the Tam claims, Omineca Mining Division; *BC Ministry of Energy, Mines and Petroleum Resources*, Assessment Report 23746, 20 pages.

Sutherland, D. and Hoffman, E.L. (2003): SGH — a new soil gas hydrocarbon technique for mineral exploration under deep cover; *Geological Association of Canada – Mineralogical Association of Canada*, Joint Annual Meeting, Program with Abstracts, 1 page.

Tipper, H.W. (1963): Nechako River map-area, British Columbia; *Geological Survey of Canada*, Memoir 324, 59 pages.

Wallis, C.S. and Fier, N.E. (2002): Technical report on the Tsacha property, British Columbia; report prepared for Southern Rio Resources, filed on SEDAR February 11, 2003.

Wallis, C.S. and Fier, N.E. (2004): Technical report on the Tam property, British Columbia; report prepared for Southern Rio Resources, filed on SEDAR September 2, 2004.

Halogens in Surface Exploration Geochemistry: Evaluation and Development of Methods for Detecting Buried Mineral Deposits (NTS 093F/03), Central British Columbia[1]

By Colin E. Dunn[2], Stephen J. Cook[3] and Gwendy E.M. Hall[4]

KEYWORDS: exploration, geochemistry, gold, copper, soil, vegetation, halogens, multielement suites

INTRODUCTION

A striking feature of the current MINFILE (2005) mineral occurrence map of BC is that a significant part of central BC has very few mineral discoveries (Fig. 1). Much of this area has a cover of Quaternary deposits and/or volcanic rocks and, given the fact that it is underlain by the generally 'fertile' Quesnel Terrane, there is good reason to be optimistic that significant buried mineralization may be present. The challenge is, therefore, to develop a method for detecting mineralization hidden beneath this cover. Various geochemical selective extraction methods are steadily being refined to assist the search for buried mineralization in BC (Cook and Dunn, 2006), and the present study aims at augmenting this 'tool box' of techniques by developing some new methodology.

The halogens comprise five nonmetallic elements whose compounds form salts. The term 'halogen' means 'salt-former' and, at room temperature, they exist in all three states of matter: solid (iodine, astatine), liquid (bromine) and gas (fluorine, chlorine). However, they all form diatomic molecules that are gases at normal temperatures and pressures, and therefore are mobile and play significant roles in the atmosphere, hydrosphere and biosphere. They are the most organophilic elemental family, such that they react with organic compounds on contact and are therefore readily absorbed by plants. Of these elements, astatine is radioactive and not considered in this study. The remaining halogens are commonly associated with the emplacement of mineral deposits, as witnessed by their presence in many minerals and in the saline fluid inclusions that are typical of many mineral deposits. Their volatility renders them good candidates to examine as 'pathfinder elements' in surface geochemical media, where they may be captured on soil particles and taken up by vegetation.

Fluorine-rich minerals are characteristic of late-stage hydrothermal systems. Fluid inclusions associated with mineral deposits are commonly rich in NaCl (*e.g.*, ~50% NaCl in inclusions within Cu porphyries), attesting to the highly saline environment of many ore-forming processes. In recent years, fluid inclusion studies have included determinations of Br and I. Furthermore, some styles of mineralization, such as the Broken Hill Sedex deposits in Australia, have high levels of F and Cl in fluorite, apatite and amphiboles. During the degradation of these mineral deposits, whether due to the reaction with subsurface waters, subtle changes in pressure or fracturing by slight seismic activity, some of the halogen component may be released.

The high contents of Br, Cl and I in seaweed have long been known. Relatively little information is available on the distribution of these elements within and among land plants, and their relationships to mineralization have received little attention except in Russia, from where detailed information is difficult to obtain. Some published and personal observations are:

- Pine needles are good indicators of F; the standard pine needle control NIST 1575a is reported to contain an average of 389 ppm F.
- Spruce needles can contain >1000 ppm Cl (C.E. Dunn, unpublished data).
- Br levels are commonly elevated in vegetation growing over Au deposits (Dunn, 1985).
- Unpublished scanning electron microscope investigations by the senior author have revealed chlorides of potassium and bismuth formed in the trunk wood of trees growing on the epithermal Au system at Mt. Washington (Vancouver Island), demonstrating the metal complexing of halogens within plant tissues.
- Iodine enrichment occurs in plants growing over porphyry deposits (Al Ajely *et al.*, 1985).

Outside of the former Soviet Union, the halogens have been little used in mineral exploration; this is partly because of inadequate easily accessible analytical methodology for determinations at low concentrations. An account of the significance of I and Br for indicating deep ore deposits has recently been made available as an English translation of a classic Russian work (Trofimov and Rychkov, 2004). They demonstrated the exceptional migrational abilities of I and Br in different geological settings, and "show these elements to be highly effective in exploring for deeply buried endogenous ore bodies and using this technique has resulted in finding new highly prospective ore bodies….up to 1,000 m depth." They stated that "within all deposits studied, iodine and bromine occupy the position most distant from ore bodies. This extreme zonal position makes it possible to use these elements as very effective indicators of hidden ore deposits." They concluded that "sec-

[1] *Geoscience BC contribution GCB003*

[2] *Consulting Geochemist, Sidney, BC*

[3] *Cook Geochemical Consulting, Victoria, BC*

[4] *Geological Survey of Canada, Ottawa, ON*

This publication is also available, free of charge, as colour digital files in Adobe Acrobat PDF format from the BC Ministry of Energy, Mines and Petroleum Resources internet website at http://www.em.gov.bc.ca/Mining/Geolsurv/Publications/catalog/catfldwk.htm

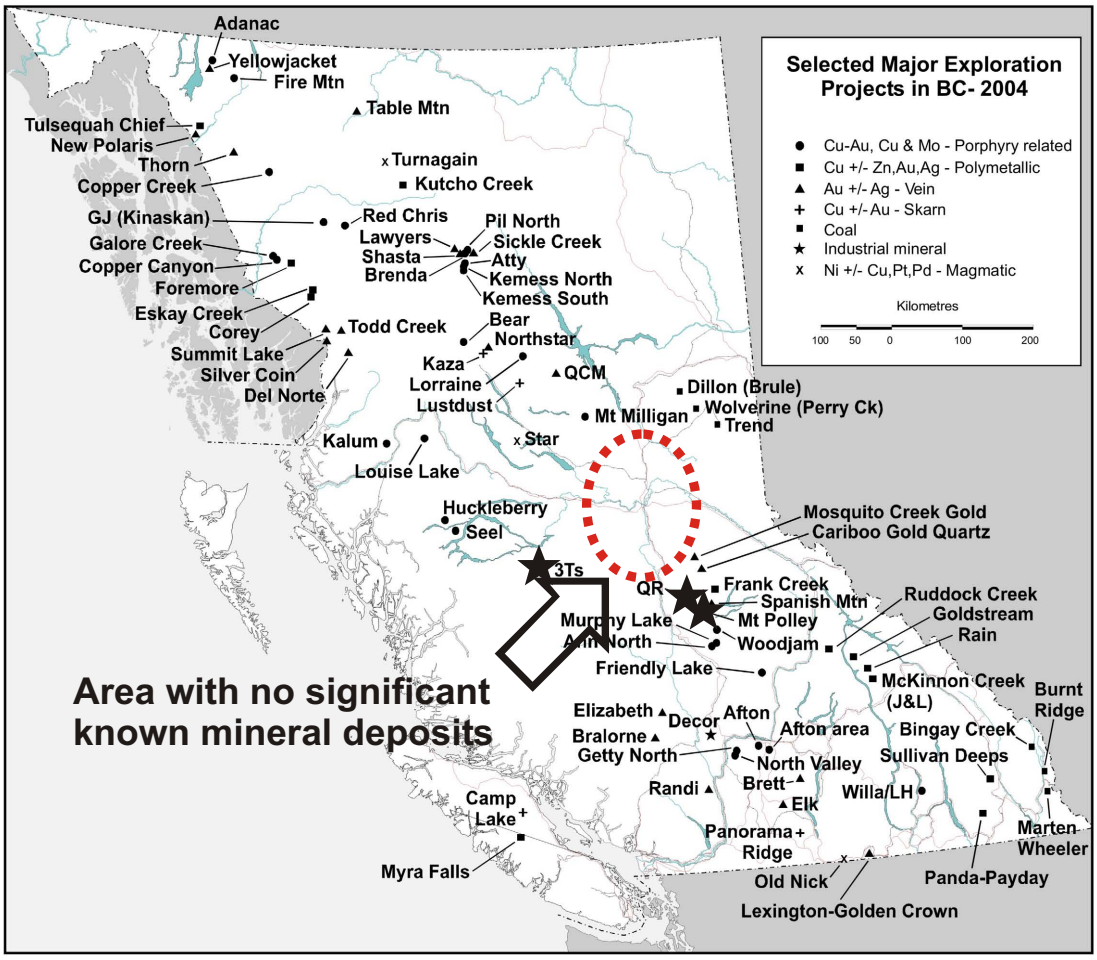


Figure 1. Area outlined for focusing on halogen geochemistry method development. Grey stars indicate areas of focused studies: Mt. Polley, QR and 3Ts. Map base from the BC Ministry of Energy, Mines and Petroleum Resources (2005).

ondary geochemical haloes ….are still insufficiently studied, and biogeochemical halos of these elements have yet to be found [because there are no reported studies]. These problems must be the primary focus of further studies. We must improve the analytical determinations of iodine and bromine and then transfer this understanding to the analytical instrumentation".

FOCUS OF FIELD STUDIES

As part of a two-year program, the focus in this first year is to obtain suitable vegetation and soil samples for analysis and investigate their geochemical signatures over a range of mineral deposit styles typically found in central BC: a Cu-Au porphyry (Mt. Polley), a Au skarn (QR) and nearby Au/Mo mineralization associated with gabbro, and a Au-Ag epithermal system (3Ts). The aims are to,

- determine the geochemical response of volatile elements (halogens) to known mineralization;
- compare these responses to trace element signatures of the same samples;
- assess the potential value of halogen geochemistry to the exploration for minerals concealed by volcanic rocks and glacial deposits;
- by evaluating and comparing commercially available analytical methods, identify gaps in analytical methodology and develop new analytical techniques (in year 2) most suited to the geological and physiographic environments of central BC; and
- develop new technology and methods for passing on to Canadian analytical laboratories and to the exploration community at large.

A summary of the samples collected in each of the three survey areas is given in Table 1. This table shows that there was a considerably larger collection of vegetation samples than of soil. This is partly because two or three different plant tissues could be collected in the time that was required for collecting the soil samples and recording relevant observations, and partly because, at the time of collection, it was unknown which plant species would be the most suitable for accumulating the halogens. Russian literature has indicated that they tend to concentrate in the foliage, so the prime sample medium at each area was foliage of common species, with pine bark as a secondary collection. In view of the ease of collection of the vegetation samples, an extra minute was spent at those sites where a third species was commonly present (*e.g.*, Mt. Polley). No single species was present at all locations. Lodgepole pine was the most common species, but foliage could not be collected because

TABLE 1. SUMMARY OF SOIL AND VEGETATION SAMPLES COLLECTED AT EACH LOCATION. PRINCIPAL VEGETATION SAMPLES SENT FOR ANALYSIS ARE SHOWN IN BOLD ITALICS

Location	Areas Sampled	Soil Sites		Vegetation Sites	
		n [1]	*Horizon*	*Species*	*n* [1]
Mt. Polley	Boundary Zone	45	B	***Western redcedar foliage***	***46***
	Boundary Zone			Engelmann spruce outer bark	41
	Pond Zone	60	B	***Subalpine fir foliage***	***54***
	Pond Zone			Western redcedar foliage	58
	Pond Zone			Engelmann spruce outer bark	21
QR	Main and West Zones[2]	0		***Douglas-fir needles (crowns)*** [2]	***100***
	Northern extension	0		Douglas-fir needles (low branches)	10
	Northern extension			Lodgepole pine outer bark	21
	Eastern IP' transect	32	B	***Engelmann spruce foliage***	***32***
	Eastern IP' transect			Lodgepole pine outer bark	31
	Cariboo Zone	24	B	***Engelmann spruce foliage***	***23***
	Cariboo			Lodgepole pine outer bark	13
3Ts	Tommy vein transect	20	B[3]	***White spruce foliage***	***43***
	Tommy vein transect			Lodgepole pine outer bark	40
	Ted vein transect	15	B[3]	***White spruce foliage***	***24***
	Ted vein transect			Lodgepole pine outer bark	24

[1] excluding field duplicates

[2] archived samples from collection made in 1988, prior to site development

[3] multi-horizon samples collected (see Cook and Dunn, 2006)

most trees were dead from mountain pine beetle infestation. Bark remained the only choice. Whereas this might have proved to be an optimal sample medium, it was desirable to obtain information on additional species (including spruce bark) because of the likelihood that millions of acres of central BC will have sparse pine populations once the dead trees have been felled.

Mt. Polley (Imperial Metals Corporation)

Located 56 km northeast of Williams Lake in central BC, the Mt. Polley mine lies between Polley and Bootjack lakes. Mineralization includes Cu-Au-Ag porphyry. The open pit Cu-Ag mine was commissioned in 1997 and ore from the Cariboo and Bell pits was mined until September 2001 when, due to low metal prices, the mine was idled. Subsequent increases in metal prices resulted in reopening of the mine in March of 2005. While the mine was closed, exploration continued and significant new zones of mineralization were discovered. Areas surrounding two recently discovered zones, the Boundary and Pond, have undergone little surface disruption and proved suitable for focusing the sampling program of the present study (Fig. 2).

Including field duplicates, 55 samples were collected north of the Boundary zone, mostly at 50 m intervals along two north-south parallel lines (100 m apart). Figure 2 shows the location of the Boundary zone and the area sampled (marked as 'Boundary zone extension'). See Figures 6–9 for detailed locations of sample sites. Sample sites extended from till-covered brecciated monzonite northward to Jurassic volcanic cover of unknown thickness. The collection, detailed in Table 1, comprised B-horizon soil, foliage of western redcedar (*Thuja plicata*)[4] and outer bark from Engelmann spruce (*Picea engelmannii*). For simplicity, the western redcedar will be referred to as 'cedar', since this is the name commonly used by those working in the forests of BC.

At the Pond zone (Fig. 2), sampling was undertaken at 75 sites at 50 m intervals, along two parallel east-west lines 100 m apart that traverse brecciated monzonite, and mineralized Triassic basalt that hosts the monzonite. The sample collection comprised B-horizon soil and foliage of subalpine fir and western redcedar. Spruce was rare, so relatively few samples of spruce outer bark were collected (details in Table 1).

QR (Cross Lake Minerals Ltd.)

Located 58 km southeast of Quesnel, the QR is a Au skarn situated near the eastern edge of the north-westerly-trending assemblage of Upper Triassic–Lower Jurassic volcanic rocks of the Quesnel Trough (Fox *et al.*, 1987). The deposits occur in association with propylitized and carbonatized fragmental mafic volcanic rocks. Ore is associated with pyrite in stockworks and in massive basaltic tuff. Associated minerals include epidote, chlorite, anhydrite and carbonate. Gold occurs with Ag as micrometre-size particles along pyrite and chalcopyrite boundaries. Details of the geology and mineralogy are given in Fox *et al.* (1987) and Melling and Watkinson (1988).

Biogeochemical studies were conducted over the QR deposit in the late 1980s, prior to mine development (Dunn, 1989; Dunn and Scagel, 1989). Archived vegetation samples from an area now stripped of vegetation were available from the Geological Survey of Canada (GSC) to comple-

[4] *Nomenclature: In February 1988* Thuja plicata *was designated the official tree of BC, but it is not a true cedar (genus* Cedrus*) and belongs to the cypress family. In order to avoid confusion with a true cedar, botanists spell the popular name 'redcedar' rather than 'red cedar'. Following somewhat dissimilar logic, the Douglas-fir is hyphenated, because it is not a true fir.*

ment new geochemical work. This unique material offered a valuable opportunity to determine the halogen signatures prior to any mine development. The 1988 and 1989 surveys indicated a strong positive response between mineralization and Au in the vegetation (*e.g.*, Fig. 3), at a time when the only development was drilling and some minor trenching.

This summer, a few samples of Douglas-fir foliage were collected to the north of the area shown in Figure 3. Sampling was limited, because a tailings pond now occupies the site of the Au anomaly in tree tops (Fig. 4). Furthermore, foliage from lower limbs has different concentrations of some elements compared to foliage at tree tops and, on this occasion, there was no opportunity to collect samples from the tops of the 20–40 m tall Douglas-firs.

A second area sampled was an IP geophysical anomaly to the east of the tailings pond (henceforth referred to as the IP zone), where Douglas-fir was rare (Fig. 4). It represented a target that exploration personnel from Cross Lake Minerals considered worth examining from a geochemical standpoint. Including controls, 32 sites at 50 m intervals were sampled northward along two parallel lines, set 100 m apart. Sample media were B-horizon soil, foliage from Engelmann spruce and outer bark from lodgepole pine. Six kilometres to the east of the area depicted in Figure 4, the Cariboo zone (Au, Cu, Mo associated with gabbro) was a third target. The area is not disturbed by any mining activities, and a single north-south line was sampled at 50 m intervals over a distance of 1250 m. The same sample media were collected as at the IP zone.

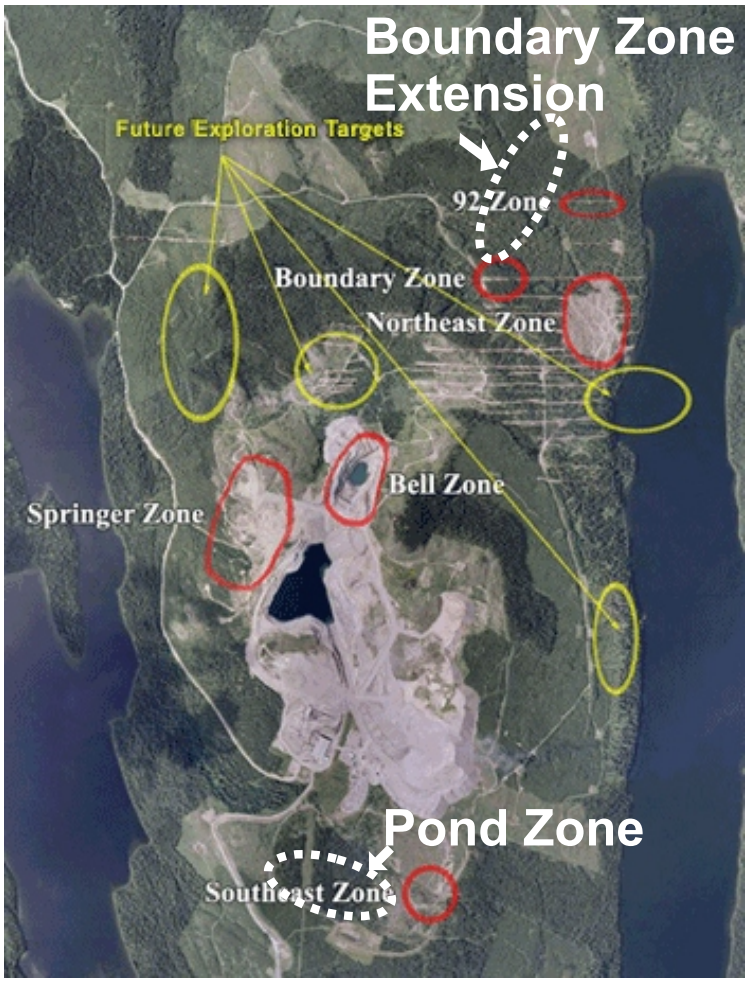


Figure 2. Locations of principal ore zones at Mt. Polley, and the two little-disturbed areas selected for this study: Boundary zone extension and Pond zone (annotated from airphoto downloaded from Imperial Metals Corporation website (http://www.imperialmetals.com/s/ MountPolley.asp) 28-Oct-05).

3Ts (Southern Rio Resources Ltd.)

Three contiguous properties, totalling 34 km^2, cover a bonanza-style, epithermal Au-Ag camp located approximately 120 km southwest of Vanderhoof. There is only minor disturbance of the ground. Geological details of this area are given in Bottomer (2003a, b) and Cook and Dunn (2006).

Fieldwork at 3Ts was complicated by the fact that, recently, easy access to the field area had been made impossible by decommissioning of the only good-quality trail. Minor trails required the use of all-terrain vehicles.

The Tommy and Ted Au-bearing quartz veins were the prime targets over which the sampling transects were designed (Fig. 5). In total, 46 B-horizon soil samples were collected at the same time as a significant collection of multi-horizon samples that are discussed in the paper by Cook and Dunn (2006). Vegetation was considerably easier to collect than the soil; approximately 150 samples were collected, comprising equal proportions of white spruce (*Picea glauca*) foliage and outer bark from lodgepole pine (*Pinus contorta*). Vegetation sampling extended across the Tommy vein eastward to the Ringer boulder showing, and eastward across the Ted vein to the Adrian West boulder showing.

SAMPLE COLLECTION AND PREPARATION

At each sample location (mostly at 50 m intervals), a B-horizon soil was collected from the typical Brunisol profile. In addition, 4–5 samples of twigs and foliage comprising the most recent 3 years of growth were placed in a porous polypropylene bag (Hubco Sentry II) and, on most traverses where available, outer bark of lodgepole pine was scraped using a hardened steel paint scraper and a standard 'kraft' paper soil bag half-filled with the scrapings (about 50 g). Many of the pines were dead or dying because of the rampant pine beetle 'kill'. However, this was not a problem for the sample integrity and quality because outer bark scales are dead tissue even when a tree is alive.

In the laboratory, soil samples were dried at 40°C and sieved to –80 ASTM (180 μm). Vegetation samples were dried at 70°C in an oven for 24 hours to remove all moisture. The foliage could then be separated from the twigs. Each foliage and bark sample was then milled to a powder in preparation for chemical analysis

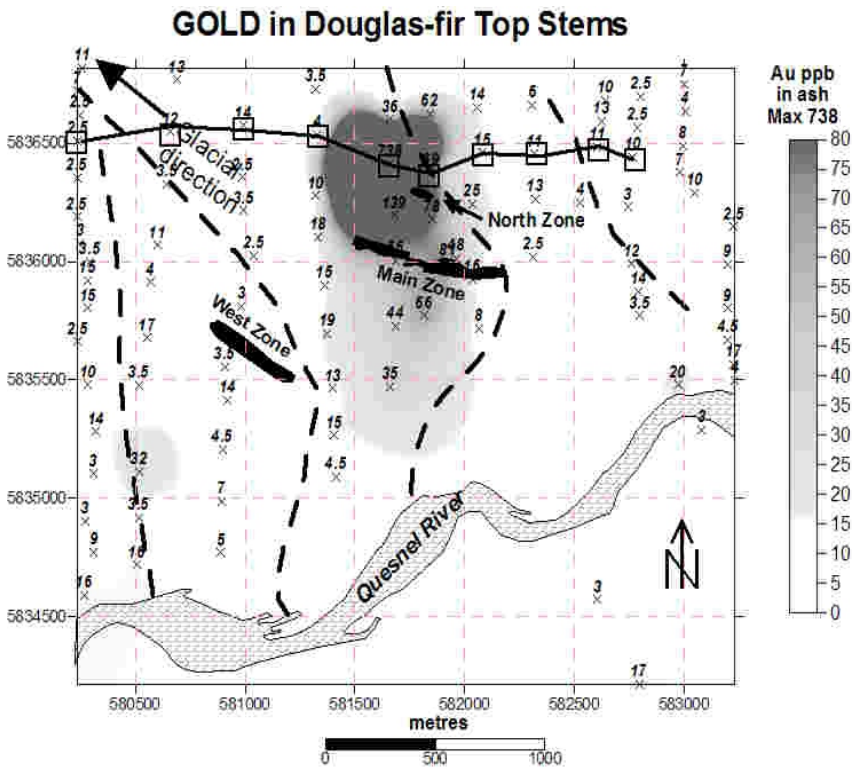


Figure 3. QR deposit: 1988 survey (Dunn and Scagel, 1989). Geological features after Fox *et al.* (1987). Deposits as known in 1988 are shown as solid black polygons. They mostly subcropped beneath the till or, as in the case of the West zone, were buried except for the northwestern and southeastern parts. Dashed lines represent faults. Sites outlined by linked squares indicate those selected as test samples for halogens in needles. Five pine bark samples (not shown) selected for testing were from a 500 m northwest-southeast traverse across the Main zone.

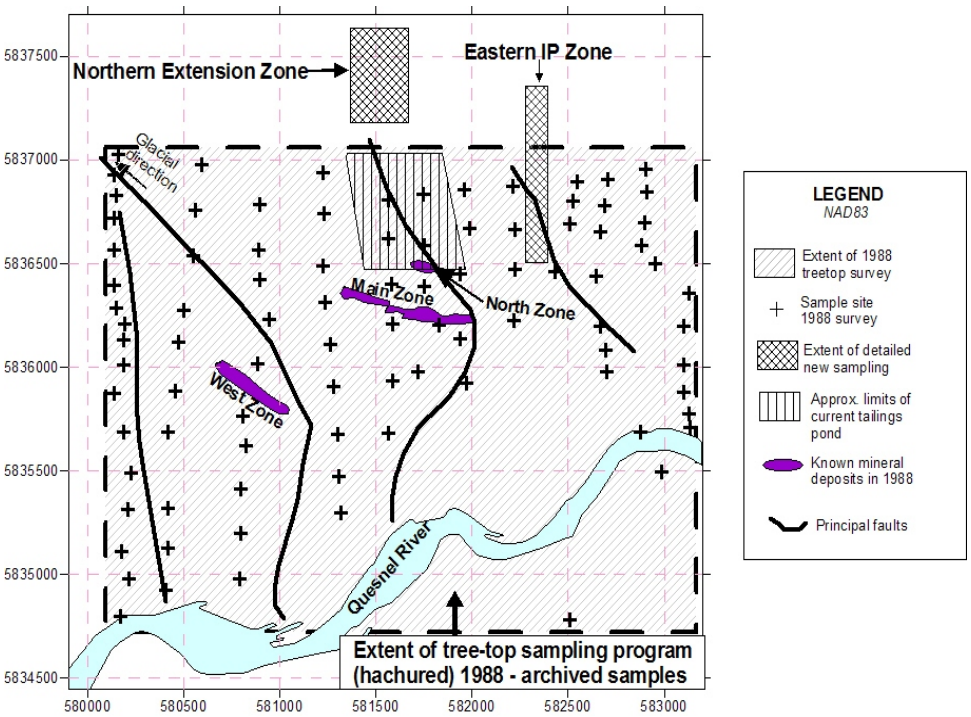


Figure 4. QR deposits: locations of the areas surveyed in 1988 and for this survey.

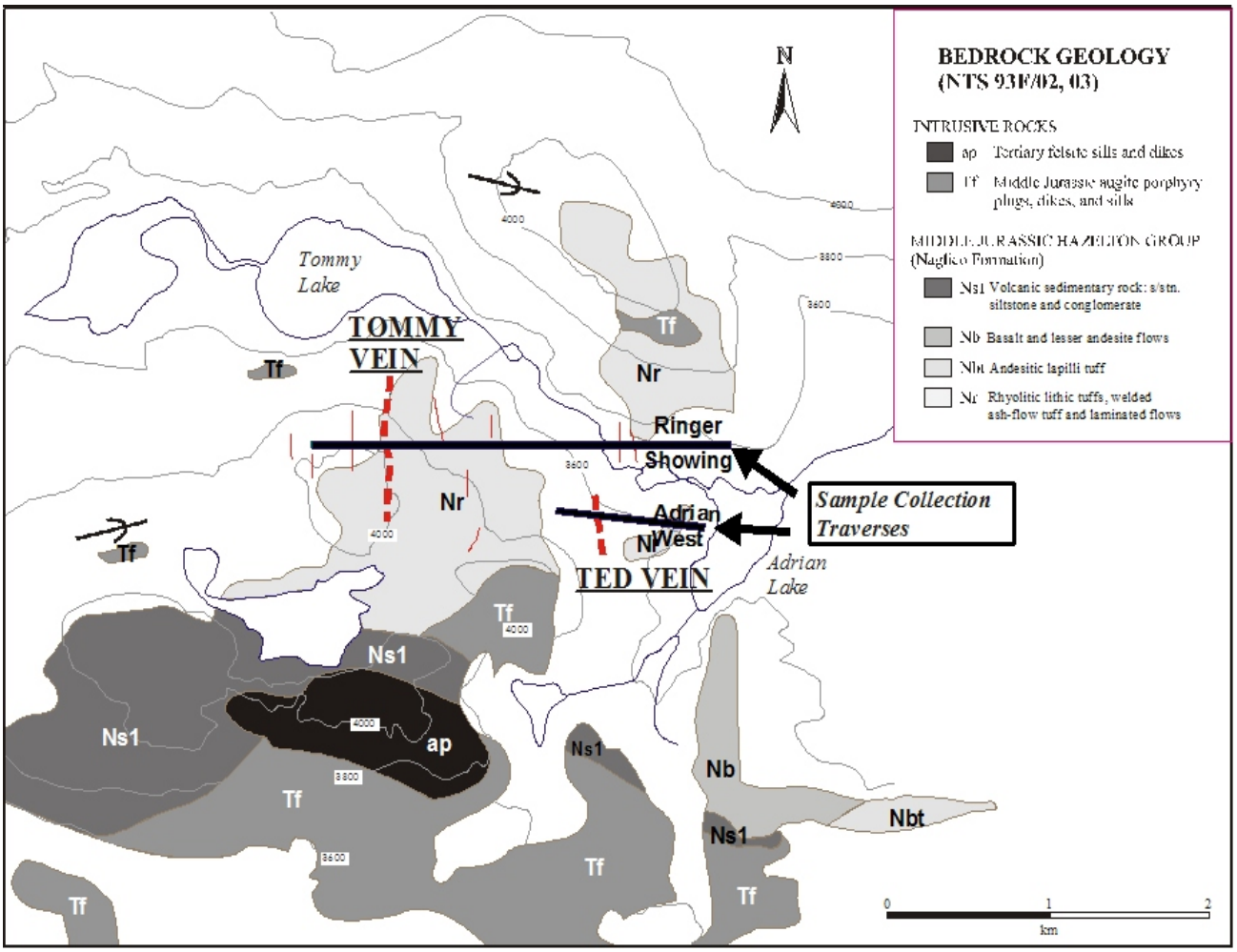


Figure 5. 3Ts: general geology, topography and location of traverses across the north-south mineralized veins and boulder occurrences (Ringer showing and Adrian West). Modified after Diakow and Webster (1994). Note that the soil sampling extended only over the western half of the traverse across the Tommy vein. Note also that unit Tf has recently been dated by Jim Mortensen to be a Late Cretaceous microdiorite intrusion (L. Bottomer, pers. comm., 2005).

ANALYSIS OF TEST SAMPLES

In order to ascertain the optimal analytical method for the halogens, a set of 35 test samples was selected for analysis by several laboratories using a variety of methods. In the final selection of the method by which all of the newly collected samples would be analyzed, consideration was to be given to both the appropriate level of sensitivity and the cost of analysis.

The vegetation test samples were Douglas-fir (*Pseudotsuga menziesii*) needles and lodgepole pine (*Pinus contorta*) outer bark collected in 1988 and 1989 from the vicinity of the QR deposit and archived at the Geological Survey of Canada in Ottawa. Ten samples of needles and five samples of bark were chosen from sites that spanned the Au biogeochemical anomaly (Fig. 3). In addition, five vegetation controls of known composition were included. They were two samples of V6, a composite of pine twigs and needles developed in 1990 by the senior author using CANMET facilities; two samples of CLV-2, CANMET spruce needles (certified values); and one sample of V13, mountain hemlock needles developed recently by the senior author and Acme Analytical Laboratories Ltd. The suite of archived samples represented suitable test material in that prior analysis had shown there to be elevated levels of Au in these samples from sites over or adjacent to known Au deposits (Fig. 3). Furthermore, some halogens have been shown to accumulate in foliage, and some limited halogen data (Cl and Br) were available for V6. Nothing was known about the halogen content of bark; however, since bark is known to accumulate many metals that are surplus to plant metabolism, the tests should determine if this would be a suitable sample medium for the halogens.

No appropriate soils were available from over known mineralization, so tests were performed on five splits each of GSC controls that had certified values for many elements. They were STSD-1 and STSD-4 (both stream sediments), and TILL-4.

Table 2 lists the suite of methods for which analyses were requested at various Canadian laboratories. At that time, it was not known if optimal results would be from a total halogen analysis (*e.g.*, INAA or XRF) or from an analysis involving a partial extraction (*e.g.*, leaching by water or pH-controlled ammonium acetate). With regard to the vegetation, it was considered that a partial extraction might yield similar results to a 'total' analysis, because of the high

solubilities of the halogens. However, for soil, there may be greater differences, because some halogens may be structurally bound in crystal lattices and therefore not readily extracted by a weak leach (*e.g.*, Cl in biotite and amphiboles; F and/or Cl in apatite). However, since the objective of this program was to investigate the distribution of halogens that might be derived from concealed mineralization, it was the labile (readily leached) portion of any halogens that would be of principal interest, and not the structurally bound halogens.

Subsequently, portions of each sample were sent to Activation Laboratories Ltd. in order to test the potential suitability for halogen determinations by high resolution ICP-MS of several experimental methods currently being developed.

RESULTS

Halogens

At the time of writing, most of the data on the test samples have been received and results indicate some significant complications with regard to obtaining consistent and accurate data. Some data sets are clearly inadequate and/or inaccurate, emphasizing the need to develop appropriate analytical methodologies. For example, for the vegetation, total F obtained by one method yielded concentrations of 60–80 ppm F, whereas values obtained by another method were <10 ppm F; furthermore, analysis by a partial (water) leach returned values for the same samples mostly in excess of 1000 ppm F. Alchemy at its best! A selection of these differences is shown in Table 3.

In the analysis of vegetation samples by ion chromatography (Dionex), F^- is the first halogen to be evolved. Whereas it may appear that F^- gives a clean positive signature, a variety of unknown organic compounds greatly en-

TABLE 2. SELECTION OF ANALYTICAL METHODS TO BE UNDERTAKEN AT VARIOUS LABORATORIES ON 20 SAMPLES OF MILLED VEGETATION AND 15 SOIL SAMPLES

INAA: epithermal neutron activation for Cl, Br and I
ICP-MS water leach: approximately 50 elements
ICP-MS ammonium acetate pH 7 leach: approximately 50 elements
ICP-ES water leach: 10 elements
ICP-ES ammonium acetate pH 7 leach: 10 elements
Ion chromatography water leach: all available anions
Ion chromatography ammonium acetate pH 7 leach: all available anions
F_water leach selective ion electrode
Cl_water leach selective ion electrode
F_fusion (Teflon bomb) selective ion electrode
Enzyme Leach^{SM}: full suite of elements including I, Br and semiquantitative Cl
XRF (high resolution): halogens

TABLE 3. VEGETATION SAMPLES ANALYZED FOR F BY SEVERAL DIFFERENT METHODS AT DIFFERENT LABORATORIES. NO CERTIFIED VALUES AVAILABLE FOR THE CONTROLS

Sample	*Lab A1* *Dionex (IC)* Water Leach *F (ppm)*	*Lab A2* *Sel. Ion Electrode* Water Leach *F (ppm)*	*Lab A3* *NaOH Fusion* *Total* *F (ppm)*	Lab B Dionex (IC) Water Leach *F (ppm)*	Lab C Dionex (IC) Water Leach *F (ppm)*	*Lab D* *XRF* *Total* *F (ppm)*
DFN_04	1241	0.36	<10	27.2	1380	75
DFN_08	1529	0.34	20	35.1	1776	
DFN_14	1324	0.2	<10	26.6	1476	78
DFN_22	839	0.24	<10	24.5	1168	86
DFN_33	1383	0.15	<10	16.3	1613	63
DFN_45	1429	0.23	<10	45.5	1623	72
DFN_60	1121	0.21	<10	26.2	1255	72
DFN_65	1253	0.15	<10	32.8	1393	68
DFN_70	1616	0.19	<10	17.6	2028	65
DFN_74	1170	0.2	<10	20.2	1318	83
LP-BK-09	74	0.14	<10	15.1	124	
LP-BK-11	64	0.11	<10	18.0	109	
LP-BK-28	99	0.14			128	
LP-BK-68	63	0.09	<10	23.9	102	
LP-BK-73	88	0.22	<10	24.2	115	
Controls:						
V6	70	1.17	<10	0.75	83	96
V6	77	0.6	<10	0.92	83	81
CLV-2	774	0.34	<10	21.2	900	<25
CLV-2	1022	0.34	<10	10.9	906	80
V13	2284	0.17	<10	33.8	2666	<42

hance the presumed fluoride signature, generating a false analysis. It seems that this is a significant analytical problem that would need to be resolved.

As a consequence of results such as those shown in Table 3, samples from the field traverses have not yet been sent for analysis (October 2005). Recently received data by other methods, however, do indicate some positive associations of F and I with the locations of the Au anomaly in tree tops shown in Figure 3. Figure 6 shows selective ion electrode determinations (SIE) of fluoride in a water leach of 1 g samples of dry vegetation. From these and other data, it appears that there are typically higher concentrations of F in foliage than bark.

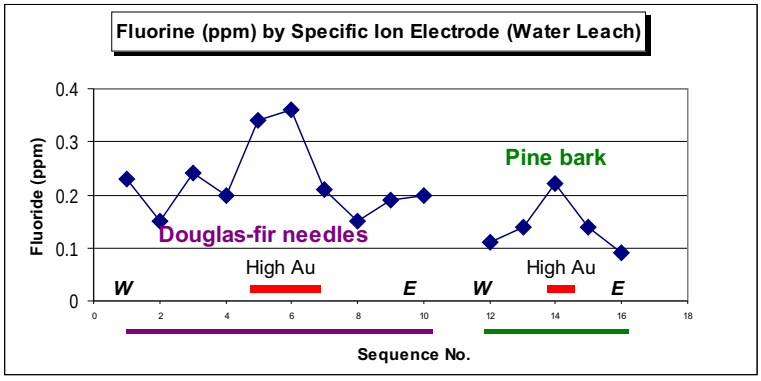


Figure 6. Concentrations of F with respect to Au biogeochemical anomalies at QR. Left profile shows dry Douglas-fir needles; right profile shows dry lodgepole pine outer bark. Samples collected in 1988 and 1989 prior to mine development. Determinations by selective ion electrode on a water leach.

With regard to halogen anomalies associated with mineralization, although Figures 6 and 7 show some increased values where there are elevated levels of Au in tree tops, it should be noted that such a relationship may not always occur, depending on the nature of the mineralization, depth of burial, and faulting and fracturing of the overlying bedrock. Trofimov and Rychkov (2004) note that an I and/or Br halo may occur marginal to a halo of other pathfinder elements (*e.g.*, As, Hg) that are themselves marginal to an ore body. As a result, the spatial relationship of the halogens may form a broad halo anomaly at the surface over a deeply buried ore deposit, with peak values surrounding the deposit. Along transects over mineralization, the appearance would be the classic 'rabbit ears' type of anomaly. These patterns will be examined when the halogen data are received.

Determinations of I in the same materials by a range of methods have generated results that are as diverse as those for fluorine. However, there is a reasonable correspondence between I determined by INAA and by enzyme leach (Fig. 7).

There was insufficient archived bark material available for running all samples by all methods; however, preliminary data from several analytical methods indicate that I is considerably more concentrated in the bark than in the foliage.

Data for Cl and Br show similar substantial variability among the various analytical methods that were tested, and neither element shows the positive response over the test traverse that was noted for F and I.

Multielement ICP-MS

Soil samples were submitted to Acme Analytical Laboratories Ltd., Vancouver, for a 53-element ICP-MS analysis by method 1F (aqua regia digestion) and pH determinations. Vegetation samples were analyzed at Acme by method 1VE-MS (nitric acid followed by aqua regia digestion). A portion of each sieved soil and milled vegetation sample was set aside for later analysis of the halogens, once a suitable method(s) had been identified.

The multielement ICP-MS results on the B-horizon soil and the principal sets of vegetation (foliage) were obtained within a few weeks of the field samples being submitted for analysis. The multielement data for these samples are required for comparison of the commodity elements (especially Au, Ag, Cu) with the data ultimately to be obtained for the halogens. Recently, data have also been acquired for some of the bark samples, in light of the relative enrichment of I (in bark compared to foliage) revealed from the test samples. More bark samples will be processed. To date, a total of approximately 60 000 analytical determinations have been made on the full set of field and test samples.

The quality-control and quality-assurance procedures for all samples were the same as those described in Cook and Dunn (2006). In brief, field duplicates were collected at every tenth sample site, and appropriate quality-control samples inserted at a minimum of one in every twenty samples.

An outline is presented, by mineral occurrence, of selected geochemical features of the large datasets acquired for the soil and vegetation tissues. Details will be provided in the final report that will prepared by March 2006.

Mt. Polley

BOUNDARY ZONE

At the more northerly of the two zones studied, the Boundary zone (Fig. 2), western redcedar foliage was se-

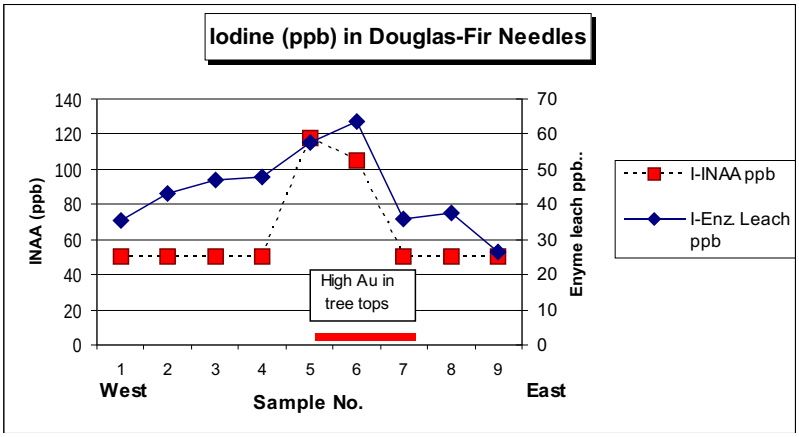


Figure 7. Concentrations of I in dry Douglas-fir needles from tree tops at QR. Comparison of results from an enzyme leach and by INAA. Detection level by INAA was 100 ppb; values below detection are shown as half detection (50 ppb).

lected as the principal vegetation sampling medium. Table 4 is a statistical summary of element concentrations in dry tissue. Table 5 shows the same statistical parameters for the soil samples.

These tables are provided for general information on element levels encountered in this environment, and serve as a yardstick against which to compare data from future surveys. In general, elements considered somewhat concentrated in the cedar foliage are Au, Cu and Mo; notable concentrations in the soil include Ag, As, Au, Cu, Hg and V.

A comparison of several commodity elements in the soil with those in the cedar foliage is instructive, in that anomalous concentrations appear at different localities (Fig. 8–11). Previous studies of concentrations in soil versus vegetation in glaciated terrain, at Beaver Dam, Nova Scotia (Dunn *et al.*, 1991) and Mt. Milligan, BC (Dunn *et al.*, 1996), have found that vegetation anomalies tend to be more directly over mineralization than the soil.

The implication from the above comparisons is that the zone of mineralization occurs in the centre of the survey area, as indicated by the vegetation, rather than farther to the south where most of the soil anomalies lie. It is considered that a significant local concentration of a metal is required in order to be reflected in the plant chemistry: there is insufficient concentration of metals in a soil anomaly (even though it constitutes a geochemical anomaly) to be reflected in the vegetation. The soil anomaly is commonly displaced by down-ice or downslope dispersion or dispersal, whereas a biogeochemical anomaly typically occurs directly over a mineralized source.

POND ZONE

Farther south, two east-west traverses were conducted over an area considered by Imperial Metals to have good potential for a continuation of the Pond zone that lies immediately to the south (Fig. 2). A short distance beyond the eastern extension of the traverses lies the Southeast zone of proven mineralization. Along these traverses, in addition to B-horizon soil samples, foliage was collected from both western redcedar and subalpine fir. The latter has been selected as the principal vegetation sampling medium for analysis, partly because this permits testing the relative sensitivity of this species, compared to the cedar from the Boundary zone, to halogen uptake.

Table 6 presents a statistical breakdown of the analysis of the subalpine fir foliage, and Table 7 gives the information from –80 mesh B-horizon soil from the same sites. Elements in the fir needles that are enriched for conifer foliage in general include Au, Cu, Zn and, most notably, Re. Notable concentrations in the soil include As, Au and Cu; Re, too, is slightly elevated in the soil.

Figure 12 presents plots of selected elements along the northernmost of the two traverses. Soil is shown on the left and vegetation on the right. Of note are the peaks at the eastern end of the line: Au, Mo and Re in both media, and Cu in soil but not in the vegetation. Copper in vegetation is anomalous in this area (background is usually around 8 ppm, and there is up to 14 ppm present), but far less so than in the west (around 300–350 m), where Cu is coincident with Au in the vegetation. The inference is that there are two different styles of mineralization present: a Cu, Au, Fe association with Cs, REEs and Cd at the western anomaly, which is displaced, like that indicated at the Boundary zone, about 50 m west of the principal multielement soil anomalies (Ag, Bi, Mo, Pb, Sb, Se, Te); and a second zone of Au enrichment in the east, where the association from the soil (Co, Cr, Ni, Mg and REEs, with an associated Hg and U signature) indicates a mafic substrate. The vegetation signature is predominantly Au, Mo, Pb, Li, Rb and Re.

QR Deposit

ANALYSIS OF ARCHIVED NEEDLES FROM DOUGLAS-FIR TOPS

Analysis of the dry needle tissue confirmed and refined the original anomalies identified from analysis of the top stems (Dunn and Scagel, 1989). Previously, no data were obtained from the needles. The correspondence of the anomalies in the dry needles (Fig. 13; by ICP-MS) compared to the ashed top stems (Fig. 3; by INAA) confirms and validates the robustness of the geochemical signature, and in fact enhances the relationship of the biogeochemical signature to the subcropping mineralization at either end of the West zone. New data from the northern extension of the principal anomaly does not indicate an extension to the north. However, the multielement dataset shows that, in general, there are quite substantial differences between needles from the tree tops collected in 1988 and those from the lower branches that were collected this year. There is no systematic increase or decrease of elements that might be attributed to either contamination from mining activities or long-term natural variations in plant chemistry.

IP ZONE

Two traverses (Fig. 4) were conducted to collect soils and spruce foliage from north-south lines about 500 m east of the Main zone anomaly (Fig. 3, 13). These lines were selected because of the presence of an IP anomaly of unknown origin. A one to three-station multielement anomaly occurs in soil along one of the two transects. Element enrichments include Ag, As, Au, Co, Cu, Mo, Ni, Sb, Se, Te and traces of Pt. Data from the spruce needles do not show any significant enrichment. However, spruce needles usually only yield very subtle indications of metal enrichments in the substrate: they were selected for this project because spruce was the only common species from which foliage could be collected in this area, and because the literature has indicated that foliage is more likely than twigs to yield enrichments of the halogens. Data are pending for a set of pine bark samples.

CARIBOO ZONE

The third area of study in the vicinity of the QR deposit lies 6 km to the east. Past surveys have demonstrated that the 'Cariboo' zone has multielement soil anomalies: notably Au, As and Sb, with Mo as another zone to the north, mostly associated with gabbro. Since this area has undergone little disturbance, it was selected for a single 1400 m north-south traverse. In addition to the soil, spruce foliage and pine bark (where available) were collected. Examples of soil data are shown in Figure 14. The soil results indicate three zones of multielement enrichment involving Ag, Au, Bi, Cu and Hg, among others. The central zone is subtle with respect to Ag, Au and Bi, but has a strong Hg and Cu signature. Only the northern zone includes a Mo signature. Several ppb Pt are present at the southern end of the line.

The vegetation signatures are considerably more subtle (again, only spruce needles have been analyzed to date) and, once again, the anomalies that do occur are displaced

TABLE 4. MT. POLLEY BOUNDARY ZONE: STATISTICAL SUMMARY FOR ANALYSIS BY ICP-MS OF DRY WESTERN REDCEDAR FOLIAGE

Element	Units	N	Mean	Std. Dev.	Minimum	Percentiles				Maximim
						50th	70th	80th	90th	
Ag	ppb	46	3.1	1.0	1	3	4	4	4	6
Al	%	46	0.005	0.001	0.005	0.005	0.005	0.005	0.006	0.01
As	ppm	46	0.09	0.05	0.05	0.05	0.1	0.1	0.13	0.3
Au	ppb	46	0.86	1.05	0.1	0.5	0.9	1.48	2.7	5
B	ppm	46	17	4.2	11	16	18	20	23	29
Ba	ppm	46	29	15.3	6.7	25	38	44	51	63
Be	ppm	46	0.05	0.007	0.05	0.05	0.05	0.05	0.05	0.1
Bi	ppm	46	0.01	0.002	0.01	0.01	0.01	0.01	0.01	0.02
Ca	%	46	1.18	0.19	0.85	1.15	1.229	1.31	1.53	1.66
Cd	ppm	46	0.03	0.02	0.005	0.03	0.04	0.05	0.06	0.07
Ce	ppm	46	0.06	0.02	0.03	0.06	0.07	0.08	0.1	0.11
Co	ppm	46	0.06	0.02	0.02	0.055	0.069	0.076	0.083	0.1
Cr	ppm	46	2.1	0.17	1.7	2.1	2.2	2.26	2.33	2.5
Cs	ppm	46	0.02	0.01	0.007	0.016	0.02	0.022	0.035	0.065
Cu	ppm	46	5.5	1.5	2.2	5.3	5.9	6.8	7.6	11.0
Fe	%	46	0.013	0.004	0.006	0.012	0.014	0.015	0.02	0.023
Ga	ppm	46	0.05	0	0.05	0.05	0.05	0.05	0.05	0.05
Ge	ppm	46	0.006	0.002	0.005	0.005	0.005	0.01	0.01	0.01
Hf	ppm	46	0.002	0.001	0.001	0.002	0.003	0.003	0.004	0.006
Hg	ppb	46	24	6.9	14	23	27	28	33	42
In	ppm	46	0.01	0	0.01	0.01	0.01	0.01	0.01	0.01
K	%	46	0.53	0.11	0.3	0.53	0.589	0.62	0.679	0.77
La	ppm	46	0.04	0.02	0.02	0.04	0.049	0.05	0.07	0.08
Li	ppm	46	0.05	0.06	0.005	0.03	0.07	0.09	0.11	0.38
Mg	%	46	0.10	0.02	0.059	0.102	0.112	0.119	0.126	0.147
Mn	ppm	46	176	97	34	159	208	248	345	412
Mo	ppm	46	1.5	1.4	0.39	1.2	1.5	1.8	2.5	10.1
Na	%	46	0.002	0	0.001	0.002	0.002	0.002	0.002	0.003
Nb	ppm	46	0.013	0.01	0.005	0.01	0.019	0.02	0.03	0.07
Ni	ppm	46	1.4	0.7	0.2	1.2	1.6	1.8	2.2	3.6
P	%	46	0.125	0.03	0.066	0.123	0.137	0.144	0.163	0.187
Pb	ppm	46	0.11	0.08	0.05	0.09	0.119	0.12	0.14	0.58
Pd	ppb	46	1	0	1	1	1	1	1	1
Pt	ppb	46	0.5	0.14	0.5	0.5	0.5	0.5	0.65	1
Rb	ppm	46	2.4	1.6	0.6	2.05	2.88	3.3	3.9	9.5
Re	ppb	46	0.7	0.31	0.5	0.5	1	1	1	2
S	%	46	0.1	0.04	0.005	0.07	0.1	0.116	0.13	0.16
Sb	ppm	46	0.04	0.05	0.01	0.02	0.04	0.05	0.06	0.34
Sc	ppm	46	0.23	0.06	0.1	0.2	0.3	0.3	0.3	0.3
Se	ppm	46	0.17	0.05	0.1	0.2	0.2	0.2	0.2	0.3
Sn	ppm	46	0.04	0.05	0.01	0.03	0.049	0.06	0.08	0.32
Sr	ppm	46	62	24	24	60	78	86	92	117
Ta	ppm	46	0.001	0	0.001	0.001	0.001	0.001	0.001	0.002
Te	ppm	46	0.01	0	0.01	0.01	0.01	0.01	0.01	0.01
Th	ppm	46	0.005	0	0.005	0.005	0.005	0.005	0.005	0.005
Ti	ppm	46	8.2	1.5	5	8	8.9	9	10	12
Tl	ppm	46	0.01	0	0.01	0.01	0.01	0.01	0.01	0.01
U	ppm	46	0.005	0	0.005	0.005	0.005	0.005	0.005	0.005
V	ppm	46	1	0	1	1	1	1	1	1
W	ppm	46	0.06	0.04	0.05	0.05	0.05	0.05	0.05	0.3
Y	ppm	46	0.03	0.01	0.013	0.03	0.034	0.037	0.049	0.061
Zn	ppm	46	11.6	2.9	5.9	12.1	12.7	13.8	15.1	20.8
Zr	ppm	46	0.06	0.09	0.02	0.05	0.05	0.05	0.07	0.68

TABLE 5. MT. POLLEY BOUNDARY ZONE: STATISTICAL SUMMARY FOR ANALYSIS BY ICP-MS OF –80 MESH B-HORIZON SOIL

Element	Units	N	Mean	Std. Dev.	Minimum	Percentiles				Maximum
						50th	70th	80th	90th	
Ag	ppb	45	262	303	35	189	248	295	565	1545
Al	%	45	2.4	0.84	1.21	2.16	2.606	2.858	3.426	6.16
As	ppm	45	6.6	3.0	2.7	5.9	7.9	8.3	10.8	15.9
Au	ppb	45	5.7	8.8	0.2	2.1	5.0	8.8	16.8	40.2
B	ppm	45	4.3	2.7	2	4	4	4	8	16
Ba	ppm	45	173	80	80	155	199	218	306	429
Be	ppm	45	0.5	0.41	0.2	0.4	0.5	0.58	0.64	3.1
Bi	ppm	45	0.15	0.12	0.07	0.12	0.14	0.15	0.21	0.83
Ca	%	45	0.54	0.252	0.24	0.47	0.58	0.67	0.90	1.37
Cd	ppm	45	0.29	0.23	0.06	0.27	0.31	0.38	0.43	1.55
Ce	ppm	45	16.3	6.4	6.5	15.4	17.8	20.5	24.7	39.3
Co	ppm	45	13.3	2.9	8.2	13.6	14.7	15.4	15.7	25
Cr	ppm	45	51	21	4.2	56	65	72	75	80
Cs	ppm	45	2.3	1.8	0.62	1.73	2.19	2.81	4.48	11.42
Cu	ppm	45	118	198	8.07	52	91	145	269	1106
Fe	%	45	3.8	0.53	2.72	3.87	4.082	4.186	4.356	5.92
Ga	ppm	45	7.4	1.7	5.1	6.7	8.1	8.5	10.0	13.8
Ge	ppm	45	-0.1		-0.1	-0.1	-0.1	-0.1	-0.1	0.1
Hf	ppm	45	0.075	0.047	0.02	0.06	0.08	0.106	0.13	0.29
Hg	ppb	45	81	91	16	45	66	106	202	469
In	ppm	45	0.03	0.009	0.02	0.03	0.03	0.03	0.04	0.06
K	%	45	0.106	0.045	0.06	0.1	0.11	0.118	0.14	0.3
La	ppm	45	9.6	4.6	3.5	8.8	10.1	11.1	14.5	28.1
Li	ppm	45	23	12.4	11.5	20	22	24	29	92
Mg	%	45	0.65	0.19	0.21	0.66	0.732	0.75	0.854	1.34
Mn	ppm	45	670	330	323	604	782	879	1040	1932
Mo	ppm	45	1.09	0.88	0.2	0.72	1.29	1.56	2.38	4.01
Na	%	45	0.011	0.004	0.006	0.01	0.013	0.014	0.016	0.028
Nb	ppm	45	0.8	0.25	0.2	0.79	0.88	1.01	1.17	1.45
Ni	ppm	45	28	14	3.1	31	35.2	38.3	42.8	73.3
P	%	45	0.122	0.073	0.026	0.105	0.156	0.178	0.217	0.422
Pb	ppm	45	10.5	13.2	4.91	7.14	9.5	11.7	14.9	94.3
Pd	ppb	45	-10		-10	-10	-10	-10	-10	-10
Pt	ppb	45	-2		-2	-2	2	2	2	2
Rb	ppm	45	10.6	3.1	6.3	10	11	12	13	25
Re	ppb	45	-1		-1	-1	1	1	1	2
S	%	45	0.002	0.014	-0.01	-0.01	0.01	0.01	0.02	0.04
Sb	ppm	45	0.26	0.1	0.14	0.24	0.26	0.3	0.44	0.58
Sc	ppm	45	4.6	2.4	2.6	4.1	4.74	5.08	6.18	18.4
Se	ppm	45	0.2	0.2	-0.1	0.1	0.2	0.3	0.64	0.7
Sn	ppm	45	0.5	0.10	0.3	0.5	0.5	0.5	0.6	0.8
Sr	ppm	45	56	21	26.2	51	59	64	86	127
Ta	ppm	45	-0.05	0	-0.05	-0.05	-0.05	-0.05	-0.05	-0.05
Te	ppm	45	0.025	0.04	-0.02	0.02	0.04	0.058	0.09	0.11
Th	ppm	45	1.95	0.82	0.7	1.8	2.12	2.5	2.92	5.5
Ti	%	45	0.10	0.03	0.073	0.1	0.1	0.1	0.2	0.2
Tl	ppm	45	0.06	0.04	0.04	0.05	0.05	0.06	0.064	0.27
U	ppm	45	0.57	0.39	0.3	0.5	0.5	0.6	0.82	2.8
V	ppm	45	113	20	67	117	124.4	128	137.8	155
W	ppm	45	0.09	0.17	-0.1	0.1	0.1	0.2	0.2	0.9
Y	ppm	45	4.8	5.8	2.1	3.2	3.9	4.8	6.6	37.2
Zn	ppm	45	100	30	53	94	121	130	142	176
Zr	ppm	45	3.75	2.16	1.5	3.2	3.62	5.32	6.9	11.9
pH		45	5.47	0.5	4.4	5.4	5.7	5.8	6.24	6.7

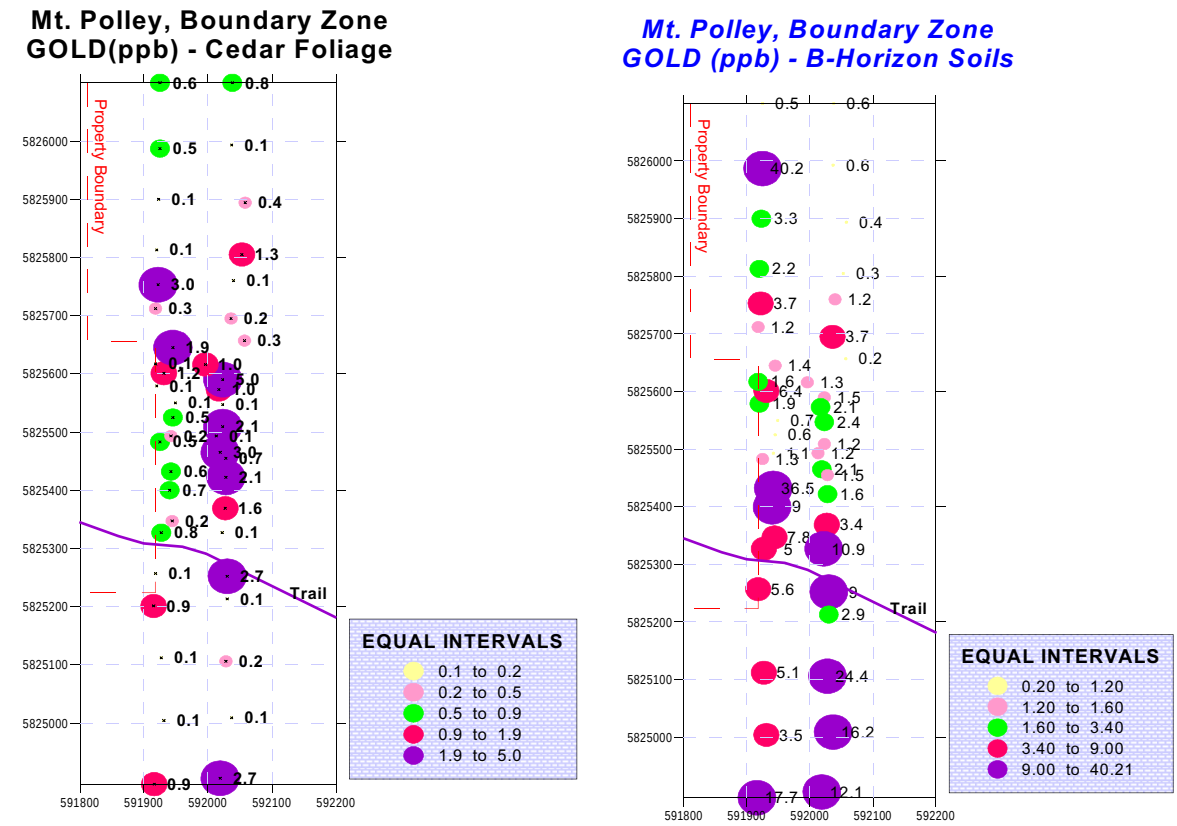


Figure 8. Mt. Polley Boundary zone: Au in dry cedar foliage compared to B-horizon soil.

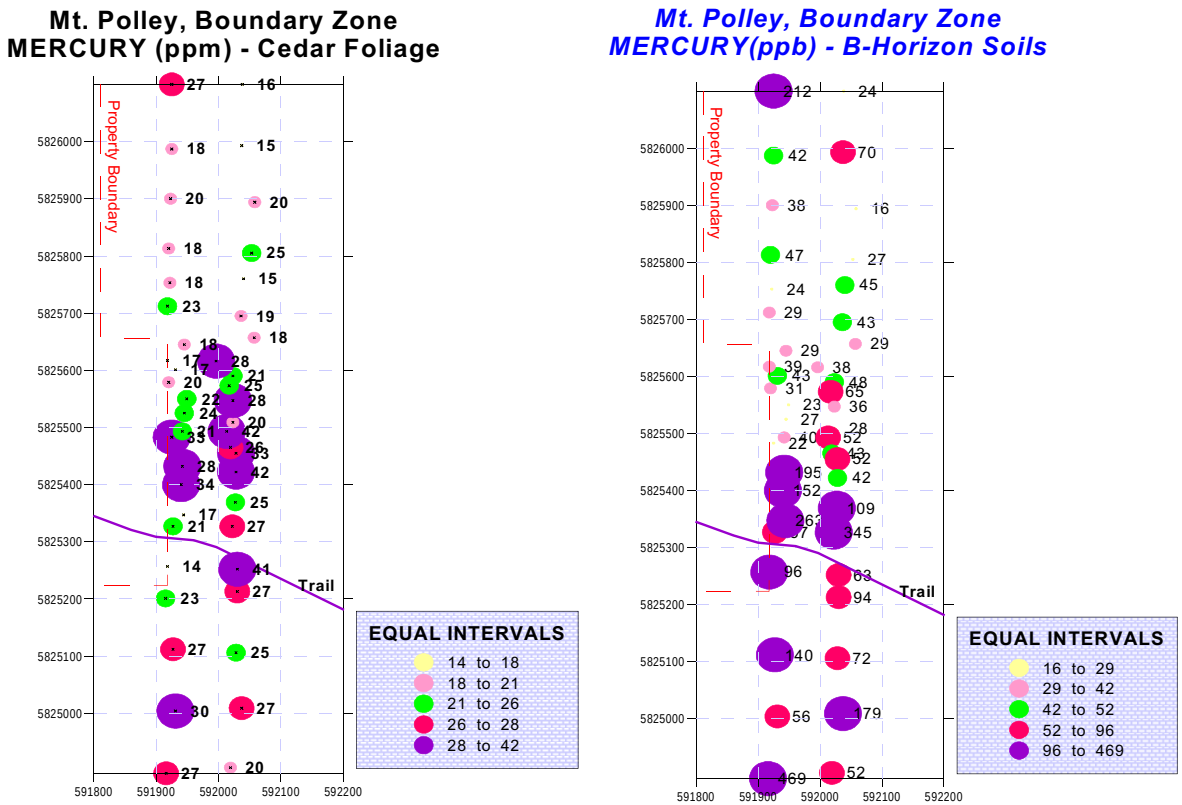


Figure 9. Mt. Polley Boundary zone: Hg in dry cedar foliage compared to B-horizon soil.

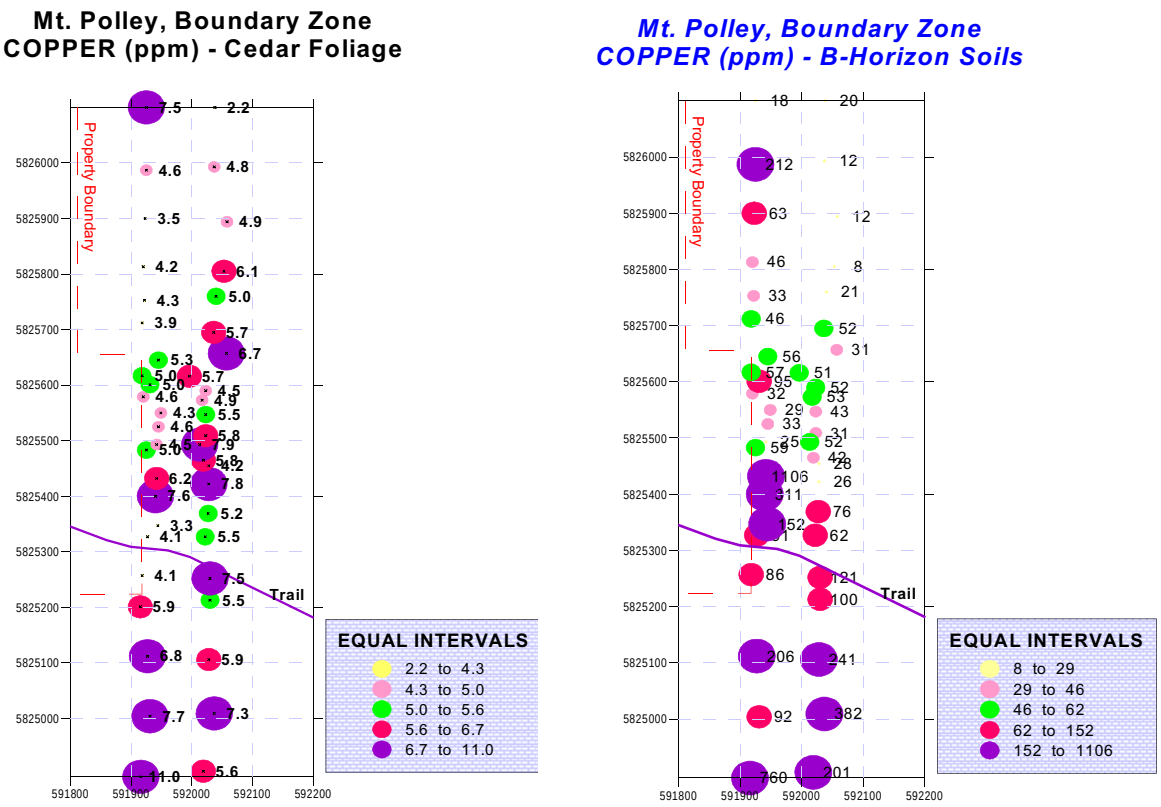


Figure 10. Mt. Polley Boundary zone: Cu in dry cedar foliage compared to B-horizon soil.

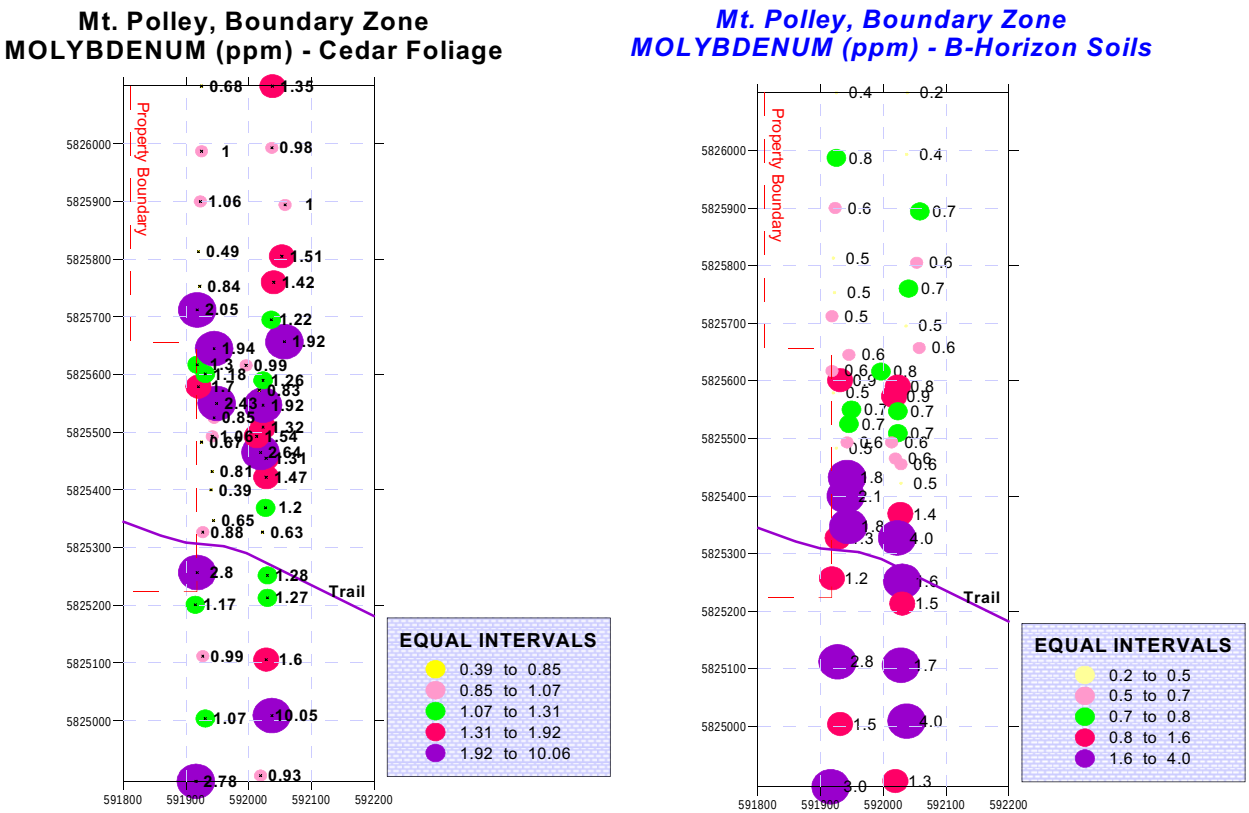


Figure 11. Mt. Polley Boundary zone: Mo in dry cedar foliage compared to B-horizon soil.

TABLE 6. POND ZONE: STATISTICAL SUMMARY FOR ANALYSIS BY ICP-MS OF DRY SUBALPINE FIR FOLIAGE

Element	Units	N	Mean	Std. Dev.	Minimum	Percentiles				Maximum
						50th	70th	80th	90th	
Ag	ppb	54	7.8	5.4	3	6	7	8	15	36
Al	%	54	0.02	0.009	0.005	0.02	0.02	0.02	0.03	0.05
As	ppm	54	0.3	0.6	0.05	0.1	0.2	0.2	0.4	3.7
Au	ppb	54	1.4	1.3	0.1	0.9	1.6	2.2	3.1	5.5
B	ppm	54	14	5	5	14	17	20	23	25
Ba	ppm	54	81	38	2.8	73	93	105	134	208
Ca	%	54	0.858	0.244	0.43	0.835	0.935	1.04	1.19	1.68
Cd	ppm	54	0.06	0.04	0.01	0.05	0.07	0.08	0.12	0.17
Ce	ppm	54	0.07	0.03	0.02	0.08	0.09	0.09	0.11	0.20
Co	ppm	54	0.12	0.05	0.04	0.11	0.14	0.15	0.17	0.28
Cr	ppm	54	1.96	0.13	1.70	2.00	2.00	2.10	2.15	2.20
Cs	ppm	54	0.065	0.113	0.006	0.032	0.056	0.078	0.154	0.779
Cu	ppm	54	11.6	4.6	4.1	10.5	12.8	14.4	16.8	33.6
Fe	%	54	0.018	0.008	0.006	0.017	0.021	0.024	0.027	0.056
Ga	ppm	54			0.05	0.1	0.1	0.1	0.1	0.1
Ge	ppm	54			0.005	0.01	0.01	0.01	0.015	0.02
Hf	ppm	54	0.002	0.001	0.001	0.002	0.002	0.003	0.003	0.005
Hg	ppb	54	26	8	11	26	31	32	37	51
In	ppm	54	0.01	0	0.01	0.01	0.01	0.01	0.01	0.01
K	%	54	0.509	0.082	0.35	0.52	0.555	0.57	0.605	0.74
La	ppm	54	0.04	0.02	0.01	0.04	0.05	0.06	0.06	0.11
Li	ppm	54	0.16	0.34	0.01	0.08	0.10	0.11	0.21	2.23
Mg	%	54	0.096	0.023	0.038	0.097	0.108	0.119	0.125	0.154
Mn	ppm	54	1253	751	346	1151	1573	1894	2150	4536
Mo	ppm	54	0.14	0.09	0.05	0.13	0.15	0.17	0.21	0.54
Na	%	54	0.002	0	0.001	0.002	0.002	0.002	0.003	0.003
Nb	ppm	54	0.011	0.01	0.005	0.01	0.01	0.01	0.03	0.06
Ni	ppm	54	0.7	0.3	0.3	0.7	0.8	0.9	1.1	2.0
P	%	54	0.152	0.025	0.099	0.15	0.163	0.168	0.18	0.233
Pb	ppm	54	0.16	0.07	0.06	0.15	0.19	0.21	0.27	0.46
Rb	ppm	54	5.3	2.4	1.1	4.8	6.2	6.9	9.5	10.9
Re	ppb	54	2.9	10.8	0.5	0.5	1	1	4.5	77
S	%	54	0.084	0.024	0.005	0.09	0.1	0.1	0.115	0.12
Sb	ppm	54	0.03	0.01	0.01	0.02	0.03	0.04	0.05	0.07
Sc	ppm	54	0.24	0.06	0.1	0.2	0.3	0.3	0.3	0.3
Se	ppm	54	0.19	0.09	0.1	0.2	0.2	0.2	0.2	0.6
Sn	ppm	54	0.03	0.02	0.01	0.02	0.03	0.04	0.05	0.1
Sr	ppm	54	26	9	6	25	28	33	40	52
Th	ppm	54	0.005	0	0.005	0.005	0.005	0.005	0.005	0.005
Ti	ppm	54	9.9	2.5	5	10	11	12	12.5	20
Tl	ppm	54	0.024	0.016	0.01	0.02	0.03	0.04	0.05	0.07
U	ppm	54	0.005	0.001	0.005	0.005	0.005	0.005	0.005	0.01
Y	ppm	54	0.05	0.02	0.01	0.04	0.05	0.06	0.07	0.12
Zn	ppm	54	47	16	12	47	55	58	66	90
Zr	ppm	54	0.04	0.01	0.02	0.03	0.04	0.05	0.05	0.09

TABLE 7. POND ZONE: STATISTICAL SUMMARY FOR ANALYSIS BY ICP-MS OF –80 MESH B-HORIZON SOIL

Element	Units	N	Mean	Std. Dev.	Minimum	Percentiles				Maximum
						50th	70th	80th	90th	
Ag	ppb	60	282	235	67	227	287	392	486	1732
Al	%	60	1.766	0.518	0.92	1.71	1.987	2.242	2.536	2.98
As	ppm	60	5.9	3.0	2.2	4.9	6.7	7.5	11.4	16.3
Au	ppb	60	15	22	-0.2	7.4	15.4	21	41	149
B	ppm	60	2.3	0.9	1	2	3	3	4	5
Ba	ppm	60	107	39	41	107	118	131	160	238
Be	ppm	60	0.42	0.15	0.2	0.4	0.5	0.6	0.6	0.9
Bi	ppm	60	0.17	0.12	0.07	0.13	0.17	0.21	0.26	0.7
Ca	%	60	0.388	0.196	0.17	0.34	0.407	0.478	0.629	1.36
Cd	ppm	60	0.22	0.11	0.09	0.2	0.25	0.28	0.39	0.59
Ce	ppm	60	17	4	10.2	16.7	18.2	19.5	21.3	33.1
Co	ppm	60	10.2	3.5	4.5	9.7	10.8	11.7	16.5	21.6
Cr	ppm	60	31	9	18	29	33	38	45	57
Cs	ppm	60	2.8	2.6	0.76	1.89	2.75	3.22	6.37	15.30
Cu	ppm	60	72	102	11	41	63	85	152	652
Fe	%	60	3.053	0.783	1.86	2.875	3.308	3.75	4.083	5.65
Ga	ppm	60	6.2	1.5	3.8	6.1	6.8	7.5	8.7	10.0
Ge	ppm	60			-0.1	-0.1	-0.1	-0.1	-0.1	0.1
Hf	ppm	60	0.048	0.022	-0.02	0.049	0.06	0.068	0.08	0.11
Hg	ppb	60	39	19	9	39	47	51	61	119
In	ppm	60	0.02	0.02	-0.02	0.02	0.02	0.03	0.03	0.04
K	%	60	0.084	0.031	0.04	0.08	0.1	0.1	0.119	0.19
La	ppm	60	9.6	1.6	6.2	9.5	10.4	11.1	11.7	13.8
Li	ppm	60	18.6	5.2	7.9	18.2	20.1	22.1	27.2	30.9
Mg	%	60	0.482	0.215	0.17	0.45	0.524	0.598	0.767	1.22
Mn	ppm	60	620	374	237	479	701	851	1165	1881
Mo	ppm	60	1.7	1.6	0.5	1.1	1.5	2.3	4.2	7.2
Na	%	60	0.008	0.004	0.005	0.007	0.008	0.009	0.01	0.031
Nb	ppm	60	0.83	0.17	0.50	0.80	0.92	0.98	1.10	1.25
Ni	ppm	60	18.4	8.4	6.6	17	21	23	31	51
P	%	60	0.104	0.057	0.032	0.089	0.111	0.134	0.204	0.292
Pb	ppm	60	7.0	2.1	4.5	6.5	7.1	8.0	10.6	13.9
Pd	ppb	60	-10	0	-10	-10	-10	-10	-10	-10
Pt	ppb	60	-2		-2	-2	-2	-2	2	2
Rb	ppm	60	13.4	4.1	7.1	13.3	14.5	16.2	20.3	23.8
Re	ppb	60		1.9	-1	-1	-1	-0.39	1.9	7
S	%	60	0.011	0.045	-0.01	0.01	0.01	0.018	0.03	0.31
Sb	ppm	60	0.29	0.08	0.15	0.28	0.33	0.36	0.41	0.52
Sc	ppm	60	3.2	1.4	1.6	2.9	3.3	3.68	4.27	10.7
Se	ppm	60	0.36	0.39	-0.1	0.2	0.387	0.48	0.7	2.2
Sn	ppm	60	0.45	0.14	0.3	0.4	0.5	0.5	0.6	1.2
Sr	ppm	60	58	39	19	44	57	77	109	232
Ta	ppm	60		0	-0.05	-0.05	-0.05	-0.05	-0.05	-0.05
Te	ppm	60	0.013	0.029	-0.02	0.02	0.03	0.03	0.05	0.09
Th	ppm	60	2.06	0.50	0.7	2.08	2.4	2.5	2.69	3.1
Ti	%	60	0.103	0.039	0.049	0.094	0.112	0.123	0.148	0.276
Tl	ppm	60	0.07	0.03	0.03	0.07	0.08	0.10	0.11	0.18
U	ppm	60	0.42	0.12	0.2	0.4	0.4	0.5	0.5	1
V	ppm	60	84	22	49	80	88	99	111	158
W	ppm	60	0.14	0.16	-0.1	0.1	0.2	0.2	0.39	0.6
Y	ppm	60	3.4	1.7	1.6	3.0	3.4	3.9	4.7	12.9
Zn	ppm	60	98	38	49	86	120	131	152	197
Zr	ppm	60	2.1	0.7	0.8	1.9	2.3	2.5	3.0	5.2
pH		59	5.1	0.5	4.3	5.1	5.2	5.4	5.8	6.4

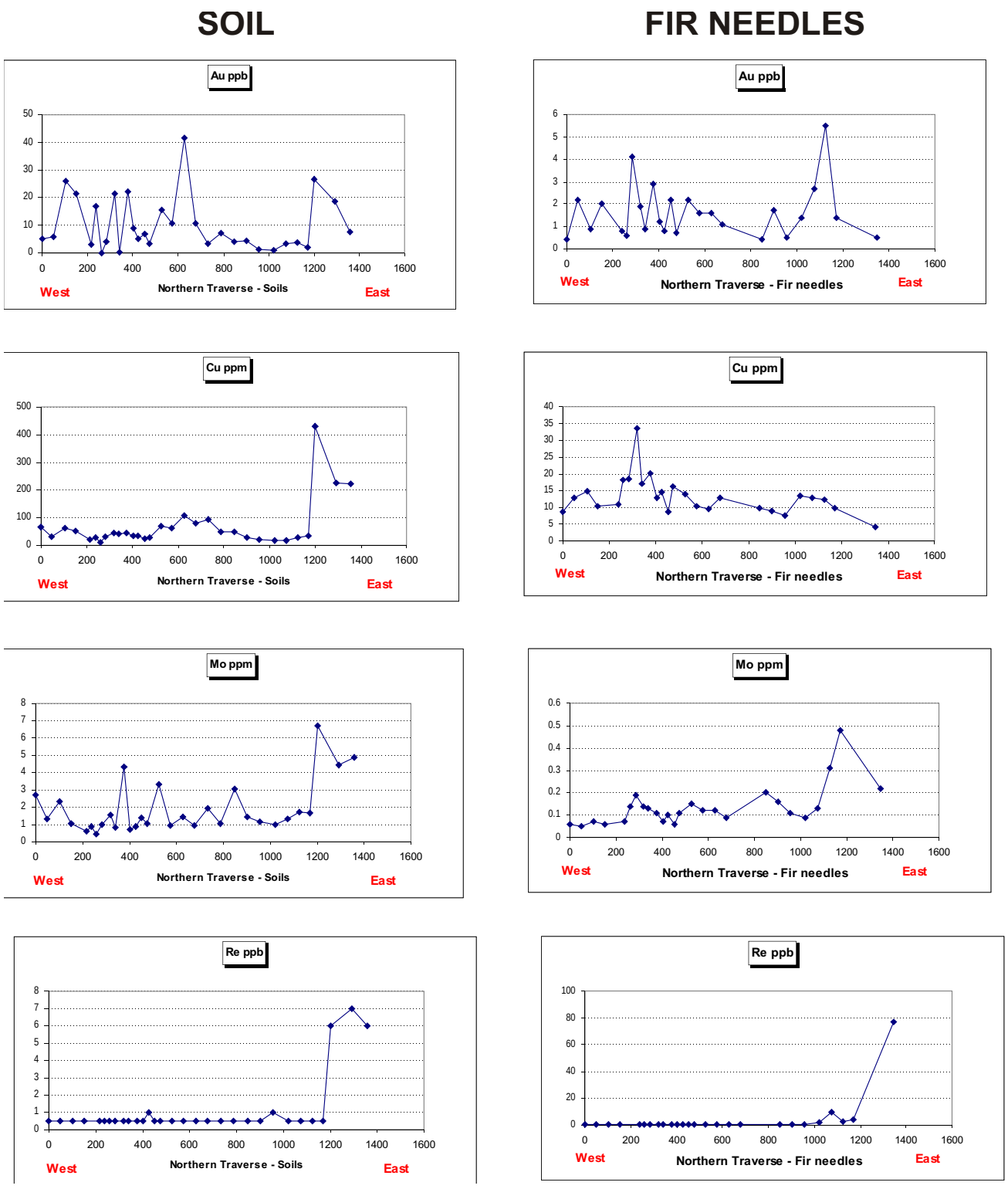


Figure 12. Pond zone: profiles of element concentrations in soil and foliage of subalpine fir along the northern east-west traverse (soil in left column, subalpine fir needles in right column).

from those in the soil by about 50 m. Figure 15 presents examples of a few elements.

3Ts Prospect

TOMMY VEIN TO THE RINGER SHOWING

The traverse covering these occurrences is shown in Figure 5. As noted, soil samples were only collected along the western half of the transect, and preliminary details of their multifaceted analyses are outlined in Cook and Dunn (2006).

Vegetation coverage is primarily white spruce, and lodgepole pine that has suffered from the mountain pine beetle kill. Sample media were spruce foliage and outer bark of the pine, and both have been analyzed. The foliage was originally selected as the priority medium for the halogens, but recent data on test samples of bark have yielded relatively high concentrations of iodine, so the bark samples will also be submitted for halogen analysis.

Near the west end of the traverse, a number of veins have been recognized and the spruce needles indicate subtle enrichment of several elements throughout this zone in general, with some enrichments closely related to the principal veins (Tommy and Larry) and, to a lesser extent, the narrower Ian vein. Farther east, the Mint vein was traversed and it, too, generates a subtle biogeochemical signature. The source of the boulders that constitute the Ringer showing has yet to be identified, and could be located at sites between the Mint vein and the Ringer showing where subtle peaks occur, since the direction of ice movement would have transported the boulders in an easterly direction. Figure 16 presents profiles of several elements in dry spruce needles that show some of these relationships. Gold is not shown because values in the sub-ppb level were too imprecise to be meaningful.

Of interest is a sharp increase in Mo at the eastern extremity of the traverse. This is evident from both the spruce foliage and the pine bark (Fig. 17), but with the bark yielding almost an order of magnitude more Mo. Iron, too, shows strong enrichment in the bark in this area. The enrichment suggests either a change in bedrock or, given the high concentrations in the bark, Mo mineralization.

TED VEIN TO ADRIAN WEST BOULDERS

The same plant species and tissues as those along the Tommy vein traverse were collected along the traverse extending from the Ted vein to the southern edge of the boulder showing near Adrian Lake (Fig. 5). Figure 18 shows the profiles across the Ted vein of S and Zn in each tissue type.

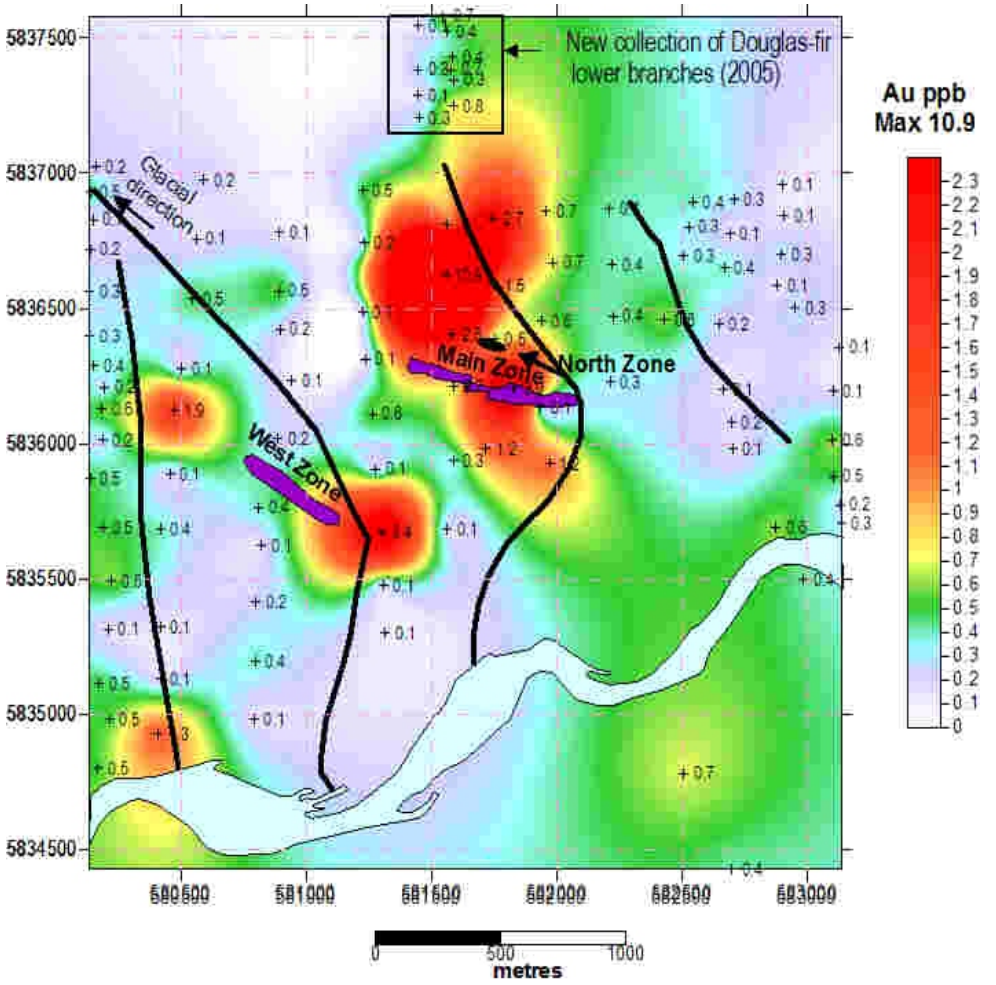


Figure 13. Plot of Au in dry Douglas-fir needles from tree tops, with cluster of samples in the north showing results of new data from lower branches.

Molybdenum enrichment at the eastern end of the line suggests some stratigraphic continuity with the end of the line to the north, in the vicinity of the Ringer showing (Fig. 5).

In general, the response of the vegetation to known mineralization is less pronounced than the signatures derived from the soil (Cook and Dunn, 2006). It remains to be seen if the halogen signatures will be more definitive.

SUMMARY AND PRELIMINARY CONCLUSIONS

Gold-rich Douglas-fir needles and lodgepole pine bark archived from GSC surveys over the QR deposit in the late 1980s have served as preliminary samples for testing and developing various methods to determine the halogen elements: F, Cl, Br and I. Several portions of each of three standard soil samples (STSD-1, STSD-4 and TILL-4) were used for developing methods appropriate for B-horizon soil.

Fifteen different methods were tested at commercial laboratories in Canada and at the GSC, of which some methods were duplicated at several of the laboratories. The test data indicate widely divergent results for most of the halogens. This is due, in part, to differences between 'total' and 'partial' analyses, but problems mostly lie in selecting appropriate digestions and instrumentation. Whereas the ion chromatograph would appear to be ideal for determining the halogens and other anions, the problems in obtaining accurate and precise data are at present sufficiently significant, especially for the vegetation, that this is not the recommended technique.

At this time, it appears that ICP-MS is the preferred technique for I, Br and probably Cl, and experimental data from various leaches will be used for the final decision on the currently optimal analytical method. Fluoride determi-

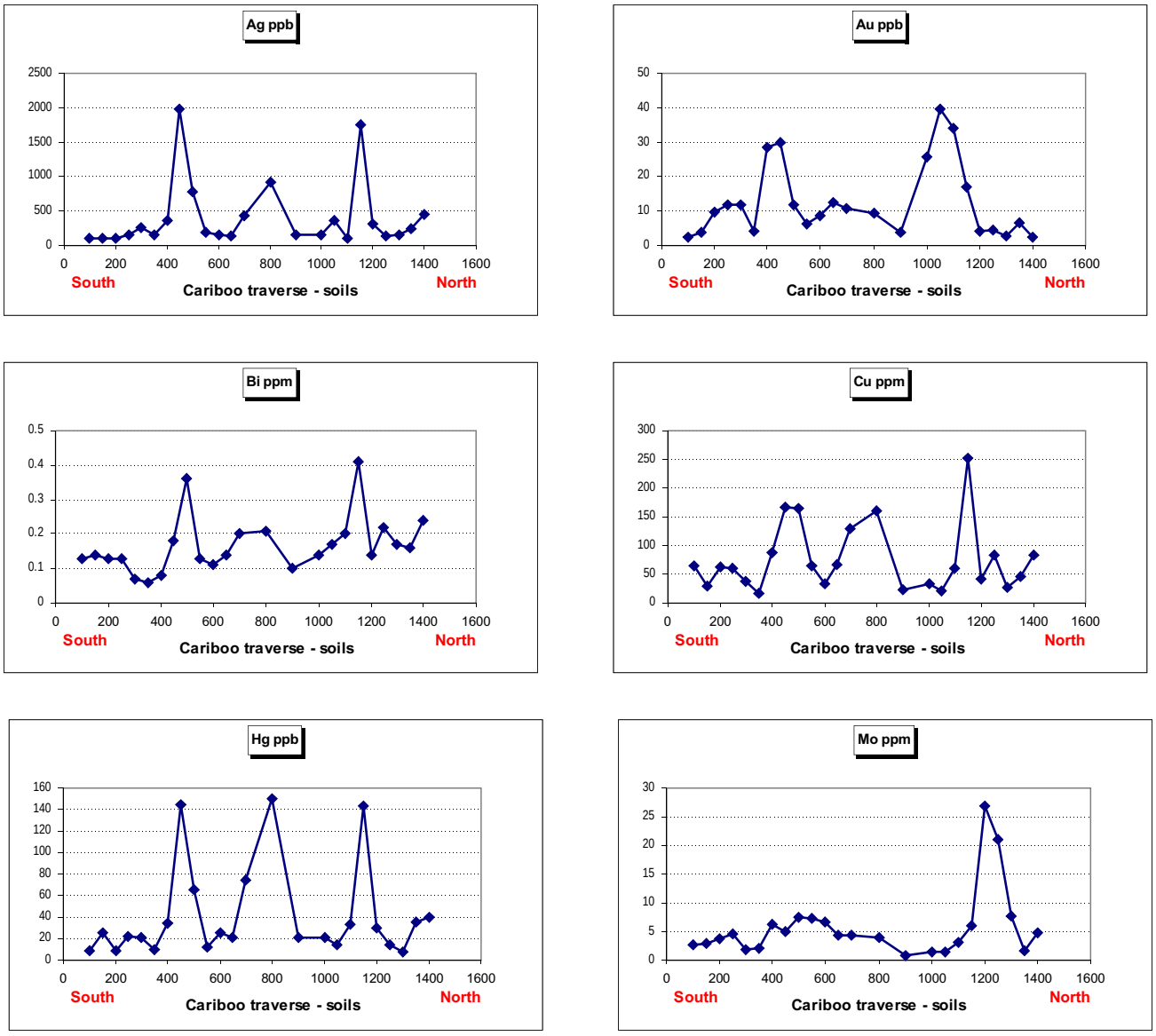


Figure 14. Cariboo zone (6 km east of QR deposit): examples of multielement signatures in B-horizon soils

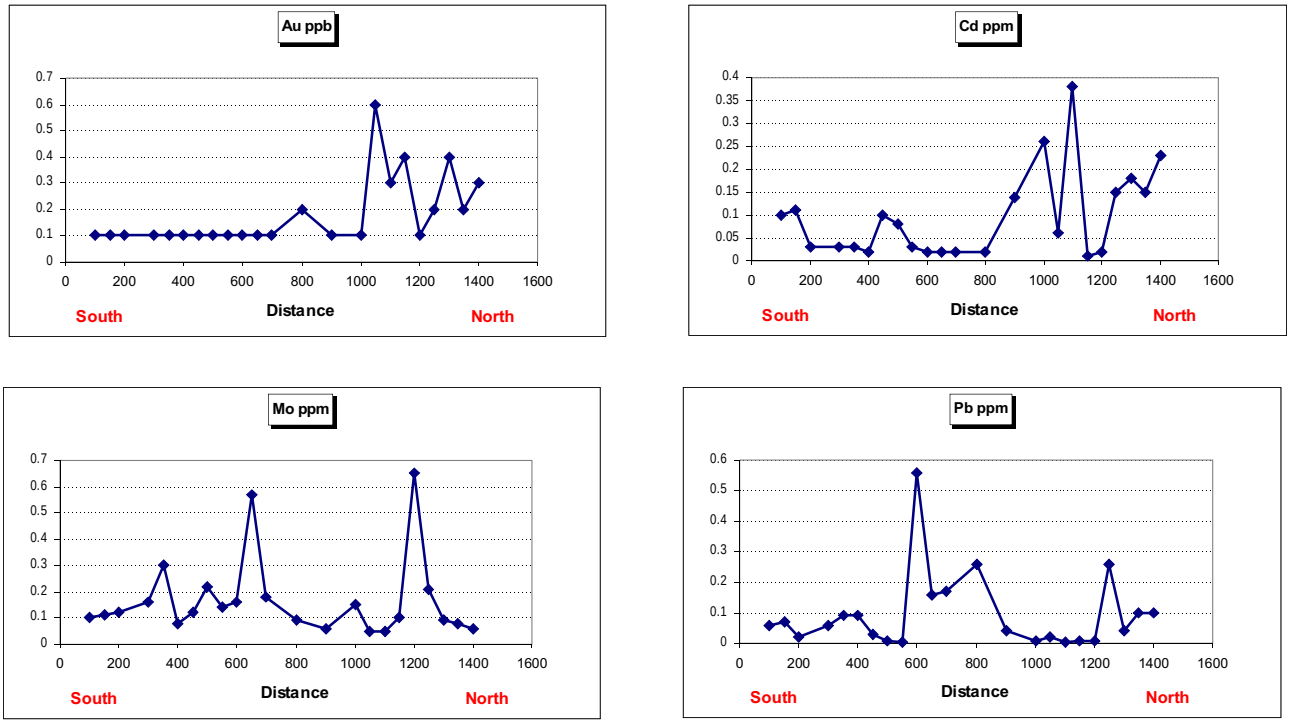


Figure 15. Cariboo zone: element concentrations in dry spruce needles.

nations are likely to be conducted using a selective ion electrode on a water leach of both soil and vegetation.

Multielement analyses (by ICP-MS for 53 elements) provide data on the distribution of elements in soil and vegetation with respect to known mineralization at the three survey areas. A few points of note are some unusually high Re results from the Mt. Polley area; some high Mo results near two mineralized boulder occurrences at 3Ts; enrichment of base and precious metals, including traces of Pt, at the Cariboo zone (east of the QR deposit). In general, the soil provides stronger signatures than the vegetation tissues that were tested, but the vegetation suggests evidence of mineralization from a number of trace elements that are not evident from the soil. Also, vegetation anomalies appear to be located more directly over concealed mineralization than anomalies present in the soil, because the latter are displaced either downslope or down-ice from mineralization.

Details of the multielement analytical data and the halogen data that have yet to be obtained will be presented in a final report submitted to Geoscience BC by March 2006.

ACKNOWLEDGMENTS

This project is funded mostly by Geoscience BC, but with significant contributions from the Geological Survey of Canada (Analytical Methodology Section, Judy Vaive and Pierre Pelchat), and the participating companies on whose properties the sampling has been undertaken: Imperial Metals Corporation (Mt. Polley), Cross Lake Minerals Ltd. (QR), and Southern Rio Resources Ltd. (3Ts). In particular we thank Patrick McAndless, VP Exploration, and his dynamic group of geologists at Mt. Polley; Jim Miller-Tait, VP Exploration, Cross Lake Minerals; Lindsay Bottomer, President, and Dan Meldrum, Southern Rio Resources. We were fortunate to have the assistance of Karen Hulme, a biogeochemistry Ph.D. student from the University of Adelaide, Australia, who valiantly conquered the alien field conditions of central BC.

We thank, too, John Gravel (Acme Analytical Laboratories Ltd.), Eric Hoffman (Activation Laboratories Ltd.) and Brenda Caughlin (ALS Chemex) who have all offered their advice and some free analytical work in order to further the objectives of this project. The incisive review comments of our industry partners (Imperial Metals, Cross Lake Minerals and Southern Rio Resources), Ray Lett (BCGS) and Rob Stevens (Geoscience BC) are greatly appreciated.

REFERENCES

Al Ajely, K.O., Andrews, M.J. and Fuge, R. (1985): Biogeochemical dispersion patterns associated with porphyry-style mineralization in the Coed Y Brenin forest, North Wales; *in* Prospecting in Areas of Glaciated Terrain, *Institution of Mining and Metallurgy*, London, Volume 6, pages 1–10.

BC Ministry of Energy, Mines and Petroleum Resources (2005): Exploration and mining in British Columbia 2004; *BC Ministry of Energy, Mines and Petroleum Resources*, Mining and Minerals Division, page 9.

Bottomer, L. (2003a): Epithermal gold-silver mineralization in the Nechako plateau, central British Columbia; *North West Mining Association*, Annual Meeting, Program with Abstracts, December 2003.

Bottomer, L. (2003b): The 3Ts epithermal gold-silver project, Nechako region, central BC; *Cordilleran Round-Up 2003*, Program with Abstracts, January 2003.

Cook, S.J. and Dunn, C.E. (2006): Preliminary results of the Cordilleran geochemistry project: a comparative assessment of soil geochemical methods for detecting buried mineral deposits, 3Ts Au-Ag prospect (NTS 093F/03), central

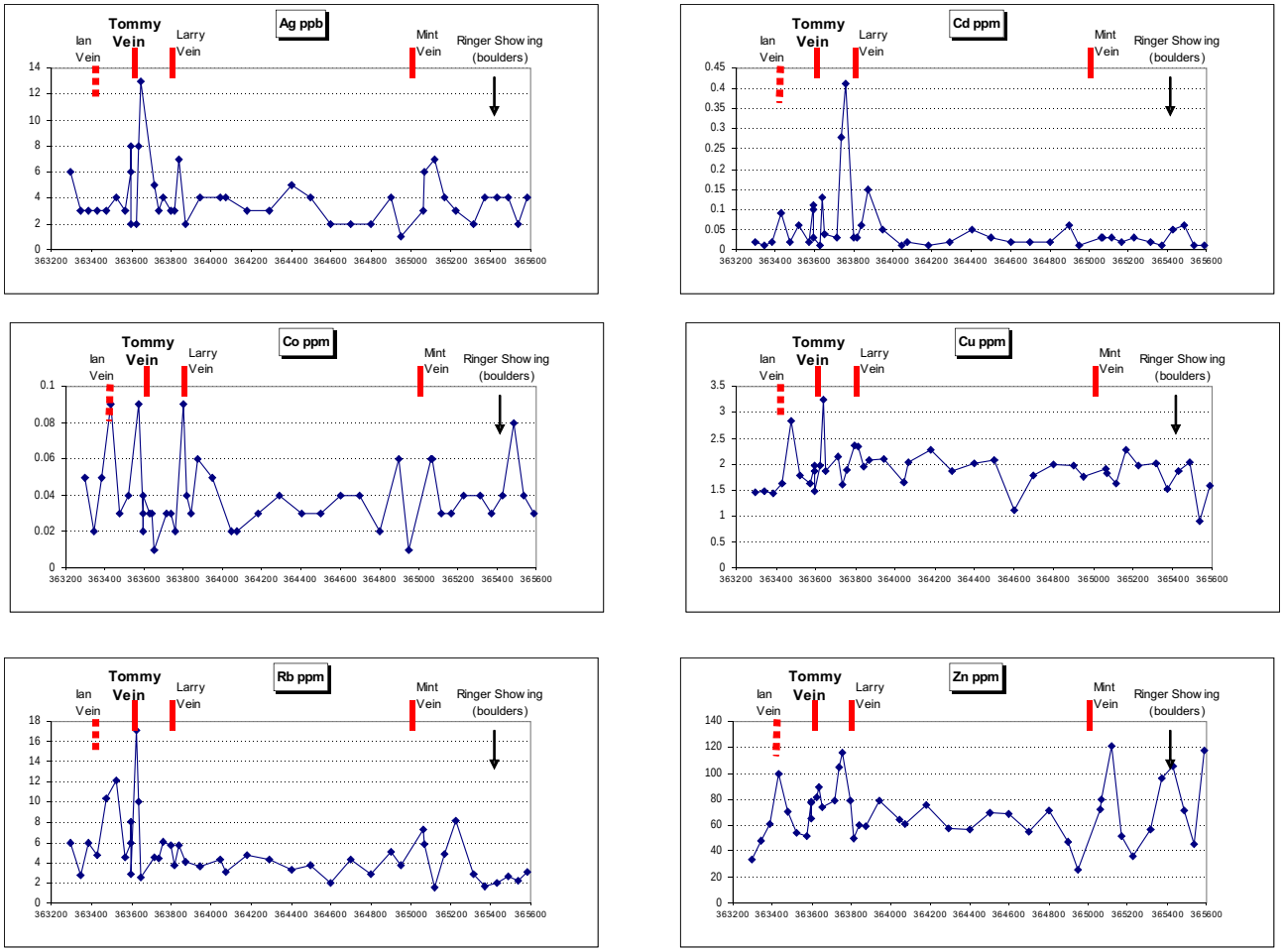


Figure 16. 3Ts prospect: concentrations of selected elements in dry spruce needles along a 2.4 km traverse across several known Au-bearing veins.

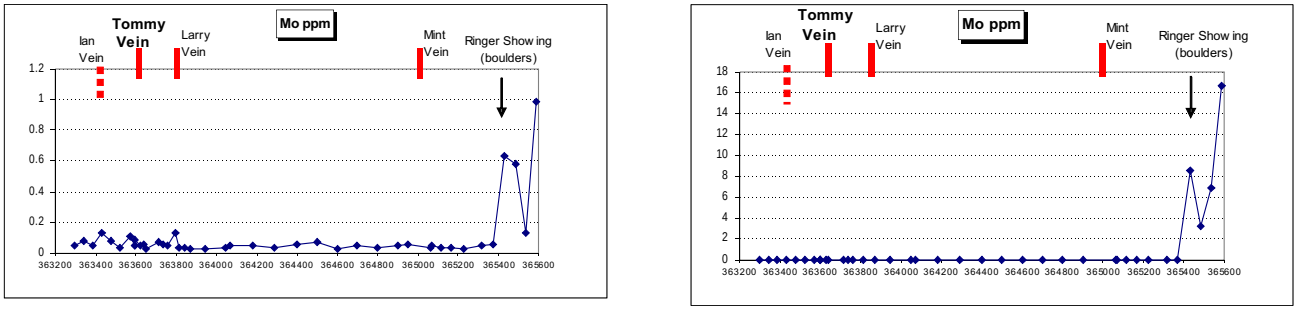


Figure 17. 3Ts prospect: profile across Au-bearing veins, showing Mo in spruce needles (left) and pine bark (right).

British Columbia; *in* Geological Fieldwork 2005, *BC Ministry of Energy, Mines and Petroleum Resources*, Paper 2006-1 and *Geoscience BC*, Report 2006-1.

Diakow, L. and Webster, C. (1994): Geology of the Fawnie Creek map area; *in* Geological Fieldwork 1993, *BC Ministry of Energy, Mines and Petroleum Resources*, Paper 1994-1, pages 15–26.

Dunn, C.E. (1985): Biogeochemical exploration for gold in the La Ronge Belt, 1985; *in* Summary of Investigations 1985, Saskatchewan Geological Survey, *Saskatchewan Energy and Mines*, Miscellaneous Report 85-4, pages 37–49.

Dunn, C.E. (1989): Airborne and surface biogeochemical surveys for precious metals in the Cordillera; *in* Cordilleran Geology and Exploration Roundup, Program and Abstracts, *BC and Yukon Chamber of Mines,* Mineral Exploration Roundup, Feb 7–10, Vancouver, BC.

Dunn, C.E., Balma, R.G. and Sibbick, S.J. (1996):Biogeochemical survey using lodgepole pine bark: Mount Milligan, central British Columbia (parts of NTS 93N/1 and 93O/4); *Geological Survey of Canada*, Open File 3290; *BC Ministry of Energy, Mines and Petroleum Resources*, Open File 1996-17.

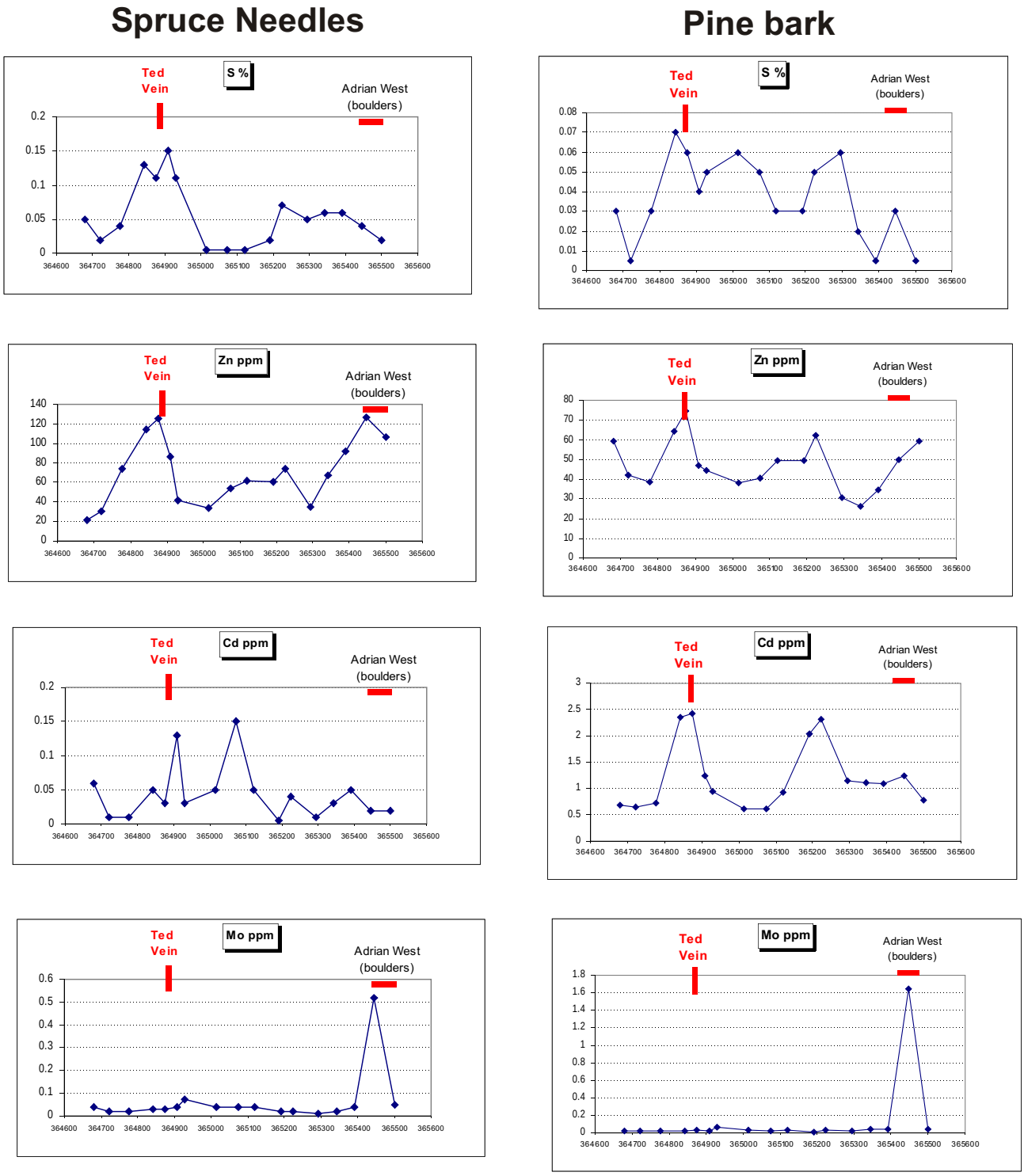


Figure 18. 3Ts prospect: southern traverse across the Ted vein, showing concentrations of S, Zn, Cd and Mo in spruce needles (left column) and pine bark (right column).

Dunn, C.E., Coker, W.B. and Rogers, P.J. (1991): Reconnaissance and detailed geochemical surveys for gold in eastern Nova Scotia using plants, lake sediment, soil and till; *Journal of Geochemical Exploration*, Volume 40, pages 143–163.

Dunn, C.E. and Scagel, R.K. (1989): Tree-top sampling from a helicopter — a new approach to gold exploration; *Journal of Geochemical Exploration*, Volume 34, pages 255–270.

Fox, P.E., Cameron, R.S. and Hoffman, S.J. (1987): Geology and soil geochemistry of the Quesnel River gold deposit, British Columbia; *in* GEOEXPO '86, *Association of Exploration Geochemists and Cordilleran Section, Geological Association of Canada*, Vancouver, BC, pages 61–71.

Melling, D.R. and Watkinson, D.H. (1988): Alteration and fragmental basaltic rocks: the Quesnel River gold deposit,

central British Columbia; in Geological Fieldwork 1987, *BC Ministry of Energy Mines and Petroleum Resources*, Paper 1988-1, pages 325–348

MINFILE (2005): MINFILE BC mineral deposits database; *BC Ministry of Energy, Mines and Petroleum Resources*, URL <http://www.em.gov.bc.ca/Mining/Geolsurv/Minfile/> [Nov 2005].

Trofimov, N.N. and Rychkov, A.I. (2004): Iodine and Bromine: Geochemical Indicators of Deep Ore Deposits; *Colorado Mountain Publishing House*, Denver, CO, 205 pages.

Targeted Energy-Resource Studies in the Bowser and Sustut Interior Basins of British Columbia[1]

By C.A. Evenchick[2], P.B. O'Sullivan[3] and J.W.F. Waldron[4]

KEYWORDS: Bowser Basin, Sustut Basin, petroleum resources, apatite fission-track thermochronology, Bowser Lake Group, Sustut Group, Hazelton Group

INTRODUCTION

The Bowser and Sustut basins are interior basins of Jurassic and Cretaceous age in north-central British Columbia (Fig. 1). They have been underexplored in terms of hydrocarbon resources because of widespread misperceptions of their prospectivity, largely due to the reconnaissance nature of all geoscience work carried out there until recently. This two-year project focuses on specific, *detailed*, energy-resource studies complementary to an ongoing *regional* project that has been a collaboration between the Geological Survey of Canada (GSC) and the BC Ministry of Energy, Mines and Petroleum Resources (BCMEMPR; Evenchick *et al.*, 2005). The project includes three elements of research and compilation: apatite fission-track thermochronology (AFTT) of the southern basins; detailed study of the early history and structural development of the Bowser Basin; and data management, integration and digital publication. The sample analysis and interpretation of AFTT data are critical to understanding petroleum systems in sedimentary basins, which is an essential element of a geoscience-resource framework on which to base sound exploration decisions. Mapping in targeted areas will provide detailed field data on the important early history and geometry of the basin. Data management, integration and publication are critical because *communication* of data and interpretations are essential to attracting investment to the region. This paper outlines the three elements of this project, describing the nature of the work and its relationship to the broader GSC project. It also presents the status of the project. Details of work on the early Bowser Basin history are presented in a separate paper (Waldron et al., 2006).

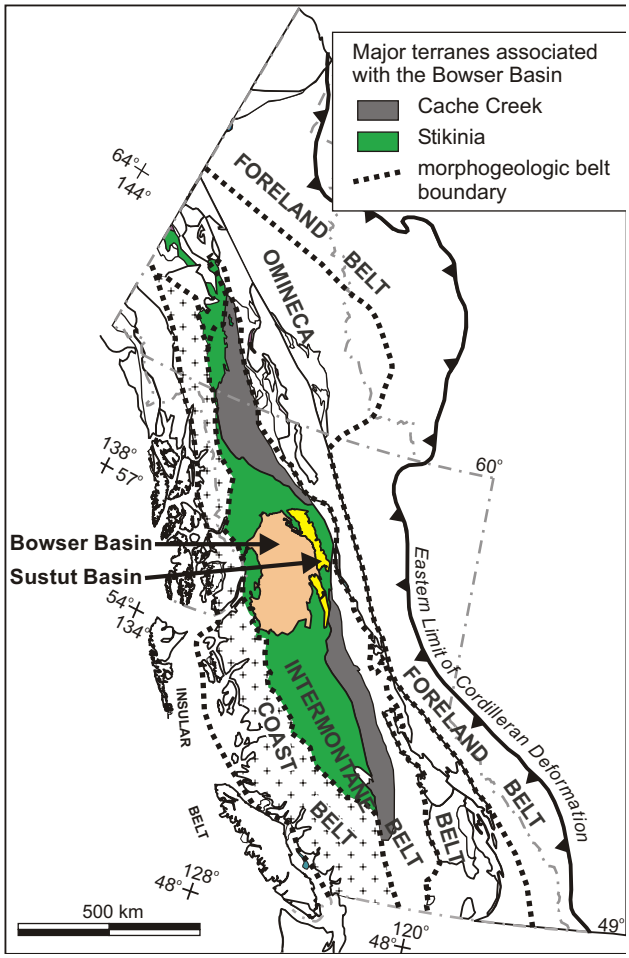


Figure 1. Location of the Bowser and Sustut basins (modified after Wheeler and McFeeley, 1991).

GEOLOGICAL AND HYDROCARBON-RESOURCE OVERVIEW OF THE BOWSER AND SUSTUT BASINS

The Bowser and Sustut basins underlie approximately 62 000 km^2 of north-central BC (Fig. 1) and are considered to be frontier hydrocarbon basins. Bowser Basin strata (the Bowser Lake Group) overlie volcanic and clastic rocks of the Early to early Middle Jurassic Hazelton Group. Bowser strata are late Middle Jurassic to mid-Cretaceous in age, and were deposited in a wide range of clastic sedimentary environments, from deep distal marine through slope, shelf, deltaic, fluvial and lacustrine (*e.g.*, Evenchick *et al.*, 2004). They contain minor carbonates and a huge volume

[1] *Geoscience BC contribution GBC004; GSC contribution 2005416*

[2] *Geological Survey of Canada, Vancouver, BC (cevenchi@nrcan.gc.ca)*

[3] *Apatite to Zircon Inc., Moscow, ID, USA*

[4] *University of Alberta, Edmonton, AB*

This publication is also available, free of charge, as colour digital files in Adobe Acrobat PDF format from the BC Ministry of Energy, Mines and Petroleum Resources internet website at http://www.em.gov.bc.ca/Mining/Geolsurv/Publications/catalog/catfldwk.htm

of dark grey siltstone and mudstone, all of which are potential source rocks. Bowser strata are overlain on the east by fluvial strata of the Upper Cretaceous Sustut Group. Most strata of the Bowser-Sustut region, except for parts of the northeastern margin of the Sustut Basin, were deformed by folds and thrust faults in the Cretaceous to form the thin-skinned Skeena fold belt (Evenchick, 1991). The style of deformation, which includes a classic triangle zone locally in the northeast, provides ample opportunities for structural traps of hydrocarbons.

The regional Bowser-Sustut project aims to provide basic regional geological and resource framework data and interpretations upon which to base more informed exploration decisions. Overviews of the regional geological framework and context of the project are presented elsewhere (*e.g.*, Evenchick *et al.*, 2003; Evenchick and Thorkelson, 2005). Fieldwork over the past three field seasons has contributed to significant refinements of the distribution of map units across the central and southern basin. Early results of regional energy-resource studies show that the basin is not entirely overmature (Evenchick *et al.*, 2002) and that there are at least three effective petroleum systems that at some point have generated, expelled and accumulated crude oil (Osadetz *et al.*, 2004). Hydrocarbon source rocks identified are a sub-Hazelton carbonate, upper Hazelton or lower Bowser marine strata and Mesozoic lacustrine strata. Recent results (Stasiuk *et al.*, 2005) indicate that the most prospective parts of the basins (in the early oil to condensate – dry gas generation stage of thermal maturation) are in the northwestern Bowser Basin and an elongate belt in the east, overlapping the Sustut Basin and eastern Bowser Basin. Energy-resource studies now need to focus on specifics of timing of petroleum generation and migration, and peak temperatures. The analytical parts of the current (Geoscience BC) project will address these through apatite fission-track thermochronology. Following up on the 2004 regional mapping, one element of this work is a detailed field examination of the early history of the Bowser Basin, which includes an interval known locally to include organic-rich shale (Thomson *et al.*, 1986).

REGIONAL BOWSER-SUSTUT PROJECT — CONTEXT FOR THE COMPLEMENTARY TARGETED ENERGY-RESOURCE STUDIES OF THIS PROJECT

The 'Integrated Petroleum Resource Potential and Geoscience Studies of the Bowser and Sustut Basins' project (referred to hereafter as the Bowser-Sustut project) is a project of the GSC's Northern Resources Development program. It started in 2003 as a collaboration between the GSC and BCMEMPR Oil and Gas Division. The primary goal of the four-year Bowser-Sustut project is to provide improved geoscience data and knowledge regarding energy resources of the Bowser and Sustut basins, in order to spark new private-sector investment. It is regional in scope, covering the breadth of the Bowser and Sustut basins. The final of many project deliverables (several of which are completed) will be a digital basin atlas, including resource assessment. The project has involved twenty-two GSC scientists and technicians; one BCMEMPR scientist (Fil Ferri); and one faculty member (Peter Mustard) and one graduate student from Simon Fraser University. This new targeted project includes one outside consultant (Paul O'Sullivan), and one faculty member (John Waldron) and two graduate students from the University of Alberta, following scoping of topics as part of the 2004 Bowser-Sustut field program. Geological Survey of Canada scientists involved in the project include specialists in a wide suite of geoscience and energy-resource studies that are all aimed at an integrated understanding of energy resources of the basins (*e.g.*, biostratigraphy, paleomagnetism, geophysics, geochronology, structural geology, basin stratigraphy, organic petrology, thermal maturity, petroleum systems, resource assessment). These are complemented by a small team dedicated to cartography, graphics, database management, information management, website creation and maintenance, development of tools for capturing field data digitally and integrating digital data for publication, and outreach. The latter group is highlighted because rapid and broad communication of results is essential in order to have the desired impacts; therefore, it is necessary to have staff dedicated to the manipulation and management of data and production of manuscripts and maps.

TARGETED ENERGY-RESOURCE STUDIES COMPLEMENTARY TO THE REGIONAL BOWSER-SUSTUT PROJECT

Apatite Fission-Track Thermochronology

The timing of hydrocarbon generation relative to the formation of structures affects petroleum-play and prospect-level risks. Organic maturity provides a maximum recording geothermometer that indicates regions of probable petroleum generation, whereas apatite fission-track thermochronology (AFTT) provides an integrated thermal history for the period when samples last cooled from approximately >110°C to approximately <60°C. Therefore, AFTT provides potential constraints on the age of structures, at various scales, that can be combined with petroleum-system models to constrain play and prospect risks for petroleum accumulation. Preliminary results of samples from parts of the northern Bowser and Sustut basins have indicated that 'pooled' AFTT ages range primarily between 45 and 35 Ma (O'Sullivan *et al.*, 2005). Results are interpreted to record rapid cooling (from temperatures greater than 100–110°C) at a time slightly before the value of the reported AFTT age, beginning at various times in different parts of the basin. Rocks presently at the surface were within the zone of thermogenic petroleum generation until either Late Cretaceous (in the north and northeast) or at least Middle Eocene (the remainder of the region sampled). Therefore, most of the samples appear to record a rapid regional event that postdates Skeena fold belt structures, highlighting the potential for structural traps in those areas.

All AFTT samples analyzed to date (O'Sullivan *et al.*, 2005) are from the northern two-thirds of the Bowser and Sustut basins (Fig. 2). These samples were collected and analyzed under a research agreement in 2002 between GSC and the BCMEMPR. New sampling in the southern basin, undertaken during this targeted project, was conducted in concert with mapping by the broader Bowser-Sustut project and addresses the following issues:

- A vertical profile in a high-relief Cretaceous intrusion will establish a well-constrained geothermal gradient for

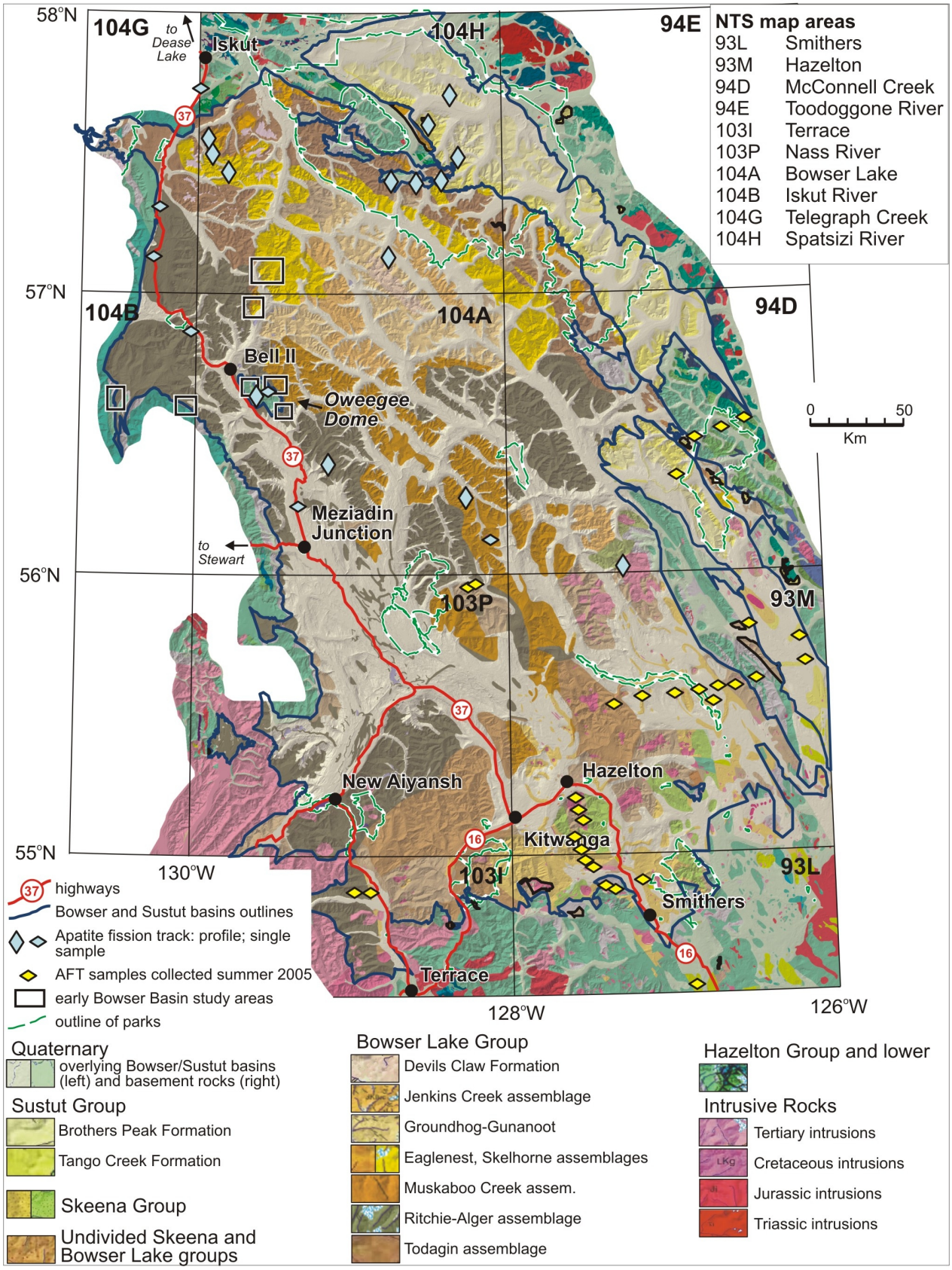


Figure 2. Geological compilation of the Bowser and Sustut basins on shaded-relief map (modified after Evenchick *et al.*, 2004), showing locations of detrital zircon samples collected in previous work and this work, and areas for field studies of the early history of the Bowser Basin.

the southern basin region, which will enhance thermal history modelling of other samples.

- Current geological maps of the southeastern Bowser Basin (*e.g.*, Richards, 1990) display a rectilinear pattern of normal faults. This interpretation is based on the presence of young rocks in valleys and a model of Tertiary extension. However, the faults are poorly exposed and alternatives exist to explain the map pattern. Results from AFTT, when combined with mapping, can elucidate the nature and significance of the faults by placing constraints on their timing and magnitude of displacement. This is important for petroleum exploration because the map pattern could be interpreted as resulting from fold-and-thrust-belt structures similar to those farther north. The geometric difference between the two interpretations is fundamental to any attempt to extrapolate structures and units to depth. Therefore, the resolution of the dominant structural style is an issue critical for petroleum assessment and planning geophysical surveys or drill programs. Mapping in 2004 in the western part of NTS 093M (Hazelton map area; Ferri *et al.*, 2005) suggested that several faults shown on the previous map (Richards, 1990) are not required by the distribution of map units.
- AFTT results from Tertiary units will provide a thermal history for a younger period than existing samples, extending into the period of inferred rapid cooling for farther north.
- AFTT results from samples collected from the southern Sustut Basin will be used to compare and contrast with those previously collected from the northern basin, and to determine when rocks in the southern Sustut Basin were within the temperature range for generating petroleum.

After initial stages of data and information are released as they become available, a final report will integrate these new data with other pertinent datasets.

STATUS OF RESEARCH

During the 2005 field season, 29 samples were collected to cover the targeted issues listed above. The location of new samples is shown in Figure 2. The samples were shipped to the laboratory in September and will be processed and analyzed. Initial data release is anticipated for the spring 2006. Field observations indicate that fold-and-thrust-belt structures are common in the southeastern Bowser Basin and affect strata below the Bowser Lake Group, all units of the Bowser Lake Group, the Skeena Group and the Sustut Group. The degree to which the present structural relief is a result of normal faults rather than contractional structures will be addressed with further analysis of the field data, and its integration with apatite fission-track thermochronology.

Early Bowser Basin History and Structural Analysis

A field study led by John Waldron (University of Alberta) focuses on potential source rocks and structures in the transition from a volcanic-dominated rifted-arc environment (Hazelton Group) to a sedimentary basin (Bowser Lake Group). Reconnaissance in 2004 as part of the regional Bowser-Sustut project identified major lateral facies changes in this transition, in the northwestern part of the Bowser Basin (Oweegee Dome area; Fig. 2). In this area, volcanic and coarse volcaniclastic rocks of the lower Hazelton Group are separated by a conspicuous unconformity from laminated, thinly bedded siltstone of the upper Hazelton Group. The latter contain tuffaceous bands, occasional intercalations of bioclastic limestone and localized spectacular mound-facies limestone; it is unknown whether the mound-facies limestone represents *in situ* reefs or olistoliths that slid in from basin margins. The upper Hazelton rocks, including the limestone, are organic rich and may have acted as source rocks for petroleum during burial and deformation of the basin. To the east of Oweegee the Dome, work in 2004 under the regional Bowser-Sustut project demonstrated a shallowing in the lower Bowser Lake Group, with the deposition of bioturbated shelf clastic rocks. In contrast, other parts of the dome appear submerged in thick turbidite successions (Evenchick *et al.*, 2005). These observations indicate that Oweegee Dome may be founded on a primary feature of the basin floor, modified by later deformation.

Bowser strata around the Oweegee dome display a pattern of folding, locally with weak cleavage development, involving intersecting northwest and northeast-trending folds, producing structural domes and basins. Evenchick (2001) suggested that the transverse folds were related to strike-slip motion. Evidence for the relative timing of the two sets of folds is contradictory.

The objectives of the work are to,

- determine stratigraphic relationships in the Hazelton-Bowser transition, in order to understand the tectonic processes involved in the initiation of the basin and the role of the Upper Hazelton as a potential source rock; and
- determine the origin and relative timing of transverse structures responsible for domes and basins within the basin, with the aim of understanding their relationship to potential petroleum traps.

As an additional benefit, the work will provide an improved regional understanding of the stratigraphic interval that farther west is extensively mineralized and contains the Eskay Creek gold mine.

The work is being undertaken by two graduate students (W. Loogman and J.-F. Gagnon) under the supervision ofJohn Waldron. Gagnon is working on relationships in the Hazelton-Bowser transition, to define the rock types, lateral relationships and tectonic setting of the sedimentary rocks. Loogman is focusing on transverse structures and folds in the Bowser Lake Group. The work is field based and initially (summer of 2005) focused in the Oweegee area in the northwest Bowser Basin (Fig. 2). Work was also undertaken to determine target areas for 2006 fieldwork.

STATUS OF RESEARCH

Field work was completed successfully and is reported in a separate paper (Waldron *et al.*, 2006)

Digital Aspects of the Field-to-Publication Process

Critical links in the path from field observation to communication and publication of the data and interpretations include a wide range of digital and organizational work be-

ing carried out in parallel with the scientific work. This includes maintaining and upgrading an application for digital capture of field data (using handheld computers); managing data in the field; follow-up checking and cleaning of databases; rectification of aerial photographs used in the cartographic process; extracting data subsets for analysis and distribution; compiling archival data from previous field work in the region with current work; maintenance of the project website; creation of CDs of recent project presentations and results for distribution at major meetings; customization of specialized tools for integration, display and communication of thematic datasets for final compilation and release; sample curation and distribution of the various sample suites to labs; digital graphics for publications; and analysis of datasets. To emphasize the time involved in the publication process alone, the deliverables for the other elements of this targeted project for 2005-2006 will require 6 weeks. This work is fundamental to communicating results and putting new data and interpretations into the hands of explorationists for decision making.

STATUS OF WORK

The primary deliverable for this work is an open file release of digital field data on CD from all mapping seasons, to be completed in 2007. Work is progressing this year on data verification, capture of past field data and design of the format for the final synthesis.

ACKNOWLEDGMENTS

The authors acknowledge the safe and efficient helicopter support provided by Canadian Helicopters pilots Tom Brooks and Darrell Adzich during sampling for the AFTT study. Sampling was done with the able assistance of Gareth Smith (Simon Fraser University), Nathan Cleven (University of British Columbia), Ruben Wesley, Jamel Joseph (GSC), David Ritcey (GSC), Paul Wodjak (BCMEMPR) and Linda Zurkirchen (volunteer). In addition, a few samples were collected by Peter Mustard (Simon Fraser University) and David Ritcey (GSC). John Waldron, Walter Loogman and J.-F. Gagnon were assisted by Ian Swan and the pilots of Quantum Helicopters, and by field assistants Jeff Samson and Shane Krepakevich. They also appreciated the hospitality of Ted Mahoney and Barrick Gold Corporation in the Eskay Creek area. The authors appreciate the efforts of Rob Stevens (Geoscience BC) and Steve Irwin (GSC) in providing helpful reviews of the manuscript.

REFERENCES

Evenchick, C.A. (1991): Geometry, evolution, and tectonic framework of the Skeena Fold Belt, north-central British Columbia; *Tectonics*, Volume 10, pages 527–546.

Evenchick, C.A. (2001): Northeast-trending folds in the western Skeena Fold Belt, northern Canadian Cordillera: a record of Early Cretaceous sinistral plate convergence; *Journal of Structural Geology,* Volume 23, pages 1123–1140.

Evenchick, C.A., Ferri, F., Mustard, P.S., McMechan, M., Osadetz, K.G., Stasiuk, L., Wilson N.S.F., Enkin, R.J., Hadlari, T. and McNicoll, V.J. (2003): Recent results and activities of the Integrated Petroleum Resource Potential and Geoscience Studies of the Bowser and Sustut basins, British Columbia; *in* Current Research, *Geological Survey of Canada*, 2003-A13, 11 pages.

Evenchick, C.A., Ferri, F., Mustard, P.S., McMechan, M.E., Ritcey, D., McNicoll, V.J., Osadetz, K.G., O'Sullivan, P.B., Stasiuk, L.D., Wilson, N.S.F., Poulton, T.P., Lowe, C., Enkin, R.J., Waldron, J., Snyder, D.B., Turner, R.J.W., Nowlan, G. and Boddy, M. (2005): Highlights of recent research in the Bowser and Sustut basins project, British Columbia; *in* Current Research, *Geological Survey of Canada*, 2005-A1, 11 pages.

Evenchick, C.A., Hayes, M.C., Buddell, K.A and Osadetz, K.G. (2002): Vitrinite reflectance data and preliminary organic maturity model for the northern two-thirds of the Bowser and Sustut basins, north-central British Columbia; *Geological Survey of Canada* Open File 4343; *BC Ministry of Energy, Mines and Petroleum Resources,* Petroleum Geology Open File 2002-1.

Evenchick, C.A., Mustard, P.S., Woodsworth, G.J. and Ferri, F. (2004): Compilation of geology of Bowser and Sustut basins draped on shaded relief map, north-central British Columbia; *Geological Survey of Canada*, Open File 4638, scale 1:500 000.

Evenchick, C.A., Poulton, T.P., Tipper, H.W. and Braidek, I. (2001): Fossils and facies of the northern two-thirds of the Bowser Basin, northern British Columbia; *Geological Survey of Canada*, Open File 3956.

Evenchick, C.A. and Thorkelson, D.J. (2005): Geology of the Spatsizi River map area, north-central British Columbia; *Geological Survey of Canada*, Bulletin 577.

Ferri, F., Mustard, P.S., McMechan, M., Ritcey, D., Smith, G.T., Evenchick, C.A. and Boddy, M. (2005). Skeena and Bowser Lake Groups, West Half Hazelton Map Area (93M); *in* Summary of Activities 2005, *BC Ministry of Energy, Mines and Petroleum Resources*, pages 113–131.

Osadetz, K.G., Jiang, C., Evenchick, C.A., Ferri, F., Stasiuk, L.D., Wilson N.S.F. and Hayes, M. (2004): Sterane compositional traits of Bowser and Sustut basin crude oils: indications for three effective petroleum systems; *in* Summary of Activities 2004, *BC Ministry of Energy, Mines and Petroleum Resources*, pages 99–112.

O'Sullivan, P.B., Donelick, R.A., Osadetz, K.G., Evenchick, C.A., Ferri, F., Wilson, N.S.F. and Hayes, M. (2005): Apatite fission-track data from seventy-one Bowser and Sustut Basin rock samples; *Geological Survey of Canada* Open File Report 4840; *BC Ministry of Energy, Mines and Petroleum Resources*, Petroleum Geology Open File 2004-3.

Richards, T.A. (1990): Geology of Hazelton map area (93M); *Geological Survey of Canada*, Open File 2322.

Stasiuk, L.D., Evenchick, C.A., Osadetz, K.G., Ferri, F., Ritcey, D., Mustard, P.S. and McMechan M. (2005): Regional thermal maturation and petroleum stage assessment using vitrinite reflectance, Bowser and Sustut basins, north-central British Columbia, *Geological Survey of Canada* Open File 4945; *BC Ministry of Energy, Mines and Petroleum Resources*, Petroleum Geology Open File 2005-2.

Thomson, R.C., Smith, P.L. and Tipper, H.W. (1986): Lower to Middle Jurassic (Pliensbachian to Bajocian) stratigraphy of the northern Spatsizi area, north-central British Columbia; *Canadian Journal of Earth Sciences*, Volume 23, pages 1963–1973.

Waldron, J.W.F., Gagnon, J.-F., Loogman, W. and Evenchick, C.A. (2006): Initiation and deformation of the Jurassic–Cretaceous Bowser Basin: Implications for Hydrocarbon Exploration in North-Central British Columbia; *in* Geological Fieldwork 2005, *BC Ministry of Energy, Mines and Petroleum Resources*, Paper 2006-1 and *Geoscience BC*, Report 2006-1.

Wheeler, J.O. and McFeeley, P. (1991): Tectonic assemblage map of the Canadian Cordillera and adjacent parts of the United States of America; *Geological Survey of Canada*, Map 1712A, scale 1:2 000 000.

ASTER Imagery for British Columbia – An Online Exploration Resource[1]

by W.E. Kilby[2] and C.E. Kilby[2]

KEYWORDS: ASTER, anaglyph, virtual reality, digital elevation model, reflectance, orthorectification

INTRODUCTION

The ASTER Imagery for British Columbia project, sponsored by Geoscience BC, increases the quantity and quality of Advanced Spaceborne Thermal Emission and Reflection Radiometer (ASTER) imagery available through the BC Ministry of Energy, Mines and Petroleum Resources' MapPlace website (www.MapPlace.ca). One hundred new images have been added to the collection, all available for analysis through the MapPlace's Image Analysis Toolbox (IAT) (Kilby *et al*., 2004; Kilby, 2005). A number of new derivative products have been generated from the imagery and made available for online viewing at the MapPlace website using the Google Earth viewer (Google, 2005). The products can also be downloaded for offline viewing.

ASTER is an imaging instrument flying on the Terra satellite, launched in late 1999. ASTER is a cooperative project between the National Aeronautics and Space Administration (NASA), Japan's Ministry of Economy, Trade and Industry and Japan's Earth Remote Sensing Data Analysis Center. The instrument has three subsystems that capture readings from different portions of the electromagnetic spectrum at different resolutions. The three subsystems are referred to as VNIR (Visible and Near Infrared), SWIR (Shortwave Infrared) and TIR (Thermal Infrared). Reflectance values in the SWIR range are particularly useful in differentiating rock and soil mineralogy related to alteration zones. An ASTER image contains 14 bands of information, 4 bands in the VNIR with 15 m resolution, 6 bands in the SWIR with 30 m resolution and 5 bands in the TIR with 90 m resolution. Two of the VNIR bands sample the same wavelength range but one is back-looking providing the ability to generate a stereo view of the scene. A single ASTER scene covers an area of approximately 60 by 60 km. The ASTER website (asterweb.jpl.nasa.gov) is an excellent source of information on the instrument, its mission, available imagery, usage examples and analysis tools.

The 39 previously existing ASTER images and 100 new images included in the IAT have been processed to relative reflectance values, a significant improvement from the calibrated radiance integer (DN) values previously available. A mask layer that filters out vegetation, clouds, water, snow and ice has been added to optionally restrict IAT image analysis processes to pixels with good ground exposure. Specialized maps with anaglyph background images (3-D images requiring red/cyan glasses) are now available through the IAT. In addition, a number of preprocessed layers are available that predict relative alteration-mineral distributions such as iron oxides, siliceous rocks, sericite and illite, and alunite and/or kaolinite. A series of video tutorials to assist in the use of the IAT and ASTER viewing tools are available on the site.

A number of products generated from the ASTER imagery are also available for downloading through the MapPlace. These include the original ASTER data, a 30 m resolution DEM (digital elevation model), a virtual reality world file, colour orthorectified anaglyph images and stereo pairs of digital images.

The new Google Earth viewer provides powerful viewing capabilities with the ability to incorporate external data. Several of the ASTER products, such as the near-natural colour image, anaglyph image and alteration-mineral images, have been incorporated into Google Earth files that are accessible through the MapPlace and provide an enhanced level of data viewing.

IMAGE ANALYSIS TOOLBOX ENHANCEMENTS

Image Preprocessing

New ASTER imagery was purchased as part of this project. Previously, ASTER imagery contained in the IAT included only those images that were available at no cost. ASTER imagery that in part covers the United States is available at no cost; imagery from all other locations is available for a handling fee of US$80 per image. The objective of this project was to obtain representative imagery from all parts of the province that could be of benefit in mineral exploration. The most recent, best quality images covering areas of interest to the mineral exploration community were selected (Fig. 1). Minimum cloud, smoke and snow cover were the primary quality factors. These conditions were usually found in images collected in late summer and early fall. If images of equal quality for a specific area were available then the most recent image was selected. Images with good ground exposure or including existing mining operations were selected initially. Imagery over the areas heavily affected by the mountain pine beetle infestations was also addressed in the hope of stimulating mineral exploration in these areas.

The ASTER images previously housed in the IAT and the new imagery were processed to bring them all to a new standard level of quality. The image data was orthorectified and atmospherically corrected. Orthorectification was per-

[1]*Geoscience BC contribution GBC005*

[2]*Cal Data Ltd., Kelowna, BC*

This publication is also available, free of charge, as colour digital files in Adobe Acrobat PDF format from the BC Ministry of Energy, Mines and Petroleum Resources internet website at http://www.em.gov.bc.ca/Mining/Geolsurv/Publications/catalog/

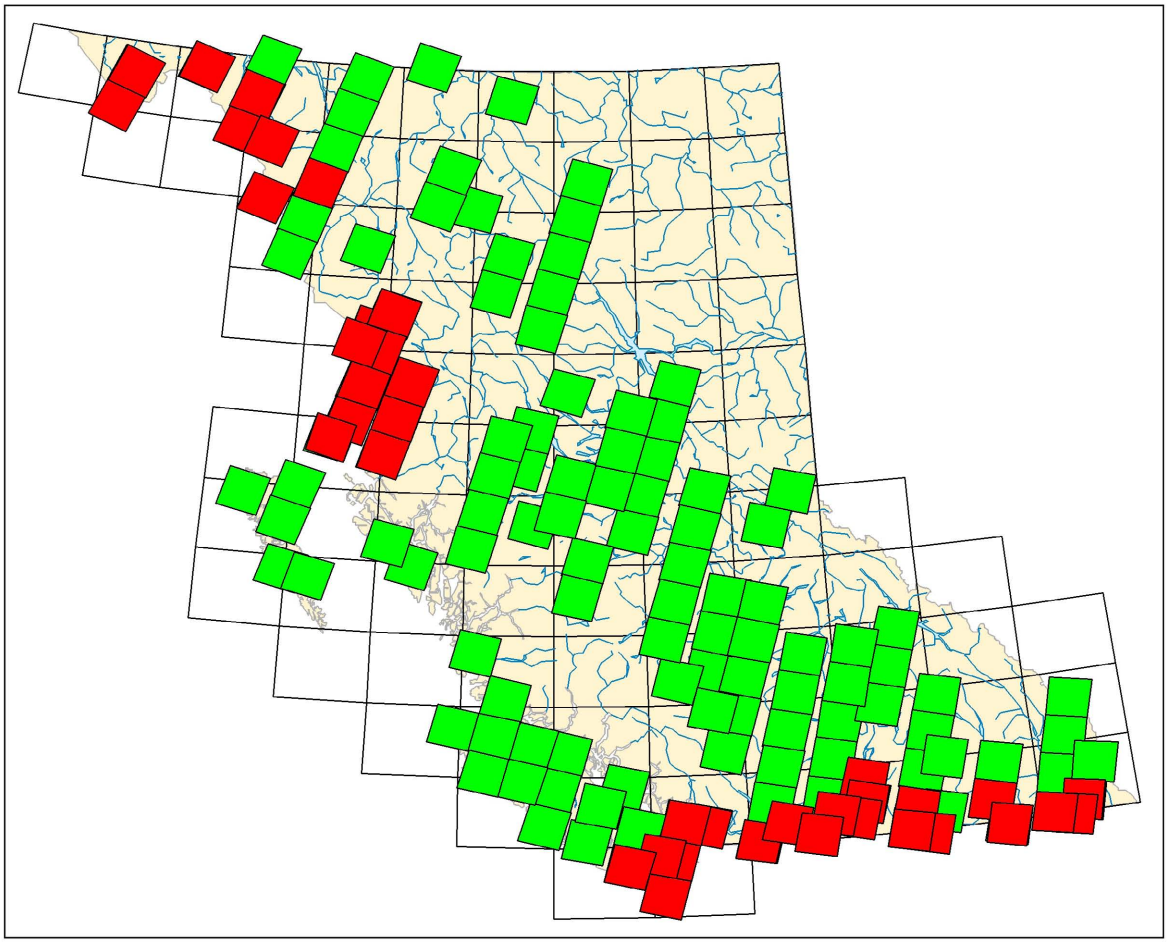


Figure 1. A display of ASTER image footprints; existing images are shown in red and the approximate locations of Geoscience BC project images are shown in green.

formed using the AsterDTM (SulSoft, 2005) add-on to the ENVI image analysis program (RSI, 2005). The orthorectified images were then manually adjusted to fit the TRIM (Terrain Resource Inventory and Mapping) 1:20 000 digital map data displayed on the MapPlace. This manual adjustment was necessary to compensate for some ASTER positioning errors: "Over the last 5 years, we have discovered several small errors that can affect the accuracy of these coordinates" (NASA Jet Propulsion Laboratory, 2005). For the purposes of this project, registration to the TRIM data provided the most appropriate adjustment.

Atmospheric corrections were performed on the VNIR and SWIR bands in all the images using the ACORN5 (Atmospheric CORrection Now) program (ImSpec, 2004). This program performs a radiance to relative reflectance correction of the image values by removing the effect of water vapour and other gases in the atmosphere using the MOTRAN4 technology. ACORN5 also corrects for atmospheric scattering as well as the shape of the solar irradiance curve that is variable by wavelength depending on solar incidence angle. ASTER imagery does not contain enough information to calculate the amount of water vapour found within an image so a standard value of 15 mm of atmospheric water was used for all images. Atmospheric water content obviously varies between ASTER scenes and within the scenes but the value of 15 mm was selected as representative after a review of the MODIS Atmosphere Profile Product record (NASA MODIS Atmosphere Discipline Group, 2005). Atmospheric correction enhances the digital information available to the IAT from simple DN (calibrated radiance) values to relative reflectance values that more accurately portray the true reflectance spectra of a ground sample area. The relative reflectance values allow comparison of the image pixel spectra with natural and man-made materials in existing reflectance spectral libraries, such as the ASTER spectral library available online (NASA, 2000).

A major problem with analyzing a large area, such as a whole ASTER image, is that many very different types of surfaces are included in the analysis, often making subtle differences in the spectra of a target area difficult to identify. A traditional method of overcoming this problem is to apply a mask that removes all but the area of interest from the calculation. Such a mask was calculated for each MapPlace image and is available in the IAT to constrain the area of the image being analyzed. The mask blacks out all areas covered by vegetation, clouds, water, snow and ice; hopefully, leaving only those pixels that sampled good ground exposures. A simple toggle button in the individual tool panels of the IAT allows the user to make use of the

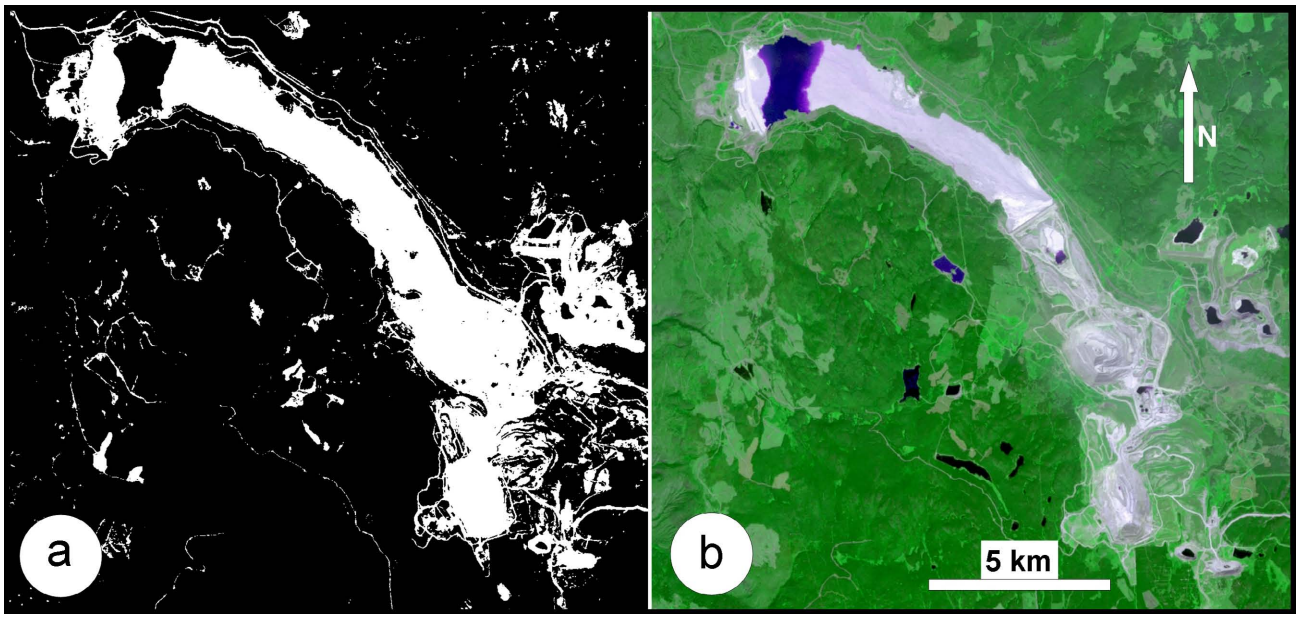


Figure 2. a) An enlarged portion of a mask and b) the corresponding coloured image. The white pixels in the mask overlay good ground exposures, such as the rock exposures in the mine, road-cuts, beaches around lakes and freshly logged areas. The mask effectively blacks out most vegetated areas and water bodies.

mask when desired. The available mask removes the vast majority of the pixels measuring nonrock surfaces but there are always some pixels which include a mixture of rock and nonrock materials (Fig. 2). The user should use caution when interpreting analysis results using this mask, a pixel of interest should be further investigated to confirm it does in fact represent a rock surface.

New IAT Options

The IAT basic functionality has been described previously (Kilby *et al.*, 2004; Kilby, 2005). The ASTER image data available to the analysis tools has been significantly improved and expanded – the major objective of this project. The major addition to ASTER analysis capability is the option for the user to include the image mask described above with several of the analysis tools.

Short video tutorials have been added to assist the first-time user though the operation of the analysis tools and also demonstrate the operation of several of the viewers that can be used to examine some of the ASTER products.

Four new selections have been added to the basic analysis tools, available when an ASTER image has been chosen for analysis. These four selections do not perform an analysis on the image but rather launch new displays related to the selected ASTER image. Figure 3 illustrates the new layout of the Image Analysis Tools panel when an ASTER image is selected for analysis in the IAT. The Anaglyph Map button will launch a new MapPlace map with the ASTER anaglyph image forming the main display. The Virtual Reality button will launch a low resolution virtual reality file of the ASTER scene draped over its DEM. If the user has a virtual reality viewer linked to their browser, it will be launched and the file immediately viewable. If no virtual reality viewer is linked then the user has the option to save the file for later viewing. The Google Earth button will launch the Google Earth package for the selected ASTER image on the client's computer, if they have Google Earth loaded. If they do not have Google Earth loaded, they have the option of saving the file for later viewing. The Download Page button launches a web page that provides access to all the downloadable products associated with the selected ASTER image.

Anaglyph Maps

A new product that is accessible through the IAT is a map display with an anaglyph ASTER image as its base. These maps are rotated so that the satellite flight line is hori-

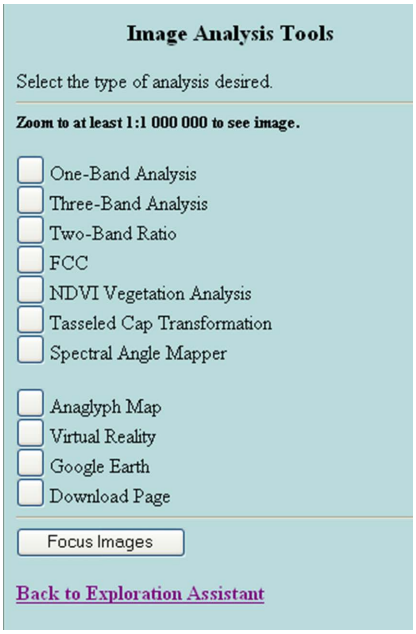


Figure 3. The ASTER Image Analysis Tools panel. The four new options are found at the bottom of the selection list.

zontal in the display, making map north to the right of the display. This aligns the viewer's eyes with the flight path and allows viewing of the image in 3-D. Anaglyph glasses are required to view the image. Glasses with red and cyan lenses are preferred but red and blue lenses will work reasonably as well. All available MapPlace layers can be overlain on these maps just as with any other MapPlace map. These images have been orthorectified and fit the existing TRIM base map data very well. Three-dimensional topographic surface views, such as these, provide an excellent tool for the interpretation of surficial and bedrock geological features.

Alteration-Mineral Images

Four alteration-mineral images have been prepared for each ASTER image and are available for viewing in the IAT. These images were produced using standard combinations of the ASTER bands. The four images can be used to map the relative abundance of siliceous rocks, iron oxides, sericite and illite, and alunite and/or kaolinite. The band combinations (J.A. Zamudio, pers comm, 2005) used to calculate each of these images are

- siliceous rocks – (B10+B11+B12)/3/(B13)
- sericite and illite – (B5+B7)/B6
- alunite and/or kaolinite – (B4+B6)/B5
- iron oxides – B2/B1

All of the alteration-mineral images were calculated using the appropriate mask as discussed above. Figure 4 contains examples of these images. It must be remembered that these images show only the results of the various band combinations given above. These ratios have been used to identify the relative abundance of the specific materials, but they may also indicate other substances. They must be used as a guide to the location of mineral substances just as with any remote sensing technique. These images are only one of many tools that can assist in defining target areas for more detailed analysis and must not be considered an absolute indicator of the target material.

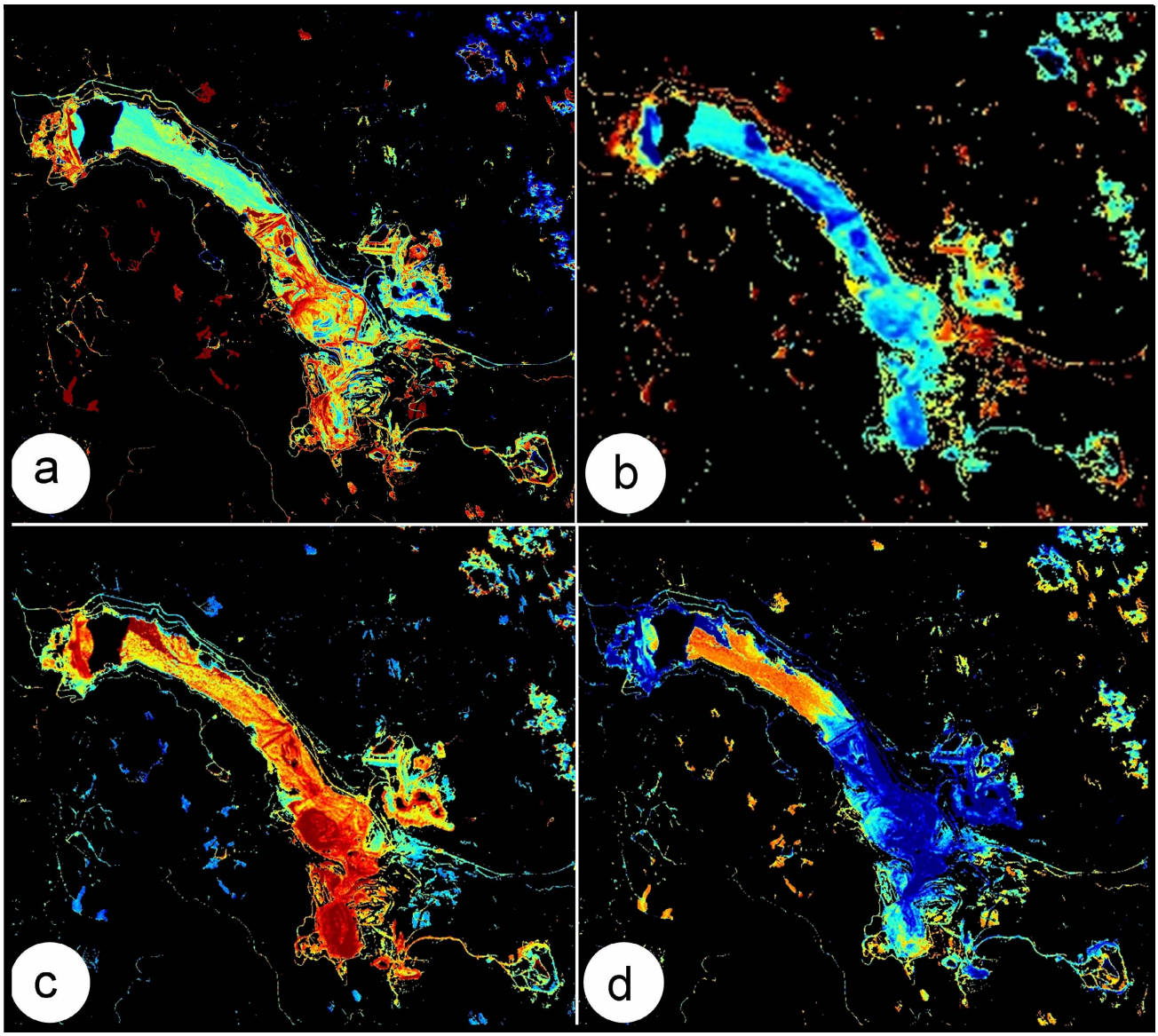


Figure 4. Alteration-mineral images from Highland Valley mine area; a) iron oxides, b) siliceous rocks, c) sericite and illite and d) alunite and/or kaolinite. The range of low to high values is shown as a range of cool to warm colours.

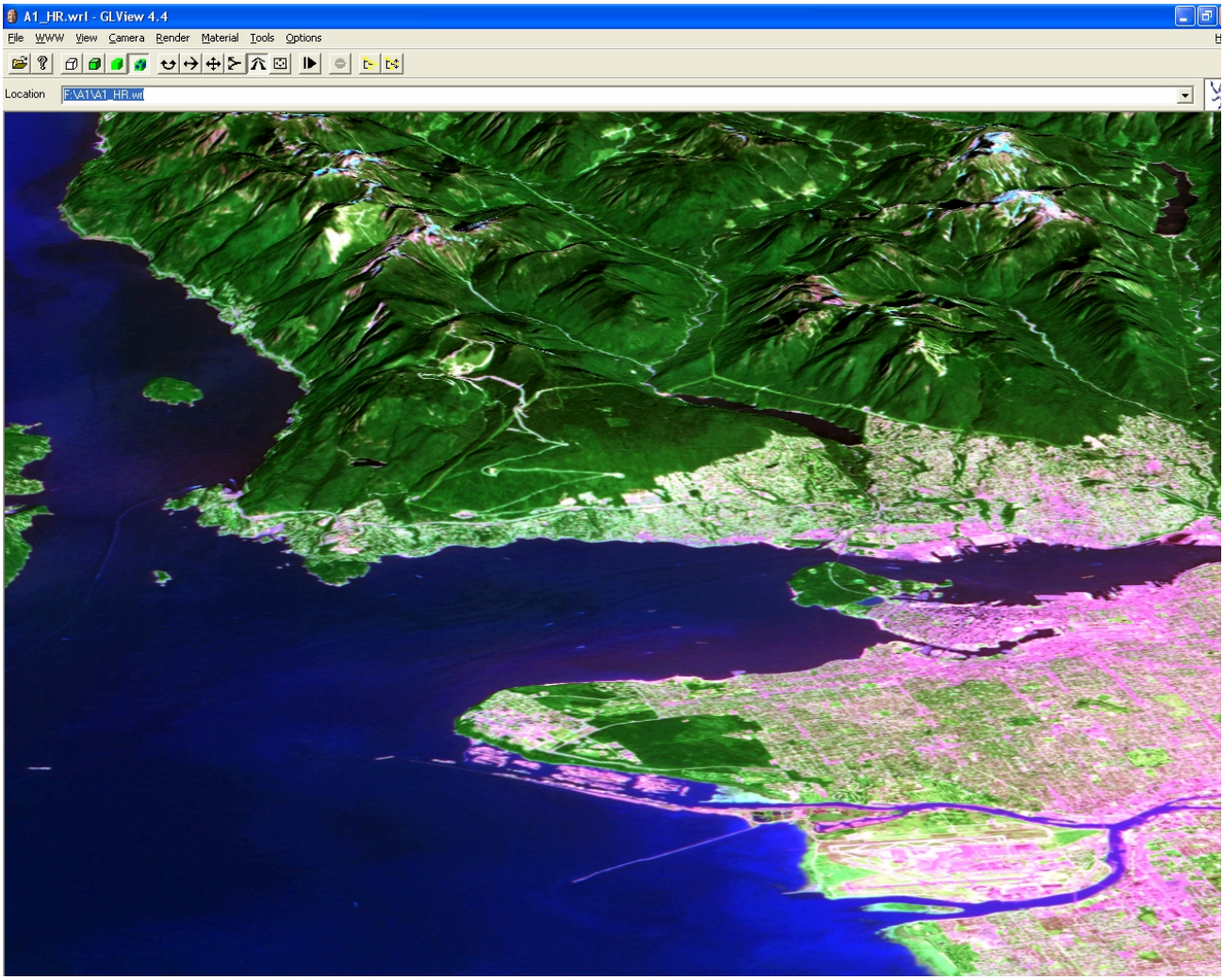


Figure 5. An example of a virtual reality viewer (GL View) with a view of ASTER image A1 (Vancouver area).

Virtual Reality

Virtual reality files (WRL format) have been produced for each image by draping the near-natural colour image over the DEM generated during the orthorectification process. When viewed with the appropriate viewing software, these files allow the user to fly through the terrain, generate perspective views and even incorporate new flight paths and viewpoints. Similar functions are available through the Google Earth products discussed below but the virtual reality files provided here are available on a much more detailed topographic base than presently available through Google Earth. The files have been prepared in two resolutions; the high resolution version is available through the download option while the low resolution version is available by direct link from the IAT map. There are a number of free virtual reality viewers available over the internet. One that works very well with these files is the GL View viewer available at http://www.snafu.de/hg (Fig. 5). The low resolution product has a DEM spacing of about 1.3 km and an image resolution of one pixel every 75 m. The high resolution product has a DEM spacing of about 160 m and an image resolution of one pixel every 15 m.

DOWNLOAD PRODUCTS

A number of products generated during this project are available for download. These products include the original ASTER imagery and a number of products generated from the imagery. The ASTER Download Page provides access to these products and is available by clicking on the Download Page button in the ASTER IAT panel.

Original ASTER Image Data

The ASTER image data, in its original format, can be downloaded for free by the user. The two original files associated with each image have been zipped together for convenience of handling but are otherwise in the original XML and HDF formats. As discussed above, images that do not include part of the United States were purchased at a cost of US$80 per image. This is a direct savings to any user wanting this data. A search of the internet will return a large number of free and high-end programs capable of manipulating this image format.

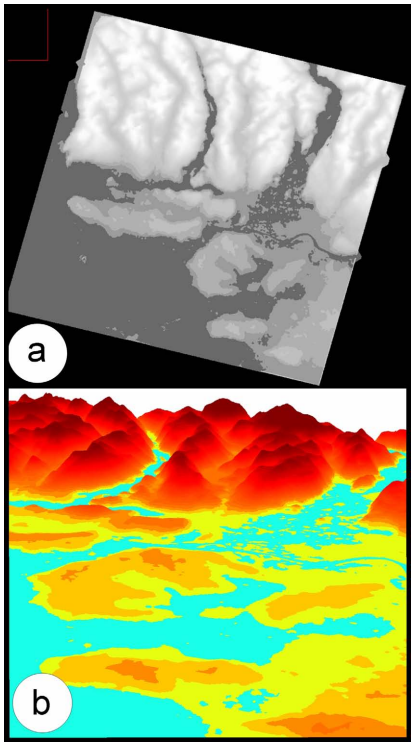


Figure 6. Two views of a DEM: a) a grey-scale map view of the dataset and b) a coloured perspective view of the same dataset.

DEM

During the orthorectification process a relative digital elevation model was constructed. This model is available for download. The model resolution is 30 m. Unlike many DEM where the grid points are interpolated from widely spaced data points, this model was generated by a calculation based on the Band 3N (Nadir) and Band 3B (back-looking) images at each grid point. The DEM is relative and has not been corrected to true elevations. A correction could be applied by the user if desired but for most applications the relative model is adequate (Fig. 6). Many of the ASTER images contain some cloud cover and the elevation of the cloud tops is what is recorded in the DEM rather than the ground elevation. Also in some images certain pixels in Band 3N or Band 3B were saturated and resulted in no elevation calculation being possible. These appear as holes in the DEM. This problem usually occurs over very large bright objects, such as glaciers. The DEM is provided in a standard DEM format, USGS DEM, which can be read by a large number of free and widely available software packages.

Virtual Reality File

The high resolution virtual reality file is only available through the download page. This product, discussed above, is too large for direct linking from a map but may be downloaded by the client and manipulated with a virtual reality viewer on the user's desktop (Fig. 5).

Stereo Pairs

Stereo pair images of the whole ASTER scene are available for download in JPEG format. These images have a 15 m resolution and when viewed with a standard stereoscope provide a 3-D view of the image scene. The files can be printed as whole images or subregions of the images may be enlarged to provide more detailed viewing. The Nadir image (vertically down-looking) has been orthorectified while the back-looking image has been left in its original state. This configuration provides stereo viewing of an orthorectified image. The Nadir image is in UTM projection (Fig. 7).

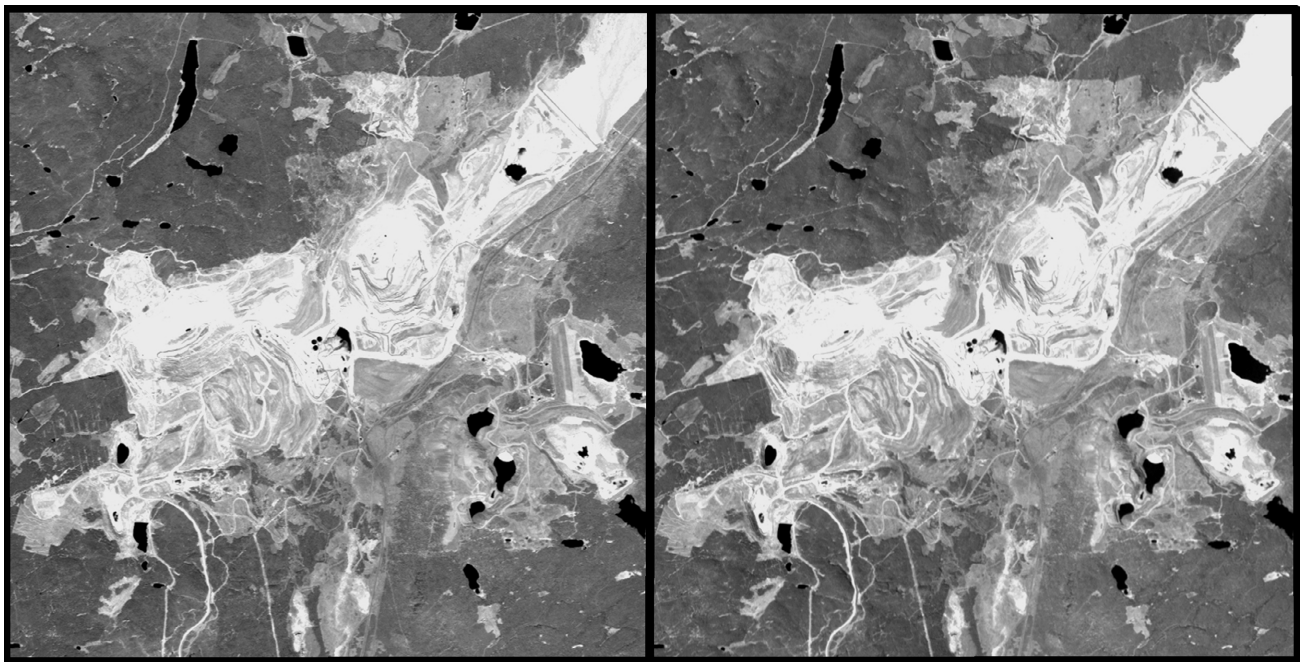


Figure 7. An example of stereo pair images from an enlarged section of the downloadable stereo pairs product. This view is of the open pits at the Highland Valley operation.

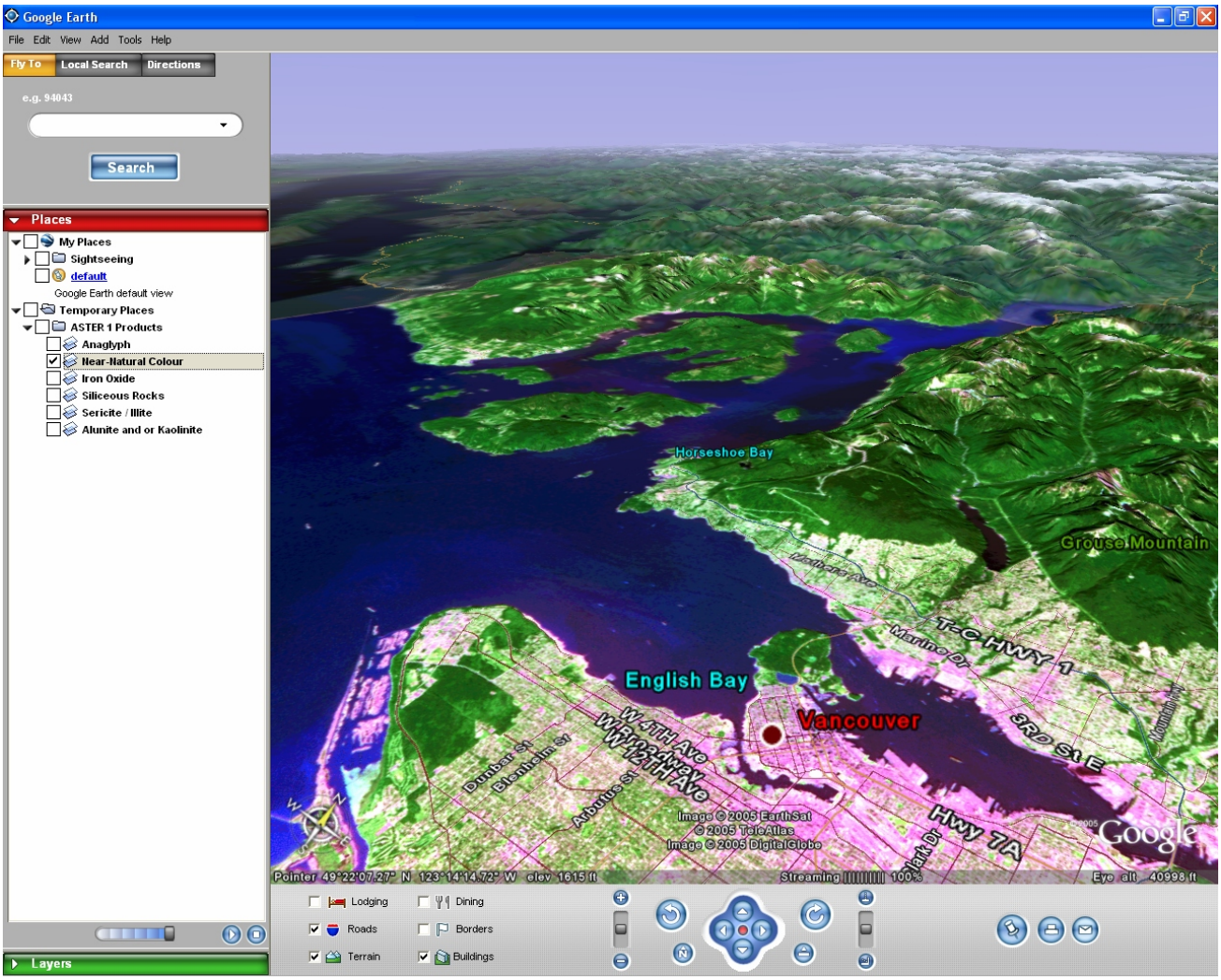


Figure 8. Google Earth viewer with Google Earth ASTER product for the Vancouver area. The near-natural colour image is displayed in this example.

GOOGLE EARTH PRODUCT

On June 28, 2005, the Google Earth viewer became publicly available. This free viewer provides a significant advancement in viewing geospatial information over the internet. The convenience and power of this viewer warranted its inclusion in the product mix provided by this project. A Google Earth display is available for each ASTER image (Fig. 8). Each display includes

- a near-natural colour image;
- an anaglyph image;
- a siliceous rock image;
- a sericite and illite image;
- an alunite and/or kaolinite image;
- an iron oxides image; and
- other imagery and spatial data available from Google Earth.

The Google Earth viewer allows the user to turn the various images off and on and adjust the opacity of a selected image. Double clicking on the anaglyph image name in the legend will cause the Google Earth viewer to rotate and zoom to the optimal position to view that anaglyph image (anaglyph glasses required). The Google Earth displays can be accessed by clicking on the Google Earth button of the ASTER IAT panel (Fig. 3). Unfortunately, use of Google Earth requires a relatively fast internet connection and computer so this product may not be readily useable by all site users. All ASTER-related information provided in the Google Earth format is also available through MapPlace map displays.

SUMMARY

ASTER imagery for a significant portion of British Columbia is now available for online analysis and downloading. The IAT provides the opportunity to remotely examine exposed ground surfaces for the presence of alteration minerals that may be associated with a variety of deposit types. Examination of vegetation variations may provide useful indications of underlying geology. Derivative products generated during this project provide a variety of 3-D visualization options. The 3-D visualizations provide powerful tools for examining and displaying ideas

about geology, exploration concepts and project planning. The site can also be used to help advance the understanding of the geology and mineral industry of British Columbia by the general public.

ACKNOWLEDGMENTS

This project was made possible by a grant from Geoscience BC. The BC Ministry of Energy, Mines and Petroleum Resources provided support in the form of internet hosting of the project products on the MapPlace website.

The authors would like to thank Joe Zamudio for his thorough review of this paper and useful suggestions regarding multispectral analysis.

REFERENCES

Google (2005): Google Earth, global Internet viewer of imagery and vector information; *Google*, URL <earth.google.com> [Oct 2005].

ImSpec (2004): ACORN5, atmospheric correction software package, Ver. 040801; *ImSpec*, URL <www.imspec.com> [Oct 2005].

Kilby, W.E., Kliparchuk, K. and McIntosh, A. (2004): Image analysis toolbox and enhanced satellite imagery integrated into the MapPlace; *in* Geological Fieldwork 2003, *BC Ministry of Energy, Mines and Petroleum Resources*, Paper 2004-1, pages 209-215.

Kilby, W.E. (2005): MapPlace.ca image analysis toolbox – phase 2; *in* Geological Fieldwork 2004, *BC Ministry of Energy, Mines and Petroleum Resources*, Paper 2005-1, pages 231-235.

NASA Jet Propulsion Laboratory (2000): ASTER spectral library, online spectral library; *NASA*, URL <speclib.jpl.nasa.gov/Search.htm> [May 2000].

NASA Jet Propulsion Laboratory (2005): Lat/long adjustment tool, ASTER spatial location correction service access page; *NASA*, URL <asterweb.jpl.nasa.gov/latlon.asp> [Oct 2005].

NASA MODIS Atmosphere Discipline Group (2005): Daily atmospheric water vapour mean display, online display of daily MODIS derivative product images; *NASA*, URL <modis-atmos.gsfc.nasa.gov/index.html> [Aug 2005].

RSI (2005): ENVI, image analysis software package, Ver 4.2; *RSI*, URL <www.rsinc.com/envi> [Oct 2005].

SulSoft (2005): AsterDTM, ASTER orthorectification software, Ver 2.2; *SulSoft*, URL <www.envi.com.br/asterdtm> [Oct 2005].

Drainage Sediment and Water Geochemical Surveys in the Anahim Lake and Nechako River Map Areas (NTS 093C and F), Central British Columbia[1]

By W. Jackaman[2]

KEYWORDS: Nechako Plateau, Fraser Plateau, mineral exploration, geochemistry, multielement, lake sediment, lake water, epithermal, gold, molybdenum, copper, porphyry deposit

INTRODUCTION

During the 2005 field season, Geoscience BC funded two reconnaissance-scale drainage sediment and water surveys that were successfully completed in previously unsurveyed regions of central British Columbia (Fig. 1). These surveys are part of an ongoing effort to complete first-level geochemical coverage of the province and provide the mining and exploration community with new, high-quality geochemical information. The program will help to,

- outline regional geochemical trends,
- identify new exploration targets, and
- profile previously explored mineral properties.

Each component of the work is being conducted according to National Geochemical Reconnaissance (NGR) and BC Regional Geochemical Survey (RGS) program standards and specifications. Resulting digital data will fit seamlessly into current NGR and RGS databases, as well as complement other geoscience information available for the region.

Regional geochemical surveys have been carried out in BC since 1976. A total of 45 1:250 000-scale NTS map sheets and numerous detailed studies have been published to date, covering approximately 500 000 km^2 of the province. Analytical results and field observations contribute to the building of a national geochemical database for resource assessment, mineral exploration, geological mapping and environmental studies. Sample collection, preparation procedures and analytical methods are strictly specified and carefully monitored to ensure consistent and reliable results regardless of the area, the year of collection or the laboratory undertaking the analyses.

SURVEY AREA DESCRIPTION

The Anahim Lake (NTS 093C) and Nechako River (NTS 093F) map sheets are situated in the Nechako Basin

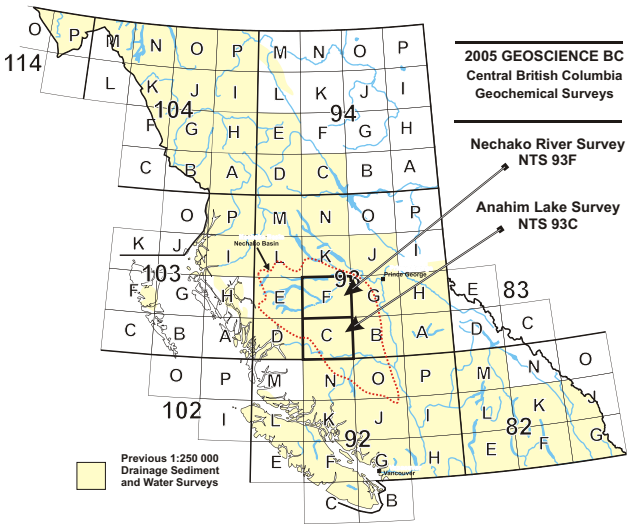


Figure 1. Location of Anahim Lake and Nechako River drainage sediment and water geochemical survey areas, central BC.

of central BC, in a region of low relief characterized by large expanses of flat and gently rolling landscape (Holland, 1976). The surface of the Nechako and Fraser plateaus is generally between 1200 and 1500 m in elevation and comprises a wide variety of physiographic environments, ranging from rocky subalpine peaks to boggy lowlands. To the north, the Fawnie and Nechako ranges break up the plateau landscape, and the Ilgachuz and Itcha ranges interrupt the Fraser Plateau. In the southwest corner, the rugged Coast Mountain Range extends into the study area. The plateaus are mostly forested with subboreal spruce and pine, and are generously dotted with small to medium-sized lakes, as well as extensive wetland systems. Throughout the region, the northern pine beetle kill has significantly impacted extensive areas of forest cover.

The Nechako Basin is a postaccretionary basin bounded to the north by the Skeena arch, to the west and south by the Cost Plutonic Complex and to the east by the Cache Creek Group (Fig. 2). The area is covered by extensive mafic to felsic volcanic flows of Tertiary to recent age, and much of the region is covered with thick glacial drift that has left very little exposed bedrock. Underlying these deposits are Middle Jurassic to Tertiary marine and nonmarine sedimentary rocks and lesser volcanic rocks.

Less than one hundred mineral occurrences (Fig. 2) are currently listed in the provincial mineral inventory database (MINFILE, 2005). Several of the more important deposits include epithermal Au-Ag occurrences. These include Wolf (093F 045) and Oboy (093C 015), hosted by Ootsa Lake Group felsic volcanic rocks, and the 3Ts devel-

[1] *Geoscience BC contribution GBC006*

[2] *Consultant, Sooke, BC*

This publication is also available, free of charge, as colour digital files in Adobe Acrobat PDF format from the BC Ministry of Energy, Mines and Petroleum Resources internet website at http://www.em.gov.bc.ca/Mining/Geolsurv/Publications/catalog/catfldwk.htm

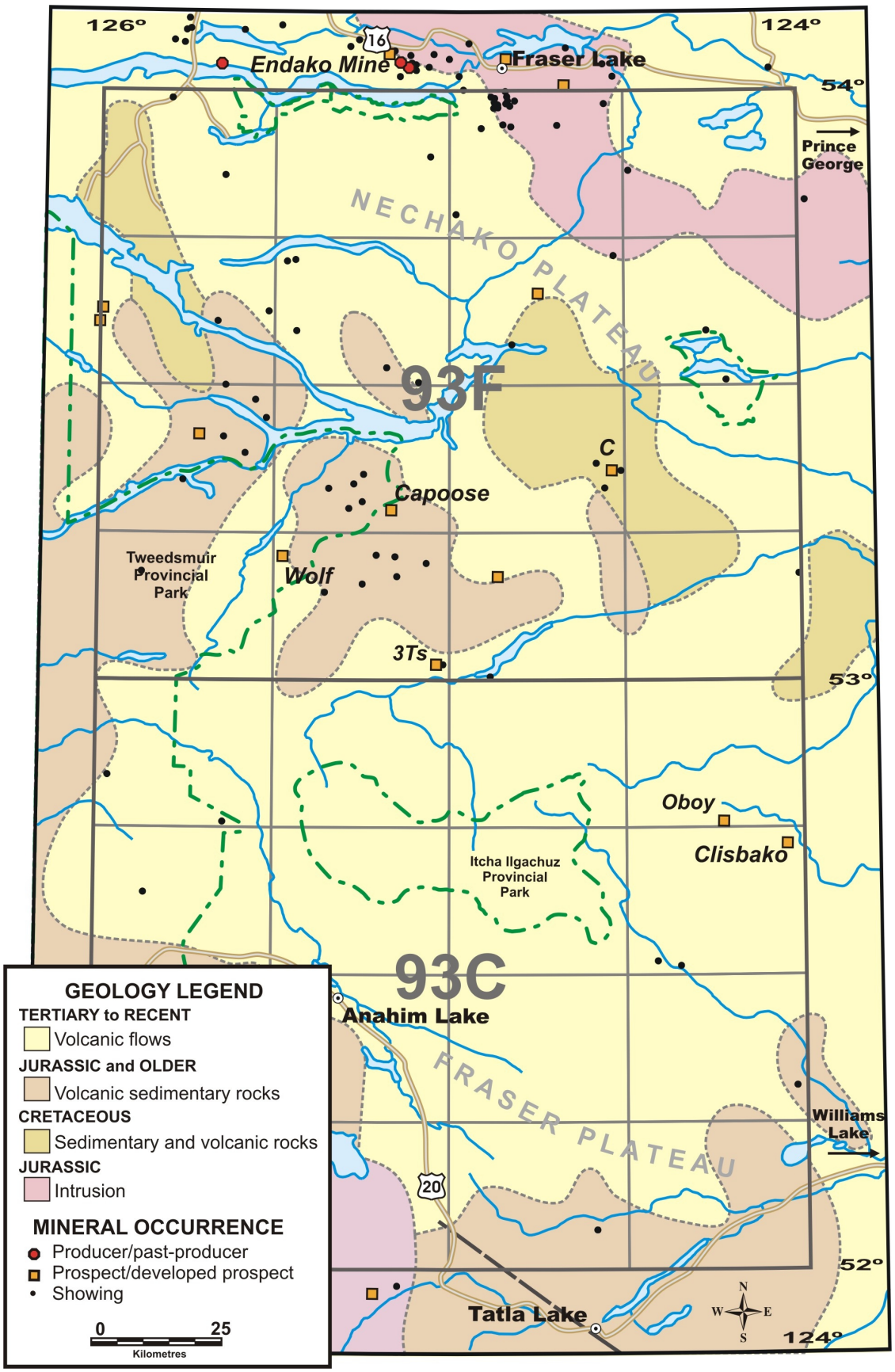


Figure 2. Simplified geological setting of the Anahim Lake and Nechako River survey areas, with MINFILE locations.

oped prospect (Tsacha [093F055], Taken [093F055] and Tam claims), occurring in Hazelton Group intermediate volcanic rocks. Also important are Mo and Cu porphyry occurrences associated with Tertiary intrusions (*e.g.*, C, 093F 004) and porphyry-related precious and base metal mineralization (*e.g.*, Capoose, 093F 040), hosted by Hazelton Group intermediate volcanic rocks associated with cross-cutting rhyolitic dikes of Cretaceous age.

PREVIOUS GEOCHEMICAL WORK

Although the region offers a favourable environment for new mineral discoveries, extensive glacial drift, poor bedrock exposure and an unproductive volcanic cover have previously hampered much of the exploration activity. In addition, a collection of comprehensive geochemical information for the Nechako and Fraser plateaus has only been developed relatively recently, starting in 1993 as part of the Interior Plateau Project (Diakow, 1997) and, more recently, the Nechako NATMAP Project (Struik *et al*., 2001). Included in these activities were a number of orientation and case studies, summarized by Cook (1997), that outline the importance of lake sediments as an effective exploration tool in the Interior Plateau region. Levson and Giles (1997) and Dunn (1997) highlighted the use of till geochemistry and biogeochemistry within the Interior Plateau. In addition, Cook and Dunn (2006) are conducting further studies dealing with property-scale surficial geochemistry.

In the Nechako Plateau, two lake sediment and water geochemistry surveys (Cook and Jackaman, 1994) were completed in the Fawnie Range and Ootsa Lake areas (Fig. 3), and several till geochemistry surveys were conducted in parts of the southern Nechako Plateau (Levson *et al*., 1994; Weary *et al*., 1997; Levson *et al*., 2001). Biogeochemical surveys have been completed in parts of the Nechako Plateau (Dunn and Hastings, 1998a, b, c, d; Dunn and Hastings, 2000a, b, c, d) and in the Clisbako area of the Fraser Plateau (Dunn, 1997). The 2005 survey areas are also completely surrounded by previous NGR and RGS reconnaissance-scale stream sediment and water geochemistry programs. A list of publicly available geochemistry data for the region has been provided in Table 1.

SURVEY METHODS AND SPECIFICATIONS

Methods and specifications are based on standard lake sediment geochemical survey strategies used elsewhere in Canada for the NGR program (Friske, 1991), as well as prior orientation studies and regional lake sediment surveys completed in BC (Cook, 1997).

Sample Collection

Helicopter-supported sample collection was carried out from July to September 2005, during which 2070 drainage sediment and water samples were systematically collected from 1957 sites (Fig. 4). Within the low-lying areas, lake sediment and water were collected from 1855 sites. In the Anahim Lake map sheet, stream sediment material was collected from 102 sites in areas of greater relief near Mount Dent and Charlotte Lake. The surveys covered a total area of 19 500 km^2 and the average sample site density was 1 site per 9.9 km^2. Field duplicate sediment and water samples were routinely collected in each analytical block of twenty samples.

Lake sites were accessed using a float-equipped Bell Jet Ranger helicopter. The sampling crews collected sediment material with a torpedo style sampler, and water samples were saved in 250 mL bottles. Samples were successfully collected from most of the lakes located in the survey area. However, some of the smaller ponds were not sampled due to poor landing conditions, and samples were not collected from several very large and deep lakes. Lake bottom material typically consisted of organic gels with varying amounts of organic matter. Field observations and site locations were manually and digitally recorded for each site.

Sample Analysis

After drying, each sample was pulverized to approximately –150 mesh (100 μm) in a ceramic ring mill, and two analytical splits (5 g and 30 g) were extracted from the material. To monitor and assess accuracy and precision of analytical results, control reference material and analytical duplicate samples were routinely inserted into each block of twenty sediment samples. The sediment samples were analyzed for base and precious metals, pathfinder elements and rare earths by instrumental neutron activation analysis (INAA) and inductively coupled plasma – mass spectrometry (ICP-MS). Loss-on-ignition and fluorine were also determined for sediment material, and fluoride, conductivity and pH were determined for the water samples. A complete list of elements and analytical detection limits is provided in Tables 2 and 3.

TABLE 1. PREVIOUS GEOCHEMICAL SURVEYS CONDUCTED IN THE ANAHIM LAKE AND NECHAKO RIVER AREAS

Survey Type	Survey Date	NTS Map Sheets	Survey Name	Reference
Till geochemistry	1994	93F/03	Fawnie Creek	Levson *et al*., 1994
Till geochemistry	1997	93F/07	Chedakuz Creek	Weary *et al*., 1997
Till geochemistry	2001	93F/05, 12	Tetachuk Creek and Marilla	Levson *et al*., 2001
Lake sediment and water geochemistry	1994	93F/02, 03	Fawnie Range	Cook and Jackaman, 1994
Lake sediment and water geochemistry	1994	93F/06, 11, 12, 13, 14	Ootsa Lake	Cook and Jackaman, 1994
Biogeochemistry	1996	93C/09	Clisbako	Dunn, 1997
Biogeochemistry	1998	93F/03, 05, 07, 12	Ootsa-Francois Lakes	Dunn and Hastings, 1998
Biogeochemistry	2000	93F/12, 13, 14	Nechako River	Dunn and Hastings, 2000

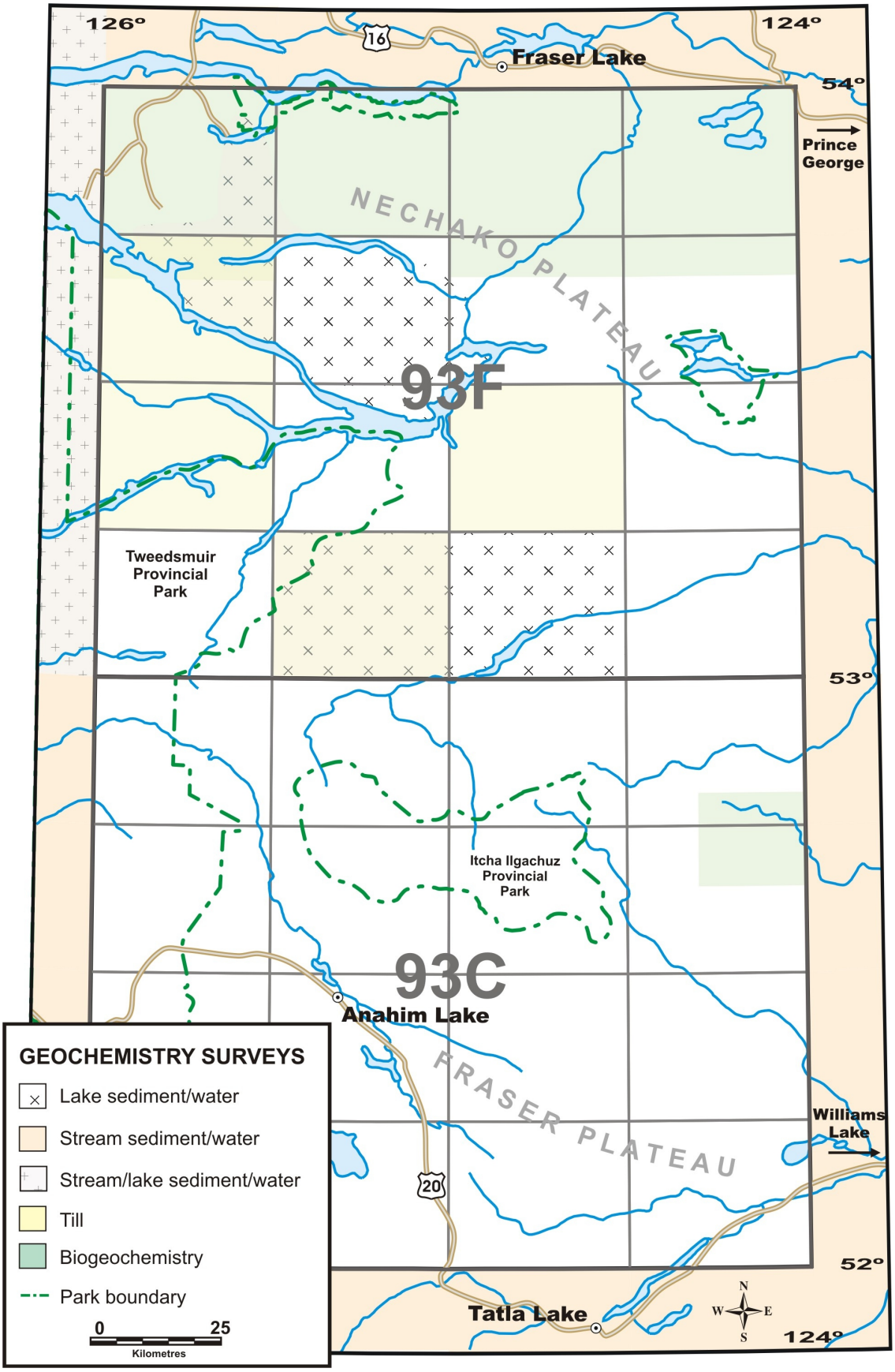


Figure 3. Location of previous geochemical surveys in the Anahim Lake and Nechako River areas.

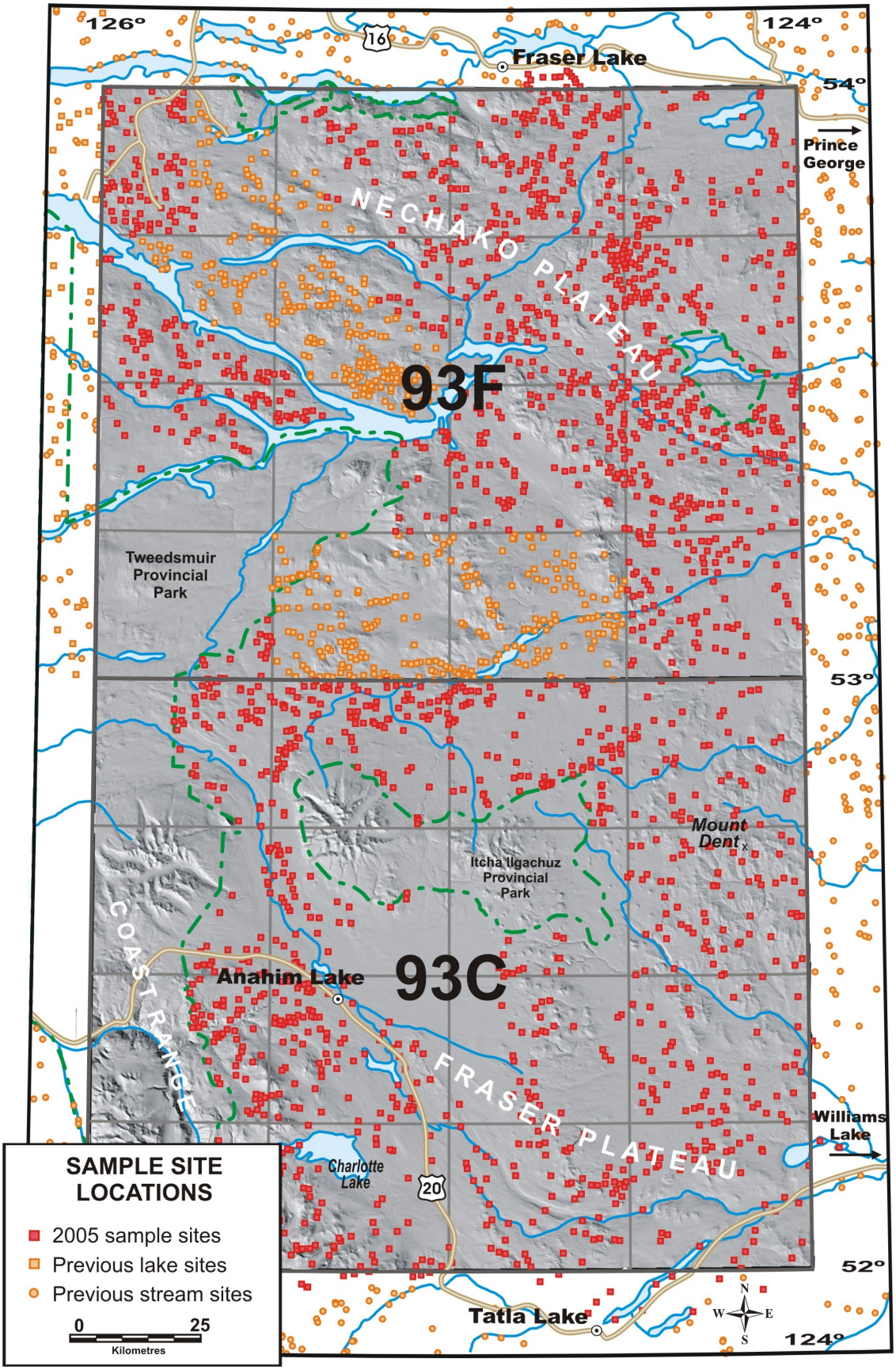


Figure 4. Location of sample sites, Anahim Lake and Nechako River survey areas.

TABLE 2. DETECTION LIMITS FOR SEDIMENT SAMPLES ANALYZED BY INDUCTIVELY COUPLED PLASMA – MASS SPECTROMETRY (ICP-MS)

Element		Detection Limit	Units
Aluminum	Al	0.01	%
Antimony	Sb	0.02	ppm
Arsenic	As	0.1	ppm
Barium	Ba	0.5	ppm
Bismuth	Bi	0.02	ppm
Cadmium	Cd	0.01	ppm
Calcium	Ca	0.01	%
Chromium	Cr	0.5	ppm
Cobalt	Co	0.1	ppm
Copper	Cu	0.01	ppm
Gallium	Ga	0.2	ppm
Iron	Fe	0.01	%
Lanthanum	La	0.5	ppm
Lead	Pb	0.01	ppm
Magnesium	Mg	0.01	%
Manganese	Mn	1	ppm
Mercury	Hg	5	ppb
Molybdenum	Mo	0.01	ppm
Nickel	Ni	0.1	ppm
Phosphorus	P	0.001	%
Potassium	K	0.01	%
Scandium	Sc	0.1	ppm
Selenium	Se	0.1	ppm
Silver	Ag	2	ppb
Sodium	Na	0.001	%
Strontium	Sr	0.5	ppm
Sulphur	S	0.02	%
Tellurium	Te	0.02	ppm
Thallium	Tl	0.02	ppm
Thorium	Th	0.1	ppm
Titanium	Ti	0.001	%
Tungsten	W	0.1	ppm
Uranium	U	0.1	ppm
Vanadium	V	2	ppm
Zinc	Zn	0.1	ppm

TABLE 3. DETECTION LIMITS FOR SEDIMENT SAMPLES ANALYZED BY INSTRUMENTAL NEUTRON ACTIVATION ANALYSIS (INAA), LOSS-ON-IGNITION (LOI) AND F, AND FOR FLUORIDE, CONDUCTIVITY AND PH OF WATER SAMPLES

Element		Detection Limit	Units
Antimony	Sb	0.1	ppm
Arsenic	As	0.5	ppm
Barium	Ba	50	ppm
Bromine	Br	0.5	ppm
Cerium	Ce	5	ppm
Cesium	Cs	0.5	ppm
Chromium	Cr	20	ppm
Cobalt	Co	5	ppm
Europium	Eu	1	ppm
Gold	Au	2	ppb
Hafnium	Hf	1	ppm
Iron	Fe	0.2	%
Lanthanum	La	2	ppm
Lutetium	Lu	0.2	ppm
Rubidium	Rb	5	ppm
Samarium	Sm	0.1	ppm
Scandium	Sc	0.2	ppm
Sodium	Na	0.02	%
Tantalum	Ta	0.5	ppm
Terbium	Tb	0.5	ppm
Thorium	Th	0.2	ppm
Tungsten	W	1	ppm
Uranium	U	0.2	ppm
Ytterbium	Yb	2	ppm
Sample weight	Wt	0.01	gm
Fluorine	F	10	ppm
Loss-on-ignition	LOI	0.1	%
pH	pH		
Conductivity	CND	0.01	µS

RELEASE DETAILS

Reconnaissance-scale drainage sediment and water surveys are widely recognized as one of the most important reconnaissance exploration tools in the Canadian Cordillera. To date, more than 70% of BC has been surveyed. These high-quality grassroots data are directly responsible for follow-up mineral exploration that is valued in the millions of dollars and has been credited with the discovery of numerous mineral prospects. Survey results from the 2005 programs will provide the exploration community access to new geochemical information for underexplored areas of high mineral potential and will help stimulate mineral exploration.

Final survey results will be compiled into an NGR-RGS – style data package that will include survey descriptions and details regarding methods; analytical and field-data listings; summary statistics; and sample location maps and maps for individual elements. In addition, existing lake sediment results from previous surveys conducted in the study area will be incorporated into the final data package. The publications will be released on a CD as PDF files and will include all raw digital data files used in the production process. The data package is scheduled for release by March 31, 2006.

ACKNOWLEDGMENTS

Companies that contributed to the successful completion of the 2005 field program include Far West Helicopters (Chilliwack), White Saddle Air Services (Bluff Lake) and McElhanney Consulting Services (Vancouver). R. Lett and T. Höy are thanked for their editorial comments and suggestions

REFERENCES

Cook, S.J. (1997): Regional and property-scale application of lake sediment geochemistry in the search for buried mineral deposits in the southern Nechako Plateau area, British Columbia; *in* Interior Plateau Geoscience Project: Summary of

Geological, Geochemical and Geophysical Studies, Diakow, L.J. and Newell, J.M., Editors, *Geological Survey of Canada*, Open File 3448 and *BC Ministry of Energy, Mines and Petroleum Resources*, Paper 1997-2, pages 175–203.

Cook, S.J. and Dunn, C.E. (2006): Preliminary results of the Cordilleran Geochemistry Project: a comparative assessment of soil geochemical methods for detecting buried mineral deposits, 3Ts Au-Ag prospect (NTS 093F/03), central British Columbia; *in* Geological Fieldwork 2005, *BC Ministry of Energy, Mines and Petroleum Resources*, Paper 2006-1 and *Geoscience BC*, Report 2006-1.

Cook, S.J. and Jackaman, W. (1994): Regional lake sediment and water geochemistry of part of the Nechako River map area (93F/2,3; parts of 93F/6, 11, 12, 13, 14); *BC Ministry of Energy, Mines and Petroleum Resources*, Open File 1994-19.

Diakow, L.J. (1997): Introduction; *in* Interior Plateau Geoscience Project: summary of geological, geochemical and geophysical studies, Diakow, L.J. and Newell, J.M., Editors, *Geological Survey of Canada*, Open File 3448 and *BC Ministry of Energy, Mines and Petroleum Resources*, Paper 1997-2, pages 1–3.

Dunn, C.E. (1997): Biogeochemical surveys in the Interior Plateau of British Columbia; in Interior Plateau Geoscience Project: Summary of Geological, Geochemical and Geophysical Studies, Diakow, L.J. and Newell, J.M., Editors, *Geological Survey of Canada*, Open File 3448 and *BC Ministry of Energy, Mines and Petroleum Resources*, Paper 1997-2, pages 205–218.

Dunn, C.E. and Hastings, N.L. (1998a): Biogeochemical survey of the Ootsa-Francois Lakes area using outer bark of lodgepole pine (NTS 93F 13/14 and part of 12, north-central British Columbia): base metals and pathfinder elements; *Geological Survey of Canada*, Open File 3587a (1 sheet of coloured maps).

Dunn, C.E. and Hastings, N.L. (1998b): Biogeochemical survey of the Ootsa-Francois Lakes area using outer bark of lodgepole pine (NTS 93F 13/14 and part of 12, north-central British Columbia): mafic suite of elements with thorium and lanthanum; *Geological Survey of Canada*, Open File 3587b (1 sheet of coloured maps).

Dunn, C.E., and Hastings, N.L. (1998c): Biogeochemical survey of the Ootsa-Francois Lakes area using outer bark of lodgepole pine (NTS 93F 13/14 and part of 12, north-central British Columbia): alkali metals, alkaline earths, manganese and aluminum; *Geological Survey of Canada*, Open File 3587c (1 sheet of coloured maps).

Dunn, C.E. and Hastings, N.L. (1998d): Biogeochemical survey of the Ootsa-Francois Lakes area using outer bark of lodgepole pine (NTS 93F 13/14 and part of 12, north-central British Columbia): digital data listings and summary notes; *Geological Survey of Canada*, Open File 3587d.

Dunn, C.E. and Hastings, N.L. (2000a): Biogeochemical survey of the Nechako River area using outer bark of lodgepole pine (NTS 93F/15, 16 and parts of 9 and 10): base metals, silver and pathfinder elements; *Geological Survey of Canada*, Open File 3594a (1 sheet of coloured maps).

Dunn, C.E. and Hastings, N.L. (2000b): Biogeochemical survey of the Nechako River area using outer bark of lodgepole pine (NTS 93F/15, 16 and parts of 9 and 10): mafic suite of elements with thorium and lanthanum; *Geological Survey of Canada*, Open File 3594b (1 sheet of coloured maps).

Dunn, C.E. and Hastings, N.L. (2000c): Biogeochemical survey of the Nechako River area using outer bark of lodgepole pine (NTS 93F/15, 16 and parts of 9 and 10): alkali metals, alkaline earths, manganese and aluminum; *Geological Survey of Canada*, Open File 3594c (1 sheet of coloured maps).

Dunn, C.E. and Hastings, N.L. (2000d): Biogeochemical survey of the Nechako River area using outer bark of lodgepole pine (NTS 93F/15, 16 and parts of 9 and 10): digital data listings and summary notes; *Geological Survey of Canada*, Open File 3594d.

Friske, P.W.B. (1991): The application of lake sediment geochemistry in mineral exploration; *in* Exploration Geochemistry Workshop; *Geological Survey of Canada*, Open File 2390, pages 4.1–4.20.

Holland, S.S. (1976): Landforms of British Columbia — a physiographic outline; *BC Ministry of Energy, Mines and Petroleum Resources*, Bulletin 48.

Levson, V.M. and Giles, T.R. (1997): Quaternary geology and till geochemistry studies in the Nechako and Fraser Plateaus, central British Columbia (NTS 93C/1, 8, 9, 10; F/2, 3, 7; L/16; M/1); *in* Interior Plateau Geoscience Project: Summary Of Geological, Geochemical And Geophysical Studies, Diakow, L.J. and Newell, J.M., Editors, *Geological Survey of Canada*, Open File 3448 and *BC Ministry of Energy, Mines and Petroleum Resources*, Paper 1997-2, pages 121–147.

Levson, V.M., Giles, T.R., Cook, S.J. and Jackaman, W. (1994): Till geochemistry of the Fawnie Creek area (93F/03); *BC Ministry of Energy, Mines and Petroleum Resources*, Open File 1994-18.

Levson, V.M., Mate, D., Stumpf, A.J. and Stewart, A. (2001): Till geochemistry of the Tetachuck Lake and Marilla map areas (NTS 93 F/5 and F/12); *BC Ministry of Energy, Mines and Petroleum Resources*, Open File 2001-15.

MINFILE (2005): MINFILE BC mineral deposits database; *BC Ministry of Energy, Mines and Petroleum Resources*, URL <http://www.em.gov.bc.ca/Mining/Geolsurv/Minfile/> [Nov 2005].

Struik, L.C., MacIntyre, D. and Hastings, N.L. (2001): Nechako NATMAP Project, geochemistry data CD-ROM; *Geological Survey of Canada*, Open File 4356 and *BC Ministry of Energy, Mines and Petroleum Resources*, Paper 2001-9.

Weary G.F., Levson, V.M. and Broster, B.E. (1997): Till geochemistry of the Chedakuz Creek map area (93F/7), British Columbia; *BC Ministry of Energy, Mines and Petroleum Resources*, Open File 1997-11.

Geology and Mineral Deposits of the Skeena Arch, West-Central British Columbia: A Geoscience BC Digital Data Compilation Project[1]

By Don MacIntyre[2]

KEYWORDS: digital data, GIS, Skeena arch, mineral deposits, geology

INTRODUCTION

The Skeena arch is a northeast-trending belt of uplifted Jurassic and older rocks that transects central British Columbia. This uplift is believed to have formed in the Middle Jurassic and resulted in separation of the Bowser and Nechako basins (Yorath, 1991). Rocks exposed along the Skeena arch represent a long-lived magmatic arc that has produced a diverse range of mineral deposits in a wide variety of geological settings. This area represents some of the most richly endowed terrain in BC and has been the site of mineral exploration for the past 125 years. Since 1985, the BC Geological Survey and the Geological Survey of Canada have been involved in regional mapping projects along the Skeena arch, first as part of the Whitesail and Smithers projects (*e.g.*, MacIntyre *et al.*, 1989) and more recently as part of the Interior Plateau (Diakow *et al.*, 1997) and Nechako NATMAP (MacIntyre *et al.*, 1996a, 1996b, 1997, 1998; MacIntyre 1998, 2001a, b; MacIntyre and Villeneuve, 2001) projects. This work has resulted in a much better understanding of the geological evolution of the arch, particularly during the metallogenically important Jurassic through Cretaceous time periods. Although there are gaps in the map coverage, a large part of the project area (80%) has now been mapped in detail. These data were originally compiled at 1:100 000 scale as part of the Mineral Potential Project (MacIntyre *et al.*, 1994) and revised and updated as part of the Digital Geology of BC Project (Massey *et al.*, 2003, 2003a). The Skeena arch Project will provide a means of bringing this and other digital datasets together as a series of standardized, digital geological maps with linked databases for structure, mineral occurrences, geochemistry, geophysics, geochronology and paleontology. A new series of 1:100 000-scale maps will be produced for the area and made available in digital and hardcopy format.

The aim and scope of this proposed two-year project is to promote new exploration along the Skeena arch by:

- compiling all existing data relevant to mineral exploration along the arch and building a GIS database, using Manifold 6.5 GIS software, for use by explorationists; various data formats will be produced in order to make the data as widely useable as possible; data will be made available on CD and possibly over the Internet in standard GIS format; and
- spatial analysis of the data and definition of exploration targets based on correlation of positive indicators, such as geochemical and geophysical anomalies and stratigraphic setting.

The project will generate the following deliverables over a two year period:

- Updated and standardized 1:100 000-scale geological, geochemical and geophysical compilation maps for the maps sheets covered by the project area (Fig. 1)
- A CD containing reports documenting the results of the project and new exploration targets, plus a complete suite of data files and maps in GIS format for use in Manifold 6.5 GIS and other popular GIS packages (ArcView®, MapInfo®, AutoCAD® Map, etc.); the CD will also contain 1:100 000-scale digital maps in PDF format portraying the geology, mineral occurrences, geochemistry and geophysics of the project area, and assessed exploration potential for key mineral deposit types
- Updated MINFILE (2005) occurrences, as required.

Projected release of final report, maps and database files is October 2006.

LOCATION OF THE PROJECT AREA

The area covered by the Skeena Arch Project is shown in Figure 1. The area includes all of the Hazelton (93M), Smithers (93L) and Whitesail (93E) maps sheets, and the south half of the McConnell Creek (94D), east half of the Terrace (103I) and southeast corner of the Nass River (103P) map sheets.

KEY DATASETS AND PRODUCTS

New geology and exploration-potential maps will be compiled and released as digital products for each of the map tiles shown in Figure 1. The digital files will include bedrock geology and exploration potential for specific mineral-deposit types, such as epithermal veins, Eskay Creek – type VMS, porphyry Cu and Mo, etc. Potential for hydrocarbons may also be included if sufficient data can be

[1] *Geoscience BC contribution GBC007*

[2] *Consulting Geologist, D.G. MacIntyre & Associates Ltd., Victoria, BC*

This publication is also available, free of charge, as colour digital files in Adobe Acrobat PDF format from the BC Ministry of Energy, Mines and Petroleum Resources internet website at http://www.em.gov.bc.ca/Mining/Geolsurv/Publications/catalog/catfldwk.htm

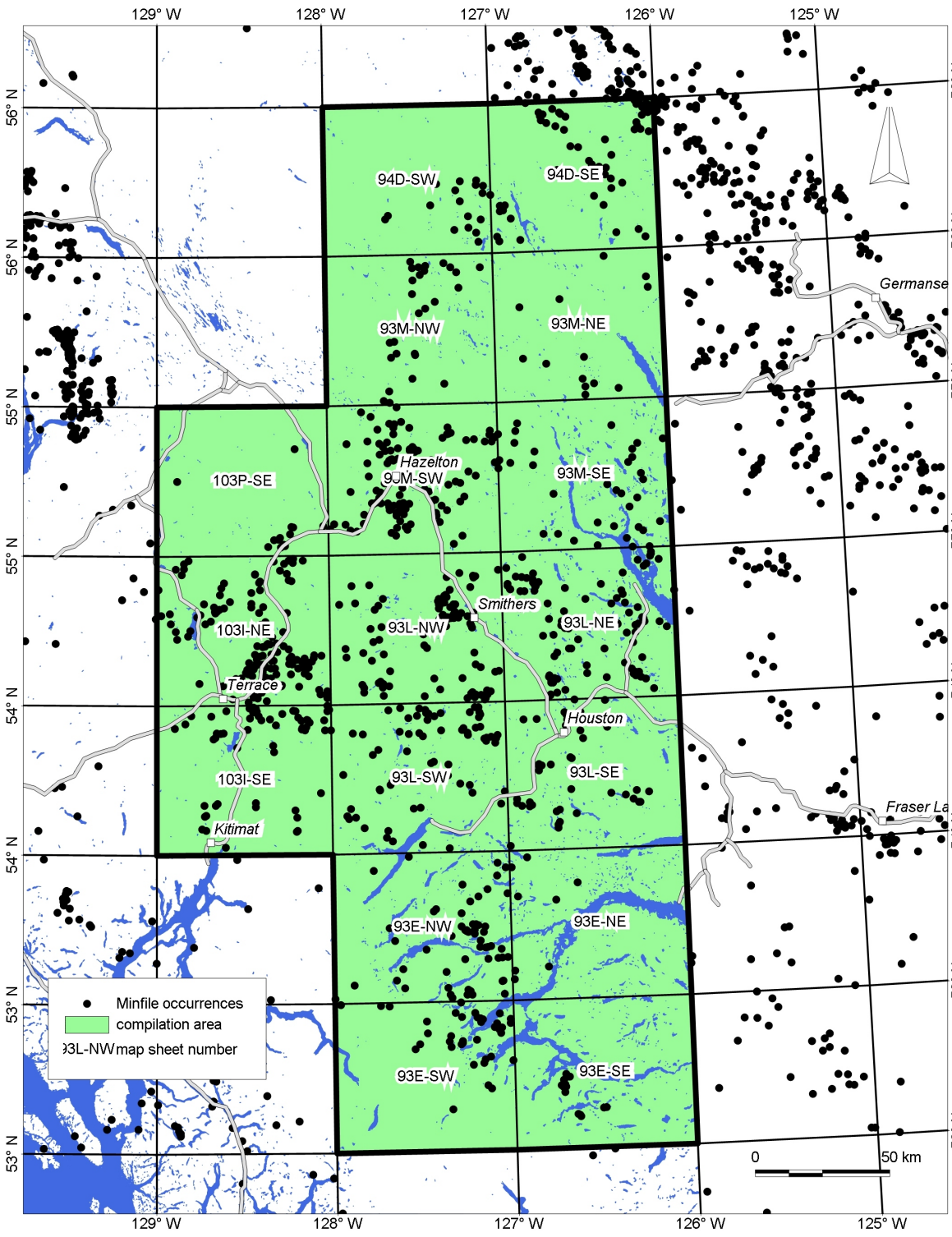


Figure 1. Skeena Arch Project area, showing map tiles to be compiled and location of MINFILE occurrences.

obtained. Digital compilation products will be derived from the datasets shown in Table 1. A key criterion for the project is that all datasets used to produce the derivative geology and exploration-potential maps and databases are available to the public for free. Unfortunately, this means that TRIM topographic data cannot be used in this project because of its high cost and distribution restrictions. However, digital elevation data are available for free from the Government of Canada GEOBASE website, and these will be used to generate contour maps and hillshade surfaces for the project area using the capabilities of the Manifold 6.5 GIS software. Manifold was chosen as the GIS platform for this project because of its exceptional functionality and low cost (currently selling for around $300 Canadian). In addi-

TABLE 1. KEY DATASETS TO BE USED IN THE SKEENA ARCH COMPILATION PROJECT

Name	Description	Source
Geology	Bedrock geology polygons, faults and related databases	BCGS
Quaternary	Quaternary cover polygons	BCGS
Age Dates	Isotopic ages	BCGS
Minfile	Mineral occcurrence locations and related databases	BCGS
ARIS	Assessment report locations and descriptions	BCGS
RGS	Regional silt, water and till geochemistry sample locations and related databases	BCGS
Minpot	Mineral potential tracts, location of known resources and related databases	BCGS
Geophysics	Airborne geophysical surveys	GSC
DEM	Digital elevation model points (used to generate contours and hillshade relief maps)	GEOBASE
Rivers	Major rivers as lines and polygons	GEOGRATIS
Lakes	Major lake polygons	GEOGRATIS
Sea	Ocean polygons	GEOGRATIS
Roads	Road network	GEOGRATIS
FSR	Logging road network	BCMOF
Cities	Cities, towns and communities	GEOGRATIS
Ice Cover	Areas of ice cover	GEOGRATIS
Parks	Location of parks	BCMENV
Grid 250K	NTS map sheet grids for 1:250K and 1:50K maps	GEOGRATIS
Grid 20K	Map sheet grid for BC 1:20K TRIM maps	BCMENV

tion to the Manifold data format, however, all files will also be made available in ESRI shapefile, MapInfo® MIF and AutoDesk® DWG format. All file formats will be available in three projections: geographic, Universal Transverse Mercator and BC Albers. These projections will be based on the North American Datum 1983.

TECTONIC SETTING

The project area is within the Intermontane Belt, which at this latitude includes the volcanic-arc Stikine (Stikinia) Terrane and a small part of the oceanic Cache Creek Terrane. The Stikine Terrane comprises Carboniferous to Middle Jurassic island-arc volcanic and sedimentary rocks and related plutonic suites (Schiarizza and MacIntyre, 1999). The Stikine Terrane is believed to have evolved in the eastern Pacific of the northern hemisphere and moved northward to dock with ancestral North America sometime during the Middle Jurassic (Monger *et al.*, 1972, 1996). The Stikine Terrane is well exposed along the Skeena arch. North of the Skeena arch, the Stikine Terrane is overlain by postaccretion Late Jurassic to Early Cretaceous marine and nonmarine sedimentary rocks of the Bowser Basin. The southern part of the Skeena arch is overlapped by Late Cretaceous and Eocene continental volcanic arc and related sedimentary rocks of the Ootsa Lake and Endako groups.

The project area spans the zone of westward-directed thrust faulting that marks the boundary between the Stikine and Cache Creek terranes (Struik *et al.*, 2001). This structural imbrication occurred prior to 165 Ma (Schiarizza and MacIntyre 1999), as indicated by isotopic ages for postkinematic plutons that cut both terranes. Folds and thrust faults related to this imbrication are offset by a complex pattern of high-angle faults. This pattern of faulting is not unique to the boundary between Stikine and Cache Creek terranes, as it is observed throughout the Smithers and Hazelton map sheets (Tipper and Richards 1976a, b; Richards 1980, 1990). Most of these faults formed during Late Cretaceous to Eocene or younger block-faulting events (MacIntyre *et al.*, 1997, 1998). In most parts of the project area, rocks of the Stikine Terrane display broad open fold patterns. The occurrence of a penetrative cleavage and metamorphic grade higher than lower greenschist facies is rare.

GEOLOGY

The geology of the Skeena Arch Project area is based on a recent compilation completed by the BC Geological Survey (Massey *et al.*, 2003a, b). This information has been used to generate Figures 2–5. Figure 6 is a schematic cross-section, extending from the Skeena arch to the Bowser basin, that shows the relationships of major lithostratigraphic map units. Also shown are the stratigraphic positions of geochronological and paleontological age controls.

Most of the project area is underlain by the Stikine Terrane, which here includes the Carboniferous to Permian Asitka Group island-arc metavolcanic rocks and limestone; Middle to Late Triassic augite-phyric basalt, andesite and related island-arc marine sedimentary rocks of the Takla Group; and Early to Middle Jurassic andesitic volcanic, volcaniclastic and related marine sedimentary rocks of the Hazelton Group island-arc to continental-arc assemblage (Fig. 2; Thorkelson *et al.*, 1995; Richards 1980, 1990). The stratified rocks are cut by the granodiorite and quartz diorite of the Late Triassic to Early Jurassic Topley intrusive suite and the newly recognized Early to Middle Jurassic Spike Peak intrusive suite (MacIntyre *et al.*, 2001), which are probably comagmatic with the Takla and Hazelton volcanic-arc successions.

In the northwest corner of the project area, the Stikine Terrane is overlain by marine to nonmarine clastic sedimentary strata of the Late Jurassic Bowser Lake and Early Cretaceous Skeena groups (Fig. 3). These rocks were de-

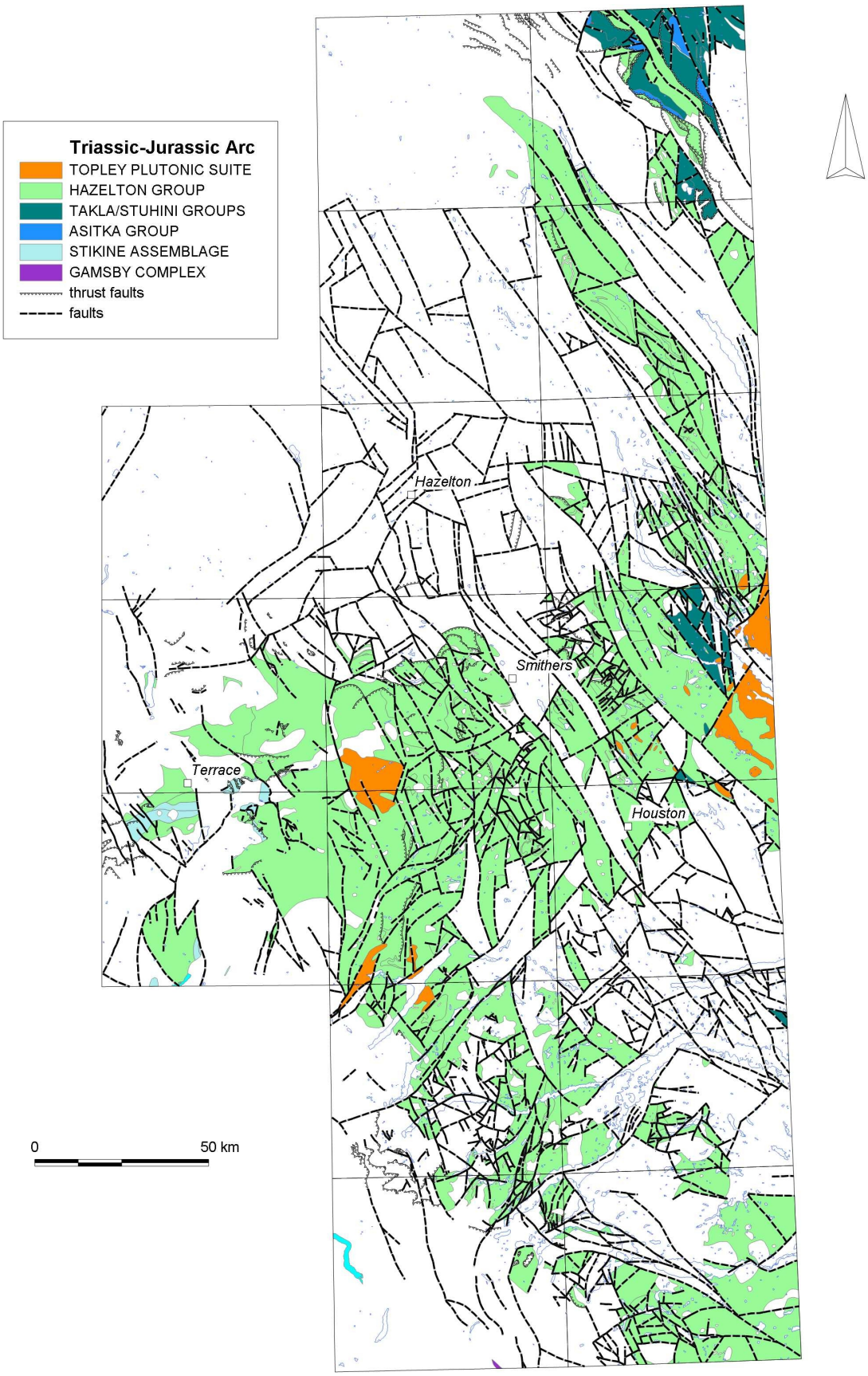


Figure 2. Distribution of Triassic and Jurassic volcanic and plutonic rocks of the Stikine Terrane.

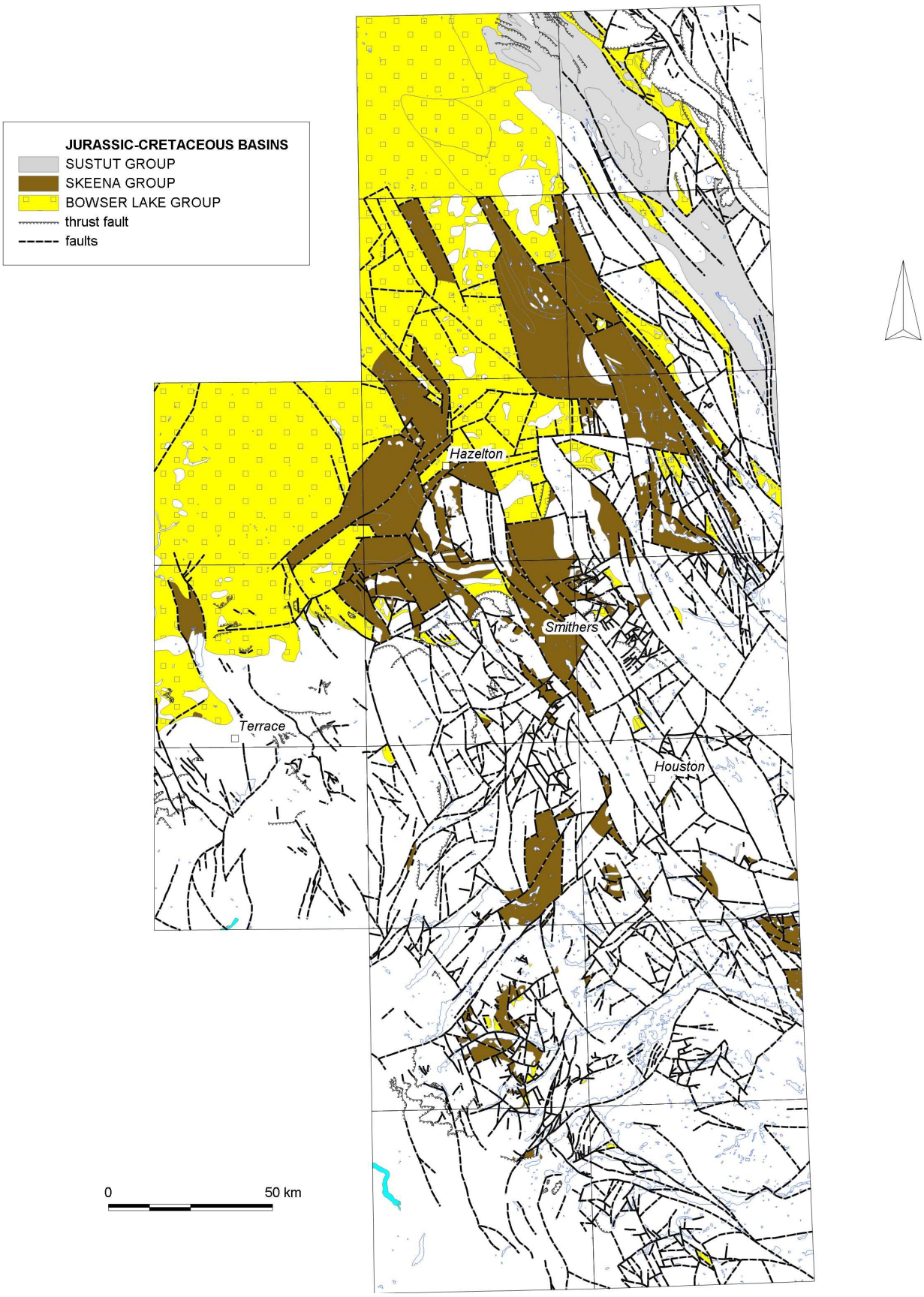


Figure 3. Distribution of Jurassic and Cretaceous sedimentary rocks of the Bowser and Skeena basins.

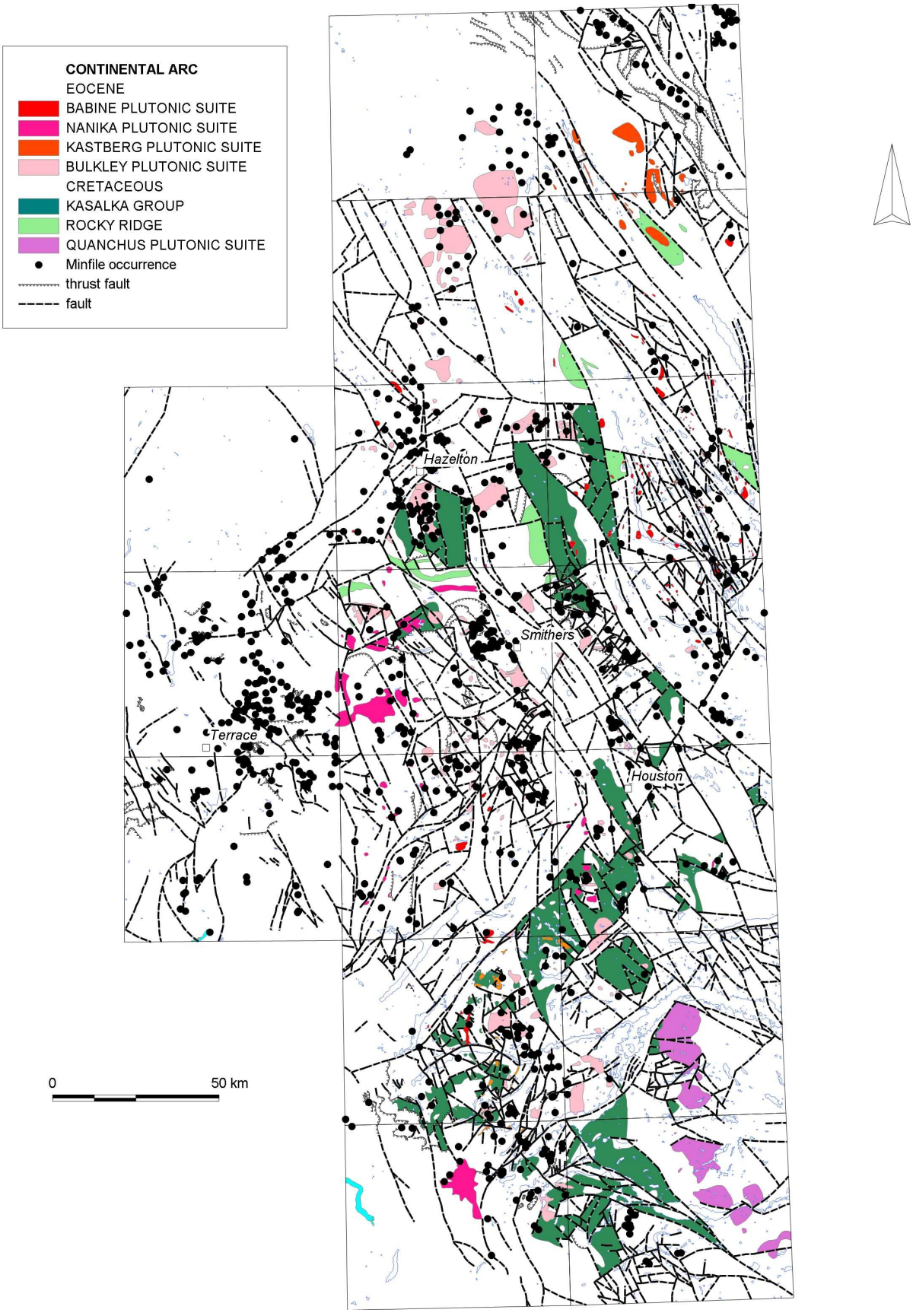


Figure 4. Distribution of Cretaceous and Tertiary volcanic-arc rocks and location of MINFILE occurrences.

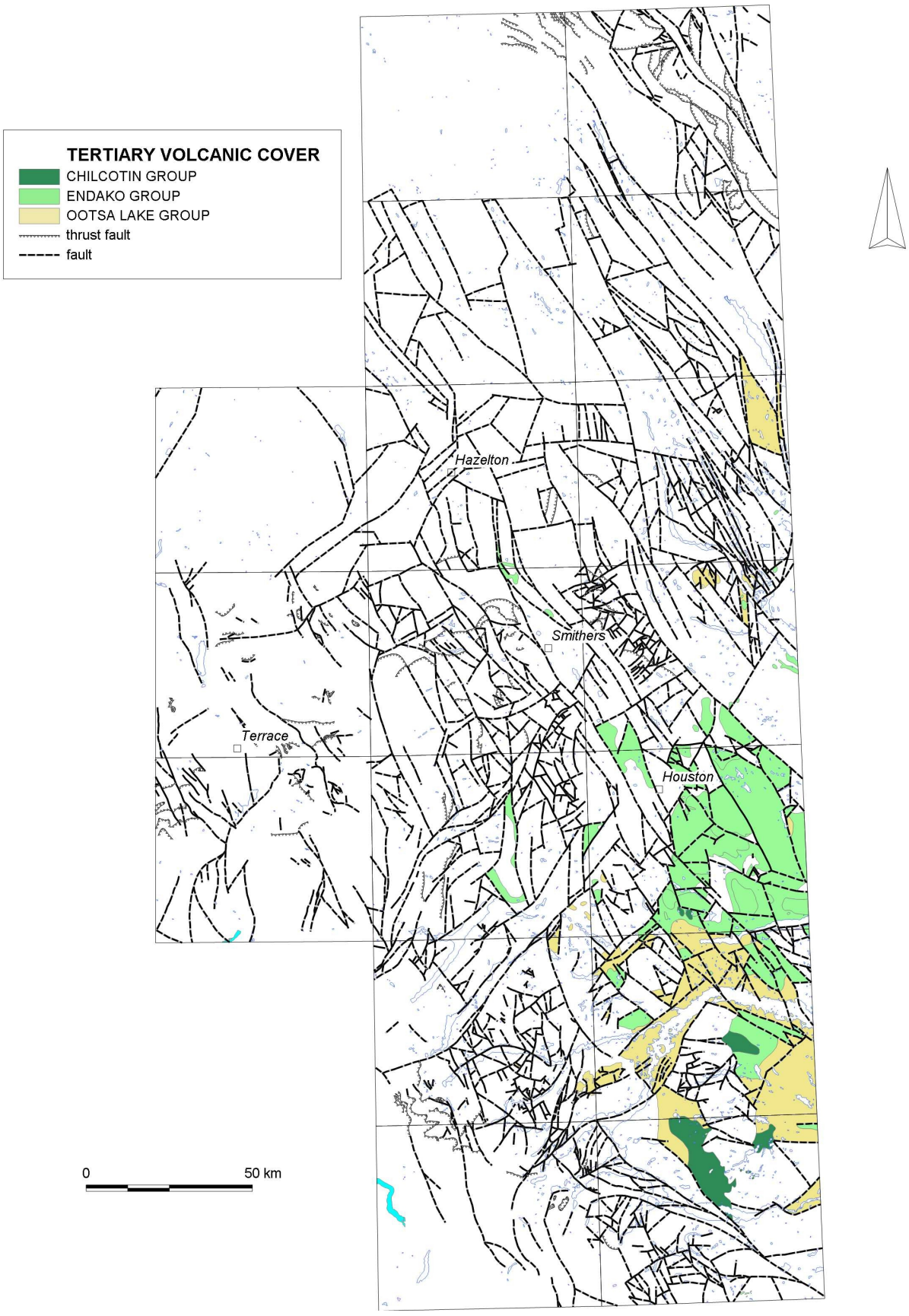


Figure 5. Distribution of Tertiary volcanic cover.

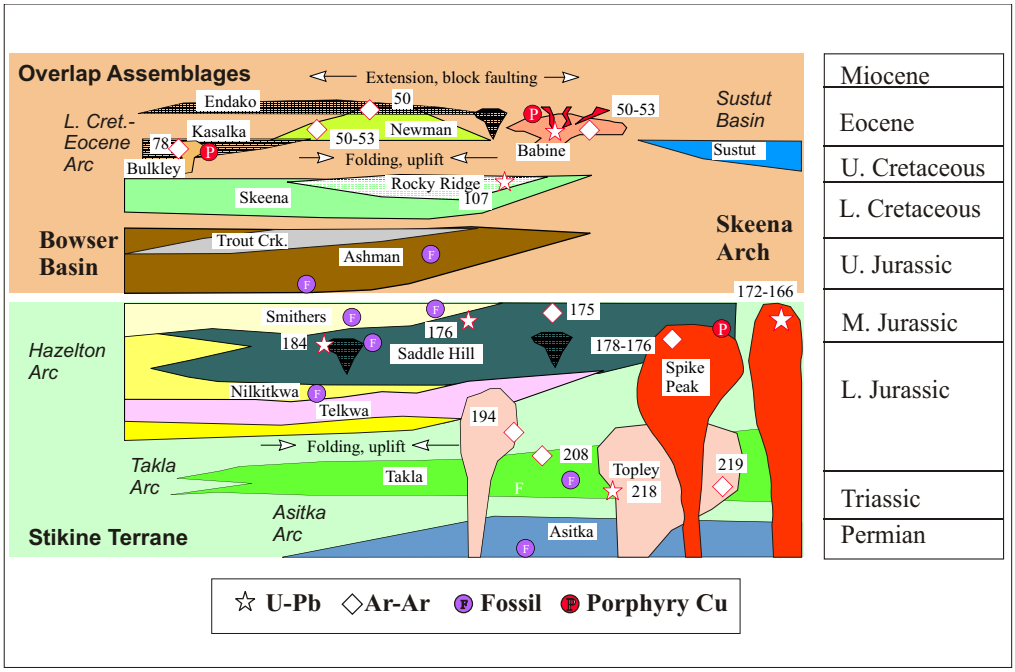


Figure 6. Schematic stratigraphic relationships, northern Skeena arch.

posited in a fluvial-deltaic to nearshore shelf environment along the southeastern margin of the Bowser Basin (Bassett, 1991; Bassett and Kleinspehn, 1996; Evenchick, 1999). A detailed discussion of these overlap assemblages is presented in MacIntyre (1998).

In the western half of the project area, Late Cretaceous to Early Eocene porphyritic andesite, basalt, rhyolite and related pyroclastic and volcaniclastic continental-arc rocks unconformably overlie both folded and uplifted rocks of the Stikine Terrane and Late Jurassic to Early Cretaceous sedimentary rocks of the Bowser Basin (Fig. 4). The younger volcanic rocks are preserved in grabens or as erosional remnants on ridge tops. The Late Cretaceous rocks include porphyritic andesite flows and lahars of the Kasalka Group and coeval granodiorite and quartz diorite plutons of the Bulkley plutonic suite (MacIntyre, 1985; Carter, 1981). In the vicinity of Babine Lake, the Stikine Terrane is unconformably overlain by porphyritic andesite flows of the Early Eocene Newman Formation and is cut by porphyritic granodiorite to quartz monzonite plutons of the Babine plutonic suite. In the southern part of the project area, small porphyritic quartz monzonite and related felsic intrusions constitute the Nanika plutonic suite. Important porphyry copper deposits are associated with the Bulkley, Babine and Nanika intrusive rocks (Carter, 1976, 1981; Carter *et al.*, 1995; MacIntyre and Villeneuve, 2001).

In the east and southeast parts of the project area, the Stikine and Cache Creek terranes are unconformably overlain by Early Eocene basalt and rhyolite flows and related pyroclastic rocks of the Endako and Ootsa Lake Groups (Fig. 5; Grainger and Anderson, 1999; Grainger *et al.*, 2001) and Miocene basalt flows of the Chilcotin Group. These younger rocks have also been block faulted and tilted during an Eocene or younger extensional tectonic event.

MINERAL DEPOSITS

The Skeena Arch Project area is richly endowed with metallic mineral deposits, with over 800 occurrences listed in the BC Geological Survey's MINFILE database. The different deposit types that have been recognized in the area are listed in Table 2. Of these, the most important types are polymetallic veins (268), subvolcanic Cu-Ag-Au-(As-Sb) (153), porphyry Cu±Mo±Au (140), volcanic redbed Cu (86), porphyry Mo (66), intrusion-related Au pyrrhotite

TABLE 2. MINERAL DEPOSIT TYPES OCCURRING IN THE SKEENA ARCH PROJECT AREA

Profile Code	Name	Count
I05	Polymetallic veins Ag-Pb-Zn Au	268
L01	Subvolcanic Cu-Ag-Au-(As-Sb)	153
L04	Porphyry Cu Mo Au	140
D03	Volcanic redbed Cu	86
L05	Porphyry Mo (low F- type)	66
I02	Intrusion-related Au pyrrhotite veins	38
K01	Cu skarns	20
G06	Noranda-Kuroko massive sulphide Cu-Pb-Zn	7
E04	Sediment-hosted Cu	6
H05	Epithermal Au-Ag (low sulphidation)	6
I01	Au-quartz veins	6
M01	Flood basalt - associated Ni-Cu	4
H04	Epithermal Au-Ag-Cu (high sulphidation)	3
I06	Cu Ag quartz veins	3
I12	W veins	3
K03	Fe skarns	3
K04	Au skarns	3
E14	Sedimentary exhalative Zn-Pb-Ag	2
G04	Besshi massive sulphide Cu-Zn	2
J01	Polymetallic manto Ag-Pb-Zn	2
K02	Pb-Zn skarns	2
L02	Porphyry-related Au	2
L03	Alkalic porphyry Cu-Au	2
		827

veins (38) and Cu skarns (20). Most of these deposits are related to the Late Cretaceous Bulkley and Eocene Babine and Nanika plutonic suites. These intrusions are part of a long-lived magmatic arc that forms the core of the Skeena arch. A schematic diagram showing the evolution of Cretaceous and Tertiary volcanic centres is shown in Fig. 4. Redbed Cu occurrences are mostly associated with basaltic flows of the Takla and Hazelton Groups.

In recent years, potential for the discovery of Eskay Creek – type volcanogenic massive sulphide deposits has been recognized. The most prospective targets are Middle Jurassic submarine volcanic rocks of the Hazelton Group (Massey, 1999; Massey *et al.*, 1999) and mid-Cretaceous bimodal volcanic rocks of the Rocky Ridge Formation (MacIntyre, 2001).

There is currently only one deposit in production in the project area: the Huckleberry porphyry Cu-Mo deposit at Tahtsa Lake, 90 km south of the town of Houston. Two other deposits are in the advanced stages of feasibility studies: the Davidson (a.k.a. Glacier Gulch or Yorke-Hardy) porphyry Mo deposit at Smithers and the Morrison porphyry Cu deposit at Babine Lake.

CONCLUSIONS

This project will help to stimulate mineral exploration by providing mineral explorationists with a comprehensive, up-to-date, all-inclusive GIS-compatible compilation of existing geoscience data in one of the most prospective areas of BC. The current database for this area is a mixture of digital and nondigital data from a wide range of projects that were done at different times and scales by different government agencies and exploration companies. The data from these projects need to be compiled, integrated and standardized into a format that can be used in a GIS. Building such a database will help explorationists identify new exploration targets and re-evaluate areas of known mineral occurrences using new geological and metallogenic models. Particular focus will be directed toward porphyry Mo and Eskay Creek – type deposits. In addition to providing a comprehensive standardized database, this project will also analyze the data and generate a list of potential target areas for consideration, thus assisting the exploration community in their evaluation of the potential for new discoveries.

REFERENCES

Bassett, K.N. (1991): Preliminary results of the sedimentology of the Skeena Group in west-central British Columbia; *in* Current Research, Part A, *Geological Survey of Canada*, Paper 91-1A, pages 131–141.

Bassett, K.N. and Kleinspehn, K.L. (1996): Mid-Cretaceous transtension in the Canadian Cordillera: evidence from the Rocky Ridge volcanics of the Skeena Group; *Tectonics*, Volume 15, pages 727–746.

Carter, N.C. (1976): Regional setting of porphyry deposits in west-central British Columbia; *in* Porphyry Deposits of the Canadian Cordillera, Sutherland-Brown, A., Editor, *Canadian Institute of Mining and Metallurgy*, Special Volume 15, pages 227–238

Carter, N.C. (1981): Porphyry copper and molybdenum deposits, west-central British Columbia; *BC Ministry of Energy, Mines and Petroleum Resources*, Bulletin 64.

Carter, N.C., Dirom, G.E. and Ogryzlo, P.L. (1995): Porphyry copper-gold deposits, Babine Lake area, west-central British Columbia; i*n* Porphyry Deposits of the Northwestern Cordillera of North America, Schroeter, T.G., Editor, *Canadian Institute of Mining, Metallurgy and Petroleum*, Special Volume 46, pages 247–255.

Diakow, L.J., Webster, I.C.L., Richards, T.A. and Tipper, H.W. (1997): Geology of the Fawnie and Nechako Ranges, southern Nechako Plateau, central British Columbia (93F/2,3,6,7); *in* Interior Plateau Geoscience Project: Summary of Geological, Geochemical and Geophysical Studies, Diakow, L.J. and Newell, J.M., Editors, *BC Ministry of Energy, Mines and Petroleum Resources*, Paper 1997-2 and *Geological Survey of Canada*, Open File 3448, pages 7–30.

Evenchick, C.A. (1999): Depositional and structural histories of the northern two-thirds of the Bowser Basin/Skeena Fold Belt, northern British Columbia: records of terrane interactions; *in* Terrane Paths 99, Circum-Pacific Terrane Conference, Abstracts and Program, Evenchick, C.A., Woodsworth, G.J. and Jongens, R., Editors, *Geological Survey of Canada – Geological Association of Canada*, pages 30–32.

Grainger, N.C. and Anderson, R.G. (1999): Geology of the Eocene Ootsa Lake Group in northern Nechako River and southern Fort Fraser map area, central British Columbia; *in* Current Research 1999-A, *Geological Survey of Canada*, pages 139–148.

Grainger, N.C., Villeneuve, M.E., Heaman, L.M. and Anderson, R.G. (2001): New U-Pb and Ar/Ar isotopic age constraints on the timing of Eocene magmatism, Fort Fraser and Nechako River Map areas, central British Columbia; *Canadian Journal of Earth Sciences*, volume 38, pages 679–696.

MacIntyre, D.G. (1985): Geology and mineral deposits of the Tahtsa Lake district, west-central British Columbia; *BC Ministry of Energy, Mines and Petroleum Resources*, Bulletin 75.

MacIntyre, D.G. (1998): Babine Porphyry District Project: bedrock geology of the Nakinilerak Lake map sheet (93M/8), British Columbia; *in* Geological Fieldwork 1997, *BC Ministry of Energy, Mines and Petroleum Resources*, Paper 1998-1, pages 2-1–2-18.

MacIntyre, D.G. (2001a): Geological compilation of the Babine porphyry copper district; *BC Ministry of Energy, Mines and Petroleum Resources*, Open File Map 2001-3.

MacIntyre, D.G. (2001b): The Mid-Cretaceous Rocky Ridge Formation — a new target for subaqueous hot-spring deposits (Eskay Creek – type) in central British Columbia; *in* Geological Fieldwork 2000, *BC Ministry of Energy, Mines and Petroleum Resources*, Paper 2001-1, pages 253–268.

MacIntyre, D.G., Ash C. and Britton, J. (1994): Nass-Skeena (93/E, L, M; 94/D; 103/G, H, I, J, P; 104/A, B), *BC Ministry of Energy, Mines and Petroleum Resources*, Open File 1994-14.

MacIntyre, D.G., Desjardins, P. and Tercier, P (1989): Jurassic stratigraphic relationships in the Babine and Telkwa ranges; i*n* Geological Fieldwork 1988, *BC Ministry of Energy, Mines and Petroleum Resources*, Paper 1989-1, pages 195–208.

MacIntyre, D.G. and Villeneuve, M.E. (2001): Geochronology and tectonic setting of mid-Cretaceous to Eocene magmatism, Babine porphyry copper district, central British Columbia; *Canadian Journal of Earth Sciences*, Volume 38, pages 639–655.

MacIntyre, D.G., Villeneuve, M.E. and Schiarizza, P. (2001): Timing and tectonic setting of Stikine Terrane magmatism, Babine-Takla lakes area, central British Columbia; *Canadian Journal of Earth Sciences*, Volume 38, pages 579–601.

MacIntyre, D.G., Webster, I.C.L. and Bellefontaine, K. (1996a). Babine Porphyry District Project: bedrock geology of the Fulton Lake map area (NTS 93L16); *in* Geological Field-

work 1995, *BC Ministry of Energy, Mines and Petroleum Resources*, Paper 1996-1, pages 11–35.

MacIntyre, D.G., Webster, I.C.L. and Bellefontaine, K. (1996b). Geology of the Fulton Lake map sheet (93L/16), *BC Ministry of Energy, Mines and Petroleum Resources*, Open File Map 1996-29.

MacIntyre, D., Webster, I.C.L. and Desjardins, P. (1998): Bedrock geology of the Old Fort Mountain map area, north-central BC; *BC Ministry of Energy, Mines and Petroleum Resources*, Open File Map 1997-10.

MacIntyre, D.G., Webster, I.C.L and Villeneuve, M. (1997). Babine Porphyry District Project: bedrock geology of the Old Fort Mountain area (93M/1), British Columbia; *in* Geological Fieldwork 1996, *BC Ministry of Energy, Mines and Petroleum Resources*, Paper 1997-1, pages 47–67.

Massey, N.W.D. (1999): Volcanogenic massive sulphide deposits in British Columbia; *BC Ministry of Energy, Mines and Petroleum Resources*, Open File 1999-2.

Massey, N.W.D., Alldrick, D.J. and Lefebure, D.V.L. (1999): Potential for subaqueous hot-spring (Eskay Creek) deposits in British Columbia; *BC Ministry of Energy, Mines and Petroleum Resources*, Open File 1999-14.

Massey, N.W.D., MacIntyre, D.G. and Desjardins, P.J., (2003b): Digital geology map of British Columbia: tile NN9 north coast BC; *BC Ministry of Energy, Mines and Petroleum Resources*, GeoFile 2003-13, scale 1:250 000.

Massey, N.W.D., MacIntyre, D.G. and Desjardins, P.J., (2003a): Digital geology map of British Columbia: tile NO9 north-central BC; *BC Ministry of Energy, Mines and Petroleum Resources*, GeoFile 2003-18, scale 1:250 000.

MINFILE (2005): MINFILE BC mineral deposits database; *BC Ministry of Energy, Mines and Petroleum Resources*, URL <http://www.em.gov.bc.ca/Mining/Geolsurv/Minfile/> [Nov 2005].

Monger, J.W.H., Gabrielse, H. and Souther, J.A. (1972): Evolution of the Canadian Cordillera: a plate tectonic model; *American Journal of Science*, Volume 272, pages 577–602.

Monger, J.W.H. and Nokleberg, W.J. (1996): Evolution of the northern North American Cordillera: generation, fragmentation, displacement and accretion of successive North American plate-margin arcs; *in* Geology and Ore Deposits of the American Cordillera, Coyner, A.R. and Fahey, P.L., Editors, *Geological Society of Nevada,* Symposium Proceedings, Reno/Sparks, Nevada, April 1995, pages 1133–1152.

Richards, T.A. (1980): Geology of the Hazelton map area (93M); *Geological Survey of Canada*, Open File 720.

Richards, T.A. (1990). Geology of the Hazelton map area (93M); *Geological Survey of Canada*, Open File 2322.

Schiarizza, P. and MacIntyre, D.G. (1999): Geology of the Babine Lake – Takla Lake area, central British Columbia; *in* Geological Fieldwork 1998, *BC Ministry of Energy, Mines and Petroleum Resources*, Paper 1999-1, pages 33–68.

Struik, L.C., Schiarizza, P., Orchard, M.J., Cordey, F., Sano, H., MacIntyre, D.G., Lapierre, H. and Tardy, M. (2001): Imbricate architecture of the upper Paleozoic to Jurassic oceanic Cache Creek Terrane, central British Columbia; *Canadian Journal of Earth Sciences*, Volume 38, pages 495–514.

Thorkelson, D.J., Mortensen, J.K., Marsden, H. and Taylor, R.P. (1995): Age and tectonic setting of Early Jurassic episodic volcanism along the northeastern margin of the Hazelton Trough, northern British Columbia; *in* Jurassic Magmatism and Tectonics of the North American Cordillera, Miller, D.M. and Busby, C., Editors, *Geological Society of America*, Special Paper 299, pages 83–94.

Tipper, H.W. and Richards, T.A. (1976a): Jurassic stratigraphy and history of north-central British Columbia; *Geological Survey of Canada*, Bulletin 270, 73 pages.

Tipper, H.W. and Richards, T.A. (1976b). Geology of the Smithers area; *Geological Survey of Canada*, Open File Map 351.

Yorath, C.J. (1991): Upper Jurassic to Paleogene assemblages; Chapter 9 *in* Geology of the Cordilleran Orogen of Canada, Gabrielse, H. and Yorath, C.J., Editors, *Geological Survey of Canada*, Geology of Canada, no 4, pages 329–371 (also Geological Society of America, The Geology of North America, Volume G-2).

Geological Setting and Mineralization Potential of the Southwestern Whitesail Lake Map Area (NTS 093E), Southwestern British Columbia: Preliminary Assessment

By J. Brian Mahoney[1], J.W. Haggart[2], R.L. Hooper[1], L.D. Snyder[1] and G.J. Woodsworth[2]

KEYWORDS: Hazelton Group, Whitesail Lake, layered mafic intrusion, Central Gneiss Complex

INTRODUCTION

The primary objective of this investigation is detailed bedrock mapping and evaluation of economic mineralization potential in the southern and western Whitesail Lake map area (NTS 093E; Fig. 1, 2). Fieldwork in 2005 concentrated on the southwestern corner of the Whitesail Lake map area (NTS 093E/03, 04, 05, 06), extending work completed to the east under the auspices of the Rocks to Riches Program (Mahoney *et al.*, 2005; Gordee *et al.*, 2005). Year 2 of the project will focus on areas to the north and northeast of the present map area (Fig. 2), with the ultimate goal of providing a comprehensive evaluation of economic mineralization potential of the southern and western Whitesail Lake map area.

REGIONAL GEOLOGICAL SETTING

The southern Whitesail Lake (NTS 093E) 1:250 000 map area is located along the transition zone between the Coast and Intermontane morphogeological belts, straddling the boundary between igneous and metamorphic rocks of the Coast Plutonic Complex on the west and Jurassic and Cretaceous volcanosedimentary successions of southwestern Stikinia on the east (Fig. 1, 2). Bedrock geological mapping and economic mineral assessment in the eastern Bella Coola (NTS 093D) map area to the south was the focus of the 2001–2004 Bella Coola Targeted Geoscience Initiative (TGI) of the Geological Survey of Canada. The TGI project focused on constraining the geological evolution of the region and assessing the economic potential of Mesozoic volcanic assemblages and plutonic belts in the region (Haggart *et al.*, 2004). The geological framework established by the Bella Coola TGI was extended to the north, into the southern Whitesail Lake map area (NTS 093E/02, 03), under the auspices of the Rocks To Riches Program in 2004. Regional mapping and economic assessment were extended to the west and northwest (NTS 093E/04, 05, 06) in 2005 by a combined research team from the University of Wisconsin – Eau Claire, the Geological Survey of Canada and the University of British Columbia. This is an ongoing project, sponsored by Geoscience BC, that is designed to improve understanding of the geological evolution and economic mineral potential of the west-central portion of the Coast Mountains (52–54°N).

The primary focus of mapping during the brief 2005 field season was the southwestern corner of the Whitesail Lake map area, including portions of the Kitlope Lake (NTS 093E/04), Tsaytis River (NTS 093E/05) and Chikamin Mountain (NTS 093E/06) 1:50 000 map areas (Fig. 1, 2). This area contains Jurassic and Cretaceous volcanic and sedimentary successions, with volcanogenic massive sulphide mineralization potential, on the western edge of Stikinia and Jurassic to Eocene plutonic bodies, which are known hosts for a variety of porphyry deposits, along the eastern margin of the Coast Plutonic Complex (Woodsworth, 1980; Dawson *et al.*, 1991; Diakow *et al.*, 2002). Stream sediment geochemistry, MINFILE (2005) data and detailed geological mapping to the north (Whitesail Lake map area) and south (eastern Bella Coola map area) indicate potential for volcanogenic massive sulphide, Cu±Mo±Au porphyry, and Ni-Cu-Cr-platinum-group-element (PGE) mineralization in Mesozoic volcanogenic successions of western Stikinia and plutonic bodies along the eastern margin of the Coast Plutonic Complex (Fig. 3).

This report briefly describes the geology of the southwestern Whitesail 1:250 000 map area (NTS 093E/04, 05, 06), documented by detailed bedrock mapping during the 2005 field season (Fig. 4). Geochemical and geochronological analyses are ongoing. The bulk of the bedrock mapping slated for this project will be conducted during the 2006 field season. This investigation will integrate regional bedrock mapping, stratigraphic and structural analyses, geochronology, plutonic and volcanic geochemistry, isotopic analyses and mineral assays into a comprehensive assessment of the geological framework and economic mineral potential of the region.

STRATIGRAPHIC SUCCESSIONS

Hazelton Group

The southern Whitesail Lake and Bella Coola map areas represent the southernmost extent of significant exposures of the Lower to Middle Jurassic Hazelton Group. In the southern Whitesail Lake area (NTS 093E/02, 03), Hazelton Group strata are widespread and well preserved,

[1]*Department of Geology, University of Wisconsin, Eau Claire, WI (mahoney@uwec.edu)*

[2]*Geological Survey of Canada, Vancouver, BC*

This publication is also available, free of charge, as colour digital files in Adobe Acrobat PDF format from the BC Ministry of Energy, Mines and Petroleum Resources internet website at http://www.em.gov.bc.ca/Mining/Geolsurv/Publications/catalog/catfldwk.htm

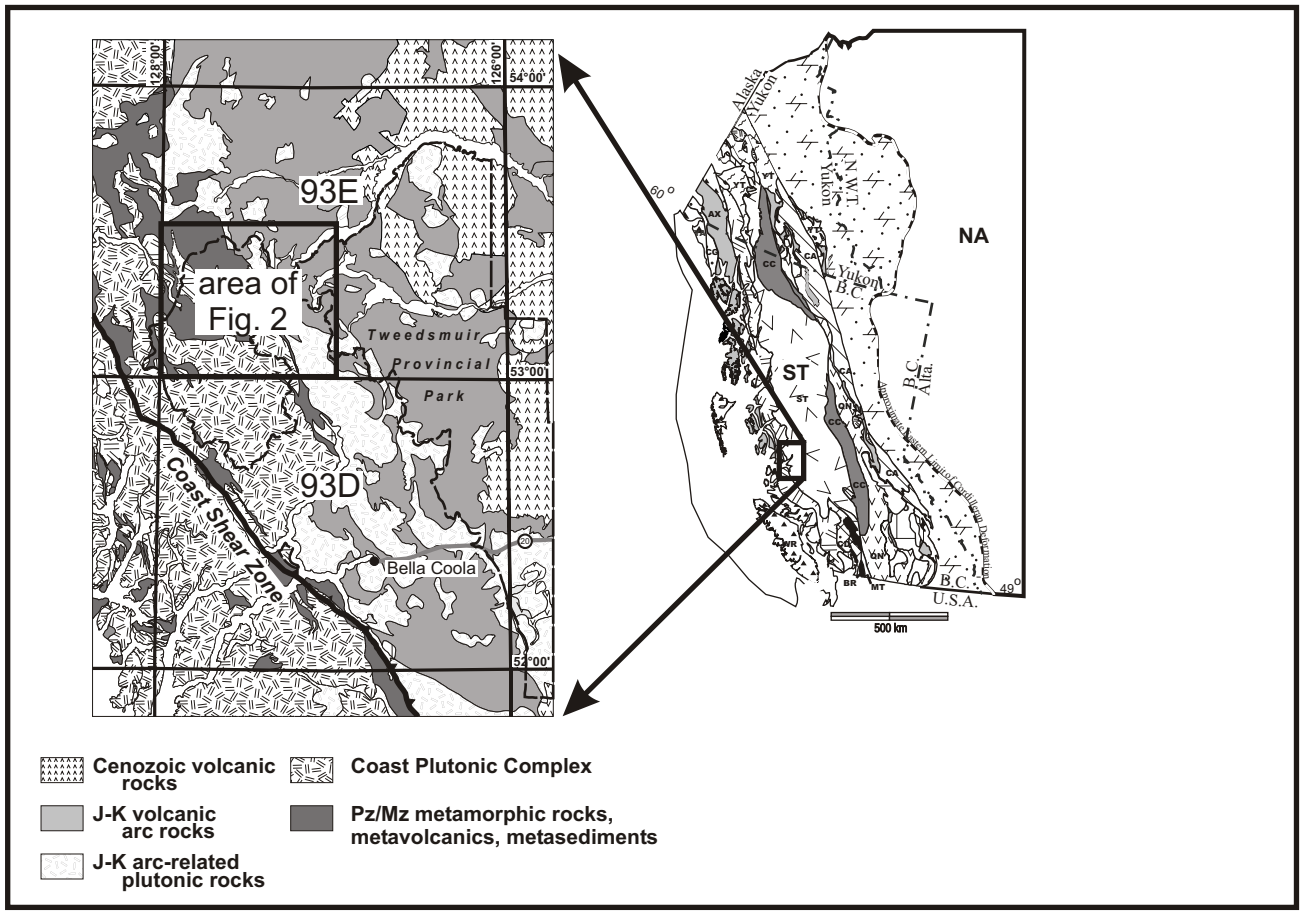


Figure 1. General geological setting of NTS 093D (Bella Coola) and 93E (Whitesail Lake) 1:250 000 map areas; inset map is a schematic terrane map of the Canadian Cordillera, modified from Wheeler and McFeeley (1991).

and occur in well-exposed, generally eastward-younging, gently dipping structural panels along the eastern margin of the Coast Plutonic Complex. These strata comprise a thick (>4 km), bimodal volcanic succession of basaltic and basaltic andesite flows and associated volcanogenic strata, interbedded with and overlain by rhyolitic tuff, lapilli tuff, tuff-breccia, tuffaceous sedimentary rocks and associated rhyolitic domes (Gordee *et al.*, 2005).

The homoclinal, eastward-dipping orientation of the Hazelton Group and available geochronological and biostratigraphic data suggest that Hazelton Group strata become progressively older to the west, with deeper levels of the volcanic system exposed adjacent to the Coast Plutonic Complex. In the southwestern Whitesail Lake map area, rocks

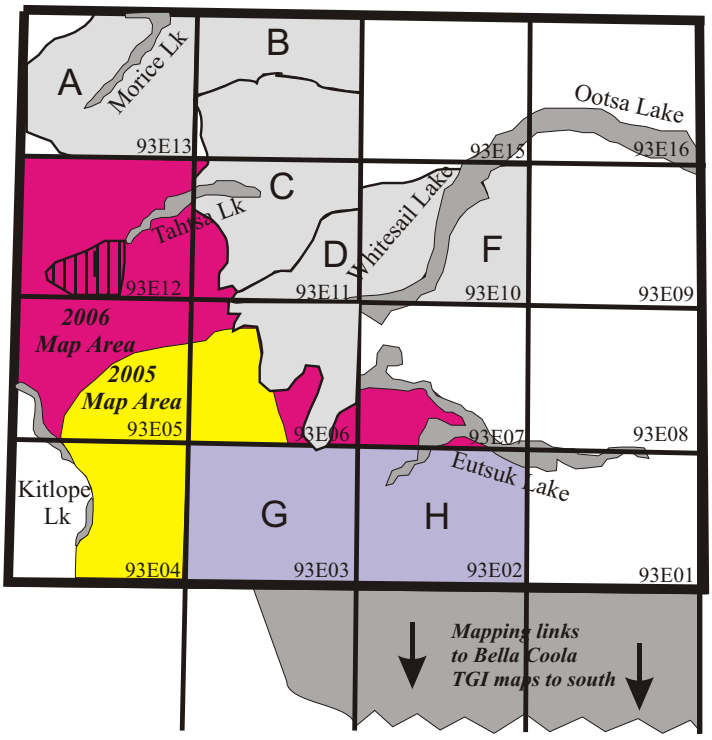


Figure 2. Geographic distribution of existing 1:50 000 geological maps in the Whitesail Lake map area, and the extent of mapping to be conducted under the Geoscience BC program. Light grey areas were mapped by BC Geological Survey teams (*ca.* 1985–1990; letters keyed to reference list); hatched area is thesis map of van der Heyden (1982); medium grey area was mapped by Bella Coola Targeted Geoscience Initiative project in Bella Coola area (NTS 093D; 2001–2003), and NTS 093E/02 and 03 were mapped under the auspices of Rocks to Riches Program (2004).

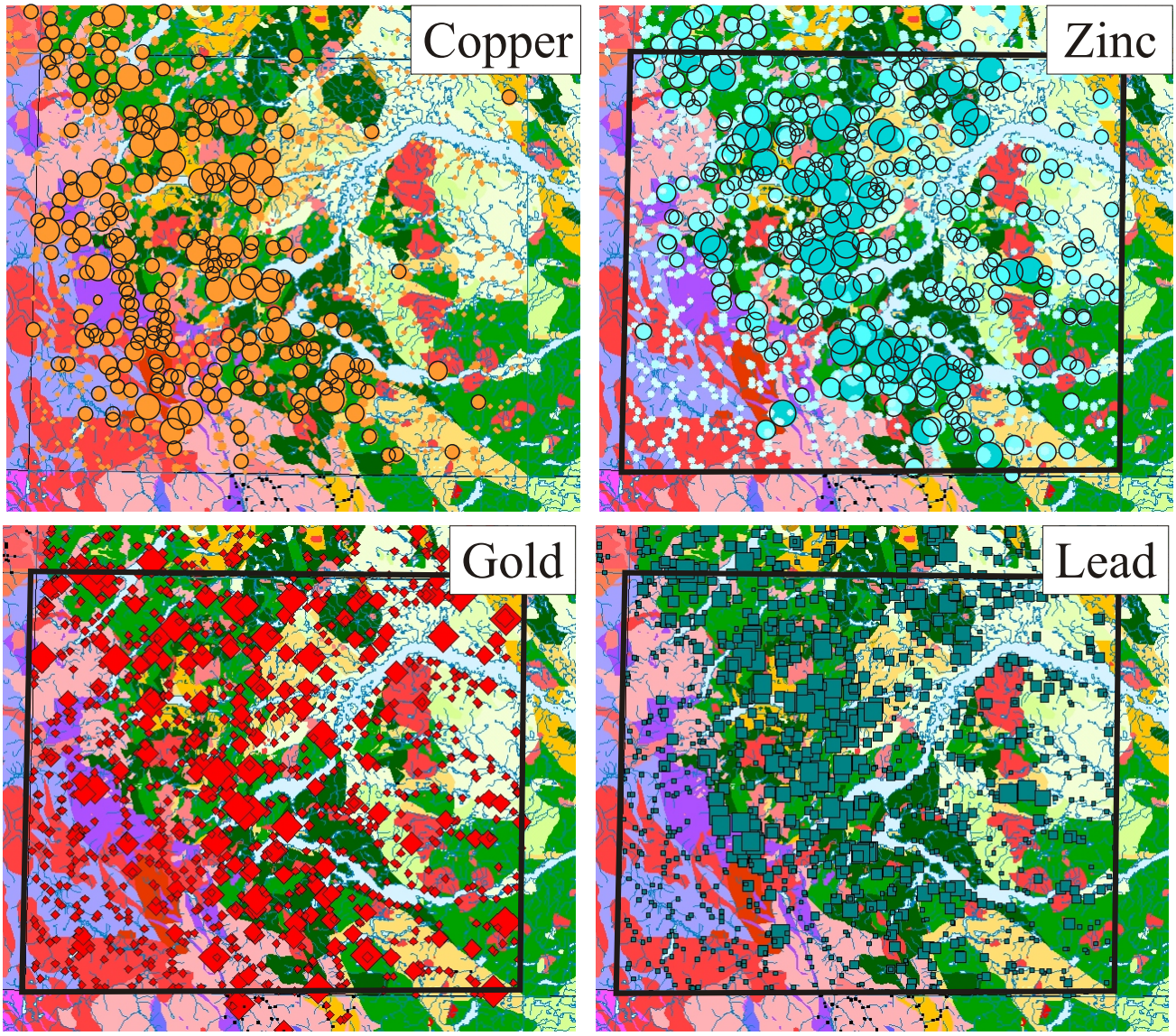


Figure 3. Regional stream sediment elemental anomaly maps for the Whitesail Lake map area. For each element, the relative size of the sample point indicates elemental abundance. Note strong concentration of anomalies along western edge of Mesozoic volcanic assemblages (BC Ministry of Energy, Mines and Petroleum Resources, 1986).

assigned to the Hazelton Group contain a higher proportion of mafic volcanic flows and lesser rhyolitic strata, and include intervals of dark, thin-bedded, fine-grained argillite, siltstone and sandstone. Sedimentary strata intercalated with andesitic flows south of Price Peak yielded a poorly preserved ammonite and bivalve fossil assemblage of Late Pliensbachian to Toarcian age (Haggart, 2005).

The east-to-west facies change to a higher proportion of fine-grained sedimentary strata intercalated with mafic volcanic flows within the Hazelton Group has resulted in previous misidentification of these strata as the Cretaceous Monarch assemblage (Mahoney *et al.*, 2005). It is now recognized, based on fossil ages on lithologically identical strata near Price Peak and on preliminary U-Pb ages (*ca.* 213 Ma) on volcanic strata north of Chatsquot Mountain, that volcanic strata in western Foresight Mountain (NTS 093E/03) and eastern Kitlope Lake (NTS 093E/04) map areas represent older, deeper components of the Hazelton Group stratigraphy. These strata are contained in a series of structural panels that are interpreted to represent an imbrication of several different stratigraphic-structural levels within a single volcanoplutonic-arc assemblage (Mahoney *et al.*, 2005). From the lowest structural level upward, these panels include 1) a foliated to nonfoliated hornblende quartz diorite complex with metavolcanic xenoliths (10–20%) and abundant, roughly east-west trending mafic dikes; 2) metavolcanic and metasedimentary screens (40–50%) within a 'matrix' of texturally and compositionally complex, locally magmatically foliated, biotite-hornblende, pyroxene-hornblende and hornblende diorite to quartz diorite; 3) massive basalt, basaltic andesite and andesite flows, associated tuff breccia and other fragmental rocks; and 4) volcaniclastic sedimentary rocks and associated pyroclastic strata. These structural panels are interpreted to represent 'slices' of a single volcanoplutonic-arc assem-

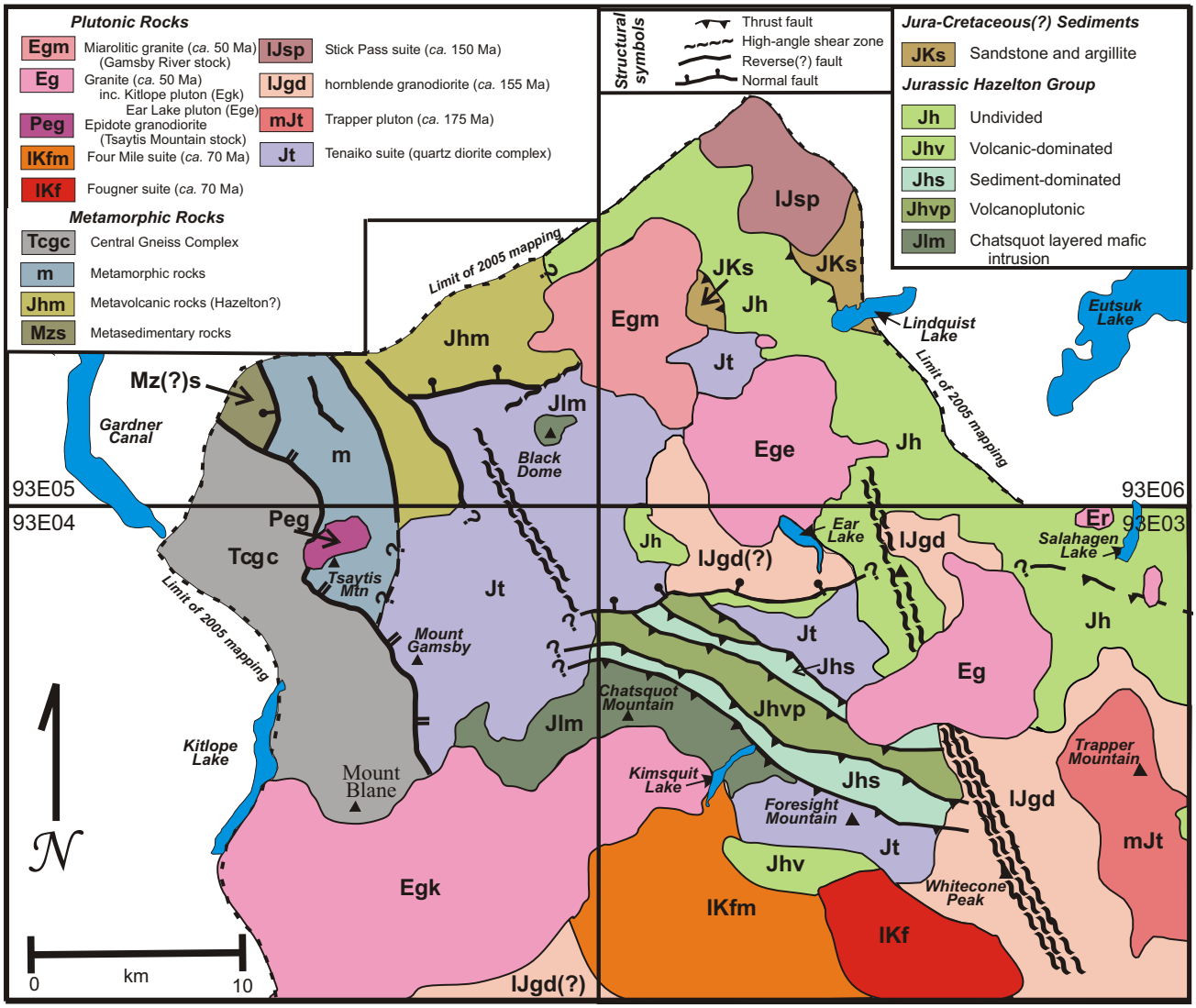


Figure 4. Generalized geology of the southwestern Whitesail Lake map area, showing major lithological units, structures and physiographic features referred to in the text.

blage, from the subvolcanic plutonic roots through the plutonic-volcanic intrusive contact to the surficial volcanic flows and associated volcanogenic sedimentary rocks (Fig. 3). In this succession, the rheologically weak sedimentary intervals tend to form décollement surfaces, whereas the massive flow units tend to be structurally resistant.

Chatsquot Layered Mafic Intrusion (Unit Jlm)

Spectacular exposures of a mineralized layered mafic intrusion (Jlm), exposed on Chatsquot Mountain and the ridges immediately to the southeast and northwest of the main massif, form an important component of the regional volcanic stratigraphy (Fig. 4, 5). Compositional banding in unit Jlm typically consists of variable proportions of olivine, pyroxene, plagioclase and magnetite, and ranges in composition from ultramafic magnetite-olivine websterite to anorthositic gabbro. The prominent foliation in the rock parallels the compositional layering and results in a distinctly layered appearance visible from several kilometres away. Typical compositional layers are less than 1 m thick, with clinopyroxene-rich gabbro (80% clinopyroxene) alternating with more plagioclase-rich layers that distinctly weather to a lighter colour (Fig. 5). Subordinate ultramafic layers include magnetite-olivine-rich rocks, apparent cumulate layers, which weather to a distinctive rusty brown, knobby surface. Along the ridge northeast of Chatsquot Mountain, unit Jlm is cut by numerous andesite porphyry dikes that locally exceed unit Jlm in volume and form intrusion breccias. Unit Jlm extends from Chatsquot Mountain to the southern end of the Mount Gamsby ridge, and also caps the high peaks near Black Dome, where the layered mafic intrusion appears as a large screen within the Tenaiko intrusive suite (Fig. 4).

Hazelton Group (Metamorphosed; Unit Jhm)

The Hazelton group consists of variably metamorphosed mafic to silicic volcanic and volcaniclastic rocks,

including andesitic to basaltic flows, tuff-breccia and tuff, with lesser argillite. The metamorphic grade varies widely and generally increases to the west. The metavolcanic rocks include abundant quartzofeldspathic schist and gneiss, epidote-chlorite schist and, locally, actinolite-bearing amphibolite. These rocks have previously been assigned to the Gamsby Group, a succession of pre – Lower Jurassic metasedimentary and metavolcanic rocks (Woodsworth, 1978, 1979, 1980), but are herein inferred to be metamorphosed equivalents of the Lower to Middle Jurassic Hazelton Group, based on their dominantly volcanic character and lack of carbonate interbeds.

Jurassic(?) Argillite and Sandstone (Unit JKs)

A thick argillite and sandstone unit forms the massif of Lindquist Peak, east of Mount Irma (Fig. 4). Although locally overturned, the succession dips to the north and northeast. The overall succession is approximately 2.5 km thick and consists of five alternating units of argillite and sandstone, although one or more of these may be thrust repeated, thereby diminishing the total thickness. Similar lithological facies make up the five sedimentary units, which are, in descending stratigraphic order: 1) an upper mixed argillite and sandstone package; 2) a dominantly argillaceous package, with minor interstratified sandstone; 3) a dominantly massive sandstone package, with minor shale interbeds; 4) a massive, strongly foliated argillite package; 5) a massive sandstone package, similar to 3; and 5) a basal mixed sandstone and argillite package.

The argillite is typically massive, often strongly bioturbated and locally includes lenticular bedding and fine sandstone and siltstone stringers with climbing ripple cross-stratification. Rounded calcareous nodules occur locally. Argillite typically displays strongly developed pencil cleavage and local orange-coloured oxidation. The sandstone is typically massive to cross-stratified, thin to medium bedded (up to 2 m) and fine to medium grained, although it can locally become coarse grained. Sandstone is micaceous but poorly sorted and mud rich, exhibiting flaser bedding and abundant bioturbation. Wood fragments are abundant and bivalve moulds are found as shell lag deposits in a fine-grained, calcareous-cemented facies.

The age of these strata is unclear, although it is likely they are post-Hazelton sedimentary rocks and possibly represent the base of the Jura-Cretaceous Bowser Lake Group in this region.

Mesozoic(?) Sedimentary Rocks (Unit Mzs)

In the southern portion of the Tsaytis River 1:50 000 map area (NTS 093E/05), a small fault block north of Tsaytis Mountain contains a rusty-weathering succession of brown to light grey, thin-bedded calcsilicate, micaceous phyllite and fine-grained quartzite. The metasedimentary rocks are tightly folded, displaying abundant mesoscale (0.25–1 m) tight to isoclinal folds. These rocks differ significantly from the metavolcanic rocks that dominate the region. These strata are potentially pre – Early Jurassic in age and may be correlative with continental margin strata of the Burke Channel assemblage described by Gehrels and Boghossian (2000).

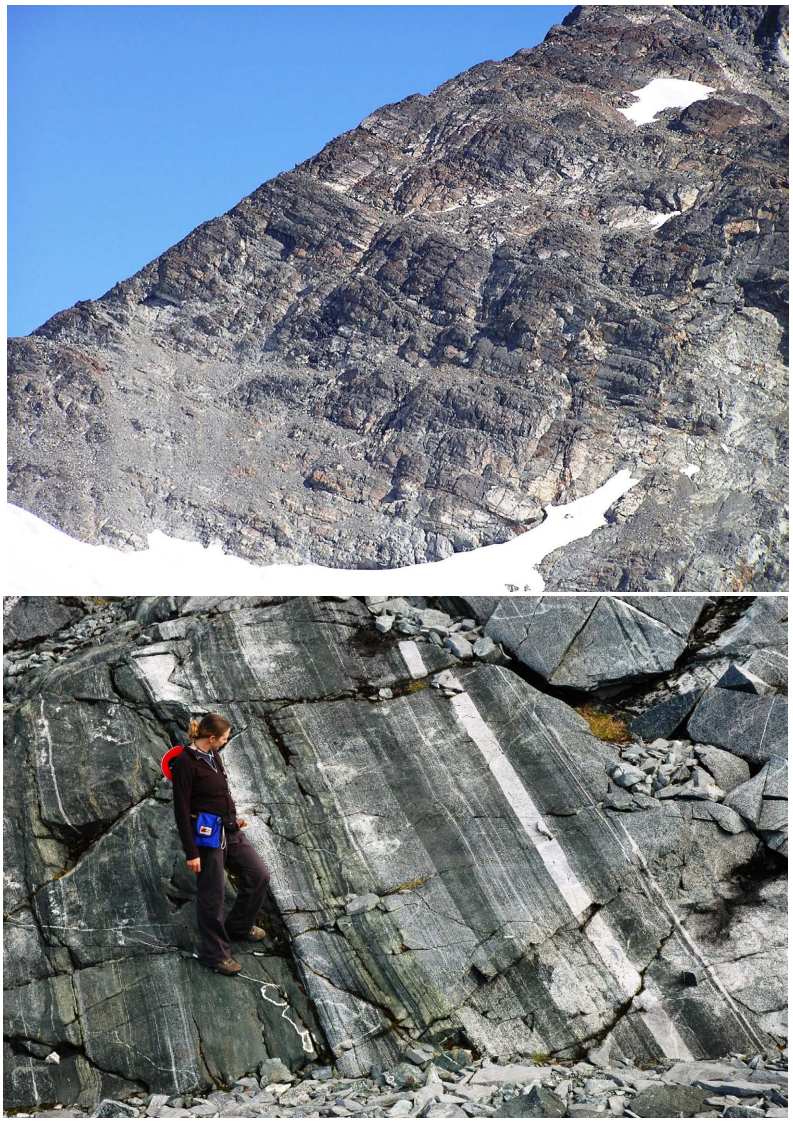


Figure 5. (Top) Layered mafic intrusion on the flanks of Chatsquot Mountain; (Bottom) distinct banding within the layered mafic intrusion on Gamsby Ridge.

PLUTONIC ASSEMBLAGES

Tenaiko Suite (Unit Jt)

The central portion of the map area is underlain by the Tenaiko Range, which is dominated by a heterogeneous assemblage of hornblende diorite to quartz diorite, characterized by complex intrusive relations with adjacent metavolcanic rocks and layered mafic intrusions (Fig. 4). The Tenaiko suite refers to a compositionally and texturally het-

erogeneous intrusive suite that ranges from a coarse-grained pyroxene-hornblende gabbro to medium to coarse-grained hornblende diorite to quartz diorite with lesser hornblende granodiorite. The suite contains locally abundant mafic and ultramafic xenoliths and metavolcanic screens ranging from a few centimetres to tens of metres in length. The density of the inclusions is variable, ranging from isolated mafic xenoliths to dense intrusion breccias with distinctive interlocking jigsaw clast boundaries (Fig. 6). Intrusive boundaries are highly irregular, with felsic stringers and dikelets invading adjacent country rock. The intrusive rocks are complexly foliated, locally displaying magmatic foliation surrounding entrained, structurally deformed metavolcanic screens, and locally displaying syndeformational folds and postdeformational tectonic foliations.



Figure 6. Tenaiko suite autoclastic breccia, consisting of angular mafic metavolcanic clasts within hornblende diorite.

The age of the Tenaiko suite is unclear. The suite is similar, in part, to rocks on Whitecone Peak and Crawford Peak that yield Late Jurassic U-Pb ages (*ca.* 154–155 Ma), and the suite clearly intrudes rocks mapped as Hazelton Group. However, the close spatial and compositional relationship between the more mafic components of the Tenaiko suite and the layered mafic intrusion (unit Jlm) suggests the Tenaiko suite may be subvolcanic with respect to unit Jlm, which is probably Early Jurassic in age. Geochronology on both packages is in progress.

Paleocene-Eocene Plutonic Rocks

TSAYTIS MOUNTAIN STOCK (PEG)

The Tsaytis Mountain stock is a medium-grained epidote-bearing biotite granodiorite to tonalite exposed on the north flank of Tsaytis Mountain (Fig. 4). The stock displays an upper intrusive contact with dark green pyroxene-hornblende gabbro and chloritic amphibolite, and an intrusive lower contact with quartzofeldspathic gneiss of the Central gneiss complex, and clearly intrudes the Central gneiss detachment fault (see below). The unit displays magmatic foliation defined by biotite segregations, and the foliation parallels the trace of the detachment structure. Geochronology for this unit is critical, as it will constrain the age of extensional faulting in the region.

KITLOPE PLUTON (UNIT EG)

The Kitlope pluton is a massive, homogeneous biotite granite to granodiorite that intrudes the Central gneiss complex southeast of Kitlope Lake. The unit is characteristically medium to coarse-grained, equigranular, locally K-feldspar porphyritic, biotite granite with clean, fresh books of biotite, white to pink K-feldspar, euhedral white plagioclase and large, anhedral quartz blebs. Oxidation of biotite leads to a distinct yellow weathering rind. The intrusive contact is generally sharp, with a locally well-developed intrusion breccia along the boundary. Preliminary age data suggest an Eocene age.

EAR LAKE PLUTON

The Ear Lake pluton is a pink, medium to coarse-grained, locally muscovite-bearing biotite granite. The unit is relatively homogeneous, with minor amounts of mafic xenoliths along the pluton margins and a minor component of aplite dikes. The pluton is cut by abundant east-trending, steeply north-dipping joints that produce blocky, angular talus. The unit intrudes rocks of the Hazelton Group and Tenaiko suite along a sharp irregular contact that seems to represent emplacement by passive inflation of overlying country rock.

GAMSBY RIVER STOCK (UNIT EGM)

The Gamsby River stock is a pink, medium to coarse-grained, miarolitic biotite granite. The pluton appears massive, homogeneous and undeformed. Adjacent to the margin, 30–50 m wide, locally flow-foliated granitic dikes with aplitic margins occur. The pluton has sharp, well-defined contacts with the Hazelton Group, associated metavolcanic rocks and the Tenaiko suite. The steep, near-vertical lateral margins, convex upward upper contact and presence of miarolitic cavities suggest diapiric emplacement at shallow crustal levels. The pluton yields a K-Ar age on biotite of 48.9 ±2.5 Ma (Wanless *et al.*, 1979), which is an uplift age, but the evidence for shallow emplacement suggests that this age approximates the timing of crystallization.

METAMORPHIC ASSEMBLAGES

Central Gneiss Complex (Unit Tvgc)

The eastern half of the Kitlope Lake (NTS 093E/04) 1:50 000 map area is underlain by a distinctive series of upper amphibolite to granulite-facies quartzofeldspathic gneisses that have been strongly deformed in a ductile fashion. These rocks are part of a broad belt of high-grade metamorphic rocks, referred to as the Central gneiss complex, that extends up the eastern edge of the Coast plutonic complex from about 53° to 56°N (Rusmore et al., 2005). In the southern Whitesail Lake map area, the Central gneiss com-



Figure 7. Tight folds with quartzofeldspathic gneiss of the Central gneiss complex, looking south toward Kitlope Lake.

plex is dominated by orthogneiss, including interleaved quartzofeldspathic gneiss, hornblende-biotite tonalitic gneiss, amphibolitic gneiss and lesser amphibolite. Mineralogy is predominantly quartz, plagioclase, hornblende and biotite, with locally abundant epidote. Pegmatitic garnet-bearing granitic dikes occur locally. Ductile deformation fabrics, primarily mesoscale (0.5–1.5 m amplitude) tight to isoclinal folds and associated axis-parallel foliation planes, are common (Fig. 7). The mean fold-axis orientation, estimated from the ridges north of Tsaytis Mountain (n = 29), is 53–143° (Fig. 8).

Paleocene(?) Metamorphic Rocks

The Central gneiss complex is exposed in the lower plate of a major low-angle extension fault that separates the gneiss complex from lower grade rocks in the upper plate (see below; Fig. 4). The upper plate consists of a series of imbricate structural panels of metaplutonic and metavolcanic rocks that distinctly decrease in metamorphic grade to the east of the detachment fault. Northwest of Black Dome, approximately 7–8 km east of the detachment fault, greenschist to locally lower amphibolite facies metavolcanic rocks are inferred to be metamorphosed Hazelton Group rocks (unit Jhm; Fig. 4). The area between these metavolcanic rocks and the detachment fault is underlain by an imbricated series of amphibolite, chloritic mafic metavolcanic rocks and strongly foliated diorite, tonalite and granodiorite that ranges in metamorphic grade from upper greenschist to upper amphibolite. The increased metamorphic grade and significantly higher proportion of metaplutonic rocks distinguish this succession from lower grade rocks to the east, and the presence of abundant chlorite distinguishes it from the Central gneiss complex to the west. The succession apparently consists of a number of imbricated structural panels that interleave metavolcanic and metaplutonic rocks of different metamorphic grade, and these rocks presumably represent a structural level intermediate between the Central gneiss complex and lower grade rocks of the upper plate to the east. Regionally, peak metamorphism in the Central gneiss complex is interpreted to be Paleocene in age (Hollister and Andronicos, 2000), and the spatial proximity and metamorphic similarity of these rocks to the Central gneiss complex suggests they are Paleocene in age.

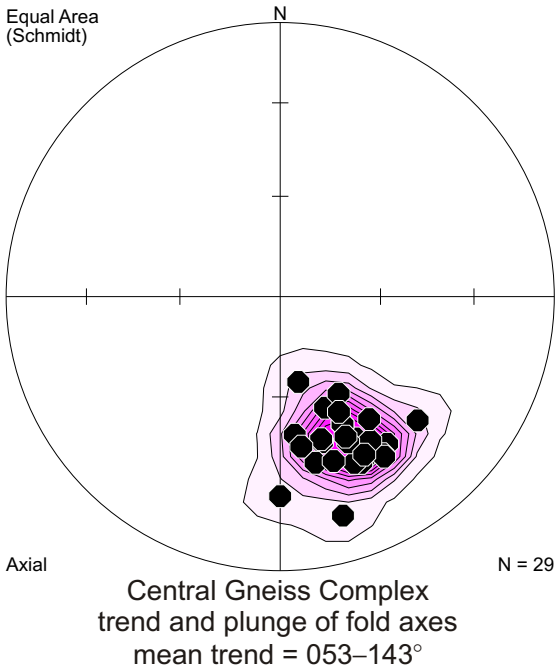


Figure 8. Stereonet of fold-axis orientations in Central gneiss complex northwest of Tsaytis Mountain.

STRUCTURAL FEATURES

Central Gneiss Detachment

The contact between high-grade gneissic rocks of the Central gneiss complex and lower grade rocks of the eastern Coast plutonic complex and western Stikine Terrane is commonly difficult to locate accurately. In the southwestern Whitesail Lake map area, upper amphibolite to granulite facies rocks of the Central gneiss complex are separated from greenschist to lower amphibolite grade rocks of the Tenaiko suite and Paleocene(?) metamorphic rocks by a low-angle, east-dipping detachment fault (Fig. 4). Northeast of Tsaytis Mountain, the upper plate of this structure contains imbricated structural panels of greenschist facies chloritic metavolcanic rocks, lower amphibolite facies metavolcanic rocks and metatonalite. The structural panels are apparently separated by steep, west-dipping faults of unknown displacement. These faults locally juxtapose amphibolitic metavolcanic rocks and metatonalite against greenschist facies metavolcanic rocks; in other cases, the metamorphic transition appears more gradational. These structurally interleaved panels decrease in metamorphic grade from west to east, and grade into subgreenschist to greenschist grade basaltic to andesitic metavolcanic rocks to the northeast. South of Mount Gamsby, the lower plate consists of the Tenaiko suite with locally abundant metavolcanic screens. The volume of plutonic rocks decreases to the south, where diorite of the Tenaiko suite intrudes mafic rocks of the Chatsquot layered mafic intrusion (Fig. 4). The detachment fault is exposed due west of Mount Gamsby, where high-grade rocks of the Central gneiss complex are structurally overlain by lower grade rocks of the Tenaiko suite across a low-angle, east-dipping shear zone. Elsewhere, the detachment structure is either not exposed or is intruded by a distinctive epidote-biotite granodiorite. However, the boundary between the upper and lower plates is readily recognized by the abundance of chloritic rocks in the upper plate and the absence of chlorite in the lower plate.

Contractional Structures

The western portion of the Foresight Mountain 1:50 000 map area (NTS 093E/03) is underlain by an imbricate stack of northeast-vergent thrust sheets that complexly imbricates various structural levels within the Hazelton Group. The primary décollement horizons are within sediment-dominated intervals, with the massive mafic volcanic units acting as structural buttresses. Regional mapping suggests this thrust system is continuous with the Late Cretaceous Mount Waddington fold-and-thrust system, exposed in the Bella Coola map area to the south (Haggart *et al.*, 2003, 2004). The system is truncated on its eastern side by a high-angle north-northwest-trending dextral shear zone that roughly parallels the Kimsquit River valley. This shear zone is cut by a biotite granite of presumed Eocene age, providing a minimum age for the contractional deformation. The northwestern extent of the thrust system is unclear. Rocks in the upper plate of the Central gneiss detachment are cut by numerous northwest-trending, steeply west-dipping structures that imbricate fault panels of differing metamorphic grade. These structures may represent deeper levels of the thrust system.

Translational Shear Zones

Several high-angle shear zones transect the area and cut all pre-Paleocene rock units. One of the larger shear zones parallels the Kimsquit River valley, extending north from the northern end of Dean Channel through Whitecone Peak and the eastern flank of Crawford Peak and continuing out of the area (Fig. 4). This shear zone continues south into the Bella Coola map area, where it apparently connects into the Pootlass shear zone (Haggart *et al.*, 2004). The shear zone is recognized in plutonic rocks by the presence of pervasive near-vertical fracture planes and locally in-

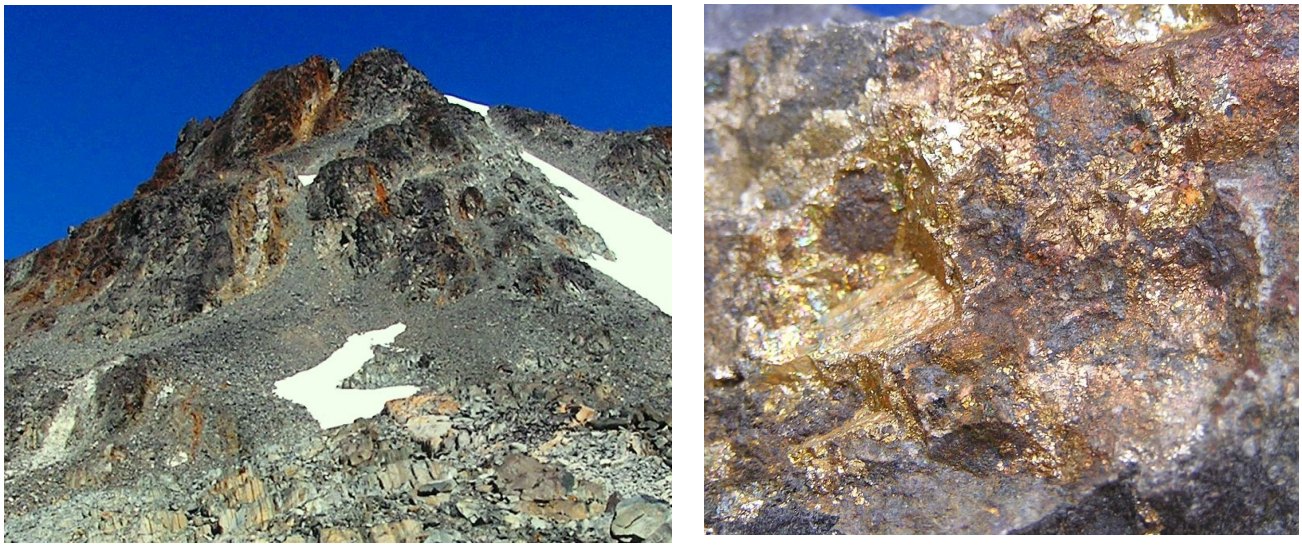


Figure 9. (Left) View looking north at the south flank of Chatsquot Mountain shows rusty gossan developed along pyrite-chalcopyrite veins near the top of the peak. (Right) Pyrite-chalcopyrite vein mineralization is most intense where localized along shear zones and along boundaries with Eocene(?) granite dikes crosscutting the Chatsquot layered mafic intrusion. Copper-nickel sulphide mineralization is also widely disseminated in individual pyroxenite and norite layers near the southern edge of the intrusion and along veins where sulphide minerals have been subsequently remobilized by hydrothermal fluids.

tense foliation development, manifested by mineral realignment and the stretching and reorientation of xenoliths and metamorphic screens. East of Crawford Peak, graphitic phyllite, chloritic schist, and clastic metasedimentary and metavolcanic rocks are incorporated into the shear zone, and dextral transpression is indicated by the orientation of kink bands and isoclinal folds with moderately plunging (30–35°) fold axes (Mahoney *et al.*, 2005). A second prominent shear zone extends from Chatsquot Mountain northwest toward Black Dome. This shear system is approximately 1–1.5 km wide and consists of chloritic schist, micaceous schist, local actinolitic schist, foliated hornblende diorite and granodiorite, and pods of pyroxene gabbro that are crosscut by syndeformational andesitic to basaltic dikes. The shear zone is characterized by northwest-trending foliation containing prominent, moderately northwest-plunging intersection and mineral-elongation lineations. The shear zone is flanked on both sides by the Tenaiko suite, suggesting a lack of major offset along the system. The shear zone must dissipate at its southern end, as it cannot be traced through the series of thrust faults mapped north of Chatsquot Mountain. The presence of high-angle shear zones at both ends of the thrust system suggests that the thrust system may represent a contractional step over at a restraining bend along a dextral transpressional system.

ECONOMIC POTENTIAL

The primary objective of this investigation is to evaluate the economic mineral potential of Mesozoic volcanogenic assemblages and Jurassic to Tertiary plutonic rocks in the southern Whitesail Lake map area. Preliminary analysis of bedrock geological mapping, both in the current map area and in areas to the east and southeast, suggests that there are three potential targets of economic importance.

Volcanogenic Massive Sulphide Deposits within the Hazelton Group

Preliminary facies analysis, geochronology and geochemistry from the southern Whitesail Lake map area (Gordee *et al.*, 2005) and the Bella Coola area to the south (Diakow *et al.*, 2003) indicate that these rocks are age equivalent to host rocks for the Eskay Creek volcanogenic massive sulphide (VMS) deposit, and are characterized by predominantly shallow-water deposition, probably in a rifted-arc setting. The similarities between these strata and those in the Eskay Creek area suggest that the Hazelton Group in the southern Whitesail Lake area is highly prospective for VMS mineralization. In a regional sense, Hazelton Group strata form an east-dipping homocline, with older, deeper strata exposed to the west. These strata also display a higher degree of structural and metamorphic alteration. However, the recognition of stratiform sulphide mineralization, primarily disseminated chalcopyrite, pyrite in bedded volcanogenic metasedimentary rocks, at several locations in metamorphosed Hazelton Group strata north of Black Dome (Fig. 4) indicates that there is VMS potential in western exposures of the Hazelton Group.

Chatsquot Layered Mafic Intrusion

The Chatsquot layered mafic intrusion (described above) may have potential for significant Cu-Ni sulphide and PGE mineralization. Some pyroxene-rich compositional layers (clinopyroxene gabbro) near the southwestern contact have substantial chalcopyrite (or Cu-Ni sulphide) mineralization, both as disseminated stratiform sulphides and sulphide veins (Fig. 9). Preliminary geochemical values in unmineralized gabbro indicate elevated Cu and Ni values (>130 ppm Cu, >400 ppm Ni); PGE assays are in progress.

Cu±Mo±Au Porphyry Mineralization

Paleocene and Eocene plutonic rocks in the southwestern Whitesail Lake map area are generally coarse grained, locally porphyritic granitic rocks that were apparently emplaced at relatively shallow levels. Intrusive contacts with adjacent country rock are generally sharp, although extensive (tens of metres) of variably mineralized intrusive breccia occur locally, and there is evidence of sulphide, primarily Cu and Mo, remobilization along some intrusive boundaries. Geochemical and geochronological studies of these plutons are underway, and assay samples collected from alteration zones adjacent to pluton margins have been submitted. The character of potential porphyry targets will be examined in detail during the course of this investigation.

ACKNOWLEDGMENTS

Danny Hodson of Rainbow West Helicopters provided outstanding helicopter support during this investigation. Adam Kjos and Kate Maclaurin provided excellent field assistance. Funding for this investigation was provided by the Geoscience BC program, the Geological Survey of Canada, the University of British Columbia and the University of Wisconsin – Eau Claire.

REFERENCES

British Columbia Ministry of Energy, Mines and Petroleum Resources (1986): Regional stream, lake sediment and water geochemical reconnaissance data, British Columbia; Geological Survey of Canada, Open File 1360, 145 pages.

Dawson, K.M., Panteleyev, A., Sutherland Brown, A. and Woodsworth, G.J. (1991): Regional metallogeny; Chapter 19 *in* Geology of the Cordilleran Orogen in Canada, Gabrielse, H. and Yorath, C.J., Editors, Geological Survey of Canada, Geology of Canada, no 4, pages 707–768.

Diakow, L.J., Mahoney, J. B., Gleason, T.G., Hrudey, M.G., Struik, L.C. and Johnson, A.D. (2002): Middle Jurassic stratigraphy hosting volcanogenic massive sulphide mineralization in the eastern Bella Coola map area (NTS 093/D), southwest British Columbia; *in* Geological Fieldwork 2001, *BC Ministry of Energy, Mines and Petroleum Resources*, Paper 2002-1, pages 119–134.

Diakow, L.J., Mahoney, J.B., Haggart, J.W., Woodsworth, G.J., Gordee, S.M., Snyder L.D., Poulton, T.P., Friedman, R.M. and Villeneuve, M. (2003): Geology of the eastern Bella Coola map area (93D), west-central British Columbia; *in* Geological Fieldwork 2003, *BC Ministry of Energy, Mines and Petroleum Resources*, Paper 2002-1, pages 65–75.

Gehrels, G.E. and Boghossian, N.D. (2000): Reconnaissance geology and U-Pb geochronology of the west flank of the Coast

Mountains between Bella Coola and Prince Rupert, coastal British Columbia; *in* Stowell, H.H. and McClelland, W.C., Editors, Tectonics of the Coast Mountains, Southern Alaska and British Columbia, Geological Society of America, Special Paper 343, pages 61–75.

Gordee, S.M., Mortensen, J.K., Mahoney, J.B. and Hooper, R.L. (2005): Volcanostratigraphy, lithogeochemistry and U-Pb geochronology of the upper Hazelton Group, west-central British Columbia: implications for Eskay Creek – type VMS mineralization in southwest Stikinia; *in* Geological Fieldwork 2004, *BC Ministry of Energy, Mines and Petroleum Resources*, Paper 2005-1, p. 311–322.

Haggart, J.W. (2005): Report on Jurassic fossils from Whitesail Lake map area (93E), British Columbia; *Geological Survey of Canada*, unpublished Paleontological Report JWH-2005-01, 2 pages.

Haggart, J.W., Diakow, L.J., Mahoney, J.B., Struik, L.C., Woodsworth, G.J. and Gordee, S.M. (2004): Geology, Bella Coola area (parts of 93D/01, D/02, D/06, D/07, D/08, D/09, D/10, D/11, D/15 and D/16), British Columbia; *Geological Survey of Canada*, Open File 4639 and *BC Ministry of Energy, Mines and Petroleum Resources*, Open File 2004-13, scale 1:150 000.

Mahoney, J.B., Hooper, R.L., Gordee, S.M., Haggart, J.W. and Mortensen, J.K. (2005): Initial evaluation of bedrock geology and economic mineralization potential of southern Whitesail Lake map area (92E/02, 03), west-central British Columbia; *in* Geological Fieldwork 2004, *BC Ministry of Energy, Mines and Petroleum Resources*, Paper 2005-1, pages 291–299.

MINFILE (2005): MINFILE BC mineral deposits database; *BC Ministry of Energy, Mines and Petroleum Resources*, URL <http://www.em.gov.bc.ca/Mining/ Geolsurv/Minfile/> [Nov 2005].

Rusmore, M.E., Woodsworth, G.J., and Gehrels, G.E., 2005, Two-stage exhumation of midcrustal arc rocks, Coast Mountains, British Columbia; Tectonics, vol. 24, TC5013, doi:10.1029/2004TC001750.

van der Heyden, P. (1982): Tectonic and stratigraphic relations between the Coast Plutonic Complex and Intermontane belt, west-central Whitesail Lake map area, British Columbia; *University of British Columbia*, M.Sc. thesis, 172 pages.

Wanless, R.K., Stevens, R.D., Lachance, G.R. and Delabio, R.N. (1990): Age determinations and geological studies, K-Ar isotopic ages, report 14; *Geological Survey of Canada*, Paper 79-2, 67 pages.

Wheeler, J.O. and McFeely, P., Compilers (1991): Tectonic assemblage map of the Canadian Cordillera and adjacent parts of the United States of America; *Geological Survey of Canada*, Map 1712A, 2 sheets at 1:2 000 000 scale.

Woodsworth, G.J. (1978) Eastern margin of the Coast Plutonic Complex in Whitesail Lake map area, British Columbia; *in* Current Research, Part A, *Geological Survey of Canada*, Paper 78-1A, pages 71–75.

Woodsworth, G.J. (1979): Geology of Whitesail Lake map-area, British Columbia; Current Research, Part A, Geological Survey of Canada Paper 79-1A, p. 25-29.

Woodsworth, G.J. (1980): Geology of Whitesail Lake (93E) map area, BC; *Geological Survey of Canada*, Open File 708, 1 map sheet at 1:250 000 scale.

ADDENDUM

PROGRAM PURPOSE AND SCOPE

This fieldwork article reports the preliminary findings of a bedrock mapping project designed to examine the western side of the Whitesail Lake, 1:250 000-scale map area. The principal goal of this investigation is detailed geologic mapping (1:50 000 scale) and economic mineral assessment of the eastern Coast Plutonic Complex and western Stikinia in the southwestern and western Whitesail Lake map-area.

Stream sediment geochemistry, MINFILE data and detailed geologic mapping farther north in Whitesail Lake map-area, and to the south (eastern Bella Coola map-area), indicate potential for volcanogenic massive sulphide, Cu±Mo±Au porphyry, and Ni-Cu-Cr-PGE mineralization.

The primary objective of this current program is to establish the geologic framework for potential economic mineralization in the region, as opposed to targeting specific mineral occurrences. Documentation of the regional structure, stratigraphy, geochemical character and geochronology benefits not only local but also regional exploration programs. The area under investigation includes the area surrounding the Kitlope Heritage area and the areas along the western edge of Tweedsmuir Park (Figure 1). Our goal is to establish the regional geologic framework with respect to potential economic mineralization. Maps from this investigation will be linked with our mapping to the east (Mahoney *et al*., 2004), south (Haggart *et al*., 2004) and the northeast (numerous BCGS maps) to provide comprehensive regional coverage of a significant portion of the eastern Coast Belt.

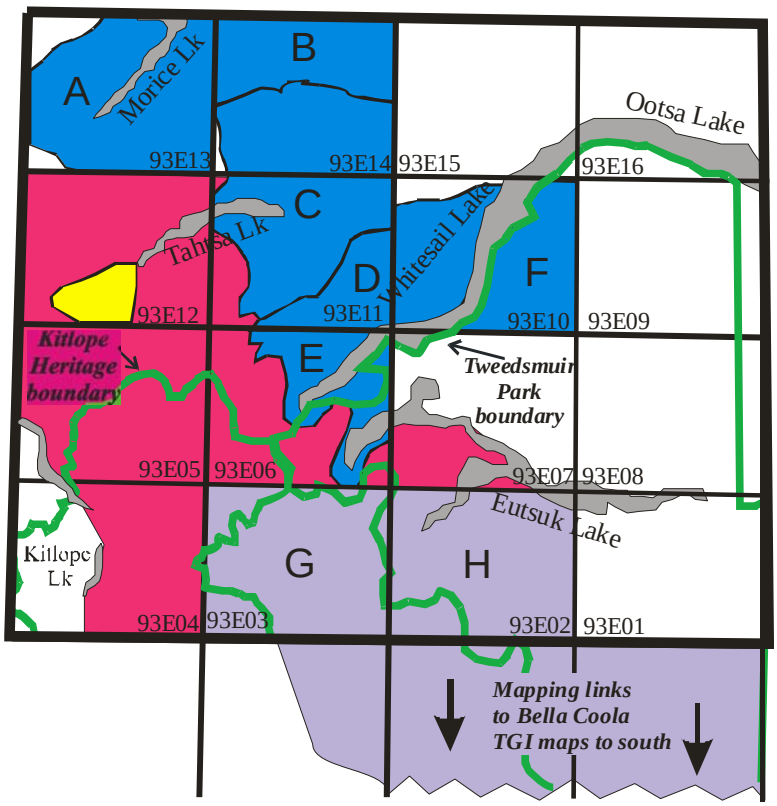


Figure 1: Geographic distribution of existing 1:50,000 geologic maps in the Whitesail Lake map area, and the extent of proposed map area (shown in red). Blue areas were mapped by BCGS teams (ca 1985-1990; letters keyed to reference list); yellow area is thesis map of van der Heyden (1982); purple area was mapped by Bella Coola TGI project in Bella Coola area (93D; 2001-2003), and 93E2/3 were mapped under auspices of Rocks to Riches program (200

Update on the Mineral Deposit Potential of the Nootka Sound Region (NTS 092E), West Coast of Vancouver Island, British Columbia[1]

By D. Marshall[2], M. Lesiczka[2], G. Xue[2], S. Close[2] and K. Fecova[2]

KEYWORDS: Nootka Sound, ore deposits, metamorphism, Sicker, Westcoast Crystalline Complex, geochemistry, layered ultramafic

INTRODUCTION

The Nootka Sound region is host to a few small ore deposits. These are skarns (Ford and Silverado) and intrusion-related Au mineralization, such as the Privateer in the Zeballos camp. The area was mapped in the 1980s by Muller *et al.* (1981), a large portion being categorized as a metamorphic complex representative of mid-crustal level rocks. This oversimplification and misidentification of metamorphic grade in the area, combined with difficult access and terrain, have made exploration difficult. Preliminary work in the Nootka Sound region indicated that the rocks in the area were locally contact metamorphosed by the Jurassic Island and Tertiary Mount Washington intrusive suites, but had not been subjected to high-grade regional metamorphism and thus could be correlated with the rock units in the southern parts of Vancouver Island (cf. Massey, 1991; Massey, 1995; Yorath *et al.*, 1999; DeBari *et al.*, 1999;). Potential correlations of these rocks with the Sicker Group also makes these rocks prospective for volcanogenic massive sulphide (VMS) – type mineralization, such as at Myra Falls (Barrett and Sherlock, 1996).

The primary goals of this study are to promote exploration in the area through improved geological mapping, lithogeochemistry, metallogeny and mineral-deposit studies. This paper summarizes this summer's mapping and some preliminary lithogeochemistry, which are part of a Geoscience BC project focused on improving the bedrock mapping in the Nootka Sound area. Basic prospecting and sampling were undertaken during the mapping. Work continues on completion of a lithogeochemistry study of the various rock types and on a revised metallogenic interpretation of the area, based on new mapping, geochemistry and geochronology.

LOCATION, ACCESS AND PHYSIOGRAPHY

The Nootka Sound region (Fig. 1) occupies a large portion of the west-central half of Vancouver Island. The study region is mostly coastal in nature and comprises many islands, fjords, channels and inlets. The most notable of these are Bligh Island, Muchalat Inlet, Tlupana Inlet, Shelter Inlet, Sydney Inlet, Stewardson Inlet, Zuciarte Channel and Millar Channel. The region is relatively rugged and heavily vegetated with rain forest, with some portions of it having been logged.



Figure 1. Location of the study area on the west coast of Vancouver Island.

Logging roads connected to the main road grid are accessed from the Gold River, Tofino, Zeballos and Tahsis roads. There are many additional logging roads not connected to the main road network, including the Conuma, Stewardson, Zuciarte, Escalante, Silverado and Houston main forestry roads (mainlines). Access to the field area this summer was by four-wheel-drive truck on logging roads connected to the main grid. Boats and fixed-wing aircraft were generally used to get to logging camps. A few weeks of coastal geological mapping were carried out using a variety of boats

PREVIOUS WORK

Previous work in the area has been carried out by a number of authors. Most notably, Muller *et al.* (1981). Two other important publications that describe similar rocks outside the study area are DeBari *et al.* (1999) and Yorath *et al.* (1999). Publications specific to mineralization in the area are Stevenson (1938, 1939, 1950), Muller *et al.* (1981), Sinclair and Hansen (1983), Hansen and Sinclair

[1] *Geoscience BC contribution GBC009*

[2] *Department of Earth Sciences, Simon Fraser University, Burnaby, BC (marshall@sfu.ca)*

This publication is also available, free of charge, as colour digital files in Adobe Acrobat PDF format from the BC Ministry of Energy, Mines and Petroleum Resources internet website at http://www.em.gov.bc.ca/Mining/Geolsurv/Publications/catalog/catfldwk.htm

(1984) and Marshall *et al.* (2004) for the intrusion-related Au or 'Zeballos'-type mineralization. The other deposit types in the area, including vein, skarn and replacement types, are listed in Muller *et al.* (1981) and the interested reader is referred to that publication for additional references.

REGIONAL GEOLOGY

The study area is part of the Insular Belt of the Canadian Cordillera comprising a number of accreted volcanic terranes (Jones *et al.*, 1977; Wheeler *et al.*, 1991). Thus, the area consists mostly of metavolcanic rocks and their plutonic counterparts. Regional deformation is not pronounced. However, some rocks locally display minor tectonic foliation. Regional metamorphic grade in the area ranges up to middle greenschist facies. Local contact metamorphism around the intrusive rocks ranges from greenschist to migmatite, with many examples of partially melted inclusions of country rock. There are abundant brittle faults in the area, ranging from local to regional in scale. In most cases, the volcanic rocks are greenschist equivalents of Sicker, Bonanza and Karmutsen volcanic rocks. The volcanic rocks are, in most cases, impossible to distinguish in the field; it is virtually impossible to distinguish Sicker and Bonanza volcanic rocks in the study region even using geochemistry. The intrusive rocks are typical of the Jurassic Island and the Tertiary Mount Washington intrusive suites. Some of the more altered intrusive rocks may also be related to Sicker volcanism.

ROCK TYPES

A preliminary geology map (Fig. 2) and stratigraphic column (Fig. 3) for the rocks of the Muchalat Inlet area have been derived from field observations, airphotos and previously published reports and maps. Most of this year's mapping was concentrated in the areas surrounding and between Muchalat and Stewardson Inlets.

Older Basement Rocks

The older basement comprises fine-grained mafic rocks and more coarse grained intrusive rocks. The finer grained rocks appear to be mostly dikes or flows and exhibit no textures characteristic of extrusive volcanic rocks. Both fine-grained and coarser grained older basement rocks have been altered. Muller *et al.* (1981) mapped these rocks as Paleozoic and Mesozoic. Distinctive geochronological relationships with most of the rocks in the area are absent, but the higher degree of alteration observed in these rocks was not seen in either the Jurassic intrusive rocks or the Triassic extrusive rocks. Thus, it is inferred that these rocks are pre-Triassic. However, the altered coarse-grained rocks may be as young as early Jurassic and experienced a higher degree of alteration due to emplacement at depth. Geochronological work is underway to determine the exact age of the rocks.

FINE-GRAINED VOLCANIC AND HIGHER LEVEL INTRUSIVE FINE-GRAINED ROCKS (UNIT PMV)

These rocks are light to medium grey on fresh surfaces and dark brown/maroon on weathered surfaces. Grain size ranges from fine-grained (aphanitic to a few millimetres) basalt-dacite to a plagioclase-phyric basalt-dacite and locally even a plagioclase-hornblende-phyric basalt-dacite. Plagioclase and hornblende phenocrysts are up to 2 mm in diameter. The contacts between the different types of volcanic rocks are diffuse. There are varying amounts of alteration, with chlorite, yellow-green epidote-quartz veinlets up to 2 cm wide, and very small stringers (0.5 mm) of sulphide minerals. The volcanic rocks are intruded by dikes up to 3 m in width, veinlets of hornblende diorite and biotite-hornblende diorite, and rhyolite dikes. Within the volcanic rocks, there are dikes, patches and veinlets of equigranular coarser grained (2–3 mm) gabbro-like material resulting from partial remelting and recrystallization. The volcanic rocks are highly fractured and deformed within brittle faults and shear zones.

COARSE-GRAINED INTRUSIVE ROCKS (UNIT PMA_V)

These rocks, which are dark grey to whitish when fresh and white to tan brown when weathered, range from diorite to hornblende diorite (with abundant mafic minerals) to hornblende granodiorite. The intrusive rocks are equigranular and coarse grained, with grain size varying from 1 to 5 mm with generally finer grained mafic phases. There is epidote alteration and epidote-quartz veining along fractures. Abundant, fine-grained, rounded to angular volcanic inclusions generally range up to 30 cm in length, with some up to 3 m. There are abundant examples of local remelting and recrystallization of some of the volcanic clasts. Some basaltic inclusions have been completely recrystallized to fine-grained hornblende diorite. The intrusive rocks are themselves intruded by many basaltic dikes up to 1.5 m wide and striking generally 330–360° with steep dips.

Mooyah Formation (Unit PMm)

The Mooyah Formation comprises sedimentary and volcaniclastic rocks of various types. The rocks are best exposed in Mooyah Bay, on Anderson Point and along the northeastern parts of Zuciarte Channel. The rocks are interbedded cherty shale, sandstone-greywacke and conglomerate of turbidite sequences. Layers are generally up to 20 cm thick, although some of the more cohesive sandstone layers are up to 1 m and some pebble conglomerate layers are up to 2 m. Finely layered (1–2 cm) shaly beds are mostly found interbedded with coarser, more massive layers of sandstone and/or siltstone-sandstone. The sandy layers are pebble rich, with abundant (30%) white-weathering feldspar-rich clasts in a sandy matrix. The silty-sandy rocks have interlayered light and dark grey laminations up to 1 m thick. Some layers contain feldspar crystals and small pebbles (4 mm) of chert, and can locally be gossanous. There are also alternating sandy and silty crystal tuffs with very subtle layering. The crystal tuffs have 3–4 mm feldspar and hornblende crystals and smaller shaly clasts. The conglomeratic rocks have well-rounded fragments of volcanic rock up to 8 cm long, smaller fragments (2 cm) of a more felsic volcanic phase, quartz and feldspar fragments, and some hornblende crystals ranging up to 5 mm in a very fine grained volcanic matrix with no visible bedding. There are also minor beds of limestone and fine-grained diopside-garnet skarn at a few locations. The finer grained sedimentary rocks can be massive and have well-developed bedding with northeasterly strikes. They are light grey to black when fresh and a buff to rusty brown colour on the weath-

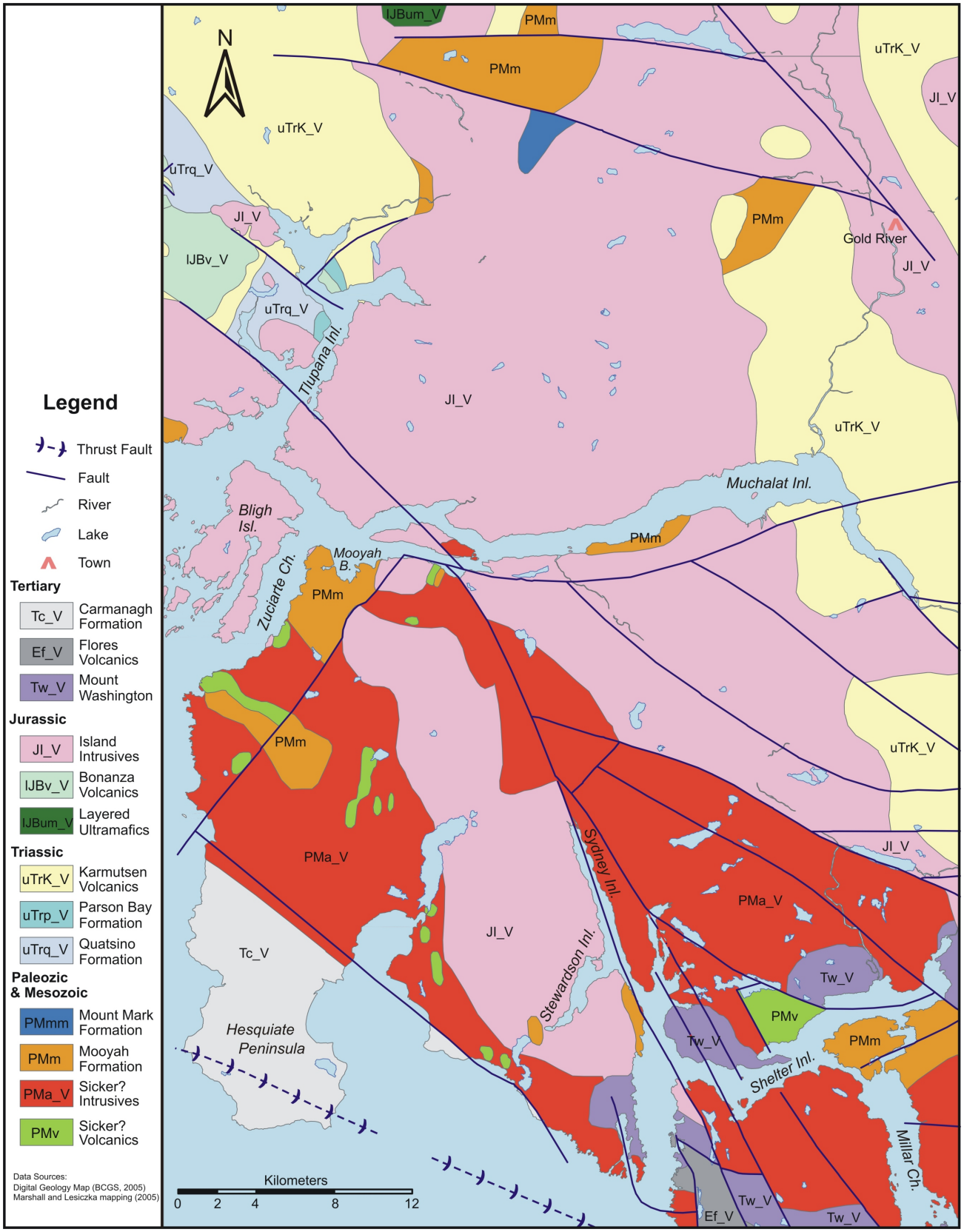


Figure 2. Preliminary geology of the study area, Nootka Sound region (after Muller *et al.*, 1981).

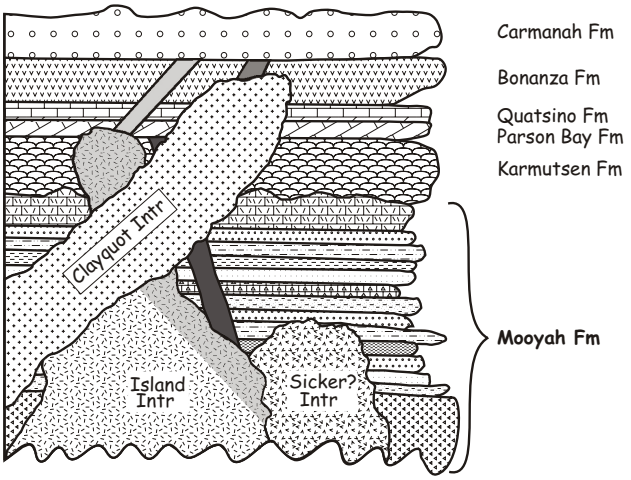


Figure 3. Idealized stratigraphic column. Unit thicknesses are not to scale. The base of the newly named Mooyah Formation is potentially equivalent to the McLaughlin Ridge Formation (Yorath *et al.*, 1999) and the lower parts of the Mooyah Formation are possibly correlative with the Fourth Lake Formation (Yorath *et al.*, 1999). The upper calcareous units of the Mooyah Formation may be possible correlatives with the Mount Mark Formation (Yorath *et al.*, 1999). Note that the intrusive rocks labelled as Sicker intrusive rocks are not dated and no contact relationships have been established in the field. Thus, these rocks may be an early generation of the Jurassic Island intrusive suite or as old as upper Paleozoic.

ered surface. Fining-upward sequences, ripple marks and rip-up clasts in number of locations indicate tops up in all locations displaying geopetal indicators.

The Mooyah Formation is intruded by diorite, rhyolite and mafic dikes (Fig. 4), and cut by quartz veins with minor epidote. There are some fine-grained epidote clasts (5 cm) and epidotized patches. The rocks are slightly deformed by fracturing and shearing, as well as by broad, low-amplitude folds that indicate antiformal closure to the north. The total thickness of the package is difficult to estimate due to possible apparent thickening from folding and fault repetition; however, the total package is estimated to be on the order of 1 km in thickness. Although the geochronology of the Mooyah Formation is not yet established, the authors have interpreted it as pre-Triassic. The volcaniclastic rocks of the lower Mooyah Formation may be correlative with the McLaughlin Ridge Formation, while the upper Mooyah Formation is probably correlative with the Fourth Lake Formation (Yorath *et al.*, 1999).

Mount Mark Formation (Unit PMmm)

The Mount Mark Formation (Yorath *et al.*, 1999) is exposed in the north-central portion of the study area (Fig. 2). The exposures here are several hundred metres thick and form highly visible light grey cliffs along the Conuma mainline. Layer thicknesses vary from a few centimetres to tens of metres. The layers are broadly to tightly folded and, in general, the Mount Mark Formation in this area is a tremolite marble, with minor occurrences of diopside marble. Marble formation is due to the intrusion of the nearby Jurassic Island intrusions.

Karmutsen Formation (Unit uTrK_V)

The Karmutsen rocks were not studied in detail. In general, the Karmutsen volcanic rocks (uTrK_V) are a relatively thick (~4 km) Triassic succession of dominantly pillow and massive basalt with comagmatic dikes and sills, and minor sedimentary and volcaniclastic rocks (Yorath *et al.*, 1999).

Quatsino and Parson Bay Formations (Units UTrq_V and UTrp_V)

The Triassic Parson Bay Formation is not well represented in the study area. The few outcrops observed were shaly limestone and were consistent with other descriptions of this rock type (cf. Muller *et al.*, 1969, 1981; Jeletzky, 1976; Yorath *et al.*, 1999). Likewise, outcrops of the Triassic Quatsino Formation are not abundant and the reader is directed to other publications for more detailed discussions of these rocks (cf. Muller *et al.*, 1974, 1981; Jeletzky, 1976; Yorath *et al.*, 1999).

Island Intrusive Suite (Unit JI_V) and Layered Ultramafic Rocks (Unit IJBum_V)

Rocks from the Jurassic Island intrusive suite vary from biotite-hornblende granodiorite to biotite-hornblende diorite (Fig. 5). The rocks are black and white on fresh surfaces and white on weathered surfaces. They are equigranular coarse grained (up to 8 mm) with occasional (1 cm) quartz veins. There are numerous volcanic inclusions that range from angular to rounded and are generally up to 30 cm in length, with few up to 1 m. The clasts can be fine-grained basalt to completely recrystallized finer grained mafic diorite. Clasts with partly recrystallized hornblende and plagioclase edges and remnant basalt cores are evidence of partial remelting and migmatization of the



Figure 4. Fine-grained felsic dike, approximately 2 m in width, cutting the flat-lying undisturbed sedimentary rocks of the Mooyah Formation at Anderson Point near Mooyah Bay, Muchalat Inlet.

clasts. Within the diorite, there are also very large screens (tens of metres) of layered Mooyah sedimentary rocks. The Island intrusive rocks are intruded by a number of different types of dikes, ranging from fine-grained granitic dikes (4 cm wide), mafic plagioclase-phyric dikes, aphanitic rhyolite/dacite dikes (1 m) and diorite dikes (40 cm wide) to mafic basalt-gabbro dikes up to 1.5 m in width. The rocks are locally fractured and sheared, but to a much lesser degree than the basement rocks. There is some vein-type mineralization along faults and shears, with minimal amounts of hydrothermal alteration comprising fine-grained chlorite, epidote and quartz along fractures.

The new ultramafic unit found on the upper reaches of the Conuma mainline consists of layered gabbro and pyroxenite (Fig. 6). The pyroxenite layers vary up to 60 cm in thickness and comprise relatively coarse grained (5 mm) equigranular pyroxene, phlogopite and plagioclase. The pyroxene constitutes 85% of the rock, with 10% phlogopite and 5% plagioclase making up the remainder. The gabbroic layers are generally thinner, ranging up to 30 cm, and comprise equal amounts of equigranular plagioclase and pyroxene, with grain sizes ranging up to 7 mm. This unit is arbitrarily assigned to the Jurassic. No contact relationships were observed with the surrounding Jurassic Island intrusive suite or the neighbouring Karmutsen rocks; thus, the layered ultramafic rocks might be Triassic.

Bonanza Group Rocks (Unit lJBv_V)

The Triassic Bonanza Group rocks are considered to be dominantly the extrusive equivalents and associated minor sedimentary rocks of the Island intrusive suite. These rocks outcrop in the northern portions of the study area and also to the west, on Nootka Island. The Bonanza rocks are calcalkaline pyroclastic rocks and associated hypabyssal rocks (Yorath *et al.*, 1999). The rocks tend to weather a slightly reddish colour and are generally dark grey on the fresh surface. The entire suite tends to be plagioclase phyric, with the plagioclase phenocrysts ranging up to several millimetres in length. These rocks were not studied in detail during this field season and no attempt has been made to subdivide the group into subunits, as in Jeletzky (1954), Muller *et al.* (1981) and Yorath *et al.* (1999).

Mount Washington Intrusive Rocks (Unit Tw_V)

Tertiary intrusive rocks are difficult to distinguish from the Jurassic Island intrusive suite. In the field, they have been distinguished by their large plagioclase phenocrysts in a finer grained matrix and fresher mafic minerals. The rocks range in composition from granodiorite to diorite, with matrix grain size varying up to 4 mm and porphyritic plagioclase ranging up to 1 cm. The mafic contents vary up to 15%, with amphibole generally the dominant mafic phase but usually accompanied by biotite. The fresh surface is generally white with black mafic minerals and aphanitic basalt to ghosted diorite clasts. Clasts are rare compared to the Island intrusive suite, but they can range in size up to 30 cm and, in some rare cases, constitute up to 10% of the rock. The weathered surface is generally a light tan to white colour.

MINERALIZATION POTENTIAL

The study region is host to a number of different deposit types. The largest of these are the Silverado mine and associated mineralization, such as the Baltic and Danzig. These are recorded as skarn and replacement-type deposits in limestone and Island intrusive rocks (MINFILE 082FSW323; MINFILE, 2005). The combined deposits

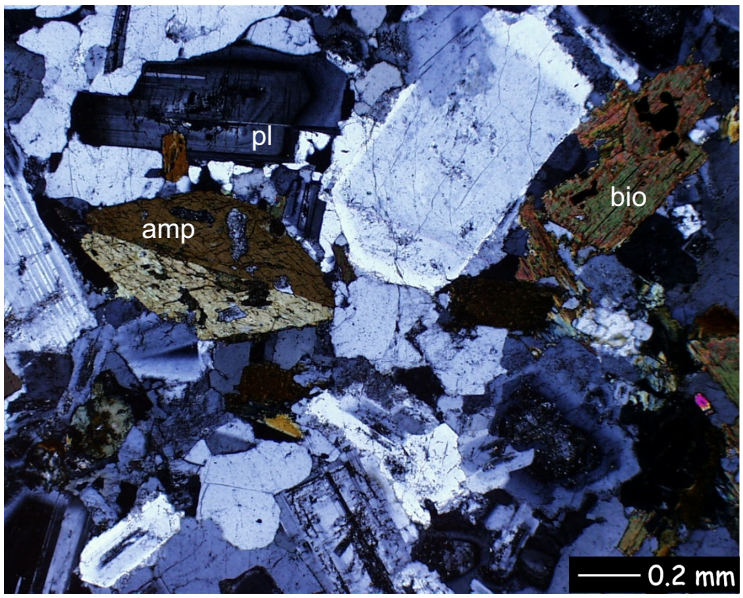


Figure 5. Thin-section photomicrograph of a slightly altered hornblende-biotite diorite from the Island intrusive suite (sample DM-05-182). Note the twinned poikiloblastic hornblende with typical amphibole (amp) cleavage intersection angles, zoned plagioclase (pl) and slightly altered biotite (bio). Photograph taken in plane-polarized light.



Figure 6. Gently eastward-dipping layered ultramafic rocks on the Conuma main forestry road. The layers consist of alternating bands of coarse-grained gabbro (gbo) and relatively finer grained peridotite (pdt). Hammer for scale.

produced 5567 g Au, 10 294 g Ag and 87 kg Cu. Other interesting mineralization types hosted within similar rocks adjacent to the study area include intrusion-related Au in the Zeballos camp, Fe-skarn mineralization (*e.g.*, the Ford mine), minor Au in pyrrhotite veins (*e.g.*, Beano on the Little Zeballos River) and VMS-type mineralization within the Sicker Group at Myra Falls.

Intrusion-Related Gold Mineralization

The study area has potential for Au mineralization similar to the intrusion-related deposits in the Zeballos camp. The Zeballos mineralization is related to the emplacement of the Tertiary Mount Washington intrusive rocks. This study has tentatively identified another large intrusion of this type in Shelter Inlet. The occurrence of the Mount Washington – type intrusive rocks in general proximity to volcanic rocks and Mooyah sedimentary rocks is prospective. Another earmark of Zeballos-type mineralization is the presence of carbonate rocks. No carbonate rocks or areas of mineralization were observed during this summer's fieldwork. However, there is still much unexplored ground in the area.

Sulphide Vein – Type Mineralization

The sulphide vein – type mineralization found on the H7000 spur north of the Stewardson mainline is similar to the mineralization at the Beano showing near the mouth of the Little Zeballos River. The mineralization at Beano consisted of three types (MINFILE): quartz-calcite-pyrrhotite stringers, disseminated pyrrhotite and lenses of massive pyrrhotite. The H7000 mineralization, which consists of a vein of massive pyrrhotite with blebs and veinlets of chalcopyrite and inclusions of altered hostrock, resembles the lenses of massive pyrrhotite from Beano. The inclusions consist of chlorite and constitute approximately 10% of the vein material. The chalcopyrite veinlets appear to cut the massive pyrrhotite within the main vein and make up as much as 2% of the rock. The vein, which strikes north-northeast and dips 80°W, is exposed at the edge of a small pond and disappears beneath the pond. The total length of the vein in outcrop is approximately 1.5 m. Preliminary geochemistry on a grab sample returned 0.5% Cu, elevated As and 0.005 ppm Au. The vein width varies from 10 to 30 cm in outcrop (Fig. 7). In polished thin section. chalcopyrite veins (Fig. 8) and blebs are abundant and appear to postdate the pyrrhotite. There is arsenopyrite associated with the chalcopyrite in thin section. Lack of exposure makes the vein hard to follow. However, a gossanous region can be seen on the other side of the valley directly along strike from the vein.

Skarn-Type Mineralization

Skarn mineralization has been reported at Silverado within the study area and nearby at a number of locations, most notably the Ford Fe-skarn north of Zeballos. The Silverado is hosted within limestone of uncertain age near the flanks of a large Jurassic Island intrusion. It is predominantly a Zn skarn with minor Ag, Au and Cu mineralization. The Ford skarn is hosted within Triassic carbonate rocks. It is magnetite skarn and is associated with the emplacement of Jurassic Island intrusions. There are two localities found this summer that have similar geological settings of calcareous rocks intruded by Jurassic Island



Figure 7. Gossanous zone containing a pyrrhotite vein cutting poorly bedded sedimentary rocks of the Mooyah Formation from the H7000 spur of the Stewardson main forestry road. The vein comprises predominantly massive pyrrhotite with minor veinlets and blebs of chalcopyrite visible in hand specimen. The vein-hostrock contacts vary from sharp to diffuse. Hammer for scale.

intrusions. The exposed areas of carbonate were limited and, although there was abundant evidence of calcsilicate skarn minerals, there was little observed sulphide mineralization. Due to limited access and heavily vegetated terrane, however, there remains abundant unprospected terrain. The first of these areas is adjacent to the sulphide vein mineralization near the H7000 spur off the Stewardson mainline. There is some skarn exposed in a roadcut. Additionally, a small stock of Mount Washington intrusive (as mapped by Muller *et al.*, 1981) in Hisnit Inlet appears to be part of the Jurassic Island intrusive suite. The intrusion was emplaced into Quatsino and Parson Bay carbonate rocks, thus making it prospective for Silverado-type mineralization. A small marble quarry occurs in the marble near the intrusive contact and indicates that metamorphic conditions are probably appropriate for skarn-type mineralization.

VMS-Type Mineralization

Some metavolcanic rocks occur in the study area. Preliminary geochemistry and the presence of the overlying Mooyah Formation indicate that some of these volcanic rocks are most likely equivalent to Sicker Group volcanic rocks and correlative with the rocks hosting the Myra Falls mine, as described by Barrett and Sherlock (1996). The rocks on the upper portions of the H7000 spur are highly gossanous (Fig. 9) and contain abundant mineralized veins, up to 15 cm wide, that are comparable to typical VMS

stockwork mineralization. The hostrocks are massive flows and volcaniclastic rocks with abundant chlorite-epidote alteration. The gossanous zones are up to 10 m in width. A grab sample from one of the highly weathered sulphide veins returned 2.5% Cu (Table 1).

Layered Ultramafic Rocks

Although not one of the targets of this project, layered ultramafic rocks (Fig. 5) were found on the Conuma mainline in the north-central portion of the study area (Fig. 2). As noted above, these rocks have been arbitrarily assigned to the Jurassic but could also be Triassic in age. Argon/argon dating is in progress. If these rocks are Triassic and thus related to the massive outpouring of mafic lavas forming oceanic plateaus during relatively short time intervals, then this rock type may be analogous to similar rocks that host such deposits as Noril'sk-Talnakh and the Thompson nickel belt. The presence of this rock type in the area certainly makes the region prospective for Ni and platinum group element – rich magmatic sulphide minerals (cf. Greene *et al.*, 2004).

MAPPING

Mapping from this summer (Fig. 2) has revealed some interesting features. Primarily, the Westcoast Crystalline Complex of Muller *et al.* (1981) is not a high-grade metamorphic complex as originally suggested and it can be subdivided into time-stratigraphic units correlative with other units on Vancouver Island. For example, the volcanic and volcaniclastic rocks found at the base of the Mooyah Formation (Fig. 3) may be correlative with the McLaughlin Ridge Formation, and the upper portions of the Mooyah Formation may be correlative with the Forth Lake Formation (Yorath *et al.*, 1999). Additionally, the Muller *et al.* (1981) map has inconsistencies relating to the identification of some intrusive rocks. This summer's efforts have identified a large stock of Mount Washington intrusive suite in Shelter Inlet; conversely a stock previously mapped as Tertiary Mount Washing Intrusive has been identified as part of the Jurassic Island intrusive suite. In both cases, these two igneous complexes can now be looked at as exploration targets for different types of mineralization.

CONCLUSIONS

Fieldwork is consistent with the rocks of the Westcoast Crystalline Complex having undergone a much lower grade of metamorphism than suggested by Muller *et al.* (1981). These preliminary results (Fig. 2) indicate that the rocks in the complex are probably correlative with other stratigraphic units on Vancouver Island, especially the sedimentary rocks of the Mooyah Formation. The basal and upper portions of the Mooyah Formation are probably correlative with the McLaughlin Ridge and Fourth Lake formations, respectively. Additionally, this summer's fieldwork has identified some exploration targets:

- at least one new occurrence of the Mount Washing intrusive suite, which is associated with Au mineralization in the neighbouring Zeballos Au camp
- a previously undocumented occurrence of layered mafic rocks near the contact between Jurassic and Triassic rocks that has potential for Ni and PGE-rich magmatic sulphide mineralization
- encouraging Cu values (2.5% Cu) from complex vein networks and possible stockwork mineralization in the altered volcanic rocks near Stewardson Inlet

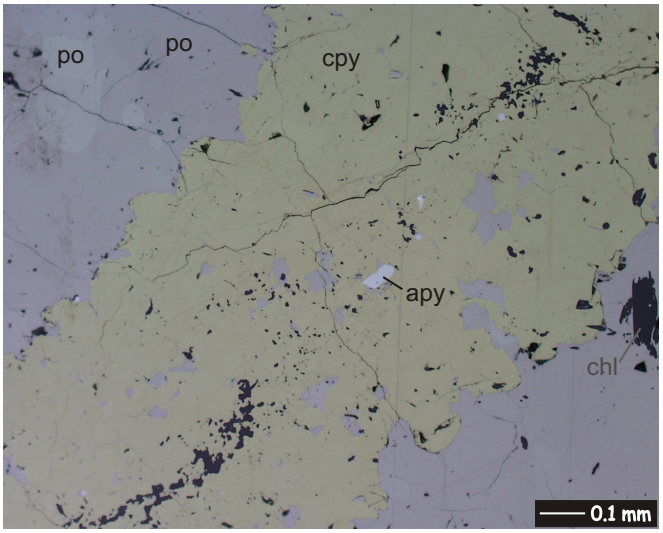


Figure 8. Polished thin-section photomicrograph of the pyrrhotite vein shown in Figure 7. A veinlet of chalcopyrite (cpy) cuts the generally massive pyrrhotite (po). Arsenopyrite (apy) is present in lesser quantities in the chalcopyrite veinlets. Inclusions of chlorite (chl) are present in both pyrrhotite and chalcopyrite. In some instances, the chlorite appears to be pseudomorphous after amphibole. Photograph taken under partly crossed polars.



Figure 9. Gossanous zone within altered mafic volcanic rocks, containing dispersed sulphide veins similar to a typical VMS stockwork zone. The vein on the extreme left (arrow) contains 2.5% Cu. The photograph is approximately 10 m in width.

TABLE 1. SELECTED GEOCHEMICAL RESULTS FOR THE GOSSANOUS VOLCANIC ROCK OCCURRENCE AND THE PYRRHOTITE VEIN (BOTH FROM THE H7000 SPUR OFF THE STEWARDSON MAIN FORESTRY ROAD)

Sample	Description	Au (ppm)	Cu (ppm)	Ni (ppm)	Pb (ppm)	Zn (ppm)	Ag (ppm)	As (ppm)	S (wt.%)	Co (ppm)	Cr (ppm)
DM05-13	VMS	NA	24700	69	11	217	17.6	6	6.7	155	24
DM05-11	Po vein	0.005	4900	260	59	5	0.5	45	37.4	462	<1

Abbreviations: NA, not analyzed; Po: pyrrhotite; VMS, stockwork-like mineralization

potential for skarn mineralization similar to the neighbouring Silverado and Ford skarns

massive pyrrhotite veins with minor chalcopyrite mineralization that are similar to the veins described from the nearby Beano Au deposit on the Little Zeballos River

ACKNOWLEDGMENTS

The authors would like to thank Geoscience BC, Simon Fraser University, the Natural Sciences and Engineering Research Council of Canada (NSERC), Interfor Ltd., Spirit Lake Contracting, Western Forest Products Inc., Hesquiat First Nations and Peter Buckland for financial aid and/or assistance in the field and/or access to properties. Nick Massey from the BC Geological Survey is gratefully acknowledge for a very helpful field visit.

REFERENCES

Barrett, T.J. and Sherlock, R.L. (1996): Volcanic stratigraphy, lithogeochemistry, and seafloor setting of the H-W massive sulfide deposit, Myra Falls, Vancouver Island, British Columbia; *Exploration and Mining Geology*, Volume 5, pages 421–458.

British Columbia Ministry of Energy, Mines and Petroleum Resources (2005): BC Geological Survey Digital Geoscience Map; *BC Ministry of Energy, Mines and Petroleum Resources*, URL < http://www.em.gov.bc.ca/Mining/Geolsurv/MapPlace/MoreDetails/geology.htm> [Nov 2005].

DeBari, S.M., Anderson, R.G. and Mortensen, J.K. (1999): Correlation among lower to upper crustal components in an island arc: the Jurassic Bonanza arc, Vancouver Island, Canada; *Canadian Journal of Earth Sciences*, Volume 36, pages 1371–1413.

Hansen, M.C. and Sinclair, A.J. (1984): A preliminary assessment of Zeballos mining camp (92L); *in* Geological Fieldwork, 1983, *BC Ministry of Energy, Mines and Petroleum Resources*, Paper 1984-1, pages 219–232.

Greene, A.R., Scoates, J.S. and Weis, D. (2004): Wrangellia Terrane on Vancouver Island, British Columbia: distribution of flood basalts with implications for potential Ni-Cu-PGE mineralization in southwestern British Columbia; *in* Geological Fieldwork 2004, *BC Ministry of Energy, Mines and Petroleum Resources*, Paper 2005-1, pages 209–220.

Jeletzky, J.A. (1954): Tertiary rocks of the Hesquiat-Nootka area, west coast of Vancouver Island, British Columbia; *Geological Survey of Canada*, Paper 53-17, 65 pages.

Jeletsky, J.A. (1976): Mesozoic and ?Tertiary rocks of Quatsino Sound, Vancouver Island, British Columbia; *Geological Survey of Canada*, Bulletin 242, 243 pages.

Jones, D.L., Silberling, N.J. and Hillhouse, J. (1977): Wrangellia — a displaced terrane in northwestern North America; *Canadian Journal of Earth Sciences*, Volume 14, pages 2565–2577.

Marshall, D., Podstawskyj, N. and Aichmeier, A. (2004): Gold mineralization and geology in the Zeballos area, Nootka Sound, British Columbia; *in* Geological Fieldwork 2004, *BC Ministry of Energy, Mines and Petroleum Resources*, Paper 2005-1, pages 301–310.

Massey, N.W.D. (1991): The geology of the Port Alberni – Nanaimo Lakes area; *BC Ministry of Energy Mines and Petroleum Resources*, Geoscience Map 1991-1.

Massey, N.W.D. (1995): Geology and mineral resources of the Alberni – Nanaimo Lakes sheet, Vancouver Island, 92 F/1W, 92 F/2E and part of 92 F/7E; *BC Ministry of Energy Mines and Petroleum Resources*, Paper 1992-2, 132 pages.

MINFILE (2005): MINFILE BC mineral deposits database; *BC Ministry of Energy, Mines and Petroleum Resources*, URL <http://www.em.gov.bc.ca/Mining/Geolsurv/Minfile/> [Nov 2005].

Muller, J.E. and Carson, D.J. (1969): Geology and mineral deposits of Alberni map-area, British Columbia, (92F); *Geological Survey of Canada*, Paper 68-50, 52 pages.

Muller, J.E., Cameron, B.E.B and Northcote, K.E. (1981): Geology and mineral deposits of the Nootka Sound map-area, Vancouver Island, British Columbia; *Geological Survey of Canada*, Paper 80-16, 53 pages.

Sinclair, A.J. and Hansen, M.C. (1983): Resource assessment of gold-quartz veins, Zeballos mining camp, Vancouver Island: a preliminary report (92L); *in* Geological Fieldwork 1982, *BC Ministry of Energy Mines and Petroleum Resources*, pages 290–303.

Stevenson, J.S. (1938): Lode-gold deposits of the Zeballos area, west coast of Vancouver Island, British Columbia; *BC Ministry of Energy Mines and Petroleum Resources,* Miscellaneous Publication, 23 pages.

Stevenson, J.S. (1939): Geology and ore deposits of the Zeballos area, British Columbia; Transactions of the Canadian Institute of Mining and Metallurgy and of the Mining Society of Nova Scotia, Volume 42.

Stevenson, J.S. (1950): Geology and mineral deposits of the Zeballos mining camp; *BC Ministry of Energy Mines and Petroleum Resources*, Bulletin 27, 145 pages.

Wheeler, J.O., Brookfield, A.J., Gabrielese, H., Monger, J.W.H., Tipper, H.W. and Woodsworth, G.J. (1991): Terrane map of the Canadian Cordillera; *Geological Survey of Canada*, Map 1713, scale 1:2 000 000.

Yorath, C.J., Sutherland Brown, A. and Massey, N.W.D. (1999): LITHOPROBE, southern Vancouver Island, British Columbia: geology; *Geological Survey of Canada*, Bulletin 498, 145 pages.

Stratigraphic and Paleotectonic Studies of the Middle Paleozoic Sicker Group and Contained VMS Occurrences, Vancouver Island, British Columbia[1]

By J.K. Mortensen[2]

KEYWORDS: Sicker Group, Paleozoic, Vancouver Island, VMS deposit, stratigraphy, U-Pb zircon geochronology, lithogeochemistry

INTRODUCTION

Volcanic strata of the mid-Paleozoic Sicker Group on Vancouver Island (Fig. 1) host the Myra Falls volcanogenic massive sulphide (VMS) deposit. With combined production and proven and probable reserves in excess of 30 million tonnes of Zn-Cu-(Au-Ag) ore, this is currently the largest and most productive VMS mine in western Canada. Other VMS deposits and occurrences are known elsewhere within the Sicker, and deposits in the Mt. Sicker area (Mt. Sicker, Lenora and Twin J; MINFILE (2005) occurrences 092B 001, 002, 003; Fig. 1) have been mined on a relatively small scale. Exploration for additional VMS deposits within the Sicker Group, however, has met with only limited success outside the immediate area of the Myra Falls deposit. Despite the considerable potential for such deposits in the Sicker and the current high base-metal prices, VMS exploration within the group has been at a low level for the past decade. A significant impediment to VMS exploration within the Sicker Group is the relatively poor overall understanding of the geology of this assemblage, which makes it difficult to develop a sound regional exploration strategy based on typical stratigraphic and volcanological criteria. Detailed studies of the group in the past have been hampered by generally poor exposure and limited access, except in the immediate vicinity of the Myra Falls deposit (e.g., Juras, 1987; Barrett and Sherlock, 1996; Robinson *et al.*, 1996). New logging-road construction in the 1980s and 1990s greatly improved access to and exposure of the Sicker Group in central Vancouver Island, and regional mapping studies of this area were carried out by personnel of the BC Geological Survey (e.g., Massey and Friday, 1987, 1989; Massey, 1995a, b, c; see also Yorath *et al.*, 1999). These studies did not include all of the exposed Sicker Group, however, and available data are still insufficient to produce a comprehensive analysis of the stratigraphy and evolution of the group.

A new integrated geological, geochemical and geochronological study of the Sicker Group on Vancouver Island, funded by Geoscience BC, was begun in 2005. This study has the following main goals:

- develop a model for the physical volcanology and eruptive history of the Sicker Group
- constrain the paleotectonic evolution of this portion of Wrangellia
- evaluate the nature and stratigraphic position(s) of VMS deposits and occurrences within the Sicker Group

Results of the study will provide a much improved framework for VMS exploration within the Sicker Group. Two weeks of reconnaissance work were carried out by the author in September of 2005, and a new Ph.D. level graduate student will begin work on the project in the summer of 2006.

REGIONAL GEOLOGY OF THE SICKER GROUP AND REVIEW OF PREVIOUS WORK

The mid-Paleozoic Sicker Group and correlative Skolai Group in Alaska represent the oldest exposed rocks in Wrangellia (e.g., Monger and Nokleberg, 1996). The Sicker Group and the Late Paleozoic Buttle Lake Group that overlies it on Vancouver Island and the Canadian Gulf Islands are exposed in four major structural uplifts: the Buttle Lake, Bedingfield, Nanoose and Cowichan Lake uplifts (Fig. 1).

Most previous investigations of the Sicker and overlying Buttle Lake groups have focused on the Buttle Lake and Cowichan Lake uplifts. This work concentrated mainly on the stratigraphy of the two groups; however. a limited amount of geochronology has also been carried out, as well as detailed biostratigraphic and lithogeochemical studies of a few localities. Stratigraphic nomenclature for the Sicker and Buttle Lake groups has changed substantially over time (Fig. 2), and this complicates comparison between data produced by the different generations of work in the different regions.

Muller (1977, 1980) subdivided volcanic-dominated Paleozoic successions on Vancouver Island into two formations, the lower Nitinat and the upper Myra Formation. He also introduced the informally named 'sediment sill unit' (thin-bedded sedimentary rocks intruded by diabase sills), which stratigraphically separates the Myra and overlying Buttle Lake formations. The most recent revision of Sicker and Buttle Lake nomenclature (Massey, 1995a, b, c; Yorath

[1] *Geoscience BC contribution GBC010*

[2] *Mineral Deposit Research Unit, Earth and Ocean Sciences, University of British Columbia, Vancouver, BC (jmortensen@eos.ubc.ca)*

This publication is also available, free of charge, as colour digital files in Adobe Acrobat PDF format from the BC Ministry of Energy, Mines and Petroleum Resources internet website at http://www.em.gov.bc.ca/Mining/Geolsurv/Publications/catalog/catfldwk.htm

et al., 1999) divides the original Sicker Group into two groups: the Sicker Group (revised), comprising the Nitinat and underlying Duck Lake formations (previously the lower Nitinat Formation), as well as the McLaughlin Ridge Formation; and the overlying Buttle Lake Group (Fig. 2). From base to top, the Buttle Lake Group comprises the Fourth Lake and the Mount Mark formations, as well as the newly identified St. Mary Lake Formation. In this stratigraphic arrangement, the McLaughlin Ridge Formation is equivalent to all of Muller's Myra Formation. This revised stratigraphic nomenclature is presently only considered valid for the Cowichan Lake uplift (Yorath *et al.*, 1999).

Juras (1987) reinterpreted the stratigraphy of the Sicker Group specifically within the Buttle Lake uplift. He retained the Sicker and Buttle Lake group divisions; however, new terminology was proposed for the subdivisions of the Sicker. According to Juras, the lowermost unit in the Sicker Group in the Buttle Lake uplift is the Price Formation (which Yorath *et al.* (1999) correlate with all of the Duck Lake Formation and the lower Nitinat Formation). Above the Price Formation is the Myra Formation, which corresponds to the upper Nitinat and lower McLaughlin Ridge formations (and is therefore not equivalent to Muller's Myra Formation; Yorath *et al.*, 1999). Juras' Thelwood and Flower Ridge formations approximately correlate with the upper McLaughlin Ridge Formation of Yorath *et al.* (1999).

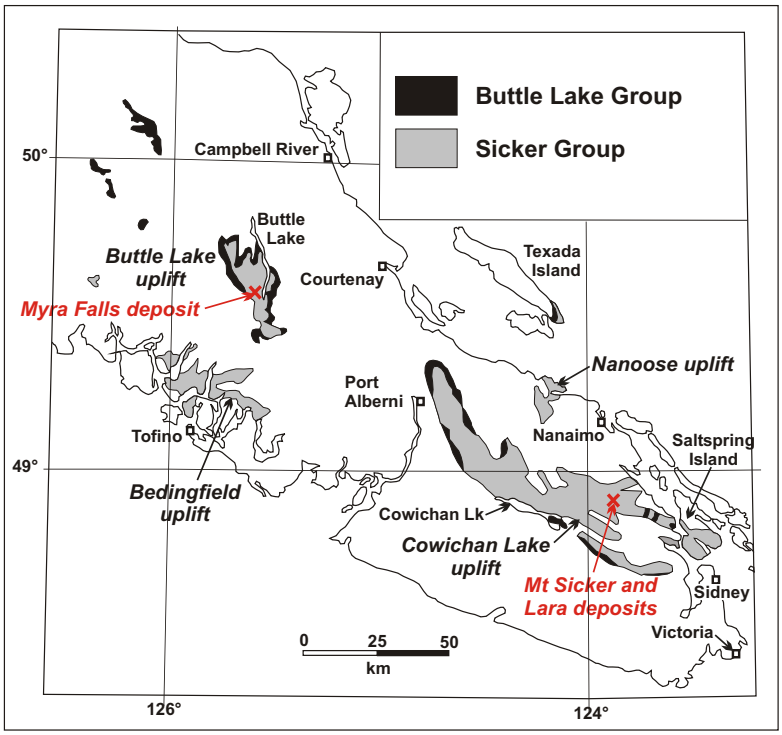


Figure 1. Distribution of Paleozoic strata of the Sicker and Buttle Lake groups on Vancouver Island and the Gulf Islands.

Collectively the Sicker Group comprises three successive volcanic and volcaniclastic formations that are thought to record the evolution of an oceanic magmatic arc. The following synthesis of Sicker Group evolution is summarized from Massey (1995a). The lowermost Duck Lake Formation consists of dominantly tholeiitic basalts, which pass upward into calcalkaline lavas. The Duck Lake Formation is interpreted to represent the oceanic crust basement and possibly the earliest stage of Sicker arc magmatism. The Duck Lake is overlain by mafic, submarine, volcanic and volcaniclastic rocks of the Nitinat Formation, which are interpreted to represent an early stage of arc development. The andesitic to mainly dacitic and rhyolitic McLaughlin Ridge Formation that overlies the Nitinat and hosts the Myra Falls deposit reflects a more evolved stage of arc activity. Eruption of Nitinat volcanic and volcaniclastic rocks occurred from several widely scattered centres, whereas the McLaughlin Ridge Formation is thought to represent eruption from one or more major volcanic edifices. One such magmatic centre is located in the Cowichan Lake uplift in the Duncan and Saltspring Island area (Fig. 1), and is defined by voluminous comagmatic felsic intrusions (Saltspring intrusions). Plant material and trace fossils indicate that at least some the McLaughlin Ridge volcanism was subaerial. Deposition of the Fourth Lake Formation of the Buttle Lake Group on top of the McLaughlin Ridge represents the end of Sicker arc magmatism, and scarce mafic volcanic rocks contained within the Fourth Lake Formation yield enriched tholeiitic rather than the calcalkaline compositions that characterize the McLaughlin Ridge. Massey (1995a) speculated that the Buttle Lake Group may represent a marginal-basin assemblage that developed on top of the Sicker arc.

The most recent study of the Sicker and Buttle Lake groups was undertaken by Sluggett (2003) as part of a B.Sc. thesis at the University of British Columbia (UBC) under the author's supervision. The study included detailed petrographic and geochemical investigation of the Sicker Group and, to a lesser extent, the Buttle Lake Group on southern Saltspring Island, as well as detailed U-Pb dating of several key rock units. Although this study focused on a very small geographic area, the results underscore the fact that substantial problems remain in our understanding of the evolution of the Paleozoic portion of southern Wrangellia. Major results of the work by Sluggett (2003) and Sluggett and Mortensen (2003) include the following:

Muller, 1977 (Vancouver Island)		Juras, 1987 (Buttle Lake Uplift)		Yorath et al., 1999 (Alberni area)	
		Buttle Lake Gp	Henshaw Fm	Buttle Lake Gp	St. Mary Lk Fm
Sicker Gp	Buttle Lk Fm		Mt Mark Fm		Mt Mark Fm
	'Sediment-sill' unit				Fourth Lk Fm
	Myra Fm	Sicker Gp	Flower Ridge Fm	Sicker Gp	McLaughlin Ridge Fm
			Thelwood Fm		
			Myra Fm		
	Nitinat Fm		Price Fm		Nitinat Fm
					Duck Lk Fm

Figure 2. Stratigraphic nomenclature for the Sicker and Buttle Lake groups on Vancouver Island.

- U-Pb zircon dating indicates that two distinct episodes of felsic magmatism are represented in this portion of the Cowichan Lake uplift. Felsic volcanic rocks of the McLaughlin Ridge Formation and most of the geochemically similar and presumably genetically related Saltspring intrusions yield U-Pb ages in the range 356.5–359.1 Ma. However, a somewhat older phase of magmatism is indicated by a U-Pb age of 369.7 Ma for a separate body of Saltspring intrusion at Burgoyne Bay on southern Saltspring Island. The extent of this older magmatic episode is unknown; however, most previous U-Pb dating studies of felsic rocks in the Sicker Group (see later discussion) have produced imprecise ages of ~370 Ma, suggesting that the bulk of the McLaughlin Ridge Formation regionally, including the host rocks for the Myra Falls deposit, may correlate with the older magmatic event recognized on Saltspring Island.
- A minor component of inherited zircon with ages up to 420 Ma occurs within the Sicker Group. This is inconsistent with the dominantly intraoceanic-arc setting that has previously been suggested for the Sicker Group. In addition, all of the Saltspring intrusions that were sampled yield weakly peraluminous compositions and two are garnet bearing; these observations are also inconsistent with an oceanic-arc setting.
- Detrital zircons recovered from a grit unit that contains felsic volcanic lapilli, in the lower portion of the Fourth Lake Formation, yield consistent U-Pb ages of ~320 Ma. This indicates that this portion of the Fourth Lake Formation is at least 40 m.y. younger than the McLaughlin Ridge Formation that it is interpreted to directly overlie. This suggests the possibility of substantial unconformities within the Sicker Group.
- Mafic sills that intrude the Fourth Lake Formation and form part of the 'sediment sill unit' of Muller (1980) yield Late Triassic U-Pb baddeleyite ages and are thus unrelated to the sedimentary rocks into which they have been emplaced. The mafic sills represent subvolcanic feeders to basalts of the overlying Karmutsen Group (e.g., Greene et al., 2005).

VMS MINERALIZATION IN THE SICKER GROUP

In a review of potential for VMS mineralization in BC, Massey (1999) identified definite or potential VMS occurrences within three of the four uplifts of Sicker Group on Vancouver Island (Buttle Lake, Cowichan Lake and Bedingfield; Fig. 1). Most known VMS occurrences are of the Kuroko type and are hosted by felsic volcanic or volcaniclastic rocks of the McLaughlin Ridge Formation or equivalents. However, examples of manganiferous and/or sulphidic chert horizons that may be exhalitive in origin are also locally present in the upper Duck Lake Formation and the lowermost Fourth Lake Formation (e.g., Massey and Friday, 1989). Occurrences such as the Mt. Sicker and Lara in the southeastern and central part of the Cowichan Lake uplift (MINFILE occurrences 092B 001-003 and -129, respectively; Fig. 1) consist of baritic laminated base metal sulphide accumulations within felsic tuffaceous units of the McLaughlin Ridge Formation, and are clearly syngenetic in origin. Descriptions of some of the other occurrences taken from BC MINFILE, however, suggest that the identification of some of these occurrences as being syngenetic in origin is somewhat more equivocal, and at least some are more likely epigenetic occurrences associated with a later mineralizing event in the region, possibly related to the emplacement of the Early to Middle Jurassic Island intrusions. However, Massey's review serves to highlight the incompletely tested VMS potential remaining within the Sicker Group. Previous studies by Godwin et al. (1988) and Andrew and Godwin (1989) indicate that it is possible to confidently discriminate between syngenetic Paleozoic mineral occurrences and younger epigenetic occurrences within the Sicker using sulphide Pb isotopes (Fig. 3).

GOALS OF THE NEW PROJECT

A review of available data regarding the nature of the Sicker Group in the various uplifts on Vancouver Island suggests that significant problems exist in terms of how individual rock units correlate from one uplift to another and at what exact stratigraphic level known VMS mineralization occurs. Volcanic and volcaniclastic assemblages in an arc setting such as the Sicker typically show rapid lateral and vertical facies changes, and it is therefore difficult to establish confident correlations between widely separated exposures. Detailed correlations within and between the various uplifts must therefore be based largely on precise

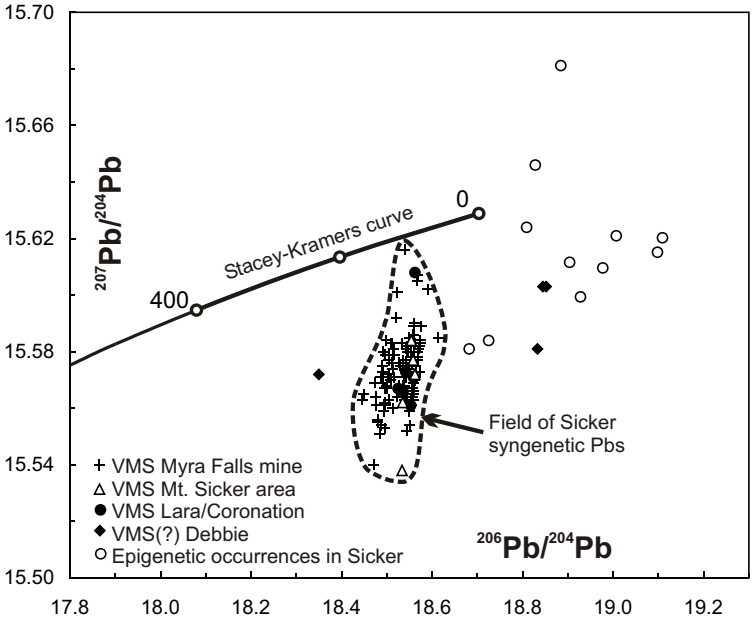


Figure 3. Lead isotopic compositions of sulphide minerals from syngenetic and epigenetic deposits and occurrences hosted within the Sicker Group. Data from Godwin *et al.* (1988) and this study.

age determinations. Existing age constraints for Sicker rock units, however, are generally very poor. Only one of the numerous published U-Pb age determinations from the Sicker Group, as reported by Juras (1987), Brandon *et al.* (1986) and Parrish and McNicoll (1992), is considered reliable (an age of 362 ±2 Ma for a quartz-feldspar porphyry body on the east side of Mt. Sicker). There are at present no reliable or precise age determinations at all from within the Buttle Lake uplift. Recent advances in U-Pb zircon dating methods have made it possible to produce much more reliable ages for Sicker samples (as evidenced by the four new ages reported by Sluggett (2003) for the McLaughlin Ridge Formation and Saltspring intrusions on Saltspring Island), with the high precision (±<2 m.y.) that is required to resolve the timing of individual magmatic events within the Sicker Group.

The most critical need in understanding the evolution of the Sicker arc is therefore to establish timelines throughout the Sicker Group that will allow direct chronological correlations to be made within and between various exposures of these units. Conodont biochronology may provide additional temporal constraints in some parts of the section, although carbonate units are rare within the Sicker Group. This temporal framework will constrain facies reconstructions of the Sicker arc and its immediately underlying basement and, together with complete geochemical and isotopic studies from throughout each section, will provide a basis for interpreting the paleotectonic evolution of the arc. It will also help constrain the metallogenic evolution of the Sicker and, in particular, establish the stratigraphic position of the Myra Falls deposit and other syngenetic base-metal occurrences in the Sicker (as identified through Pb isotopic analyses of sulphide minerals).

WORK COMPLETED AND IN PROGRESS

A two-week field program was carried out by the author in September of 2005. This work was aimed at gaining a better regional understanding of the geology of the Sicker Group, especially in the Cowichan Lake uplift, and also assessing the access to and exposure of the units in this region. As a result of recent and current logging activity, access and exposure are much improved since Massey (1995a, b, c) did his work in the area. In particular, several days were spent examining the geology and mineralization within the southeastern portion of the Cowichan Lake uplift in the vicinity of the Mt. Sicker and Lara deposits (Fig. 1). Forty-two samples were collected and have been analyzed for complete major, trace and rare earth elements at ALS Chemex Ltd. to more completely constrain the geochemical characteristics of the main Sicker rock types. These results are currently being compiled with existing lithogeochemical data from the Cowichan Lake uplift from Massey (1995a, b, c) and Sluggett (2003), and data from the Sicker Group in the Buttle Lake uplift from Barrett and Sherlock (1996). In addition, 15 samples were collected from throughout the Cowichan Lake uplift for U-Pb zircon dating using the laser-ablation inductively coupled plasma – mass spectrometry (ICP-MS) U-Pb dating technique that has recently been established at the Pacific Centre for Isotopic and Geochemical Research laboratory at UBC. This method makes it possible to generate reliable and precise U-Pb zircon ages much more quickly and at considerably lower cost than using conventional thermal ionization mass spectrometry methods. An additional five(+) U-Pb zircon dating samples will be collected later in the fall from the immediate mine stratigraphy at the Myra Falls mine in the Buttle Lake uplift. These data are critical to establish a comparative chronostratigraphy between the Buttle Lake and Cowichan Lake uplifts.

Existing Pb isotopic data from VMS and epigenetic mineral occurrences hosted by the Sicker Group on Vancouver Island are shown in Figure 3, together with several new Pb isotopic analyses of sulphide minerals from epigenetic vein occurrences in the Cameron River area, southeast of Port Alberni, that have been generated during the present study. Sulphide Pb compositions in VMS occurrences within the McLaughlin Ridge Formation form a well-defined cluster that differs markedly from Pb analyses from epigenetic occurrences within the Sicker (Fig. 3). This demonstrates that Pb isotopes provide an effective tool for discriminating between syngenetic and younger mineralization in the Sicker. Three analyses reported by Godwin *et al.* (1988) from the Debbie (Mineral Creek) occurrence (MINFILE 092F 079) in the northwestern portion of the Cowichan Lake uplift are identified on the plot. The Debbie occurrence is hosted within the Duck Lake Formation and comprises a variety of styles mineralization. Most previous and current work has focused on Au-bearing veins and shear zones; however sulphide-bearing cherty horizons are also present within the Duck Lake basalt on the property. There are no descriptions of the three sulphide samples that were analyzed for Pb isotopes; however, two fall within the broad array of analyses from other epigenetic occurrences in the Sicker, but one gives a Pb isotopic composition that is slightly less radiogenic than sulphide minerals from syngenetic occurrences hosted by the McLaughlin Ridge Formation. This would be consistent with this sample being syngenetic in origin with a somewhat older depositional age than the other VMS occurrences in the Sicker. The age of the Duck Lake Formation is not well constrained at this point, but it is certainly older than the McLaughlin Ridge Formation. Additional sampling for Pb isotopes is planned in the Debbie area to further investigate the range of styles of mineralization present and, in particular, the potential for VMS mineralization within the Duck Lake Formation.

ACKNOWLEDGMENTS

This project is funded by a Geoscience BC grant as well as a Natural Sciences and Engineering Research Council of Canada (NSERC) Discovery Grant to the author. I thank Nick Massey for discussions and insights into the geology of the Sicker Group. I also thank several prospectors, consultants and explorationists working on Vancouver Island, especially Allen Francis, Jacques Houle, Herb McMaster and Sy Tresierra, for sharing their time and knowledge of Sicker geology and mineralization with me.

REFERENCES

Andrew, A. and Godwin, C.I. (1989): Lead- and strontium-isotope geochemistry of Paleozoic Sicker Group and Jurassic Bonanza Group volcanic rocks and Island Intrusions, Vancouver Island, British Columbia; *Canadian Journal of Earth Sciences*, Volume 26, pages 894–907.

Barrett, T.J. and Sherlock, R.L. (1996): Volcanic stratigraphy, lithogeochemistry, and seafloor setting of the H-W massive sulfide deposit, Myra Falls, Vancouver Island, British Co-

lumbia; *Exploration and Mining Geology*, Volume 5, pages 421–458.

Brandon, M.T., Orchard, M.J., Parrish, R.R., Sutherland Brown, A. and Yorath, C.J. (1986): Fossil ages and isotopic dates from the Paleozoic Sicker Group and associated intrusive rocks, Vancouver Island, British Columbia; *in* Current Research, Part A, *Geological Survey of Canada*, Paper 86-1A, pages 683–696.

Godwin, C.I., Gabites, J.E. and Andrew, A. (1988): Leadtable: A galena lead isotope database for the Canadian Cordillera; *BC Ministry of Energy, Mines and Petroleum Resources*, Paper 1988-4, 214 pages.

Greene, A.R., Scoates, J.S. and Weis, D. (2005): Wrangellia Terrane on Vancouver Island, British Columbia: distribution of flood basalts with implications for potential Ni-Cu-PGE mineralization in southwestern British Columbia; *in* Geological Fieldwork 2004, *BC Ministry of Energy, Mines and Petroleum Resources*, Paper 2005-1, pages 209–220.

Juras, S.J. (1987): Geology of the polymetallic volcanogenic Buttle Lake Camp, with emphasis on the Price Hillside, central Vancouver Island, British Columbia, Canada; Ph.D. thesis, *University of British Columbia*, Vancouver, BC, 279 pages.

Massey, N.W.D. (1995a): Geology and mineral resources of the Duncan sheet, Vancouver Island, 92B/13; *BC Ministry of Energy, Mines and Petroleum Resources*, Paper 1992-4.

Massey, N.W.D. (1995b): Geology and mineral resources of the Alberni-Nanaimo Lakes sheet, Vancouver Island, 92F/1W, 92F/2E and part of 92F/7E; *BC Ministry of Energy, Mines and Petroleum Resources*, Paper 1992-2.

Massey, N.W.D. (1995c): Geology and mineral resources of the Cowichan Lake sheet, Vancouver Island, 92C/16; *BC Ministry of Energy, Mines and Petroleum Resources*, Paper 1992-3.

Massey, N.W.D. (1999): Volcanogenic massive sulphide deposits in British Columbia; *BC Ministry of Energy, Mines and Petroleum Resources*, Open File 1999-2.

Massey, N.W.D. and Friday, S.J. (1987): Geology of the Chemainus River – Duncan area, Vancouver Island (92C/16; 92B/13); *BC Ministry of Energy, Mines and Petroleum Resources*, Paper 1988-1, pages 81–91.

Massey, N.W.D. and Friday, S.J. (1989): Geology of the Alberni-Nanaimo Lakes area, Vancouver Island (92F/1W, 92F/2E and part of 92F/7); *BC Ministry of Energy, Mines and Petroleum Resources*, Open File 1987-2.

MINFILE (2005): MINFILE BC mineral deposits database; *BC Ministry of Energy, Mines and Petroleum Resources*, URL <http://www.em.gov.bc.ca/Mining/Geolsurv/Minfile/> [Nov 2005].

Monger, J.W.H. and Nokleberg, W.J. (1996): Evolution of the northern North American Cordillera: generation, fragmentation, displacement and accretion of successive North American plate-margin arcs; *in* Geology and Ore Deposits of the American Cordillera, Symposium Proceedings, Reno, Nevada, April 10–13, 1995, Coyner, A.R. and Fahey, P.L., Editors, *Geological Society of Nevada*, Volume III, pages 1133–1152.

Muller, J.E. (1977): Evolution of the Pacific margin, Vancouver Island and adjacent regions; *Canadian Journal of Earth Sciences*, Volume 14, pages 2062–2085.

Muller, J.E. (1980): The Paleozoic Sicker Group of Vancouver Island, British Columbia; *Geological Survey of Canada*, Paper 79-30, 24 pages.

Parrish, R.R. and McNicoll, V.J. (1992): U-Pb age determinations from the southern Vancouver Island area, British Columbia; Radiogenic Age and Isotopic Studies: Report 5, *Geological Survey of Canada*, Paper 91-2, pages 79–86.

Robinson, M., Godwin, C.I. and Stanley, C.R. (1996): Geology, lithogeochemistry and alteration of the Battle volcanogenic zone, Buttle Lake camp, Vancouver Island; *Economic Geology*, Volume 91, pages 527–548.

Sluggett, C.L. (2003): Uranium-lead age and geochemical constraints on Paleozoic and Early Mesozoic magmatism in Wrangellia terrane, Saltspring Island, British Columbia; B.Sc. thesis, *University of British Columbia*, Vancouver, BC, 56 pages.

Sluggett, C.L. and Mortensen, J.K. (2003): U-Pb age and geochemical constraints on the paleotectonic evolution of the Paleozoic Sicker Group on Saltspring Island, southwestern British Columbia; *Geological Association of Canada – Mineralogical Association of Canada*, Joint Annual Meeting, Program with Abstracts, Volume 28.

Yorath, C.J., Sutherland Brown, A. and Massey, N.W.D. (1999): LITHOPROBE, southern Vancouver Island, British Columbia: geology; *Geological Survey of Canada*, Bulletin 498, 145 pages.

Glacial and Stream Sediments Sampling in Support of Kimberlite Exploration in Northeastern British Columbia[1]

by A. Plouffe[2], I.R. Smith[3], M. McCurdy[2], P. Friske[2], T. Ferbey, J. Bednarski[4], V.M. Levson, T.E. Demchuk[5], M. Trommelen[5], S. Day[2] and A.S. Hickin

KEYWORDS: geochemistry, kimberlite, mineral exploration, till, stream sediments, glaciofluvial sediments

INTRODUCTION

The objective of this project is to evaluate the mineral potential of the region northeast of Fort Nelson, BC, in particular the potential to host diamondiferous kimberlites, with the intended benefit of promoting future investment in natural resources exploration. The project is funded by the Geological Survey of Canada (GSC) and by Geoscience BC (GBC). The Resource Development and Geoscience Branch (RDGB) of the BC Ministry of Energy, Mines and Petroleum Resources (BC MEMPR) also has been conducting Quaternary geology studies in the region and in collaboration with the GSC have undertaken a surficial geology mapping project in this area since 2003. The new project outlined here builds on that collaborative work and receives additional benefit from two Masters theses projects, which are aimed at mapping surficial geology and reconstructing the glacial history of regions on and adjacent to the Etsho Plateau (Demchuk *et al.*, 2005; Trommelen *et al.*, 2005).

This project was stimulated by the announcement of the first recorded occurrence of kimberlite indicator minerals (KIMs) in northeastern BC by members of this joint provincial-federal research group at the Mineral Exploration Roundup 2005 (Simandl, 2005). KIMs were found in 14 out of 22 samples of glaciofluvial sediment submitted for analysis (Levson *et al.*, 2004; Fig. 1). Soon after the official release of results, mineral staking occurred in six areas of northeastern BC.

The current GBC project builds on activities conducted as part of the existing collaborative surficial geology project by the BC MEMPR and the GSC. British Columbia Oil and Gas Development Strategy funding was provided to the RDGB in 2002 to initiate a project with the principal objective of identifying new granular aggregate resources to improve and develop access roads in the extensive gas fields of northeastern BC (Johnsen *et al.*, 2004; Levson *et al.*, 2004, 2005; Ferbey *et al.*, 2005). In the following year, the GSC and BC MEMPR instigated a four-year collaborative project in northeastern BC under the GSC's Northern Resource Development Program and the Targeted Geoscience Initiative (TGI-2) to provide geoscience information in support of exploration for not only granular aggregate resources, but also shallow gas reservoirs in unconsolidated Tertiary – Quaternary sediments, and the potential presence of kimberlites. The study area of this collaborative project extends into northwestern Alberta where similar objectives are being pursued by the GSC and the Alberta Geological Survey (for an example of results, see Smith *et al.*, 2005).

The composition of KIMs in glaciofluvial sediment samples collected as part of this collaborative project (Levson *et al.*, 2004) was reported by Simandl *et al.* (2005a, b). Simandl *et al.* (2005b) suggested that northeastern BC "could be more favorable for diamond exploration than previously thought." The authors indicated that the source of the KIMs is still unknown and that they could be derived locally, from the Northwest Territories to the northeast and/or Alberta to the east. In light of the initial positive KIMs results, it was decided that additional sampling of glacial sediments and stream sediments and waters in the Etsho Plateau region would help elucidate potential sources of the KIMs, and in so doing, help to encourage investment in this area by the diamond exploration industry.

PHYSIOGRAPHY AND GEOLOGY OF THE STUDY AREA

The study area lies within the Fort Nelson Lowlands, part of the Alberta Plateau, which is a dominantly flat to gently rolling region situated below an elevation of 600 m above sea level. More specifically, it is centred on the Etsho Plateau, a subdivision of the Fort Nelson Lowlands, where KIMs were first reported in glaciofluvial sediments (Fig. 1; Simandl *et al.*, 2005a). The subdued topography of the region is inherited from the underlying horizontal to gently dipping sedimentary bedrock. The region is poorly drained, secondary streams are not deeply incised, except those situated in former glacial spillways, and organic deposits abound. In contrast, the Etsho Plateau stands approximately 300 m above the surrounding lowlands with a denser network of streams along its flanks compared to the adjacent lowlands. Drainage radiates from the Etsho Plateau into the Petitot River to the north, Sahtaneh River to the west, Kotcho River to the southeast and Shekilie River to the east. The Petitot and Sahtaneh rivers ultimately drain

[1]*Geoscience BC contribution GBC011*

[2]*Geological Survey of Canada, Ottawa, ON*

[3]*Geological Survey of Canada, Calgary, AB*

[4]*Geological Survey of Canada, Sidney, BC*

[5]*University of Victoria, Victoria, BC*

This publication is also available, free of charge, as colour digital files in Adobe Acrobat PDF format from the BC Ministry of Energy, Mines and Petroleum Resources internet website at http://www.em.gov.bc.ca/Mining/Geolsurv/Publications/catalog/catfldwk.htm

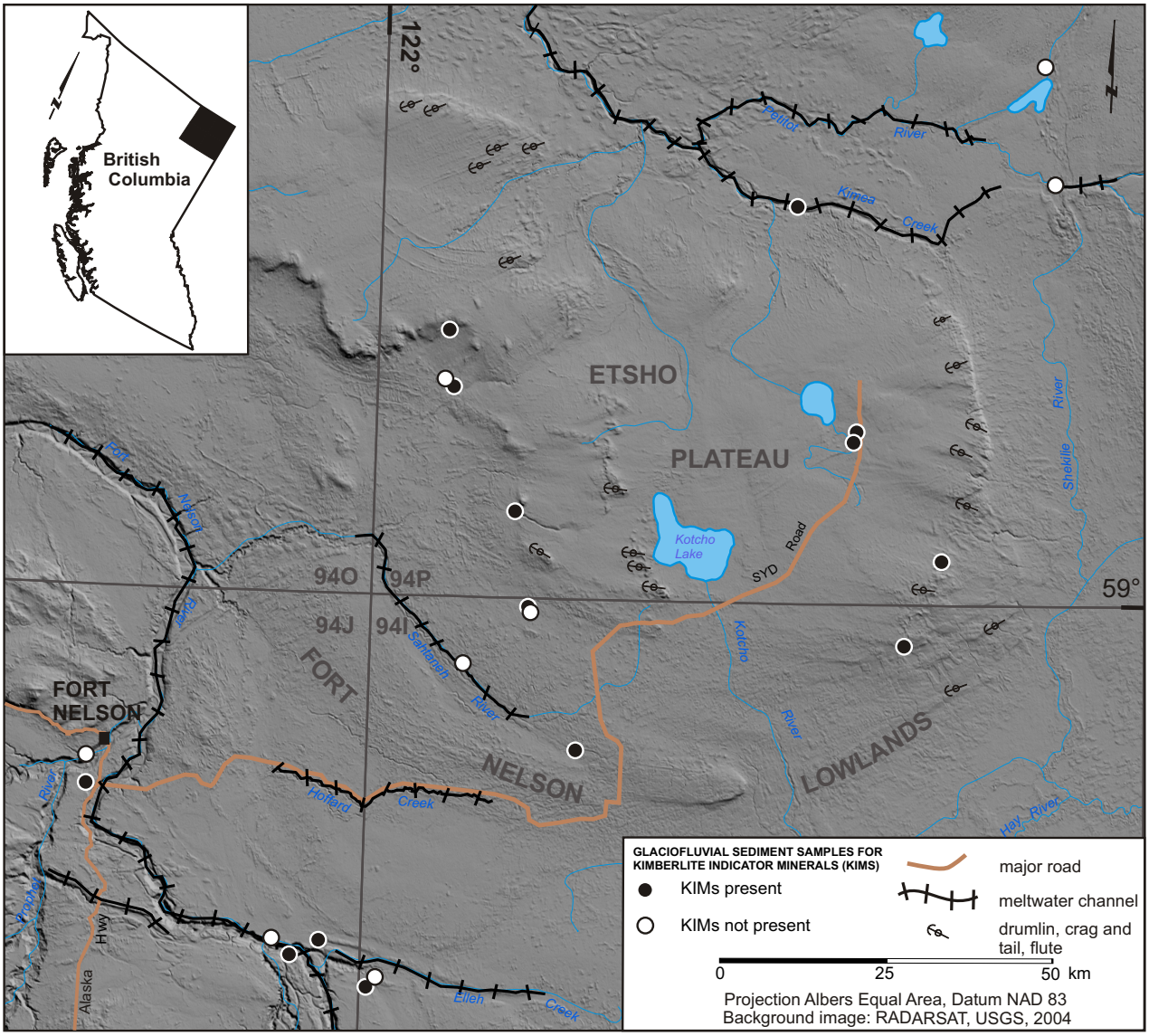


Figure 1. Location map of study area showing major ice-flow direction indicators and glaciofluvial sample sites. See Simandl *et al.* (2005a, b) for details on the KIM survey results.

to the Liard River while the Kotcho and Shekilie rivers flow to the Hay River, and then ultimately into the Mackenzie River and Beaufort Sea. Access to the region is limited to the Sierra-Yoyo-Desan (SYD) Road and a limited number of secondary all-season roads, which can rapidly deteriorate in wet weather conditions owing to their construction with clay-rich glacial sediment.

During the Late Wisconsinan glaciation, northeastern BC was completely covered by ice which flowed west and southwest across this region from the Keewatin ice divide of the Laurentide ice sheet (Fig. 1). The glaciers eroded the soft fine-grained Cretaceous sedimentary bedrock along with the glaciolacustrine sediments deposited at the advancing ice margin, resulting in a fine-grained silt and clay-rich regional till cover. The clast content in the tills is generally low (<10%), and rock fragments largely consist of the harder rock types derived from the Canadian Shield to the northeast with lesser amounts of carbonate and sandstone clasts derived from Cambrian to Devonian strata situated along the western Shield margin. Clasts of local sandstone and shale are found in small amounts. During deglaciation, large glacial lakes formed along the glacier margins where ice blocked the regional eastward drainage of rivers (Mathews, 1980). Extensive meltwater channels flowing from the retreating ice front and outlets of glacial lakes were incised into the glacial sediments and in some places bedrock (Fig. 1). Glaciofluvial sediments associated with these former meltwater channels are the focus of some KIM sampling as they are thought to provide a greater regional signature compared to till samples and is appropriate to the reconnaissance-scale exploration being conducted here. Nonetheless, in much of the study area, extensive bogs and fens with more than a metre of accumulated organic material greatly impede the systematic sampling of glacial sediments.

Northeastern BC is underlain by Archean and Proterozoic basement rocks (Gehrels and Ross, 1998; Simandl, 2004; Simandl *et al.*, 2005b) that extend into Alberta where diamondiferous kimberlites have been reported (Dufresne *et al.*, 1996; Carlson *et al.*, 1999; Eccles *et al.*, 2003;

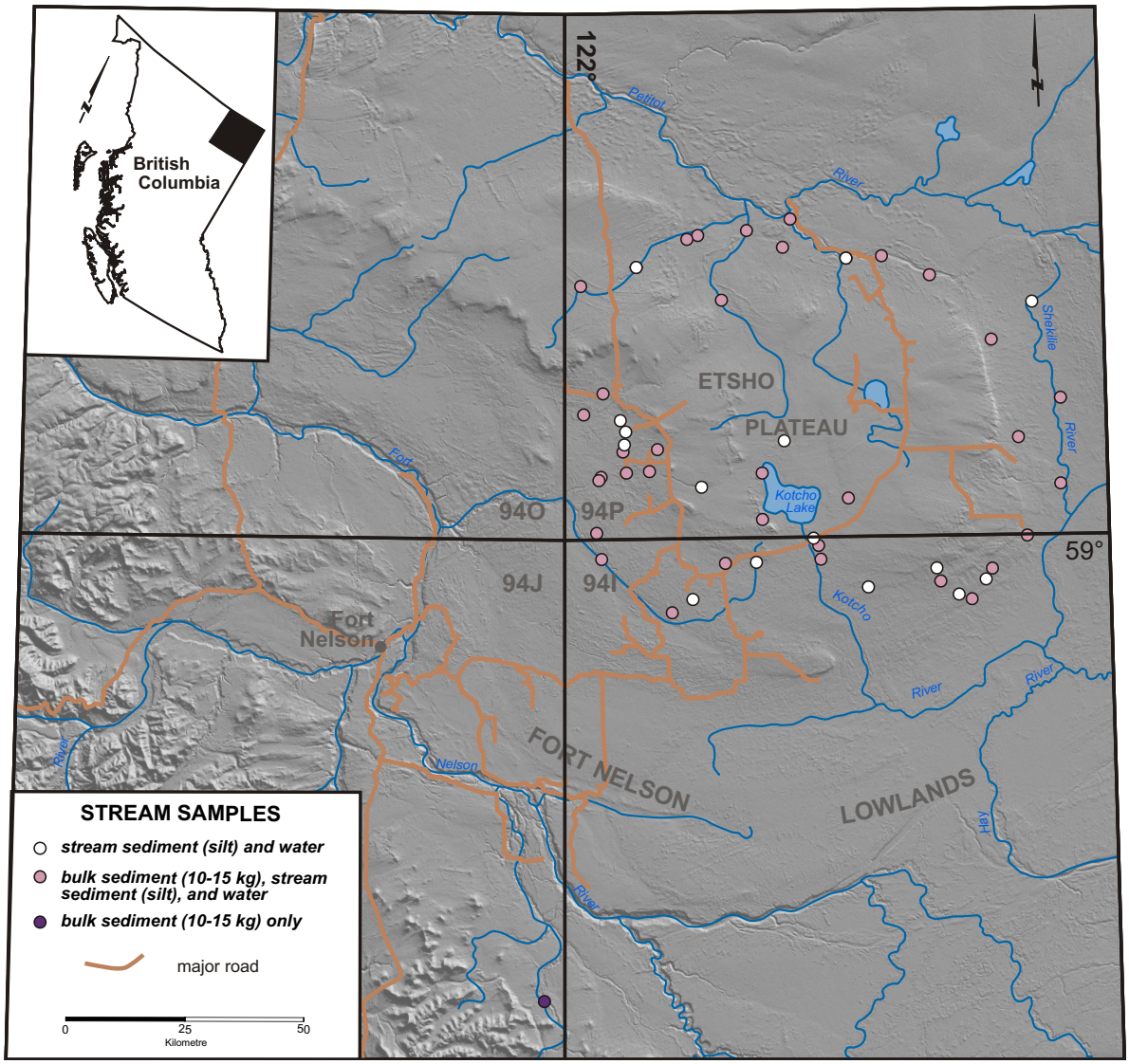


Figure 2. Location map of stream sediment and water sample sites, collected during the fall of 2005. Projection: Albers Equal Area, Datum NAD 83. Background image: RADARSAT, USGS, 2004.

Skelton *et al.*, 2003). The basement rocks are overlain by a succession of Paleozoic and Mesozoic sedimentary rocks including the Cretaceous Shaftesbury and Dunvegan formations, which outcrop in a limited number of places. As a result, the prospecting methodology used by this project restricts potential discoveries of kimberlites to those younger than or contemporaneous with the Cretaceous host rocks. Local kimberlites older than the Cretaceous rocks and thus overlain by them would not contribute indicator minerals to the surficial sediments. Furthermore, it is possible that older or Cretaceous kimberlites have been eroded and contributed KIMs into the Cretaceous bedrock. Consequently, the KIM content of a limited number of Cretaceous bedrock samples will be evaluated.

PROJECT DESCRIPTION AND OBJECTIVES

As part of a multidisciplinary effort to investigate the resource potential for kimberlite, diamonds, gold, base metal and other economic commodities in northeastern BC, an integrated glacial sediment survey over one year and a stream sediment, water and heavy mineral concentrate survey over two years are being completed in northeastern BC. Results obtained from both components of this project will complement each other.

Stream Sediment and Water Geochemistry

The main objective in the first year (2005) of this activity is to fully evaluate the effectiveness of stream sediment and water geochemistry at detecting potential kimberlites in the region of the Etsho Plateau. Based on the results of the sampling completed in 2005 (Fig. 2), a second year of stream sediment and water sampling (2006) covering the equivalent of one or two 1:50 000-scale map sheets will be undertaken. Geochemical surveys combining the collection of stream silt, water and coarse sediment for heavy mineral concentrates has proven effective at detecting kimberlites in the Buffalo Head Hills region of Alberta (Friske *et al.*, 2003), where the physiography is similar to the Etsho Plateau.

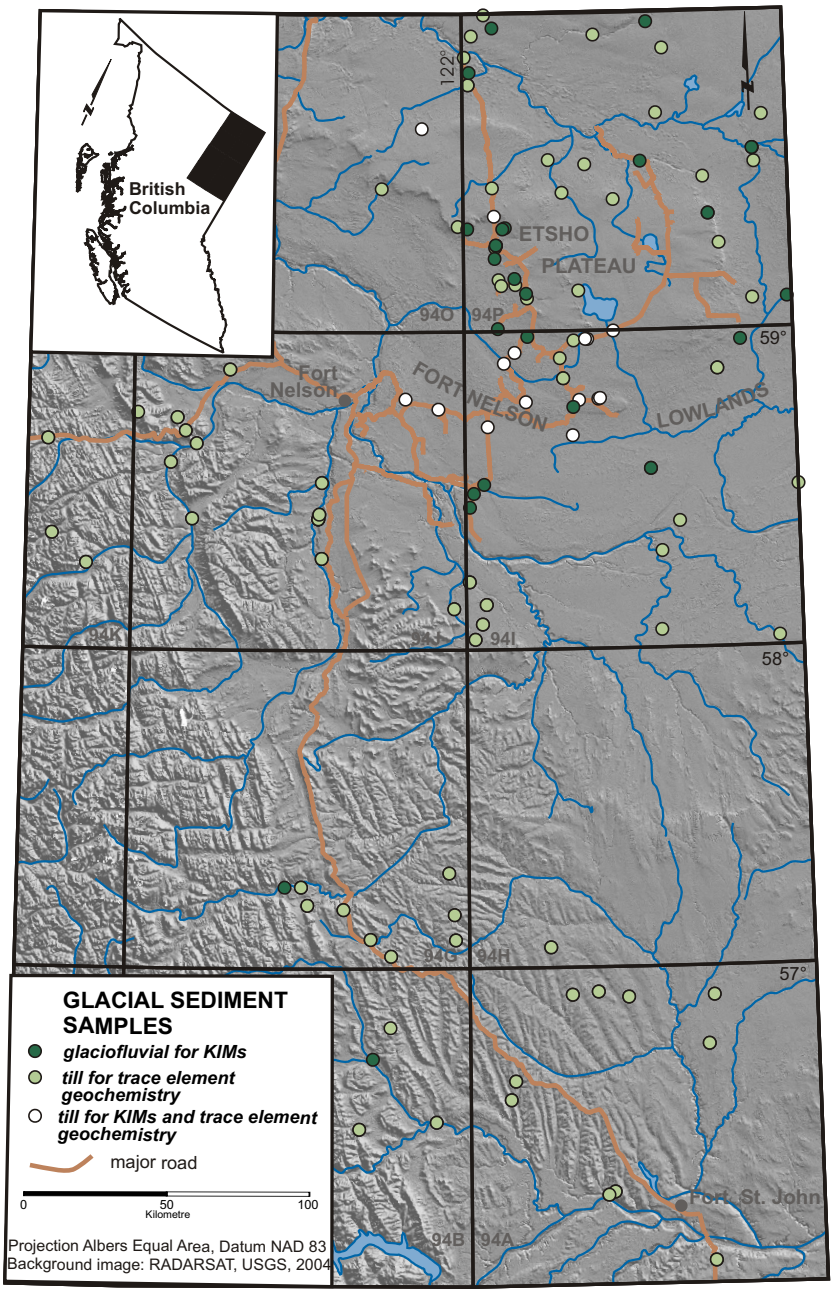


Figure 3. Location map of the glacial sediment sample sites, collected during the summer and fall of 2005.

Glacial Sediment Survey

Sampling of glacial sediments was completed during the summer and fall of 2005 (Fig. 3). It was principally focussed in the vicinity of the Etsho Plateau in the region where KIMs were previously reported. The main objective of this component is to better define the extent of the region where KIMs occur in glacial sediments and the potential source area. As part of the sampling program, till and glaciofluvial sediments have been sampled. Till samples generally reflect a more local source and glaciofluvial sediments can reflect a proximal or distal source depending on their nature and genesis. Therefore, sampling of these two sediments will provide additional information as to the source of the KIMs.

Increased helicopter access, gained from the funding provided by GBC, will also allow an improvement in the quality and accuracy of the surficial geology maps produced as part of the ongoing GSC and BC MEMPR collaborative project. Surficial geology maps are one of the fundamental sources of information necessary to reconstruct the glacial and ice-flow histories of the region, which are crucial elements to trace mineralogical or geochemical anomalies identified in the surficial sediment cover. Two surficial geology maps have been released from this area (Bednarski, 2005a, b) while full coverage of NTS 094I and 094P is expected to be completed by spring 2007. A further added benefit of the improved regional access gained through this project is the support it provides for exploration and assessment of new granular aggregate resources in

the more inaccessible areas. Local aggregate sources are critical to the promotion and sustainable development of petroleum resources in northeastern BC.

METHODOLOGY

Stream Sediment and Water Sample Collection

The integrated stream sediment, water and coarse sediment survey consists of two components:

- the collection of stream sediments and stream water samples at every site; and
- the additional collection of a bulk sediment sample (10–15 kg wet-screened through a 12-mesh [1.68 mm] sieve) from every second site (on average), from which the heavy mineral fraction is derived.

Stream sediment (silt) and water samples are collected at predetermined sites at an average density of one sample per 13 km^2. At the stream sites (first or second-order streams), a clean water sample(s) and a silt-clay – rich sediment sample are collected. Access is usually by helicopter, but also includes the more cost-effective use of trucks along existing roads, and all-terrain vehicle access along winter roads, pipeline right-of-ways and seismic lines. At sites selected for bulk sediment sampling (1 sample/25 km^2), coarse sediment (ideally from upstream points of mid-channel bars) is wet-sieved through a 12-mesh (1.68 mm) screen to collect 10 to 15 kg of material. Routine stream sediment samples (silt) and one or two water samples are also collected at the coarse sediment sample sites. Sample locations are recorded with a global positioning system (GPS) receiver, field observations are noted and the site is flagged.

Glacial Sediment Sample Collection

As with the stream sediment survey, two types of glacial sediment samples were collected:

- large bulk samples (equivalent to a 15 gallon pail) of till or glaciofluvial sediment for KIM analyses; and
- smaller samples (approximately 2 kg) of bulk till for geochemical analyses (Fig. 3).

The glacial sediment survey follows a methodology which has proven successful at identifying the presence of kimberlites throughout Canada; bulk glacial sediment samples are analyzed for their KIM content (McClenaghan *et al.*, 2002; McClenaghan, 2005). Using this method, bulk glacial sediment samples are collected below the depth of the oxidized soil horizon from road cuts, river bluffs, hand-dug pits, borrow pits and sump pits. Till sampling for geochemical analyses was completed in the Etsho Plateau region and was extended to the west and south of the study area to provide reconnaissance-scale evaluation of the mineral potential of this vast territory. Furthermore, in addition to the large bulk sediment samples collected in the Etsho Plateau region, two large glaciofluvial sediment samples were collected approximately 150 km northwest of Fort St. John (Fig. 3). Glacial sediment sample sites were recorded with a GPS receiver, field observations were noted, and sites were flagged.

Sample Processing and Analysis

Glacial and stream sediment samples are shipped to a commercial laboratory, which conducts the heavy mineral separation using a combination of a shaking table and heavy liquid to separate the nonferromagnetic heavy mineral fraction. This heavy mineral fraction is picked for KIMs and other indicators, such as gold, in the same laboratory. Potential KIMs are sent to the GSC for microprobe analysis. Spiked and duplicate samples are included in the samples sent to the laboratories to monitor analytical quality. Clasts from the glacial sediment samples are retained for glacial transport study.

Bulk sediment subsamples are sent to a separate laboratory for geochemical analyses. Inductively coupled plasma mass spectrometry analyses are conducted on the silt and clay-sized fraction (-250 mesh or <0.063 mm) of the till samples only. Analytical quality will be monitored with standard and duplicate samples.

ACHIEVEMENTS TO DATE

Field activities for both components of this project were conducted in the summer and fall of 2005. Stream sediment and water samples were collected at 51 sites including 36 sites with bulk sediment samples (10–15 kg; Fig. 2). A total of 123 glacial sediment samples were collected including 25 glaciofluvial samples and 98 till samples (Fig. 3). Sampling was hindered by wet weather conditions and the rarity of sediment exposures suitable for the collection of adequate KIM sediment samples.

The samples will be analyzed in the winter of 2006. Results will be released in 2006 in the form of open file reports.

ACKNOWLEDGMENTS

Jamie Andrews from Land and Water British Columbia and Kirsten Brown provided field assistance. Helicopter services were provided by Highland Helicopters and Vancouver Island Helicopters. Accommodation and services provided by Kledo Construction Ltd. Camp 102 were greatly appreciated.

REFERENCES

Bednarski, J.M. (2005a): Surficial geology, Estsine Lake, British Columbia (NTS 94P/13); *Geological Survey of Canada*, Open File 4825, scale 1:50 000.

Bednarski, J.M. (2005b): Surficial geology, Gote Creek, British Columbia (NTS 94P/12); *Geological Survey of Canada*, Open File 4846, scale 1:50 000.

Carlson, S.M., Hillier, W.D., Hood, C.T., Pryde, R.P. and Skelton, D.N. (1999): The Buffalo Hills kimberlites: a newly-discovered diamondiferous kimberlite province in north-central Alberta, Canada; *in* Proceedings of the VIIth International Kimberlite Conference, Volume 1, Gurney, J.J., Gurney, J.L., Pascoe, M.D. and Richardson, S.H., Editors, *Red Roof Design*, Capetown, pages 109–116.

Demchuk, T.E., Ferbey, T., Kerr, B.J. and Levson, V.M. (2005): Surficial geology and aggregate potential mapping in northeast British Columbia using Lidar imagery; *in* Summary of Activities 2005, *BC Ministry of Energy, Mines and Petroleum Resources*, pages 51–59.

Dufresne, M.B., Eccles, D.R., McKinstry, B., Schmitt, D.R., Fenton, M.M., Pawlowicz, J.G. and Edwards, W.A.D. (1996): The diamond potential of Alberta; *Alberta Geological Survey*, Bulletin No. 63, 158 pages.

Eccles, D.R., Pana, D.I., Paulen, R.C., Olson, R.A. and Magee, D. (2003): Discovery and geological setting of the northern Alberta kimberlite province; *in* Slave Province and Northern Alberta Field Trip Guidebook, VIIIth International Kimberlite Conference, Kjarsgaard, B.A., Editor, pages 1–10.

Ferbey, T., Hickin, A.S., Demchuk, T.E. and Levson, V.M. (2005): Northeast British Columbia aggregate mapping program: a summary of selected aggregate occurrences northeast of Fort Nelson; *in* Summary of Activities, *BC Ministry of Energy, Mines and Petroleum Resources*, pages 60–68.

Friske, P.W.B., Prior, G.J., McNeil, R.J., McCurdy, M.W. and Day, S.J.A. (2003): National geochemical reconnaissance (NGR) stream sediment and water survey in the Buffalo Head Hills area, northern Alberta (parts of NTS 84B, 84C, 84F and 84G) including analytical mineralogical and kimberlite indicator mineral data from silts, heavy mineral concentrates and waters; *Alberta Geological Survey*, Special Report 66 / *Geological Survey of Canada*, Open File 1790, CD ROM.

Gehrels, G.E. and Ross, G.M. (1998): Detrital zircon geochronology of Neoproterozoic to Permian miogeoclinal strata in British Columbia and Alberta; *Canadian Journal of Earth Sciences*, Volume 35, pages 1380–1401.

Holland, S.S. (1976): Landforms of British Columbia, a physiographic outline; *BC Ministry of Energy, Mines and Petroleum Resources*, Bulletin 48, 138 pages.

Johnsen, T., Ferbey, T., Levson, V.M. and Kerr, B. (2004): Quaternary geology and aggregate potential of the Fort Nelson airport area; *in* Summary of Activities, *BC Ministry of Energy, Mines and Petroleum Resources*, Resource Development and Geoscience Branch, pages 19–28.

Levson, V.M., Ferbey, T., Kerr, B., Johnsen, T., Bednarski, J.M., Smith, R., Blackwell, J. and Jonnes, S. (2004): Quaternary geology and aggregate mapping in northeast British Columbia: applications for oil and gas exploration and development; *in* Summary of Activities, *BC Ministry of Energy, Mines and Petroleum Resources*, Resource Development and Geoscience Branch, pages 29–40.

Levson, V.M., Ferbey, T., Hickin, A.S., Bednarski, J., Smith, I. R., Demchuk, T.E., Trommelen, M.S., Kerr, B. and Church, A. (2005): Surficial geology and aggregate studies in the boreal plains of northeast British Columbia; *in* Summary of Activities 2005, *BC Ministry of Energy, Mines and Petroleum Resources*, pages 42–50.

Mathews, W.H. (1980): Retreat of the last ice sheets in northeastern British Columbia and adjacent Alberta; *Geological Survey of Canada*, Bulletin 331, 22 pages.

McClenaghan, M.B. (2005): Indicator mineral methods in mineral exploration; *Geochemistry: Exploration, Environment, Analysis*, Volume 5, pages 233–245.

McClenaghan, M.B., Ward, B.C., Kjarsgaard, I.M., Kjarsgaard, B.A., Kerr, D.E. and Dredge, L.A. (2002): Indicator mineral and till geochemical dispersal patterns associated with the Ranch Lake kimberlite, Lac de Gras region, NW Territories, Canada; *Geochemistry: Exploration, Environment, Analysis*, Volume 2, pages 299–320.

Simandl, G.J. (2004): Concepts for diamond exploration in "on/off craton" areas - British Columbia; *Lithos*, Volume 77, pages 749–764.

Simandl, G.J. (2005): Diamond potential - new advances in British Columbia; *in* Mineral Exploration Roundup 2005, Abstract Volume, Vancouver, BC, *British Columbia and Yukon Chamber of Mines*, page 10.

Simandl, G.J., Ferbey, T., Levson, V.M., Demchuk, T.E., Hewett, T., Smith, I.R. and Kjarsgaard, I. (2005a): Heavy mineral survey and its significance for diamond exploration, Fort Nelson area, British Columbia, Canada; *BC Ministry of Energy, Mines and Petroleum Resources*, Geofile 2005-13.

Simandl, G.J., Ferbey, T., Levson, V.M., Demchuk, T.E., Mallory, S., Smith, I.R. and Kjarsgaard, I. (2005b): Kimberlite indicator minerals in the Fort Nelson area, northeastern British Columbia; *in* Geological Fieldwork 2004, *BC Ministry of Energy, Mines and Petroleum Resources*, pages 325–343.

Skelton, D.N., Clements, B., McCandless, T.E., Hood, C., Aulbach, S., Davies, R. and Boyer, L.P. (2003): The Buffalo Head Hills kimberlite province, Alberta; *in* Slave Province and Northern Alberta Field Trip Guidebook, VIIIth International Kimberlite Conference, Kjarsgaard, B.A., Editor, pages 11–19.

Smith, I.R., Paulen, R.C., Plouffe, A., Kowalchuk, C. and Peterson, R. (2005): Surficial mapping and granular aggregate resource assessment in northwest Alberta; *in* Summary of Activities 2005, *BC Ministry of Energy, Mines and Petroleum Resources*, pages 80–95.

Trommelen, M.S., Levson, V.M., Hickin, A. and Ferbey, T. (2005): Quaternary geology of Fort Nelson (NTS 094J/SE) and Fontas River (NTS 094I/SW), northeastern British Columbia; *in* Summary of Activities 2005, *BC Ministry of Energy, Mines and Petroleum Resources*, pages 96–112.

2005 Regional Geochemical Survey, NTS Areas 083C, 083D, 083E and 082N, Southeastern British Columbia[1]

By C.O. Naas[2]

KEYWORDS: geochemistry, regional geochemical survey

INTRODUCTION

Reconnaissance-scale stream sediment and water surveys have a history of success in British Columbia and are widely recognized as one of the more important exploration tools in the Cordillera. In 2005, this important geochemical data source was expanded with a new program conducted in the Valemount and Golden areas.

The stream sediment and water survey in NTS map sheets 083C (Brazeau Lake), 083D (Canoe River), 083E (Mount Robson) and 082N (Golden) will complete the coverage in the southeastern portion of the province. Funding for this program was made available by Geoscience BC.

The 2005 Regional Geochemical Survey program was carried out between August 26 and October 23, 2005 by CME Managing Consultants Inc. The survey covered a total of 21 560 km^2 (including approximately 7% glacier and icefield coverage) at an average density of approximately one sample site per 15 km^2.

Samples were collected from a total of 1409 sites. Sample sites were accessed via truck, trail bike or helicopter. Sample collection, data recording, drying, packing and shipping standards were undertaken according to standards set by the BC Geological Survey and the Geological Survey of Canada for the Regional Geochemical Survey program, which is part of the Federal National Geochemical Reconnaissance program.

REGIONAL SETTING

Location

The area surveyed covers southeastern BC from 51° to 53°N and from 116° to 120°W (Fig. 1). Sampling was not undertaken in national or provincial parks.

Physiography

From east to west, the study area consists of the Rocky Mountains, the Rocky Mountain Trench, the Columbia Mountains and the Quesnel and Shuswap highlands (Holland, 1976). The Quesnel and Shuswap highlands make up a small portion of the study area, as they occur in the southwestern corner of map sheet 83D. The Columbia Mountains, from north to south, consist of the Cariboo, Monashee, Selkirk and Purcell mountains.

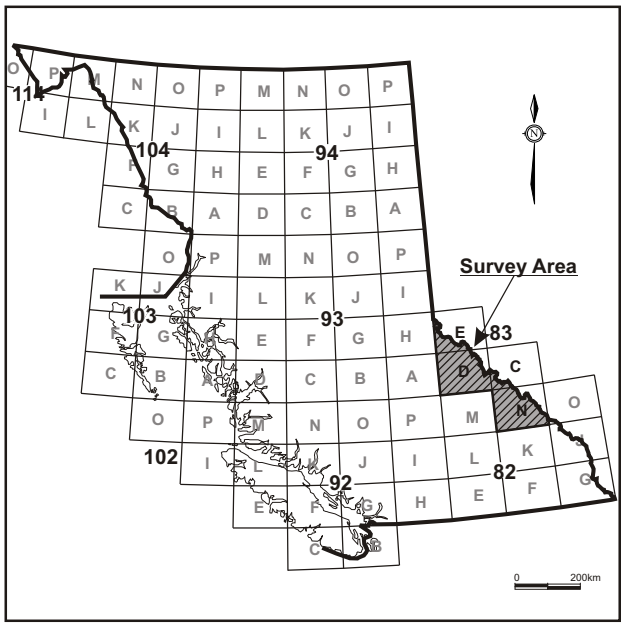


Figure 1. Location of 2005 regional geochemical survey.

Both the Rocky and Columbia mountains are glaciated and consist of extremely rugged terrain. Massive and bold sharp peaks are separated by deep and narrow valleys. The peaks and ridges are predominantly exposed bedrock and typically range between 2500 and 3000 m in elevation. The steeply sloping valley sides are covered with talus and colluvium, and the valley bottoms with alluvium and till.

Geology

The survey area includes parts of two of the five morphotectonic belts that constitute the Canadian segment of the North American Cordillera. These are the Foreland Belt to the east and the Omineca Belt to the west.

Several gneissic bodies crop out adjacent to and along the Rocky Mountain Trench. To the east of the Rocky Mountain Trench, rocks of the Main Ranges of the Rocky Mountains form an imbricate thrust package of Hadrynian to Triassic metasedimentary and sedimentary rocks of the ancestral North American craton (Mountjoy, 1992).

---

[1] *Geoscience BC contribution GBC012*

[2] *CME Managing Consultants Inc., Richmond, BC*

This publication is also available, free of charge, as colour digital files in Adobe Acrobat PDF format from the BC Ministry of Energy, Mines and Petroleum Resources internet website at http://www.em.gov.bc.ca/Mining/Geolsurv/Publications/catalog/catfldwk.htm

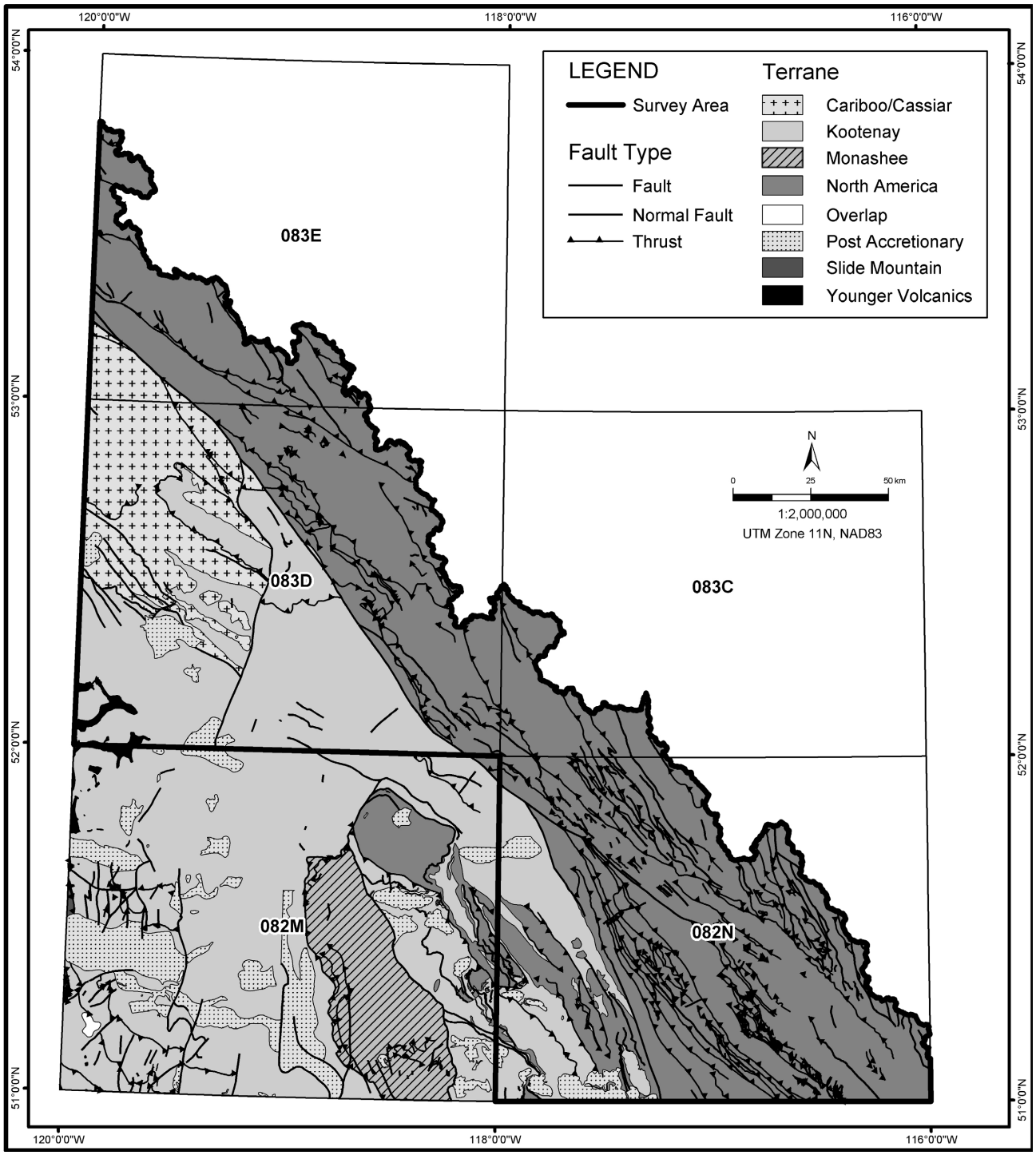


Figure 2. Terrane map, east-central British Columbia.

To the west of the Rocky Mountain Trench in the Canoe River and Mount Robson map areas are the Kootenay and Cassiar-Cariboo terranes (Fig. 2). Rocks of the Kootenay Terrane include the Hadrynian Horsethief Creek Group and the overlying Kaza and Cariboo groups (Mountjoy, 19932. The Cassiar-Cariboo Terranes include Late Proterozoic to Late Triassic passive continental margin sedimentary rocks displaced along the Rocky Mountain Trench transcurrent faults (Wheeler *et al.*, 1988). East of the Rocky Mountain Trench is the Foreland Belt, represented by the Rocky Mountains. In this area, the Foreland Belt consists primarily of a sequence of quartzite, carbonate and pelite from the Hadrynian Miette Group through the Late Cambrian Gog Group to the Middle Cambrian Chancellor Group (MINFILE 083D001; MINFILE, 2005).

Hadrynian rocks on both sides of the Rocky Mountain Trench have been intensely deformed by at least three folding events and affected by Barrovian metamorphism

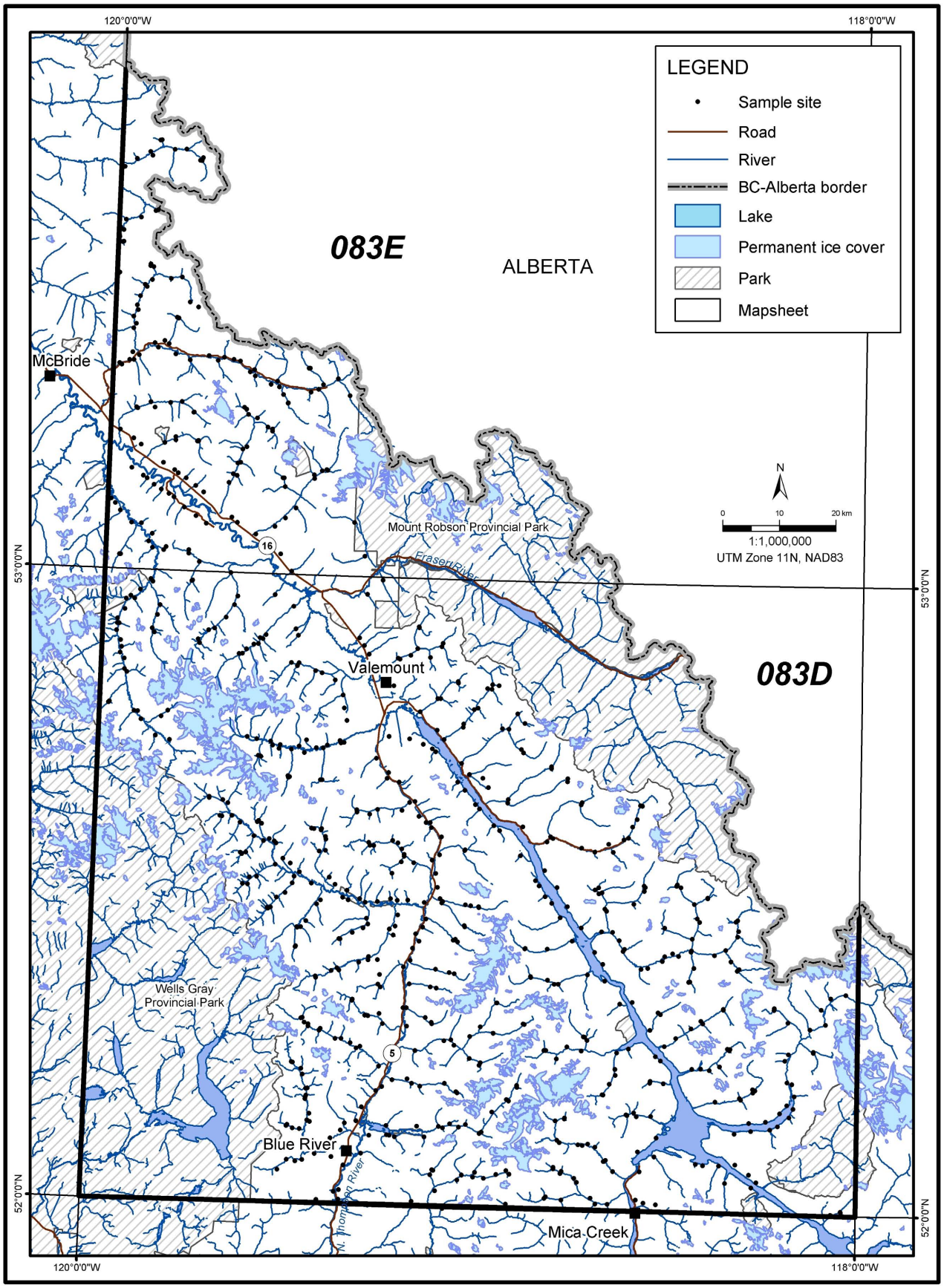


Figure 3. Sample site locations, NTS areas 083D and 083E.

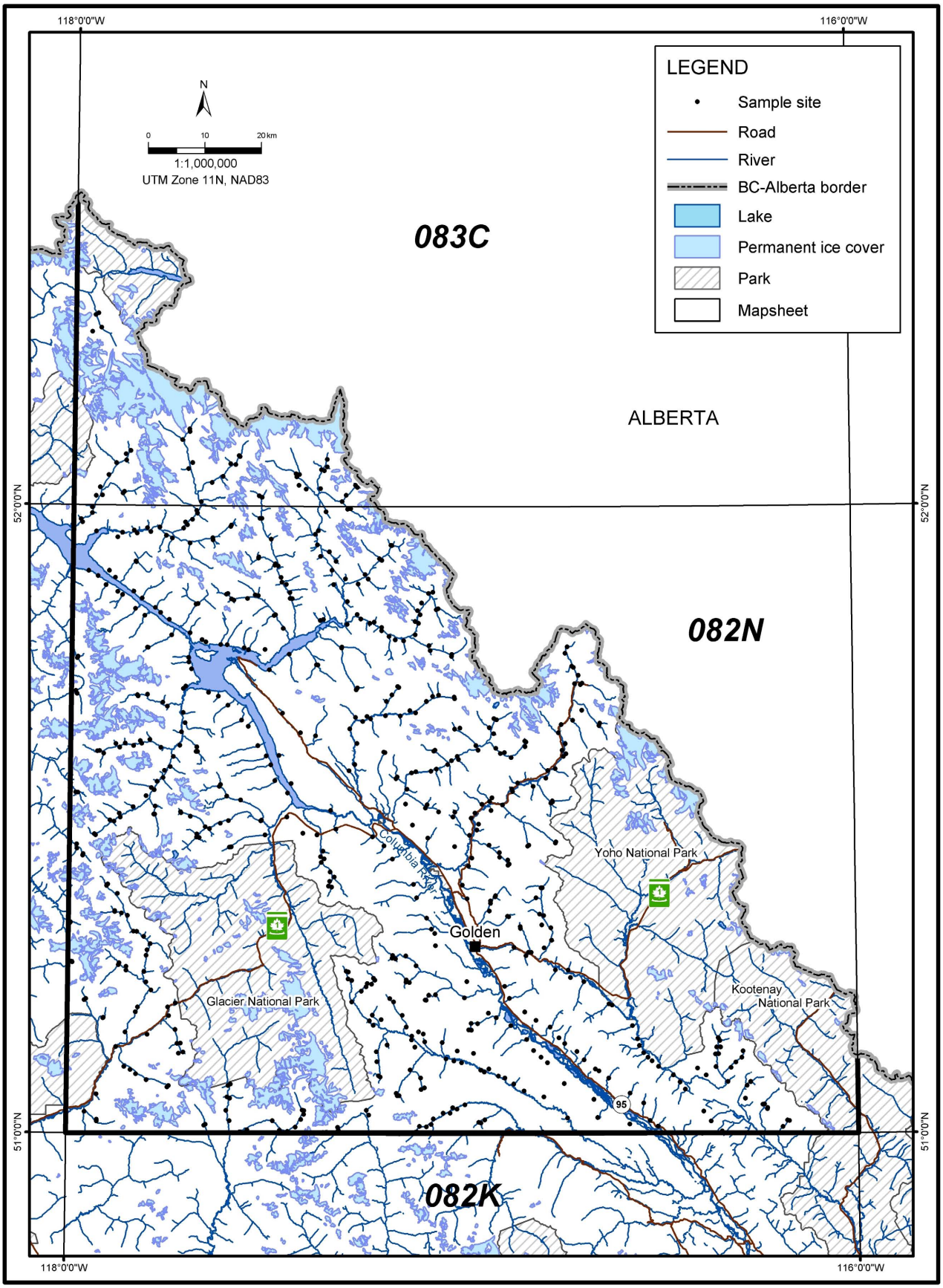


Figure 4. Sample site locations, NTS areas 082N and 083C.



Figure 5. Helicopter sampling in the Mount Robson map area.

(~160–60 Ma; Crowley *et al.*, 2000), ranging in grade from the biotite to the sillimanite zone (Mountjoy, 1992).

West of the Rocky Mountain Trench in the Golden area lies the Purcell Anticlinorium, within which a thick succession of Proterozoic (*i.e.*, Horsethief Creek and Miette groups) and Paleozoic (Hamill, Lardeau and Gog groups; Eager, Badshot, Mohican, Donald, Reno, Laib and Quartzite Range formations) miogeoclinal rocks has been deformed by imbricate thrust faults, normal faults, complex folds and widespread penetrative deformation (Owsiacki, 1993).

Mineralization

In the Canoe River and Brazeau Lake map areas, most of the known mineral occurrences are located adjacent to or west of the Rocky Mountain Trench and consist of industrial mineral as well as precious and base metal occurrences. The precious and base metal occurrences are dominated by Pb-Zn-Ag showings, with lesser numbers of Au showings. Industrial mineral occurrences of mica and kyanite, with lesser garnet and beryllium, are generally hosted in the semipelite-amphibolite unit of the Hadrynian Horsethief Creek Group (Mountjoy, 1992).

Several small alkaline ultramafic diatremes, intruding Late Cambrian carbonate strata, have been discovered and explored in the Bush River area for diamonds (Mountjoy, 1992).

A number of carbonatite and nepheline syenite layers occur within the semipelite-amphibolite unit of the Horsethief Creek Group in the Monashee Mountains. These have been examined for their vermiculite, U, Nb and Ta potential.

The documented occurrences in the Golden map area are evenly distributed on both sides of the Rocky Mountain Trench. Approximately two-thirds of the total occurrences are Pb-Ag-Zn-(Cu-Au) replacement-type mineralization hosted primarily in carbonate rocks, and Pb-Ag-Zn-(Au-Cu-W) quartz veins in metasedimentary rocks, chiefly slate, graphitic slate, schist and argillite. Industrial mineral occurrences make up the remaining third of the occurrences in the Golden map area (Owsiacki, 1993).



Figure 6. Sample collection site in the Golden map area.

REGIONAL GEOCHEMICAL SURVEY PROGRAM

CME Managing Consultants Inc. of Richmond, BC was selected by competitive bid to manage and carry out the 2005 regional geochemical survey sampling program in southeastern BC.

Sample Collection

The sample-collection team consisted of three samplers and a crew chief. The sample preparation facility was supervised by a lab manager. Field operations were conducted from several strategically located base camps. Sample collection, data recording, drying, packing and shipping were in accordance with standards set by the BC Geological Survey and required by Geoscience BC.

Stream sediment and streamwater samples were collected from 42 sites in the Brazeau Lake map area (83C), 603 sites in the Canoe River map area (83D), 152 sites in the Mount Robson map area (83E) and 612 sites in the Golden map area (82N; Fig. 3, 4).

The surveys covered approximately 21 560 km^2 at an average density of approximately one sample site per 15 km^2. Sampling was not undertaken in national or provincial parks. Approximately 7% of the area surveyed is covered by glaciers and icefields.

Access to the sample sites was gained by truck or trail bike for 36% of the sites, with the remainder being accessed by helicopter (Fig. 5).

In general, sample sites were restricted to primary and secondary drainages having catchment basins of less than 10 km^2 (Fig. 6). Contaminated or poor-quality sample sites were avoided by choosing an alternative stream or sampling a minimum of 50 m upstream from the identified problem.

Sample Preparation

Collected samples were field processed by CME at a central facility in Valemount. Sediment samples were dried and sediment material finer than 1.7 mm was recovered by sieving each sample through a –10 mesh ASTM screen.

Sediment samples were further sieved to –80 mesh ASTM to produce a minimum of 50 g of material. Blind duplicate samples and control reference materials were inserted into each analytical batch of 20 sediment samples. Control reference water standards were also inserted into each analytical batch of 20 water samples.

Analytical Procedures

The –80 mesh material and water samples were delivered to Eco Tech Laboratories of Kamloops, BC for analytical testing.

Analysis of sediments will include 37 elements by inductively couple plasma – mass spectrometry, 35 elements by neutron activation, fluorine, and loss-on-ignition. Water analysis will include pH, conductivity and fluorine.

In order to monitor the integrity of the geochemical database and to provide a measure of precision, accuracy and confidence, a quality-control program was implemented for all samples. Field site duplicates, blind analytical duplicates and control reference materials were used to ensure that analytical data satisfy the quality-control standards established by the BC Geological Survey.

The expected release date for the results is early spring 2006.

ACKNOWLEDGMENTS

The author gratefully acknowledges the financial support from Geoscience BC. The author also acknowledges the dedicated work provided by the field crew, in particular Larry Crittenden, Ted VanderWart and Evert Van Leeuwen. Ray Lett is thanked for the timely supply of geochemical references and Henry Awmack for his review and comments on the manuscript.

REFERENCES

Crowley, J.L, Ghent, E.D., Carr, S.D., Simony, P.S. and Hamilton, P.A. (2000): Multiple thermotectonic events in a continuous metamorphic sequence, Mice Creek area, southeastern Canadian Cordillera; *Geological Materials Research*, Volume 2, no 2, page 1.

Holland, S.S. (1976): Landforms of British Columbia, a physiographic outline; *BC Ministry of Energy, Mines and Petroleum Resources*, Bulletin 48.

MINFILE (2005): MINFILE BC mineral deposits database; *BC Ministry of Energy, Mines and Petroleum Resources*, URL <http://www.em.gov.bc.ca/Mining/ Geolsurv/Minfile/> [Nov 2005].

Mountjoy, K.J., Compiler (1992): Canoe River and Brazeau (NTS 083D, C); *BC Ministry of Energy and Mines and Petroleum Resources*, MINFILE digital data, 47 occurrences, URL <www.em.gov.bc.ca/Mining/Geolsurv/Minfile/mapareas/83dccov.htm> [Dec 2005].

Owsiacki, G., Compiler (1993): Golden and Calgary (NTS 082N, O); *BC Ministry of Energy and Mines and Petroleum Resources*, MINFILE digital data, 92 occurrences, URL <www.em.gov.bc.ca/Mining/Geolsurv/Minfile/mapareas/82nocov.htm> [Dec 2005].

Wheeler, J.O., Brookfield, A.J., Gabielse, H., Monger, J.W.H., Tipper, H.W. and Woodsworth, G.J. (1988): Terrane map of the Canadian Cordillera; *Geological Survey of Canada*, Open File 1894, 9 pages and 1 map.

Initiation and Deformation of the Jurassic-Cretaceous Bowser Basin: Implications for Hydrocarbon Exploration in North-Central British Columbia[1]

By J.W.F. Waldron[2], J.-F. Gagnon[2], W. Loogman[2] and C.A. Evenchick[3]

KEYWORDS: Hazelton Group, Bowser Basin, Bowser Lake Group, structure, folds

INTRODUCTION

The Bowser Basin is a large (~53 000 km^2) sedimentary basin located over the Stikine Terrane in the north-central Cordillera of British Columbia (Fig. 1). The basin is filled by up to ~6 km of Jurassic to Cretaceous sedimentary rocks, mainly assigned to the Bowser Lake Group but potentially also including upper units of the Early to Middle Jurassic Hazelton Group, as well as Cretaceous strata of the Skeena Group in the southern part of the basin (Tipper and Richards, 1976; Ricketts *et al.*, 1992; Bassett and Kleinspehn, 1997; Evenchick and Thorkelson, 2005). The economic significance of the basin includes, at the base, mineralized units (*e.g.*, the Eskay Creek Au-Ag deposit; Anderson, 1993; Roth *et al.*, 1999). Higher in the succession, the Bowser Lake Group contains significant coal beds and units with potential as petroleum source and reservoir rocks. The structure of the basin, dominated by folds, provides numerous potential traps. The petroleum potential of the basin has been discussed by Osadetz *et al.* (2003), and Evenchick *et al.* (2003).

The aims of this study are to 1) improve understanding of the structural and sedimentological conditions during the initiation of Bowser Basin subsidence; and 2) examine the Cretaceous-Tertiary deformation of the basin, with the goal of distinguishing and understanding deformation episodes in the Skeena fold belt. Organic-rich shale units at the base of the succession deposited in the Bowser Basin were investigated by Ferri and Boddy (2005), who reported total organic carbon contents up to 6% in samples from mature to overly mature parts of the basin; they suggested that original organic contents may have been 2–4 times greater, representing the greatest source potential in the basin. An improved understanding of the stratigraphic and structural relationships of these rocks (objective 1) is therefore important for an assessment of the petroleum potential of the basin. Structurally, the Skeena fold belt contains overprinted folds of at least two generations, producing dome-and-basin fold-interference patterns (*e.g.*, Evenchick 1991, 2001). Structural domes represent potential traps; an improved understanding of the origin and timing of folding, and the relationships between folds and faults (objective 2), may assist in the location of such structures in the subsurface.

Fieldwork in 2005 focused on selected regions (Fig. 1), chosen on the basis of previous mapping by Greig and Evenchick (1993), Evenchick *et al.* (2000), Evenchick (2001) and Evenchick and Thorkelson (2005) as displaying either field relations at the base of the Bowser succession or potential overprinting relationships between folds of different generations, or both. The results presented here are preliminary, and are based entirely on field results; thin-section, paleontological and analytical work will be carried out later in the project.

REGIONAL STRATIGRAPHIC UNITS

Units of the Stikine Terrane underlying the Bowser Lake Group represent a variety of Late Paleozoic to early Mesozoic arc environments, and are dominated by volcanic rocks. The Triassic (Carnian-Norian) Stuhini Group is characterized by pyroxene-phyric basalt, whereas Early to early Middle Jurassic volcanic and volcaniclastic rocks of the overlying Hazelton Group include bimodal lavas and abundant volcaniclastic rocks (Anderson, 1993). Interfingering with these, distinctive mixed sedimentary and volcanic successions of Early Jurassic to early Middle Jurassic (Pliensbachian to Bajocian) age have historically been assigned to the upper Hazelton Group and have been given a variety of formation names (*e.g.*, Thomson *et al.*, 1986; for a review, see also Marsden and Thorkelson, 1992). In the vicinity of the study areas, the term Salmon River Formation has been applied to these strata (Anderson, 1993; Greig and Evenchick, 1993; Lewis, 1996), and they are largely within the belt of the Eskay Creek and Troy Ridge facies of Anderson (1993). As elsewhere, the unit is characterized in the study areas by very thinly bedded, blocky, siliceous, very fine brown sandstone and siltstone, including fine, pale-coloured tuffaceous mudstone, which locally imparts a conspicuous striped appearance (Fig. 2). These strata are known informally as 'pyjama beds'.

At many locations visited in this study, the lower and upper Hazelton rocks are separated by a mappable angular unconformity. In contrast, the contact between the Spatsizi Formation (and its equivalents) and the overlying Bowser Lake Group is typically broadly concordant and appears transitional in many locations, though affected by later deformation. Hence, for the purposes of understanding basin evolution, it is helpful to treat the upper Hazelton and Bowser Lake groups together. The informal term 'Bowser suc-

[1] *Geoscience BC contribution GBC013; ESS contribution #2005442*

[2] *Department of Earth and Atmospheric Sciences, University of Alberta, Edmonton AB (john.waldron@ualberta.ca)*

[3] *Geological Survey of Canada, Vancouver, BC*

This publication is also available, free of charge, as colour digital files in Adobe Acrobat PDF format from the BC Ministry of Energy, Mines and Petroleum Resources internet website at http://www.em.gov.bc.ca/Mining/Geolsurv/Publications/catalog/catfldwk.htm

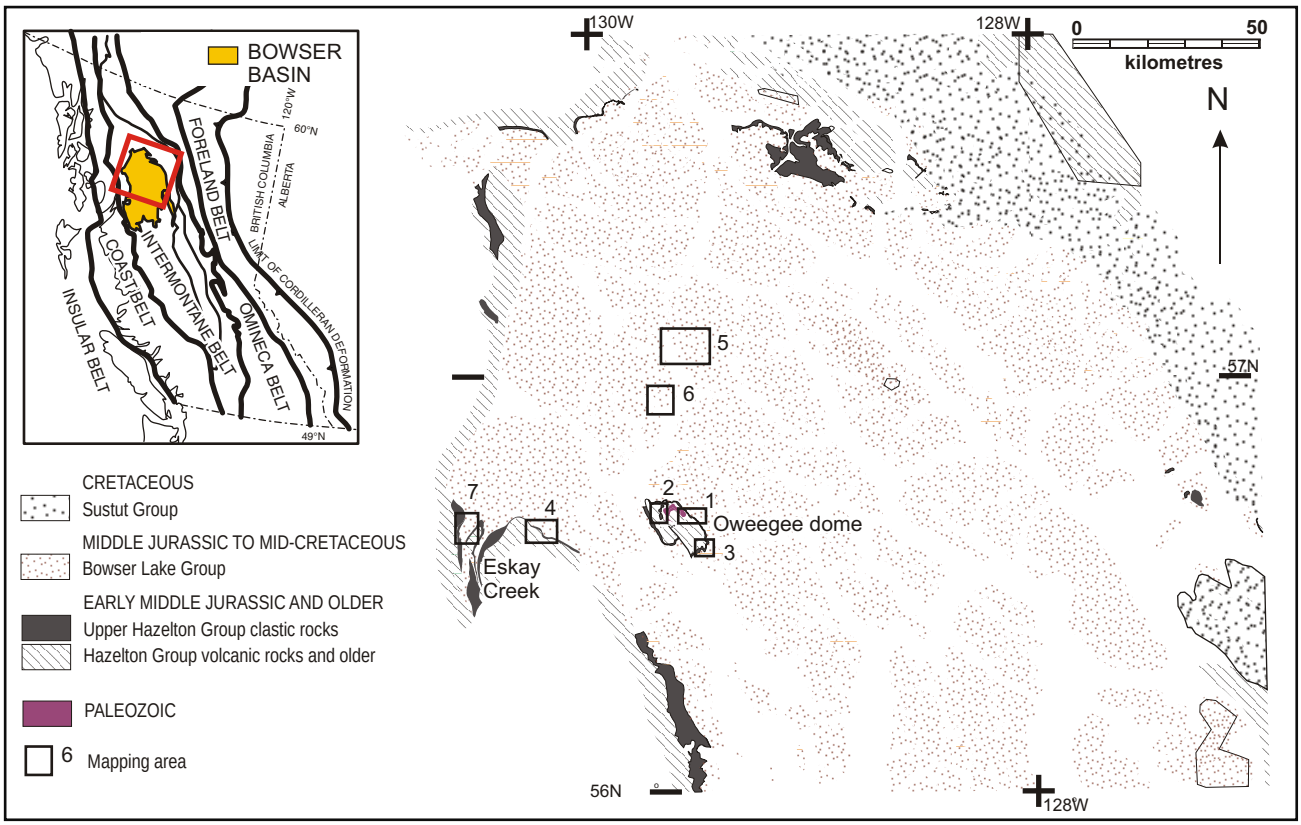


Figure 1. Simplified geology of the northern two-thirds of the Bowser Basin, showing areas of detailed study in 2005. Inset shows the location of the Bowser Basin in relation to principal belts of the Cordilleran Orogen in British Columbia, with the area covered by the main map indicated by the red rectangle.

cession' is used herein to refer to this package of mainly sedimentary strata.

The overlying Bowser Lake Group consists predominantly of shale and sandstone, and, in the north and northeast, chert-pebble conglomerate (*e.g.*, Evenchick and Thorkelson, 2005) The sandstone and siltstone are less siliceous than those of the upper Hazelton Group. Petrographic investigations summarized by Evenchick and Thorkelson (2005) have revealed an abundance of detrital chert clasts, interpreted to have been derived from the Cache Creek Terrane to the northeast. The Bowser Lake Group has been informally divided by Evenchick and Thorkelson (2005) into facies assemblages based on features such as sedimentary structures, nature of cyclicity and proportions of rock types, and are interpreted to represent distinct depositional environments. Three of these assemblages were examined in the course of the 2005 field season: the Richie-Alger, Muskaboo and Skelhorne assemblages, representing submarine fan, shallow marine (Fig. 3) and deltaic environments of deposition.

STRATIGRAPHIC RELATIONSHIPS OBSERVED AT THE BASE OF THE BOWSER SUCCESSION

Lower Hazelton and Older Rocks

Relationships at the base of the Bowser succession are well displayed around the Oweegee Dome, in areas 1–3 (Fig. 1). Immediately below the base of the Bowser succession is the largely volcanic succession of the lower Hazelton Group. Good exposures of the lower Hazelton Group dip gently (20°) southwest in area 2 in the northwestern part of the Oweegee Dome (Fig. 1). The lowest unit observed consists of medium beds of weakly calcareous green chert interbedded with fine layers of fissile dust tuff, passing laterally into well-stratified maroon and green volcaniclastic sandstone interbedded with pebble to cobble conglomerate, debris flows, minor andesitic volcanic flows and pinkish volcanic breccia. Pyroclastic rocks, such as clay-altered flaky ash tuff and highly feldspathic lapilli tuff, are common within this unit. Upsection, there is a gradual increase of reworked volcanic material, producing more characteristically sedimentary rocks. Volcaniclastic siltstone and sandstone with high proportions of igneous clasts display parallel laminations, moderate sorting and fining-upward sequences. These units are overlain by an ~30 m thick unit of felsic porphyritic rhyolite.

In the vicinity of Teigen Lake (area 4, Fig. 1), the lower Hazelton Group is characterized by well-stratified, greenish grey, poorly sorted, matrix-supported pebble conglomerate with soft thin interbeds of ash and lapilli tuff. These volcaniclastic rocks are highly siliceous and locally show significant evidence of reworking by water, such as fining-upward cycles and well-sorted bands. Matrix-supported debris-flow units are also present. Volcanic flows of quartz-phyric rhyolite, and hornblende-phyric andesitic lava with calcite amygdules, are common.

Rocks of the Hazelton Group west of the Eskay Creek mine in area 7 are thinly bedded felsic volcanic tuff interbedded with intermediate plagioclase-hornblende-phyric flows. These rocks are greenish grey on fresh surfaces and usually altered to an intense reddish brown colour. Calcite and quartz veins are common.

Upper Hazelton Group

The overlying upper Hazelton Group consists of thinly interbedded sandstone and shale, localized conglomerate, occasional fissile green tuff beds and thin beds of limestone. In area 1, the basal contact of the upper Hazelton Group is clearly mappable as an angular unconformity, though rarely well exposed. Massive grey-green volcanic breccia of the lower Hazelton Group is overlain by clast-supported, poorly sorted, quartz-rich pebble conglomerate with occasional mafic pebbles. The conglomerate is indicative of a high-energy environment and likely a relatively shallow water depth. Clasts range from angular to well rounded, suggesting provenance from a range of distances. The conglomerate passes transitionally upward into more characteristic 'pyjama beds' that are similar to parts of the Salmon River Formation elsewhere. The overlying siltstone, shale and laterally continuous tuff beds suggest a lower energy, deeper water setting, with continuing distal volcanic activity. Sectional exposures of the upper Hazelton Group overlain by turbidites of the Bowser Lake Group (Ritchie-Alger assemblage) occur along the east side of Oweegee Dome (area 1). The section in Figure 4 shows the upper portion of the Hazelton Group and the basal Bowser Lake Group.

In area 2, a sharp irregular contact between green andesitic volcanic rocks and overlying polymictic cobble conglomerate is interpreted as the basal unconformity of the upper Hazelton Group. The basal conglomerate unit has a discontinuous fining-upward gradation from cobble-size clasts to coarsely laminated arkosic sandstone over a 1 m interval. This unit is mostly clast supported and contains a matrix of poorly sorted coarse to very coarse sandstone. Clasts are angular and include diorite, maroon and green lapilli and ash tuff, chert, lithic fragments and very fine grained fossiliferous limestone containing corals and crinoid fragments. Overlying conglomerate units with very similar characteristics show a cyclicity of multiple fining-upward sequences (Fig. 5). The basal conglomerate fines upward gradually into moderately calcareous arkosic sandstone beds that show cross-laminations, mud intraclasts and current ripples. Higher up, finely laminated beds of tuffaceous pale silt and orange-weathered fine sand resemble typical 'pyjama beds' (Fig. 2KB063b) and display such sedimentary structures as parallel laminations and ripples, and rusty orange–weathering carbonate lenses. Centimetre-scale normal faults and slump folds, soft-sediment deformation and bed pinchouts probably signify synsedimentary tectonism. Carbonate concretions occur at various locations throughout the sedimentary section. These can be up to 50 cm in diameter but are more commonly 5 cm. The distribution of concretions is sporadic, but they tend to be concentrated in certain beds.

A 2 m thick enigmatic unit of light to dark limestone with complex boundstone textures (Fig. 6) is present in area 3, close to the top of the Hazelton Group. The limestone includes shell fragments and is locally bioturbated. Freshly broken pieces smell of bitumen. Unfortunately, the contacts of this unit are not exposed, but the presence of thin limestone units elsewhere in the laterally equivalent successions suggest that it is an *in situ* carbonate unit and not an exotic block.

Massive sandstone occurring in the higher 'pyjama beds' represents a gradational transition between the underlying upper Hazelton Group and the overlying Bowser Lake Group. Thick beds of fine grey sandstone, alternating



Figure 2. Thinly interbedded siliceous mudstone, siltstone and fine sandstone with pale bands interpreted as tuff, characteristic of the upper Hazelton Group, area 3.



Figure 3. Bioturbated siltstone and mudstone containing the trace fossil *Scolicia*, suggesting shallow marine deposition, probably Muskaboo Creek assemblage, area 5.

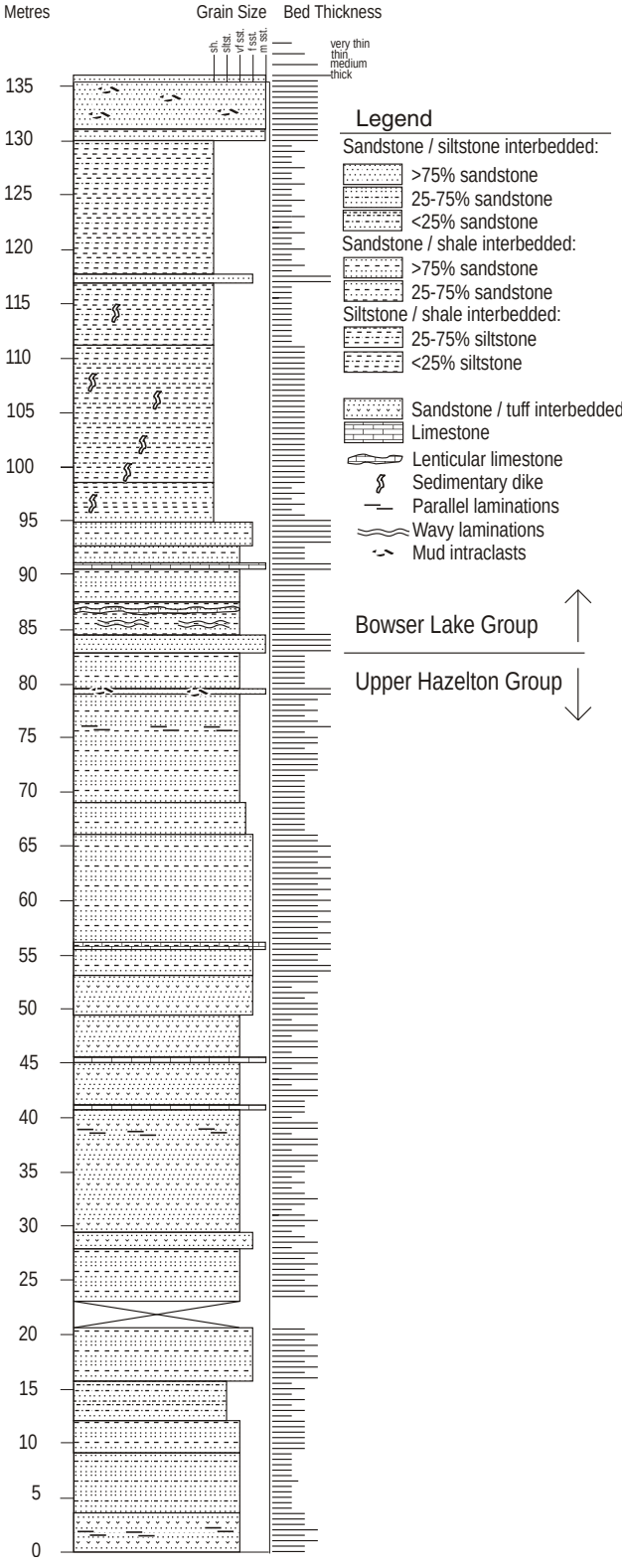


Figure 4. Stratigraphic section in upper Hazelton Group and lower Bowser Lake Group, area 1.

with thick successions of black fissile shale, represent the basal Bowser Lake Group.

In the Teigen Lake area (area 4, Fig. 1), the boundary between the volcanic-dominated lower Hazelton Group and the more sedimentary-dominated upper Hazelton Group is marked by a 30–40 m band of orange to brown-weathered outcrop. A sharp contact of lapilli tuff overlain by an arkosic medium sandstone bed emphasizes the contact, but no angular discordance was seen. The contact is offset about 30 m in a dextral sense by a small north-northeast-striking fault. Abundant marine fossils (belemnites, bivalves) occur on the top of a thick pebbly sandstone bed just above the inferred base of the upper unit. Higher in the section, finely laminated thin beds of dark grey siltstone are overlain by thickly bedded arkosic sandstone. The dark grey siltstone is locally calcareous and contains well-preserved belemnites. The very fine parallel laminations and the interbeds of black shale within this unit again suggest a deep-water depositional environment. The stratigraphically higher sandstone unit is well sorted overall and includes centimetre-thick bands of coarse grains and many rounded mud intraclasts (up to 25 cm). The rapid change of grain size in both fining and coarsening-upward sequences, and erosional features such as scoured bases and intraclasts, indicate rapid deposition in a high-energy marine environment.

Sedimentary rocks similar to those described above were observed at a single locality in area 7 (location A in Fig. 7). The limited extent of these units suggests that their contact with the purely igneous rocks of the lower Hazelton Group might be faulted.

Bowser Lake Group

The base of the Bowser Lake Group is marked by medium beds of medium-grained grey sandstone; the sandstone has a smoother appearance on weathered surfaces and is less siliceous than those of the upper Hazelton Group. The overlying succession is dominated by fine to medium sandstone beds and fissile black shale, in cyclic successions that are each several metres thick. These are representative of the Ritchie-Alger turbidite assemblage.

Approximately 15 m above the base of the Bowser Lake Group in area 1, medium-grained beige sandstone sheets are observed to cut bedding in black shale units at low to high angles (Fig. 4). Some of these sheets are planar, whereas others are tightly to ptygmatically folded, probably in response to compaction of the surrounding mud. These sheets are interpreted as sedimentary dikes, representing extensional fissures infilled by sand from above. In some locations, the dikes show offset of bedding, indicating that the fissures displayed a component of normal-sense fault motion.

The transition from the upper Hazelton Group to Bowser Lake Group sedimentary rocks is rather abrupt in area 4. There is an overall increase in the quartz content of the sandstone and mudrock becomes more fissile upward. The overlying thick succession of turbidites with Bouma sequences and interbedded fine sandstone and shale is typical of the Ritchie-Alger assemblage. Diagenetic carbonate concretions and pyrite are locally present in the siltstone. A well-defined submarine-fan channel, characterized by well-sorted chert-pebble conglomerate, locally cuts through the finer sedimentary rocks. East-trending

syndepositional normal faults and sandstone dikes (Fig. 8) attest to tectonic instability.

No direct contact between the Hazelton Group and the Bowser Lake Group was observed in area 7; however, because the transition is abrupt, occurring over a relatively small unexposed distance (~50 m), and lacks transitional facies seen elsewhere, the contact is here interpreted to be a fault. The Bowser Lake Group consists of interbedded shale, dark grey siltstone and light grey fine-grained sandstone with parallel laminations. Sedimentary structures, such as flame structures, convolute laminations and partial (bcd) Bouma sequences, suggest that these rocks were deposited as turbidites in a submarine-fan setting. Distorted fossils, such as ammonites and belemnites, are common in this rock type and attest to the marine environment.

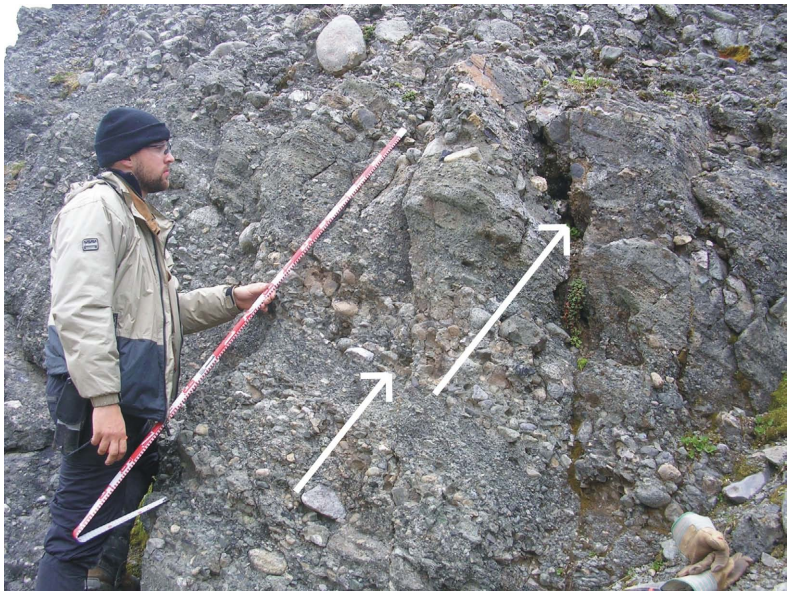


Figure 5. Conglomerate at base of upper Hazelton Group, area 2.

DEFORMATION

Deformation in the Lower Hazelton Group

The lower Hazelton Group on the margins of Oweegee Dome displays numerous faults that do not appear to continue, based on this summer's observations, into the overlying Bowser succession. The scale of faulting ranges from meso to macroscopic, but only the larger faults have associated gouge. Faults with gouge dip steeply, with strikes ranging from southwest to west. Volcaniclastic rocks display protomylonitic texture, with localized C-S fabric indicating a component of dextral shear, adjacent to a conspicuous west-striking fault zone with extensive fault gouge and orange-weathering gossan. These observations suggest that deformation occurred close to the brittle-ductile transition. Numerous veins are present, filled by both calcite and quartz; in some cases, intersecting veins indicate multiple generations of fracturing and movement of hydrothermal fluid. Veins are typically quartz where they cut chert and rhyolite, but calcite in the pyroclastic rocks, intermediate lava flows and sedimentary rocks.

On the west side of the dome (area 2), at least two well-developed foliation fabrics are developed in the lower Hazelton Group: a steeply dipping (80º) east-trending cleavage and a shallower (20º) fabric with similar orientation to bedding, which dips gently west-southwest. The intersection lineation created by the superimposed cleavages results in an elongated pencil-like breaking habit. The foliations are best developed in maroon and green volcaniclastic rocks and in the fine-grained sedimentary rocks; they are difficult to see in the more competent units, such as chert, rhyolite and conglomerate. Extensional features, including joint and vein sets, are common in this area.

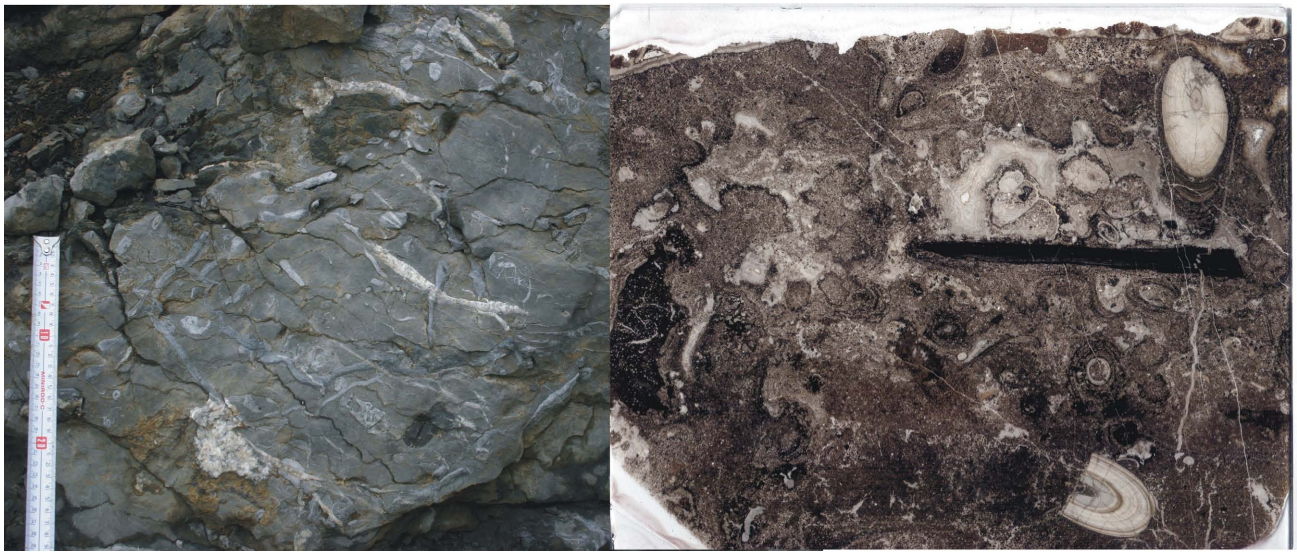


Figure 6. Complex boundstone unit at the top of the Hazelton Group, area 3. Field photograph (left) and large-format thin section (right). Field of view of thin section ~10 cm.

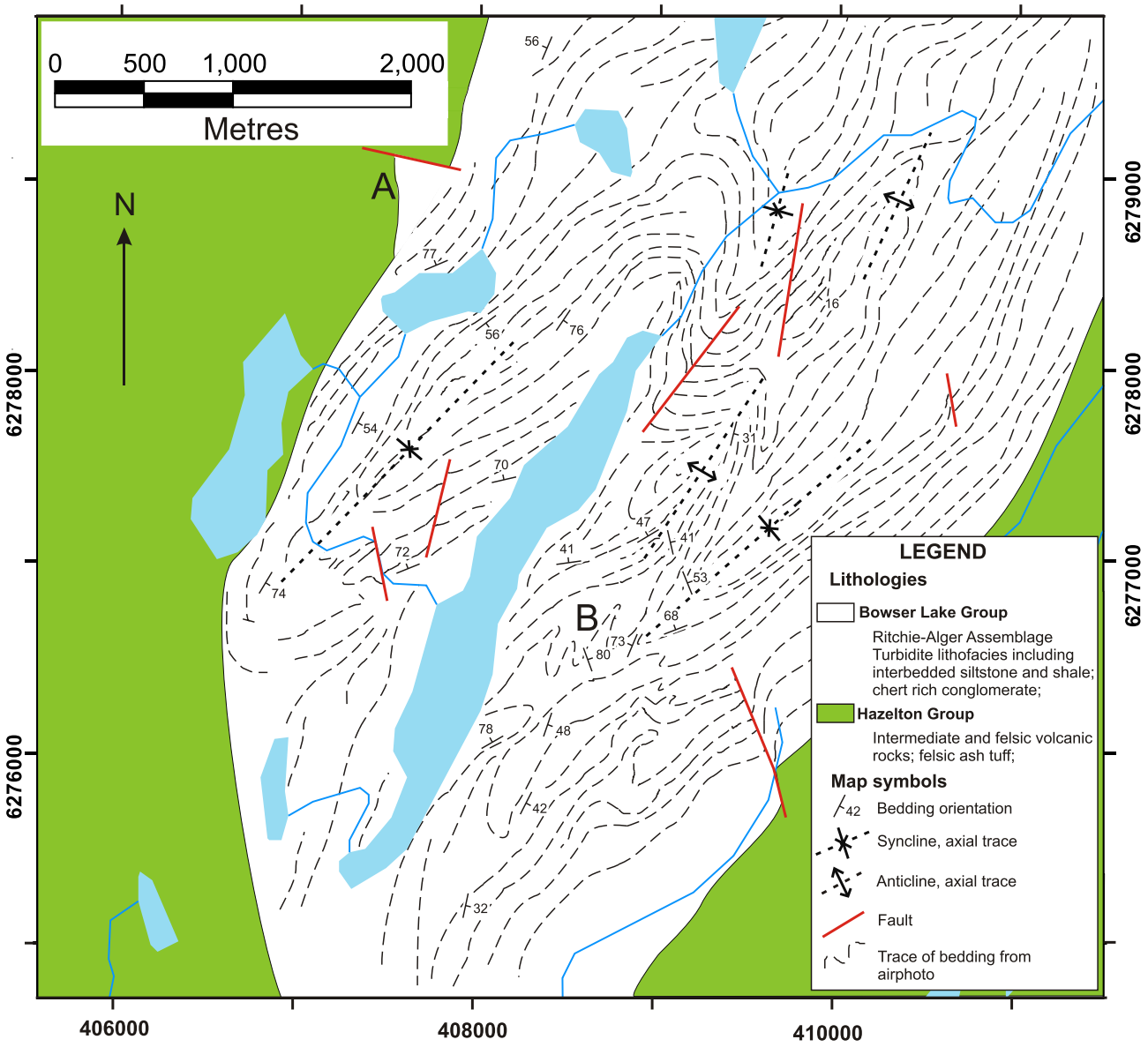


Figure 7. Generalized geology of area 7, showing traces of bedding and major structures based on mapping and airphoto interpretation, and locations A and B.

Deformation in the Bowser Succession

REGIONAL FOLDS AND CLEAVAGE

Oweegee Dome Area

Previous mapping was carried out in the Oweegee Dome area by Greig and Evenchick (1993). The authors have examined selected areas in detail (Fig. 1), confirming the map-scale structures shown by them. Folds, with wavelengths estimated to range from hundreds of metres to kilometres, occur in the Bowser Lake Group overlying the Oweegee Dome. In general, the amplitude of folding increases away from the margins of the dome, suggesting that shortening in higher parts of the stratigraphy is balanced by faults or ductile shearing deeper in the succession. At least some of the folds are therefore probably detachment folds (*e.g.*, Jamison, 1987) related to shearing in the lower shaly strata of the Bowser Lake Group. Most folds trend southeast in this area and plunge gently; south-southwest and north-northeast-plunging folds are present locally. Figure 9 displays a typical kink-fold pair, with fold hinges plunging gently north-northwest. Smaller folds, with wavelengths of metres to tens of metres, are locally abundant, particularly in area 3. Plots of poles to bedding from selected areas around the Oweegee Dome clearly show girdle distributions related to the predominant fold axes that trend south-southeast (Fig. 10, 11), consistent with the major structures mapped by Greig and Evenchick (1993).

Cleavage is very sporadically developed around the Oweegee Dome; cleavage orientations are also plotted in Figures 10 and 11. Local pencil fabric was observed, resulting from simultaneous splitting of the rock along tectonic cleavage and a strong bed-parallel fabric. On the east margin of the dome, a majority of cleavage orientations strike south-southeast and could be consistent with an axial-planar relationship to the main folds. However, they are much

more widely dispersed than the bedding poles. At the south margin of the dome, the scattered cleavage observations show a predominant east-southeasterly strike, again scattered in a diffuse girdle about a steeply south-southwest-plunging axis. These relationships are consistent with an early development of cleavage, perhaps associated with east-southeast-trending F_1 folds and subsequent refolding by F_2 folds with a Cordilleran (north-northwest) trend.

Because of the difficulty of resolving the relative timing of fold generations, an area of previously recorded diverse fold orientations (area 5) was selected for study near Tumeka Creek. Kilometre-scale northwest-trending chevron folds are observable from several locations. Locally, concentric and kink folds occur at the cores of larger structures, with planar bedding on the flanks. However, plotted bedding orientations show a diffuse cluster, with no clear girdle distribution (Fig. 12). Cleavage is well developed in this area, particularly in the dark grey siltstone. Cleavage predominantly strikes north-northeast, with steep dips. In contrast to the observed fold hinges, which mainly trend south-southeast, bedding-cleavage intersection lineations show a wide scatter, including predominant north-northeasterly trends. Cleavage orientations are also significantly more dispersed than bedding, forming a short segment of a girdle distribution about a steeply plunging axis (Fig. 12). These observations suggest that cleavage predates the majority of observed folds and was refolded about a steeply plunging axis by development of south-southeast-striking F_2 folds.

Folds are rare at the basin margin near Teigen Lake (area 4), but penetratively foliated shale contains at least two different cleavages (oriented 089°/84°S and 217°/75°W) that form a steep pencil lineation. Although the sequence of deformation is uncertain because of poor outcrop, it again appears that the steeper, south-dipping fabric (S_2) cuts an older northwest-dipping S_1.

The Bowser Lake rocks in area 7 show an overall structural pattern dominated by tight, northeast-plunging, steeply inclined anticlines and synclines (Fig. 7, 13). This generation of folds is associated with a penetrative cleavage with a mean orientation of 053°/80°S. The map-scale folds are commonly surrounded by outcrop-scale parasitic folds with a cleavage trace that is nearly parallel to the axial plane (047°). At location B (Fig. 7, 14), the northeast-trending cleavage is disturbed and changes direction significantly by more than 30° at outcrop scale. The deflection of both F_1 folds and their associated cleavage (S_1) indicates that a second generation of open F_2 folds is present, with an average axial trace striking 120°. A second, locally developed disjunctive cleavage (S_2) associated with the F_2 folds shows constant orientation of 315°/85°E, without any sign of curvature, and is therefore believe to be related to a later and different episode of deformation. On a regional scale, the superimposed F_2 folds create a distortion of the F_1 folds by gently bending their limbs (Fig. 7). The overprinting of the two cleavage planes locally creates a steeply north-plunging L_2 intersection lineation.

STRUCTURES ASSOCIATED WITH THE BASE OF THE BOWSER SUCCESSION

Outcrop-scale structures are well exposed in the upper Hazelton Group adjacent to the Oweegee Dome. On the east margin of the dome, the formation contains thrust faults that cut bedding and terminate in outcrop-scale fault-propagation folds with chevron geometry and kink-like fault-bend folds, related to ramp-flat geometries on the faults. These have fold hinges with a shallow plunge to the northwest. South-striking centimetre-scale extensional faults are also present, but there is no clear evidence of their timing relative to the thrusts.

Farther upsection, the upper Hazelton Group and the overlying Bowser Lake Group are separated in area 1 by a zone of intense veining, folding and fabric development in shale, defining a shear zone between the two formations. Shale within this shear zone displays multiple orientations



Figure 8. Synsedimentary dikes in basal Bowser Lake Group, area 4.



Figure 9. View of kink-style folds in area 3. Field of view approximately 300 m wide.

of fabric (Fig. 15). The first fabric generation suggests that the shear zone initially behaved as a southwest-directed thrust fault, producing a shear fabric oblique to the fault. Later reactivation of the fault with a normal sense of displacement produced an intermediate upright fabric in response to the change in sense of movement.

In area 4, the regional moderate to steep northeaster dip of bedding is relatively constant. However, a tight synform and antiform in 'pyjama beds' plunge gently southeast. This style of deformation is only observed in upper Hazelton and Bowser Lake sedimentary rocks and seems to be absent in the older Hazelton volcaniclastic rocks. Therefore, a décollement at the top of the lower Hazelton Group might have occurred during the formation of the Skeena fold belt.

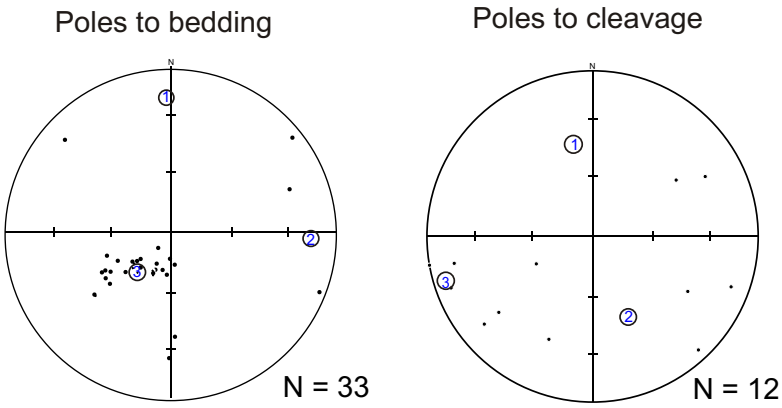


Figure 10. Lower hemisphere, equal-area projections showing the orientation of structures in area 1. Circled numbers 1, 2 and 3 represent eigenvectors of the distribution.

STEEP BRITTLE STRUCTURES IN THE BOWSER SUCCESSION

Steep brittle structures are seen at other localities. On the west side of the Oweegee Dome, brittle structures are developed in the lowest stratigraphic unit of the upper Hazelton Group, a unit of heavily sheared silicified conglomerate that shows intense veining. Multiple quartz veins recut each other in variable directions along a 5 m band that strikes 032°. The white-weathering colour of the rock is likely to be the result of siliceous fluids circulating in the fractures. Systematic conjugate joints sets (015°/75°E; 322°/75°E) are also present in the competent conglomerate unit, suggesting north-south compression consistent with sinistral shear on the north-northeast-striking fault. The fault zone continues into an adjacent section of 'pyjama beds'.

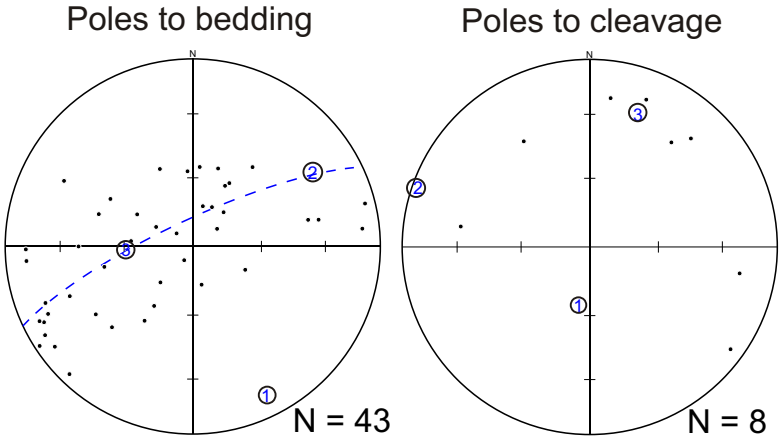


Figure 11. Lower hemisphere, equal-area projections showing the orientation of structures in area 3. Circled numbers 1, 2 and 3 represent eigenvectors of the distribution. Dashed line represents best-fit great circle to girdle distribution.

Veining is locally intense in folded regions north of the Oweegee Dome at Tumeka Creek (area 5); veins are dominantly filled by quartz. However, anhydrite veins with brecciated sandstone clasts were noted, distributed over an area several hundred metres square. Faults are also abundant in this area. The largest of these is a southwest-striking dextral strike-slip fault.

Faults in area 7 strike predominantly southeast, roughly parallel to the second (S_2) cleavage. Since the S_1 cleavage seems to be distorted and cut by multiple small-scale faults, the timing of faulting is clearly post F_1. One recorded fault, striking 290º, shows Riedel shears that suggest sinistral motion. Locally, veins show an 'en échelon' arrangement and are believed to be synthetic Riedel shears formed during strike-slip movement associated with the second folding event (F_2).

DISCUSSION

Figure 16 shows comparative sections through the base of the Bowser succession, based on the authors' observations in areas 1–4. The predominantly volcanic rocks of the lower Hazelton Group are interpreted (following Thorkelson *et al.*, 1995) as representing volcanic-arc environments that existed during the final stages in the existence of Stikinia as an independent terrane. The observations made at Mount Skowill (area 2) in the northern part of Oweegee Dome show that there is a gradual increase of more convincingly sedimentary rocks upsection in the Hazelton Group, suggesting a progressive decline in volcanic activity; several debris flows suggest that the basin was still tectonically unstable. The boundary between the lower and upper Hazelton Group is an unconformity, as clearly illustrated by the map relationships at the Oweegee Dome (Greig and Evenchick, 1993). The basal conglomerate of the upper Hazelton Group progressively fines upward through feldspathic medium sandstone to black shale. This overall transgressive sequence indicates an increase in the basin depth in response to some combination of sea-level change, tectonics and thermal subsidence. Variations in the thickness and facies of the upper Hazelton Group suggest transgression over an uneven surface (Fig. 16). The thinness of the Richie-Alger assemblage on the east side of the Oweegee Dome (area 1) suggests that the domal structure possibly originated during the development of the basin (Evenchick *et al.*, 2005). The abundance of fractures and brittle deformation structures in the lower Hazelton Group support significant deformation and suggest that the Bowser Basin was developed over a topography developed by

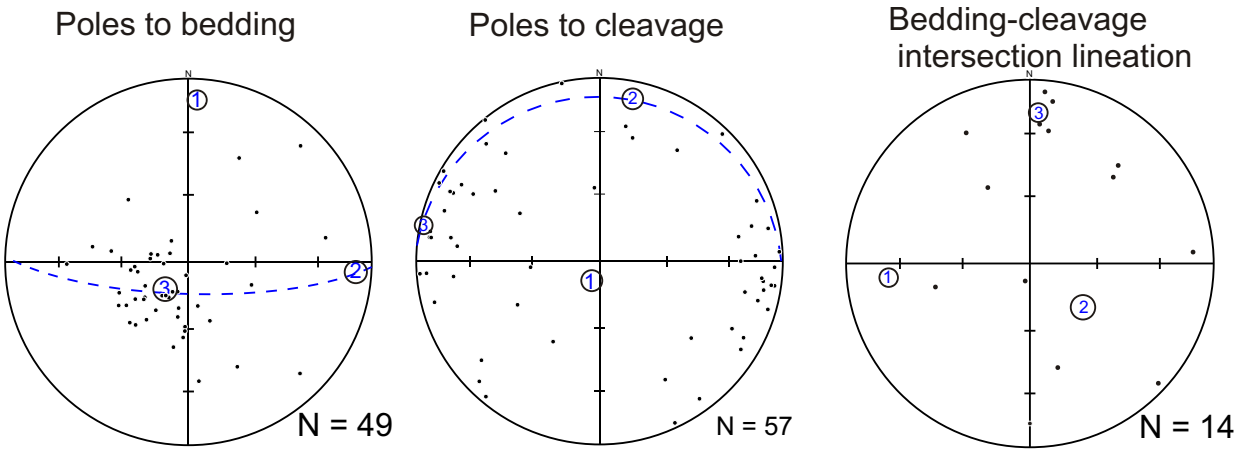


Figure 12. Lower hemisphere, equal-area projections showing the orientation of structures in area 5. Circled numbers 1, 2 and 3 represent eigenvectors of the distribution. Dashed line represents best-fit great circle to girdle distribution.

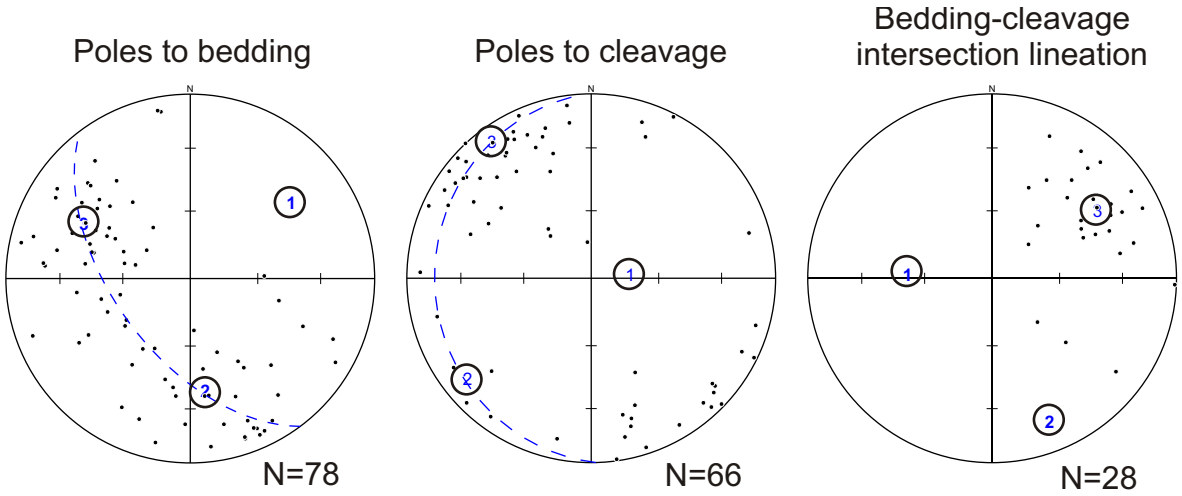


Figure 13. Lower hemisphere, equal-area projections showing the orientation of structures in area 7. Circled numbers 1, 2 and 3 represent eigenvectors of distribution. Dashed line represents best-fit great circle to girdle distribution.

faulting of the underlying Stikinia Terrane. Tectonic instability continued during deposition of the early Bowser Lake Group, indicated by an abundance of synsedimentary dikes.

Following deposition of the Bowser Lake Group, major deformation by folding occurred. Cleavage was also developed locally in the shaly units. Most of the mapped areas show some indication of overprinted fold generations and, in most areas, either northeast or northwest-trending folds predominate, confirming the observations of Evenchick (2001). Where evidence for overprinting is present, the authors noted a consistent overprinting of generally northeast-trending early folds or northeast-striking cleavage by later folds, with less well developed cleavage, that display 'Cordilleran' northwest or southeast trends. These results are consistent with earlier interpretations (Evenchick, 2001) that the northeast-trending folds were related to an early phase of Mesozoic sinistral transpression in the development of the Cordillera. The Cordilleran F_2 folds increase in amplitude with stratigraphic height above the base of the Bowser succession, suggesting that detachment occurred at this level, in addition to those below and above interpreted by Evenchick (1991). Low-angle thrusts that postdate S_1 cleavage, observed near the base of the succession, were probably developed as a result of this process.

At several locations, minor extensional structures were observed that appear to postdate F_2 folding. The authors speculate that these developed during Cenozoic extension, or perhaps dextral transtension.

Northeast-trending F_1 and S_1 structures are much more intensely developed in area 7 than elsewhere. This area coincides with the region of back-arc extension, or Eskay rift (e.g. Anderson, 1993; Alldrick *et al.*, 2005), a major structure in the underlying Hazelton Group that controls the distribution of facies and mineralization. The authors speculate that the faults associated with extension were inverted during the early stages of shortening in the Bowser Basin, and that the northeast-trending structures roughly follow pre-Bowser extensional features in underlying Stikinia. Since the Eskay Creek mine is located in a fault-bounded anticline, understanding the timing of the different structural elements that characterize the Bowser Lake rocks is potentially useful for predicting the location of the Eskay horizon (and possible mineral deposits) that might occur in the shallow subsurface. In addition, inversion structures are likely to propagate throughout the overlying Bowser succession, providing potential targets for hydrocarbon explo-

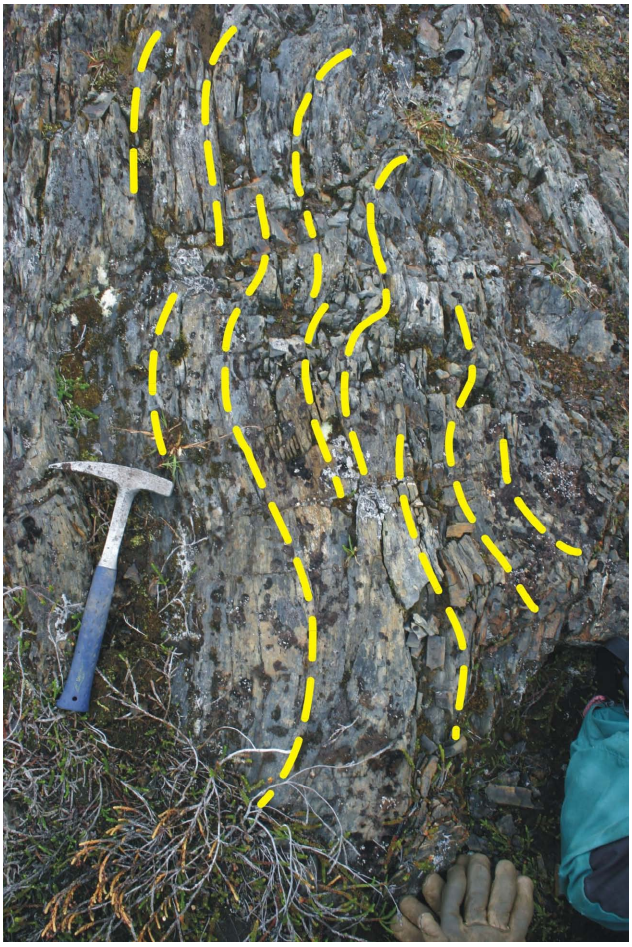


Figure 14. F_2 folds distorting S_1 cleavage, area 7.

ration that juxtapose thick successions of organic-rich upper Hazelton Group in the deep subsurface with anticlinal and or fault traps in potential reservoir rocks at higher stratigraphic levels. Further detailed geological mapping is needed to assess the timing relationship between faults and the two fold generations on a larger scale, and to improve the constraints on the geometry and timing of structures.

ACKNOWLEDGMENTS

The authors thank Geoscience BC for supporting this research through a grant to the Geological Survey of Canada. Additional field costs were supported by Natural Sciences and Engineering Research Council of Canada (NSERC) Discovery Grant A8508 to the senior author. Steve Samson and Shane Kepakevich assisted in the field. Helicopter support was provided by Quantum Helicopters. We acknowledge useful discussions with Peter Mustard, Margot McMechan, Dave Ritcey, Dani Alldrick and Joanne Nelson. Murray Gingras, Steve Irwin and Rob Stevens provided helpful comments on earlier versions of the manuscript.

REFERENCES



Figure 15. Shear zone containing fabric with multiple orientations. At A, the fabric dips steeply northeast, consistent with southwest shearing on shear zone (indicated by dashed line). At B and C, the fabric is progressively rotated to a moderate northwesterly dip, in-

Alldrick, D.J., Nelson, J.L. and Barresi, T. (2005): Geology and mineral occurrences of the Upper Iskut River area: tracking the Eskay rift through northern British Columbia (Telegraph Creek NTS 104G/1, 2; Iskut River NTS 104B/9, 10, 15, 16); *in* Geological Fieldwork 2004, *BC Ministry of Energy, Mines and Petroleum Resources*, Paper 2005-1, pages 1–30.

Anderson, R.G. (1993): A Mesozoic stratigraphic and plutonic framework for northwestern Stikinia (Iskut River area), northwestern British Columbia, Canada; *in* Mesozoic Paleogeography of the Western United States – II; Dunne, G. and McDougall, K., Editors, *Pacific Section, Society of Economic Paleontologists and Mineralogists*, Book 71, pages 477–494.

Bassett, K.N. and Kleinspehn, K.L. (1997): Early to Middle Cretaceous paleogeography of north-central British Columbia: stratigraphy and basin analysis of the Skeena Group; *Canadian Journal of Earth Sciences*, Volume 34, pages 1644–1669.

Greig, C.J. and Evenchick, C.A. (1993): Geology of Oweegee Dome (geochemistry and paleontology), Delta Peak (104A/12) and Taft Creek (104A/11W) map areas, northwestern British Columbia; *Geological Survey of Canada*, Open File 2688.

Evenchick, C.A. (1991): Structural relationships of the Skeena Fold Belt west of the Bowser Basin, northwest British Columbia; *Canadian Journal of Earth Sciences,* Volume 28, pages 973–983.

Evenchick, C.A. (2001): Northeast-trending folds in the western Skeena Fold Belt, northern Canadian Cordillera: a record of Early Cretaceous sinistral plate convergence; *Journal of Structural Geology*, Volume 23, pages 1123–1140.

Evenchick, C.A., Mustard, P.S., Greig, C.J., Porter, J.S. and McNeill, P.D. (2000): Geology, Bowser Lake (NTS 104A), British Columbia; *Geological Survey of Canada*, Open File 3918.

Evenchick, C.A., Ferri, F., Mustard, P.S., McMechan, M.E., Osadetz, K.G., Stasiuk, L.D., Wilson, N.S.F., Enkin, R.J. and McNicoll, V.J. (2003): Recent results and activities of the integrated petroleum resource potential and geoscience studies of the Bowser and Sustut basins, British Columbia; *Geological Survey of Canada*, Current Research 2003-A13, 11 pages.

Evenchick, C.E., Ferri, F., Mustard, P.S., McMechan, M.E., Ritcey, D., McNicoll, V.J., Osadetz, K.G., O'Sullivan, P.B., Stasiuk, L.D., Wilson, N.S.F., Poulton, T.P., Lowe, C., Enkin, R.J., Waldron, J., Snyder, D.B., Turner, R.J.W., Nowlan, G. and Boddy, M. (2005): Highlights of recent research in the Bowser and Sustut Basins Project, British Columbia; *Geological Survey of Canada*, Current Research 2005-A1, 11 pages.

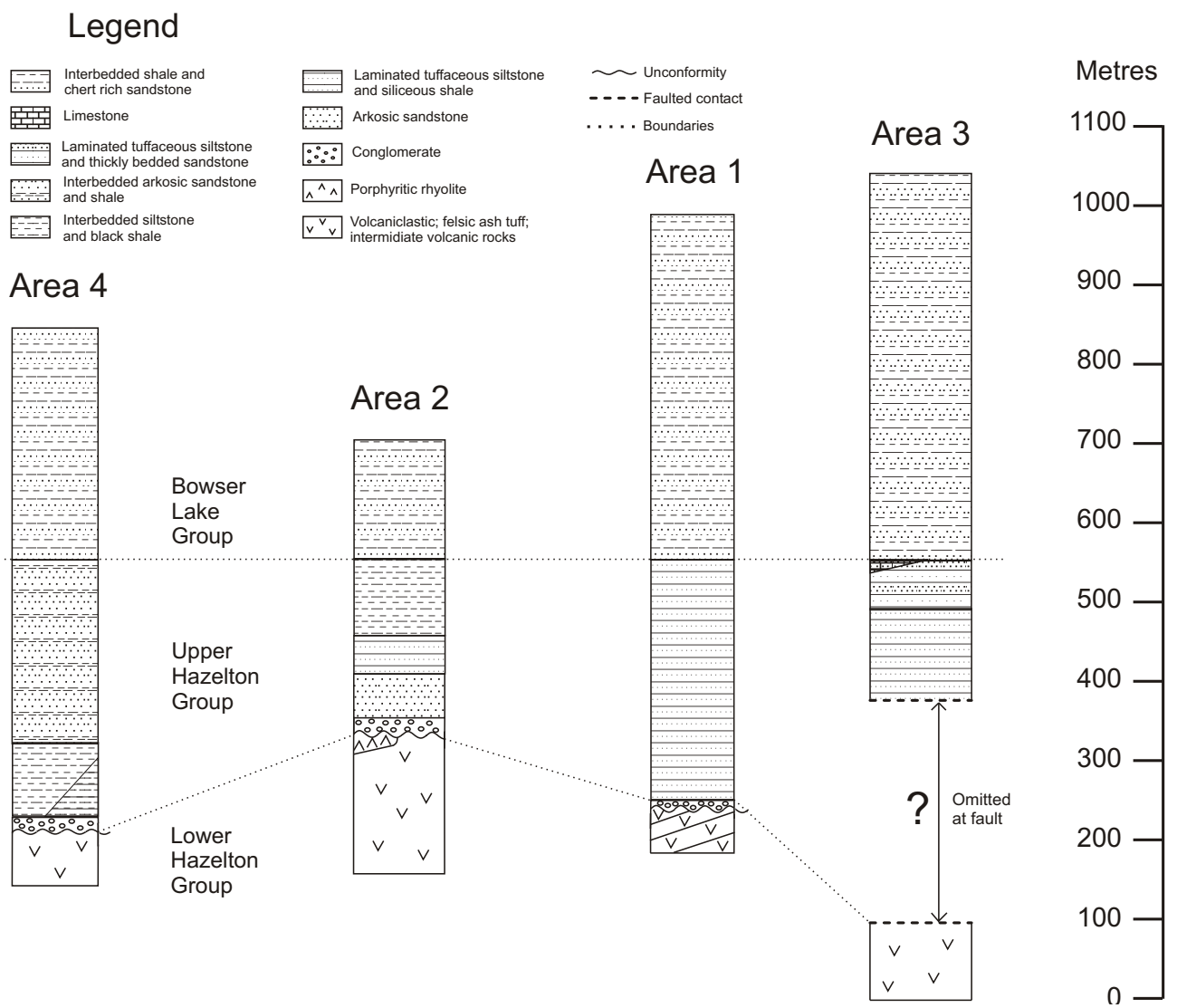


Figure 16. Comparative stratigraphic sections through the upper Hazelton Group in areas 1–4.

Evenchick, C.A. and Thorkelson, D.J. (2005): Geology of the Spatsizi River map area, north-central British Columbia; *Geological Survey of Canada*, Bulletin 577.

Ferri, F. and Boddy, M. (2005): Geochemistry of Early to Middle Jurassic organic-rich shales, intermontane basins, British Columbia; *in* Summary of Activities 2005, *BC Ministry of Energy, Mines and Petroleum Resources,* pages 132–151.

Greig, C.J. and Evenchick, C.A. (1993): Geology of Oweegee Dome (geochemistry and paleontology), Delta Peak (104A/12) and Taft Creek (104A/11W) map areas, northwestern British Columbia; *Geological Survey of Canada*, Open File 2688.

Jamison, R.J. (1987): Geometric analysis of fold development in overthrust terranes; *Journal of Structural Geology*, Volume 9, pages 207–219.

Lewis, P.D., Toma, A. and Tosdal, R.M., Compilers (1996): Metallogenesis of the Iskut River area, northwestern British Columbia; University of British Columbia, Mineral Deposit Research Unit, Special Publication 1, 325 pages plus maps at 1:50 000 scale (CD-ROM).

Marsden, H. and Thorkelson, D.J. (1992): Geology of the Hazelton volcanic belt in British Columbia: implications for the Early to Middle Jurassic evolution of Stikinia; *Tectonics*, Volume 11, pages 1266–1287.

Osadetz, K.G., Evenchick, C.A., Ferri, F., Stasiuk, L.D. and Wilson, N.S.F. (2003): Indications for effective petroleum systems in Bowser and Sustut basins, north-central British Columbia; *in* Geological Fieldwork 2002, *BC Ministry of Energy, Mines and Petroleum Resources*, Paper 2003-1, pages 257–264.

Ricketts, B.D., Evenchick, C.A., Anderson, R.G. and Murphy, D.C. (1992): Bowser Basin, northern British Columbia: constraints on the timing of initial subsidence and Stikinia – North America terrane interactions; *Geology*, Volume 20, pages 1119–1122.

Roth, T., Thompson, J.F.H. and Barrett, T.J. (1999): The precious metal – rich Eskay Creek deposit, northwestern British Columbia; *in* Volcanic-Associated Massive Sulfide Deposits: Processes and Examples in Modern and Ancient Settings, Barrie, C.T. and Hannington, M.D., Editors, *Reviews in Economic Geology,* Volume 8, pages 357–373.

Tipper, H.W. and Richards, T.A. (1976): Jurassic stratigraphy and history of north-central British Columbia; *Geological Survey of Canada*, Bulletin 270.

Thomson, R.C., Smith, P.L. and Tipper, H.W. (1986): Lower to Middle Jurassic (Pliensbachian to Bajocian) stratigraphy of the northern Spatsizi area, north-central British Columbia; *Canadian Journal of Earth Sciences*, Volume 23, pages 1963–1973.

Thorkelson, D.J., Mortensen, J.K., Marsden, H. and Taylor, R.P. (1995): Age and tectonic setting of Early Jurassic volcanism along the northeastern margin of the Hazelton Trough, northern British Columbia; *in* Jurassic Magmatism and Tectonics of the North American Cordillera, Miller, D.M. and Busby, C., Editors, *Geological Society of America*, Special Paper 299, pages 83–94.